

cover



Taub's
**Principles of
Communication Systems**

Fourth Edit ion

ABOUT THE AUTHORS



Goutam Saha, a BTech. and PhD holder from IIT Kharagpur, joined the faculty of Electronics and Electrical Communication Engineering at IIT Kharagpur in 2000. Dr Saha has undergone a short Management Training at XLRI, Jamshedpur. During 1990-1994, he worked with Tata Steel. In 2006, he served University of Southern California, USA, for one semester under the faculty exchange program. He also worked as a visiting scientist at Trento University, Italy briefly and has been a member of Indian delegations to leading universities in Canada. Dr. Saha has given many invited lectures in India and abroad in his research areas which include investigation in health care, and audio analysis related to surveillance system. He was declared a winner in DST-Lockheed Martin India Innovation Growth Program 2009. He has published papers in leading international journals and conference proceedings and has filed several patents. Dr. Saha is co-author of two popular engineering textbooks, *Digital Principles and Applications* and *Principles of Communication Systems*, published by McGraw Hill Education (India). He has served many administrative positions and is currently, the Program Coordinator of National Service Scheme (NSS), IIT Kharagpur.



Taub's
**Principles of
Communication Systems**

Fourth Edit ion

(Late) Herbert Taub

Formerly Vice President for Academic Affairs and Dean of the Faculty City University of New York

Donald L Schilling

City University of New York

Goutam Saha

Program Coordinator of National Service Scheme (NSS) Department of Electronics and Electrical Communication Engineering IIT Kharagpur, West Bengal, India



McGraw Hill Education (India) Private Limited

NEW DELHI

McGraw Hill Education Offices New York St Louis San Francisco Auckland Bogotá Caracas Kuala Lumpur Lisbon London Madrid Mexico City Milan Montreal San Juan Santiago Singapore Sydney Tokyo Toronto



McGraw Hill Education (India) Private Limited

Principles of Communication Systems, 4e (SIE)

Indian Adaptation done by arrangement with The McGraw-Hill Companies, Inc., New York

Sales Territories: India, Pakistan, Nepal, Bangladesh, Sri Lanka and Bhutan

Copyright © 2013, 2008, by The McGraw-Hill Companies, Inc. All Rights reserved. No part of this publication may be reproduced or distributed in any form or by any means, electronic, mechanical, photocopying, recording, or otherwise or stored in a database or retrieval system without the prior written permission of The McGraw-Hill Companies, 1221 Avenue of the Americas, New York, NY, 10020 including, but not limited to, in any network or other electronic storage or transmission, or broadcast for distance learning.

McGraw Hill Education (India) Edition 2013

ISBN (13): 978-1-25-902985-1

ISBN (10): 1-25-902985-9

Vice President and Managing Director: *Ajay Shukla*

Head—Higher Education Publishing and Marketing: *Vibha Mahajan*

Publishing Manager—SEM & Tech Ed.: *Shalini Jha*

Editorial Executive: *Koyel Ghosh*

Manager—Production Systems: *Satinder S Baveja*

Asst. Manager—Editorial Services: *Sohini Mukherjee*

Sr. Production Manager: *P L Pandita*

Asst. General Manager—Higher Education (Marketing): *Vijay Sarathi*

Sr. Product Specialist —SEM & Tech. Ed.: *Tina Jajoriya*

Sr. Graphic Designer—Cover: *Meenu Raghav*

General Manager—Production: *Rajender P Ghansela*

Production Manager: *Reji Kumar*

Information contained in this work has been obtained by McGraw Hill Education (India), from sources believed to be reliable. However, neither McGraw Hill Education (India) nor its authors guarantee the accuracy or completeness of any information published herein, and neither McGraw Hill Education (India) nor its authors shall be responsible for any errors, omissions, or damages arising out of use of this information. This work is published with the understanding that McGraw Hill Education (India) and its authors are supplying information but are not attempting to render engineering or other professional services. If such services are required, the assistance of an appropriate professional should be sought.

Typeset at The Composers, 260, C.A. Apt., Paschim Vihar, New Delhi 110 063, and printed at

Cover Printer:

**

CONTENTS

Preface

1. Introduction: Signal and Spectra

1.1 An Overview of Electronic Communication Systems

Self-Test Questions

1.2 Signal and its Properties

Self-Test Questions

1.3 Fourier Series Expansion and its Use

Self-Test Questions

1.4 The Fourier Transform

Self-Test Questions

1.5 Orthogonal Representation of Signal

Self-Test Questions

Matlab

Summary

Problems

References

2. Amplitude-Modulation Systems

2.1 Need for Frequency Translation

2.2 Double Side Band—Suppressed Carrier (DSB-SC) Modulation

Self-Test Questions

2.3 Amplitude Modulation: Double Side Band with Carrier (DSB-C)

Self-Test Questions

2.4 Single Side Band Modulation (SSB)

Self-Test Questions

2.5 Other AM Techniques and Frequency Division Multiplexing

Self-Test Questions

2.6 Radio Transmitter and Receiver

Self-Test Questions

Matlab

Summary

Problems

References

3. Angle Modulation

3.1 Angle Modulation

Self-Test Questions

3.2 Spectrum of Tone Modulated Signal

Self-Test Questions

3.3 Arbitrary Modulated FM Signal

Self-Test Questions

- 3.4 FM Modulators and Demodulators

Self-Test Questions

- 3.5 Stereophonic FM Broadcasting

Self-Test Questions

Matlab

Summary

Problems

References

4. Pulse Modulation and Digital Transmission of Analog Signals

- 4.1 Analog to Digital: The Need

Self-Test Questions

- 4.2 Pulse Amplitude Modulation and Concept of Time Division Multiplexing

- 4.3 Pulse Width Modulation and Pulse Position Modulation

Self-Test Questions

- 4.4 Digital Representation of Analog Signal

Self-Test Questions

- 4.5 Certain issues in Digital Transmission

- 4.6 Differential Pulse Code Modulation

- 4.7 Delta Modulation

Self-Test Questions

- 4.8 Voice Coders (Vocoders)

Self-Test Questions

Matlab

Summary

Problems

References

5. Digital Modulation and Transmission

- 5.1 Binary Phase Shift Keying (BPSK)

- 5.2 Differential Phase Shift Keying (DPSK)

- 5.3 Differentially Encoded Phase Shift Keying (DEPSK)

- 5.4 Quadrature Phase Shift Keying (QPSK)

- 5.5 M-ary Phase Shift Keying

Self-Test Questions

- 5.6 Quadrature Amplitude Shift Keying (QASK)

- 5.7 Binary Frequency Shift Keying (BFSK)

- 5.8 M-ary FSK

- 5.9 Minimum Shift Keying (MSK)

Self-Test Questions

- 5.10 Pulse Shaping to Reduce Interchannel and Intersymbol Interference

Self-Test Questions

- 5.11 Some Issues in Transmission and Reception

5.12 Orthogonal Frequency Division Multiplexing (OFDM)

Self-Test Questions

Matlab

Summary

Problems

6. Random Variables and Processes

6.1 Probability

Self-Test Questions

6.2 Random Variables

Self-Test Questions

6.3 Useful Probability Density Functions

Self-Test Questions

6.4 Useful Properties and Certain Application Issues

Self-Test Questions

6.5 Random Processes

Self-Test Questions

Matlab

Summary

Problems

References

7. Mathematical Representation of Noise

7.1 Some Sources of Noise

7.2 Frequency-domain Representation of Noise

Self-test Questions

7.3 Superposition of Noises

7.4 Linear Filtering of Noise

Self-Test Questions

7.5 Quadrature Components of Noise

7.6 Representation of Noise using Orthonormal Coordinates

Self-test Questions

Matlab

Summary

Problems

References

8. FM Reception Performance Under Noise

8.1 Framework for Amplitude Demodulation

8.2 Single Sideband Suppressed Carrier (SSB-SC)

8.3 Double Sideband Suppressed Carrier (DSB-SC)

Self-test Questions

8.4 Double Sideband with Carrier (DSB-C)

8.5 Comparison of AM Systems: A Figure of Merit

8.6 Threshold Effect in AM Reception

Self-Test Questions

Matlab

Summary

Problems

Reference

9. FM Reception Performance Under Noise

9.1 An FM Receiving System

9.2 Calculation of Signal to Noise Ratio

9.3 Comparison of FM and AM

Self-test Questions

9.4 Preemphasis and Deemphasis and SNR Improvement

9.5 Phase Modulation (PM) and Multiplexing Issues

Self-test Questions

9.6 Threshold in Frequency Modulation

Self-test Questions

9.7 Calculation of Threshold in an FM Discriminator

9.8 The FM Demodulator using Feedback (FMFB)

Self-Test Questions

Matlab

Summary

Problems

Reference

10. Phase-Locked Loops

10.1 PLL Characteristics

10.2 Analog PLL and Frequency Demodulation

Self-test Questions

10.3 Digital Phase-Locked Loop

10.4 All Digital PLL and Software PLL

Self-Test Questions

10.5 Applications of Phase-Locked Loops

Self-Test Questions

Matlab

Summary

Problems

References

11. Optimal Reception of Digital Signal

11.1 A Baseband Signal Receiver

11.2 Probability of Error

Self-Test Questions

11.3 Optimal Receiver Design

Self-test Questions

11.4 Reception of PSK, FSK, QPSK, DPSK Signal

Self-Test Questions

11.5 Signal Space Representation and Probability of Error

Self-Test Questions

11.6 Probability of Error Calculation for M-ary Signal

11.7 Probability of Error in a QPR System

11.8 Comparison of Modulation Systems

Self-Test Questions

Matlab

Summary

Problems

References

12. Noise in Pulse Code Modulation and Delta Modulation Systems

12.1 PCM Transmission

Self-Test Questions

12.2 Delta Modulation (DM) Transmission

Self-Test Questions

12.3 Comparison of PCM and DM

12.4 The Space Shuttle ADM

Self-Test Questions

Matlab

Summary

Problems

References

13. Information Theoretic Approach to Communication

13.1 Discrete Messages and Information Content

Self-Test Questions

13.2 Source Coding and Increase of Average Information

Self-Test Questions

13.3 Shannon's Theorem, Channel Capacity

13.4 Use of Orthogonal Signals to Attain Shannon's Limit

13.5 Mutual Information and Channel Capacity

13.6 Rate Distortion Theory and Lossy Source Coding

Self-Test Questions

13.7 Information Theory and Optimum Modulation System

13.8 Feedback Communication

Self-Test Questions

Matlab

Summary

Problems

References

14. Error-Control Coding

- 14.1 Introduction to Error-Control Codes
- 14.2 Upper Bound of the Probability of Error with Coding
- 14.3 Block Codes—Coding and Decoding
 - Self-Test Questions*
- 14.4 Burst Error Correction
- 14.5 Convolutional Coding
- 14.6 Comparison of Error Rates in Coded and Uncoded Transmission
- 14.7 Turbo Codes
- 14.8 Low Density Parity Check Codes
 - Self-Test Questions*
- 14.9 Automatic Repeat Request (ARQ)
- 14.10 Trellis-Decoded Modulation
 - Self-Test Questions*
 - Matlab*
 - Summary*
 - Problems*

15. Communication Systems and Component Noises

- 15.1 Resistor Noise
- 15.2 Networks with Reactive Elements
- 15.3 Available Power
- 15.4 Noise Temperature
 - Self-Test Questions*
- 15.5 Two Ports: Equivalent Noise Temperature and Noise Figure
 - Self-Test Questions*
- 15.6 Antennas
 - Self-Test Questions*
 - Matlab*
 - Summary*
 - Problems*

16. Spread Spectrum Modulation

- 16.1 Use of Spread Spectrum
- 16.2 Direct Sequence (DS) Spread Spectrum
- 16.3 Spread Spectrum and Code Division Multiple Access (CDMA)
- 16.4 Ranging Using DS Spread Spectrum
 - Self-Test Questions*
- 16.5 Frequency Hopping (FH) Spread Spectrum
- 16.6 Pseudorandom (PN) Sequences: Generation and Characteristics
 - Self-Test Questions*
- 16.7 Synchronization in Spread Spectrum Systems
 - Self-Test Questions*
 - Matlab*

Summary

Problems

17. Miscellaneous Topics in Communication Systems

17.1 Telephone Switching

Self-Test Questions

17.2 Computer Communication

17.3 Optical Communication

Self-Test Questions

17.4 Mobile Telephone Communication—The Cellular Concept

Self-Test Questions

17.5 Satellite Communication

Self-Test Questions

Summary

Problems

References

Appendix A

Appendix B

Index

PREFACE

Overview

The work for the fourth edition of *Principles of Communication Systems* started with a review on the third edition by faculty members drawn from US engineering schools, namely, University of Texas at Arlington, University of Illinois at Urbana Champaign, University of Illinois at Chicago, University of Florida, North Eastern University at Boston, and Michigan State University. The aim was to have a feedback on major revision carried out in the third edition and how it could be further improved to serve a larger international community. The appreciation of the effort made and the encouragement to go forward led us to this new edition. Some of these comments are shared below.

“The addition of the new material has enhanced the usability of the book, and I think the new edition will be a welcome addition to the market of undergraduate texts on communication systems.”

“Most significant strength is the illustration of various systems through self-explanative figures.”

“Geometrical representation of modulated signals is a welcome change from most other books in this area...”

“The main strength of the chapters is MATLAB examples, the chapter introduction and self-test questions....”

If this review was the starting point for the work on the fourth edition, there were numerous thought inputs from faculty, students here and, of course, from literature in communication technology and research space. The revision work of this edition emphasizes on strengthening the digital communication aspect in the text. Accordingly, the analog communication part has been modified to fit the time budget for a one-semester or two-semester-long course. The relatively obsolete topics are given less weightage in this edition. This makes the title ready for any curriculum revision exercise where two-semester-long communication courses are not strictly divided into analog and digital communication modules. A summary of the changes made are given next. Besides new text and

examples, twenty-four new or revised figures, there are new problem sets and MATLAB examples.

Chapter Organization and Changes

Among the major changes, the unanimous view was to shift the chapter “Random Variables and Processes” later and bring discussion on modulations after the introductory chapter. This chapter is now brought before “Mathematical Treatment of Noise” which leads to discussions on reception of signal, corrupted with noise. The other major change was to split the chapter “Information Theory and Coding” to two different chapters, given the increasing focus on digital communication.

In Chapter 1, the introduction to digital signal representation and transmission, stands improved. The concept of negative frequency is introduced through phasor representation. Sampling of analog signals through an impulse train to get the corresponding digital signal is included through an example. Use of duality theorem in convolution-multiplication relationship is referenced to signal modulation.

Chapter 2 now is the first chapter to deal with modulation at system level. Emphasis is increased on block-diagram-level representations that connect mathematical equations to system components. Simple pictorial representation of frequency domain characteristics is an added feature of this edition. These are placed alongside individual blocks in block diagrams to help understand their functionality.

The major change in Chapter 4 is to discuss Discrete Fourier Transform (DFT) in detail with new text and examples. The section on Z-Transform is also improved. These help in formulation as well as in understanding of important digital communication concepts that come later. A short introduction to probability density function is made which makes analysis of quantization error easier in the digitization step of analog-to-digital conversion.

In Chapter 5, Orthogonal Frequency Domain Multiplexing (OFDM) and Gaussian Minimum Shift Keying (GMSK) are added as new topics. These are new discourses giving important insights related to digital communication, especially in cell phone application space.

In line with the suggestion made by reviewers, the discussion on “Random Variables and Processes” is shifted to Chapter 6. This is followed by a discussion on “Mathematical Representation of Noise” in Chapter 7.

In Chapter 10, a discussion on mathematical analysis of digital Phase Locked Loop (PLL) is included with new text and examples.

Chapter 13 is now dedicated to information theoretic approach to communication. The text has been rewritten to accommodate the change. New MATLAB examples on “Rate Distortion Theory” give the readers a hands-on experience of trade-off between data rate and distortion.

Accordingly, Chapter 14 is a new chapter dedicated to “Error Control Coding”. Necessary changes have been made in the text of the previous edition to suit the need of a new chapter, and a new topic “Low Density Parity Check (LDPC) codes” is included.

In all chapters, changes are made to improve readability. Text is rewritten at several places with revision of figures or inclusion of new figures. For example, better clarity is sought between frequency and phase modulation in Chapter 3, the discussion on threshold effect on AM reception is rationalized in Chapter 8, the section dealing with multipath fading and RAKE receiver is improved in Chapter 16, the topic ‘Optical Communication’ is strengthened in Chapter 17, etc.

A new component named ‘Facts and Figures’ was introduced in the third edition. These were anecdotes relevant to each chapter from the history of communication engineering, aiming to motivate young students. This was very highly appreciated by the reviewers and more of these were recommended. In this edition, the contribution to this segment is doubled which we hope will doubly motivate the students!

Salient Features

- Communication Systems dealt with detailed mathematical analysis
- Comprehensive coverage of Noise and Noise Performances
- Elaboration of concepts of Information Theory and Coding Theory
- Focus on Noise and its Impact on System Performances
- Pedagogy revised to suit curriculum requirements:
 - *104 Solved Examples*
 - *58 MATLAB Examples*
 - *36 Additional Problems*
 - *545 Problems*
 - *420 Diagrams*

Online Learning Centre

The Online Learning Centre of this book can be accessed at <https://www.mhhe.com/taub/cs4/sie> and contains the following material:

For Instructors: Updated Solution Manual and PowerPoint slides *For Students:* Supplementary Study Material for further reading

Acknowledgements

The revision work for this edition came to a full circle with each revised chapter getting reviewed by faculty members from institutions like Illinois Institute of Technology, Florida A&M University, Auburn University, Virginia Tech, New Mexico State University, CA State Polytechnic University, George Mason University, and University of Florida. They lauded the work, and some of their comments in the general section of the review that highlights the strength of the title, are given next.

“The overall treatment of the subject in the chapters is very good. The mathematical treatment is quite complete. Examples given generally after each section are very useful and appropriate and also the “self-test” questions in the text are useful aids in allowing the reader to re-review the material. The MATLAB based simulations are very appropriate. The historical perspectives in the chapters are very meaningful.”

“The overall organization and order is appropriate and logical. The early coverage of prerequisite material on signals is good. The illustrations are adequately tied to the text and are fine. Having illustrations for this course are very helpful.”

“The writing style is appropriate for senior-level communications courses. The writing is very detailed and comprehensive. It is clear and accurate. The illustrations are done professionally.” A number of Indian faculty members also reviewed the script and I extend my heartfelt thanks to all of them.

Finally, sincere thanks to all faculty who helped by providing valuable review comments. Thanks are due to my faculty colleagues and my dear students. I refrain from taking individual names as the list will be too long. I also thank the entire publishing team of McGraw Hill Education (India), more specifically Raghu Srinivasan and Michael Hays for initiating the work through their India visit; Peter Massar, Darlene Schueller, and Jane Mohr for following it up; Vibha Mahajan, Shalini Jha, Koyel Ghosh, Satinder Singh Baveja, Piyaray Lal Pandita, Sohini Mukherjee, and Baldev Raj of McGraw Hill Education (India) for providing necessary support.

At this point, I humbly remember my father, the late G. N. Saha. Last but not the least, I must mention the help and support I received from my big family—my mother, my parents-in-law, my wife, Sanghita, and my daughter, Upasana.

GOUTAM SAHA

Publisher's Note

Do you have any further request or a suggestion? We are always open to new ideas (the best ones come from you!). You may send your comments to tmh.ecefeedback@gmail.com

Piracy-related issues may also be reported!

1

INTRODUCTION: SIGNAL AND SPECTRA

CHAPTER OBJECTIVE

This chapter aims to give an introduction to modern communication systems through a brief overview. It also intends to develop necessary background on signals and their spectral information, to be exploited in later chapters. The discussion includes characterization of signals, basic signal operations, characterization of periodic signal by Fourier series and aperiodic signal by Fourier transform and finally, representation of a signal in vector space. Fourier analysis brings out the frequency information of a signal, which in communication context is very important. References to necessary Fourier series and Fourier transform properties are made at appropriate places. Besides illustrative numerical examples, the chapter also presents a wide variety of MATLAB based simulations. The MATLAB examples are developed in a manner that is interesting to a beginner.

FACTS AND FIGURES

“Yesterday was my 21st birthday, at that age Newton and Pascal had already acquired many claims to immortality.” Thus wrote Fourier in one of his letters in 1789. Born in a tailor family as the ninth of twelve children, he briefly served priesthood, was imprisoned for revolutionary activity, but his love of mathematics continued. In 1807, his famous theory on Fourier series was published but initially faced opposition of the then famous Lagrange and Laplace.

In 1980, the Fortran MATLAB, was invented, an interactive matrix calculator which had no m-files, toolboxes, Fourier transform or graphics. In 1984, Jack Little, Steve Bangert and Cleve Moler founded The Mathworks and released the commercial version, MATLAB 1.0. It was targeted to MS-DOS PCs and was implemented in C. Some of those codes are still used in current versions of MATLAB.

1.1 AN OVERVIEW OF ELECTRONIC COMMUNICATION SYSTEMS

Imagine a world without television, radio, telephone—fixed or mobile, fax machines, internet, email, Automatic Teller Machines—credit or debit cards, global positioning systems, radar, satellites, aircraft or ship guidance system Most of us will be dreading to think about it and consider that evolution to be in reverse gear and that we are back to Stone Age again! How do we then communicate with humans or machines? Only a few hundred years back we were dependent only on physical mode of communication, i.e. someone had to carry the message physically from one place to another. The speed of transmission was severely limited, cost huge and reliability of service poor —constrained by geo-political situation on ground. How come the situation is different today? The development in electronic communication system by which a signal moves with the speed of light is changing the face of human civilization. With a click of a mouse you find details of a place which is continents apart; click your remote to switch to a favourite TV channel—see a live soccer match or how people are rescued after tsunami; press few buttons and you are connected within seconds to your near or dear ones on the other side of the globe. Today all these are everyday realities and we perhaps cannot live without them.

The important question is—how communication is made so simple, so close to our life? What is the technology behind it? Yes, we'll try to unfurl the mystery slowly but steadily in this book. Our emphasis will be more on fundamental principles but adequate references on emerging trends will also be made. Before we get into detail, let us have a quick overview of important issues related to electronic communication systems.

1.1.1 Block-Diagram Representation of an Electronic Communication System

A simple block-diagram representation of an electronic communication system is shown in Fig. 1.1. We'll simply describe the functioning of each block here and more stories about them will appear in the later part of this book. We begin our discussion with the block named *channel*. Note that, *communication is the process of transferring information from one place to another*. The information generated at *source* side may need to travel hundreds or thousands of miles via channel to reach *destination*. *Communication channel is the media by which information is sent*. The

channel could be a *wired* line such as copper wire or *wireless* such as atmosphere. Placing a physical wire from source to destination is definitely a costlier and less convenient proposition than use of atmosphere as media. But there are other issues too. Consider the block called noise and distortion feeding to *channel*. *Distortion is the process of changing shape of the communicating signal that may mislead the destination about the content of the message.* This occurs due to inability of the channel to convey all frequency, phase, amplitude information truthfully from one side to another, a limitation that characterizes a channel. Distortion parameters can vary linearly, termed *linear distortion* as well as nonlinearly, termed *nonlinear distortion*. The loss in amplitude or strength of the signal as it travels through a channel is called *attenuation*. Noise is different from distortion and is a serious issue in a communication system. *Noise can be defined as random, unwanted interference on transmitted signal.* The block, channel is a major source of noise though other blocks also contribute to it. *External noise*, as the name suggests, are interference from other sources like lightning, electrical switching, automobile ignition, other communicating signals etc. *Internal noise* is due to thermal motion of electrons or random emission, diffusion, recombination of carriers. The channel is also characterized by another important parameter called *bandwidth*. This is the amount of space available in frequency domain that is not distorted by the channel; of course, the more the bandwidth, the better. Signal bandwidth, on the other hand, is the range of frequencies over which the signal is present. Often the major part of the energy of a signal is spread over a particular frequency band and it is much less, though not entirely zero, in other frequencies. This gives rise to several practical definitions of signal bandwidth, e.g. in one case it is defined as the band that has 98 percent of the signal energy. No problem is envisaged if channel bandwidth is more than signal bandwidth.

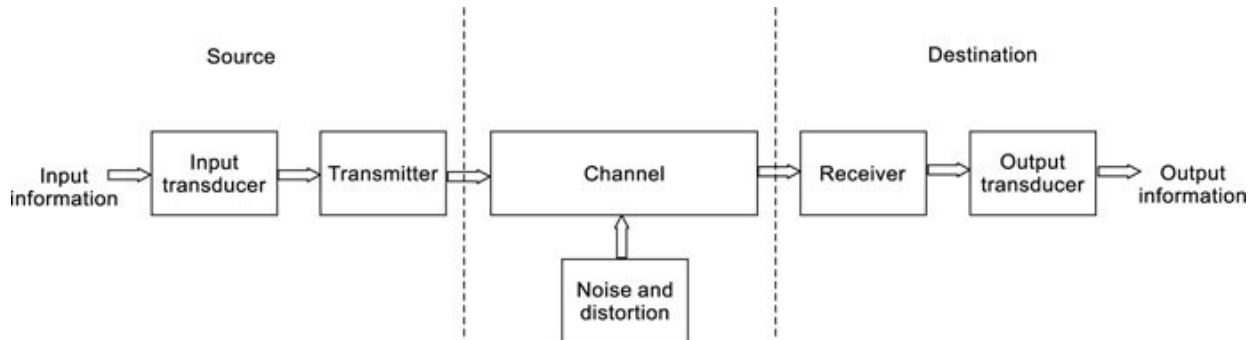


Fig. 1.1 A block-diagram representation of electronic communication system.

From this discussion we find that there are several issues and related trade-offs to choose a particular media for communication. In reality, many different types of media coexist. Among wired lines we have coaxial cables or fibre-optic links that are superior to copper lines offering very high bandwidth. Today we have trans-oceanic submarine cables connecting continents. Atmosphere as propagating media is used by electromagnetic waves while communication via satellites partly uses free space as communication channel. In Sec. 1.1.4 we present a discussion on transmission media.

Now we turn our attention to two blocks adjacent to *channel*. On source side there is *transmitter*, a device that makes input electrical information suitable for efficient transmission over a given channel. It is obvious that for different channels we have different types of transmitters. Also, if channel characteristics vary, the transmitter has to adjust itself to maintain a desired quality of communication service. In general, the transmitter modulates or changes some parameter say, amplitude or frequency of a high-frequency carrier signal by original electrical information input which is also known as *baseband signal*. Transmitter also multiplexes, i.e. puts number of signals in a common pool and effects simultaneous transmission of number of input signal. On the destination side receiver is the device that receives information from channel and extract intended electrical message from it. Other than demodulation, the reverse of modulation and demultiplexing, the reverse of multiplexing the receiver also amplify and remove noise, distortion from the noise contaminated, distorted, attenuated received signal.

Finally, we discuss the blocks *input* and *output transducers*. The *input transducer* converts the information to be transmitted to its electrical equivalent message signal. As we discussed before we are interested in sending the signal as fast as possible and electrical signals that move with the speed of light remains our choice and hence, these transducers are important. The input information can be speech, image, video, text, etc. Microphone is an input transducer which converts audio input like speech to an electrical signal. The *output transducer* converts electrical input to a form of message required by user, e.g. speech, image, video, text, etc. The loud-speaker is an example of output transducer where electrical input is converted to an audio output.

1.1.2 Analog vs. Digital Communication

As a student of communication or simply from user's point of view you may be aware of these two terms, *analog communication* and *digital communication*. Before we discuss them in detail later in this book, let us spend sometime here understanding what exactly are they. The electrical message signal that needs to be communicated can be *analog*, i.e. *continuously varying with time* or *digital*, i.e. *has finite number of discrete levels*. Speech, video, variation in temperature with time, all are analog in nature while text, data are primarily digital signal. In analog communication, the message in electrical form is considered to be an analog signal, i.e. continuously varying. Here, when a signal of digital nature like data is sent, it is converted to some analog form before sending. The example is, data communication through telephone line using a modem (abbreviation of modulator-demodulator).

In digital communication, the message is discrete in nature. However, the number of different symbols that can be sent is limited because of certain constraints. In M -ary communication, M different symbols are used. In binary digital communication, only two symbols are used. This is the most common form of digital communication and symbols are represented by digits '0' and '1'. From your knowledge of earlier courses you can very well write numerical data '12' in decimal as '1100' in binary. But how to write texts like 'A', 'a', 'B', 'b', '.', '%' etc. in binary? American Standard Code for Information Interchange (ASCII) has 7 bit representation for each of these alphabets or special characters, e.g. 'A' is represented as '1000001' while 'a' as '1100001'. A complete list of ASCII representation of characters is given in Table A1 of Appendix A.

Analog signal is converted to digital if sent using digital communication mode. Figure 1.2a gives an idea of analog-to-digital conversion, the details is discussed in Chapter 4. This involves sampling the analog signal at certain interval and quantizing the voltage level of that instant with its binary equivalent, i.e. each sample is represented by a finite set of '0's and '1's. In Fig. 1.2, sampling is done at time instants 1, 2, 3 seconds etc., and number of levels are eight: 0, $V/8$, $2V/8$, ..., $7V/8$. this corresponds to digital representation of analog signals as 010, 010, 100, etc. Since each level is represented by three binary digits, three pulses are inserted between two successive samples for digital transmission where $-V$ represents 0 and $+V$ represents 1. Note that, the variation in analog signal at time 0 and 1 are not

accurately reflected in digital due to quantization of amplitude information. This is equivalent to addition of some noise in the quantization process, termed as *quantization noise* and can be reduced by increasing the number of levels. This would require more than three bits to represent one sample. For example, with 4-bit representation we can use up to 16 levels. However, now between two samples 1 second apart, 4 pulses or bits are to be inserted. This increases bit rate from 3 bits per second to 4 bits per second, i.e. 33.33 percent more data is to be pushed through the channel. We'll see later that if time samples are sufficiently close then there is no error on account of time sampling. Now, at the destination end, if analog representation is required, Digital to Analog conversion is done which is some sort of averaging to find out in-between time information from digital samples.

Analog communication is older than digital communication. It does not require Analog-Digital conversion for naturally occurring signals which are analog and avoids conversion related error. The required bandwidth for analog communication is relatively less and cost of components less costly. Digital communication is newer and scores over analog in terms of quality of service. It is less affected by noise and for long distance communication can effectively use *regenerative repeater*. This is a device placed at intermediate places, removes noise, regenerates original binary information '0's and '1's and retransmits them. Figure 1.2c shows a typical representation of digital signal at the end of a transmission channel. If decision on binary value of the signal is delayed a little as shown in the figure, we can use that to get a clean digital signal of Fig. 1.2d. In a regenerative repeater this clean signal can be retransmitted and such regeneration scheme can be employed before the signal deteriorates much. In analog communication, repeater can only attenuate noise which is not in the same frequency band as message but cannot regenerate the original signal as shown for digital signal. Further amplification in repeater amplifies both signal and in-band noise. The quality of transmission is decided by parameter, Signal-to-Nose ratio (SNR) in analog and by bit (abbreviation of binary digit) error rate (BER) in digital. In digital communication we can employ different coding techniques to improve BER and compression techniques to reduce the required bit rate which in turn reduces bandwidth. This is not possible in analog communication. Every 2-3 years, digital hardware cost reduces by half while its capacity doubles. Storage and indexing of digital signals is easy and inexpensive. Also digital hardware

implementation is flexible in nature that helps moving to newer technology standard with relative ease. All these help digital communication in getting more and more space though analog communication is very much in use. A lot of digital communication concepts owe their development to field of analog communication. Keeping this in mind, this text will emphasize on digital communication concept but will also dwell on fundamentals of analog communication.

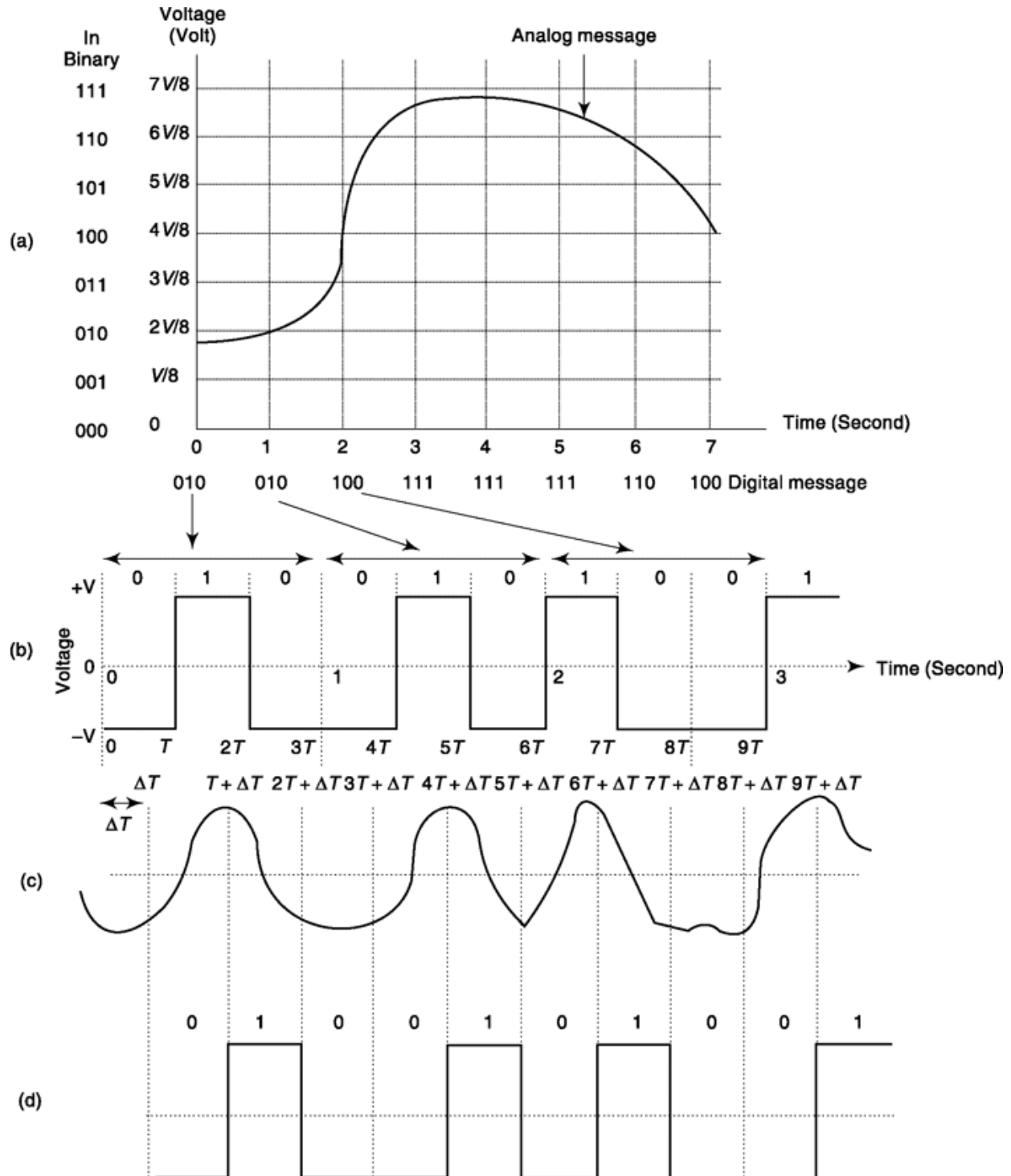


Fig. 1.2 (a) Digital equivalence of an analog message by discretizing time and amplitude axis (b) PCM coded digital signal in the period 0-3 second for onward digital communication, (c) Distorted, noisy signal at receiver end after its passage through a transmission channel, (d) Cleaned digital signal at receiver with a delay of AT . In regenerative repeater it can be retransmitted.

1.1.3 Modulation and Multiplexing

As discussed in Sec. 1.1.1, modulation is the process of varying one attribute of a signal by message signal. In electronic communication modulation plays a very important role and a good number of chapters in any communication text is devoted to it. Why at all we need to modulate the message signal? There are several reasons. The first comes from an important practical consideration. For wireless communication the electromagnetic wave needs to be radiated. This requires an antenna the diameter of which is required to be approximately one-tenth of signal wavelength or of that order. Now, let us do a quick calculation.

If c is speed of light and frequency of electromagnetic wave to be transmitted is f then its wavelength $\lambda = c/f$.

To radiate a signal of frequency 4 kHz, the antenna diameter needs to be $0.1 \times 3 \times 10^8 / 4000 = 75000$ meter or 7.5 km while a 1 GHz signal needs an antenna size of $0.1 \times 3 \times 10^8 / 10^9 = 0.03$ meter or 3 cm.

Of course, the first one is impractical and we should have a mechanism to translate original baseband signal to a very high frequency to reduce the antenna size. This is usually achieved by linearly or proportionately varying one attribute of a high-frequency signal called *carrier* (called so as *carries message* or *message rides on it*) be it amplitude, frequency or phase. Note that, such frequency translation is required at the transmitter end for both analog and digital signal before the signal is put to channel unless it is a baseband transmission.

There is another advantage behind modulating message signal. The original message signal occupies lower baseband frequencies, which for example in speech is 0.3 to 3.4 kHz. If two persons want to communicate over the same channel simultaneously then two baseband signals will interfere with each other. However, if one signal is placed between 0 to 4 kHz and the other say 4 to 8 kHz then there is no such conflict. Using a carrier to shift the frequency band of a message signal for simultaneous transmission is known as frequency division multiplexing (FDM). For digital signal, multiplexing can be achieved by dividing the time between two samples of signals in various time slots and using each time slot to send one digital signal. Such a method of simultaneous transmission is known as time division multiplexing (TDM). Consider the example shown in Fig. 1.2. If we want to send two message signals of that type (both sampled at 1 sample per second rate and 3 bits representing each sample) using TDM, we have to place 6 bits in 1 second interval. This reduces pulse width by half

and increases data rate to 6 bit-second. Now, if the transmission system can support a data rate of say, 24 bits/sec then we can used TDM to send 8 signals simultaneously.

1.1.4 Transmission Media

Different types of transmission media being in use today are discussed here briefly, the major varieties with some of their characteristics are the following:

Open wire Lines

The original telephone and telegraph transmission lines are still in use today but on their way of phasing out. They have low attenuation (typically 0.04 dB/km) for voice frequency range and useful for long distance communication. A loss of 3 dB refers to signal strength being reduced by nearly 50 percent which in this media can happen after $3/0.04=75$ km of transmission. More about dB scale is discussed in Sec. 1.1.6. Open wire lines are susceptible to environmental, weather and human abuse.

paired Cables

This is used in telephone networks within short distances - inside building, building to local office, etc. Often a large number of such cables are put in a bundle. The loss here is typically 0.05 dB/km.

Quad Cables

A quad cable includes four conductors arranged as two differential pairs for carrying the differential signals. It uses insulators and shielding materials. It offers higher bandwidth, i.e. more frequency range of operation and finds its use among other things in railway communication. It gives nearly 0.25 dB/km of attenuation.

Coaxial Cables

It consists of a single wire conductor at the centre of a cylindrical cable and an outer conductor typically a wire mesh separated by a dielectric (Fig. 1.3a). It gives bandwidth in MHz range and is used for television

connection, local area networks for computers, etc. But the attenuation in this is relatively high, typically greater than 5 dB/km at maximum frequency.

Radio

Radio is a wireless propagation where atmosphere or free space is used as transmission media. Radio frequency signals are radiated into them as electromagnetic signal through antenna. Since it acts as a common media for number of communication channel a stringent frequency allocation policy is followed. This is further discussed in Sec. 1.1.5.

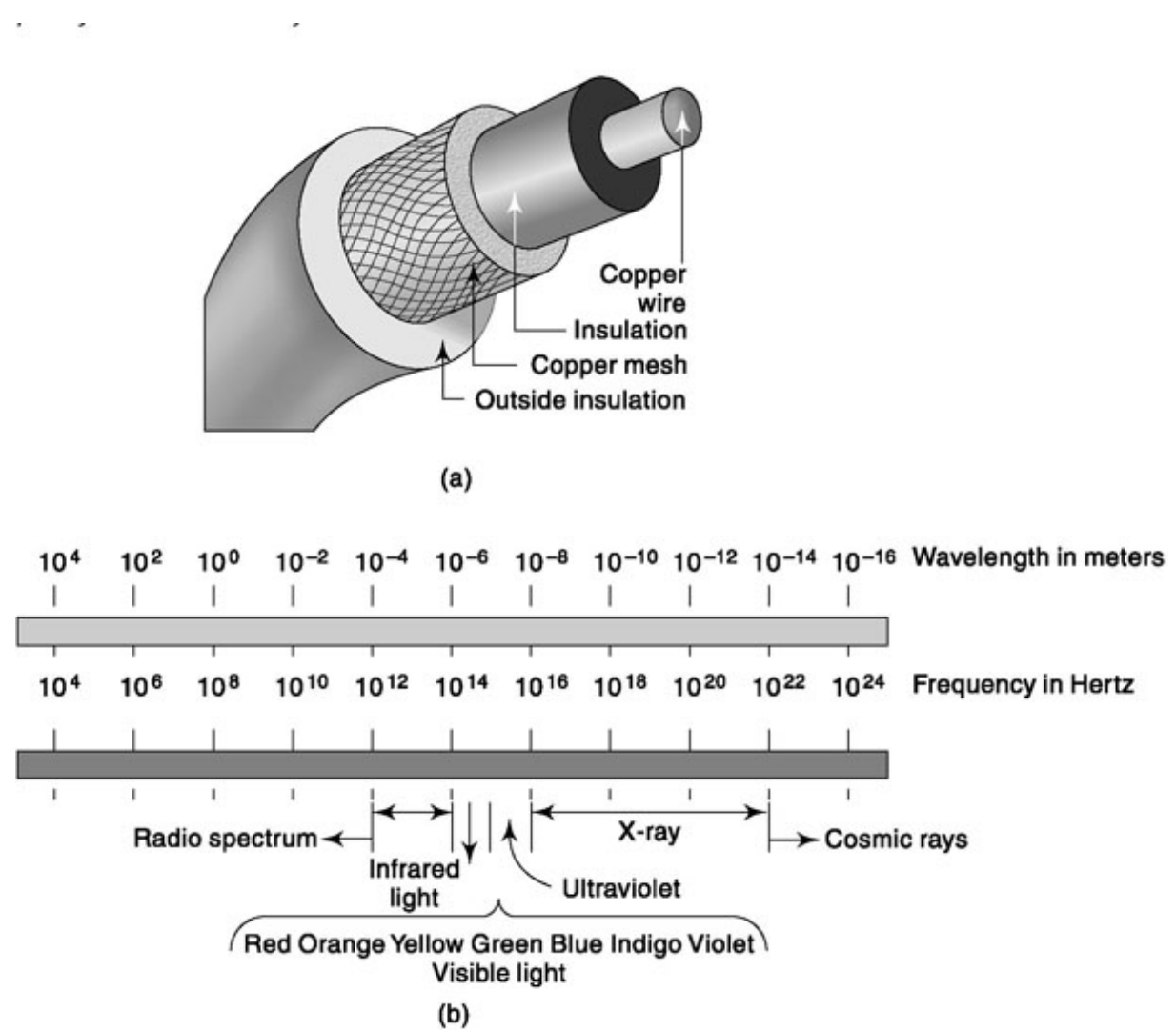


Fig. 1.3 (a) A coaxial transmission cable (b) The range of electromagnetic wave spectrum.

Waveguide

This is a hollow conductor of rectangular, circular or elliptical cross section typically feeding or receiving signal from transmitter or receiver antenna in radio propagation. It offers very high bandwidth, in the range of hundreds of MHz and attenuation is approximately 5 dB over 100m, the maximum height typically seen for an antenna tower.

Optical Fibre

It is made up of a very fine fibre core that allows light wave to propagate through it with minimum loss. An outer layer called cladding ensures total internal reflection. A final protective layer protects it from physical damages. Optical fibre allows message signal to be coded in the form of light and offers very high rate of signal transfer in GHz range. Transmission loss is typically 0.2-0.4 dB/km. Light emitting diodes or lasers are used in transmission and photodiodes are used in reception of signal. This mode of transmission is not susceptible to electromagnetic interferences. Optical fibers are increasingly used as media in long as well as short distance wired communication that requires high bandwidth.

1.1.5 Frequency Spectrum and Filtering

The frequency spectrum available and the extent we are able to use it for electronic communication is a major issue in modern communication system. In reality, one frequency band is analogous to one independent communication channel. And you hear so much about spectrum licensing policies, demand of more spectrum, fight among competing operators over its use. Let us take a quick look at how electromagnetic wave spectrum is used for communication. Refer to Fig. 1.3b. The frequencies below infrared, termed as *radio spectrum* is available for wireless communication. The infrared frequency range 43-430 THz ($1 \text{ THz} = 10^{12} \text{ Hz}$), wavelength range 0.7-7 mm ($1 \text{ mm} = 10^{-6} \text{ m}$), visible light 430-750 THz, 0.4-0.7 mm and ultraviolet 750-3000 THz, 0.1-0.4 mm are being used in optical communication system where fibre optic cable is used as channel.

How the radio spectrum is used for different types of needs is described in Table 1.1. You can see there is a crowding towards middle. The lower frequencies are unsuitable for higher antenna size while the technology for higher frequencies is still at experimental stage. The cell phones usually operate at either of 900, 1800, 1900 MHz frequencies. However, with

increasing subscriber bases they are looking for more spectrum to avoid congestion.

Filtering is the technique by which one component is taken out from a mix. In communication, filtering refers to separation of a frequency band from the entire signal (Illustrated later in Fig. 1.27a and Fig. 1.27b). A low pass filter (LPF) passes low frequencies from 0 Hz to some upper cut-off, say 4 kHz and attenuates the rest from incoming signal. Similarly, a band pass filter (BPF) of cut-off frequencies say, 70 (lower cutoff) and 75 (upper cutoff) MHz has its output signal primarily containing frequency components between 70-75 MHz. An ideal filter output will have no signal components that contain frequencies outside the pass band. But all practical filters outputs have such components which are usually greatly attenuated but acceptable for most practical purposes.

Table 1.1 *Radio Spectrum and its Uses*

<i>Frequency band</i>	<i>Name</i>	<i>Some of the uses</i>
3–30 kHz	Very Low Frequency (VLF)	Sonar, Long range navigation
30–300 kHz	Low Frequency (LF)	Navigation
300–3000 kHz	Medium Frequency (MF)	AM (Amplitude Modulated) radio, maritime radio
3–30 MHz	High Frequency (HF), Short Waves (SW)	SW radio, telephone, telegraph, FAX, ship
30–300 MHz	Very High Frequency (VHF)	FM (Frequency Modulated) radio, television, air traffic control, mobile radio, navigation, police
0.3–3 GHz	Ultra High Frequency (UHF), Microwave (above 1 GHz) band	Television (wired), radar, satellite communication, navigation, mobile, military
3–30 GHz	Super High Frequency (SHF), Microwave band	Satellite communication, microwave links, radar
30–300 GHz	Extremely High Frequency (EHF)	Radar, experimental
300–3000 GHz	Milimeter waves	Experimental

1.1.6 Signal-to-Noise Ratio, Bandwidth, Channel Capacity and Coding

Besides spectrum, there are few other important parameters in electronic communication which we briefly discuss here and in details later. A quantity that gives relative strength of the Signal to Noise is called Signal to Noise Ratio (SNR) and is an often used term in communication text. This is usually expressed in decibel or dB, the definition of which is as follows

$$\text{SNR in dB} = 10 \log_{10} (\text{Signal energy}/\text{Noise energy})$$

From above, SNR of zero dB means signal energy is equal to noise energy, 10 dB refers to signal energy is 10 times more than noise energy. The unit dBW is used to give a measure of signal strength referenced to 1 watt where, zero dBW = 1 watt. Similarly, dBm gives signal strength referenced to 1 milliwatt where zero dBm = 1 milliwatt.

Now, the power that can be transmitted is always finite and the usual noise spectrum is flat (also called *white*) in nature. Bandwidth of a channel is already defined as the range of frequencies which can be transmitted through it, within acceptable degradation. For any given bandwidth of the channel, the higher the signal power, the higher the SNR and the better the quality of reception. Note that a certain minimum SNR is required for effective communication. If in the originating signal, power is distributed over a narrower signal bandwidth, and we have BPF to filter out unwanted frequencies at receiver end then effect of noise addition is observed only on signal bandwidth and signal to noise ratio is higher.

There is another issue in this SNR-bandwidth story which may appear as conflicting but is not really so. Please follow the argument given next, carefully. To transmit any given message if we use larger bandwidth then signal power required to send it for any given quality is usually less. This depends on how an input message is encoded into an electrical signal and the technical aspect of this will be taken up later. If channel bandwidth is increased by a factor of n, then required SNR is approximately reduced to its $1/n$ -th root. Small increase in bandwidth reduces SNR requirement to a great extent. And thus there is a *bandwidth required—SNR trade-off*. Notice the word ‘required’ in SNR in this part of the discussion while previous paragraph talked about increase of signal strength to achieve or exceed this required SNR.

The capacity of a channel to support a particular rate of information is defined as *channel capacity* and is an important measure in digital communication. The upper limit of channel capacity, C comes from Shannon’s equation

$$C=B \log_2 (1 + \text{SNR}) \text{ bits/sec}$$

The significance of this equation is that digital data theoretically can be sent at any rate less than C without any error. Practical systems of course, are yet to achieve this upper limit and we employ various coding techniques for this purpose. A complex coding technique can come close to this capacity but

issues like time and other overhead may limit its use. Formally speaking, *coding is the technique of changing characteristics of a signal to make it more suitable for intended application*, e.g. removal of redundancy from input message through *source coding* that reduces required transmission bandwidth; introduction of calibrated redundancy to reduce effect of noise in transmission through *channel coding*; joint source-channel coding, etc. The issue of redundancy or information content of a message comes from what is known as *information theory* which states that the more

the uncertainty, the more the information content. Of course, waves in an ocean are no information but a tsunami is, as the former is a certainty while the latter is not.

Coming back to significance of Shannon's equation, we find it also highlights trade-off between received SNR and channel bandwidth for a given information rate. It clearly shows that increase of B reduces required SNR when information rate is constant and vice versa. Also if noise energy is zero then $C = \infty$, i.e. theoretically, under no noise condition any information rate is supported. For channel with white noise or flat noise spectrum of strength N_0 the above equation can be modified to

$$C = B \log_2 [1 + S/(N_0 B)] \text{ bits/sec}$$

where S is the signal strength. Note that, B in the denominator inside log and B in the numerator outside log give an interesting characteristics curve which we'll discuss later. But you are free to explore its consequence yourself if you love number game. Before we move to next topic let's do some auick math.

Consider,	$B = 4 \text{ kHz}, \text{SNR} = 20 \text{ dB} = 10^{20/10} = 100 \text{ then}$
	$C = 4000 \log_2(1+100) \text{ bits/sec}$
	$= 26.63 \text{ kbit/sec}$

Next consider, $B = 1 \text{ MHz}$, C required is as above, i.e. 26.63 kbit/sec

$$\text{Then required SNR} = 2^{26.630/1000000} - 1 = 0.0184 = -17.3525 \text{ dB}$$

Notice the reduction in required SNR once bandwidth is increased.

SELF-TEST QUESTION

1. Is modulation done at transmitter end while demodulation at receiver end?

2. Can regenerative repeater be used in analog communication?
3. What frequencies are used in microwave communication?
4. Is channel capacity related to SNR?

1.2 SIGNAL AND ITS PROPERTIES

In previous section we had a bird's-eye-view of electronic communication systems. Let us start looking into conceptual details with basic description of a signal. We have seen in Sec. 1.1.1 that input message has to be converted to an electrical signal for electronic transmission. Generally speaking, *a signal is a single-valued function of one or more independent variables*. For speech signal, time is the independent variable and can be represented by voltage v as $v(t)$ called function of t , i.e. time, the image information can be represented by $v(x,y)$ where x and y are space coordinates. However, if image information is to be sent from one place to another via a communication channel the transmitted signal itself will vary with time. Thus for communication purposes, *signal is a time varying quantity*. Signal is processed by a system through addition, deletion or alteration of certain components of it. In following discussion, we'll use time as the independent variable but this can be extended to other types of independent variables too.

1.2.1 signal Energy and Power

We have had a brief discussion on importance of signal energy in Sec. 1.1.6. Signal power is its time derivative. They, in a way, represent the strength of a signal. Mathematically, energy of a signal $v(t)$ is defined as,

$$E = \int_{-\infty}^{+\infty} |v(t)|^2 dt \quad (1.1)$$

The absolute value of $v(t)$ within integral makes this definition valid for both real and complex valued signal. Strictly speaking, if $v(t)$ is voltage signal, E is the energy spent by that signal on a 1 ohm resistor and can be considered normalized energy referenced to 1 ohm. The unit of E then will be Joule and not Volts² as appears from above equation. Still, E gives a useful measure of signal strength that is related to energy. Note that, the above equation will converge to a finite value only if $|v(t)| \rightarrow 0$ as $t \rightarrow \pm\infty$. Hence, for a periodic signal, a ramp or an exponentially increasing signal E cannot be calculated.

Power is represented by average power in communication text. For a signal $v(t)$ it can be defined

$$S = \lim_{T \rightarrow \infty} \frac{1}{T} \int_{-T/2}^{+T/2} |v(t)|^2 dt \quad (1.2)$$

Similar to E , the quantity S too is the average power spent across a 1-ohm resistor and should be called normalized power referenced to 1 ohm. However, this too like E is a very useful measure of the signal strength. Note that, for S to be finite, $v(t)$ must be periodic or have some statistical regularity and should not be constantly increasing like a ramp or exponentially increasing function. Here, S is also known as mean square power and its square root is known as Root Mean Square power or RMS power.

Next, we discuss a different measure involving power that is very relevant to a communication system. Suppose that in some system we encounter at one point and another normalized powers S_1 and S_2 respectively. If the ratio of these powers is of interest, we need but to evaluate, say, S_2IS_1 . It frequently turns out to be more convenient not to specify this ratio directly but instead to specify the quantity K defined by

$$K \equiv 10 \log \frac{S_2}{S_1} \quad (1.3)$$

Like the ratio S_2IS_1 , the quantity K is dimensionless. However, in order that one may know whether, in specifying a ratio we are stating the number S_2IS_1 or the number K , the term *decibel* (abbreviated dB) is attached to the number K . Thus, for example, suppose $S_2IS_1 = 100$, then $\log S_2IS_1 = 2$ and $K = 20$ dB. The advantages of the use of the decibel are twofold. First, a very large power ratio may be expressed in decibels by a much smaller and therefore often more convenient number. Second, if power ratios are to be multiplied, such multiplication may be accomplished by the simpler arithmetic operation of addition if the ratios are first expressed in decibels. Suppose that S_2 and S_1 are, respectively, the normalized power associated with sinusoidal signals of amplitudes V_2 and V_1 . Then $S_2 = V_2^2 / 2$, $S_1 = V_1^2 / 2$ (Refer to Example 1.2) and

$$K = 10 \log \frac{V_2^2/2}{V_1^2/2} = 20 \log \frac{V_2}{V_1} \quad (1.4)$$

The use of the decibel was introduced in the early days of communications systems in connection with the transmission of signals over telephone lines. (The “bel” in decibel comes from the name Alexander Graham Bell.) In those days the decibel was used for the purpose of specifying ratios of *real* powers, not normalized powers. Because of this early history, occasionally some confusion occurs in the meaning of a ratio expressed in decibels. To point out the source of this confusion and, we hope, thereby to avoid it, let us consider the situation represented in Fig. 1.4. Here a waveform $v_i(t) = V_i \cos \omega t$ is applied to the input of a linear amplifier of input impedance R_i . An output signal $v_o(t) = V_o \cos(\omega t + \theta)$ then appears across the load resistor R_o . A real power $P_i = V_i^2/2R_i$ is supplied to the input, and the real power delivered to the load is $P_o = V_o^2/2R_o$. The real power gain P_o/P_i of the amplifier expressed in decibels is

$$K_{\text{real}} = 10 \log \frac{V_o^2/2R_o}{V_i^2/2R_i} \quad (1.5)$$

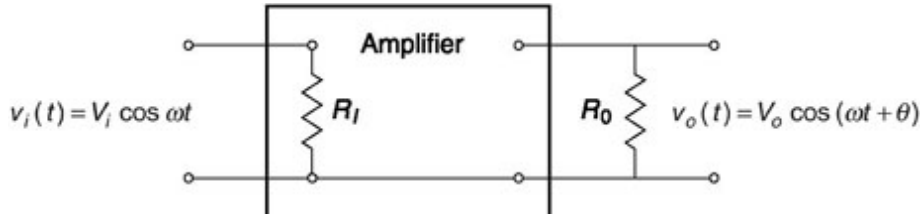


Fig. 14 An amplifier of input impedance R_i with load R_o .

If it should happen that $R_i = R_o$, then K_{real} may be written as in Eq. (1.4).

$$K_{\text{real}} = 20 \log \frac{V_o}{V_i} \quad (1.6)$$

But if $R_i \neq R_o$, then Eq. (1.6) does not apply. On the other hand, if we calculate the normalized power gain, then we have

$$K_{\text{norm}} = 10 \log \frac{V_o^2/2}{V_i^2/2} = 20 \log \frac{V_o}{V_i} \quad (1.7)$$

So far as the normalized power gain is concerned, the impedances R_i and R_o in Fig. 1.4 are *absolutely irrelevant*. If it should happen that $R_i = R_o$, then

$K_{\text{real}} = K_{\text{norm}}$, but otherwise they would be different.

Example 1.1

Calculate energy of the signal $u(t) = 2e^{-3t}$, $t \geq 0$ and $v(t) = 0$ elsewhere.

Solution

Substituting $v(t) = 2e^{-3t}$ in Eq. 1.1 and considering $v(t) = 0$ for $t < 0$, we get

$$\begin{aligned} E &= \int_0^{+\infty} 4e^{-6t} dt = 4 \int_0^{+\infty} e^{-6t} dt \\ &= 4e^{-6t}/(-6) \Big|_0^{+\infty} \\ &= -(2/3) [e^{-6\infty} - e^{-6 \cdot 0}] \\ &= -(2/3) [0 - 1] = 2/3 \end{aligned}$$

Example 1.2

Calculate power of the signal $v(t) = 2 \sin 0.5\pi t$.

Solution

Since, $v(t)$ is periodic, i.e. repetitive, averaging over $-\infty$ to ∞ and $-T_0/2$ to $T_0/2$ will give same result, where T_0 is the time period of $v(t)$.

Here, $T_0 = 2\pi/(0.5\pi) = 4$. From Eq. 1.2

$$\begin{aligned} S &= \frac{1}{4} \int_{-2}^{+2} 4 \sin^2 (0.5\pi t) dt \\ &= \int_{-2}^{+2} \sin^2 (0.5\pi t) dt \\ &= 2 \int_0^{+2} \sin^2 (0.5\pi t) dt \\ &= 2 \int_0^{+2} 0.5 [1 - \cos (\pi t)] dt \\ &= 2 \times 0.5 [t \Big|_0^{+2} - \cos (\pi t)/\pi \Big|_0^{+2}] \\ &= [2 - 0] - [\cos(2\pi) - \cos(0\pi)]/\pi \\ &= 2 - 0 = 2 \end{aligned}$$

Following above steps, we can find for any $v(t) = A \sin \omega t$, power $S = A^2/2$ and RMS power $= \sqrt{S} = A/\sqrt{2}$.

1.2.2 Classification of signals

Here we briefly classify signals in different categories based on their properties or presentation. This is useful in explaining the behavior of a communication system for signal of a particular type.

Real and Complex signals

As the name suggests real signals have only real components while complex signal has both real and imaginary components. Complex signal representation has an important place in communication as it conveys both amplitude and phase. Signals described in Example 1.1 and 1.2 are real signals. A complex signal in exponential form can be written as follows

$$v(t) = A e^{j\omega t} \quad \text{where } j = \sqrt{(-1)}$$

The magnitude information of above is given by $|v(t)| = A$ and phase information is given by $-v(t) = \omega t$. Figure 1.5 shows a phasor (phase vector) representation of a complex signal and the concept of +ve and -ve frequency. We can see that real signal is nothing but the projection of a rotating phasor with a specific angular velocity.

Analog and Digital signals

We have already discussed these in Sec. 1.1.2 (Fig. 1.2). Analog signals are continuous in nature while digital signals are generated from discrete events or are sampled version of analog signal, with amplitude axis quantized. Analog signals are represented as $v(t)$ where t is continuous in time while digital signals are represented by $v(n)$ where n is sampling time index. If sampling is done at regular interval of time gap T then

$$v(n) = v(t) \mid_{t=nT}, n = \text{integer}$$

The above assumes that there are infinite numbers of quantization levels for amplitude axis. In reality, this is finite but quantization error can be reduced by increasing number of quantization levels. *Nyquist theory* states that to represent an analog signal by its sampled version, the sampling frequency should be greater than or equal to twice the maximum frequency content present in the analog signal. We discuss more about it in Chapter 4.

Periodic and Aperiodic signals

You are familiar with periodic signals in the form of sine, cosine functions. A periodic signal is repetitive in nature and is defined as, $v(t) = v(t + T)$ where T is the time period of repetition. For discrete periodic signals the relation to be obeyed is $v(n) = v(n + N)$ where N is an integer. For aperiodic signals these relationships are not obeyed. Note that, a sampled version of analog periodic signal need not be periodic. This occurs when TIN is an irrational number.

Even and Odd Signals

An even signal is symmetric about $t = 0$ axis such that $v(t) = v(-t)$ and an odd signal shows anti-symmetry for the same where $v(t) = -v(-t)$. The signal $v(t) = A \cos \omega t$ is an even signal while $v(t) = A \sin \omega t$ is an odd signal. Any arbitrary signal $v(t)$ can be written as sum of even and odd parts as follows (subscript e and o stand for even and odd respectively).

$$v(t) = v_e(t) + v_o(t)$$

where,

$$v_e(t) = [v(t) + v(-t)]/2 \quad \text{and} \quad v_o(t) = [v(t) - v(-t)]/2$$

Energy and power Signals

We have defined signal energy and power in Sec. 1.2.1. A signal with finite energy is known as energy signal while a signal with finite but greater than zero power is known as power signal. Signal in Example 1.1 is an energy signal but not power signal because if it is averaged over T (' produces zero. Signal in Example 1.2 of course, is a power signal.

Deterministic and Random Signals

A deterministic signal is completely specified in any form be it mathematical, graphical, etc. The quantity $v(t)$ in $v(t) = A \sin \omega t$ is a deterministic signal. Random signals by the very name of it related to random values and are described in probabilistic terms like mean, variance, distribution function etc. The message signal in a communication problem is always random in nature. The whole of sixth chapter is used in understanding random variables and processes.

Causal and Noncausal Signals

A causal signal $v(t)$ is the one for which $v(t) = 0$ for $t < 0$ while for noncausal signal it is not. Practical real-life signals are causal in nature. The causal nature of the signal poses an interesting constraint on realizable systems which we'll discuss after we discuss frequency description of a signal by Fourier method in the later part of this chapter.

Singularity Functions

These are functions that are not finite or do not have finite derivatives everywhere. Two such functions are of primary interest to us. One is *unit impulse function*, also called *delta function or Dirac-delta function* and is represented by $d(t)$. The other is termed as *unit step function*, $u(t)$. They are defined as follows.

Unit impulse function is defined as

$$\begin{aligned}\delta(t) &= \infty \text{ for } t = 0 \\ &= 0 \text{ for } t \neq 0\end{aligned}$$

Such that,

$$\begin{aligned}\int_{-\infty}^{+\infty} \delta(t) dt &= 1 \text{ and} \\ \int_{-\infty}^{+\infty} v(t) \delta(t) dt &= v(0)\end{aligned}\tag{1.8}$$

Fig. 1.5 Phasor representation of a complex exponential signal, (a) Phasor OP represents $v(t) = Ae^{j(M+e)}$. The projection on real axis represents $\operatorname{Re}(v(t)) = A\cos(\omega t + \phi)$ and on imaginary axis represents $\operatorname{Im}(v(t)) = A\sin(\omega t + \phi)$. The counterclockwise sense of rotation represents +ve frequency, (b) Phasor OP' represents $v(t) = Ae^{-j(cat + \phi)}$. Clockwise sense of rotation represents -ve frequency.

The first integral points to a limiting condition when $v(t)$ is a rectangular pulse of width say, e at origin, its height is 1 and $e > 0$. This makes area under $d(t) = 1$ as shown in this integral. The second integral comes from the earlier definition of $d(t)$ where it is 0 for $t \neq 0$, so that $v(0)$ only is of consequence. If the constant (over interval e) term $v(0)$ is taken out then what is left with is the first integral whose value according to definition is one. Such a signal is useful in describing point source or point charges and also in describing other signal mathematically as shown in Eq. (1.9). We'll see later that it gives a flat frequency spectrum, i.e. all frequencies are present with same magnitude. This is useful in probing a communication system to find its frequency response.

Unit step function is defined as follows:

$$\begin{aligned} u(t) &= 1 \text{ for } t \geq 0 \\ &= 0 \text{ for } t < 0 \end{aligned}$$

Note that, $u(t)$ does not have finite derivative at $t = 0$.

The relation between $\delta(t)$ and $u(t)$ is as follows.

$$\int_{-\infty}^t \delta(\tau) d\tau = u(t) \text{ and } du(t)/dt = \delta(t)$$

The first relation comes from the fact that for $t < 0$, the integral = 0 and for $t \geq 0$ this is 1. The second relation comes directly from the first.

Note that, $\sum_{n=-\infty}^{\infty} \delta(t - nT)$ represents a periodic impulse train of time period T . This is a useful representation in communication context.

1.2.3 shifting, Inversion, scaling and Convolution of a signal

These are some of the useful signal properties or operations related to independent variable, time. In Fig. 1.2, we have already seen how a digital signal looks like at the reception side as a time-shifted version of transmitted signal. We'll discuss other signal operations in next subsection and later in this book.

Time Shifting

This is an operation by which signal is shifted in time using simple mathematical change of the independent variable time. If $v(t)$ is the original signal, then $w(t) = v(t + T)$ is a time shifted version of $v(t)$. If T is negative then the signal is shifted towards right and if T is positive it is shifted towards left. This is because whatever occurs for $v(t)$ in time t , occurs for $w(t)$ in time $t + T$. This is illustrated in Fig. 1.6a. Since, $d(t - t)$ will be shifted version $d(t)$ along t axis by amount t , from definition of delta function and Eq. (1.8), we can write

$$\int_{-\infty}^{+\infty} v(\tau) \delta(t - \tau) d\tau = v(t) \quad (1.9)$$

Time inversion

This operation inverts the signal along time axis so that we get a mirror image of the signal with $t = 0$ being the reflecting line. If $v(t)$ is original signal then $x(t) = v(-t)$ is a time inverted version of $v(t)$ such that what occurs at t for $v(t)$, the same occurs for $x(t)$ at $-t$. An illustration of this is shown in Fig. 1.6b.

Time Scaling

This operation compresses or expands a signal along the time axis. If $v(t)$ is original signal then $y(t) = v(at)$ is a time scaled version of $v(t)$. Note that, in general $a > 0$ and a negative a signifies both time scaling and time inversion, the inversion comes from the negative sign. If $a < 1$ then $y(t)$ is an expanded version of $v(t)$ and if $a > 1$ then $y(t)$ is a compressed version of $v(t)$. This is because whatever occurs for $v(t)$ in time at , occurs for $w(t)$ in time t . This is illustrated in Fig. 1.6c. Note that $a = 1$ gives the original signal and $a = -1$ gives the time inverted signal of the original.

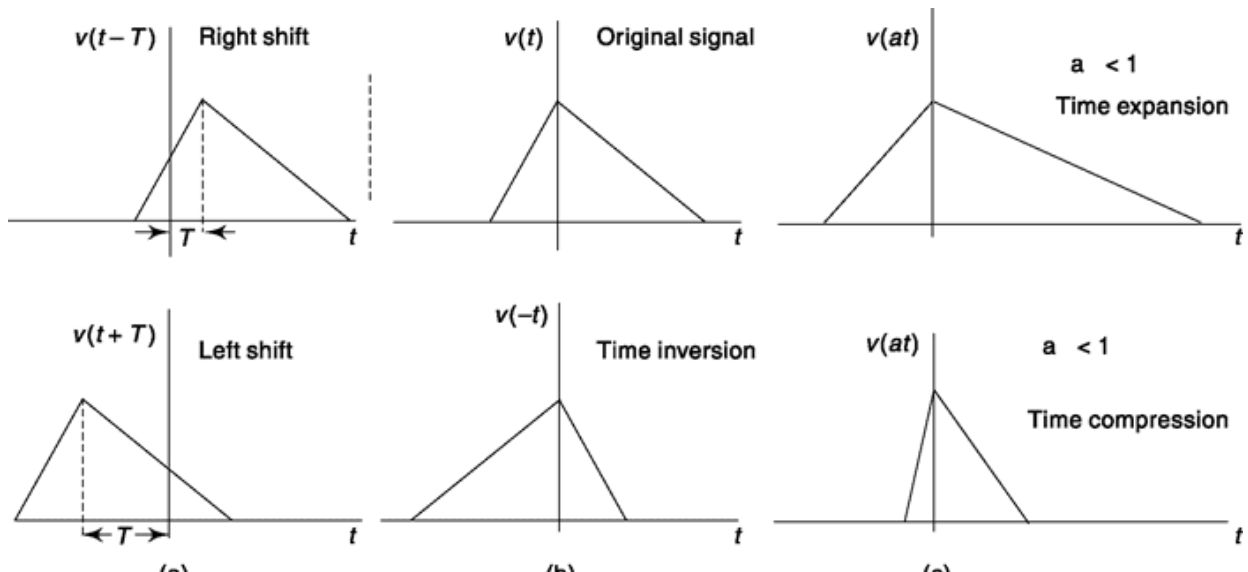


Fig. 1.6 (a) Time shifting, (b) Time inversion, and (c) Time scaling of original signal given in top of (b).

Convolution

This is a process by which one signal is time reversed, shifted, multiplied with another signal and then its integral is calculated to generate a third signal. This operation is useful in describing output of a system by convolving input signal and its unit impulse response. Mathematically, convolution is represented as shown in Eq. (1.10) where $w(t)$ is the convolved output and $v(t)$, $h(t)$ are the signals being convolved. The symbol ‘ \otimes ’ is often used as a convolution operator.

$$w(t) = v(t) \otimes h(t) = \int_{-\infty}^{+\infty} v(\tau) h(t - \tau) d\tau \quad (1.10)$$

Note that, $v(t) \otimes h(t) = h(t) \otimes v(t)$. Compare Eq. (1.10) with Eq. (1.9) and you can see how input and output of a system is related. You can visualize $h(t)$ as the output generated by the system when $d(t)$ is input. The system that obeys this is known as *linear-time-invariant* system. *Linear system* are those for which principle of superposition is valid, i.e. if inputs $v_x(t)$ and $v_2(t)$ generate output $w_x(t)$ and $w_2(t)$ respectively then input $[av(t) + bv_2(t)]$ will generate output $[aw(t) + bw_2(t)]$. For a *time-invariant* system, if input is shifted in time by T_{unit} then output too is shifted by same amount. Please refer to Example 1.8 and its graphical illustration (Fig. 1.11) to understand how convolution operation works.

1.2.4 Correlation and Autocorrelation

The correlation between waveforms is a measure of the similarity or relatedness between the waveforms. Suppose that we have waveforms $v_x(t)$ and $v_2(t)$, not necessarily periodic nor confined to a finite time interval. Then the correlation between them, or more precisely the *average cross correlation* between $v_x(t)$ and $v_2(t)$, is $R_{12}(t)$ defined as

$$R_{12}(\tau) \equiv \lim_{T \rightarrow \infty} \frac{1}{T} \int_{-T/2}^{T/2} v_1(t)v_2(t + \tau) dt \quad (1.11)$$

If $v_1(t)$ and $v_2(t)$ are periodic with the same fundamental period T_0 , then the average cross correlation is

$$R_{12}(\tau) = \frac{1}{T_0} \int_{-T_0/2}^{T_0/2} v_1(t)v_2(t + \tau) dt \quad (1.12)$$

If $v_x(t)$ and $v_2(t)$ are waveforms of finite energy (for example, nonperiodic pulse-type waveforms), then the cross correlation is defined as

$$R_{12}(\tau) = \int_{-\infty}^{\infty} v_1(t)v_2(t + \tau) dt \quad (1.13)$$

The need for introducing the parameter t in the definition of cross correlation may be seen by the example illustrated in Fig. 1.7. Here the two waveforms, while different, are obviously related. They have the same period and nearly the same form. However, the integral of the product $v_x(t)v_2(t)$ is zero since at all times one or the other function is zero. The function $v_2(t + \tau)$ is the

function $v_2(t)$ shifted to the left by amount t . It is clear from the figure that while $R_{12}(0) = 0$, $R_{12}(t)$ will increase as t increases from zero, becoming a maximum when $t = t_0$. Thus t is a “searching” or “scanning” parameter which may be adjusted to a proper time shift to reveal, to the maximum extent possible, the relatedness or correlation between the functions. The term *coherence* is sometimes used as a synonym for correlation. Functions for which $R_{12}(t) = 0$ for all t are described as being *uncorrelated* or *noncoherent*.

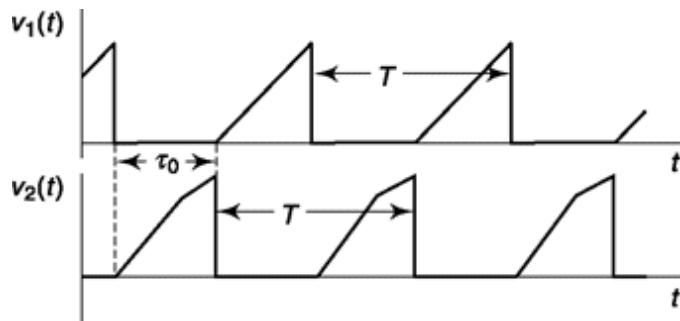


Fig. 17 Two related waveforms. The timing is such that the product $v_1(t)v_2(t) = 0$.

In scanning to see the extent of the correlation between functions, it is necessary to specify which function is being shifted. In general, $R_{12}(t)$ is not equal to $R_{21}(t)$. It is readily verified (Prob. 1.40) that

$$R_{21}(\tau) \equiv \lim_{T \rightarrow \infty} \frac{1}{T} \int_{-T/2}^{T/2} v_1(t + \tau) v_2(t) dt = R_{12}(-\tau) \quad (1.14)$$

with identical results for periodic waveforms or waveforms of finite energy.

Correlation coefficient is also used as a measure of similarity. For two signals $v_x(t)$ and $v_2(t)$ with energy E_x and E_2 respectively, it is defined as

$$c = \frac{1}{\sqrt{E_1 E_2}} \int_{-\infty}^{+\infty} v_1(t) v_2(t) dt = \frac{R_{12}(0)}{\sqrt{E_1 E_2}} \quad (1.15)$$

Division by terms square root of E_x and E_2 in Eq. (1.15) effectively make each of $v_x(t)$ and $v_2(t)$ normalized to unit energy. Thus if $v_x(t) = v_2(t)$, $c = 1$ and if $v_x(t) = -v_2(t)$, $c = -1$. For c positive it is called positive correlation, i.e. if $v_x(t)$ increases then $v_2(t)$ also shows increasing trend and c negative is known as negative correlation where trend is reverse. What if $c = 0$? This makes two signals orthogonal to each other where one does not influence the

other in any way, +ve or -ve. This is a very important concept which we shall investigate further in this chapter.

Power and Cross Correlation

Let $v_x(t)$ and $v_2(t)$ be waveforms which are not periodic nor confined to a finite time interval. Suppose that the normalized power of $v_x(t)$ is S_1 and the normalized power of $v_2(t)$ is S_2 . What, then, is the normalized power of $v_x(t) + v_2(t)$? Or, more generally, what is the normalized power S_{12} of $v_x(t) + v_2(t + \tau)$? We have

$$S_{12} = \lim_{T \rightarrow \infty} \frac{1}{T} \int_{-T/2}^{T/2} [v_1(t) + v_2(t + \tau)]^2 dt \quad (1.16)$$

$$= \lim_{T \rightarrow \infty} \frac{1}{T} \left\{ \int_{-T/2}^{T/2} v_1^2(t) dt + \int_{-T/2}^{T/2} [v_2(t + \tau)]^2 dt + 2 \int_{-T/2}^{T/2} v_1(t)v_2(t + \tau) dt \right\} \quad (1.17)$$

$$= S_1 + S_2 + 2R_{12}(\tau) \quad (1.18)$$

In writing Eq. (1.18), we have taken account of the fact that the normalized power of $v_2(t + \tau)$ is the same as the normalized power of $v_2(t)$. For, since the integration in Eq. (1.17) extends eventually over the entire time axis, a time shift in v_2 will clearly not affect the value of the integral.

From Eq. (1.18) we have the important result that if two waveforms are uncorrelated, that is, $R_{12}(t) = 0$ for all t , then no matter how these waveforms are time-shifted with respect to one another, the normalized power due to the superposition of the waveforms is the sum of the powers due to the waveforms individually. Similarly, if a waveform is the sum of any number of mutually uncorrelated waveforms, the normalized power is the sum of the individual powers. It is readily verified that the same result applies for periodic waveforms. For finite energy waveforms, the result applies to the normalized energy.

Suppose that two waveforms $v_1(t)$ and $v_2(t)$ are uncorrelated. If dc components V_1 and V_2 are added to the waveforms, then the waveforms $v_x(t) = v_1(t) + V_1$ and $v_2(t) = v_2(t) + V_2$ will be correlated with correlation $R_{12}(t) = V_1V_2$. In most applications where the correlations between waveforms is of concern, there is rarely any interest in the dc component. It is customary,

then, to continue to refer to waveforms as being uncorrelated if the only source of the correlation is the dc components.

Autocorrelation

The correlation of a function with itself is called the *autocorrelation*. Thus with $v_x(t) = v_2(t)$, $R_{12}(t)$ becomes $R(t)$ given, in the general case, by

$$R(t) = \lim_{T \rightarrow \infty} \frac{1}{T} \int_{-T/2}^{T/2} v(t)v(t + \tau) dt \quad (1.19)$$

A number of the properties of $R(t)$ are listed in the following:

$$(a) \quad R(0) = \lim_{T \rightarrow \infty} \frac{1}{T} \int_{-T/2}^{T/2} [v(t)]^2 dt = S \quad (1.20)$$

That is, the autocorrelation for $\tau = 0$ is the average power S of the waveform.

$$(b) \quad R(0) \geq R(\tau) \quad (1.21)$$

This result is rather intuitively obvious since we would surely expect that similarity between $v(t)$ and $v(t + \tau)$ be a maximum when $t = 0$. The student is guided through a more formal proof in Prob. 1.42.

$$(c) \quad R(\tau) = R(-\tau) \quad (1.22)$$

Thus the autocorrelation function is an even function of t . To prove Eq. (1.22), assume that the axis $t = 0$ is moved in the negative t direction by an amount t . Then the integrand in Eq. (1.19) would become $v(t - t)v(t)$, and $R(t)$ would become $R(-t)$. Since, however, the integration eventually extends from $-'$ to $'$, such a shift in time axis can have no effect on the value of the integral. Thus, $R(t) = R(-t)$.

The three characteristics given in Eqs (1.20) to (1.22) are features not only of $R(t)$ defined by Eq. (1.19) but also for $R(t)$ as defined by Eqs (1.12) and (1.13) for the periodic case and the non-periodic case of finite energy. In the latter case, of course, $R(0) = E$, the energy rather than the power.

Example 1.3

Plot the signal $u(t - t)$ against t .

Solution

Refer to Fig. 1.8. We have used time shifting and time inversion operation to get $u(t - t)$ from $u(t)$.

Example 1.4

Plot the signal $u(t) - u(t - \tau)$ where τ is a positive constant.

Solution

Refer to Fig. 1.9.

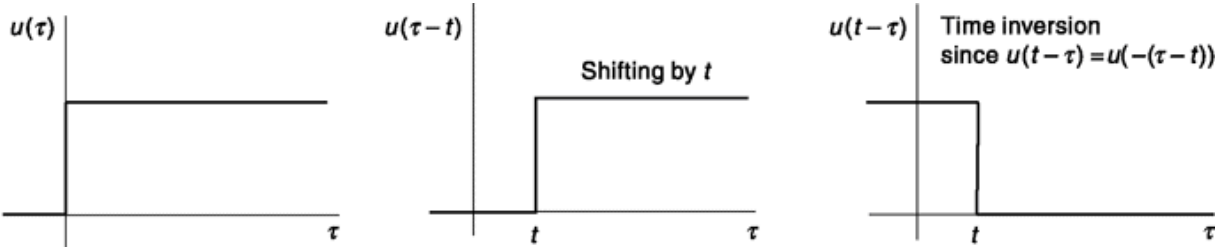


Fig. 1.8 Plot of $u(t - \tau)$ against τ

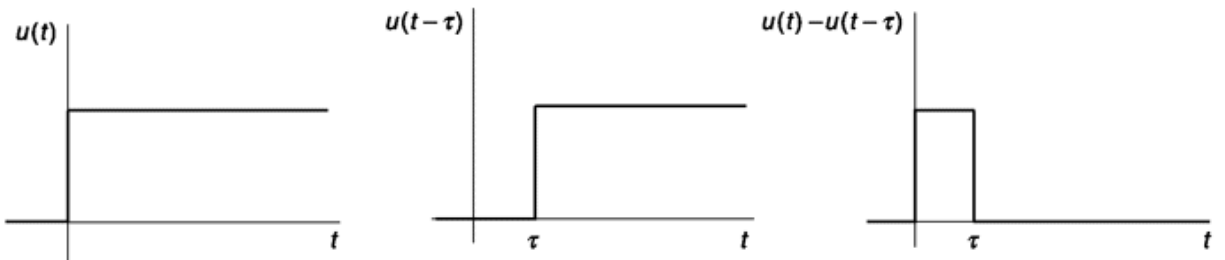


Fig. 1.9 Plotting of $u(t) - u(t - \tau)$.

Example 1.5

Find cross-correlation term $R_{12}(0)$, autocorrelation terms $R_1(0)$, $R_2(0)$ and energy E_1 , E_2 and hence correlation coefficient of two signals defined as follows $v_1(t) = u(t) - u(t - 5)$ and $v_2(t) = 2t(u(t) - u(t - 3))$

Solution

The signals $v_1(t)$ and $v_2(t)$ are shown in Fig. 1.10(a) and (b) respectively.

From definition of $R_{12}(0)$ and noting that $v_1(t)$ is nonzero for $0 < t < 5$ and $v_2(t)$ is nonzero for $0 < t < 3$, we get

$$R_{12}(0) = \int_0^{+3} 2t \, dt = 2 \cdot t^2/2 \Big|_0^{+3} = 3^2 = 9$$

$$E_1 = \int_0^{+5} 1 \cdot dt = t \Big|_0^{+5} = 5$$

$$E_2 = \int_0^{+3} 4t^2 \, dt = 2 \cdot t^3/3 \Big|_0^{+3} = (2/3) \cdot 3^3 = 18$$

Thus $c = 9/\sqrt{5 \times 18} = 0.9487$

Since $v_1(t)$ and $v_2(t)$ are aperiodic, from definition

$$R_1(0) = E_1 = 5 \text{ and } R_2(0) = E_2 = 18$$

Example 1.6

Find $R_{12}(-l)$ and $R_{12}(l)$ for signals given in Example 1.5.

Solution

Note that, from its definition $R_{12}(-1)$ uses $v_1(t)$ and $v_2(t - 1)$ inside the integral. $v_2(t - 1)$ is $v_2(t)$ shifted to right by 1 unit. Refer to Fig. 1.106. Thus, the overlap of $v_1(t)$ and $v_2(t - 1)$ exists within $1 < t < 4$. Since, $v_2(t)$ remains same in the new overlap the integral gives same value as that of $R_{12}(0) = 9$.

Now, $R_{12}(1)$ uses $v_1(t)$ and $v_2(t + 1)$ where $v_2(t + 1)$ is $v_2(t)$ shifted to left by 1 unit. Thus, the overlap of $v_1(t)$ and $v_2(t + 1)$ is within $0 < t < 2$. Here, the overlap is one unit less than before. Thus, the integral becomes

$$\begin{aligned} R_{12}(1) &= \int_0^{+2} 2(t+1) \cdot 1 \, dt = (2 \cdot t^2/2 + 2t) \Big|_0^{+2} \\ &= 2^2 + 2 \times 2 = 8 \end{aligned}$$

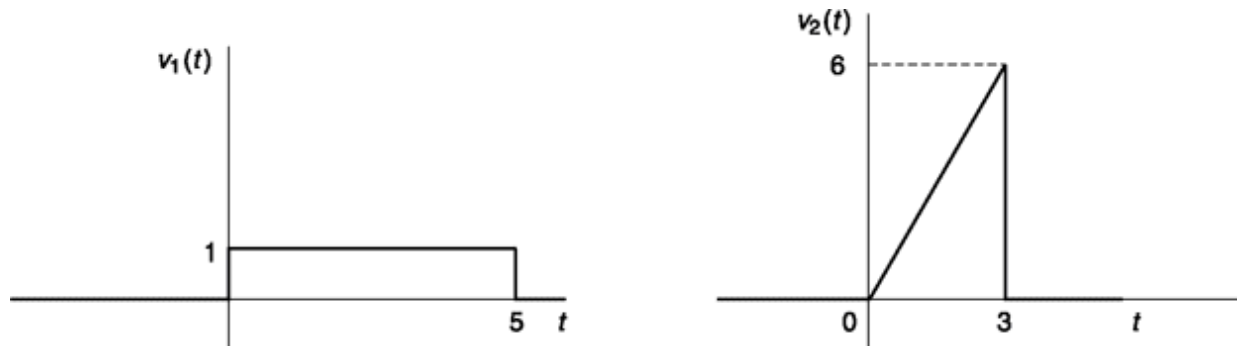


Fig. 1.10 Signals for Example 1.5(a) $v_1(t) = u(t) - u(t - 5)$, (b) $v_2(t) = 2t(u(t) - u(t - 3))$.

Example 1.7

Find $R_{12}(t)$ for signals given in Example 1.5.

Solution

From discussion in Example 1.6, we find there are 3 distinct regions of t for which there is a overlap between two signals.

For $0 < t < 3$, there is a left shift of $v_2(t)$ and overlap can be written in terms of t , as shown within integral given next

$$\begin{aligned} R_{12}(\tau) &= \int_0^{3-\tau} 2(t + \tau) \cdot 1 \, dt = (2 \cdot t^2/2 + 2\tau \cdot t)|_0^{3-\tau} \\ &= (3 - \tau)^2 + 2 \cdot \tau \cdot (3 - \tau) = 9 - \tau^2 \end{aligned}$$

For $-2 \leq \tau \leq 0$, overlap does not change $R_{12}(\tau) = R_{12}(0) = 9$

For $-5 \leq \tau \leq -2$, there is a right shift of $v_2(t)$ and overlap can be written in terms of τ , as shown within integral given next

$$\begin{aligned} R_{12}(\tau) &= \int_{-\tau}^5 2(t + \tau) \cdot 1 \, dt = (2 \cdot t^2/2 + 2\tau \cdot t)|_{-\tau}^5 \\ &= (5^2 - \tau^2) + 2 \cdot \tau \cdot (5 + \tau) \\ &= 25 + 10\tau + \tau^2 \end{aligned}$$

Example 1.8

Find convolution product $w(t)$ of two signals given in Example 1.5.

Solution

We know, $w(t) = v_1(t) \otimes v_2(t) = v_2(t) \otimes v_1(t)$

$$w(t) = v_2(t) \otimes v_1(t) = \int_{-\infty}^{+\infty} v_2(\tau) v_1(t - \tau) \, d\tau$$

Since, $v_1(t - t)$ is the time reversed rectangular pulse that is shifted to right on $v_2(t)$ (Fig. 1.11) the overlap is from 0 to t for $0 < t < 3$. The overlap is constant 0 to 3 for $3 < t < 5$. For $5 < t < 8$, the overlap is from $(t - 5)$ to 3. Note that for $t < 0$ and $t > 8$ there is no overlap of $v_2(t)$ and $v_1(t - t)$ and convolution product for those region is zero.

For $0 \leq t \leq 3$,

$$w(t) = \int_0^t 2\tau \cdot 1 \, d\tau = (2 \cdot \tau^2/2)|_0^t = t^2$$

For $3 \leq t \leq 5$,

$$w(t) = \int_0^3 2\tau \cdot 1 \, d\tau = (2 \cdot \tau^2/2)|_0^3 = 9$$

For $5 \leq t \leq 8$,

$$\begin{aligned} w(t) &= \int_{t-5}^3 2\tau \cdot 1 \, d\tau = (2 \cdot \tau^2/2)|_{t-5}^3 \\ &= 3^2 - (t-5)^2 = 10t - t^2 - 16 \end{aligned}$$

For other t , $w(t) = 0$.

SELF-TEST QUESTION

5. What is the RMS power of a sinusoidal signal of amplitude A ?
6. Complex signal is characterized by both magnitude and phase while real signal carries only magnitude information. Is it correct?
7. Is $v(t) = A\cos(\omega t + 0.5)$ an even signal?
8. Is $v(2t)$ a time compressed version of the signal $v(t)$?

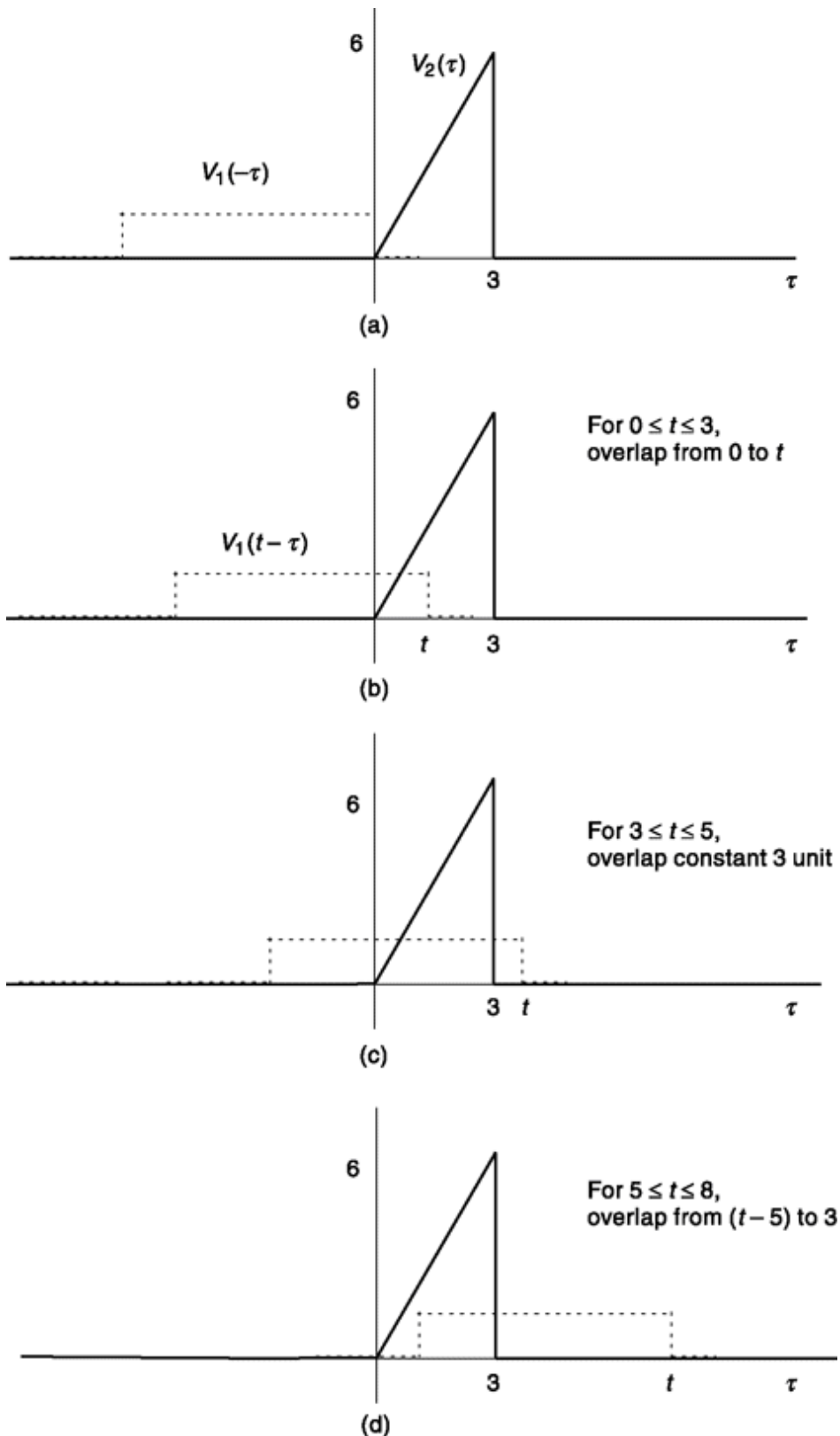


Fig. 1.11 Convolution process for Example 1.8.

1.3 FOURIER SERIES EXPANSION AND ITS USE

A periodic function of time $v(t)$ having a fundamental period T_0 can be represented as an infinite sum of sinusoidal waveforms. This summation, called a *Fourier series*, may be written in several forms. One such form is the following:

$$v(t) = A_0 + \sum_{n=1}^{\infty} A_n \cos \frac{2\pi n t}{T_0} + \sum_{n=1}^{\infty} B_n \sin \frac{2\pi n t}{T_0} \quad (1.23)$$

The constant A_0 is the average value of $v(t)$ given by

$$A_0 = \frac{1}{T_0} \int_{-T_0/2}^{T_0/2} v(t) dt \quad (1.24)$$

while the coefficients A_n and B_n are given by

$$A_n = \frac{2}{T_0} \int_{-T_0/2}^{T_0/2} v(t) \cos \frac{2\pi n t}{T_0} dt \quad (1.25)$$

and $B_n = \frac{2}{T_0} \int_{-T_0/2}^{T_0/2} v(t) \sin \frac{2\pi n t}{T_0} dt \quad (1.26)$

An alternative form for the Fourier series is

$$v(t) = C_0 + \sum_{n=1}^{\infty} C_n \cos \left(\frac{2\pi n t}{T_0} - \phi_n \right) \quad (1.27)$$

where C_0 , C_n and ϕ_n are related to A_0 , A_n and B_n by the equations

$$C_0 = A_0 \quad (1.28a)$$

$$C_n = \sqrt{A_n^2 + B_n^2} \quad (1.28b)$$

and $\phi_n = \tan^{-1} \frac{B_n}{A_n} \quad (1.28c)$

The Fourier series of a periodic function is thus seen to consist of a summation of harmonics of a fundamental frequency $f = 1/T_0$. The coefficients C_n are called *spectral amplitudes*; that is, C_n is the amplitude of the *spectral component* $C_n \cos (2\pi n f t - \phi_n)$ at frequency $n f_0$. A typical *amplitude spectrum* of a periodic waveform is shown in Fig. 1.12. Here, at each harmonic frequency, a vertical line has been drawn having a length equal to the spectral amplitude associated with each harmonic frequency. Of

course, such an amplitude spectrum, lacking the phase information, does not specify the waveform $v(t)$.

Note that, the information carried by j_n if plotted along f at intervals off will give phase spectrum of $v(t)$. It is important to know that Fourier series transformable signals should follow Dirichlet's conditions, i.e. (i) it should be single valued within period T_0 , (ii) should have finite number of maxima and minima within a finite time period, (iii) should have at most finite number of discontinuities in finite time period, and (iv) it must be absolutely integrable, i.e. $\int |v(t)| dt < \infty$. If you feel jittery about all these preconditions, be assured that the signals we handle in communication systems, obey these conditions and we don't need to be unduly concerned about.

The V_n 's are the *spectral amplitudes* of the *spectral components* $V_n e^{j2\pi nt/T_0}$. The amplitude spectrum of the V_n 's shown in Fig. 1.126 corresponds to the amplitude spectrum of the C_n 's shown in Fig.

We shall discuss orthogonality issue and usefulness of sinusoidal basis function and its employment in Fourier series expansion later in this chapter.

Exponential Form of the Fourier Series The exponential form of the Fourier series finds extensive application in communication theory. This form is given by

$$v(t) = \sum_{n=-\infty}^{\infty} V_n e^{j2\pi nt/T_0} \quad (1.29)$$

where V_n is given by

$$V_n = \frac{1}{T_0} \int_{-T_0/2}^{T_0/2} v(t) e^{-j2\pi nt/T_0} dt \quad (1.30)$$

The coefficients V_n have the property that V_n and V_{-n} are complex conjugates of one another, that is, $V_n = V_{-n}^*$. These coefficients are related to the C_n 's in Eq. (1.27) by

$$V_0 = C_0 \quad (1.31a)$$

$$V_n = \frac{C_n}{2} e^{-j\phi_n} \quad (1.31b)$$

1.12a. Observe that while $V_0 = C_0$, otherwise each spectral line in 1.12a at frequency f is replaced by the 2 spectral lines in 1.126, each of half amplitude, one at frequency f and one at frequency $-f$. The amplitude

spectrum in 1.12a is called a *single-sided* spectrum, while the spectrum in 1.126 is called a *two-sided* spectrum. We shall find it more convenient to use the two-sided amplitude spectrum and shall consistently do so from this point on.

Note that, though not conventional but we can also write amplitude spectrum of periodic signal $|V(f)|$

$$V(f) = \sum_{n=-\infty}^{\infty} V_n \delta(f - nf_0) \text{ where } f_0 = 1/T_o$$

This is not conventional as the quantity $V(f)$ in communication text usually refers to Fourier transform which we discuss shortly.

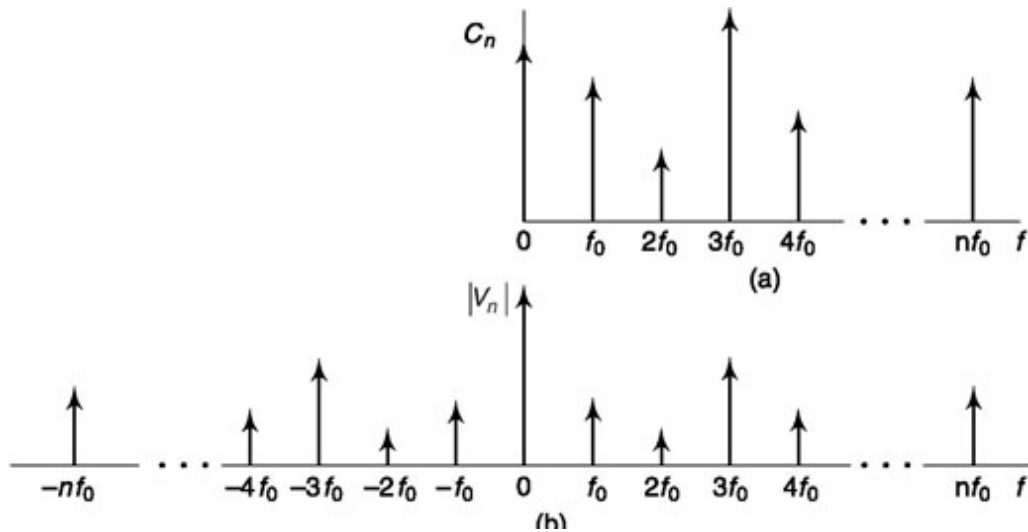


Fig. 1.12 (a) A one-sided plot of spectral amplitude of periodic waveform, (b) The corresponding two-sided plot.

Example 1.9

Consider the periodic impulse train shown in Fig. 1.13a. Find its Fourier coefficients. Hence, represent it as a (i) trigonometric Fourier series and (ii) exponential Fourier series. Note that these impulse trains can be considered as a sampler for analog to digital conversion in digital communication as discussed in reference to the example of Fig. 1.2.

Solution

The periodic impulse train is written

$$v(t) = I \sum_{k=-\infty}^{\infty} \delta(t - kT_0) \quad (1.32)$$

Using Eqs (1.24) and (1.25),

$$A_0 = \frac{I}{T_0} \int_{-T_0/2}^{T_0/2} \delta(t) dt = \frac{I}{T_0} \quad (1.33)$$

$$A_n = \frac{2I}{T_0} \int_{-T_0/2}^{T_0/2} \delta(t) \cos \frac{2\pi nt}{T_0} dt = \frac{2I}{T_0} \quad (1.34)$$

and, using Eq. (1.26),

$$B_n = \frac{2I}{T_0} \int_{-T_0/2}^{T_0/2} \delta(t) \sin \frac{2\pi nt}{T_0} dt = 0 \quad (1.35)$$

Further we have, using Eq. (1.28),

$$C_0 = \frac{I}{T_0}, \quad C_n = \frac{2I}{T_0}, \quad \phi_n = 0 \quad (1.36)$$

and from Eq. (1.31),

$$V_0 = V_n = \frac{I}{T_0} \quad (1.37)$$

Hence, $v(t)$ may be written in the forms

$$\begin{aligned} v(t) &= I \sum_{k=-\infty}^{\infty} \delta(t - kT_0) \\ &= \frac{I}{T_0} + \frac{2I}{T_0} \sum_{n=1}^{\infty} \cos \frac{2\pi nt}{T_0} \\ &= \frac{I}{T_0} \sum_{n=-\infty}^{\infty} e^{j2\pi nt/T_0} \end{aligned} \quad (1.38)$$

Note that, for even function B_n will be zero and for odd function A_n will be zero.

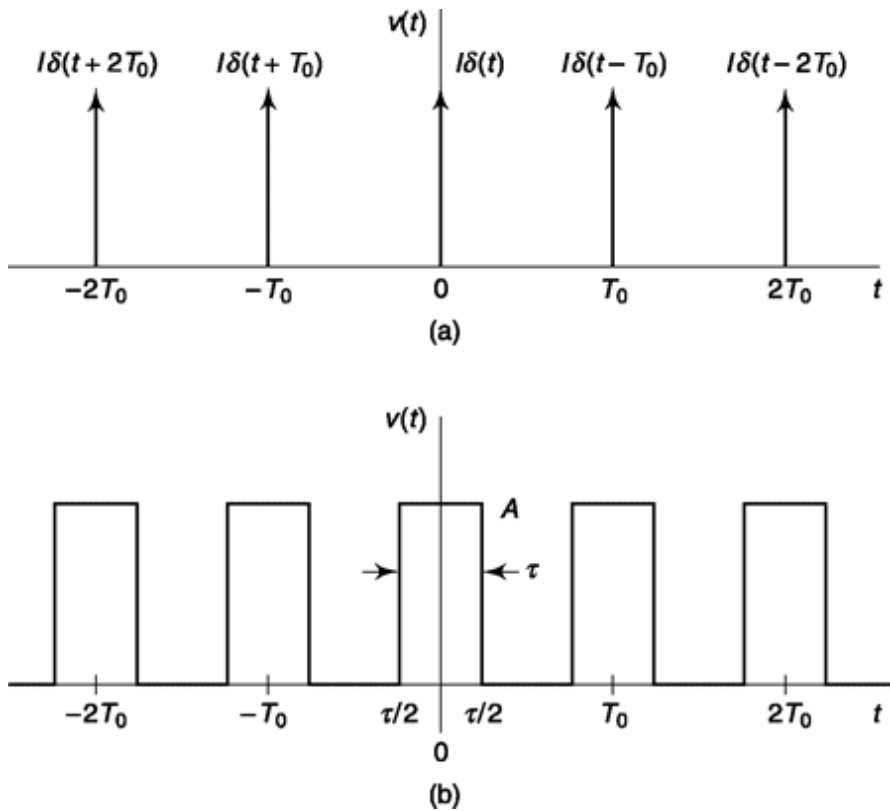


Fig. 1.13 Examples of periodic functions. (a) A periodic train of impulses, (b) A periodic train of pulses of duration t .

Example 1.10

Find Fourier coefficients of the periodic train of pulses of amplitude A and duration t , as shown in Fig. 1.13b.

Solution

We follow the method shown in previous example.

$$A_0 = C_0 = V_0 = \frac{1}{T_0} \int_{-T_0/2}^{T_0/2} v(t) dt = \frac{A\tau}{T_0} \quad (1.39)$$

$$\begin{aligned} A_n = C_n = 2V_n &= \frac{2}{T_0} \int_{-T_0/2}^{T_0/2} v(t) \cos \frac{2\pi nt}{T_0} dt \\ &= \frac{2A\tau}{T_0} \frac{\sin(n\pi\tau/T_0)}{n\pi\tau/T_0} \end{aligned} \quad (1.40)$$

$$\text{and} \quad B_n = 0 \quad \phi_n = 0 \quad (1.41)$$

Thus,

$$v(t) = \frac{A\tau}{T_0} + \frac{2A\tau}{T_0} \sum_{n=1}^{\infty} \frac{\sin(n\pi\tau/T_0)}{n\pi\tau/T_0} \cos \frac{2\pi nt}{T_0} \quad (1.42a)$$

$$= \frac{A\tau}{T_0} \sum_{n=-\infty}^{\infty} \frac{\sin(n\pi\tau/T_0)}{n\pi\tau/T_0} e^{j2\pi nt/T_0} \quad (1.42b)$$

Suppose that in the waveform of Fig. 1.13b we reduce t while adjusting A so that $A\tau$ is a constant, say $A\tau = I$. We would expect that in the limit, as $t \rightarrow 0$, the Fourier series for the pulse train in Eq. (1.42) should reduce to the series for the impulse train in Eq. (1.38). It is readily verified that such is indeed the case since as $t \rightarrow 0$

$$\begin{aligned} \tau &\rightarrow 0 \\ \frac{\sin(n\pi\tau/T_0)}{n\pi\tau/T_0} &\rightarrow 1 \end{aligned} \quad (1.43)$$

The Sampling Function

A function frequently encountered in spectral analysis is the sampling function $Sa(x)$ defined by

$$Sa(x) \equiv \frac{\sin x}{x} \quad (1.44)$$

[A closely related function is sinc x defined by sinc $x = (\sin nx)/nx$.] The function $Sa(x)$ is plotted in Fig. 1.14. It is symmetrical about $x = 0$, and at $x = 0$ has the value $Sa(0) = 1$. It oscillates with an amplitude that decreases with increasing x . The function passes through zero at equally spaced intervals at values of $x = \pm np$, where n is an integer other than zero. Aside from the peak at $x = 0$, the maxima and minima occur *approximately* midway between the zeros, i.e., at $x = \pm (n + 1/2)p$,

where $|\sin x| = 1$. This approximation is poorest for the minima closest to $x = 0$ but improves as x becomes larger. Correspondingly, the approximate value of $Sa(x)$ at these extremal points is

$$Sa\left[\pm\left(n + \frac{1}{2}\right)\pi\right] = \frac{2(-1)^n}{(2n+1)\pi} \quad (1.45)$$

We encountered the sampling function in Example 1.10 in Eq. (1.42) which expresses the spectrum of a periodic sequence of rectangular pulses.

In that equation, we have $x = npt/T_0$. The spectral amplitudes of Eq. (1.42b) are plotted in Fig. 1.14b for the case $A = 4$ and $t/T_0 = 1$. The spectral components appear at frequencies which are multiples of the fundamental frequency $f_0 = 1/T_0$, that is, at frequencies $f = nf_0 = n/T_0$. The envelope of the spectral components of $Sa(ptf)$ is also shown in the figure. Here we have replaced x by

$$x = n\pi \tau/T_0 = \pi \tau nf_0 = \pi \tau f \quad (1.46)$$

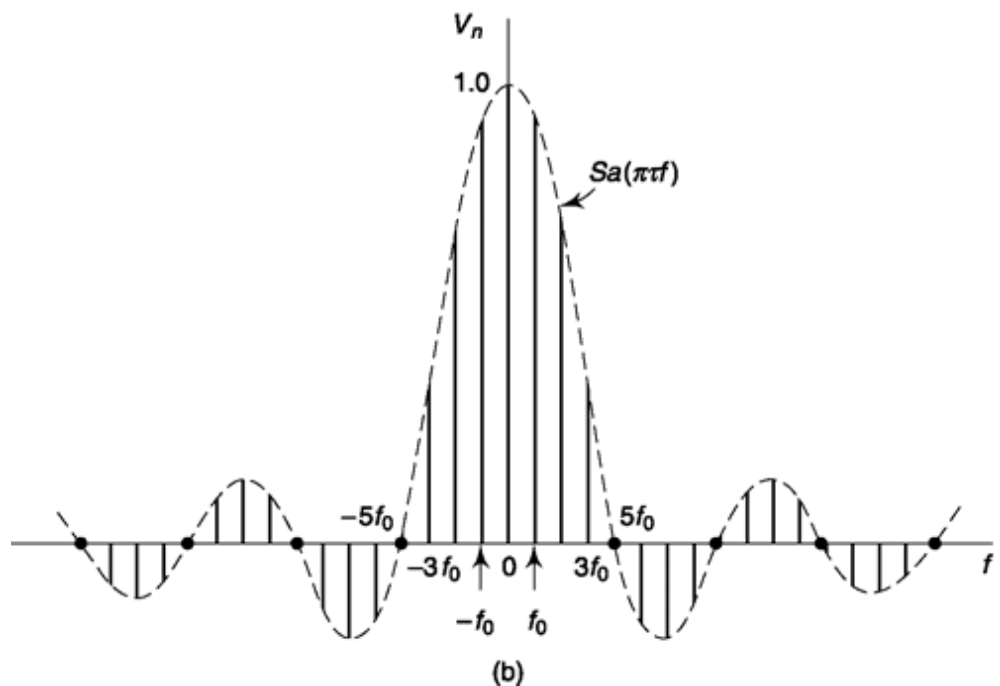
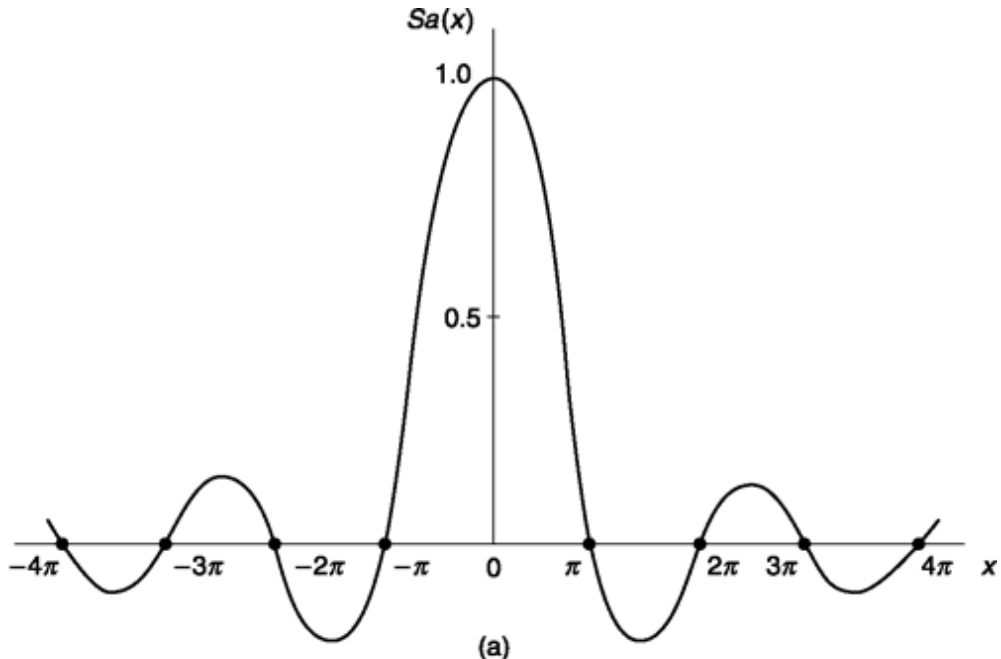


Fig. 1.14 (a) The function $Sa(x)$. (b) The spectral amplitudes V_n of the two-sided Fourier representation of the pulse train or Fig. 1.3.1b for $A = 4$ and $t/T_0 = - .4$

1.3.1 useful Fourier Series properties

Here, we present some of the interesting properties of Fourier series. We consider in each case the original signal is represented as

$$v(t) = \sum_{n=-\infty}^{\infty} V_n e^{j 2\pi n t / T_0}$$

Time Scaling

Fourier series representation of $v(at)$ is given by

Time Shift

Fourier series representation of $v(t + \tau)$, that is $v(t)$ shifted by t can be written as

$$\sum_{n=-\infty}^{\infty} V_n e^{j 2\pi n (t+\tau) / T_0} = \sum_{n=-\infty}^{\infty} V_n' e^{j 2\pi n t / T_0} \quad (\text{separating the exponential}) \quad (1.47)$$

where,

$$V_n' = V_n e^{j 2\pi n \tau / T_0}$$

Time Inversion

Fourier series representation of $v(-t)$ is given by

$$\sum_{k=-\infty}^{\infty} V_k e^{j 2\pi k (-t) / T_0} = \sum_{n=-\infty}^{\infty} V_n e^{j 2\pi n t / T_0} \quad (1.48)$$

i.e. magnitude of V_n remains constant, phase is shifted by 1800° . In trigonometric representation this is equivalent to A_n remaining same, B_n becoming negative.

$$\sum_{n=-\infty}^{\infty} V_n e^{j 2\pi n (at) / T_0} = \sum_{n=-\infty}^{\infty} V_n e^{j 2\pi n t / T_0'} \quad (\text{including } a \text{ within } T_0') \quad (1.49)$$

where $T_0' = T_0/a$, i.e. V_n remains constant but shifts to new frequencies na/T_0 from original locations n/T_0 . It is interesting to note that, for $a > 1$, *the signal is compressed in time domain* (refer to Sec. 1.2.3) *but gets expanded in frequency domain* with V_n appearing a times apart (at frequencies $na f_0$ instead of $n f_0$, $f_0 = 1/T_0$). For $a < 1$, the signal is expanded in time domain but contracted in frequency domain.

Time Derivative

Taking first derivative with time for the original expression, we get

$$\begin{aligned}
dv/dt &= \sum_{n=-\infty}^{\infty} d(V_n e^{j2\pi nt/T_0})/dt = \sum_{n=-\infty}^{\infty} (j2\pi n/T_0) V_n e^{j2\pi nt/T_0} \\
&= \sum_{n=-\infty}^{\infty} V'_n e^{j2\pi nt/T_0}
\end{aligned} \tag{1.50}$$

where,

$$V'_n = j2\pi n V_n / T_0$$

Integration

The integration of $v(t)$ can be represented as

$$\begin{aligned}
\int_0^t v(\tau) d\tau &= \sum_{n=-\infty}^{\infty} \int_0^t V_n e^{j2\pi nt/T_0} d\tau \\
&= \sum_{n=-\infty}^{\infty} V_n \int_0^t e^{j2\pi nt/T_0} d\tau = \sum_{n=-\infty}^{\infty} V_n / (j2\pi n/T_0) e^{j2\pi nt/T_0} \\
\text{or} \quad \int_0^t v(\tau) d\tau &= \sum_{n=-\infty}^{\infty} V'_n e^{j2\pi nt/T_0} \quad \text{where, } V'_n = V_n / (j2\pi n/T_0)
\end{aligned} \tag{1.51}$$

1.3.2 response of a Linear System

The Fourier trigonometric series is by no means the only way in which a periodic function may be expanded in terms of other functions.² As a matter of fact, the number of such possible alternative expansions is limitless. However, what makes the Fourier trigonometric expansion especially useful is the distinctive and unique characteristic of the sinusoidal waveform, this characteristic being that when a sinusoidal excitation is applied to a linear system, the response everywhere in the system is similarly sinusoidal and has the same frequency as the excitation. That is, the sinusoidal waveform preserves its waveshape. And since the wave-shape is preserved, then, in order to characterize the relationship of the response to the excitation, we need but to specify how the response amplitude is related to the excitation amplitude and how the response phase is related to the excitation phase. Therefore, with sinusoidal excitation, two numbers (amplitude ratio and phase difference) are all that are required to deduce a response. It turns out to be possible and very convenient to incorporate these two numbers into a single complex number.

Let the input to a linear system be the spectral component

$$v_i(t, \omega_n) = V_n e^{j2\pi nt/T_0} = V_n e^{j\omega_n t} \quad \text{where, } \omega_n = \frac{2\pi n}{T_0} \tag{1.52}$$

The waveform $v(t, \omega_n)$ may be, say, the voltage applied to the input of an electrical filter as in Fig. 1.15. Then the filter output $v_o(t, \omega_n)$ is related to the input by a complex transfer function

$$H(\omega_n) = |H(\omega_n)| e^{-j\theta(\omega_n)} \quad (1.53)$$

that is, the output is

$$\begin{aligned} v_o(t, \omega_n) &= H(\omega_n)v_i(t, \omega_n) = |H(\omega_n)| e^{-j\theta(\omega_n)} V_n e^{j\omega_n t} \\ &= |H(\omega_n)| V_n e^{j[\omega_n t - \theta(\omega_n)]} \end{aligned} \quad (1.54)$$

Actually, the spectral component in Eq. (1.52) is not a physical voltage. Rather, the physical input voltage $v_{ip}(t)$ which gives rise to this spectral component is the sum of this spectral component and its complex conjugate, that is,

$$v_{ip}(t, \omega_n) = V_n e^{j\omega_n t} + V_{-n} e^{-j\omega_n t} = V_n e^{j\omega_n t} + V_n^* e^{-j\omega_n t} = 2 \operatorname{Re}(V_n e^{j\omega_n t}) \quad (1.55)$$

The corresponding *physical* output voltage is $v_{op}(t, \omega_n)$ given by

$$v_{op}(t, \omega_n) = H(\omega_n)V_n e^{j\omega_n t} + H(-\omega_n)V_n^* e^{-j\omega_n t} \quad (1.56)$$

Since $v(t, \omega_n)$ must be real, the two terms in Eq. (1.56) must be complex conjugates, and hence we must have that $H(\omega_n) = H^*(-\omega_n)$. Therefore, since $H(\omega_n) = |H(\omega_n)| e^{-j\theta(\omega_n)}$, we must have that

$$|H(\omega_n)| = |H(-\omega_n)| \quad (1.57)$$

and

$$\theta(\omega_n) = -\theta(-\omega_n) \quad (1.58)$$

that is, $|H(\omega_n)|$ must be an even function and $\theta(\omega_n)$ an odd function of ω_n .

If, then, an excitation is expressed as a Fourier series in exponential form as in Eq. (1.29), the response is

$$v_o(t) = \sum_{n=-\infty}^{\infty} H(\omega_n)V_n e^{j2\pi n t/T_0} \quad (1.59)$$

If the form of Eq. (1.27) is used, the response is

$$v_o(t) = H(0)C_0 + \sum_{n=1}^{\infty} |H(\omega_n)| C_n \cos\left[\frac{2\pi n t}{T_0} - \phi_n - \theta(\omega_n)\right] \quad (1.60)$$

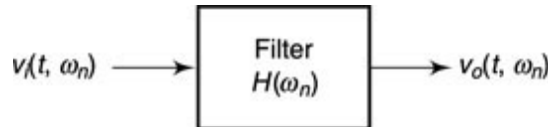


Fig. 1.15 A sinusoidal waveform $v_i(t, \omega_n)$ of angular frequency ω_n is applied at the input to a network (filter) whose transfer characteristic at ω_n is $H(\omega_n)$. The output $v_o(t, \omega_n)$ differs from the input only in amplitude and phase.

Given a periodic waveform, the coefficients in the Fourier series may be evaluated. Thereafter, if the transfer function $H(\omega_n)$ of a system is known, the response may be written out formally as in, say, Eq. (1.59) or Eq. (1.60). Actually, these equations are generally of small value from a *computational* point of view. For, except in rather special and infrequent cases, we should be hard-pressed indeed to recognize the waveform of a response which is expressed as the sum of an infinite (or even a large) number of sinusoidal terms. On the other hand, the *concept* that a response may be written in the form of a linear superposition of responses to individual spectral components, as, say, in Eq. (1.59), is of inestimable value.

1.3.3 Normalized power in a Fourier Expansion

Let us consider two typical terms of the Fourier expansion of Eq. (1.27). If we take, say, the fundamental and first harmonic, we have

$$v'(t) = C_1 \cos\left(\frac{2\pi t}{T_0} - \phi_1\right) + C_2 \cos\left(\frac{4\pi t}{T_0} - \phi_2\right) \quad (1.61)$$

To calculate the normalized power S' of $v'(t)$, we must square $v'(t)$ and evaluate

$$S' = \frac{1}{T_0} \int_{-T_0/2}^{T_0/2} [v'(t)]^2 dt \quad (1.62)$$

When we square $v'(t)$, we get the square of the first term, the square of the second term, and then the cross-product term. However, the two cosine functions in Eq. (1.61) are *orthogonal*. That is, when their product is integrated over a complete period, the result is zero. Hence in evaluating the normalized power, we find no term corresponding to this cross product. We find actually that S' is given by

$$S' = \frac{C_1^2}{2} + \frac{C_2^2}{2} \quad (1.63)$$

By extension, it is apparent that the normalized power associated with the entire Fourier series is

$$S = C_0^2 + \sum_{n=1}^{\infty} \frac{C_n^2}{2} \quad (1.64)$$

Hence, we observe that because of the orthogonality of the sinusoids used in a Fourier expansion, the total normalized power is the sum of the normalized power due to each term in the series separately. If we write a waveform as a sum of terms which are not orthogonal, this very simple and useful result will not apply. We may note here also that in terms of the A's and B's of the Fourier representation of Eq. (1.23), the normalized power is

$$S = A_0^2 + \sum_{n=1}^{\infty} \frac{A_n^2}{2} + \sum_{n=1}^{\infty} \frac{B_n^2}{2} \quad (1.65)$$

It is to be observed that power and normalized power are to be associated with a *real* waveform and not with a *complex* waveform. Thus suppose we have a term $A_n \cos(2\pi nt/T_0)$ in a Fourier series. Then the normalized power contributed by this term is $A^2/2$ quite independently of all other terms. And this normalized power comes from averaging, over time, the product of the term $A_n \cos(2\pi nt/T)$ by *itself*. On the other hand, in the complex Fourier representation of Eq. (1.29) we have terms of the form $V_n e^{j2\pi nt/T_0}$. The average value of the square of such a term is zero. We find as a matter of fact that the contributions to normalized power come from product terms

$$V_n e^{j2\pi nt/T_0} V_{-n} e^{-j2\pi nt/T_0} = V_n V_{-n} = V_n V_n^* \quad (1.66)$$

The total normalized power is

$$S = \sum_{n=-\infty}^{+\infty} V_n V_n^* \quad (1.67)$$

Thus, in the complex representation, the power associated with a particular *real* frequency $n/T_0 = nf_0$ (f_0 is the fundamental frequency) is associated neither with the spectral component at nf_0 nor with the component at $-nf_0$, but rather with the *combination* of spectral components, one in the positive-frequency range and one in the negative-frequency range. This power is

$$V_n V_n^* + V_{-n} V_{-n}^* = 2 V_n V_n^* \quad (1.68)$$

It is nonetheless a procedure of great convenience to associate one-half of the power in this combination of spectral components (that is, $V_n V_n^*$) with the frequency nf_0 and the other half with the frequency $-nf_0$. Such a procedure will always be valid provided that we are careful to use the procedure to calculate only the *total* power associated with frequencies nf_0

and $-nf_0$. Thus, we may say that the power associated with the spectral component at nf_0 is $V_n V^*$ and the power associated with the spectral component at $-nf_0$ is similarly $V_n V^*$ ($= V_{-n} V_{-n}$). If we use these associations only to arrive at the result that the total power is $2 V_n V^*$, we shall make no error.

In correspondence with the one-sided and two-sided spectral amplitude pattern of Fig. 1.12, we may construct one-sided and two-sided spectral (normalized) power diagrams. A two-sided power spectral diagram is shown in Fig. 1.16. The vertical axis is labeled S_n , the power associated with each spectral component. The height of each vertical line is $|V_n|^2$. Because of its greater convenience and because it lends a measure of systemization to very many calculations, we shall use the two-sided amplitude and power spectral pattern throughout this text.

We shall similarly use a two-sided representation to specify the transmission characteristics of filters. Thus, suppose we have a low-pass filter which transmits without attenuation all spectral components up to a frequency f_M and transmits nothing at a higher frequency. Then the magnitude of the transfer function will be given as in Fig. 1.17. The transfer characteristic of a bandpass filter will be given as in Fig. 1.18.

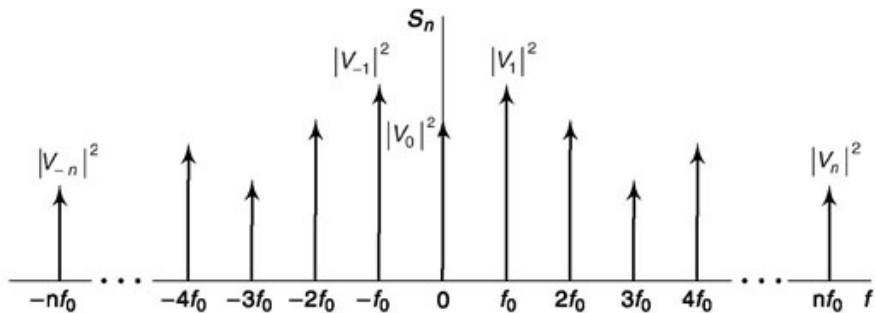


Fig. 1.16 A two-sided power spectrum.

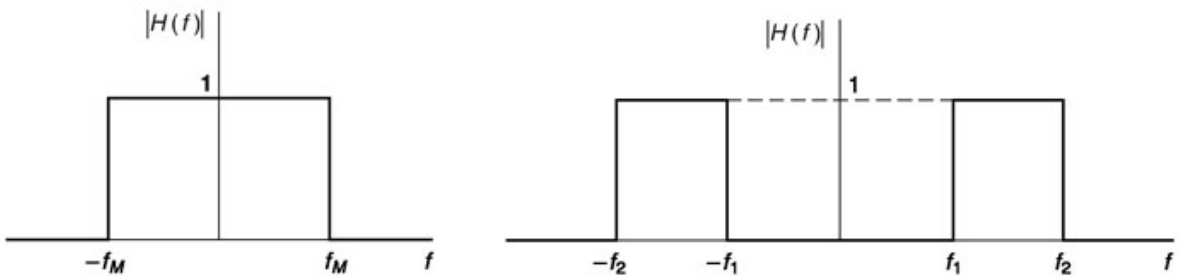


Fig. 1.17 The transfer characteristic of Fig. 1.18 The transfer characteristic of an idealized an idealized low-pass filter. bandpass filter with passband from f_1 to f ,

1.3.4 power Spectral density (pSD)

Suppose that in Fig. 1.16 where S_n is given for each spectral component, we start at $f = -'$ and then, moving in the positive-frequency direction, we add the normalized powers contributed by each power spectral line up to the frequency f . This sum is $S(f)$, a function of frequency. $S(f)$ typically will have the appearance shown in Fig. 1.19. It does not change as f goes from one spectral line to another, but jumps abruptly as the normalized power of each spectral line is added. Now let us

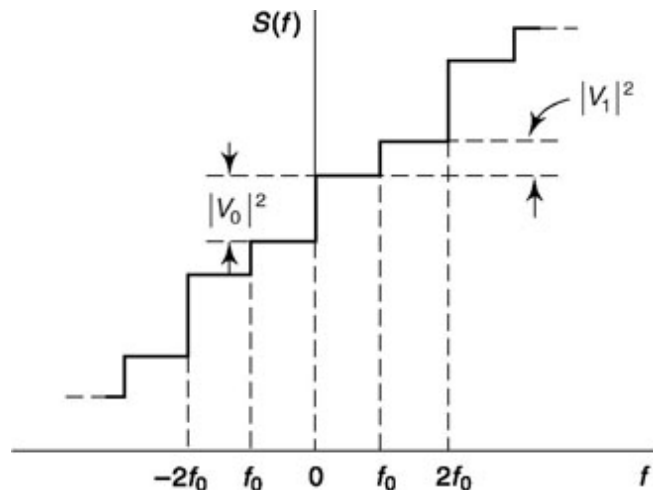


Fig. 1.19 The sum $S(f)$ of the normalized power in all spectral components from $f = -'$ to f

inquire about the normalized power at the frequency f in a range df . This quantity of normalized power $dS(f)$ would be written

$$dS(f) = \frac{dS(f)}{df} df \quad (1.69)$$

The quantity $dS(f)/df$ is called the (normalized) *power spectral density* $G(f)$; thus

$$G(f) \equiv \frac{dS(f)}{df} \quad (1.70)$$

The power in the range df at f is $G(f) df$. The power in the positive-frequency range f_1 to f_2 is

$$S(f_1 \leq f \leq f_2) = \int_{f_1}^{f_2} G(f) df \quad (1.71)$$

The power in the negative-frequency range $-f_2$ to $-f_1$ is

$$S(-f_2 \leq f \leq -f_1) = \int_{-f_2}^{-f_1} G(f) df \quad (1.72)$$

The quantities in Eqs (1.71) and (1.72) do not have physical significance. However, the total power in the *real* frequency range f_1 to f_2 does have physical significance, and this power $S(f_1 \leq |f| \leq f_2)$ is given by

$$S(f_1 \leq |f| \leq f_2) = \int_{-f_2}^{-f_1} G(f) df + \int_{f_1}^{f_2} G(f) df \quad (1.73)$$

To find the power spectral density, we must differentiate $S(f)$ in Fig. 1.19. Between harmonic frequencies we would have $G(f) = 0$. At a harmonic frequency, $G(f)$ would yield an impulse of strength equal to the size of the jump in $S(f)$. Thus, we would find

$$G(f) = \sum_{n=-\infty}^{\infty} |V_n|^2 \delta(f - nf_0) \quad (1.74)$$

If, in plotting $G(f)$, we were to represent an impulse by a vertical arrow of height proportional to the impulse strength, then a plot of $G(f)$ versus f as given by Eq. (1.74) would have exactly the same appearance as the plot of S_n shown in Fig. 1.16.

1.3.5 Effect of transfer Function on pSD

Let the input signal $v(t)$ to a filter have a power spectral density $G_i(f)$. If V_{in} are the spectral amplitudes of this input signal, then, using Eq. (1.74)

Let the output signal of the filter be $v_o(t)$. If V_{on} are the spectral amplitudes of this output signal, then the corresponding power spectral density is

$$G_0(f) = \sum_{n=-\infty}^{\infty} |V_{on}|^2 \delta(f - nf_0) \quad (1.77)$$

where

$$V_{on} = \frac{1}{T_0} \int_{-T_0/2}^{T_0/2} v_o(t) e^{-j2\pi nt/T_0} dt \quad (1.78)$$

As discussed in Sec. 1.3.2, if the transfer function of the filter is $H(f)$, then the output coefficient V_{on} is related to the input coefficient by

$$V_{on} = V_{in} H(f = nf_0) \quad (1.79)$$

Hence,

$$|V_{on}|^2 = |V_{in}|^2 |H(f = nf_0)|^2 \quad (1.80)$$

Substituting Eq. (1.80) into Eq. (1.77) and comparing the result with Eq. (1.75) yields the important result

$$G_0(f) = G_i(f) |H(f)|^2 \quad (1.81)$$

Equation (1.81) is of the greatest importance since it relates the power spectral density, and hence the power, at one point in a system to the power spectral density at another point in the system. Equation (1.81) was derived for the special case of periodic signals; however, it applies to nonperiodic signals and signals represented by random processes (Sec. 6.5) as well.

As a special application of interest of the result given in Eq. (1.81), assume that an input signal $v_i(t)$ with power spectral density $G_i(f)$ is passed through a differentiator. The differentiator output $v_o(t)$ is related to the input by

$$v_o(t) = \tau \frac{d}{dt} v_i(t) \quad (1.82)$$

where τ is a constant. The operation indicated in Eq. (1.82) multiplies each spectral component of $v_i(t)$ by $j2\pi f\tau = j\omega\tau$. Hence $H(f) = j\omega\tau$, and $|H(f)|^2 = \omega^2\tau^2$. Thus from Eq. (1.81) the spectral density of the output is

$$G_0(f) = \omega^2 \tau^2 G_i(f) \quad (1.83)$$

Example 1.11

Find Fourier coefficients of the square waveform shown in Fig. 1.20a. Hence, find its power spectral density.

Solution

Note that time period $T_0 = 4$. Then $f_0 = 1/4$

From definition,

$$\begin{aligned} V_n &= \frac{1}{4} \int_{-2}^2 v(t) e^{-j2\pi nt/T_0} dt \\ &= \frac{1}{4} \int_{-1}^1 v(t) e^{-j2\pi nt/T_0} dt + \frac{1}{4} \int_1^3 v(t) e^{-j2\pi nt/T_0} dt \\ &= \frac{1}{4} \int_{-1}^1 1 \cdot e^{-j2\pi nt/4} dt + \frac{1}{4} \int_1^3 (-1) e^{-j2\pi nt/4} dt \end{aligned}$$

$$\begin{aligned} &= \frac{1}{4} \cdot 1/(-j2\pi n/4)[e^{-j2\pi nt/4}]_{-1}^1 - e^{-j2\pi nt/4}]_1^3 \\ &= j/(2\pi n) [e^{-j2\pi n/4} - e^{j2\pi n/4} - e^{-j2\pi n3/4} + e^{-j2\pi n/4}] \\ &= j/(2\pi n) [e^{-j2\pi n/4} - e^{j2\pi n/4} - e^{-j2\pi n(1-1/4)} + e^{-j2\pi n/4}] \\ &= j/(2\pi n) [2e^{-j2\pi n/4} - 2e^{j2\pi n/4}] \text{ as } e^{-j2\pi n} = 1 \\ &= j/(2\pi n) [4j \sin(-2\pi n/4)] \\ &= -2j^2/(\pi n) \sin(\pi n/2) \\ &= 2/(\pi n) \sin(\pi n/2) \\ &= \text{sinc}(n/2) \end{aligned}$$

Note that, since $v(t)$ is an even function, only A_n terms (real) are necessary. Also, since the dc component is zero (symmetric about time axis) $A_0 = 0$.

From definition, Power Spectral Density,

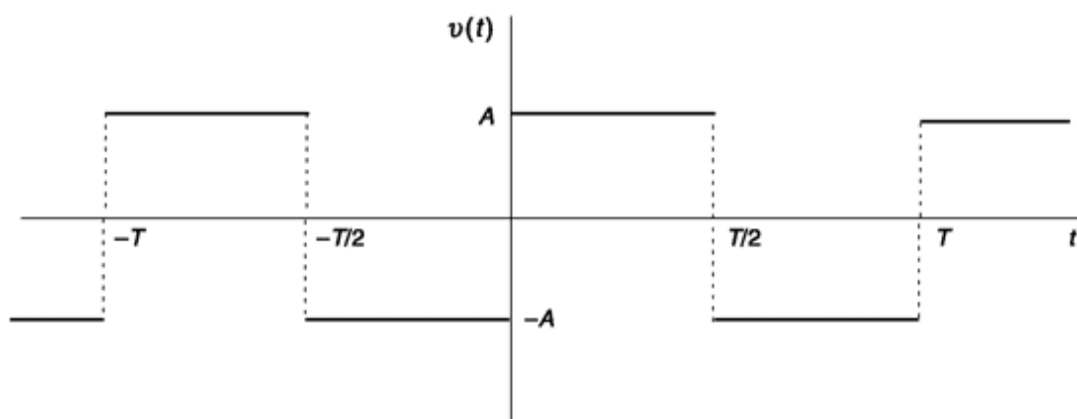
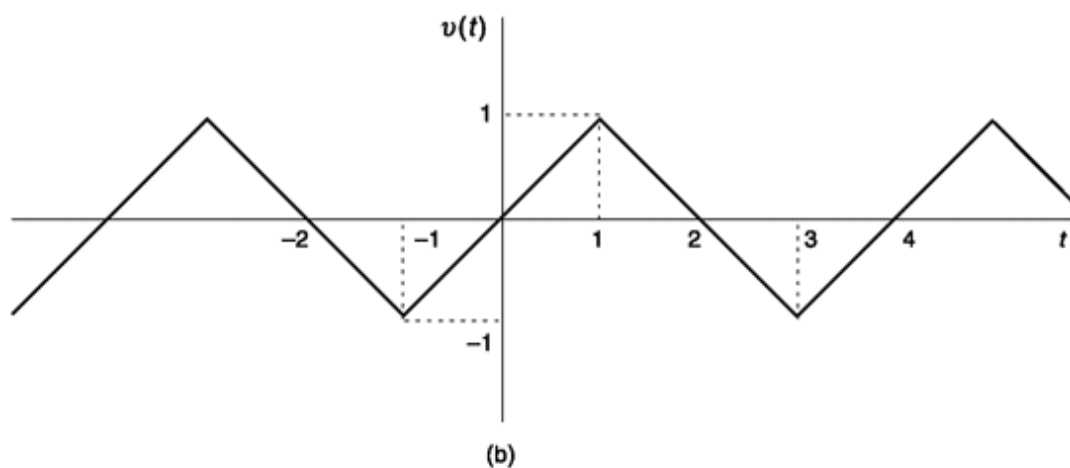
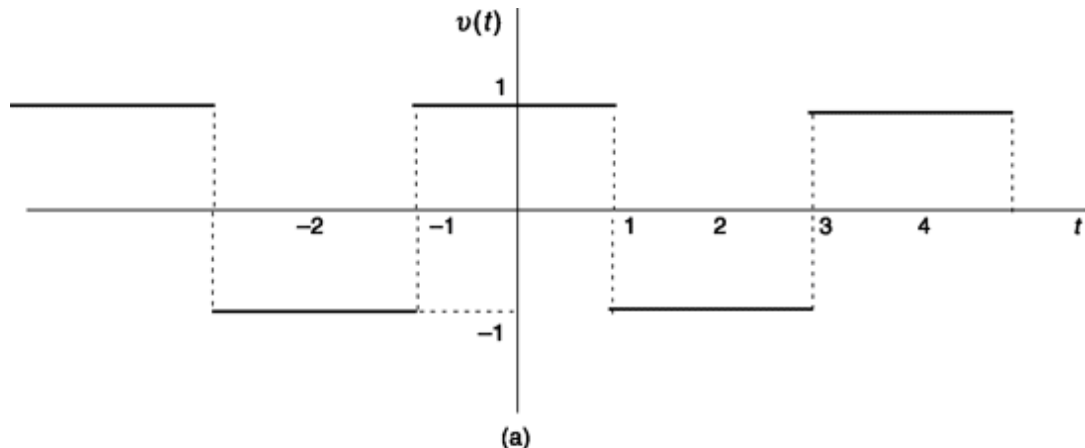
$$\begin{aligned} G(f) &= \sum_{n=-\infty}^{\infty} |V_n|^2 \delta(f - n/4) \\ &= 4 \sum_{n=-\infty}^{\infty} \frac{1}{(\pi n)^2} \sin^2(\pi n/2) \delta(f - n/4) \end{aligned}$$

Example 1.12

Find Fourier coefficients of the triangular waveform shown in Fig. 1.20b.

Solution

Note that, the triangular waveform is integral of the square waveform shown in Fig. 1.20a for which $V_n = 2/(p n) \sin(p n/2)$.



(c)

Fig. 1.20 Signals for (a) Example 1.11, (b) Example 1.12, and (c) Example 1.13.
From Fourier series properties (Eq. 1.51) of integral coefficients here are

$$\begin{aligned} V'_n &= V_n / (j2\pi n/T_0) = [2/(\pi n) \sin (\pi n/2)] / (j2\pi n/4) \\ &= -4j \sin (\pi n/2) / (\pi^2 n^2) \end{aligned}$$

Note that, the triangular signal is an odd signal and hence $A_n = 0$.

You can check yourself that by applying derivative property we can get back coefficients of square wave.

Example 1.13

Give trigonometric expansion of the signal shown in Fig. 1.20c.

Solution

Since, the signal is antisymmetric $A_n = 0$.

$$\begin{aligned}
 B_n &= \frac{2}{T} \int_{-T/2}^{T/2} A \sin(2\pi n/T) dt \\
 &= \frac{2A}{T} \int_0^{T/2} \sin(2\pi n/T) dt \\
 &\quad + \frac{2A}{T} \int_{T/2}^0 (-1) \cdot \sin(2\pi n/T) dt \\
 &= \frac{4A}{T} \int_0^{T/2} \sin(2\pi n/T) dt \\
 &= \frac{4A}{T} \cdot \frac{1}{(2n\pi/T)} \cdot (-\cos(2n\pi t/T)) \Big|_0^{T/2} \\
 &= -\frac{2A}{n\pi} \cdot \left[\cos\left(\frac{2n\pi T/2}{T}\right) - 1 \right] \\
 &= \frac{A}{n\pi} \cdot [1 - \cos(n\pi)]
 \end{aligned}$$

Thus, $B_n = 0$ for $n = \text{even}$ [as $\cos(n\pi) = 1$]

And $= \frac{2A}{n\pi}$ for $n = \text{odd}$ [as $\cos(n\pi) = -1$]

Please refer to MATLAB Example 1.4 for more interesting insights of this expansion and how we approximate the square wave by including more and more components of this.

SELF-TEST QUESTION

9. Does Dirichlet's condition require a signal to be absolutely integrable?
10. In Fourier series expansion, for even function B_n will be zero and for odd function A_n will be zero. Is it true?

11. Does compression in time domain lead to compression in frequency domain?

12. For a linear system, sinusoidal excitation retains its shape and frequency. Is it true?

1.4 THE FOURIER TRANSFORM

A periodic waveform may be expressed, as a sum of spectral components. These components have finite amplitudes and are separated by finite frequency intervals $f_0 = 1/T_0$. The normalized power of the waveform is finite, as is also the normalized energy of the signal in an interval T_0 . Now suppose we increase without limit the period T_0 of the waveform. Thus, say, in Fig. 1.136 the pulse centered around $t = 0$ remains in place, but all other pulses move outward away from $t = 0$ as $T_0 \rightarrow \infty$. Then eventually we would be left with a single-pulse nonperiodic waveform.

As $T_0 \rightarrow \infty$, the spacing between spectral components becomes infinitesimal. The frequency of the spectral components, which in the Fourier series was a discontinuous variable with a one-to-one correspondence with the integers, becomes instead a continuous variable. The normalized energy of the nonperiodic waveform remains finite, but, since the waveform is not repeated, its normalized power becomes infinitesimal. The spectral amplitudes similarly become infinitesimal. The Fourier series for the periodic waveform

$$v(t) = \sum_{n=-\infty}^{\infty} V_n e^{j2\pi n f_0 t} \quad (1.84)$$

becomes (see Prob. 1.19)

$$v(t) = \int_{-\infty}^{\infty} V(f) e^{j2\pi f t} df \quad (1.85)$$

The finite spectral amplitudes V_n are analogous to the infinitesimal spectral amplitudes $V(f) df$. The quantity $V(f)$ is called the *amplitude spectral density* or more generally the *Fourier transform* of $v(t)$. The Fourier transform is given by

$$V(f) = \int_{-\infty}^{\infty} v(t) e^{-j2\pi f t} dt \quad (1.86)$$

in correspondence with V_n , which is given by

$$V_n = \frac{1}{T_0} \int_{-T_0/2}^{T_0/2} v(t) e^{-j2\pi n f_0 t} dt \quad (1.87)$$

Again, in correspondence with Eq. (1.59), let $H(f)$ be the transfer function of a network. If the input signal is $v_i(t)$, then the output signal will be $v_o(t)$ given by

$$v_o(t) = \int_{-\infty}^{\infty} H(f) V(f) e^{j2\pi f t} df \quad (1.88)$$

Comparing Eq. (1.88) with Eq. (1.85), we see that the Fourier transform $V_o(f) \equiv \mathcal{F}[v_o(t)]$ is related to the transform $V_i(f)$ of $v_i(t)$ by

$$\mathcal{F}[v_o(t)] = H(f) \mathcal{F}[v_i(t)] \quad (1.89)$$

or $V_o(f) = H(f) V_i(f) \quad (1.90)$

as indicated in Fig. 1.21.

Note that, to have Fourier transform the signal should follow Dirichlet's condition as discussed for Fourier series. We'll conclude definition of Fourier transform by expressing it in terms of angular frequency ω . Since, $\omega = 2\pi f$ and $d\omega = 2\pi df$, a factor 2π is required in one of the Fourier transform pair equations. Usually, this is associated with $v(t)$ (Eq. 1.86) and the Fourier transform pair in alternate form is expressed as follows

$$V(\omega) = F[v(t)] = \int_{-\infty}^{\infty} v(t) e^{-j\omega t} dt \quad (1.91)$$

$$v(t) = F^{-1}[V(\omega)] = \frac{1}{2\pi} \int_{-\infty}^{\infty} V(\omega) e^{j\omega t} d\omega \quad (1.92)$$

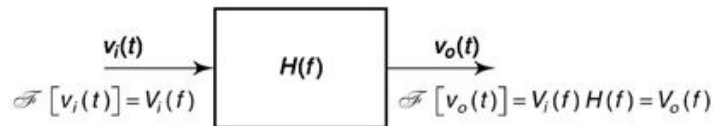


Fig. 1.21 A waveform $v_i(t)$ of transform $V_i(f)$ is transmitted through a network of transfer function $H(f)$. The output waveform $v_o(t)$ has a transform $V_o(f) = V_i(f)H(f)$.

Discrete Fourier Transform

Discrete Fourier Transform (DFT) is the discrete representation of Discrete Time Fourier Transform. This is used in getting frequency information of discrete time signal and is discussed in Chapter 4. An N -point DFT gives frequency information of in terms of N frequency samples spaced between frequencies 0 and f_s (sampling frequency) that makes each sample $\Delta f = f_s/N$ apart. Since, a discrete signal has frequency spectrum periodic in frequency axis with period that of sampling frequency f_s , the DFT values are periodic with period N . It can be shown that amplitude spectrum is symmetric and phase spectrum is antisymmetric about $f/2$ (or $N/2$). Using periodicity and symmetry property, DFT coefficients are usually calculated with an efficient numerical technique called Fast Fourier Transform (FFT) when N is integer power of 2. In digital hardware or computers, Fourier transform of analog signal also needs to be represented by discrete samples and thus certain sampling frequency (usually very high) is assumed. In MATLAB simulations using a digital computer, all representations eventually are in digital form. This will be clearer when we take up some MATLAB exercises at the end of this chapter.

Example 1.14

If $v(t) = \cos \omega_0 t$, find $V(f)$.

Solution

The function $v(t) = \cos \omega_0 t$ is periodic, and therefore has a Fourier series representation as well as a Fourier transform.

The exponential Fourier series representation of $v(t)$ is

$$v(t) = \frac{1}{2} e^{+j\omega_0 t} + \frac{1}{2} e^{-j\omega_0 t} \quad \omega_0 = \frac{2\pi}{T_0} \quad (1.93)$$

Thus

$$V_1 = V_{-1} = \frac{1}{2} \quad (1.94)$$

$$\text{and } V_n = 0 \quad n \neq \pm 1 \quad (1.95)$$

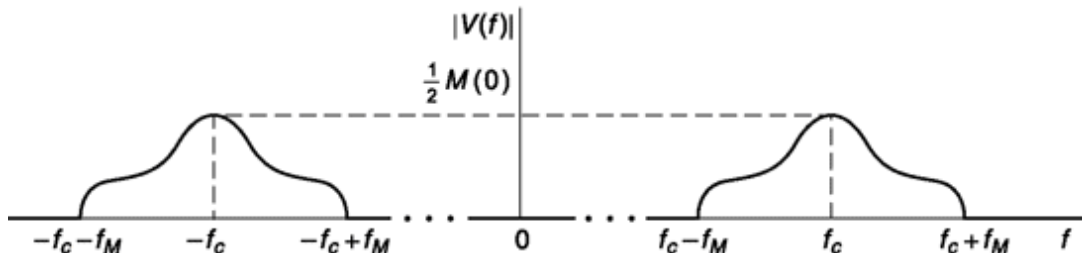
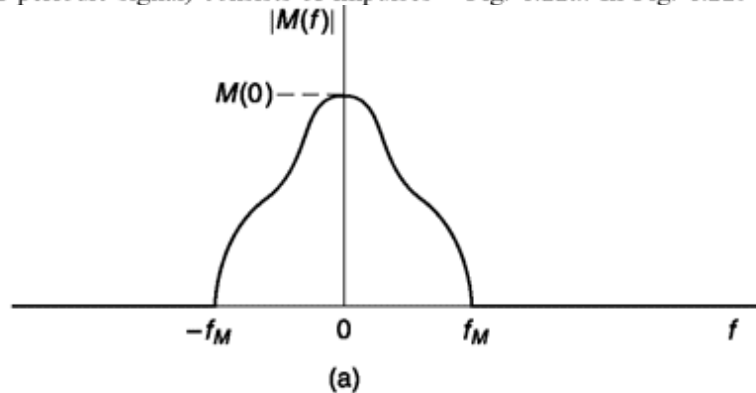
The Fourier transform $V(f)$ is found using Eq. (1.86):

$$\begin{aligned} V(f) &= \int_{-\infty}^{\infty} (\cos \omega_0 t) e^{-j2\pi f t} dt \\ &= \frac{1}{2} \int_{-\infty}^{\infty} e^{-j2\pi(f-f_0)t} dt \\ &\quad + \frac{1}{2} \int_{-\infty}^{\infty} e^{-j2\pi(f+f_0)t} dt \end{aligned} \quad (1.96a)$$

$$= \frac{1}{2} \delta(f-f_0) + \frac{1}{2} \delta(f+f_0) \quad (1.96b)$$

[See Eq. (1.114).]

From Eqs (1.93) and (1.95) we draw the following conclusion: The Fourier transform of a sinusoidal signal (or other periodic signal) consists of impulses



located at each harmonic frequency of the signal, i.e. at $f_n = n/T_0 = nf_0$. The strength of each impulse is equal to the amplitude of the Fourier coefficient of the exponential series.

Example 1.15

A signal $m(t)$ is multiplied by a sinusoidal waveform of frequency f_c . The product signal is

$$v(t) = m(t) \cos 2\pi f_c t \quad (1.97)$$

If the Fourier transform of $m(t)$ is $M(f)$, that is,

$$M(f) = \int_{-\infty}^{\infty} m(t) e^{-j2\pi f t} dt \quad (1.98)$$

find the Fourier transform of $v(t)$.

Solution

Since

$$m(t) \cos 2\pi f_c t = \frac{1}{2} m(t) e^{j2\pi f_c t} + \frac{1}{2} m(t) e^{-j2\pi f_c t} \quad (1.99)$$

then the Fourier transform $V(f)$ is given by

$$\begin{aligned} V(f) &= \frac{1}{2} \int_{-\infty}^{\infty} m(t) e^{-j2\pi(f+f_c)t} dt \\ &\quad + \frac{1}{2} \int_{-\infty}^{\infty} m(t) e^{-j2\pi(f-f_c)t} dt \end{aligned} \quad (1.100)$$

Comparing Eq. (1.100) with Eq. (1.98), we have the result that

$$V(f) = \frac{1}{2} M(f+f_c) + \frac{1}{2} M(f-f_c) \quad (1.101)$$

The relationship of the transform $M(f)$ of $m(t)$ to the transform $V(f)$ of $m(t) \cos 2\pi f_c t$ is illustrated in Fig. 1.22a. In Fig. 1.22b we see the spectral pattern

Fig. 1.22 (a) The amplitude spectrum of a waveform with no spectral component beyond f_M . (b) The amplitude spectrum of the waveform in (a) multiplied by $\cos 2p f_c t$.

of $M(f)$ replaced by two patterns of the same form. Example 1.16 One is shifted to the right and one to the left, each

, — — , , ... A pulse of amplitude A extends from $t = -\tau/2$ to $t = \tau/2$ by amount f_c . Further, the amplitudes of each of these J_n are $+A$ at $t = \pm \tau/2$. Find its Fourier transform $V(f)$. Consider also

two spectral patterns is one-half the amplitude of the the Fourier series for a periodic sequence of such

attempt (J pulses separated by intervals T_0 . Compare the Fourier A case of special interest arises when the waveform series coefficients V_n with the transform in the limit $m(t)$ is itself sinusoidal. Thus assume $m(t) = m \cos 2p f_m t$ (1.102)

where m is a constant. We then find that $V(f)$ is given *Solution* by We have directly

$$\begin{aligned} V(f) &= \frac{m}{4} \delta(f + f_c + f_m) \\ &+ \frac{m}{4} \delta(f + f_c - f_m) + \frac{m}{4} \delta(f - f_c + f_m) \\ &+ \frac{m}{4} \delta(f - f_c - f_m) \end{aligned} \quad (1.103)$$

This spectral pattern is shown in Fig. 1.23. Observe that the pattern has four spectral lines corresponding to two real frequencies $f_c + f_m$ and $f_c - f_m$.

The waveform itself is given by

$$\begin{aligned} v(t) &= \frac{m}{4} [e^{j2\pi(f_c + f_m)t} + e^{-j2\pi(f_c + f_m)t}] \\ &+ \frac{m}{4} [e^{j2\pi(f_c - f_m)t} + e^{-j2\pi(f_c - f_m)t}] \end{aligned} \quad (1.104a)$$

$$= \frac{m}{4} [\cos 2\pi(f_c + f_m)t + \cos 2\pi(f_c - f_m)t] \quad (1.104b)$$

$$V(f) = \int_{-\tau/2}^{\tau/2} A e^{-j2\pi f t} dt = A\tau \frac{\sin \pi f \tau}{\pi f \tau} \quad (1.105)$$

The Fourier series coefficients of the periodic pulse train are given by Eq. (1.42b) as

$$V_n = \frac{A\tau}{T_0} \frac{\sin(n\pi\tau/T_0)}{n\pi\tau/T_0} \quad (1.106)$$

The fundamental frequency in the Fourier series is $f_0 = 1/T_0$. We shall set $f_0 \equiv \Delta f$ in order to emphasize that $f_0 \equiv \Delta f$ is the frequency interval between spectral lines in the Fourier series. Hence, since $1/T_0 = \Delta f$, we may rewrite Eq. (1.106) as

$$V_n = A\tau \frac{\sin(\pi n \Delta f \tau)}{\pi n \Delta f \tau} \Delta f \quad (1.107)$$

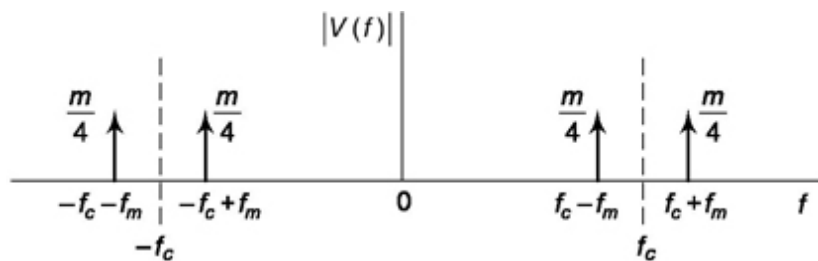


Fig. 1.23 The two-sided amplitude spectrum of the product waveform $v(t) = m \cos 2p f_c t$.

In the limit, as $T_0 \rightarrow 0$, $Af \rightarrow 0$. We then may replace Af by df and replace n Af by a continuous variable f . Equation (1.107) then becomes

$$\lim_{\Delta f \rightarrow 0} V_n = A\tau \frac{\sin \pi ft}{\pi ft} \quad (1.108)$$

Thus, we confirm our earlier interpretation of $V(f)$ as an *amplitude spectral density*.

Example 1.17

- (a) Find the Fourier transform of $S(t)$, an impulse of unit strength.
- (b) Given a network whose transfer function is $H(f)$. An impulse $S(t)$ is applied at the input. Show that the response $v_o(t) = h(t)$ at the output is the inverse transform of $H(f)$, that is, show that $h(t) = F^{-1}[H(f)]$.

Solution

- (a) The impulse $\delta(t) = 0$ except at $t = 0$ and, further, has the property that

$$\text{Hence, } V(f) = \int_{-\infty}^{\infty} \delta(t) e^{-j2\pi ft} dt = 1 \quad (1.111)$$

Thus the spectral components of $\delta(t)$ extend with uniform amplitude and phase over the entire frequency domain.

- (b) Using the result given in Eq. (1.90), we find that the transform of the output $v_o(t) = h(t)$ is $V_o(f)$ given by

$$V_o(f) = 1 \times H(f) \quad (1.112)$$

since the transform of $\delta(t)$, $F[\delta(t)] = 1$. Hence the inverse transform of $V_o(f)$, which is the function $h(t)$, is also the inverse transform of $H(f)$. Specifically, for an impulse input, the output is

We may use the result given in Eq. (1.113) to arrive at a useful representation of $d(t)$ itself. If $H(f) = 1$, then the response $h(t)$ to an impulse $d(t)$ is the impulse itself, Hence, setting $H(f) = 1$ in Eq. (1.113), we find

$$h(t) = \int_{-\infty}^{\infty} H(f) e^{j2\pi ft} df \quad (1.113)$$

$$\delta(t) = \int_{-\infty}^{\infty} e^{j2\pi ft} df = \int_{-\infty}^{\infty} e^{-j2\pi ft} df \quad (1.114)$$

1.4.1 useful Fourier transform properties

Here, we present some of the useful properties of Fourier transform. We'll discuss convolution, correlation and Parseval's theorem related properties in the following subsections.

We use notation $v(t)$ ($V(f)$) as Fourier transform pairs to describe the properties. The logic behind writing these relations in most of the cases follows a similar procedure adopted in deriving properties of Fourier series and hence not repeated. The conclusions are also similar, e.g. compressing the signal in time domain expands it in frequency domain.

Time Shift

$$v(t + \tau) \leftrightarrow V(f) e^{j2\pi f\tau} \quad (1.115)$$

Time Inversion

$$v(-t) \leftrightarrow V(-f) \quad (1.116)$$

Time Scaling

$$v(at) \leftrightarrow \frac{1}{|a|} V\left(\frac{f}{a}\right) \quad (1.117)$$

Derivative with Time

$$\frac{dv}{dt} \leftrightarrow j2\pi f V(f) \quad (1.118)$$

Integration

$$\int_0^t v(\tau) d\tau \leftrightarrow \frac{1}{j2\pi f} V(f) + \pi V(0) \delta(f) \quad (1.119)$$

where, $V(0) = \int_{-\infty}^{\infty} v(\tau) d\tau$, i.e. area under $v(t)$. This for zero dc signal is zero and the 2nd term on the right-hand side of above equation vanishes.

Frequency Shifting

$$v(t) e^{j2\pi f_c t} \leftrightarrow V(f - f_c) \quad (1.120)$$

The above is a useful property in communication and we discussed it in Example 1.14 in multiplying a signal in time domain with $\cos 2\pi f_c t$ which can be written as

$$\frac{1}{2} (e^{j2\pi f_c t} + e^{-j2\pi f_c t})$$

Derivative with Frequency

$$-j2\pi t v(t) \leftrightarrow dV(f)/df \quad (1.121)$$

The above is similar to derivation of Eq. (1.116) that arrives from differentiation of both sides w.r.t. f of basic definition given in Eq. (1.86).

Duality or Symmetry

$$V(t) \leftrightarrow v(-f) \text{ or } V(t) \leftrightarrow 2\pi v(-\omega) \quad (1.122)$$

The above comes from similarity in the Fourier and inverse Fourier transform, the difference being in sign of quantity under exponential and also in proportionality constant in the angular frequency relation.

Linearity

$$av_1(t) + bv_2(t) \leftrightarrow aV_1(f) + bV_2(f) \quad (1.123)$$

where,

$$v_1(t) \leftrightarrow V_1(f) \text{ and } v_2(t) \leftrightarrow V_2(f)$$

1.4.2 Convolution

Suppose that $v_x(t)$ has the Fourier transform $V_1(f)$ and $v_2(t)$ has the transform $V_2(f)$. What then is the waveform $v(t)$ whose transform is the product $V_1(f)V_2(f)$? This question arises frequently in spectral analysis and is answered by the *convolution theorem*, which says that

$$v(t) = \int_{-\infty}^{\infty} v_1(\tau)v_2(t - \tau) d\tau \quad (1.124)$$

or equivalently

$$v(t) = \int_{-\infty}^{\infty} v_2(\tau)v_1(t - \tau) d\tau \quad (1.125)$$

The integrals in Eq. (1.124) or (1.125) are called *convolution integrals*, and the process of evaluating $v(t)$ through these integrals is referred to as *taking the convolution* of the functions $v_1(t)$ and $v_2(t)$.

To prove the theorem, we begin by writing

$$v(t) = \mathcal{F}^{-1}[V_1(f)V_2(f)] \quad (1.126a)$$

$$= \frac{1}{2\pi} \int_{-\infty}^{\infty} V_1(f)V_2(f)e^{j\omega t} d\omega \quad (1.126b)$$

By definition, we have

$$V_1(f) = \int_{-\infty}^{\infty} v_1(\tau)e^{-j\omega\tau} d\tau \quad (1.127)$$

Substituting $V_1(f)$ as given by Eq. (1.127) into the integrand of Eq. (1.126b), we have

$$v(t) = \frac{1}{2\pi} \int_{-\infty}^{\infty} \int_{-\infty}^{\infty} v_1(\tau)e^{-j\omega\tau} d\tau V_2(f)e^{j\omega t} d\omega \quad (1.128)$$

Interchanging the order of integration, we find

$$v(t) = \int_{-\infty}^{\infty} v_1(\tau) \left[\frac{1}{2\pi} \int_{-\infty}^{\infty} V_2(f)e^{j\omega(t-\tau)} d\omega \right] d\tau \quad (1.129)$$

We recognize that the expression in brackets in Eq. (1.129) is $v_2(t - \tau)$, so that finally

$$v(t) = \int_{-\infty}^{\infty} v_1(\tau)v_2(t - \tau) d\tau \quad (1.130)$$

Examples of the use of the convolution integral are given in Probs. 1.30 and 1.31. These problems will also serve to recall to the reader the relevance of the term *convolution*.

A special case of the convolution theorem of great utility is arrived at through the following considerations. Suppose a waveform $v_i(t)$ whose transform is $V_i(f)$ is applied to a linear network with transfer function $H(f)$. The transform of the output waveform is $V_o(f)H(f)$. What then is the waveform of $v_o(t)$?

In Eq. (1.130) we identify $v_1(\tau)$ with $v_i(\tau)$ and $v_2(t)$ with the inverse transform of $H(f)$. But we have seen [in Eq. (1.113)] that the inverse transform of $H(f)$ is $h(t)$, the impulse response of the network. Hence Eq. (1.130) becomes

$$v_o(t) = \int_{-\infty}^{\infty} v_i(\tau)h(t - \tau) d\tau \quad (1.131)$$

in which the output $v_o(t)$ is expressed in terms of the input $v_i(t)$ and the impulse response of the network. Note that, from duality theorem we can

arrive at another useful relationship. It is easy to prove the following method adopted before that multiplication in time domain is equivalent to convolution in frequency domain. In analog or digital modulation, often a message signal is multiplied with a high-frequency carrier signal and then sent. One can find the spectrum of this modulation signal using this convolution property.

If $v(f) = v_1(t)v_2(t)$ then $V(f) = V_1(f) \otimes V_2(f)$ or $V(f) = V_2(f) \otimes V_1(f)$

In integral form $V(f) = \int_{-\infty}^{+\infty} V_1(f)V_2(f - \lambda) d\lambda$ or $V(f) = \int_{-\infty}^{+\infty} V_2(f)V_1(f - \lambda) d\lambda$

1.4.3 parseval's theorem

We saw that for periodic waveforms we may express the normalized power as a summation of powers due to individual spectral components. We also found for periodic signals that it was appropriate to introduce the concept of *power spectral density*. Let us keep in mind that we may make the transition from the periodic to the nonperiodic waveform by allowing the period of the periodic waveform to approach infinity. A nonperiodic waveform, so generated, has a finite *normalized energy*, while the normalized power approaches zero. We may therefore expect that for a nonperiodic waveform, the energy may be written as a continuous summation (integral) of energies due to individual spectral components in a continuous distribution. Similarly we should expect that with such nonperiodic waveforms it should be possible to introduce an *energy spectral density*.

The normalized energy of a periodic waveform $v(t)$ in a period T_n is

$$E = \int_{-T_0/2}^{T_0/2} [v(t)]^2 dt \quad (1.132)$$

From Eq. (1.67) we may write E as

$$E = T_0 S = T_0 \sum_{n=-\infty}^{n=+\infty} V_n V_n^* \quad (1.133)$$

Again, as in the illustrative Example 1.95, we let $\Delta f \leq 1/T_0 = f_0$, where f_0 is the fundamental frequency, that is, Δf is the spacing between harmonics. Then we have

$$V_n V_n^* = \frac{V_n}{\Delta f} \frac{V_n^*}{\Delta f} (\Delta f)^2 \quad (1.134)$$

and Eq. (1.133) may be written

$$E = \sum_{n=-\infty}^{\infty} \frac{V_n}{\Delta f} \frac{V_n^*}{\Delta f} \Delta f \quad (1.135)$$

In the limit, as $\Delta f \rightarrow 0$, we replace Δf by df , we replace $V_n/\Delta f$ by the transform $V(f)$ [see Eq. (1.109)], and the summation by an integral. Equation (1.135) then becomes

$$E = \int_{-\infty}^{\infty} V(f) V^*(f) df = \int_{-\infty}^{\infty} |V(f)|^2 df = \int_{-\infty}^{\infty} [v(t)]^2 dt \quad (1.136)$$

Introduction: Signal and Spectra 45

This equation expresses *Parseval's theorem*. Parseval's theorem is the extension to the nonperiodic case of Eq. (1.67) which applies for periodic waveforms. Both results simply express the fact that the power (periodic case) or the energy (nonperiodic case) may be written as the superposition of power or energy due to individual spectral components separately. The validity of these results depends on the fact that the spectral components are orthogonal. In the periodic case the spectral components are orthogonal over the interval T_0 . In the nonperiodic case this interval of orthogonality extends over the entire time axis, i.e. from $-'$ to $+'$.

From Eq. (1.136), we find that the *energy density* is $G_E(f)$ given by

$$G_E(f) \equiv \frac{dE}{df} = |V(f)|^2 \quad (1.137)$$

in correspondence with Eq. (1.74), which gives the power spectral density for a periodic waveform.

Parseval's theorem may be derived more formally by a direct application of the convolution theorem and by other methods (see Prob. 1.26).

1.4.4 power and Energy Transfer through a Network

Suppose that a periodic signal $v_i(t)$ is applied to a network of transfer function $H(f)$ which yields an output $v_o(t)$. If $v_i(t)$ is written

$$v_i(t) = \sum_{n=-\infty}^{\infty} V_n e^{j2\pi n f_0 t} \quad (1.138)$$

then

$$v_o(t) = \sum_{n=-\infty}^{\infty} H(n f_0) V_n e^{j2\pi n f_0 t} \quad (1.139)$$

The power of $v_i(t)$ is

$$S_i = \sum_{n=-\infty}^{\infty} |V_n|^2 \quad (1.140)$$

while the power of $v_o(t)$ is

$$S_0 = \sum_{n=-\infty}^{\infty} |H(n f_0)|^2 |V_n|^2 \quad (1.141)$$

Thus, it is seen from Eq. (1.141) that depending on $H(n f_0)$, the power associated with particular spectral components may be increased or decreased. Suppose for example that $H(n f_0) = h$ (a constant) for values of n between $n = i$ and $n = j$, and that $H(n f_0) = 0$ otherwise. Then the power associated with spectral components outside the range $i < |n| < j$ will be *lost*, and the network output waveform will be

$$v_o(t) = \sum_{n=-j}^{-i} h V_n e^{j2\pi n f_0 t} + \sum_{n=i}^j h V_n e^{j2\pi n f_0 t} \quad (1.142)$$

while the power output will be

$$S_0 = \sum_{n=-j}^{-i} h^2 |V_n|^2 + \sum_{n=i}^j h^2 |V_n|^2 = 2 \sum_{n=i}^j h^2 |V_n|^2 \quad (1.143)$$

1.4.5 distortion due to Bandlimiting and Effect on digital pulse transmission

Rather generally, waveforms, periodic or nonperiodic, have spectral components which extend, at least in principle, to infinite frequency. Periodic waveforms may or may not have a dc component. Nonperiodic waveforms usually have spectral components extending to zero or near-zero frequency. Therefore, again, at least in principle, if an arbitrary waveform is to pass through a network without changing its shape, the transfer function of the network must not discriminate among spectral components. All spectral amplitudes must be increased or decreased by the same amount, and

each spectral component must be delayed equally. A network which introduces no distortion, therefore, has the transfer function

$$H(f) = h_0 e^{-j\theta f T_D} \quad (1.146)$$

in which h_0 is a constant and T_D is the delay time introduced by the network. An example of a network which produces no distortion is a length of transmission line of uniform cross section, having no losses and properly terminated.

A signal may have spectral components which extend in the upper-frequency direction only up to a maximum frequency f_M . Such a signal is described as being *bandlimited* (at the high-frequency end) to f_M . If such a signal is passed through a network (filter) for which $H(f) = 1$ for $f < f_M$, the signal will be transmitted without distortion. Suppose, however, the signal is not precisely bandlimited to f_M but nonetheless, a very large part of its power or energy lies in spectral components below f_M . For example, suppose 99 percent of the power or energy lies below f_M . Then we may reasonably expect that the filter will introduce no serious distortion. Similarly, a signal may be bandlimited at the low-frequency end to a frequency f_L . And, again, if the signal is not precisely so bandlimited, but if a negligible fraction of the signal energy or power lies below f_L , a filter with low frequency cutoff at f_L will produce negligible distortion.

We shall frequently have occasion to deal with waveforms which are not of themselves bandlim-ited but are passed through filters, introducing bandlimiting and hence producing distortion. The effect of such bandlimiting may be seen in a general sort of way by considering the response of the networks shown in Fig. 1.24 to a step function. We select the step function because it represents a combination of the fastest possible rate of change of voltage (rise time equal to zero) and the slowest possible (zero) rate of change of voltage after the abrupt rise. We select the circuit of Fig. 1.24a because it produces bandlimiting (albeit not abrupt) at the high-frequency end, while the circuit in Fig. 1.24b produces bandlimiting at the low-frequency end.

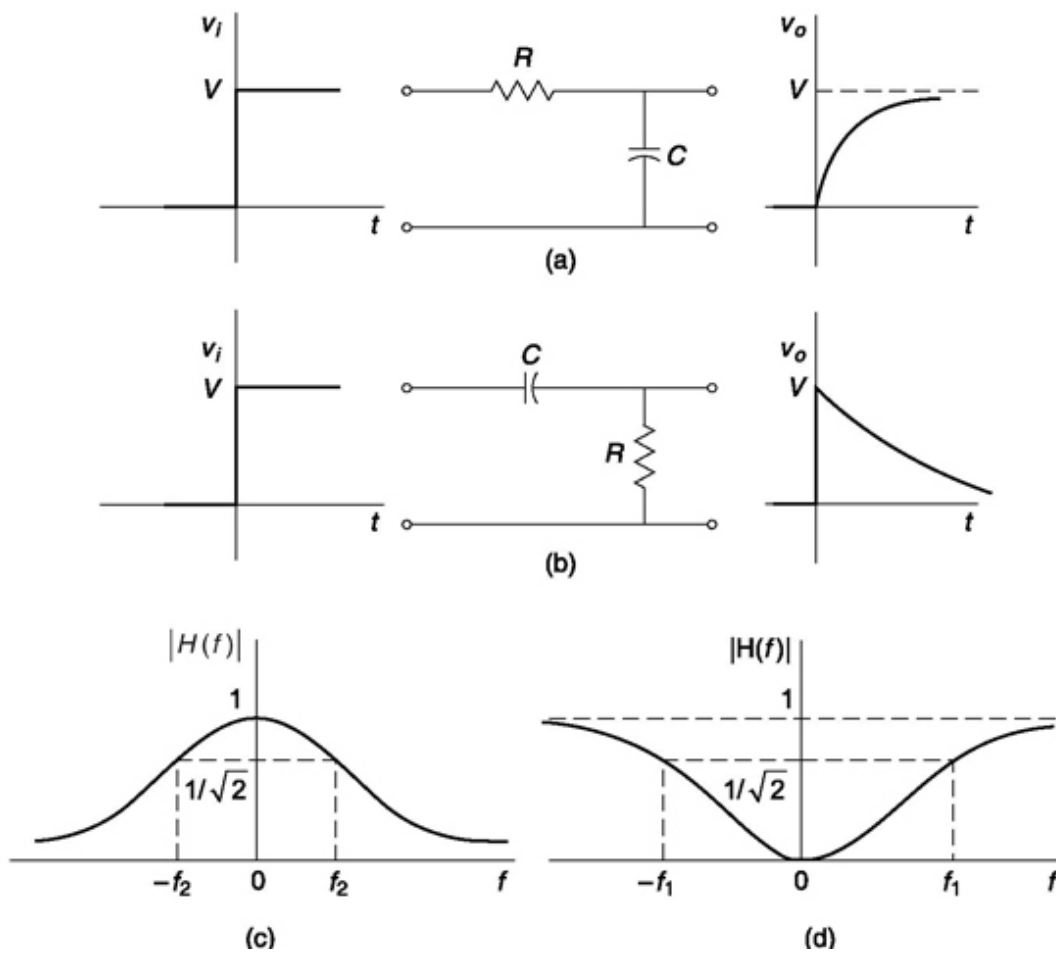


Fig. 1.24 (a) A low-pass RC circuit. (b) A high-pass RC circuit. (c) $|H(f)|$ for the circuit in (a). (d) $|H(f)|$ for the circuit in (b).

The low-pass RC circuit of Fig. 1.24a has a transfer function

$$H(f) = \frac{1}{1 + jf/f_2} \quad (1.147)$$

where $f_2 = 1/(2\pi RC)$. The magnitude of $H(f)$ is plotted in Fig. 1.24c. At the frequency $f = f_2$, $|H(f)|$ has fallen to the value $1/\sqrt{2} = 0.707$, corresponding to a reduction of 3 dB from its value at $f = 0$. The frequency f_2 is called the 3 dB frequency of the network and is sometimes referred to as the *passband* of the network. For a step input of amplitude V_0 the output is

$$v_o(t) = V_0(1 - e^{-t/RC}) = V_0(1 - e^{-2\pi f_2 t}) \quad (1.148)$$

The essential distortion which has been introduced by the frequency discrimination of the network is that the output rises gradually rather than abruptly as does the input. We thus associate with the output waveform a *rise time*. This rise time may be defined in a variety of ways. One definition commonly employed is that the rise time is the time required for the output $v_o(t)$ to change from $0.1V_0$ to $0.9V_0$. It may be verified from Eq. (1.148) that this rise time t_r is related to f_2 by

$$t_r f_2 = 0.35 \quad (1.149)$$

This rise time is a measure of the promptness with which the output responds to a voltage change at the input. A long rise time indicates a sluggish response. We note then from Eq. (1.149) that the more the upper-frequency range of the transfer function is restricted, the longer the rise time becomes.

The principle enunciated in Eq. (1.149) is of general validity. Even for filter circuits of much greater complexity and sharper cutoff than the simple RC circuit of Fig. 1.24a, the product $t_r f_2$ remains approximately constant. By way of example, suppose we postulate an ideal (unrealizable) filter. Such a filter has an arbitrarily sharp cutoff. That is, $H(f) = 1$ for $0 < f < f_M$, and $H(f) = 0$ for $f > f_M$. Then in this case it turns out that $t_r f_2 = 0.44$. On the other hand, Eq. (1.149) will often be encountered in texts and in literature with a rather different constant. For example, the result for the ideal filter is often given as $t_r f_2 = 1$. These differences result from different definitions of the rise time.

If the input to the RC low-pass filter is a pulse, then there will be a rise time associated with the leading and trailing edges of the pulse. Let the pulse duration be t . Then as a rule of thumb it is generally considered that to preserve the waveshape of the pulse with reasonable fidelity, it is necessary that the bandwidth f_2 be at least large enough to satisfy the condition $f_2 t = 1$. For combining this condition with Eq. (1.149), we find $t_r = 0.351$. In this case, with the rise time about one-third the pulse duration, the output pulse waveform has the form shown in Fig. 1.25a.

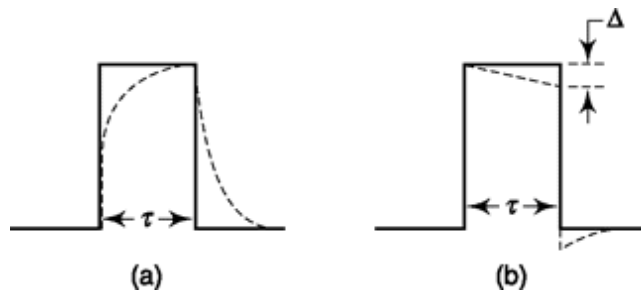


Fig. 1.25 (a) A rectangular pulse (solid) and the response (dashed) of a low-pass RC circuit. The rise time $t_r = 0.35T$. (b) The response of a high-pass RC circuit for $f_1t = 0.02$.

The high-pass RC circuit of Fig. 1.246 has a transfer function

$$H(f) = \frac{1}{1 - jf_1/f} \quad (1.150)$$

where

$$f_1 = \frac{1}{2\pi RC} \quad (1.151)$$

The magnitude of $H(f)$ is plotted in Fig. 1.24d. The frequency f is the 3dB frequency of the network and is generally described as the low-frequency cutoff of the network. For a step input of amplitude V_0 , the output is

$$v_o(t) = V_0 e^{-t/RC} = V_0 e^{-2\pi f_1 t} \quad (1.152)$$

The essential distortion introduced by the frequency discrimination of this network is that the output does not sustain a constant voltage level when the input is constant. Instead, the output begins immediately to decay towards zero, which is its asymptotic limit. From Eq. (1.152), we have

$$\frac{1}{V_o} \frac{dv_o}{dt} = -\frac{1}{RC} = -2\pi f_1 \quad (1.153)$$

Thus the low-frequency cutoff f_1 alone determines the percentage drop in voltage per unit time. Again the importance of Eq. (1.153) is that, at least as a reasonable approximation, it applies to high-pass networks quite generally, even when the network is very much more complicated than the simple RC circuit.

If the input to the RC high-pass circuit is a pulse of duration t , then the output has the waveshape shown in Fig. 1.25b. The output exhibits a tilt and an undershoot. As a rule of thumb, we may assume that the pulse is reasonably faithfully reproduced if the tilt A is no more than $0.1 V_0$. Correspondingly, the condition requires that f_1 be no higher than given by the condition

fit = 0.02 (1.154)

1.4.6 Autocorrelation of a Periodic Waveform

When the function is periodic, we may write

$$v(t) = \sum_{n=-\infty}^{\infty} V_n e^{j2\pi nt/T_0} \quad (1.155)$$

and, using the correlation integral in the form of Eq. (1.12), we have

$$R(\tau) = \frac{1}{T_0} \int_{-T_0/2}^{T_0/2} \left(\sum_{m=-\infty}^{\infty} V_m e^{j2\pi mt/T_0} \right) \left(\sum_{n=-\infty}^{\infty} V_n e^{j2\pi n(t+\tau)/T_0} \right) dt \quad (1.156)$$

The order of integration and summation may be interchanged in Eq. (1.156). If we do so, we shall be left with a double summation over m and n of terms $I_{m,n}$ given by

$$I_{m,n} = \frac{1}{T_0} e^{j2\pi nt/T_0} \int_{-T_0/2}^{T_0/2} V_m V_n e^{j2\pi(m+n)t/T_0} dt \quad (1.157a)$$

$$= V_m V_n e^{j2\pi n\tau/T_0} \frac{[\sin \pi(m+n)]}{\pi(m+n)} \quad (1.157b)$$

Since m and n are integers, we see from Eq. (1.157b) that $I_{m,n} = 0$ except when $m = -n$ or $m + n = 0$. To evaluate $I_{m,n}$ in this latter case, we return to Eq. (1.157a) and find

$$I_{m,n} = I_{-n,n} = V_m V_{-n} e^{j2\pi n\tau/T_0} \quad (1.158)$$

Finally, then,

$$R(\tau) = \sum_{n=-\infty}^{\infty} V_n V_{-n} e^{j2\pi n\tau/T_0} = \sum_{n=-\infty}^{\infty} |V_n|^2 e^{j2\pi n\tau/T_0} \quad (1.159a)$$

$$= |V_0|^2 + 2 \sum_{n=1}^{\infty} |V_n|^2 \cos 2\pi n \frac{\tau}{T_0} \quad (1.159b)$$

We note from Eq. (1.159b) that $R(\tau) = R(-\tau)$ as anticipated, and we note as well that for this case of a periodic waveform the correlation $R(\tau)$ is also periodic with the same fundamental period T_0 .

We shall now relate the correlation function $R(\tau)$ of a periodic waveform to its power spectral density. For this purpose we compute the Fourier transform of $R(\tau)$. We find, using $R(\tau)$ as in Eq. (1.159a), that

$$\mathcal{F}[R(\tau)] = \int_{-\infty}^{\infty} \left(\sum_{n=-\infty}^{\infty} |V_n|^2 e^{j2\pi n\tau/T_0} \right) e^{-j2\pi f\tau} d\tau \quad (1.160)$$

Interchanging the order of integration and summation yields

$$\mathcal{F}[R(\tau)] = \sum_{n=-\infty}^{\infty} |V_n|^2 \int_{-\infty}^{\infty} e^{-j2\pi(f-n/T_0)\tau} d\tau \quad (1.161)$$

Using Eq. (1.114), we may write Eq. (1.161) as

$$\mathcal{F}[R(\tau)] = \sum_{n=-\infty}^{\infty} |V_n|^2 \delta\left(f - \frac{n}{T_0}\right) \quad (1.162)$$

Comparing Eq. (1.162) with Eq. (1.74), we have the interesting result that for a periodic waveform

$$G(f) = \mathcal{F}[R(\tau)] \quad (1.163)$$

and, of course, conversely

$$R(\tau) = \mathcal{F}^{-1}[G(f)] \quad (1.164)$$

Expressed in words, we have the following: *The power spectral density and the correlation function of a periodic waveform are a Fourier transform pair.*

1.4.7 Autocorrelation of a Nonperiodic waveform of Finite Energy

For pulse-type waveforms of finite energy, there is a relationship between the correlation function of Eq. (1.19) and the energy spectral density which corresponds to the relationship given in Eq. (1.163) for the periodic waveform. This relationship is that the correlation function $R(t)$ and the *energy* spectral density are a Fourier transform pair. This result is established as follows.

We use the convolution theorem. We combine Eqs (1.124) and (1.126) for the case where the waveforms $v_1(t)$ and $v_2(t)$ are the same waveforms, that is, $v_1(t) = v_2(t) = v(t)$, and get

$$\mathcal{F}^{-1}[V(f)V(f)] = \int_{-\infty}^{\infty} v(\tau)v(t-\tau) d\tau \quad (1.165)$$

Since $V(-f) = V^*(f) = \mathcal{F}[v(-t)]$, Eq. (1.165) may be written

$$\mathcal{F}^{-1}[V(f)V^*(f)] = \mathcal{F}^{-1}[|V(f)|^2] = \int_{-\infty}^{\infty} v(\tau)v(\tau-t) d\tau \quad (1.166)$$

The integral in Eq. (1.166) is a function of t , and hence this equation expresses $\mathbf{F}^{-1}[V(f)V^*(f)]$ as a function of t . If we want to express $\mathbf{F}^{-1}[V(f)V^*(f)]$ as a function of t without changing the form of the function, we need but to interchange t and τ . We then have

$$\mathcal{F}^{-1}[V(f)V^*(f)] = \int_{-\infty}^{\infty} v(t)v(t-\tau) dt \quad (1.167)$$

The integral in Eq. (1.167) is precisely $R(\tau)$, and thus

$$\mathcal{F}[R(\tau)] = V(f)V^*(f) = |V(f)|^2 \quad (1.168)$$

which verifies that $R(\tau)$ and the energy spectral density $|V(f)|^2$ are Fourier transform pairs.

1.4.8 autocorrelation of other waveforms

In the preceding sections we discussed the relationship between the autocorrelation function and power or energy spectral density of *deterministic* waveforms. We use the term “deterministic” to indicate that at least, in principle, it is possible to write a function which specifies the value of the function at all times. For such deterministic waveforms, the availability of an autocorrelation function is of no particularly great value. The autocorrelation function does not include within itself complete information about the function. Thus we note that the autocorrelation function is related only to the amplitudes and not to the phases of the spectral components of the waveform. The waveform cannot be reconstructed from a knowledge of the autocorrelation functions. Any characteristic of a deterministic waveform which may be calculated with the aid of the autocorrelation function may be calculated by direct means at least as conveniently.

On the other hand, in the study of communication systems we encounter waveforms which are not deterministic but are instead random and unpredictable in nature. There we shall find that for such random waveforms no explicit function of time can be written. The waveforms must be described in statistical and probabilistic terms. It is in connection with such waveforms that the concepts of correlation and autocorrelation find their true usefulness. Specifically, it turns out that even for such random waveforms, the autocorrelation function and power spectral density are a Fourier transform pair. The proof³ that such is the case is formidable and will not be undertaken here.

Example 1.18

Find Fourier transform of the signal $v(t) = e^{-at}u(t)$ where $u(t)$ is unit step function.

Solution

From definition

$$e^{-at} u(t) \leftrightarrow \frac{1}{a + j2\pi f}$$

Using differentiation with frequency property (Eq. 1.121)

$$\begin{aligned}-j2\pi t e^{-at} u(t) &\leftrightarrow d\left(\frac{1}{a + j2\pi f}\right)/df = \frac{-j2\pi}{(a + j2\pi f)^2} \\ te^{-at} u(t) &\leftrightarrow \frac{1}{(a + j2\pi f)^2}\end{aligned}$$

Example 1.19

Find Fourier transform of the signal $v(t) = te^{-at} u(t)$ where $u(t)$ is the unit step function.

Solution

In Example 1.17, we have seen,

Solution

The signal $v(t)$ can be written as

$$v(t) = e^{-at}u(t) + e^{at}u(-t)$$

Fourier transform of first term on right-hand side of the above equation has already been calculated in Example 1.17 as,

$$e^{-at}u(t) \leftrightarrow \frac{1}{a + j2\pi f}$$

Note that, the 2nd term is time reversed version of first term. Using time inversion property (Eq. 1.116) and above result we can write

$$e^{at}u(-t) \leftrightarrow \frac{1}{a + j2\pi(-f)} = \frac{1}{a - j2\pi f}$$

Combining, (from linearity property)

$$\begin{aligned}V(f) &= \frac{1}{a + j2\pi f} + \frac{1}{a - j2\pi f} \\ &= \frac{2a}{a^2 + 4\pi^2 f^2}\end{aligned}$$

Example 1.20

Find Fourier transform of the signal $v(t) = e^{-alt}$ Solution

The signal $v(t)$ can be written as $v(t) = e^{-at}u(t) + e^{at}u(-t)$

Fourier transform of first term on right-hand side of the above equation has already been calculated in Example 1.17 as,

$$e^{-at}u(t) \leftrightarrow \frac{1}{a + j2\pi f}$$

Note that, the 2nd term is time reversed version of first term. Using time inversion property (Eq. 1.116) and above result we can write

$$e^{at}u(-t) \leftrightarrow \frac{1}{a + j2\pi(-f)} = \frac{1}{a - j2\pi f}$$

Combining, (from linearity property)

$$\begin{aligned} V(f) &= \frac{1}{a + j2\pi f} + \frac{1}{a - j2\pi f} \\ &= \frac{2a}{a^2 + 4\pi^2 f^2} \end{aligned}$$

Example 1.21

- (a) Find Fourier transform of function $\text{sgn}(t)$ [Fig. 1.26a] defined as follows
 $\text{sgn}(t) = u(t) - u(-t)$
- (b) Find $h(t)$ where $H(\omega) = -j \text{sgn}(\omega)$ [Fig. 1.26b]

Solution

- (a) We can write, $\text{sgn}(t) = \lim_{a \rightarrow 0} [e^{-at}u(t) - e^{at}u(-t)]$
 From Example 1.19 and linearity property

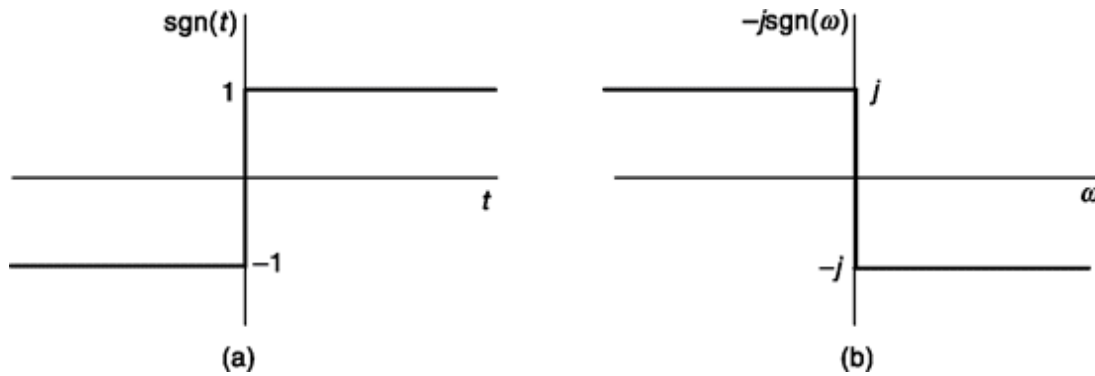


Fig. 1.26 (a) $\text{sgn}(t)$ vs. t and (b) $-j \text{sgn}(\omega)$ vs. ω .

$$\begin{aligned}
F[\text{sgn}(t)] &= \lim_{a \rightarrow 0} \left[\frac{1}{a + j2\pi f} - \frac{1}{a - j2\pi f} \right] \\
&= \lim_{a \rightarrow 0} \left[\frac{-j4\pi f}{a^2 + 4\pi^2 f^2} \right] \\
&= \frac{1}{j\pi f}
\end{aligned}$$

(b) We can write, in terms of angular frequency

$$F[\text{sgn}(t)] = \frac{2}{j(2\pi f)} = \frac{2}{j\omega}$$

Now,

$$\begin{aligned}
h(t) &= F^{-1}[-j \text{sgn}(\omega)] = j F^{-1}[\text{sgn}(-\omega)] = j \cdot \\
&\quad \frac{2}{j2\pi t} \quad [\text{Duality property (Eq. 1.122)}] = \frac{1}{\pi t}
\end{aligned}$$

A filter that has a frequency response such as this is known as *quadrature filter*.

$$H_{BPF}(f) = H_{LPF}(f + f_c) + H_{LPF}(f - f_c)$$

Define, $h_{LPF}(t) = F^{-1}[H_{LPF}(f)]$ and

$$h_{BPF}(t) = F^{-1}[H_{BPF}(f)]$$

$$\begin{aligned}
\text{Then, } h_{BPF}(t) &= F^{-1}[H_{LPF}(f + f_c)] + F^{-1}[H_{LPF}(f - f_c)] \\
&= h_{LPF}(t) e^{j2\pi f_c t} + h_{LPF}(t) e^{-j2\pi f_c t} \\
&\quad [\text{from Eq. 1.120}] \\
&= 2 h_{LPF}(t) \cos(2\pi f_c t) \\
&\quad [\text{as } e^{jx} = \cos x + j\sin x]
\end{aligned}$$

Example 1.22

Find $W(f)$, Fourier transform of output $w(t)$ which is produced when signal $v(t) = e^{-at}u(t)$ passes through a quadrature mirror filter having impulse response

Solution

From convolution relation,

$$w(t) = \int_{-\infty}^{\infty} v(\tau)h(t - \tau) d\tau$$

$$\begin{aligned}
\text{And } W(f) &= V(f)H(f) \\
&\quad [\text{From convolution property}]
\end{aligned}$$

$$\text{Now, } V(f) = \frac{1}{a + j2\pi f} \quad [\text{From Example 1.17}]$$

From, Example 1.20, we have seen that

$$\begin{aligned} H(f) &= F\left(\frac{1}{\pi t}\right) = -j \operatorname{sgn}(\omega) \\ &= -j \operatorname{sgn}(2\pi\omega f) \end{aligned}$$

As the factor 2π only scales frequency axis, $H(f) = -j \operatorname{sgn}(f)$

$$\text{Hence, } W(f) = \frac{-j \operatorname{sgn}(f)}{a + i 2\pi f}$$

$$h(t) = Pt. p t$$

Note that, a signal that passes through a quadrature mirror filter is said to have undergone *Hilbert transform*. This gives a phase shift of $-p/2$ to the input signal equivalent to a phase delay of $-p/2$ to all the frequency components. This is a useful feature which will be used later in this text.

Example 1.23

An ideal low pass filter (LPF) of cut-off frequency $B/2$ is shown in Fig. 1.27a. Show one technique to get a bandpass (BPF) filter of bandwidth B centred at f_c from it.

Solution

The frequency response the bandpass filter is shown in Fig. 1.276. We can write,

$$H_{BPF}(f) = H_{LPF}(f + f_c) + H_{LPF}(f - f_c)$$

Define, $h_{LPF}(t) = F^{-1}[H_{LPF}(f)]$ and

$$h_{BPF}(t) = F^{-1}[H_{BPF}(f)]$$

Then, $h_{BPF}(t) = F^{-1}[H_{LPF}(f + f_c)] + F^{-1}[H_{LPF}(f - f_c)]$

$$= h_{LPF}(t) e^{j 2\pi f_c t} + h_{LPF}(t) e^{j 2\pi f_c t}$$

[from Eq. 1.120]

$$= 2 h_{LPF}(t) \cos(2\pi f_c t)$$

[as $e^{jx} = \cos x + j\sin x$]

For linear time invariant system,

$$\begin{aligned} h_{BPF}(t - \tau) &= 2 h_{LPF}(t - \tau) \cos(2\pi f_c(t - \tau)) \\ &= 2 h_{LPF}(t - \tau) [\cos(2\pi f_c t) \cos(2\pi f_c \tau) \\ &\quad + \sin(2\pi f_c t) \sin(2\pi f_c \tau)] \\ &= [2 \cos(2\pi f_c \tau) h_{LPF}(t - \tau)] \cos(2\pi f_c t) \\ &\quad + [2 \sin(2\pi f_c \tau) h_{LPF}(t - \tau)] \sin(2\pi f_c t) \end{aligned}$$

$$= [\{2 \cos(2\pi f_c t) \cdot \delta(t - \tau)\}$$

$$h_{LPF}(t - \tau)] \cos(2\pi f_c t)$$

$$+ [\{2 \sin(2\pi f_c t) \cdot \delta(t - \tau)\}$$

$$h_{LPF}(t - \tau)] \sin(2\pi f_c t)$$

Thus, if $8(t - t)$ is input to the system drawn from above equation (Fig. 1.27c, for $\theta = 0$) then its output is $h_{BPF}(t - t)$. From time invariance property, if $8(t)$ is input, output will be $h_{BPF}(t)$. Hence, Fig. 1.27c shows BPF design from LPF. Note that, if all the multiplying cosine or sine signals have same phase difference (say, 0), then result does not change.

Note that, for any arbitrary signal $v(t)$, fed as input to circuit in Fig. 1.27bc, the output of LPF1 is usually represented by $v_c(t)$ and is called in phase component and the output of LPF2 is represented by $v_s(t)$ and is called in quadrature component. Thus, a bandpass or band-limited signal can in general be represented as

$$v(t) = v_c(t) \cos(2\pi f_c t) + v_s(t) \sin(2\pi f_c t) \quad (1.169)$$

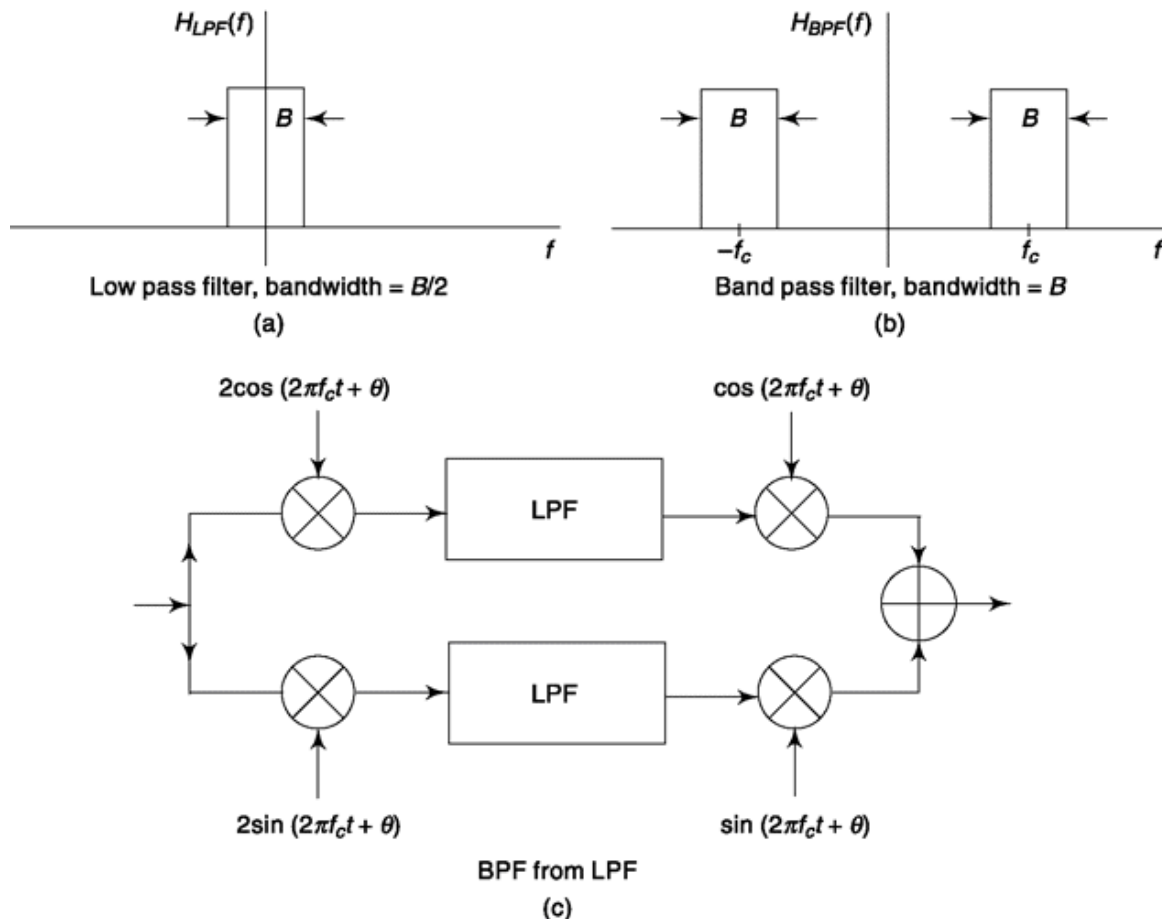


Fig. 1.27 (a) An ideal LPF, (b) An ideal BPF, (c) BPF from LPF.

Ideal and Practical Filter The frequency responses shown for LPF and BPF are ideal, i.e. it does not pass any frequency outside the passband. Such a

filter is not practically realizable. Consider the case of ideal LPF shown in Fig. 1.27a. Its inverse Fourier transform will be a sinc function from Example 1.16 which extends up to $t = -\infty$. Clearly, that cannot be impulse response $h(t)$ of a practical system which is causal. Depending on how much delay is tolerable, $h(t)$ is shifted to right as $h(t - t_0)$ which is equivalent to have a frequency response $H(f) e^{-j2\pi f t_0}$ from time shift property and then truncate what is to left of $t = 0$. The sufficient and necessary condition for realizable filter $f \int_{-\infty}^{\infty} |H(f)|^2 df < \infty$ which does not allow $|H(f)| = 0$ over any finite frequency band. In short, if $H(f)$ is desired frequency response, then for a practical realizable filter $h(t)$ will be only $t > 0$ part of inverse Fourier transform of $H(f) e^{-j2\pi f t_0}$ where t_0 is allowable delay. A practical filter transfer function $H(f)$ will be Fourier transform of this delayed, truncated impulse response.

SELF-TEST QUESTION

13. Can DFT be considered as a digital representation of frequency information?
14. In frequency domain, what is equivalent to convolution in time domain?
15. What is the inference of Parseval's theorem?
16. Are autocorrelation function and energy (aperiodic signal)/power (periodic signal) spectral density Fourier transform pair?

1.5 ORTHOGONAL REPRESENTATION OF A SIGNAL

Orthogonal representation of signal is a useful technique to represent any arbitrary signal in terms of orthogonal basis functions. It also leads to vector representation of signal, especially in digital communication, that simplifies estimation problems to be discussed later in this book. Here, first we discuss expansions in terms of orthogonal functions.

Let us consider a set of functions $g_1(x), g_2(x), \dots, g_n(x) \dots$, defined over the interval $x_1 < x < x_2$ and which are related to one another in the very special way that any two different ones of the set satisfy the condition

$$\int_{x_1}^{x_2} g_i(x)g_j(x) dx = 0 \quad (1.170)$$

That is, when we multiply two different functions and then integrate over the interval from x_1 to x_2 the result is zero. A set of functions which has this property is described as being *orthogonal over the interval from x_x to x_2* . The term “orthogonal” is employed here in correspondence to a similar situation which is encountered in dealing with vectors. The *scalar* product of two vectors \mathbf{V}_i and \mathbf{V}_j (also referred to as the *dot* product or as the *inner* product) is a scalar quantity V_H defined as

$$V_{ij} = |\mathbf{V}_i||\mathbf{V}_j| \cos (\mathbf{V}_i, \mathbf{V}_j) = V_{ji} \quad (1.171)$$

In Eq. (1.171), $|\mathbf{V}_j|$ and $|\mathbf{V}_j|$ are the magnitudes of the respective vectors and $\cos (\mathbf{V}_i, \mathbf{V}_j)$ is the cosine of the angle between the vectors. If it should turn out that $V_i = 0$ then (ignoring the trivial cases in which $\mathbf{V}_x = 0$ or $\mathbf{V}_i = 0$) $\cos (\mathbf{V}_i, \mathbf{V}_j)$ must be zero and correspondingly it means that the vectors

\mathbf{V}_i and \mathbf{V}_j are perpendicular (i.e. orthogonal) to one another. Thus vectors whose scalar product is zero are physically orthogonal to one another and, in correspondence, functions whose integrated product, as in Eq. (1.170) is zero are also orthogonal to one another.

Now consider that we have some arbitrary function $f(x)$ and that we are interested in $f(x)$ only in the range from x_1 to x_2 , i.e. in the interval over which the set of functions $g(x)$ are orthogonal. Suppose further that we undertake to write $f(x)$ as a linear sum of the functions $g_n(x)$. That is, we write

$$f(x) = C_1g_1(x) + C_2g_2(x) + \cdots + C_ng_n(x) + \cdots \quad (1.172)$$

in which the C 's are numerical coefficients. Assuming that such an expansion is indeed possible, the orthogonality of the g 's makes it very easy to compute the coefficients C_n . Thus to evaluate C_n we multiply both sides of Eq. (1.172) by $g_n(x)$ and integrate over the interval of orthogonality. We have

$$\begin{aligned} \int_{x_1}^{x_2} f(x)g_n(x) dx &= C_1 \int_{x_1}^{x_2} g_1(x)g_n(x) dx \\ &\quad + C_2 \int_{x_1}^{x_2} g_2(x)g_n(x) dx + \cdots + C_n \int_{x_1}^{x_2} g_n^2(x) dx + \cdots \end{aligned} \quad (1.173)$$

Because of the orthogonality, *all of the terms on the right-hand side of Eq. (1.173) become zero with a single exception* and we are left with

$$\int_{x_1}^{x_2} f(x)g_n(x) dx = C_n \int_{x_1}^{x_2} g_n^2(x) dx \quad (1.174)$$

so that the coefficient that we are evaluating becomes

$$C_n = \frac{\int_{x_1}^{x_2} f(x)g_n(x) dx}{\int_{x_1}^{x_2} g_n^2(x) dx} \quad (1.175)$$

The mechanism by which we use the orthogonality of the functions to “drain” away all the terms except the term that involves the coefficient we are evaluating is often called the “orthogonality sieve.”

Next suppose that each $g_n(x)$ is selected so that the denominator of the right-hand member of Eq. (1.175) (which is a numerical constant) has the value

$$\int_{x_1}^{x_2} g_n^2(x) dx = 1 \quad (1.176)$$

In this case,

$$C_n = \int_{x_1}^{x_2} f(x)g_n(x) dx \quad (1.177)$$

When the orthogonal functions $g_n(x)$ are selected as in (1.176) they are described as being *normalized*. The use of normalized functions has the merit that the C_n 's can then be calculated from Eq. (1.177) and thereby avoids the need to evaluate $\int_{x_1}^{x_2} g_n^2(x) dx$ in each case as called for in Eq. (1.175). A set of functions which is both orthogonal and normalized is called an *orthonormal* set.

1.5.1 Completeness of an Orthogonal set: the Fourier series

Suppose on the one hand we expand a function $f(x)$ in terms of orthogonal functions as

$$f(x) = C_1s_1(x) + C_2s_2(x) + C_3s_3(x) + \cdots \quad (1.178)$$

and on the other hand, we expand it as

$$f(x) = C_1s_1(x) + C_3s_3(x) + \cdots \quad (1.179)$$

That is, in the second case, we have deliberately omitted one term. A moment's review of the procedure, described in the previous section, for evaluating coefficients makes it apparent that all the coefficients C_1 , C_3 , etc., that appear in both expansions will turn out to be *the same*. Hence, if one expansion is correct the other is in error. We might be suspicious of the expansion of Eq. (1.179) on the grounds that a term is missing. But then how do we know that a term is not missing in the expansion of Eq. (1.178)? The point is that simply having a set of orthogonal functions and having a procedure for evaluating coefficients does not guarantee that the series so developed can represent an arbitrary function. Such can well be the case even when the orthogonal set consists of an infinite number of independent functions. When, however, the orthogonal set does indeed include all the functions necessary to allow an error-free expansion of an arbitrary function then the set is said to be *complete*.

A most important orthogonal set which is complete is the set of sinusoidal functions (both sines and cosines) which generate the *Fourier series*. In this case, because of the periodicity of the functions, it is not necessary to specify the *end points* of the interval over which the expansion is to be valid but only to specify the *length* of the interval. (It may, however, be useful to specify the interval end points for the sake of computational convenience in connection with evaluating the coefficients.) Specifically, if the variable of interest is time t and the length of time interval is T , then the Fourier expansion of a function $v(t)$ is

$$v(t) = \sum_{n=0}^{\infty} A_n \cos \frac{2\pi n t}{T} + \sum_{n=0}^{\infty} B_n \sin \frac{2\pi n t}{T} \quad (1.180)$$

We take account of the fact that $\cos 0 = 1$ and $\sin 0 = 0$, and applying the normalized procedure of Sec. 1.5 we can express the expansion of $v(t)$ in terms of orthogonal functions as

$$v(t) = \frac{A_0}{\sqrt{T}} + \sum_{n=1}^{\infty} A_n \sqrt{2/T} \cos \frac{2\pi n t}{T} + \sum_{n=1}^{\infty} B_n \sqrt{2/T} \sin \frac{2\pi n t}{T} \quad (1.181)$$

The orthonormal functions are

$$1/\sqrt{T}; \sqrt{2/T} \cos 2\pi n t/T, n \neq 0; \text{ and } \sqrt{2/T} \sin 2\pi n t/T.$$

Any two such different functions when multiplied and integrated over T yields zero, and any function squared and integrated over T yields unity.

In the general case, an expansion is valid only over the finite interval T of orthogonality. In the present case we observe from Eq. (1.181) that the expansion is periodic with period T . If it should happen that $v(t)$ is also periodic with period T then the expansion is valid for all t . Thus, a periodic function with period T can be expanded into a Fourier series as in Eq. (1.181) in which the coefficients are given by

$$A_0 = \frac{1}{\sqrt{T}} \int_T v(t) dt \quad (1.182a)$$

1.5.2 the Gram-Schmidt Procedure

Orthogonal sets of functions that are complete for the purpose of representing an arbitrary function inevitably have an infinite number of components. It turns out however that it is useful, on occasion, to be able to construct an orthogonal set which is complete for the purpose of allowing valid expansions of only a finite number of functions. In such cases the orthogonal set itself has only a finite number of functions and the Gram-Schmidt procedure which we now describe allows us to construct this orthogonal (or orthonormal) set.

Let us call the time functions which are to be expanded: $s_1(t), s_2(t), \dots, s_N(t)$, and the orthonormal functions $u_1(t), u_2(t), \dots, u_N(t)$. Then we require, given the functions $s(t)$, to find the functions $u(t)$ and to evaluate the coefficients s_y in the expansions:

$$s_1(t) = s_{11}u_1(t) + s_{12}u_2(t) + \cdots + s_{1N}u_N(t) \quad (1.183a)$$

$$s_2(t) = s_{21}u_1(t) + s_{22}u_2(t) + \cdots + s_{2N}u_N(t) \quad (1.183b)$$

$$\begin{matrix} \vdots & \vdots & \vdots & \vdots \\ s_N(t) = s_{N1}u_1(t) + s_{N2}u_2(t) + \cdots + s_{NN}u_N(t) \end{matrix} \quad (1.183c)$$

or, using a shorter notation

$$s_i(t) = \sum_{j=1}^N s_{ij}u_j(t) \quad i = 1, 2, \dots, N \quad (1.184)$$

The orthogonality of the functions $u(t)$ over the interval T is expressed by

$$\int_T u_j(t)u_k(t) dt = \begin{cases} 1 & \text{if } j=k \\ 0 & \text{if } j \neq k \end{cases} \quad (1.185)$$

The Gram-Schmidt method proceeds as follows:

Step 1.

In Eq. (1.183a) we set to zero all the coefficients except s_{11} . We then have

$$s_1(t) = s_{11}u_1(t) \quad (1.186a)$$

Since $u_1(t)$ is to be a normalized function we find that

$$s_{11} = \left[\int_T s_1^2(t) dt \right]^{1/2} \quad (1.186b)$$

and $u_1(t) \doteq s_1(t)/s_{11}$ is now determined.

Step 2.

In Eq. (1.183b) we set to zero all coefficients except the first two, s_{21} and s_{22} . We then have

$$s_2(t) = s_{21}u_1(t) + s_{22}u_2(t) \quad (1.187)$$

Step 4.

We continue the procedure until we have used all N equations and shall finally have N orthonormal functions $u_1(t), u_2(t), \dots, u_N(t)$. We shall also have evaluated the coefficients s needed to express the functions $s_x(t), s_2(t), \dots, s_N(t)$ in terms of the $w(t)$'s.

It is assumed in this discussion that the N functions $s(t)$ are linearly independent, that is that no one of the $s(t)$'s can be expressed as a linear sum of the other $s(t)$'s. Suppose, on the other hand, that such is not the case. Assume, for example, that $s_3(t) = C_1s_1(t) + C_2s_2(t)$, C_1 and C_2 being constants.

Then since $s_1(t)$ and $s_2(t)$ can be expressed in terms of $u_1(t)$ and $u_2(t)$ so also would $s_3(t)$ be expressible in terms of $u_1(t)$ and $u_2(t)$. Thus, in Eq. (1.192), we would find that $s_{33} = 0$ and our procedure would not generate a

new function $u_3(t)$. In general, if there are N functions $s_i(t)$ but only M of them are linearly independent, then the procedure will generate $M (< N)$ orthonormal functions in terms of which we shall be able to express all N functions $s_i(t)$.

Given N functions $s_i(t)$ we are, of course, at liberty to number them in any manner we please. Correspondingly, $u_1(t)$ will be determined by which of the functions we please to call $s_1(t)$, $u_2(t)$ will then be determined by this selection of $s_1(t)$ and the subsequent selection of $s_2(t)$, etc. In short, the set of orthonormal functions generated by our procedure is not *unique*. There are, in general, as many sets as there are ways to assign the numbers 1 through N to N functions.

Example 1.24

Two functions $s_1(t)$ and $s_2(t)$ are given in Fig. 1.28a. Here the interval of interest extends from $t = 0$ to $t = T$. Use the Gram-Schmidt procedure to express these functions in terms of orthonormal components.

Solution

We find from Eq. (1.186b) that

$$s_{11} = \left[\int_0^T s_1^2(t) dt \right]^{1/2} = \left(\int_0^T 2^2 dt \right)^{1/2} = 2\sqrt{T}$$

$$u_1(t) = \frac{s_1(t)}{s_{11}} = \frac{s_1(t)}{2\sqrt{T}} \quad (1.195)$$

From Eq. (1.188), we have

$$s_{21} = \int_0^T s_2(t) u_1(t) dt = \int_0^{T/2} 4 \left(\frac{2}{\sqrt{4T}} \right) dt = 2\sqrt{T}$$

From Eq. (1.190),

$$s_{22} = \left\{ \int_0^T [s_2(t) - s_{21}u_1(t)]^2 dt \right\}^{1/2}$$

The function $[s_2(t) - s_{21}u_1(t)]$ and $[s_2(t) - s_{21}u_1(t)]^2$ and drawn in Fig. 1.28b. We have, accordingly,

$$s_{22} = \left(\int_0^T 4 dt \right)^{1/2} = 2\sqrt{T}$$

and finally from Eq. (1.191) we find $u_2(t)$ to be

$$\begin{aligned} u_2(t) &= \frac{1}{2\sqrt{T}} \left[s_2(t) - \frac{2\sqrt{T}s_1(t)}{2\sqrt{T}} \right] \\ &= \frac{1}{2\sqrt{T}} [s_2(t) - s_1(t)] \end{aligned}$$

The orthonormal functions $u_1(t)$ and $u_2(t)$ are shown in Fig. 1.28c. Finally, we have

$$s_2(t) = 2\sqrt{T}u_1(t) + 2\sqrt{T}u_2(t) \quad (1.196)$$

An alternative set of orthonormal functions can be generated by interchanging $s_1(t)$ and $s_2(t)$ (see Prob. 1.41).

1.5.3 Correspondence between Signals and Vectors

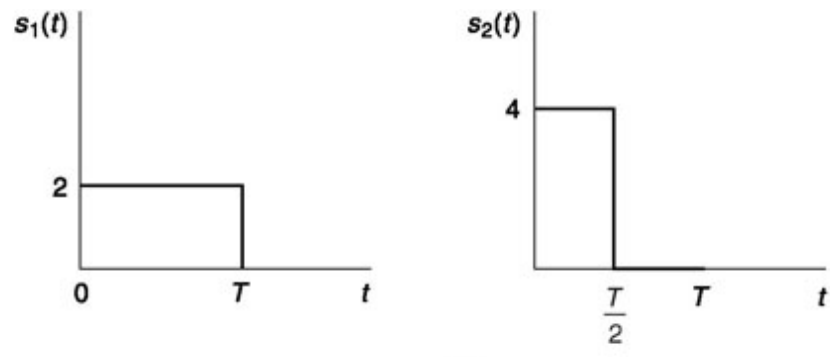
In this section we shall draw an analogy and show a correspondence between the specification of a vector in terms of orthonormal vector components and of a signal in terms of orthonormal functions.

In Fig. 1.29a, a vector A is represented in an XYZ coordinate system. We have defined three unit vectors i , j and k in the X, Y and Z directions, respectively. These unit vectors have the property that the scalar products of a unit vector with itself are

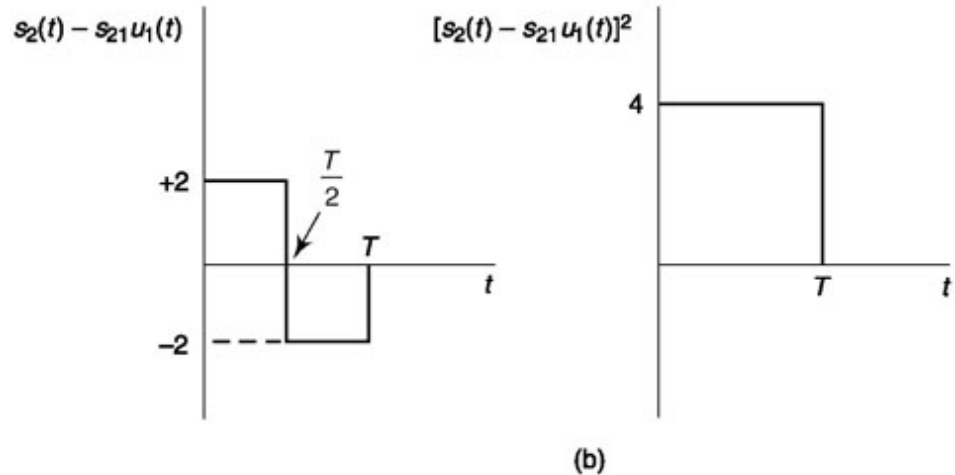
$$i \cdot i = j \cdot j = k \cdot k = 1 \quad (1.197)$$

We note a correspondence between the characteristic noted in Eq. (1.185) and the characteristic of the orthonormal function discussed here that

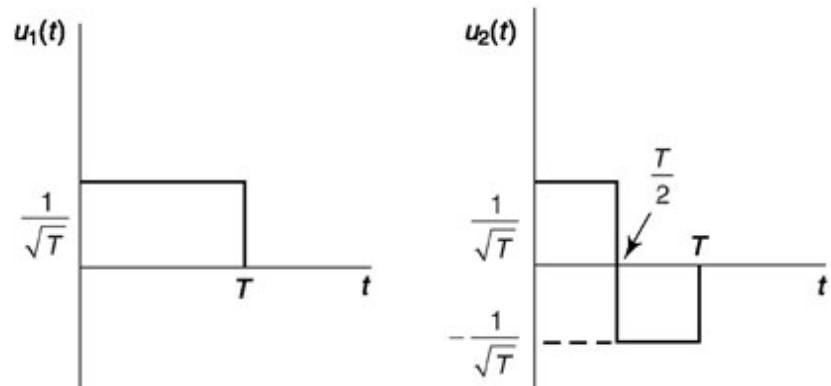
$$\int_T u_i(t) \cdot u_i(t) dt = 1 \quad (1.198)$$



(a)



(b)



(c)

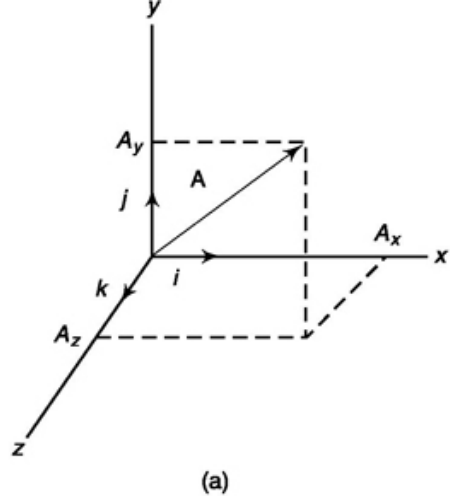
Fig. 1.28 Decomposition of two signals using the Gram-Schmidt technique, (a) The original signals.
(b) Evaluating s_{22} . (c) Orthonormal functions $u_1(t)$ and $u_2(t)$.

Further, the unit vectors have the property that

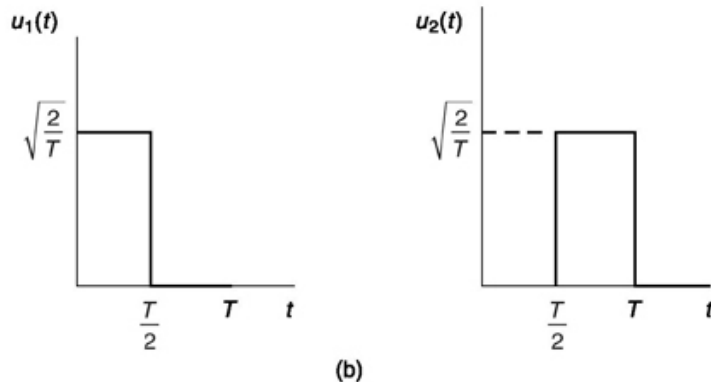
$$i \cdot j = j \cdot k = k \cdot i = 0 \quad (1.199)$$

in correspondence with the property of the orthonormal functions

$$\int_T u_i(t) \cdot u_j(t) dt = 0 \quad (i \neq j) \quad (1.200)$$



(a)



(b)

Fig. 1.29 (a) Expressing a vector \mathbf{A} in a three-dimensional cartesian coordinate system. (b) Unit vectors u_1 and u_2 .

An arbitrary vector \mathbf{A} can be written in terms of its components as

$$\mathbf{A} = A_x i + A_y j + A_z k \quad (1.201)$$

While an arbitrary function $s(t)$ can be written as

$$s(t) = C_1 u_1(t) + C_2 u_2(t) + \cdots + C_N u_N(t) \quad (1.202)$$

If we want to evaluate a vector component, say A_y , we can do so by multiplying Eq. (1.201) by j . For then we have

$$\begin{aligned} j \cdot \mathbf{A} &= A_n j \cdot i + A_y j \cdot j + A_z j \cdot k \\ &= 0 + A_y + 0 \end{aligned}$$

so that

$$A_y = j \cdot \mathbf{A} \quad (1.203)$$

correspondingly, if we want to evaluate, say C_2 in Eq. (1.202) we do so by multiplying by $u_2(t)$ and integrating. For then we have

$$\begin{aligned}
\int_T s(t) u_2(t) dt &= C_1 \int_T u_1(t) \cdot u_2(t) dt + C_2 \int_T u_2(t) \cdot u_2(t) dt + \dots \\
&\quad + C_N \int_T u_N(t) \cdot u_2(t) dt \\
&= 0 + C_2 + \dots + 0
\end{aligned} \tag{1.204}$$

so that

$$C_2 = \int_T s(t) u_2(t) dt$$

Thus we see that the *sieve* technique serves effectively in both cases. The vector, finally, can be expressed specifically by its components in the three orthonormal directions, i.e.

$$A = \{A_x, A_y, A_z\} \tag{1.205a}$$

Correspondingly, the function $s(t)$ can be expressed by specifying its components in N orthonormal “directions,” i.e.

$$s(t) = \{C_1, C_2, \dots, C_N\} \tag{1.205b}$$

There is of course a substantive difference between vectors (force, acceleration, etc.) and functions. In the case of vectors the coordinate system, in which we specify our vectors, is always a system in which the axes extend in three orthogonal directions in a physical space. With functions, the coordinates extend in N “directions” in some “function space” and not in a physical space. Still, continuing our comparisons we note that a vector \mathbf{A} has a magnitude $|A|$ which is calculated

$$|A| = [\mathbf{A} \cdot \mathbf{A}]^{1/2} = [A_x^2 + A_y^2 + A_z^2]^{1/2} \tag{1.206a}$$

Correspondingly we can take the “magnitude” of $s(t)$, $|s(t)|$ to be defined by

$$|s(t)| = \left[\int_T s^2(t) dt \right]^{1/2} \tag{1.206b}$$

Note that the magnitude squared of $s(t)$ is the *signal energy*. From Eq. (1.202), taking into account the orthonormality of the functions $u_1(t), u_2(t), \dots, u_N(t)$ it is readily verified (Prob. 1.50) that

$$|s(t)|^2 = [C_1^2 + C_2^2 + \dots + C_N^2] \tag{1.206c}$$

In Summary

To represent any vector, we first establish and define a coordinate system by introducing three orthogonal unit vectors i, j and k . The vector is expressed as a linear combination of these unit vectors as in Eq. (1.201). The vector can then be represented by the coefficients A_x, A_y and A_z which are the *components* of the vector in the specified coordinate system. In a second coordinate system, oriented differently from the first; with unit vectors i', j' and k , the components will be different from what they were in the first coordinate system. Of course, however, intrinsic properties of the vector such as magnitude will be invariant to the selection of the coordinate system.

In function space, to represent N signals $s_1(t)$, we first establish and define a coordinate system by introducing N orthonormal functions, $u_1(t), u_2(t), \dots,$

$u_N(t)$. The signals are then expressed as a linear combination of these orthonormal functions as in Eq. (1.202). Thus, the signal is represented by the coefficients C_1, C_2, \dots, C_N which are the *components* of the function in the specified coordinate system. In a second coordinate system, “oriented” differently from the first, with “unit functions” $u_1(t), u_2(t), \dots, u'_N(t)$ the components will be different from what they were in the first coordinate system. Of course, intrinsic properties of the functions $s_i(t)$, such as the energy of each signal, are invariant to the choice of coordinate system.

In the Gram-Schmidt procedure, we start by orienting the function space coordinate system in such a manner that the first function $s_x(t)$ [see Eq. (1.186a)] points in the direction of one of the coordinate axes. Hence the first function $s_x(t)$ has only a single component s_n , all other components being zero. Next we rotate the coordinate system about the $u_1(t)$ axis until the second function lies in a “plane” defined by the two axes $u_1(t)$ and $u_2(t)$. Hence, $s_2(t)$ has only two components s_{21} and s_{22} . Proceeding in this manner we find that each successive function $s_i(t)$ has one additional component provided that it is independent of those which have preceded it in the procedure. We have already noted that we are free to number the functions $s_i(t)$ as we please. Each new numbering order yields a different function space coordinate system. These different coordinate systems are “rotated” with respect to one another and correspondingly have different components C_1, C_2, \dots, C_N for the same function $s(t)$.

The application of the Gram-Schmidt procedure yields a function-space coordinate system which has a special orientation with respect to the functions $s(t)$. However, we can, if we please, easily generate a limitless number of function-space coordinate systems which have no special orientation with respect to the functions $s(t)$ so that, in the general case, every $s(t)$ has as many non-zero components as there are coordinates. The procedure for generating such coordinate systems with no special orientation (having again an exact correspondence with the procedure applicable to vectors in real space) will be illustrated by the following example involving just two functions. The generalization to an arbitrary number of functions will be readily apparent.

Example 1.25

In Example 1.24, we started with the functions $s_1(t)$ and $s_2(t)$ of Fig. 1.28a and found the expansions for $s_1(t)$ and $s_2(t)$ to 6e as given in Eqs (1.194) and (1.195), that is,

$$s_1(t) = 2\sqrt{T} u_1(t)$$

$$s_2(t) = 2\sqrt{T} u_1(t) + 2\sqrt{T} u_2(t)$$

where $u_1(t)$ and $u_2(t)$ are given in Fig. 1.28c. That is, $s_1(t)$ and $s_2(t)$ expressed in terms of components are

$$s_1(t) = \{ 2\sqrt{T}, 0 \} \quad (1.207a)$$

$$s_2(t) = \{ 2\sqrt{T}, 2\sqrt{T} \} \quad (1.207b)$$

Find more general orthonormal functions $u'_1(t)$ and $u'_2(t)$ which generate coordinate systems which have no special orientation with respect to the function $s_1(t)$ and $s_2(t)$.

Solution

We take $U_j'(t)$ to be a linear combination of the orthonormal functions $u_x(f)$ and $u_2(t)$, say a parts of $u_2(t)$ to one part of $u_x(t)$. We multiply this linear combination by a number N_1 which we shall later adjust to arrange

that $u'_1(t)$ be normalized. Thus, altogether we write

$$u'_1(t) = N_1[u_1(t) + \alpha u_2(t)] \quad (1.208a)$$

Correspondingly, we set

$$u'_2(t) = N_2[u_1(t) + \beta u_2(t)] \quad (1.208b)$$

It is essential that α and β not be the same for otherwise $u'_1(t)$ and $u'_2(t)$ would be the same functions except for a multiplicative constant. Since $u_1(t)$ and $u_2(t)$ are orthonormal and we require that $u'_1(t)$ and $u'_2(t)$ also be orthonormal, we find that (see Prob. 1.52)

$$1 + \alpha\beta = 0 \quad (1.209)$$

Equation (1.209) constitutes the only constraint on α and β . Within this constraint we are at liberty to select α and β as we please, and thereby are able to generate a limitless number of different function-space coordinate systems. Having selected α and β we can then adjust N_1 and N_2 to normalize $u'_1(t)$ and $u'_2(t)$.

As a specific example, let us assume $\alpha = 1$ so that $\beta = -1$. In this case we readily find, using $u_1(t)$ and $u_2(t)$ as given in Fig. 1.30, that $N_1 = N_2 = 1/\sqrt{2}$ and $u'_1(t)$ and $u'_2(t)$ appear as shown. We find further

that $s_1(t)$ and $s_2(t)$ are expressed in terms of these new orthonormal functions as

$$s_1(t) = \sqrt{2T}u'_1(t) + \sqrt{2T}u'_2(t) \quad (1.210a)$$

$$s_2(t) = 2\sqrt{2T}u'_1(t) \quad (1.210b)$$

In terms of components in this coordinate system in which the unit functions are $u'_1(t)$ and $u'_2(t)$, we find

$$s_1(t) = \{\sqrt{2T}, \sqrt{2T}\} \quad (1.211a)$$

$$s_2(t) = \{2\sqrt{2T}, 0\} \quad (1.211b)$$

In conclusion, we have drawn in Fig. 1.30 a coordinate system in which the unit functions are $u_1(t)$ and $u_2(t)$ and, in this coordinate system, using the components given in Eq. (1.207) we have located the functions $s_1(t)$ and $s_2(t)$. We have also drawn the coordinate system in which the unit functions are $u'_1(t)$ and $u'_2(t)$ in which the components of the functions $s_1(t)$ and $s_2(t)$ are given in Eq. (1.211).

Fig. 1.30 Geometrical representation of orthonormal functions.

1.5.4 Distinguishability of Signals

In the general case, then (for two independent functions $s_1(t)$ and $s_2(t)$), the expansion of the function $s_i(t)$ into an orthonormal series yields the geometric representation of Fig. 1.31. A coordinate system is defined by the unit orthonormal vectors $u_1(t)$ and $u_2(t)$. The functions $s_1(t)$ and $s_2(t)$ are then represented by their components, that is the coordinates (s_{11}, s_{12}) and (s_{21}, s_{22}) or by the function vectors themselves drawn from the origin of the system to the coordinate point. Thus, s_{11} is the component of $s_1(t)$ in the direction of $u_1(t)$, etc. A change in the selection of the unit vectors would generate a rotation of the coordinate system. Under such a rotation, however, the magnitude of each vector $s_1(t)$ and $s_2(t)$, and the angle between them would remain invariant just as in the case of real vectors in physical space.

As we shall describe more fully in Chap. 5, the set of N waveforms $s_1(t)$, $s_2(t)$, ..., $s_N(t)$ can be used to represent N different messages which we may want to transmit from one place to another. Depending on the message we want to transmit, we transmit one or another of the signals. At the

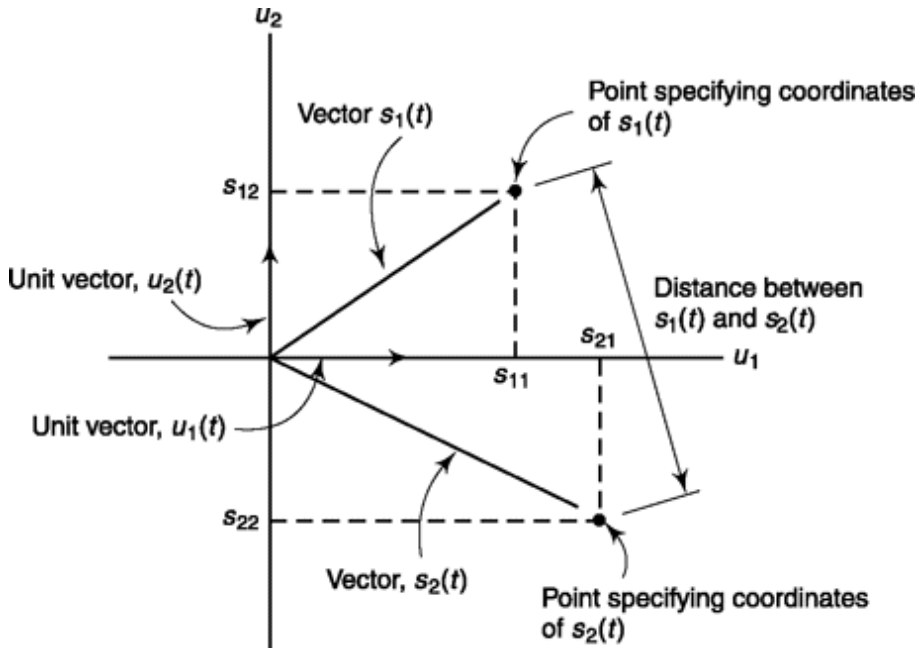


Fig. 1.31 Decomposition of two signal vectors $s_1(t)$ and $s_2(t)$ in terms of the orthonormal vectors $u_1(t)$ and $u_2(t)$.

receiver, the repertory of possible messages and corresponding signals is known and the task there is simply to distinguish the received signal from all

possible signals. If the signals were received as transmitted, there would be no problem at all. More generally however, in transmission, the signal will become mixed with noise. In Chap. 6 we show that because of the characteristics of the noise, no matter how little is added to the signal, the noise will generate a finite probability that an error will be made at the receiver in judging which signal has been transmitted. It seems intuitively reasonable that to minimize the probability of error, it would be advantageous to make the individual signals $s_i(t)$ as “distinguishable” from one another as possible. The question is now how to measure distinguishability. Referring to Fig. 1.31, it again seems reasonable to suggest that distinguishability is measured by the “distance” between the two coordinate points representing $s_1(t)$ and $s_2(t)$, that is by the magnitude of the difference between the two signal vectors.

$$|s_1(t) - s_2(t)| = [(s_{11} - s_{21})^2 + (s_{12} - s_{22})^2]^{1/2} \quad (1.212)$$

In Chap. 11 we shall see that this surmise is indeed valid. Applying the principle to the present two signal case, it then appears that we should make the magnitude of the two signals as large as possible and select signals where the angle between them is 1800° .

Consider the four signals $s_1(t)$, $s_2(t)$, $s_3(t)$, and $s_4(t)$ given by the relation:

$$s_i(t) = \sqrt{2 P_s} \cos\left[\omega_0 t + (2i-1)\frac{\pi}{4}\right] \quad (1.213)$$

i = 1, 2, 3, 4 for $0 \leq t \leq T$. Assume $2\omega_0 T = n\pi$.

- (a) Find a set of orthonormal coordinates.
- (b) Plot the four signals using the orthonormal coordinates.

Solution

$s_i(t)$ can be expanded and written as

$$\begin{aligned} s_i(t) &= \sqrt{2 P_s} \left[\cos(2i-1)\frac{\pi}{4} \right] \cos \omega_0 t \\ &\quad - \sqrt{2 P_s} \left[\sin(2i-1)\frac{\pi}{4} \right] \sin \omega_0 t \end{aligned}$$

We shall choose

$$u_1(t) = \sqrt{\frac{2}{T}} \cos \omega_0 t \quad (1.214)$$

$$\text{and} \quad u_2(t) = \sqrt{\frac{2}{T}} \sin \omega_0 t \quad (1.215)$$

Then $s_i(t)$ can be rewritten as

$$\begin{aligned} s_i(t) &= \sqrt{P_s T} \left[\cos(2i-1) \frac{\pi}{4} \right] u_1(t) \\ &\quad - \sqrt{P_s T} \left[\sin(2i-1) \frac{\pi}{4} \right] u_2(t) \end{aligned} \quad (1.216)$$

The results for $i = 1, 2, 3$ and 4 are shown in Fig. 1.32. Note that the distance d between, say, $s_1(t)$ and $s_2(t)$ is $d = \sqrt{2 P_s T}$.

It is important to note that the magnitude of the signal vectors shown in Fig. 1.32 is equal to the square root of the signal energy. Thus, in Eq. (1.213) each signal $s_i(t)$ has a power P_s and a duration T . Thus the

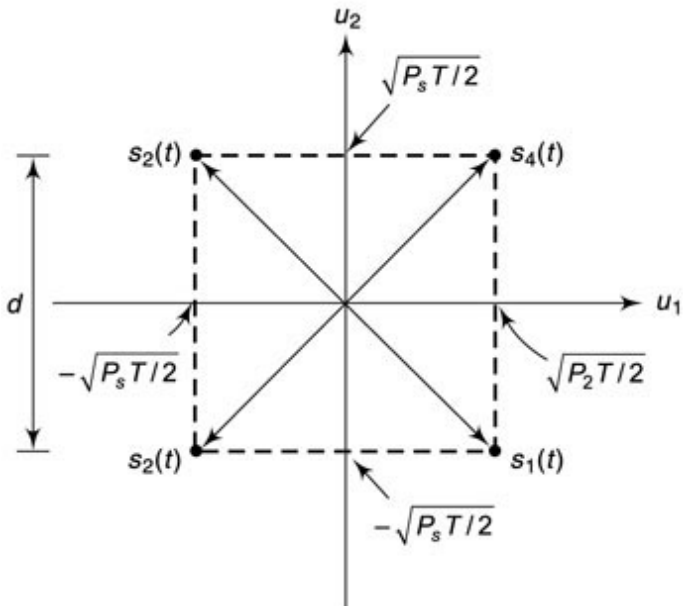


Fig. 1.32 Signal vectors representing the four signals of Eq. (1.213).

SELF-TEST QUESTION

17. Is it a necessary requirement for orthogonality to have zero scalar product?

18. Gram-Schmidt procedure allows to develop a finite orthogonal set to represent a finite number of function. Is it true?
19. What is orthonormal set?
20. Three signals have same magnitude. What phase value will make them maximally distinguishable?

Facts and Figures

It was literally a race against time for the attorney of Alexander Graham Bell (from whom the term *decibel* or *dB* that represents gain has been coined) to be able to file the patent of the telephone at the U.S. Patent office on February 14, 1876, only a few hours before Elisha Gray. Bell won all the court cases and got the sole right to produce telephones in the U.S. for the next 19 years. This patent was valued less than USD 0.1 million by a large company of that time. This prompted Bell and his associates to form Bell Telephone Company in 1877. Bell was only 30 years at that time. In two years, the patent was worth more than USD 25 million and Bell Company became hugely successful.

Alexander Graham Bell has been credited with many other developments like photophone, metal detector, hydrofoil boat, metal jacket for assisted breathing, audiometer to detect minor hearing problems, device to detect icebergs, separation of salt from sea water, etc. His inventions on techniques of teaching to the deaf may have been rooted in the fact that both his mother and wife were deaf. This quote from Bell, a few months before he died in 1922, shows what made this remarkable journey possible. Bell said, “There cannot be mental atrophy in any person who continues to observe, to remember what he observes, and to seek answers for his unceasing hows and whys about things.”

MATLAB

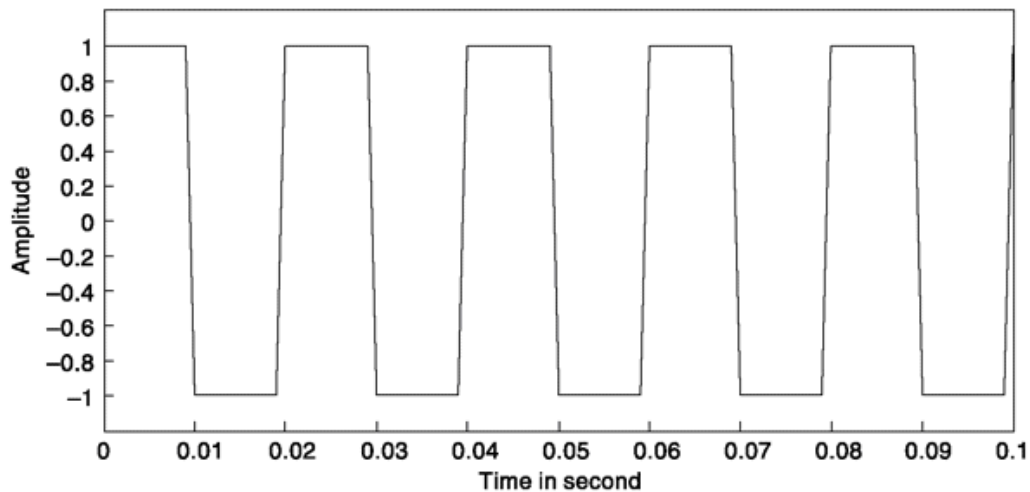
This section presents MATLAB implementation of important concepts developed in this chapter. We provide sufficient comments to make each program self-explanatory. If you are a beginner in MATLAB, please follow the sequence in which the examples are presented. You’ll also learn all necessary MATLAB basics from it. We prefer the term *Experiment* over *Example* as we expect after coding in your computer you will change various parameters yourself and experiment on it to have a deeper understanding of the principles. For each experiment, please write the code (may omit

comment statements after ‘%’ symbol though it is a good practice to include them) in a new .m file in MATLAB editor, save it in some name say ‘exp1.m’ for Experiment 1 and then at MATLAB command prompt, simply type ‘exp1’ press ‘return’ and the result is available. If any syntax error comes, check typing error in the line, column mentioned in the command prompt. To know more about each in-built function used type ‘help *function name*’ at command prompt. If you want the value of a variable to be echoed in the command window, then remove ‘;’ after corresponding instruction. The command ‘who’ and ‘whos’ at command prompt gives you active variables. The value of an active variable can be seen simply by typing its name (no semicolon) and pressing ‘return’ - it will be echoed in the command window. You’ll learn many more things as you start playing with the code.

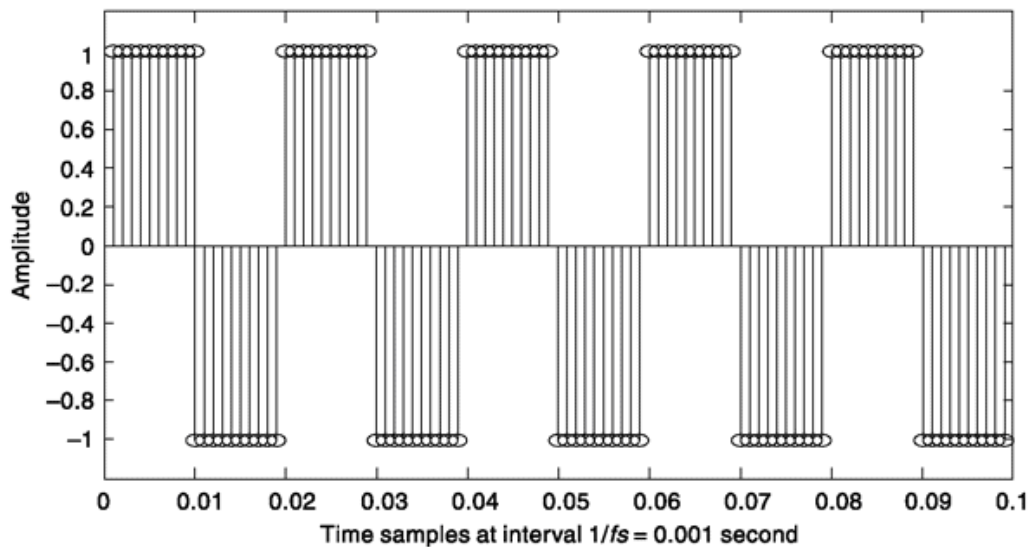
```
%Experiment 1

%Generation of square wave
f = 50; D = 50; %fundamental frequency f, duty cycle in percentage D
fs = 1000; %sampling frequency fs, in each cycle fs/f samples
t = 0:1/fs:0.1; %sampling time 0 to 0.1 second at interval of 1/fs
v = square(2*pi*f*t,D); %generating square wave using in built function
plot(t,v); %continuous plot, made continuous by interpolation
axis ([0 0.1 -1.2 1.2]); % defining axis else in default mode
xlabel('time in second');
ylabel('amplitude');
```

Continuous plot exp1, sq. wave duty cycle 50%, f = 50 Hz, fs = 1000 Hz



Discrete plot exp1, sq. wave duty cycle 50%, f = 50 Hz, fs = 1000 Hz



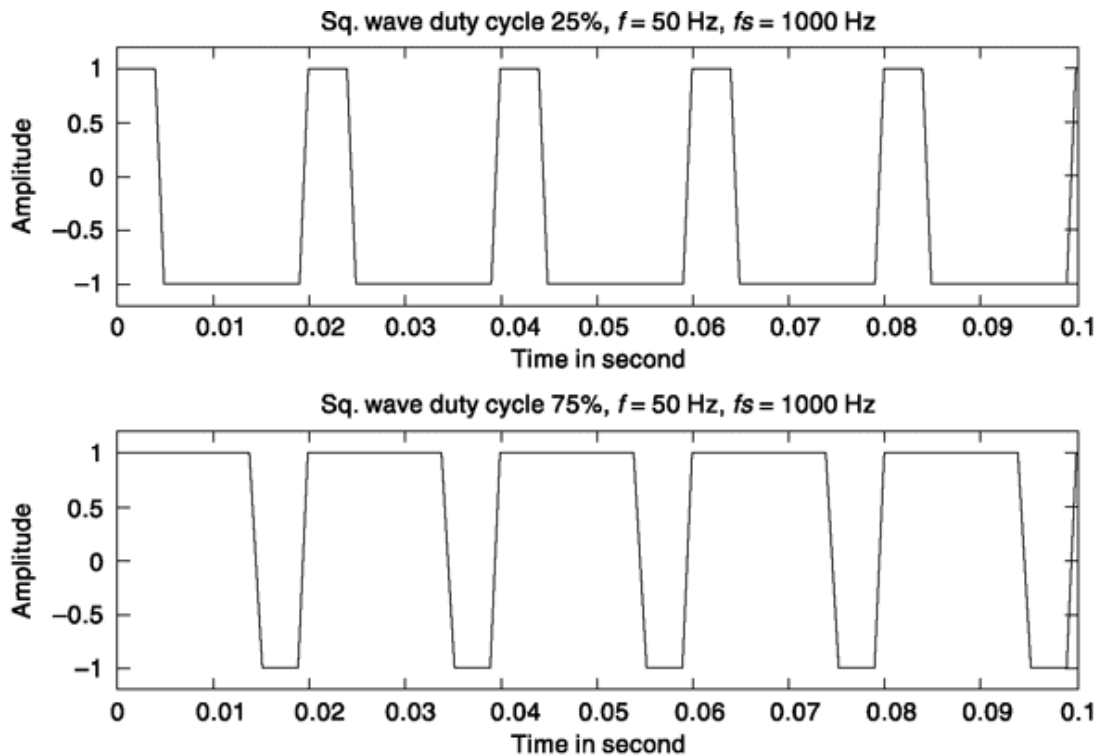
```

title('continuous plot exp1, sq. wave duty cycle 50%, f=50Hz, fs=1000 Hz')
figure % opens a new graphical figure window
stem(t,v); % discrete plot, actual one
axis ([0 0.1 -1.2 1.2]); % again defining axis else in default mode
xlabel('time samples at interval 1/fs = 0.001 second');
ylabel('amplitude');
title('discrete plot exp1, sq. wave duty cycle 50%, f=50Hz, fs=1000 Hz')

%Experiment 1a

%Generation of square wave of different duty cycles and plotting
f=50; fs=1000; t = 0:1/fs:0.1; %As in Experiment 1
v1 = square(2*pi*f*t,25); %duty cycle of 25 percent
v2 = square(2*pi*f*t,75); %duty cycle of 75 percent

```



```

subplot (2,1,1)%divides plot window into 2x1, select 1, ','optional
plot(t,v1); axis ([0 0.1 -1.2 1.2]); % As in Experiment 1
xlabel('time in second');
ylabel('amplitude');
title('sq. wave duty cycle 25%, f=50Hz, fs=1000 Hz')
subplot (2,1,2)%divides plot window into 2x1 matrix, 2nd selected
plot(t,v2); axis ([0 0.1 -1.2 1.2]); % As in Experiment 1
xlabel('time in second'); ylabel('amplitude');
title('sq. wave duty cycle 75%, f=50Hz, fs=1000 Hz')
%Experiment 2
%Generation of pulse wave and sine wave
% Note changes in graphical display 2x1 to 1x2.

f=50; fs=1000; t = 0:1/fs:0.1; %As in Experiment 1

% We generate pulse wave between 0 and 1, duty cycle D percent by
% dc shift of square wave (becomes between 0 to 2) and dividing by 2

v1 =0.5*(square(2*pi*f*t,25)+1); % Duty cycle is 25 percent

% Sine wave is generated by using in built function sine

v2 = sin(2*pi*f*t);

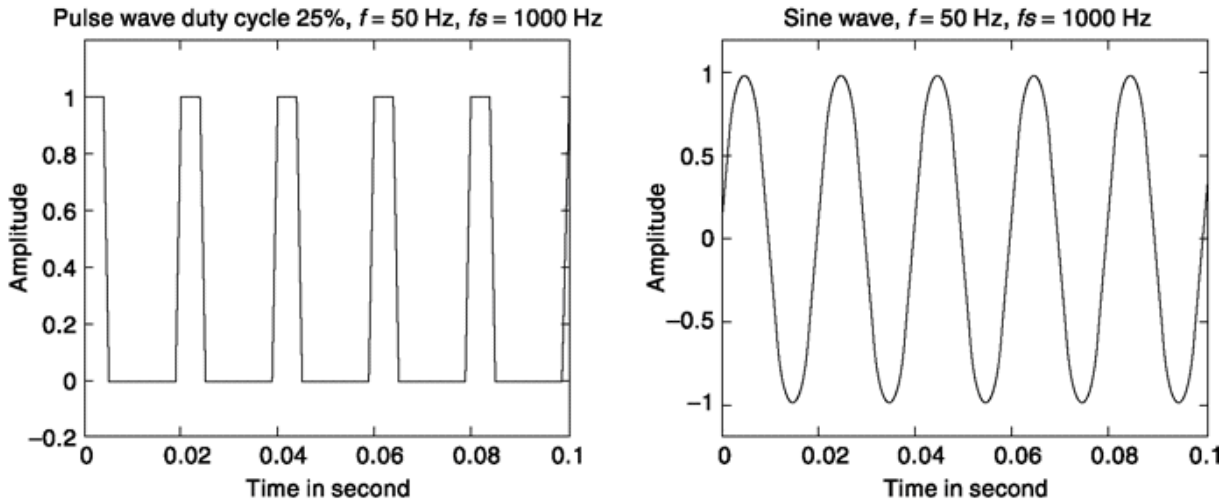
subplot (1,2,1); plot(t,v1); axis ([0 0.1 -0.2 1.2]);
xlabel('time in second'); ylabel('amplitude');
title('pulse. wave duty cycle 25%, f=50Hz, fs=1000 Hz')
subplot (1,2,2); plot(t,v2); axis ([0 0.1 -1.2 1.2]);
xlabel('time in second'); ylabel('amplitude');
title('sine wave, f=50Hz, fs=1000 Hz')

```

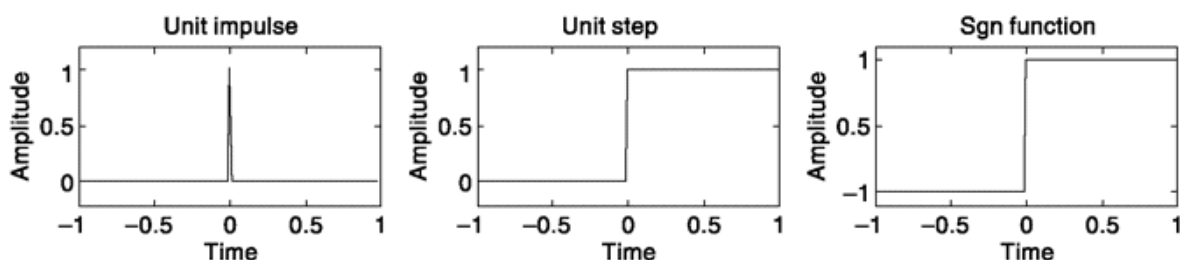
```
%Experiment 2a
%Generation of unit impulse, unit step and sgn function
%Note use of in built function 'zeros' and 'ones', note subplot use

fs=100;
t=-1:1/fs:1; %Total samples=100(- time)+1(origin)+100(+ time) = 201

unit_impulse = [zeros(1,100) 1 zeros(1,100)];
unit_step = [zeros(1,100) ones(1,101)];
```



```
sgn = [-ones(1,100) 0 ones(1,100)];
subplot(1,3,1); plot(t, unit_impulse); axis([-1 1 -0.2 1.2]);
xlabel('time'), ylabel ('amplitude'); title('unit impulse');
subplot(1,3,2); plot(t, unit_step); axis([-1 1 -0.2 1.2]);
xlabel('time'), ylabel ('amplitude'); title('unit step');
subplot(1,3,3); plot(t, sgn); axis([-1 1 -1.2 1.2]);
```



Here, we introduce the concept of a function. *If we're doing repetitive task then it is preferred to code that task in a function and make function call when that task is necessary.* In Experiment 3, we write the function which is used in Experiment 3 a. To see how this function works, code both the experiments - save codes of 3 in *function name.m* (here *unit_impulse.m*) and that of 3a in any name say '*exp3a.m*'. Then in MATLAB command prompt, type '*exp3a*' and press return, the result will be available.

```

%Experiment 3

%Writing a function that generates unit impulse signal
%The file is to be saved in function name, i.e. as unit_impulse.m

%Input to be given are t1=start time in second, t2=end time in second,
%d=shift in second, fs=sampling frequency

function [x,t]=unit_impulse(t1,t2,fs,d)

t=t1:1/fs:t2;
n=abs(d)*fs; %No. of samples that needs to be shifted

temp = [zeros(1,-t1*fs) 1 zeros(1,t2*fs)]; % Original no shift signal
l=length(temp);

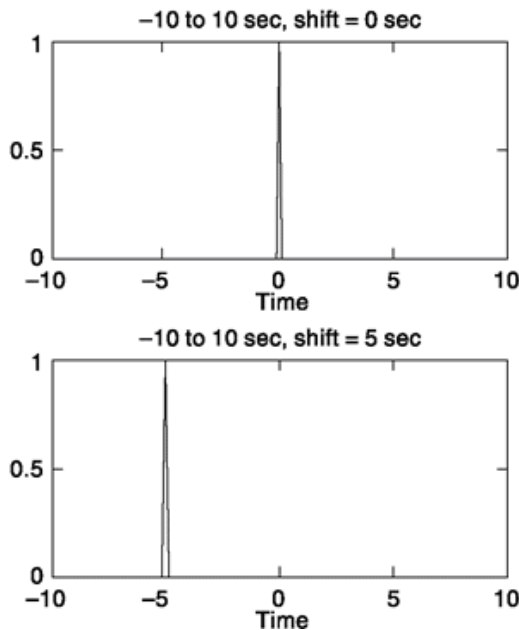
if d == 0
    x=temp; %if d=0 no shift
elseif d > 0
    x=[temp(n+1:l) zeros(1,n)]; %d +ve, then left shift by n samples
else
    x=[zeros(1,n) temp(1:l-n)]; %d -ve, right shift by n samples
end

%Experiment 3a

%Use of function that we have written - unit_impulse.m in expt. 3

[x,t]=unit_impulse(-10,10,10,0);
subplot(2,2,1); plot(t,x);
xlabel('time'); title('-10 to 10 sec, shift = 0 sec');
[x,t]=unit_impulse(-5,15,10,0);

```



```

subplot(2,2,2); plot(t,x);
xlabel('time'); title('-5 to 15 sec, shift = 0 sec');
[x,t]=unit_impulse(-10,10,10,5);
subplot(2,2,3); plot(t,x);
xlabel('time'); title('-10 to 10 sec, shift = 5 sec');
[x,t]=unit_impulse(-10,10,10,-3);
subplot(2,2,4); plot(t,x);
xlabel('time'); title('-10 to 10 sec, shift = -3 sec');

% Experiment 4

% Here we write a function that reconstructs a square wave from its
% Fourier coefficients. T = Time period, N = No. of harmonics used
% don't forget to save this in fs_square.m, the function name chosen

function [x,ti]=fs_square(T,N)

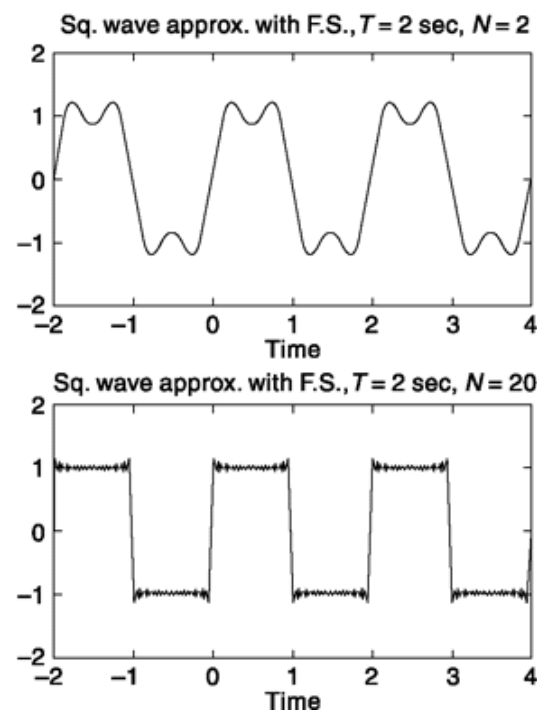
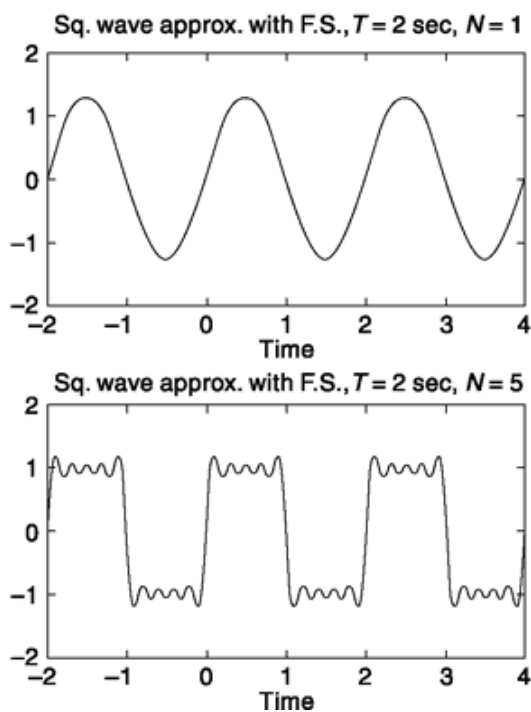
f0=1/T;      % Fundamental frequency
ti=-1*T:1/(100*f0):2*T; % Three cycles generated(-T to 2T), fs = 100*f0
x=0;

for i=1:N
    n=2*(i-1)+1;      % Only odd harmonics of sin function are present
    x=x+(4*sin(2*pi*f0*n*ti))/(pi*n); % From Fourier expansion
end

%Experiment 4a

%Use of function that we have written - fs_square.m
%to see the effect of inclusion of more and more harmonics

```



```

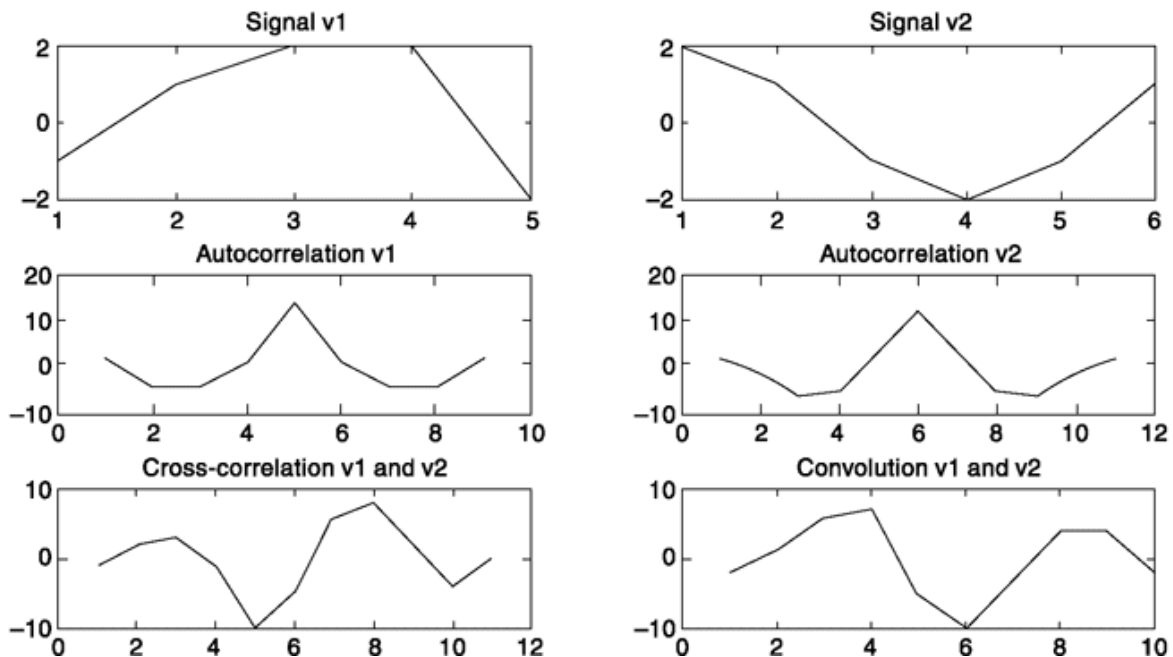
%that approximates a signal better, uses function fs_square of expt. 4
[x,t]=fs_square(2,1); %Time period chosen 2 second, only fundamental
subplot(2,2,1); plot(t,x);
xlabel('time'); title('Sq. wave approx. with F.S.,T=2 sec, N=1');
[x,t]=fs_square(2,2); %Two components
subplot(2,2,2); plot(t,x);
xlabel('time'); title('Sq. wave approx. with F.S.,T=2 sec, N=2');
[x,t]=fs_square(2,5); %Five components
subplot(2,2,3); plot(t,x);
xlabel('time'); title('Sq. wave approx. with F.S.,T=2 sec, N=5');
[x,t]=fs_square(2,20); %Twenty components
subplot(2,2,4); plot(t,x);
xlabel('time'); title('Sq. wave approx. with F.S.,T=2 sec, N=20');

%Experiment 5
% Calculation of autocorrelation, cross correlation and convolution
% and correlation coefficient, use v1, v2 defined next
v1=[-1 1 2 2 -2];
v2=[2 1 -1 -2 -1 1];

ac_1=xcorr(v1) %calculates autocorrelation, without ; result is echoed
ac_2=xcorr(v2)
xc_12=xcorr(v1,v2) % size is 2M-1, M larger of two, shorter zero padded
cv_12=conv(v1,v2) % size M+N-1

subplot(3,2,1); plot(v1); title('signal v1');
subplot(3,2,2); plot(v2); title('signal v2');
subplot(3,2,3); plot(ac_1); title('Autocorrelation v1');
subplot(3,2,4); plot(ac_2); title('Autocorrelation v2');

```



```

subplot(3,2,5); plot(xc_12); title('Cross-correlation v1 and v2');
subplot(3,2,6); plot(cv_12); title('Convolution v1 and v2');

% To find correlation coefficient vectors must be of same length.
% Let us zero pad v1 to make its size equal to v2.

v1 =[v1 0]; % zero padding
cf_12=corrcoef(v1,v2) % calculates correlation coefficient and echos it

```

After execution command window echoes following values

```

ac_1 = 2.0000 -4.0000 -4.0000 1.0000 14.0000 1.0000 -4.0000 -4.0000 2.0000
ac_2 = 2.0000 -1.0000 -6.0000 -5.0000 4.0000 12.0000 4.0000 -5.0000 -6.0000 -1.0000 2.0000
xc_12 = -1.0000 2.0000 3.0000 -1.0000 -10.0000 -5.0000 6.0000 8.0000 2.0000 -4.0000 0
cv_12 = -2 1 6 7 -5 -10 -3 4 4 -2
cf_12 = 1.0000 -0.3953
           -0.3953 1.0000

```

%Experiment 6

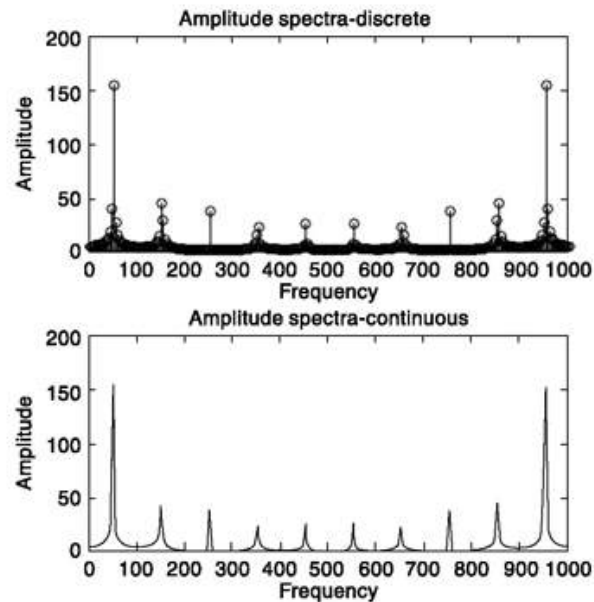
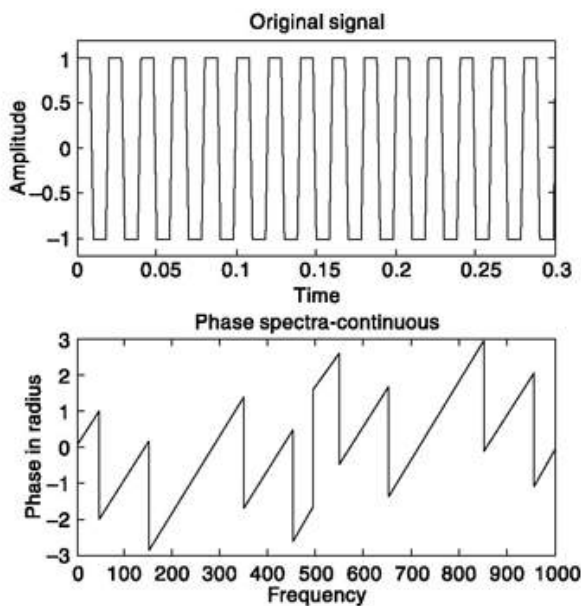
%This finds frequency content of a square wave through FFT

```

f0=50; D=50; %fundamental frequency f, duty cycle in percentage D
fs=1000; %sampling frequency fs, in each cycle fs/f samples
t = 0:1/fs:0.3; %sampling time 0 to 0.1 second at interval of 1/fs
v = square(2*pi*f0*t,D);
vf=fft(v,256); %256 point fft, truncates or zero pads a signal to size
va=abs(vf); %amplitude spectra
vp=angle(vf); %phase (in radian) spectra
f=0:fs/255:fs; %setting frequency axis, 256 points, thus 255 intervals

subplot(221); plot(t,v); axis([0 0.3 -1.2 1.2]);
xlabel('time'); ylabel('amplitude'); title('original signal');
subplot(222); stem(f,va); % stem gives discretized plot

```



```

xlabel('frequency'); ylabel('amplitude');
title('amplitude spectra-discrete');
subplot(224); plot(f,va);
xlabel('frequency'); ylabel('amplitude');
title('amplitude spectra-continuous');
subplot(223); plot(f,vp);
xlabel('frequency'); ylabel('phase in radian');
title('phase spectra-continuous');

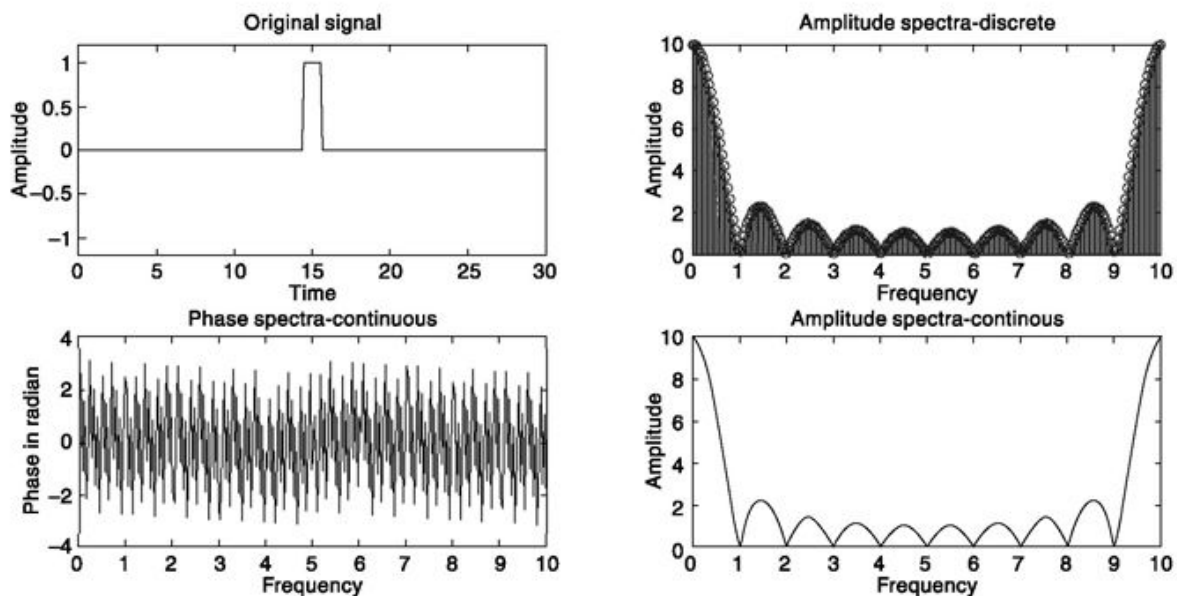
%Experiment 6a

%This finds frequency content of a rectangular pulse through FFT

fs=10; %sampling frequency fs, in each cycle fs/f samples
t = 0:1/fs:30; %sampling time 0 to 30 second at interval of 1/fs
v = [zeros(1,145) ones(1,10) zeros(1,146)]; % pulse width 10/fs=1 sec
vf=fft(v,256); %256 point fft, truncates or zero pads a signal to size
va=abs(vf); %amplitude spectra
vp=angle(vf); %phase (in radian) spectra
f=0:fs/255:fs; %setting frequency axis, 256 points, thus 255 intervals

subplot(221); plot(t,v); axis([0 30 -1.2 1.2]);
xlabel('time'); ylabel('amplitude'); title('original signal');
subplot(222); stem(f,va); % stem gives discretized plot
xlabel('frequency'); ylabel('amplitude');
title('amplitude spectra-discrete');
subplot(224); plot(f,va);
xlabel('frequency'); ylabel('amplitude');
title('amplitude spectra-continuous');
subplot(223); plot(f,vp);
xlabel('frequency'); ylabel('phase in radian');
title('phase spectra-continuous');

```



```

%Experiment 3

%Writing a function that generates unit impulse signal
%The file is to be saved in function name, i.e. as unit_impulse.m

%Input to be given are t1=start time in second, t2=end time in second,
%d=shift in second, fs=sampling frequency

function [x,t]=unit_impulse(t1,t2,fs,d)

t=t1:1/fs:t2;
n=abs(d)*fs; %No. of samples that needs to be shifted

temp = [zeros(1,-t1*fs) 1 zeros(1,t2*fs)]; % Original no shift signal
l=length(temp);

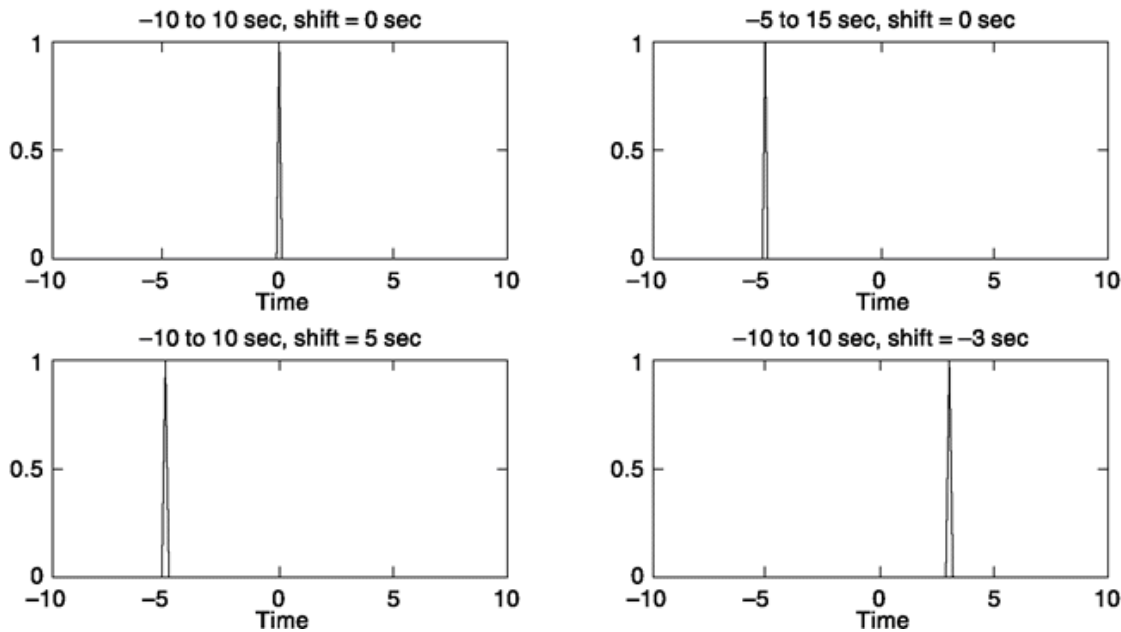
if d == 0
    x=temp; %if d=0 no shift
elseif d > 0
    x=[temp(n+1:l) zeros(1,n)]; %d +ve, then left shift by n samples
else
    x=[zeros(1,n) temp(1:l-n)]; %d -ve, right shift by n samples
end

%Experiment 3a

%Use of function that we have written - unit_impulse.m in expt. 3

[x,t]=unit_impulse(-10,10,10,0);
subplot(2,2,1); plot(t,x);
xlabel('time'); title('-10 to 10 sec, shift = 0 sec');
[x,t]=unit_impulse(-5,15,10,0);

```



SUMMARY

The chapter begins with an overview of the electronic communication systems. Using a system-level block diagram, it introduces concepts like modulation, multiplexing, distortion, noise interference, signal to noise ratio, bandwidth, channel capacity, coding and use of spectrum. This follows a discussion on classification of signals, means to characterize it, e.g. energy, power, correlation, etc., and certain basic signal operations like shifting, scaling, etc. A detailed discussion on Fourier series expansion, useful for identifying frequency information of periodic signals and Fourier transform, useful for aperiodic signals is presented. In each cases, important properties are discussed, judicious application of which makes many complex problems look simple. The chapter also discusses orthogonal representation of signal and presents technique like Gram-Schmidt rotation that uses only a finite set of signals for orthogonal representation. Correspondence between signals and vectors are discussed with its use in enhancing distinguishability between various types of signals. More emphasis is given to the understanding of digital signals in digital communication context. At the end, an extensive illustration of various concepts developed in this chapter is presented through MATLAB simulations.

PROBLEMS

- 1.1 What size of antenna is required to radiate signal of 150 MHz frequency?
- 1.2 Find channel capacity for bandwidth = 4 kHz, SNR = 30 dB
- 1.3 Find bandwidth requirement for 256 kbps channel when SNR is 20 dB.
- 1.4 Calculate energy of the signal $v(t) = ae^{-bt}u(t)$.
- 1.5 Calculate power of the signal $\omega(t) = A \sin(\omega t + \theta)$
- 1.6 Find cross-correlation term $R_{12}(0)$ for $v_1(t) = (u(t) - u(t - 5)) \sin 2\pi t/5$ and $v_2(t) = 3t(u(t) - u(t - 10))$.
- 1.7 Verify the relationship of C_n and ϕ_n to A_n and B_n as given by Eq. (1.28).
- 1.8 Calculate A_n , B_n , C_n and ϕ_n for a waveform $v(t)$ which is a symmetrical square wave and which makes peak excursions to $+\frac{3}{4}$ volt and $-\frac{1}{4}$ volt, and has a period $T = 1$ sec. A positive going transition occurs at $t = 0$.
- 1.9 Verify the relationship of the complex number V_n to C_n and ϕ_n as given by Eq. (1.31).
- 1.10 The function

$$p(t) = \begin{cases} e^{-t} & 0 \leq t \leq 1 \\ 0 & \text{elsewhere} \end{cases}$$

is repeated every $T = 1$ sec. Thus, with $u(t)$ the unit step function

$$v(t) = \sum_{n=-\infty}^{\infty} p(t-n)u(t-n)$$

Find V_n and the exponential Fourier series for $v(t)$.

- 1.11 The impulse function can be defined as

$$\delta(t) = \lim_{a \rightarrow \infty} \frac{a}{2} e^{-at}$$

Discuss.

that the Fourier series does approximate the train of impulses.

- 1.13 $Sa(x) = (\sin x)/x$. Determine the maxima and minima of $Sa(x)$ and compare your result with the approximate maxima and minima obtained by letting $x = (2n + 1)(/2, n = 1, 2, ..$

- 1.14 A train of rectangular pulses, making excursions from zero to 1 volt, have a duration of 2 /ms and are separated by intervals of 10 ms.

- (a) Assume that the center of one pulse is located at $t = 0$. Write the exponential Fourier series for this pulse train and plot the spectral amplitude as a function of frequency. Include at least 10 spectral components on each side of $f = 0$, and draw also the envelope of these spectral amplitudes.

- (b) Assume that the left edge of a pulse rather than the center is located at $t = 0$. Correct the Fourier expansion accordingly. Does this change affect the plot of spectral amplitudes? Why not?

- 1.15 (a) A periodic waveform $v_i(t)$ is applied to the input of a network. The output $v_o(t)$ of the

network is $v_o(t) = t[dv_i(t)/dt]$, where t is a constant. What is the transfer function $H(w)$ of this network?

(b) A periodic waveform $v_i(t)$ is applied to the RC network shown, whose time constant is $\tau = RC$. Assume that the highest frequency spectral component of $v_i(t)$ is of a frequency $f \neq 1/\tau$. Show that, under these circumstances, the output $v_o(t)$ is approximately $v_o(t) = t [dv_i(t)/dt]$.

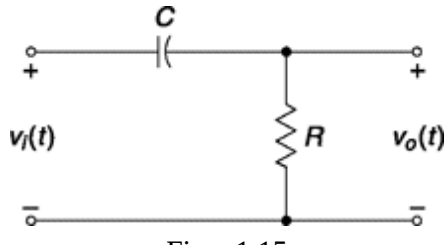


Fig. p1.15

1.16 A voltage represented by an impulse train of strength I and period T is filtered by a low-pass RC filter having a 3 dB frequency f_c .

- (a) Find the Fourier series of the output voltage across the capacitor.
- (b) If the third harmonic of the output is to be attenuated by 1000, find $f_c T$.

1.17 Measurements on a voltage amplifier indicate a gain of 20 dB.

- (a) If the input voltage is 1 volt, calculate the output voltage.
- (b) If the input power is 1 mw, calculate the output power.

1.18 A voltage gain of 0.1 is produced by an attenuator.

- (a) What is the gain in decibels?
- (b) What is the power gain (not in decibels)?

1.19 A periodic triangular waveform $v(t)$ is defined by

$$v(t) = \frac{2t}{T} \quad \text{for} \quad -\frac{T}{2} < t < \frac{T}{2}$$

and

$$v(t \pm T) = v(t)$$

and has the Fourier expansion

$$v(t) = \frac{2}{\pi} \sum_{n=1}^{\infty} \frac{(-1)^{n+1}}{n} \sin 2\pi n \frac{t}{T}$$

Calculate the fraction of the normalized power of this waveform which is contained in its first three harmonics.

- 1.20 The complex spectral amplitudes of a periodic waveform are given by

$$V_n = \frac{1}{|n|} e^{-j \arctan(n/2)} \quad n = \pm 1, \pm 2, \dots$$

Find the ratio of the normalized power in the second harmonic to the normalized power in the first harmonic.

- 1.21 Find $G(f)$ for the following voltages:

- (a) An impulse train of strength I and period T .
- (b) A pulse train of amplitude A , duration $\tau = I/A$, and period T .

- 1.22 Plot $G(f)$ for a voltage source represented by an impulse train of strength I and period nT for $n = 1, 2, 10, \infty$. Comment on this limiting result.

- 1.23 $G_i(f)$ is the power spectral density of a *square-wave* voltage of peak-to-peak amplitude 1 and period 1. The square wave is filtered by a low-pass RC filter with a 3 dB frequency 1. The output is taken across the capacitor.

- (a) Calculate $G_i(f)$.
- (b) Find $G_0(f)$.

- 1.24 (a) A symmetrical square wave of zero mean value, peak-to-peak voltage 1 volt, and period

1 sec is applied to an ideal low-pass filter. The filter has a transfer function $|H(f)| = \frac{1}{2}$ in the frequency range $-3.5 \leq f \leq 3.5$ Hz, and $H(f) = 0$ elsewhere. Plot the power spectral density of the filter output.

- (b) What is the normalized power of the input square wave? What is the normalized power of the filter output?

- 1.25 In Eqs (1.29) and (1.30), write $f_0 \equiv 1/T_0$. Replace f_0 by Δf , i.e., Δf is the frequency interval between harmonics. Replace $n \Delta f$ by f , i.e. as $\Delta f \rightarrow 0$, f becomes a continuous variable ranging from 0 to ∞ as n ranges from 0 to ∞ . Show that in the limit as $\Delta f \rightarrow 0$, so that Δf may be replaced by the differential df , Eq. (1.29) becomes

$$v(t) = \int_{-\infty}^{\infty} V(f) e^{j2\pi ft} df$$

in which $V(f)$ is

$$V(f) = \lim_{\substack{f_0 = \Delta f \rightarrow 0 \\ nf_0 \rightarrow f}} \int_{-1/2f_0}^{1/2f_0} v(t) e^{-j2\pi n f_0 t} dt = \int_{-\infty}^{\infty} v(t) e^{-j2\pi f t} dt$$

- 1.26 Find the Fourier transform of $\sin \omega_0 t$. Compare with the transform of $\cos \omega_0 t$. Plot and compare the power spectral densities of $\cos \omega_0 t$ and $\sin \omega_0 t$.
- 1.27 The waveform $v(t)$ has the Fourier transform $V(f)$. Show that the waveform delayed by time t_d , i.e. $v(t - t_d)$ has the transform $V(f)e^{-j\omega t_d}$.
- 1.28 (a) The waveform $v(t)$ has the Fourier transform $V(f)$. Show that the time derivative $(d/dt)v(t)$ has the transform $(j2\pi f)V(f)$.
- (b) Show that the transform of the integral of $v(t)$ is given by

$$\mathcal{F}\left[\int_{-\infty}^t v(\lambda) d\lambda\right] = \frac{V(f)}{j2\pi f}$$

- 1.29 Derive the convolution formula in the frequency domain. That is, let $V_1(f) = \mathcal{F}[v_1(t)]$ and $V_2(f) = \mathcal{F}[v_2(t)]$. Show that if $V(f) = \mathcal{F}[v_1(t)v_2(t)]$, then

$$V(f) = \frac{1}{2\pi} \int_{-\infty}^{\infty} V_1(\lambda)V_2(f - \lambda) d\lambda$$

or

$$V(f) = \frac{1}{2\pi} \int_{-\infty}^{\infty} V_2(\lambda)V_1(f - \lambda) d\lambda$$

- 1.30 (a) A waveform $v(t)$ has a Fourier transform which extends over the range from $-f_M$ to $+f_M$. Show that the waveform $v^2(t)$ has a Fourier transform which extends over the range from $-2f_M$ to $+2f_M$. (Hint: Use the result of Prob. 1.29.)
- (b) A waveform $v(t)$ has a Fourier transform $V(f) = 1$ in the range $-f_M$ to $+f_M$ and $V(f) = 0$ elsewhere. Make a plot of the transform of $v^2(1)$.
- 1.31 A filter has an impulse response $h(t)$ as shown. The input to the network is a pulse of unit amplitude extending from $t = 0$ to $t = 2$. By graphical means, determine the output of the filter.

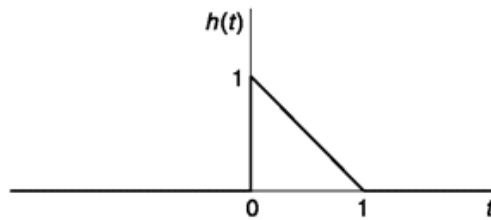


Fig. P1.31

- 1.32 The energy of a nonperiodic waveform $v(t)$ is

$$E = \int_{-\infty}^{\infty} v^2(t) dt$$

- (a) Show that this can be written as

$$E = \int_{-\infty}^{\infty} dt v(t) \int_{-\infty}^{\infty} V(f) e^{j2\pi f t} df$$

- (b) Show that by interchanging the order of integration we have

$$E = \int_{-\infty}^{\infty} V(f)V^*(f) df = \int_{-\infty}^{\infty} |V(f)|^2 df$$

which proves Eq. (1.136). This is an alternate proof of Parseval's theorem.

- 1.33 If $V(f) = AT \sin 2\pi fT/2\pi fT$, find the energy E contained in $v(t)$.
 1.34 A waveform $m(t)$ has a Fourier transform $M(f)$ whose magnitude is as shown.
 (a) Find the normalized energy content of the waveform.
 (b) Calculate the frequency f_1 such that one-half of the normalized energy is in the frequency range $-f_1$ to f_1 .

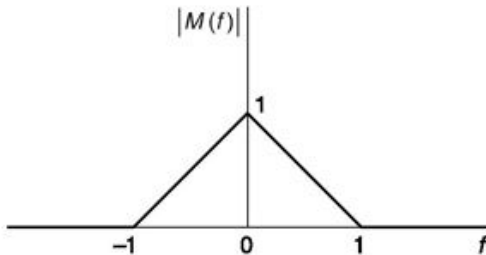
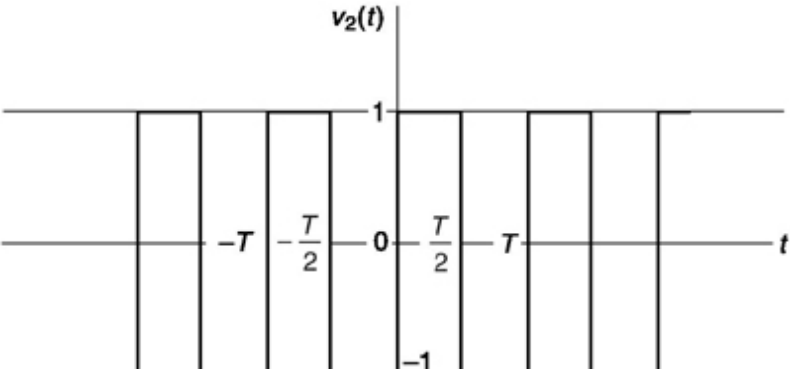
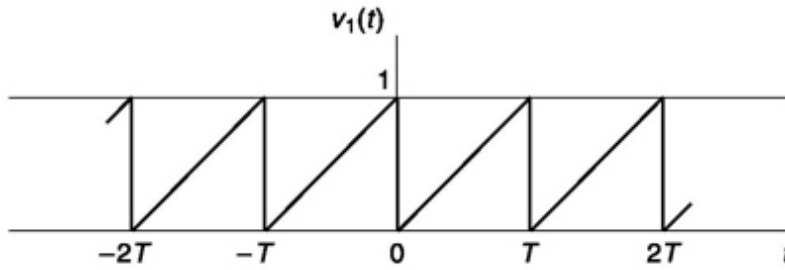


Fig. P1.34

- 1.35 The signal $v(t) = \cos \omega_0 t + 2 \sin 3\omega_0 t + 0.5 \sin 4\omega_0 t$ is filtered by an RC low-pass filter with a 3dB frequency $f_c = 2f_0$.
 (a) Find $G_i(f)$.
 (b) Find $G_o(f)$.
 (c) Find S_o .
 1.36 The waveform $v(t) = e^{-t/\tau} u(t)$ is passed through a high-pass RC circuit having a time constant equal to τ .
 (a) Find the energy spectral density at the output of the circuit.
 (b) Show that the total output energy is one-half the input energy.
 1.37 (a) An impulse of strength I is applied to a low-pass RC circuit of 3 dB frequency f_2 . Calculate the output waveform.
 (b) A pulse of amplitude A and duration τ is applied to the low-pass RC circuit. Show that, if $\tau \ll 1/f_2$, the response at the output is approximately the response that would result from the application to the circuit of an impulse of strength $I' = A\tau$. Generalize this result by considering any voltage waveform of area I' and duration τ .
 1.38 A pulse extending from 0 to A volts and having a duration τ is applied to a high-pass RC circuit. Show that the area under the response waveform is zero.
 1.39 Find the cross correlation of the functions $\sin \omega t$ and $\cos \omega t$.
 1.40 Show that two signals if time advanced or time delayed by the same unit will generate the same amount of correlation.
 1.41 Find the cross-correlation function $R_{12}(\tau)$ of the two periodic waveforms shown. (Fig. P1.41)



1.42

$$R(f) = \lim_{T \rightarrow \infty} \frac{1}{T} \int_{-T/2}^{T/2} v(t)v(t + \tau) dt$$

Prove that $R(0) \geq R(\tau)$. Hint: Consider

$$I = \lim_{T \rightarrow \infty} \frac{1}{T} \int_{-T/2}^{T/2} [v(t) - v(t + \tau)]^2 dt$$

Is $I \geq 0$? Expand and integrate term by term. Show that

$$I = 2[R(0) - R(\tau)] \geq 0$$

- 1.43 Determine an expression for the correlation function of a square wave having the values 1 or 0 and a period T .
- 1.44 (a) Find the power spectral density of a square-wave voltage by Fourier transforming the correlation function. Use the results of Prob. 1.43.
 (b) Compare the answer to (a) with the spectral density obtained from the Fourier series (Prob. 1.15a) itself.
- 1.45 If $v(t) = \sin \omega_0 t$,
 (a) Find $R(\tau)$.
 (b) If $G(f) = \mathcal{F}[R(\tau)]$, find $G(f)$ directly and compare.
- 1.46 A waveform consists of a single pulse of amplitude A extending from $t = -\tau/2$ to $t = \tau/2$.
 (a) Find the autocorrelation function $R(\tau)$ of this waveform.
 (b) Calculate the energy spectral density of this pulse by evaluating $G_E(f) = \mathcal{F}[R(\tau)]$.
 (c) Calculate $G_E(f)$ directly by Parseval's theorem and compare.
- 1.47 Interchange the labels $s_1(t)$ and $s_2(t)$ on the waveforms of Fig. 1.28a and with this new labeling apply the Gram-Schmidt procedure to find expansions of the waveforms in terms of orthonormal functions.
- 1.48 Use the Gram-Schmidt procedure to express the functions in Fig. P1.48 in terms of orthonormal components.

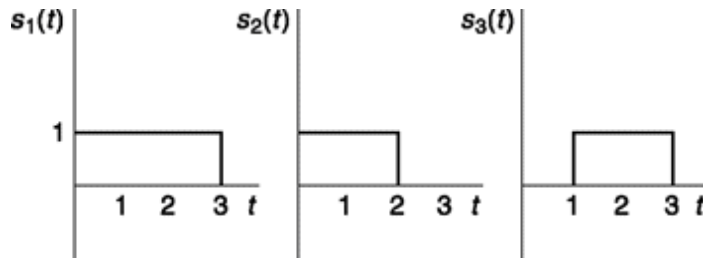


Fig. P1.48

1.49 A set of signals ($k = 1, 2, 3, 4$) is given by

$$s_k(t) = \begin{cases} \cos\left(\omega_0 t + k \frac{\pi}{2}\right) & 0 \leq t \leq k \frac{2\pi}{\omega_0} = 0 \\ = 0 & \text{otherwise} \end{cases}$$

Use the Gram–Schmidt procedure to find an orthonormal set of functions in which the functions $s_k(t)$ can be expanded.

1.50 A signal is completely specified by a finite number of orthonormal components. Show that the signal energy is the sum of squares of orthonormal components.

- 1.51 (a) Show that the pythagorean theorem applies to signal functions. That is, show that if $s_1(t)$ and $s_2(t)$ are orthogonal then the square of the length of $s_1(t)$ (defined as in Eq. (1.206b)) plus the square of the length of $s_2(t)$ is equal to the square of the length of the sum $s_1(t) + s_2(t)$.
 (b) Let $s_1(t)$ and $s_2(t)$ be the signals shown in Fig. P1.51. Draw the signal $s_1(t) + s_2(t)$. Show that $s_1(t)$ and $s_2(t)$ are orthogonal. Show that $|s_1(t) + s_2(t)|^2 = |s_1(t)|^2 + |s_2(t)|^2$.

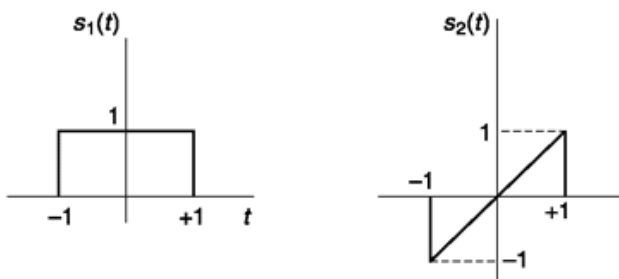


Fig. p1.51

1.52 From two orthonormal functions given, how many different pairs of orthonormal functions can be generated? Find the condition that governs this.

1.53 (a) Refer to Fig. 1.30 and Eq. (1.209). Verify that the parameter a in Eq. (1.209) is the tangent of the angle between the axes of the u_1 , u_2 coordinate system and the u'_1 / u'_2 coordinate system.
 (b) Expand the functions $s_x(t)$ and $s_2(t)$ of Fig. 1.28 in terms of orthonormal functions $u_1(t)$ and $u_2(t)$ which are the axes of a coordinate system which is rotated 600° counterclockwise from the coordinate system whose axes are $u_1(t)$ and $u_2(t)$ of the same figure.

Introduction: Signal and Spectra 83

1.54 Apply the Gram-Schmidt procedure to the eight signals of Eq. (1.217). Verify that two orthonormal components suffice to allow a representation of any of the signals. Show that in a coordinate system of these two orthonormal signals, the geometric representation of the eight signals is as shown in Fig. 1.33.

1.55 A set of signals is $s_{a1}(t) = (2p_a \sin w_0 t - s_{a2}) V^2 Pa \sin w_0 t$. A second set of signals is $s_{b2} = y/2p_b \sin w_0 t$, $s_{b2} = j2p_b \sin (w_0 t + pI2)$. If the two sets of signals are to have the same distinguishability, what is the ratio P_b/P_a ?

1.56 Given two signals

$$S1(t) = f(t) \quad 0 < t < T; \quad S2(t) = -f(t) \quad 0 < t < T$$

Show that independently of the form of $f(t)$ the distinguishability of the signals is given by $V^2 E$ where E is the normalized energy of the waveform $f(t)$.

1.57 (a) Use the Gram-Schmidt procedure to express the functions in Fig. P1.57 in terms of orthonormal components. In applying the procedure, involve the functions in the order $s_x(t)$, $s_2(t)$, $s_3(t)$ and $s_4(t)$. Plot the functions as points in a coordinate system in which the coordinate axes are measured in units of the orthonormal functions.

(b) Repeat part (a) except that the functions are to be involved in the order $s_1(t)$, $s_2(t)$, $s_3(t)$ and $s_4(t)$. Plot the functions.

(c) Show that the procedures of parts (a) and (b) yield the same distances between function points.

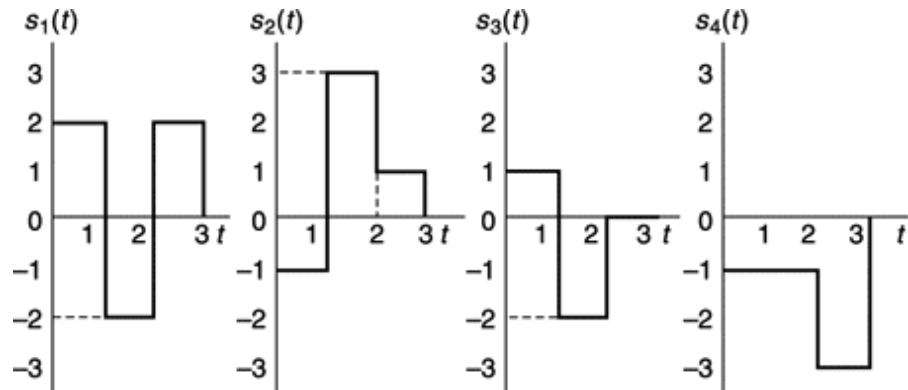


Fig. P1.57

1.58 Find Fourier series expansion coefficients of a sawtooth wave, one period of which is defined by $v(t) = t(u(t) - u(t - 1))$.

1.59 Find Fourier series expansion coefficients of rectangular pulse train of amplitude A, angular frequency w_c and duty cycle 50% symmetrically spaced about $t = 0$ axis.

1.60 Find exponential Fourier series of the signal $v(t) = \cos w_c t + \sin^2 w_c t$

1.61 Find Fourier transform of $v(t) = AS(t)$.

1.62 Find Fourier transform of $v(t) = AS(t - t)$.

1.63 Find Fourier Transform of $v(t) = A$.

1.64 Find Fourier transform of a rectangular pulse of height 0.5, that extends from -1 second to +1 (can be defined as $A \operatorname{rect}(t/T)$ where $A = 0.5$, $T = 2$).

1.65 Find the Fourier transform of train of unit impulses ($S(t - nT)$)
 $n = \dots$

1.66 Find the relation between Fourier series of a periodic signal given by ($v(t)S(t - nT)$) and
 $n = \dots$

Fourier transform of $v(t)$ where $v(t)$ is zero everywhere except $-T/2 < t < T/2$.

$|1 - |t|/T| < T$

1.67 If $v(t) = \{0 \quad |t| > T\}$ then find $V(f)$.

1.68 In digital communication, one can employ a scheme called Amplitude Shift Keying (ASK) where amplitude of a high-frequency sinusoidal carrier is changed according to a digital pulse stream. Find the spectrum of a sinusoid signal of frequency f_c switched by a rectangular pulse of height A and width t.

REFERENCES

1. Javid, M., and E. Brenner: "Analysis of Electric Circuits," 2d ed., McGraw-Hill Book Company, New York, 1967.

Papoulis, A.: "The Fourier Integral and Applications," McGraw-Hill Book Company, New York, 1963.

2. Churchil, R. V.: "Fourier Series," McGraw-Hill Book Company, New York, 1941.
3. Papoulis, A.: "Probability, Random Variables, and Stochastic Processes," McGraw-Hill Book Company, New York, 1965.

2

AMPLITUDE-MODULATION SYSTEMS

CHAPTER OBJECTIVE

One of the basic problems of communication engineering is the design and analysis of systems which will allow many individual messages to be transmitted simultaneously over a single communication channel. A method by which such multiple transmission, called multiplexing, may be achieved consists of translating each message to different positions in the frequency spectrum. This frequency multiplexing needs use of a carrier, with certain attributes of it varying according to the message signal. We discuss amplitude modulation techniques in this chapter that varies amplitude of a carrier according to the message input. Besides illustrative examples, the chapter also presents a variety of MATLAB based simulations. These are developed in a manner that helps one go beyond mathematical representations, play with waveforms by changing simulation parameters and feel confident about important issues in different types of amplitude modulation. At the end we discuss basic issues behind working of radio transmitter and receiver in general but Amplitude Modulation system in particular. Since it is the very first chapter on modulation-demodulation, a large number of block diagrams are presented that can be mapped to governing mathematical equations. This is to help one understand the implementation issues and also how to convert a mathematical description to its block-diagram-level realization in communication context.

FACTS AND FIGURES

In 1831, M. Faraday discovered electromagnetic induction from his pioneering experiments. J. Maxwell followed it up and in 1873, first described the theoretical basis of the propagation of electromagnetic waves. Between 1886 and 1888, H. R. Hertz validated Maxwell's theory, showed that radio radiation follows all the properties of waves and gave wave

equations. Marconi patented the radio transmitter for telegraph messages (dot and dash) in 1897 and was able to send them across the Atlantic in 1901.

The Canadian-born American physicist R. Fessenden first showed that amplitude modulation (AM) of radio waves can be used to send messages other than telegraph. He got a patent in 1901 for this new type of radio transmitter. Five years later, on Christmas Eve of 1906, the first audio broadcast

was made from Brant Rock, Massachusetts. Ships at sea heard Fessenden playing ‘O Holy Night’ on violin or reading passages from the Bible.

2.1 NEED FOR FREQUENCY TRANSLATION

It is often advantageous and convenient, in processing a signal in a communication system, to translate the signal from one region in the frequency domain to another region. Suppose that a signal is bandlimited, or nearly so, to the frequency range extending from a frequency f to a frequency f_2 . The process of frequency translation is one in which the original signal is replaced with a new signal whose spectral range extends from f' to f and which **new** signal bears, in recoverable form, the same **information** as was borne by the original signal. We discuss now a number of useful purposes which may be served by frequency translation. Note that frequency translation is useful for both analog and digital signals.

Frequency Multiplexing

Suppose that we have several different signals, all of which encompass the same spectral range. Let it be required that all these signals be transmitted along a single communication channel in such a manner that, at the receiving end, the signals be separately recoverable and distinguishable from each other. The single channel may be a single pair of wires or the free space that separates one radio antenna from another. Such multiple transmissions, i.e. multiplexing, may be achieved by translating each one of the original signals to a different frequency range. Suppose, say, that one signal is translated to the frequency range f to f_2 , the second to the range f_1 to f_2' , and so on. If these new frequency ranges do not overlap, then the signal may be separated at the receiving end by appropriate bandpass filters, and the outputs of the

filters processed to recover the original signals. Refer to Fig. 2.1. It shows how three signals having overlapping spectrum may be frequency multiplexed with separate frequency bands for each of the signals and a guard band in between.

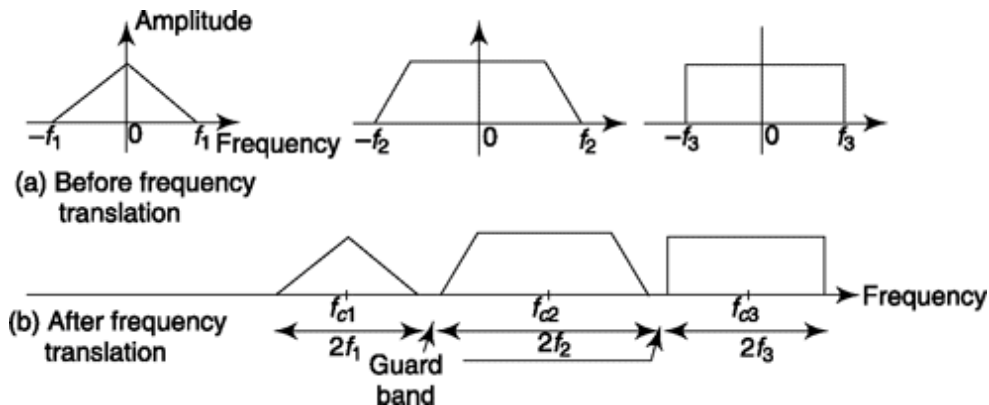


Fig. 21 *An example of frequency multiplexing. (a) Spectrum of three signals in original form having frequency overlap. (b) Spectrum of three signals of (a) after frequency translation. There is no frequency overlap now and it is suitable for transmission in this form.*

Practicability of Antennas

When free space is the communication channel, antennas radiate and receive the signal. It turns out that antennas operate effectively only when their dimensions are of the order of magnitude of the wavelength of the signal being transmitted. A signal of frequency 1 kHz (an audio tone) corresponds to a wavelength of 300,000 m, an entirely impractical length. The required length may be reduced to the point of practicability by translating the audio tone to a higher frequency.

Narrowbanding

Returning to the matter of the antenna, just discussed, suppose that we wanted to transmit an audio signal directly from the antenna, and that the inordinate length of the antenna were no problem. We would still be left with a problem of another type. Let us assume that the audio range extends from, say, 50 to 10^4 Hz. The ratio of the highest audio frequency to the lowest is 200. Therefore, an antenna suitable for use at one end of the range would be entirely too short or too long for the other end. Suppose, however, that the audio spectrum were translated so that it occupied the range, say, from $(10^6 + 50)$ to $(10^6 + 10^4)$ Hz. Then the ratio of highest to lowest frequency would

be only 1.01. Thus, the processes of frequency translation may be used to change a “wideband” signal into a “narrowband” signal which may well be more conveniently processed. The terms “wideband” and “narrowband” are being used here to refer not to an absolute range of frequencies but rather to the fractional change in frequency from one band edge to the other.

Common Processing

It may happen that we may have to process, in turn, a number of signals similar in general character but occupying different spectral ranges. It will then be necessary, as we go from signal to signal, to adjust the frequency range of our processing apparatus to correspond to the frequency range of the signal to be processed. If the processing apparatus is rather elaborate, it may well be wiser to leave the processing apparatus to operate in some fixed frequency range and instead to translate the frequency range of each signal in turn to correspond to this fixed frequency. An example of this concept is the design of a superheterodyne receiver where a common processing block is tuned to different frequencies by using a local oscillator, this is discussed in Section 2.6.4.

2.1.1 A Method for Frequency Translation

A signal may be translated to a new spectral range by ***multiplying*** the signal with an auxiliary sinusoidal signal. To illustrate the process, let us consider initially that the signal is sinusoidal in waveform and given by

$$v_m(t) = A_m \cos \omega_m t = A_m \cos 2\pi f_m t \quad (2.1a)$$

$$= \frac{A_m}{2} (e^{j2\pi f_m t} + e^{-j2\pi f_m t}) \quad (2.1b)$$

in which A_m is the constant amplitude and $f_m = \omega_m/2\pi$ is the frequency. The two-sided spectral amplitude pattern of this signal is shown in Fig. 2.2a. The pattern consists of two lines, each of amplitude $A_m/2$, located at $f = f_m$ and at $f = -f_m$. Consider next the result of the multiplication of $v_m(t)$ with an auxiliary sinusoidal signal

$$v_c(t) = A_c \cos \omega_c t = A_c \cos 2\pi f_c t \quad (2.2)$$

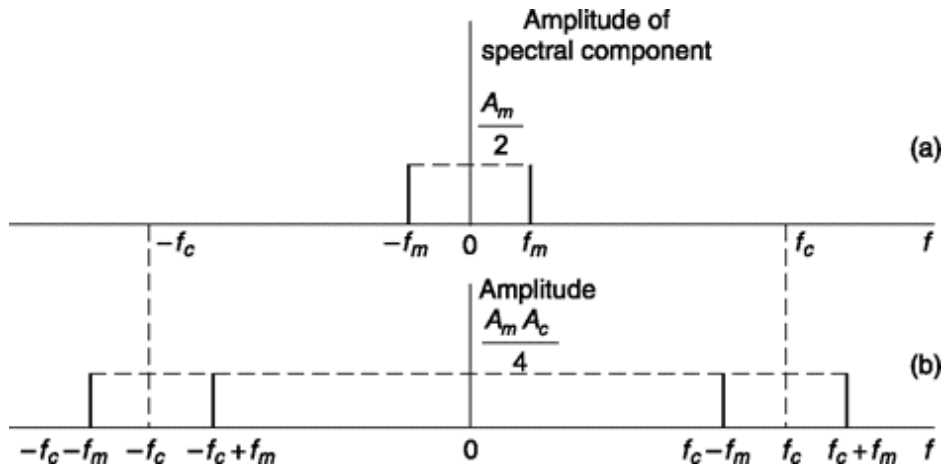


Fig. 2.2 (a) Spectral pattern of the waveform $A_m \cos \omega_m t$. (b) Spectral pattern of the product waveform $A_m A_c \cos \omega_m t \cos \omega_c t$.

in which A_c is the constant amplitude and f is the frequency. From Example 1.15.

$$\begin{aligned} v_m(t)v_c(t) &= A_m A_c \cos \omega_m t \cos \omega_c t \\ &= \frac{A_m A_c}{4} (e^{j(\omega_c + \omega_m)t} + e^{-j(\omega_c + \omega_m)t} + e^{j(\omega_c - \omega_m)t} + e^{-j(\omega_c - \omega_m)t}) \end{aligned} \quad (2.3)$$

The new spectral amplitude pattern is shown in Fig. 2.2b. Observe that the two original spectral lines have been **translated**, both in the positive-frequency direction by amount f_c and also in the negative-frequency direction by the same amount. There are now four spectral components resulting in two sinusoidal waveforms, one of frequency $f_c + f_m$ and the other of frequency $f_c - f_m$. Note that while the product signal has four spectral components each of amplitude $A_m A_c / 4$, there are only two frequencies, and the amplitude of each sinusoidal component is $A_m A_c / 2$.

A generalization of Fig. 2.2 is shown in Fig. 2.3. Here a signal is chosen which consists of a superposition of four sinusoidal signals, the highest in frequency having the frequency f_M . Before translation by multiplication, the two-sided spectral pattern displays eight components centered around zero frequency. After multiplication, we find this spectral pattern is translated both in the positive- and the negative-frequency directions. The 16 spectral components in this two-sided spectral pattern give rise to eight sinusoidal waveforms. While the original signal extends in range up to a frequency f_M ,

the signal which results from multiplication has sinusoidal components covering a range $2f_M$ from $f_c - f_M$ to $f_c + f_M$.

2.2 DOUBLE SIDEBAND—SUPPRESSED CARRIER (DSB-SC) MODULATION

Continuing from the previous discussion, we take up a more general presentation of input signal here and effect similar frequency translation. Consider in Fig. 2.4 the situation in which the signal to be translated may not be represented as a superposition of a number of sinusoidal components at sharply defined frequencies. Such would be the case if the signal were of finite energy and nonperiodic. In this case the signal is represented in the frequency domain in terms of its Fourier

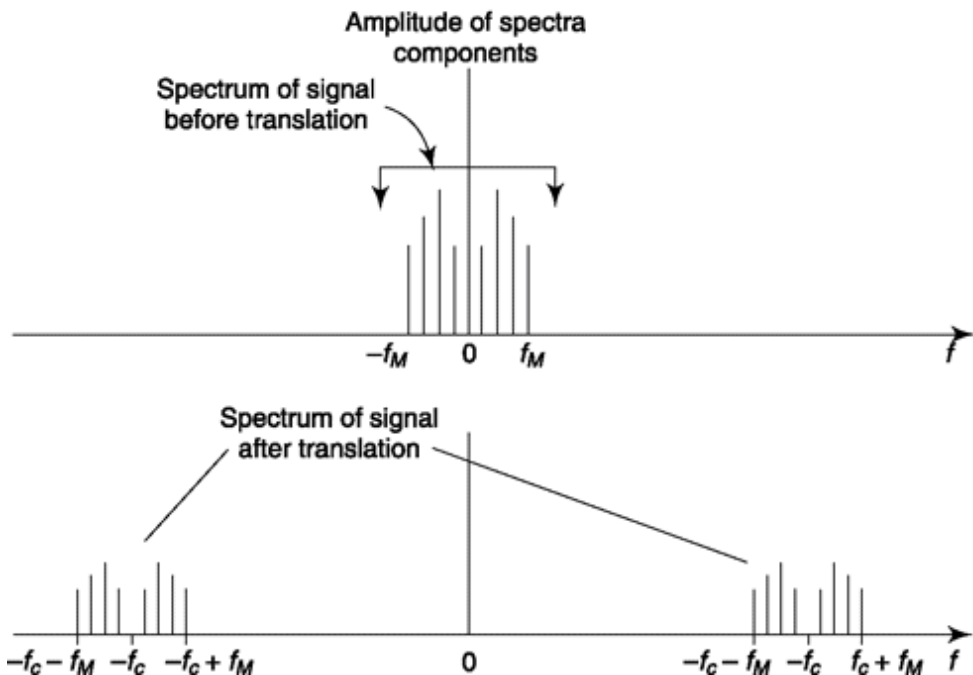


Fig. 2.3 An original signal consisting of four sinusoids of differing frequencies is translated through multiplication and becomes a signal containing eight frequencies symmetrically arranged about f_c .

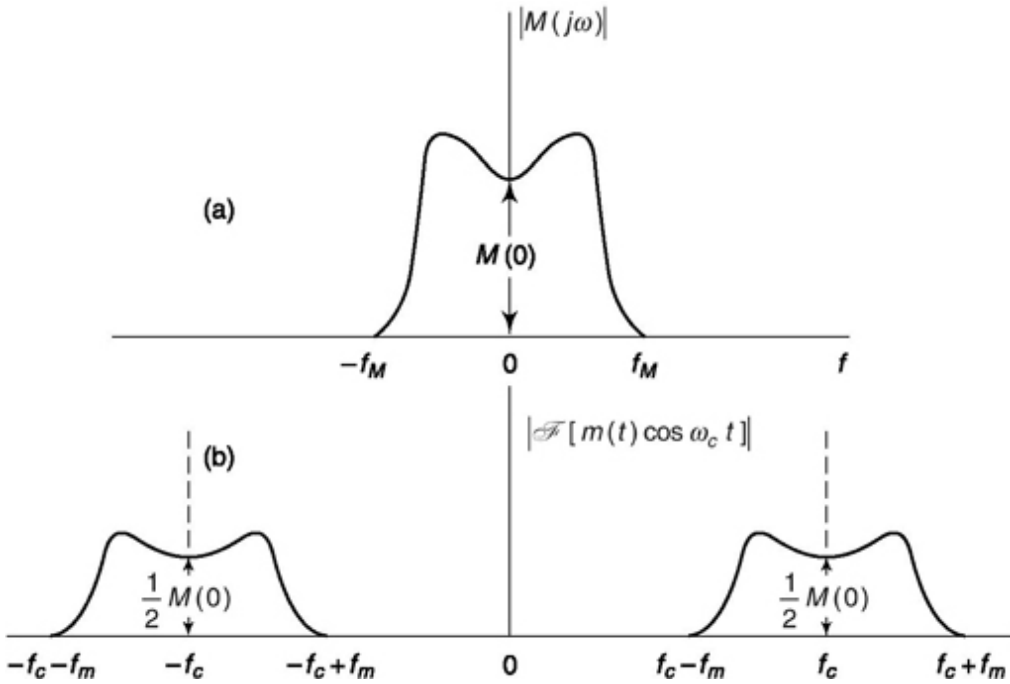


Fig. 2.4 (a) The spectral density $|M(j\omega)|$ of a nonperiodic signal $m(t)$. (b) The spectral density of $m(t) \cos 2\pi f_c t$.

transform, that is, in terms of its spectral density. Thus, let the signal $m(t)$ be bandlimited to the frequency range 0 to f_M . Its Fourier transform is $M(j\omega) = \mathcal{F}[m(t)]$. The magnitude $|M(j\omega)|$ is shown in Fig. 2.4a. The transform $M(j\omega)$ is symmetrical about $\omega = 0$ since we assume that $m(t)$ is a real signal. The spectral density of the signal which results when $m(t)$ is multiplied by $\cos \omega_c t$

is shown in Fig. 2.4b. This spectral pattern is deduced as an extension of the results shown in Figs 2.2 and 2.3. Alternatively, from Example 1.15 if $M(j\omega) = \mathcal{F}[m(t)]$, then

$$\mathcal{F}[m(t) \cos \omega_c t] \frac{1}{2} = [M(\omega + \omega_c) + M(\omega - \omega_c)] \quad (2.4)$$

The spectral range occupied by the original signal is called the **baseband frequency range** or simply the **baseband**. On this basis, the original signal itself is referred to as the baseband signal. The operation of multiplying a signal with an auxiliary sinusoidal signal is called **mixing** or **heterodyning**. In the translated signal, the part of the signal which consists of spectral components **above** the auxiliary signal, in the range f_c to $f_c + f_M$, is called the **upper-sideband** signal. The part of the signal which consists of spectral components below the auxiliary signal, in the range $f_c - f_M$ to f_c , is called the **lower-sideband** signal. The two sideband signals are also referred to as the

sum and the **difference** frequencies, respectively. The auxiliary signal of frequency f_c is variously referred to as the **local oscillator signal**, the **mixing signal**, the **heterodyning signal**, or as the **carrier signal**, depending on the application. The student will note, as the discussion proceeds, the various contexts in which the different terms are appropriate. The modulation scheme discussed here is also known as Double Side Band-Suppressed Carrier modulation or in short DSB-SC. It is called DSB because when transmitted both upper and lower sidebands are transmitted each of which has identical message contents. It is called SC as we are not sending carrier signal separately. Why this is an issue will be clear shortly.

We may note that the process of translation by multiplication actually gives us something somewhat different from what was intended. Given a signal occupying a baseband, say, from zero to f_M , and an auxiliary signal f_c , it would often be entirely adequate to achieve a simple translation, giving us a signal occupying the range f_c to $f_c + f_M$, that is, the upper sideband. We note, however, that translation by multiplication results in a signal that occupies the range $f_c - f_M$ to $f_c + f_M$. This feature of the process of translation by multiplication may, depending on the application, be a nuisance, a matter of indifference, or even an advantage. Hence, this feature of the process is, of itself, neither an advantage nor a disadvantage. It is, however, to be noted that there is no other operation so simple which will accomplish translation.

2.2.1 DsB-sC Modulator

We have described a “multiplier” as a device that yields as an output a signal which is the product of two input signals. Actually no simple physical device now exists which yields the product alone. On the contrary, all such devices yield, at a minimum, not only the product but the input signals themselves. Suppose, then, that such a device has as inputs a carrier $\cos w_c t$ and a modulating baseband signal $m(t)$. The device output will then contain the product $m(t) \cos w_c t$ and also the signals $m(t)$ and $\cos w_c t$. Ordinarily, the baseband signal will be bandlimited to a frequency range very much smaller than $f_c = w_c/2\pi$. Suppose, for example, that the baseband signal extends from zero frequency to 1000 Hz, while $f_c = 1$ MHz. In this case, the carrier and its sidebands extend from 999,000 to 1,001,000 Hz, and the baseband signal is easily removed by a filter.

The overall result is that the devices available for multiplication yield an output carrier as well as the lower- and upper-sideband signals. Such output is called amplitude-modulated signal which is a double sideband with carrier. We will characterize such signal and discuss its use in next section. If we require the product signal alone, we must take steps to cancel or ***suppress*** the carrier. Such

a suppression may be achieved by adding, to the amplitude-modulated signal, a signal of carrier frequency equal in amplitude but opposite in phase to the carrier of the amplitude modulated signal. Under these circumstances only the sideband signals will remain.

Balanced Modulator

An alternative arrangement for carrier suppression is shown in Fig. 2.5. Here two ***physical*** multipliers, as discussed in the first paragraph of this section, are used and labeled in the diagram as ***amplitude modulators***. The carrier inputs to the two modulators are of reverse polarity, as are the modulating signals. The modulator outputs are added with consequent suppression of the carrier. We observe a cancellation not only of the carrier but of the baseband signal $m(t)$ as well. This last feature is not of great importance, since, as noted previously, the baseband signal is easily eliminated by a filter. We note that the product terms of the two modulators reinforce. The arrangement of Fig. 2.5 is called a ***balanced modulator***.

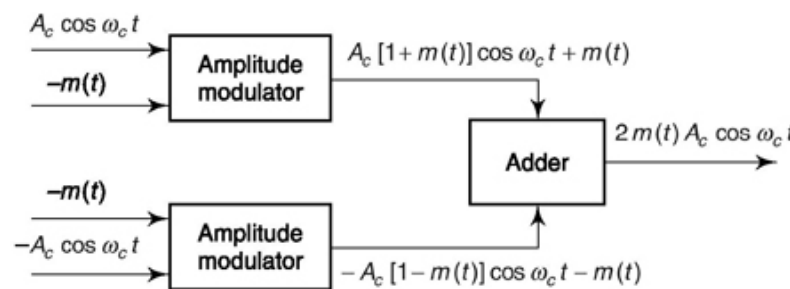


Fig. 2.5 Showing how the outputs of two amplitude modulators are combined to produce a double-sideband suppressed-carrier output.

Nonlinear Modulator

Refer to Fig. 2.6. If compared with Fig. 2.5 the Amplitude Modulation block represents a nonlinear device which generates output $w(t)$ if input is $v(t)$ following relation $w(t) = av(t) + bv^2(t)$.

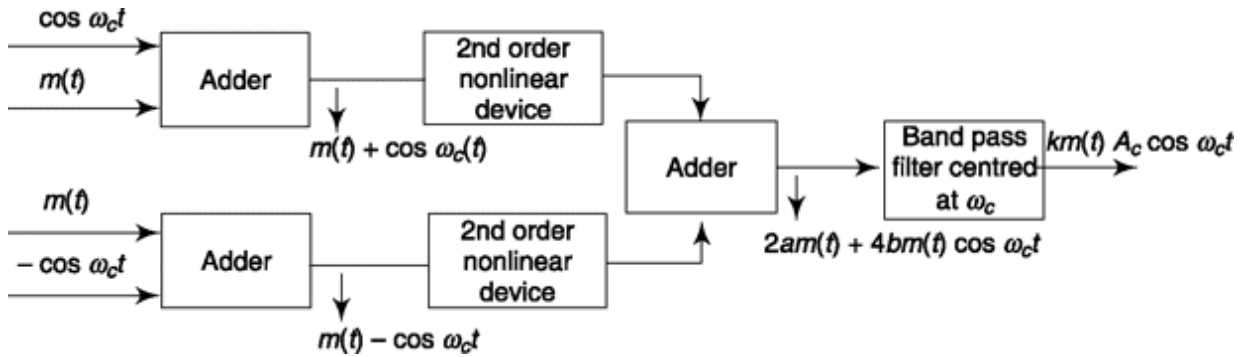


Fig. 26 Double sideband—suppressed carrier generation using nonlinear device.

Note that, for upper block input $v_1(t) = m(t) + \cos \omega_c t$ and lower block input is $v_2(t) = m(t) - \cos \omega_c t$. Thus, the summer output, $s(t) = a[v_1(t) - v_2(t)] + b[v_1^2(t) - v_2^2(t)]$

Substituting $v_1(t)$ and $v_2(t)$, expanding the square term and simplifying we get output as,

$$s(t) = 2am(t) + 4bm(t)\cos \omega_c t \quad (2.5)$$

The first term is the baseband signal while the second term is the desired DSB-SC signal. Using a BPF after summer block in Fig. 2.6 which is centred around ω_c with cutoff frequencies $\omega_c \pm \omega_m$ (ω_m is maximum frequency of message signal) we get the desired DSB-SC signal. Note that this arrangement though uses balanced modulator principle is not fully so as it generates $m(t)$ and requires a BPF to remove it. Refer to Example 2.1 for other DSB-SC generation technique.

Example 2.1

Consider the simple switching modulator circuits shown in Fig. 2.7a. The BPF passes frequency $\omega_c \pm \omega_m$ where ω_m is maximum frequency of message signal, ω_c is frequency with which switch is made on and off and on-off times are equal. Show if this arrangement can generate a DSB-SC signal. Show one circuit that can be used as a switch which can be operated by a sinusoidal carrier signal.

Solution

The switching action can be approximated by a pulse train (Prob. 1.59 of Chapter 1) as

$$s(t) = \frac{1}{2} + \frac{2}{\pi} \left(\cos \omega_c t - \frac{1}{3} \cos 3\omega_c t + \frac{1}{5} \cos 5\omega_c t - \frac{1}{7} \cos 7\omega_c t + \dots \right)$$

Now the message $m(t)$ will appear at the output when the switch is on and otherwise not. Mathematically, the output of the switch can be written as

$$y(t) = m(t)s(t) = m(t) \left[\frac{1}{2} + \frac{2}{\pi} \left(\cos \omega_c t - \frac{1}{3} \cos 3\omega_c t + \frac{1}{5} \cos 5\omega_c t - \frac{1}{7} \cos 7\omega_c t + \dots \right) \right]$$

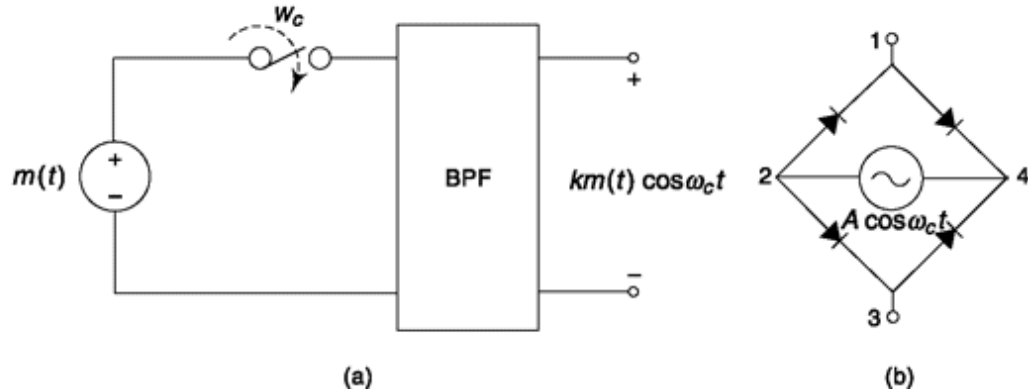


Fig. 2.7 (a) DSB-SC generation using switching circuit. (b) A switching circuit.

Thus, $y(t)$ has baseband signal as well as translated signal around w_c , $3w_c$, $5w_c$ etc. A BPF filter that passes $2w_c \pm w_m$ will bring out $-m(t)\cos w_c(t)$ which clearly is a DSB-SC signal. Figure 2.7b shows an electronic 8[1-3] in one half-cycle when all the diodes conduct (potential of 2 > potential 4) with zero input voltage fed to BPF. In the other half-cycle none of the diode conducts making terminals 1-3 open and entire $m(t)$ is available to BPF input. Note that, the diodes considered here are ideal.

However, if strength of carrier signal is larger than message signal we get close performance as discussed here.

Don't confuse the diode bridge circuit shown here with full-wave rectifier (FWR) you might have studied at some other course. Compare the orientation of diodes there and here. In FWR a pair of diode conducts in each half cycle.

2.2.2 Recovery of the Baseband signal: DsB-sC Demodulator

We have seen that for effective communication, a baseband signal requires frequency translation. We have also seen how a signal $m(t)$ has been translated out of its baseband through multiplication with $\cos \omega_c t$. The question to be addressed now—how is the baseband signal recovered or detected from the modulated signal? Here, we discuss two principles. At first, we discuss coherent technique that requires a carrier signal at the receiver (demodulator) side which is in coherence with the carrier at transmitter side. Next, we discuss noncoherent technique that though complicated does not require coherent carrier for recovery.

Coherent Detection

Here, the signal recovery is done by a reverse frequency translation by multiplying the translated signal with $\cos \omega_c t$. That such is the case may be seen by drawing spectral plots as in Fig. 2.3 or 2.4 and noting that the difference-frequency signal obtained by multiplying $m(t) \cos \omega_c t$ by $\cos \omega_c t$ is a signal whose spectral range is back at baseband. Alternatively, we may simply note that

$$[m(t) \cos \omega_c t] \cos \omega_c t = m(t) \cos^2 \omega_c t = m(t) \left(\frac{1}{2} + \frac{1}{2} \cos 2\omega_c t \right) \quad (2.6a)$$

$$= \frac{m(t)}{2} + \frac{m(t)}{2} \cos 2\omega_c t \quad (2.6b)$$

Thus, the baseband signal $m(t)$ reappears. We note, of course, that in addition to the recovered baseband signal there is a signal whose spectral range extends from $2f_c - f_M$ to $2f_c + f_M$. As a matter of practice, this latter signal cause no difficulty. For most commonly $f_c @ f_M$, and consequently the spectral range of this double-frequency signal and the baseband signal are widely separated. Therefore the double-frequency signal is easily removed by a low-pass filter. A block diagram of this demodulation scheme and frequency representation at input and output of each block is shown in Fig. 2.8.

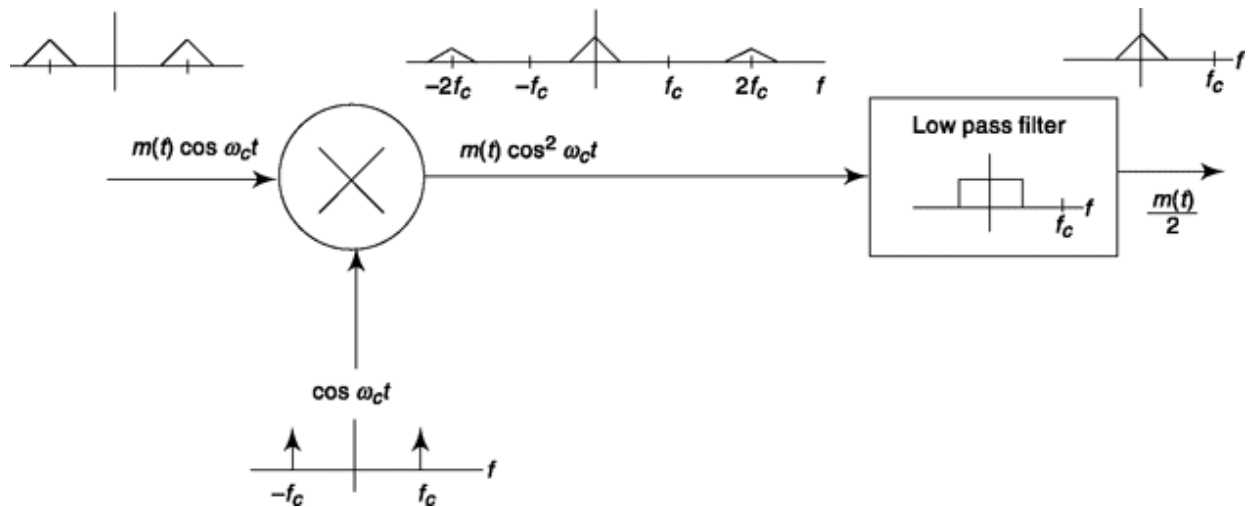


Fig. 2.8 Double sideband—suppressed carrier demodulation with frequency domain representation.

This method of signal recovery, for all its simplicity, is beset by an important inconvenience when applied in a physical communication system. Suppose that the auxiliary signal used for recovery differs in phase from the auxiliary signal used in the initial translation. If this phase angle is δ , then, as may be verified (Example 2.2), the recovered baseband waveform will be proportional to $m(t) \cos \delta$. Therefore, unless it is possible to maintain $\delta = 0$, the signal strength at recovery will suffer. If it should happen that $\delta = \pi/2$, the signal will be lost entirely. Or consider, for example, that δ drifts back and forth with time. Then in this case the signal strength will wax and wane, in addition, possibly, to disappearing entirely from time to time.

Alternatively, suppose that the recovery auxiliary signal is not precisely at frequency f_c but is instead at $f_c + Df$. In this case we may verify (Prob. 2.4) that the recovered baseband signal will be proportional to $m(t) \cos 2\pi Dft$, resulting in a signal which will wax and wane or even be entirely unacceptable if Df is comparable to, or larger than, the frequencies present in the baseband signal. This latter contingency is a distinct possibility in many an instance, since usually $f_c @ f_M$ so that a small percentage change in f_c will cause a Df which may be comparable or larger than f_M . In telephone or radio systems, an offset $Df < 30$ Hz is deemed acceptable.

We note, therefore, that signal recovery using a second multiplication requires that there be available at the recovery point a signal which is precisely **synchronous** with the corresponding auxiliary signal at the point of the first multiplication. In such a **synchronous** or **coherent** system a **fixed** initial phase discrepancy is of no consequence since a simple phase shifter will correct the matter. Similarly it is not essential that the recovery auxiliary

signal be sinusoidal (see Prob. 2.5). What is essential is that, in any time interval, the number of cycles executed by the two auxiliary-signal sources be the same. Of course, in a physical system, where some signal distortion is tolerable, some lack of synchronism may be allowed.

We'll discuss how to recover carrier at later part of the text.

squaring synchronizer

When the use of a common auxiliary signal is not feasible, it is necessary to resort to rather complicated means to provide a synchronous auxiliary signal at the location of the receiver. One commonly employed scheme is indicated in Fig. 2.9 that also shows corresponding frequency domain representation. To illustrate the operation of the synchronizer, we assume that the baseband signal is a sinusoidal $\cos w_m t$. Then the received signal is, say $s_i(t) = A \cos w_m t \cos w_c t$, with A a constant amplitude. This signal $s_i(t)$ does not have a spectral component at the angular frequency w_c . The output of the squaring circuit is

$$s_i^2(t) = A^2 \cos^2 w_m t \cos^2 w_c t \quad (2.7a)$$

$$= A^2 \left(\frac{1}{2} + \frac{1}{2} \cos 2w_m t \right) \left(\frac{1}{2} + \frac{1}{2} \cos 2w_c t \right) \quad (2.7b)$$

$$= \frac{A^2}{4} \left[1 + \frac{1}{2} \cos 2(w_c + w_m)t + \frac{1}{2} \cos 2(w_c - w_m)t + \cos 2w_m t + \cos 2w_c t \right] \quad (2.7c)$$

The filter selects the spectral component $(A^2/4) \cos 2w_c t$, which is then applied to a circuit which divides the frequency by a factor of 2. (See Prob. 2.6) This frequency division may be accomplished by using, for example, a bistable multivibrator. The output of the divider is used to demodulate (multiply) the incoming signal and thereby recover the baseband signal $\cos w_m t$.

Note that, a Phase Locked Loop (PLL) block before the frequency divider block in Fig. 2.9 will be able to track the carrier frequency (actually, $2w_c$) in a better way and helps in attaining synchronism.

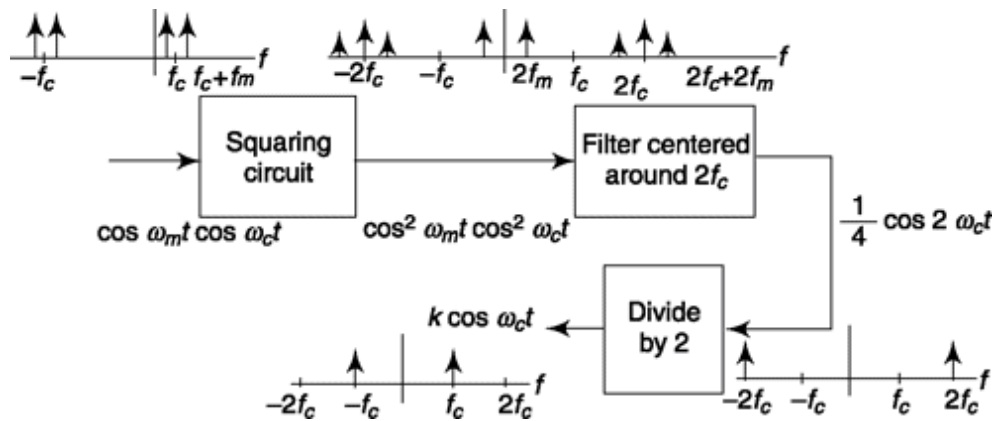


Fig. 2.9 A simple squaring synchronizer.

PLL is discussed in detail in Sec. 10.2 of Chapter 10. In fact, we devote Sec. 10.5.1 of Chapter 10 to discuss carrier recovery that includes other methods like Costas loop.

Example 2.2

Show the effect of phase error in coherent detection of DSB-SC signal

Solution

The DSB-SC signal $m(t)\cos \omega_c t$ is multiplied by a locally generated carrier in coherent detection. Let a phase-error of 9° is there between carriers of transmitter and receiver side. Then receiver carrier can be represented by $\cos(\omega_c t + 9^\circ)$.

After multiplication we get $s(t)$

$$= m(t) \cos \omega_c t [\cos(\omega_c t + \theta)]$$

$$\begin{aligned}
 &= \frac{m(t)}{2} [\cos(\omega_c t + \theta - \omega_c t) + \cos(\omega_c t + \theta - \omega_c t)] \\
 &= \frac{m(t)}{2} \cos\theta + \frac{m(t)}{2} \cos(2\omega_c t)
 \end{aligned}$$

A low pass filter that passes frequency $\pm\omega_m$ where ω_m is maximum frequency of message signal will have its output demodulated message signal as $\frac{m(t)}{2} \cos\theta$

Thus for a phase error of $\theta = \pi/2$, the output will be zero and if θ varies randomly the strength of received message signal will also vary.

SELF-TEST QUESTION

1. Is it true that frequency translation help in reducing size of antenna?
2. Is it true that diode bridge used in switching regulator based DSB-SC generation rectifies carrier signal?
3. Which of frequency or amplitude is affected due to phase error in synchronizing carrier in demodulation of DSB-SC signal?

2.3 AMPLITUDE MODULATION: DOUBLE SIDEBAND WITH CARRIER (DSB-C)

A frequency-translated signal from which the baseband signal is easily recoverable is generated by adding, to the product of baseband and carrier, the carrier itself and is named amplitude modulation. The presence of carrier gives it another name, Double SideBand with Carrier (DSB-C). In

demodulation carrier recovery is simpler if coherent detection is employed. Also one can employ noncoherent detection scheme for such modulation. If $m(t)$ represents the message signal and $A_c \cos w_c t$ the carrier, we can represent amplitude modulation (AM in short) as

$$v(t) = A_c[1 + m(t)] \cos w_c t \quad (2.8)$$

We observe, from Eq. (2.8) as well as from Fig. 2.10, that the resultant waveform is one in which the carrier $A_c \cos w_c t$ is **modulated in amplitude**.

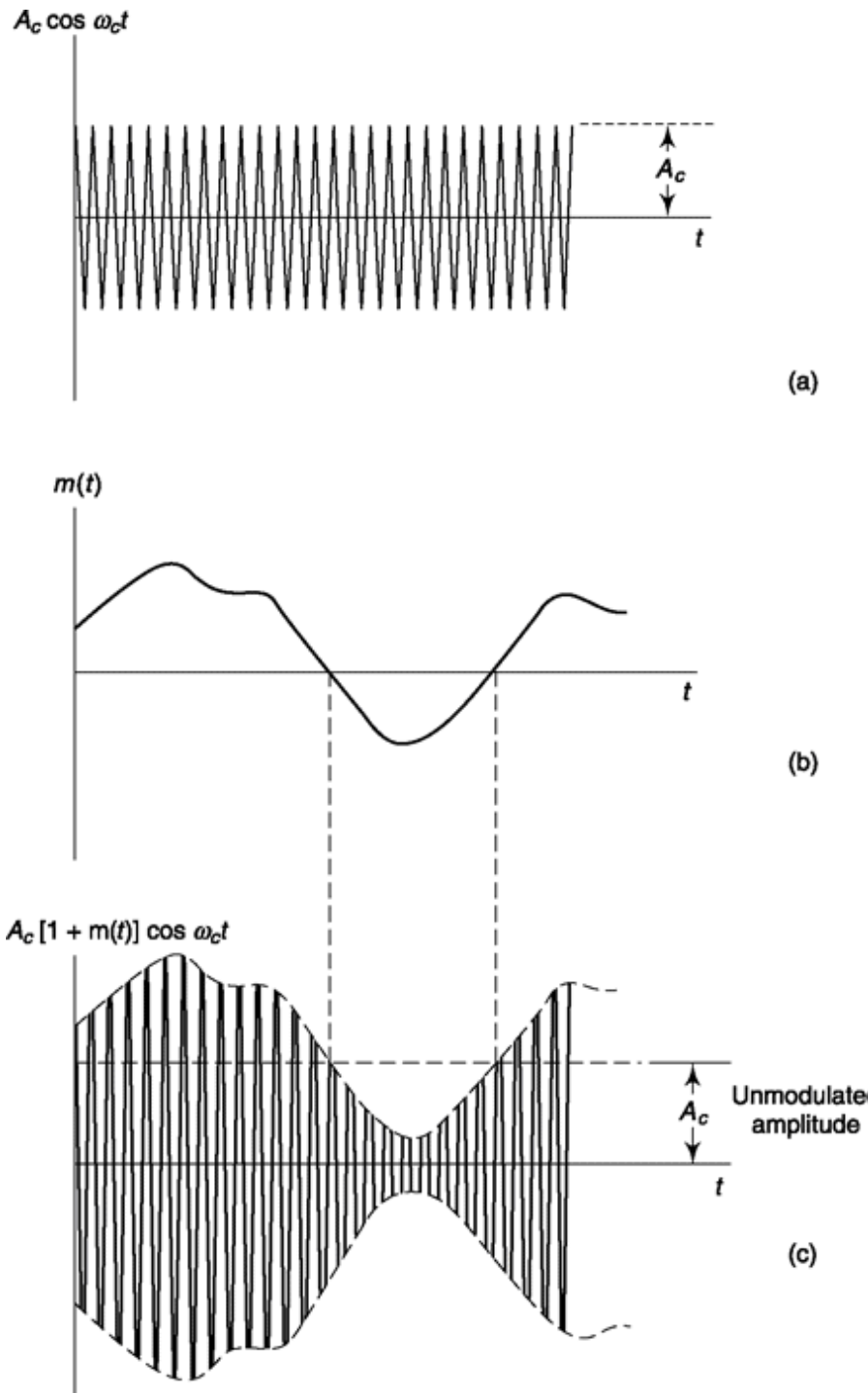


Fig. 2.10 (a) A sinusoidal carrier, (b) A modulating waveform, (c) The sinusoidal carrier in (a) modulated by the waveform in (b).

2.3.1 DsB-C Modulator

The DSB-C modulator can be generated as discussed in Sec. 2.2.1 by using a mixer (multiplier) that generates the sidebands as well as carrier signal and

the baseband message signal. For DSB-C modulator only the baseband message is to be filtered out. Also in any DSB-SC generator if carrier is added by a summer we get DSB-C modulation. However, for switching modulator (Example 2.1) a simpler circuit will do.

Consider the simple switching modulator circuits with only one diode as shown in Fig. 2.11. The BPF passes frequency $w_c \pm w_m$ where w_m is maximum frequency of message signal; carrier is represented by $A\cos w_c t$. Consider the diode is ideal and carrier is stronger than message. The diode conducts when the combined signal (message plus carrier) is positive. Since, carrier is stronger than message signal the switching of diode is regulated by carrier only. The switching action can be approximated by a pulse train (Prob. 1.59) as

$$s(t) = \frac{1}{2} + \frac{2}{\pi} \left[\cos \omega_m t - \frac{1}{3} \cos 3\omega_m t + \frac{1}{5} \cos 5\omega_m t - \frac{1}{7} \cos 7\omega_m t + \dots \right] \quad (2.9)$$

Now the combined signal message $m(t) + A\cos w_c t$ will appear at the output when the diode is switched on and otherwise not. Mathematically, diode output can be written as

$$y(t) = [m(t) + A \cos \omega_c t]s(t)$$

$$= [m(t) + A \cos \omega_c t] \left[\frac{1}{2} + \frac{2}{\pi} \left(\cos \omega_c t - \frac{1}{3} \cos 3\omega_c t + \frac{1}{5} \cos 5\omega_c t - \frac{1}{7} \cos 7\omega_c t + \dots \right) \right]$$

or $y(t) = \frac{m(t)}{2} + \frac{A}{2} \cos \omega_c t + \frac{2}{\pi} m(t) \cos \omega_c t + \frac{2A}{\pi} \cos \omega_c^2 t - \dots$

Thus $y(t)$ has baseband signal (1st), a dc term (from 4th), carrier (2nd), and higher harmonics of carrier. The BPF filter that passes $\omega_c \pm \omega_m$ will bring out $\frac{2}{\pi} m(t) \cos \omega_c t$ and the carrier component $\frac{A}{2} \cos \omega_c t$ which clearly is an AM or DSB-C signal.

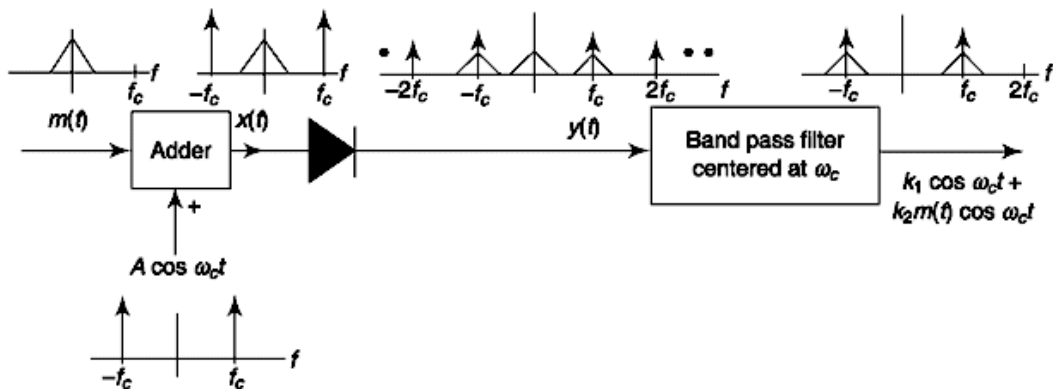


Fig. 2.11 An AM (DSB-C) modulator and its frequency domain representation.

2.3.2 DsB-C Demodulator

Envelope Detector

The merit of the amplitude-modulated carrier signal is the ease with which the baseband signal can be recovered. This is accomplished with the simple circuit of Fig. 2.12a, which consists of a diode **D** and the resistor-capacitor **RC** combination. We now discuss the operation of this circuit briefly and qualitatively. For simplicity, we assume that the amplitude-modulated carrier which is applied at the input terminals is supplied by a voltage source of zero internal impedance. We assume further that the diode is ideal, i.e. of zero or infinite resistance, depending on whether the diode current is positive or the diode voltage negative.

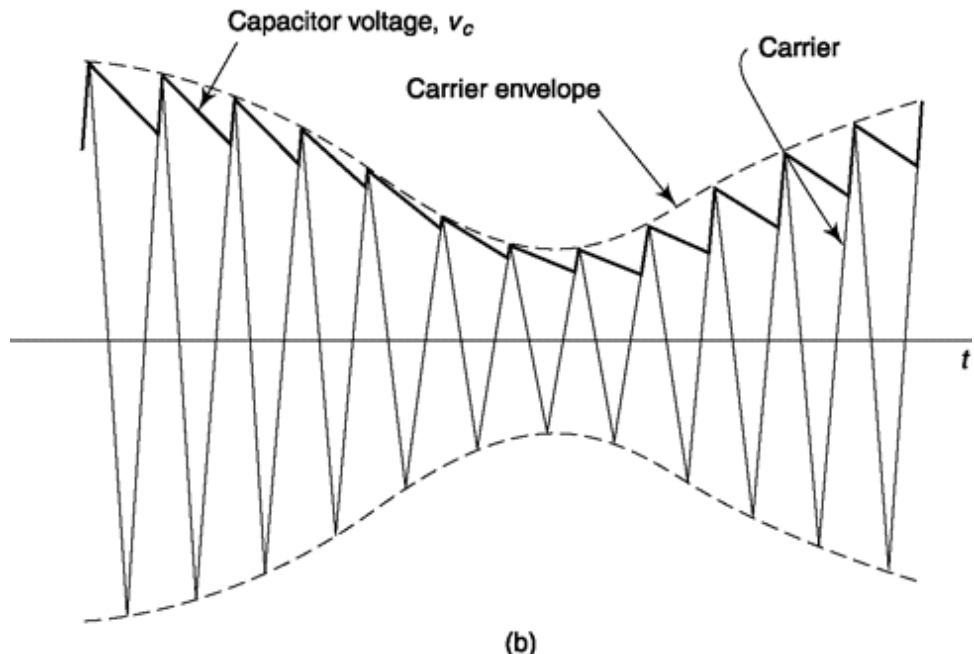
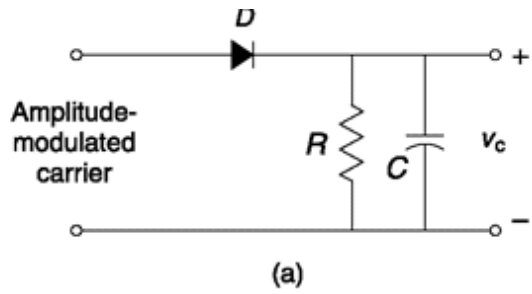


Fig. 2.12 (a) A demodulator for an AM signal, (b) Input waveform and output voltage v_c across capacitor.

Let us initially assume that the input is of fixed amplitude and that the resistor R is not present. In this case, the capacitor charges to the peak positive voltage of the carrier. The capacitor holds this peak voltage, and the diode would not again conduct. Suppose now that the input-carrier amplitude is increased. The diode again conducts, and the capacitor charges to the new higher carrier peak. In order to allow the capacitor voltage to follow the carrier peaks when the carrier amplitude

is decreasing, it is necessary to include the resistor R , so that the capacitor may discharge. In this case the capacitor voltage v_c has the form shown in Fig. 2.12b. The capacitor charges to the peak of each carrier cycle and decays slightly between cycles. The time constant RC is selected so that the change in v_c between cycles is at least equal to the decrease in carrier

amplitude between cycles. This constraint on the time constant RC is explored in Prob 2.7.

It is seen that the voltage v_c follows the carrier envelope except that v_c also has superimposed on it a sawtooth waveform of the carrier frequency. In Fig. 2.12b the discrepancy between v_c and the envelope is greatly exaggerated. In practice, the normal situation is one in which the time interval between carrier cycles is extremely small in comparison with the time required for the envelope to make a sizeable change. Hence, v_c follows the envelope much more closely than is suggested in the figure. Further, again because the carrier frequency is ordinarily much higher than the highest frequency of the modulating signal, the sawtooth distortion of the envelope waveform is very easily removed by a filter.

A General Approach to rectifier Detector

Using switching principle discussed in the previous section and in Example 2.1, we can present rectifier based detection in a more general way. We use Fig. 2.12b to describe the scheme. Note that we have a LPF with cutoff frequency w_m followed by capacitor which blocks dc component. The input to LPF is the rectifier output which is periodic pulse train multiplied DSB-C modulated signal and can be written as (using Eq. 2.9)

$$y(t) = [A + m(t)] \cos \omega_c t \left[\frac{1}{2} + \frac{2}{\pi} \left(\cos \omega_c t - \frac{1}{3} \cos 3\omega_c t + \frac{1}{5} \cos 5\omega_c t - \frac{1}{7} \cos 7\omega_c t + \dots \right) \right] \quad (2.10)$$

Thus $y(t)$ has a dc term A/p coming from $\cos^2 \omega_c t$ term and $m(t)$ between 0 to w_c which is passed by LPF. We can apply a dc blocker capacitor in series after this to remove the dc term and get back the message signal.

2.3.3 Maximum Allowable Modulation for rectifier Detection

If we are to avail ourselves of the convenience of demodulation by the use of the simple diode circuit of Fig. 2.12, we must limit the extent of the modulation of the carrier. That such is the case may be seen from Fig. 2.13. In Fig. 2.13a is shown a carrier modulated by a sinusoidal signal. It is apparent that the envelope of the carrier has the waveshape of the

modulating signal. The modulating signal is sinusoidal; hence $m(t) = A_m \cos \omega_m t$, where m is a constant. Equation (2.8) becomes

$$v(t) = A_c(1 + A_m \cos \omega_m t) \cos \omega_c t \quad (2.11)$$

In Fig. 2.13b we have shown the situation which results when, in Eq. (2.11), we adjust $A_m > 1$. Observe now that the diode demodulator which yields as an output the positive envelope (a negative envelope if the diode is reversed) will not reproduce the sinusoidal modulating waveform. In this latter case, where $A_m > 1$, we may recover the modulating waveform but not with the diode modulator. Recovery would require the use of a coherent demodulation scheme such as was employed in connection with the signal furnished by a multiplier.

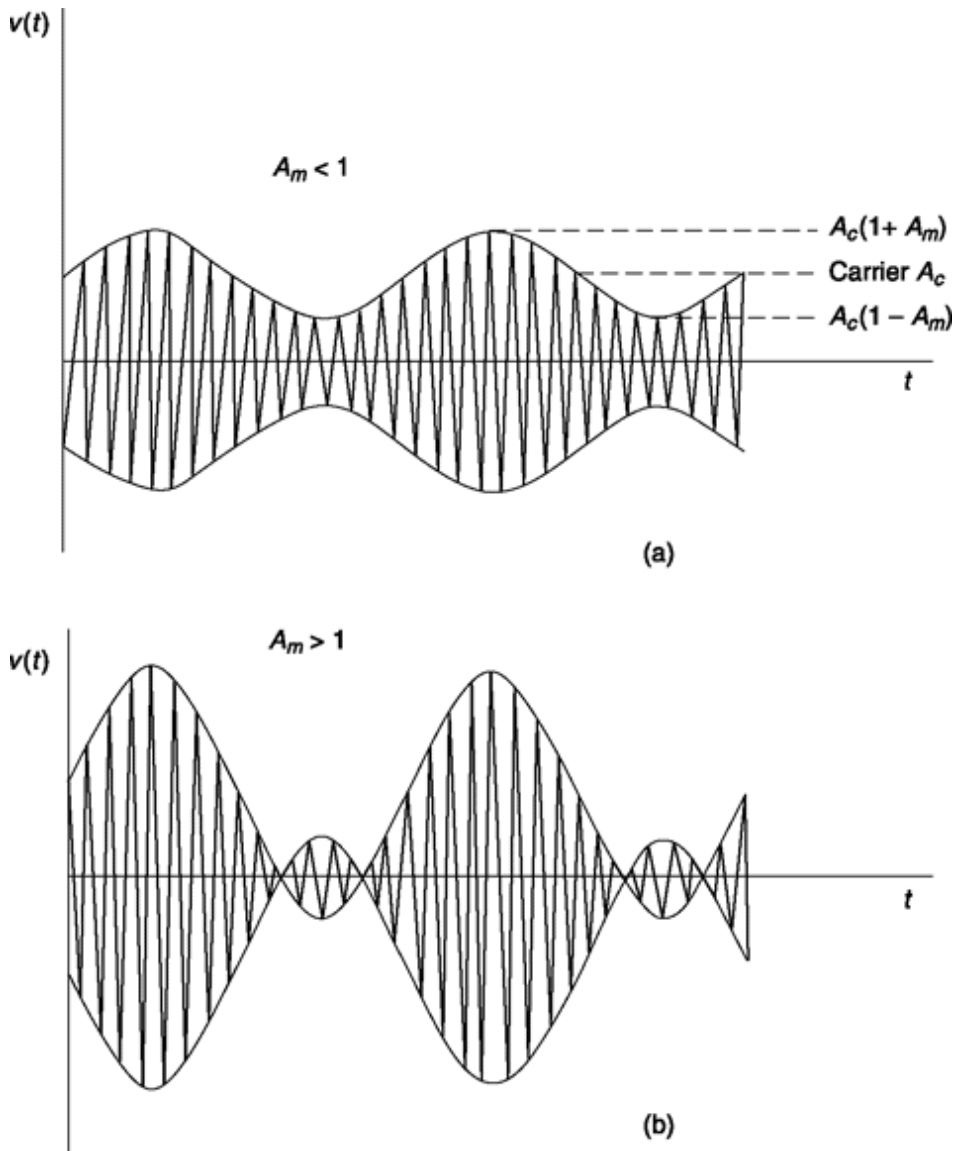


Fig. 2.13 (a) A sinusoidally modulated carrier ($A_m < 1$). (b) A carrier overmodulated ($A_m > 1$) by a sinusoidal modulating waveform.

It is therefore necessary to restrict the excursion of the modulating signal in the direction of decreasing carrier amplitude to the point where the carrier amplitude is just reduced to zero. No such similar restriction applies when the modulation is increasing the carrier amplitude. With sinusoidal modulation, as in Eq. (2.11), we require that $|A_m| < 1$. More generally in Eq. (2.8) we require that the maximum negative excursion of $m(t)$ be **-1**.

The extent to which a carrier has been amplitude-modulated is expressed in terms of a **percentage modulation**. Let A_c , $A_c(\max)$ and $A_c(\min)$, respectively, be the unmodulated carrier amplitude and the maximum and

minimum carrier levels. Then if the modulation is symmetrical, the percentage modulation is defined as P , given by

$$\frac{P}{100\%} = \frac{A_c(\max) - A_c}{A_c} = \frac{A_c - A_c(\min)}{A_c} = \frac{A_c(\max) - A_c(\min)}{2A_c} \quad (2.12)$$

In the case of sinusoidal modulation, given by Eq. (2.11) and shown in Fig. 2.13, $P = A_m \times 100$ percent.

Having observed that the signal $m(t)$ may be recovered from the waveform $A_c[1 + m(t)] \cos w_c t$ by the simple circuit of Fig. 2.12a, it is of interest to note that a similar easy recovery of $m(t)$ is not possible from the waveform $m(t) \cos w_c t$. That such is the case is to be seen from Fig. 2.14. Figure 2.14a shows the carrier signal. The modulation or baseband signal $m(t)$ is shown in Fig. 2.14b, and the product $m(t) \cos w_c t$ is shown in Fig. 2.14c. We note that the envelope in Fig. 2.14c has the waveform not of $m(t)$ but rather of $|m(t)|$, the ***absolute value*** of $m(t)$. Observe the reversal of phase of the carrier in Fig. 2.14c whenever $m(t)$ passes through zero.

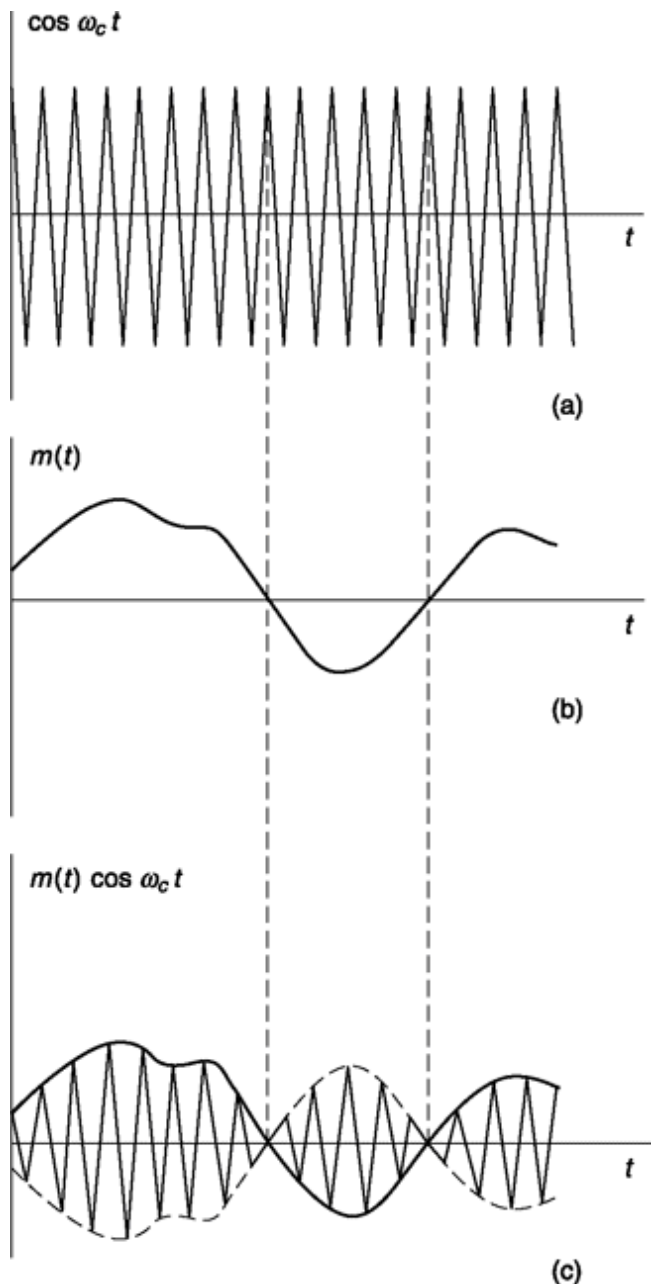
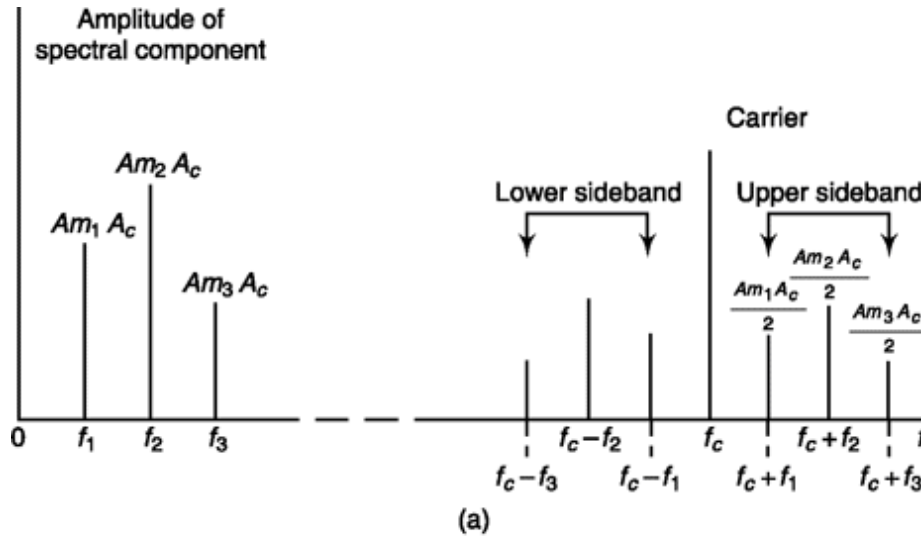


Fig. 2.14 (a) A carrier $\cos \omega_c t$. (b) A baseband signal $m(t)$. (c) The product $m(t) \cos \omega_c t$ and its envelope.

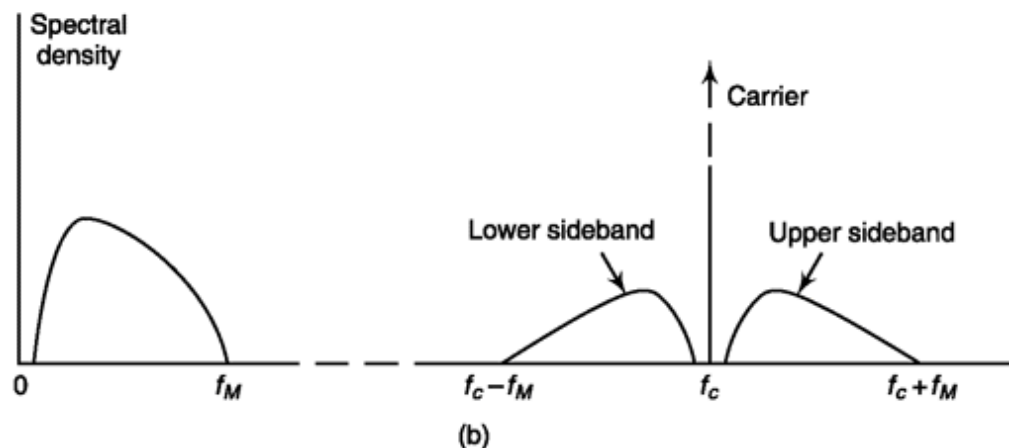
2.3.4 spectrum and power Efficiency

The spectrum of an amplitude-modulated signal is similar to the spectrum of a signal which results from multiplication except, of course, that in the former case a carrier of frequency f_c is present. If in Eq. (2.8) $m(t)$ is the superposition of three sinusoidal components $m(t) = Am_1 \cos w_1 t + Am_2 \cos$

$w_2 t + A m_3 \cos w_3 t$, then the (one-sided) spectrum of this baseband signal appears as at the left in Fig. 2.15a. The spectrum of the modulated carrier is shown at the right. The spectral lines at the sum frequencies $f_c + f_1$, $f_c + f_2$, and $f_c + f_3$ constitute the **upper-sideband** frequencies. The spectral lines at the difference frequencies constitute the **lower sideband**.



(a)



(b)

Fig. 2.15 (a) At left the one-sided spectrum of $m(t)A_C$, where $m(t)$ has three spectral components. At right the spectrum of $A_C[i + m(t)] \cos 2\pi f_c t$. (b) Same as in (a) except $m(t)$ is a nonperiodic signal and the vertical axis is spectral density rather than spectral amplitude.

The spectrum of the baseband signal and modulated carrier are shown in Fig. 2.15b for the case of a bandlimited nonperiodic signal of finite energy. In this figure the ordinate is the spectral density,

i.e. the magnitude of the Fourier transform rather than the spectral amplitude, and consequently the carrier is represented by an impulse.

At this point we discuss something very important related to AM transmission. This is the issue of power associated with AM modulation. The basic equation of AM modulation given in Eq. 2.8 is

$$v(t) = A_c[1 + m(t)]\cos \omega_c t$$

Expanding above,

$$v(t) = A_c \cos \omega_c t + A_c m(t) \cos \omega_c t \quad (2.13)$$

The first term in Eq. (2.13) represents power needed to transmit the carrier, $P_c = AC / 2$ and the 2nd term represents the power transmitted in the sidebands, P_s (say). Since, carrier power does not carry any message information but helps in demodulation process, we consider P_s is not useful from message point of view. The useful power is the power in sideband, P_s . The power efficiency in AM transmission is thus given as a ratio of useful power to total power

$$\eta = \frac{P_s}{P_c + P_s} = \frac{P_s}{0.5 A_c^2 + P_m} \quad (2.14)$$

For tone modulation, discussed in the previous section, we can write $m(t) = A_m \cos \omega_m t$ where $|m| \leq 1$ and is known as depth of modulation. Then, (Eq. 2.13) becomes

$$\begin{aligned} v(t) &= A_c \cos \omega_c t + A_c A_m \cos \omega_c t \cos \omega_m t \\ &= A_c \cos \omega_c t + \frac{A_c A_m}{2} [\cos(\omega_c + \omega_m)t + \cos(\omega_c - \omega_m)t] \end{aligned}$$

$$\text{Thus, useful sideband power } P_S = \frac{1}{2} \left[\frac{(A_c A_m)^2}{2} + \frac{(A_c A_m)^2}{2} \right] = 0.5(A_c A_m)^2$$

Substituting in (Eq. 2.14), $\eta = \frac{A_m^2}{2 + A_m^2}$. Since the maximum $A_m = 1$, maximum power efficiency that

can be achieved in case of tone modulation is $1/3 = 33\%$ which for practical cases have a lower figure than this. Thus, we find the simplicity in AM modulation comes with a major burden of high power budget.

Note that, using coherent detection, i.e. multiplying the modulated signal with $\cos \omega_c t$, we can recover message signal for any value of modulation index and η can be very high. [Check MATLAB Experiment 16.] But then the simplicity of the envelop detector will not be of any use.

Example 2.3

The input to an envelope detector of a tone modulated signal is given as $v(t) = A_c[1 + A_m \cos \omega_m t] \cos \omega_c t$. Find the maximum value of time constant RC of the detector that can always follow the message envelop.

Solution

Refer to Fig. 2.12. If the peak voltage across capacitor in any time $t = t_1$ is V_1 then the discharging voltage till the next high of carrier signal comes at $t = t_2$ can be written as

$$v(t) = V_1 e^{-t/(RC)} \quad t_1 \leq t \leq t_2 \text{ and } t_2 - t_1 \text{ is of the order of } (1/T) \text{ where } T = 2\pi/\omega_c$$

From power series expansion of the exponential term,

$$v(t) = V_1 \left[1 - \frac{t}{RC} + \frac{1}{2!} \left(\frac{t}{RC} \right)^2 - \dots \right]$$

Since in the above interval $RC \gg t$, neglecting higher

$$\text{order term } v(t) = V_1 \left[1 - \frac{t}{RC} \right] \quad (2.15)$$

The requirement is that the rate of discharge, i.e. magnitude of slope of $v(t)$ must be more than that of envelop.

For tone modulated AM, envelope $v(t) = [1 + A_m \cos \omega_m t_1]$

$$\text{Then } \frac{dv(t)}{dt} = -A_c A_m \sin \omega_m t$$

The magnitude of slope across the capacitor

$$\left| \frac{dv(t)}{dt} \right| = \frac{V_1}{RC} = \frac{A_c}{RC} [1 + A_m \cos \omega_m t_1]$$

And the requirement is $\frac{A_c}{RC} [1 + A_m \cos \omega_m t_1] \leq A_c A_m \sin \omega_m t$

Since, $t_2 - t_1$ is small compared to message time period $2\pi/\omega_m$, we may write,

$$\frac{A_c}{RC} [1 + A_m \cos \omega_m t_1] = \frac{A_c}{RC} [1 + A_m \cos \omega_m t]$$

Hence, the inequality becomes $\frac{A_c}{RC} [1 + A_m \cos \omega_m t] \leq A_c A_m \sin \omega_m t$

$$\text{or } RC \leq \frac{1 + A_m \cos \omega_m t}{A_m \omega_m \sin \omega_m t} \quad (2.16)$$

Since the above holds for every t , RC should be less than equal to what we get when RHS goes minimum for a particular value of t . Differentiating RHS with t and equating it to zero, we get $\cos \omega_m t = -A_m$. Substituting and simplifying,

$$RC \leq \frac{1}{\omega_m} \left(\frac{\sqrt{1 - A_m^2}}{A_m} \right) \quad (2.17)$$

Example 2.4

Find transmission power efficiency for a tone modulated signal when modulated index is 0.25, 0.5 and 0.75.

Solution

From Sec. 2.3.4, power efficiency

$$\eta = \frac{A_m^2}{2 + A_m^2} \times 100\%$$

Substituting,	for $A_m = 0.25$,	$\eta = 3.03\%$
	for $A_m = 0.5$,	$\eta = 11.11\%$
	for $A_m = 0.75$,	$\eta = 21.95\%$

Note that we have already seen that the best result obtained for $A_m = 1$ is 33.33%.

SELF-TEST QUESTION

4. Is it true that use of simple rectifier-low pass filter based demodulator circuit a big advantage for AM?
5. How can message be recovered from an AM signal if modulation index is greater than one?

6. Is it true that for envelop detector based AM system power efficiency cannot exceed 33%?

2.4 SINGLE SIDEBAND MODULATION (SSB)

We have seen that the baseband signal may be recovered from a double-sideband suppressed-carrier signal by multiplying a second time, with the same carrier. It can also be shown that the baseband signal can be recovered in a similar manner even if only one sideband is available. Suppose a spectral component of the baseband signal is multiplied by a carrier $\cos w_c t$, giving rise to an upper sideband at $w_c + w$ and a lower sideband at $w_c - w$. Now let us assume that we have filtered out one sideband and are left with, say, only the upper sideband at $w_c + w$. If now this sideband signal is again multiplied by $\cos w_c t$, we shall generate a signal at $2w_c + w$ and the original baseband spectral component at w . If we had used the lower sideband at $w_c - w$, the second multiplication would have yielded a signal at $2w_c - w$ and again restored the baseband spectral component. Since it is possible to recover the baseband signal from a single sideband, there is an obvious advantage in doing so, since spectral space is used more economically. In principle, two single-sideband (abbreviated SSB) communications systems can now occupy the spectral range previously occupied by a single amplitude-modulation system or a double-sideband suppressed-carrier system.

The baseband signal may **not** be recovered from a single-sideband signal by the use of a diode modulator. That such is the case is easily seen by considering, for example, that the modulating signal is a sinusoid of frequency f . In this case, the single-sideband signal will consist also of a single sinusoid of frequency, say, $f_c + f$, and there is no amplitude variation at all at the baseband frequency to which the diode modulator can respond.

Now, let us try to find a mathematical representation of SSB signal. This will also give us idea about how to generate an SSB signal. We start with the discussion of how to represent the lower sideband (SSB-L). Refer to Fig. 1.26. We find, SSB-L can be obtained from DSB provided it is multiplied with a transfer function as shown in Fig. 2.16(c). This can be derived from sgn function which we used in Example 1.21 and 1.22 of Chapter 1. If $M(w)$ is baseband representation of original message $m(t)$, $M_{DSB}(w)$ is its DSB

representation (multiplied by carrier $\cos \omega_c t$) and $M_{DSB-L}(\omega)$ is the spectrum of lower sideband of SSB signal, we can write,

$$\begin{aligned}
M_{DSB}(\omega) &= 0.5[M(\omega + \omega_c) + M(\omega - \omega_c)] \\
M_{SSB-L}(\omega) &= 0.5M_{DSB}(\omega)[\operatorname{sgn}(\omega + \omega_c) - \operatorname{sgn}(\omega - \omega_c)] \\
&= 0.25[M(\omega + \omega_c) + M(\omega - \omega_c)] [\operatorname{sgn}(\omega + \omega_c) - \operatorname{sgn}(\omega - \omega_c)] \\
&= 0.25[-M(\omega + \omega_c)\operatorname{sgn}(\omega - \omega_c) + M(\omega - \omega_c)\operatorname{sgn}(\omega + \omega_c) \\
&\quad + M(\omega + \omega_c)\operatorname{sgn}(\omega + \omega_c) - M(\omega - \omega_c)\operatorname{sgn}(\omega - \omega_c)]
\end{aligned} \tag{2.18}$$

Now, $-\operatorname{sgn}(\omega - \omega_c) = 1$ for $\omega < \omega_c$ and $\operatorname{sgn}(\omega + \omega_c) = 1$ for $\omega > -\omega_c$. Using these two first terms within third bracket,

$$\begin{aligned}
M_{SSB-L}(\omega) &= 0.25[M(\omega + \omega_c) + M(\omega - \omega_c)] + 0.25[M(\omega + \omega_c)\operatorname{sgn}(\omega + \omega_c) \\
&\quad - M(\omega - \omega_c)\operatorname{sgn}(\omega - \omega_c)]
\end{aligned} \tag{2.19}$$

The first term within bracket on inverse transform gives familiar DSB-SC signal $0.5m(t)\cos \omega_c t$. Let us see what the second term offers. Refer to our discussion of Example 1.21 and 1.22 of Chapter 1.

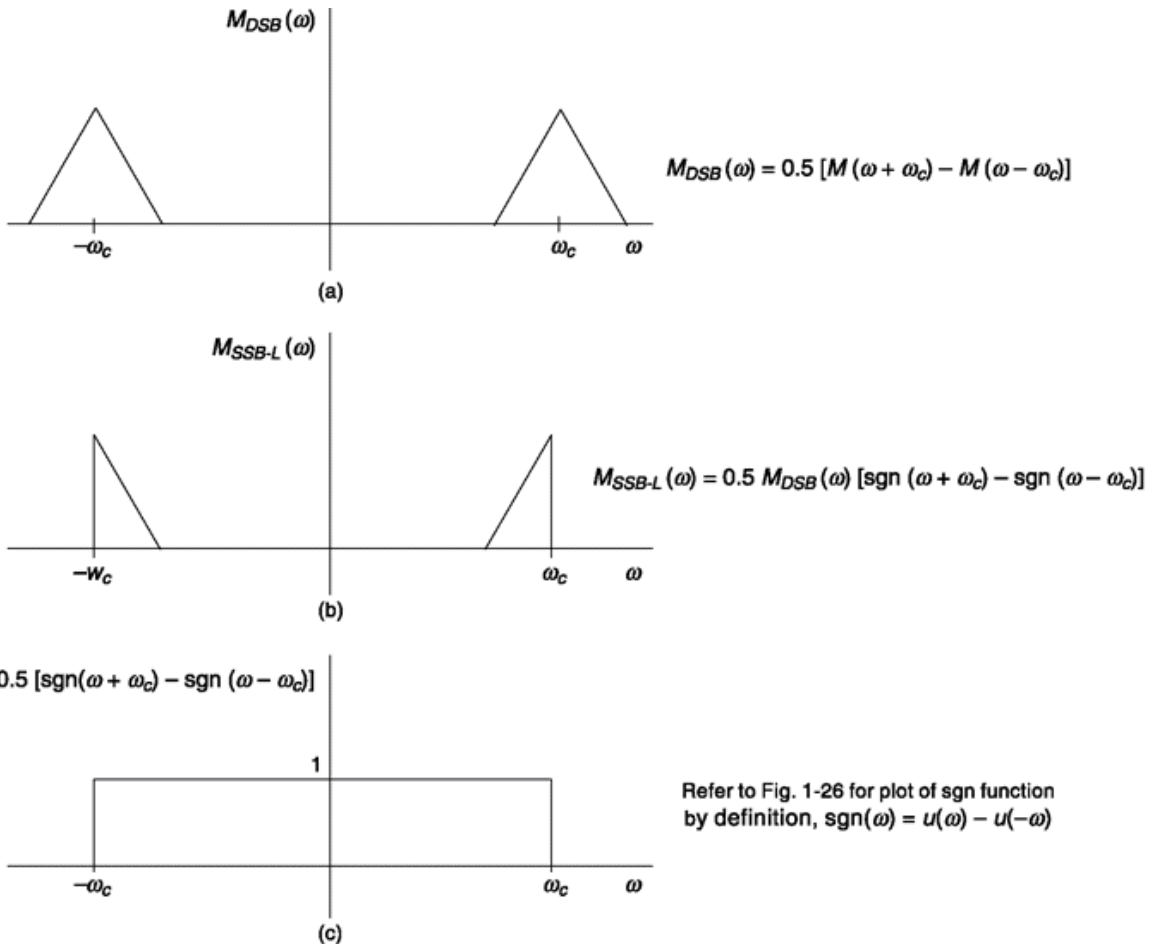


Fig. 2.16 SSB spectrum, lower sideband (SSB-L) from DSB spectrum.

Any signal $m(t)$ when delayed by a phase of $\pi/2$ is said to have undergone Hilbert transform (which is passing through a filter having impulse response $h(t) = 1/(\pi t)$ and has frequency representation

$$-j\operatorname{sgn}(\omega)M(\omega) \xrightarrow[F^{-1}]{F} m_h(t) \quad \text{where } m_h(t) \text{ is } m(t) \text{ delayed by } \pi/2$$

$$\text{From Hilbert transformer relation, } m_h(t) = \frac{1}{\pi} \int_{-\infty}^{\infty} \frac{m(\tau)}{t - \tau} d\tau \quad (2.20)$$

From frequency shifting property of Fourier transform (Eq. 1.120)

$$-j\operatorname{sgn}(\omega - \omega_c)M(\omega - \omega_c) \xrightarrow[F^{-1}]{F} m_h(t) e^{j\omega_c t} \quad (2.21a)$$

$$\text{and } -j\operatorname{sgn}(\omega + \omega_c)M(\omega + \omega_c) \xrightarrow[F^{-1}]{F} m_h(t) e^{-j\omega_c t} \quad (2.21b)$$

Using Eq. (2.21) in Eq. (2.19) we get inverse Fourier transform of $M_{SSB-L}(\omega)$ as

$$\begin{aligned} m_{SSB-L}(t) &= 0.5m(t)\cos \omega_c t + \frac{0.25}{-j} [m_h(t)e^{-j\omega_c t} - m_h(t)e^{j\omega_c t}] \\ &= 0.5m(t)\cos \omega_c t + \frac{0.25m_h(t)}{-j} [-2j\sin \omega_c t] \end{aligned}$$

or, $m_{SSB-L}(t) = 0.5m(t)\cos \omega_c t + 0.5m_h(t)\sin \omega_c t$ (2.22a)

Similarly, the SSB upper sideband can be represented as

$$m_{SSB-H}(t) = 0.5m(t)\cos \omega_c t - 0.5m_h(t)\sin \omega_c t \quad (2.22b)$$

SSB finds its application in telephone communication.

2.4.1 SSB Modulator

SSB Modulation by Multistage Filtering

Multistage filtering as a concept is used in SSB modulation to overcome the practical constraint associated with design of very sharp cutoff filter. Refer to Fig. 2.17. Here the baseband signal and a carrier are applied to a balanced modulator. The output of the balanced modulator bears both the upper- and lower-sideband signals. One or the other of these signals is then selected by a filter. The filter is a bandpass filter whose passband encompasses the frequency range of the sideband selected. The filter must have a cutoff sharp enough to separate the selected sideband from the other sideband. The frequency separation of the sidebands is twice the frequency of the lowest frequency spectral components of the baseband signal. Human speech contains spectral components as low as about 70 Hz. However, to alleviate the sideband filter selectivity requirements in an SSB system, it is common to limit the lower spectral limit of speech to about 300 Hz. It is found that such restriction does not materially affect the intelligibility of speech. Similarly, it is found that no serious distortion results if the upper limit of the speech spectrum is cut off at about 3000 Hz. Such restriction is advantageous for the purpose of conserving bandwidth. Altogether, then, a typical sideband filter has a passband which, measured from f_c , extends from about 300 to 3000 Hz and in which range its response is quite flat. Outside this passband the response falls off sharply, being down about 40 dB at 4000 Hz and rejecting the unwanted sideband also be at least 40 dB. The filter may also serve, further, to suppress the carrier itself. Of course, in principle, no carrier should appear at the output of a balanced modulator. In practice,

however, the modulator may not balance exactly, and the precision of its balance may be subject to some variation with time. Therefore, even if a pilot carrier is to be transmitted, it is well to suppress it at the output of the modulator and to add it to the signal at a later point in a controllable manner.

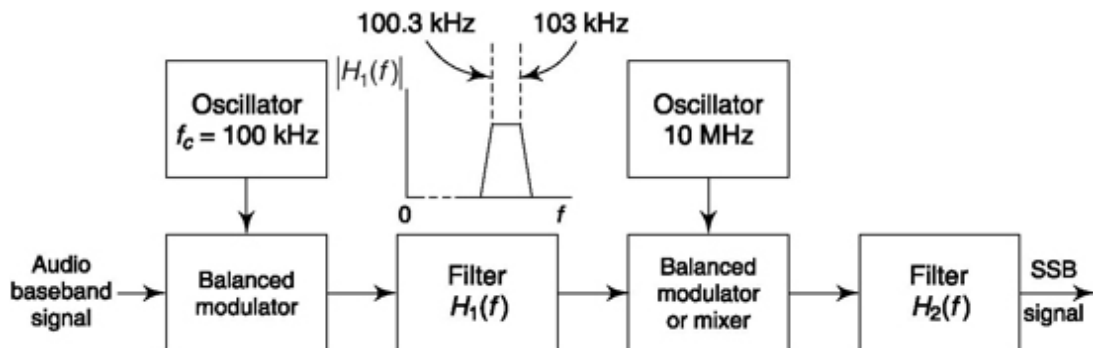


Fig. 2.17 Block diagram of the filter method of generating a single-sideband signal.

Now consider that we desire to generate an SSB signal with a carrier of, say, 10 MHz. Then we require a passband filter with a selectivity that provides 40 dB of attenuation within $2 \times 300 \text{ Hz} = 600 \text{ Hz}$ at a frequency of 10 MHz, a percentage frequency change of 0.006 percent. Filters with such sharp selectivity are very elaborate and difficult to construct. For this reason, it is customary to perform the translation of the baseband signal to the final carrier frequency in several stages. Two such stages of translation are shown in Fig. 2.17. Here we have selected the first carrier to be of frequency 100 kHz. The upper sideband, say, of the output of the balanced modulator ranges from 100.3 to 103 kHz. The filter following the balanced modulator which selects this upper sideband need now exhibit a selectivity of only a hundredth of the selectivity (40 dB in 0.6 percent frequency change) required in the case of a 10 MHz carrier. Now let the filter output be applied to a second balanced modulator, supplied this time with a 10 MHz carrier. Let us again select the upper sideband. Then the second filter must provide 40 dB of attenuation in a frequency range of $2 \times 100.3 \text{ kHz} = 200.6 \text{ kHz}$, which is nominally 2 percent of the carrier frequency.

If the second frequency-translating device in Fig. 2.17 were a mixer rather than a multiplier, then in addition to the upper and lower sidebands, the output would contain a component encompassing the range 100.3 to 103 kHz as well as the 10 MHz carrier. The range 100.3 to 103 kHz is well out of the range of the second filter intended to pass the range 10,100,300 to 10,103,000 Hz. And it is realistic to design a filter which will suppress the 10 MHz carrier, since the carrier frequency is separated from the lower edge

of the upper sideband (10,100,300) by nominally a 1-percent frequency change.

Altogether, then, we note in summary that when a single-sideband signal is to be generated which has a carrier in the megahertz or tens-of-megahertz range, the frequency translation is to be done in more than one stage—frequently two but not uncommonly three. If the baseband signal has spectral components in the range of hundreds of hertz or lower (as in an audio signal), the first stage invariably employs a balanced modulator, while succeeding stages may use mixers.

SSB Modulation by phase shift

This alternative scheme comes from our mathematical presentation of SSB signal in Eq. (2.22). Refer to Fig. 2.18. The carrier signals of angular frequency ω_c which are applied to the modulators differ in phase by 900° . Similarly, the baseband signal, before application to the modulators, is passed through a 900° phase-shifting network so that there is a 900° phase shift between any spectral component of the baseband signal applied to one modulator and the like-frequency component applied to the other modulator.

To see most simply how the arrangement of Fig. 2.18 operates, let us assume that the baseband signal is sinusoidal and appears at the input to one modulator as $\cos \omega_m t$ and hence as $\sin \omega_m t$ at the other. Let the carrier be $\cos \omega_c t$ at one modulator and $\sin \omega_c t$ at the other. Then the outputs of the balanced modulators (multipliers) are

$$\cos \omega_m t \cos \omega_c t = \frac{1}{2} [\cos (\omega_c - \omega_m)t + \cos (\omega_c + \omega_m)t] \quad (2.23)$$

$$\sin \omega_m t \sin \omega_c t = \frac{1}{2} [\cos (\omega_c - \omega_m)t - \cos (\omega_c + \omega_m)t] \quad (2.24)$$

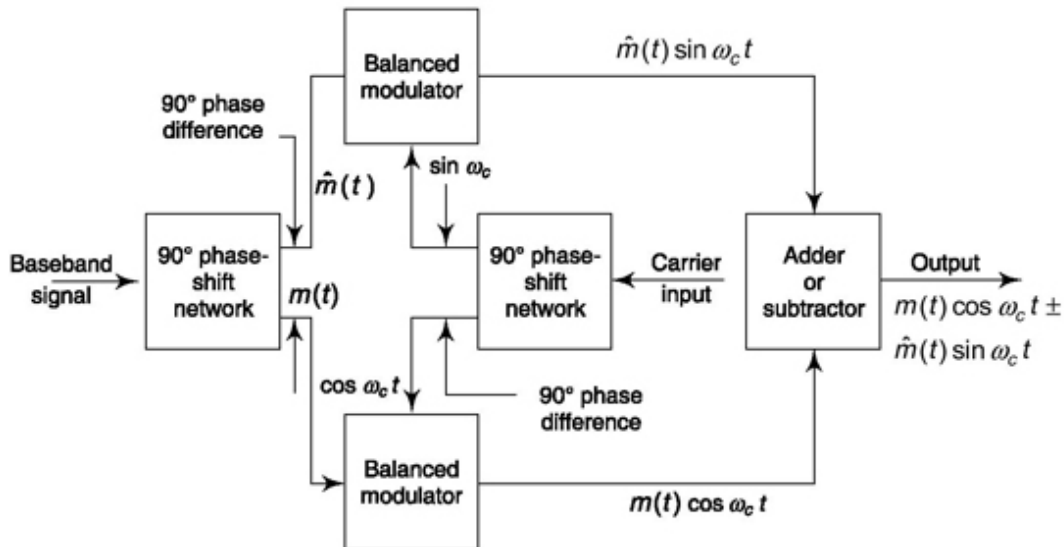


Fig. 2.18 A method of generating a single-sideband signal using balanced modulators and phase shifters.

If these waveforms are added, the lower sideband results; if subtracted, the upper sideband appears at the output. In general, if the modulation $m(t)$ is given by

$$m(t) = \sum_{i=1}^m A_i \cos(\omega_i t + \theta_i) \quad (2.25)$$

then, using Fig. 2.18, we see that the output of the SSB modulator is in general

$$m(t) \cos \omega_c t \pm \hat{m}(t) \sin \omega_c t \quad (2.26)$$

where

$$\hat{m}(t) \equiv \sum_{i=1}^m A_i \sin(\omega_i t + \theta_i) \quad (2.27)$$

The single-sideband generating system of Fig. 2.18 generally enjoys less popularity than does the filter method. The reason for this lack of favor is the need of precise 90 degree shift of phase shifter over a large frequency range, each modulator carefully balanced, etc.

2.4.2 SSB Demodulator

Coherent Detector

Baseband recovery is achieved at the receiving end of the single-sideband communications channel by heterodyning the received signal with a local

carrier signal which is synchronous (coherent) with the carrier used at the transmitting end to generate the sideband. As in the double-sideband case it is necessary, in principle, that the synchronism be exact and, in practice, that synchronism be maintained to a high order of precision. The effect of a lack of synchronism is different in a double-sideband system and in a single-sideband system. Suppose that the carrier received is $\cos w_c t$ and that the local carrier is $\cos (w_c t + \theta)$. Then with DSB-SC, as noted in Sec. 2.2.2, the spectral component $\cos wt$ will, upon demodulation, reappear as $\cos wt \cos \theta$. In SSB, on the other hand, the

spectral component, $\cos wt$ will reappear (Prob. 2.14) in the form $\cos (wt - \theta)$. Thus, in one case a phase offset in carriers affects the amplitude of the recovered signal and, for $\theta = \pi/2$, may result in a total loss of the signal. In the other case the offset produces a phase change but not an amplitude change. As discussed in Section 1.4.5, a human being is less sensitive to phase distortion in audio signal and thus SSB can be used for speech transmission even if the local carrier has phase offset.

Alternatively, let the local oscillator carrier have an angular frequency offset $A\omega$ and so be of the form $\cos (w_c + A\omega)t$. Then as already noted, in DSB-SC, the recovered signal has the form $\cos wt \cos A\omega t$. In SSB, however, the recovered signal will have the form $\cos (w + A\omega)t$. Thus, in one case the recovered spectral component $\cos wt$ reappears with a “warble,” that is, an amplitude fluctuation at the rate $A\omega$. In the other case, the amplitude remains fixed, but the frequency of the recovered signal is in error by amount $A\omega$.

When the carrier frequency is very high, even quartz crystal oscillators may be hard pressed to maintain adequate frequency stability for at transmitter and receiver end. In such cases it is necessary to transmit the carrier itself along with the sideband signal. At the receiver the carrier may be separated by filtering and used to synchronize a local carrier generator. When used for such synchronization, the carrier is referred to as a “pilot carrier” and may be transmitted at a substantially reduced power level.

Note that the squaring circuit used to recover the frequency and phase information of the DSB-SC system cannot be used here.

Figure 2.19 represents coherent detection scheme for SSB modulated signal. Mathematically speaking, from Eq. (2.22).

$$\begin{aligned}
m_{SSB}(t) &= 0.5m(t)\cos \omega_c t \pm 0.5m_h(t)\sin \omega_c t \\
y(t) &= m_{SSB}(t) \cos \omega_c t = 0.5m(t)\cos^2 \omega_c t \pm 0.5m_h(t)\sin \omega_c t \cos \omega_c t \\
&= 0.25 m(t)[1 + \cos 2 \omega_c t] \pm 0.25m_h(t)\sin 2 \omega_c t
\end{aligned} \tag{2.28}$$

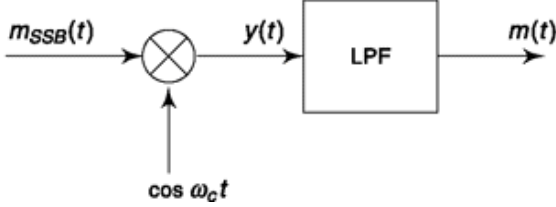


Fig. 2.19 SSB demodulation.

This signal when passed through a LPF of bandwidth that of $m(t)$ suppresses components around $2 \omega_c t$ and recovers the first term, the message signal. It is left as an exercise to students to draw frequency-domain representation at various points of SSB demodulation blocks.

Envelope Detector for ssB signal with Carrier

Suppose a carrier of angular frequency ω_c is amplitude modulated by a sinusoid of angular frequency ω_m to the extent where the resultant signal displays a percentage modulation m . Then the waveform is

$$f_1(t) = A(1 + A_m \cos \omega_m t) \cos \omega_c t \tag{2.29}$$

$$= A \cos \omega_c t + \frac{A_m A}{2} [\cos (\omega_c + \omega_m)t + \cos (\omega_c - \omega_m)t] \tag{2.30}$$

If one of the sidebands is removed, leaving, however, the carrier, we have

$$f_2(t) = A \cos \omega_c t + \frac{A_m A}{2} \cos (\omega_c + \omega_m)t \quad (2.31)$$

To calculate the response of a diode demodulator to $f_2(t)$ we need to have the form of the envelope of $f_2(t)$. We have

$$\begin{aligned} f_2(t) &= A \cos \omega_c t + \frac{A_m A}{2} \cos \omega_c t \cos \omega_m t - \frac{A_m A}{2} \sin \omega_c t \sin \omega_m t \\ &= A \left(1 + \frac{A_m}{2} \cos \omega_m t \right) \cos \omega_c t - \frac{A_m A}{2} \sin \omega_m t \sin \omega_c t \end{aligned} \quad (2.32)$$

The amplitude $A(t)$ of $f_2(t)$ is

$$\begin{aligned} A(t) &= \sqrt{A^2 \left(1 + \frac{A_m}{2} \cos \omega_m t \right)^2 + \left(\frac{A_m A}{2} \sin \omega_m t \right)^2} \\ &= \sqrt{A^2 \left(1 + \frac{A_m^2}{4} \right) + A^2 A_m \cos \omega_m t} \end{aligned} \quad (2.33)$$

and for $A_m \ll 1$,

$$A(t) \approx A \left(1 + \frac{A_m}{2} \cos \omega_m t \right) \quad (2.34)$$

We note that if A_m is small, the diode demodulator does demodulate a signal which is lacking one sideband. Comparing the amplitude $A(t)$ given in Eq. (2.34) with the factor in parentheses in Eq. (2.29), we observe that the baseband signal output with one sideband suppressed is half as large as it would be if both sidebands had been present, a result to have been anticipated.

The diode-demodulator method for SSB application is of interest since it allows recovery of the baseband signal with a receiving system intended for double-sideband amplitude-modulation signals. Many amplitude-modulation “communications” type receivers are equipped with an adjustable oscillator which can be adjusted in frequency to serve as the local carrier and then added to a single-sideband signal. Hence, such AM receivers may demodulate SSB signals, with, however, some distortion.

This technique should be compared with the use of the synchronous demodulator. Although the synchronous demodulator yields no distortion when the carrier phase is perfectly adjusted, the diode demodulator introduces some distortion (see Prob. 2.20). However, for synchronous

demodulation we need, at the receiver, information about both the frequency and phase of the carrier. With a diode demodulator we need to know only the frequency.

Example 2.5

Explain the nature of SSB spectrum if the modulating signal is $m(t) = \cos 2\pi \cdot 1000t + \cos 2\pi \cdot 2000t$ and carrier is given by $c(t) = \cos 2\pi \cdot 10000t$

Solution

$$\text{Given, } m(t) = \cos 2\pi \cdot 1000t + \cos 2\pi \cdot 2000t$$

$$\begin{aligned} m_h(t) &= m(t) \text{ shifted in phase by } \pi/2 \\ &= \cos(2\pi \cdot 1000t - \pi/2) + \cos(2\pi \cdot 2000t - \pi/2) \\ &= \sin 2\pi \cdot 1000t + \sin 2\pi \cdot 2000t. \end{aligned}$$

From Eq. (2.22),

$$\begin{aligned} m_{SSB}(t) &= 0.5m(t)\cos \omega_c t \pm 0.5m_h(t)\sin \omega_c t \\ &= 0.5[\cos 2\pi \cdot 1000t \end{aligned}$$

$$\begin{aligned} &\quad + \cos 2\pi \cdot 2000t] \cos 2\pi \cdot 10000t \\ &\quad \pm 0.5[\sin 2\pi \cdot 1000t \\ &\quad \quad + \sin 2\pi \cdot 2000t] \sin 2\pi \cdot 10000t \\ &= 0.5[\cos 2\pi \cdot (10000 \pm 1000)t \\ &\quad + \cos 2\pi \cdot (10000 \pm 2000)t] \end{aligned}$$

Thus, for SSB with lower sideband,

$$\begin{aligned} m_{SSB-L}(t) &= 0.5[\cos 2\pi \cdot (10000 - 1000)t \\ &\quad + \cos 2\pi \cdot (10000 - 2000)t] \\ &= 0.5[\cos 2\pi \cdot 9000t + \cos 2\pi \cdot 8000t] \end{aligned}$$

Frequencies present in lower sideband are ± 8000 Hz and ± 9000 Hz [since real signal has both +ve and -ve frequencies]. Similarly, frequencies present in upper sideband are ± 11000 Hz and ± 12000 Hz.

SELF-TEST QUESTION

7. Both lower sideband and upper sideband carry the same message information. Is it correct?
8. Is it true that a Hilbert transformer provides 90 degree phase shift?
9. Is it possible to use envelope detector for SSB demodulation?

2.5 OTHER AM TECHNIQUES AND FREQUENCY DIVISION

MULTIPLEXING

In this section we discuss two other techniques under amplitude modulation and certain important use of amplitude modulation as in Frequency Division Multiplexing (FDM). While describing vestigial side band modulation we use commercial television broadcasting as an illustration.

2.5.1 vestigial sideBand (vsB) Modulation

Vestigial SideBand (VSB) modulation is something in between SSB and DSB-SC modulation which provides certain advantages at small cost. This is so called because a vestige or appendage is added here to SSB spectrum. The practical issues which we'll discuss shortly requires a gradual tapering of SSB spectrum over carrier frequency in an antisymmetric fashion. Here, the

difficulty of SSB generation, i.e. requirement of a sharp cutoff filter or phase shifter is avoided and also the spectrum requirement is not as high as DSB-SC. The additional spectrum required is usually less than one-fourth of one side band. The modulation here uses coherent detection like other cases that multiplies the modulated signal with synchronized carrier and low pass filters the message signal spectrum $M(\omega)$. Let us now mathematically represent a VSB signal. We use Fig. 2.20 for it where we consider generating VSB signal by filtering DSB-SC signal with $H(\omega)$.

From Eq. (2.4), DSB-SC signal spectrum, $M_{DSB}(\omega) = \frac{1}{2} [M(\omega + \omega_c) + M(\omega - \omega_c)]$

$$\text{Then, VSB spectrum, } M_{VSB}(\omega) = H(\omega)M_{DSB}(\omega) = \frac{1}{2} H(\omega)[M(\omega + \omega_c) + M(\omega - \omega_c)] \quad (2.35)$$

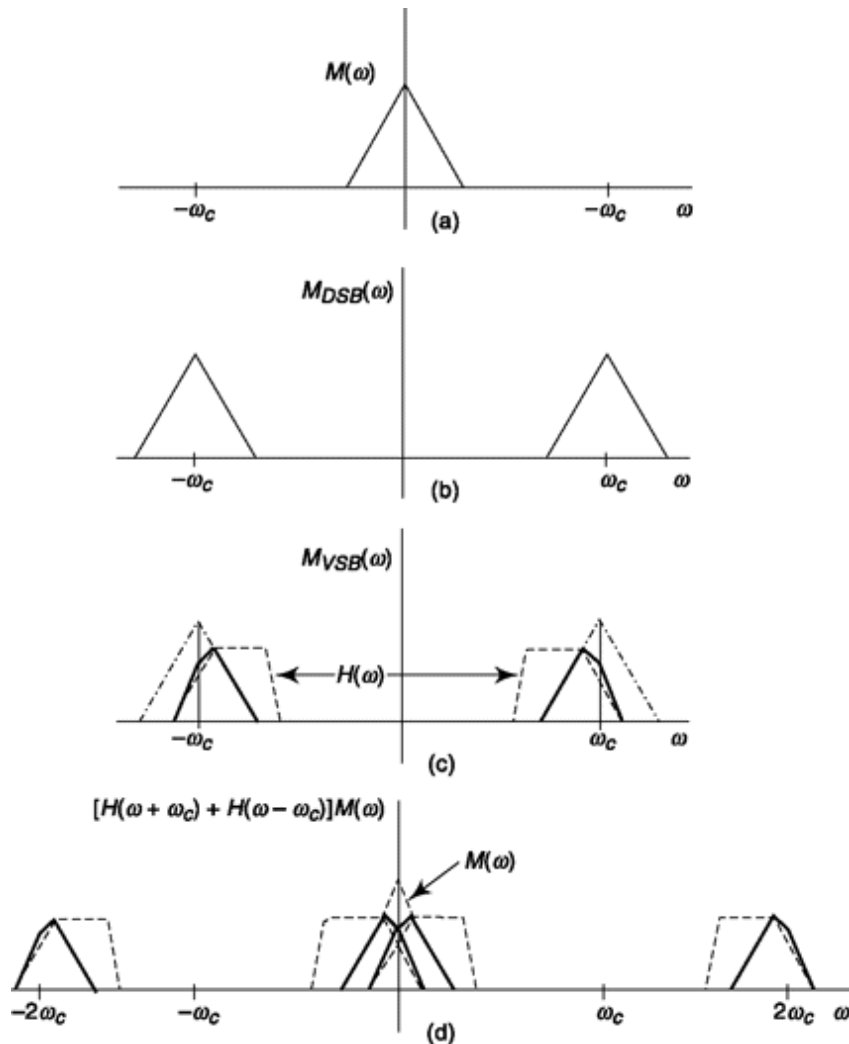


Fig. 2.20 VSB modulation and demodulation. (a) Spectrum of message signal (b) Spectrum of DSB-SC signal, (c) VSB modulation from DSB-SC modulation, (d) VSB demodulation by coherent detection.

In the demodulation process, (similar to Fig. 2.19, input is now only VSB signal) the multiplier output,

$$\begin{aligned}
 y(t) &= m_{VSB}(t) \cos \omega_c t \\
 Y(\omega) &= \frac{1}{2} [M_{VSB}(\omega + \omega_c) + M_{VSB}(\omega - \omega_c)] \\
 &= \frac{1}{4} [H(\omega + \omega_c) M(\omega + \omega_c + \omega_c) + H(\omega + \omega_c) M(\omega - \omega_c + \omega_c)] \\
 &\quad + \frac{1}{4} [H(\omega - \omega_c) M(\omega + \omega_c - \omega_c) + H(\omega - \omega_c) M(\omega - \omega_c - \omega_c)] \quad \text{using Eq. (2.35)} \\
 &= \frac{1}{4} [H(\omega + \omega_c) + H(\omega - \omega_c)] M(\omega) + \frac{1}{4} [H(\omega + \omega_c) M(\omega + 2 \omega_c) \\
 &\quad + H(\omega - \omega_c) M(\omega - 2 \omega_c)]
 \end{aligned}$$

The low pass filter removes the second term which is centred around $2\omega_c$ and has a transfer function $H_R(\omega)$. Then final demodulated output will be

If, $H_R(w)[H(w + w_c) + H(w - w_c)]$ is constant within our frequency of interest, i.e. $|w| < 2pB$ then the output of LPF is $km(t)$ where k is a constant. Again for $H_R(w) = 1$ in baseband, (usual for LPF) we need $[H(w + w_c) + H(w - w_c)] = \text{Constant}$ and this condition requires a band pass filter $H(w)$ to be applied on DSB-SC signal which is antisymmetric or odd-symmetric about w_c . More about VSB is discussed in an illustrative example related to television broadcasting in the next section.

2.5.2 VSB and Television Broadcasting

The principal application of VSB is found in commercial television broadcasting. The television picture signal, i.e. the video signal occupies a bandwidth of nominally 4.5 MHz. A carrier, amplitude-modulated with such a signal, would give rise to a signal extending over 9 MHz comprising of two sidebands. Single sideband for bandwidth conservation is not feasible because of the complexity it must introduce into each of the millions of receivers. A workable compromise between the spectrum-conserving characteristic of single-sideband modulation and the demodulation simplicity of double-sideband amplitude modulation is found in the vestigial-sideband system which is standard in television broadcasting.

In the vestigial-sideband system, an amplitude-modulated signal, carrier plus double sideband, is passed through a filter before transmission to the receiving end. The response of the filter is plotted in Fig. 2.21a as a function of the deviation Df of the frequency from the carrier frequency. (The sound which accompanies the video signal is transmitted by frequency modulation,

discussed in the next chapter, on a carrier located 4.5 MHz above the picture carrier for better quality than AM transmission. A frequency range of 100 kHz is allowed on each side of the sound carrier for the sound sidebands.) The upper sideband of the picture carrier is transmitted without attenuation up to 4 MHz. Thereafter, the sideband is attenuated so that it does not interfere with the lower sideband of the sound carrier. The lower sideband of the picture carrier is transmitted without attenuation over the range 0.75 MHz and is entirely attenuated at 1.25 MHz. Thus, the picture signal is transmitted double sideband over the range 0 to 0.75 MHz, single sideband over the range 1.25 MHz and above, while in the intermediate range, 0.75 to 1.25 MHz, the transition is made from one to the other. Altogether, however, the entire transmission is confined to a range of about **6** MHz, a saving of **one-third** of the bandwidth that would be required for full double-sideband transmission.

We noted above that when only a single sideband is present, the output of a diode demodulator is half the output yielded when both sidebands are present. Therefore, with a vestigial-sideband signal, the relative demodulator output, plotted against frequency for a fixed percentage modulation, has the form shown in Fig. 2.21b. This lack of uniformity is corrected at the receiver by passing the received signal through a filter before demodulation. The relative response of this filter is shown in Fig. 2.21c. Over the range 1.25 MHz on either side of the picture carrier the response varies linearly as shown. As a result, for modulating frequencies up to 1.25 MHz, the **sum** of the amplitudes of the two sidebands, and hence of the demodulator output, is the same as is yielded by the single sideband above

1.25 MHz. This result is easily verified. For example, the received signal frequency component at $Df = 0$ is attenuated by a factor of 2. Referring to Fig. 2.21b, we see that this reduces the modulation to 1 when $Df = 0$. As a second illustration, let $Df = \pm 0.75$. The sideband amplitude due to $Df = -0.75$ is 0.2, while the sideband amplitude due to $Df = +0.75$ is 0.8. The sum is again unity, as expected.

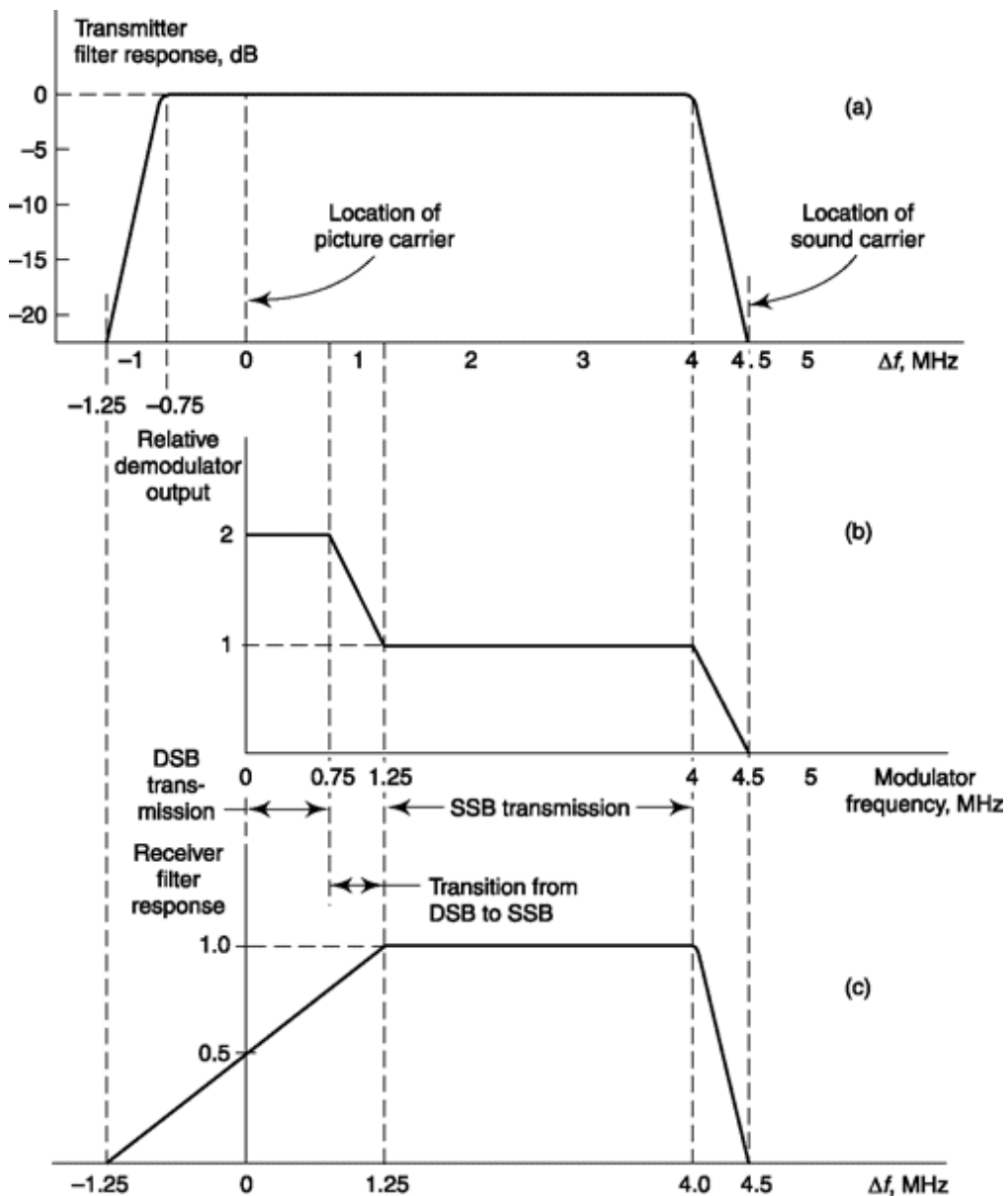


Fig. 2.21 *Vestigial-sideband transmission, (a) Transmitter filter response. (b) Relative diode demodulator output. (c) Receiver filter response.*

It is, of course, to be anticipated that the vestigial-sideband system will introduce some distortion into the demodulated signal, especially at high-percentage modulation. The experimental fact is, however, that in the transmission of picture information the distortion can be kept within tolerable levels. We may even wonder why the cutoff frequency of the filter which removes the lower sideband is not adjusted to be even closer to the carrier frequency thereby conserving additional bandwidth. It is found rather generally, in real filters, that spectral components which lie within the passband but close to the cutoff frequency suffer distortion-producing phase

shifts, even when the amplitude response of the filter is maintained uniform. The nature of the picture signal is such that its waveforms suffer substantial distortion from relatively small phase shifts of its low-frequency components. Thus, the decision to leave a *vestige* of the nominally suppressed sideband is dictated by an engineering compromise between bandwidth economy and faithfulness of reproduction of the picture.

Example 2.6

Give time domain representation of VSB signal discussed in Sec. 2.5.1.

Solution

From Eq. (2.35), $M_{VSB}(\omega) = H(\omega)M_{DSB}(\omega)$. If $h(t)$ is inverse of $H(\omega)$, noting multiplication in frequency domain is equivalent to convolution in time domain we can write,

$$\begin{aligned} m_{VSB}(t) &= h(t) \otimes m_{DSB}(t) \\ &= h(t) \otimes m(t)\cos \omega_c t \\ &\quad [\text{From DSB-SC representation}] \\ &= \int_{-\infty}^{\infty} h(\tau)m(t-\tau)\cos \omega_c(t-\tau) d\tau \\ &= \int_{-\infty}^{\infty} h(\tau)m(t-\tau)(\cos \omega_c t \cos \omega_c \tau + \sin \omega_c t \sin \omega_c \tau) d\tau \end{aligned}$$

$$\begin{aligned} &+ \sin \omega_c t \sin \omega_c \tau) d\tau \\ &= \cos \omega_c t \int_{-\infty}^{\infty} h(\tau)m(t-\tau)\cos \omega_c \tau d\tau \\ &+ \sin \omega_c t \int_{-\infty}^{\infty} h(\tau)m(t-\tau)\sin \omega_c \tau d\tau \\ &= m_c(t)\cos \omega_c t + m_s(t)\sin \omega_c t \end{aligned} \quad (2.36)$$

where, in phase component of $m(t)$ is defined as

$$m_c(t) = \int_{-\infty}^{\infty} h(\tau)m(t-\tau)\cos \omega_c \tau d\tau$$

and in quadrature component of $m(t)$ is defined as

$$m_s(t) = \int_{-\infty}^{\infty} h(\tau)m(t-\tau)\sin \omega_c \tau d\tau$$

Note that $m_s(t) = m_h(t)$, i.e. Hilbert transform of $m(t)$ for SSB and $m_s(t) = 0$ for DSB-SC.

2.5.3 Quadrature amplitude Modulation (QAM)

The quadrature amplitude modulation (QAM) is similar to DSB-SC but sends two message signals over the same spectrum. One of this message signals, say $m_x(t)$ is sent in phase, i.e. by multiplying it with $\cos \omega_c t$ and the other message signal, $m_2(t)$ is sent in quadrature by multiplying it with $\sin \omega_c t$ and finally adding these two signals. A QAM signal is thus represented as

$$m_{QAM}(t) = m_1(t)\cos \omega_c t + m_2(t)\sin \omega_c t \quad (2.37)$$

The demodulation uses coherent detection, i.e. multiplication by carrier and then baseband low pass filtering. If $m_{QAM}(t)$ is multiplied with $\cos \omega_c t$ we get $m_x(t)$ back and if it is multiplied with $\sin \omega_c t$ we get $m_2(t)$ back. This can be shown from following calculations.

$$\begin{aligned}
m_{QAM}(t)\cos \omega_c t &= m_1(t)\cos^2 \omega_c t + m_2(t)\sin \omega_c t \cos \omega_c t \\
&= \frac{1}{2} [(1 + \cos \omega_c t) m_1(t) + m_2(t)\sin 2\omega_c t] \\
&= \frac{1}{2} [m_1(t) + m_1(t)\cos \omega_c t + m_2(t)\sin 2\omega_c t]
\end{aligned} \tag{2.38a}$$

Similarly,

$$\begin{aligned}
m_{QAM}(t)\sin \omega_c t &= m_1(t)\sin \omega_c t \cos \omega_c t + m_2(t)\sin^2 \omega_c t \\
&= \frac{1}{2} [m_1(t)\sin 2\omega_c t + m_2(t) - m_2(t)\cos 2\omega_c t]
\end{aligned} \tag{2.38b}$$

Thus, low-pass filtering brings out $m_x(t)$ from Eq. (2.38a) and $m_2(t)$ from Eq. (2.38b) by suppressing components around frequency $2\omega_c$. Figure 2.22 shows generation and detection of QAM signal. The QAM gives SSB like performance with easy manipulation but there could be a serious problem with QAM demodulation if local carrier has some phase error. This gives co-channel interference. Multiplying Eq. (2.37) with $\cos(\omega_c t + 0)$ where 0 is phase error and separating the baseband component

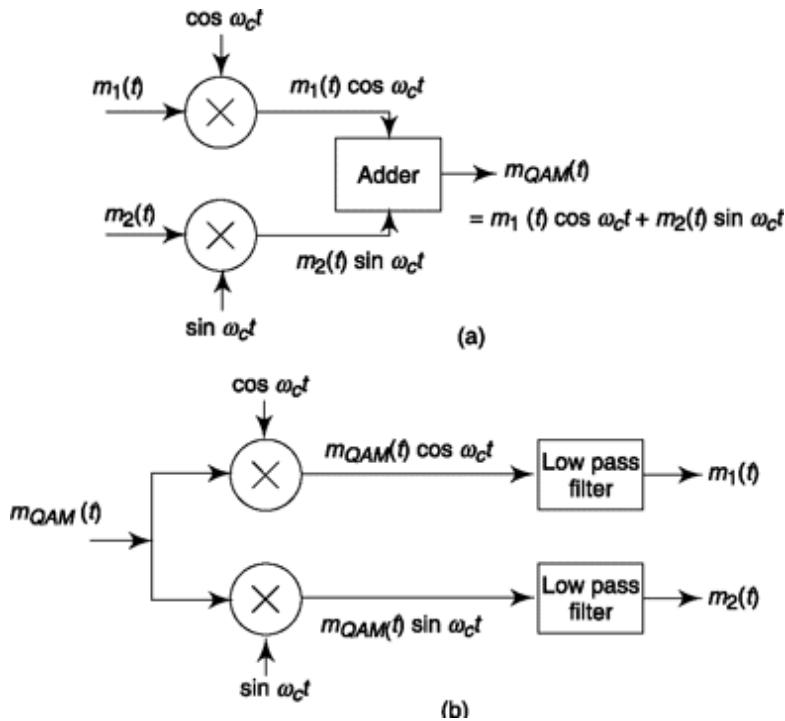


Fig. 2.22 Block-diagram representation of (a) Analog QAM modulator, and (b) Analog QAM demodulator.

(LPF output), we get $m_x(t)\cos 0 - m_2(t)\sin 0$ instead of $m_x(t)$. Similar interference occurs for quadrature component too. [Refer to MATLAB Experiment 17.] In practical communication problems, like transmission of

multiplexed chrominance signal in television, carrier synchronization is maintained by periodically sending carrier in between messages. Note that there is a digital equivalent of QAM which we shall take up later. To avoid ambiguity, we can call QAM discussed here as analog QAM.

2.5.4 Frequency Division Multiplexing

We have explored the principles of operation of a number of amplitude-modulation **modems** (systems of modulation and demodulation). The manner in which such systems are used for multiplexing (i.e. transmitting many baseband signals over a common communications channel) is shown in Fig. 2.23. The individual baseband signals $m_1(t)$, $m_2(t)$, ..., $m_n(t)$, each bandlimited to f_M , are applied to individual modulators, each modulator being supplied as well with carrier waveforms of frequency f_1, f_2, \dots, f_n . The individual modulator-output signals extend over a limited range in the neighborhood of the individual carrier frequencies. Most importantly, the carrier frequencies are selected to the spectral ranges of the modulator-output signals do not overlap. This separation in frequency is precisely the feature that allows the eventual recovery of the individual signals, and for this reason this multiplexing system is referred to as **frequency multiplexing**. As a matter of fact, to facilitate this separation of the individual signals, the carrier frequencies are selected to leave a comfortable margin (guard band) between the limit of one frequency range and the beginning of the next. The combined output of all the modulators, i.e. the **composite** signal, is applied to a common communications channel. In the case of radio transmission, the channel is free space, and coupling to the channel is made by means of an antenna. In other cases wires are used.

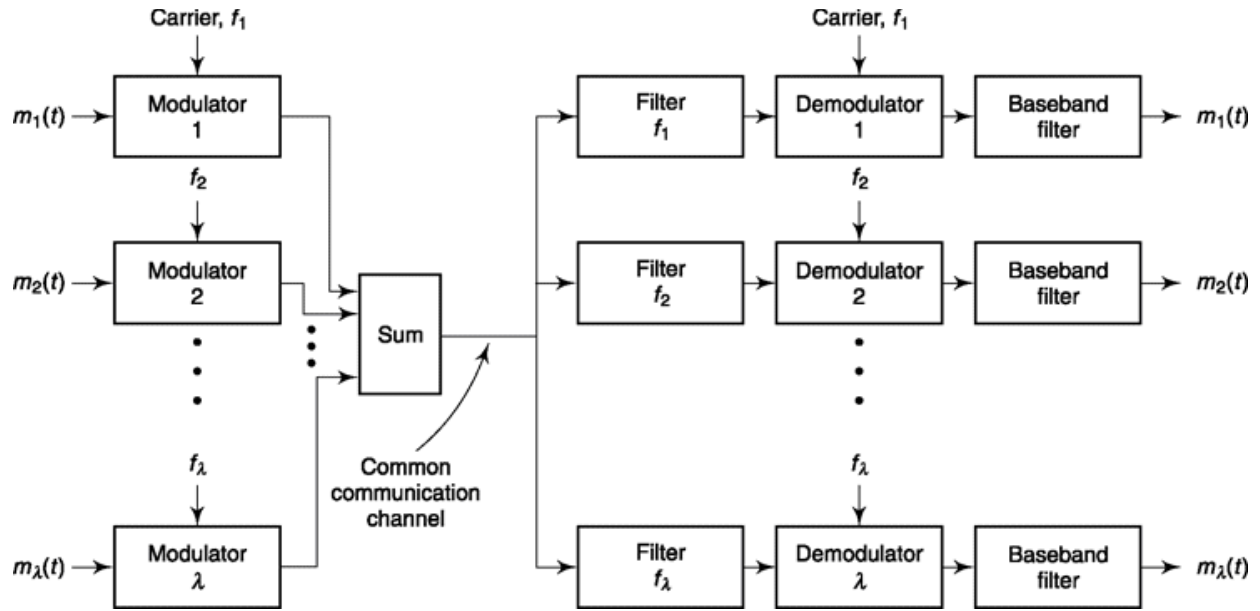


Fig. 2.23 Multiplexing many baseband signals over a single communications channel.

At the receiving end the composite signal is applied to each of a group of bandpass filters whose passbands are in the neighborhood f_1, f_2, \dots . The filter f_1 is a bandpass filter which passes only the spectral range of the output of modulator 1 and similarly for the other bandpass filters. The signals have thus been separated. They are then applied to individual demodulators which extract the baseband signals from the carrier. The carrier inputs to the demodulators are required only for synchronous demodulation and are not used otherwise.

The final operation indicated in Fig. 2.23 consists in passing the demodulator output through a baseband filter. The baseband filter is a low-pass filter with cutoff at the frequency f_M to which the baseband signal is limited. This baseband filter will pass, without modification, the baseband signal output of the modulator in this sense serves no function in the system as described up to the present point. We shall, however, see in Chapters 8 and 9 that such baseband filters are essential to suppress the noise which invariably accompanies the signal.

2.5.5 Amplitude Modulation and Linearity

All the modulation schemes considered up to the present point have two principal features in common. In the first place, each spectral component of the baseband signal gives rise to one or two spectral components in the modulated signal. These components are separated from the carrier by a

frequency difference equal to the frequency of the baseband component. Most importantly, the nature of the modulators is such that the spectral components which they produce depend only on the carrier frequency and the baseband frequencies. The amplitudes of the spectral components of the modulator output may depend on the amplitude of the input signals; however, the frequencies of the spectral components do not. In the second place, all the operations performed on the signal (addition, subtraction and multiplication) are linear operations so that superposition applies. Thus, if a baseband signal $m_1(t)$ introduces one spectrum of components into the modulated signal and a second signal $m_2(t)$ introduces a second spectrum, the application of the sum $m_1(t) + m_2(t)$ will introduce a spectrum which is the sum of the spectra separately introduced. All these systems are referred to under the designation “amplitude or linear modulation.” This terminology must be taken with some reservation, for we have noted that, at least in the special case of single sideband using modulation with a single sinusoid, there is no amplitude variation at all. And even more generally, when the amplitude of the modulated signal does vary, the carrier envelope need not have the waveform of the baseband signal.

SELF-TEST QUESTION

10. Is it true that VSB uses more spectrum than SSB but less than DSB?
11. Commercial TV broadcasting uses VSB for both video and audio transmission. Is it correct?
12. Cochannel interference is a serious issue in QAM. What causes that?

2.6 RADIO TRANSMITTER AND RECEIVER

Let us now discuss wireless transmission of AM signal. For this we shall briefly study a radio transmitter and receiver. Note that this will be useful for other types of modulation, including digital modulation that uses air interface. In a radio transmitter, the baseband signal is translated to a radio frequency by a modulation process which is then amplified by a power amplifier and radiated through antenna assembly. A simple block diagram shown in Fig 2.24 shows these steps. What is not apparent in this diagram but will be discussed later, is the role of impedance matching networks in connecting one stage with the other. The frequency translation and amplification of the signal can be done in several stages.

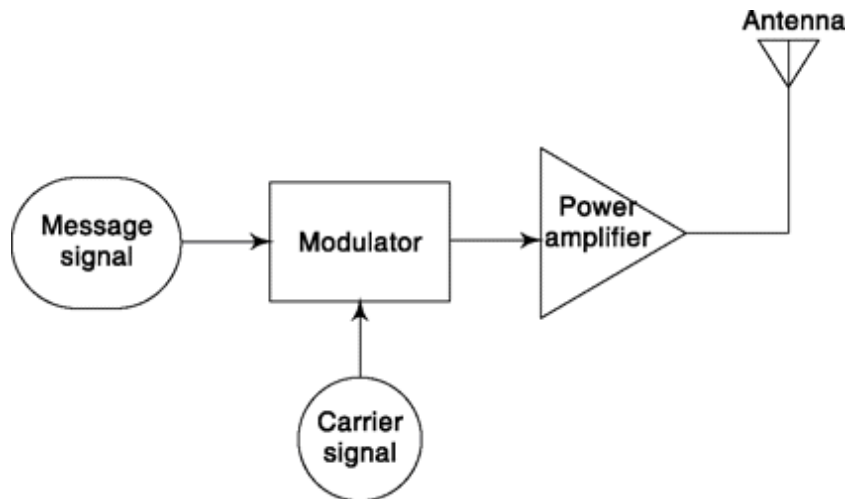


Fig 2.24 A simple block diagram of radio transmitter.

An AM broadcast transmitter occupies 10 kHz bandwidth, i.e. if the carrier signal is of 600 kHz frequency then it occupies frequency range of 595-605 kHz. The oscillator used for carrier is usually made up from crystal as **LC** oscillators tend to drift with time and are not as stable. The oscillator output passes through a buffer amplifier which increases its power level but more importantly serves as an isolator that prevents variation of load affecting frequency of the oscillator.

2.6.1 power amplifier

A typical modulator output has few mW of power while a commercial AM broadcast transmitter radiates several kW of power. This is usually a two-step process as shown in Fig. 2.25. The driver amplifier provides intermediate power boost followed up by final power amplifier. The diagram also shows how impedance matching networks are placed.

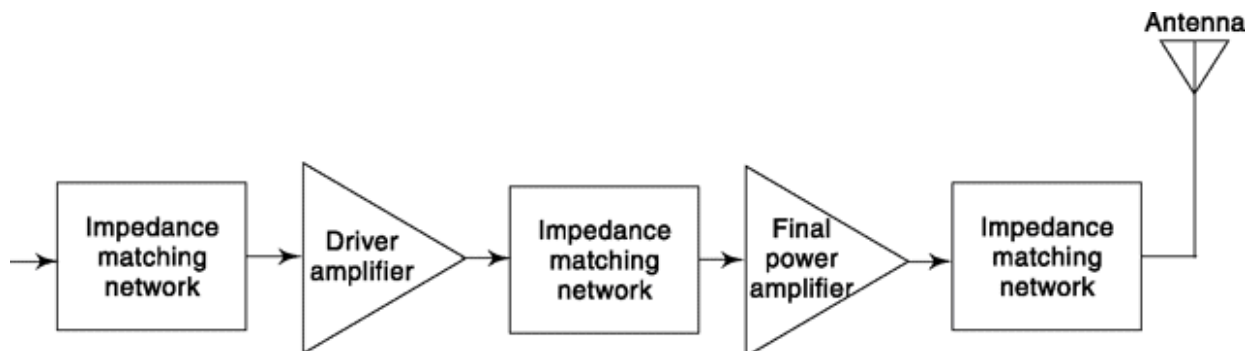


Fig. 2.25 Power amplification blocks in radio transmitter.

A class C amplifier is usually used for power amplification. These amplifiers conduct less than 50% of the input signal and the distortion at the output is high, but up to 90% of power efficiency can be achieved. In RF transmitters this distortion can vastly be reduced by using tuned loads. Refer to Fig. 2.26 which will be used in explaining the working principle. The input signal switches the amplifying device, usually a transistor, on and off, which causes pulses of current to flow through an **LC** tuned circuit. The tuned circuit will only resonate at particular frequencies linked to fundamental or some harmonics and suppresses other frequencies. Note that if n-th harmonic is tuned to then it can serve as a **frequency multiplier** that multiplies the input carrier frequency by a factor of n. Class A amplifier is used in buffer stage discussed in previous section that offers higher bandwidth and full 360-degree amplification. But its power efficiency is low (below 50%) as it conducts current even when input signal is absent which consumes power.

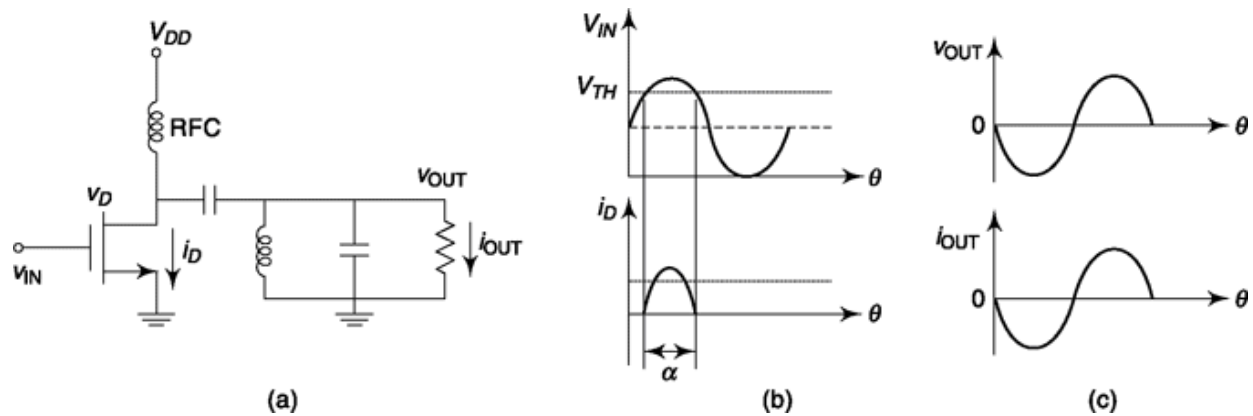


Fig. 2.26 (a) A Class C amplifier with tuned output. (b) Amplification for conduction angle $\alpha < 180^\circ$. (c) Output of tuned section.

Figure 2.26a shows a MOSFET based Class C amplifier which conducts when $V_{IN} > V_{TH}$ the threshold voltage. The corresponding current flow i_D is shown in Fig 2.26b. You can see that i_D is available only for conduction angle, $\alpha < 180^\circ$ in a full cycle because $V_{TH} > 0$. The **LC** resonator is tuned to fundamental and exchange of energy between **L** and **C** provides oscillation that is sent to antenna via RF coil or choke (RFC) and radiated from there. Since, the modulated signal will have some variation over the original carrier frequency the **LC** circuit should be capable of tuned to that and hence need to have some bandwidth around carrier, ± 5 kHz for AM. Note that, **Q factor** of a resonator circuit is an important parameter that is

defined as ratio of resonating frequency to its bandwidth. A too high Q will clip sideband of the modulated signal while a too low Q will distort the signal and the shape will deviate from being sinusoidal.

2.6.2 Impedance Matching Network

Impedance matching network in radio transmitter facilitates efficient power coupling between two stages. They also do filtering job and provide **selectivity** to the network. Selectivity is the ability of a circuit to accept a given band of frequency and reject unwanted or interfering signals. The principle of making output impedance of one stage equal to input impedance of the next stage is required for maximum power transfer and this is generally followed. But small adjustment is often required in practice to take care of parasitic values and the necessity of obtaining maximum output from next stage. Usually, **LC** networks are useful in impedance matching, but transformers, or specially designed baluns (between balanced and unbalanced load) are also used in radio transmitters. Balanced load refers to circuits where two wires are used and signal is considered as difference of two. The

external interferences affect two lines almost equally and the differential signal is not affected much. In unbalanced circuit the signal is carried by single line with ground as reference.

Now let us illustrate how impedance matching is done. We use an **LC** network based that has narrowband characteristics (good selectivity) and useful for RF system. Consider, the arrangement shown in Fig. 2.27 where our objective is to match two purely resistive loads R_1 , (output impedance of previous stage) and R_2 , (input impedance of next stage). We consider first $R_1 < R_2$, and discuss later what should be done if it is otherwise in notes of Example 2.7.

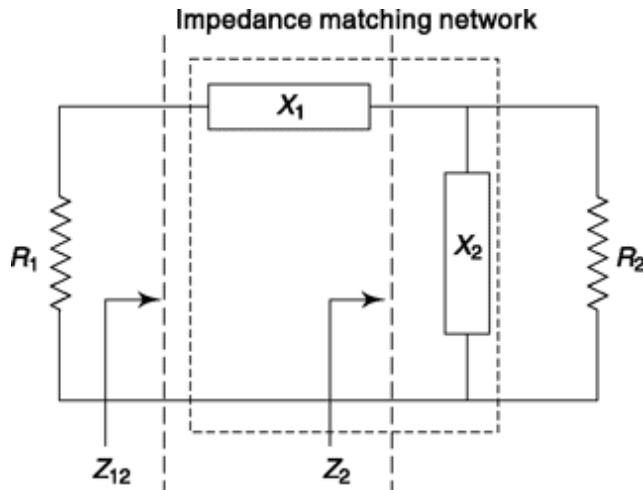


Fig. 2.27 **Impedance matching by L-network ($R_X > R_2$)**.

For above circuit, the combined equivalent impedance of R_2 and X_2 in parallel can be written as,

$$Z_2 = \frac{jR_2 X_2}{R_2 + jX_2} = \frac{jR_2 X_2 (R_2 - jX_2)}{R_2^2 + X_2^2} = \frac{R_2 X_2^2}{R_2^2 + X_2^2} + \frac{jR_2^2 X_2}{R_2^2 + X_2^2} \quad (2.39)$$

This makes Z_2 and X_1 in series and their combined impedance can be written as,

$$Z_{12} = Z_2 + jX_1 = \frac{R_2 X_2^2}{R_2^2 + X_2^2} + \frac{jR_2^2 X_2}{R_2^2 + X_2^2} + jX_1 \quad (2.40)$$

For impedance matching we want, $R_1 = Z_{12}$

Hence, equating real and imaginary part,

$$R_1 = \frac{R_2 X_2^2}{R_2^2 + X_2^2} \quad \text{and} \quad X_1 = \frac{R_2^2 X_2}{R_2^2 + X_2^2} \quad (2.41a \text{ and } 2.41b)$$

We haven't assumed so far if X_1 , X_2 are resistive or reactive. But Eq. (2.41) shows they have to be of opposite sign. In usual cases, X_1 is a capacitive element (C) and X_2 is an inductive element (L). Similar procedure can be followed if loads to be matched are complex and also if the network is cascaded is L-network and T or p network. The later have three reactive elements arranged in the fashion of a T or p and is more flexible than L-network.

Transformer-based impedance matching makes judicious use of turns ratio to match loads and uses special type of core materials like ferrite or powdered iron (also called **toroid**). This has a copper winding and does not let magnetic energy to escape or radiate at such a high frequency. As

already mentioned baluns are used to match balanced and unbalanced load and has a special type of winding on a toroid usually with 1:1 turns ratio.

Baluns are useful in matching impedance between an antenna and its previous stage.

2.6.3 Antenna

Antenna is the final subsystem of a radio transmitter. When current enters antenna, an electrical conductor, it creates a magnetic field around it. This magnetic field creates an electric field in the surrounding space which in turn induces another magnetic field, which again induces another electric field, and so on. These way electric and magnetic fields (together called electromagnetic fields) induce each other and move with the speed of light in a direction away from the antenna. If the electrical field remains horizontal to earth, produced by a horizontal antenna it is called horizontal polarization and if vertical known as vertical polarization. The shape and size of an antenna can have a wide variety but always depends on the wavelength of operation. The simplest of them is a half wave dipole which is a simple wire piece of length half the wavelength it can radiate.

When an electrical signal enters antenna, a part of it can be reflected back. The remaining power that feeds the antenna (P_{in}) partly provides for ohmic loss (P) and the rest (P_{rad}) is used for radiation purposes. Radiation resistance (R_a) of an antenna is an equivalent resistance that provides same ohmic loss as P_{rad} . Note that R_a does not depend on conductivity of the antenna material but antenna geometry and its ability to radiate power. For half wave dipole, radiation resistance is nearly 72 ohms. The efficiency (η) of an antenna is defined as the ratio of radiated power to input power, i.e.

$$\eta = P_{rad}/P_{in} \quad (2.42)$$

Let us now discuss few other parameters that is used to define an antenna. The directivity function, $D(\theta, F)$ of an antenna is defined as the ratio of power radiated per unit solid angle in any direction (R, θ, F defines polar coordinate) to average power radiated per unit solid angle. If you don't immediately recollect your solid geometry fundamentals use Fig. 2.28a where we define solid angle for your convenience. The gain, $G(\theta, F)$ of an antenna is similarly defined as the ratio of power radiated per unit solid angle to average power input to antenna, per unit solid angle. Thus, we can write

$$D(\theta, \phi) = \frac{dP_{\text{rad}}/d\Omega}{P_{\text{rad}}/4\pi} \quad \text{and} \quad G(\theta, \phi) = \frac{dP_{\text{rad}}/d\Omega}{P_{\text{in}}/4\pi} \Rightarrow G(\theta, \phi) = \eta D(\theta, \phi) \quad (2.43)$$

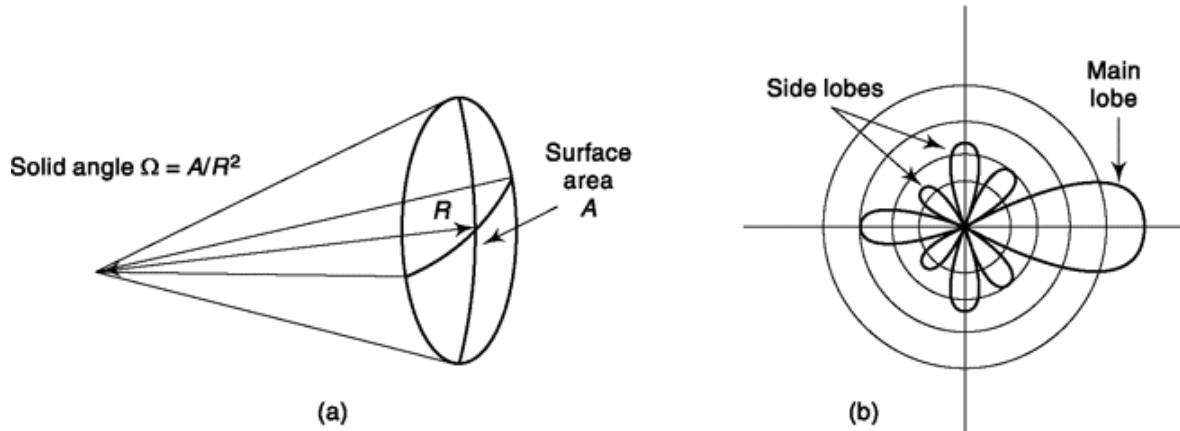


Fig. 2.28 (a) Solid angle, (b) Typical radiation pattern of an antenna.

Directivity, D and gain, G are defined as maximum of their respective functions so that

$$G = \eta D \quad (2.44)$$

Often we need antenna to radiate in a specified direction or directions. This is accomplished by designing it to have a proper radiation pattern. Figure 2.28b shows a typical antenna plot in polar coordinate that has one main lobe and few side lobes. It radiates power more in the direction of the main lobe. The beam width of an antenna is a measure of the directivity of an antenna and is usually defined by the angles where the pattern drops to one half of its peak value or known as the 3dB points. If the antenna is uniformly excited (uniform distribution of current over it) this beam width is about $50/D$ degrees. The next lobe in the pattern, usually called the first side lobe, will be about one-twentieth of the value of the main lobe and others will be of even less. Note that the antenna behaves in a reciprocal manner when used as a receiver, i.e. if it radiates power in one direction more than others as transmitter, it will receive power more from that direction as receiver. In the receiving antenna the electromagnetic wave induces current which is amplified and then further processed to find out the transmitted message. This is discussed in the next section. AM radio stations transmit at high powers to compensate for the suboptimal receiver antenna heights. For satellites that are millions of miles away NASA uses antenna dishes that are 200 feet or more wide.

2.6.4 Radio Receiver

We discuss the principle of a radio frequency receiver here with respect to AM system. The demodulator block only is changed if any other modulation scheme is used. The frequency modulation and demodulation is discussed in the next chapter.

A system for processing an amplitude-modulated carrier and recovering the base-band modulating system is shown in Fig. 2.29. We assume that the signal has suffered great attenuation during the course of its transmission over the communication channel and hence is in need of amplification. The input to the system might be a signal furnished by a receiving antenna which receives its signal from a transmitting antenna. The carrier of the received signal is called a **radio-frequency** (RF) carrier, and its frequency is the **radio** frequency f_{rf} . The input signal is amplified in an RF amplifier and then passed on to a **mixer**. In the mixer, the modulated RF carrier is mixed (i.e. multiplied) with a sinusoidal waveform generated by a local oscillator which operates at a frequency f_{osc} . The process of mixing is also called **heterodyning**, and since, as is to be explained, the heterodyning local-oscillator frequency f_{osc} is selected to be **above** the radio frequency f_{rf} , the system is often referred to as a **superheterodyne** system.

The process of mixing generates sum and difference frequencies. Thus, the mixer output consists of a carrier of frequency $f_{osc} + f_{rf}$ and a carrier $f_{osc} - f_{rf}$. Each carrier is modulated by the baseband signal to the same extent as was the input RF carrier. The sum frequency is rejected by a filter. This filter is not shown explicitly in Fig. 2.29 and may be considered to be part of the mixer. The difference-frequency carrier is called the **intermediate frequency** (IF) carrier, that is, $f_f = f_{osc} - f_{rf}$. The modulated IF carrier is applied to an IF amplifier. The process just described, in which a modulated RF carrier is replaced by a modulated IF carrier, is called **conversion**. The combination of the mixer and local oscillator is called a **converter**.

The IF amplifier output is passed, through an IF carrier filter, to the demodulator in which the baseband signal is recovered, and finally through a baseband filter. The baseband filter may include an amplifier, not explicitly indicated in Fig. 2.29. If synchronous demodulation is used, a synchronous signal source will be required.

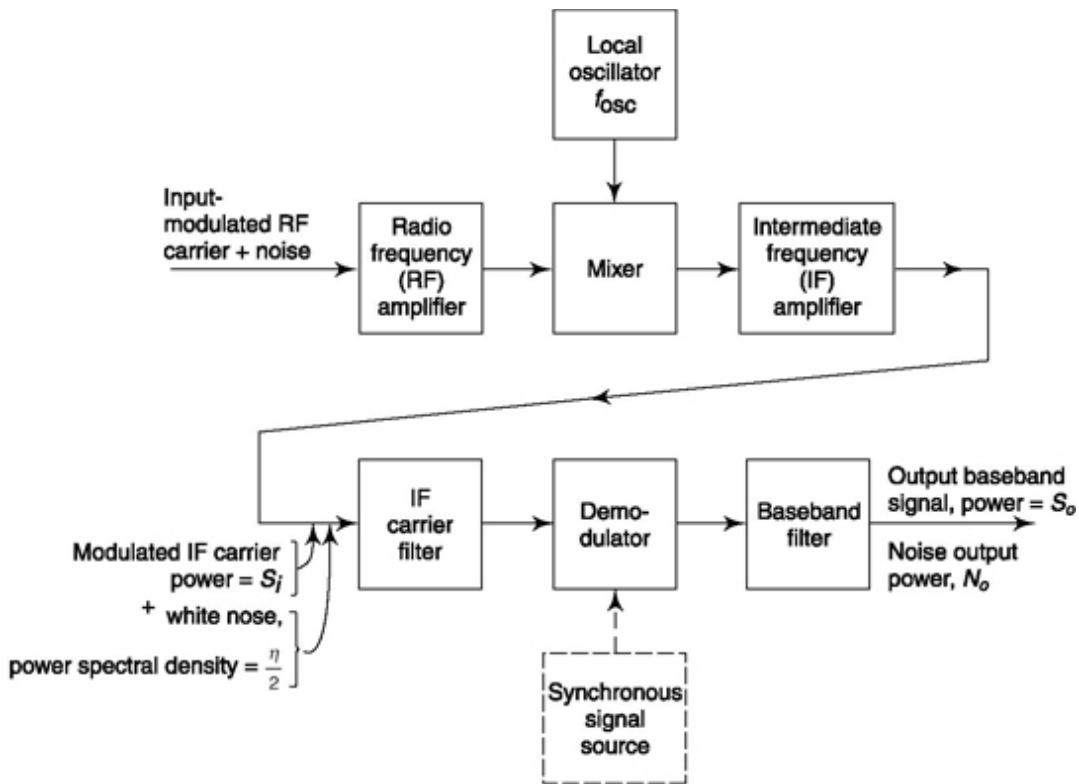


Fig. 2.29 A receiving system for an amplitude-modulated signal.

The only absolutely essential operation performed by the receiver is the process of frequency translation back to baseband. This process is, of course, the inverse of the operation of modulation in which the baseband signal is frequency-translated to a carrier frequency. The process of frequency translation is performed in the system of Fig. 2.29 in part by the converter and in part by the demodulator. For this reason the converter is sometimes referred to as the ***first detector***, while the demodulator is then called the ***second detector***. The only other components of the system are the linear amplifiers and filters, none of which would be essential if the signal were strong enough and there were no need for multiplexing.

It is apparent that there is no essential need for an initial conversion before demodulation. The modulated RF carrier may be applied directly to the demodulator. However, the superheterodyne principle, which is rather universally incorporated into receivers, has great merit, as discussed in the next section.

Before we move to the next section, let us discuss what is known as ***Automatic Gain Control*** (AGC). The voltage gain available at the receiver from antenna to demodulator in several stages of amplification is very high so that it can amplify even a very weak signal..What about the signal which

is much stronger? If same gain is maintained the signal is likely to be distorted with some of the amplifiers reaching saturation level. We need to have a mechanism which will measure the strength of the input signal and accordingly adjust the gain. AGC does precisely this job and improves the dynamic range of the antenna to 60-100 dB by adjusting gain of the IF (and sometimes the RF) stages.

2.6.5 advantage of the superheterodyne principle

A signal furnished by an antenna to a receiver may have a power as low as some tens of picowatts, while the required output signal may be of the order of tens of watts. Thus, the magnitude of the required gain is very large. In addition, to minimize the noise power presented to the demodulator, filters are used which are no wider than is necessary to accommodate the baseband signal. Such filters should be rather flat-topped and have sharp skirts. It is more convenient to provide gain in sharp flat-topped filters at low frequencies than at high. By way of example, in commercial FM broadcasting, the RF carrier frequency is in the range of 100 MHz, while at the FM receiver the IF frequency is 10.7 MHz.

Thus, in Fig. 2.29 the largest part, by far, of the required gain is provided by the IF amplifier, and the critical filtering done by the IF filter. While Fig. 2.29 suggests a separate amplifier and filter, actually in physical receivers these two usually form an integral unit. For example, the IF amplifier may consist of a number of amplifier stages, each one contributing to the filtering. Some filtering will also be incorporated in the RF amplifier. But this filtering is not critical. It serves principally to limit the total noise power input to the mixer and thereby avoids **overloading** the mixer with a noise waveform of excessive amplitude.

RF amplification is employed whenever the incoming signal is very small. This is because of the fact that RF amplifiers, such as masers, are **low-noise** devices; i.e. an RF amplifier can be designed to provide relatively high gain while generating relatively little noise. When RF amplification is not employed, the signal is applied directly to the mixer. The mixer provides relatively little gain and generates a relatively large noise power. Calculations showing typical values of gain and noise power generation in RF, mixer, and IF amplifiers are presented in Sec. 15.6.1.

Multiplexing

An even greater merit of the superheterodyne principle becomes apparent when we consider that we shall want to tune the receiver to one or another of a number of different signals, each using a different RF carrier. If we were not to take advantage of the superheterodyne principle, we would require a receiver in which many stages of RF amplification were employed, each stage requiring tuning. Such tuned-radio-frequency (TRF) receivers were, as a matter of fact, commonly employed during the early days of radio communication. It is difficult enough to operate at the higher radio frequencies; it is even more difficult to **gang-tune** the individual stages over a wide band, maintaining at the same time a reasonably sharp flat-topped filter characteristic of constant bandwidth.

In a **superheterodyne** receiver, however, we need but change the frequency of the local oscillator to go from one RF carrier frequency to another. Whenever f_{osc} is set so that $f_{osc} - f_{rf} = ff$, the mixer will convert the input modulated RF carrier to a modulated carrier at the IF frequency, and the signal will proceed through the demodulator to the output. Of course, it is necessary to gang the tuning of the RF amplifier to the frequency control of the local oscillator. But again this ganging is not critical, since only one or two RF amplifiers and filters are employed.

Finally, we may note the reason for selecting f_{osc} higher than f_{rf} . With this higher selection the fractional change in f_{osc} required to accommodate a given range of RF frequencies is smaller than would be the case for the alternative selection.

Note that, FM transmitter is discussed in Chap. 3 and FM receiver in Chap. 9. The noise and its effect in the receiving system are discussed in Chap. 8 onwards. An important discussion on effect of thermal noise which is an important issue in Radio transmitter-receiver is taken up in Chap. 13. It also gives more details on antenna and other subsystems.

Example 2.7

A class C power amplifier has output load of 10 ohm. This is to be matched with an antenna of impedance 50 ohms by an L-network. Find value of L and C if the carrier frequency to be used is 500 kHz.

Solution

Given, input impedance of matching network, $R_1 = 10$,
output impedance of matching network, $R_2 = 50$

$$\text{From Eq. (2.41a), } 10 = \frac{50 \times X_2^2}{2500 + X_2^2}$$

$$\text{or, } 40X_2^2 = 25000 \rightarrow X_2 = 25 \text{ ohms}$$

Note that if $R_1 > R_2$, then X_2^2 will come as negative which is absurd. For those cases the L-network is arranged in a reverse fashion. The capacitor comes in parallel with R , followed by inductor in series.

Substituting X_2 in Eq (2.41b),

$$X_1 = \frac{2500 \times 25}{2500 + 625} \rightarrow = -20 \text{ ohm}$$

$$\begin{aligned} |X_1| &= |j\omega L| = \omega L = 20 \text{ and } |X_2| = |1/j\omega C| = 1/\omega C \\ &= 25 \rightarrow L/C = 500 \end{aligned} \quad (2.45)$$

The operating range of ω needs to be near resonant frequency for necessary frequency selectivity. This requires, $\omega_c^2 = \frac{1}{LC}$,

Example 2.8

Solution

Total equivalent resistance seen by the current = 12 + 48 = 60 ohm

$$\begin{aligned} \text{Total power used in antenna, } P_{\text{in}} &= \frac{1}{2} (0.1)^2 \times 60 \\ &= 0.3 \text{ watt} \end{aligned}$$

$$\text{Power used in radiation, } P_{\text{rad}} = \frac{1}{2} (0.1)^2 \times 48 = 0.24 \text{ watt}$$

$$\text{Efficiency of the antenna, } \eta = P_{\text{rad}}/P_{\text{in}} = 0.24/0.3 = 0.8$$

$$\text{Gain of antenna} = \text{efficiency} \times \text{directivity} = 0.8 \times 2 = 1.6$$

Note that antenna is a passive device and a gain greater than one refers to redistribution of power so that it is more in one direction compared to average.

Thus, $LC = \frac{1}{(2\pi \times 0.5 \times 10^6)^2} \approx 10^{-3}$ (2.46)

Multiplying Eq. (2.45) and (2.46),

$$L^2 = 50 \times 10^{-14} \rightarrow L = 0.71 \mu\text{H}$$

Using this in (2.49), $C = 1.4 \text{ nF}$

An antenna has ohmic loss resistance of 12 ohm, radiation resistance of 48 ohm and directivity 2. Find the gain of the antenna and power radiated into space. Given, input current = $0.1\cos(2p10^6t)$.

SELF-TEST QUESTION

13. Is it true that class C amplifiers have higher power efficiency than class A amplifiers?
14. Baluns are a kind of transformer that is used to match balanced systems? Is that correct?
15. Antenna has a gain though it is a passive device. Is that correct?
16. Is the frequency of local oscillator in superheterodyne receiver less than that of RF carrier?

Facts and Figures

The credit of developing the first working television goes to J. L. Baird who gave its first public demonstration on 26 January, 1926 in London. The system used 30 scan lines per image and transmitted 12.5 images per second. Baird used the concept of scanning disk developed by P. J. Nipkow in 1884, who first proposed the idea of an electromechanical television system but could not develop a working model.

It was a battle of two geniuses, Philo Farnsworth and Vladimir Zworykin, to get the honour of inventing the first electronic television using the electronic scanning system. With the might of RCA (Radio Corporation of America) backing Zworykin, it became a high-stake legal battle. Zworykin patented the idea in 1923 but it did not work beyond his laboratory. Farnsworth held a public demonstration on 3 September, 1928 and got the patent in 1930. In a run-up to the legal battle, RCA proudly proclaimed, “RCA earns royalties, it does not pay them”. After getting the final verdict in 1939, RCA agreed to pay Farnsworth USD 1 million, in addition to license payments, to use his patents.

MATLAB

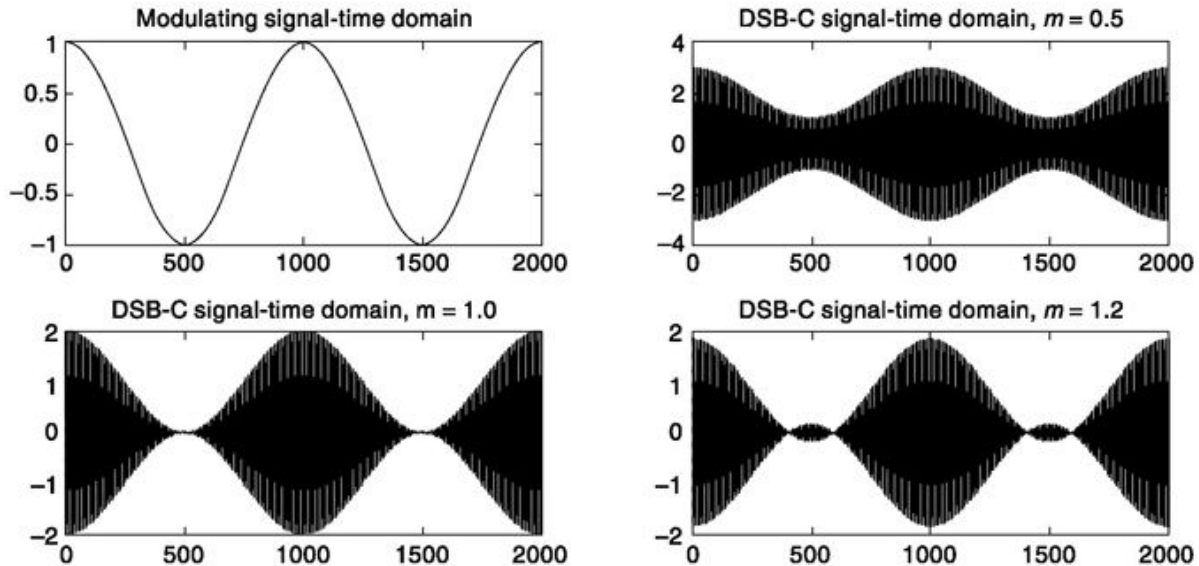
```

% Experiment 13
% Amplitude Modulation : DSB-C with tone input
% In built function to be used y = modulate(x,fc,fs,'method',opt)
% x= modulating signal, fc=carrier frequency, fs=sampling frequency
% method = 'amdsb-tc' i.e. AM double sideband, transmitted carrier
% 'opt' decides amount of carrier, used as y = (x-opt).*cos(2*pi*fc*t)
% Comparing our equation y = A(1+m(t))cos(2*pi*fc*t) we see opt=-A
% and when x is a tone, modulation index, m = 1/A or A=1/m

fc=100000;      % Carrier frequency
fs=1000000;      % Sampling frequency
f=1000;          % Tone modulation
m=0.5;           % Modulation index
A=1/m;           % Amplitude of carrier from above relation for modulate.m
opt=-A;          % From definition and syntax of modulate.m

t=0:1/fs:((2/f)-(1/fs)); %Gives exact two cycles of modulating signal
x=cos(2*pi*f*t);

```



```

y = modulate(x,fc,fs,'amdsb-tc',opt);
subplot(221); plot(x); title('modulating signal-time domain')
subplot(222); plot(y); title('DSB-C signal-time domain, m=0.5')

m=1.0; opt=-1/m;
y = modulate(x,fc,fs,'amdsb-tc',opt);
subplot(223); plot(y); title('DSB-C signal-time domain, m=1.0')

m=1.2; opt=-1/m;
y = modulate(x,fc,fs,'amdsb-tc',opt);
subplot(224); plot(y); title('DSB-C signal-time domain, m=1.2')

% Experiment 14
% Amplitude Modulation : DSB-SC and SSB
% In built function to be used y = modulate(x,fc,fs,'method')
% x= modulating signal, fc=carrier frequency, fs=sampling frequency
% method = 'amdsb-sc' or 'amssb'
% DSB-SC eqn. used : y = x.*cos(2*pi*fc*t)
% SSB eqn. used : y = x.*cos(2*pi*fc*t)+imag(hilbert(x)).*sin(2*pi*fc*t)

fc=2000; % Carrier frequency
fs=10000; % Sampling frequency
f=200; % Single tone modulation

t=0:1/fs:((2/f)-(1/fs)); %Gives exact two cycles of modulating signal
x=cos(2*pi*f*t);
y_dsb_sc = modulate(x,fc,fs,'amdsb-sc');
y_ssbb = modulate(x,fc,fs,'amssb');
f_dsb_sc = abs(fft(y_dsb_sc,1024));
f_ssbb = abs(fft(y_ssbb, 1024));
f_dsb_sc=[f_dsb_sc(514:1024) f_dsb_sc(1:513)];
f_ssbb=[f_ssbb(514:1024) f_ssbb(1:513)];
f=(-511*fs/1024):(fs/1024):(512*fs/1024);

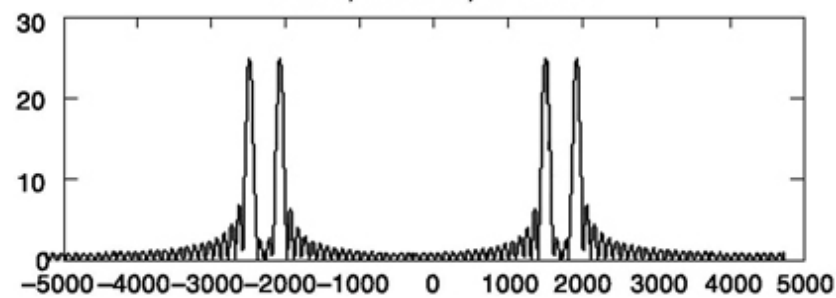
subplot(221); plot(f,f_dsb_sc);
title('DSB-SC spectrum for single tone modulation, f=200,fc=2000,fs=10000')
subplot(223); plot(f,f_ssbb);
title('SSB spectrum for single tone modulation, f=200,fc=2000,fs=
10000')
xlabel('frequency in Hz'); ylabel('amplitude');

f1=200; f2=400; %Two tone modulation
x2=cos(2*pi*f1*t)+cos(2*pi*f2*t);
y2_dsb_sc = modulate(x2,fc,fs,'amdsb-sc'); %Repetition for new signal
y2_ssbb = modulate(x2,fc,fs,'amssb');
f2_dsb_sc = abs(fft(y2_dsb_sc,1024));
f2_ssbb = abs(fft(y2_ssbb, 1024));
f2_dsb_sc=[f2_dsb_sc(514:1024) f2_dsb_sc(1:513)];
f2_ssbb=[f2_ssbb(514:1024) f2_ssbb(1:513)];

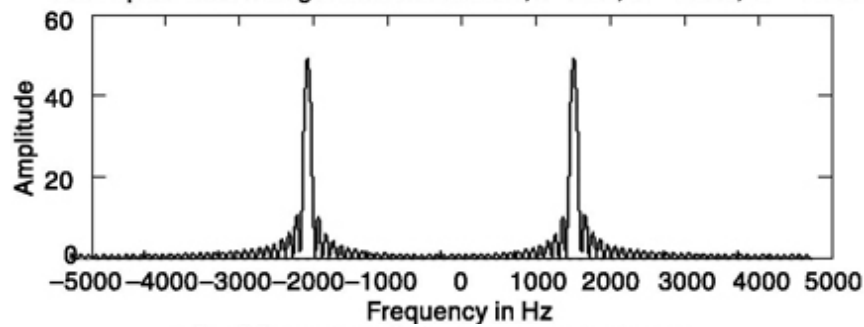
subplot(222); plot(f,f2_dsb_sc);
title('DSB-SC spectrum for two tone modulation,f=200 & 400,fc=2000,fs=10000')

```

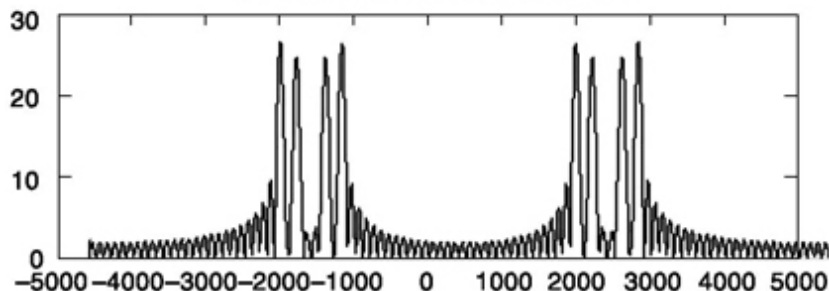
DSB-SC spectrum for single tone modulation,
 $f = 200$, $fc = 2000$, $fs = 10000$



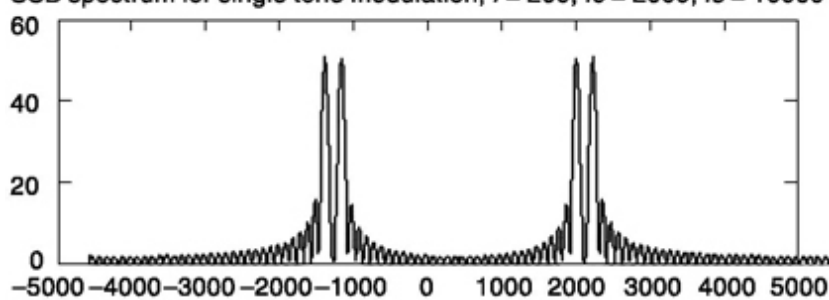
SSB spectrum for single tone modulation, $f = 200$, $fc = 2000$, $fs = 10000$



DSB-SC spectrum for single tone modulation,
 $f = 200 \& 400$, $fc = 2000$, $fs = 10000$



SSB spectrum for single tone modulation, $f = 200$, $fc = 2000$, $fs = 10000$



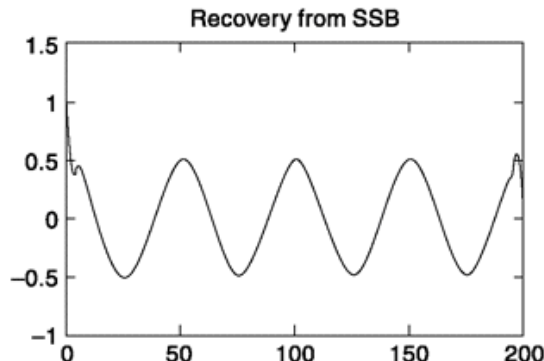
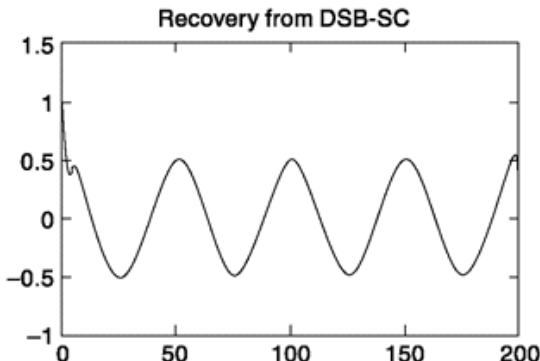
```

subplot(224); plot(f,f2_ss);
title('SSB spectrum for two tone modulation, f=200 & 400,fc=2000,fs=10000')

% Experiment 15
% Demodulation, syntax x = demod(y,fc,fs,'method')
% Method is as specified in experiment 13 and 14
% The function demod.m can be used for coherent detection
% of AM DSB-C too. This is shown in Experiment 16a.

clear;
exp14; % We have used 4 cycles for better illustration by changing one
       % line of the code as t=0:1/fs:((4/f)-(1/fs)) in exp14 % saving it.
x1=demod(y_dsb_sc,fc,fs,'amdsb-sc');
subplot(121); plot(x1); %axis([0 2000 0 2]);
title('Recovery from DSB-SC');
x2=demod(y_ss,fc,fs,'amssb');
subplot(122); plot(x2);%axis([0 2000 0 2]);
title('Recovery from SSB');

```



```

% Experiment 16
% Writing a matlab function that simulates envelop detection
% Save it as envdet_my.m
% Input y=Amplitude modulated signal,
% f=max. fre. of modulating signal, fs=sampling frequency.
% By AM modulation basic assumption carrier freq. fc>>f

```

```

function [x]=envdet_my(y,f,fs)
le=length(y);

for i=1:le      % The following simulates the performance
    if y(i)<0    % of an ideal diode.
        y(i)=0;
    end
end

[b,a]=butter(1,2*pi*f/fs);    % RC filter approximated by 1st order
x=filter(b,a,y);              % Butterworth filter, cut-off freq. f

**

```

```

% Experiment 16a

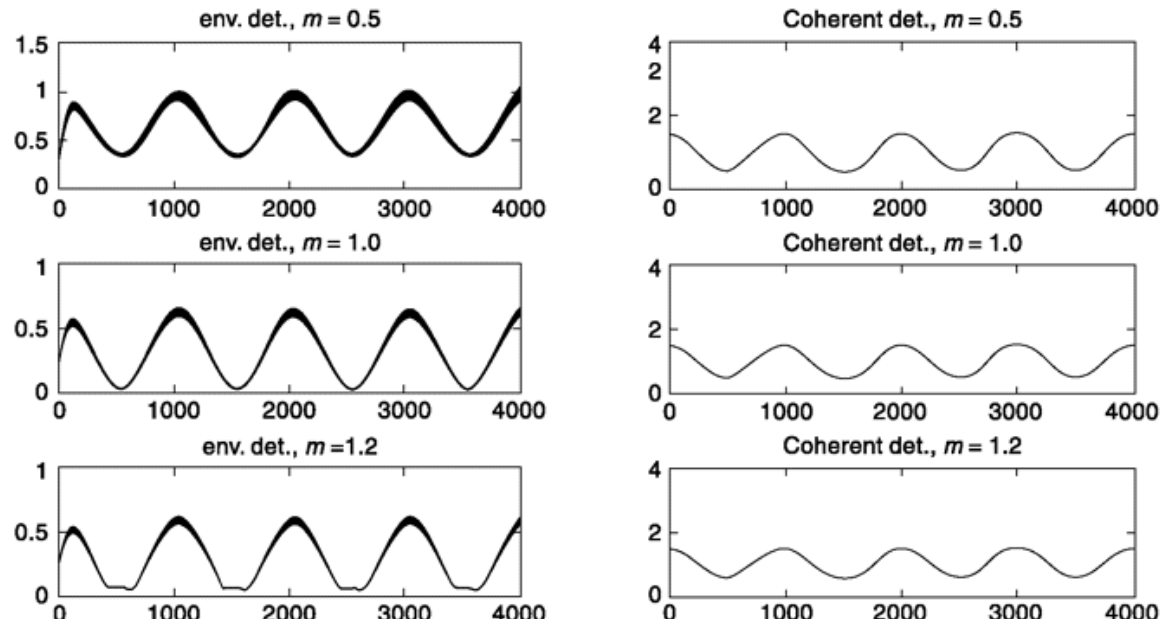
% AM demodulation by envelop detection and coherent detection
% We use envdet_my.m written in Experiment 16 for envelop detection
% and demod.m, a MATLAB in-built function for coherent detection

% We use AM modulated data generated in exp13.m

clear;
exp13; % We have used 4 cycles for better illustration by changing one
        % line of the code as t=0:1/fs:((4/f)-(1/fs)) in exp13
[x1]=envdet_my(y1,f,fs); subplot(321); plot(x1); title('env. det., m=0.5');
[x2]=envdet_my(y2,f,fs); subplot(323); plot(x2); title('env. det., m=1.0');
[x3]=envdet_my(y3,f,fs); subplot(325); plot(x3); title('env. det., m=1.2');

[x1]=demod(y1,fc,fs,'amdsb-tc');
subplot(322); plot(x1); title('coherent det., m=0.5');
[x2]=demod(y1,fc,fs,'amdsb-tc');
subplot(324); plot(x1); title('coherent det., m=1.0');
[x3]=demod(y1,fc,fs,'amdsb-tc');
subplot(326); plot(x1); title('coherent det., m=1.2');

```



```

% Experiment 17
% Quadrature Amplitude Modulation
% We write our own code to understand the effect of phase error better
% You can use MATLAB in built function modulate.m and demod.m too.


```

```

fc=1000; % Carrier frequency
fs=10000; % Sampling frequency
f1=200; f2=300; % We use two single tone message signal

```

```

t=0:1/fs:((4/f1)-(1/fs)); %Gives exact four cycles of modulating signal
x1=cos(2*pi*f1*t); % message 1
x2=cos(2*pi*f2*t); % message 2

% Modulation
y=x1.*cos(2*pi*fc*t)+x2.*sin(2*pi*fc*t); %Generation of QAM signal

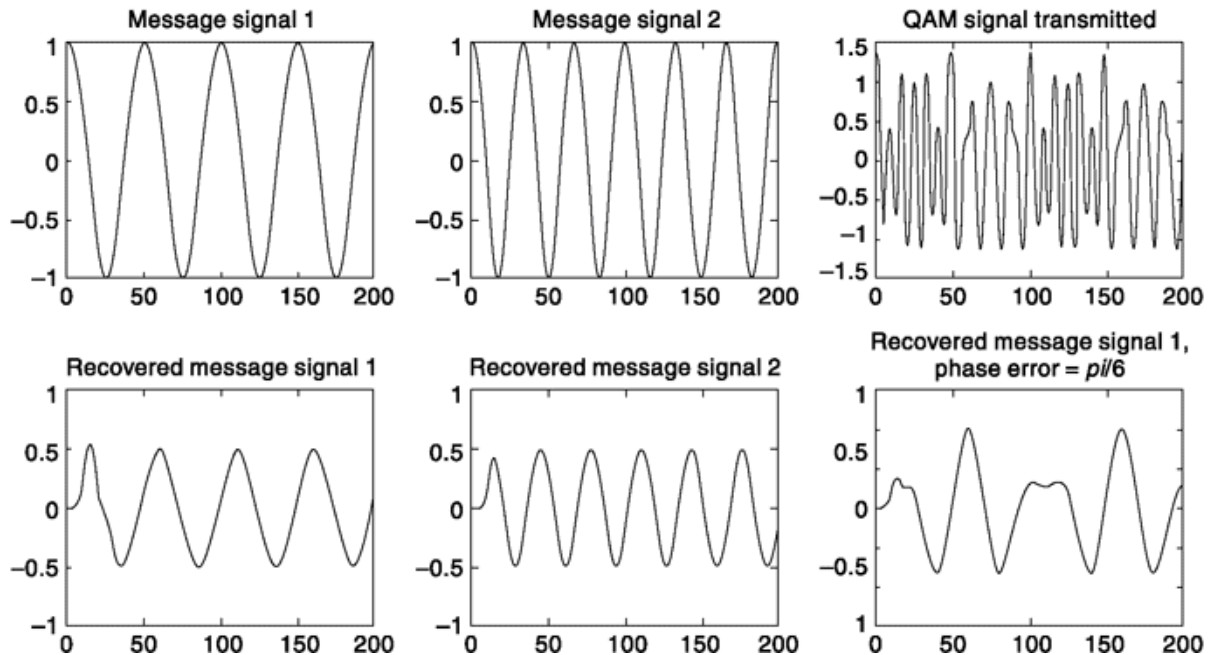
subplot(231);plot(x1); title('message signal 1');
subplot(232);plot(x2); title('message signal 2');
subplot(233);plot(y); title('QAM signal transmitted');

%Demodulation
y1=y.*cos(2*pi*fc*t); %Extracting in phase component
y2=y.*sin(2*pi*fc*t); %Extracting in quadrature component
[b,a]=butter(10,2*pi*max(f1,f2)/fs); %Designing 10th order butterworth LPF
x1_recov=filter(b,a,y1); % In phase component recovered
x2_recov=filter(b,a,y2); % In quadrature component recovered

subplot(234);plot(x1_recov); title('recovered message signal 1');
subplot(235);plot(x2_recov); title('recovered message signal 2');

%Introducing phase error in demodulation
pe=pi/6; %phase error, you can vary to understand its effect
y1_pe=y.*cos(2*pi*fc*t+pe);
x1_recov_pe=filter(b,a,y1_pe); %Recovery of message signal 1
subplot(236);plot(x1_recov_pe);
title('recovered message signal 1, phase error = pi/6')

```



SUMMARY

This chapter begins with a discussion on the need of frequency translation. It discusses how simple multiplication by a high-frequency sinusoidal signal translates the message to a new frequency band in the frequency spectrum. A detailed discussion on various types of amplitude modulation schemes along with demodulation principles and circuits are discussed. These includes double sideband suppressed carrier (DSB-SC), double sideband with carrier (DSB-C) or simple amplitude modulation (AM), single sideband (SSB), vestigial sideband (VSB), quadrature amplitude modulation (QAM). In each case, mathematical representation of signal is presented along with modultation-demodulation scheme. The simplicity of AM detector is highlighted while note is made on its lower power efficiency. Carrier recovery and synchronization issues are addressed for modulation schemes that require coherent detection. Application in television broadcasting and frequency domain multiplexing are followed by a discussion on radio transmitter and receiver.

PROBLEMS

- 2.1 A signal $v_m(t)$ is bandlimited to the frequency range 0 to f_M . It is frequency-translated by multiplying it by the signal $v_c(t) = \cos 2\pi f_c t$. Find f_c so that the bandwidth of the translated signal is 1 percent of the frequency f_c .
- 2.2 The Fourier transform of $m(t)$ is $\mathcal{F}[m(t)] \equiv M(f)$. Show that

$$\mathcal{F}[m(t) \cos 2\pi f_c t] = \frac{1}{2} [M(f + f_c) + M(f - f_c)]$$

2.3 The signals

$$v_1(t) = 2 \cos \omega_1 t + \cos 2\omega_1 t$$

and

$$v_2(t) = 2 \cos \omega_2 t + 2 \cos 2\omega_2 t$$

are multiplied. Plot the resultant amplitude-frequency characteristic, assuming that $\omega_2 > 2\omega_1$, but is not a harmonic of ω_1 . Repeat for $\omega_2 = 2\omega_1$.

- 2.4 The baseband signal $m(t)$ in the frequency-translated signal $v(t) = m(t) \cos 2\pi f_c t$ is recovered by multiplying $v(t)$ by the waveform $\cos 2\pi(f_c + \Delta f)t$. The product waveform is transmitted through a low-pass filter which rejects the double-frequency signal. Find the output signal of the filter.
- 2.5 (a) The baseband signal $m(t)$ in the frequency-translated signal $v(t) = m(t) \cos 2\pi f_c t$ is to be recovered. There is available a waveform $p(t)$ which is periodic with period $1/f_c$. Show that $m(t)$ may be recovered by appropriately filtering the product waveform $p(t)v(t)$.
- (b) Show that $m(t)$ may be recovered as well if the periodic waveform has a period n/f_c , where n is an integer. Assume $m(t)$ bandlimited to the frequency range from 0 to 5 kHz and let $f_c = 1$ MHz. Find the largest n which will allow $m(t)$ to be recovered. Are all periodic waveforms acceptable?
- 2.6 The signal $m(t)$ in the DSB-SC signal $v(t) = m(t) \cos(\omega_c t + \theta)$ is to be reconstructed by multiplying $v(t)$ by a signal derived from $v^2(t)$.
- (a) Show that $v^2(t)$ has a component at the frequency $2f_c$. Find its amplitude.
- (b) If $m(t)$ is bandlimited to f_M and has a probability density

$$f(m) = \frac{1}{\sqrt{2\pi}} e^{-m^2/2} \quad -\infty \leq m \leq \infty$$

find the expected value of the amplitude of the component of $v^2(t)$ at $2f_c$.

- 2.7 The envelope detector shown in Fig. 2.12a is used to recover the signal $m(t)$ from the AM signal $v(t) = [1 + m(t)] \cos \omega_c t$, where $m(t)$ is a square wave taking on the values 0 and -0.5 volt and having a period $T \gg 1/f_c$. Sketch the recovered signal if $RC = T/20$ and $4T$.
- 2.8 The signal $v(t) = (1 + m \cos \omega_m t) \cos \omega_c t$ is detected using a diode envelope detector. Sketch the detector output when $m = 2$.
- 2.9 The signal $v(t) = [1 + 0.2 \cos(\omega_M/3)t] \cos \omega_c t$ is demodulated using a square-law demodulator having the characteristic $v_o = (v + 2)^2$. The output $v_o(t)$ is then filtered by an ideal low-pass filter having a cutoff frequency at f_M Hz. Sketch the amplitude-frequency characteristics of the output waveform in the frequency range $0 \leq f \leq f_M$.
- 2.10 Repeat Prob. 2.9 if the square-law demodulator is centered at the origin so that $v_o = v^2$.
- 2.11 The signal $v(t) = [1 + m(t)] \cos \omega_c t$ is square-law detected by a detector having the characteristic $v_o = v^2$. If the Fourier transform of $m(t)$ is a constant M_0 extending from $-f_M$ to $+f_M$, sketch the Fourier transform of $v_o(t)$ in the frequency range $-f_M < f < f_M$. Hint: Convolution in the frequency domain is needed to find the Fourier transform of $m^2(t)$. See Prob. 1.30.
- 2.12 The signal $v(t) = (1 + 0.1 \cos \omega_1 t + 0.1 \cos 2\omega_1 t) \cos \omega_c t$ is detected by a square-law detector, $v_o = 2v^2$. Plot the amplitude-frequency characteristic of $v_o(t)$.
- 2.13 (a) Show that the signal

$$v(t) = \sum_{i=1}^N [\cos \omega_c t \cos (\omega_i t + \theta_i) - \sin \omega_c t \sin (\omega_i t + \theta_i)]$$

is an SSB-SC signal ($\omega_c \gg \omega_N$). Is it the upper or lower sideband?

- (b) Write an expression for the missing sideband.
- (c) Obtain an expression for the total DSB-SC signal.
- 2.14 The SSB signal in Prob. 2.13 is multiplied by $\cos \omega_c t$ and then low-pass filtered to recover the modulation.
- (a) Show that the modulation is completely recovered if the cutoff frequency of the low-pass filter f_0 is $f_M < f_0 < 2f_c$.
- (b) If the multiplying signal were $\cos(\omega_c t + \theta)$, find the recovered signal.
- (c) If the multiplying signal were $\cos(\omega_c + \Delta\omega)t$, find the recovered signal. Assume that $\Delta\omega \ll \omega_1$.
- 2.15 Show that the squaring circuit shown in Fig. 2.9 will not permit the generation of a local oscillator signal capable of demodulating an SSB-SC signal.
- 2.16 A baseband signal, bandlimited to the frequency range 300 to 3000 Hz, is to be superimposed on a carrier of frequency of 40 MHz as a single-sideband modulation using the filter method. Assume that bandpass filters are available which will provide 40 dB of attenuation in a frequency interval which is about 1 percent of the filter center frequency. Draw a block diagram of a suitable system. At each point in the system draw plots indicating the spectral range occupied by the signal present there.
- 2.17 The system shown in Fig. 2.18 is used to generate a single-sideband signal. However, an ideal 90° phase-shifting network which is independent of a frequency is unattainable. The 90° phase shift is approximated by a lattice network having the transfer function

$$H(f) = e^{-j \arctan(f/30)}$$

The input to this network is $m(t)$, given by Eq. (2.25). If $f_1 = 300$ Hz and $f_M = 3000$ Hz show that $H(f) \approx e^{-j\pi/2} e^{j30f}$, for $f_1 \leq f \leq f_M$.

- 2.18 In the SSB generating system of Fig. 2.18, the carrier phase-shift network produces a phase shift which differs from 90° by a *small* angle α . Calculate the output waveform and point out the respects in which the output no longer meets the requirements for an SSB waveform. Assume that the input is a single spectral component $\cos \omega_m t$.
- 2.19 Repeat Prob. 2.18 except, assume instead, that the baseband phase-shift network produces a phase shift differing from 90° by a *small* angle α .
- 2.20 A received SSB signal in which the modulation is a single spectral component has a normalized power of 0.5 volt². A carrier is added to the signal, and the carrier plus signal are applied to a diode demodulator. The carrier amplitude is to be adjusted so that at the demodulator output 90 percent of the normalized power is in the recovered modulating waveform. Neglect dc components. Find the carrier amplitude required.
- 2.21 The characteristics of a VSB filter $H(\omega)$ which filters LSB and a vestige from USB is similar to what is shown in Fig. 2.20. The carrier frequency is ω_c , the modulating signal is combination of two single tone sinusoids ω_1 and ω_2 such that $\omega_c + \omega_1$ is a part of the vestige but $\omega_c + \omega_2$ is not. If $H(\omega) = 1$ in the flat region and is linear with a slope -0.5 around ω_c show that original signal can be obtained by synchronous demodulation.

REFERENCES

1. Bell Telephone Laboratories: "Transmission Systems for Communications," Western Electric Company, Tech. Pub., Winston-Salem, N.C., 1964.
2. Norgaard, D. E.: A Third Method of Generation and Detection of Single-sideband Signals, *Proc. IRE*, December, 1956.
3. Voelcker, H.: Demodulation of Single-sideband Signals Via Envelope Detection, *IEEE Trans. on Communication Technology*, pp. 22-30, February, 1966.

3

ANGLE MODULATION

CHAPTER OBJECTIVE

In the amplitude-modulation systems described in the previous chapter, the modulator output was a high-frequency carrier signal with varying amplitude, the variation containing information of the modulating message. In this chapter, we discuss modulation systems in which the modulator output is of constant amplitude. Here, the message signal is superimposed on the carrier by varying its frequency and phase, together called angle. Following the qualitative and quantitative presentation of underlying principles, we discuss a variety of modulation and demodulation techniques. Examples are chosen to highlight important aspects of theoretical concepts. At the end, MATLAB based simulation examples make one play with various parameters discussed in the text and see its effect in angle-modulated waveform and its spectrum.

Facts and Figures

In 1922, J. R. Carson first used the term “frequency modulation” which was in principle totally different from the then popular “amplitude modulation”. He showed that the bandwidth required for frequency modulation is at least twice the highest modulating frequency. But he was wrong when he said “I have proved, mathematically, that this type of modulation inherently distorts without any compensating advantages whatsoever.”

It required the genius of E.H. Armstrong to catch Carson off-guard on this count. A prolific inventor, Armstrong invented regenerative circuits in his college days (1912), superheterodyne receiver in 1918 and was the holder of 42 patents. On June 9, 1934, he conducted the first field test on FM transmission by sending an organ recital, via both AM and FM, from the top of the Empire State Building to the home of a trusted old friend on Long Island. The FM organ came through loud and clear with a better quality than AM. And he had this to say, “I could never accept findings based almost

exclusively on mathematics. It ain't ignorance that causes all the trouble in this world. It's the things people know that ain't so."

3.1 ANGLE MODULATION

We discussed amplitude modulation in the previous chapter. Angle modulation has certain important differences. The spectral components in the modulated waveform depend on the amplitude as well as the frequency of the spectral components in the baseband signal. Furthermore, the modulation system is *not* linear and superposition does *not* apply. Such a system results when, in connection with a carrier of constant amplitude, the phase angle is made to respond in some way to a baseband signal. Such a signal has the form

$$v(t) = A \cos [\omega_c t + \phi(t)] \quad (3.1)$$

in which A and ω_c are constant but in which the phase angle $\phi(t)$ is a function of the baseband signal.

3.1.1 Phase Modulation (PM) and Frequency Modulation (FM)

To review some elementary ideas in connection with sinusoidal waveforms, let us recall that the function $A \cos \omega_c t$ can be written as

$$A \cos \omega_c t = \text{real part } (A e^{j\omega_c t}) \quad (3.2)$$

The function $A e^{j\theta}$ is represented in the complex plane by a phasor of length A and an angle θ measured counterclockwise from the real axis. Refer to Fig. 1.5 here. If $\theta = \omega_c t$, then the phasor rotates in the counterclockwise direction with an angular velocity ω_c . With respect to a coordinate system which also rotates in the counterclockwise direction with angular velocity ω_c , the phasor will be stationary. If in Eq. (3.1), f is actually not time-dependent but is a constant, then $v(t)$ is to be represented precisely in the manner just described. But suppose $f = f(t)$ does change with time and makes positive and negative excursions. Then $v(t)$ would be represented by a phasor of amplitude A which runs ahead of and falls behind the phasor representing $A \cos \omega_c t$. We may, therefore, consider that the angle $\omega_c t + f(t)$, of $v(t)$,

undergoes a *modulation* around the angle $\theta = w_c t$. The waveform of $v(t)$ is, therefore, a representation of a signal which is *modulated in phase*.

If the phasor of angle $\theta + f(t) = w_c t + f(t)$ alternately runs ahead of and falls behind the phasor $\theta = w_c t$, then the first phasor must alternately be rotating more, or less, rapidly than the second phasor. Therefore we may consider that the angular velocity of the phasor of $v(t)$ undergoes a modulation around the nominal angular velocity w_c . The signal $v(t)$ is, therefore, an angular-velocity-modulated waveform. The angular velocity associated with the argument of a sinusoidal function is equal to the time rate of change of the argument (i.e. the angle) of the function. Thus, we have that the instantaneous radial frequency $w = d(\theta + f)/dt$, and the corresponding frequency $f = w/\ln$ is

$$f = \frac{1}{2\pi} \frac{d}{dt} [\omega_c t + \phi(t)] = \frac{\omega_c}{2\pi} + \frac{1}{2\pi} \frac{d}{dt} \phi(t) \quad (3.3)$$

The waveform $v(t)$ is, therefore, *modulated in frequency*.

In initial discussions of the sinusoidal waveform, it is customary to consider such a waveform as having a fixed frequency and phase. In the present discussion we have generalized these concepts somewhat. To acknowledge this generalization, it is not uncommon to refer to the frequency f in Eq. (3.3) as the *instantaneous frequency* and $f(t)$ as the *instantaneous phase*. If the frequency variation about the nominal frequency w_c is small, that is, if $df(t)/dt \ll w_c$, then the resultant waveform

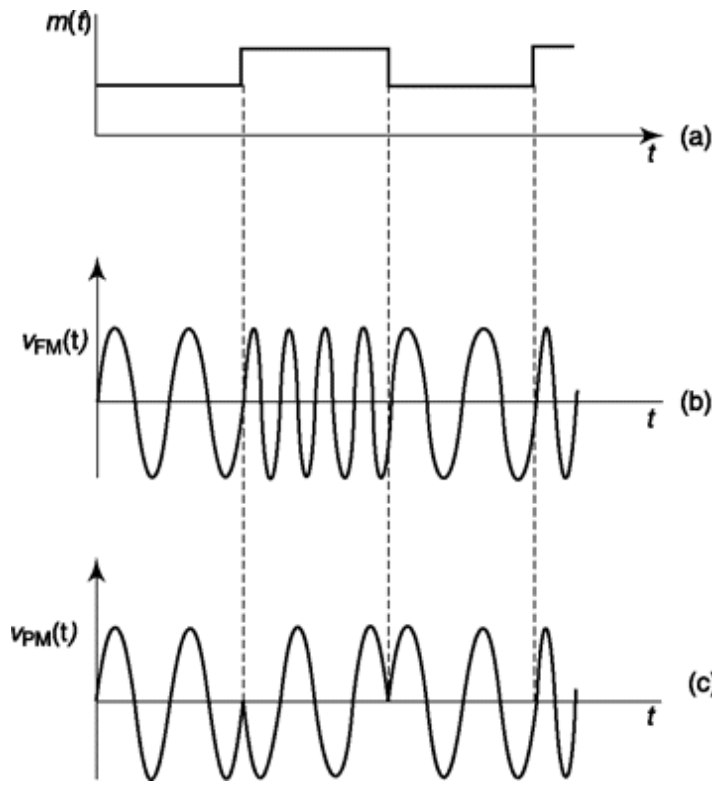


Fig. 3.1 Angle-modulated waveform. (a) Modulation signal. (b) Frequency-modulated sinusoidal carrier signal. (c) Phase-modulated sinusoidal carrier signal.

will have an appearance readily recognizable as a “sine wave,” albeit with a period which changes somewhat from cycle to cycle. Such a waveform is represented in Fig. 3.1a. In this figure the modulating signal is a square wave. The frequency-modulated signal changes frequency whenever the modulation changes level. A phase-modulated signal is shown in Fig. 3.1c.

Among the possibilities which suggest themselves for the design of a modulator are the following. We might arrange that the phase $f(t)$ in Eq. (3.1) be directly proportional to the modulating signal, or we might arrange a direct proportionality between the modulating signal and the derivative, $df(t)/dt$. From Eq. (3.3), with $f = coJ2n$

$$\frac{d\phi(t)}{dt} = 2\pi(f - f_c) \quad (3.4)$$

where f is the instantaneous frequency. Hence, in this latter case, the proportionality is between modulating signal and the departure of the instantaneous frequency from the carrier frequency. Using standard terminology, we refer to the modulation of the first type as *phase*

modulation, or PM in short and the term *frequency modulation* or FM in short refers only to the second type.

3.1.2 Relationship Between phase and Frequency Modulation

The relationship between phase and frequency modulation may be visualized further by a consideration of the diagrams of Fig. 3.2. In Fig. 3.2a, the phase-modulator block represents a device which furnishes an output $v(t)$ which is a carrier, phase-modulated by the input signal $m_i(t)$. Thus,

$$v(t) = A \cos [\omega_c t + k_p m_i(t)] \quad (3.5)$$

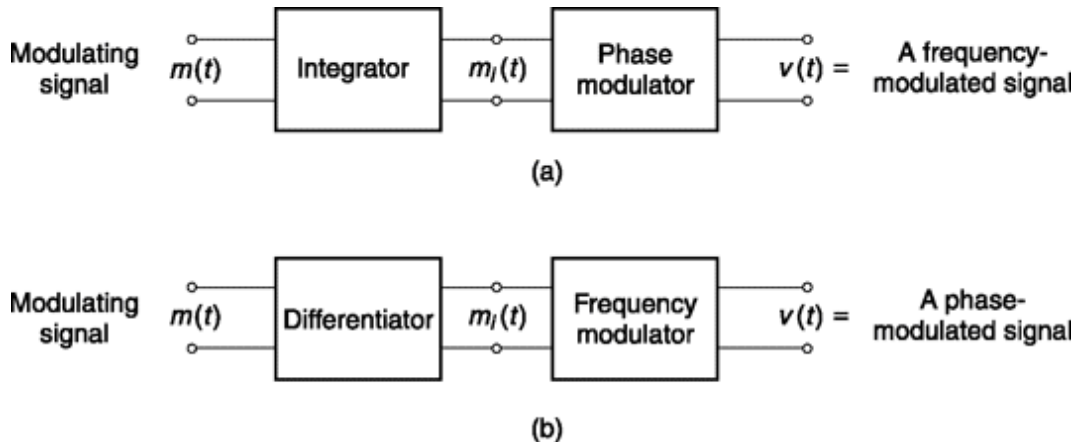


Fig. 3.2 Illustrating the relationship between phase and frequency modulation.

k_p being a constant. Let the waveform $m_i(t)$ be derived as the integral of the modulating signal $m(t)$ so that

$$m_i(t) = k'' \int_{-\infty}^t m(t) dt \quad (3.6)$$

in which k'' is also a constant. Then with $k_f = kk_p$, we have

$$v(t) = A \cos \left[\omega_c t + k_f \int_{-\infty}^t m(t) dt \right] \quad (3.7)$$

The instantaneous angular frequency is

$$\omega = \frac{d}{dt} \left[\omega_c t + k_f \int_{-\infty}^t m(t) dt \right] = \omega_c + km(t) \quad (3.8)$$

The deviation of the instantaneous frequency from the carrier frequency $\omega_c/2\pi$ is

$$v \equiv f - f_c = \frac{k}{2\pi} m(t) \quad (3.9)$$

Since the deviation of the instantaneous frequency is directly proportional to the modulating signal, the combination of *integrator* and *phase modulator* of Fig. 3.2a constitutes a device for producing a *frequency-modulated output*. Similarly, the combination in Fig. 3.2b of the differentiator and frequency modulator generates a *phase-modulated output*, i.e. a signal whose phase departure from the carrier is proportional to the modulating signal. Note that the integration being a linear operation does not change the number of frequency components present. Thus, if f_M is the maximum frequency component of $m(t)$, it will be same for $m(t)$ too.

3.1.3 Modulation Index

In the waveform of Eq. (3.1), the maximum value attained by $f(t)$, that is, the maximum phase deviation of the total angle from the carrier angle $\omega_c t$, is called the *phase deviation*. Similarly, the maximum departure of the instantaneous frequency from the carrier frequency is called the *frequency deviation*.

When the angular (and consequently the frequency) variation is sinusoidal with frequency f_m , we have, with $\omega_m = 2\pi f_m$

$$v(t) = A \cos (\omega_c t + \beta \sin \omega_m t) \quad (3.10)$$

where β is the peak amplitude of $\phi(t)$. In this case β which is the maximum phase deviation, is usually referred to as the *modulation index*. The instantaneous frequency is

$$f = \frac{\omega_c}{2\pi} + \frac{\beta \omega_m}{2\pi} \cos \omega_m t \quad (3.11a)$$

$$= f_c + \beta f_m \cos \omega_m t \quad (3.11b)$$

The maximum frequency deviation is defined as Δf and is given by

$$\Delta f = \beta f_m \quad (3.12)$$

Equation (3.10) can, therefore, be written

$$v(t) = A \cos \left(\omega_c t + \frac{\Delta f}{f_m} \sin \omega_m t \right) \quad (3.13)$$

While the instantaneous frequency f lies in the range $f_c \pm \Delta f$, it should not be concluded that all spectral components of such a signal lie in this range. In fact, in the early days of FM, bandwidth was mistakenly conceived as this. In the next section, we shall discuss spectrum of FM signal and find out effective bandwidth.

Example 3.1

Show that DSB-SC amplitude modulation is linear while phase modulation is not.

Solution

Let, $m_1(t)$ and $m_2(t)$ be two message signals and corresponding DSB-SC modulated signals are $m_{DSB1}(t)$ and $m_{DSB2}(t)$ while phase-modulated signals are $m_{PM1}(t)$ and $m_{PM2}(t)$ respectively.

Example 3.2

Consider an angle-modulated signal $x(t) = 3\cos[2\pi 10^6 t + 2\sin(2\pi 10^3 t)]$.

Find its (a) instantaneous frequency at time (i) $t = 0.25 \text{ ms}$ and (ii) $t = 0.5 \text{ ms}$, (b) maximum phase deviation and (c) maximum frequency deviation.

Solution

If w_c = carrier frequency then from definition of DSB-SC, (Eq. 2.4)

$$m_{DSB1}(t) = m_1(t)\cos \omega_c t$$

$$m_{DSB2}(t) = m_2(t)\cos \omega_c t$$

For combined input $[m_1(t) + m_2(t)]$, DSB-SC signal,

$$\begin{aligned} m_{DSB12}(t) &= [m_1(t) + m_2(t)] \cos \omega_c t \\ &= m_1(t)\cos \omega_c t + m_2(t)\cos \omega_c t \\ &= m_{DSB1}(t) + m_{DSB2}(t) \end{aligned}$$

Hence, DSB-SC is linear.

For angle-modulated signal, we can write (Eq. 3.5),

$$m_{PM1}(t) = A\cos[\omega_c t + k m_1(t)]$$

where, k = constant.

$$m_{PM2}(t) = A\cos[\omega_c t + k m_2(t)]$$

$$(a) \text{ phase } \Phi(t) = 2\pi 10^6 t + 2\sin(2\pi 10^3 t)$$

$$\text{Instantaneous frequency} = d\Phi(t)/dt = 2\pi 10^6 + 4\pi 10^3 \sin(2\pi 10^3 t)$$

$$\text{Substituting, (i) Inst. freq. at } t = 0.25 \text{ ms}$$

$$= 2\pi 10^6 + 4\pi 10^3 \sin\left(2\pi 10^3 \frac{10^{-3}}{4}\right)$$

$$= 2\pi(1.002)10^6 \text{ rad/s} = (1.002)10^6 \text{ Hz.}$$

(ii) Inst. freq. at $t = 0.5$ ms $= 2\pi 10^6 + 4\pi 10^3 \sin \left(2\pi 10^3 \frac{10^{-3}}{2} \right)$ $= 2\pi 10^6 \text{ rad/s} = 10^6 \text{ Hz}$	(b) Maximum phase deviation = $\max[2\sin(2\pi 10^3 t)]$ $= 2 \text{ rad}$ (c) Maximum frequency deviation = $\max[4\pi 10^3 \sin(2\pi 10^3 t)] = 4\pi 10^3 \text{ rad/s} = 2000 \text{ Hz}$
----------------------------------------------------------------------------------------------------------------------------------------------------------------	----------------------------------------------------------------------------------------------------------------------------------------------------------------------------------------------------

SELF-TEST QUESTION

1. Is frequency modulation a linear modulation?
2. Is it true that amplitude of transmitted carrier doesn't carry any message information in phase modulation?
3. Is phase information obtained by differentiating frequency with time?

3.2 SPECTRUM OF TONE MODULATED SIGNAL

First, we shall look into the frequency spectrum of an angle-modulated signal that is modulated by a single sinusoidal signal or tone. The modulated signal, in general, can be written as

$$v(t) = \cos(\omega_c t + \beta \sin \omega_m t) \quad (3.14)$$

which is the signal of Eq. (3.10) with the amplitude arbitrarily set at unity as a matter of convenience. One point is to be noted here. If a tone $\sin \omega_m t$ is used for phase modulation, then from Eq. (3.5), β of Eq. (3.14) is $\beta_p = k_p$. Next, if a tone $\cos \omega_m t$ is used for frequency modulation, then also we arrive at a similar expression as Eq. (3.14) by using Eq. (3.6). Then β of Eq. (3.14) is $\beta_f = k_f / \omega_m$ where the factor ω_m comes from integration. In subsequent analysis, we shall use the term β for convenience in place of writing both β_p or β_f and FM in place of both PM and FM. Note that the abbreviation AM is used for Amplitude Modulation and we cannot use it here for Angle Modulation. We shall highlight the difference between FM and PM wherever required as in Section 3.2.4. Continuing with our analysis of Eq. (3.14), we have

$$\cos(\omega_c t + \beta \sin \omega_m t) = \cos \omega_c t \cos(\beta \sin \omega_m t) - \sin \omega_c t \sin(\beta \sin \omega_m t) \quad (3.15)$$

Consider now the expression $\cos(\beta \sin \omega_m t)$ which appears as a factor on the right-hand side of Eq. (3.15). It is an *even*, periodic function having an angular frequency ω_m . Therefore it is possible to expand this expression in a Fourier series in which $\omega_m/2\pi$ is the fundamental frequency. We shall not undertake the evaluation of the coefficients in the Fourier expansion of $\cos(\beta \sin \omega_m t)$ but shall instead simply write out the results. The coefficients are, of course, functions of β , and, since the function is *even*, the coefficients of the odd harmonics are zero. The result is

$$\begin{aligned} \cos(\beta \sin \omega_m t) &= J_0(\beta) + 2J_2(\beta) \cos 2\omega_m t + 2J_4(\beta) \cos 4\omega_m t \\ &\quad + \cdots + 2J_{2n}(\beta) \cos 2n\omega_m t + \cdots \end{aligned} \quad (3.16)$$

while for $\sin(\beta \sin \omega_m t)$, which is an *odd* function, we find the expansion contains only odd harmonics and is given by

$$\begin{aligned} \sin(\beta \sin \omega_m t) &= 2J_1(\beta) \sin \omega_m t + 2J_3(\beta) \sin 3\omega_m t \\ &\quad + \cdots + 2J_{2n-1}(\beta) \sin (2n-1)\omega_m t + \cdots \end{aligned} \quad (3.17)$$

Observe that the spectrum is composed of a carrier with an amplitude $J_0(b)$ and a set of sidebands spaced symmetrically on either side of the carrier at frequency separations of w_m , $2w_m$, $3w_m$, etc. In this respect the result is unlike that which prevails in the amplitude-modulation systems discussed earlier, since in AM a sinusoidal modulating signal gives rise to only one sideband or one pair of sidebands. A second difference, which is left for verification by the student (Prob. 3.8), is that the present modulation system is nonlinear, as anticipated from the discussion of Sec. 3.1.

3.2.1 some Features of the Bessel Coefficient

Several of the Bessel functions which determine the amplitudes of the spectral components in the Fourier expansion are plotted in Fig. 3.3. We note that, at $b = 0$, $J_0(0) = 1$, while all other J_n 's are zero. Thus, as expected when there is no modulation, only the carrier, of normalized amplitude unity, is present, while all sidebands have zero amplitude. When b departs slightly from zero, $J(b)$ acquires a magnitude which is significant in comparison with unity, while all higher-order J 's are negligible in comparison. That such is the case may be seen either from Fig. 3.3 or from the approximations³ which apply when $b \neq 1$, that is,

$$J_0(\beta) \approx 1 - \left(\frac{\beta}{2}\right)^2 \quad (3.21)$$

$$J_n(\beta) \approx \frac{1}{n!} \left(\frac{\beta}{2}\right)^n \quad n \neq 0 \quad (3.22)$$

Accordingly, for b very small, the FM signal is composed of a carrier and a single pair of sidebands with frequencies $w_c \pm w_m$. An FM signal which is so constituted, that is, a signal where b is small enough so that only a single sideband pair is of significant magnitude, is called a *narrowband* FM signal. We see further, in Fig. 3.3, as b becomes somewhat larger, that the amplitude J_x of the first sideband pair increases and that also the amplitude J_2 of the second sideband pair becomes significant. Further, as b continues to increase, J_3 , J_4 , etc., begin to acquire significant magnitude, giving rise to sideband pairs at frequencies $w_c \pm 2w_m$, $w_c \pm 3w_m$, etc.

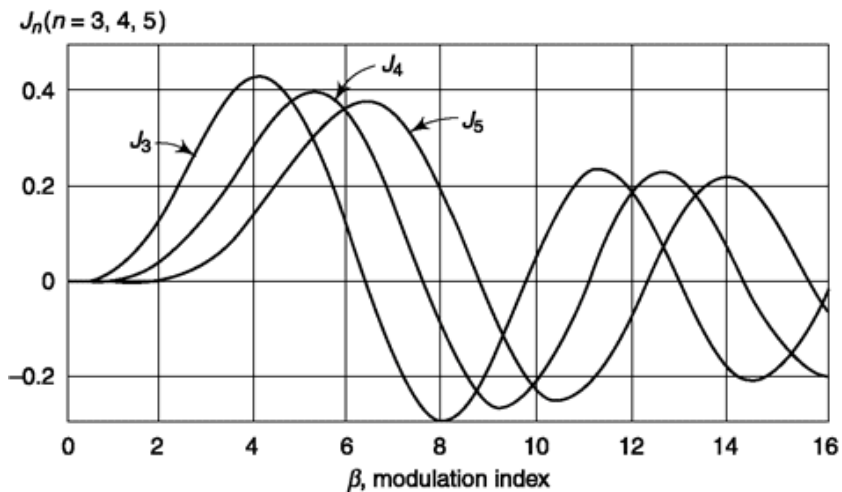
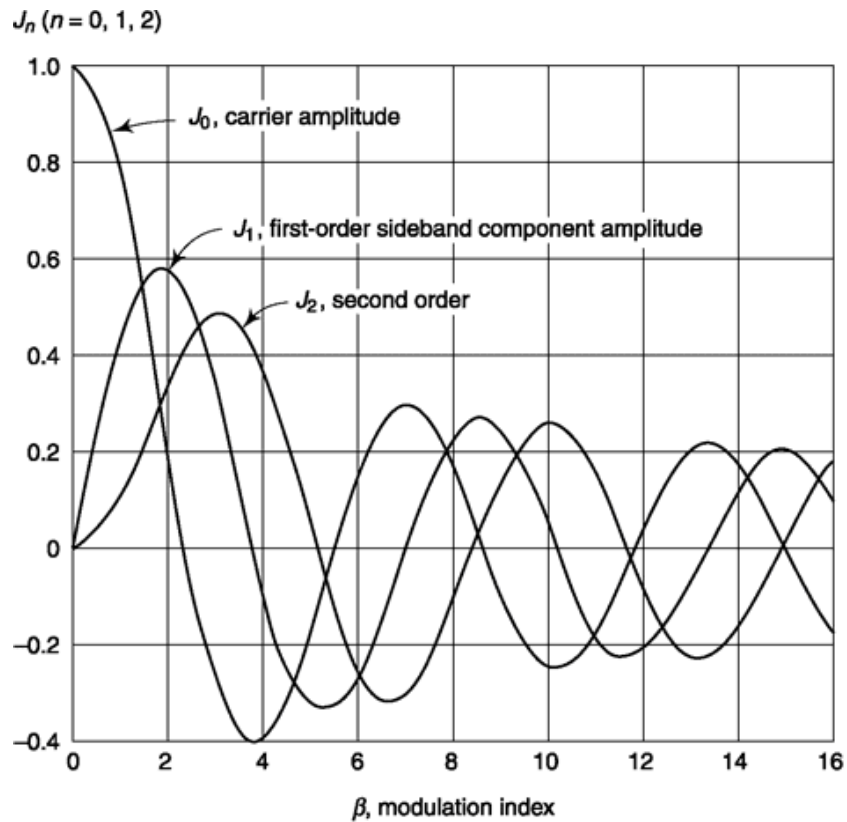


Fig. 3.3 The Bessel functions $J_n(b)$ plotted as a function of b for $n = 0, 1, 2, 5$.

power of FM signal

Another respect in which FM is unlike the linear-modulation schemes described earlier is that in an FM signal the amplitude of the spectral component at the carrier frequency is not constant independent of b . It is to be expected that such should be the case on the basis of the following considerations. The envelope of an FM signal has a constant amplitude.

Therefore the power of such a signal is a constant independent of the modulation, since the power of a periodic waveform depends only on the square of its amplitude and not on its frequency. The power of a unit amplitude signal, as in Eq. (3.14), is $P_v = 1$ (Refer to Example 1.2) and is independent of ft . When the carrier 2 is modulated to generate an FM signal, the power in the sidebands may appear only at the expense of the power originally in the carrier. Another way of arriving at the same conclusion is to make use of the identity³ $J_0^2 + 2 J_1^2 + 2 J_2^2 + 2 J_3^2 + \dots = 1$. We calculate the power P_v by squaring $v(t)$ in Eq. (3.20) and then averaging $v^2(t)$. Keeping in mind that cross-product terms average to zero, we find, independently of b , that

$$P_v = \frac{1}{2} \left(J_0^2 + 2 \sum_{n=1}^{\infty} J_n^2 \right) = \frac{1}{2} \quad (3.23)$$

as expected. We observe in Fig. 3.3 that, at various values of b , $J_0(b) = 0$. At these values of b all the power is in the sidebands and none in the carrier.

3.2.2 Bandwidth of a tone-Modulated FM signal

In principle, when an FM signal is modulated, the number of sidebands is infinite and the bandwidth required to encompass such a signal is similarly infinite in extent. As a matter of practice, it turns out that for any b , so large a fraction of the total power is confined to the sidebands which lie within some finite bandwidth that no serious distortion of the signal results if the sidebands outside this bandwidth are lost. We see in Fig. 3.3 that, except for $J_0(b)$, each $J_n(b)$ hugs the zero axis initially and that as n increases, the corresponding J_n remains very close to the zero axis up to a larger value of b . For any value of b only those J_n need be considered which have succeeded in making a significant departure from the zero axis. How many such sideband components need to be considered may be seen from an examination of Table A3 where $J_n(b)$ is tabulated for various values of n and b . It is found experimentally that the distortion resulting from bandlimiting an FM signal is tolerable as long as 98 percent or more of the power is passed by the bandlimiting filter. This definition of the bandwidth of a filter is, admittedly, somewhat vague, especially since the term “tolerable” means

different things in different applications. However, using this definition for bandwidth, one can proceed with an initial tentative design of a system. When the system is built, the bandwidth may thereafter be readjusted, if necessary. In each column of Table A3, a line has been drawn after the entries which account for at least 98 percent of the power. To illustrate this point, consider $b = 1$. Then the power contained in the terms $n = 0, 1$ and 2 is

$$\begin{aligned} P &= \frac{1}{2} J_0^2(1) + J_1^2(1) + J_2^2(1) \\ &= 0.289 + 0.193 + 0.013 = 0.495 \end{aligned} \quad (3.24)$$

The sum 0.495 is 99 percent of the power in the FM signal, which is $\frac{1}{2}$.

We note that the horizontal lines in Table A3, which indicate the value of n for 98 percent power transmission, always occur just after $n = b + 1$. Thus, for sinusoidal modulation the bandwidth required to transmit or receive the FM signal is

$$B = 2(\beta + 1)f_m \quad (3.25)$$

By way of example, when $\beta = 5$, the sideband components furthest from the carrier which have adequate amplitude to require consideration are those which occur at frequencies $f_c \pm 6f_m$. From the table of Bessel functions published in Jahnke and Emde² it may be verified on a numerical basis that the rule given in Eq. (3.25) holds without exception up to $\beta = 29$, which is the largest value of β for which J_m is tabulated there.

Using Eq. (3.12), we may put Eq. (3.25) in a form which is more immediately significant. We find

$$B = 2(\Delta f + f_m) \quad (3.26)$$

Expressed in words, *the bandwidth is twice the sum of the maximum frequency deviation and the modulating frequency*. This rule for bandwidth is called *Carson's rule*.

We deduced Eqs (3.25) and (3.26) as a generalization from Table A3, which begins with $\beta = 1$. We may note, however, that the bandwidth approximation applies quite well even when $\beta \ll 1$. For, in that case, we find that Eq. (3.25) gives $B = 2f_m$, which we know is correct from our earlier discussion of narrowband FM.

The spectra of several FM signals with sinusoidal modulation are shown in Fig. 3.4 for various values of b . These spectra are constructed directly from the entries in Table A3 except that the signs of the terms have been ignored. The spectral lines have, in every case, been drawn upward even when the corresponding entry is negative. Hence, the lines represent the *magnitudes* only of the spectral components. Not all spectral components have been drawn. Those, far removed from the carrier, which are too small to be drawn conveniently to scale, have been omitted.

3.2.3 Modulation Index: AM vs. FM

The modulation index b plays a role in FM which is not unlike the role played by the parameter A_m in connection with AM. In the AM case, and for sinusoidal modulation, we established that to avoid distortion we must observe $A_m = 1$ as an upper limit. It was also apparent that when it is feasible to do so, it is advantageous to adjust A_m to be close to unity, that is, 100 percent modulation; by doing so, we keep the magnitude of the recovered baseband signal at a maximum. On this same basis, we expect the advantage to lie with keeping b as large as possible. For, again, the larger is b , the stronger will be the recovered signal. While in AM the constraint that $A_m < 1$ is imposed by the necessity to avoid distortion, there is no similar absolute constraint on b .

There is, however, a constraint which needs to be imposed on b for a different reason. From Eq. (3.25) for $b \neq 1$ we have $B @ 2bf_m$. Therefore the maximum value we may allow for b is determined by the maximum allowable bandwidth and the modulation frequency. In comparing AM with FM, we may then note, in review, that in AM the recovered modulating signal may be made progressively larger subject to the onset of distortion in a manner which keeps the occupied bandwidth constant. In FM there is no similar limit on the modulation, but increase in the magnitude of the recovered signal is achieved at the expense of bandwidth. A more complete comparison is deferred to chapters 8 and 9, where we shall take account of the presence of noise and also of the relative power required for transmission.

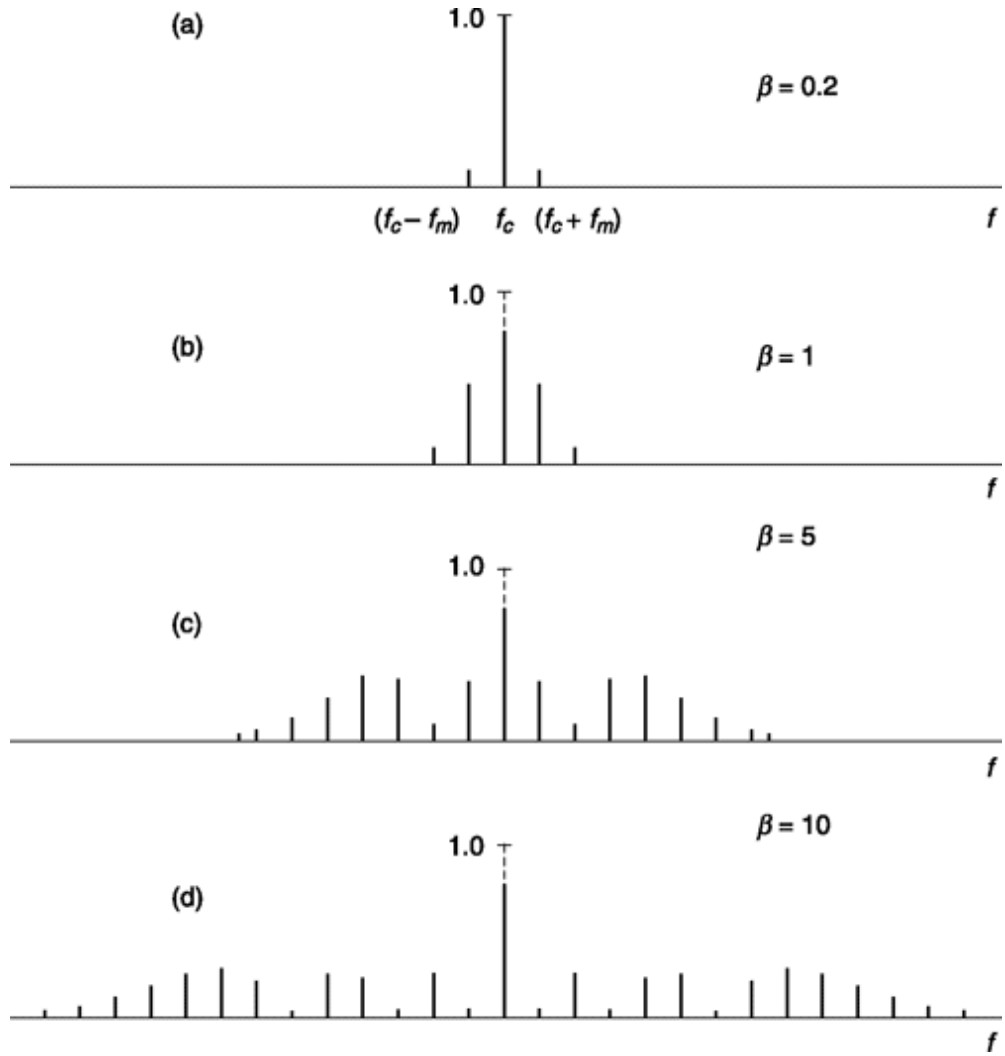


Fig. 3.4 The spectra of sinusoidally modulated FM signals for various values of b as discussed in Section 2.3.3.

3.2.4 spectrum of 'Constant Bandwidth' FM

Let us consider that we are dealing with a modulating signal voltage $v_m \cos 2\pi f_m t$ with v_m the peak voltage. In a phase-modulating system the phase angle $\phi(t)$ would be proportional to this modulating signal so that $\phi(t) = k' v_m \cos 2\pi f_m t$, with k' a constant. The phase deviation is $\beta = k' v_m$, and, for constant v_m , the bandwidth occupied increases linearly with modulating frequency since $B \equiv 2\beta f_m = 2k' v_m f_m$. We may avoid this variability of bandwidth with modulating frequency by arranging that $\phi(t) = (k/2\pi f_m) v_m \sin 2\pi f_m t$ (k a constant). For, in this case

$$\beta = \frac{k v_m}{2\pi f_m} \quad (3.27)$$

and the bandwidth is $B \cong (2k/2\pi)v_m$, independently of f_m . In this latter case, however, the instantaneous frequency is $\omega = \omega_c + kv_m \cos 2\pi f_m t$. Since the instantaneous frequency is proportional to the modulating signal, the initially phase-modulated signal has become a frequency-modulated signal. Thus a signal intended to occupy a nominally constant bandwidth is a frequently-modulated rather than an phase-modulated signal.

In Fig. 3.5 we have drawn the spectrum for three values of β for the condition that βf_m is kept constant. The nominal bandwidth $B \cong 2 \Delta f = 2\beta f_m$ is consequently constant. The amplitude of the unmodulated carrier at f_c is shown by a dashed line. Note that the extent to which the actual bandwidth extends beyond the nominal bandwidth is greatest for small β and large f_m and is least for large β and small f_m .

Fig. 3.5 Spectra of sinusoidally modulated FM signals. The nominal bandwidth $B \sim 2pf_m = 2Df$ is kept fixed.

In commercial FM broadcasting, the Federal Communications Commission allows a frequency deviation $Df = 75$ kHz. If we assume that the highest audio frequency to be transmitted is 15 kHz, then at this frequency $b = Df/f_m = 75/15 = 5$. For all other modulation frequencies b is larger than 5. When $b = 5$, there are $b + 1 = 6$ significant sideband pairs so that at $f_m = 15$ kHz the bandwidth required is $B = 2 \times 6 \times 15 = 180$ kHz, which is to be compared with $2 Df = 150$ kHz. When $b = 20$, there are 21 significant sideband pairs, and $B = 2 \times 21 \times 15/4 = 157.5$ kHz. In the limiting case of very large b and correspondingly very small f_m , the actual bandwidth becomes equal to the nominal bandwidth $2Df$.

3.2.5 Phasor Diagram: AM vs. FM

With the aid of a phasor diagram we shall be able to arrive at a rather physically intuitive understanding of how so odd an assortment of sidebands as in Eq. (3.20) yields an FM signal of constant amplitude. The diagram will also make clear the difference between AM and narrowband FM (NBFM). In both of these cases there is only a single pair of sideband components

Let us consider first the case of narrowband FM. From Eqs (3.10), (3.21), and (3.22) we have for $\beta \ll 1$ that

$$v(t) = \cos(\omega_c t + \beta \sin \omega_m t) \quad (3.28a)$$

$$\cong \cos \omega_c t - \frac{\beta}{2} \cos(\omega_c - \omega_m)t + \frac{\beta}{2} \cos(\omega_c + \omega_m)t \quad (3.28b)$$

Refer to Fig. 3.6a. Assuming a coordinate system which rotates counter-clockwise at an angular velocity w_c , the phasor for the carrier-frequency term in Eq. (3.28) is fixed and oriented in the horizontal direction. In the

same coordinate system, the phasor for the term $(b/2) \cos(\omega_c + \omega_m)t$ rotates in a counter-clockwise direction at an angular velocity ω_m , while the phasor for the term $-(b/2) \cos(\omega_c - \omega_m)t$ rotates in a clockwise direction, also at the angular velocity ω_m . At the time $t = 0$, both phasors, which represent the sideband components, have maximum projections in the horizontal direction. At this time one is parallel to, and one is antiparallel to, the phasor representing the carrier, so that the two cancel. The situation depicted in Fig. 3.6a corresponds to a time shortly after $t = 0$. At this time, the rotation of the sideband phasors which are in opposite directions, as indicated by the curved arrows, have given rise to a sum phasor A_x . In the coordinate system in which the carrier phasor is stationary, the phasor A_x always stands perpendicularly to the carrier phasor and has the magnitude

$$\Delta_1 = \beta \sin \omega_m t \quad (3.29)$$

The carrier, now slightly reduced in amplitude, and A_1 combine to give rise to a resultant R . The angular departure of R from the carrier phasor is f . It is readily seen from Fig. 3.6a that since $b \neq 1$, the maximum value of $f \cdot \tan f = b$, as is to be expected. The small variation in the amplitude of the resultant which appears in Fig. 3.6a is only the result of the fact that we have neglected higher-order sidebands.

Now let us consider the phasor diagram for AM. The AM signal is

$$(1 + m \sin \omega_m t) \cos \omega_c t = \cos \omega_c t + \frac{m}{2} \sin (\omega_c + \omega_m)t - \frac{m}{2} \sin (\omega_c - \omega_m)t \quad (3.30)$$

and the individual terms are represented as phasors in Fig. 3.6a. Comparing Eqs (3.28) and (3.30), we see that there is a 900° phase shift in the phases of the sidebands between the FM and AM cases. In Fig. 3.6b the sum A of the sideband phasors is given by

$$\Delta = m \sin \omega_m t \quad (3.31)$$

The important difference between the FM and AM cases is that in the former the sum A_1 is always perpendicular to the carrier phasor, while in the latter the sum A is always parallel to the carrier phasor. Hence in the AM case, the resultant R does not rotate with respect to the carrier phasor but instead varies in amplitude between $1 + m$ and $1 - m$.

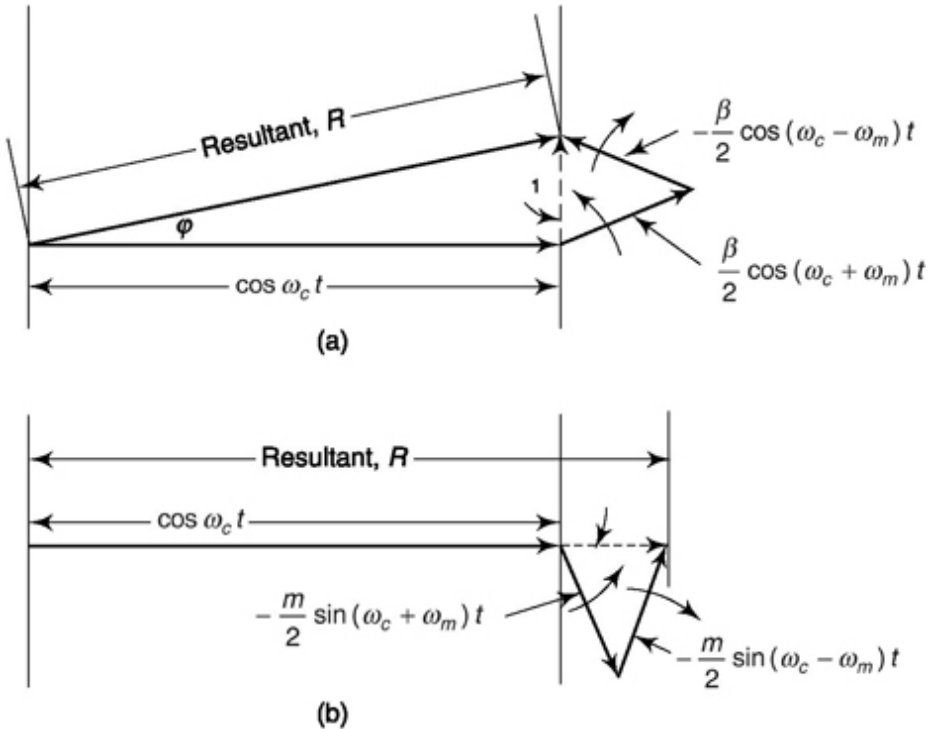


Fig. 3.6 (a) Phasor diagram for a narrowband FM signal, (b) Phasor diagram for an AM signal.

Another way of looking at the difference between AM and NBFM is to note that in NBFM where $\beta \ll 1$

$$v(t) \approx \cos \omega_c t - \beta \sin \omega_m t \sin \omega_c t \quad (3.32)$$

while in AM

$$v(t) = \cos \omega_c t + m \sin \omega_m t \cos \omega_c t \quad (3.33)$$

Note that in NBFM the first term is $\cos \omega_c t$, while the second term involves $\sin \omega_c t$, a *quadrature* relationship. In AM both first and second terms involve $\cos \omega_c t$, an *in-phase* relationship.

To return now to the FM case and to Fig. 3.6a, the following point is worth noting. When the angle ϕ completes a full cycle, that is, Δ_1 varies from $+\beta$ to $-\beta$ and back again to $+\beta$, the magnitude of the resultant R will have executed *two* full cycles. For R is a maximum at $\Delta_1 = \beta$, a minimum at $\Delta_1 = 0$, a maximum again when $\Delta_1 = -\beta$, and so on. On this basis, it may well be expected that if an additional sideband pair is to be added to the first to make R more nearly constant, this new pair must give rise to a resultant Δ_2 which varies at the frequency $2\omega_m$. Thus, we are not surprised to find that as the phase deviation β increases, a sideband pair comes into existence at the frequencies $\omega_c \pm 2\omega_m$.

As long as we depend on the first-order sideband pair only, we see from Fig. 3.6a that ϕ cannot exceed 90° . A deviation of such magnitude is hardly adequate. For consider, as above, that $\Delta f = 75$ kHz and that $\phi_m = 50$ Hz. Then $\omega_m = 75,000/50 = 1500$ rad, and the resultant R must, in this case, spin completely about $1500/2\pi$ or about 240 times. Such wild whirling is made possible through the effect of the higher-order sidebands. As noted, the first-order sideband pair gives rise to a phasor $\Delta_1 = J_1(\beta) \sin \omega_m t$, which phasor is perpendicular to the carrier phasor. It may also be established by inspection of Eq. (3.20) that the second-order sideband pair gives rise to a phasor $\Delta_2 = J_2(\beta) \cos 2\omega_m t$ and that this phasor is *parallel* to the carrier phasor. Continuing, we easily establish that all odd-numbered sideband pairs give rise to phasors

which are parallel to the carrier phasor. Thus, phasors A_x , A_2 , A_3 , etc., alternately perpendicular and parallel to the carrier phasor, are added to carry the end point of the resultant phasor R completely around as many times as may be required, while maintaining R at constant magnitude. It is left as an exercise for the student to show by typical examples how the superposition of a carrier and sidebands may swing a constant-amplitude resultant around through an arbitrary angle (Prob. 3.16).

Example 3.3

Give a generalized representation of bandwidth for single tone sinusoidal modulating signal of amplitude A_m , frequency w_m ($= 2\pi f_m$), carrier amplitude A_c , frequency w_c ($= 2\pi f_c$) for both PM and FM. Assume, proportionality constant for phase modulation k_p and proportionality constant for frequency modulation k_f

$$v(t) = A_c \cos[\omega_c t + k_p m(t)] \quad (3.36)$$

$$v(t) = A_c \cos\left[\omega_c t + k_f \int_{-\infty}^t m(t) dt\right] \quad (3.37)$$

Bandwidth calculation for PM: For single-tone case, from Eq. (3.36)

$$v(t) = A_c \cos[\omega_c t + k_p A_m \sin(\omega_m t)]$$

$$\text{Instantaneous frequency } \omega_i = d[\omega_c t + k_p A_m \sin(\omega_m t)]/dt$$

$$\text{or, } \omega_i = \omega_c t + k_p A_m \omega_m \cos(\omega_m t) \quad (3.38)$$

$$\text{Maximum frequency deviation, } \Delta f = \Delta\omega/(2\pi) = \max |k_p A_m \omega_m \cos(\omega_m t)|/(2\pi)$$

$$\text{or, } \Delta f = k_p A_m f_m \quad (3.39)$$

$$\text{From Eq. (3.26), bandwidth for PM} = 2(f_m + \Delta f) = 2(1 + k_p A_m) f_m \quad (3.40)$$

Bandwidth calculation for FM: From Eq. (3.37)

$$\begin{aligned} \text{Instantaneous frequency } \omega_i &= \left[\omega_c t + k_f \int_{-\infty}^t m(t) dt \right] / dt \\ &= \omega_c + k_f m(t) \end{aligned}$$

For single tone case $\omega_i = \omega_c + k_f A_m \sin(\omega_m t)$ (3.41)

Maximum frequency deviation, $\Delta f = \Delta\omega/(2\pi) = \max |k_f A_m \sin(\omega_m t)|/(2\pi)$

or, $\Delta f = k_f A_m$ (3.42)

From Eq. (3.26), bandwidth for FM = $2(f_m + \Delta f) = 2(f_m + k_f A_m)$ (3.43)

Note that inclusion of f_m in Δf calculation for PM makes its bandwidth increase/decrease faster with increase/decrease of f_m when compared with FM. Since bandwidth can be written in terms of modulation index β as $2(\beta + 1) f_m$, for PM and FM we can write (for single tone case)

From Eq. (3.40), modulation index for frequency modulation, $\beta_p = k_p A_m$ (3.44)

From Eq. (3.40), modulation index for phase modulation, $\beta_f = k_f A_m / f_m$ (3.45)

Thus, β_p is insensitive to f_m variation but β_f is inversely proportional to f_m

Example 3.4

Consider a modulating signal $m(t) = 2\sin(2\pi 10^3 t)$ is used to modulate a carrier of frequency 10^6 Hz. Find the bandwidth for (a) phase modulation and frequency modulation for above also, (b) when modulating frequency is doubled and (c) when amplitude of modulating signal is halved, thereafter. Use $\beta_p = 10$ and $\beta_f = 10$ unit.

Solution

(a) $A_m = 2, f_m = 1000, \beta_p = 10$ and $\beta_f = 10$.

For PM, from Eq. (3.25), bandwidth = $2(1 + 10)1000 = 22000$ Hz

SELF-TEST QUESTIONS

4. Does an FM signal have infinite bandwidth?
5. Why the strength of carrier in FM spectrum is not constant like AM?
6. In phasor representation of AM, length of carrier phasor is varied while in FM the angle is varied. Is it correct?

3.3 ARBITRARY MODULATED FM SIGNAL

In previous section we put emphasis on tone modulation, i.e. modulating signal had sinusoidal variation or single frequency component. Here, we relax that constraint and investigate more general type of modulating signal.

3.3.1 spectrum of Narrowband Angle Modulation

Previously, we considered the spectrum, in NBFM, which is produced by sinusoidal modulation. We found that, just as in AM, such modulation gives rise to two sidebands at frequencies $w_c + w_m$ and $w_c - w_m$. We extend the result now to an arbitrary modulating waveform.

We may readily verify (Prob. 3.19) that superposition applies in narrowband angle modulation just as it does to AM. That is, if $b_1 \sin w_1 t + b_2 \sin w_2 t$ is substituted in Eq. (3.28a) in place of $b \sin w_m t$, the sidebands which result are the sum of the sidebands that would be yielded by either modulation alone. Hence even if a modulating signal of waveform $m(t)$, with a continuous distribution of spectral components, is used in either AM or narrowband angle modulation, the forms of the sideband spectra will be the same in the two cases.

More formally, we have in AM, when the modulating waveform is $m(t)$, the signal is

$$v_{AM}(t) = A[1 + m(t)] \cos \omega_c t = A \cos \omega_c t + Am(t) \cos \omega_c t \quad (3.46)$$

Let us assume, for simplicity, that $m(t)$ is a finite energy waveform with a Fourier transform $M(j\omega)$. We use the theorem that if the Fourier transform $\mathcal{F}[m(t)] = M(j\omega)$, then $\mathcal{F}[m(t) \cos \omega_c t]$ is as given in Eq. (2.4). We then find that

$$\mathcal{F}[v_{AM}(t)] = \frac{A}{2} [\delta(\omega + \omega_c) + \delta(\omega - \omega_c)] + \frac{A}{2} [M(j\omega + j\omega_c) + M(j\omega - j\omega_c)] \quad (3.47)$$

The narrowband angle-modulation signal of Eq. (3.28), except of amplitude A and with phase modulation $m(t)$, may be written, for $|m(t)| \ll 1$,

$$v_{PM}(t) \cong A \cos \omega_c t - Am(t) \sin \omega_c t \quad (3.48)$$

so that

$$\mathcal{F}[v_{PM}(t)] = \frac{A}{2} [\delta(\omega + \omega_c) + \delta(\omega - \omega_c)] + \frac{A}{2} e^{-j\pi/2} [M(j\omega + j\omega_c) - M(j\omega - j\omega_c)] \quad (3.49)$$

Comparing Eq. (3.47) with Eq. (3.49), we observe that

$$|\mathcal{F}[v_{AM}]|^2 = |\mathcal{F}[v_{PM}]|^2 \quad (3.50)$$

Thus, if we were to make plots of the energy spectral densities of $v_{AM}(t)$ and of $v_{PM}(t)$, we would find them identical. Similarly, if $m(t)$ were a signal of finite power, we would find that plots of power spectral density would be the same.

3.3.2 spectrum of Wideband FM (WBFM)

In this section we engage in a heuristic discussion of the spectrum of a wideband FM signal. We shall not be able to deduce the spectrum with the precision that is possible in the NBFM case described in the previous section. As a matter of fact, we shall be able to do no more than to deduce a means of expressing approximately the power spectral density of a WBFM signal. But this result is important and useful.

Previously, to characterize an FM signal as being narrowband or wideband, we had used the parameter $b = Af/f_m$, where Af is the frequency deviation and f_m the frequency of the sinusoidal modulating signal. The signal was then NBFM or WBFM depending on whether $b \ll 1$ or $b \gg 1$. Alternatively we distinguished one from the other on the basis of whether one or many sidebands were produced by each spectral component of the modulating signal, and on the basis of whether or not superposition applies. We consider now still another alternative.

Let the symbol $v = f - f_c$ represent the frequency difference between the instantaneous frequency f and the carrier frequency f_c ; that is, $v(t) = (k/2\pi)m(t)$ [see Eq. (3.9)]. The period corresponding to v is $T = 1/v$. As f varies, so also will v and T . The frequency v is the frequency with which the resultant phasor R in Fig. 3.6 rotates in the coordinate system in which the carrier phasor is fixed. In WBFM this resultant phasor rotates through many complete revolutions, and its speed of rotation does not change radically from revolution to revolution. Since, the resultant R is constant, then if we were to examine the plot as a function of time of the projection of R in, say, the horizontal direction, we would recognize it as a sinusoidal waveform because its frequency would be changing very slowly. No appreciable change in frequency would take place during the course of a cycle. Even a long succession of cycles would give the appearance of being of rather constant frequency. In NBFM, on the other hand, the phasor R simply oscillates about the position of the carrier phasor. Even though, in this case, we may still formally calculate a frequency v , there is no corresponding time interval during which the phasor makes complete revolutions at approximately a constant rate v .

Now let us consider that a carrier is wideband FM-modulated by a signal $m(t)$ such as, say, an audio signal. The message signal is random in nature. If deterministic, then it need not be sent from one place to another and can be generated at the receiver side by using the deterministic relation. Though

random message signal shows some probabilistic distribution, i.e. a certain value of it is more probable than others. Probability density function gives a functional representation of this probability. We shall discuss it in detail in Section 6.2.3. For this discussion, let us consider that the modulation

$m(t)$ is characterized by the probability density function $f(m)$. Then the fraction of the time that $m(t)$ spends in the range between m_1 and $m_1 + dm$ is the probability that $m(t)$ lies between m_1 and $m_1 + dm$, that is, $f(m_1) dm$. Corresponding to each value of $m(t)$, the value of the frequency deviation $v(t) = (k/2p)m(t)$. Hence, during the time $m(t)$ is in the range m_1 and $m_1 + dm$, v is in the range v_1 and $v_1 + dv$. As we have seen in WBFM, the frequency v changes only relatively slowly. Thus, the assignment of a frequency v to a waveform during the interval when $m(t)$ has a value corresponding to v has a physical as well as a purely mathematical significance. On this basis, it is reasonable to say that of the total power in the FM waveform, the fraction of the power in the frequency range between v_1 and $v_1 + dv$ is proportional to the time $m(t)$ spends in the range m_1 to $m_1 + dm$. With $G(v)$, the power spectral density (Refer to Section 1.3.4) of the FM waveform, we have the result that $G(v_1) dv$ is proportional to $f(m_1) dm$. Finally, since dv is proportional to dm , we have the most important result that $G(v)$ is proportional to $f(m)$. Expressed in words, the *power spectral density G(v) of a WBFM waveform is determined by, and has the same form as, the density function f(m) of the modulating waveform.*

Example 3.5

In the WBFM signal

$$v(t) = A \cos \left[2\pi f_c t + k \int_{-\infty}^t m(\lambda) d\lambda \right] \quad (3.51)$$

$m(t)$ is defined by a probability density function

$$f(m) = \begin{cases} \frac{1}{M} & -\frac{M}{2} \leq m \leq \frac{M}{2} \\ 0 & \text{elsewhere} \end{cases} \quad (3.52)$$

Obtain an expression for $G(f)$, the power spectral density of $v(t)$.

Solution

Since $G(v)$ (with $v \equiv f - f_c$) is proportional to $f(m)$, we have

$$G(v) = \alpha f(m) \quad (3.53)$$

where α is a constant of proportionality. Since $v(t) = km(t)/2\pi$,

$$G(v) = \begin{cases} \frac{\alpha}{M} & -\frac{kM}{4\pi} \leq v \leq \frac{kM}{4\pi} \\ 0 & \text{elsewhere} \end{cases} \quad (3.54)$$

Replacing v by $f - f_c$, and expressing the power spectral density for both positive and negative frequencies (i.e. a two-sided density), we have

$$G(f) = \begin{cases} \frac{\alpha}{2M} & f_c - \frac{kM}{4\pi} \leq |f| \leq f_c + \frac{kM}{4\pi} \\ 0 & \text{elsewhere} \end{cases} \quad (3.55)$$

To evaluate α , we note that the power of the FM waveform is $A^2/2$. Hence,

$$\int_{-\infty}^{\infty} G(f) df = \frac{A^2}{2} \quad (3.56)$$

From Eqs (3.55) and (3.56) we find $\alpha = \pi A^2/k$, so that

$$G(f) = \begin{cases} \frac{\pi A^2}{2kM} & f_c - \frac{kM}{4\pi} \leq |f| \leq f_c + \frac{kM}{4\pi} \\ 0 & \text{elsewhere} \end{cases} \quad (3.57)$$

Note that many physically encountered signals can be approximated by a bell-shaped probability density function termed *Gaussian shape*. More about this distribution will be discussed in Section 6.3.1. What we note here is that power spectral density of such signals will also show Gaussian shape as shown in Fig. 3.7 and 98% bandwidth can be calculated as

$$B = 4.6\Delta f_{\text{rms}} \quad (3.58)$$

where Δf_{rms} is standard deviation of spectral density (Refer to web supplement for details.)

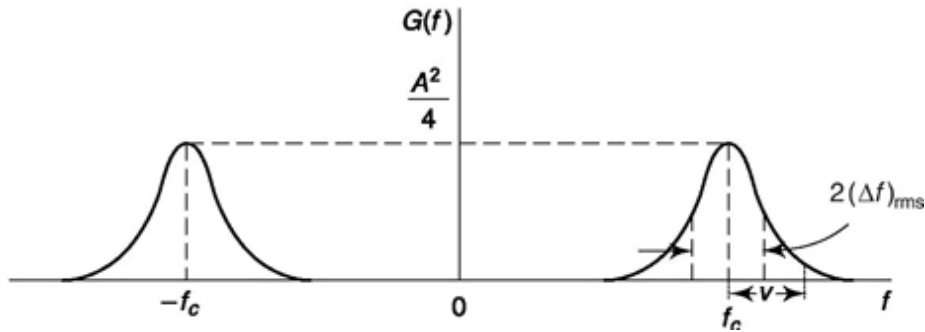


Fig. 3.7 The power spectral density of a carrier f frequency-modulated by a baseband signal with a Gaussian amplitude distribution. The variable v measures the departure of frequency from the carrier frequency. A is the amplitude of FM waveform.

SELF-TEST QUESTION

7. Is it true that for wideband FM, $b \neq 1$?
8. Narrowband PM with magnitude of modulating signal $\neq 1$ and AM have identical energy/power spectral density. Is that true?
9. Does a Gaussian modulating signal produce Gaussian power spectral density for wideband FM?
10. Will the WBFM bandwidth be different if two Gaussian message signals have same variance
but are otherwise arbitrary?

3.4 FM MODULATORS AND DEMODULATORS

In this section, we discuss FM modulators and demodulators. The aim is to address all the major principles and their representative systems. Though we emphasize on FM modulators and demodulators we show towards the end how PM modulators and demodulators can be obtained from the same.

3.4.1 FM Generation by parameter variation Method

The generator which produces the carrier of an FM waveform is, in many instances, a tuned circuit oscillator. Such oscillator circuits furnish a sinusoidal waveform whose frequency is very largely determined by, and is very nearly equal to, the resonant frequency of an inductance-capacitance combination. Thus, the frequency of oscillation is $f = (2\pi/LC)^{-1}$, in which L is the inductance and C the capacitance. Such an LC combination, a parallel combination in this case, is shown in Fig. 3.8. The capacitor consists here of

a fixed capacitor C_0 , which is shunted by a voltage-variable capacitor C_v . A voltage-variable capacitor, commonly called a *varicap*, is one whose capacitance value depends

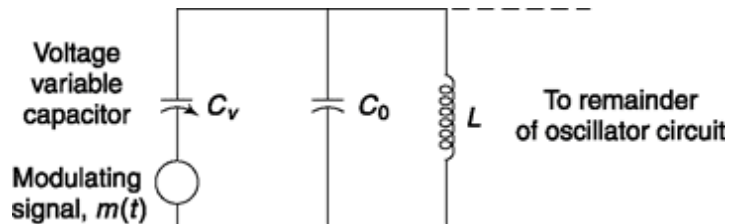


Fig. 3.8 A voltage-variable capacitor is used to frequently-modulate an LC oscillator.

on the dc biasing voltage maintained across its electrodes. Semiconductor diodes, when operated with a reverse bias, have characteristics suitable to permit their use as voltage-variable capacitors.

In the circuit of Fig. 3.8 the modulating signal varies the voltage across C_v . As a consequence, the capacitance of C_v changes and causes a corresponding change in the oscillator frequency. Ordinarily the modulating frequency is very small in comparison with the oscillator frequency. Therefore the fractional change in C_v may be very small during the course of many cycles of the oscillator signal. We may consequently expect that even with this variable capacitance, the instantaneous oscillator frequency will be given by $f = (2\pi\sqrt{LC})^{-1}$. Then we have the result that the system suggested in Fig. 3.8 will generate an oscillator output signal whose instantaneous frequency depends on the instantaneous value of the modulating signal. Any oscillator whose frequency is controlled by the modulating-signal voltage is called a *voltage-controlled oscillator*, or VCO.

Frequency modulation may be achieved by the variation of any element or parameter on which the frequency depends. If the frequency variation is to occur in response to a modulating signal $m(t)$, then a component must be available, capacitor, resistor, or inductor, whose value can be varied with an electrical signal. We have noted that reversed-biased junctions may serve as voltage-variable capacitors. Similarly, PIN diodes and FETs (field-effect transistors) have found application as variable resistors. The inductance of a magnetic-cored inductor, called a saturable reactor, can, be varied by changing the dc biasing current through the winding, and thereby changing the core permeability.

Let us now look at a mathematical representation of VCO by considering this as a block to which a variable voltage $v(t)$ is input and $v_{osc}(t)$ output. The block level relation can be written as

$$v_{osc}(t) = B \cos \left[\omega_c t + G_0 \int_{-\infty}^t v(\lambda) d\lambda \right] \quad (3.59)$$

where, B is the amplitude of the output of VCO and ω_c the angular frequency in absence of any frequency-controlling voltage; G_0 is the frequency sensitivity in radian/volt, i.e. rate of change of instantaneous angular frequency w.r.t. frequency controlling voltage $v(t)$. Thus, instantaneous angular frequency

$$\omega_i(t) = \omega_c + G_0 v(t) \quad (3.60)$$

Note that, frequency modulation is achieved if $v(t)$ is the modulating message signal $m(t)$.

A principal difficulty with the parameter-variation method of frequency modulation is the difficulty it entails when we require that the carrier frequency [the signal frequency when the modulation signal $m(t) = 0$] be maintained constant to a high order of precision over extended periods of time. There is a certain measure of inconsistency in requiring that a device have *long-time* frequency stability and yet be able to respond readily to a modulating signal. We turn our attention in the next section to a system of frequency modulation in which the carrier generator is *not* required to respond to a modulating signal. The carrier generator is isolated from the remainder of the circuitry and may be designed without the need to make compromises with its frequency stability. Thus, we find that, when the frequency range is appropriate, the carrier generator is invariably a crystal-controlled oscillator which is much more stable than LC oscillator.

3.4.2 FM Generation by Armstrong's Indirect Method

A phase-modulated waveform in which the modulating waveform is $m(t)$ is written $\cos [\omega_c t + m(t)]$. If the modulation is narrowband [$|m(t)| \ll 1$], then we may use the approximation

$$\cos [\omega_c t + m(t)] \approx \cos \omega_c t - m(t) \sin \omega_c t \quad (3.61)$$

The term $m(t) \sin w_c t$ is a DSB-SC waveform in which $m(t)$ is the modulating waveform and $\sin w_c t$ the carrier. We note that the carrier of the FM waveform, that is, $\cos w_c t$, and the carrier of the DSB-SC waveform are in quadrature. We may note in passing that if the two carriers are in phase, the result is an AM signal since

$$\cos w_c t + m(t) \cos w_c t = [1 + m(t)] \cos w_c t \quad (3.62)$$

A technique used in commercial FM systems to generate NBFM, which is based on our observation in connection with Eq. (3.61), is shown in Fig. 3.9. Here a balanced modulator is employed to generate the DSB-SC signal using $\sin w_c t$ as the carrier of the modulator. This carrier is then shifted in phase by 900° and, when added to the balanced modulator output, thereby forms an NBFM signal. However, the signal so generated will be phase-modulated rather than frequency-modulated. If we desire that the frequency rather than the phase be proportional to the modulation $m(t)$, then, as discussed in Sec. 3.1.2 and illustrated in Fig. 3.2, we need merely integrate the modulating signal before application to the modulator.

If the system of Fig. 3.9 is to yield an output signal whose phase deviation is directly proportional to the amplitude of the modulating signal, then the phase deviation must be kept small. That such is the case is readily to be seen in Fig. 3.6a. If we neglect the small second-order correction in the carrier amplitude and assume it to be of unit magnitude, we have $\tan f = D_1$. Since, however, $D_1 (= b \sin w_m t)$ is proportional to the modulating signal, we actually require that $f = D_1$. In order that we may replace $\tan f$ by f , we require that at all times $f \neq 1$. In this case $b \neq 1$, and then $f = b \sin w_m t$.

The restriction that $f \neq 1$ imposes a similar constraint on the allowable frequency deviation $Df (= bw_m/2\pi)$ when the system of Fig. 3.9 is adapted for use as a frequency-modulation system by the addition of an integrator. In the next section we discuss how the frequency deviation, and the phase deviation as well, of a narrowband signal may be increased by the process of frequency multiplication.

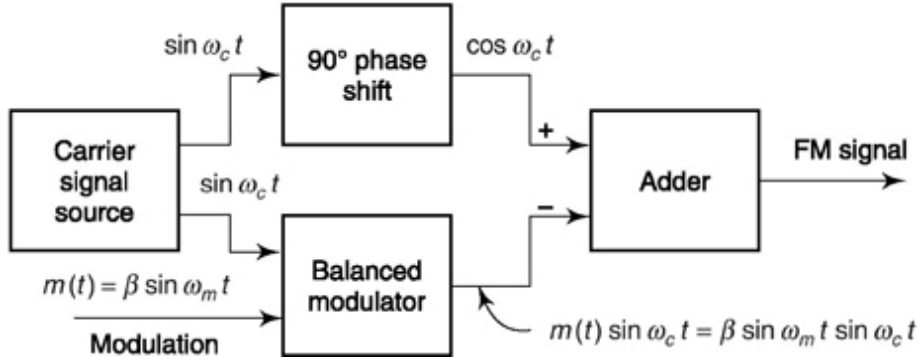


Fig. 3.9 Illustrating the principle of the Armstrong system of generating a PM signal.

3.4.3 Frequency Multiplication and Application to FM

A *frequency multiplier* is a combination of a nonlinear element and a bandpass filter. One such possible combination is shown in Fig. 3.10. We consider the operation, qualitatively, in order to see the relevance of the process to our present interest of increasing the frequency deviation of an FM signal.

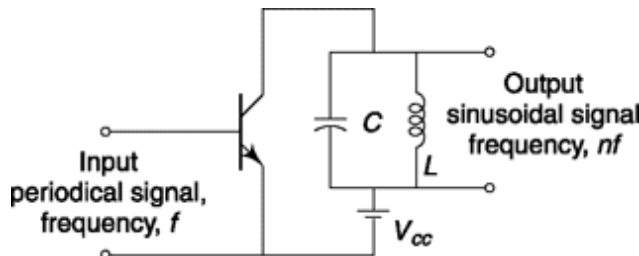


Fig. 3.10 A frequency-multiplier circuit.

Assume that the input signal to the transistor in the circuit of Fig. 3.10 is a periodic signal, possibly sinusoidal but not necessarily so. The amplitude of the input signal is large enough, and the biasing (not shown) is such that the transistor operates nonlinearly. Typically, the transistor operates in the *class C* mode. In this mode of operation the transistor is in the cutoff region for more than half of the period of the input signal. During intervals in the neighborhood of the peak positive excursions of the input signal, the transistor is driven into the active region, possibly even into saturation. Collector current flows, not continuously, but rather in spurts, forming pulses, one pulse for each cycle of the input driving signal. The collector-current waveform has the same fundamental period as has the driving signal but is rich in higher-frequency harmonics. The *LC* parallel resonant circuit is tuned to resonance at the *n*th harmonic of the frequency *f* of the input signal. The sharpness of the resonance is such that the impedance presented by the

resonant circuit is very small at all harmonic frequencies except the n th. All components of collector current except the component at frequency nf pass through the resonant circuit without developing appreciable voltage. However, in response to this n th harmonic current component, there appears across the resonant circuit a very nearly sinusoidal voltage waveform of frequency nf . The resonant circuit serves as a bandpass filter to selectively single out the n th harmonic of the driving waveform. The process of *frequency multiplication* performed by the multiplier under consideration is one in which a periodic signal of frequency f serves to generate a second periodic signal of frequency nf , with n an integer.

In principle, we may multiply by an arbitrary integral number n by simply tuning the resonant circuit to nf . In practice, of course, most periodic waveforms encountered in engineering applications, such as the collector-current pulse waveform of the transistor of Fig. 3.10, are characterized by a progressive decrease of amplitude of harmonic with increasing harmonic number. As a result, we find that as the order of multiplication increases, the output signal becomes progressively smaller. Circuits such as in Fig. 3.10 are commonly used for multiplication by factors from about 2 to 5. Where higher orders of multiplication are required, multipliers may be cascaded. Cascaded multipliers of order n_b , n_2 , n_3 , ... yield an overall multiplication of order $n_x n_2 n_3 \dots$.

Now let us consider the result of the application to a frequency multiplier of an FM signal. If we think of an FM signal as a "sinusoidal" signal in which the frequency changes from moment to moment, then at each instant we may expect that the output frequency will be n times the input frequency. Hence, if the input consists of a carrier of frequency f_c which ranges through a frequency deviation $\pm Af$, the output will have a carrier frequency nf_c and will range through the deviation $\pm n Af$. The multiplier multiplies both the carrier and the deviation frequency. Also, since the modulation index is proportional to the frequency deviation, for a fixed modulation frequency, the multiplier increases the modulation index by the same factor n .

By way of example, consider the case of commercial FM broadcasting in the United States. Here, the allowable frequency deviation is 75 kHz, so that for a modulation frequency $f_m = 50$ Hz, $\beta = \Delta f/f_m = 1500$. Even if we allow ϕ in Fig. 3.6a to attain a maximum value as large as $\phi = 0.5$, then the multiplication needed is $1500/0.5 = 3000$. On the other hand, at the high-frequency end of the baseband spectrum, say, $f_m = 15$ kHz, $\beta = 75/15 = 5$. Correspondingly, with a multiplication by a factor of 3000, the phase ϕ in Fig. 3.6a need to attain only a maximum value $5/3000 = 1.7 \times 10^{-3}$. Thus, it is to be seen that the required multiplication is determined by the low-frequency limit of the baseband spectrum.

3.4.4 Armstrong FM system: An Example

The block diagram of Fig. 3.11 represents an Armstrong FM system which supplies a signal whose carrier is at 96 MHz (which is near the center of the commercial FM broadcasting band). It allows direct *phase modulation* of the carrier, before multiplication, to the extent of $f_m = 0.5$. Thus, at $Af = 50$ Hz, we have $Af = 25$ Hz. Note that at higher modulating frequencies, f_m is less than 0.5 rad. The carrier frequency before multiplication has been selected at 200 kHz, a frequency at which very stable crystal oscillators and balanced modulators are readily constructed.

As already noted, if we require that $Af = 75$ kHz, then a multiplication by a factor of 3000 is required. In Fig. 3.11 the multiplication is actually 3072 (= 64×48). The values were selected so that the multiplication may be done by factors of 2 and 3, that is, $64 = 2^6$, $48 = 3 \times 2^4$. Direct multiplication would yield a signal of carrier frequency

$$200 \text{ kHz} \times 3072 = 614.4 \text{ MHz}$$

This signal might then be heterodyned with a signal of frequency, say, $614.4 - 96.0 = 518.4$ MHz. The difference signal output of such a mixer would be a signal of carrier frequency 96 MHz. Note particularly that a mixer, since it yields sum and difference frequencies, will translate the frequency spectrum of an FM signal but will have no effect on its frequency deviation. In the system of Fig. 3.11, in order to avoid the inconvenience of heterodyning at a frequency in the range of hundreds of megahertz, the frequency translation has been accomplished at a point in the chain of multipliers where the frequency is only in the neighborhood of approximately 10 MHz.

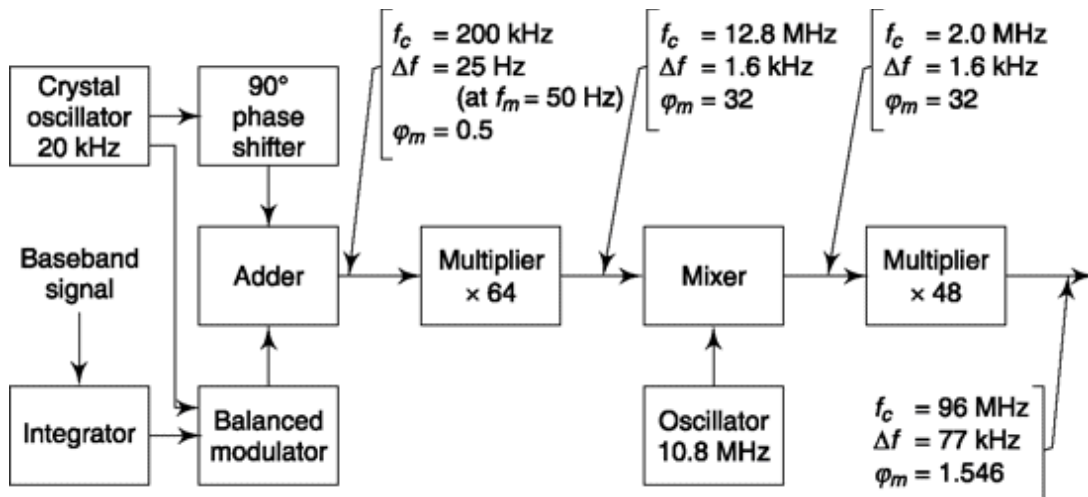


Fig. 3.11 Block diagram of an Armstrong system of generating an FM signal using multipliers to increase the frequency deviation.

A feature, not indicated in Fig. 3.11 but which may be incorporated, is to derive the 10.8 MHz mixing signal not from a separate oscillator but rather through multipliers from the 0.2 MHz crystal oscillator. The multiplication required is $10.8/0.2 = 54 = 2 \times 3^3$. Such a derivation of the 10.8 MHz signal will suppress the effect of any drift in the frequency of this signal (see Prob. 3.31).

3.4.5 FM Demodulator

With a view towards describing how we can recover the modulating signal from a frequency-modulated carrier, we consider the situation represented in Fig. 3.12. Here a waveform of frequency f_0 and input amplitude A_i is applied to a frequency selective network which then yields an output of amplitude A_o . The ratio of amplitudes A_o/A_i is the absolute value of the transfer function of the network that is, $|H(j\omega)|$. This output waveform is then applied to a diode AM demodulator (see Fig. 3.9). The diode demodulator generates an output which is equal to the peak value of the sinusoidal input so that the diode demodulator output is equal to A_o . Suppose now that the input waveform, instead of being of fixed frequency f_0 , is actually a frequency modulated waveform. Then even for a fixed input amplitude A_i , the output amplitude A_o will not remain fixed but instead be modulated because of the frequency selectivity of the transmission network. Correspondingly the diode demodulator output will follow the variation of A_o .

In short, a fixed amplitude, frequency-modulated input will generate, at the output of the frequency selective network, a waveform which is not only frequency modulated but also amplitude modulated. The diode demodulator will ignore the frequency modulation but will respond to the amplitude modulation. (In general, the frequency-selective network will not only give rise to an amplitude change but will also generate a frequency-dependent phase change, as noted in Fig. 3.12. But such a phase change is simply additional angle modulation which the envelope detector will ignore.)

What we require of an FM demodulator is that the instantaneous output signal A_o be proportional to the instantaneous frequency deviation of the received signal from the carrier frequency. If the

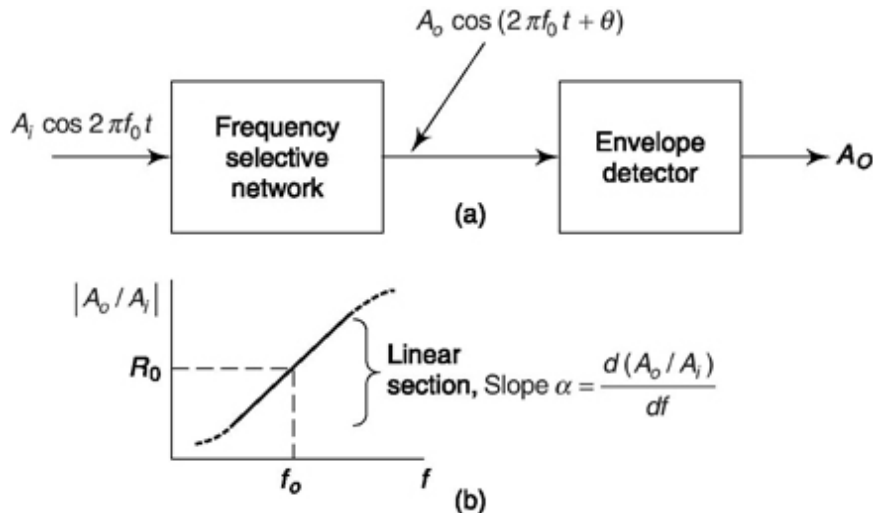


Fig. 3.12 (a) FM demodulation. (b) Frequency selective network, typically an LC circuit.

carrier frequency is f_0 then we require a linear relationship between A_o and $(f - f_0)$ where f is the instantaneous frequency. Such a linear relationship is indicated in the plot of Fig. 3.12b. We require actually that the linearity extend only as far as is necessary to accommodate the maximum frequency deviation to which the carrier is subject.

As indicated in Fig. 3.12b let us consider that the frequency selective network has a linear transfer characteristic of slope a over an adequate range in the neighborhood of the carrier frequency f_0 , and that, at $f=f_0$, $|A_o/A_i| = R_0 = |H(f=f_0)|$. Then we shall have, as required

$$A_o = R_0 A_i + \alpha A_i (f - f_0) \quad (3.63)$$

the term R_0A_i in Eq. (3.63) is a term of fixed value which displays no response to frequency deviation and the second term $aA_i(f - f_0)$ provides the required response to the instantaneous frequency deviation of the input frequency-modulated signal.

We observe however from Eq. (3.63) that if the amplitude A_t of the input signal is not fixed then the demodulator output will respond to the input amplitude variations as well as to frequency deviations. Ordinarily, in a frequency-modulated communication system the amplitude of the transmitted signal will not be modulated deliberately so that any such modulation which does appear will be due to noise. Hence it is of advantage, for the purpose of suppressing the noise, to reduce the dependence of A_o on A_t in Eq. (3.63). This is accomplished by passing the incoming signal through a hard limiter as shown in Fig. 3.13. The purpose of the hard limiter (or comparator) is to insure that variations of $A_i(t)$ are removed. Figure 3.13 shows the original FM waveform with amplitude variations at the output of the hard limiter. Since the waveform has been reduced to a frequency modulated "square wave" a bandpass filter is inserted to extract to first harmonic frequency f_0 . The resulting FM waveform is now applied to the FM demodulator.

Unfortunately, one cannot construct a network having the precisely linear transfer characteristic shown in Eq. (3.63). Indeed, in practical networks the output amplitude appears as

$$A_o = R_0A_i + \alpha A_i(f - f_0) + \beta A_i(f - f_0)^2 + \dots \quad (3.64)$$

The balanced FM demodulator shown in Fig. 3.14 can be used to remove the constant term R_0A_i and all even harmonics, thereby reducing the distortion produced by the nonlinearity of the bandpass filters. Here two demodulators are employed, differing only in that in one case the frequency-selec-

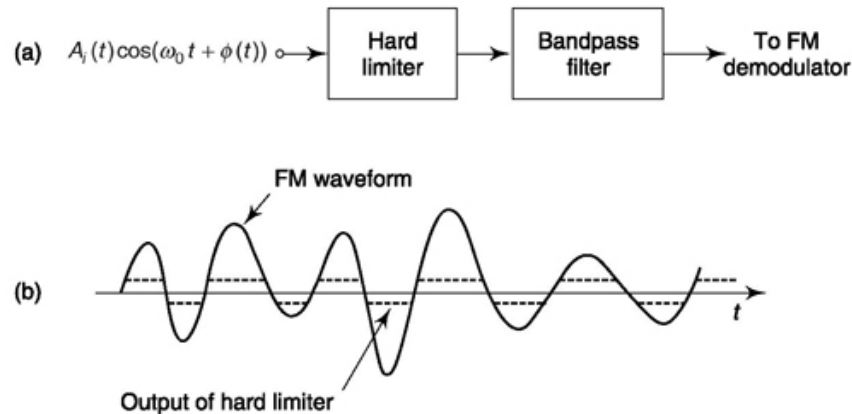


Fig. 3.13 (a) Hard limiter (or comparator) input to FM demodulator, (b) FM waveform at input and output of hard limiter.

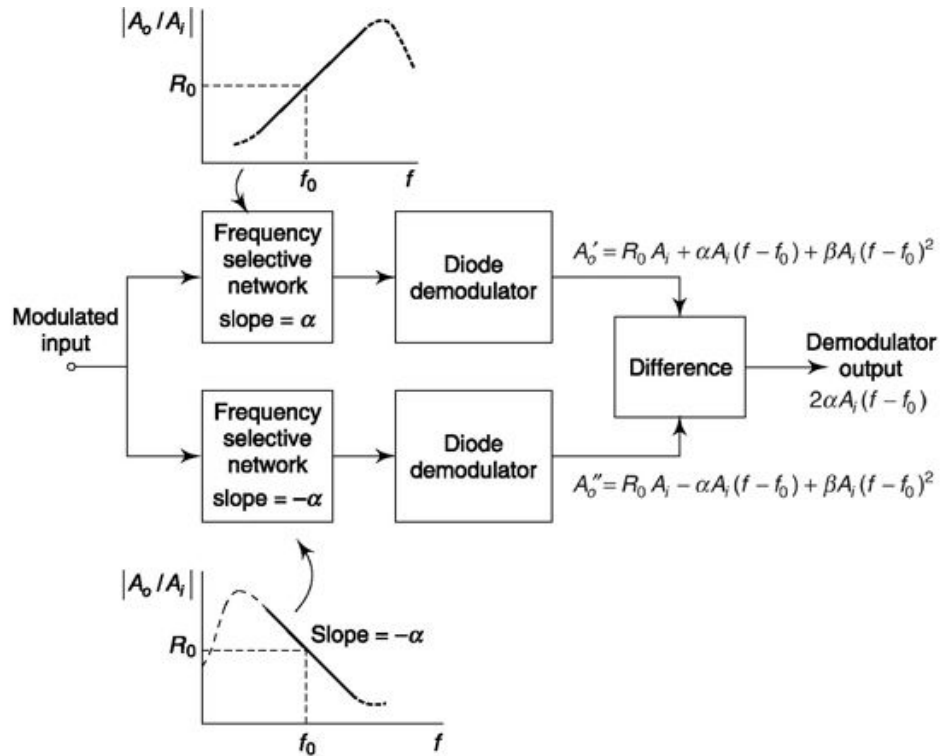


Fig. 3.14 A balanced FM demodulator.

tive network has a slope α and in the other the slope is $-\alpha$. The output provided by this balanced modulator is the difference between the two individual demodulators. These individual outputs are (assuming a second-order nonlinearity):

$$A'_o = R_0 A_i + \alpha A_i (f - f_0) + \beta A_i (f - f_0)^2 \quad (3.65)$$

and

$$A''_o = R_0 A_i - \alpha A_i (f - f_0) + \beta A_i (f - f_0)^2 \quad (3.66)$$

The difference output is then

$$A_o = 2\alpha A_i (f - f_0) \quad (3.67)$$

and we see that the linearity of the output of the FM demodulator has been improved.

In practice an *LC* tuned circuit is used as the frequency selective network. The relationship between the center frequency of each of the two tuned circuits and their bandwidths on the linearity of the FM demodulator is explored in Prob. 3.36.

It has also been shown in the literature that a hard limiter is not required when using a balanced discriminator and that any overdriven amplifier (i.e. an amplifier which is driven between cutoff and saturation) can be used.

Note that, phase locked loop (PLL) provides a better frequency discriminator circuit which we discuss in detail in Chapter 10.

Pulse Averaging Discriminator

Here we discuss a simple Integrated Circuit based demodulation scheme. Figure 3.15 shows one such block diagram which is known as pulse averaging discriminator. The FM signal when passes through a zero-crossing detector or a hard limiter produces rectangular pulses, the frequency of which is decided by the instantaneous frequency of the FM signal. These pulses then feed a monoshot multivibrator which at each trigger of the rectangular pulse generates a pulse of fixed width. This width is so chosen that it is less than the period of highest frequency in the input FM signal. Finally, these trains of fixed width pulses are fed to an averaging filter that could be a RC low pass filter which produces time averages of the dc pulses. Obviously, when the frequency of input is high within a particular time frame we have more number of such pulses and the averaged output will be high. The reverse happens when input frequency is low. Since, the input frequency variation is due to message input, and the pulse averaged output follows that frequency variation, it in turn follows message signal.

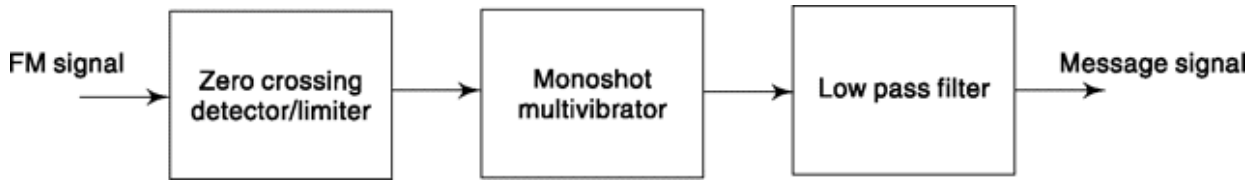


Fig. 3.15 FM demodulation by pulse averaging discriminator.

3.4.6 pm Modulator and Demodulator

We have seen in our discussion at Sec. 3.1.2 the relation between frequency and phase modulation (Fig. 3.2). If we have a frequency modulator in place we can use that for phase modulator too by sending the modulating signal first through a differentiator and then to FM modulator. The Armstrong's FM generation system described in Fig. 3.11 is basically a phase modulator unit. It is made to act like an FM system by incorporating an integrator at the input side removal of which will make it a phase modulator.

A similar argument follows for PM demodulators too. We have noted that, a frequency discriminator generates an output $y(t)$ which can be approximated in our linear region of interest as

$$y(t) \propto m(t)$$

where $m(t)$ is message signal. Again, we know if $\theta(t)$ is phase of the FM system then $\theta(t) \propto m(t)$. Thus,

$$y(t) \propto d[\theta(t)]/dt$$

For a phase-modulated input signal, $\theta(t) \propto m(t)$. Thus, discriminator output $y(t) \propto d[m(t)]/dt$, i.e.

$$y(t) = k \frac{d\theta(t)}{dt} \quad (3.68)$$

where, k is a proportionality constant. Hence, by placing an integrator after frequency discriminators discussed in FM demodulation we can get phase demodulator that recovers message signal from a phase modulated input.

Example 3.6

Show that weak sinusoidal interferences on carrier has negligible effect on angle-modulated systems.

Solution

Let, the carrier being interfered has amplitude A and angular frequency ω_c . Let the interfering signal has frequency close to ω_c to interfere with it, represented by $\omega_c + \Delta\omega$. Let the amplitude of the interfering signal be B .

$$\begin{aligned} \text{Then, received signal } r(t) &= A \cos \omega_c t + B \cos(\omega_c + \Delta\omega)t \\ &= [A + B \cos(\Delta\omega)t] \cos \omega_c t - B \sin \omega_c t \sin(\Delta\omega)t \end{aligned}$$

$$\text{Define, } R^2(t) = [A + B \cos(\Delta\omega)t]^2 + [B \sin(\Delta\omega)t]^2$$

$$\cos \theta(t) = \frac{A + B \cos(\Delta\omega)t}{R}, \quad \sin \theta(t) = \frac{B \sin(\Delta\omega)t}{R}$$

$$\text{Then, } r(t) = R(t) \cos[\omega_c t + \theta(t)]$$

In angle modulation, we are concerned with phase of the signal.

$$\begin{aligned} \text{Phase deviation, } \theta(t) &= \tan^{-1} \frac{B \sin(\Delta\omega)t}{A + B \sin(\Delta\omega)t} \approx \tan^{-1} \\ &\left[\frac{B \sin(\Delta\omega)t}{A} \right] \approx \frac{B}{A} \sin(\Delta\omega)t \text{ since, } A \ll B \end{aligned}$$

Now deviation due to interference is inversely proportional to carrier amplitude, the stronger it is the weaker is the interference.

This suppression of weak interference by angle modulation system is advantageous when compared with amplitude modulation system. This phenomenon of stronger carrier capturing (suppressing) weaker one is also known as capture effect.

Solution

Frequency response of RC 1st order high pass filter is given by,

Example 3.7

The FM signal defined in Eq. (3.37) is applied to high-pass RC filter where $RC \gg 1/\omega$ for ω representing the FM frequency band. Show if an envelop detector after the filter can demodulate the FM signal.

$$H(\omega) = \frac{R}{R + 1/(j\omega C)} = \frac{j\omega RC}{1 + j\omega RC} \approx j\omega RC$$

since, $RC \gg 1/\omega$

From Eq. (1.118) of Chapter 1, we find following Fourier transform pair

$$dv(t)/dt \leftrightarrow j\omega V(\omega)$$

Thus, the high pass filter output in time domain will be $RCdv(t)/dt$ where $v(t)$ is input FM signal. Thus filter output from Eq. (3.37) and above is

$$\begin{aligned} RCdv(t)/dt &= RCd \left[A_c \cos \left\{ \omega_c t + k_f \int_{-\infty}^t m(t) dt \right\} \right] /dt \\ &= -A_c RC [\omega_c + k_f m(t)] \sin \left\{ \omega_c t + k_f \int_{-\infty}^t m(t) dt \right\} \end{aligned}$$

The envelop detector acts like an AM demodulator and gives output $A_c RC [\omega_c + k_f m(t)]$ which is required message signal plus a dc bias. Hence, this scheme can act like an FM demodulator.

Note that noise interference in general for FM signal is discussed in detail in chapters 9 and 10.

SELF-TEST QUESTION

11. Is long term stability a major concern for parameter-based FM generation?
12. Frequency multiplication is useful in increasing the deviation. Is it correct?
13. Does a frequency selective network generate only amplitude variation at its output?

3.5 STEREOPHONIC FM BROADCASTING

In *monophonic* broadcasting of sound, a single audio baseband signal is transmitted from broadcasting studio to a home receiver. At the receiver, the audio signal is applied to a loudspeaker which then reproduces the original sound. The original source of the baseband waveform is a single microphone at the broadcasting studio. (If more than one microphone is used, as, for example, where a large orchestra is involved, the outputs of the individual microphones are combined to generate a single audio baseband signal.) In stereophonic broadcasting, two microphones (or two groups of microphones) are used. Two audio baseband signals are transmitted to the receiver where they are applied to two individual loudspeakers. At the broadcast studio, the microphones are located some distance apart from one another, and at the receiver the two loudspeakers are also physically separated. The advantage of such stereophonic broadcasting is that it yields at the receiver a more “natural” sound. The sound heard at the receiver is more nearly what the listener would hear if he were located at the broadcasting studio itself, where his two ears would receive somewhat different sounds.

The earliest commercial FM broadcasts were monophonic and conformed in transmission characteristics to standards established by the Federal Communications Commission. These standards required that the carrier frequencies of stations occupying adjacent frequency channels be separated by 200 kHz. To give reasonable assurance that there would be no interference between adjacent stations, the maximum allowable instantaneous-frequency deviation was limited by the FCC to 75 kHz. With sinusoidal modulation of the carrier frequency at the modulating frequency f_m and a frequency deviation Df , the bandwidth requirement is $B = 2(Df_m + f_m)$. If we assume a maximum audio frequency $f_m = 20$ kHz, and even if we imagine the extreme case that all the allowable baseband power is located at that frequency, then we find $B = 2(75 + 20) = 190$ kHz.

By the time commercial stereo broadcasting began to be contemplated, monophonic broadcasting was well established, and there were already many millions of monophonic FM receivers in use. Accordingly the FCC ruled that no proposed stereo scheme would be acceptable unless it were entirely *compatible* in the sense that a standard FM receiver, without modification, would be able to receive a monophonic version of a stereo transmission. Additionally the FCC required that the bandwidth occupied by a stereo transmission be no greater than the bandwidth already allocated for

monophonic transmission. Many possible stereo systems were considered. We discuss now the system finally adopted in 1961 and presently in use.

Transmitted signal

At the broadcast studio two microphones or microphone groups generate a left-hand audio signal $L(t)$ and a right-hand signal $R(t)$, as indicated in Fig. 3.16a. These signals are added and subtracted to generate $L(t) + R(t)$ and $L(t) - R(t)$. These sum and difference signals are each band limited to 15 kHz by filters not explicitly indicated in Fig. 3.16a. An oscillator makes available a sinusoidal waveform, referred to as a *pilot* carrier at a frequency $f_p = 19$ kHz. The pilot carrier is applied to a frequency doubler which generates a sinusoidal *subcarrier* at the frequency $f_{sc} = 2 \times f_p = 38$ kHz. The subcarrier and the difference signal are applied to the input of a balanced modulator, and the output of that modulator is $[L(t) - R(t)] \cos 2\pi f_{sc} t$. By combining the modulator output, the sum signal, and the oscillator output, a composite signal $M(t)$ is formed, where

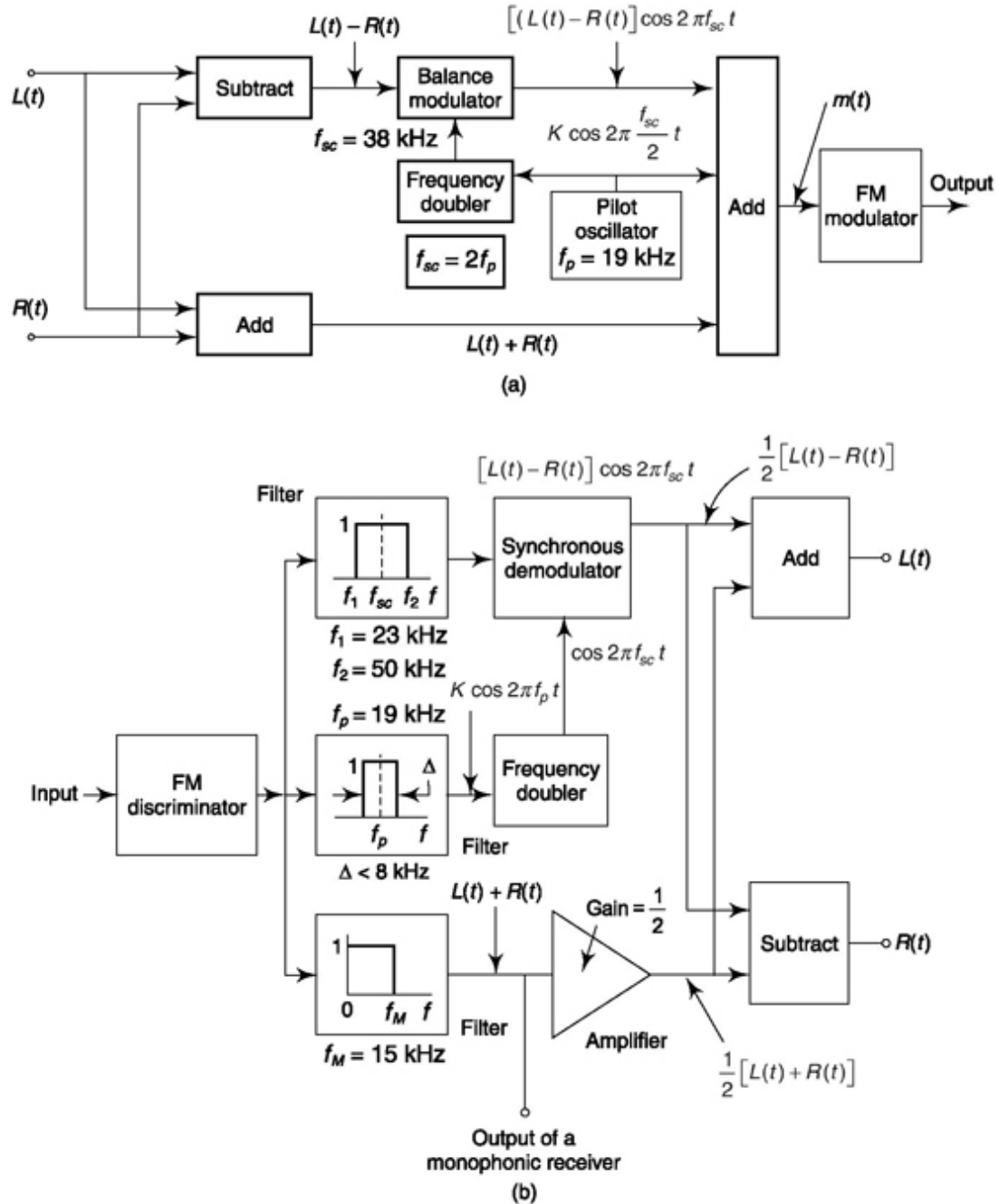


Fig. 3.16 Stereophonic broadcasting system. (a) Transmitter, (b) Receiver.

from 23 (that is, $38 - 15$) to 38 kHz and an upper sideband which extends from 38 to 53 (that is, $38 + 15$). Note that there is no subcarrier at 38 kHz. The pilot carrier at 19 kHz is present, as shown in the figure. This composite-signal $M(t)$ frequency modulates a carrier, and this modulated carrier is delivered to a transmitting antenna.

Operation of Receiver

At a stereo receiver, the composite signal $M(t)$ is recovered from the frequency-modulated carrier. One way to sort $M(t)$ into its components is shown in Fig. 3.16b. Here the individual components of the composite signal are separated by filters. The pilot carrier, applied to a frequency doubler, regenerates the subcarrier. The availability of this subcarrier now permits synchronous demodulation of the double-sideband suppressed-carrier waveform. The output of the synchronous demodulator is proportional to the difference waveform $L(t) - R(t)$, while the output of the baseband filter is proportional to $L(t) + R(t)$.

We have seen that the transmission of the pilot carrier allows us to regenerate, at the receiver, the required subcarrier waveform. We may see from Fig. 3.17 the reason on account of which the 38 kHz subcarrier was not itself transmitted directly. Such a subcarrier is not separated by any appreciable frequency interval from the spectral components of its accompanying sidebands. Hence, to extract such a subcarrier would require a very narrow and sharply tuned filter. On the other hand, the pilot carrier occupies an isolated place in the spectrum, there being no other spectral components present over a range of 4 kHz on either side.

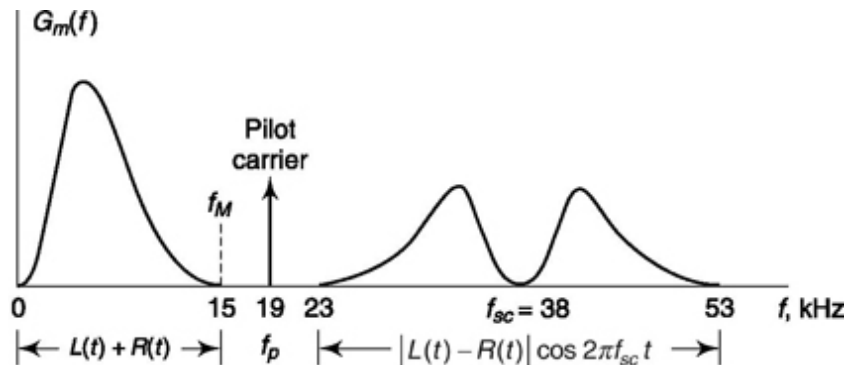


Fig. 3.17 Spectral density of a typical composite stereo baseband signal.

Now having available the sum signal $L(t) + R(t)$, and the difference signal $L(t) - R(t)$, then, as indicated in Fig. 3.16b, the individual signals $L(t)$ and $R(t)$ respectively, are recovered by adding and subtracting.

The system is entirely compatible with the requirements of a monophonic receiver. In such a receiver, the sum signal $L(t) + R(t)$ passes through the baseband filter while the pilot carrier and the suppressed-carrier signal do not. Hence these latter two signals contribute nothing to the output of a monophonic receiver and neither do they interfere with the receiver's operation.

Interleaving

A monophonic receiver makes use only of the $L + R$ signal in the stereo transmission. In order that the monophonic receiver output be as loud and disturbance-free as possible, it is necessary that the sum signal $V_s = L + R$, which modulates the FM carrier, be as large as possible. If the only component of the modulation waveform were the sum signal V_s , we would be at liberty to increase the peak excursion of V_s to the point where the corresponding peak instantaneous-frequency deviation of the carrier would be ± 75 kHz. However, in order to accommodate to the requirements of the stereo receiver, the composite modulating waveform must include as well the DSB-SC signal $V_d = (L - R) \cos 2pf_{sc} t$. We now require that the peak excursion of $V_s + V_d$ be no larger than the peak excursion previously allowed to V_s alone, i.e. the peak must correspond to a frequency deviation no larger than ± 75 kHz. These considerations suggest that, when V_d is added to V_s , the level of V_s needs to be reduced and that, as a consequence, monophonic reception of a stereo transmission would be inferior to monophonic reception of a monophonic transmission. We shall now show that,

as a matter of practice, such is not the case. We shall show that with V_s itself adjusted to produce a peak allowable frequency deviation, V_d may be added without exceeding the allowable frequency deviation. This characteristic of the stereo system under consideration is known as *interleaving*.

We recognize at the outset that, although $L(t)$ and $R(t)$ are different, they will ordinarily not be greatly different. After all, the microphones which generate the two signals are intended to represent a person's two ears. Hence, if naturalness in sound it to be achieved, presumably the placement of the microphones at the studio will take this fact into account. Thus, we may expect that the levels of the signal outputs of the two microphones will be comparable. The maximum excursion L_m of $L(t)$ and the maximum excursion R_m of $R(t)$ will be about the same. We must allow for the fact that from time to time both $L(t)$ and $R(t)$ will attain a maximum at about the same time. Therefore we set the maximum of the sum signal V_{sm} at

$$V_{sm} = L_m + R_m \approx 2L_m \approx 2R_m \quad (3.70)$$

Turning now to the composite signal $M(t)$ in Eq. (3.69), we note that $\cos 2pf_{sc}t$ oscillates rapidly between +1 and -1, and, ignoring temporarily the pilot carrier, we have that $M(t)$ oscillates rapidly between $M(t) = 2L(t)$ and $M(t) = 2R(t)$. The maximum attained by $M(t)$ is then $M_m = 2L_m$ or $M_m = 2R_m$. From Eq. (3.70) $M_m = V_{sm}$. Hence, in summary, we find that the addition of the difference signal V_d to the sum signal V_s does not increase the peak signal excursion.

Effect of the Pilot Carrier

Unlike the DSB-SC signal, the pilot carrier, when added to the other components of the composite modulating signal, does produce an increase in peak excursion. Hence, the addition of the pilot carrier calls for a reduction in the sound signal modulation level. A low-level pilot carrier allows greater sound signal modulation, while a high-level pilot carrier eases the burden of extracting the pilot carrier at the receiver. As an engineering compromise, the FCC standards call for a pilot carrier of such level that the peak sound modulation amplitude has to be reduced to about 90 percent of what would be allowed in the absence of a carrier. This 10 percent reduction corresponds to a loss in signal level of less than 1 dB.

SELF-TEST QUESTION

14. What is a stereophonic sound?
15. Stereophonic FM broadcast requires generation of sum and difference signals of left and right audio. Is that correct?

Facts and Figures

Stereophonic, or stereo, sound generates a more realistic and pleasing sound by playing two or more recordings and is used by today's radio programs, movies, television shows, and music industries. The first stereo sound was demonstrated by Clement Ader in 1881. In a Paris opera show he placed several telephone transmitters on stage. These were in turn connected to telephone receivers in another building 3 km apart. The audience experience was enthralling and there came remarks like, ".in listening with both ears at the two telephones, the sound takes a special character of relief and localization which a single receiver cannot produce."

Radio's first stereo broadcast was made in 1925 by BBC, where one channel was sent by long wave and another by medium wave, both modulated by AM. In a 1952 demonstration at Chicago, one channel was sent by AM while the other by FM. Full FM stereo broadcasting in USA started in 1961. In music-oriented TV shows of the sixties, the stereo sound was delivered by a local FM radio station and this required reel-to-reel manual synchronization between the radio and TV stations.

MATLAB

```
% Experiment 18

% Frequency modulation and demodulation
% Y = MODULATE(X,Fc,Fs,'fm',OPT)
% OPT is a scalar which specifies the constant of frequency modulation kf.
% kf=(Fc/Fs)*2*pi/max(max(abs(X))) makes maximum frequency deviation Fc Hz.

fc=10000;           % Carrier frequency
fs=100000;          % Sampling frequency
f1=200; f2=500;    % First single tone message signal and then combined

t=0:1/fs:((2/f1)-(1/fs));    %Gives exact two cycles of modulating signal
x1=cos(2*pi*f1*t);         % single tone meassage 1
x2=cos(2*pi*f1*t)+cos(2*pi*f2*t);    %combined, message 2
kf=2*pi*(fc/fs)*(1/max(max(x1)));    %frequency deviation = fc
kf=kf*(f1/fc);             % makes frequency deviation = f1;

% Modulation

opt=10*kf;                % At first let deviation = 10*f1
y1=modulate(x1,fc,fs,'fm',opt);
subplot(521);plot(x1); title('original single tone message, fs=100000')
subplot(522);plot(y1); title('time domain FM,single
tone,fc=10000,fm=200,dev=10*fm')
fx1 = abs(fft(y1,1024)); fx1 =[fx1(514:1024) fx1(1:513)];
f=(-511*fs/1024):(fs/1024):(512*fs/1024);
subplot(524);plot(f,fx1); title('freq. description,single tone, dev=10*fm')
**

% Demodulation

x1_recov=demod(y1,fc,fs,'fm',opt); subplot(523);plot(x1_recov);
title('time domain recovered, single tone, dev=10*fm')

%Repeat for different frequency deviation

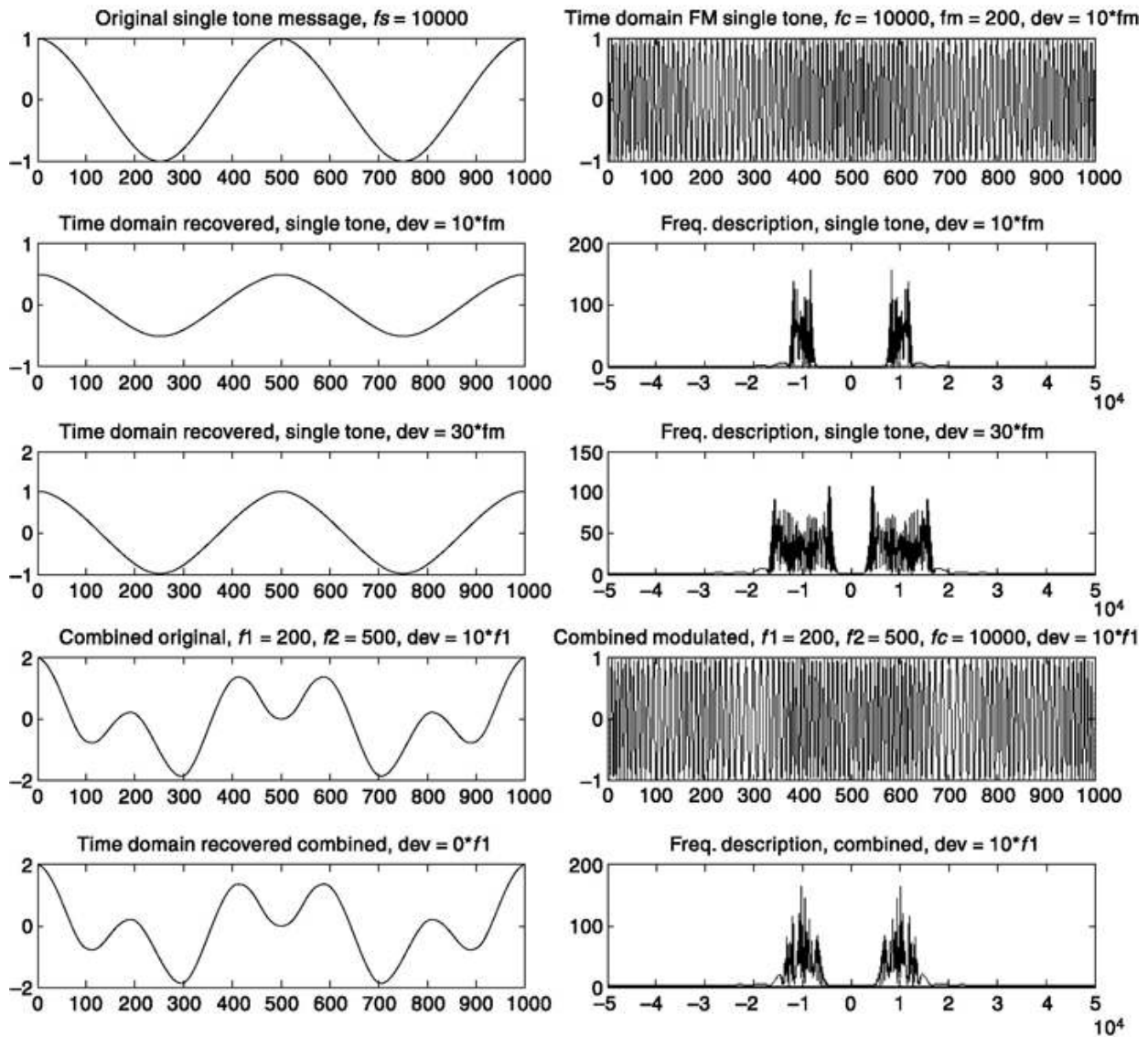
opt=30*kf;                % Let deviation be 30 times f1
y1=modulate(x1,fc,fs,'fm',opt); fx1 = abs(fft(y1,1024));
fx1 =[fx1(514:1024) fx1(1:513)];subplot(526);plot(f,fx1);
title('freq. description,single tone, dev=30*fm')
x1_recov=demod(y1,fc,fs,'fm',opt); subplot(525);plot(x1_recov);
```

```

title('time domain recovered, single tone, dev=30*fm')

% modulation demodulation for combined signal
opt=10*kf; % Let deviation be 10 times f1
y2=modulate(x2,fc,fs,'fm',opt); fx2 = abs(fft(y2,1024));
subplot(527),plot(x2);title('combined original,f1=200,f2=500,dev=10*f1');
subplot(528),plot(y2);title('combined modulated,f1=200,f2=500,fc=10000,dev=10*f1');
fx2 =[fx2(514:1024) fx2(1:513)];subplot(5,2,10);plot(f,fx2);
title('freq. description, combined, dev=10*f1')
x2_recov=demod(y2,fc,fs,'fm',opt); subplot(529);plot(x2_recov);
title('time domain recovered, combined, dev=10*f1')

```



Play with the parameter 'kf' and see how the waveform changes. Check what happens when maximum deviation exceeds fc.

```

% Experiment 19

% Phase modulation and demodulation
% Y = MODULATE(X,Fc,Fs,'pm',OPT)
% OPT is a scalar which specifies the constant of phase modulation kp.
% kp = pi/max(max(abs(x))) makes maximum phase deviation pi radian.

fc=10000;           % Carrier frequency
fs=100000;          % Sampling frequency
f1=200; f2=500;     % First single tone message signal and then combined

t=0:1/fs:((2/f1)-(1/fs));    %Gives exact two cycles of modulating signal
x1=cos(2*pi*f1*t);         % single tone meassage 1
x2=cos(2*pi*f1*t)+cos(2*pi*f2*t);   %combined, message
2 kp=pi/max(max(x1));       %phase deviation = pi

% Modulation

opt=kp/6;             % At first let phase deviation = pi/6
y1=modulate(x1,fc,fs,'pm',opt);
subplot(521);plot(x1); title('original single tone message, fs=100000')
subplot(522);plot(y1);title('time domain PM,single
tone,fc=10000,fm=200,dev=pi/6')
fx1 = abs(fft(y1,1024)); fx1 =[fx1(514:1024) fx1(1:513)];
f=(-511*fs/1024):(fs/1024):(512*fs/1024);
subplot(524);plot(f,fx1); title('freq. description,single tone, dev=pi/6')

% Demodulation

x1_recov=demod(y1,fc,fs,'pm',opt); subplot(523);plot(x1_recov);
title('time domain recovered, single tone, dev=pi/6')

%Repeat for different phase deviation

opt=kp/3;             % Let deviation =pi/3
y1=modulate(x1,fc,fs,'pm',opt); fx1 = abs(fft(y1,1024));
fx1 =[fx1(514:1024) fx1(1:513)];subplot(526);plot(f,fx1);
title('freq. description,single tone, dev=pi/3')
x1_recov=demod(y1,fc,fs,'pm',opt); subplot(525);plot(x1_recov);
title('time domain recovered, single tone, dev=pi/3')

% modulation demodulation for combined signal
opt=kp/6;             % Let deviation=pi/6
y2=modulate(x2,fc,fs,'pm',opt); fx2 = abs(fft(y2,1024));
subplot(527),plot(x2);title('combined
original,f1=200,f2=500,dev=pi/6');
subplot(528),plot(y2);title('combined
modulated,f1=200,f2=500,fc=10000,dev=pi/6');
fx2 =[fx2(514:1024) fx2(1:513)];subplot(5,2,10);plot(f,fx2);
title('freq. description, combined, dev=pi/6')
x2_recov=demod(y2,fc,fs,'pm',opt); subplot(529);plot(x2_recov);
title('time domain recovered, combined, dev=pi/6')

```

SUMMARY

The chapter begins with definition of angle modulation and derives important relations between phase modulation (PM) and frequency modulation(FM). The theoretical development is first carried out for single-tone modulating signal which includes definition of modulation index, bandwidth, spectrum and phasor representation. This is followed up by discussion where modulating signal is arbitrary in nature and modulation can be narrowband or wideband. Different types of FM generation schemes are discussed with Armstrong's system taken up as a case study. The demodulator discussion, besides traditional ones refers to Integrated Circuit based techniques. The way to get PM modulators and demodulators from its FM counterpart is also discussed. The relative immunity of FM and PM signals to weak interference is highlighted through an example. Finally, we present a detailed scheme of FM stereophonic broadcasting and MATLAB simulation experiments.

PROBLEMS

- 3.1 Consider the signal $\cos [\omega_c t + \phi(t)]$ where $\phi(t)$ is a square wave taking on the values $\pm\pi/3$ every $2/f_c$ sec.
- Sketch $\cos [\omega_c t + \phi(t)]$.
 - Plot the phase as a function of time.
 - Plot the frequency as a function of time.
- 3.2 If the waveform $\cos (\omega_c t + k \sin \omega_m t)$ is a phase-modulated carrier, sketch the waveform of the modulating signal. Sketch the waveform of the modulating signal if the carrier is frequency-modulated.
- 3.3 What are the dimensions of the constants k' , k'' and k that appear in Eqs (3.5), (3.6), and (3.7)?
- 3.4 An FM signal is given by

$$v(t) = \cos \left[\omega_c t + \sum_{k=1}^K \beta_k \cos(k\omega_0 t + \theta_k) \right]$$

- If $\theta_k = 0$ and $K = 1, 2$, find the maximum frequency deviations.
 - If each θ_k is an independent random variable, uniformly distributed between $-\pi$ and π , find the rms frequency deviation.
 - Under the condition of (b) calculate the rms phase deviation.
- 3.5 If $v(t) = \cos \left[\omega_c t + k \int_{-\infty}^t m(\lambda) d\lambda \right]$, where $m(t)$ has a probability density

$$f(m) = \frac{1}{\sqrt{2\pi}} e^{-m^2/2}$$

calculate the rms frequency deviation.

- 3.6 A carrier which attains a peak voltage of 5 volts has a frequency of 100 MHz. This carrier is frequency-modulated by a sinusoidal waveform of frequency 2 kHz to such extent that the frequency deviation from the carrier frequency is 75 kHz. The modulated waveform passes through zero and is increasing at time $t = 0$. Write an expression for the modulated carrier waveform.
- 3.7 A carrier of frequency 10^6 Hz and amplitude 3 volts is frequency-modulated by a sinusoidal modulating waveform of frequency 500 Hz and of peak amplitude 1 volt. As a consequence, the frequency deviation is 1 kHz. The level of the modulating waveform is changed to 5 volts peak, and the modulating frequency is changed to 2 kHz. Write the expression for the new modulated waveform.
- 3.8 A carrier is angle-modulated by two sinusoidal modulating waveforms simultaneously so that

$$v(t) = A \cos (\omega_c t + \beta_1 \sin \omega_1 t + \beta_2 \sin \omega_2 t)$$

- Show that this waveform has sidebands separated from the carrier not only at multiples of ω_1 and of ω_2 but also has sidebands as well at separations of multiples of $\omega_1 + \omega_2$ and of $\omega_1 - \omega_2$.
- 3.9 Bessel functions are said to be *almost periodic* with a period of almost 2π . Demonstrate this by recording the values of β , for $J_0(\beta)$ and $J_1(\beta)$, required to make these functions equal to zero.
- 3.10 The primary difference between the Bessel functions and the sine wave is that the envelope of the Bessel function decreases.
- Tabulate the magnitude of all peak values of $J_0(\beta)$, positive and negative peaks, as a function of β .
 - Plot the magnitude of the peak values obtained in part (a) versus β and draw a smooth curve through the points.
 - Show that the magnitude decreases as $\frac{1}{\sqrt{\beta}}$.
- 3.11 An FM carrier is sinusoidally modulated. For what values of β does all the power lie in the sidebands (i.e. no power in the carrier)?
- 3.12 A bandwidth rule sometimes used for space communication systems is $B = (2\beta + 1)f_M$. What fraction of the signal power is included in that frequency band? Consider $\beta = 1$ and 10.
- 3.13 A carrier is frequency-modulated by a sinusoidal modulating signal of frequency 2 kHz, resulting in a frequency deviation of 5 kHz. What is the bandwidth occupied by the modulated waveform? The amplitude of the modulating sinusoid is increased by a factor of 3 and its frequency lowered to 1 kHz. What is the new bandwidth?
- 3.14 Plot the spectrum of $\cos(2\pi \times 4t + 5 \sin 2\pi t)$. Note that the spectrum indicates the presence of a dc component. Plot the waveform as a function of time to indicate that the dc component is to have been expected.
- 3.15 $v(t) = \cos \omega_c t + 0.2 \cos \omega_m t \sin \omega_c t$.
- Show that $v(t)$ is a combination AM-FM signal.
 - Sketch the phasor diagram at $t = 0$.
- 3.16 Consider the angle-modulated waveform $\cos(\omega_c t + 2 \sin \omega_m t)$, i.e., $\beta = 2$, so that the waveform may be approximated by a carrier and three pairs of sidebands. In a coordinate system in which the carrier phasor Δ_0 is at rest, determine the phasors Δ_1 , Δ_2 and Δ_3 , representing respectively

the first, second and third sideband pairs. Draw diagrams combining the four phasors for the cases $\omega_m t = 0, \pi/4, \pi/2, 3\pi/4$ and π . For each case calculate the magnitude of the resultant phasor.

- 3.17 (a) Show with a phasor diagram that $v(t)$ given by

$$v(t) = \cos(2\pi \times 10^6 t) + 0.02 \cos[2\pi \times (10^6 + 10^3)t]$$

represents a carrier which is modulated both in amplitude and frequency.

- (b) Show that, on the basis of the relative magnitudes of the two terms in $v(t)$, the amplitude and the frequency variations both vary approximately sinusoidally with time with frequency 10^3 Hz.
(c) Express $v(t)$ in the form

$$v(t) \approx (1 + m \cos 2\pi \times 10^3 t) \cos(2\pi \times 10^6 t + \beta \sin 2\pi \times 10^3 t)$$

Find m and β . Write an expression for the instantaneous frequency as a function of time.

- 3.18 Consider the angle-modulated waveform $\cos(\omega_c t + 6 \sin \omega_m t)$, i.e., $\beta = 6$, so that the waveform may be approximated by a carrier and seven pairs of sidebands. In a coordinate system in which the carrier phasor Δ_0 is at rest, determine the phasor Δ_1, Δ_2 , etc., representing the first, second, etc., sideband pairs at a time when $\sin \omega_m t = 1$. For this time draw a phasor diagram showing each phasor Δ_i and the resultant phasor.
3.19 Verify the comment made in Sec. 3.3.1 that superposition applies in NBFM. To do this, consider $v(t) = \cos[\omega_c t + \phi(t)]$ where $\phi(t) = \beta_1 \sin \omega_1 t + \beta_2 \omega_2 t$. Let β_1 and β_2 be sufficiently small so that $|\phi(t)| \ll \pi/2$. Show that $v(t) \approx \cos \omega_c t - (\beta_1 \sin \omega_1 t + \beta_2 \sin \omega_2 t) \sin \omega_c t$.
3.20 The frequency of a laboratory oscillator is varied back and forth extremely slowly and at a uniform rate between the frequencies of 99 and 101 kHz. The amplitude of the oscillator output is constant at 2 volts. Make a plot of the two-sided power spectral density of the oscillator output waveform.
3.21 If the probability density of the amplitude of $m(t)$ is Rayleigh:

$$f(m) = \begin{cases} me^{-m^2/2} & m \geq 0 \\ 0 & \text{elsewhere} \end{cases}$$

Find the power spectral density $G_v(f)$ of the FM signal

$$v(t) = \cos \left[\omega_c t + k \int_{-\infty}^t m(\lambda) d\lambda \right]$$

- 3.22 Repeat Prob. 3.21 if the probability density of $m(t)$ is $f(m) = \frac{1}{2}e^{-|m|}$.
3.23 The frequency of a laboratory oscillator is varied back and forth extremely slowly and in such a manner that the instantaneous frequency of the oscillator varies sinusoidally with time between the limits of 99 and 101 kHz. The amplitude of the oscillator output is constant at 2 volts.
(a) Find a function of frequency $g(f)$ such that $g(f) df$ is the fraction of the time that the instantaneous frequency is in the range between f and $f + df$.
(b) Make a plot of the two-sided power spectral density of the oscillator output waveform.

- 3.24 Consider that the WBFM signal having a power spectral density is filtered by a Gaussian filter having the bandpass characteristic

$$|H(f)|^2 = e^{-(f-f_c)^2/2B^2} + e^{-(f+f_c)^2/2B^2}$$

Assume $f_c \ll B$:

- (a) Sketch $|H(f)|^2$ as a function of f .
- (b) Calculate the 3 dB bandwidth of the filter in terms of B .
- (c) Find B so that 98 percent of the signal power of the WBFM signal is passed.

- 3.25 The two independent modulating signals $m_1(t)$ and $m_2(t)$ are both gaussian and both of zero mean and variance 1 volt². The modulating signal $m_1(t)$ is connected to a source which can be frequency modulated in such manner that, when $m_1(t) = 1$ volt (constant), the source frequency, initially 1 MHz, increases by 3 kHz. The modulating signal $m_2(t)$ is connected in such a manner that, when $m_2(t) = 1$ volt (constant), the source frequency decreases by 4 kHz. The carrier amplitude is 2 volts. The two modulating signals are applied simultaneously. Write an expression for the power spectral density of the output of the frequency-modulated source.

- 3.26 Consider the FM signal

$$v(t) = \cos \left[\omega_c t + \sum_{k=1}^K \beta_k \cos(\omega_k t + \theta_k) \right]$$

Let $\beta_k \omega_k = 1$ for each k .

- (a) Find B if $B \equiv 2[(\Delta f)_1 + (\Delta f)_2 + \dots + (\Delta f)_K]$.
- (b) Find B if $B \equiv 2[(\Delta f)_{1\text{rms}} + (\Delta f)_{2\text{rms}} + \dots + (\Delta f)_{K\text{rms}}]$.

- 3.27 Refer to Fig. 3.7. If $G(f)$ is Gaussian given as

$$G(f) = \frac{A^2}{4\sqrt{2\pi}\Delta f_{\text{rms}}} \left[e^{-(f-f_c)^2/2(\Delta f_{\text{rms}})^2} + e^{-(f+f_c)^2/2(\Delta f_{\text{rms}})^2} \right]$$

find its root mean square (r.m.s.) bandwidth which is defined as

$$B = 2 \left[\frac{\int_{-\infty}^{\infty} v^2 G(v) dv}{\int_{-\infty}^{\infty} G(v) dv} \right]^{1/2}$$

- 3.28 In Fig. 3.8 the voltage-variable capacitor is a reversed-biased *pn* junction diode whose capacitance is related to the reverse-biasing voltage v by $C_v = (100/\sqrt{1+2v})$ pF. The capacitance $C_0 = 200$ pF and L is adjusted for resonance at 5 MHz when a fixed reverse voltage $v = 4$ volts is applied to the capacitor C_v . The modulating voltage is $m(t) = 4 + 0.045 \sin 2\pi \times 10^3 t$. If the oscillator amplitude is 1 volt, write an expression for the angle-modulated output waveform which appears across the tank circuit.

- 3.29 (a) In the multiplier circuit of Fig. 3.10 assume that the transistor acts as a current source and is so biased and so driven that the collector current consists of alternate half-cycles of a sinusoidal waveform with a peak value of 50 mA. The input frequency of the driving signal is 1 MHz, and the multiplication by a factor of 3 is to be accomplished. If $C = 200$ pF and the inductor $Q = 30$, find the inductance of the inductor and calculate the amplitude of the third harmonic voltage across the tank.

- (b) If multiplication by 10 is to be accomplished, calculate the amplitude of the tank voltage. Assume that the resonant impedance of the tank remains the same as in part (a).

- 3.30 (a) Consider the narrowband waveform $v(t) = \cos(\omega_c t + \beta \sin \omega_m t)$, with $\beta \ll 1$ and $\omega_m \ll \omega_c$. Show that $v(t)$, which has a frequency deviation $\Delta f = \beta f_m$, may be written approximately as

$$v(t) = \cos \omega_c t - \beta/2 \cos (\omega_c - \omega_m)t + \beta/2 \cos (\omega_c + \omega_m)t$$

and that this approximation is consistent with the general expansion for an angle-modulated waveform as given by Eq. (3.20). Use the approximations of Eqs (3.21) and (3.22).

- (b) Let $v(t)$ be applied as the input to a device whose output is $v^2(t)$ (i.e., the device is nonlinear and is to be used for frequency multiplication by a factor of 2). Square the approximate expression for $v(t)$ as given in part (a). Compare the spectrum of $v^2(t)$ so calculated with the exact spectrum for an angle-modulated waveform with frequency deviation $2\beta f_m$.

- 3.31 Assume that the 10.8 MHz signal in Fig. 3.11 is derived from the 200 kHz oscillator by multiplying by 54 and that the 200 kHz oscillator drifts by 0.1 Hz.

- (a) Find the drift, in hertz, in the 10.8 MHz signal.
 (b) Find the drift in the carrier of the resulting FM signal.

- 3.32 In an Armstrong modulator, as shown in Fig. 3.11, the crystal-oscillator frequency is 200 kHz. It is desired, in order to avoid distortion, to limit the maximum angular deviation to $\phi_m = 0.2$. The system is to accommodate modulation frequencies down to 40 Hz. At the output of the modulator the carrier frequency is to be 108 MHz and the frequency deviation 80 kHz. Select multiplier and mixer oscillator frequencies to accomplish this end.

- 3.33 The narrowband phase modulator of Fig. 3.9 is converted to a frequency modulator by preceding the balanced modulator with an integrator. The input signal is a sinusoid of angular frequency ω_m .

- (a) Show that, unless the frequency deviation is kept small, the modulator output, when de-modulated, will yield not only the input signal but also its odd harmonics.
 (b) If the modulation frequency is 50 Hz, find the allowable frequency deviation if the normalized power associated with the third harmonic is to be no more than 1 percent of the fundamental power.

- 3.34 (a) Consider the FM demodulator of Fig. 3.12. Let the frequency selective network be an RC integrating network. The 3 dB frequency of the network is $f_2 (= 1/2\pi RC)$. If the carrier frequency of the FM waveform is f_c , how should f_2 be selected so that the demodulator has the greatest sensitivity (i.e. greatest change in output per change in input frequency)?
 (b) With f_2 selected for maximum sensitivity and with $f_c = 1$ MHz, find the change in demodulator output for a 1 Hz change in input frequency.

- 3.35 A “zero-crossing” FM discriminator operates in the following manner. The modulated waveform

$$v(t) = A \cos \left[2\pi f_c t + k \int_{-\infty}^t m(\lambda) d\lambda \right]$$

is applied to an electronic circuit which generates a narrow pulse on each occasion when $v(t)$ passes through zero. The pulses are of fixed polarity, amplitude and duration. This pulse train is applied to a low-pass filter, say an RC low-pass network of 3 dB frequency f_2 . Assume that the bandwidth of the baseband waveform $m(t)$ is f_M . Discuss the operation of this discriminator. Show that if $f_c \ll f_2 \ll f_M$ the output of the low-pass network is indeed proportional to the instantaneous frequency of $v(t)$.

- 3.36 (a) A frequency selective network is shown in Fig. P3.36. Calculate the ratio $|V_o(f)/V_i(f)|$, i.e., the ratio of the amplitude of the output to the amplitude of the input, as a function of frequency. Verify that

$$\left| \frac{V_o(f)}{V_i(f)} \right| = \left\{ 1 + \frac{Q_0^2}{(f/f_0)^2} [(f/f_0)^2 - 1]^2 \right\}^{1/2}$$

in which $f_0 = 1/2\pi\sqrt{1/LC}$ is the resonant frequency and $Q_0 = R/2\pi f_0 L$ is the energy storage factor of the resonant network at f_0 .

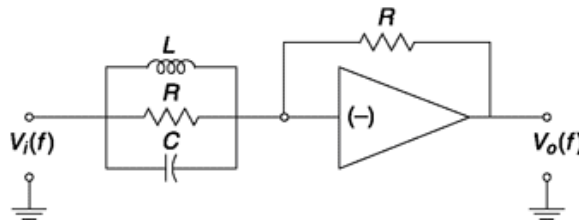


Fig. P3.36

- (b) Find the frequencies at which $|V_o/V_i|$ is higher by 3 dB than its value at the resonant frequency. Show that, for large Q_0 , these frequencies are $f = f_0(1 \pm 1/Q_0)$. Calculate the slope of $|V_o/V_i|$ at the frequency $f_H = f_0(1 + 1/Q_0)$. A frequency modulated waveform with carrier frequency f_H is applied as $V_i(f)$. What is the ratio of the change in amplitude $\Delta V_o(f)$ to the change, Δf , of the instantaneous frequency of the input?
- (c) In the discriminator of Fig. 3.12 let the two frequency selective networks be the network shown in Fig. P3.36. The resonant frequencies of the two networks are to be $f_H = f_c(1 + 1/Q_0)$ and $f_L = f_c(1 - 1/Q_0)$, f_c being the carrier frequency of an input frequency modulated waveform. Make a plot of the discriminator output as a function of the instantaneous frequency of the input. Use $Q_0 = 50$.

REFERENCES

1. Bell Telephone Laboratories: "Transmission Systems for Communications," Western Electric Company, Tech. Pub., Winston-Salem, N.C., 1964.
2. Jahnke, E., and F. Emde: "Tables of Functions," Dover Publications Inc., New York, 1945.
3. Pipes, L. A.: "Applied Mathematics for Engineers and Physicists," McGraw-Hill Book Company, New York, 1958.
4. Blachman, N.: Calculation of the Spectrum of an FM Signal Using Woodward's Theorem, *IEEE Trans. Communication Technology*, August, 1969.
5. Kahn, L. R.: Compatible Single Sideband. *Proc. IRE*, vol. 49, pp. 1503-1527, October, 1961.

4

PULSE MODULATION AND DIGITAL TRANSMISSION OF ANALOG SIGNALS

CHAPTER OBJECTIVE

In the previous two chapters, we discussed modulation techniques which can send multiple message signals simultaneously by positioning them separately over a frequency band. A similar thing can be done in time domain when message is represented in the form of pulses and putting number of pulses coming from different sources one after another in a time band by what is known as Time Division Multiplexing (TDM). These discrete time signals when coded in binary offer advantages like storage, error correction, greater immunity to noise, etc. In this chapter, we first discuss sampling and related issues required to faithfully represent an analog data by its discrete samples. For practical needs, these samples are of finite width in the form of pulses. When message information is carried by amplitude of the pulse, it is called Pulse Amplitude Modulation (PAM), if by its width then Pulse Width Modulation (PWM) and if by its position then Pulse Position modulation (PPM). Among pulse modulation schemes, PAM is suitable both for TDM and digital representation. The binary coding of waveform goes through a process called quantization and invariably is an approximation of analog signal; the error is reflected in what is known as quantization noise. We discuss different waveform coding techniques including design of linear predictors. Finally, we discuss coding of voice signals in detail. Like previous chapters we have numerical and MATLAB based examples to support principal issues discussed in the chapter.

FACTS AND FIGURES

The first great invention of Thomas Alva Edison was the tinfoil phonograph in 1877. While working to improve the efficiency of a telegraph transmitter,

he observed that the tape of the machine produced a noise, resembling spoken words when played at a high speed. Further experiments led him to try a stylus on a tinfoil cylinder, which, to his great surprise, played back the short message he recorded, "Mary had a little lamb." He was invited to demonstrate his phonograph to the then US president Rutherford B. Hayes. By 1888, certain recording standards emerged where a cylinder of 2-inch diameter and 4-inch length at 90 RPM could record 4 minutes of speech and in 120-160 RPM version 2-2.5 minutes of music.

Harry Nyquist, in 1928, first described the criteria for what we know today as sampled data systems. His contributions include the first quantitative explanation of thermal noise and important studies on signal transmission which laid the foundation for modern information theory and data transmission. He also invented vestigial sideband transmission system now widely-used in television broadcasting and the well-known Nyquist diagram for determining the stability of feedback systems.

4.1 ANALOG TO DIGITAL: THE NEED

We consider a basic problem associated with the transmission of a signal over a noisy communication channel. For the sake of being specific, suppose we require that a telephone conversation be transmitted from New York to Los Angeles. If the signal is transmitted by radio, then, when the signal arrives at its destination, it will be greatly attenuated and also combined with noise due to thermal noise present in all receivers (Chap. 15), and to all manner of random electrical disturbances which are added to the radio signal during its propagation across country. (We neglect as irrelevant, for the present discussion, whether such direct radio communication is reliable over such long channel distances.) As a result, the received signal may not be distinguishable against its background of noise. The situation is not fundamentally different if the signal is transmitted over wires. Any physical wire transmission path will both attenuate and distort a signal by an amount which increases with path length. Unless the wire path is completely and perfectly shielded, as in the case of a perfect coaxial cable, electrical noise and crosstalk disturbances from neighboring wire paths will also be picked up in amounts increasing with the path length. In this connection it is of interest to note that even coaxial cable does not provide complete freedom from crosstalk. External low-frequency magnetic fields will penetrate the outer conductor of the coaxial cable and thereby induce signals on the cable.

In telephone cable, where coaxial cables are combined with parallel wire signal paths, it is common practice to wrap the coax in Permalloy for the sake of magnetic shielding. Even the use of fiber optic cables which are relatively immune to such interference, does not significantly alter the problem since receiver noise is often the noise source of largest power.

One attempt to resolve this problem is simply to raise the signal level at the transmitting end to so high a level that, in spite of the attenuation, the received signal substantially overrides the noise. (Signal distortion may be corrected separately by equalization.) Such a solution is hardly feasible on the grounds that the signal power and consequent voltage levels at the transmitter would be simply astronomical and beyond the range of amplifiers to generate, and cables to handle. For example, at 1 kHz, a telephone cable may be expected to produce an attenuation of the order of 1 dB per mile. For a 3000 mile run, even if we were satisfied with a received signal of 1 mV, the voltage at the transmitting end would have to be 10^{147} volts.

An amplifier at the receiver will not help the above situation, since at this point both signal and noise levels will be increased together. But suppose that a repeater (repeater is the term used for an amplifier in a communications channel) is located at the midpoint of the long communications path. This repeater will raise the signal level; in addition, it will raise the level of only the noise introduced in the first half of the communications path. Hence, such a midway repeater, as contrasted with an amplifier at the receiver, has the advantage of improving the received signal-to-noise ratio.

This midway repeater will relieve the burden imposed on transmitter and cable due to higher power requirements when the repeater is not used.

The next step is, of course, to use additional repeaters, say initially at the one-quarter and three-quarter points, and thereafter at points in between. Each added repeater serves to lower the maximum power level encountered on the communications link, and each repeater improves the signal-to-noise ratio over what would result if the corresponding gain were introduced at the receiver.

In the limit we might, conceptually at least, use an infinite number of repeaters. We could even adjust the gain of each repeater to be infinitesimally greater than unity by just the amount to overcome the attenuation in the infinitesimal section between repeaters. In the end, we would thereby have constructed a channel which had no attenuation. The

signal at the receiving terminal of the channel would then be the unattenuated transmitted signal. We would then, in addition, have at the receiving end all the noise introduced at all points of the channel. This noise is also received without attenuation, no matter how far away from the receiving end the noise was introduced. If now, with this finite array of repeaters, the signal-to-noise ratio is not adequate, there is nothing to be done but to raise the signal level or to make the channel quieter.

The situation is actually somewhat more dismal than has just been intimated, since each repeater (transistor amplifier) introduces some noise on its own accord. Hence, as more repeaters are cascaded, each repeater must be designed to more exacting standards with respect to noise figure (see Sec. 15.5.3). The limitation of the system we have been describing for communicating over long channels is that once noise has been introduced any place along the channel, we are “stuck” with it.

If we now were to transmit a digital signal over the same channel, we would find that significantly less signal power would be needed in order to obtain the same performance at the receiver. The reason for this is that the significant parameter is now not the signal-to-noise ratio but the probability of mistaking a digital signal for a different digital signal. In practice we find that signal-to-noise ratios of 40-60 dB are required for analog signals while 10-12 dB are required for digital signals. This reason and others, to be discussed subsequently, have resulted in a large commercial and military switch to digital communications.

4.1.1 Sampling Theorem and Low Pass Signal

We consider at the outset the fundamental principle of digital communications; the sampling theorem:

Let $m(t)$ be a signal which is bandlimited such that its highest frequency spectral component is f_M . Let the values of $m(t)$ be determined at regular intervals separated by times $T_s \leq 1/2f_M$ that is, the signal is periodically sampled every T_s seconds. Then these samples $m(nT)$, where n is an integer, uniquely determine the signal, and the signal may be reconstructed from these samples with no distortion.

The time T_s is called the *sampling time*. Note that the theorem requires that the *sampling rate* be rapid enough so that at least two samples are taken during the course of the period corresponding to the highest-frequency

spectral component. We shall now prove the theorem by showing how the signal may be reconstructed from its samples.

The baseband signal $m(t)$ which is to be sampled is shown in Fig. 4.1a. A periodic train of pulses $S(t)$ of unit amplitude and of period T_s is shown in Fig. 4.1b. The pulses are arbitrarily narrow, having a width dt . The two signals $m(t)$ and $S(t)$ are applied to a multiplier as shown in Fig. 4.1c, which

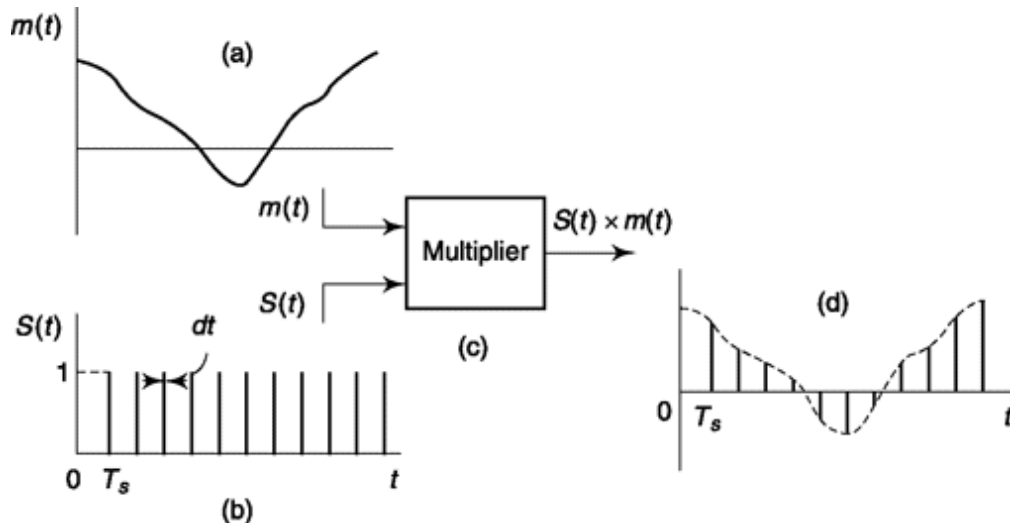


Fig. 4-1 (a) A signal $m(t)$ which is to be sampled. (b) The sampling function $S(t)$ consists of a train of very narrow unit amplitude pulses. (c) The sampling operation is performed in a multiplier, (d) The samples of the signal $m(t)$.

then yields as an output the product $S(t)m(t)$. This product is seen in Fig. 4.1d to be the signal $m(t)$ *sampled* at the occurrence of each pulse. That is, when a pulse occurs, the multiplier output has the same value as does $m(t)$, and at all other times the multiplier output is zero.

The signal $S(t)$ is periodic, with period T_s , and has the Fourier expansion [see Eq. (1.38) with $I = dt$ and $T_0 = T_s$]

$$S(t) = \frac{dt}{T_s} + \frac{2}{T_s} \left(\cos 2\pi \frac{t}{T_s} + \cos 2 \times 2\pi \frac{t}{T_s} + \dots \right) \quad (4.1)$$

For the case $T_s = 1/2f_M$, the product $S(t)m(t)$ is

$$S(t)m(t) = \frac{dt}{T_s} m(t) + \frac{dt}{T_s} [2m(t) \cos 2\pi(2f_M)t + 2m(t) \cos 2\pi(4f_M)t + \dots] \quad (4.2)$$

We now observe that the first term in the series is, aside from a constant factor, the signal $m(t)$ itself. Again, aside from a multiplying factor, the second term is the product of $m(t)$ and a sinusoid of frequency $2f_M$. This product then, as discussed in Sec. 2.1.1, gives rise to a double-sideband suppressed-carrier signal with carrier frequency $2f_M$. Similarly, succeeding terms yield DSB-SC signals with carrier frequencies $4f_M$, $6f_M$, etc.

Let the signal $m(t)$ have a spectral density $M(j\omega) = \mathcal{F}[m(t)]$ which is as shown in Fig. 4.2a. Then $m(t)$ is bandlimited to the frequency range below f_M . The spectrum of the first term in Eq. (4.2) extends from 0 to f_M . The spectrum of the second term is symmetrical about the frequency $2f_M$ and extends from $2f_M - f_M = f_M$ to $2f_M + f_M = 3f_M$. Altogether the spectrum of the sampled signal has the appearance shown in Fig. 4.2b. Suppose then that the sampled signal is passed through an ideal low-pass filter with cutoff frequency at f_M . If the filter transmission were constant in the passband and if the cutoff were infinitely sharp at f_M , the filter would pass the signal $m(t)$ and nothing else.

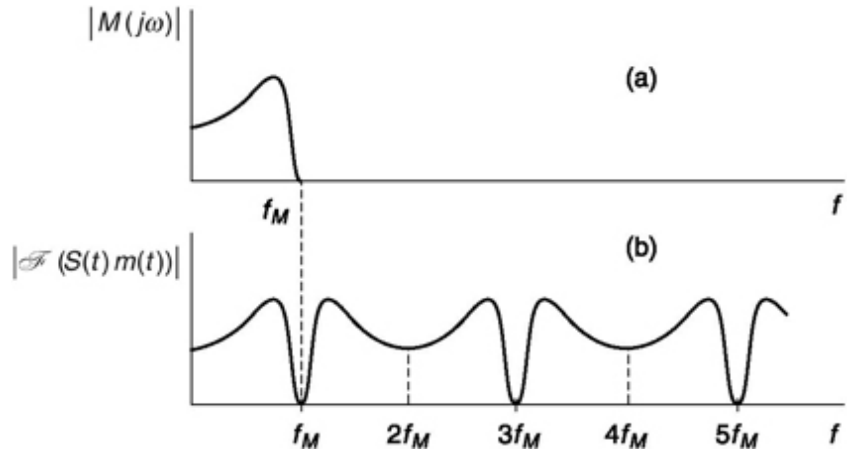


Fig. 4-2 (a) The magnitude plot of the spectral density of a signal bandlimited to f_M . (b) Plot of amplitude of spectrum of sampled signal.

The spectral pattern corresponding to Fig. 4.2b is shown in Fig. 4.3a for the case in which the sampling rate $f_s = 1/T_s$ is larger than $2f_M$. In this case there is a gap between the upper limit f_M of the spectrum of the baseband signal and the lower limit of the DSB-SC spectrum centered around the carrier frequency $f_s > 2f_M$. For this reason the low-pass filter used to select the signal $m(t)$ need not have an infinitely sharp cutoff. Instead, the filter attenuation may begin at f_M but need not attain a high value until the frequency $f_s - f_M$. This range from f_M to $f_s - f_M$ is called a *guard band* and is always required in practice, since a filter with infinitely sharp cutoff is, of course, not realizable. Typically, when sampling is used in connection with voice messages on telephone lines, the voice signal is limited to $f_M = 3.3$ kHz, while f_s is selected at 8.0 kHz. The guard band is then $8.0 - 2 \cdot 3.3 = 1.4$ kHz.

The situation depicted in Fig. 4.3b corresponds to the case where $f_s < 2f_M$. Here we find an overlap between the spectrum of $m(t)$ itself and the spectrum of the DSB-SC signal centered around f_s . Accordingly, no filtering operation will allow an exact recovery of $m(t)$. This phenomenon is known as aliasing.

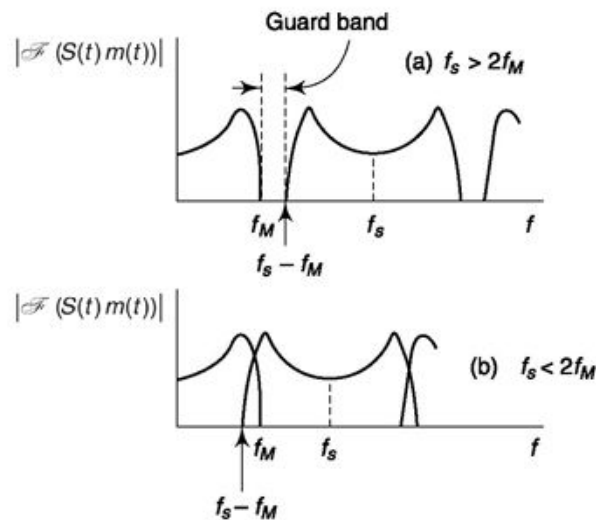


Fig. 4-3 (a) A guard band appears when $f_s > 2f_M$. (b) Over-lapping of spectra when $f_s < 2f_M$.

as aliasing in frequency domain. When necessary, to avoid aliasing we use an *antialiasing filter*, a low pass filter that limits the frequency band of the message signal $m(t)$ within frequency $f/2$.

We have just proved the *sampling theorem* since we have shown that, in principle, the sampled signal can be recovered exactly when $T_s < 1/2f_M$. It has also been shown why the minimum allowable sampling rate is $2f_M$. This minimum sampling rate is known as the *Nyquist rate*. An increase in sampling rate above the Nyquist rate increases the width of the guard band, thereby easing the problem of filtering. On the other hand, we shall see that an increase in rate extends the bandwidth required for transmitting the sampled signal. Accordingly an engineering compromise is called for.

An interesting special case is the sampling of a sinusoidal signal having the frequency f_M . Here, *all* the signal power is concentrated precisely at the

cutoff frequency of the low-pass filter, and there is consequently some ambiguity about whether the signal frequency is inside or outside the filter passband. To remove this ambiguity, we require that $f_s > 2f_M$ rather than that $f_s > 2f_M$. To see that this condition is necessary, assume that $f_s = 2f_M$ but that an initial sample is taken at the moment the sinusoid passes through zero. Then all successive samples will also be zero. This situation is avoided by requiring $f_s > 2f_M$.

4.1.2 sampling of Bandpass signal

For a signal $m(t)$ whose highest-frequency spectral component is f_M , the sampling frequency f_s must be no less than $f_s = 2f_M$ only if the lowest-frequency spectral component of $m(t)$ is $f_L = 0$. In the more general case, where $f_L \neq 0$, it may be that the sampling frequency need be no larger than $f_s = 2(f_M - f_L)$. For example, if the spectral range of a signal extends from 10.0 to 10.1 MHz, the signal may be recovered from samples taken at a frequency $f_s = 2(10.1 - 10.0) = 0.2$ MHz.

To establish the sampling theorem for such bandpass signals, let us select a sampling frequency $f_s = 2(f_M - f_L)$ and let us initially assume that it happens that the frequency f_L turns out to be an integral multiple of f_s , that is, $f_L = nf_s$ with n an integer. Such a situation is represented in Fig. 4.4. In part *a* is shown the two-sided spectral pattern of a signal $m(t)$ with Fourier transform $M(j\omega)$. Here it has been arranged that $n = 2$; that is, f_L coincides with the second harmonic of the sampling frequency, while the sampling frequency is exactly $f_s = 2(f_M - f_L)$. In part *b* is shown the spectral pattern of

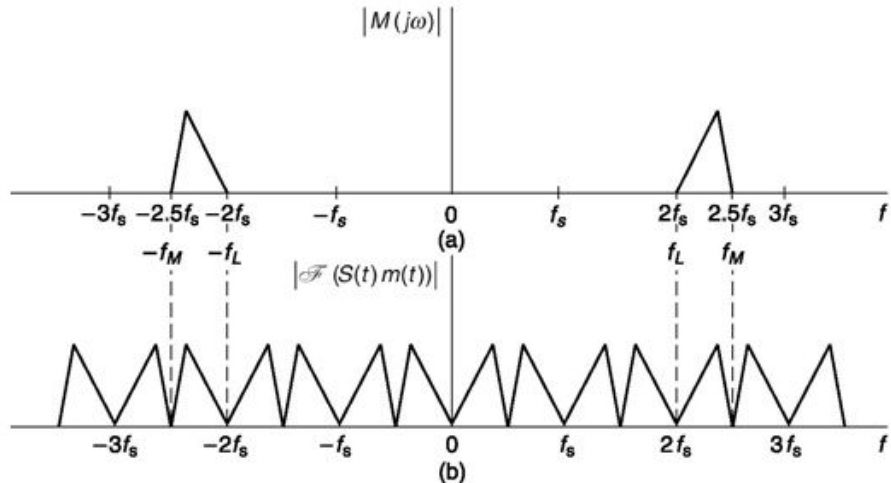


Fig 4.4 (a) The spectrum of a bandpass signal. (b) The spectrum of the sampled bandpass signal.

the sampled signal $S(t)m(t)$. The product of $m(t)$ and the dc term of $S(t)$ [Eq. (4.1)] duplicates in part *b* the form of the spectral pattern in part *a* and leaves it in the same frequency range from f_L to f_M . The product of $m(t)$ and the spectral component in $S(t)$ of frequency $f_s (= l/T_s)$ gives rise in part *b* to a spectral pattern derived from part *a* by shifting the pattern in part *a* to the

right and also to the left by amount f_s . Similarly, the higher harmonics of f_s in $S(t)$ give rise to corresponding shifts, right and left, of the spectral pattern in part *a*. We now note that if the sampled signal $S(t)m(t)$ is passed through a bandpass filter with arbitrarily sharp cutoffs and with passband from f_L to f_M , the signal $m(t)$ will be recovered exactly.

In Fig. 4.4 the spectrum of $m(t)$ extends over the first half of the frequency interval between harmonics of the sampling frequency, that is, from $2.0f$, to $2.5f_s$. As a result, there is no spectrum overlap, and signal recovery is possible. It may also be seen from the figure that if the spectral range of $m(t)$ extended over the second half of the interval from $2.5f_s$ to $3.0f$,, there would similarly be no overlap. Suppose, however, that the spectrum of $m(t)$ were confined neither to the first half nor to the second half of the interval between sampling-frequency harmonics. In such a case, there would be overlap between the spectrum patterns, and signal recovery would not be possible. Hence the minimum sampling frequency allowable is $f_s = 2(f_M - f_L)$ provided that either f_M or f_L is a harmonic of f_s .

If neither f_M nor f_L is a harmonic of f_s , a more general analysis is required. In Fig. 4.5a we have reproduced the spectral pattern of Fig. 4.4. The positive-frequency part and the negative-frequency part of the spectrum are called PS and NS respectively. Let us, for simplicity, consider separately PS and NS and the manner in which they are shifted due to the sampling and let us consider initially what constraints must be imposed so that we cause no overlap over, say, PS.

The product of $m(t)$ and the dc component of the sampling waveform leaves PS unmoved and it is this part of the spectrum which we propose to selectively draw out to reproduce the original signal. If we select the minimum value of f_s to be $f_s = 2(f_H - f_L) = 2B$ then the shifted PS patterns will not overlap PS. The NS will also generate a series of shifted patterns to the left and to the right. The left shiftings cannot cause an overlap of PS. However, the right shiftings of NS might cause an overlap and these right shiftings of NS are the only possible source of such overlap over PS.

Shown in Fig. 4.5b are the right shifted patterns of NS due to the $(N - 1)$ st and N th harmonics of the sampling waveform. It is clear that to avoid overlap it is necessary that in which $k > N$ since $f_s > 2B$. Equations (4.7) and (4.8) establish the constraint which must be observed to avoid an overlap on

PS. It is clear from the symmetry of the initial spectrum and the symmetry of the shiftings required that this same constraint assures that there will be no overlap on NS.

$$(N - 1)f_s - f_L \leq f_L \quad (4.3)$$

and

$$Nf_s - f_M \geq f_M \quad (4.4)$$

so that, with $B \equiv f_M - f_L$ we have

$$(N - 1)f_s \leq 2(f_M - B) \quad (4.5)$$

and

$$Nf_s \geq 2f_M \quad (4.6)$$

If we let $k \equiv f_M/B$, Eqs (4.5) and (4.6) become

$$f_s \leq 2B \left(\frac{k-1}{N-1} \right) \quad (4.7)$$

and

$$f_s \geq 2B \left(\frac{k}{N} \right) \quad (4.8)$$

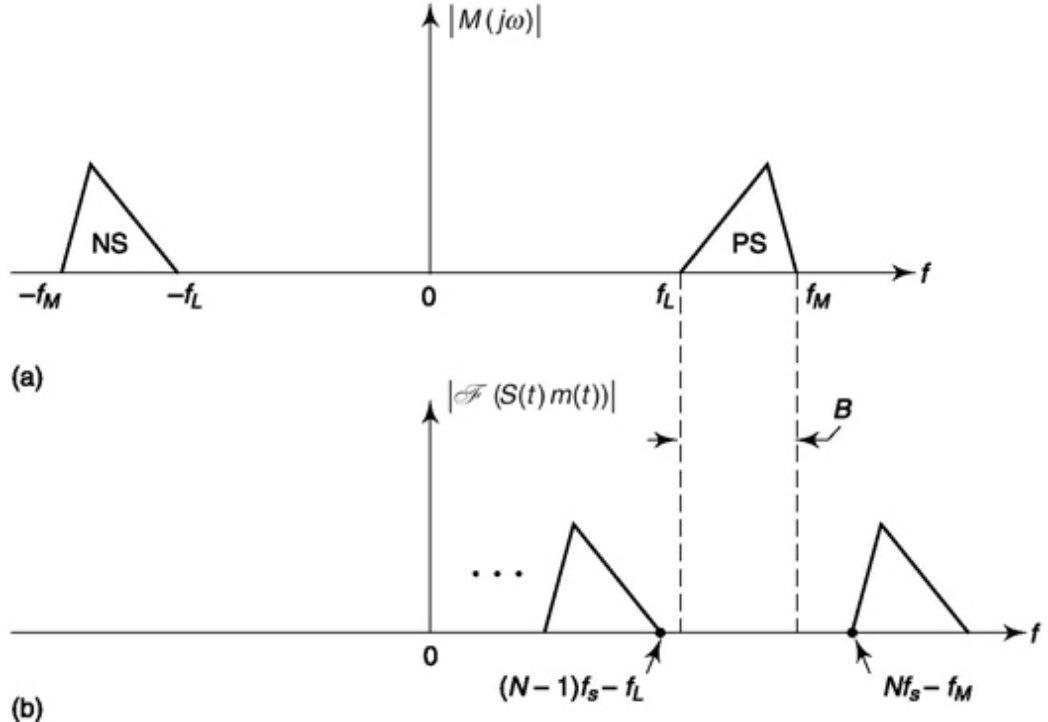


Fig. 4.5 (a) Spectrum of the bandpass signal. (b) Spectrum of NS shifted by the $(N - i)$ st and the N th harmonic of the sampling waveform.

Equations (4.7) and (4.8) have been plotted in Fig. 4.6 for several values of N . The shaded regions are the regions where the constraints are satisfied, while in the unshaded regions the constraints are not satisfied and overlap will occur. As an example of the use of these plots, consider a case in which a baseband signal has a spectrum which extends from $f_L = 2.5$ kHz to $f_M =$

3.5 kHz. Here $B = 1$ kHz and $k = f_M/B = 3.5$. On the plot of Fig. 4.6, we have accordingly erected a dashed vertical line at $k = 3.5$. We observe that for this value of k , the selection of a sampling frequency $f_s = 2B = 2$ kHz brings us to a point in an overlap region. As f_s is increased there is a small range of f_s , corresponding to $N = 3$, where there is no overlap. Further increase in f_s again takes us to an overlap region, while still further increase in f_s provides a nonoverlap range, corresponding to $N = 2$ (from $f_s = 3.5B$ to $f_s = 5B$). Increasing f_s further we again enter an overlap region while at $f_s = 7B$ we enter the nonoverlap region for $N = 1$. When $f_s > 7B$ we do not again enter an overlap region. (This is the region where $f_s > 2f_M$; that is, we assume we have a lowpass rather than a bandpass signal.)

From this discussion, we can write bandpass sampling theorem as follows —*A bandpass signal with highest frequency f_H and bandwidth B , can be recovered from its samples through bandpass filtering by sampling it with frequency $f_s = 2f_H/k$, where k is the largest integer not exceeding f_H/B . All frequencies higher than f_s but below $2f_H$ (lower limit from low pass sampling theorem) may or may not be useful for bandpass sampling depending on overlap of shifted spectrums.*

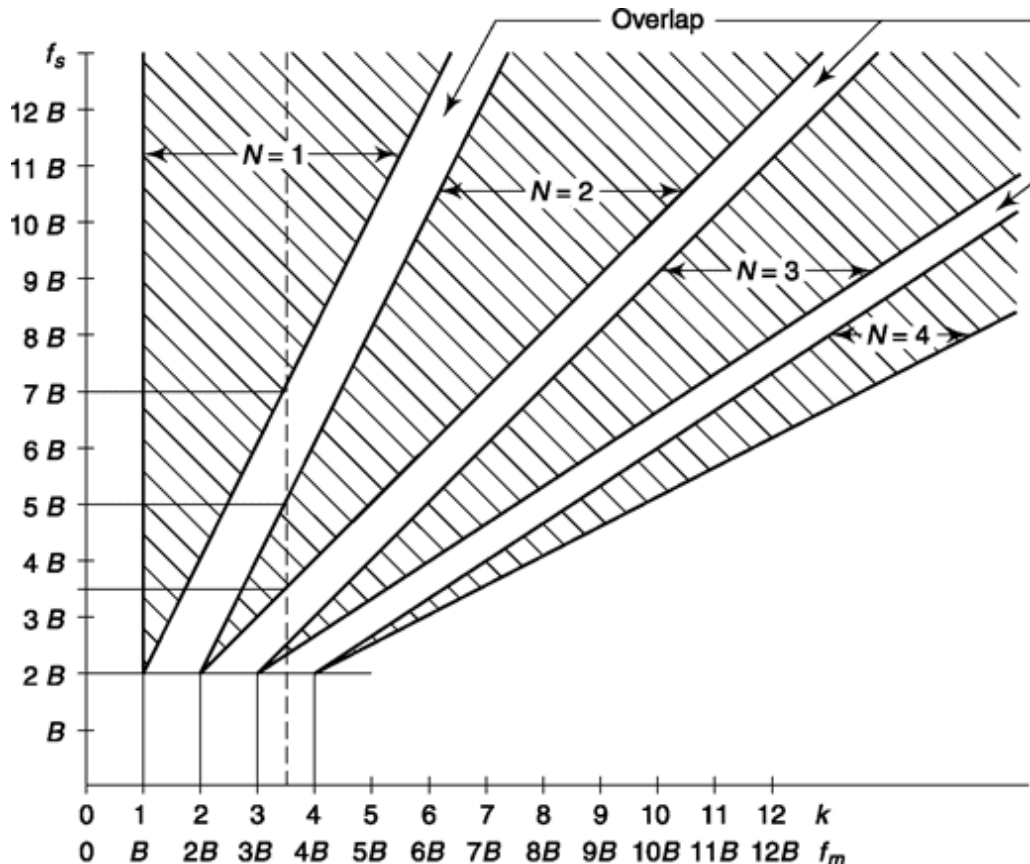


Fig. 4-6 Showing the regions (shaded) in which both Eqs (4.7) and (4.8) are satisfied.

4-1-3 The Discrete Fourier Transform

There are occasions when the only information available about a signal is a set of sample values, N in number, taken at regularly spaced intervals T_s over a period of time T_0 . From this sampled data we should often like to be able to arrive at some reasonable approximation of the spectral content of the signal. If the sample period and the number of samples is adequate to give us some confidence that what has been observed of the signal is representative of the signal generally, we may indeed estimate its spectral content.

We pretend that the signal is periodic with period T_0 and we pretend, as well, that the sampling rate is adequate to satisfy the Nyquist criterion. A typical set of sample values is shown in Fig. 4.7. Here, for simplicity we have assumed an even number of samples so that we can place them symmetrically in the period interval T_0 and symmetrically about the origin of the coordinate system. The sample values are located at $\pm T_s/2, \pm 3T_s/2$, etc. If

there are N samples then the samples most distant from the origin are at $\pm[(N - 1)/2] T$.

If the waveform to be sampled is $m(t)$, then after sampling, the waveform we have available is $m(t)S(t)$, where $S(t)$ is the sampling function, i.e. $S(t) = 1$ during the sampling duration dt , as shown in Fig. 4.7, and $S(t) = 0$ elsewhere. We note from Figs 4.2 and 4.3a that the spectrum of $m(t)$ and the part of the spectrum of $m(t)S(t)$ up to f_M are identical in form. Hence, to find the spectrum of $m(t)$ we may evaluate instead the spectrum of $m(t)S(t)$. The spectral amplitudes of $m(t)S(t)$ from En. (1 30) are'

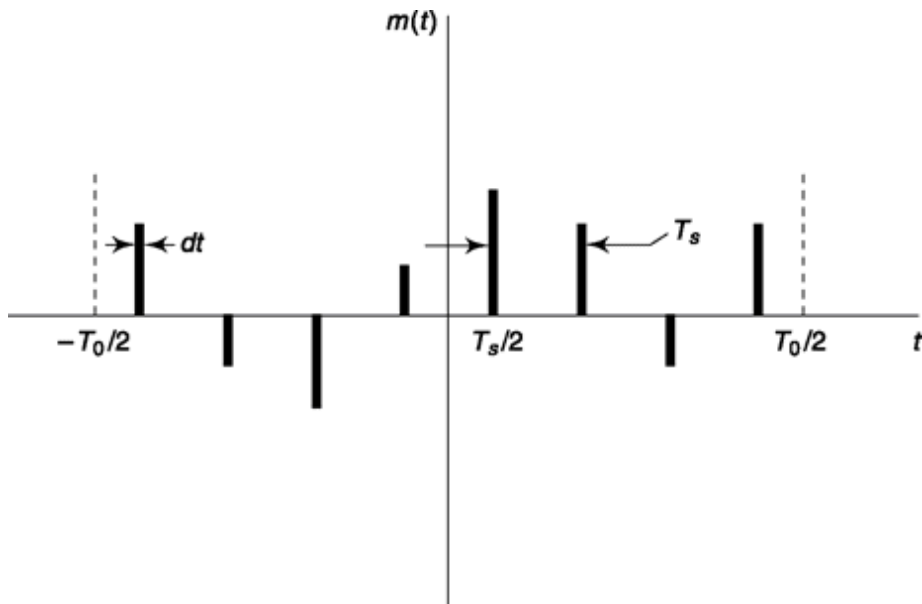


Fig. 4.7 A possible set of sample values of a waveform $m(t)$, taken every T_s over a time interval T .

$$M_n = \frac{1}{T_0} \int_{-T_0/2}^{T_0/2} m(t) e^{-j2\pi nt/T_0} dt \quad (4.9)$$

If there are N samples in all, then the sample times are

$$-\left(\frac{N-1}{2}\right)T_s, -\left(\frac{N-1}{2}\right)T_s + T_s, -\left(\frac{N-1}{2}\right)T_s + 2T_s, \dots, \left(\frac{N-1}{2}\right)T_s + \dots$$

Using these values for t in the integrand, we find that Eq. (4.9) becomes:

$$M_n = \frac{dt}{T_0} \sum_{k=-(N-1)/2}^{k=(N-1)/2} m(kT_s) e^{-j2\pi nkT_s/T_0} \quad (4.10)$$

As a purely mathematical exercise, we could use Eq. (4.10) to calculate spectral components M_n for any value of n . But consistently with our assumptions, the largest value of n allowable is determined by the Nyquist criterion. The highest frequency component should have a period which is $2T_s$ so that

$$f_n(\max) = \frac{1}{2T_s} \quad (4.11)$$

The fundamental period is T_0 so that the fundamental frequency is therefore $f_0 = 1/T_0$. Since $T_0 = NT_s$, we have

$$f_n(\max) = \frac{N}{2} \frac{1}{T_0} = \frac{N}{2} f_0 \quad (4.12)$$

Hence, the highest value of n for which Eq. (4.10) should be used is $n = N/2$.

Now, from the definition of Fourier Transform in Eq. (1.86), we can write

$$M(f) = \int_{-T_0/2}^{T_0/2} m(t) e^{-j2\pi ft} dt \quad (4.13)$$

or

$$M(f) = \lim_{T_s \rightarrow 0} \sum_{k=-(N-1)/2}^{(N-1)/2} m(kT_s) e^{-j2\pi f k T_s} T_s \quad (4.14)$$

where $t = kT_s$ and $dt = T_s$

Let us try to relate M_n of Eq. (4.10) with $M(f)$ of Eq. (4.14). We can see that M_n can be related to the n -th sample of $M(f)$ at $f = n/T_0$ or $f = nf_0$ where $f_0 = 1/T_0$, the separation between two consecutive frequency samples. We are now in position to formally define Discrete Fourier Transform (DFT) of a sampled discrete-time signal as

$$M_q = \sum_{k=0}^{N-1} m_k e^{-j2\pi q k / N}, \quad q = 0, 1, 2, \dots, N-1 \quad (4.15a)$$

where $M_q = M(qf_0)$ and $m_k = m(kT_s)$. This puts N uniformly spaced frequency samples between frequency 0 to sampling frequency $f_s = 1/T_s$. Note that (i) $M_q = M_{q+iN}$ for any integer i from Eq. (4.15a) as $e^{-j2\pi(q+iN)k/N} = e^{-j2\pi q k / N} \cdot e^{-j2\pi i k} = e^{-j2\pi q k / N}$, i.e. M_q is periodic with periodicity N , and also (ii) $M_q = M_{q+N/2}^*$ where * stands for complex conjugate, i.e. it is symmetric about $N/2$ (See Example 4.3). Thus, $N/2$ number of frequency samples give the estimate as discussed before. This periodicity and anti-symmetry property help in deriving DFT by a faster algorithm called Fast Fourier Transform (FFT) that reduces the number of multiplications from N^2 [for each value of q in Eq. (4.15a), N multiplications are needed and q is N long] to $\frac{N}{2} \log_2 N$ multiplications. The Inverse Discrete Fourier Transform (IDFT) that gives back the time samples is defined as

$$m_k = \frac{1}{N} \sum_{q=0}^{N-1} M_q e^{j2\pi q k / N}, \quad k = 0, 1, 2, \dots, N-1 \quad (4.15b)$$

Equation (4.15b) can be arrived at by substituting M_q from Eq. (4.15a) and noting

$$\sum_{q=0}^{N-1} e^{j2\pi q(k-l)/N} = N \text{ for } l = k \quad \text{and} \quad \sum_{q=0}^{N-1} e^{j2\pi q(k-l)/N} = 0 \text{ for } l \neq k \quad (4.16)$$

The DFT relation shows that we can have N frequency samples if the number of time samples available is N with frequency resolution f_s/N . If we want to increase frequency resolution to say f_s/M where ($M > N$), we can simply pad $(M - N)$ number of zeros to m_k to increase its length to M and then apply Eq. (4.15a). If we conduct IDFT on this then we shall get back M samples, of which the last $(M - N)$ samples will be zero and can be discarded.

It is often convenient to write DFT and IDFT relations in matrix form.

If $\mathbf{M} = [M_0 \ M_1 \ M_2 \ \dots \ M_{N-1}]^T$, $\mathbf{m} = [m_0 \ m_1 \ m_2 \ \dots \ m_{N-1}]^T$

and

$$W_N = \begin{bmatrix} 1 & 1 & .. & 1 \\ 1 & W_N^1 & .. & W_N^{(N-1)} \\ .. & .. & .. & .. \\ 1 & W_N^{(N-1)} & W_N^{2(N-1)} & W_N^{(N-1)^2} \end{bmatrix} \quad \text{where } W_N = e^{-j2\pi/N}$$

Then Eq. (4.15a) and Eq. (4.15b) can respectively be written as

$$\mathbf{M} = W_N \mathbf{m} \quad (4.17a)$$

$$\mathbf{m} = \frac{1}{N} W_N^* \mathbf{M} \quad (4.17b)$$

Substituting \mathbf{M} from Eq. (4.17a) in Eq. (4.17b), we get

$$W_N^* W_N = N I_{N \times N} \quad \text{or} \quad W_N^* = N W_N^{-1} \quad (4.18)$$

Frequency representation by samples is very useful when we use digital hardware. While discussing orthogonal frequency division multiplexing (OFDM), we shall further see how the concept of DFT-IDFT is exploited in communication that uses multiple carriers. The DFT relation of Eq. (4.15a) depicting frequency samples can be rewritten to describe the discrete time signal's frequency characteristic in continuous form (not sampled) as $M(e^{j\omega}) = \sum_{k=0}^{N-1} m_k e^{-j\omega k}$ where $\omega = 2\pi f$ for a periodic signal and more generally for any signal, periodic or aperiodic in the form

$$M(e^{j\omega}) = \sum_{k=0}^{\infty} m_k e^{-j\omega k} \quad (4.19)$$

This is known as Discrete Time Fourier Transform (DTFT). One can see that DFT coefficients are sampled version of DTFT such that $M_q = M(e^{j\omega})|_{\omega=2\pi q/N}$. Further generalization is used to describing a discrete time signal by z -transform defined as

$$M(z) = \sum_{k=0}^{\infty} m_k z^{-k} \quad (4.20)$$

where, $z = re^{j\omega}$. The value assigned to r is a real number and when $r = 1$, the z -transform is same as DTFT. Compared to DTFT, z -transform is more popular in describing discrete-time system as it ensures convergence of more signals because of the r^{-n} factor in the expansion equation. We shall take up more aspects of z -transform later when it is necessary to understand a few specific discussions involving discrete time systems.

Example 4.1

A single-tone 4 kHz message signal is sampled with

- (a) *10 kHz signal and 7 kHz signal. Describe the frequency spectrum in each case.*
- (b) *What will be the output if the sampled signals are passed through a low pass filter in each case?*

Solution

For 10 kHz sampling, frequencies present will be ± 4 kHz, $\pm(10 - 4) = \pm 6$ kHz, $\pm(10 + 4) = \pm 14$ kHz, $\pm(2 \times 10 - 4) = \pm 16$ kHz, $\pm(2 \times 10 + 4) = \pm 24$ kHz, etc.

For 7 kHz sampling, frequencies present will be ± 4 kHz, $\pm(7 - 4) = \pm 3$ kHz, $\pm(7 + 4) = \pm 11$ kHz, $\pm(2 \times 7 - 4) = \pm 10$ kHz, $\pm(2 \times 7 + 4) = \pm 18$ kHz, etc.

- (b) For 10 kHz case, the maximum frequency a LPF can be designed to pass is $< 10/2 = 5$ kHz. Hence, it can pass 4 kHz signal, and reconstructs the original signal.

For 7 kHz case, the maximum frequency a LPF can be designed to pass is $< 7/2 = 3.5$ kHz. Hence, it can pass 3 kHz signal, and gives a completely different signal from the original sampled.

Note that, the second case is that of under-sampling where Nyquist rate is not followed.

Example 4.2

A signal $m(t) = 2\cos 6000nt + 4\cos 8000nt + 6 \cos 10000pt$ is to be truthfully represented by its samples. What is the minimum sampling rate from

- (a) low pass sampling theorem consideration and
- (b) band pass consideration?

Solution

The signal given has two frequency components.

Highest frequency, $f_H = 10000/2 = 5000$ Hz

Lowest frequency, $f_L = 6000/2 = 3000$ Hz

- (a) Minimum sampling frequency from low pass consideration = $2 \times f_H = 2 \times 5000 = 10000$ Hz
- (b) $B = f_H - f_L = 5000 - 3000 = 2000$ Hz, $k = \text{floor}(f_H/B)$ = $\text{floor}(5000/2000) = \text{floor}(2.5) = 2$
where, $\text{floor}(x)$ gives the largest integer that does not exceed x .

Then required sampling frequency = $2f_H/k = 2 \times 5000/2 = 5000$ Hz.

Draw the spectrum of $m(t)$ in both the cases and you'll have a greater understanding of sampling phenomena and sampling frequency.

Example 4.3

Four samples of a discrete-time signals sampled at 8000Hz are 1, 0, 2, -1. (i) Find its frequency samples through DFT. What is the frequency resolution? (ii) Show how to double the frequency resolution by zero padding. (iii) Conduct IDFT of (i) to get back the original signal.

Solution

We use matrix multiplication technique for computational ease. Also, it is easy to employ in a digital

computer.

- (i) Here, $N = 4$. Thus we have to conduct 4-point DFT operation, i.e. $W_4 = e^{-j2\pi/4} = -j$

$$\mathbf{m} = [1 \ 0 \ 2 \ -1]^T \text{ and}$$

$$W_4 = \begin{bmatrix} 1 & 1 & 1 & 1 \\ 1 & -j & (-j)^2 & (-j)^3 \\ 1 & (-j)^2 & (-j)^4 & (-j)^6 \\ 1 & (-j)^3 & (-j)^6 & (-j)^9 \end{bmatrix} = \begin{bmatrix} 1 & 1 & 1 & 1 \\ 1 & -j & -1 & j \\ 1 & -1 & 1 & -1 \\ 1 & j & -1 & -j \end{bmatrix}$$

From Eq. (4.17a),

$$M = \begin{bmatrix} 1 & 1 & 1 & 1 \\ 1 & -j & -1 & j \\ 1 & -1 & 1 & -1 \\ 1 & j & -1 & -j \end{bmatrix} \begin{bmatrix} 1 \\ 0 \\ 2 \\ -1 \end{bmatrix} = \begin{bmatrix} 2 \\ -1-j \\ 4 \\ -1+j \end{bmatrix}$$

$$\text{Frequency resolution} = 8000/4 = 2000 \text{ Hz}$$

This means frequency samples are at 0, 2000, 4000, 6000 Hz and valued 2, $-1-j$, 6, $-1+j$ respectively. The symmetry about 4000 Hz can be seen; sample values at 2000 Hz and 6000 Hz are complex conjugate and magnitude of both are $\sqrt{2}$.

- (ii) To double frequency resolution, consider $N = 8$ and after zero padding, $\mathbf{m} = [1 \ 0 \ 2 \ -1 \ 0 \ 0 \ 0 \ 0]^T$

We can use matrix route but to avoid writing 8×8 matrix describing W_8 let us use Eq. (4.15a). Substituting $N = 8$,

$$M_q = \sum_{k=0}^7 m_k e^{-j\pi q k / 4}$$

$$M_0 = 1 + 0 + 2 + -1 + 0 + 0 + 0 + 0 = 2$$

The last 4 terms in summation for all values of q are zero as $m_k = 0$ for $k = 4, 5, 6, 7$.

$$\begin{aligned} M_1 &= 1 + 0 + 2 \cdot e^{-j\pi 2/4} + -1 \cdot e^{-j\pi 3/4} \\ &= 1 - 2j + \frac{1}{\sqrt{2}} + \frac{j}{\sqrt{2}} = 1.707 - j 1.293 \end{aligned}$$

$$\begin{aligned} M_2 &= 1 + 0 + 2 \cdot e^{-j\pi 4/4} + -1 \cdot e^{-j\pi 5/4} \\ &= 1 - 2 - j = -1 - j \end{aligned}$$

$$\begin{aligned} M_3 &= 1 + 0 + 2 \cdot e^{-j\pi 6/4} + -1 \cdot e^{-j\pi 6/4} \\ &= 1 + 2j - \frac{1}{\sqrt{2}} + \frac{j}{\sqrt{2}} = 0.293 + j 2.707 \end{aligned}$$

$$M_4 = 1 + 0 + 2 \cdot e^{-j\pi/4} + -1 \cdot e^{-j\pi/2/4} \\ = 1 + 2 + 1 = 4$$

From symmetry property,

$$M_5 = M_1^* = 1.707 + j 1.293$$

(Symmetry about 8/2 = 4)

$$M_6 = M_2^* = -1 + j$$

$$M_7 = M_3^* = 0.293 - j 2.707$$

Frequency resolution = $8000/8 = 1000$ and frequency samples $M_0, M_1, M_2, \dots, M_7$ are at frequencies 0, 1000, 2000, ..., 7000 Hz respectively. Note that in both sample values at 0, 2000, 4000, 6000 Hz are same for both (i) and (ii). This should be the case as by zero padding frequency resolution is only increased.

(iii) For IDFT of (i), we go back to matrix multiplication method and use Eq. (4.17b). By conjugate operation,

$$W_4^* = \begin{bmatrix} 1 & 1 & 1 & 1 \\ 1 & j & -1 & -j \\ 1 & -1 & 1 & -1 \\ 1 & -i & -1 & i \end{bmatrix}$$

Then,

$$\mathbf{m} = \frac{1}{4} \begin{bmatrix} 1 & 1 & 1 & 1 \\ 1 & j & -1 & -j \\ 1 & -1 & 1 & -1 \\ 1 & -i & -1 & i \end{bmatrix} \begin{bmatrix} 2 \\ -1-j \\ 4 \\ -1+i \end{bmatrix} = \begin{bmatrix} 1 \\ 0 \\ 2 \\ -1 \end{bmatrix}$$

SELF-TEST QUESTION

1. The more the path length for a signal to travel, the more is the attenuation and distortion. Is it correct?
2. For the same performance, an analog signal requires less signal power compared to digital. Is it true?
3. Is it advisable to sample a single-tone signal of frequency f with frequency $2f$?
4. Is it true that the sampling frequency for a bandpass signal need not be more than double the maximum frequency present in the signal?

4.2 PULSE AMPLITUDE MODULATION AND CONCEPT OF TIME DIVISION MULTIPLEXING

A technique by which we may take advantage of the sampling principle for the purpose of time-division multiplexing is illustrated in the idealized representation of Fig. 4.8. At the transmitting end on the left, a number of bandlimited signals are connected to the contact point of a rotary switch. We assume that the signals are similarly bandlimited. For example, they may all be voice signals, limited to 3.3 kHz. As the rotary arm of the switch swings around, it samples each signal sequentially. The rotary switch at the receiving end is in synchronism with the switch at the sending end. The two switches make contact simultaneously at similarly numbered contacts. With each revolution of the switch, one sample is taken of each input signal and presented to the correspondingly numbered contact of the receiving-end

switch. The train of samples at, say, terminal 1 in the receiver, pass through low-pass filter 1, and, at the filter output, the original signal $m_x(t)$ appears reconstructed. Of course, if f_M is the highest-frequency spectral component present in any of the input signals, the switches must make at least $2f_M$ revolutions per second.

When the signals to be multiplexed vary slowly with time, so that the sampling rate is correspondingly slow, mechanical switches, indicated in Fig. 4.8, may be employed. When the switching speed required is outside the range of mechanical switches, electronic switching systems may be employed. In either event, the switching mechanism, corresponding to the switch at the left in Fig. 4.8, which samples the signals, is called the *commutator*. The switching mechanism which performs the function of the switch at the right in Fig. 4.8 is called the *decommutator*. The commutator samples and combines samples, while the decommutator separates samples belonging to individual signals so that these signals may be reconstructed.

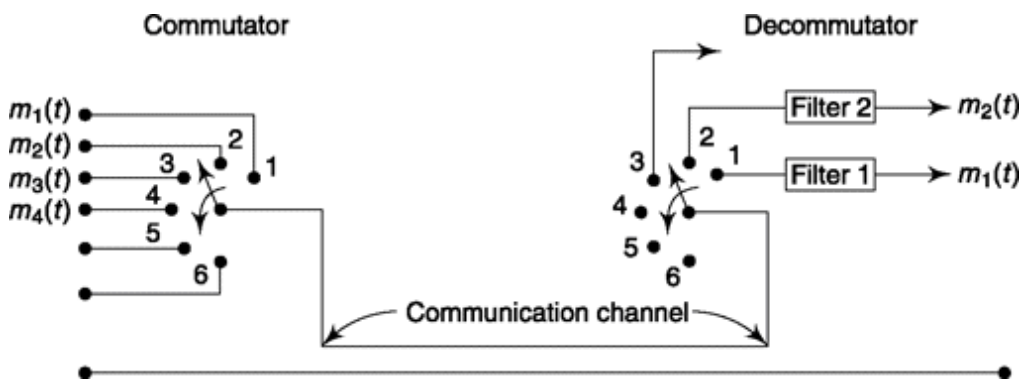


Fig. 4.8 Illustrating how the sampling principle may be used to transmit a number of bandlimited signals over a single communications channel.

The interlacing of the samples that allows multiplexing is shown in Fig. 4.9. Here, for simplicity, we have considered the case of the multiplexing of just two signals $m_1(t)$ and $m_2(t)$. The signal $m_1(t)$ is sampled regularly at intervals of T_s and at the times indicated in the figure. The sampling of $m_2(t)$ is similarly regular, but the samples are taken at a time different from the sampling time of $m_1(t)$. The input waveform to the filter numbered 1 in Fig. 4.8 is the train of samples of $m_1(t)$, and the input to the filter numbered 2 is the train of samples of $m_2(t)$. The timing in Fig. 4.9 has been deliberately drawn to suggest that there is room to multiplex more than two signals. We shall see shortly, in principle, how many signals may be multiplexed.

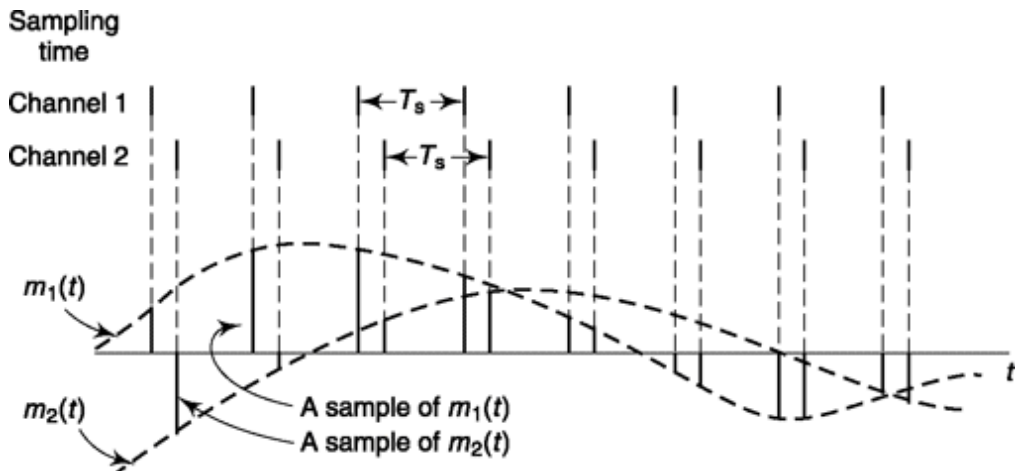


Fig. 4.9 The interlacing of two baseband signals.

We observe that the train of pulses corresponding to the samples of each signal are *modulated in amplitude* in accordance with the signal itself. Accordingly, the scheme of sampling is called *pulse-amplitude modulation* and abbreviated PAM.

Multiplexing of several PAM signals is possible because the various signals are kept distinct and are separately recoverable by virtue of the fact that they are sampled at different times. Hence, this system is an example of a *time-division multiplex* (TDM) system. Such systems are the counterparts in the time domain of the systems of Chapter 2. There, the signals were kept separable by virtue of their translation to different portions of the frequency domain, and those systems are called frequency-division multiplex (FDM) systems.

If the multiplexed signals are to be transmitted directly, say, over a pair of wires, no further signal processing need be undertaken. Suppose, however, we require to transmit the TDM-PAM signal from one antenna to another. It would then be necessary to amplitude-modulate or frequency-modulate a high-frequency carrier with the TDM-PAM signal; in such a case the overall system would be referred to, respectively, as PAM-AM or PAM-FM. Note that the same terminology is used whether a single signal or many signals (TDM) are transmitted.

4.2.1 Channel Bandwidth for pAM

Suppose that we have N independent baseband signals $m_1(t)$, $m_2(t)$, etc., each of which is bandlimited to f_M . What must be the bandwidth of the communications channel which will allow all N signals to be transmitted

simultaneously using PAM time-division multiplexing? We shall now show that, in principle at least, the channel need not have a bandwidth larger than Nf_M .

The baseband signal, say $m_x(t)$, must be sampled at intervals not longer than $T_s = 1/2f_M$. Between successive samples of $m_x(t)$ will appear samples of the other $N - 1$ signals. Therefore, the interval of separation between successive samples of different baseband signals is $1/2f_M N$. The composite signal, then, which is presented to the transmitting end of the communications channel, consists of a sequence of samples, that is, a sequence of *impulses*. If the bandwidth of the channel were arbitrarily great, the waveform at the receiving end would be the same as at the sending end and demultiplexing could be achieved in a straightforward manner.

If, however, the bandwidth of the channel is restricted, the channel response to an instantaneous sample will be a waveform which may well persist with significant amplitude long after the time of selection of the sample. In such a case, the signal at the receiving end at any particular sampling time may well have significant contributions resulting from previous samples of other signals. Consequently the signal which appears at any of the output terminals in Fig. 4.8 will not be a single baseband signal but will be instead a combination of many or even all the baseband signals. Such combining of baseband signals at a communication system output is called *crosstalk* and is to be avoided as far as possible.

Let us assume that our channel has the characteristics of an ideal low-pass filter with angular cutoff frequency $\omega_c = 2\pi f_c$, unity gain, and no delay. Let a sample be taken, say, of $m_1(t)$, at $t = 0$. Then at $t = 0$ there is presented at the transmitting end of the channel an impulse of strength $I_1 = m_1(0) dt$. The response at the receiving end is $s_{R1}(t)$ given by (see Prob. 4.15)

$$s_{R1} = \frac{I_1 \omega_c}{\pi} \frac{\sin \omega_c t}{\omega_c t} \quad (4.21)$$

The normalized response $\pi s_R(t)/\omega_c$ is shown in Fig. 4.10 by the solid plot. At $t = 0$ the response attains a peak value proportional to the strength of the impulse $I_1 = m_1(0) dt$, which is in turn proportional

to the value of the sample $m_1(0)$. This response persists indefinitely. Observe, however, that the response passes through zero at intervals which are multiples of $\pi/\omega_c = 1/2f_c$. Suppose, then, that a sample of $m_2(t)$ is taken and transmitted at $t = 1/2f_c$. If $I_2 = m_2(t = 1/2f_c) dt$,

$$s_{R2}(t) = \frac{I_2 \omega_c}{\pi} \frac{\sin \omega_c(t - 1/2f_c)}{\omega_c(t - 1/2f_c)} \quad (4.22)$$

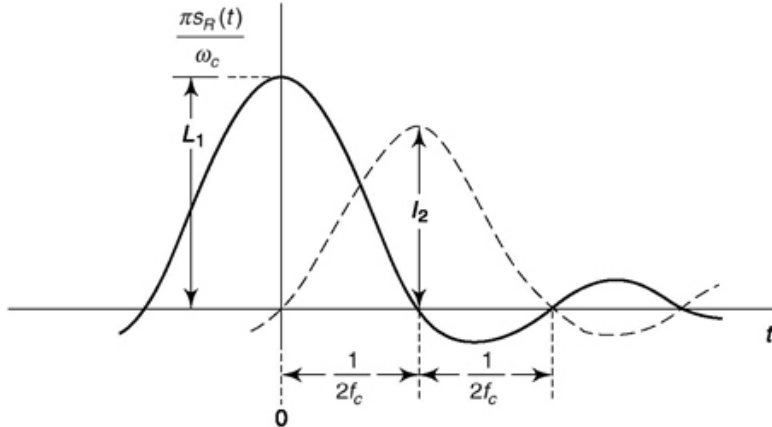


Fig. 4.10 The response of an ideal low-pass filter to an instantaneous sample at $t = 0$ (solid plot). The response at $t = 1/2f_c$ (dashed plot).

This response is shown by the dashed plot. Suppose, finally, that the demultiplexing is done also by instantaneous sampling at the receiving end of the channel, for $m_1(t)$ at $t = 0$ and for $m_2(t)$ at $t = 1/2f_c$. Then, in spite of the persistence of the channel response, there will be no crosstalk, and the signals $m_1(t)$ and $m_2(t)$ may be completely separated and individually recovered. Similarly, additional signals may be sampled and multiplexed, provided that each new sample is taken synchronously, every $1/2f_c$ s. The sequence must, of course, be continually repeated every $1/2f_M$ s, so that each signal is properly sampled.

We have then the result that with a channel of bandwidth f_c we need to separate samples by intervals $1/2f_c$. The sampling theorem requires that the samples of an individual baseband signal be separated by intervals not longer than $1/2f_M$. Hence the total number of signals which may be multiplexed is $N = f_c/f_M$, or $f_c = Nf_M$ as indicated earlier.

In principle then, multiplexing a number of signals by PAM time division requires no more bandwidth than would be required to multiplex these signals by frequency-division multiplexing using single-sideband transmission.

4.2.2 Natural sampling

It was convenient, for the purpose of introducing some basic ideas, to begin our discussion of time multiplexing by assuming instantaneous commutation and decommutation. Such instantaneous sampling, however, is hardly feasible. Even if it were possible to construct switches which could operate in an arbitrarily short time, we would be disinclined to use them. The reason is that instantaneous samples at the transmitting end of the channel have infinitesimal energy, and when transmitted through a bandlimited channel give rise to signals having a peak value which is infinitesimally small. We recall that in Fig. 4.10 $I_I = m_x(0) dt$. Such infinitesimal signals will inevitably be lost in background noise.

A much more reasonable manner of sampling, referred to as *natural sampling*, is shown in Fig. 4.11. Here the sampling waveform $S(t)$ consists of a train of pulses having duration t and separated by the sampling time T_s . The baseband signal is $m(t)$, and the sampled signal $S(t)m(t)$ is shown in Fig. 4.11c. Observe that the sampled signal consists of a sequence of pulses of varying amplitude whose tops are not flat but follow the waveform of the signal $m(t)$.

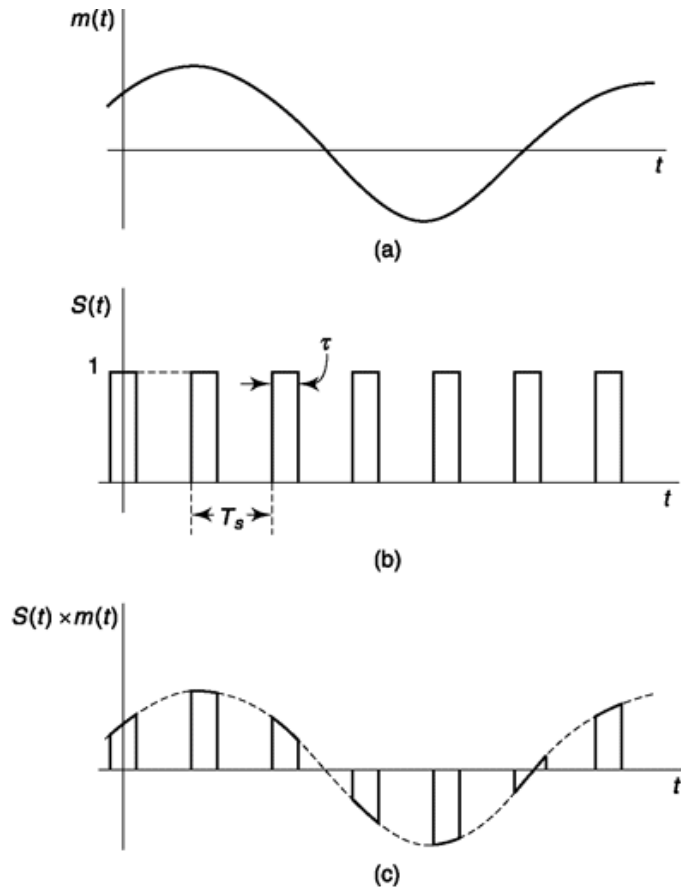


Fig. 4.11 (a) A baseband signal $m(t)$. (b) A sampling signal $S(t)$ with pulses of finite duration. (c) The naturally sampled signal $S(t)m(t)$.

With natural sampling, as with instantaneous sampling, a signal sampled at the Nyquist rate may be reconstructed exactly by passing the samples through an ideal low-pass filter with cutoff at the frequency f_M , where f_M is the highest-frequency spectral component of the signal. To prove this, we note that the sampling waveform $S(t)$ shown in Fig. 4.11 is given by [see Eq. (1.42) with $A = 1$ and $T_0 = T_s$]

$$S(t) = \frac{\tau}{T_s} + \frac{2\tau}{T_s} \left(C_1 \cos 2\pi \frac{t}{T_s} + C_2 \cos 2 \times 2\pi \frac{t}{T_s} + \dots \right) \quad (4.23)$$

with the constant C_n given by

$$C_n = \frac{\sin(n\pi\tau/T_s)}{n\pi\tau/T_s} \quad (4.24)$$

This sampling waveform differs from the sampling waveform of Eq. (4.1) for instantaneous sampling only in that dt is replaced by τ and by the fact that the amplitudes of the various harmonics are not the same. The sampled baseband signal $S(t)m(t)$ is, for $T_s = 1/2f_M$,

$$S(t)m(t) = \frac{\tau}{T_s} m(t) + \frac{2\tau}{T_s} [m(t)C_1 \cos 2\pi(2f_M)t + m(t)C_2 \cos 2\pi(4f_M)t + \dots] \quad (4.25)$$

Therefore, as in instantaneous sampling, a low-pass filter with cutoff at f_M will deliver an output signal $s_o(t)$ given by

$$s_o(t) = \frac{\tau}{T_s} m(t) \quad (4.26)$$

which is the same as is given by the first term of Eq. (4.2) except with dt replaced by t .

With samples of finite duration, it is not possible to completely eliminate the crosstalk generated in a channel, sharply bandlimited to a bandwidth f_c . If N signals are to be multiplexed, then the maximum sample duration is $t = T_s/N$. It is advantageous, for the purpose of increasing the level of the output signal, to make t as large as possible. For, as is seen in Eq. (4.18), $s_o(t)$ increases with t . However, to help suppress crosstalk, it is ordinarily required that the samples be limited to a duration much less than T_s/N . The result is a large *guard time* between the end of one sample and the beginning of the next.

4.2.3 Flat-Top sampling

Pulses of the type shown in Fig. 4.11, with tops contoured to follow the waveform of the signal, are actually not frequently employed. Instead *flat-topped* pulses are customarily used, as shown in Fig. 4.12a. A flat-topped pulse has a constant amplitude established by the sample value of the signal at some point within the pulse interval. In Fig. 4.12a we have arbitrarily sampled the signal at the beginning of the pulse. In sampling of this type the baseband signal $m(t)$ cannot be recovered exactly by simply passing the samples through an ideal low-pass filter. However, the distortion need not be large. Flat-top sampling has the merit that it simplifies the design of the electronic circuitry used to perform the sampling operation.

To show the extent of the distortion, consider the signal $m(t)$ having a Fourier transform $M(j\omega)$. We have seen (see Figs 4.2 and 4.3) how to deduce the transform of the sampled signal, when the sampling is instantaneous. The transform of the sampled signal for flat-top sampling is determined by considering that the flat-top pulse can be generated by passing the instantaneously sampled signal through a network which broadens a pulse of duration dt (an impulse) into a pulse of duration t . The transform of a pulse of unit amplitude and width dt is

$$\mathcal{F}[\text{impulse of strength } dt \text{ at } t = 0] = dt \quad (4.27)$$

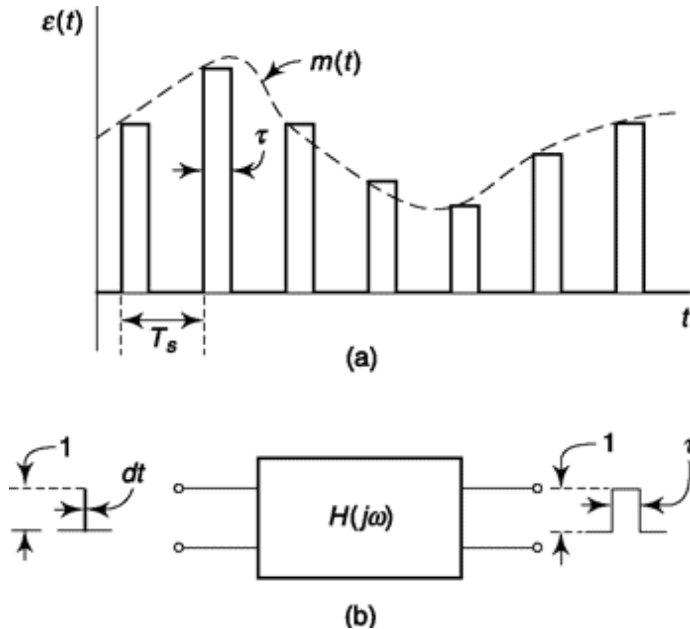


Fig. 4.12 (a) Flat-topped sampling, (b) A network with transform $H(j\omega)$ which converts a pulse of width dt into a rectangular pulse of like amplitude but of duration t

The transform of a pulse of unit amplitude and width τ is [see Eq. (1.105)]

$$\mathcal{F}\left[\text{pulse, amplitude} = 1, \text{extending from } t = -\frac{\tau}{2} \text{ to } t = \frac{\tau}{2}\right] = \tau \frac{\sin(\omega\tau/2)}{\omega\tau/2} \quad (4.28)$$

Hence, the transfer function of the network shown in Fig. 4.12b, is required to be

$$H(j\omega) = \frac{\tau}{dT} \frac{\sin(\omega\tau/2)}{\omega\tau/2} \quad (4.29)$$

Let the signal $m(t)$, with transform $M(j\omega)$, be bandlimited to f_M and be sampled at the Nyquist rate or faster. Then in the range 0 to f_M the transform of the flat-topped sampled signal is given by the product $H(j\omega)M(j\omega)$ or, from Eqs (4.27), (4.28), and (4.29)

$$\mathcal{F}[\text{flat-topped sampled } m(t)] = \frac{\tau}{T_s} \frac{\sin(\omega\tau/2)}{\omega\tau/2} M(j\omega) \quad 0 \leq f \leq f_M \quad (4.30)$$

To illustrate the effect of flat-top sampling, we consider for simplicity that the signal $m(t)$ has a flat spectral density equal to M_0 over its entire range from 0 to f_M , as is shown in Fig. 4.13a. The form of the transform of the instantaneously sampled signal is shown in Fig. 4.13b. The sampling frequency $f_s = 1/T_s$ is assumed large enough to allow for a guard band between the spectrum of the baseband signal and the DSB-SC signal with carrier f_s . The spectrum of the flat-topped sampled signal is shown in Fig. 4.13d. We are, of course, interested only in the part of the spectrum in the range 0 to f_M . If, in this range, the spectra of the sampled signal and the original signal are identical, than the original signal may be recovered by a low-pass filter as has already been discussed. We observe, however, that such is not the case and that, as a result, distortion will result. This distortion results from the fact that the original signal was “observed” through a finite rather than an infinitesimal time “aperture” and is hence referred to as *aperture effect* distortion.

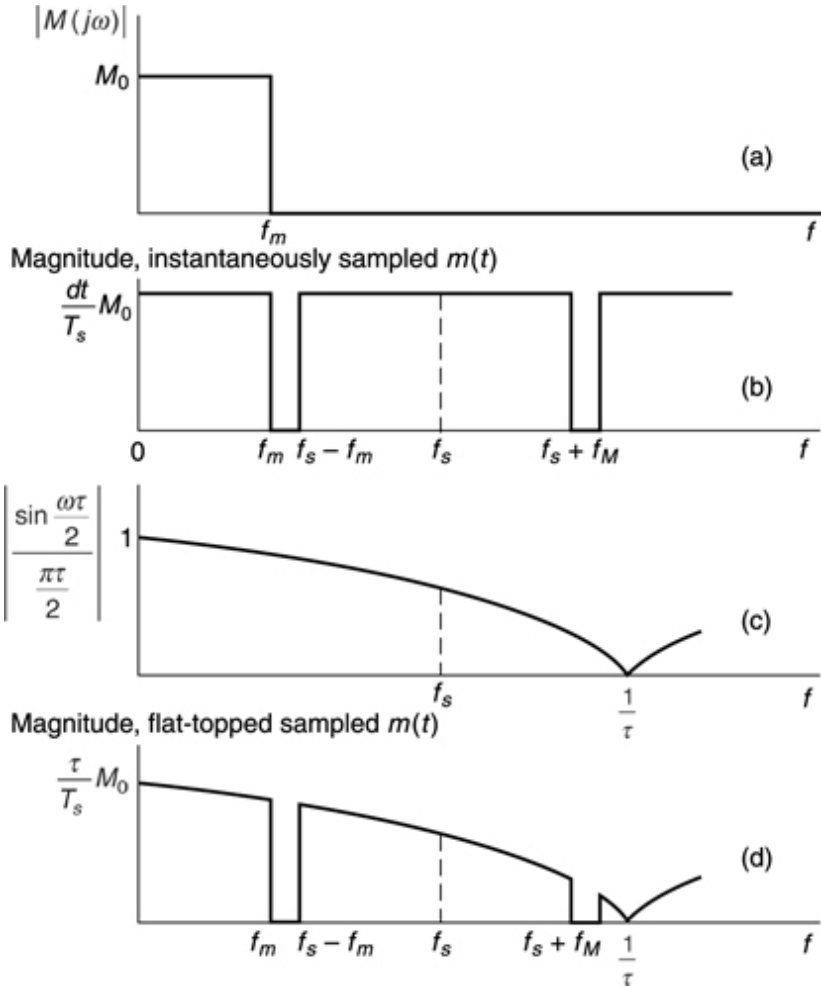


Fig. 4.13 (a) An idealized spectrum of a baseband signal. (b) The spectrum of the signal with instantaneous sampling. (c) The form $[(\sin x)/x]$, with $x = \omega t/2$, of the distortion factor (aperture effect) introduced by flat-topped sampling, (d) The spectrum of the signal with flat-topped sampling.

The distortion results from the fact that the spectrum is multiplied by the sampling function $Sa(x) = (\sin x)/x$ (with $x = \omega t/2$). The magnitude of the sampling function (see Sec. 1.3) falls off slowly with increasing x in the neighborhood of $x = 0$ and does not fall off sharply until we approach $x = n$, at which point $Sa(x) = 0$. To minimize the distortion due to the aperture effect, it is advantageous to arrange that $x = n$ correspond to a frequency very large in comparison with f_M . Since $x = n\omega t/2$, the frequency f_0 corresponding to $x = n$ is $f_0 = 1/t$. If $f_0 @ f_M$, or, correspondingly, if $t! 1/f_M$, the aperture distortion will be small. The distortion becomes progressively smaller with decreasing t . And, of course as $t \rightarrow 0$ (instantaneous sampling), the distortion similarly approaches zero.

Equalization^{1, 2}

As in the case of natural sampling, so also in the present case of flat-top sampling, it is advantageous to make t as large as practicable for the sake of increasing the amplitude of the output signal. If, in a particular case, it should happen that the consequent distortion is not acceptable, it may be corrected by including an *equalizer* in cascade with the output low-pass filter. An equalizer, in the present instance, is a passive network whose transfer function has a frequency dependence of

the form $x/\sin x$, that is, a form inverse to the form of $H(jw)$ given in Eq. (4.29). The equalizer in combination with the aperture effect will then yield a flat overall transfer characteristic between the original baseband signal and the output at the receiving end of the system. The equalizer $x/\sin x$ cannot be exactly synthesized, but can be approximated.

If N signals are multiplexed, $t < 1/2f_M N$, and hence for large N $t \approx 1/f_M$ and $x/\sin x \approx 1$. In this case the equalizer is not needed as negligible distortion results.

4.2.4 signal Recovery Through Holding

We have already noted that the maximum ratio t/T_s , of the sample duration to the sampling interval, is $t/T_s = 1/N$, N being the number of signals to be multiplexed. As N increases, t/T_s becomes progressively smaller, and, as is to be seen from Eq. (4.26), so correspondingly does the output signal. We discuss now an alternative method of recovery of the baseband signal which raises the level of the output signal (without the use of amplifiers which may introduce noise). The method has the additional advantage that rather rudimentary filtering is often quite adequate, but has the disadvantage that some distortion must be accepted.

The method is illustrated in Fig. 4.14, where the baseband signal $m(t)$ and its flat-topped samples are shown. At the receiving end, and after *demultiplexing*, the sample pulses are extended; that is, the sample value of each individual baseband signal is *held* until the occurrence of the next sample of that same baseband signal. This operation is shown in Fig. 4.14 as the dashed extension of the sample pulses. The output waveform consists then, as shown, of an up and down staircase waveform with no blank intervals.

A method, in principle, by which this holding operation may be performed is shown in Fig. 4.15. The switch S operates in synchronism with the occurrence of input samples. This switch, ordinarily open, closes somewhat after the occurrence of the leading edge of a sample pulse and opens somewhat before the occurrence of the trailing edge. The amplifier, whose gain, if any, is incidental to the present discussion, has a low-output impedance. Hence, at the closing of the switch, the capacitor C charges abruptly to a voltage proportional to the sample value, and the capacitor holds this voltage until the operation is repeated for the next sample. In Fig. 4.14 we have idealized the situation somewhat by showing the output waveform maintaining a perfectly constant level throughout the sample pulse interval and its following holding interval. We have also indicated abrupt transitions in voltage level from one sample to the next. In practice, these voltage transitions will be somewhat rounded as the capacitor charges and discharges exponentially. Further, if the received sample pulses are natural samples rather than flat-topped samples, there will be some departure from a constant voltage level during the sample interval itself. As a matter of practice however, the sample interval is very small in comparison with the interval between samples, and the voltage variation of the baseband signal during the sampling interval is small enough to be neglected.

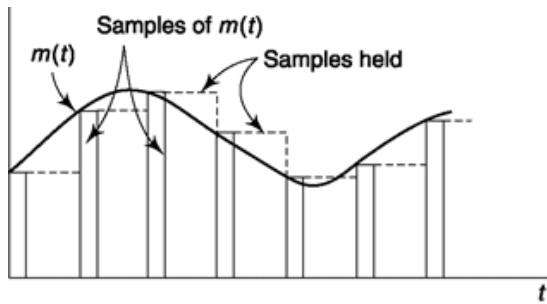


Fig. 4.14 Illustrating the operation of holding.

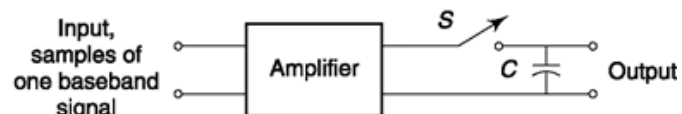


Fig. 4.15 Illustrating a method of performing the operation of holding.

If the baseband signal is $m(t)$ with spectral density $M(jw) = F[m(t)]$, we may deduce the spectral density of the sampled and held waveform in the manner of Sec. 4.2.3 and in connection with flat-topped sampling. We consider that the flat tops have been stretched to encompass the entire interval between instantaneous samples. Hence the spectral density is given as in Eq. (4.30) except with t replaced by the time interval between samples. We have, then,

$$\mathcal{F}[m(t), \text{sampled and held}] = \frac{\sin(\omega T_s/2)}{\omega T_s/2} M(j\omega) \quad 0 \leq f \leq f_M \quad (4.31)$$

In Fig. 4.16 we have again assumed for simplicity that the band-limited signal $m(t)$ has a flat spectral density of magnitude M_0 . In Fig. 4.16a is shown the spectrum of the instantaneously sampled signal. In Fig. 4.16b has been drawn the magnitude of the aperture factor $(\sin x)/x$ (with $x = \omega T_s/2$), while in Fig. 4.16c is shown the magnitude of the spectrum of the sampled-and-held signal. These plots differ from the plots of Fig. 4.13 only in the location of the nulls of the factor $(\sin x)/x$. In Fig. 4.16 the first null occurs at the sampling frequency f_s . We observe that, as a consequence, the

Magnitude, instantaneously sampled signal

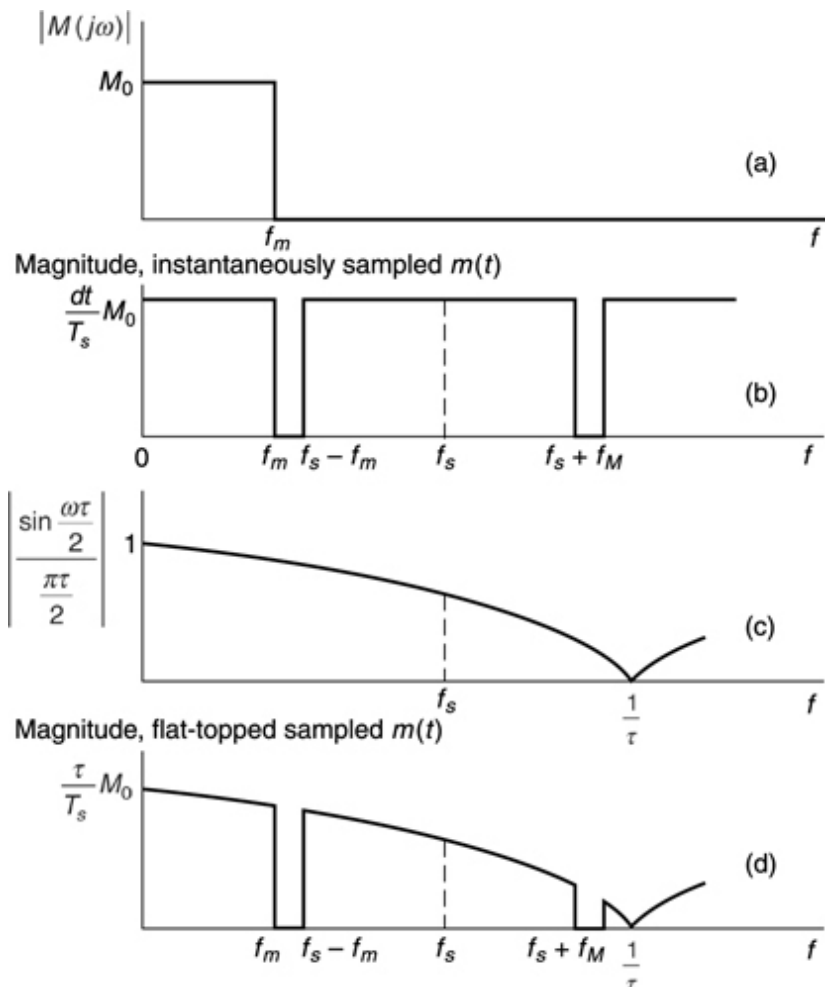


Fig. 4.16 (a) Spectrum of instantaneously sampled signal $m(t)$ with $m(t)$ having idealized spectrum shown in Fig. 4.13a. (b) The magnitude of the aperture effect factor, (c) Spectrum of sampled-and-held signal.

aperture effect, which is responsible for the $(\sin x)/x$ term, has accomplished most of the filtering which is required to suppress the part of the spectrum of the output signal above the bandlimit f_M . Of course, the filtering is not perfect, and some additional filtering may be required. We also note that, as in the case of flat-top sampling, there will be some distortion introduced by the unequal transmission of spectral components in the range 0 to f_M . If the distortion is not acceptable, then, as before, it may be corrected by an $x/\sin x$ equalizer.

Most importantly we note in comparing Eq. (4.31) with Eq. (4.30) that, aside from the relatively small effect of the $(\sin x)/x$ terms in the two cases, the sampled-and-held signal has a magnitude larger by the factor TJt than the signal of sample duration t . This increase in amplitude is, of course, intuitively to have been anticipated.

4.3 PULSE WIDTH MODULATION AND PULSE POSITION MODULATION

Before we move to digital representation of PAM signal, let us discuss two other analog modulation techniques involving pulse train and sampling. In one method, known as Pulse Width Modulation (PWM), the message modulates the width of the pulse and in the other, called Pulse Position Modulation (PPM), the position of the arrival of a fixed width pulse in each sample period is modulated by the message signal. Clearly, the randomness of the width in PWM and randomness in position in PPM do not make them suitable for time division multiplexing scheme. As a consequence their contribution to communication is limited. PWM finds application in motor control, in delivery of power which is precisely regulated by regulating the width of the pulse. Together, PWM and PPM are known as Pulse Time Modulation or PTM. The modulation and demodulation of these two schemes are closely connected.

Let us begin with the simplest method for PWM generation. Refer to Fig. 4.17a. We have a comparator, one input of which is fed by input message signal and the other by a sawtooth signal which operates at carrier frequency. The maximum of the input signal (considering both \pm ve side) should be less than that of sawtooth signal (Fig. 4.18). If that is so we'll get PWM signal at the output of comparator as shown in third waveform of Fig. 4.18. Note that, PWM pulses occur at regular interval, its rising edge coinciding with the falling edge of sawtooth signal. This is because when sawtooth signal is at

its minimum, which is always less than the minimum of input signal, the +ve input of the comparator is at higher potential and hence comparator output is positive. Next, when the sawtooth signal rises with a fixed slope and crosses input signal value, the -ve input of comparator is at higher potential and the comparator output will be -ve. The duration, for which the comparator stays at high is thus dependent on input signal magnitude and this decides the width of the pulse generated. Thus message information gets reflected in the time during which comparator output is at HIGH (+ve) or the width of the pulse generated at its output which is directly proportional to the amplitude of the message signal at that instant.

Now, we turn our attention to PPM generation which usually is a post processing of PWM signal and as shown in Fig. 4.17b. The PWM signal generated as above is sent to an inverter which reverses polarity of the pulses. If it is followed by a differentiator we'll have +ve spikes where in original PWM signal pulse was going from HIGH to LOW and -ve spikes where LOW to HIGH. This is shown in fourth waveform of Fig. 4.18. These spikes are then fed to a +ve edge triggered fixed width pulse generator which generates pulses of fixed width when a +ve spike appears, coinciding with the falling edge of original PWM signal. Note that, the occurrences of these falling edges were dependent (proportional to amplitude of message) on input message and hence the delay in occurrence of these fixed width pulses are proportional to the amplitude of the input message at that instant. These are the PPM outputs where positions of the pulses in a sample period carry input message information (the last waveform of Fig. 4.18).

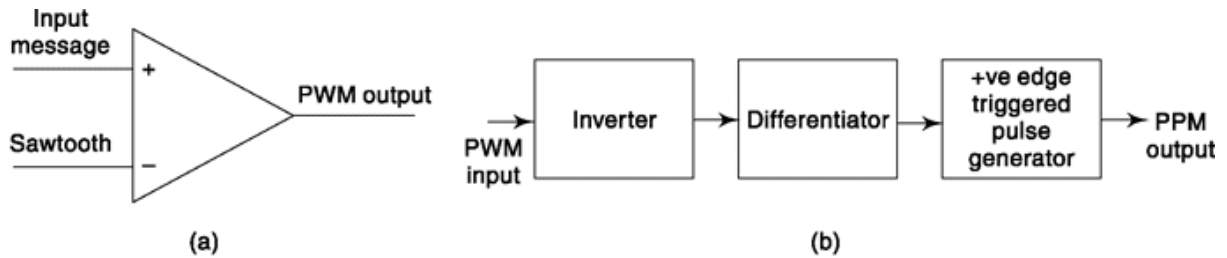


Fig. 4.17 (a) PWM generation by a comparator, (b) PPM generation from PWM.

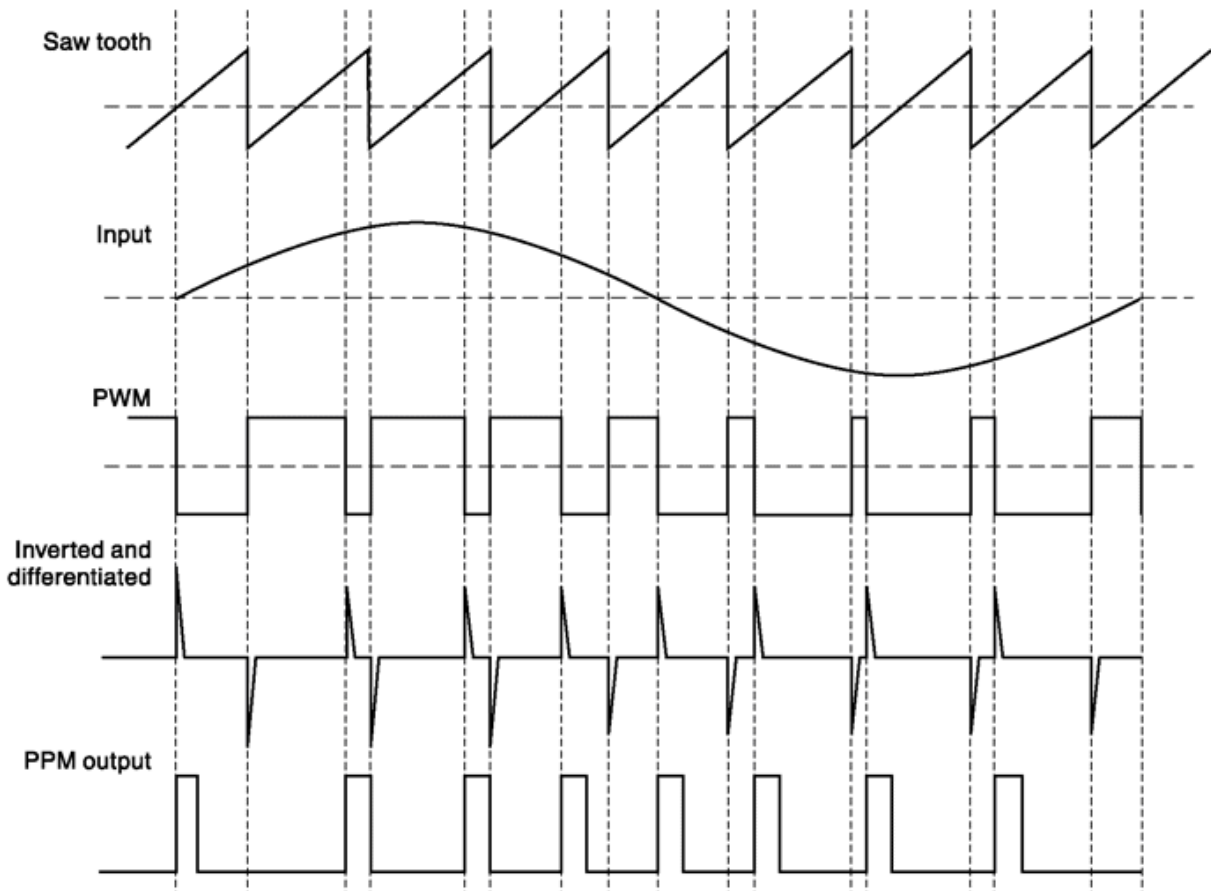


Fig. 4.18 Principle of PWM and PPM generation.

The method we discussed just now is known as *direct method*. The other direct method uses addition of message signal with sawtooth-like signal(slope in other direction, i.e. the signal first shows

a step and then linear fall) and setting a comparator level in such a manner that it always cuts in that triangular region once in every cycle. In *indirect method*, a PAM signal from input message is generated to which this sawtooth-like signal is added and then comparator does the slicing action in a similar way. The more the message amplitude, the cut is more towards the base of the triangle, the more is the pulse width and vice versa.

Note that, IC710 can be used as comparator. The inverter-differentiator block of Fig. 4.176 can be designed together using an op-amp and RC components. The fixed width pulse generator can be a monoshot device like IC74121, IC555, etc. A suitable arrangement of IC555 with RC differentiator can generate PWM signal and for a different arrangement, the PPM modulator.

Before we go to demodulation, can we find a simple technique to convert PPM signal to PWM? We have done the reverse in Fig. 4.17. Look at the simple arrangement shown in Fig. 4.19. The SR edge triggered Flip-Flop is set by +ve edge of the clock. It remains set so that output Q is high, till a +ve edge from PPM resets it. The more the delay in arrival, the longer the duration Q remains high. It is again set in the next clock period by the rising edge of the clock pulse. Thus the output of the Flip-Flop is a train of pulses, the width of which is decided by how late PPM pulses arrive in a particular clock period in which again the message information is contained. Thus we get a PWM output at the flip-flop output, the width of which in each cycle is proportional to the amplitude of

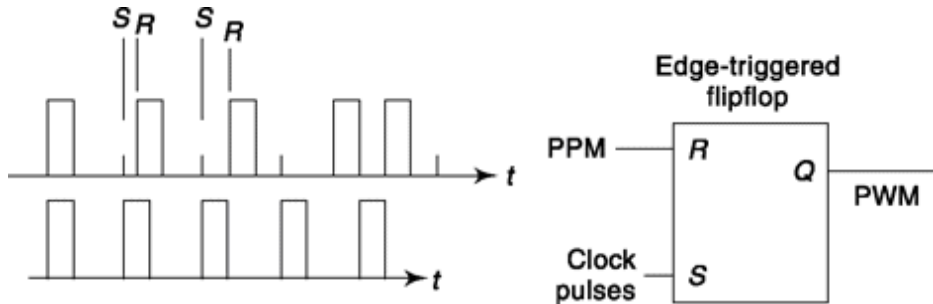


Fig. 4.19 PWM from PPM. the message signal.

Now let us discuss *demodulation* of PWM and PPM. For PWM demodulation, we would like to start a ramp at the positive edge and stop it when the negative edge comes. Since, the widths are different these ramps will reach different heights in each cycle which is directly proportional to pulse width and in turn the amplitude of the modulating message. This when passed through a low pass filter will follow the envelop, i.e. the message signal and the demodulation is done. Refer to Example 4.4. In PPM demodulation, a similar scheme is employed but now the ramp starts at one positive edge of the pulse and stops at the positive edge of the next pulse. Thus the delay between the pulses decides the height of the ramp generated and in turn closely follows the modulating message amplitude. A low-pass filter after that filters out the envelop information as demodulated signal.

Transistor and RC combinations can be used both for ramp generation and filtering to implement a demodulator circuit.

Note that, if synchronous clock is available then PPM can be converted to PWM (Fig. 4.19) and then PWM demodulator can be used to get the message signal back. Between PWM and PPM, the latter gives better performance in a noisy system.

Example 4.4

Figure 4.20 shows a PAM-TDM representation. (a) If each pulse is of width 150 ms, find the guard time. (b) If same guard time is maintained and we want to transmit 10 PAM messages time multiplexed how narrow the pulses should be?

Solution

One cycle is of period, $T = 1 \text{ ms} = 1000 \mu\text{s}$

- (a) Since, there are 5 messages multiplexed each utilizes $1000/5 = 200 \mu\text{s}$
Guard time = Allocated time-pulse width = $200 - 150 = 50 \mu\text{s}$.
- (b) For 10 messages multiplexed in $1000 \mu\text{s}$, time allocated for each = $1000/10 = 100 \mu\text{s}$.
If same guard time is to be maintained we require narrower pulses of width = $100 - 50 = 50 \mu\text{s}$

Example 4.5

Show that, PWM demodulation can be achieved by simple time averaging of PWM pulses by an averaging low pass filter.

Solution

If $x(t)$ is the modulated signal, the width, $W(t)$ of which in each cycle of time period T is proportional to message $m(t)$, then time averaged output of $x(t)$ can be written as,

$$\begin{aligned}
x_{av}(t) &= \frac{1}{T} \int_0^T x(t) dt \\
&= \frac{1}{T} \int_0^{W(t)} x_{HIGH}(t) dt + \frac{1}{T} \int_{W(t)}^T x_{LOW}(t) dt \\
&= \frac{1}{T} \int_0^{W(t)} 1 \cdot dt + \frac{1}{T} \int_{W(t)}^T 0 \cdot dt = \frac{W(t)}{T}
\end{aligned}$$

Thus, $x_{av}(t)$ is directly proportional to $W(t)$ and hence modulating signal $m(t)$.

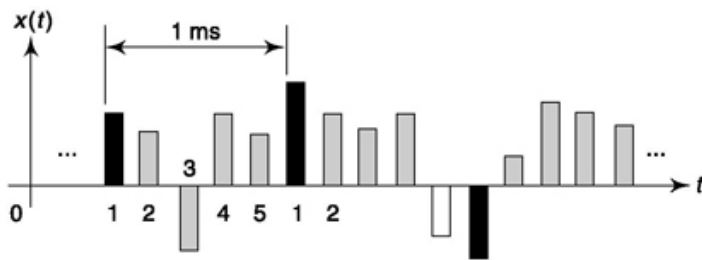


Fig. 4.20 A PAM-TDM system for Example 4.4.

SELF-TEST QUESTION

5. Instantaneous sampling is not preferred as the sample energy becomes too low which makes it susceptible to noise. Is that correct?
6. Crosstalk can be suppressed but not avoided with samples of finite duration. Is that true?
7. Which of these two approximates equalizer transfer function, $x/\sin x$ or $\sin x/x$?
8. Is PPM signal related to differentiation of PWM or the reverse?

4.4 DIGITAL REPRESENTATION OF ANALOG SIGNAL

We return to our journey towards complete digital representation of analog signal. We have already gone through an important step of sampling the time axis, i.e. discrete-time representation of analog signal. Now we need to discretize the amplitude axis and then represent that signal in terms of binary digits to complete the process.

4.4.1 Quantization of signals

The limitation of the system we have been describing for communicating over long channels is that once noise has been introduced at any place along

the channel, we are “stuck” with it. We now describe how the situation is modified by subjecting a signal to the operation of quantization. When quantizing a signal $m(t)$, we create a new signal $m_q(t)$ which is an approximation to $m(t)$. However, the quantized signal $m_q(t)$ has the great merit that it is, in large measure, separable from the additive noise.

The operation of quantization is represented in Fig. 4.21. Here we contemplate a signal $m(t)$ whose excursion is confined to the range from V_L to V_H . We have divided this total range into M equal intervals each of size S . Accordingly S , called the *step size*, is $S = (V_H - V_L)/M$. In Fig. 4.21 we show the specific example in which $M = 8$. In the center of each of these steps we locate *quantization levels* m_0, m_1, \dots, m_7 . The quantized signal $m_q(t)$ is generated in the following way: Whenever $m(t)$ is in the range A_0 , the signal $m_q(t)$ maintains the constant level m_0 ; whenever $m(t)$ is in the range A_j , $m_q(t)$ maintains the constant level m_j ; and so on. Thus the signal $m_q(t)$ will at all times be found at one of the levels m_0, m_1, \dots, m_7 . The transition in $m_q(t)$ from $m_q(t) = m_0$ to $m_q(t) = m_1$ is made abruptly when $m(t)$ passes the transition level L_{01} which is midway between m_0 and m_1 and so on. To state the matter in an alternative fashion, we say that, at every instant of time, $m_q(t)$ has the value of the quantization level to which $m(t)$ is closest. Thus the signal $m_q(t)$ does not change at all with time or it makes a “quantum” jump of step size S . Note the disposition of the quantization levels in the range from V_L to V_H . These levels are each separated by an amount S , but the separation of the extremes V_L and V_H each from its nearest quantization level is only $S/2$. Also, at every instant of time, the quantization error $m(t) - m_q(t)$ has a magnitude which is equal to or less than $S/2$.

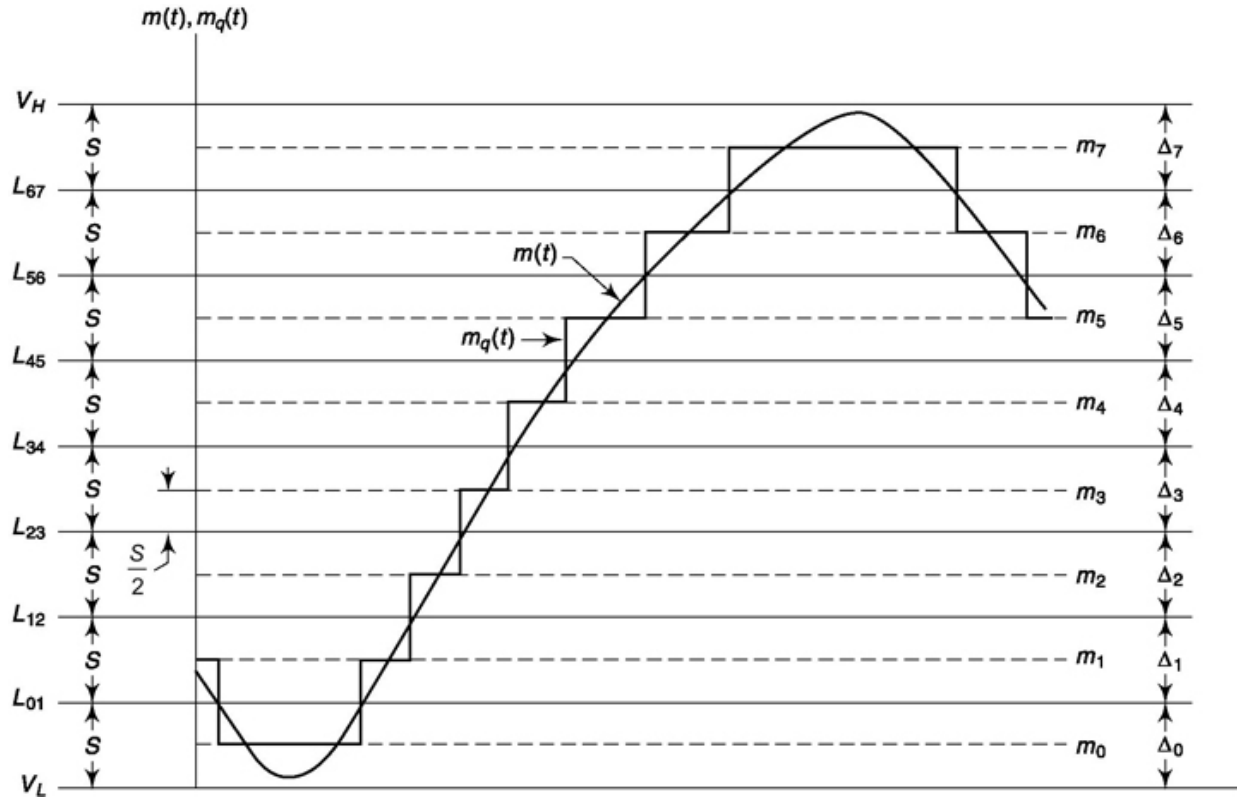


Fig. 4.21 The operation of quantization.

We see, therefore, that the quantized signal is an approximation to the original signal. The quality of the approximation may be improved by reducing the size of the steps, thereby increasing the number of allowable levels. Eventually, with small enough steps, the human ear or the eye will not be able to distinguish the original from the quantized signal. To give the reader an idea of the number of quantization levels required in a practical system, we note that 256 levels can be used to obtain the quality of commercial color TV, while 64 levels gives only fairly good color TV performance. These results are also found to be valid when quantizing voice.

Now let us consider that our quantized signal has arrived at a repeater somewhat attenuated and corrupted by noise. This time our repeater consists of a quantizer and an amplifier. There is noise superimposed on the quantized levels of $m_q(t)$. But suppose that we have placed the repeater at a point on the communications channel where the instantaneous noise voltage is almost always less than half the separation between quantized levels. Then the output of the quantizer will consist of a succession of levels duplicating the original quantized signal and *with the noise removed*. In rare instances the noise results in an error in quantization level. A noisy quantized signal is shown in Fig. 4.22a. The allowable quantizer output levels are indicated by

the dashed lines separated by amount S . The output of the quantizer is shown in Fig. 4.22b. The quantizer output is the level to which the input is closest. Therefore, as long as the noise has an instantaneous amplitude less than $S/2$, the noise will not appear at the output. One instance in which the noise does exceed $S/2$ is indicated in the figure, and, correspondingly, an error in level does occur. The statistical nature of noise is such that even if the average noise magnitude is much less than $S/2$, there is always a finite probability that from time to time, the noise magnitude will exceed $S/2$. Note that it is never possible to suppress completely level errors such as the one indicated in Fig. 4.22.

We have shown that through the method of signal quantization, the effect of additive noise can be significantly reduced. By decreasing the spacing of the repeaters, we decrease the attenuation suffered by $m_q(t)$. This effectively decreases the relative noise power and hence decreases the probability P_q of an error in level. P_q can also be reduced by increasing the step size S . However, increasing S results in an increased discrepancy between the true signal $m(t)$ and the quantized signal $m_q(t)$. This difference $m(t) - m_q(t)$ can be regarded as noise and is called *quantization noise*. Hence, the received signal is not a perfect replica of the transmitted signal $m(t)$. The difference between them is due to errors caused by additive noise and quantization noise. These noises are discussed further in Chap. 12.

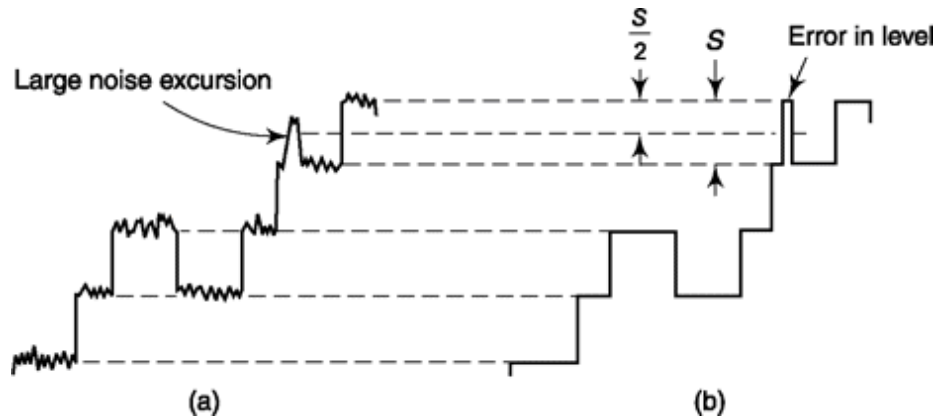


Fig. 4.22 (a) A quantized signal with added noise. (b) The signal after requantization. One instance is recorded in which the noise level is so large that an error results.

4.4.2 Quantization Error

It has been pointed out that the quantized signal and the original signal from which it was derived differ from one another in a random manner. This difference or error may be viewed as a noise due to the quantization process and is called *quantization error*. We now calculate the mean-square quantization error e^2 , where e is the difference between the original and quantized signal voltages.

Let us divide total peak-to-peak range of the message signal $m(t)$ into M equal voltage intervals, each of magnitude S volts. At the center of each voltage interval we locate a quantization level m_1, m_2, \dots, m_M as shown in Fig. 4.23a. The dashed level represents the instantaneous value of the message signal $m(t)$ at a time t . Since, in this figure, $m(t)$ happens to be closest to the level m_k , the quantizer output will be m_k , the voltage corresponding to that level. The error is $e = m(t) - m_k$.

Before calculating quantization error, let us develop a working level understanding of probability density function. Detailed analysis is postponed till Chapter 6 (Alternatively, you can come back to this discussion later, after studying Chapter 6). We have seen variation of $m(t)$ w.r.t. t in Fig. 4.21

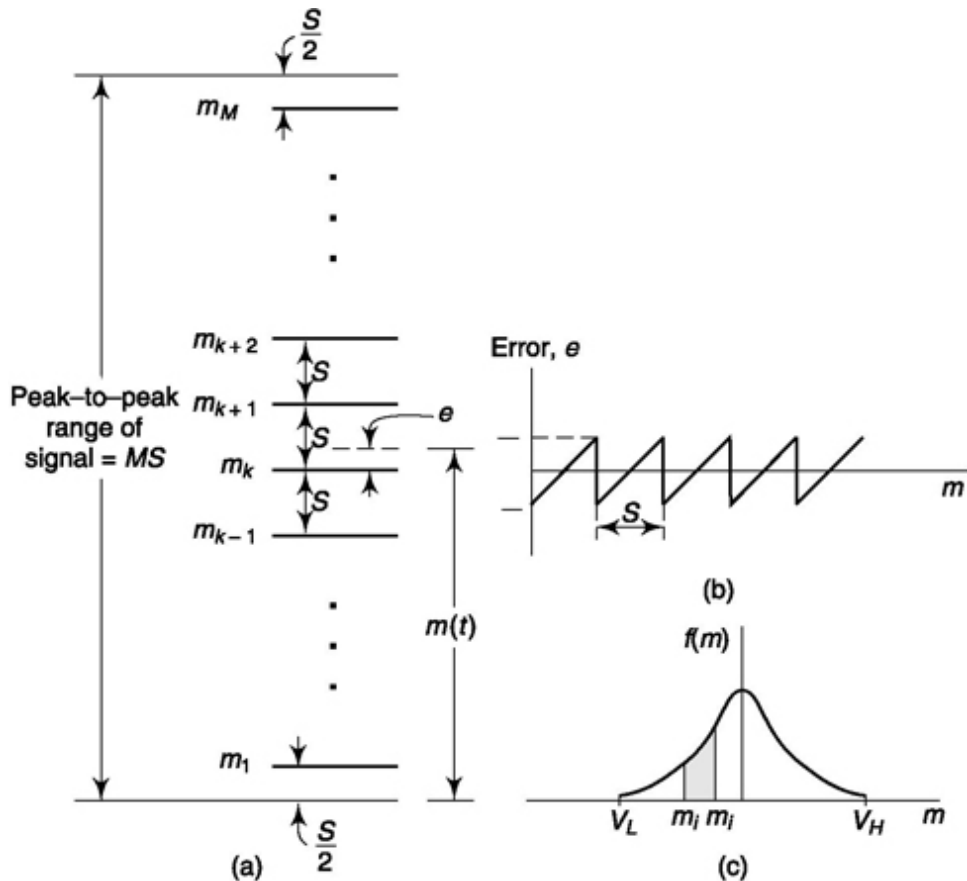


Fig. 4.23 (a) A range of voltage over which signal $m(t)$ makes excursions is divided into M quantization ranges each of size S . The quantization levels are located at the centre of the range. (b) The error voltage $e(t)$ as a function of the instantaneous value of the signal $m(t)$. (c) An arbitrary probability distribution function $f(m)$. The probability that $m(t)$ lies between m_t and m_j is given by the area of the shaded region.

where the independent variable that appears along X-axis is t and dependent variable that appears along γ -axis is magnitude m . In Fig. 4.23c, we draw magnitude m along X-axis as an independent variable and a function $f(m)$ related to relative occurrence or probability of $m(t)$ at a particular value of m along γ -axis which we term as probability density function (PDF). If $f(m_2) > f(m_1)$ then there is higher probability of $m(t)$ taking a value of m_2 than m_1 and vice versa. The relation between PDF and probability is that the probability of $m(t)$ lying between $m - dm/2$ to $m + dm/2$ is $f(m)dm$. Thus, the probability that $m(t)$ lies between m_t than m_j is given by the shaded area in Fig. 4.23c and defined as

$$P(m_i \leq m \leq m_j) = \int_{m_i}^{m_j} f(m) dm \quad (4.32)$$

Since the probability of $m(t)$ lying between $-\infty$ and $+\infty$ is 1, we can write

$$\int_{-\infty}^{\infty} f(m) dm = 1 \quad (4.33)$$

In this discussion, $m(t)$ lies between V_L and V_H for which $\int_{V_L}^{V_H} f(m) dm = 1$. Note that the shape of $f(m)$ depends on the nature of the signal and the most widely discussed is the Gaussian shape that we shall take up in Chapter 6. If the probability density is uniform over all possible values then the shape of PDF will be flat in the given range. From Eq. (4.33), in this particular case for uniform PDF $f(m) = 1/(V_H - V_L)$.

Let us come back to the discussion on calculation of quantization error. We are now in a position to define mean-square *quantization error* as

$$\overline{e^2} = \int_{m_1-S/2}^{m_1+S/2} f(m)(m - m_1)^2 dm + \int_{m_2-S/2}^{m_2+S/2} f(m)(m - m_2)^2 dm + \dots \quad (4.34)$$

Now, ordinarily the probability density function $f(m)$ of the message signal $m(t)$ will certainly not be constant. However, suppose that the number M of quantization is large, so that the step size S is small in comparison with the peak-to-peak range of the message signal. In this case, it is certainly reasonable to make the approximation that $f(m)$ is constant within each quantization range. Then in the first term of Eq. (4.34) we set $f(m) = f^{(1)}$, a constant. In the second term $f(m) = f^{(2)}$, etc. We may now remove $f^{(1)}, f^{(2)}$, etc., from inside the integral sign. If we make the substitution $x \equiv m - m_k$, Eq. (4.24) becomes

$$\overline{e^2} = (f^{(1)} + f^{(2)} + \dots) \int_{-S/2}^{S/2} x^2 dx = (f^{(1)} + f^{(2)} + \dots) \frac{S^3}{12} \quad (4.35a)$$

$$= (f^{(1)}S + f^{(2)}S + \dots) \frac{S^2}{12} \quad (4.35b)$$

Now $f^{(1)}S$ is the probability that the signal voltage $m(t)$ will be in the first quantization range, $f^{(2)}S$ is the probability that m is in the second quantization range, etc. Hence the sum of terms in the parentheses in Eq. (4.35b) has a total value of unity. Therefore, the mean-square quantization error is

$$\overline{e^2} = \frac{S^2}{12} \quad (4.36)$$

4.4.3 Pulse Code Modulation (PCM)

A signal which is to be quantized prior to transmission is usually sampled as well. The quantization is used to reduce the effects of noise, and the sampling allows us to time-division multiplex a number of messages if we choose to do so. The combined operations of sampling and quantizing generate a quantized PAM waveform, that is, a train of pulses whose amplitudes are restricted to a number of discrete magnitudes.

We may, if we choose, transmit these quantized sample values directly. Alternatively we may represent each quantized level by a code number and transmit the code number rather than the sample value itself. The merit of doing so will be developed in the subsequent discussion. Most frequently the code number is converted, before transmission, into its representation in

binary arithmetic, i.e. base-2 arithmetic. The digits of the binary representation of the code number are transmitted as pulses. Hence the system of transmission is called (binary) *pulse-code modulation* (PCM).

We review briefly some elementary points about binary arithmetic. The binary system uses only two digits, 0 and 1. An arbitrary number N is represented by the sequence... $k_2k_xk_0$, in which the k 's are determined from the equation

$$N = \dots + k_2 2^2 + k_1 2^1 + k_0 2^0 \quad (4.37)$$

with the added constraint that each k has the value 0 or 1. The binary representations of the decimal numbers 0 to 15 are given in Table 4.1. Observe that to represent the four (decimal) numbers 0 to 3, we need only two binary digits k_1 and k_0 . For the eight (decimal) numbers from 0 to 7 we require only three binary places, and so on. In general, if M numbers 0, 1, ..., $M - 1$ are to be represented, then an N binary digit sequence $k_{N-1} \dots k_0$ is required, where $M = 2^N$.

Table 4.1 Equivalent Numbers in Decimal and Binary Representation

<i>Binary</i>				<i>Decimal</i>
k_3	k_2	k_1	k_0	
0	0	0	0	0
0	0	0	1	1
0	0	1	0	2
0	0	1	1	3
0	1	0	0	4
0	1	0	1	5
0	1	1	0	6
0	1	1	1	7
1	0	0	0	8
1	0	0	1	9
1	0	1	0	10
1	0	1	1	11
1	1	0	0	12
1	1	0	1	13
1	1	1	0	14
1	1	1	1	15

The essential features of binary PCM are shown in Fig. 4.1. We assume that the analog message signal $m(t)$ is limited in its excursions to the range from -4 to +4 volts. We have set the step size between quantization levels at 1 volt. Eight quantization levels are employed, and these are located at -3.5, -2.5, ..., +3.5 volts. We assign the code number 0 to the level at -3.5 volts, the code number 1 to the level at -2.5 volts, etc., until the level at +3.5 volts, which is assigned the code number 7. Each code number has its representation in binary arithmetic ranging from 000 for code number 0 to 111 for code number 7.

In Fig. 4.24, in correspondence with each sample, we specify the sample value, the nearest quantization level, and the code number and its binary representation. If we were transmitting the analog signal, we would transmit the sample values 1.3, 3.6, 2.3, etc. If we were transmitting the quantized signal, we would transmit the quantized sample values 1.5, 3.5, 2.5, etc. In binary PCM we transmit the binary representations 101, 111, 110, etc.

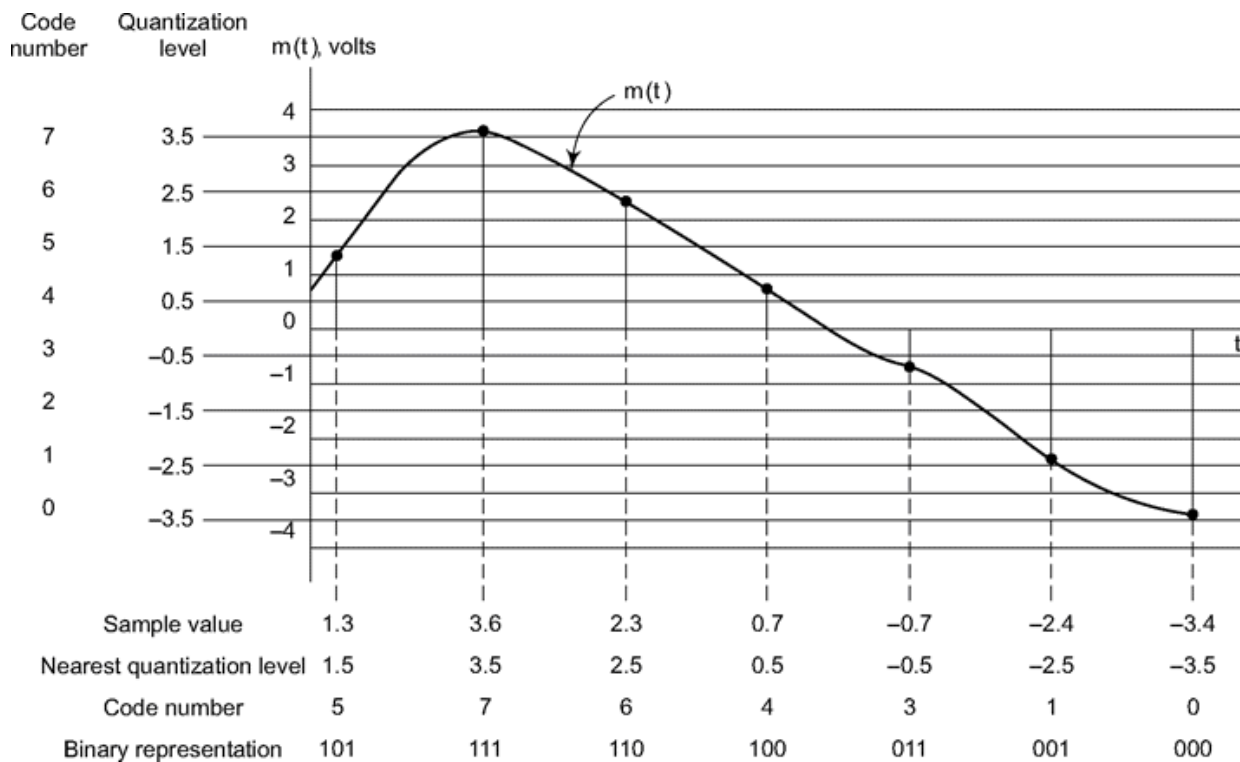


Fig. 4.24 A message signal is regularly sampled. Quantization levels are indicated. For each sample the quantized value is given and its binary representation is indicated.

4.4.4 Electrical Representation of Binary Digits

As intimated in the previous section, we may represent the binary digits by electrical pulses in order to transmit the code representations of each

quantized level over a communication channel. Such a representation is shown in Fig. 4.25. Pulse time slots are indicated at the top of the figure, and, as shown in Fig. 4.25a, the binary digit 1 is represented by a pulse, while the binary digit 0 is represented by the absence of a pulse. The row of three-digit binary numbers given in Fig. 4.25 is the binary representation of the sequence of quantized samples in Fig. 4.24. Hence the pulse pattern

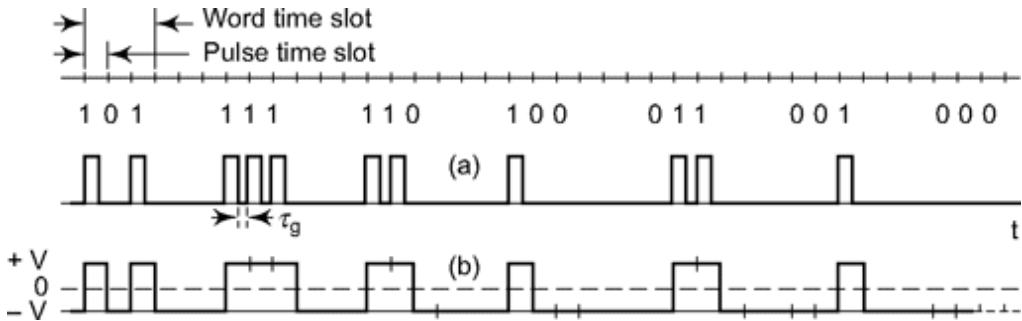


Fig. 4.25 (a) Pulse representation of the binary numbers used to code the samples in Fig. 4.24. (b) Representation by voltage levels rather than pulses.

in Fig. 4.25a is the (binary) PCM waveform that would be transmitted to convey to the receiver the sequence of quantized samples of the message signal $m(t)$ in Fig. 4.24. Each three-digit binary number that specifies a quantized sample value is called a *word*. The spaces between words allow for the multiplexing of other messages.

At the receiver, in order to reconstruct the quantized signal, all that is required is that a determination be made, within each pulse time slot, about whether a pulse is present or absent. The exact amplitude of the pulse is not important. There is an advantage in making the pulse width as wide as possible since the pulse energy is thereby increased and it becomes easier to recognize a pulse against the background noise. Suppose then that we eliminate the guard time t_g between pulses. We would then have the waveform shown in Fig. 4.25a. We would be rather hard put to describe this waveform as either a sequence of positive pulses or of negative pulses. The waveform consists now of a sequence of transitions between two levels. When the waveform occupies the lower level in a particular time slot, a binary 0 is represented, while the upper voltage level represents a binary 1.

Suppose that the voltage difference of $2V$ volts between the levels of the waveform of Fig. 4.25b is adequate to allow reliable determination at the receiver of which digit is being transmitted. We might then arrange, say, that the waveform make excursions between 0 and 2 V volts or between $-V$ volts

and $+V$ volts. The former waveform will have a dc component, the latter waveform will not. Since the dc component wastes power and contributes nothing to the reliability of transmission, the latter alternative is preferred and is indicated in Fig. 4.256.

We shall discuss other electrical representation in Section 4.5.1 when we discuss line coding.

4.4.5 The PCM System

The Encoder

A PCM communication system is represented in Fig. 4.26. The analog signal $m(t)$ is sampled, and these samples are subjected to the operation of quantization. The quantized samples are applied to an *encoder*. The encoder responds to each such sample by the generation of a unique and identifiable binary pulse (or binary level) pattern. In the example of Figs 4.24 and 4.25 the pulse pattern happens to have a numerical significance which is the same as the order assigned to the quantized levels. However, this feature is not essential. We could have assigned any pulse pattern to any level. At the receiver, however, we must be able to identify the level from the pulse pattern. Hence it is clear that not only does the encoder number the level, it also assigns to it an identification code.

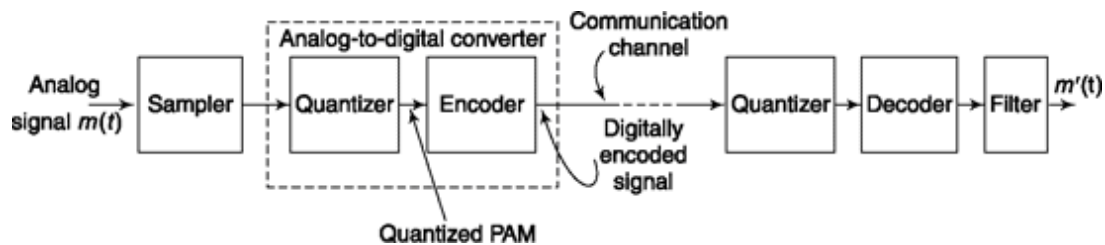


Fig. 4.26 A PCM communication system.

The combination of the quantizer and encoder in the dashed box of Fig. 4.26 is called an *analog-to-digital converter*, usually abbreviated A/D converter. In commercially available A/D converters there is normally no sharp distinction between that portion of the electronic circuitry used to do the quantizing and that portion used to accomplish the encoding. In summary, then, the A/D converter accepts an analog signal and replaces it with a succession of *code symbols*, each symbol consisting of a train of pulses in which each pulse may be interpreted as the representation of a *digit*.

in an arithmetic system. Thus the signal transmitted over the communications channel in a PCM system is referred to as a digitally encoded signal.

The Decoder

When the digitally encoded signal arrives at the receiver (or repeater), the first operation to be performed is the separation of the signal from the noise which has been added during the transmission along the channel. As noted previously, separation of the signal from the noise is possible because of the quantization of the signal. Such an operation is again an operation of *requantization*; hence the first block in the receiver in Fig. 4.26 is termed a quantizer. A feature which eases the burden on this quantizer is that for each pulse interval it has only to make the relatively simple decision of whether a pulse has or has not been received or which of the two voltage levels has occurred. Suppose the quantized sample pulses had been transmitted instead, rather than the binary-encoded codes for such samples. Then this quantizer would have yielded, in each pulse interval, not a simple yes or no decision, but rather a more complicated determination about which of the many possible levels had been received. In the example of Fig. 4.25, if a quantized PAM signal had been transmitted, the receiver quantizer would have to decide which of the levels 0 to 7 was transmitted, while with a binary PCM signal the quantizer only distinguish between two possible levels. The relative reliability of the yes or no decision in PCM over the multivalued decision required for quantized PAM constitutes an important advantage for PCM.

The receiver quantizer then, in each pulse slot, makes an educated and sophisticated estimate and then decides whether a positive pulse or a negative pulse was received and transmits its decisions, in the form of a reconstituted or regenerated pulse train, to the decoder. (If repeater operation is intended, the regenerated pulse train is simply raised in level and sent along the next section of the transmission channel.) The decoder, also called a *digital-to-analog (D/A) converter*, performs the inverse operation of the encoder. The decoder output is the sequence of quantized multilevel sample pulses. The quantized PAM signal is now reconstituted. It is then filtered to reject any frequency components lying outside of the baseband. The final output signal $m'(t)$ is identical with the input $m(t)$ except for quantization

noise and the occasional error in yes-no decision making at the receiver due to the presence of channel noise.

4.4.6 Companding

Referring again to Figs 4.21 and 4.23 let us consider that we have established a quantization process employing M levels with step size S , the levels being established at voltages to accommodate a signal $m(t)$ which ranges from a low voltage V_L to a high voltage V_H . We can readily see that if the signal $m(t)$ should make excursions beyond the bounds V_H and V_L the system will operate at a disadvantage. For, within these bounds, the instantaneous quantization error never exceeds $\pm S/2$ while outside these bounds the error is larger.

Further, whenever $m(t)$ does not swing through the full available range the system is equally at a disadvantage. For, in order that $m_q(t)$ be a good approximation to $m(t)$ it is necessary that the step size S be small in comparison to the *range over which $m(t)$ swings*. As a very pointed example of this consideration consider a case in which $m(t)$ has a peak-to-peak voltage which is less than S and never crosses one of the transition levels in Fig. 4.21. In such a case $m_q(t)$ will be a fixed (dc) voltage and will bear no relationship to $m(t)$.

To explore this latter point somewhat more quantitatively, let us consider that $m(t)$ is a signal, such as the sound signal output of a microphone, in which $V_H = -V_L = V$, i.e. a signal without dc components, and with (at least approximately) equal positive and negative peaks. Further, for simplicity, let us assume that in the range $\pm V$ the signal $m(t)$ is characterized by a uniform probability density. The probability density is then equal to $1/2V$ and the normalized average signal power of the applied input signal is

$$S_i = \overline{m^2(t)} = \int_{-V}^{+V} m^2(t) \frac{1}{2V} dm = \frac{V^2}{3} \quad (4.38)$$

The quantization noise, as given by Eq. (4.36) is

$$N_Q = \frac{S^2}{12} \quad (4.39)$$

If the number of quantization levels is M , then $MS = 2V$ so that

$$V = \frac{MS}{2} \quad (4.40)$$

Combining Eqs (4.38), (4.39) and (4.40) we have that the input signal-to-quantization noise power ratio is

$$\frac{S_i}{N_Q} = M^2 \quad (4.41)$$

Eventually, the received quantized signal will be smoothed out to generate an output signal with power S_o . If we have a useful communication system then presumably the effect of the quantization noise is not such as to cause an easily perceived difference between input and output signal. In such a case the output power S_o may be taken to be the same as the input power, i.e. $S_o \approx S_i$ so that finally we may replace Eq. (4.41) by

$$\frac{S_o}{N_Q} = M^2 \quad (4.42)$$

If there are M quantization levels then the code which singles out the closest quantization to the signal $m(t)$ will have to have N bits with $M = 2^N$. Hence, Eq. (4.42) becomes

$$\frac{S_o}{N_Q} = (2^N)^2 = 2^{2N} \quad (4.43)$$

In decibels we have

$$\left[\frac{S_o}{N_Q} \right]_{\text{dB}} = 10 \log_{10} \left[\frac{S_o}{N_Q} \right] = 10 \log_{10} 2^{2N} = 6N \quad (4.44)$$

Equation (4.44) has the interpretation that, in a system where the signal is quantized using an N -bit code (i.e. the number of quantization levels is 2^N), and where the signal amplitude is capable of swinging through all available quantization regions without extending beyond the outermost ranges, the output *signal-to-quantization noise ratio* is $6N$ dB. In voice communication we use $N = 8$ corresponding to 256 quantization regions and $S/N_q = (6)(8) = 48$ dB. If the signal is reduced in amplitude so that not all quantization ranges are used then S_o/N_Q becomes smaller, since N_Q , depending as it does only on step S is not affected by the amplitude reduction, while S_o is reduced. For example, if the amplitude were reduced by a factor of 2, the power is then reduced by a factor of 4 reducing the signal-to-noise ratio by 6

dB. It is interesting to observe that the effective number of quantization levels is also reduced by a factor of 2. Correspondingly, the number N of code bits is reduced by 1. In summary, the dependence of $SJNq$ on the input signal power S_t is such that as the number of code bits needed decreases, S_o/Nq decreases by 6 dB/bit.

It is generally required, for acceptable voice transmission, that the received signal have a ratio $SJNq$ not less than 30 dB, and that this minimum 30 dB figure hold even though the signal power itself may vary by 40 dB. (The signal, in this case, is described as having a 40 dB *dynamic range*.) In an 8-bit system, at maximum signal level we have $S_o/Nq @ S/Nq = 48$ dB. Now Nq is fixed, and depends only on step size. If we are to allow S/Nq to drop to no lower than 30 dB then the dynamic range would be restricted to $48 - 30 = 18$ dB.

The dynamic range can be materially improved by a process called *companding* (a word formed by combining the words *compressing* and *expanding*). As we have seen, to keep the signal-to-quantization noise ratio high we must use a signal which swings through a range which is large in comparison with the step size. This requirement is not satisfied when the signal is small. Accordingly before applying the signal to the quantizer we pass it through a network which has an input-output characteristic as shown in Fig. 4.27. Note that at low amplitudes the slope is larger than at large amplitudes. A signal transmitted through such a network will have the extremities of its waveform *compressed*. The peak signal which the system is intended to accommodate will, as before, range through all available quantization regions. But now, a small amplitude signal will range through *more* quantization regions than would be the case in the absence of compression. Of course, the compression produces signal distortion. To undo the distortion, at the receiver we pass the recovered signal through an *expander* network. An expander network has an input-output characteristic which is the inverse of the characteristic of the compressor. The inverse distortions of compressor and expander generate a final output signal without distortion.

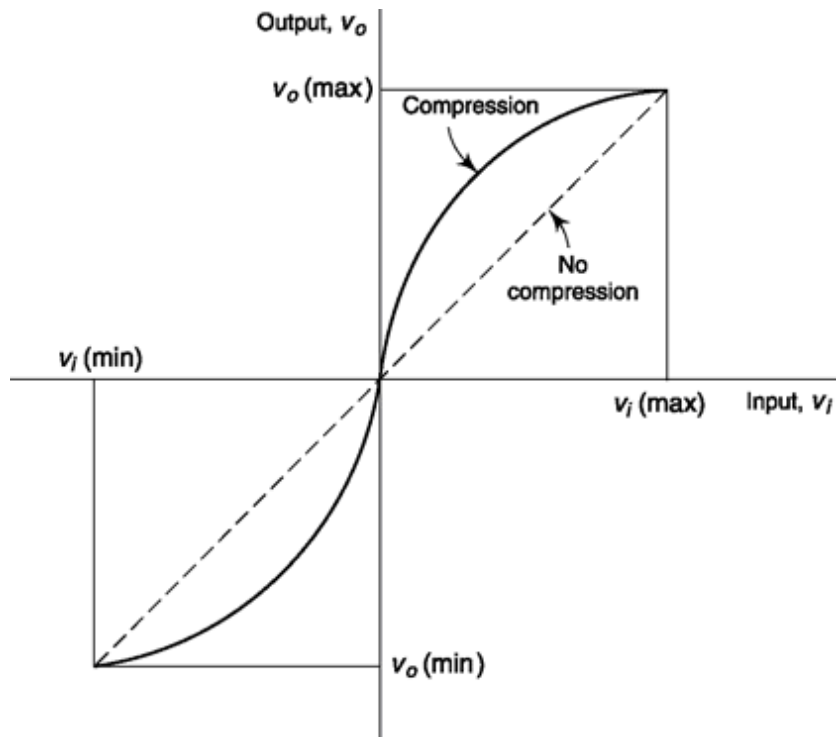


Fig. 4.27 An input-output characteristic which provides compression.

The determination of the form of the compression plot of Fig. 4.27 is a somewhat subjective matter. In the United States, Canada and Japan, a *m-law* compandor is used (see Example 4.7) and it differs somewhat from the *A-law* compander (see Prob. 4.29) used by the rest of the world. The “I” and the “A” refer to parameters which appear in the equations for the compression and expansion characteristic.

In implementing the compression characteristic, the analog signal $m(t)$ is left unmodified and, instead, the step size is tapered so that the quantization levels are close together at low signal amplitudes and progressively further apart in regions attained as the signal increases in amplitude. To see one way in which the step sizes are altered consider again an 8-bit PCM system employing $2^8 = 256$ quantization levels. In such a system, the A/D converter shown in Fig. 4.26 would ordinarily be an 8-bit converter. Each input sample would generate an 8-bit output code identifying the closest quantization level. If the total range of the input was $\pm V$ then the step size would be $S = 2V/2^8$. Let us start however with a 12-bit A/D converter so that the step size is $2 V/2^{12}$. This 12-bit PCM signal is not applied to the communication channel directly but is instead applied to the address pins of a read-only memory (ROM) whose content is to be described. The ROM has 12 address

pins and 8 output data pins. The signal transmitted is the 8-bit data output of the ROM.

The content of the ROM is as follows: As shown in Fig. 4.28, in each successive memory location in the region where the step size is to be smallest (i.e. step size = $2V/2^{12} = A$), there are written successive 8-bit code words. Hence in this region a change in analog signal of step size A will change the code word presented for transmission by the amount A. This one-to-one correspondence between addresses and transmitted code applies as shown for the middle 64 addresses. For the next 64 addresses (32 on one side and 32 on the other side of the original 64), we arrange that at the memory locations specified by pairs of addresses, i.e. for two adjacent addresses the *same* code word

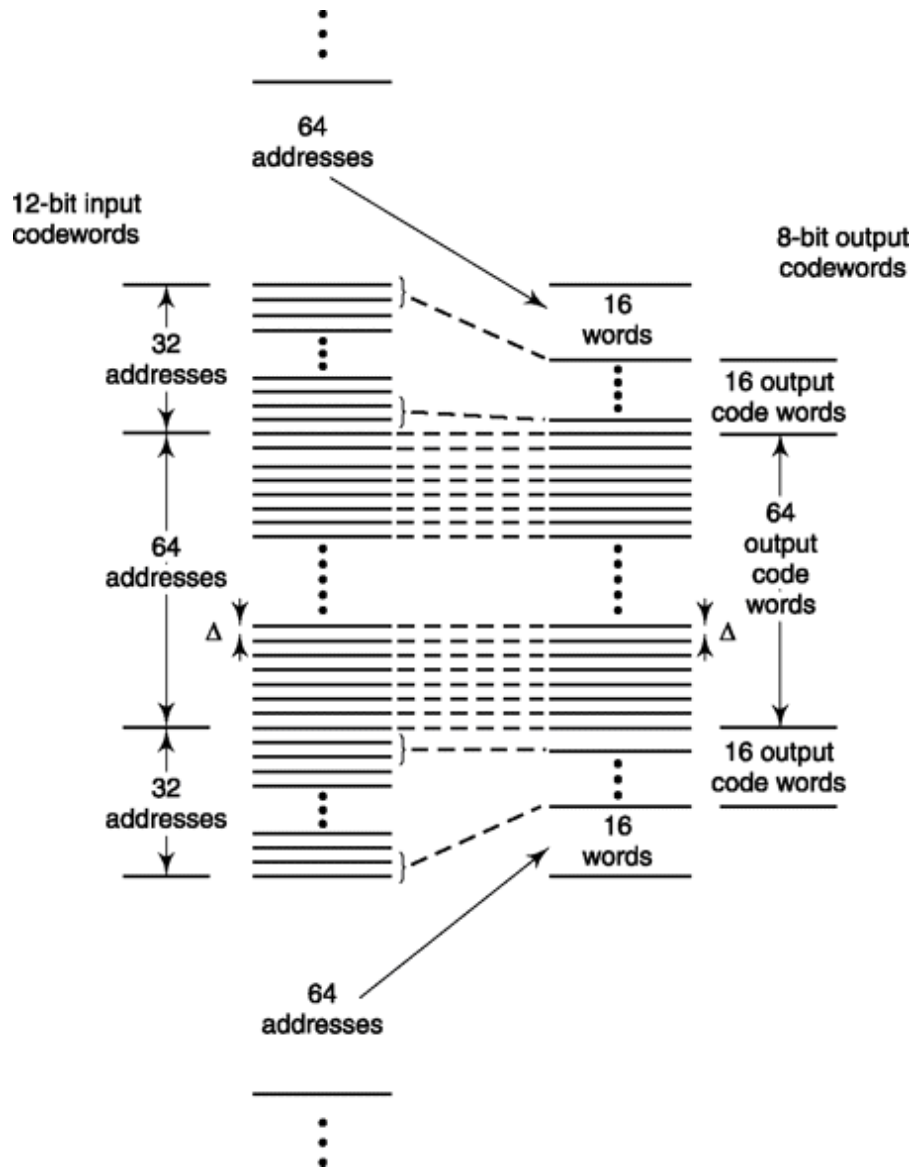


Fig. 4.28 ROM characteristic for compression.

is written into the memory. Hence, the transmitted code word will change at every *second* addresses change and correspondingly the step size is 2D. Next we arrange that for the next 128 addresses (64 above + 64 below) the *same* code word is written into the locations of *four* successive memory locations so that the step size is 4D. We proceed in this manner, each time doubling the number of successive memory locations which contain the same code word. As can be verified, when we have used all $2^{12} = 4096$ addresses we shall have generated $2^8 = 256$ code words. At the receiver we have a mechanism for generating the quantization corresponding to each code word.

It is interesting to observe that for the smallest 64 levels, the input and output signals are the same, i.e. small signals are *not* companded. One reason for this is that signals other than voice are often digitized using the same PCM system employed for voice. If a nonvoice signal is subjected to the compression algorithm the result is usually a degradation of performance. Therefore, to avoid this possibility, such non-voice signals are kept 40 dB below the peak level of a voice signal.

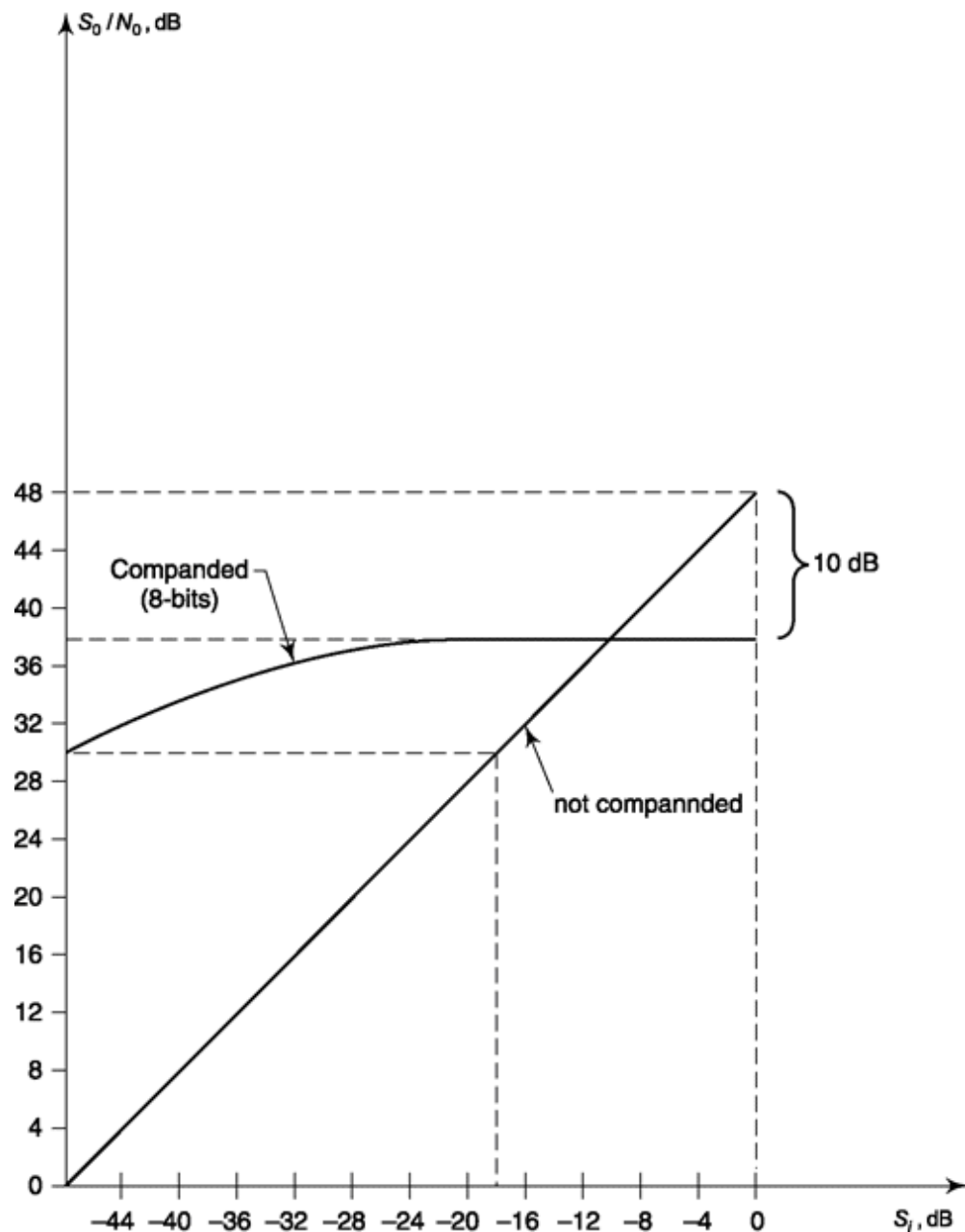


Fig. 4.29 Comparison of companded and uncompanded systems.

In conclusion, we refer to Fig. 4.29 which compares the variation of output signal-to-noise ratio as a function of input signal power when companding is used, to the case of an uncompanded system. Note that the companded system has a far greater dynamic range than the uncompanded system and that theoretically the companded system has an output signal-to-noise ratio which exceeds 30 dB over a dynamic range of input signal power of 48 dB, while the uncompanded system has a dynamic range of 18 dB for the same conditions. It should be noted however, that the penalty paid using companding is approximately 10 dB. Thus, an 8-bit uncompanded system, when operating at maximum amplitude, produces a signal-to-noise ratio of 48 dB. The same 8-bit system, using a compandor, yields a 38 dB SNR.

Example 4.6

The discrete samples of an analog signal is to be uniformly quantized for PCM system. If the maximum value of the analog sample is to be represented within 0.1% accuracy, find the minimum number of binary digits required.

Solution

Let A be the maximum value of the discrete samples.

Error tolerated is 0.1%, i.e. $0.001A$. If Δ is the step size then possible maximum error = $\Delta/2$.

Thus, $\Delta/2 = 0.001A$ or, $A/\Delta = 1000/2 = 500$

Thus no. of levels required = 500.

Minimum no. of binary digits required =

$$(\log_2 500)_{\text{rounded to next higher integer}} = 9$$

Example 4.7

A μ -law compander is defined as $y = \pm \frac{\ln(1 + \mu|x|)}{\ln(1 + \mu)}$,

$|x| < 1$, where x is input and y is output. The +sign is

used when x is +ve and - sign is used when x is negative. If the peak of input is 10 V and no. of bits available for quantization are 8 then find the smallest and largest separation between levels. Consider $\mu = 255$.

Solution

The y axis is uniformly quantized with step size = $\frac{1}{2^8/2-1} = \frac{1}{127}$ in both +ve and -ve direction between ± 1 when peak of input varies between ± 1 . The smallest step in x direction occurs nearest to $x = 0$, i.e. between $y_1 = 0$ and $y_2 = \frac{1}{127}$

Then, $0 = \frac{\ln(1+255x_1)}{\ln(1+255)}$ or $x_1 = 0$ and

$$\frac{1}{127} = \frac{\ln(1+255x_2)}{\ln(1+255)} \text{ or } x_2 = 1.75 \times 10^{-4}$$

Thus, smallest step-size is $10 \times (x_2 - x_1) = 1.75 \times 10 - 3 = 1.75$ mV

The largest step size occurs when x is at its extreme between $y_1 = 1 - \frac{1}{127} = \frac{126}{127}$ and $y_2 = 1$

Again substituting, $\frac{126}{127} = \frac{\ln(1+255x_1)}{\ln(1+255)}$ or $x_1 = 0.957$

$$\text{and } 1 = \frac{\ln(1+255x_2)}{\ln(1+255)} \text{ or, } x_2 = 1$$

Thus, largest step-size is $10 \times (x_2 - x_1) = 0.43$ V

Note that, without compander for uniform quantization the step size is $10/127 = 0.079$ V.

SELF-TEST QUESTION

9. Is it true that reduction in step size reduces quantization error?
10. Can the reduction of repeater distance in digital communication keep error arbitrarily low?
11. Is it true that a reduction in amplitude of input signal by a factor of 2 reduces signal-to-quantization noise ratio by 6 dB in (-law companding)?
12. The distortion caused by compressor is removed by expander in companding scheme. Is that correct?

4.5 CERTAIN ISSUES IN DIGITAL TRANSMISSION

Having been able to code analog data into digital let us address some pertinent questions related to digital transmission. We'll return to discussion on other coding options in Sec. 4.6 which will use basic PCM coded data in a variety of ways with an aim to reduce bit rate and in turn bandwidth required. We start our discussion here with line coding and then address

issues like scrambling to improve timing recovery, followed by discussion of a practical PCM system.

4.5.1 line Coding

We know how to represent an analog data in binary, i.e. in terms of two symbols 0 and 1. But how do we assign electrical voltages to them that suits communication over an electrical line? This issue is addressed in line coding which looks into factors like (i) power and bandwidth required for transmission, (ii) ability to extract timing information, (iii) presence of low frequency or dc component which is unsuitable for ac coupled circuits, (iv) error monitoring ability, etc. Here, we make a comparative assessment of different line codes typically used in digital system. Figure 4.30 gives a compact presentation of these codes. We shall show how to find spectrum of line codes by taking up calculation of PSD of two different waveforms later in Section 6.5.4; in one there will be presence of dc component (Fig. 4.30c) and in the other, there will be no dc component (Fig. 4.30f).

Unipolar NRZ

This code is unipolar as logic 0 is represented by 0V and logic 1 by a constant signal level, say + V during its entire bit interval (T_0 where bit rate is $1/T_0$) and hence called non return to zero (NRZ). This is simple in the sense that it mimics the binary representation but has certain serious problems. Figure 4.30(a) describes its timing diagram, PSD and also the 3 dB bandwidth. It can be seen that this code has high dc as well as low frequency components. Network that limits low frequency passage makes this unusable when there is a long string of 1's. This is explained later taking bipolar NRZ as an example case. Note that long string of 1's and 0's also make clock recovery difficult and causes synchronization problem.

Unipolar RZ

This code is again unipolar as excursion is between 0V and + V. But logic 1 here is represented by a pulse which returns to zero (RZ) after a brief period (usually half bit period) within bit interval. Figure 4.30(6) describes its timing diagram and PSD. It can be seen that its dc component is lower

compared to unipolar NRZ. Also clock recovery can be better as it has significant energy at $1/T_0$.

Bipolar NRZ

This code is bipolar as excursion is between $+V$ and $-V$. But pulses don't return to zero and stays at that level for entire bit duration. Figure 4.30(c) describes its timing diagram and PSD. The PSD is similar to unipolar NRZ but has higher power budget. In presence of noise this performs better than unipolar as voltage excursion is more. We qualitatively discuss the effect of low frequency limiting for such signals when there is a long string of 1's present in the code (Fig. 4.31a). The low frequency network can be approximated by an RC circuit as shown in Fig. 4.31b and its output is plotted in Fig. 4.31c. The validity of this result can be seen by keeping in mind the following two considerations: (a) when the input is constant the output decays exponentially (with time constant RC) to zero volts; (b) when the output changes abruptly by amount $2V$ the output changes by an equal amount since an instantaneous change in the capacitor voltage is not possible.

We shall find that the most effective way of distinguishing, at the receiver, a 1 from a 0 is to measure the area under the received waveform during the time of a bit. A positive area indicates a 1, a negative area a 0. In Fig. 4.31 we show a case in which there is a long uninterrupted sequence of 1's. We observe that as the sequence persists and even for a time after the sequence ends, the area available to assure that a 1 has been transmitted is severely depressed. Of course, a corresponding difficulty results from a long string of 0's.

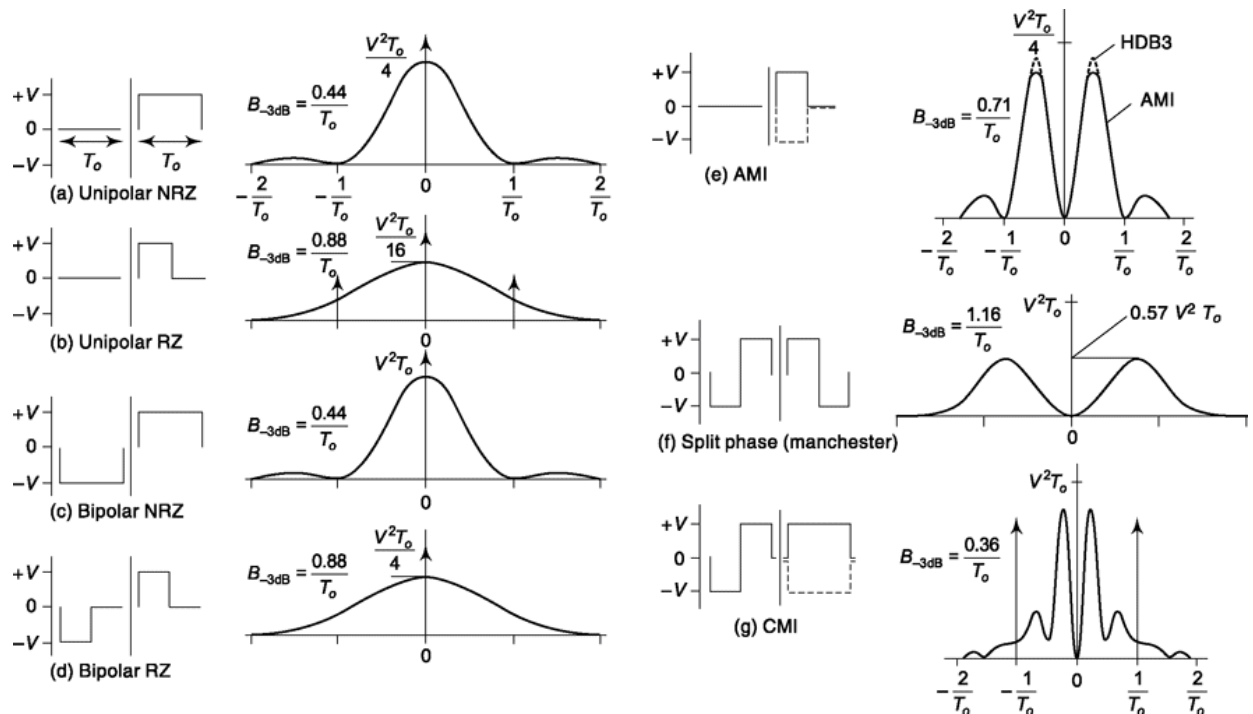


Fig. 4.30 Typical line codes and their PSD (a) Unipolar NRZ, (b) Unipolar RZ, (c) Bipolar NRZ, (d) Bipolar RZ, (e) Alternate Mark Inversion, (f) Biphase (Split phase) or Manchester coding, (g) Coded Mark Inversion.

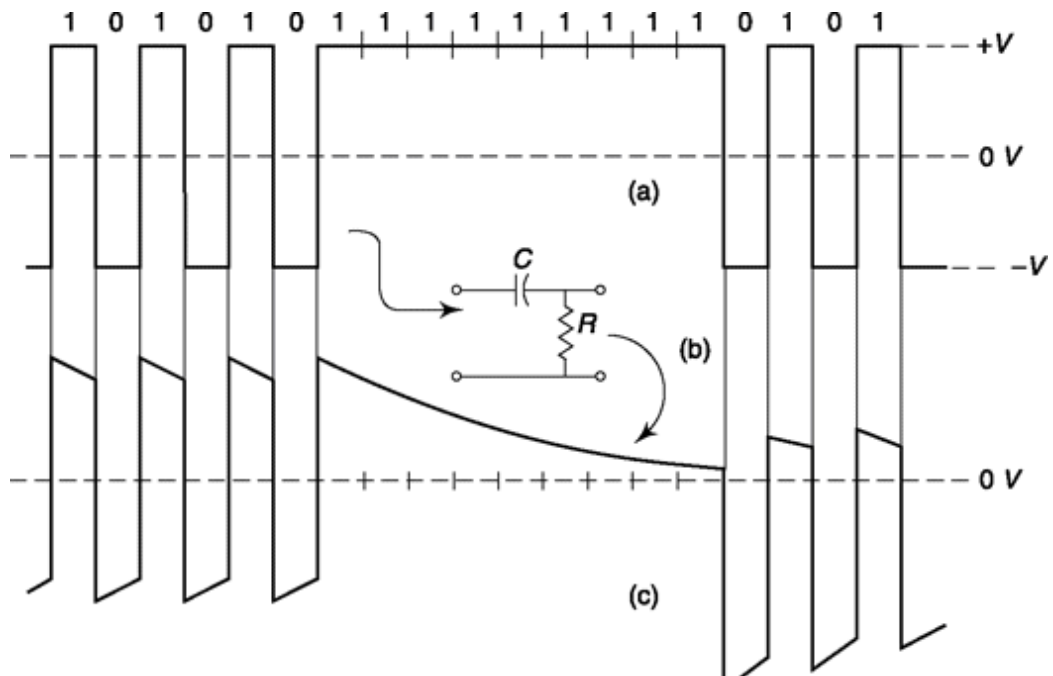


Fig. 4.31 (a) An NRZ binary waveform, (b) A circuit whose transmission discriminates against low frequency, (c) The output which results when the waveform in (a) is transmitted through the circuit in (b).

Bipolar RZ

This code is bipolar as excursion is between $+V$ and $-V$. Both logic 1 and 0 are represented by pulses that return to zero within the bit interval. Figure 4.30(d) describes its timing diagram and PSD. The PSD is similar to unipolar RZ but has higher power budget though in presence of noise it performs better. Note that, in some literature instead of ‘bipolar’, the term ‘polar’ is used and AMI, discussed next, is referred as bipolar code.

AMI

This is abbreviation of Alternate Mark Inversion. Figure 4.30e shows the abridged timing diagram and PSD. We explain it in more details now. In Fig. 4.32a we show again an NRZ waveform which we have just judged inadequate and in (b) we have shown an alternative more suitable waveform. A logic-0 is represented by zero volts over the whole bit interval. A logic-1 is rep-

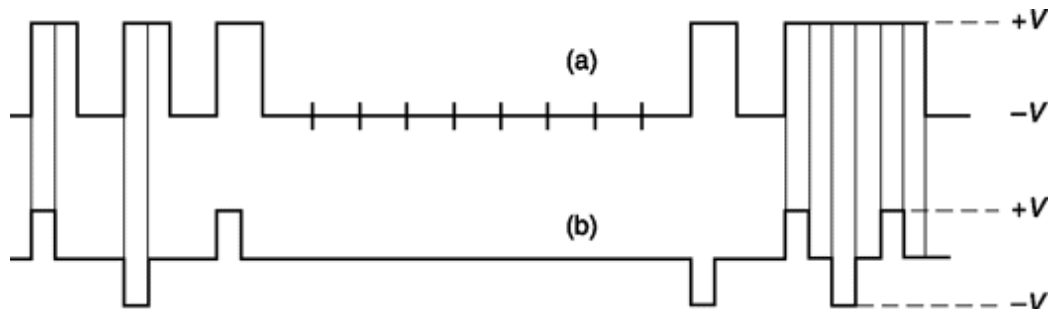


Fig. 4.32 (a) An NRZ binary waveform, (b) An alternate Mark Inversion equivalent to the waveform in (a).

resented by $+V$ or $-V$ which persists for a fraction of the bit interval. The fraction is referred to as the duty cycle and is often of the order of 50 percent. Most importantly, observe that these 50 percent duty cycle pulses *alternate*. Two successive 1’s whether they occur in neighboring bit intervals or are separated by 0’s are represented by pulses of *opposite* polarity. Such a waveform is called an *alternate mark inversion* (AMI) signal, the word “mark” being a telegrapher’s term for a logic-1. It is apparent that neither a persistent sequence of 1’s nor of 0’s will generate the accumulation of a “dc component”. Observe also that if the receiver should encounter two successive pulses of the *same* polarity it would be recognized as a *violation* of the waveform standards.

HDB

A modified version of *AMI* is known as High Density Bipolar code which deliberately introduces 1's when a long string of zeros appear in *AMI*. The 1's are inserted in such a manner that they generate violations, i.e. they do not alternate (unlike original 1's). This additional 1's is helpful in clock synchronization. In HDB-3 code, if there are more than 3 zeros in a string the 4th one is replaced by a violation pulse.

Biphase (Split-Phase) or (Manchester Coding)

Here, for logic 1, a positive pulse is followed by a negative pulse, each of half-bit duration and for logic-0, a negative pulse is followed by a positive pulse (Fig. 4.30f). Average voltage here is exactly zero and recovery of clock is easier. But note that bandwidth is roughly double of NRZ scheme due to half-bit transitions.

CMI

Abbreviation Coded Mark Inversion code, this is a two level NRZ code where logic 0 is represented by a negative pulse followed by a positive pulse, each half bit duration and logic 1 is represented alternatively by +V and -V for full bit interval (Fig. 4.30g). This code is compared with *AMI* and has higher clock content.

2B1Q

The abbreviation stands for 2 binary digits encoded into 1 quaternary symbol. This is a block code where block size is 2. The block to symbol transformation is as follows: 00 (-3 V, 01 (-1V, 10 (+1V, 11 (+3 V. This results in 4-level PAM signal having zero dc component, less bandwidth and better performance w.r.t inter symbol interference and certain type of cross talk when compared with linear codes.

4.5.2 Scrambling

Scrambling is a process by which data is randomized. It is difficult to decipher a scrambled data unless we do its reverse operation through unscrambling. You'll find its use in digital transmission of television signals where even if you have data available at your set top box you cannot view

the channel unless it is properly unscrambled. Now, why we got curious about security feature of data at this stage of discussion? Well, this is because a scrambler also removes a pattern while randomizing the data. Thus, it can remove long string of 1's or 0's which can help clock recovery and synchronization. We take a simple example to explain how this works.

Let, the digital data input to the scrambler be represented by $d(k)$ and its output is $b(k)$. Define a scrambling process as given next,

$$zb(k) = d(k) \oplus b(k-2) \oplus b(k-4) \quad (4.45)$$

where, $b(k-j)$ represents j -th last value of $b(k)$. Let us consider that input data are all 1's and past values of $b(k)$ to begin with are all zero, i.e. delay elements are all initialized with 0's. Table 4.2 illustrates what will be available as output of scrambler. The Ex-OR operation of three variables in RHS of Eq. (4.45) gives $b(k) = 1$ whenever there is odd no. of 1's present. In the table, delayed values diagonally move up till $b(k-4)$. We see that the long string of 1's is broken by scrambler by periodic insertion of 1 after certain number of 0's. This helps in recovering timing information at the receiver end. However, it does not assure that it will show improvement in same manner for all kind of data input. Refer to Example 4.9.

Table 4.2 Scrambling Operation

k	1	2	3	4	5	6	7	8	9	10	11	12	13	14
$d(k)$	1	1	1	1	1	1	1	1	1	1	1	1	1	1
$b(k-4)$	0	0	0	0	1	1	0	0	0	0	1	1	0	0
$b(k-3)$	0	0	0	1	1	0	0	0	0	1	1	0	0	0
$b(k-2)$	0	0	1	1	0	0	0	0	1	1	0	0	0	0
$b(k-1)$	0	1	1	0	0	0	0	1	1	0	0	0	0	1
$b(k)$	1	1	0	0	0	0	1	1	0	0	0	0	1	1

The unscrambling process as said before will be reverse of Eq. (4.45) that recovers $d(k)$. The corresponding equation, for this example is

$$\hat{d}(k) = b(k) \oplus b(k-2) \oplus b(k-4) \quad (4.46)$$

Table 4.3 can illustrate the recovery of original data where the delayed input data moves diagonally downwards. The Eqs (4.45) and (4.46) in general can be extended for other and more number of delay elements.

Table 4.3 Descrambling Operation

k	1	2	3	4	5	6	7	8	9	10	11	12	13	14
$b(k)$	1	1	0	0	0	1	1	0	0	0	0	1	1	1
$b(k-1)$	0	1	1	0	0	0	1	1	0	0	0	0	1	
$b(k-2)$	0	0	1	1	0	0	0	0	1	1	0	0	0	0
$b(k-3)$	0	0	0	1	1	0	0	0	1	1	0	0	0	0
$b(k-4)$	0	0	0	0	1	1	0	0	0	0	1	1	0	0
$\hat{d}(k)$	1	1	1	1	1	1	1	1	1	1	1	1	1	1

And we see $\hat{d}(k)$ is same as transmitted message $d(k)$.

4.5.3 The T1 Digital System

Figure 4.33 shows the basic time-division multiplexing scheme, called the T1 digital system, which is used to convey multiple signals over telephone lines using wideband coaxial cable. It accommodates 24 analog signals which we shall refer to as s_1 through s_{24} . Each signal is bandlimited to

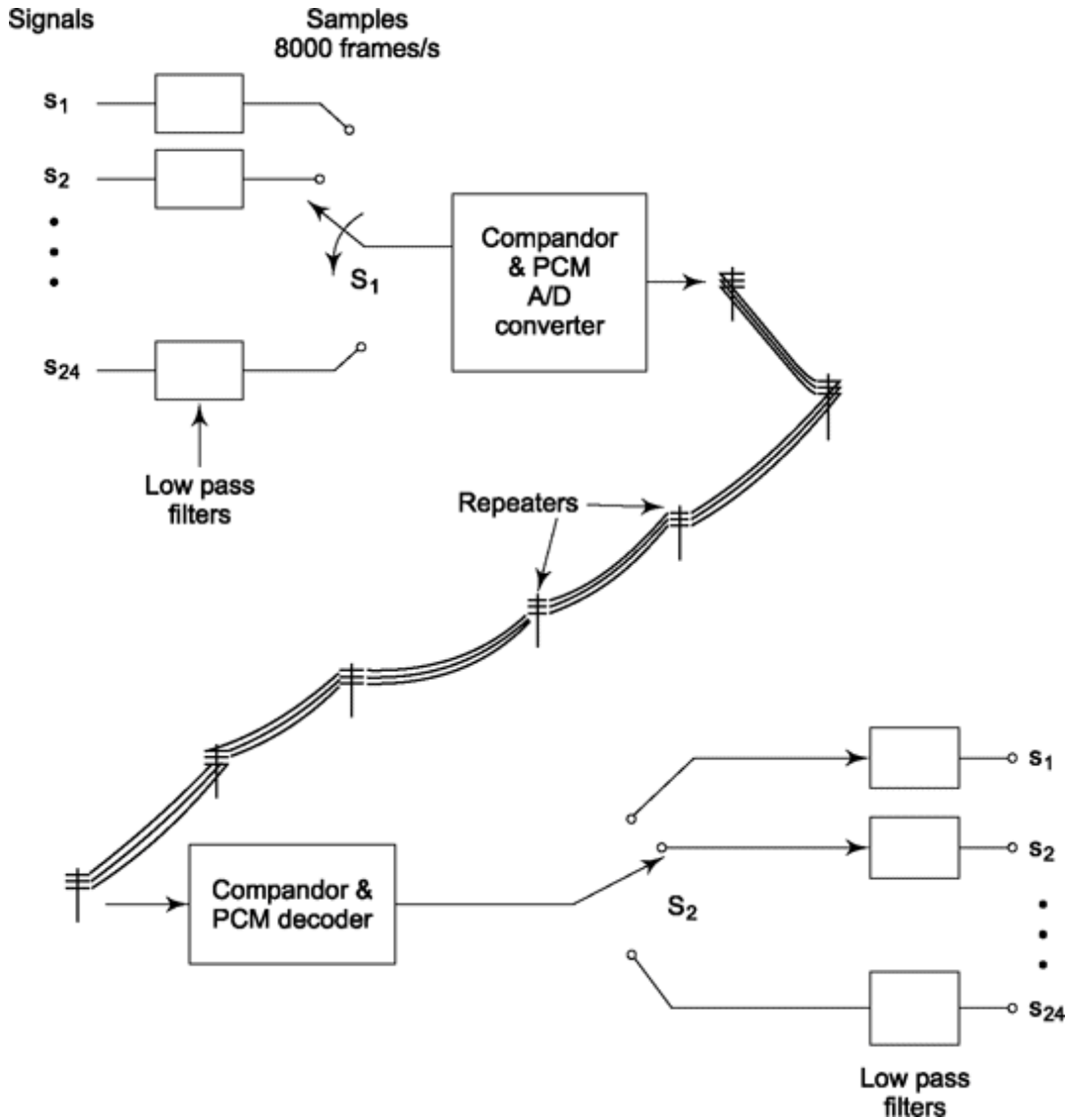


Fig. 4.33 A T1 digital system.

approximately 3.3 kHz and is sampled at the rate 8 kHz which exceeds, by a comfortable margin, the Nyquist rate of $2 \times 3.3 = 6.6$ kHz. Each of the time division multiplexed signals (still analog) is next A/D converted and companded as described in Sec. 4.4.6. The resulting digital waveform is transmitted over a coaxial cable, the cable serving to minimize signal

distortion and serving to suppress signal corruption due to noises from external sources. Periodically, at approximately 6000 ft intervals, the signal is regenerated by amplifiers called repeaters and then sent on towards its eventual destination. The repeater eliminates from each bit the effect of the distortion introduced by the channel. Also, the repeater removes from each bit any superimposed noise and thus, even having received a distorted and noisy signal, it retransmits a distortionless and noise-free duplicate of the signal originally sent. Such is, of course, the case for all bits except those infrequent bits which arrive so corrupted by noise that the bit is misread. At the destination the signal is companded, decoded and demultiplexed, making available, individually, the 24 original signals.

Bits/Frame

The commutators sweep continuously from s_1 to s_{24} and back to s_x , etc., at the rate of 8000 revolutions per second thereby providing 8000 samples per second of each signal. Each sample is encoded into eight bits (corresponding to $2^8 = 256$ quantization levels). The digital signal generated during the course of one complete sweep of the commutator is therefore $24 \times 8 = 192$ bits.

Frame Synchronization

It is necessary to make available at the receiver not only the bits into which the signals have been encoded but also some synchronizing information. Without such synchronization (i.e. timing) information, the receiver cannot know which bits correspond to which of the original signals. To provide such synchronization an extra single bit is made available immediately preceding the 192 bits that carry the encoded signals. The 192 bit slots assigned to the encoded signal together with the one extra timing bit, for a total of 193 bits, is called a *frame*. The time slots for the 24 signals together with the extra frame-synchronizing bit *F* is shown in Fig. 4.34.

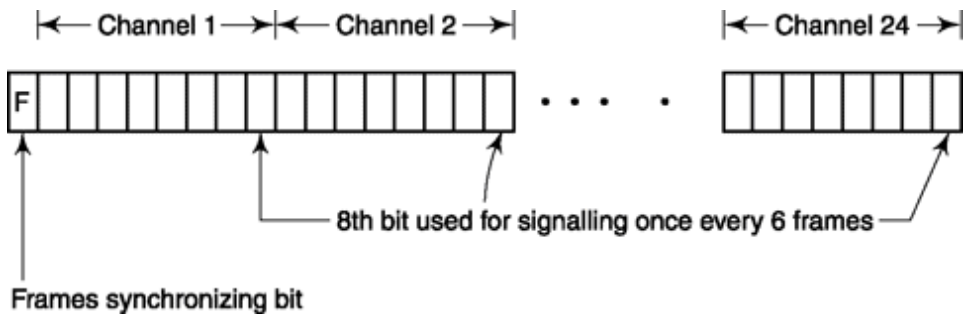


Fig. 4.34 The PCM T1 frame using channel associated signaling.

Twelve successive F slots are used to transmit a 12-bit code. The code happens to be 110111001000. This code is transmitted repetitively once every 12 frames and is used at the receiver to establish synchronization.

Bit Rate

Each signal is sampled 8000 times per second so that a complete frame occupies a time

$$T_p = 1/8000 = 125 \mu\text{s}$$

This time T_p accommodates 193 bits so that the bit rate on a $T1$ channel is

$$f_b(T1) = \frac{193}{125} \text{ Mb/s} = 1.544 \text{ Mb/s}$$

Bits in the frame synchronizing code occur once per frame, or every 125 μs . Hence the frame synchronization code repeats every 1.5 ms and the frame rate is 667 frames/s.

Signaling

A telephone system must be able to transmit not only the speech communication but also certain other signaling and supervisory information. Thus information needs to be conveyed that a call is being initiated or terminated, specifying the address of the called party, etc. When analog

transmission is employed, the signaling information is often conveyed over a channel separate from that which carries the voice. In the $T1$ digital system, a process of bit-slot sharing is used to allow the single channel to transmit both voice and signaling. In this sharing scheme, the eighth (least-significant) bit of each encoded sample is used for both voice transmission and also for signaling. During five successive samplings (and hence during five successive frames), each sample is encoded into eight bits. But during the sixth frame the samples are encoded into only seven bits, the eighth bit being used for signaling. This pattern is repeated every six frames. Thus, in six frames the number of bits used for quantization encoding is $5 \times 8 + 1 \times 7 = 47$

so that samples are encoded on the average into $47/6 = 7$ bits. The frequency of the bits used for signaling is $1/6$ th of the frame bit rate, or 6

$$f_b(T1)_{(\text{signaling})} = \frac{1}{6}(8000) = 1,333 \text{ Hz}$$

This type of signaling is called *channel-associated* signaling.

Line Coding for T1 System

The line code used for T1 system uses AMI waveform discussed in Sec. 4.5.1 but with a difference. We have noted that PCM receiver requires a bit synchronizer. That is, at receiver end, we must reestablish the clock waveform which provides the timing for the transmitter. This can be generated from AMI waveform (The clock recovery is discussed in Chapter 10) itself but we need to prevent dropping out of synchronization for extended period of zeros. Here, if eight or more consecutive zeros occur, the least significant bit of a word in the string is changed to 1 to break the pattern.

4.5.4 Multiplexing T1 Lines-The T2, T 3 and T 4 Lines

To take further advantage of the merits of TDM and digital transmission, the common carriers employ a hierarchy of further multiplexing as shown in Fig. 4.35. Four T1 lines are multiplexed in an M12 multiplexer to generate a *T2* transmission system, seven *T2* lines convert to a *T3* line in an M23 multiplexer and six *T3* lines convert to a *T4* line in an M34 multiplexer. At each stage additional frame synchronizing bits must be added as with the first order multiplexing so that at each multiplexer output it would be possible to distinguish which bits belong to which input.

There is a problem that arises in connection with the higher orders of multiplexing that does not occur at the first order. In the first order multiplexing there is just a single clock to contend with, that is the clock that drives the commutator. However, the four input lines in the *M12* multiplexer come from physically widely separated locations and employ four *separate* unsynchronized clocks. These clocks are very stable crystal controlled oscillators which are, of course, set to operate at the same nominal frequency as nearly as possible. Since, however, they do not have a means of communicating with one another, they are not synchronized and will hence experience a relative frequency drift. Design specifications allow a drift from the nominal set frequency of ± 130 parts/million. As may be verified, if then two clocks have frequencies which differ by $2 \times 130 = 260$

parts/million, the faster clock will have generated one more time slot than the slower clock in the course of just 20 frames. For proper interleaving of bits at the M12 level it is necessary that all input bit streams have or be made to appear to have the same rate. To put the matter most simplistically, the process of adjusting bit rates to make them equal involves adding bits to the slower bit stream in an operation referred to as “pulse stuffing.” Further bits must then be added to all bit streams to allow the

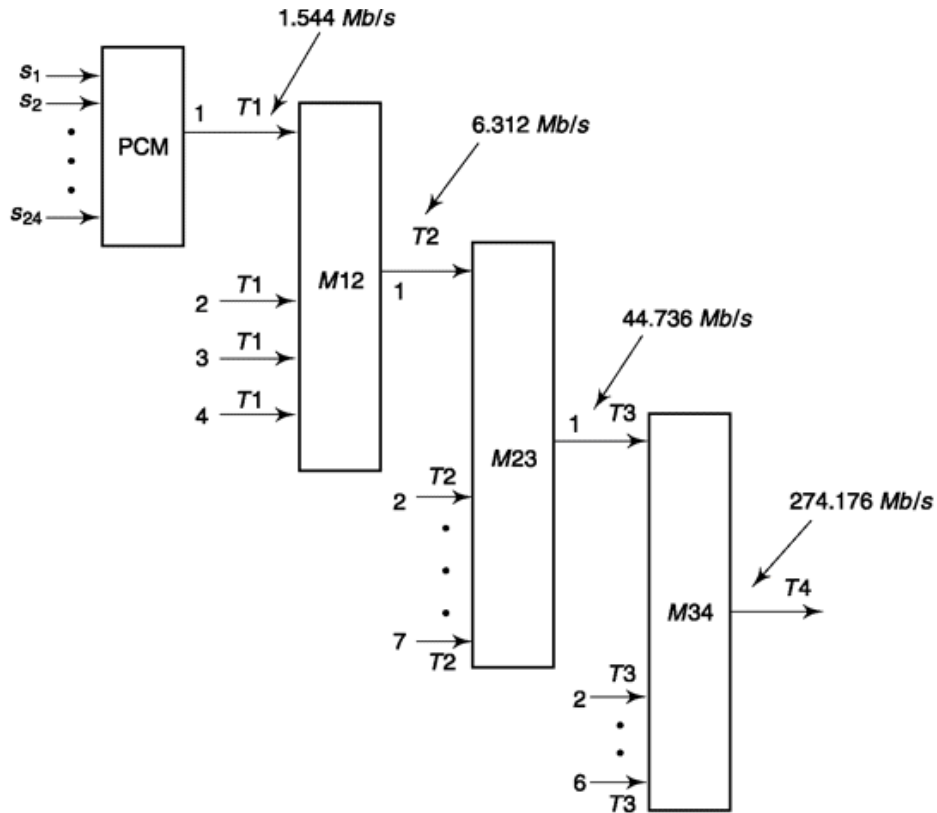


Fig. 4.35 TDM hierarchy.

receiver of the composite signal to distinguish time slots which carry information from slots which carry the “stuffed” bits.

Bit Rate

The M_{12} multiplexer adds nominally 17 bits for frame synchronization and pulse stuffing. Hence the number of bits per frame is

$$193 \times 4 + 17 = 789 \text{ bits/frame}$$

The T_2 line bit rate is therefore

$$\begin{aligned} f_b(T_2) &= 789 \text{ bits/frame} \times 8000 \text{ frames/s} \\ &= 6.312 \text{ Mb/s} \end{aligned}$$

The M_{23} multiplexer adds nominally 69 bits for synchronization and pulse stuffing; hence the number of bits per frame for a T_3 line is

$$789 \times 7 + 69 = 5592 \text{ bits/frame}$$

and

$$f_b(T_3) = 5592 \times 8000 = 44.736 \text{ Mb/s}$$

The M_{34} multiplexer adds nominally 720 bits for synchronization and pulse stuffing and therefore the T_4 system has a bit rate

$$f_b(T_4) = 274.176 \text{ Mb/s}$$

A detailed analysis of the architecture and operation of these digital systems is to be found in Ref. 3.

Example 4.8

(a) Consider Fig. 4.36a. If that represents an AMI line code give the logic values of the digital input at each bit interval. (b) Identify the line code given in Fig. 4.36b which represents the same bit sequence as Fig. 4.36a.

Solution

(a) Presence of alternate Marks in first two intervals give corresponding logic value 1, 1. Absence of Mark in the next interval means presence of logic 0. Proceeding this way we can identify input bit stream as {1, 1, 0, 1, 0, 0, 1}.

(b) Since the second waveform represents same set of data bit as above we find logic 1 has positive pulse followed by negative and logic 0, its reverse. Hence, from definition this represents split-phase or Manchester coding.

Solution We prepare a similar table (Table 4.4) as in Sec. 4.5.2 where $b(k)$ is the output.

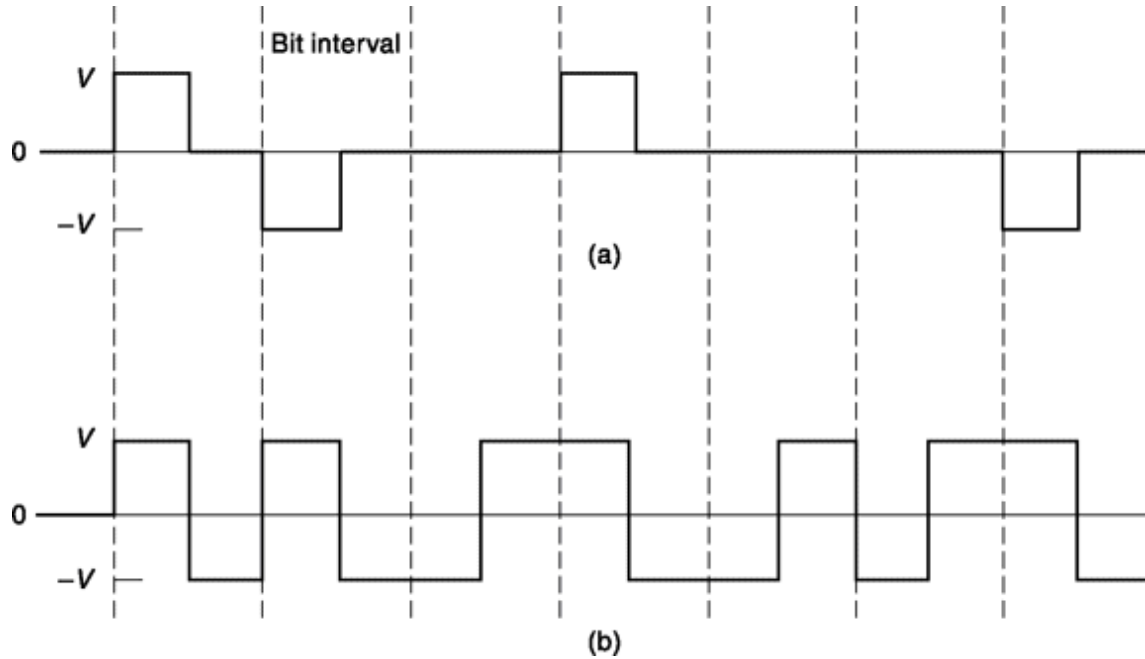


Fig. 4.36 Line code waveform for Example 4.8.

Example 4.9 Solution

Show the output of the scrambler defined in Sec. 4.5.2 if input signal is stream of alternate 1 and 0's.

Table 4.4 Scrambling Operation for Example 4.9

<i>k</i>	1	2	3	4	5	6	7	8	9	10	11	12	13	14
<i>d(k)</i>	1	0	1	0	1	0	1	0	1	0	1	0	1	0
<i>b(k - 4)</i>	0	0	0	0	1	0	0	0	0	0	1	0	0	0
<i>b(k - 3)</i>	0	0	0	1	0	0	0	0	0	1	0	0	0	0
<i>b(k - 2)</i>	0	0	1	0	0	0	0	0	1	0	0	0	0	0
<i>b(k - 1)</i>	0	1	0	0	0	0	0	1	0	0	0	0	0	1
<i>b(k)</i>	1	0	0	0	0	1	0	0	0	0	0	0	1	0

Note that $b(k)$ has less clock related information (longer string of zeros) than original signal. This shows that the primary job of scrambler is to break pattern.

4.6 DIFFERENTIAL PULSE CODE MODULATION

In a system in which a baseband signal $m(t)$ is transmitted by sampling, there is available a scheme of transmission which is an alternative to transmitting the sample values (quantized or not) at each sampling time. We can instead, at each sampling time, say the k th sampling time, transmit the *difference* between the sample value $m(k)$ at sampling time k and the sample value $m(k - 1)$ at time $k - 1$. If such changes are transmitted, then simply by adding up (accumulating) these changes we shall generate at the receiver a waveform identical in form to $m(t)$. There can be a difference in dc components between transmitted and received signals but, almost invariably, such dc components are of no interest.

Such a differential scheme has special merit when these differences are to be transmitted by pulse code modulation. For we may well anticipate that the differences $m(k) - m(k - 1)$ will be smaller than the sample values themselves. Hence, fewer levels will be required to quantize the difference than are required to quantize $m(k)$ and correspondingly, fewer bits will be needed to encode the levels. For example, suppose that $m(k)$ extends over a range $V_H - V_L$, and using PCM, $m(k)$ is encoded using $2^8 = 256$ levels. Then the step size is $S = (V_H - V_L)/2^8$, that is $V_H - V_L = 256S$. If, however, the difference signal $m(k) - m(k - 1)$ extends only over the range $\pm 2S$ then the quantized levels needed are at $\pm 0.5S$ and at $\pm 1.5S$. There are now only four levels and two bits per sample difference are adequate.

In an analog system, where we are able, at least in principle, to transmit the differences exactly, the differential system described above would operate in accordance with our description. In a digital (quantized) system we encounter the complication that the differences are not generally transmitted exactly because of the quantization. Further, we have the

problem that the difference may be larger than the maximum that can be accommodated because of the restricted number of encoding bits we have provided. Hence it might well be that at some time there might be a large discrepancy between the original signal $m(t)$ and the signal $m(t)$ generated at the receiver by accumulation. Suppose that over a number of samplings, while $m(t)$ is increasing, the transmitted differences were too small so that $m(k)$ had fallen substantially short of keeping up with $m(t)$. Suppose, further, that in the interval sampling times k and $k + 1$, $m(t)$ should decrease slightly. Clearly if we transmitted the negative change of $m(t)$ we would be giving the wrong signal.

In a digital differential system, we circumvent the difficulty we have just described by making available at the transmitter a duplicate of the receiver accumulator so that at the transmitter we have available the same signal $m(t)$. Then we arrange that the transmitted signal should not convey the most recent change in $m(t)$ but conveys instead the difference between $m(t)$ and $m(t)$. In an analog system, this difference $m(t) - m(t)$ is precisely the last change in $m(t)$. In a quantized system, as we have noted, such is not the case. In short, in a quantized system we add or subtract from $m(t)$ a value which is appropriate to bring $m(t)$ closer to $m(t)$. The waveform $m(t)$ is generally referred to as the *approximation* to $m(t)$.

Altogether, then, the quantized differential transmission scheme is as shown in Fig. 4.37. (We ignore initially the “predictors” that appear in the figure.) The receiver consists of an accumulator which adds up the received quantized differences $Ag(k)$ and a filter which smooths out the quantization noise. The output of the accumulator is the signal approximation $m(k)$ which becomes $m(t)$ at the filter output. At the transmitter we need to know whether $m(t)$ is larger or smaller than $m(t)$, and by how much. We may then determine whether the next difference $Ag(k)$ needs to be positive or

negative and of what amplitude in order to bring $m(t)$ as close as possible to $m(t)$. For this reason, we have a duplicate accumulator at the transmitter. At each sampling time, the transmitter difference amplifier compares $m(t)$ and $m(t)$ and the sample and hold circuitry holds the result of that comparison $A(t)$ for the duration of the interval between sampling times. The quantizer generates the signal $s_0(t) = Ag(k)$ both for transmission to the receiver and to provide input to the receiver accumulator in the transmitter. In a practical system the quantized differences would first be encoded into a binary bit

stream before transmission and decoded at the receiver. For simplicity the encoder and decoder are not included in Fig. 4.37.

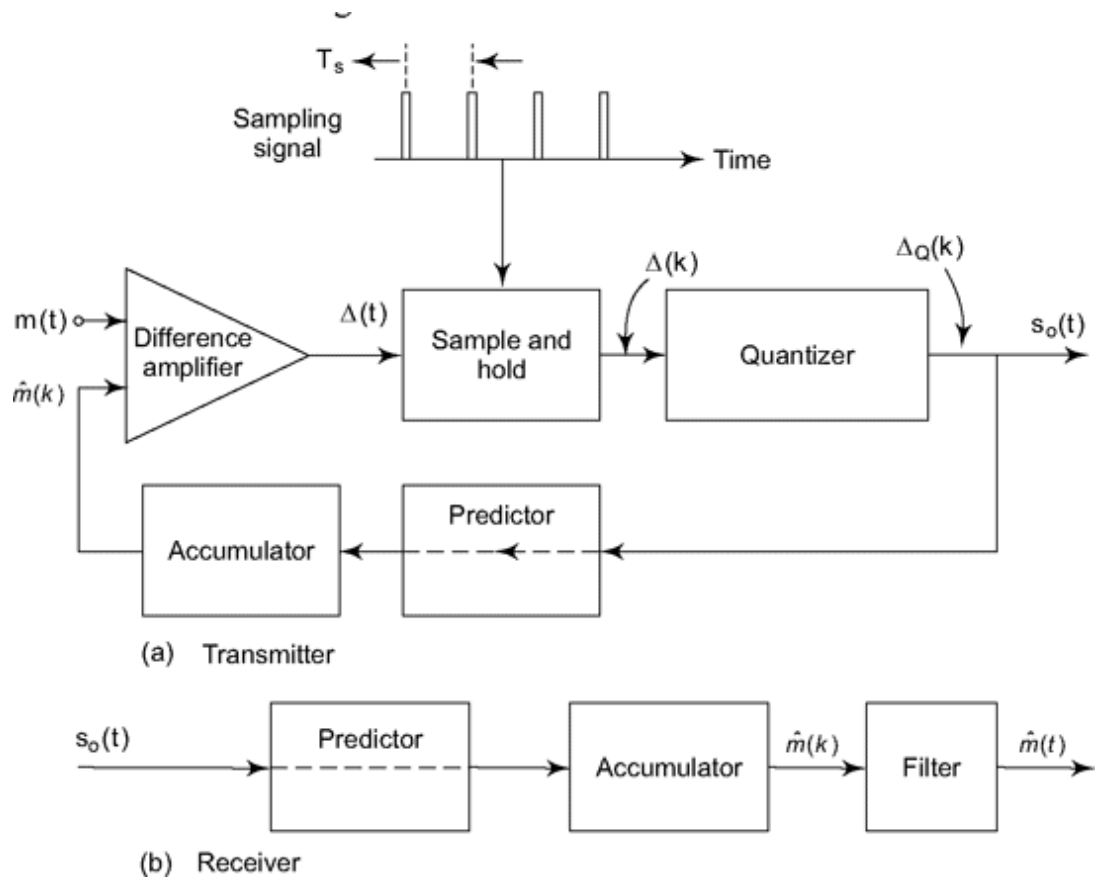


Fig. 4.37 Representation of the basic principle of differential PCM.

It needs to be emphasized that the basic limitation of the scheme we have just described is that the transmitted differences are quantized and are of limited maximum value. The quantization means that almost never will the increment $\Delta q(k)$ added to $m(k)$ make $m(t)$ precisely equal to $m(t)$. The limitation on the maximum value of $\Delta q(k)$ means that when $m(t)$ changes monotonically at a rapid rate, $m(t)$ may simply not be able to keep up.

Need for a Predictor

The DPCM scheme we have described in this section turns out, as a matter of practice, not to be effective. When the sampling rate is set at the Nyquist rate it generates unacceptably excessive quantization noise in comparison to PCM. The quantization noise can be reduced by significantly increasing the sampling rate. With increased rate the differences from sample to sample are smaller and the rate of producing large quantization errors is reduced.

Suppose, then, that in DPCM we increase the sampling rate, above the Nyquist rate, to the point where we get a quality of sound transmission which is comparable to that available from PCM operating at the Nyquist rate. Then again it turns out that DPCM is at a disadvantage because it has been demonstrated that the bit rate of DPCM (bits per sample \times sample rate) exceeds that required for PCM.

The situation in DPCM can be improved by recognizing that there is a correlation between successive samples of the signal $m(t)$ and of $A(t)$ if the signal is sampled at a rate exceeding the Nyquist rate. Hence, a knowledge of past sample values or differences allows us to *predict*, with some probability of being correct, the range of the next required increment. To take advantage of this correlation, a *predictor* is included in the DPCM system shown in Fig. 4.37. The predictor will generally be a moderately sophisticated system; it will need to incorporate the facility for storing past differences and for carrying out some algorithm to predict the next required increment.

Altogether, the quality of voice or video transmission using DPCM can be made comparable to that of PCM by increasing the sampling rate (which reduces the differences and increases the correlation between samples) and by using a predictor. Most importantly, by these expedients, DPCM can operate at approximately one-half of the bit rate of PCM with a consequent saving of spectrum space.

4.6.1 Linear Predictor Design

Here, we discuss in brief a scheme to design a linear predictor which is optimal in Mean Square Error (MSE) sense. We shall modify Fig. 4.37 little to work solely on discrete data by shifting the sample-hold and accumulator outside the predictor loop. Refer to definition of z-transform in Section 4.1.3. Let us describe input samples to a discrete time system as $\{x(n)\}$ and output samples as $\{y(n)\}$ and corresponding z-transform as $X(z)$ and $Y(z)$ respectively. Then the ratio $H(z) = Y(z)/X(z)$ is known as transfer function of the discrete time system. Following Eq. (4.20), we can write,

$$H(z) = \sum_{n=0}^{\infty} h(n) z^{-n} \quad (4.47)$$

The quantity $h(n)$ represents impulse response of the system and in popular Finite Impulse Response (FIR) system (which for obvious reason is always stable) of N -th order, extend from $h(1), \dots, h(N)$. In linear predictor design, we shall consider it as a FIR system and optimality in MSE sense tries to find $h(n)$, $n = 1, \dots, N$ that minimizes some error criterion. The convolution relation of two signals $x(n)$ and $h(n)$ in discrete-domain that generates $y(n)$ is shown in Eq. (4.48a). This relation is equivalent to multiplication in z -domain (Eq. 4.48b) as we have seen in case of convolution of continuous signal and their Fourier transforms. In fact, they follow linearity (Eq. 4.47) and other properties on an equivalent basis. If $X(z)$ and $Y(z)$ are z -transforms of $x(n)$ and $y(n)$ respectively we can write,

Convolution:
$$y(n) = \sum_{k=0}^{\infty} x(k) h(n-k) \quad (4.48a)$$

$$Y(z) = X(z)H(z) \quad (4.48b)$$

Linearity:
$$ax(n) + by(n) \xleftrightarrow[z]{z^{-1}} aX(z) + bY(z) \quad (4.49)$$

In designing predictor for DPCM (Fig. 4.48), our objective is to minimize the error $e(n)$ that is quantized and transmitted. The less is its variance compared to original signal $m(n)$, the better will be the performance of DPCM system which can use more number of levels to code a smaller range of data and hence smaller step size.

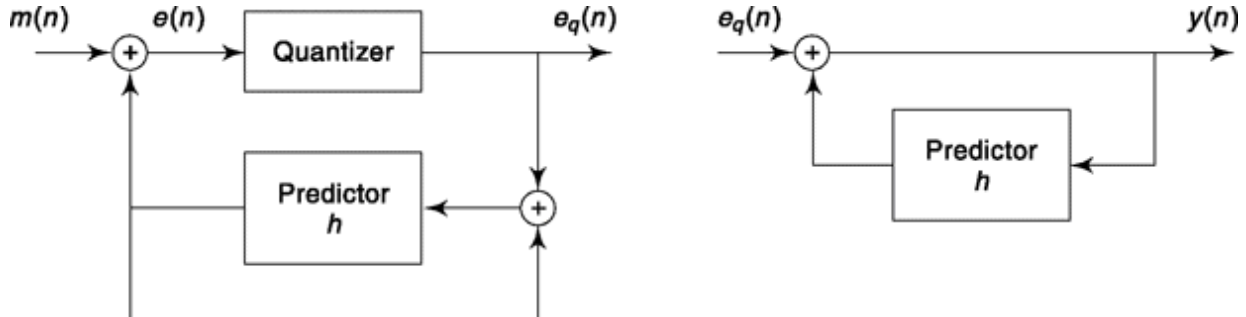


Fig. 4.38 A discrete time representation of DPCM system.

First, we write the equations that describes above system, the quantities used are defined in Fig. 4.38 itself by sum and difference operators. Predictor output (Eq. 4.50e) is convolution of its input $m(n)$ and impulse response $h(n)$.

Quantization error,	$q(n) = e_q(n) - e(n)$	(4.50a)
Prediction error,	$e(n) = m(n) - \hat{m}(n)$	(4.50b)
Input to predictor,	$\bar{m}(n) = e_q(n) + \hat{m}(n)$	(4.50c)
Output equation,	$y(n) = e_q(n) + \hat{y}(n)$	(4.50d)
Linear prediction,	$\hat{m}(n) = \bar{m}(n) \otimes h(n)$	(4.50e)

Converting above equations in z-domain and using convolution (Eq. 4.48) and linearity (Eq. 4.49) property we can write after simple algebraic manipulation,

$$E_q(z) = M(z) - H(z)\bar{M}(z) + Q(z) \quad (4.51a)$$

$$\bar{M}(z) = \hat{M}(z) + E_q(z) = H(z)(z) + [M(z) - H(z)\bar{M}(z) + Q(z)] = M(z) + Q(z) \quad (4.51b)$$

$$Y(z) = \frac{E_q(z)}{1-H(z)} = \frac{M(z)-H(z)[M(z)+Q(z)]+Q(z)}{1-H(z)} = M(z) + Q(z) \quad (4.51c)$$

Thus, we have, $Y(z) = \bar{M}(z)$, i.e. decoded receiver output $y(n)$ is same as $\bar{m}(n)$ available at the encoder side.

Let us now look beyond mathematical representation of DPCM system and calculate predictor coefficients which are optimal in MSE sense. The linear predictor output of Fig. 4.38 can be written as,

$$\hat{m}(n) = h(1)\bar{m}(n-1) + h(2)\bar{m}(n-2) + \dots + h(N)\bar{m}(n-N) \quad (4.52)$$

We assume input message $\{m(n)\}$ is a zero mean stationary random process with autocorrelation

$$R_m(k) = E[m(n)m(n-k)] = R_m(-k) \quad (4.53)$$

where, k is the discrete time(sample) shift and E is the expectation operator defined as

$$E[x(n)] = \lim_{N \rightarrow \infty} \frac{1}{N} \sum_{n=0}^{N-1} x(n) \quad (4.54)$$

As stated before, our objective is to minimize variance of $e(n)$, i.e. $E\{e^2(n)\}$. Since it is to be done w.r.t $h(j) = h_j$, we differentiate and equate each term to zero as $\frac{\partial}{\partial h_j} E\{e^2(n)\} = 0$. This after

manipulation using above relations and considering message and quantization noise are orthogonal gives $R_m(j) = \sum_{i=1}^N h_i R_m(j-i)$. As a system of linear equation we can write,

$$\begin{bmatrix} R_m(1) \\ \dots \\ R_m(N) \end{bmatrix} = \begin{pmatrix} R_m(0) & \dots & R_m(N-1) \\ \dots & \searrow & \dots \\ R_m(N-1) & \dots & R_m(0) \end{pmatrix} \begin{bmatrix} h(1) \\ \dots \\ h(N) \end{bmatrix} \quad (4.55a)$$

In matrix form, the above can be written as $\mathbf{R}_m = \mathbf{R}_N \mathbf{h}$ (4.55b)

That gives our optimal predictor coefficients $\mathbf{h} = \mathbf{R}_N^{-1} \mathbf{R}_m$ (4.56)

With \mathbf{h} as above, minimum error variance turns out to be,

$$\sigma_e^2|_{\min} = E\{e^2(n)\}|_{\min} = R_m(0) - \mathbf{R}_m^T \mathbf{R}_N^{-1} \mathbf{R}_m \quad (4.57)$$

You can see that the first term $R_m(0)$ of Eq. (4.57) is the input signal variance which is quantized in PCM system. The variance of $e(n)$ is less by the term appearing after that. If $m(n)$ and $e(n)$ have similar distribution SNR improvement in case of DPCM over PCM is by $10 \log_{10} \frac{\sigma_m^2}{\sigma_e^2}$. For audio, DPCM encoding saves nearly 25% bits compared to PCM for same audio quality.

4.6.2 Adaptive Linear Prediction: Least Mean Square Algorithm

The previous discussion assumes that the characteristics of input signal to be coded is not varying and we have all necessary autocorrelation values $R_m(j)$ available when we calculate filter coefficients h_j . (Note that we are continuing with the notations defined in previous section.) If one or both of these are not true we can employ adaptive linear prediction. Here, we start from some initial values of h_j and then iteratively update it by a simple algorithm, the most popular being Least Mean Square or *LMS algorithm*. As more and more data enters the system, updated h_j tries to seek the minimum position in error surface (may not get exactly) in a zigzag manner. The updated values of the weight in iteration $(n + 1)$ of LMS algorithm is given as

$$h_j(n+1) = h_j(n) - \mu g_k(n) \quad (4.58)$$

where, μ is step-size or learning parameter and $g_k(n) = \frac{\partial}{\partial h_j} E\{e^2(n)\}$. The second term on right hand side of Eq. (4.58) ensures that coefficients move in a direction opposite to gradient of error surface thereby reducing the error. The quantity μ , if small, takes more number of iterations and in turn time to adapt the coefficients and if it is large it may skip the minima resulting oscillatory behaviour. Using instantaneous values for estimation of autocorrelations and following some algebraic manipulations we get adaptation algorithm for predictor coefficients as

$$\hat{h}_j(n+1) = \hat{h}_j(n) + \mu m(n-j)e(n) \quad (4.59a)$$

where, prediction error, $e(n) = m(n) - \sum_{i=1}^N \hat{h}_j(n)m(n-i)$ (4.59b)

Like before, the symbol \hat{A} stands for estimate. If error $e(n)$, remains zero, the coefficients are not updated as that is not necessary. Also note that number of additions and more importantly multiplication increases *linearly* with number of filter coefficients which is considered as a computationally efficient scheme. In Adaptive Differential Pulse Code Modulation (ADPCM) the predictor coefficients updated using an adaptation scheme and LMS algorithm (Eq. 4.59) can be employed for the same.

For audio coding, ADPCM is popular like PCM and gives nearly 50% savings of bits.

4.7 DELTA MODULATION

Delta modulation (DM) is a DPCM scheme in which the difference signal $A(t)$ is encoded into just a *single* bit. The single bit, providing for just two possibilities, is used to increase or decrease the estimate $m(t)$.

One way in which a delta modulator can be assembled is shown in Fig. 4.39. This scheme is called linear delta modulation. The baseband signal $m(t)$ and its quantized approximation $m(t)$ are applied as inputs to a comparator. A comparator, as its name suggests, simply makes a comparison between inputs. As indicated in the plot shown in Fig. 4.39, the comparator has one fixed output $V(H)$ when $m(t) > m(t)$ and a different output $V(L)$ when $m(t) < m(t)$. Ideally, the transition between $V(H)$ and $V(L)$ is arbitrarily abrupt as $m(t) - m(t)$ passes through zero. The comparator replaces the difference amplifier and quantizer of Fig. 4.37, since in the present special case we need to know only whether $m(t)$ is larger or smaller than $m(t)$ and not the magnitude of the difference.

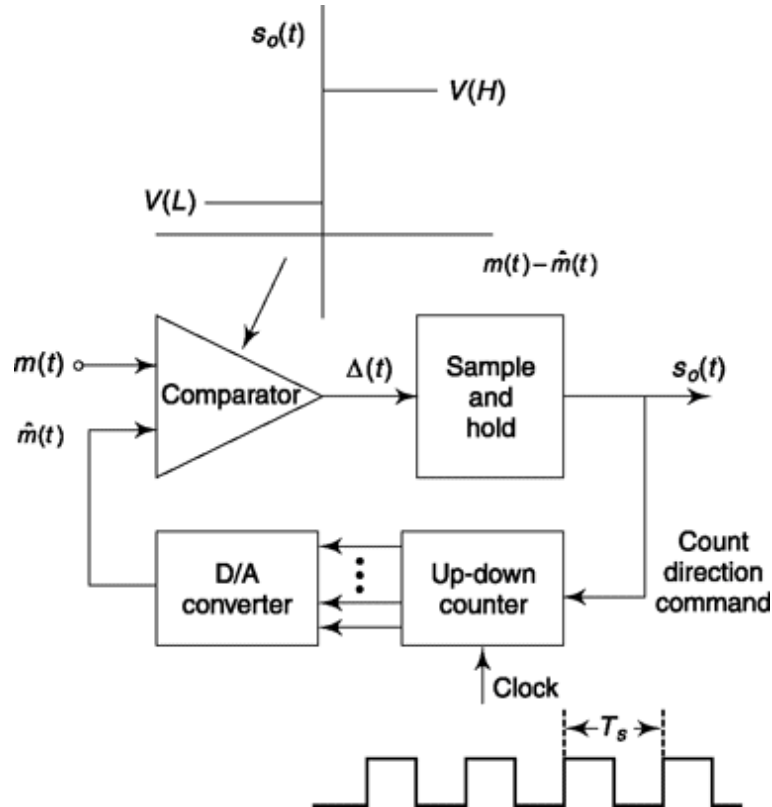


Fig. 4.39 A delta modulator.

The up-down counter increments or decrements its count by 1 at each active edge of the clock waveform. (The active edge is either the rising or falling edge of the clock, depending on the hardware design of the counter. The sampling time is the time of occurrence of this active edge.) The count direction, i.e., incrementing or decrementing, is determined by the voltage levels at the “count direction command” input to the counter. When this binary input, which is also the transmitted output $s_o(t)$, is at the level $V(H)$, the counter counts-up and when it is at the level $V(L)$ the counter counts down. In the present case the counter serves as the accumulator shown in Fig. 4.37, since it adds or subtracts increments as directed and stores the accumulated result. The digital output of the counter is converted to the analog quantized approximation $m(t)$ by the D/A converter. The waveforms of Fig. 4.40 are the waveforms for the system of Fig. 4.39, assuming that the active clock edge is the falling edge.

For a time preceding t_1 , we find $m(t) > m(t)$ so that $s_o(t) = V(H)$. At t_1 , when the active clock edge appears, the counter is incremented and immediately (ignoring propagation delays in the counter and D/A converter) the signal $m(t)$ jumps up by an amount equal to the step size S . At t_2 we still

find $m(t) > m(t)$, so $s_o(t)$ remains at $V(H)$ and there is another upward jump in $m(t)$. At t_3 , $m(t) < m(t)$, so $s_o(t)$ becomes $s_o(t) = V(L)$, the counter decrements, and there is a consequent downward jump in $m(t)$ by amount S , and so on.

We note that at start-up, there may be a brief interval when $m(t)$ may be a poor approximation to the baseband signal $m(t)$. This feature is illustrated in Fig. 4.41. Hence we note an initial large discrepancy between $m(t)$ and $m(t)$ and the stepwise approach of $m(t)$ to $m(t)$. We note further that even when $m(t)$ has caught up to $m(t)$, and even though $m(t)$ remains unvarying, $m(t)$ hunts, swinging up or down, above and below $m(t)$.

We have noted previously the limited ability of DPCM to accommodate to large increments in $m(t)$. For DM, this limitation is illustrated in Fig. 4.42. Here we have a signal $m(t)$, which, over an extended time, exhibits a slope which is so large that $m(t)$ cannot keep up with it. As a consequence the error $m(t) - m(t)$ becomes progressively larger, by far exceeding $S/2$. The excessive disparity between $m(t)$ and $m(t)$ is described as a *slope-overload error* and occurs whenever $m(t)$ has a slope larger than the “slope” S/T_n which can be sustained by the waveform $m(t)$.

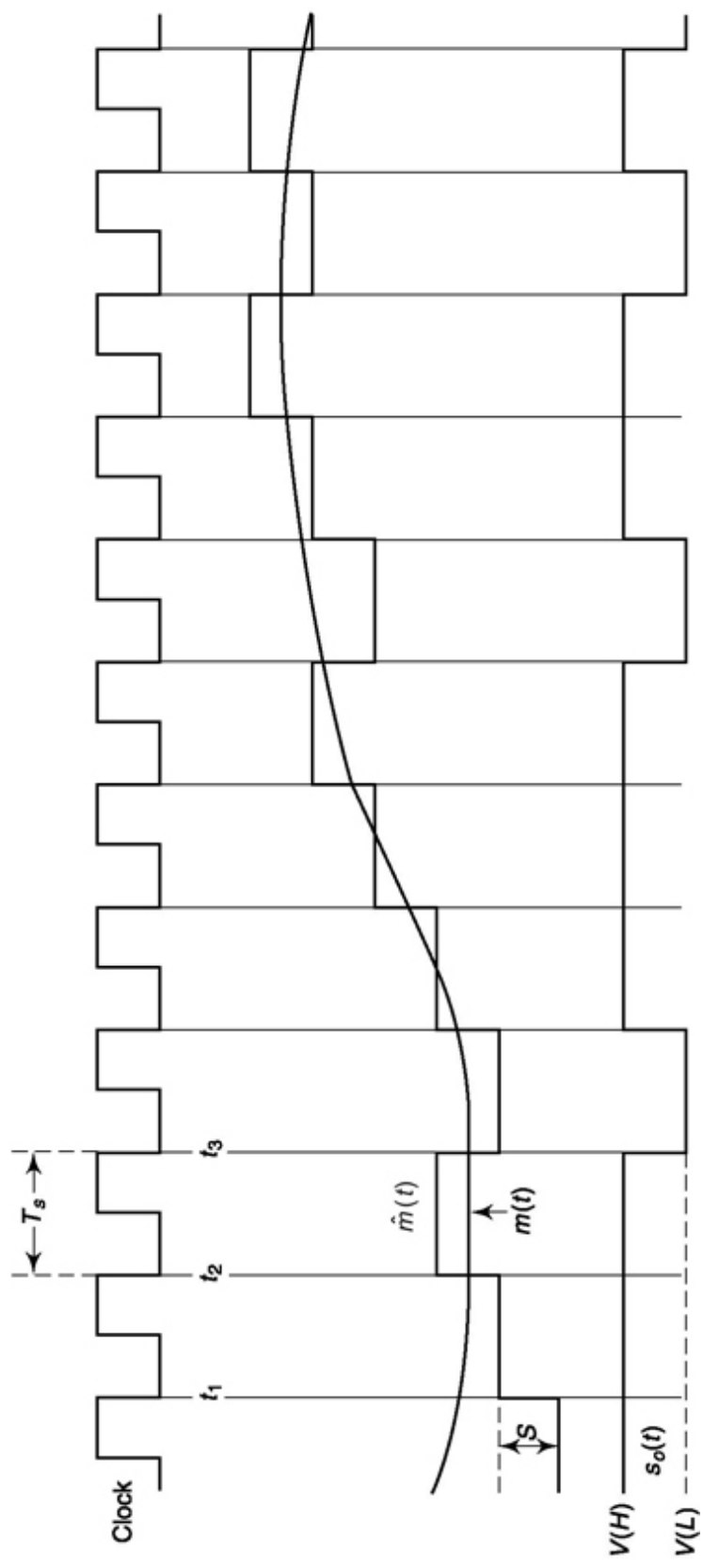
$$\text{Mathematically speaking, slope overload can be avoided if } \frac{S}{T} > \left| \frac{dm(t)}{dt} \right|_{\max} \quad (4.60)$$

The quantization noise can be calculated from Eq. (4.38) noting that error could be $\pm S$ and equally likely. This makes quantization noise for DM

$$N_Q = S^2/3 \quad (4.61)$$

The linear form of $m(t)$ in Fig. 4.42 accounts for the name *linear delta modulation* being associated with the DM system we have described. Linear delta modulation has the delightful elegance of primitive simplicity yet it suffers from severe limitations on account of which it finds almost no applications in real systems. As an example of the difficulty, consider the use of DM for speech transmission. In designing an appropriate system we would initially select a step size S which is small enough to assure acceptable quantization noise. As noted, $S = (V_H - V_L)/256$ is a reasonable selection. If now, because of the small size of S , slope overload should develop, we can hope to overcome the overload by increasing the sampling rate above the rate initially selected to satisfy the Nyquist criterion. Since we need only one bit per sample rather than eight, as in PCM, we can

E



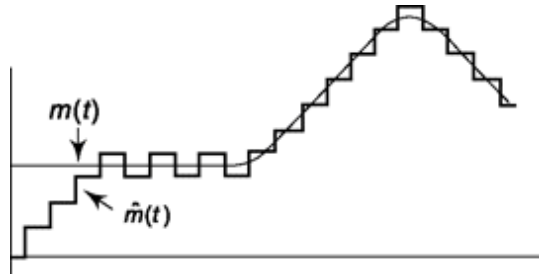


Fig. 4.41 Illustrating the “start-up” response in delta modulation and the “hunting” of $m(t)$ about $m(t)$.

increase the sampling rate eightfold before we reach the rate required in PCM. Now it has been determined experimentally that DM will transmit speech without significant slope overload provided that the DM system is able to transmit a sinusoid of frequency $f = 800$ Hz whose amplitude is the same as the amplitude of the speech waveform. A sinusoid of amplitude A and frequency f has a maximum slope of $2\pi f A$ as it passes through zero. If slope overload is to be avoided then we require that the sampling rate $f_s (= 1/T_s)$ must satisfy the condition

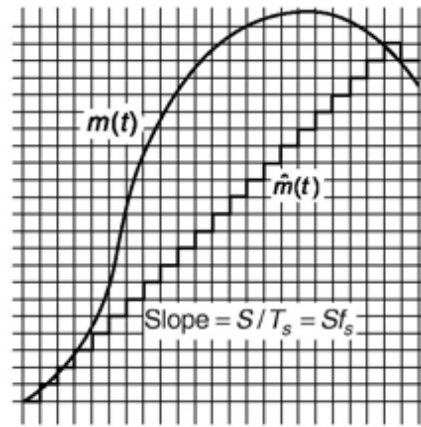


Fig. 4.42 Slope-overload in the linear DM.

$$Sf_s \geq 2\pi f A \quad (4.62)$$

$$\text{or} \quad f_s \geq \pi f \frac{2A}{S} = 256\pi f \cong 640 \text{ kHz} \quad (4.63)$$

where we have set $f = 800$ Hz. This frequency, which is also the bit rate, is to be compared with the bit rate in PCM. Assume that the highest frequency component of the speech signal is 3 kHz. Then the Nyquist rate is 6 kHz. To allow a margin of safety, let us use a sampling rate of 8 kHz. Then with 8 bits per sample the bit rate is $8 \text{ kHz} \times 8 = 64 \text{ kHz}$. Hence DM is not a practical alternative to PCM.

4.7.1 Adaptive Delta Modulation

We now consider a modification of DM called *adaptive DM* in which the step size is not kept fixed. Rather, when slope overload occurs the step size becomes progressively larger, thereby allowing $m(t)$ to catch up with $m(t)$ more rapidly.

We describe now an ADM system designed and constructed at the Communications System Laboratory at CCNY. It is represented by the block diagram of Fig. 4.43. We shall not examine the details of the hardware of the *processor* but only describe what it does. The processor has an accumulator and, at each active edge of the clock waveform, generates a step S which augments or diminishes the accumulator. The step S is not of fixed size but it is always a multiple of a basic step S_0 . The algorithm by which S is generated is as follows: In response to the k th active edge of the clock waveform the processor, to start with, generates a step equal in magnitude to the step generated in response to the $(k - 1)$ st clock edge. This step is added to m or subtracted from the accumulator, as required, to move (t) towards $m(t)$. Further however, if the direction of the step at clock edge k is the *same* as at edge $k - 1$ then the processor *increases* the magnitude of the step by amount S_0 . If the directions are *opposite* then the processor *decreases* the magnitude of the step size by S_0 . As the algorithm is

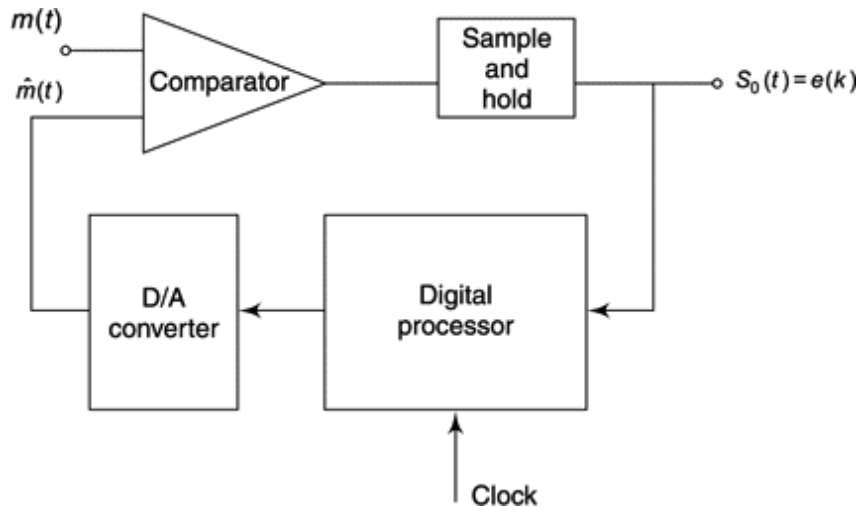


Fig. 4.43 An *adaptive DM*.

carried out there are clock edges when the total step $S = 0$. In this case, at the next clock edge the step is S_0 in the direction again to move $m(t)$ towards $m(t)$.

In Fig. 4.43 the output $S_0(t)$ is called $e(k)$. The symbol $e(k)$ represents the error, i.e., the discrepancy between $m(t)$ and $\hat{m}(t)$ and, as indicated in Fig. 4.39 is either $V(H)$ or $V(L)$. To express the algorithm by which the step size is determined it is convenient to arrange that:

$$\begin{aligned} e(k) &= +1 \text{ if } m(t) > \hat{m}(t) \text{ immediately before the } k\text{th edge} \\ e(k) &= -1 \text{ if } m(t) < \hat{m}(t) \text{ immediately before the } k\text{th edge} \end{aligned}$$

We can now specify that at sampling time k the step size $S(k)$ is to be given by:

$$S(k) = |S(k-1)| e(k) + S_0 e(k-1) \quad (4.64)$$

The important features of this adaptive scheme are shown in Fig. 4.44. Observe that as long as the condition $m(t) > \hat{m}(t)$ persists, the jumps in $m(t)$ become progressively larger. The estimate $\hat{m}(t)$ catches up with $m(t)$ sooner than would be the case with linear delta modulation as shown by the waveform $m'(t)$. On the other hand, when, in response to a large slope in $m(t)$, $\hat{m}(t)$ develops large jumps, it may require a large number of clock cycles for these jumps to decay in amplitude when they are no longer needed. Such a situation is to be seen in Fig. 4.44 in the neighborhood where $\hat{m}(t)$ first catches up with $m(t)$. Altogether, then, while this ADM system reduces slope error, it does so at the expense of increasing quantization error. The dashed waveform $m'(t)$ corresponding to linear DM has small quantization error but extremely large slope error.

Note, also, incidentally that when $m(t)$ remains constant (within an interval S_0) $m(t)$ oscillates about $\hat{m}(t)$ but that the oscillation frequency is one-half the clock frequency.

It turns out that in the matter of speech transmission the reduced slope error provides a net advantage in spite of the increased quantization error and that this adaptive delta modulator can operate at bit rates of 32 kb/s with performance comparable to that obtained when using PCM at 64 kb/s. Furthermore, the ADM can operate at 16 kb/s with only a slight degradation of performance.

It has been shown that more than 90 percent of the step sizes are less than or equal to $2S_0$ and that the probability of a step exceeding $15S_0$ is about 1 percent. In addition, the spurious frequency components introduced into the reconstructed signal by slope-overload error are principally in the low frequency range, while quantization error introduces principally high-frequency components. The

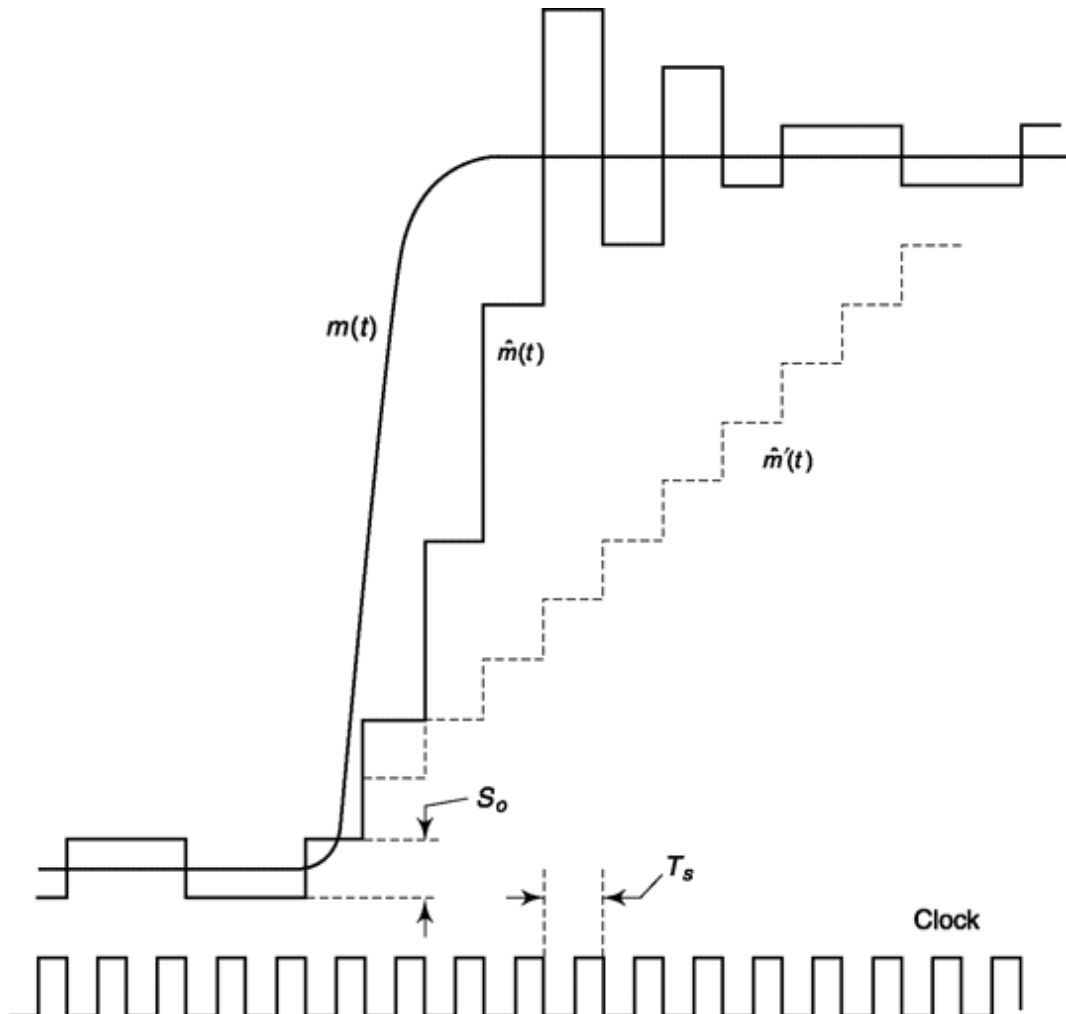


Fig. 4.44 Waveforms comparing the response of the ADM and LDM.

power in speech is concentrated largely in the low-frequency components, and these low-frequency components are also the ones which must principally be reproduced without error in order to preserve intelligibility. Hence if we pass the reconstructed signal through a low-pass filter, we shall be able to discriminate against the high-frequency quantization error without materially degrading the voice signal. A variation of this algorithm is used on the Space Shuttle.

Continuously Variable Slope Delta Modulator (CVSD)

A DM system which adjusts its step size to any given value is shown in Fig. 4.45. The amplifier has a variable gain. That is, its gain is a function of the voltage applied at its gain-control terminal. We assume that the characteristics of the amplifier are such that when the gain-control voltage is

zero, its gain is low, and that the gain increases with increasing positive gain-control voltage. The resistor-capacitor combination serves as an integrator, the voltage across C being proportional to the integral of the pulse signal $p_o(t)$. The voltage across C is used to control the gain of the amplifier. The square-law device ensures that whatever the polarity of the voltage across C , a positive voltage will be applied to the gain-control terminal of the amplifier.

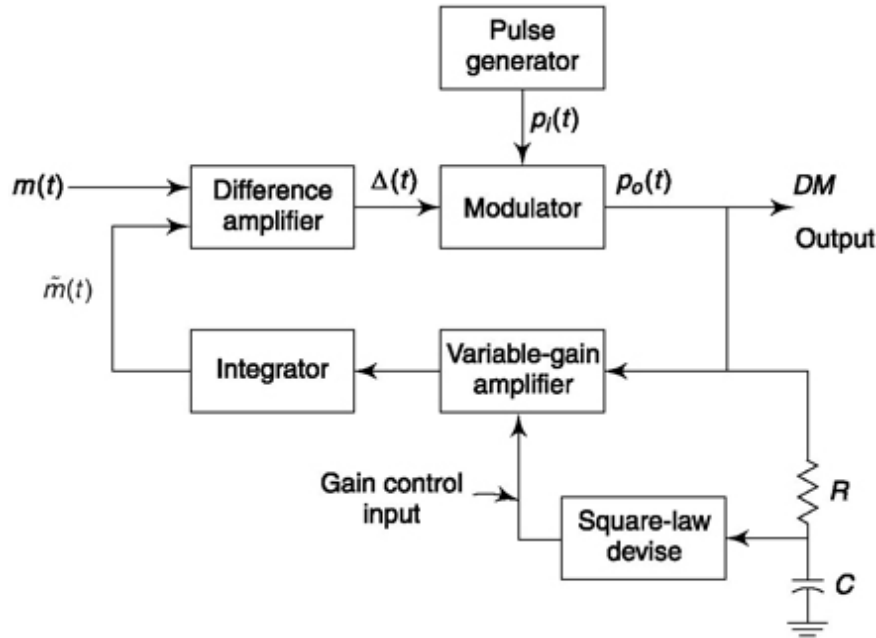


Fig. 4.45 An adaptive delta modulator.

Assume now that $m(t)$ is making only small excursions so that the modulator does not follow. The output $p_o(t)$ consists then of alternate polarity pulses. These pulses, when integrated, yield an average output of almost zero. The gain-control input is, hence, almost zero, the gain is low, and consequently the step size is reduced. Next consider the case of slope overload. If $m(t)$ increases positively or negatively at too rapid a rate, $m(t)$ cannot follow. The output $p_o(t)$ is then a train of all positive or all negative pulses. The integrator averages and provides a large voltage to increase the gain of the amplifier. Because of the squaring circuit the amplifier gain will increase no matter what the polarity of the integrator voltage. The end result is an increase in step size and a reduction in slope overload. It is of course, necessary that there be an adaptive adjustment of the step size at the receiver, as well. Thus, the receiver consists of the variable-gain amplifier,

square-law device, RC filter and integrator shown in the feedback path of Fig. 4.45.

Example 4.10

A 2nd order predictor is to be designed using LMS algorithm where input is defined as $\{m(n)\} = \{1, 2, 3, 4, 5, \dots\}$. Show how predictor coefficients are updated up to $n = 4$ where $n = 0$ signifies the start time from which adaptation begins and $\{m(n)\}$ is causal. Consider the predictor is initialized with $h_1(0)=0$, $h_2(0)=0$ and learning parameter $m = 0.1$.

Solution

Using Eq. 4.59b for error calculation, Eq. 4.59a for coefficient (weight) upgradation and considering $m(-1) = 0$, $m(-2) = 0$ as causal we can write

For $n = 0$,

$$\begin{aligned} e(0) &= m(0) - \hat{h}_1(0)m(0-1) - \hat{h}_2(0)m(0-2) \\ &= 1 - 0 \times 0 - 0 \times 0 = 1 \\ \hat{h}_1(1) &= \hat{h}_1(0) + 0.1m(0-1)e(0) \\ &= 0 + 0.1 \times 0 \times 1 = 0 \\ \hat{h}_2(1) &= \hat{h}_2(0) + 0.1m(0-2)e(0) \\ &= 0 + 0.1 \times 0 \times 1 = 0 \end{aligned}$$

For $n = 1$,

$$\begin{aligned} e(0) &= m(1) - \hat{h}_1(1)m(1-1) - \hat{h}_2(1)m(1-2) \\ &= 2 - 0 \times 1 - 0 \times 0 = 2 \\ \hat{h}_1(2) &= \hat{h}_1(1) + 0.1m(1-1)e(1) \\ &= 0 + 0.1 \times 1 \times 2 = 0.2 \end{aligned}$$

$$\begin{aligned}\hat{h}_2(2) &= \hat{h}_2(1) + 0.1m(1-2)e(1) \\ &= 0 + 0.1 \times 0 \times 2 = 0\end{aligned}$$

For $n = 2$,

$$\begin{aligned}e(2) &= m(2) - \hat{h}_1(2)m(2-1) - \hat{h}_2(2)m(2-2) \\ &= 3 - 0.2 \times 2 - 0 \times 1 = 2.6 \\ \hat{h}_1(3) &= \hat{h}_1(2) + 0.1m(2-1)e(2) \\ &= 0.2 + 0.1 \times 2 \times 2.6 = 0.72 \\ \hat{h}_2(3) &= \hat{h}_2(2) + 0.1m(2-2)e(2) \\ &= 0 + 0.1 \times 1 \times 2.6 = 0.26\end{aligned}$$

For $n = 3$,

$$\begin{aligned}e(3) &= m(3) - \hat{h}_1(3)m(3-1) - \hat{h}_2(3)m(3-2) \\ &= 4 - 0.72 \times 3 - 0.26 \times 2 = 1.32 \\ \hat{h}_1(4) &= \hat{h}_1(3) + 0.1m(3-1)e(3) \\ &= 0.72 + 0.1 \times 3 \times 1.32 = 1.116 \\ \hat{h}_2(4) &= \hat{h}_2(3) + 0.1m(3-2)e(3) \\ &= 0.26 + 0.1 \times 2 \times 1.32 = 0.524\end{aligned}$$

For $n = 4$,

$$\begin{aligned}e(4) &= m(4) - \hat{h}_1(4)m(4-1) - \hat{h}_2(4)m(4-2) \\ &= 5 - 1.116 \times 4 - 0.524 \times 3 = -1.036 \\ \hat{h}_1(5) &= \hat{h}_1(4) + 0.1m(4-1)e(4) \\ &= 1.116 + 0.1 \times 4 \times (-1.036) = 0.7016 \\ \hat{h}_2(5) &= \hat{h}_2(4) + 0.1m(4-2)e(4) \\ &= 0.524 + 0.1 \times 3 \times (-1.036) = 0.2132\end{aligned}$$

Example 4.11

Derive the expression for maximum signal to quantization noise ratio for a sinusoidal message input. Waveform coding is to be done by Delta Modulator under no slope overload condition.

Solution

Consider, input $m(t) = A \cos \omega t$ From Eq. (4.60) for no slope overload,

$$\begin{aligned}\frac{S}{T} &> \left| \frac{d(A \cos \omega t)}{dt} \right|_{\max} \\ \text{or } \frac{S}{T} &> -A\omega \sin \omega t \Big|_{\max} = A\omega \\ \text{or } \frac{A}{S} &> \frac{1}{\omega T} \quad (4.65)\end{aligned}$$

Signal energy = $A^2/2$ (since, sinusoidal), Noise energy = $S^2/3$ (from Eq. 4.61)

Example 4.12

Determine maximum SNR for a DM system that samples a 400 Hz sinusoid with a sampling rate of (a) 8 kHz and (b) 16 kHz when no post reconstruction filter is used. (c) Repeat above if a 1 kHz low pass post reconstruction filter is used assuming quantization noise is uniform over frequency band 0 to sampling frequency.

Solution

Substituting in Eq. (4.64),

(a) $f=400, f_s=8000, \text{SNR}|_{\max} = 15.1892 = 11.8179 \text{ dB}$

(b) $f=400, f_s=16000, \text{SNR}|_{\max} = 60.7927 = 13.8385 \text{ dB}$

(c) Use of post reconstruction low pass filter effectively reduces quantization noise. Since, noise is distributed uniformly, use of filter reduces it by a factor of (f_c/f_s) where f_c is cut-off frequency of the LPF. Also noise goes to denominator of Eq. (4.64) which, we can rewrite for this case as

$$\text{SNR}|_{\max} = \frac{3f_s^2}{8\pi^2 f^2} \left(\frac{f_s}{f_c} \right) = \frac{3f_s^3}{8\pi^2 f^2 f_c} \quad (4.68)$$

(d) Substituting, for $f=400, f_s=8000, \text{SNR}|_{\max} = 121.5854 = 20.8488 \text{ dB}$

for $f=400, f_s=16000, \text{SNR}|_{\max} = 972.6834 = 29.8797 \text{ dB}$

SELF-TEST QUESTION

13. The objective behind DPCM coding is to reduce the variance of the signal to be encoded. Is that correct?
14. Is it true that an FIR digital filter is always stable because its impulse response is finite?
15. The slope overload error in DM can be reduced by increasing (a) step size, (b) sampling frequency, (c) both. Which one is correct?
16. Is the step size in ADM variable?

4.8 VOICE CODERS (VOCODERS)

Suppose we listen, in turns, to one person after another pronouncing a word or a sequence of words. One has a high-pitched voice, another a low pitch. One speaks with a foreign accent, another has no accent. One enunciates clearly, another slurs words and so on. Yet we understand each speaker. These considerations make it clear that there is a variability (within limits) that can be allowed in the waveform that must impinge on a listener's ear before there appears a loss of recognition of the spoken word. It therefore occurs to us that to transmit speech we need not transmit the precise waveform generated by the speaker. Rather we can transmit information from which a waveform can be reconstructed at the receiver which is only similar to, rather than identical to, the waveform generated by the speaker. We anticipate that by allowing ourselves this latitude, we can operate a digital source coded transmission system at a lower bit rate. This expectation is indeed borne out. The source coders employed are called *vocoders* (voice coders) and they operate at a significantly lower bit rate than even ADM. Typically, vocoder bit rates are in the range 1.2 to 2.4 kb/s. However, the resulting reproduced voice has a synthetic-sounding and a somewhat artificial quality. As a result, vocoders are employed for special applications where it is acceptable to trade speech quality for the advantage of low bit rate. Applications are found in military communications, operator recorded messages, etc.

The people who developed vocoders studied and took account of the physiology of the vocal cords, the larynx, the throat, the mouth and the nasal passages, all of which have a bearing on speech generation. They also studied the physiology of the ear and the psychology associated with the

manner in which the brain interprets sounds heard. A discussion of these matters is, however, beyond the scope of this text and the interested reader should see the references⁵.

Voice Model

It appears that speech consists of, or, at least, can be well approximated by a sequence of *voiced* and *unvoiced* sounds that are passed through a filter. The voiced sounds are sounds that are generated by the vibrations of the vocal cords. The unvoiced sounds are generated when a speaker pronounces such letters as; “s” , “f” , “p” , etc. In this latter case the sounds are formed by expelling air through lips and teeth. A generalized representation of a vocoder is shown in Fig. 4.46. The filter represents the effect, on the generated sounds, of the mouth, throat and nasal passages of the speaker. In the vocoder, the voiced sounds are simulated by an impulse generator whose frequency is the fundamental frequency of vibration of the vocal cords. The unvoiced sounds are simulated by a noise source. Altogether, all vocoders employ the scheme shown in Fig. 4.46 to generate a synthesized approximation to a speech waveform. They differ only in the techniques employed to generate the voiced and unvoiced sounds and in the characteristics, and design of the filter.

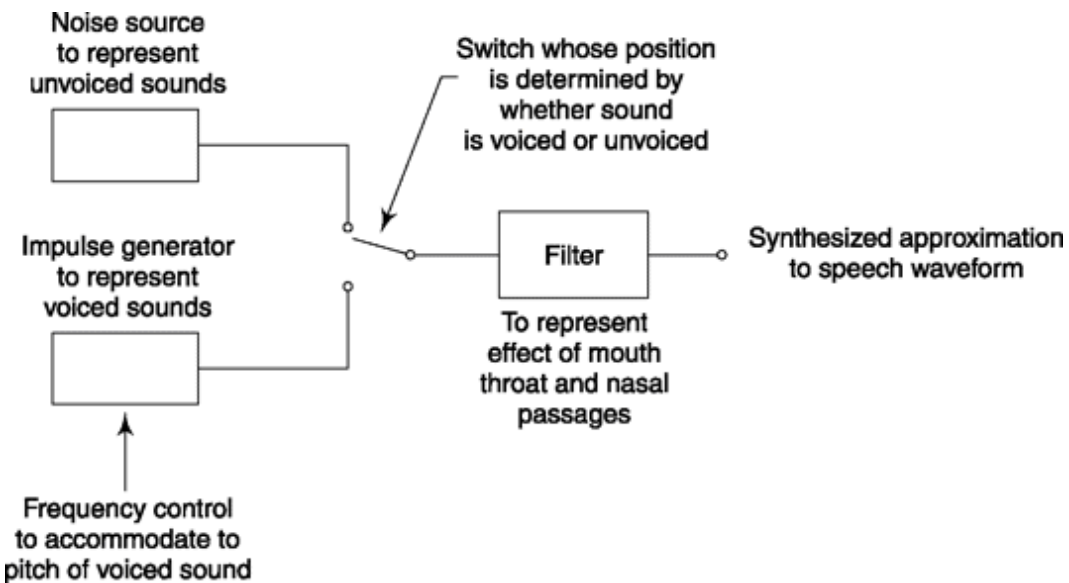


Fig. 4.46 Speech model used in vocoders.

4.8.1 Channel Vocoder

One of the many vocoder systems is the *channel vocoder* shown in Fig. 4.47. In this encoding system, the spectrum of the input speech is divided into 15 frequency ranges each of bandwidth 200 Hz. If the output of one of the bandpass filters were a sinusoidal waveform of fixed amplitude then the cascaded rectifier and 20 Hz low-pass filter would provide a dc voltage of magnitude proportional to that amplitude. In the real case represented in Fig. 4.47 each 20 Hz low-pass filter will provide instead a voltage which is proportional to the amplitude at the output of its associated 200 Hz bandpass filter.

Additionally, the input speech is applied to a frequency discriminator followed by a 20 Hz low-pass filter. When the signal is voiced, the output of the filter provides a voltage which is proportional to the voice frequency. This frequency is the *pitch* of the voice. The discriminator-filter combination is special in that when the speech is unvoiced the output of the filter is a smaller voltage than we encounter for voiced speech. Using a detector we can then determine, by noting the output of the discriminator-filter combination, whether the speech is voiced or unvoiced, and, if voiced, the voltage detected is determined by the pitch.

The outputs of the 16, 20 Hz low-pass filters are sampled, multiplexed and A/D converted. If the sampling is at the Nyquist rate of 40 samples/s (corresponding to signals of 20 Hz bandwidth) and if we use 3 bits/sample to represent each voltage sample, the bit rate is

$$R = 40 \frac{\text{samples/s}}{\text{filter}} \times 16 \text{ filters} \times 3 \text{ bits/sample}$$

$$= 1.9 \times 10^3 \text{ bits/s} \quad (4.69)$$

In any particular case the bit rate will depend on the number of low-pass filters, their passbands and the number of bits allowed per sample. Typical bit rates vary from 1.2×10^3 to 2.4×10^3 b/s.

At the vocoder receiver, as is to be seen in Fig. 4.47, the signal is demultiplexed and decoded, that is, converted back to analog form. Corresponding to each filter-rectifier combination at the en-

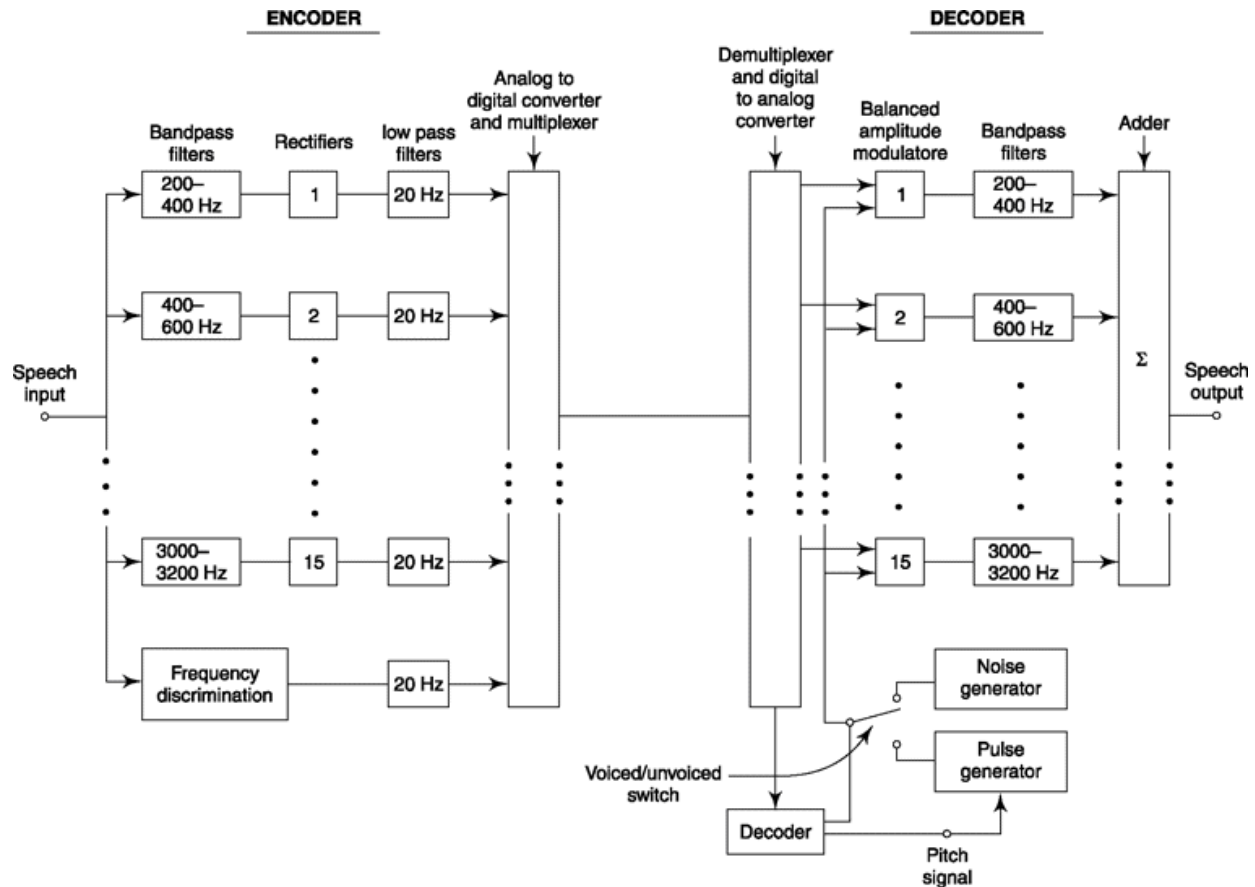


Fig. 4.47 Vocoder.

coder, there is provided, at the decoder, a balanced amplitude modulator and a bandpass filter with identical pass band. It will be recalled that a balanced modulator is a modulator that provides zero carrier output at zero modulation input. The carrier input to each modulator is the noise or pulse generator waveform. The modulation input is the amplitude signal (of each of the 15 rectifier-filters) provided by the encoder. At each sampling, the amplitude information is updated as is the information about whether the speech waveform is voiced or unvoiced and, if voiced, the pitch is provided by the discriminator.

Suppose, now, that in some sampling interval it happens that the speech is voiced and that the fundamental frequency of the generated sound is 450 Hz. This sound will generate an amplitude signal at the output associated with rectifier 2. The sound will have harmonics, so that there may be amplitude outputs at frequencies $2 \times 450 = 900$ Hz, $3 \times 450 = 1350$ Hz, etc., which will be seen at the outputs of rectifiers 4, 6, etc. The decoder will receive the information that the speech is voiced. Hence the decoder switch will connect to the pulse generator and the pulse generator frequency will be set to the

pitch of the voice. The pulse generator waveform then constitutes a carrier input to all modulators. However, only modulators 2, 4, 6, etc., will generate outputs. These outputs are amplitude modulated reproductions of the pulse-generator waveform and hence are comprised of a fundamental and a succession of harmonics. However, the filter following modulator 2 will suppress all except the fundamental, the filter following modulator 4 will suppress all except the second harmonic, etc. All these waveforms are added and the resultant output waveform consists of a combination of a fundamental and harmonics with the same relative amplitudes as existed in the speech input. When the speech input is unvoiced the sound is noiselike and its spectrum extends through the entire speech-frequency range although not necessarily in a uniform manner. In this case we can expect that all paths in the encoder will provide an output as will all paths in the decoder.

It is interesting to note that a vocoder can also be designed which transmits only the largest envelope detector outputs, completely ignoring the remaining outputs. For example if the largest three outputs are sent, 4 bits/filter \times 3 filters = 12 additional bits would be transmitted to tell the receiver which three filter outputs are sent. In this case, the bit rate becomes

$$R = 40 \frac{\text{samples/s}}{\text{filter}} \times 3 \text{ filters} \times 3 \text{ bits/sample} + 40 \text{ samples/s} \times \frac{12 \text{ bits}}{\text{sample}} \\ = 840 \text{ bits/s} \quad (4.70)$$

Unfortunately, the quality of the signal is severely degraded. However, the bit rate is significantly reduced.

4.8.2 Linear Predictive Coder

We observe, referring to Fig. 4.47, that the mechanism by which we regenerate speech at the decoder is the following: We make available at the decoder a noise generator and a pulse generator. We provide to the decoder information about whether the speech is voiced or unvoiced and, if voiced, the pitch. The outputs of these sound generators, i.e. the noise and pulse generator, are then passed through a *filter* with *adjustable parameters*. The filter is composed of the amplitude modulators and band pass filters. The adjusting signals are the modulating inputs to the modulators. These signals determine the relative proportions of fundamental and harmonics which are combined at the decoder output.

It occurs to us that we can improve the performance of the vocoder system in the following ways: First, let us employ a filter which has a greater versatility in its ability to be adjusted. Next, let us make this same filter available at the encoder. We shall then be able to regenerate the speech not only at the decoder but at the encoder as well. Thus the encoder will be able to “hear” how the speech will sound when regenerated at the decoder. Finally let us compare, at the encoder, the original speech and its regenerated version and, as in any feedback control system, use the differences, i.e. the error signal that appears, to adjust the filter parameters to minimize the error.

The *linear predictive coder* shown in Fig. 4.48 operates in this manner. As in the simpler encoder, a frequency discriminator and other hardware is provided to make available a pitch and a voiced-unvoiced signal. A single rectifier and filter is used to generate just one amplitude signal. We also provide the hardware necessary to regenerate the speech, that is a pulse generator, a noise generator, a switch, and a balanced modulator. The signal which is used to adjust the parameters of the adjustable filter is the difference (error) signal between the original speech and its regenerated form as it is formed at the filter output. This error signal is applied to a device which calculates and generates the signals which need to be applied to the adjustable filter to minimize the error signal. The decoder is shown in Fig. 4.49. It receives the amplitude, voiced-unvoiced and pitch signals. These are used in connection with the modulator, and pulse and noise generators, as at the encoder, to provide an input to the adjustable filter. The filter-parameter adjusting signals are also received and are used, as at the encoder, to adjust the filter characteristics for optimum voice regeneration.

Not explicitly shown in Figs 4.48 and 4.49, but nonetheless to be understood is that, as in the simpler vocoder of Fig. 4.47, the transmitted signal must be the time-division multiplex of the individual signals to be transmitted. Typically, 18 filter-adjusting signals a_t are employed. If, as before we sample at the rate 40 samples/s and encode each sample value into three bits, the bit rate R is

$$\begin{aligned} R &= (18 + 3) \text{ signals} \times 40 \frac{\text{sample/s}}{\text{signal}} \times 3 \text{ bits/sample} \\ &= 2.52 \text{ kb/s} \end{aligned} \tag{4.71}$$

4.8.3 Multi-Pulse Excited linear Prediction (MPLP or MPE)

The Multi-Pulse Excited Linear Prediction (MPLP or MPE) uses an excitation sequence that consists of multiple non-uniformly spaced pulses (Fig. 4.50). During analysis at encoder stage both amplitude and locations of the pulses are determined such that error (weighted mean square error) is minimized. The weights are derived from perceptual aspect of speech and the error is the difference between original speech and replica of synthetic speech at analysis side. For this reason, this approach is also known as Analysis by Synthesis (AbS) method. The multipulse algorithm typically uses 4-6 pulses every 5 ms. The synthesis filter uses both short term and long term predictor to produce synthetic speech. The short term predictor is usually of 10th order while long term predictor works on the residual of that. Assuming the speech signal as stationary, the free parameters of synthesis filter is calculated from first 10-30 ms of actual speech input which is open loop. Error minimization is done in close loop for 5-15 ms subframes of speech that addresses the non-stationarity of speech. The decoder receives quantized synthesis filter parameters and quantized excitation parameters from the encoder and uses them to produce the synthetic speech at receiver side that mimics the original speech input at encoder. Medium rate (9.6 kbps) MPLP coder gives good toll quality audio.

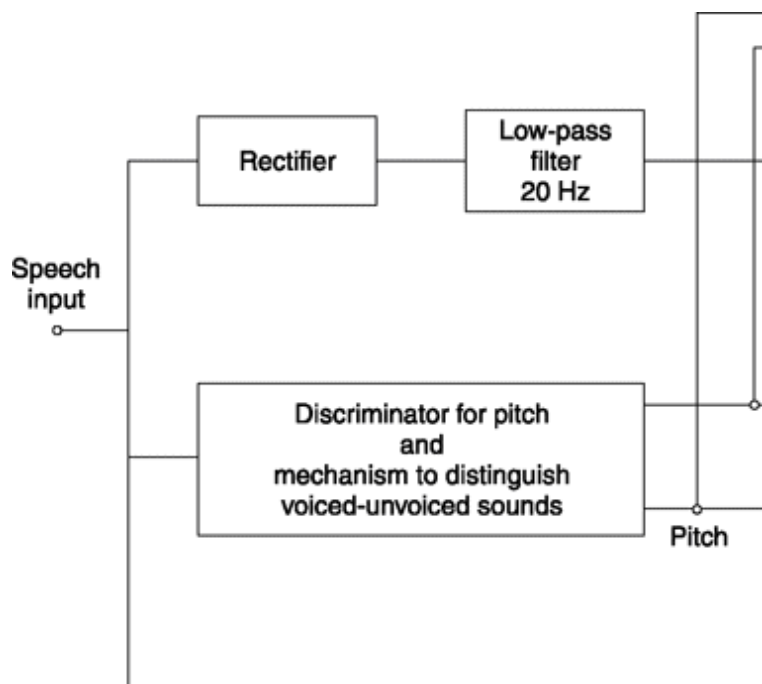


Fig.4.48 A simplified linear predictive encoder.

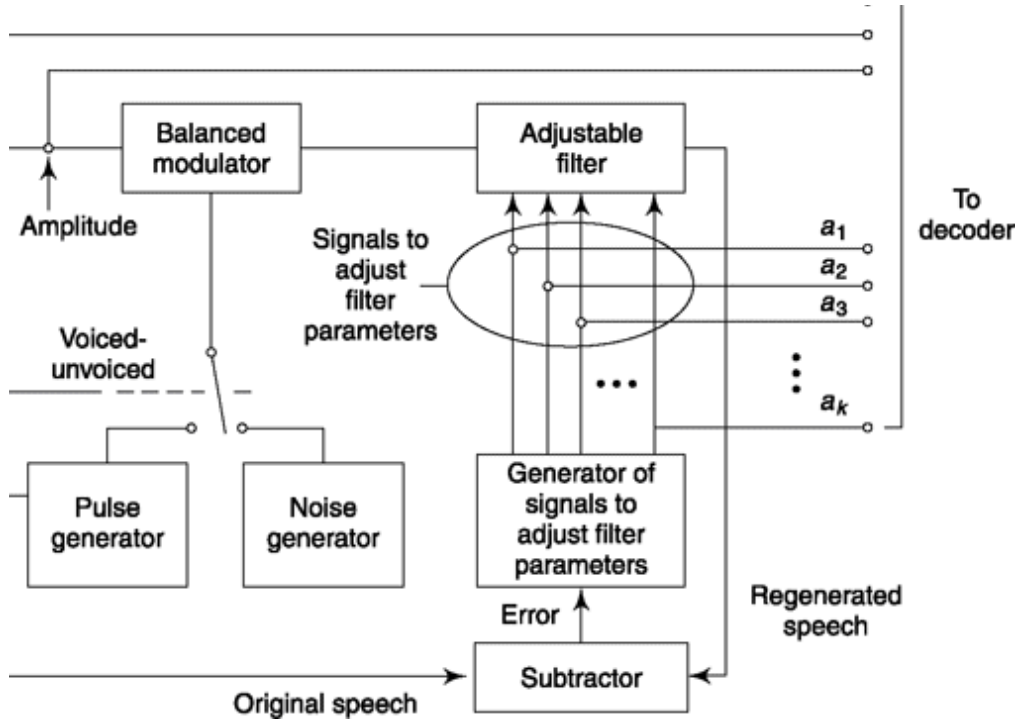


Fig. 4.49 A simplified linear predictive decoder.

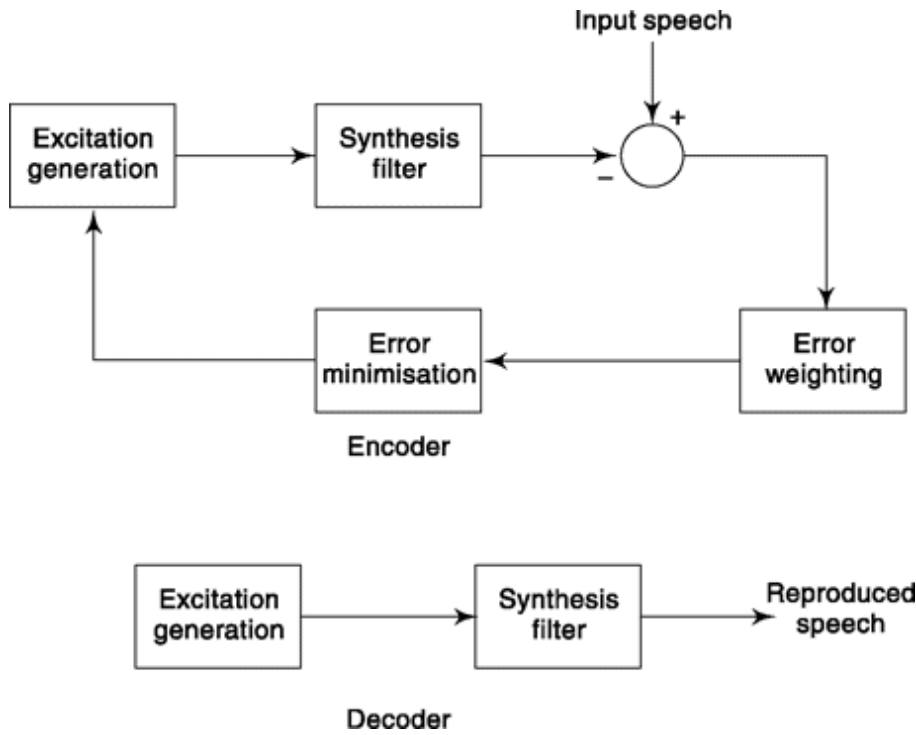


Fig.4.50 Analysis by synthesis scheme of MPLP codec.

Regular Pulse Excited (RPE) coder-decoder is similar to MPLP but there the pulse intervals are common within a frame. A typical spacing for RPE is 3 to 4 and location of first pulse is updated every 5 millisecond. Its

amplitude is determined by solving a set of linear equations. RPE at 13 kbps can give toll quality speech.

4.8.4 Code-Excited Linear Prediction (CELP)

The MPLP and RPE scheme are good for medium rate of data transmission but inadequate for lower bit rate. This is due to the large amount of information that must be transmitted about the excitation pulses positions and amplitudes. Any attempt to reduce the bit rate by using fewer pulses, or coarsely quantizing their amplitudes deteriorates the reconstructed speech quality rapidly. Code-Excited Linear Prediction is a popular technique for low bit rate coding which too follows Analysis by Synthesis approach. This encodes the excitation using a codebook of Gaussian sequences which is supposed to represent typical residues of the synthesis filter (Fig. 4.51). The codebooks are usually large and could be 1024 vectors each of 5 ms length. The codebook when divided into two blocks has one fixed that represents the Gaussian or stochastic input and the other adaptive which adapts to the speech input. A gain factor following it, scales the excitation sequence which is fed to synthesis filter that has short and long term predictors. The code vector is chosen in an optimal manner that minimizes perceptually weighted mean square error. The adaptive codebook first finishes updating and then fixed codebook is chosen. Speech quality in CELP coder can be enhanced by doing post-processing on speech sequence. This uses long and short term filters in cascade and emphasizes formant and pitch information. Fast algorithms are needed to reduce the computational overload for appropriate code vector search. Fig. 4.51 shows a typical CELP decoder. The encoder uses this decoder in synthesis stage followed by a synthesis filter block comprising of short and long predictor. This output is used to calculate error comparing input speech which is fed to a perceptually weighted MSE calculation block that in turn optimizes different parameters.

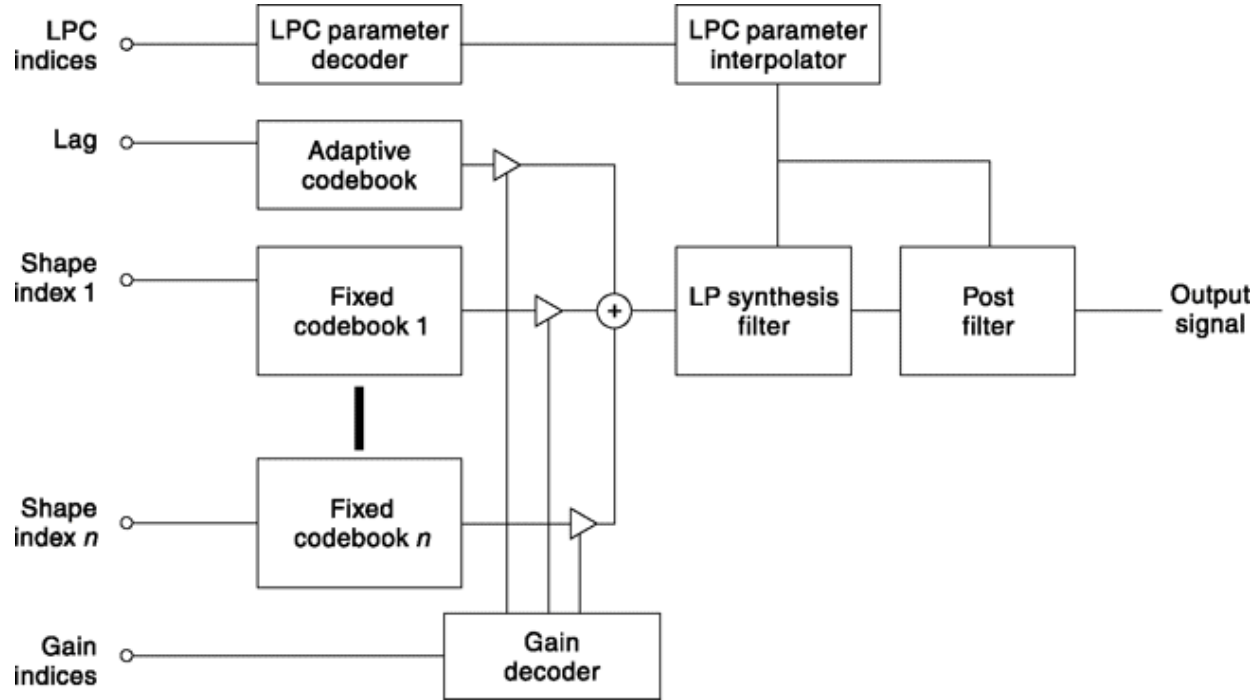


Fig. 4.51 A typical CELP decoder.

Thus, what needs to be transmitted from CELP coder is the codebook index that is represented by 10 bits (for codebook size of 1024 entries) and the gain parameter that is coded with about 5 bits. This makes bit rate necessary to transmit the excitation information to around 15 bits compared to the 47 bits used for example in RPE codec. A bit rate of 4.8 kbps gives toll grade quality for CELP codec. At the receiver a copy of the codebook is available which is selected by the index arrived. A synthesis filter is used to produce synthetic version of original speech which is further processed by post processing filter to improve the quality.

4.8.5 Mixed Excitation Linear Prediction (MELP)

Traditional LPC based vocoders discussed before, if subjected to low bit rates compromises audio quality to a great extent as it sounds mechanical or buzzy and may have in between thumping or tonal noises. This is due to the inadequacy of two state excitation models specially during voicing transitions. The MELP vocoder, besides traditional LPC parametric model has components like (i) Mixed pulse and noise excitation, (ii) Periodic or aperiodic impulses, (iii) Adaptive spectral enhancement, (iv) Pulse spreading filter, and (v) Fourier magnitude calculation of residual. Mixed excitation aims to reduce the noise and is implemented by a multiband mixing model. This model uses adaptive technique to simulate frequency dependent voicing information. For voiced speech synthesis, aperiodic pulses are used near transition regions and periodic pulses for other places. Pulse spreading filter reduces the harshness of synthetic speech by spreading the excitation energy within a pitch period. The adaptive spectral enhancement filter enhances formant structure in the synthetic speech and is based on the poles of LPC vocal tract filter. The first ten Fourier magnitudes of the residuals are used to enhance perceptual quality of speech derived from lower frequency region. Note that, Line Spectral Pair (LSP), also called Line Spectral Frequencies (LSF) is used to represent LPC coefficients for transmission as it is less sensitive to quantization. The whole scheme in block diagram form is shown in Fig. 4.52.

Some of the specifications for above blocks are given next. For Analyzer, the filter is a 4th order Chebychev, Type II filter with cutoff frequency 60 Hz (note that in US power line frequency is 60 Hz), Bandpass voicing analysis is done by five 6th order Butterworth filters in frequency bands : 0–500 Hz, 500–1000 Hz, 1000–2000 Hz, 2000–3000 Hz, 3000–4000 Hz. The LPC analysis filter is of 10th order. In synthesizer, the pulse generator uses pitch information while noise generator uses a random number generator. Pulse filters are sum of band pass filters having coefficients for voiced frequency bands while noise filter is similar but meant for unvoiced frequency bands. Adaptive spectral enhancement filter is a 10th order IIR filter and pulse dispersion filter is a 65th order FIR filter derived from spectrally flattened triangular pulse. The calculation of bit rate for MELP is as follows. For each 22.5 ms frame of 8 kHz sampled speech, pitch index is coded by 7 bits, jitter flag 1, bandpass voicing decision 4, gain 8, ten line spectrum pairs of frequencies 25, Fourier magnitude for ten harmonics 8, synchronization bit 1. This makes total 54 bits per frame. Thus bit rate required = $54 \times 1000/22.5 = 2400$ bits/second.

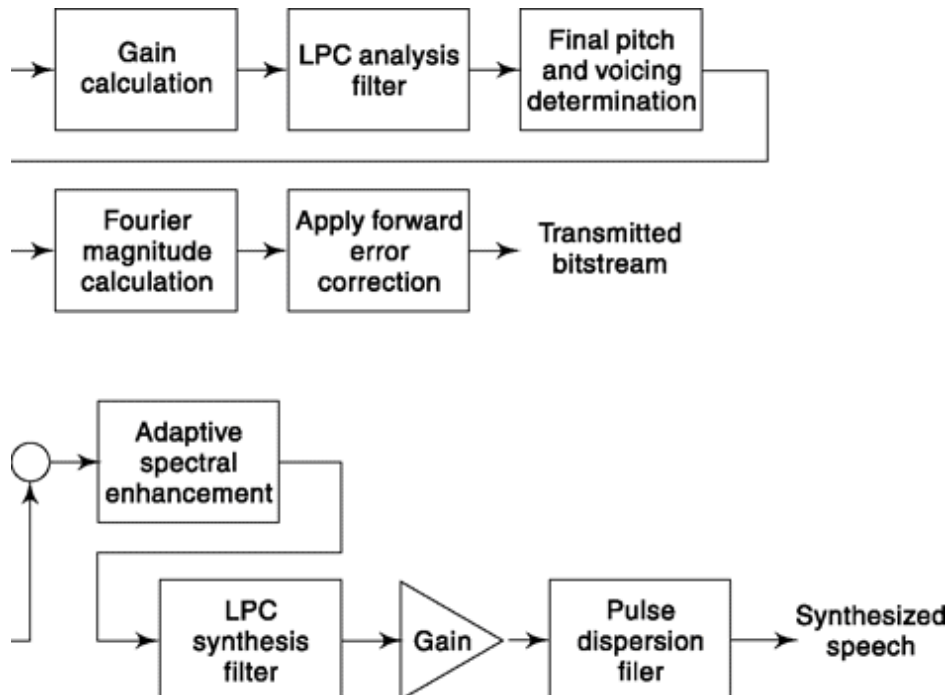
SELF-TEST QUESTIONS

17. Vcoders are different from waveform coders like PCM, DPCM as they emphasize on perceptual aspect of speech and not on faithful representation of waveform. Is that correct?
18. In LPC or analysis by synthesis system, encoder is such that it is able to hear how speech will sound at the decoder. How far is this true?
19. What is the basic difference between MPLP and RPE codecs?
20. The codebook search is a major deterrent for fast implementation of CELP. Is that correct?

FACTS AND FIGURES

The prospect of artificial production of human speech excited researchers for long. In 1779, a model of the human vocal tract was given by Christian Kratzenstein that could produce five vowel sounds:

Fig. 4.52 *Encoding and decoding of MELP.*



‘a’, ‘e’, ‘i’, ‘o’ and ‘u’. In 1791, Wolfgang Kempelen presented a bellows-operated ‘Acoustic-Mechanical Speech Machine’ that used an improved model to produce vowels and consonants. Though Kempelen is regarded as a pioneer in phonetics, during his lifetime he was more famous for his invention, the *Turk*. This was an automatic chess-playing machine, first unveiled in 1769, but later it turned out to be a hoax.

Homer Dudley was born in 1896 and started his career as a school teacher. However, he found it difficult to control students in class and looked for an alternative career. After taking courses on the then new area of ‘electronic engineering’ at Pennsylvania State University, he got employment in Bell Laboratories. Here he started experimenting with human speech in 1928. Dudley gets the credit of being the first to produce speech from an electronic system named VODER (Voice Operated Demonstrator) and was granted a patent in 1938. VODER was demonstrated as a Bell Laboratory exhibit to the public in the 1939 New York World’s Fair, where according to a report, “A girl stroked its keys and it emitted recognizable speech. No human vocal cords entered into the procedure at any point; the keys simply combined some electronically produced vibrations and passed these on to a loudspeaker.”

MATLAB

```
%Experiment 20

% This experiment shows how Nyquist rate affects sampling

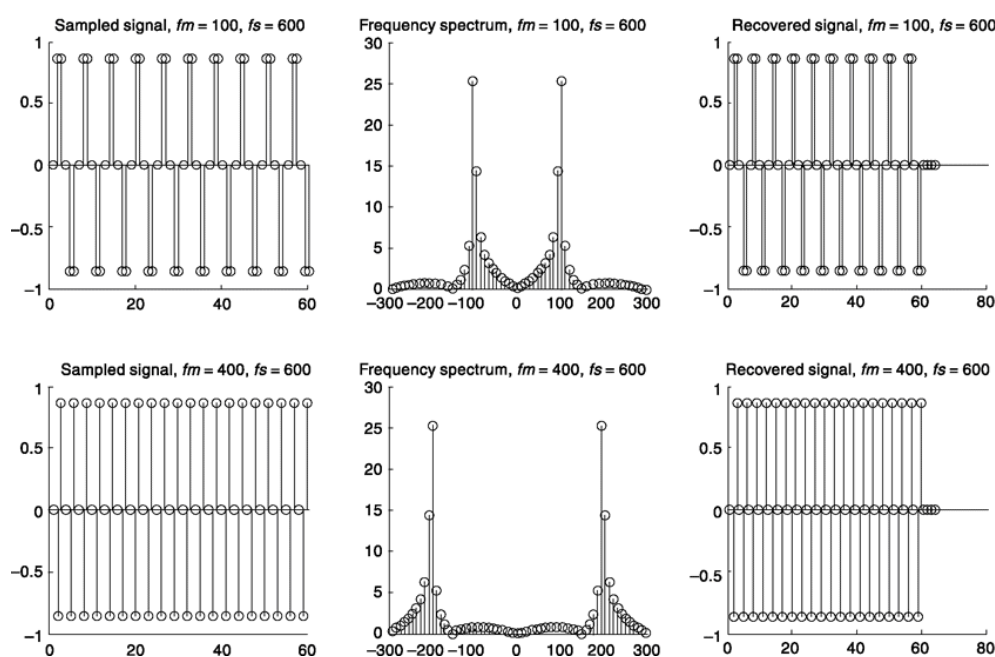
% Oversampling : fs > 2fm

fm=100;
fs=600; t=0:1/fs:((10/fm)-(1/fs)); %10 cycles 60 samples
x = sin(2*pi*fm*t); fx=fft(x,64); xr=ifft(fx,64); %inv fft generates
64 samples
f=(-31*fs/64):(fs/64):(32*fs/64); fx =[fx(34:64) fx(1:33)];
subplot(231),stem(x),title('sampled signal, fm=100, fs=600');
subplot(232),stem(f, abs(fx)), axis([-300 300 0 30]);
title('frequency spectrum, fm=100, fs=600');
subplot(233),stem(xr),title('recovered signal, fm=100, fs=600');

% Undersampling : fs < 2fm

fm=400; x = sin(2*pi*fm*t);
fx=fft(x, 64); xr=ifft(fx, 64); fx =[fx(34:64) fx(1:33)];
subplot(234),stem(x),title('sampled signal, fm=400, fs=600');
subplot(235),stem(f, abs(fx)),axis([-300 300 0 30]);
title('frequency spectrum, fm=400, fs=600');
subplot(236),stem(xr),title('recovered signal, fm=400, fs=600');
```

You can play with fm and fs. Change fm = 500 Hz in above. You will see a frequency spectrum which is exactly same as that of fm = 100 Hz case. Since, we have used 64 point FFT and IFFT on data of length 60, the last 4 value comes as zero in recovered signal. This is because the FFT process pads zero if data length is smaller.



```

% Experiment 21

% Pulse Width Modulation
% Y = MODULATE(X,Fc,Fs,'pwm')
% Input X must be within range [0,1]

fc=1000;      % Carrier frequency
fs=10000;     % Carrier frequency
f1=200; f2=300; % First single tone message signal and then combined

t=0:1/fs:((2/f1)-(1/fs));    %Gives exact two cycles of modulating signal f1
x1=0.4*cos(2*pi*f1*t)+0.5;  % single tone meassage 1 to be [0,1]
x2=0.2*(cos(2*pi*f1*t)+cos(2*pi*f2*t))+0.5; %combined, message 2 to be [0,1]

% Modulation

y1=modulate(x1,fc,fs,'pwm');
subplot(421);plot(x1); title('original single tone message,f1=500, fs=10000')
subplot(422);plot(y1); axis([0 500 -0.2 1.2]);
title('PWM, one cycle of f1, fc=1000,f1=200')
fx1 = abs(fft(y1,1024)); fx1 =[fx1(514:1024) fx1(1:513)];
f=(-511*fs/1024):(fs/1024):(512*fs/1024);
subplot(424);plot(f,fx1); title('freq. description PWM,single tone,fc=1000')

% Demodulation

x1_recov=demod(y1,fc,fs,'pwm'); subplot(423);plot(x1_recov);
title('time domain recovered, single tone, f1=200')

% modulation demodulation for combined signal

y2=modulate(x2,fc,fs,'pwm'); fx2 = abs(fft(y2,1024));
subplot(425),plot(x2);title('combined original,f1=200,f2=300,fs=10000');
subplot(426),plot(y2); axis([0 500 -0.2 1.2]);
title('combined PWM,f1=200,f2=300,fc=1000');
fx2 =[fx2(514:1024) fx2(1:513)];subplot(428);plot(f,fx2);
title('freq. description, combined, fc=1000')
x2_recov=demod(y2,fc,fs,'pwm'); subplot(427);plot(x2_recov);
title('time domain recovered, combined, f1=200,f2=300')

% Experiment 22

% Pulse Position Modulation
% Y = MODULATE(X,Fc,Fs,'ppm')

```

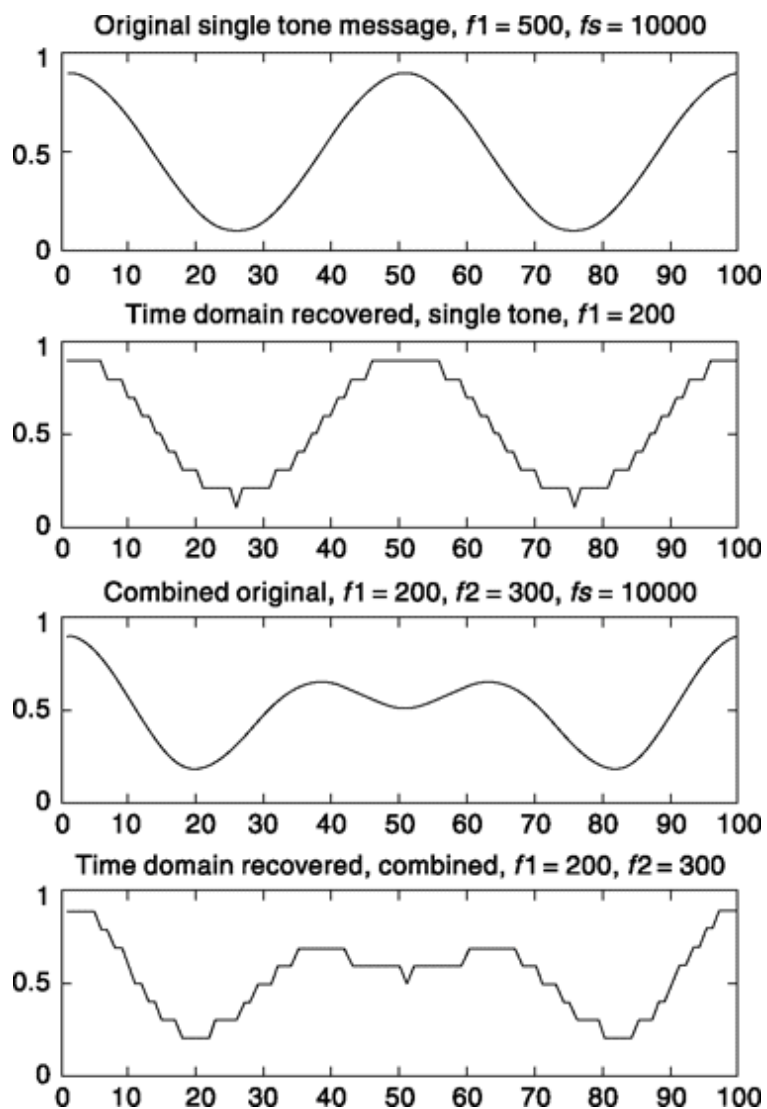
In program written for PWM, replace 'pwm' by 'ppm', save in a file say exp21.m and run. The ppm modulation and demodulation for single tone and mixed signal will be done. The figure generated will look as follows. Note the difference in frequency spectrum.

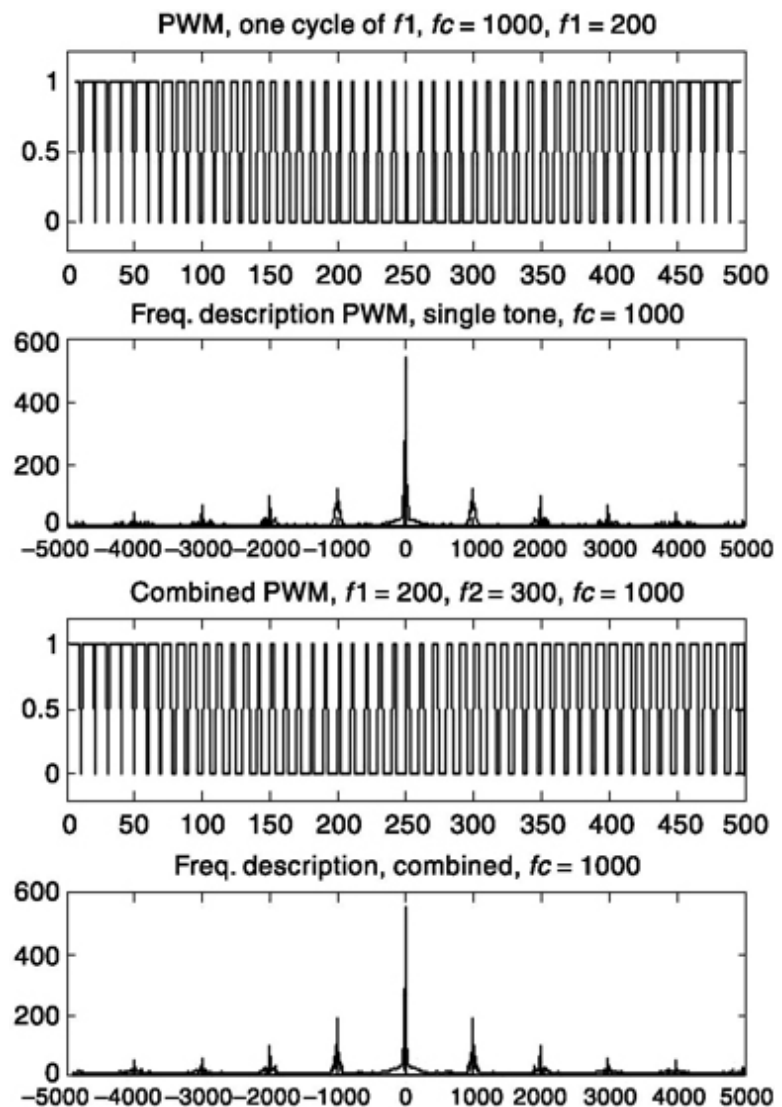
```

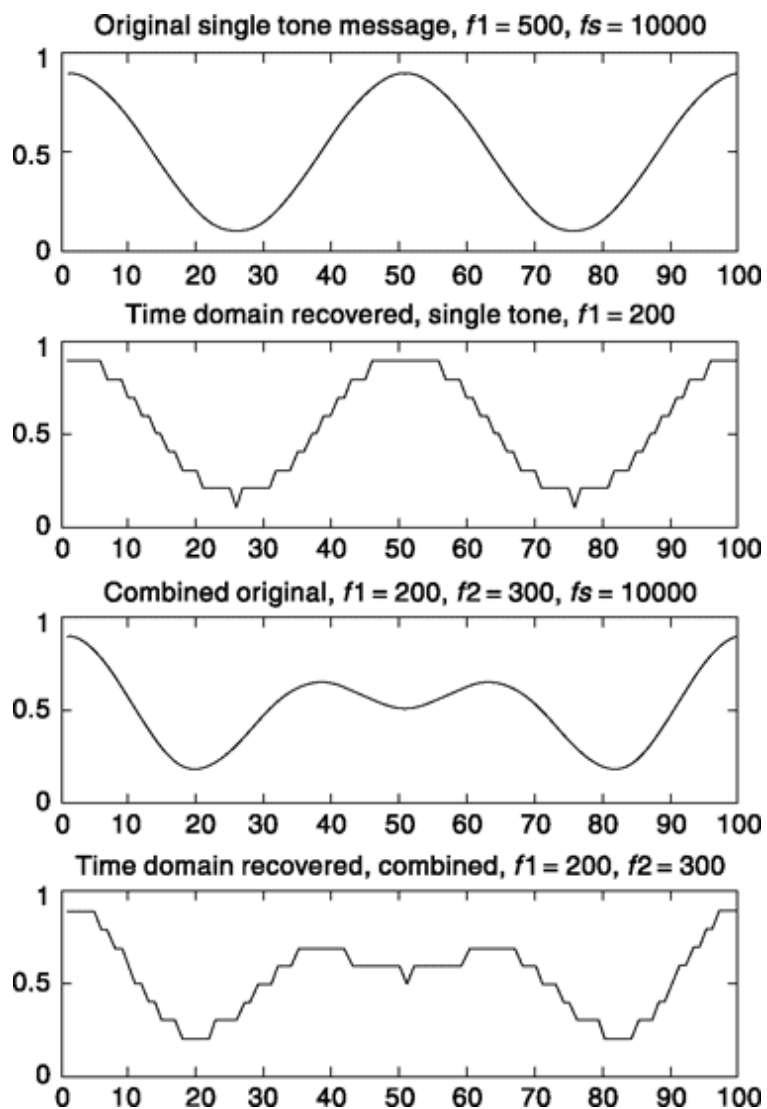
% Experiment 23

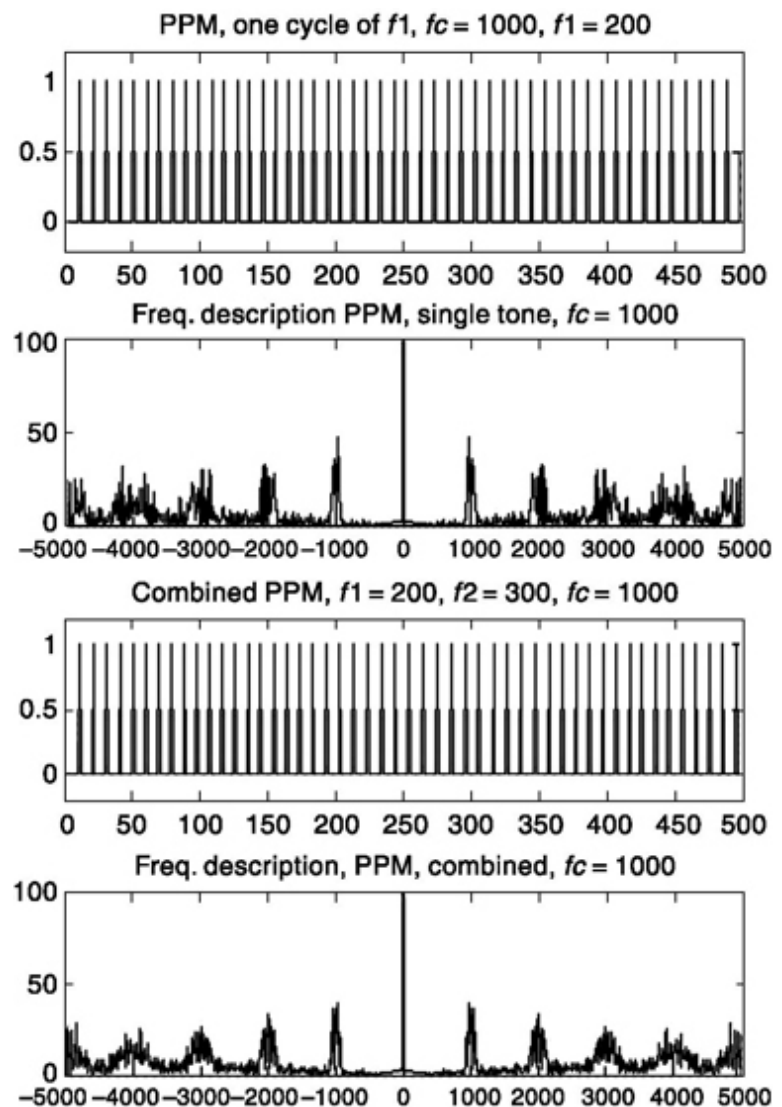
% This shows coding of a sinusoidal signal by delta modulation

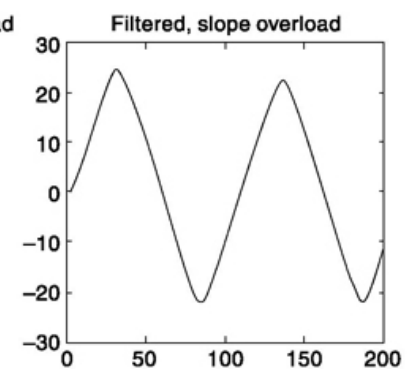
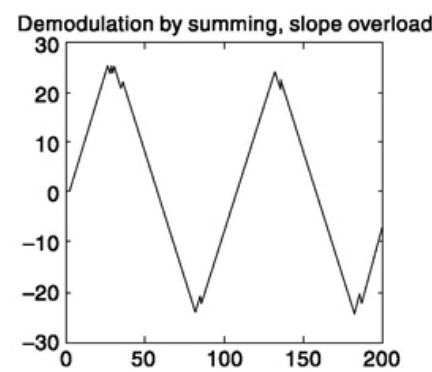
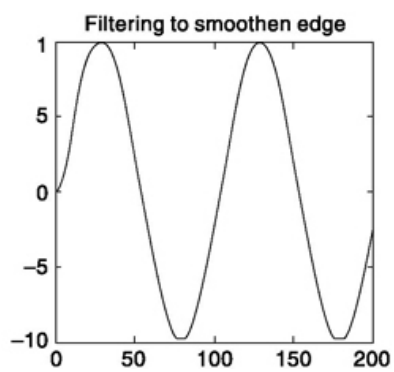
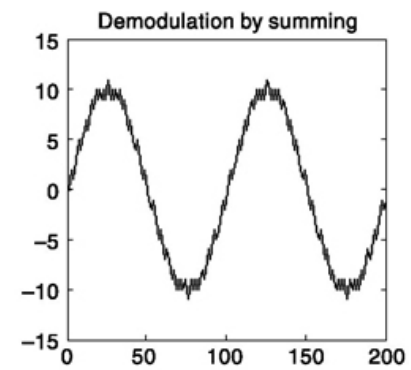
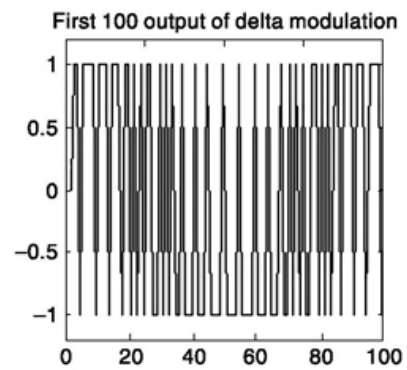
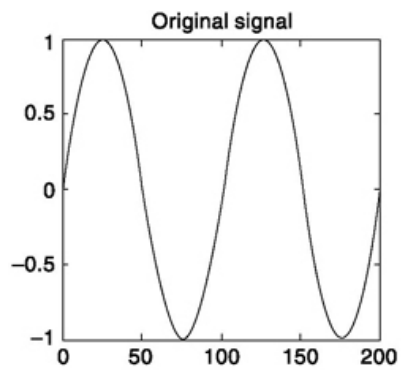
```











```

% It also shows slope overload cases

step=0.1;          % step size
fs=1000;           % dT=0.001, slope=step/dt=100
fm = 10; A=1;      % maximum slope=2*pi*fm*A=62.8, no slope overloading

t=0:1/fs:((2/fm)-(1/fs)); % Two cycles
x=A*sin(2*pi*fm*t); subplot(231), plot(x), title('original signal');

% Modulation

xq(1)=0; d(1)=0;
for n=2:length(x),
    d(n)=sign(x(n)-xq(n-1));
    xq(n)=xq(n-1)+d(n)*step;
end
subplot(232), plot(d(1:100)), axis([0 100 -1.2 1.2]);
title('First 100 output of delta modulation')

% Demodulation
y=0;
for n=2:length(d)
    y(n)=y(n-1)+d(n);
end;
subplot(233), plot(y); title('demodulation by summing');
xr=filter([0.125*ones(1,8)],1,y); %8th order moving average filter
subplot(234), plot(xr), title('filtering to smoothen edge')
A=2.5; x=A*x; %max. slope=2.5*62.8=157, slope overloading
% Modulation
xq(1)=0; d(1)=0;
for n=2:length(x),
    d(n)=sign(x(n)-xq(n-1)); xq(n)=xq(n-1)+d(n)*step;
end
% Demodulation y=0;
for n=2:length(d)
    y(n)=y(n-1)+d(n);
end;
subplot(235), plot(y); title('demodulation by summing, slope overload')
xr=filter([0.125*ones(1,8)],1,y);
subplot(236), plot(xr), title('filtered, slope overload')

```

SUMMARY

The chapter begins with a discussion on the need of transition towards digital communication systems and the role of repeaters. This is followed by a discussion on how to represent messages in the form of pulses. Sampling theorems for both low pass and band pass signals are discussed. The technique of representing message signal by modulating an attribute of sampled pulses like amplitude (PAM), width (PWM), position (PPM) are discussed with their merits and demerits. It is shown that PAM is ideally

suited for time division multiplexing (TDM) and digital encoding. Different digital encoding

schemes with related quantization errors are discussed. The role of linear prediction is highlighted. Standard voice coding schemes are presented which form the basis of digital voice communication. Numerical and MATLAB examples are used to enhance conceptual development.

PROBLEMS

- 4.1 It is required to transmit telephone messages across the United States, a 3000 mile run. The signal level is not to be allowed to drop below 1 millivolt before amplification and the signal is not to be allowed to be larger than 15 volts in order to avoid amplifier overload. Assuming that repeaters are to be located with equal spacings, how many repeaters will be required?
- 4.2 Consider a signal, say speech which is bandlimited to 4000 Hz. This is sampled at 8000 Hz and from this, 1000 samples are taken. If 1000-point DFT is computed, (i) what is the spacing between frequency samples, and (ii) what is the frequency in Hz for the 100th frequency sample?
- 4.3 Four samples of a sampled signal are {1, 1, 1, 0}. (i) Find its 4-point DFT. (ii) Perform IDFT on these DFT coefficients to get back the sampled signal. (iii) Perform zero padding and compute 8-point DFT of the sampled signal. (iv) Plot magnitude of DFT coefficients for both 4-point and 8-point DFT considering 1 kHz sampling rate.
- 4.4 Perform 16-point DFT on a sequence of samples given by $m_k = \left(\frac{1}{4}\right)^k$
- 4.5 The N -point DFT of a sampled sequence is available. How can you get L -point DFT from it?
- 4.6 A bandpass signal has a spectral range that extends from 20 to 82 kHz. Find the acceptable range of the sampling frequency f_s .
- 4.7 A bandpass signal has a center frequency f_0 and extends from $f_0 - 5$ kHz to $f_0 + 5$ kHz. The signal is sampled at a rate $f_s = 25$ kHz. As the center frequency f_0 varies from $f_0 = 5$ kHz to $f_0 = 50$ kHz find the ranges of f_0 for which the sampling rate is adequate.
- 4.8 The signal $v(t) = \cos 5\pi t + 0.5 \cos 10\pi t$ is instantaneously sampled. The interval between samples is T_s .
- (a) Find the maximum allowable value for T_s .
 - (b) If the sampling signal is $S(t) = \sum_{k=-\infty}^{\infty} \delta(t - 0.1k)$, the sampled signal $v_s(t) = v(t)S(t)$ consists of a train of impulses, each with a different strength $v_s(t) = \sum_{k=-\infty}^{\infty} I_k \delta(t - 0.1k)$. Find I_0 , I_1 , and I_2 and show that $I_k = I_{4+k}$.
 - (c) To reconstruct the signal $v_s(t)$ is passed through a rectangular low-pass filter. Find the minimum filter bandwidth to reconstruct the signal without distortion.
- 4.9 We have the signal $v(t) = \cos 2\pi f_0 t + \cos 2 \times 2\pi f_0 t + \cos 3 \times 2\pi f_0 t$. Our interest extends, however, only to spectral components up to and including $2f_0$. We therefore sample at the rate $5f_0$ which is adequate for the $2f_0$ component of the signal.
- (a) If sampling is accomplished by multiplying $v(t)$ by an impulse train in which the impulses are of unit strength, write an expression for the sampled signal.
 - (b) To recover the part of the signal of interest, the sampled signal is passed through a rectangular low-pass filter with passband extending from 0 to slightly beyond $2f_0$. Write an expression for the filter output. Is the part of the signal of interest recovered exactly? If we want to reproduce the first two terms of $v(t)$ without distortion, what operation must be performed at the very outset?

- 4.10 The bandpass signal $v(t) = \cos 10\omega_0 t + \cos 11\omega_0 t + \cos 12\omega_0 t$ is sampled by an impulse train $S(t) = I \sum_{k=-\infty}^{\infty} \delta(t - kT_s)$.

- (a) Find the maximum time between samples, T_s , to ensure reproduction without error.
- (b) Using the result obtained in (a), obtain an expression for $v_s(t) = S(t)v(t)$.
- (c) The sampled signal $v_s(t)$ is filtered by a rectangular low-pass filter with a bandwidth $B = 2f_0$. Obtain an expression for the filter output.
- (d) The sampled signal $v_s(t)$ is filtered by a rectangular bandpass filter extending from $2f_0$ to $4f_0$. Obtain an expression for the filter output.

- 4.11 The bandpass signal $v(t) = \cos 10\omega_0 t + \cos 11\omega_0 t + \cos 12\omega_0 t$ is sampled by an impulse train, $S(t) = I \sum_{k=-\infty}^{\infty} \delta(1 - k/8f_0)$. The sampled signal $v_s(t) = S(t)v(t)$ is then filtered by a rectangular low-pass filter having a bandwidth $B = 2f_0$. Obtain an expression for the filter output.

- 4.12 Let us view the waveform $v(t) = \cos \omega_0 t$ as a bandpass signal occupying an arbitrarily narrow frequency band. On this basis we find that the required sampling rate is $f_s = 0$. Discuss.

- 4.13 The TDM system shown in Fig. 4.8 is used to multiplex the four signals $m_1(t) = \cos \omega_0 t$, $m_2(t) = 0.5 \cos \omega_0 t$, $m_3(t) = 2 \cos 2\omega_0 t$ and $m_4(t) = \cos 4\omega_0 t$.

- (a) If each signal is sampled at the same sampling rate, calculate the minimum sampling rate f_s .
- (b) What is the commutator speed in revolutions per second.
- (c) Design a commutator which will allow each of the four signals to be sampled at a rate faster than is required to satisfy the Nyquist criterion for the individual signal.

- 4.14 Three signals m_1 , m_2 and m_3 are to be multiplexed. m_1 and m_2 have a 50 kHz bandwidth, and m_3 has a 10 kHz bandwidth. Design a commutator switching system so that each signal is sampled at its Nyquist rate.

- 4.15 Show that the response of a rectangular low-pass filter, with a bandwidth f_c , to the impulse function $I \delta(t - k/2f_c)$ is

$$S_R(t) = \frac{I\omega_c}{\pi} \frac{\sin \omega_c(t - k/2f_c)}{\omega_c(t - k/2f_c)}$$

Assume that in its passband the filter has $H(f) = 1$.

- 4.16 Four signals, $m_1(t) = 1 \cos \omega_0 t$, $m_2(t) = 1 \sin \omega_0 t$, $m_3(t) = -1 \cos \omega_0 t$ and $m_4(t) = -1 \sin \omega_0 t$ are sampled every $1/2f_0$ sec by the sampling function

$$S(t) = 1 \sum_{k=-\infty}^{\infty} \delta\left(t + \frac{k}{2f_0}\right)$$

The signals are then time-division multiplexed. The TDM signal is filtered by a rectangular low-pass filter having a bandwidth $f_c = 4f_0$ and then decommutated.

- (a) Sketch the four outputs of the decommutator.
- (b) Each of the four output signals is filtered by a rectangular low-pass filter having a bandwidth f_0 . Show that the four signals are reconstructed without error.

- 4.17 The four signals of Prob. 4.16 are sampled, as indicated in that problem, and time-division multiplexed. The TDM signal is filtered by a rectangular low-pass filter having a bandwidth $f_c = 2f_0$ and then decommutated. Sketch the output at the decommutator switch segment where the samples of $m_1(t)$ should appear and show that $m_1(t)$ cannot be recovered.

- 4.18 The signal $v(t) = \cos \omega_0 t + \cos 8\omega_0 t$ is sampled by using *natural sampling*.
- Determine the minimum sampling rate f_s .
 - Sketch $v_s(t) = S(t)v(t)$ if $S(t)$ is a train of pulses having unit height, occurring at the rate f_s ; and $S(t) = 1$ for $nT - \tau/2 \leq t \leq nT + \tau/2$. The pulse duration is $\tau = 1/32f_0$.
 - Repeat (b) if $\tau = 1/320f_0$
- 4.19 Show that an impulse function $I \delta(t)$ can be stretched to have a width τ by passing the impulse function through a filter $(1 - e^{-j\omega\tau})/j\omega$. Show that this operation is identical with integrating the impulse for τ sec, that is, that the output $v_o(t)$ is given by

$$v_o(t) = \begin{cases} \int_0^t I \delta(t) dt & 0 \leq t \leq \tau \\ = 0 & \text{otherwise} \end{cases}$$

- 4.20 For the quantizer characteristic shown in Fig. 4.23b.
- Plot the error characteristic $e = v_o - v_i$ versus v_i . Assume that $S = 1$, that is, $m_{k+1} - m_k = 1$ volt.
 - Since the error $e = v_o - v_i$ is periodic, it can be expanded in a Fourier series. Write the Fourier series for the error $e = e(v_i)$.
 - If $v_i = S \sin \omega_0 t$, find the component of the error e at the angular frequency ω_0 .
- 4.21 Show that if the signal is uniformly distributed, Eq. (4.36) results even if M is not large.
- 4.22 Consider a signal having a probability density

$$f(v) = \begin{cases} Ke^{-|v|} & -4 < v < 4 \\ 0 & \text{elsewhere} \end{cases}$$

- Find K .
 - Determine the step size S if there are four quantization levels.
 - Calculate the variance of the quantization error when there are four quantization levels. Do not assume that $f(v)$ is constant over each level. Compare your result with Eq. (4.36).
- 4.23 Consider a signal having a probability density

$$f(v) = K(1 - |v|) \quad -1 \leq v \leq 1$$

Calculate (a) to (c) of Prob. 4.22.

- 4.24 Show that the numbers 0 to 7 can be written using 3 binary digits (bits). How many bits are required to write the numbers 0 to 5?
- 4.25 Consider that the signal $\cos 2\pi t$ is quantized into 16 levels. The sampling rate is 4 Hz. Assume that the sampling signal consists of pulses each having a unit height and duration dt . The pulses occur every $t = k/4$ sec, $-\infty < k < \infty$.
- Sketch the binary signal representing each sample voltage.
 - How many bits are required per sample?
- 4.26 A D/A converter is shown in Fig. P4.26. Using the set-reset flip-flops shown explain the operation of the device.
- 4.27 An A/D converter is shown in Fig. P4.27. Using trigger flip-flops as indicated explain the operation of the device.

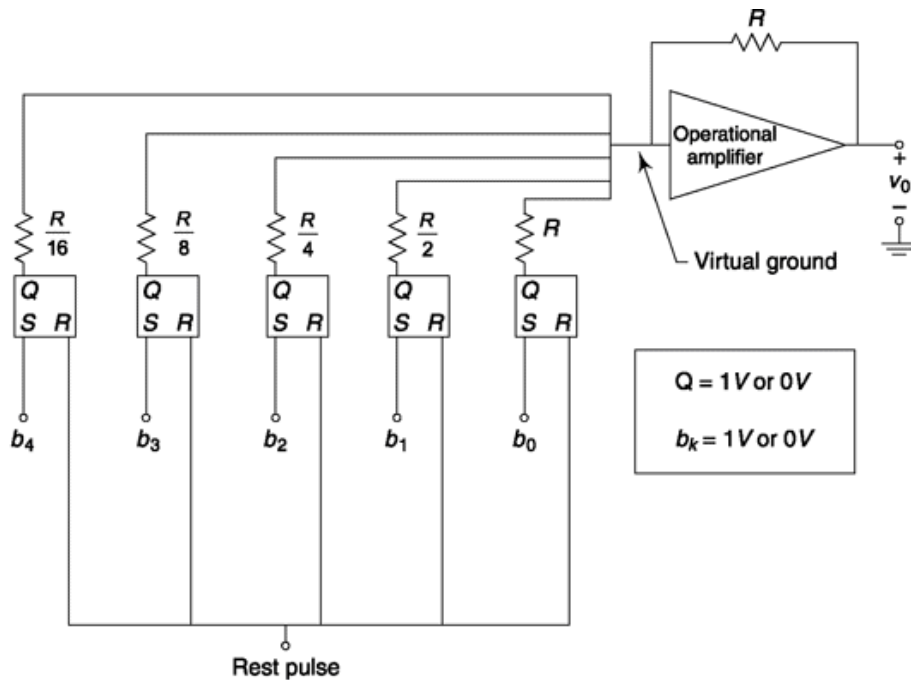


Fig. P4.26

4.28 A μ -law compander uses a compressor which relates output to input by the relation

$$y = \pm \frac{\log(1 + \mu|x|)}{\log(1 + \mu)}$$

Here the + sign applies when x is positive and the - sign applies when x is negative. Also $x \equiv v_i/V$ and $y = v_o/V$ where v_i and v_o are the input and output voltages and the range of allowable voltage is $-V$ to $+V$. The parameter μ determines the degree of compression.

- A commonly used value is $\mu = 255$. For this value make a plot of y versus x from $x = -1$ to $x = +1$.
- If $V = 40$ volts and 256 quantization levels are employed what is the voltage interval between levels when there is no compression? For $\mu = 255$ what is the minimum and what is the maximum effective separation between levels?

4.29 An A -law compander uses a compressor which relates output to input by the relations

$$y = \pm \frac{A|x|}{1 + \log A} \quad \text{for} \quad |x| \leq \frac{1}{A}$$

$$y = \pm \frac{1 + \log A|x|}{1 + \log A} \quad \text{for} \quad \frac{1}{A} \leq |x| \leq 1$$

Here the + sign applies when x is positive and the - sign when x is negative. Also $x \equiv v_i/V$ and $y = v_o/V$ where v_i and v_o are the input and output voltages and the range of allowable voltage is $-V$ to $+V$. The parameter A determines the degree of compression.

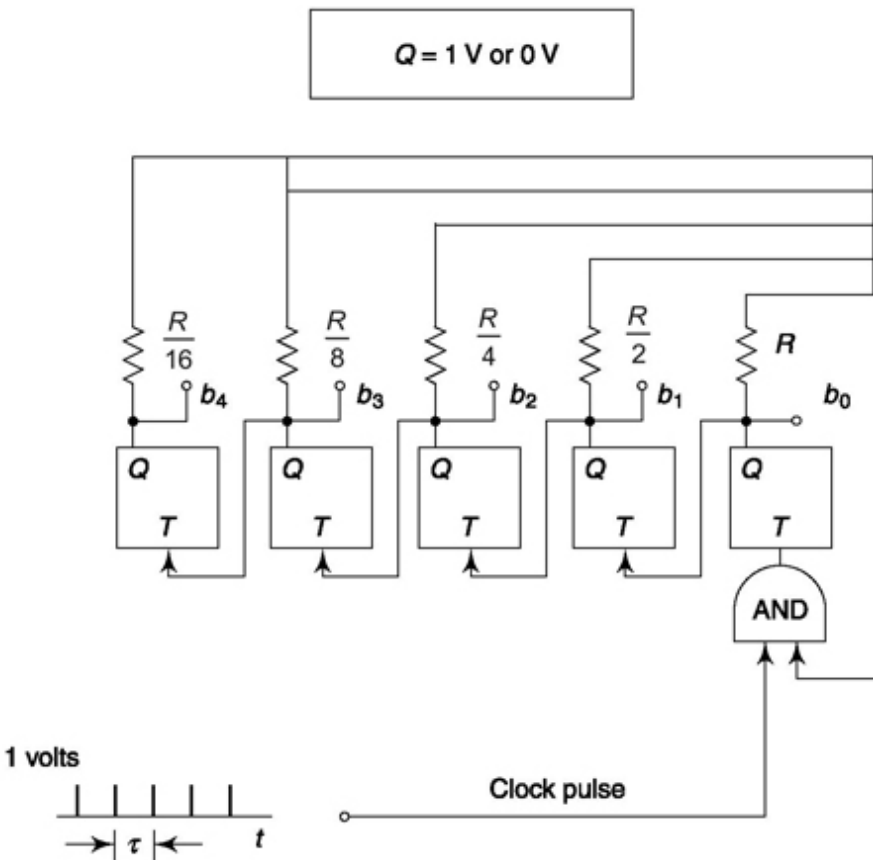
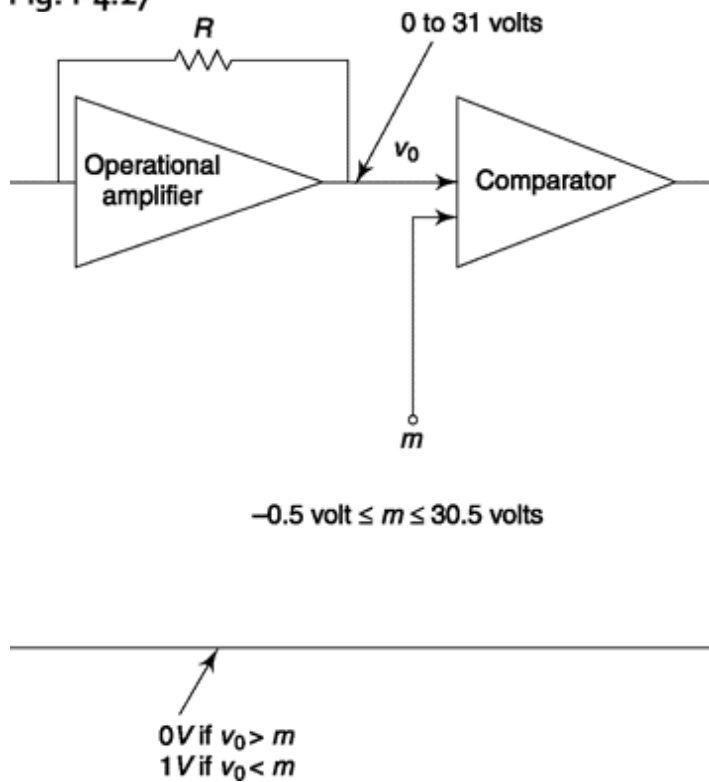


Fig. P4.27



- (a) A commonly used value is $A = 87.6$. For this value make a plot of y versus x from $x = -1$ to $x = +1$.
- (b) If $\pm V = \pm 10$ volts and 256 quantization levels are employed, what is the voltage interval between levels when there is no compression? For $A = 87.6$ what is the minimum and the maximum effective separation between levels?

4.30 An analog signal $m(t)$ has a probability density function

$$f(x) = 1 - |x| \quad -1 \leq x \leq +1$$

This signal is quantized by a quantizer that has eight quantization levels.

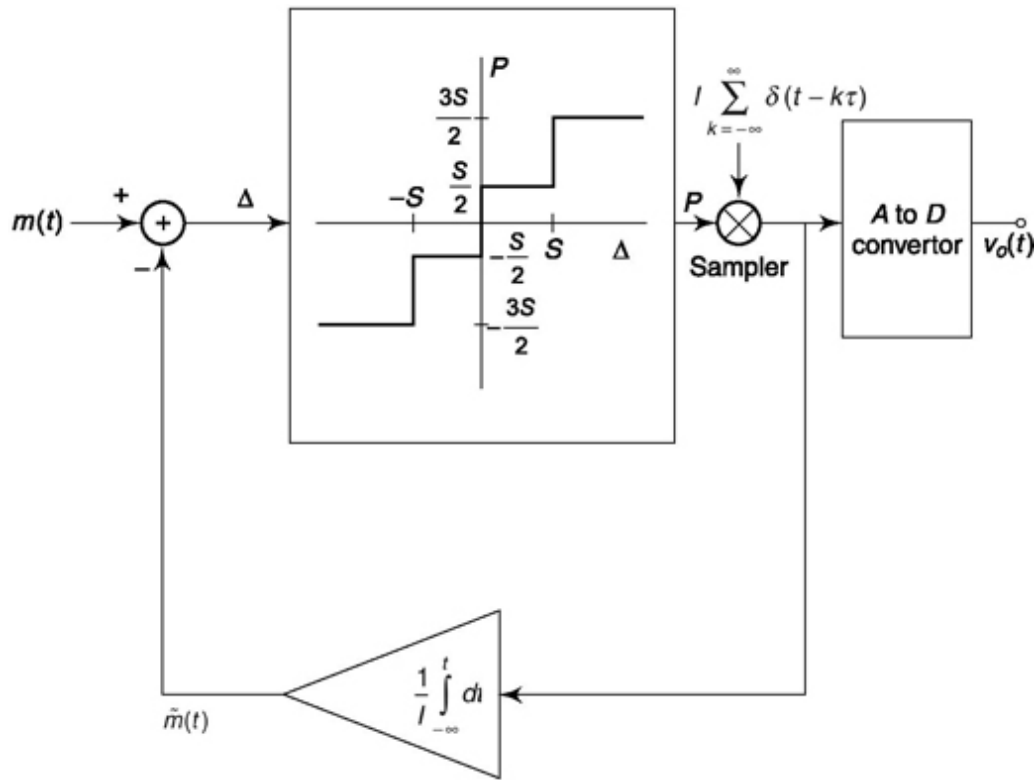
- (a) Determine the voltages at which the quantization levels should be located so that there shall be equal probabilities that $m(t)$ is between any two adjacent levels or between the extreme levels and the +1 and -1 extreme voltages.
- (b) If a quantizer is used with equal spacings between quantization levels, make an input-output plot of the compander that must precede the quantizer to satisfy the requirement of part (a).

4.31 An analog signal $m(t)$ has a probability density function

$$f(x) = 1 - |x| \quad \text{for} \quad -1 \leq x \leq -1$$

The signal is applied to a quantizer with two quantization levels at ± 0.5 volts. Calculate the mean square quantization error and compare with the result that would be given if Eq. (4.39) were applied.

- 4.32 Verify that the procedure described in the text and represented in Fig. 4.25 for setting the content of the ROM yields $2^8 = 256$ code words for $2^{12} = 4096$ addresses. What is the ratio between the smallest quantization Δ and the largest quantization level?
- 4.33 (a) An NRZ waveform as in Fig. 4.31 consists of alternating 1's and 0's. The waveform swings between $+V$ and $-V$ and the bit duration is T_b . The waveform is passed through an RC network as in Fig. 4.31b whose time constant is $RC = T_b$. Calculate all the voltage levels of the output waveform for the circumstances that the NRZ waveform has persisted for a long time.
 (b) For the circumstances of part (a) calculate the area under the waveform during the bit time T_b . Now consider that a sequence of 10 successive 1's appears. Calculate the area under the waveform during the 10th 1 bit and compare the area calculated for the case when 1's and 0's alternate.
- 4.34 Draw an AMI waveform corresponding to a binary bit stream 100110010101. The polarity of the first pulse in the waveform may be set arbitrarily.
- 4.35 Two of the T_1 inputs to the $M12$ multiplexer of Fig. 4.35 are generated in systems whose clocks have frequencies which are different by 50 parts/million. In how long a time will the faster clock have generated one more time slot than the slower clock. In this time interval, how many frames will have been generated?
- 4.36 Consider the delta PCM system shown in Fig. P4.36.
 - (a) Explain its operation.
 - (b) Sketch the receiver.
 - (c) If $m(t) = 0.05 \sin 2\pi t$, find $\bar{m}(t)$ and $\Delta(t)$ graphically.



- 4.37 (a) Write the nonlinear difference equation of the delta modulator shown in Fig. 4.39. Let $m(t) = 18 \times 10^{-3} \sin 2\pi t$ and let the samples occur every 0.05 sec starting at $t = 0.01$ sec. The step size is 5 mV.
- (b) Write and run a computer program to solve for $\Delta(t)$.
- (c) Repeat (b) if the samples occur every 0.1 sec.
- (d) Compare the results of (b) and (c).
- 4.38 The input to a DM is $m(t) = 0.01t$. The DM operates at a sampling frequency of 20 Hz and has a step size of 2 mV. Sketch the delta modulator output, $\Delta(t)$ and $\tilde{m}(t)$.
- 4.39 The input to a DM is $m(t) = kt$. Prove, by graphically determining $\tilde{m}(t)$, that slope overload occurs when k exceeds a specified value. What is this value in terms of the step size S and the sampling frequency f_s ?
- 4.40 If the step size is S , the sampling frequency is $f_s^{(\Delta)}$, and $m(t) = M \sin \omega t$, explain what happens to $\tilde{m}(t)$ if $2M < S$. This is called *step-size limiting*.
- 4.41 The signal $m(t) = M \sin \omega_0 t$ is to be encoded by using a delta modulator. If the step size S and sampling frequency $f_s^{(\Delta)}$ are selected so as to ensure that neither slope overloads [Eq. (4.62)] nor step-size limiting (Prob. 4.40) occurs, show that $f_s^{(\Delta)} > 3f_0$.
- 4.42 The adaptive delta-modulation system described in Sec. 4.7.1 has an input which is $m(t) = 0$ until time $t = 0$ and thereafter $m(t) = 1250 \sin 2\pi t$. An inactive edge of the clock occurs at $t = 0$ and the clock period is 0.05 sec. On a single set of coordinate axes draw the clock waveform, the input $m(t)$ and the approximation $\hat{m}(t)$. Extend the plot through a full cycle of $m(t)$.
- 4.43 An adaptive delta modulator is shown in Fig. P4.43. The gain K is variable and is adjusted using the following logic. If $p_o(t)$ alternates between +1 and -1, $K = 1$; if a sequence of N positive or N negative pulses occurs, K increases by N ; if after a sequence of N pulses the

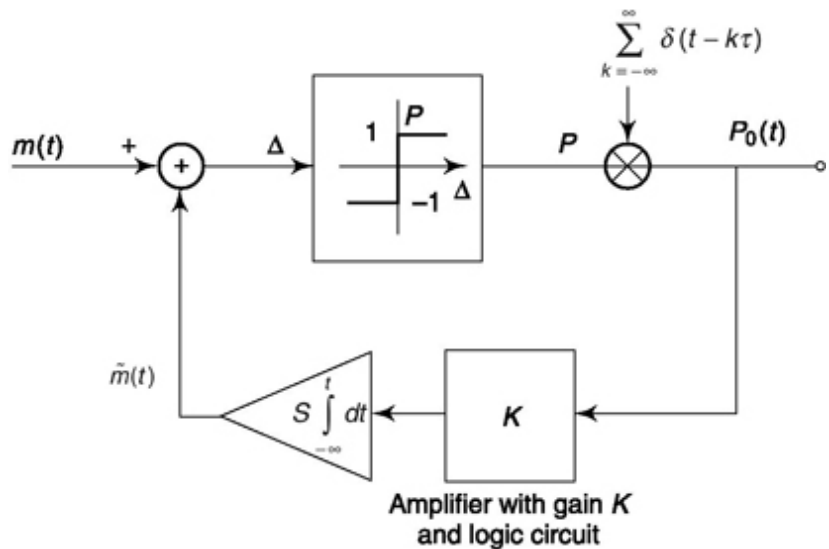


Fig. P443

polarity changes, $|K|$ decreases by 2. Thus, consider the sequence 1, 1, 1. Then $K = 1, 2, 3, 1, 2$.

Find $\tilde{m}(t)$ if $m(t) = \sin 2\pi t$. Perform the analysis graphically. Consider a sampling time of 0.05 sec, and at $t = 0.01$ sec a sample occurs. At this time the step size $S = 1$ volt when $K = 1$.

REFERENCES -

1. Lucky, R. W., J. Salz, and E. J. Weldon, Jr.: "Principles of Data Communication," pp. 61-87, McGraw-Hill Book Company, New York, 1968.
2. Lucky, R. W., J. Salz, and E. J. Weldon, Jr.: "Principles of Data Communication," pp. 128-165, McGraw-Hill Book Company, New York, 1968.
3. Bell Telephone Laboratories: "Telecommunications Transmission Engineering," Vol II, AT&T, Western Electric Company, Tech. Pub., Winston-Salem, N.C., 1977.
4. de Jager, F.: Deltamodulation: A Method of PCM Transmission Using a 1-unit Code, *Philips Res. Rept.* 7, pp. 442-446, 1952.
5. Jayant, N. S., and P. Noll: "Digital Coding of Waveforms," Prentice-Hall Inc., Englewood Cliffs, N.J., 1984.

5

DIGITAL MODULATION AND TRANSMISSION

CHAPTER OBJECTIVE

In the previous chapter, we discussed digital representation of signal and certain techniques useful for baseband pulse transmission. In chapters 2 and 3, we understood the need and frequency of translation and how to effect passband transmission for analog message signal. In this chapter, we first discuss how to do that for a digital message through different means of carrier signal modulation. Here, in place of ‘modulation’, the term ‘keying’ that means switching is used. In Amplitude Shift Keying (ASK), amplitude of the carrier is switched from one value to another depending on modulating digital input. Similarly, we have Frequency Shift Keying (FSK), Phase Shift Keying (PSK), etc., in digital passband transmission. Next in this chapter, we take up the discussion on interchannel and intersymbol interference in digital transmission and ways to reduce its ill effect. This gives us an opportunity to understand a relatively new but widely used technique called Orthogonal Frequency Division Multiplexing (OFDM). Some important topics related to digital transmission and reception like regenerative repeater, equalizer, eye pattern are taken up towards the end. We use signal space representation or constellation diagram widely within the text and in MATLAB simulations. This helps in understanding how in one technique a denser signal space spacing helps in increasing data rate which at the same time decreases the distinguishability of a signal and makes it less immune to noise. The effect of noise in digital data reception is discussed in Chapter 11. However, in MATLAB examples we made a simple introduction of error rates to help reader understand the relation between signal space representation and distinguishability of a signal.

FACTS AND FIGURES

Before World War II erupted fully, the United States and the United Kingdom were using transatlantic high-frequency radio for voice communications between senior leaders. It used some early scrambling techniques and was vulnerable to anyone with sophisticated unscrambling capability using clues from audio spectrum. To solve this, in 1943, Bell Telephone Laboratory, USA introduced SIGSALY service, a new digital transmission technique, on which Churchill and Roosevelt talked in total secrecy.

A 1983 review of Institute of Electrical and Electronic Engineers (IEEE) attributes eight “firsts” to SIGSALY. They are as follows: (i) the first realization of enciphered telephony, (ii) the first quantized speech transmission, (iii) the first transmission of speech by Pulse Code Modulation (PCM), (iv) the first use of companded PCM, (v) the first examples of multilevel Frequency Shift Keying (FSK), (vi) the first useful realization of speech bandwidth compression, (vii) the first use of FSK-FDM as a viable transmission method over a fading medium, (viii) the first use of a multilevel “eye pattern” to adjust the sampling intervals.

5.1 BINARY PHASE SHIFT KEYING (BPSK)

Ever wondered what happens in the background when we use a laptop to connect to the outside world in a wireless environment? We may have seen a decrease in data rate when channel condition worsens. If that is the external manifestation, internally there is a move to a more noise-robust but lower data rate digital modulation scheme. That is binary phase-shift keying (BPSK) with which we start discussion on different digital modulation techniques.

In BPSK the transmitted signal is a sinusoid of fixed amplitude. It has one fixed phase when the data is at one level and when the data is at the other level the *phase* is different by 1800° . Figure 5.1a shows a BPSK modulated carrier signal and corresponding digital message. If the sinusoid is

of amplitude A , it has a power $P_s = \frac{1}{2} A^2$ so that $A = \sqrt{2P_s}$. Thus the transmitted signal is either

$$v_{\text{BPSK}}(t) = \sqrt{2P_s} \cos(\omega_0 t) \quad (5.1)$$

or $v_{\text{BPSK}}(t) = \sqrt{2P_s} \cos(\omega_0 t + \pi) \quad (5.2a)$

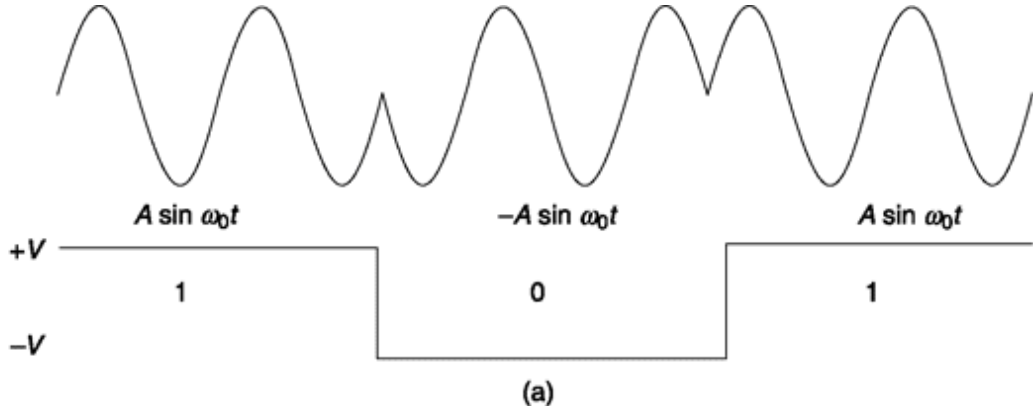
$$= \sqrt{2P_s} \cos(\omega_0 t) \quad (5.2b)$$

In BPSK the data $b(t)$ is a stream of binary digits with voltage levels which, as a matter of convenience, we take to be at +1 V and -1 V. When $b(t) = 1$ V, we say it is at logic level 1 and when $b(t) = -1$ V we say it is at logic level 0. Hence $v_{\text{BPSK}}(t)$ can be written, with no loss of generality, as

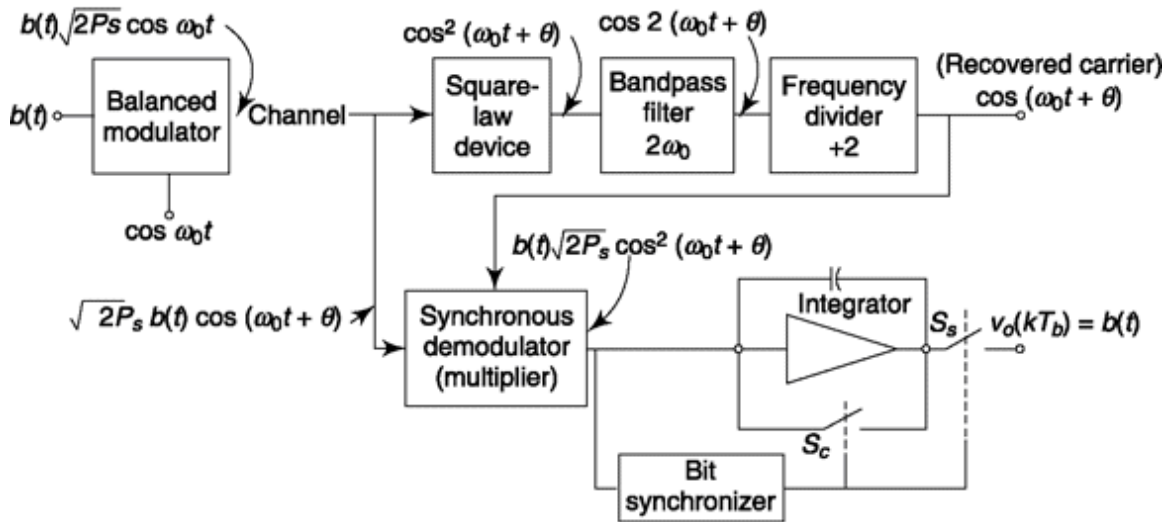
$$v_{\text{BPSK}}(t) = b(t) \sqrt{2P_s} \cos \omega_0 t \quad (5.3)$$

From our discussion in Sec. 2.2.1, we find that Eq. (5.3) resembles a DSB-SC signal and BPSK effectively is related to amplitude modulation. It does not resemble phase modulation because phase change is discrete.

In practice, a BPSK signal is generated by applying the waveform $\cos \omega_0 t$, as a carrier, to a *balanced* modulator and applying the baseband signal $b(t)$ as the modulating waveform. In this sense BPSK can be thought of as an AM signal. We have seen in Sec. 2.3.4 that DSB-SC is more power efficient than DSB-C though both take the same bandwidth. Similarly BPSK is more power efficient than ASK (where amplitudes of a sinusoidal carrier is changed from one to another according to digital message signal following AM principle) though they occupy the same bandwidth.



(a)



(b)

Fig. 5.1 (a) BPSK modulated sinusoidal carrier signal and modulating digital signal. (b) A scheme for BPSK transmission and reception.

5.1.1 Reception of BPSK

The received signal has the form

$$v_{\text{BPSK}}(t) = b(t) \sqrt{2P_s} \cos(\omega_0 t + \theta) = b(t) \sqrt{2P_s} \cos \omega_0(t + \theta/\omega_0) \quad (5.4)$$

Here θ is a nominally fixed phase shift corresponding to the time delay $6/\omega_0$ which depends on the length of the path from transmitter to receiver and the phase shift produced by the amplifiers in the “front-end” of the receiver preceding the demodulator. The original data $b(t)$ is recovered in the demodulator. The demodulation technique usually employed is called synchronous demodulation and requires that there be available at the demodulator the waveform $\cos(\omega_0 t + \theta)$. A scheme for generating the

carrier at the demodulator and for recovering the baseband signal is shown in Fig. 5.1b.

The received signal is squared to generate the signal

$$\cos^2(\omega_0 t + \theta) = \frac{1}{2} + \frac{1}{2} \cos 2(\omega_0 t + \theta) \quad (5.5)$$

The dc component is removed by the bandpass filter whose passband is centered around $2f_0$ and we then have the signal whose waveform is that of $\cos 2(\omega_0 t + \theta)$. A frequency divider (composed of a Flip-Flop and narrow-band filter tuned to f_0) is used to regenerate the waveform $\cos(\omega_0 t + \theta)$. Only the waveforms of the signals at the outputs of the squarer, filter and divider are relevant to our discussion and not their amplitudes. Accordingly in Fig. 5.1 we have arbitrarily taken each amplitude to be unity. In practice, the amplitudes will be determined by features of these devices which are of no present concern. In any event, the carrier having been recovered, is multiplied with the received signal to generate

$$b(t)\sqrt{2P_s} \cos^2(\omega_0 t + \theta) = b(t)\sqrt{2P_s} \left[\frac{1}{2} + \frac{1}{2} \cos 2(\omega_0 t + \theta) \right] \quad (5.6)$$

which is then applied to an integrator as shown in Fig. 5.1.

We have included in the system a *bit synchronizer*. This device is able to recognize precisely the moment which corresponds to the end of the time interval allocated to one bit and the beginning of the next. At that moment, it closes switch S_c very briefly to discharge (*dump*) the integrator capacitor and leaves the switch S_c open during the entire course of the ensuing bit interval, closing switch S_c again very briefly at the end of the next bit time, etc. (This circuit is called an “integrate-and-dump” circuit.) The output signal of interest to us is the integrator output at the end of a bit interval but immediately before the closing of switch S_c . This output signal is made available by switch S_s which samples the output voltage just prior to dumping the capacitor. Let us assume for simplicity that the bit interval T_b is equal to the duration of an integral number n of cycles of the carrier of frequency f_0 , that is, $n \cdot 2p = \omega_0 T_b$. In this case the output voltage $v_0(kT_b)$ at the end of a bit interval extending from time $(k - 1)T_b$ to kT_b is, using Eq. (5.6)

$$v_0(kT_b) = b(kT_b) \sqrt{2P_s} \int_{(k-1)T_b}^{kT_b} \frac{1}{2} dt + b(kT_b) \sqrt{2P_s} \int_{(k-1)T_b}^{kT_b} \frac{1}{2} \cos 2(\omega_0 t + \theta) dt \quad (5.7a)$$

$$= b(kT_b) \sqrt{\frac{P_s}{2}} T_b \quad (5.7b)$$

since the integral of a sinusoid over a whole number of cycles has the value zero. Thus we see that our system reproduces at the demodulator output the transmitted bit stream $b(t)$. The operation of the bit synchronizer allows us to sense each bit independently of every other bit. The brief closing of both switches, after each bit has been determined, wipes clean all influence of a preceding bit and allows the receiver to deal exclusively with the present bit.

Our discussion has been rather naive since it has ignored the effects of thermal noise, frequency jitter in the carrier and random fluctuations in propagation delay. When these perturbing influences need to be taken into account a phase-locked synchronization system is called for as discussed in Sec. 10.5.1.

5.1.2 Spectrum and Inter Channel, Intersymbol Interference

The waveform $b(t)$ is a NRZ (non-return-to-zero) binary waveform whose power spectral density is derived in the next chapter and we shall here only use the expression as given in Eq. (5.150) for a waveform which makes excursions between $+\sqrt{P_s}$ and $-\sqrt{P_s}$. We have

$$G_b(f) = P_s T_b \left(\frac{\sin \pi f T_b}{\pi f T_b} \right)^2 \quad (5.8)$$

The BPSK waveform is the NRZ waveform multiplied by $\sqrt{2} \cos \omega_0 t$. Thus following the analysis of Sec. 2.1.1 we find that the power spectral density of the BPSK signal is

$$G_{\text{BPSK}}(f) = \frac{P_s T_b}{2} \left\{ \left[\frac{\sin \pi(f - f_0) T_b}{\pi(f - f_0) T_b} \right]^2 + \left[\frac{\sin \pi(f + f_0) T_b}{\pi(f + f_0) T_b} \right]^2 \right\} \quad (5.9)$$

Equations (5.8) and (5.9) are plotted in Fig. 5.2.

Note that, in principle at least, the spectrum of $G_b(f)$ extends over all frequencies and correspondingly so does $G_{\text{BPSK}}(f)$. Suppose then that we tried to multiplex signals using BPSK, using different carrier frequencies for different baseband signals. There would inevitably be overlap in the spectra of the various signals and correspondingly a receiver tuned to one carrier would also receive, albeit at a lower level, a signal in a different channel. This overlapping of spectra causes *interchannel* interference.

Since efficient spectrum utilization is extremely important in order to maximize the number of simultaneous users in a multi-user communication

system, the FCC and CCITT require that the side-lobes produced in BPSK be reduced below certain specified levels. To accomplish this we employ a filter to restrict the bandwidth allowed to the NRZ baseband signal. For example, before modulation we might pass the bit stream $b(t)$ through a low-pass filter which suppresses (but does not completely eliminate) all the spectrum except the principal lobe. Since 90 percent of the power of the waveform is associated with this lobe the suggestion is not unreasonable. There is, however, the difficulty that such spectrum suppression distorts the signal and as a result, as we shall see, there is a partial overlap of a bit (symbol) and its adjacent bits in a single channel. This overlap is called *intersymbol interference* (ISI). Intersymbol interference can be somewhat alleviated by the use of *equalizers* at the receiver. Equalizers are filter-type structures used to undo the adverse effects of filters introduced, intentionally or unavoidably, at other places in a communications channel. Many other issues related to Inter Symbol Interference will be discussed later in this chapter.

5.1.3 Signal Space Representation of BPSK Signals

Referring to Sec. 1.5 we see that a BPSK signal can be represented, in terms of one orthonormal signal $M_j(t) = j(2/T_b) \cos \omega_0 t$ as [see Eq. (5.1)]

$$v_{\text{BPSK}}(t) = [\sqrt{P_s T_b} b(t)] \sqrt{\frac{2}{T_b}} \cos \omega_0 t = [\sqrt{P_s T_b} b(t)] u_1(t) \quad (5.10)$$

The binary PSK signal can then be drawn as shown in Fig. 5.3. Note that the distance d between signals is

$$d = 2 \sqrt{P_s T_b} = 2 \sqrt{E_b} \quad (5.11)$$

where $E_b = P_s T_b$ is the energy contained in a bit duration. We show in Sec. 11.5.1 that the distance d is inversely proportional to the probability that we make an error when, in the presence of noise, we try to determine which of the levels of $b(t)$ is being received.

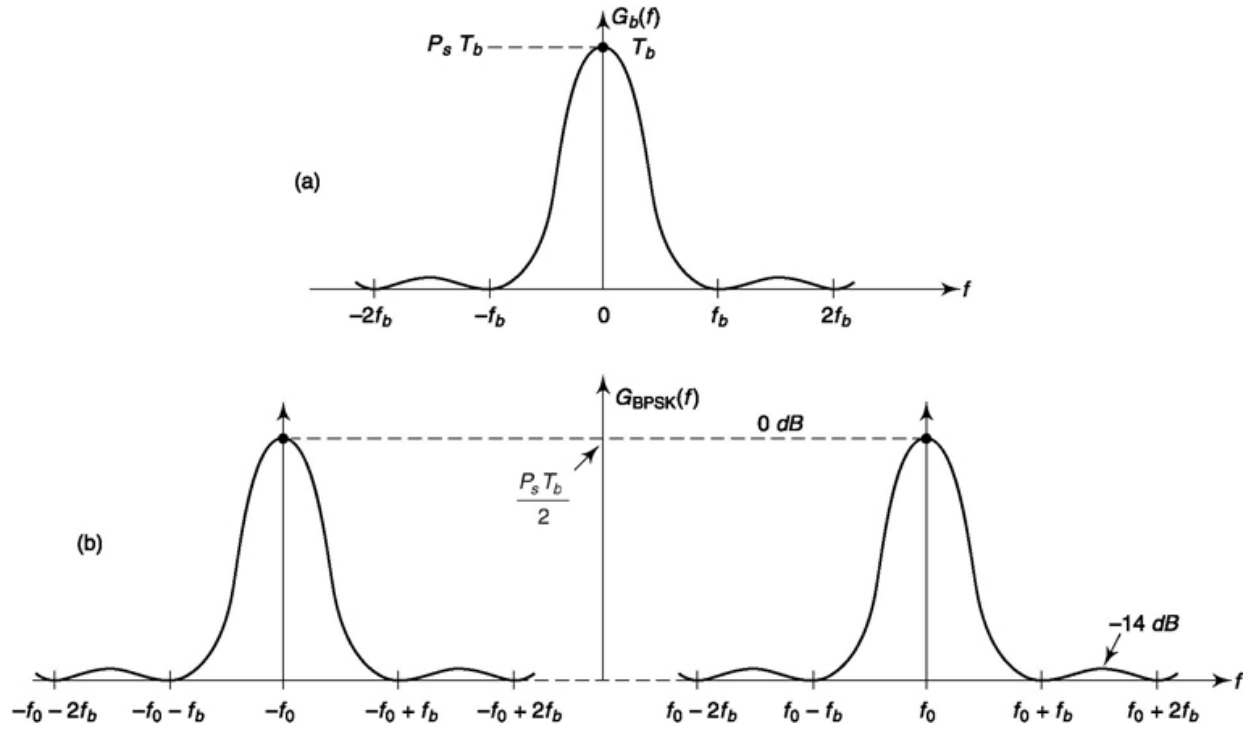


Fig. 5.2 (a) Power spectral density of NRZ data $b(t)$. **(b)** Power spectral density of binary PSK.

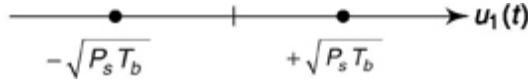


Fig. 53 Geometrical representation of BPSK signals.

5.2 DIFFERENTIAL PHASE SHIFT KEYING (DPSK)

We observed in Fig. 5.1 that, in BPSK, to regenerate the carrier we start by squaring $b(t)(J 2 P_s \cos w_0 t)$. Accordingly, if the received signal were instead $-b(t)$ ($2P_s \cos w_0 t$), the recovered carrier would remain as before. Therefore we shall not be able to determine whether the received baseband signal is the transmitted signal $b(t)$ or its negative $-b(t)$.

Differential phase-shift keying (DPSK) and differential encoded PSK (DEPSK) which is discussed in Sec. 5.3 are modifications of BPSK which have the merit that they eliminate the ambiguity about whether the demodulated data is or is not inverted. In addition DPSK avoids the need to provide the synchronous carrier required at the demodulator for detecting a BPSK signal.

A means for generating a DPSK signal is shown in Fig. 5.4. The data stream to be transmitted, $d(t)$, is applied to one input of an exclusive-OR

logic gate. To the other gate input is applied the output of the exclusive or gate $b(t)$ delayed by the time T_b allocated to one bit. This second input is then $b(t - T_b)$. In Fig. 5.5 we have drawn logic waveforms to illustrate the response $b(t)$ to an input $d(t)$. The upper level of the waveforms corresponds to logic 1, the lower level to logic 0. The truth table for the exclusive-OR gate is given in Fig. 5.4 and with this table we can easily verify that the waveforms for $d(t)$, $b(t - T_b)$, and $b(t)$ are consistent with one another. We observe that, as required, $b(t - T_b)$ is indeed $b(t)$ delayed by one bit time and that in any bit interval the bit $b(t)$ is given by $b(t) = d(t) \oplus b(t - T_b)$. In the ensuing discussion we shall use the symbolism $d(k)$ and $b(k)$ to represent the logic levels of $d(t)$ and $b(t)$ during the k th interval.

Because of the feedback involved in the system of Fig. 5.5 there is a difficulty in determining the logic levels in the interval in which we start to draw the waveforms (interval 1 in Fig. 5.5).

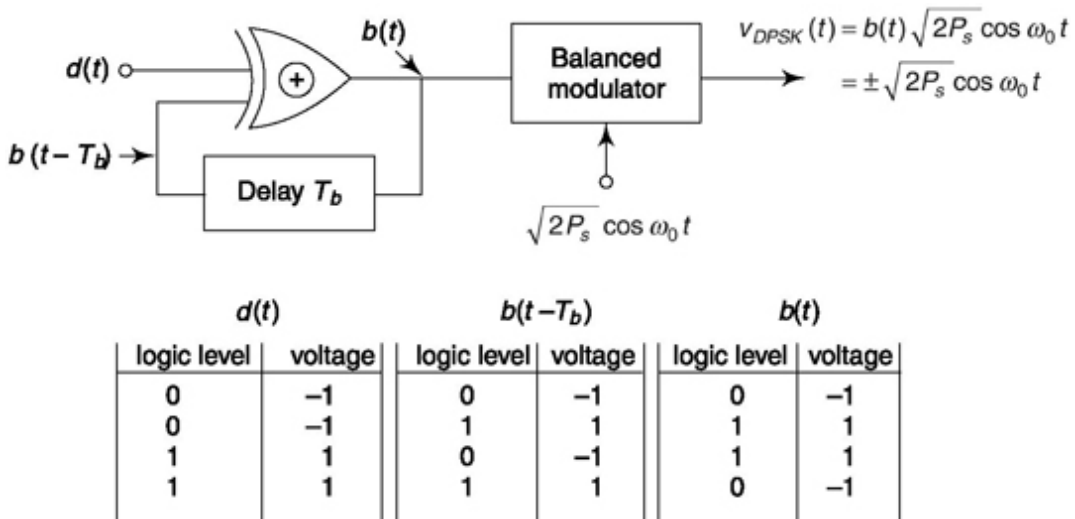


Fig. 5.4 Means of generating a DPSK signal.

Because of the feedback involved in the system of Fig. 5.5 there is a difficulty in determining the logic levels in the interval in which we start to draw the waveforms (interval 1 in Fig. 5.5). We cannot determine $b(t)$ in this first interval of our waveform unless we know $b(k = 0)$. But we cannot determine $b(0)$ unless we know both $d(0)$ and $b(-1)$, etc. Thus, to justify any set of logic levels in an initial bit interval we need to know the logic levels in the preceding interval. But such a determination requires information about the interval two bit times earlier and so on. In the waveforms of Fig. 5.5 we have circumvented the problem by *arbitrarily assuming* that in the first

interval $b(0) = 0$. It is shown below that in the demodulator, the data will be correctly determined regardless of our assumption concerning $b(0)$.

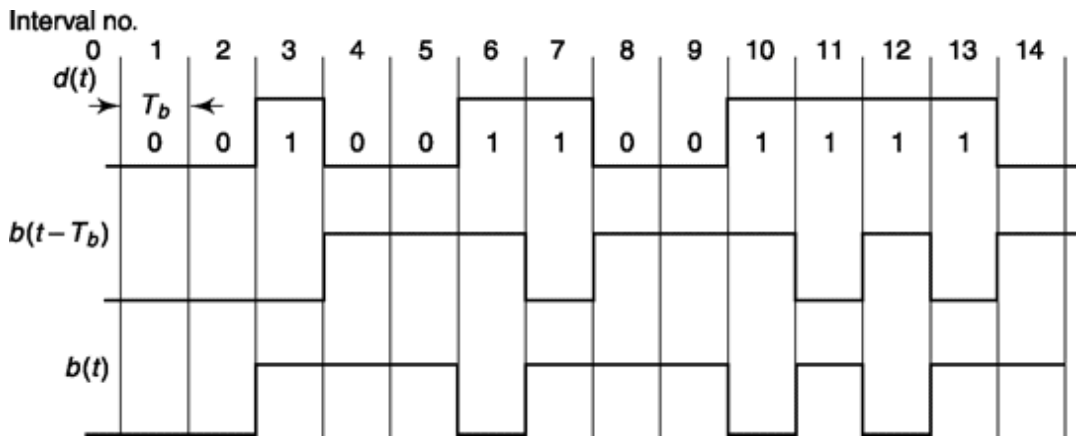


Fig. 5.5 Logic waveforms to illustrate the response $b(t)$ to an input $d(t)$.

We now observe that the response of $b(t)$ to $d(t)$ is that $b(t)$ *changes* level at the beginning of each interval in which $d(t) = 1$ and $b(t)$ does not change level when $d(t) = 0$. Thus during interval 3, $d(3) = 1$, and correspondingly $b(3)$ *changes* at the beginning at that interval. During intervals 6 and 7, $d(6) = d(7) = 1$ and there are *changes* in $b(t)$ at the beginning of both intervals. During bits 10, 11, 12 and 13 $d(t) = 1$ and there are *changes* in $b(t)$ at the beginning of each of these intervals. This behavior is to be anticipated from the truth table of the exclusive-OR gate. For we note that when $d(t) = 0$, $b(t) = b(t - T_b)$ so that, whatever the initial value of $b(t - T_b)$, it reproduces itself. On the other hand when $d(t) = 1$ then $b(t) = b(t - T_b)$. Thus, in each successive bit interval $b(t)$ changes from its value in the previous interval. Note that in some intervals where $d(t) = 0$ we have $b(t) = 0$ and in other intervals when $d(t) = 0$ we have $b(t) = 1$. Similarly, when $d(t) = 1$ sometimes $b(t) = 1$ and sometimes $b(t) = 0$. Thus, there is no correspondence between the levels of $d(t)$ and $b(t)$, and the only invariant feature of the system is that a *change* (sometimes up and sometimes down) in $b(t)$ occurs whenever $d(t) = 1$, and that no change in $b(t)$ will occur whenever $d(t) = 0$.

Finally, we note that the waveforms of Fig. 5.5 are drawn on the assumption that, in interval 1, $b(0) = 0$. As is easily verified, if not intuitively apparent, if we had assumed $b(0) = 1$, the invariant feature by which we have characterized the system would continue to apply. Since $b(0)$ must be either $b(0) = 0$ or $b(0) = 1$, there being no other possibilities, our result is valid quite generally. If, however, we had started with $b(0) = 1$ the levels $b(1)$ and $b(0)$ would have been inverted.

As is seen in Fig. 5.4 b(t) is applied to a balanced modulator to which is also applied the carrier $\cos \omega_0 t$. The modulator output, which is the transmitted signal is

$$\begin{aligned} v_{\text{DPSK}}(t) &= b(t) \sqrt{2P_s} \cos \omega_0 t \\ &= \pm \sqrt{2P_s} \cos \omega_0 t \end{aligned} \quad (5.12)$$

Thus altogether when $d(t) = 0$ the phase of the carrier does *not* change at the beginning of the bit interval, while when $d(t) = 1$ there is a phase change of magnitude p .

A method of recovering the data bit stream from the DPSK signal is shown in Fig. 5.6. Here the received signal and the received signal delayed by the bit time T_b are applied to a multiplier. The multiplier output is

$$\begin{aligned} &b(t)b(t - T_b)(2P_s) \cos(\omega_0 t + \theta) \cos[\omega_0(t - T_b) + \theta] \\ &= b(t)b(t - T_b)P_s \left\{ \cos \omega_0 T_b + \cos \left[2\omega_0 \left(t - \frac{T_b}{2} \right) + 2\theta \right] \right\} \end{aligned} \quad (5.13)$$

and is applied to a bit synchronizer and integrator as shown in Fig. 5.1 for the BPSK demodulator. The first term on the right-hand side of Eq. (5.13) is, aside from a multiplicative constant, the waveform $b(t)b(t - T_b)$ which, as we shall see is precisely the signal we require. As noted previously in connection with BPSK, and so here, the output integrator will suppress the double frequency term. We should select $\omega_0 T_b$ so that $\omega_0 T_b = 2np$ with n an integer. For, in this case we shall have $\cos \omega_0 T_b = +1$ and the signal output will be as large as possible. Further, with this selection, the bit duration encompasses an integral number of clock cycles and the integral of the double-frequency term is exactly zero.

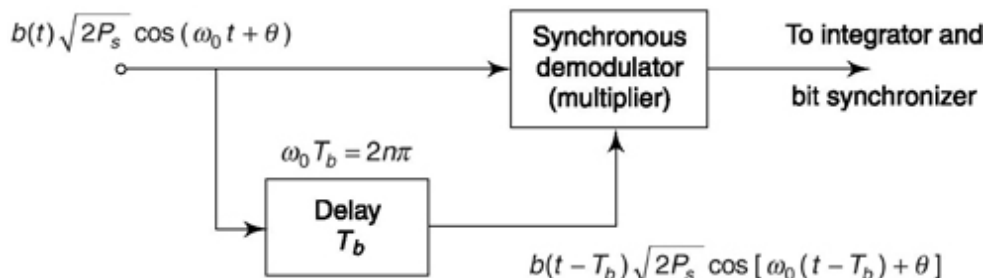


Fig. 5.6 Method of recovering data from the DPSK signal.

The transmitted data bit $d(t)$ can readily be determined from the product $b(t)b(t - T_b)$. If $d(t) = 0$ then there was no phase change and $b(t) = b(t - T_b)$ both being +1 V or both being -1 V. In this case $b(t)b(t - T_b) = 1$. If however, $d(t) = 1$ then there was a phase change and either $b(t) = 1V$ with $b(t - T_b) = -1V$ or vice versa. In either case $b(t)b(t - T_b) = -1$.

The differentially coherent system, DPSK, which we have been describing has a clear advantage over the coherent BPSK system in that the former avoids the need for complicated circuitry used to generate a local carrier at the receiver. To see the relative disadvantage of DPSK in comparison with PSK, consider that during some bit interval the received signal is so contaminated by noise that in a PSK system an error would be made in the determination of whether the transmitted bit was a 1 or a 0. In DPSK a bit determination is made on the basis of the signal received in two successive bit intervals. Hence noise in one bit interval may cause errors to two bit determinations.

The error rate in DPSK is therefore greater than in PSK, and, as a matter of fact, there is a tendency for bit errors to occur in pairs. It is not inevitable however that errors occur in pairs. Single errors are still possible. Consider a case in which the received signals in k th and $(k + 1)$ st bit intervals are both somewhat noisy but that the signals in the $(k - 1)$ st and $(k + 2)$ nd intervals are noise free. Assume further that the k th interval signal is *not* so noisy that an error results from the comparison with the $(k - 1)$ st interval signal and assume a similar situation prevails in connection with the $(k + 1)$ st and the $(k + 2)$ nd interval signals. Then it may be that only a single error will be generated, that error being the result of the comparison of the k th and $(k + 1)$ st interval signals both of which are noisy.

5.3 DIFFERENTIALLY ENCODED PHASE SHIFT KEYING (DEPSK)

As is noted in Fig. 5.6 the DPSK demodulator requires a device which operates at the carrier frequency and provides a delay of T_b . Differentially encoded PSK eliminates the need for such a piece of hardware. In this system, synchronous demodulation recovers the signal $b(t)$, and the decoding of $b(t)$ to generate $d(t)$ is done at baseband.

The transmitter of the DEPSK system is identical to the transmitter of the DPSK system shown in Fig. 5.4. The signal $b(t)$ is recovered in exactly the

manner shown in Fig. 5.1 for a BPSK system. The recovered signal is then applied directly to one input of an exclusive-OR logic gate and to the other input is applied $b(t - T_b)$ (see Fig. 5.7). The gate output will be at one or the other of its levels depending on whether $b(t) = b(t - T_b)$ or $b(t) = b(t - T_b)$. In the first case $b(t)$ did not change level and therefore the transmitted bit is $d(t) = 0$. In the second case $d(t) = 1$.

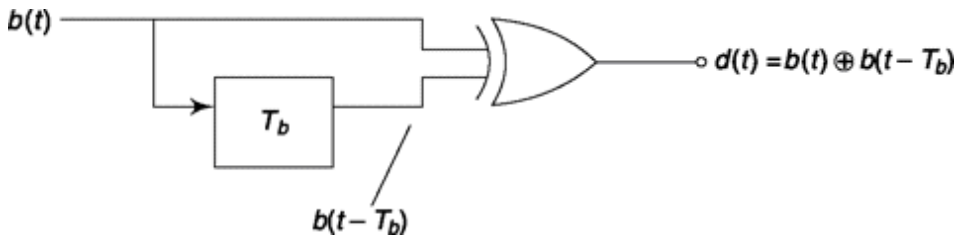


Fig. 5.7 Baseband decoder to obtain $d(t)$ from $b(t)$.

We have seen that in DPSK there is a tendency for bit errors to occur in pairs but that single bit errors are possible. In DEPSK errors *always* occur in pairs. The reason for the difference is that in DPSK we do not make a hard decision, in each bit interval about the phase of the received signal. We simply allow the received signal in one interval to compare itself with the signal in an adjoining interval and, as we have seen, a single error is not precluded. In DEPSK, a firm definite hard decision is made in each interval about the value of $b(t)$. If we make a mistake, then errors must result from a comparison with the preceding and succeeding bit. This result is illustrated in Fig. 5.8. In Fig. 5.8a is shown the error-free signals $b(k)$, $b(k - 1)$ and $d(k) = b(k) \oplus b(k - 1)$. In Fig. 5.8b we have assumed that $b'(k)$ has a single error. Then $b'(k - 1)$ must also have a single error. We note that the reconstructed waveform d (k) now has two errors.

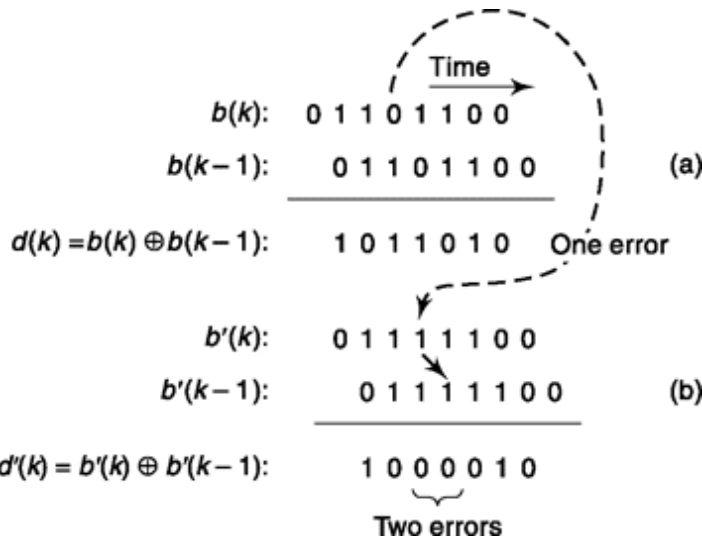


Fig. 5.8 Errors in differentially encoded PSK occur in pairs.

5.4 QUADRATURE PHASE SHIFT KEYING (QPSK)

We have seen that when a data stream whose bit duration is T_b is to be transmitted by BPSK the channel bandwidth must be nominally $2f_b$ where $f_b = 1/T_b$. Quadrature phase-shift keying, as we shall explain, allows bits to be transmitted using half the bandwidth. In describing the QPSK system we shall have occasion to use the type-D Flip-Flop as a one bit storage device. We therefore digress, very briefly, to remind the reader of the essential characteristics of this Flip-Flop.

Type-D Flip-Flop

The type-D Flip-Flop represented in Fig. 5.9a has a single data input terminal (D) to which a data stream $d(t)$ is applied. The operation of the Flip-Flop is such that at the “active” edge of the clock waveform the logic level at D is transferred to the output Q . Representative waveforms are shown in Fig. 5.9b. We assume arbitrarily that the negative-going edge of the clock waveform is the active edge. At the active edge numbered 1, we find that $d(t) = 0$. Hence, after a short delay (the delay is not shown) from the time of occurrence of this edge we shall find that $Q = 0$. The delay results from the fact that some time is required for the input data to propagate through the Flip-Flop to the output Q . (On the basis of the waveform $d(t)$ shown, we have no basis on which to determine Q at an earlier time.) At active edge 2 it appears that the clock edge occurs precisely at the time when $d(t)$ is

changing. If such were indeed the case, the response of the Flip-Flop would be ambiguous. As a matter of practice, the change in $d(t)$ will occur slightly after the active edge. Such is the case because, rather inevitably, the change in $d(t)$ is itself the response of some digital component (gate, Flip-Flop, etc.) to the very same clock waveform which is driving our type-D Flip-Flop. (The delays referred to are normally not indicated on a waveform diagram as in Fig. 5.9 because these delays are ordinarily very small in comparison with the bit time T_b .) In any event, the fact is that at active edge 2 we have $d(t) = 0$ and Q remains at $Q = 0$. The remainder of the waveforms are easily verified on the same basis. Observe that the Q waveform is the $d(t)$ waveform delayed by one bit interval T_b . The relevant point about the Flip-Flop in the matter of our present concern is the following: Once the Flip-Flop, in response to an active clock edge, has registered a data bit, it will hold that bit until updated by the occurrence of the next succeeding active edge.

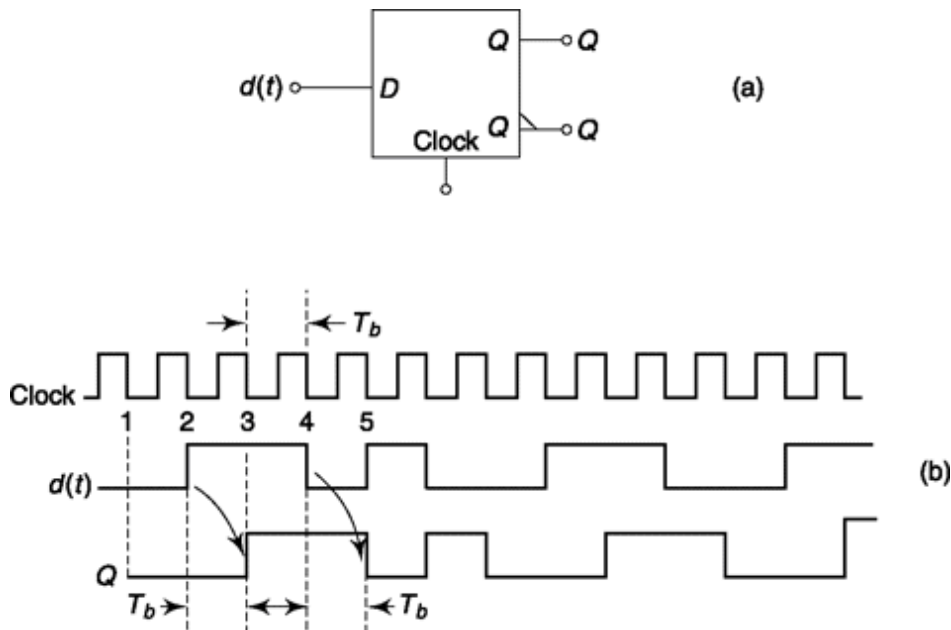


Fig. 5.9 (a) Type-D Flip-Flop symbol. (b) Waveforms showing Flip-Flop characteristics.

5.4.1 QpsK Transmitter

The mechanism by which a bit stream $b(t)$ generates a QPSK signal for transmission is shown in Fig. 5.10 and relevant waveforms are shown in Fig. 5.11. In these waveforms we have arbitrarily assumed that in every case the active edge of the clock waveforms is the downward edge. The toggle Flip-

Flop is driven by a clock waveform whose period is the bit time T_b . The toggle Flip-Flop generates an odd clock waveform and an even waveform. These clocks have periods $2T_b$. The active edge of one of the clocks and the active edge of the other are separated by the bit time T_b . The bit stream

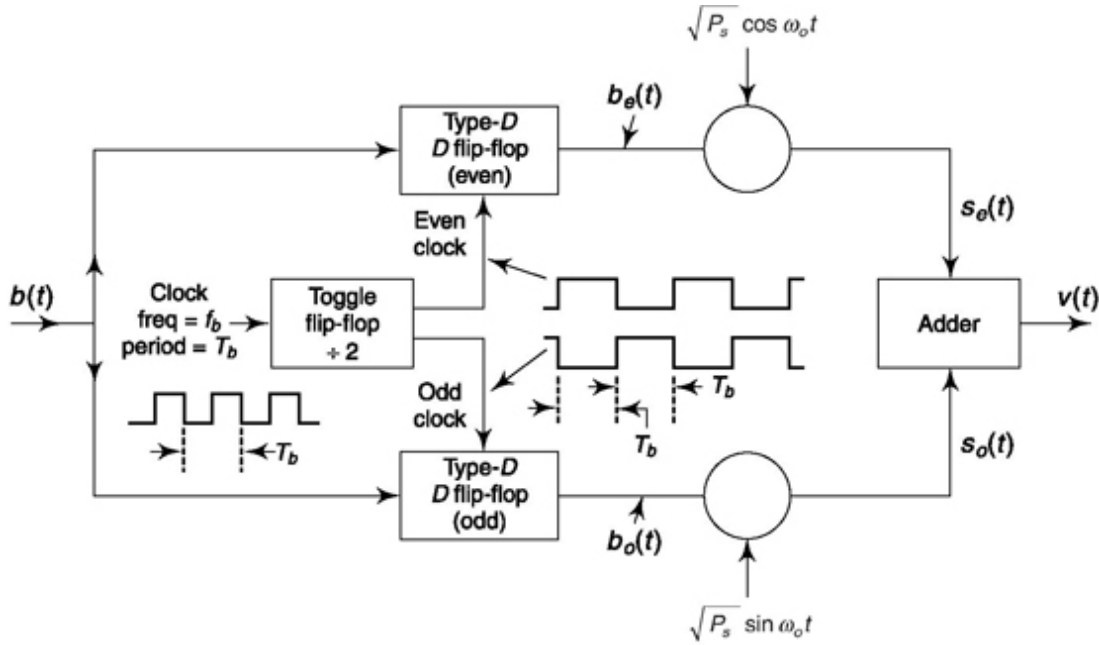


Fig. 5.11 Waveforms for the QPSK transmitter of Fig. 6.10.

$b(t)$ is applied as the data input to both type-D Flip-Flops, one driven by the odd and one driven by the even clock waveform. The Flip-Flops register alternate bits in the stream $b(t)$ and hold each such registered bit for two bit intervals, that is for a time $2T_b$. In Fig. 5.11 we have numbered the bits in $b(t)$. Note that the bit stream $b_o(t)$ (which is the output of the Flip-Flop driven by the odd clock) registers bit 1 and holds that bit for time $2T_b$, then registers bit 3 for time $2T_b$, then bit 5 for $2T_b$, etc. The even bit stream $b_e(t)$ holds, for times $2T_b$ each, the alternate bits numbered 2, 4, 6 etc. The bit stream $b_e(t)$ (which, as usual, we take to be $b_e(t) = \pm 1$ volt) is superimposed on a carrier

$P_s \cos \omega_0 t$ and the bit stream $b_o(t)$ (also ± 1 volt) is superimposed on a carrier $\sin \omega_0 t$ by the use of two multipliers (i.e. balanced modulators) as shown, to generate two signals $s_e(t)$ and $s_o(t)$. These signals are then added to generate the transmitted output signal $v_m(t)$ which is

$$v_m(t) = \sqrt{P_s} b_o(t) \sin \omega_0 t + \sqrt{P_s} b_e(t) \cos \omega_0 t \quad (5.14)$$

As may be verified, the total normalized power of $v_m(t)$ is P_s . Compare Eq. (5.14) with Eq. (2.37) and you can find QPSK corresponds to QAM signal. As we have noted in BPSK, a bit stream with bit time T_b multiplies a carrier, the generated signal has a nominal bandwidth $2 \times 1/T_b$. In the waveforms $b_o(t)$ and $b_e(t)$ the bit times are each $1/2T_b$, hence both $s_e(t)$ and $s_o(t)$ have nominal bandwidths which are half the bandwidth in BPSK. Both $s_e(t)$ and $s_o(t)$ occupy the same spectral range but they are nonetheless individually identifiable because of the phase quadrature of their carriers.

When $b_o = 1$ the signal $s_o(t) = \sqrt{P_s} \sin \omega_0 t$, and $s_o(t) = -\sqrt{P_s} \sin \omega_0 t$ when $b_o = -1$. Correspondingly, for $b_e(t) = \pm 1$, $s_e(t) = \pm \sqrt{P_s} \cos \omega_0 t$. These four signals have been represented as phasors in Fig. 5.12. They are in mutual phase quadrature. Also drawn are the phasors representing the four possible output signals $v_m(t) = s_o(t) + s_e(t)$. These four possible output signals have equal amplitude $\sqrt{2P_s}$ and are in phase quadrature; they have been identified by their corresponding values of b_o and b_e . At the end of each bit interval (i.e. after each time T_b) either b_o or b_e can change, but both cannot change at the same time. Consequently, the QPSK system shown in Fig. 5.10 is called *offset* or *staggered* QPSK and abbreviated OQPSK. After each time T_b , the transmitted signal, if it changes, changes phase by 900° rather than by 1800° as in BPSK.

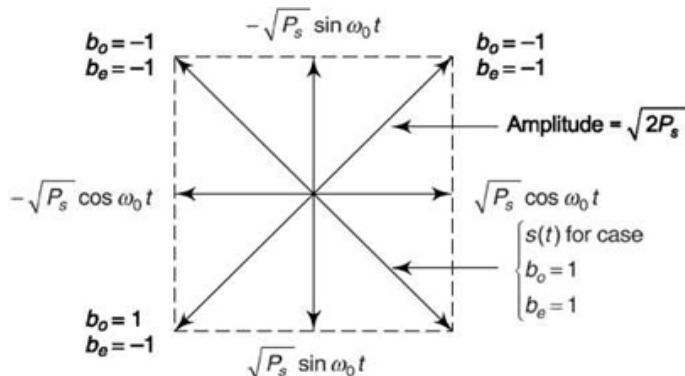


Fig. 5.12 Phasor diagram for sinusoids in Fig. 5.10.

5.4.2 Non-offset QpsK

Suppose that in Fig. 5.10 we introduce an additional Flip-Flop before either the odd or even Flip-Flop. Let this added Flip-Flop be driven by the clock

which runs at the rate f_b . Then one or the other bit streams, odd or even, will be delayed by one bit interval. As a result, we shall find that two bits which occur in time sequence (i.e. serially) in the input bit stream $b(t)$ will appear at the same time (i.e. in parallel) at the outputs of the odd and even Flip-Flops. In this case $b_e(t)$ and $b_o(t)$ can change at the same time, after each time $2T_b$, and there can be a phase change of 1800° in the output signal. There is no difference, in principle, between a staggered and non-staggered system.

In practice, there is often a significant difference between QPSK and OQPSK. At each transition time, T_b for OQPSK and $2T_b$ for QPSK, one bit for OQPSK and perhaps two bits for QPSK change from 1V to $-1V$ or $-1V$ to 1V. Now the bits $b_e(t)$ and $b_o(t)$ can, of course, not change instantaneously and, in changing, must pass through zero and dwell in that neighborhood at least briefly. Hence there will be brief variations in the *amplitude* of the transmitted waveform. These variations will be more pronounced in QPSK than in OQPSK since in the first case both $b_e(t)$ and $b_o(t)$ may be zero simultaneously so that the signal amplitude may actually be reduced to zero temporarily. There is a second mechanism through which amplitude variations are caused at the transmitter. In QPSK as in BPSK a filter is used to suppress sidebands. It turns out that when waveforms which exhibit abrupt phase changes, are filtered, the effect of the filter, at the time of the abrupt phase changes, is to cause substantial changes again in the *amplitude* of the waveform. Here too, we expect larger changes in QPSK where phase changes of 1800° are possible than in OQPSK where the maximum phase change is 900° .

The amplitude variations can cause difficulty in QPSK communication systems which employ repeaters, i.e. stations which receive and rebroadcast signals, such as earth satellites. For such stations generally employ output power stages which operate nonlinearly, the nonlinearity being deliberately introduced because such nonlinear stages can operate with improved efficiency. However, precisely because of their nonlinearity, when presented with amplitude variations, they generate spectral components outside the range of the main lobe, thereby undoing the effect of the band limiting filter and causing interchannel interference. Further filtering to suppress the effect of amplitude variation has an effect on the phase of the signal and it is, of course, precisely the phase which conveys the signal message.

symbol versus Bit Transmission

In BPSK we deal individually with each bit of duration T_b . In QPSK we lump two bits together to form what is termed a *symbol*. The symbol can have any one of four possible values corresponding to the two-bit sequences 00, 01, 10, and 11. We therefore arrange to make four distinct signals available for transmission. At the receiver each signal represents *one symbol* and, correspondingly, *two bits*. When bits are transmitted, as in BPSK, the signal changes occur at the bit rate. When symbols are transmitted the changes occur at the symbol rate which is one-half the bit rate. Thus the symbol time is $T_s = 2T_b$.

5.4.3 The QpsK Receiver

A receiver for the QPSK signal is shown in Fig. 5.13. Synchronous detection is required and hence it is necessary to locally regenerate the carriers $\cos w_0 t$ and $\sin w_0 t$. The scheme for carrier regeneration is similar to that employed in BPSK. In that earlier case we squared the incoming signal, extracted a waveform at twice the carrier frequency by filtering, and recovered the carrier frequency by dividing by two. In the present case, it is required that the incoming signal be raised to the fourth power after which filtering recovers a waveform at four times the carrier frequency and finally frequency division by four regenerates the carrier. In the present case, also, we require both $\sin w_0 t$ and $\cos w_0 t$. It is left as a problem (see Prob. 5.7) to verify that the scheme indicated in Fig. 5.13 does indeed yield the required waveforms $\sin w_0 t$ and $\cos w_0 t$.

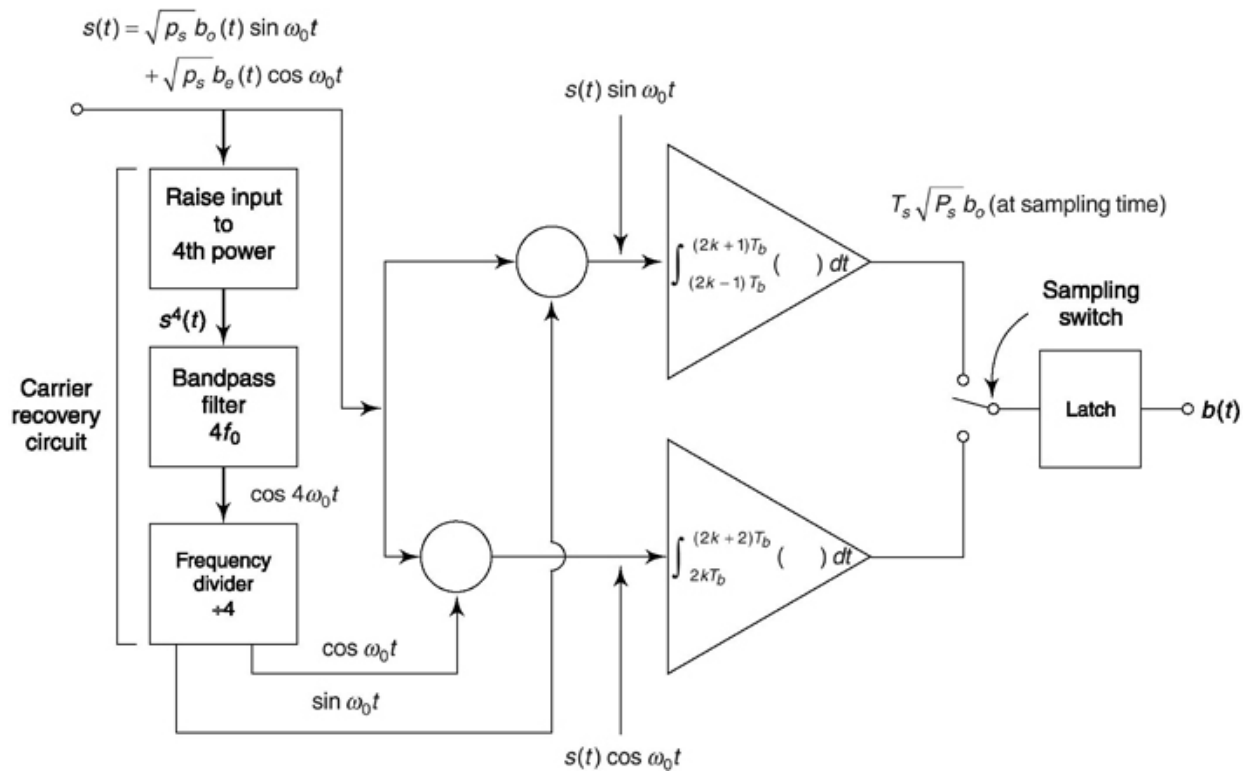


Fig. 5.13 A QPSK receiver.

The incoming signal is also applied to two synchronous demodulators consisting, as usual, of a multiplier (balanced modulator) followed by an integrator. The integrator integrates over a two-bit interval of duration $T_s = 2T_b$ and then dumps its accumulation. As noted previously, ideally the interval $2T_b = T_s$ should encompass an integral number of carrier cycles. One demodulator uses the carrier $\cos \omega_0 t$ and the other the carrier $\sin \omega_0 t$. We recall that when sinusoids in phase quadrature are multiplied, and the product is integrated over an integral number of cycles, the result is zero. Hence the demodulators will selectively respond to the parts of the incoming signal involving respectively $b_e(t)$ or $b_o(t)$.

Of course, as usual, a bit synchronizer is required to establish the beginnings and ends of the bit intervals of each bit stream so that the times of integration can be established. The bit synchronizer is needed as well to operate the sampling switch. At the end of each integration time for each individual integrator, and just before the accumulation is dumped, the integrator output is sampled. Samples are taken alternately from one and the other integrator output at the end of each bit time T_b and these samples are

held in the latch for the bit time T_b . Each individual integrator output is sampled at intervals $2T_b$. The latch output is the recovered bit stream $b(t)$.

The voltages marked on Fig. 5.13 are intended to represent the waveforms of the signals only and not their amplitudes. Thus the actual value of the sample voltages at the integrator outputs depends on the amplitude of the local carrier, the gain, if any, in the modulators and the gain in the integrators. We have however indicated that the sample values depend on the normalized power P_s of the received signal and on the duration T_s of the symbol.

The mechanism used in Fig. 5.13 to regenerate the local carriers is a source of phase ambiguity. That is, the carrier may be 180° out of phase with the carriers at the transmitter and as a result the demodulated signals may be complementary to the transmitted signal. This situation can be corrected, as before, by using differential encoding and decoding as in Figs 5.7 and 5.8.

5.4.4 signal space Representation

In Sec. 1.5.4, we investigated four quadrature signals. Equation (1.213), repeated here, is

$$v_m(t) = \sqrt{2P_s} \cos \left[\omega_0 t + (2m+1) \frac{\pi}{4} \right] \quad m = 0, 1, 2, 3 \quad (5.15)$$

These signals were then represented in terms of the two orthonormal signals $u_1(t) = \sqrt{(2/T)} \cos \omega_0 t$ and $u_2(t) = \sqrt{(2/T)} \sin \omega_0 t$. The result in Eq. (1.216), repeated here, is

$$v_m(t) = \left[\sqrt{P_s T} \cos (2m+1) \frac{\pi}{4} \right] \sqrt{\frac{2}{T}} \cos \omega_0 t - \left[\sqrt{P_s T} \sin (2m+1) \frac{\pi}{4} \right] \sqrt{\frac{2}{T}} \sin \omega_0 t \quad (5.16)$$

The QPSK signal $v_m(t)$ in Eq. (5.14) can be put in the form of Eq. (5.16) by setting

$$b_e = \sqrt{2} \cos (2m+1) \frac{\pi}{4} \quad (5.17a)$$

and

$$b_o = -\sqrt{2} \sin (2m+1) \frac{\pi}{4} \quad (5.17b)$$

Thus

$$v_m(t) = \sqrt{E_b} b_e(t)u_1(t) - \sqrt{E_b} b_o(t)u_2(t) \quad (5.18)$$

where $T = 2T_b = T_s$. Now Fig. 1.9.9 can be redrawn as shown in Fig. 5.14, to show the geometrical representation of QPSK. The points in signal space corresponding to each of the four possible transmitted signals are indicated by dots. From each such signal we can recover two bits rather than one. The distance of a signal point from the origin is $\sqrt{E_s}$ which is the square root of the signal energy associated with the symbol, that is $E_s = P_s T_s = P_s(2T_b)$. As we have noted earlier and will verify in Sec. 11.5.2, our ability to determine a bit without error is measured by the distance in signal space between points corresponding to the different values of the bit. We note in Fig. 5.14 that points which differ in a single bit are separated by the distance

$$d = 2\sqrt{P_s T_b} = 2\sqrt{E_b} \quad (5.19)$$

where E_b is the energy contained in a bit transmitted for a time T_b . This distance for QPSK is the same as for BPSK (see Eq. (5.11)). Hence, altogether, we have the important result that, in spite of the reduction by a factor of two in the bandwidth required by QPSK in comparison with BPSK, the noise immunities of the two systems are the same.

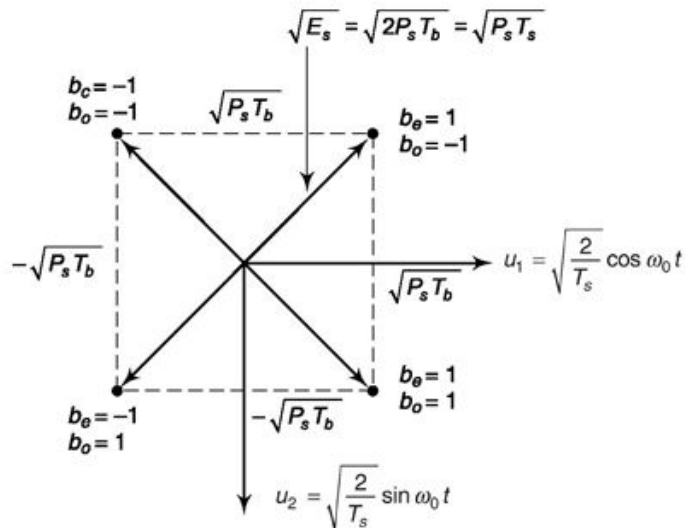


Fig. 5.14 The four QPSK signals drawn in signal space.

5.5 M-ARY PHASE SHIFT KEYING

In BPSK, we transmit each bit individually. Depending on whether $b(t)$ is logic 0 or logic 1, we transmit one or another of a sinusoid for the bit time T_b , the sinusoids differing in phase by $2\pi/2 = 180^\circ$. In QPSK we lump together two bits. Depending on which of the four two-bit words develops, we transmit one or another of four sinusoids of duration $2T_b$, the sinusoids differing in phase by amount $2\pi/4 = 90^\circ$. The scheme can be extended. Let us lump together N bits so that in this N -bit symbol, extending over the time

NT_b , there are $2^N = M$ possible symbols. Now let us represent the symbols by sinusoids of duration $NT_b = T_s$ which differ from one another by the phase $2\pi/M$. Hardware to accomplish such M-ary communication is available.

Thus in M-ary PSK the waveforms used to identify the symbols are

$$v_m(t) = \sqrt{2P_s} \cos(\omega_0 t + \phi_m) \quad (m = 0, 1, \dots, M-1) \quad (5.20)$$

with the symbol phase angle given by

$$\phi_m = (2m + 1) \frac{\pi}{M} \quad (5.21)$$

The waveforms of Eq. (5.20) are represented by the dots in Fig. 5.15 in a signal space in which the coordinate axes are the orthonormal waveforms $u_1(t) = \sqrt{(2/T_s)} \cos \omega_0 t$ and $u_2(t) = \sqrt{(2/T_s)} \sin \omega_0 t$. The distance of each dot from the origin is $\sqrt{E_s} = \sqrt{P_s T_b}$.

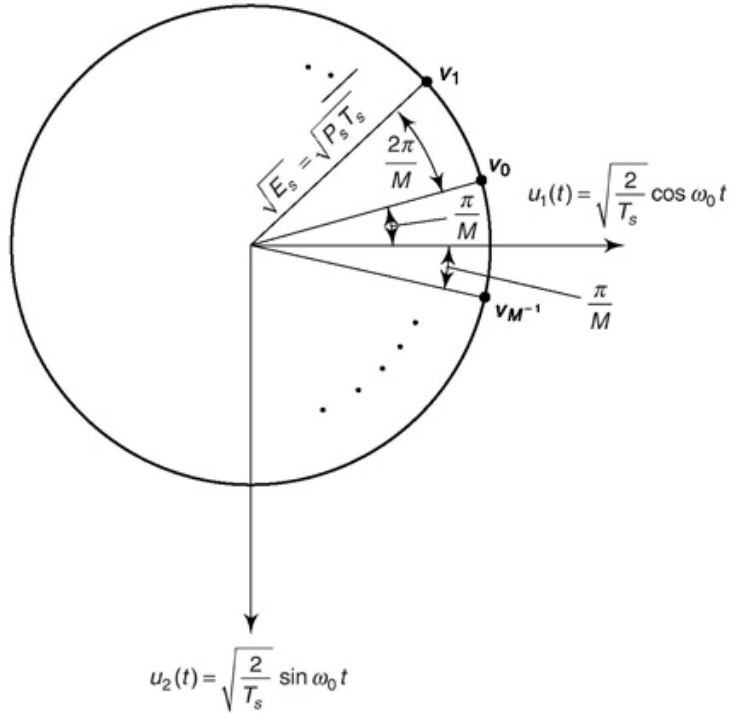
From Eq. (5.20) we have

$$v_m(t) = (\sqrt{2P_s} \cos \phi_m) \cos \omega_0 t - (\sqrt{2P_s} \sin \phi_m) \sin \omega_0 t \quad (5.22)$$

Defining p_e and p_o by

$$p_e = \sqrt{2P_s} \cos \phi_m \quad (5.23a)$$

$$p_o = \sqrt{2P_s} \sin \phi_m \quad (5.23b)$$



Equation (5.22) becomes

$$v_m(t) = p_e \cos \omega_0 t - p_o \sin \omega_0 t \quad (5.24)$$

Both p_e and p_o can change every $T_s = NT_b$ and can assume any of M possible values. The quantities p_e , p_o and ϕ_m are random processes. The power spectral densities of p_e and p_o are derived in the next chapter and given by Eq.(6.158) as

$$G_e(f) = \frac{\overline{|P_e(f)|^2}}{T_s} = 2P_s T_s \overline{\cos^2 \phi_m} \left(\frac{\sin \pi f T_s}{\pi f T_s} \right)^2 \quad (5.25)$$

and

$$G_o(f) = \frac{\overline{|P_o(f)|^2}}{T_s} = 2P_s T_s \overline{\sin^2 \phi_m} \left(\frac{\sin \pi f T_s}{\pi f T_s} \right)^2 \quad (5.26)$$

However, since ϕ_m is uniformly distributed

$$\overline{\cos^2 \phi_m} = \overline{\sin^2 \phi_m} = \frac{1}{2} \quad (5.27)$$

so that

$$G_e(f) = G_o(f) = P_s T_s \left(\frac{\sin \pi f T_s}{\pi f T_s} \right)^2 \quad (5.28)$$

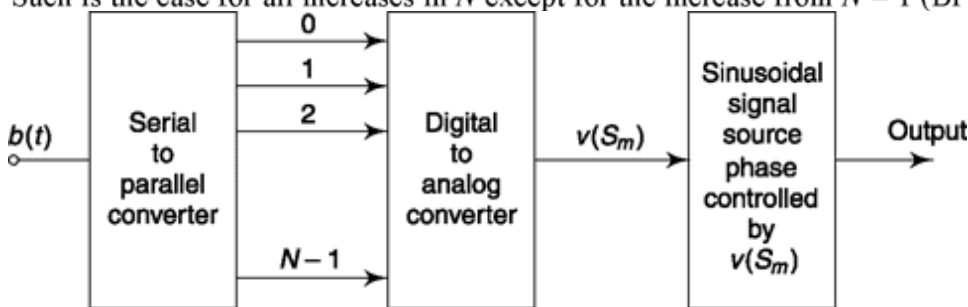
As we have already noted, when signals with spectral density given by Eq. (5.28) are multiplied by a carrier, the resultant spectrum is centered at the carrier frequency and extends nominally over a bandwidth

$$B = \frac{2}{T_s} = 2f_s = 2 \frac{f_b}{N} \quad (5.29)$$

We thus note that as we increase the number of bits N per symbol the bandwidth becomes progressively smaller. On the other hand as we can see from Fig. 5.15 the distance between symbol signal points becomes smaller. We readily calculate (using the law of cosines) that this distance is

$$d = \sqrt{4E_s \sin^2(\pi/M)} = \sqrt{4N E_b \sin^2(\pi/2^N)} \quad (5.30)$$

where E_s is the symbol energy $P_s \times (NT_b) = P_s T_s = NE_b$ and $E_b = P_s T_b$ is the energy associated with one bit. Thus as we increase N , i.e. as we increase the duration of the symbol, the bandwidth decreases, the distance d decreases and, as we shall see, the probability of error becomes higher. Such is the case for all increases in N except for the increase from $N = 1$ (BPSK) to $N = 2$ (QPSK).



M-ARY TRANSMITTER AND RECEIVER

The physical implementation of an M-ary PSK transmission system is moderately elaborate. Such hardware is only of incidental concern to us in this text so we shall describe the M-ary transmitter-receiver somewhat superficially.

As shown in Fig. 5.16, at the transmitter, the bit stream $b(t)$ is applied to a *serial-to-parallel converter*. This converter has facility for storing the N bits of a symbol. The N bits have been presented serially, that is, in time sequence, one after another. These N bits, having been assembled, are then presented all at once on N output lines of the converter, that is they are presented in *parallel*. The converter output remains unchanged for the duration NT_b of a symbol during which time the converter is assembling a new group of N bits. Each symbol time the converter output is updated.

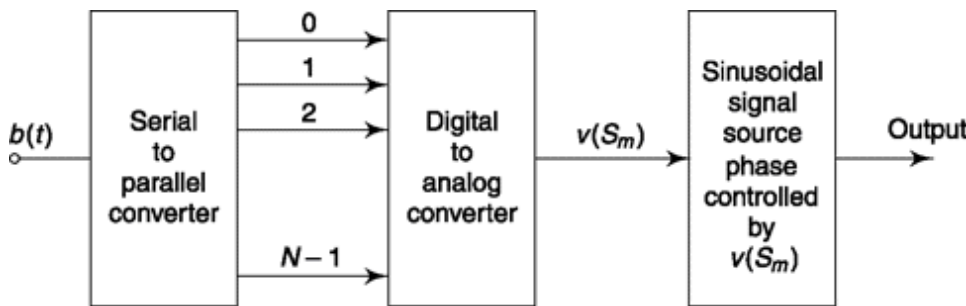


Fig. 5.16 M-ary PSK transmitter.

The converter output is applied to a D/A converter. This D/A converter generates an output voltage which assumes one of $2^N = M$ different values in a one-to-one correspondence to the M possible symbols applied to its input. That is, the D/A output is a voltage $v(S_m)$ which depends on the symbol S_m ($m = 0, 1, \dots, M-1$). Finally, $v(S_m)$ is applied as a control input to a special type of constant-amplitude sinusoidal signal source whose phase f_m is determined by $v(S_m)$. Altogether, then, the output is a fixed amplitude, sinusoidal waveform, whose phase has a one-to-one correspondence to the assembled N -bit symbol. The phase can change once per symbol time.

The receiver, shown in Fig. 5.17 is similar to the nonoffset QPSK receiver. The carrier recovery system requires, in the present case a device to raise the received signal to the M th power, filter to extract the Mf_0 component and then divide by M . The signals indicated in Fig. 5.13 are intended to represent the waveforms only and not the amplitude. Since there is no staggering of parts of the symbol, the integrators extend their integration over the same time interval. Of course, again, a bit synchronizer is needed. The integrator

outputs are voltages whose amplitudes are proportional to $T_s p_e$ and $T_s p_o$ respectively and change at the symbol rate. These voltages measure the components of the received signal in the directions of the quadrature phasors $\sin w_0 t$ and $\cos w_0 t$. Finally the signals $T_s p_e$ and $T_s p_o$ are applied to a device which reconstructs the digital N -bit signal which constitutes the transmitted signal.

There may or may not be a need to regenerate the bit stream. As a matter of fact, the idea of transmitting information one bit at a time by a bit stream $b(t)$ arises when we have a system, like BPSK which can handle only one bit at a time. If, on the other hand, our system handles M -bit symbols, then the data may originate as M -bit words. In such a case the serial to parallel converter shown in Fig. 5.16 is not needed.

Current operating systems are common in which $M = 16$. In this case the bandwidth is $B = 2f_b/4 = f_b/2$ in comparison to $B = f_b$ for QPSK. PSK systems transmit information through signal phase and not through signal amplitude. Hence such systems have great merit in situations where, on account of the vagaries of the transmission medium, the received signal varies in amplitude (i.e. fading channels).

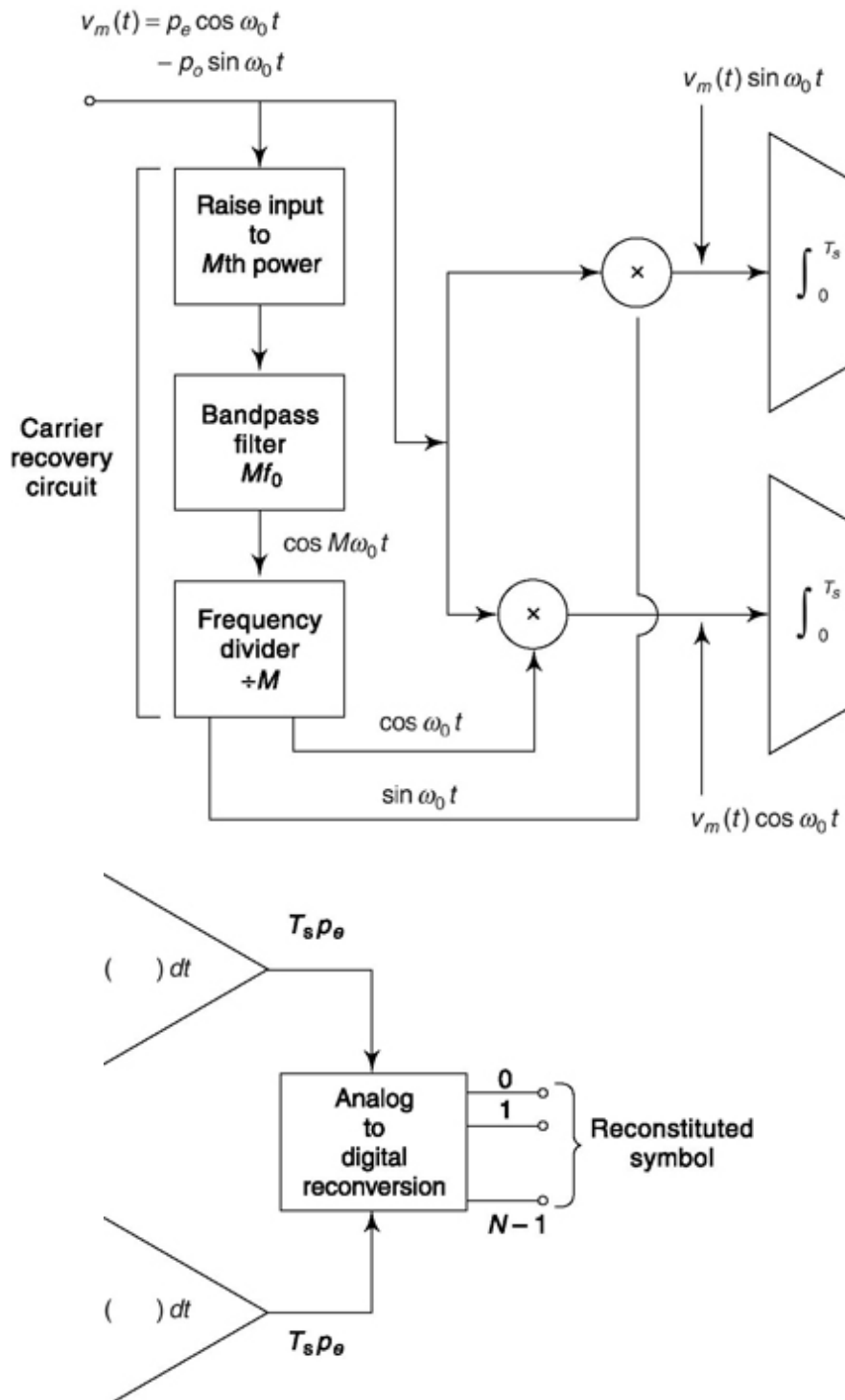


Fig. 5.17 M-ary PSK receiver.

Example 5.1

How does the phase of carrier vary for message $\{m(n)\} = \{1, 0, 1, 1, 0, 1, \dots\}$ in (a) BPSK, (b) DPSK and (c) DEPSK system?

Solution

- (a) From Eq. 5.1 and 5.2, after balance modulator the phase of the carrier will be $\{0, p, 0, 0, p, 0, \dots\}$.
- (b) In DPSK the input to balance modulator of Fig. 5.4, $b(t) = d(t) \oplus b(t - T_b)$ (5.31) represents the Ex-OR operation. Now, the sampled version of $d(t)$ is input $m(n)$. Hence, sampled version of $b(t)$ can be written as, $b(n) = m(n) \oplus b(n - 1)$. Considering, initial value of storage element = 0, $\{b(n)\} = \{1, 1, 0, 1, 1, 0, \dots\}$. Then the phase of the carrier will be $\{0, 0, p, 0, p, \dots\}$ and carrier amplitude $\{c(n)\} = \{+1, +1, -1, +1, +1, -1, \dots\}$. Considering, initial value of storage element = 1, $\{b(n)\} = \{0, 0, 1, 0, 0, 1, \dots\}$. Then the phase of the carrier will be $\{\pi, \pi, 0, \pi, \pi, 0, \dots\}$ and amplitude $\{c(n)\} = \{-1, -1, +1, -1, -1, +1, \dots\}$.
- (c) DEPSK transmitter output is same as DPSK shown in (b).

Example 5.2

Show decoded output in (a) DPSK and (b) DEPSK of Example 5.1.

Solution

- (a) The output here(Fig. 5.6) is obtained from multiplier which in sampled version can be written as,

$$y(n) = c(n)c(n-1) \quad (5.32)$$

For $\{c(n)\} = \{+1, +1, -1, +1, +1, -1, \dots\}$, considering initial value of storage element 0, i.e. -1 as in transmitter we get $\{y(n)\} = \{-1, +1, -1, -1, +1, -1, \dots\} = \{0, 1, 0, 0, 1, 0, \dots\}$

For $\{c(n)\} = \{-1, -1, +1, -1, -1, +1, \dots\}$, considering initial value of storage element 1, i.e. $+1$ as in transmitter we get $\{y(n)\} = \{-1, +1, -1, -1, +1, -1, \dots\} = \{0, 1, 0, 0, 1, 0, \dots\}$

Putting an inverter after multiplier and ignoring the first term we get $\{y(n)\} = \{1, 0, 1, 1, 0, 1, \dots\}$ same as message signal $\{m(n)\}$ of Example 5.1.

Note that, in absence of inverter after multiplier we'll get complement of transmitted binary message. The initial value of the storage element affects the first value only and not the rest which in practical cases is not a major concern.

- (b) The DPSK decoder output from Fig. 5.7 in sampled form can be written as

$$y(n) = b(n) \oplus b(n-1) \quad (5.33)$$

For $\{b(n)\} = \{1, 1, 0, 1, 1, 0, \dots\}$, considering initial value of storage element 0 as in transmitter we get $\{y(n)\} = \{1, 0, 1, 1, 0, 1, \dots\}$

For $\{b(n)\} = \{0, 0, 1, 0, 0, 1, \dots\}$, considering initial value of storage element 1 as in transmitter we get $\{y(n)\} = \{1, 0, 1, 1, 0, 1, \dots\}$

Note that, the initial value of the storage element affects the first value only and not the rest which again in practical cases is not a major issue.

SELF-TEST QUESTION

1. Can BPSK be considered a kind of DSB-SC signal?
2. Overlapping of spectra of BPSK signals leads to which of inter channel or inter symbol interference?
3. How important is initial value of storage/delay element in DPSK method?
4. Is it true that in DEPSK system error always occurs in pairs?
5. Does channel bandwidth requirement reduces by a factor of four in QPSK compared to BPSK?

5.6 QUADRATURE AMPLITUDE SHIFT KEYING (QASK)

In BPSK, QPSK and M-ary PSK, we transmit, in any symbol interval, one signal or another which are distinguished from one another in phase but are all of the *same amplitude*. In each of these individual systems the end points of the signal vectors in signal space falls on the circumference of a circle. Now we have noted that our ability to distinguish one signal vector from another in the presence of noise will depend on the distance between the vector end points. It is hence rather apparent that we shall be able to improve the noise immunity of a system by allowing the signal vectors to differ, not only in their phase but also in amplitude. We now describe such an *amplitude and phase shift keying* system. Like QPSK it involves direct (balanced) modulation of carriers in *quadrature* (i.e. $\cos w_0 t$ and $\sin w_0 t$) and hence might be abbreviated QAPSK. However, the accepted abbreviation is QASK or more simply Quadrature Amplitude Modulation (QAM). To distinguish it from Analog QAM we have discussed in Sec. 2.5.3, we shall use a prefix like 16-QAM when 16 symbols are used, 64-QAM when 64 symbols are used, etc.

As an example of a QASK system, let us consider that we propose to transmit a symbol for every 4 bits. There are then $2^4 = 16$ different possible symbols and we shall have to be able to generate 16 distinguishable signals. One possible geometrical representation of 16 signals is shown in Fig. 5.18. In this configuration each signal point is equally distant from its nearest neighbors, the distance being $d = 2a$. We have placed the points symmetrically about the origin of the signal space to simplify the hardware design of the system while keeping the energy per signal near a minimum. Figure 5.18 also shows one mapping of group of 4 bits representing one symbol in signal space.

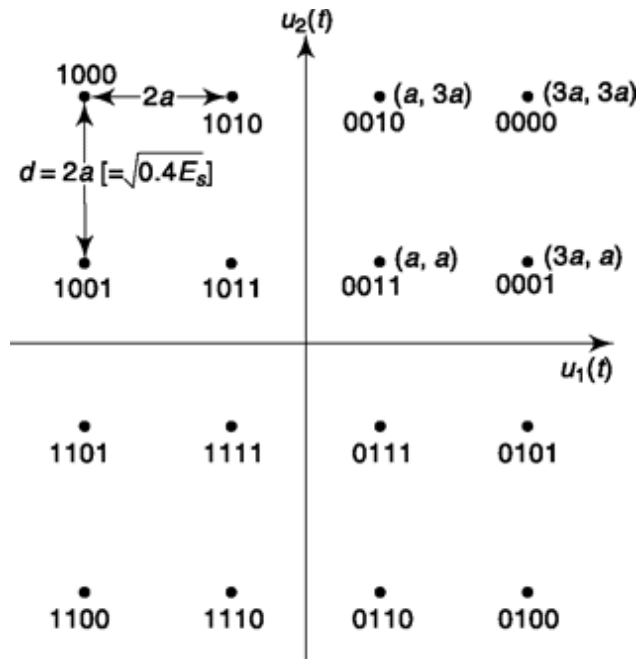


Fig. 5.18 Geometrical representation of 16 signals in a QASK system. Equivalently known as signal constellation diagram of a 16-QAM system.

This is also known as signal constellation or constellation diagram. One may note that there can be many different combinations of these association between symbols and group of 4 bits. In Prob. 12, a different constellation diagram for 16-QAM is shown.

Let us assume (quite reasonably as a matter of practice) that all 16 signals are equally likely. Because of the symmetry displayed in Fig. 5.18 we can determine the average energy associated with a signal, from the four signals in the first quadrant. The average normalized energy of a signal is

$$\begin{aligned} E_s &= \frac{1}{4} [(a^2 + a^2) + (9a^2 + a^2) + (a^2 + 9a^2) + (9a^2 + 9a^2)] \\ &= 10a^2 \end{aligned} \quad (5.34)$$

so that $a = \sqrt{0.1E_s}$ (5.35)

and $d = 2\sqrt{0.1E_s}$ (5.36)

In the present case since each symbol represents 4 bits, the normalized symbol energy is $E_s = 4E_b$ where E_b is the normalized bit energy. Hence,

$$a = \sqrt{0.1E_s} = \sqrt{0.4E_b} \quad \text{and} \quad d = 2\sqrt{0.4E_b} \quad (5.37)$$

This distance is significantly less than the distance between adjacent QPSK signals where, from Eq. (5.19) $d = 2\sqrt{E_b}$; however the distance is greater for 16 QASK or 16 QAM than for 16 MPSK, where, from Eq. (5.30),

$$d = \sqrt{16E_b \sin^2 \frac{\pi}{16}} = 2\sqrt{0.15E_b} \quad (5.38)$$

Thus, 16 QASK will be shown to have a lower error rate than 16 MPSK, but a higher error rate than QPSK.

A typical signal in Fig. 5.18 is

$$v_{\text{QASK}} = k_1 a u_1(t) + k_2 a u_2(t) \quad (5.39)$$

in which k_1 and k_2 are each equal to ± 1 or ± 3 . Since we have that $u_1(t) = \sqrt{(2/T_s)} \cos \omega_0 t$, $u_2(t) = \sqrt{(2/T_s)} \sin \omega_0 t$ and $a = \sqrt{0.1E_s}$ we can write Eq. (5.39) as

$$v_{\text{QASK}} = k_1 \sqrt{0.2 \frac{E_s}{T_s}} \cos \omega_0 t + k_2 \sqrt{0.2 \frac{E_s}{T_s}} \sin \omega_0 t \quad (5.40)$$

and since $E_s/T_s = P_s$ we have

$$v_{\text{QASK}} = k_1 \sqrt{0.2P_s} \cos \omega_0 t + k_2 \sqrt{0.2P_s} \sin \omega_0 t \quad (5.41)$$

A generator of a QASK signal for 4-bit symbol is shown in Fig. 5.19. The 4-bit symbol $b_{k+3} b_{k+2} b_{k+1} b_k$ is stored in the 4-bit register made up of four Flip-Flops. A new symbol is presented once per interval $T_s = 4T_b$ and the content of the register is correspondingly updated at each active edge

Fig. 5.19 Generation of QASK signal.

of the clock which also have a period T_s . Two bits are presented to one D/A converter and two bits to a second converter. The converter output $A_e(t)$ modulates the balanced modulator whose input carrier is the even function $\cos \omega_0 t$ and $A_o(t)$ modulates the modulator with odd-function carrier. The transmitted signal is then

$$v_{\text{QASK}}(t) = A_e(t) \sqrt{P_s} \cos \omega_0 t + A_o(t) \sqrt{P_s} \sin \omega_0 t \quad (5.42)$$

Comparing Eq. (5.41) with Eq. (5.42), we find that

$$A_e, A_o = \pm \sqrt{0.2} \quad \text{or} \quad \pm 3\sqrt{0.2} \quad (5.43)$$

Also, since all four values of A_e and A_o are equally likely, we readily verify that

$$\overline{A_e^2} = \overline{A_o^2} = 1 \quad (5.44)$$

Thus each of the quadrature terms in Eq. (5.44) conveys on the average, one half of the average total transmitted power.

Bandwidth of a QAsK signal

The power spectral density and bandwidth of a QASK signal can be calculated by the procedure applied in the case of M-ary PSK, since Eq. (5.41) is similar to Eq. (5.22). Thus, we have that the power spectral density is (see Prob. 5.18)

$$G_{\text{QASK}}(f) = \frac{P_s T_s}{2} \left[\frac{\sin \pi(f - f_0)T_s}{\pi(f - f_0)T_s} \right]^2 + \frac{P_s T_s}{2} \left[\frac{\sin \pi(f + f_0)T_s}{\pi(f + f_0)T_s} \right]^2 \quad (5.45)$$

where $T_s = NT_b$. The bandwidth of the QASK signal is

$$B = 2f_b/N \quad (5.46)$$

which is the same as in the case of M-ary PSK. For the present case of QASK with $N = 4$ corresponding to 16 possible distinguishable signals we have $B_{\text{QASK}(16)} = f_b/2$ which is one-fourth of the bandwidth required for binary PSK.

5.6.1 The QAsK receiver

The QASK receiver shown in Fig. 5.20 is similar to the QPSK receiver of Fig. 5.13. As in QPSK, a local set of quadrature carriers for synchronous demodulation is generated by raising the received signal to the fourth power, extracting the component at frequency $4f_0$ and then dividing the frequency by 4. In the present case, since the coefficients A_e and A_o are not of fixed value, it behoves us to inquire whether there is still a recoverable carrier. We have

$$v_{\text{QASK}}^4(t) = P_s(A_e(t) \cos \omega_0 t + A_o(t) \sin \omega_0 t)^4 \quad (5.47)$$

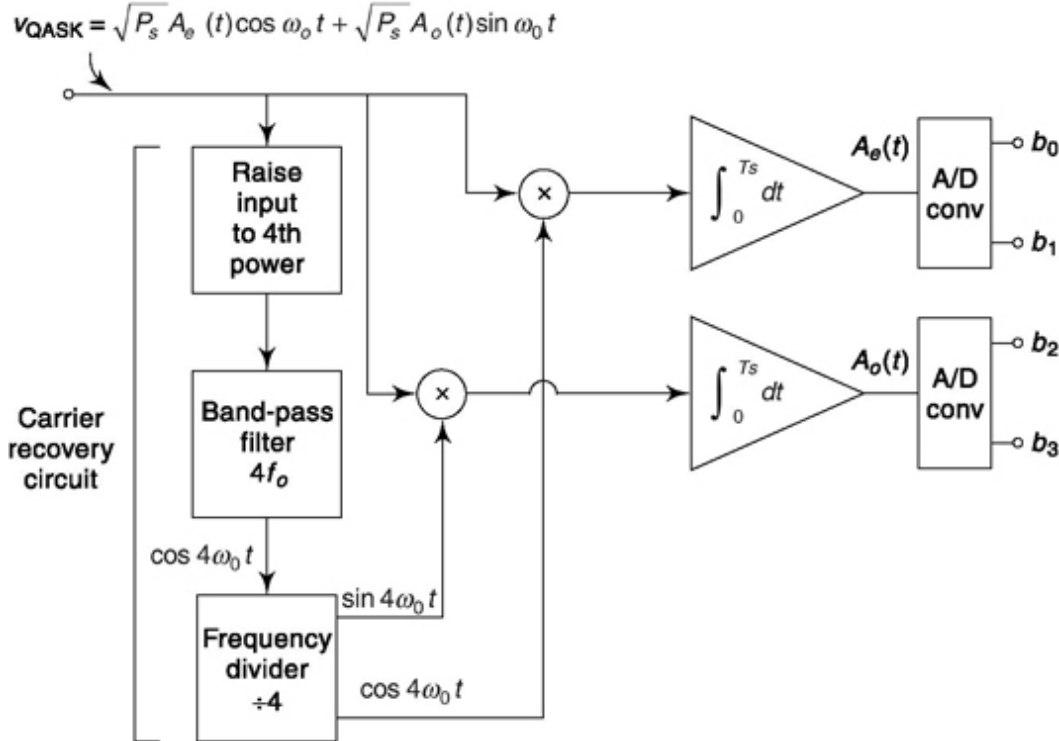


Fig. 5.20 The QASK receiver.

Neglecting all terms not at the frequency $4f_0$ we are left with

$$\begin{aligned} \frac{v_{\text{QASK}}^4(t)}{P_s} &= \left[\frac{A_e^4(t) + A_o^4(t) - 6A_e^2(t)A_o^2(t)}{8} \right] \cos 4\omega_0 t \\ &\quad + \left[\frac{A_e(t) + A_o(t)[A_e^2(t) - A_o^2(t)]}{2} \right] \sin 4\omega_0 t \end{aligned} \quad (5.48)$$

The average value of the coefficient of $\cos 4\omega_0 t$ is not zero while the average value of the coefficient of $\sin 4\omega_0 t$ is zero. Thus, a narrow bandwidth filter centered at $4f_0$ will recover a signal at frequency $4f_0$.

The quadrature carriers being available, two balanced modulators are used together with two integrators as shown to recover the signals $A_e(t)$ and $A_o(t)$. The integrators have an integration time equal to the symbol time T_s and, of course, as usual, symbol time synchronizers (not shown) are required. Finally, the original input bits are recovered by using A/D converters.

5.7 BINARY FREQUENCY SHIFT KEYING (BFSK)

In binary frequency-shift keying (BFSK) the binary data waveform $d(t)$ generates a binary signal

$$v_{\text{BFSK}}(t) = \sqrt{2P_s} \cos [\omega_0 t + d(t)\Omega t] \quad (5.49)$$

Here $d(t) = +1$ or -1 corresponding to the logic levels 1 and 0 of the data waveform. The transmitted signal is of amplitude $\sqrt{2P_s}$ and is either

$$v_{\text{BFSK}}(t) = s_H(t) = \sqrt{2P_s} \cos (\omega_0 + \Omega)t \quad (5.50)$$

or $v_{\text{BFSK}}(t) = s_L(t) = \sqrt{2P_s} \cos (\omega_0 - \Omega)t \quad (5.51)$

and thus has an angular frequency $\omega_0 + \Omega$ or $\omega_0 - \Omega$ with Ω a constant offset from the nominal carrier frequency ω_0 . We shall call the higher frequency $\omega_H (= \omega_0 + \Omega)$ and the lower frequency $\omega_L (= \omega_0 - \Omega)$. We may conceive that the BFSK signal is generated in the manner indicated in Fig. 5.21. Two balanced modulators are used, one with carrier ω_H and one with carrier ω_L . The voltage values of $p_H(t)$ and of $p_L(t)$ are related to the voltage values of $d(t)$ in the following manner

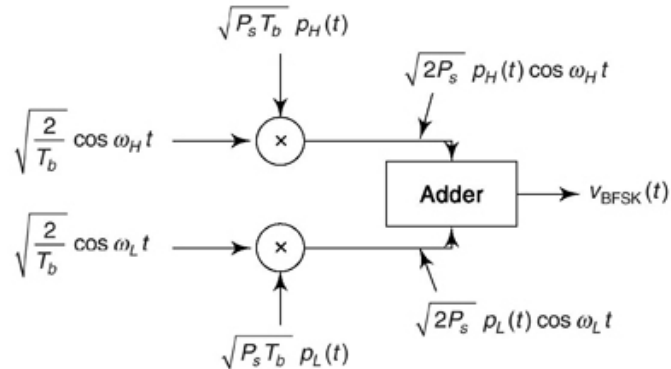


Fig. 5.21 A representation of a manner in which a BFSK signal can be generated.

$d(t)$	$p_H(t)$	$p_L(t)$
+1V	+1V	0V
-1V	0V	+1V

Thus when $d(t)$ changes from +1 to -1, p_H changes from 1 to 0 and p_L from 0 to 1. At any time either p_H or p_L is 1 but not both so that the generated signal is either at angular frequency ω_H or at ω_L .

5.7.1 spectrum of BFsk

In terms of the variables p_H and p_L , the BFSK signal is

$$v_{\text{BFSK}}(t) = \sqrt{2P_s} p_H \cos (\omega_H t + \theta_H) + \sqrt{2P_s} p_L \cos (\omega_L t + \theta_L) \quad (5.52)$$

where we have assumed that each of the two signals are of independent and random, uniformly distributed phase. Each of the terms in Eq. (5.52) looks like the signal $(2P_s b(t) \cos \omega_0 t)$ which we encountered in BPSK [see Eq. (5.3)] and for which we have already deduced the spectrum, but there is an important difference. In the BPSK case, $b(t)$ is bipolar, i.e. it alternates between +1 and -1 while in the present case p_H and p_L are unipolar, alternating between +1 and 0. We may, however, rewrite p_H and p_L as the sums of a constant and a bipolar variable, that is

$$p_H(t) = \frac{1}{2} + \frac{1}{2} p'_H(t) \quad (5.53a)$$

$$p_L(t) = \frac{1}{2} + \frac{1}{2} p'_L(t) \quad (5.53b)$$

In Eq. (5.53), p_H and p_L are bipolar, alternating between +1 and -1 and are complementary. When p_H is +1, p'_L = -1 and vice versa. We have then

$$v_{\text{BFSK}}(t) = \sqrt{2P_s} p_H \cos(\omega_H t + \theta_H) + \sqrt{2P_s} p_L \cos(\omega_L t + \theta_L) \quad (5.52)$$

The first two terms in Eq. (5.54) produce a power spectral density which consists of two impulses, one at f_H and one at f_L . The last two terms produce the spectrum of two binary PSK signals (see Fig. 5.2a) one centered about f_H and one about f_L . The individual power spectral density patterns of the last two terms in Eq. (5.54) are shown in Fig. 5.22 for the case $f_H - f_L = 2f_b$. For this separation between f_H and f_L we observe that the overlapping between the two parts of the spectra is not large and we may expect to be able, without excessive difficulty, to distinguish the levels of the binary waveform $d(t)$. In any event, with this separation the bandwidth of BFSK is

$$BW(\text{BFSK}) = 4f_b \quad (5.55)$$

which is twice the bandwidth of BPSK.

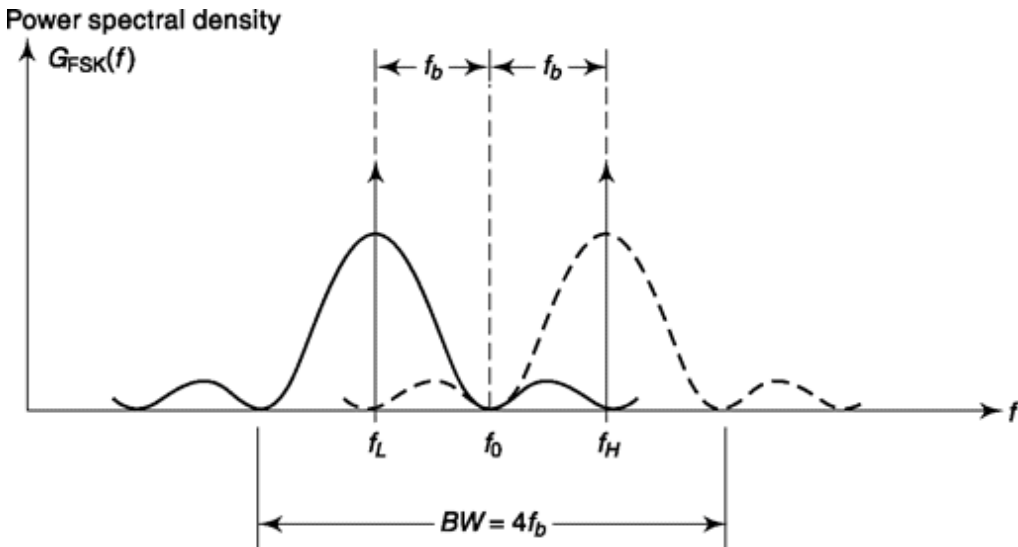


Fig. 5.22 The power spectral densities of the individual terms in Eq. (5.54).

5.7.2 The BFSK Receiver

A BFSK signal is typically demodulated by a receiver system as in Fig. 5.23. The signal is applied to two bandpass filters one with center frequency at f_H the other at f_L . Here we have assumed, as

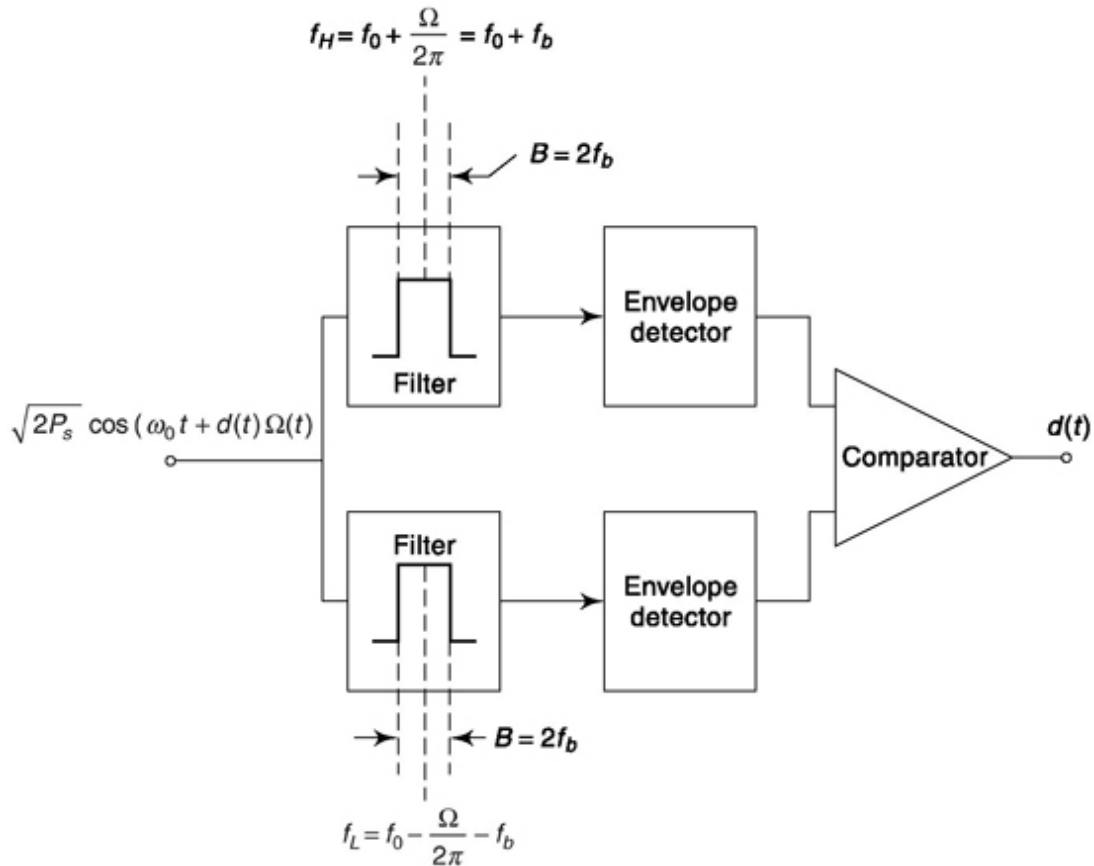


Fig. 5.23 A receiver for a BFSK signal.

above, that $f_H - f_L = 2(W/2p) = 2f_b$. The filter frequency ranges selected do not overlap and each filter has a passband wide enough to encompass a main lobe in the spectrum of Fig. 5.22. Hence one filter will pass nearly all the energy in the transmission at f_H , the other will perform similarly for the transmission at f_L . The filter outputs are applied to envelope detectors and finally the envelope detector outputs are compared by a comparator. A comparator is a circuit that accepts two input signals. It generates a binary output which is at one level or the other depending on which input is larger. Thus, at the comparator output the data $d(t)$ will be reproduced.

When noise is present, the output of the comparator may vary due to the systems response to the signal and noise. Thus, practical systems use a bit synchronizer and an integrator and sample the comparator output only once at the end of each time interval T_b .

5.7.3 signal space representation of Orthogonal BFSK

We noted, in M-ary phase-shift keying and in quadrature-amplitude shift keying, that any signal could be represented as $Qu(t) + C_2u_2(t)$. There $u_x(t)$ and $u_2(t)$ are the orthonormal vectors in signal space,

that is, $u_x(t) = yj2/T_s \cos w_0t$ and $u_2(t) = (21 T_s \sin w_0t)$. The functions u_1 and u_2 are orthonormal over the symbol interval T_s and, if the symbol is a single bit, $T_s = T_b$. The coefficients C_1 and C_2 are constants. The normalized energies associated with $C_1u_1(t)$ and with $C_2u_2(t)$ are respectively C_j^2 and C_2^2 and the total signal energy is $C_j^2 + C_2^2$. In M-ary PSK and QASK, the orthogonality of the vectors u_1 and u_2 results from their *phase quadrature*. In the present case of BFSK it is appropriate that the orthogonality should result from a special *selection of the frequencies* of the unit vectors. Accordingly, with m and n integers, let us establish unit vectors

$$u_1(t) = \sqrt{\frac{2}{T_b}} \cos 2\pi m f_b t \quad (5.56)$$

and

$$u_2(t) = \sqrt{\frac{2}{T_b}} \cos 2\pi n f_b t \quad (5.57)$$

in which, as usual, $f_b = 1/T_b$. The vectors u_1 and u_2 are the m th and n th harmonics of the (fundamental) frequency f_b . As we are aware, from the principles of Fourier analysis, different harmonics ($m \pm n$) are orthogonal over the interval of the fundamental period $T_b = 1/f_b$.

If now the frequencies f_H and f_L in a BFSK system are selected to be (assuming $m \pm n$)

$$f_H = m f_b \quad (5.58a)$$

$$f_L = n f_b \quad (5.58b)$$

then the corresponding signal vectors are

$$s_H(t) = \sqrt{E_b} u_1(t) \quad (5.59a)$$

$$s_L(t) = \sqrt{E_b} u_2(t) \quad (5.59b)$$

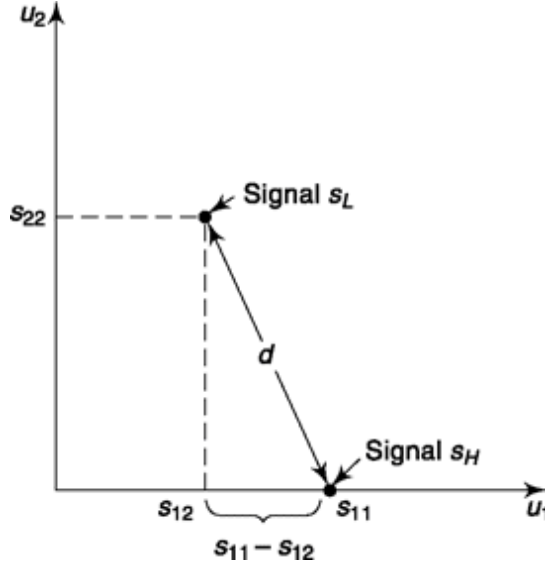


Fig. 5.25 Signal space representation of BFSK when $s_H(t)$ and $s_L(t)$ are not orthogonal.

Using Eq. (5.61b) we first determine s_{12} by multiplying both sides of the equation by $u_1(t)$ and integrating from $0 \leq t \leq T_b$. The result is

$$\begin{aligned} s_{12} &= \sqrt{2P_s} \int_0^{T_b} u_1(t) \cos \omega_L t \, dt \\ &= \frac{E_b}{s_{11}} \left[\frac{\sin(\omega_H - \omega_L)T_b}{(\omega_H - \omega_L)T_b} + \frac{\sin(\omega_H + \omega_L)T_b}{(\omega_H + \omega_L)T_b} \right] \end{aligned} \quad (5.64a)$$

To arrive at this result we have used Eq. (5.61a) where

$$u_1(t) = (\sqrt{2P_s}/s_{11}) \cos \omega_H t \quad (5.64b)$$

Finally, s_{22} is found from Eq. (5.61a) by squaring both sides of the equation and then integrating from 0 to T_b . Since u_1 and u_2 are orthogonal, the result is

$$\int_0^{T_b} s_L^2(t) \, dt = 2P_s \int_0^{T_b} \cos^2 \omega_L t \, dt = s_{12}^2 + s_{22}^2 \quad (5.65a)$$

Hence

$$s_{12}^2 + s_{22}^2 = E_b \left[1 + \frac{\sin 2\omega_L T_b}{2\omega_L T_b} \right] \quad (5.65b)$$

The distance d between s_H and s_L given in Eq. (5.62) can now be determined by substituting Eqs (5.63), (5.64a) and (5.65b) into Eq. (5.62). The result is:

$$d^2 = E_b \left[1 + \frac{\sin 2\omega_H T_b}{2\omega_H T_b} \right] - 2E_b \left[\frac{\sin(\omega_H - \omega_L)T_b}{(\omega_H - \omega_L)T_b} + \frac{\sin(\omega_H + \omega_L)T_b}{(\omega_H + \omega_L)T_b} \right] + E_b \left[1 + \frac{\sin 2\omega_L T_b}{2\omega_L T_b} \right] \quad (5.66)$$

Equation (5.66) can be simplified by recognizing that

$$\left| \frac{\sin 2\omega_H T_b}{2\omega_H T_b} \right| \ll 1$$

$$\left| \frac{\sin 2\omega_L T_b}{2\omega_L T_b} \right| \ll 1$$

and

$$\left| \frac{\sin (\omega_H + \omega_L) T_b}{(\omega_H + \omega_L) T_b} \right| \ll \left| \frac{\sin (\omega_H - \omega_L) T_b}{(\omega_H - \omega_L) T_b} \right|$$

The final result is then

$$d^2 \approx 2E_b \left[1 - \frac{\sin (\omega_H - \omega_L) T_b}{(\omega_H - \omega_L) T_b} \right] \quad (5.67)$$

Note that when $s_H(t)$ and $s_L(t)$ are orthogonal $(\omega_H - \omega_L)T_b = 2\pi(m - n)f_bT_b = 2\pi(m - n)$ and Eq. (5.67) gives $d = \sqrt{2E_b}$ as expected. Note also that if $(\omega_H - \omega_L)T_b = 3\pi/2$, the distance d is increased and becomes

$$d_{\text{opt}} = \left[2E_b \left(1 + \frac{2}{3\pi} \right) \right]^{1/2} \approx \sqrt{2.4E_b} \quad (5.68)$$

an increase in d^2 by 20 percent.

5.7.5 Comparison of BFSK and BPSK

Let us start with the BFSK signal of Eq. (5.49). Using the trigonometric identity for the cosine of the sum of two angles and recalling that $\cos d = \cos (-d)$ while $\sin d = -\sin (-d)$ we are led to the alternate equivalent expression

$$v_{\text{BFSK}}(t) = \sqrt{2P_s} \cos \Omega t \cos \omega_0 t - \sqrt{2P_s} d(t) \sin \Omega t \sin \omega_0 t \quad (5.69)$$

Note that the second term in Eq. (5.69) looks like the signal encountered in BPSK, i.e. a carrier $\sin \omega_0 t$ multiplied by a data bit $d(t)$ which changes the carrier phase. In the present case however, the carrier is not of fixed amplitude but rather the amplitude is shaped by the factor $\sin \Omega t$. We note further the presence of a quadrature reference term $\cos \Omega t \cos \omega_0 t$ which contains no information. Since this quadrature term carries energy, the energy in the information bearing term is thereby diminished. Hence we may expect that BFSK will not be as effective as BPSK in the presence of noise. For orthogonal BFSK, each term has the same energy, hence the information bearing term contains only one-half of the total transmitted energy.

5.8 M-ARY FSK

An M -ary FSK communications system is shown in Fig. 5.26. It is an obvious extension of a binary FSK system. At the transmitter an N -bit symbol is presented each T_s to an N -bit D/A converter.

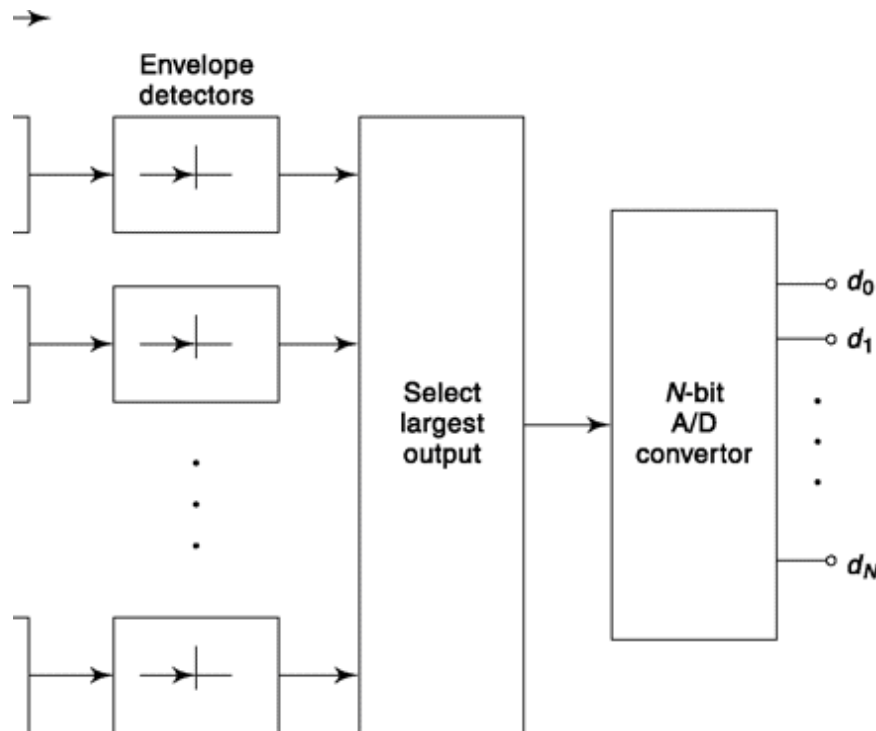


Fig. 5.26 An M -ary communications system.

The converter output is applied to a frequency modulator, i.e. a piece of hardware which generates a carrier waveform whose frequency is determined by the modulating waveform. The transmitted signal, for the duration of the symbol interval, is of frequency f_0 or f_1 ... or f_{M-1} with $M = 2^N$. At the receiver, the incoming signal is applied to M paralleled bandpass filters each followed by an envelope detector. The bandpass filters have center frequencies f_0, f_1, \dots, f_{M-1} . The envelope detectors apply their outputs to a device which determines which of the detector indications is the largest and transmits that envelope output to an N -bit A/D converter.

As we shall see (Sec. 11.5.4) the probability of error is minimized by selecting frequencies f_0, f_1, \dots, f_{M-1} so that the M signals are mutually orthogonal. One commonly employed arrangement simply provides that the carrier frequency be successive even harmonics of the symbol frequency $f_s =$

$1/T_s$. Thus, the lowest frequency, say f_0 is $f_0 = kf_s$ while $f = (k + 2)f_s$, $f_2 = (k + 4)f_s$, etc. In this case, the spectral density patterns of the individual possible transmitted signals overlap in the manner shown in Fig. 5.27, which is an extension to M -ary FSK of the pattern of Fig. 5.22 which applies to binary FSK. We observe that to pass M -ary FSK the required spectral range is

$$B = 2Mf_s \quad (5.70)$$

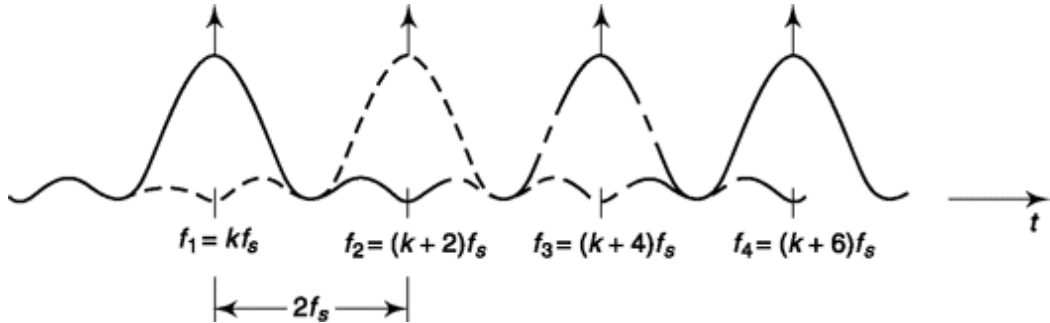


Fig. 5.27 Power spectral density of M -ary FSK (four frequencies are shown).

Since $f_s = f_b/N$ and $M = 2^N$, we have

$$B = 2^{N+1} f_b/N \quad (5.71)$$

Note that M -ary FSK requires a considerably increased bandwidth in comparison with M -ary PSK. However, as we shall see, the probability of error for M -ary FSK *decreases* as M increases, while for M -ary PSK, the probability of error increases with M .

Signal Space Representation of M-Ary Fsk

In Fig. 5.24, we provided a signal space representation for the case of orthogonal binary FSK. The case of M -ary orthogonal FSK signals is clearly an extension of this figure. We simply conceive of a coordinate system with M mutually orthogonal coordinate axes. The signal vectors are then parallel to these axes. The best we can do pictorially is the three-dimensional case shown in Fig. 5.28. As usual, and as is indicated in the figure, the square of the length of the signal vector is the normalized signal energy. Note that, as in Fig. 5.24, the distance between signal points is

$$d = \sqrt{2E_s} = \sqrt{2NE_b} \quad (5.72)$$

Note that this value of d is greater than the values of d calculated for M -ary PSK with the exception of the cases $M = 2$ and $M = 4$. It is also greater than d in the case of 16 QAM.

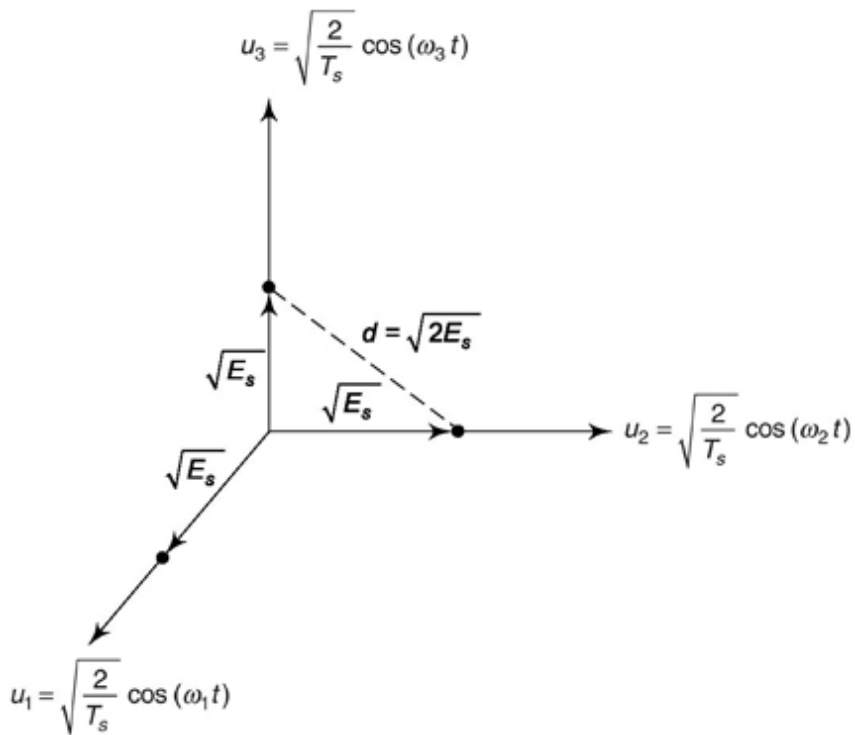


Fig. 5.28 Geometrical representation of orthogonal M -ary FSK ($M = 3$) when the frequencies are selected to generate orthogonal signals.

5.9 MINIMUM SHIFT KEYING (MSK)

In digital radio communication, one of the key concerns is the power in the sidelobes. A spectrum rich in harmonic content is likely to cause interference with the nearby channels. The abrupt change in phase in PSK gives rise to spectral components in high frequencies. Minimum Shift Keying (MSK) addresses this by changing phase in a continuous manner and is also known as Continuous Phase Modulation (CPM). Gaussian Minimum Shift Keying (GMSK) where the abrupt change in digital data is smoothed by passing it through a Gaussian shaped filter before modulating a carrier is used in Global System for Mobile Communications (GSM).

5.9.1 The Effect of sidelobe

In discussing *minimum shift keying*, we shall want to make a number of comparisons between MSK and QPSK. One of these comparisons will concern the spectra of the two systems. For this reason we review briefly some matters concerning the spectrum of QPSK. In offset QPSK the transmitted signal is Tsee Eq. (5.14)1

$$v_{\text{OQPSK}}(t) = \sqrt{P_s} b_e(t) \cos \omega_0 t + \sqrt{P_s} b_o(t) \sin \omega_0 t \quad (5.73)$$

To find the power spectral density of this signal we start with the power spectral density of the baseband waveform $b_e(t)$. The waveform $p(t) = \sqrt{P_s} \equiv b_e(t)$ is a random sequence of rectangular waveforms, flat topped for symbol duration $T_s = 2T_b$, and having an amplitude $\pm\sqrt{P_s}$. Its power spectral density $G(f)$ is given by the general formula (Eq. (6.140))

$$G_p(f) = \frac{\overline{|P(f)|^2}}{T_s} \quad (5.74)$$

where $P(f)$ is the Fourier transform $p(t)$. We readily calculate that the two-sided power spectral density of $p(t)$ is, with $f_s = 1/T_s = f_b/2$ and $P_s = E_b/T_b$

$$G_p(f) = 2E_b \left(\frac{\sin 2\pi f/f_b}{2\pi f/f_b} \right)^2 \quad (5.75)$$

The spectral density of $\sqrt{P_s} b_e(t) \cos \omega_0 t$ is generated by translating the two-sided pattern of Eq. (5.75) to $+f_0$ and also to $-f_0$, each such translated pattern being reduced in magnitude by 4 because the multiplication of $\sqrt{P_s} b_e(t)$ by $\cos \omega_0 t$ translates one-half of the voltage spectrum to f_0 and the other half to $-f_0$. (See Sec. 2.1.1.) Thus, the voltage of each term is reduced by 2 and the power by 4. The power spectral density of the second term in Eq. (5.73), that is the term $\sqrt{P_s} b_o(t) \sin \omega_0 t$ is identical to the density of the first. Finally we note that the two terms are not correlated since $b_e(t)$ and $b_o(t)$ are quite independent of one another. Hence the total power density is twice the density generated by either term. Altogether then we find

$$G_{\text{OQPSK}}(f) = E_b \left\{ \left[\frac{\sin 2\pi(f-f_0)/f_b}{2\pi(f-f_0)/f_b} \right]^2 + \left[\frac{\sin 2\pi(f+f_0)/f_b}{2\pi(f+f_0)/f_b} \right]^2 \right\} \quad (5.76)$$

Earlier, upon examining the pattern for the power spectral density (see Fig. 5.2) we took the attitude that the bandwidth of QPSK (QPSK and OQPSK yield the same result) is $B = f_b$ because such a bandwidth is adequate to encompass the main lobe. The main lobe contains 90 percent of the signal energy. Still, the inconsiderable power outside the main lobe is a source of trouble when QPSK is to be used for multichannel communication on adjacent carriers. If, say, we establish additional channels at carrier frequencies $f'_0 = f_0 \pm f_b$, then the side lobe associated with the first channel, having a peak value at frequency $f_0 + 3f_b/4$, will be a source of serious interchannel interference. These side lobes, as is to be noted in Fig. 5.2, are smaller than the main lobe by only 14 dB.

This difficulty, i.e. the wide spectrum of QPSK, is due to the character of the baseband signal. This signal consists of *abrupt changes*, and abrupt changes give rise to *spectral components at high frequencies*. In short, the baseband spectral range is very large and multiplication by a carrier translates the spectral pattern without changing its form. We might try to alleviate the difficulty by passing the baseband signal through a low-pass filter to suppress the many side lobes. Such filtering will cause intersymbol interference. The problem of interchannel interference in QPSK is so serious that regulatory and standardization agencies such as the FCC and CCIR will not permit these systems to be used except with bandpass filtering at the carrier frequency (i.e. at the transmitter output) to suppress the side lobes.

The filtering which we have just described does not, in certain situations, necessarily resolve the problem of interchannel interference. We shall discuss the matter qualitatively: We recall that QPSK (staggered or not) is a system in which the signal is of constant amplitude, the information content being borne by phase changes. In both QPSK and OQPSK there are abrupt phase changes in the signal. In QPSK these changes can occur at the symbol rate $1/T_s = 1/2T_b$ and can be as large

as 1800° . In OQPSK phase changes of 900° can occur at the bit rate. Now it turns out that when such waveforms with abrupt phase changes, are filtered to suppress sidebands, the effect of the filter, at the times of the abrupt phase

changes, is to cause substantial changes in the *amplitude* of the waveform. Such amplitude variations can cause problems in QPSK communication systems which employ repeaters, i.e. stations which receive and rebroadcast signals such as earth satellites. For such stations often employ nonlinear power output stages in their transmitters. These nonlinear stages suppress the amplitude variations. However, precisely because of their nonlinearity, they generate spectral components outside the range of the main lobe thereby undoing the effect of the bandlimit-ing filtering and causing interchannel interference. In this matter QPSK with its 1800° phase changes is a substantially worse offender than OQPSK with only 900° phase changes.

5.9.2 MsK as FsK

There are two important differences between QPSK and MSK:

1. In MSK the baseband waveform, that multiplies the quadrature carrier, is much “smoother” than the abrupt rectangular waveform of QPSK. While the spectrum of MSK has a main center lobe which is 1.5 times as wide as the main lobe of QPSK, the side lobes in MSK are relatively much smaller in comparison to the main lobe, making filtering much easier.
2. The waveform of MSK exhibits *phase continuity*, that is, there are no abrupt phase changes as in QPSK. As a result we avoid the intersymbol interference caused by nonlinear amplifiers.

The waveforms of MSK are shown in Fig. 5.29. In (a) we start with a typical data bit stream $b(t)$. This bit stream is divided into an odd and an even bit stream in (b) and (c), as in the manner of OQPSK. The odd stream $b_o(t)$ consists of the alternate bits b_1, b_3, \dots , and the even stream $b_e(t)$ consists of b_2, b_4, \dots . Each bit in both streams is held for two bit intervals $2T_b = T_s$, the symbol time. The staggering, which is optional in QPSK, is essential in MSK as we shall see. Observe again, as we noted earlier, the effect of the staggering is that the changes in the odd and even stream do not occur at the same time.

Also generated at the MSK transmitter are the waveforms $\sin 2p(t/4T_b)$ and $\cos 2p(t/4T_b)$ as in (d). These waveforms, and their phases with respect to the bit streams $b_o(t)$ and $b_e(t)$, meet the essential requirements that $\sin 2p(t/4T_b)$ passes through zero precisely at the end of the symbol time in $b_e(t)$ and $\cos 2p(t/4T_b)$ passes through zero at the end of the symbol time in $b_o(t)$.

We now generate the products $b_e(t) \sin 2\pi(t/4T_b)$ and $b_o(t) \cos 2\pi(t/4T_b)$ which are shown in (e) and (f).

In MSK the transmitted signal is

$$v_{MSK}(t) = \sqrt{2P_s} \left[b_e(t) \sin 2\pi \left(\frac{t}{4T_b} \right) \right] \cos \omega_0 t + \sqrt{2P_s} \left[b_o(t) \cos 2\pi \left(\frac{t}{4T_b} \right) \right] \sin \omega_0 t \quad (5.77)$$

(As is readily verified, the coefficient J_p in Eq. (5.73) needs to appear as $(2P_s$ in Eq. (5.77) in order that P_s shall continue to represent the total signal power.) Thus, in comparing Eq. (5.73) and Eq. (5.77) we observe that in OQPSK the quadrature carriers $\cos \omega_0 t$ and $\sin \omega_0 t$ are multiplied by the rectangular abruptly changing odd and even bit streams. In MSK, in contrast, the carriers are multiplied by the “smoother” waveforms shown in Fig. 5.29(e) and (f). As we may expect and as we shall verify, the side lobes generated by these smoother waveforms will be smaller than those associated with the rectangular waveforms and hence easier to suppress as is required to avoid interchannel interference.

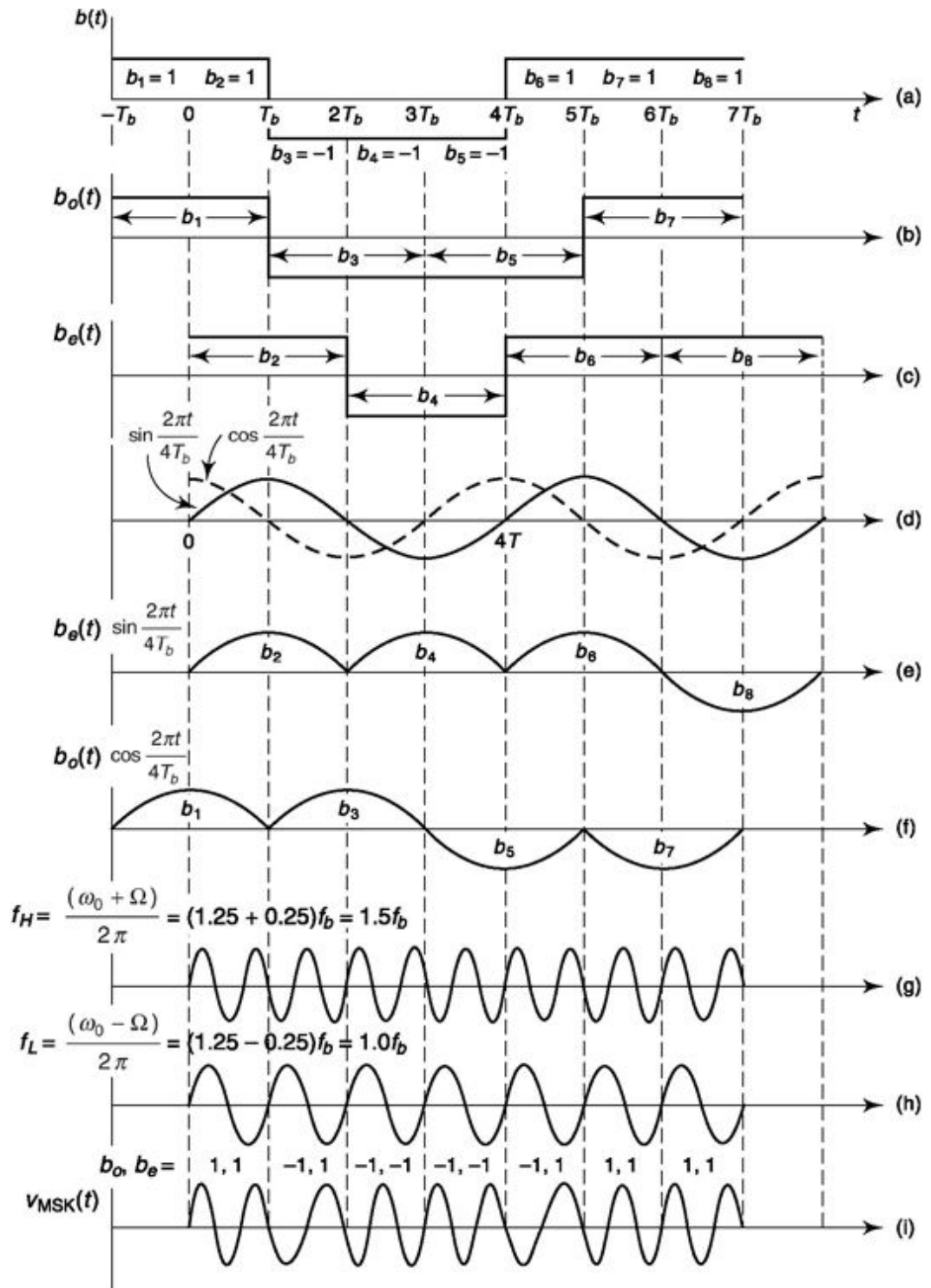


Fig. 5.29 MSK waveforms.

In Eq. (5.77), MSK appears as a modified form of OQPSK, which we can call “shaped QPSK”. We can, however, rewrite the equation to make it apparent that MSK is an FSK system. Applying the trigonometric identities for the products of sinusoids we find that Eq. (5.77) can be written:

$$v_{\text{MSK}}(t) = \sqrt{2P_s} \left[\frac{b_o(t) + b_e(t)}{2} \right] \sin(\omega_0 + \Omega)t + \sqrt{2P_s} \left[\frac{b_o(t) - b_e(t)}{2} \right] \sin(\omega_0 - \Omega)t \quad (5.78a)$$

where

$$\Omega = \frac{2\pi}{4T_b} = 2\pi \left(\frac{f_b}{4} \right) \quad (5.78b)$$

If we define: $C_H = (b_o + b_e)/2$, $C_L = (b_o - b_e)/2$, $\omega_H = \omega_0 + \Omega$, $\omega_L = \omega_0 - \Omega$ then Eq. (5.78) becomes

$$v_{\text{MSK}}(t) = \sqrt{2P_s} C_H(t) \sin \omega_H t + \sqrt{2P_s} C_L(t) \sin \omega_L t \quad (5.79)$$

Now $b_o = \pm 1$ and $b_e = \pm 1$, so that as is easily verified, if $b_o = b_e$ then $C_L = 0$ while $C_H = b_o = \pm 1$. Further, if $b_o = -b_e$ then $C_H = 0$ and $C_L = b_o = \pm 1$. Thus, depending on the value of the bits b_o and b_e in each bit interval, the transmitted signal is at angular frequency ω_H or at ω_L precisely as in FSK and the magnitude of the amplitude is always equal to $\sqrt{2P_s}$.

In MSK, the two frequencies f_H and f_L are chosen to insure that the two possible signals are orthogonal over the bit interval T_b . That is, we impose the constraint that

$$\int_0^{T_b} \sin \omega_H t \sin \omega_L t dt = 0 \quad (5.80)$$

As may be verified, Eq. (5.80) will be satisfied provided it is arranged, with m and n integers, that

$$2\pi(f_H - f_L)T_b = n\pi \quad (5.81a)$$

and

$$2\pi(f_H + f_L)T_b = m\pi \quad (5.81b)$$

Furthermore, using Eq. (5.78b):

$$f_H = f_0 + \frac{f_b}{4} \quad (5.82a)$$

and

$$f_L = f_0 - \frac{f_b}{4} \quad (5.82b)$$

Using Eq. (5.82) and Eq. (5.81) we find that

$$f_b T_b = f_b \cdot \frac{1}{f_b} = 1 = n \quad (5.83a)$$

and

$$f_0 = \frac{m}{4} f_b \quad (5.83b)$$

Equation (5.83a) shows that since $n = 1$, f_H and f_L are as close together as possible for orthogonality to prevail. It is for this reason that the present system is called “minimum shift keying.” Equation (5.83b) shows that the carrier frequency f_0 is an integral multiple of $f_b/4$. Thus,

$$f_H = (m + 1) \frac{f_b}{4} \quad (5.84a)$$

and

$$f_L = (m - 1) \frac{f_b}{4} \quad (5.84b)$$

5.9.3 signal space representation of MsK

The signal space representation of MSK is shown in Fig. 5.30. The orthonormal unit vectors of the coordinate system are given by $u_H(t) = (\sqrt{2/T_s} \sin \omega_H t)$ and $u_L(t) = (\sqrt{2/T_s} \sin \omega_L t)$. The end points of the four possible signal vectors are indicated by dots. The smallest distance between signal points is

$$d = \sqrt{2E_s} = \sqrt{4E_b}$$

just as for the case of QPSK.

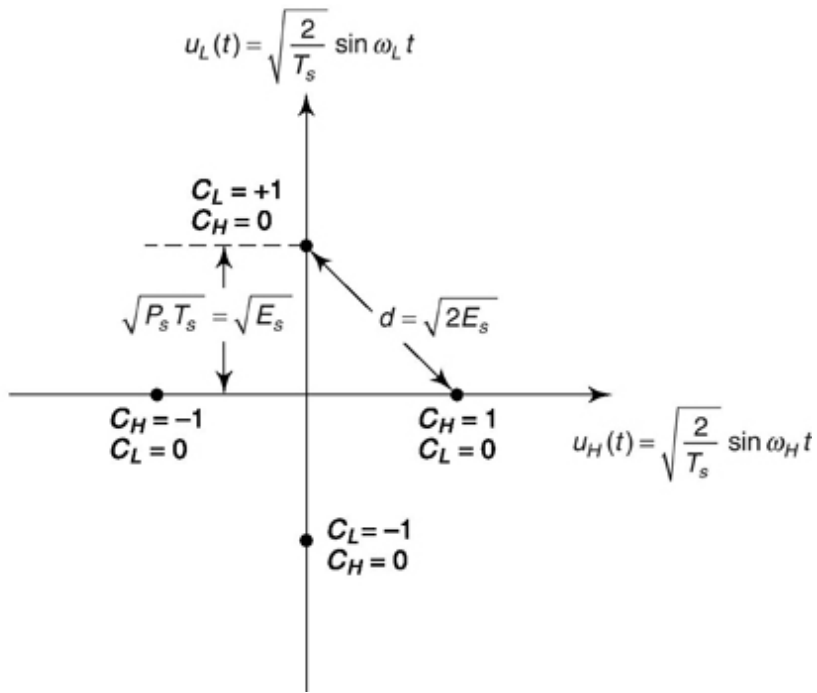


Fig. 5.30 Signal space representation of MSK.

We recall that QPSK generates two BPSK signals which are orthogonal to one another by virtue of the fact that the respective carriers are in phase quadrature. Such phase quadrature can also be characterized as *time* quadrature since, at a carrier frequency f_0 a phase shift of $\pi/2$ is accomplished by a time shift in amount $1/4f_0$, that is $\sin 2\pi f_0(t + 1/4f_0) = \sin(2\pi f_0 t + \pi/2) = \cos(2\pi f_0 t)$. It is of interest to note, in contrast, that in MSK we have again two BPSK signals [i.e. the two individual terms in Eq. (5.79)]. Here, however, the respective carriers are orthogonal to one another by virtue of the fact that they are in *frequency* quadrature.

5.9.4 phase Continuity in MsK

A most important and useful feature of MSK is its *phase continuity*. This matter is illustrated in Fig. 5.29 in waveforms in (g), (h) and (i). Here we have assumed that $f_0 = 5f_b/4$ so that

$$f_H = f_0 + f_b/4 = 5f_b/4 + f_b/4 = 1.5f_b$$

and also $f_L = f_0 - f_b/4 = 1.0f_b$. Carriers of frequencies f_H and f_L are shown in (g) and (h). We also find, from Eq. (5.78a), that for the various combinations of b_o and b_e , $v_{MSK}(t)/\sqrt{2P_s}$ is given in Table 5.1.

b_e	b_o	$v_{MSK}(t)/\sqrt{2P_s}$
-1	-1	$-\sin(\omega_0 + \Omega)t$
-1	1	$\sin(\omega_0 - \Omega)t$
1	-1	$-\sin(\omega_0 - \Omega)t$
1	1	$\sin(\omega_0 + \Omega)t$

For the bit sequences b_o and b_e in Fig. 5.29b and c the corresponding waveform $v_{MSK}(t)$ is shown in (i). The values of b_o and b_e are tabulated in (i) for each bit intervals. We note, of course, that because of the staggering, b_o and b_e do not change simultaneously. The waveform for $v_{MSK}(t)$ is generated in the following way: In each bit interval we determine from Eq. (5.80) or the table presented below, whether to use the carrier of frequency f_H or of frequency f_L , and also whether or not the carrier waveform is to be inverted. Having made such a determination, the waveform of $v_{MSK}(t)$ is one or the other carrier, inverted or not, *in that same bit interval*. We now observe that the waveform $v_{MSK}(t)$ is “smooth” and exhibits no abrupt changes in phase. Hence, in MSK we avoid the difficulty described above which results from the abrupt phase changes in the waveform of QPSK. We shall now show that the phase continuity displayed in Fig. 5.29 is a general characteristic of MSK. For this purpose we note from Table 5.1 that the $v_{MSK}(t)$ waveform of Eq. (5.78) or (5.79) can be written as

$$v_{\text{MSK}}(t) = b_o(t) \sqrt{2P_s} \sin [\omega_0 t + b_o(t)b_e(t)\Omega t] \quad (5.86)$$

The equivalence of Eq. (5.78) or (5.79) and Eq. (5.86) can be established by comparing the two in each of the four cases corresponding to $b_o(t) = \pm 1$ and $b_e(t) = \pm 1$. Now let us turn our attention to the instantaneous phase $\phi(t)$ of the sinusoid in Eq. (5.86) where

$$\phi(t) = \omega_0 t + b_o(t)b_e(t)\Omega t \quad (5.87)$$

For convenience we represent the phase as $\phi_+(t)$ or $\phi_-(t)$ where

$$\phi_+(t) = (\omega_0 + \Omega)t; \quad b_o(t) \cdot b_e(t) = +1 \quad (5.88a)$$

$$\text{and} \quad \phi_-(t) = (\omega_0 - \Omega)t; \quad b_o(t) \cdot b_e(t) = -1 \quad (5.88b)$$

In Fig. 5.31 we have plotted $\phi_+(t)$ and $\phi_-(t)$.

The term $b_o(t) \cdot b_e(t)$ in Eq. (5.86) can change at times kT_b (k an integer). Whenever $b_o(t) b_e(t)$ changes from $+1$ to -1 or vice versa we see from Fig. 5.31 that there is an abrupt phase change in $\phi(t)$ of magnitude $2 \cdot \Omega \cdot kT_b = k\pi$. The occurrence and the magnitudes of these abrupt changes are shown in the figure. Now we recall that $b_o(t)$ and $b_e(t)$ do not change at the same time and that, if $b_o(t)$ does change, it changes at times $t = kT_b$ with k odd, while $b_e(t)$ can only change when k is even. Consider, then, first a change in $b_e(t)$. Such a change will cause a phase change which is a multiple of 2π , which is equivalent to no change at all. Next consider the effect of a change in $b_o(t)$. In this case the phase change in $\phi(t)$ will be an odd multiple of π , that is, a phase change equivalent to π . But now, looking back at Eq. (5.86) we take note of the coefficient $b_o(t)$, which multiplies $\sqrt{2P_s} \sin [\phi(t)]$. Whenever there is a change in $b_o(t)$ to change the phase $\phi(t)$ by π , the coefficient $b_o(t)$ will also change sign, yielding an additional π phase change. Hence, a change in $b_o(t)$ produces no net phase discontinuity.

Thus, we have established that Eq. (5.77) assures the phase continuity that we have been seeking.

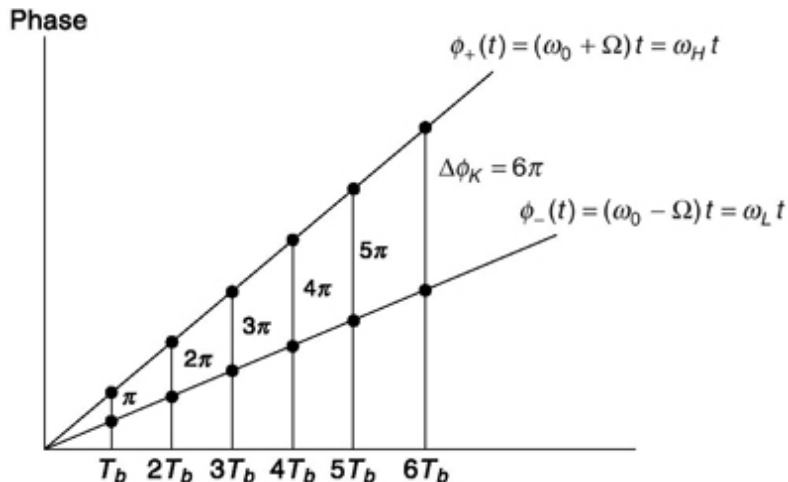


Fig. 5.31 Illustrating why the phase in MSK is continuous.

5.9.5 power spectral Density of MsK

Referring to Eq. 5.77 we see that the baseband waveform which multiplies the $\sin w_0 t$ in MSK is

$$p(t) = \sqrt{2P_s} b_o(t) \cos \frac{\pi}{2} f_b t \quad -T_b \leq t \leq T_b \quad (5.89)$$

As can be verified (Prob. 5.31), the waveform $p(t)$ has a power spectral density $G_p(f)$ given by (since again $P_s = E_b/T_b$)

$$G_p(f) = \frac{32E_b}{\pi^2} \left[\frac{\cos 2\pi f/f_b}{1 - \left(\frac{4f}{f_b} \right)^2} \right]^2 \quad (5.90)$$

Proceeding as we did above in the case of QPSK, we find that the power spectral density for the total MSK signal of Eq. (5.77) is

$$G_{\text{MSK}}(f) = \frac{8}{\pi^2} E_b \left(\left\{ \frac{\cos 2\pi(f-f_0)/f_b}{1 - \left[\frac{4(f-f_0)}{f_b} \right]^2} \right\}^2 + \left\{ \frac{\cos 2\pi(f+f_0)/f_b}{1 - \left[\frac{4(f+f_0)}{f_b} \right]^2} \right\}^2 \right) \quad (5.91)$$

A comparison of the baseband spectral densities of QPSK (which is the same as OQPSK) and MSK is shown in the plots of Fig. 5.32. Observe that the main lobe in MSK is wider than the main lobe in QPSK. In MSK the bandwidth required to accommodate this lobe is $2 \times 3/4f_b = 1.5f_b$ while it is only $1.0f_b$ in QPSK. However in MSK, the side lobes are very greatly suppressed in comparison to QPSK. This result is to be anticipated since, except near $f = 0$ (or $f = f_0$), in QPSK, $G(f)$ falls off as $1/f^2$ while in MSK $G(f)$ falls off as $1/f^4$. It turns out that in MSK 99 percent of the signal power is contained in a bandwidth of about $1.2f_b$ while in QPSK the corresponding bandwidth is about $8f_b$.

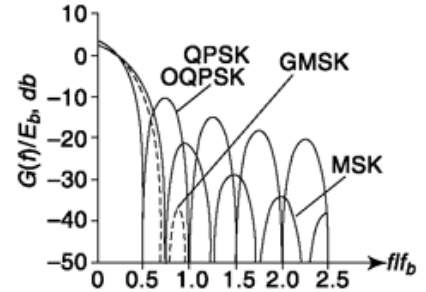


Fig. 5.32 Power spectral density of QPSK, OQPSK, MSK and GMSK (Discussed later in Sec. 5.9.7)

5.9.6 Generation and reception of MsK

One way to generate an MSK signal is the following: We start with $\sin \Omega t$ and $\sin \omega_0 t$, and use 90° phase shifters to generate $\sin(\Omega t + \pi/2) = \cos \Omega t$ and $\sin(\omega_0 t + \pi/2) = \cos \omega_0 t$. We then use multipliers to form the products $\sin \Omega t \cos \omega_0 t$ and $\cos \Omega t \sin \omega_0 t$. Additional multipliers generate $\sqrt{2P_s} b_e(t) \sin \Omega t \cos \omega_0 t$ and $\sqrt{2P_s} b_o(t) \cos \Omega t \sin \omega_0 t$. Finally an adder is used to form the sum as called for in Eq. (5.77). An alternative and more favored scheme is shown in Fig. 5.33a. This technique has the merit that it avoids the need for precise 90° phase shifters at angular frequencies ω_0 and Ω . It is left as a student exercise (Prob 5.32) to verify that, in Fig. 5.33a, the waveforms named $x(t)$ and $y(t)$ are as given and that the output is indeed identical to $v_{\text{MSK}}(t)$ given in Eq. (5.77).

The MSK receiver is shown in Fig. 5.33b. Detection is performed synchronously, i.e. by determining the correlation of the received signal with the waveform $x(t) = \cos \Omega t \sin \omega_0 t$ to determine bit $b_o(t)$, and with $y(t) = \sin \Omega t \cos \omega_0 t$ to determine bit $b_e(t)$. As is customary, such correlation is performed by multiplication and integration over the symbol interval. As is to be noted, the integrators integrate over staggered overlapping intervals of symbol time $T_s = 2T_b$. At the end of each integration time the integrator output is stored and then the integrator output is dumped. (The dumping is not explicitly indicated in Fig. 5.33b.) The switch at the output swings back and forth at the bit rate so that finally the output waveform is the original data bit stream $d_k(t)$.

Of course, to make the receiver effective we need to reconstruct the waveforms $x(t)$ and $y(t)$. A method for locally regenerating $x(t)$ and $y(t)$ is shown in Fig. 5.34. From Eq. (5.79) we see that MSK consists of transmitting one of two possible BPSK signals, the first at frequency $\omega_0 - \Omega$ and the second at frequency $\omega_0 + \Omega$. Thus as in BPSK detection, we first square and filter the incoming signal. The output of the squarer has spectral components at the frequency $2\omega_H = 2(\omega_0 + \Omega)$ and at $2\omega_L = 2(\omega_0 - \Omega)$. These are separated out by bandpass filters. Division by 2 yields waveforms $\frac{1}{2} \sin \omega_H t$ and $\frac{1}{2} \sin \omega_L t$ from which, as indicated, $x(t)$ and $y(t)$ are regenerated by addition and subtraction respectively. Further, the multiplier and low-pass filter shown regenerate a waveform at the symbol rate $f_s = f_b/2$ which can be used to operate the sampling switches in Fig. 5.32.

The reader will, at this point, want to know how the bandpass filters, divided by 2 circuits work, if, for a long period of time, say, $C_L = 0$, that is, only the high frequency signal is transmitted. The answer to this question is given in detail in Sec. 10.5.1 which is concerned with Phase Locked Loop synchronization. For the present let us just note that the bandpass filter—divided by 2 circuits are actually oscillators built to operate at frequencies $2\omega_H$ and $2\omega_L$. The incoming signal at each frequency merely provides phase synchronizing information and does not effect the oscillator frequency or amplitude. If, say, only ω_H is transmitted for an extended period of time then the signal $\frac{1}{2} \sin \omega_L t$ would have some phase jitter present which indeed would result in degradation of system performance.

5.9.7 gaussian Minimum shift Keying (GMSK)

In Fig. 5.32, we have seen that MSK has a greater spectral efficiency compared to QPSK with a considerably reduced sidelobe height. We use a sinusoidal shaped pulse in MSK. Could there be any advantage if we use a pulse of any other shape? In GMSK, the spectral efficiency is further

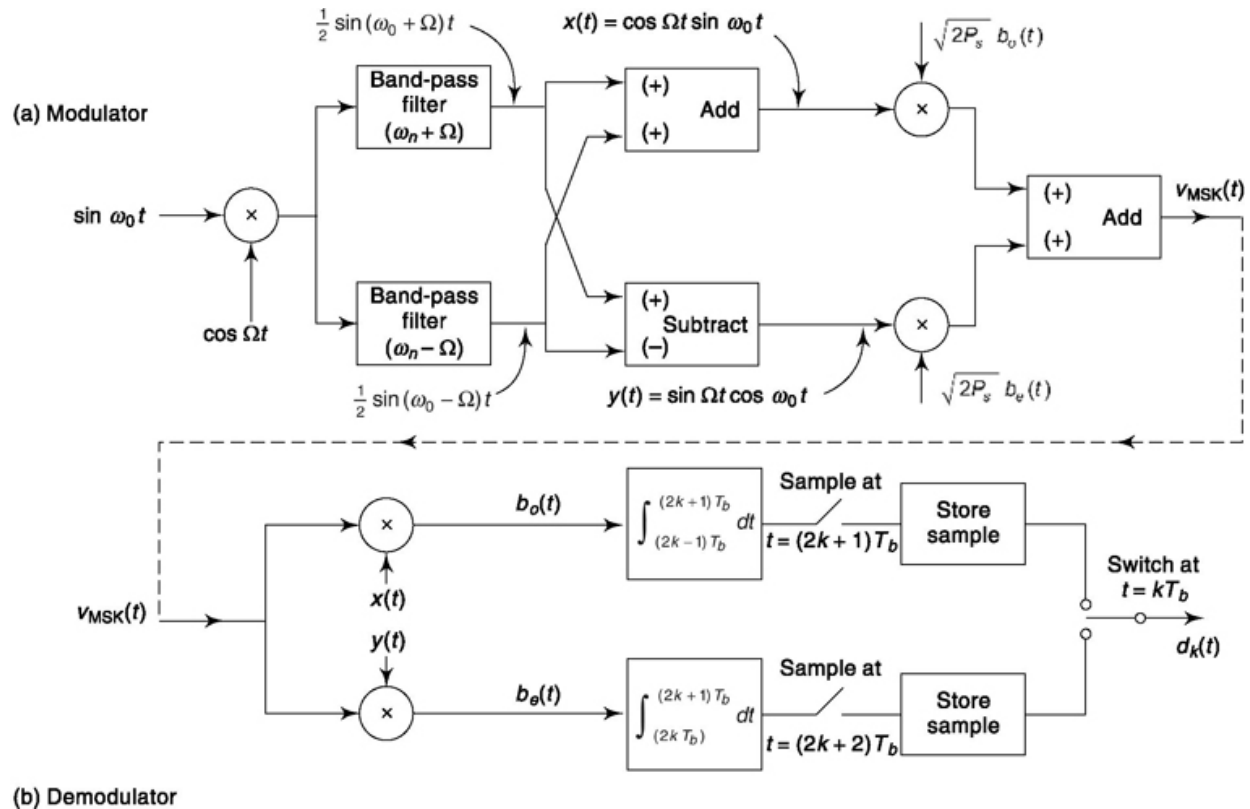
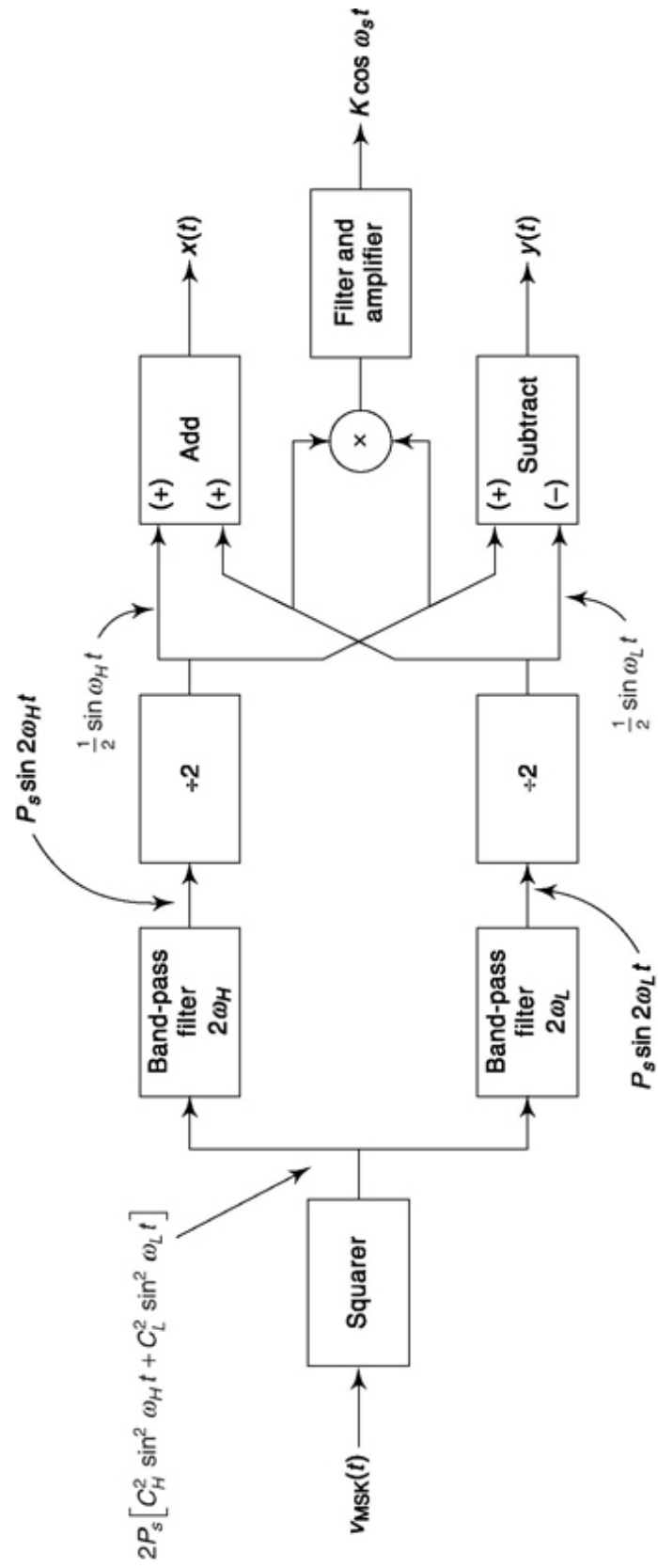


Fig- 5-33 Method of modulating and demodulating MSK.



improved by further reduction in sidelobe height (Fig. 5.32). This is achieved by passing the digital signal through a Gaussian shaped filter that generates a Gaussian shaped pulse and subject it to MSK modulation. However, this increases spread of a symbol and it becomes susceptible to InterSymbol Interference (ISI) and there lies the trade-off. If B is the 3 dB bandwidth of the Gaussian low pass filter, i.e. at frequency B the gain of the filter is -3 dB, then its transfer function is given by

$$H(f) = \exp\left[-\frac{1}{\sqrt{\ln 2}}\left(\frac{f}{B}\right)^2\right] \quad (5.92)$$

GMSK is used in GSM cellular communication. If bit period is represented by T_b then GSM designers prefer $BT_b = 0.3$ for their system. This choice generates a power spectral density for GMSK as shown in Fig. 5.32, which is obtained by simulation as analytical computation is quite involved. One can see that the sidelobe height is considerably reduced and higher harmonics are absent. Unlike MSK, which inherently does not introduce ISI, this arrangement cannot avoid that but remains at tolerable level. Usually, $BT_b < 0.3$ is not used unless additional processing is done to take care of ISI. For $BT_b = 0.5$, ISI will be lower but sidelobe height will be higher. For $BT_b = 1$, GMSK is equivalent to MSK. Note that more the ISI, more is the difficulty in detection of the pulse and it is less tolerant to noise and distortion. Like MSK, GMSK is also a constant-envelope waveform and does not require a linear amplifier. A low-cost nonlinear amplifier can be used in its implementation.

Example 5.3

Describe the transmitted signal for (a) 16 MPSK and (b) 16 QASK when binary messages to be transmitted are $\{m(n)\} = \{1, 0, 1, 1, 0, 1, 0, 0, 1, 1, 1, 0, \dots\}$. Use signal space representation of Fig. 5.15 and 5.18. Consider, digital message input data rate is 10 kbps and average energy per bit is 0.02 unit and carrier frequency = 1 MHz.

Solution

Both 16 MPSK and 16 QASK use 16 symbols, each of which considers four bits at a time. Here the symbols will be combination $S_9 = \{1, 0, 1, 1\}$, $S_4 = \{0, 1, 0, 0\}$, $S_{14} = \{1, 1, 1, 0\}$... where the suffix represents corresponding decimal equivalent.

We know signal power, $P_s = E_b/f_b$ where, E_b = Energy per bit and f_b = message fundamental frequency.

Thus, $P_s = 0.02/10000 = 2 \times 10^{-6}$. Also, no. of symbols $M = 16$.

- (a) From Eq. 5.20 and 5.21, the transmitted carriers in sequence are

$$S_9 = \sqrt{2 \times 2 \times 10^{-6}} \cos \left[2\pi 10^6 t + (2 \times 9 + 1) \frac{\pi}{16} \right]$$

$$= -.002 \cos \left[2\pi 10^6 t + \frac{3\pi}{16} \right]$$

$$S_4 = \sqrt{2 \times 2 \times 10^{-6}} \cos \left[2\pi 10^6 t + (2 \times 4 + 1) \frac{\pi}{16} \right]$$

$$= .002 \cos \left[2\pi 10^6 t + \frac{9\pi}{16} \right]$$

$$S_{14} = \sqrt{2 \times 2 \times 10^{-6}} \cos \left[2\pi 10^6 t + (2 \times 14 + 1) \frac{\pi}{16} \right]$$

$$= .002 \cos \left[2\pi 10^6 t + \frac{3\pi}{16} \right]$$

- (b) In Eq. (5.42), consider the following scheme. First two bits combination in the symbol $\{00, 01, 10, 11\}$ corresponds to $A_e = \{-\sqrt{0.2}, \sqrt{0.2}, -3\sqrt{0.2}, 3\sqrt{0.2}\}$ respectively and last two bits combination $\{00, 01, 10, 11\}$ corresponds to $A_o = \{-\sqrt{0.2}, \sqrt{0.2}, -3\sqrt{0.2}, 3\sqrt{0.2}\}$ respectively.

Then, the transmitted carriers in sequence are

$$S_9 = -3\sqrt{0.2 \times 2 \times 10^{-6}} \cos[2\pi 10^6 t]$$

$$+ 3\sqrt{0.2 \times 2 \times 10^{-6}} \sin[2\pi 10^6 t]$$

$$= 6\sqrt{2 \times 10^{-7}} \cos[2\pi 10^6 t + 3\pi/4]$$

$$\begin{aligned}
S_4 &= \sqrt{0.2 \times 2 \times 10^{-6}} \cos[2\pi 10^6 t] \\
&\quad - \sqrt{0.2 \times 2 \times 10^{-6}} \sin[2\pi 10^6 t] \\
&= 2\sqrt{2 \times 10^{-7}} \cos[2\pi 10^6 t - \pi/4] \\
S_{14} &= 3\sqrt{0.2 \times 2 \times 10^{-6}} \cos[2\pi 10^6 t] \\
&\quad - 3\sqrt{0.2 \times 2 \times 10^{-6}} \sin[2\pi 10^6 t] \\
&= 6\sqrt{2 \times 10^{-7}} \cos[2\pi 10^6 t - \pi/4]
\end{aligned}$$

Example 5.4

If digital message input data rate is 8 kbps and average energy per bit is 0.01 unit, find (a) bandwidth required for transmission of the message through BPSK, QPSK, 16 MPSK, orthogonal BFSK, MSK and 16 MFSK. (b) Put these schemes in order of their susceptibility to noise after calculating minimum separation in signal space.

Solution

Solution Energy per bit, $E_b = 0.01$ and fundamental frequency of message, $f_b = 8$ kHz

No. of symbols $M = 16$. $N = \log_2 16 = 4$.

- (a) Bandwidth required for BPSK = $2f_b = 16$ kHz,
for QPSK = $f_b = 8$ kHz

for 16MPSK = $f_b/2 = 4$ kHz

for BFSK = $4f_b = 32$ kHz

for MSK = $1.5f_b = 12$ kHz

for 16MFSK = $2Mf_b = 256$ kHz

- (b) Minimum distance in signal space,

for BPSK = $2\sqrt{E_b} = 0.2$

for QPSK = $2\sqrt{E_b} = 0.2$

for 16MPSK

$$= \sqrt{4NE_b \sin^2(\pi/16)}$$

$$= 0.0152$$

for ortho. BFSK = $\sqrt{2E_b} = 0.1414$

for MSK = $2\sqrt{E_b} = 0.2$

for 16MFSK = $\sqrt{2NE_b} = 0.2828$

The best method that provides least noise susceptibility is 16MFSK, next comes any of BPSK, QPSK, MSK, then orthogonal BFSK and at last 16MPSK.

Take note of the bandwidth requirement vis-à-vis noise susceptibility for each of the above scheme by comparing results of (a) and (b).

SELF-TEST QUESTION

6. Is it true that error rate in QASK is lower than 16 MPSK but higher than QPSK?
7. The minimum distance in signal space for non-orthogonal BFSK cannot be more than orthogonal BFSK. Is it correct?
8. MSK has lower inter symbol interference compared to QPSK because the baseband signal is smoother. Is that true?
9. Can we say that QPSK signals are in time quadrature while MSK signals are in frequency quadrature?

5.10 PULSE SHAPING TO REDUCE INTERCHANNEL AND INTERSYMBOL INTERFERENCE

We usually associate rectangular pulse shape with digital data. In discussing MSK and GMSK, we have seen that other pulse shapes are useful. We know

that if we can reduce the bandwidth then we can reduce interchannel interference and fit more number of channels in a given spectrum. At the same time we need to consider intersymbol interferences that comes from pulse spreading which is a practical reality. What type of pulse shapes can avoid that—we discuss its theoretical (Nyquist criterion) and implementation issues. We start our discussion with popular duobinary encoding scheme.

5.10.1 Duobinary encoding

We have had frequent occasion to note the bandwidth characteristics of a modulated carrier. An amplitude modulated carrier has the spectral pattern of the baseband signal except duplicated in mirror images on both sides of the carrier frequency. If f_M is the frequency of the *maximum frequency spectral component of the baseband waveform*, then, in AM, the bandwidth is $B = 2f_M$. In frequency modulation, if the modulating waveform were a sinusoid of frequency f_M , and if the frequency deviation was Df , then by Carson's rule [see Eq. (3.26)] the bandwidth would be:

$$B = 2Df + 2f_M \quad (5.93)$$

Even if the modulating waveform is not a sinusoid, but if f_M is the frequency of the highest frequency spectral component of significant power, Eq. (5.93) is a reasonable approximation to the bandwidth. In wideband FM, $Df @ f_M$ and the bandwidth is determined principally by Df . In narrowband FM, Df and f_M are comparable, or it may be that $Df! f_M$. In this narrowband case it is advantageous to minimize f_M if we want to constrain the bandwidth.

Altogether, it is apparent that bandwidth decreases with decreasing f_M , regardless of the modulation technique employed. We consider now a mode of encoding a binary bit stream, called *duobinary encoding* which effects a reduction of the maximum frequency in comparison to the maximum frequency of the unencoded data. Thus, if a carrier is amplitude or frequency modulated by a duobinary encoded waveform, the bandwidth of the modulated waveform will be smaller than if the unencoded data were used to AM or FM modulate the carrier.

There are a number of methods available for duobinary encoding and decoding. One popular scheme is shown in Fig. 5.35. The signal $d(k)$ is the data bit stream with bit duration T_b . It makes excursions between logic 1 and

logic 0, and, as had been our custom, we take the corresponding voltage levels to be +1 V and -1 V. The signal $b(k)$, at the output of the differential encoder also makes excursions between +1 V and -1 V. The waveform $v_D(k)$ is therefore

$$v_D(k) = b(k) + b(k - 1) \quad (5.94)$$

which can take on the values $v_D(k) = +2$ V, 0 V and -2 V. The value of $v_D(k)$ in any interval k depends on both $b(k)$ and $b(k - 1)$. Hence there is a correlation between the values of $v_D(k)$ in any two successive intervals. For this reason the coding of Fig. 5.35 is referred to as *correlative* coding.

The correlation can be made apparent in another way. When the transition is made from one interval to the next, *it is not possible for $v_D(k)$ to change from +2 V to -2 V or vice versa*. In short, in any interval, $v_D(k)$ cannot always assume any of the possible levels independently of its level in the previous intervals. Finally, we note that the term *duobinary* is appropriate since in each bit interval, the generated voltage $v_D(k)$ results from the *combination of two bits*.

The decoder, shown in Fig. 5.35, consists of a device that provides at its output the magnitude (absolute value) of its input cascaded with a logical inverter. For the inverter we take it that logic 1 is +1 V or greater and logic 0 is 0 V. (Different devices can, of course, have different voltages representing the logic levels 1 and 0.) We can now verify that the decoded data $d(k)$ is indeed the input data $d(k)$. For this purpose we prepare the following truth table:

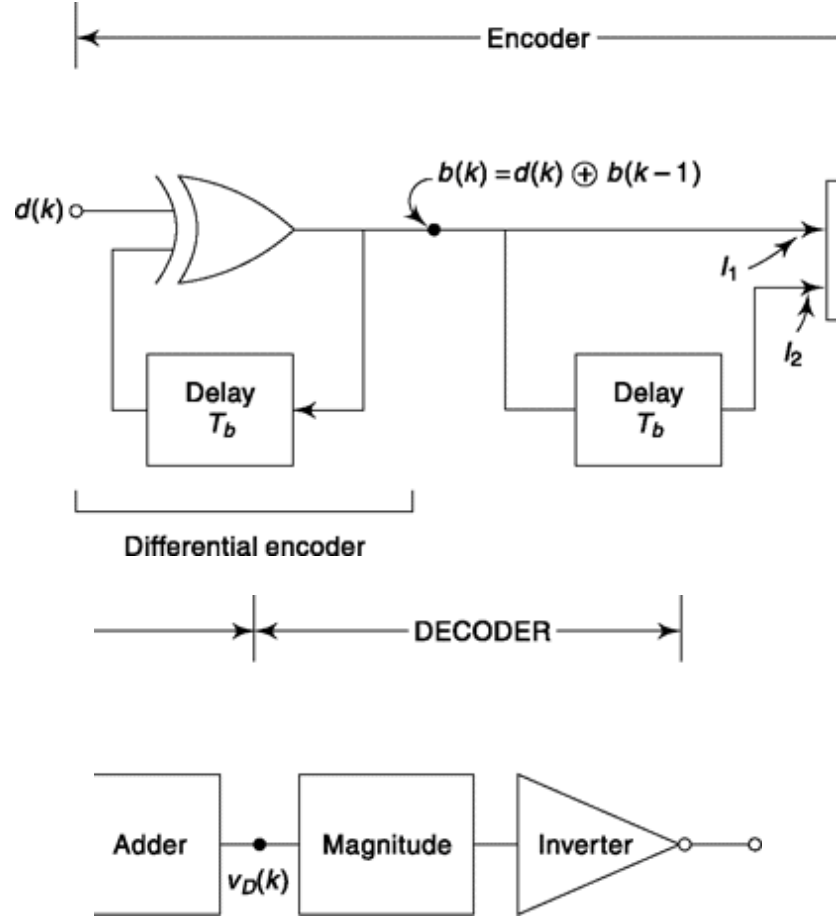


Fig. 5.35 The duobinary encoder/decoder system.

Adder Input 1 I_1		Adder Input 2 I_2		Adder output $v_D(k)$		Magnitude output (Inverter Input)		Inverter output, $d(k)$
voltage	logic	voltage	logic	input voltage	voltage	logic	logic	
-1 V	0	-1 V	0	-2 V	2 V	1	0	
-1 V	0	1 V	1	0 V	0 V	0	1	
1 V	1	-1 V	0	0 V	0 V	0	1	
1 V	1	1 V	1	2 V	2 V	1	0	

From the table we see that the inverter output is $I_1 \oplus I_2$. The differential encoder (called a precoder in the present application) output is:

$$I_1 = b(k) = d(k) \oplus b(k-1) \quad (5.95)$$

The input $I_2 = b(k-1)$ so that the inverter output $\hat{d}(k)$ is:

$$\hat{d}(k) = I_1 \oplus I_2 = d(k) \oplus b(k-1) \oplus b(k-1) = d(k) \quad (5.96)$$

Spectrum of a Duobinary Encoded Signal

The more rapidly $d(k)$ switches back and forth between logic levels the higher will be the frequencies of the spectral components generated. When

$d(k)$ switches at each time T_b , the switching speed is at a maximum. The waveform $d(k)$, under such circumstances, has the appearance of a square wave of (period $2T_b$ and frequency $1/2T_b$ as shown in Fig. 5.36a. If $d(k)$ is the input to the duobinary encoder (of Fig. 5.35 then, as can be verified, $b(k)$ appears as in Fig. 5.36b and the waveform, $v_D(k)$ which is

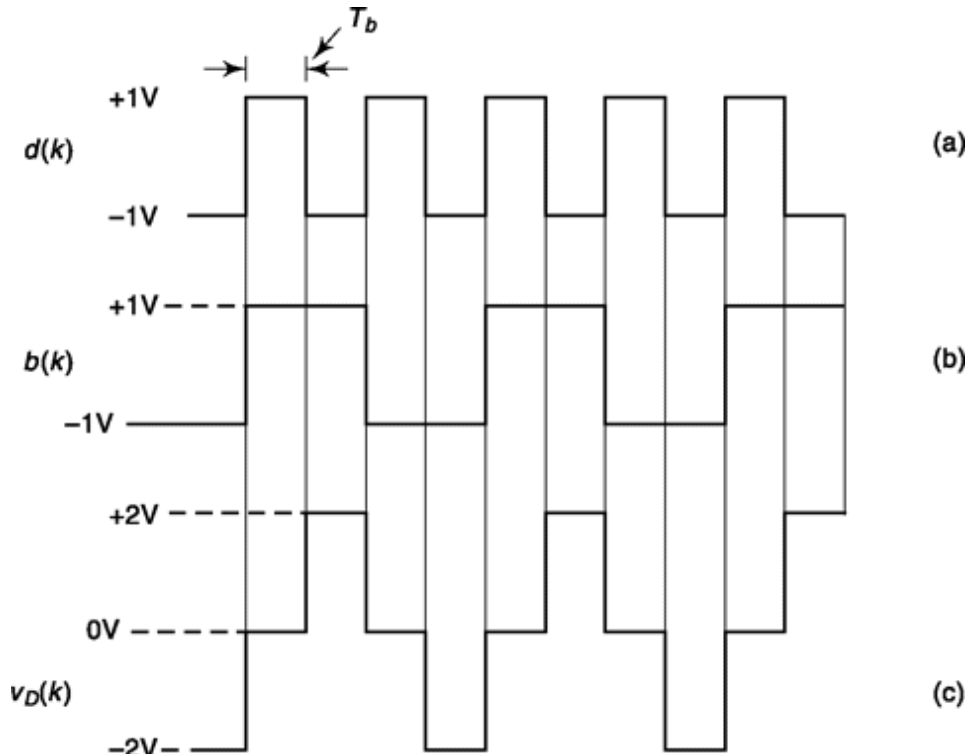


Fig. 5.36 Waveforms of $d(k)$, $b(k)$ and $v_D(k)$.

to be transmitted appears as in Fig. 5.36c. Observe that the period of $v_D(k)$ is $4T_b$ with corresponding frequency $1/4T_b$. Thus, the frequency of $v_D(k)$ is half the frequency of the original unencoded waveform $d(k)$. If we are inclined to make a moderately crude approximation, we might even think of the waveform $d(k)$ as a sinusoid of frequency $1/2T_b$ and of the waveform $v_D(t)$ as a sinusoid of frequency $1/4T_b$. If we were free to select either $d(k)$ or $v_D(k)$ as a modulating waveform for a carrier, and if we were interested in conserving bandwidth, we would choose $v_D(k)$. For, persisting in our crude approximation, if amplitude modulation were involved, the bandwidth of the modulated waveform would be $2(1/4T_b) = f_b/2$ using $v_D(k)$ since the modulating frequency is $f_M = 1/4T_b$, and would be $2(1/2T_b) = f_b$ using $d(k)$. With frequency modulation, if the peak-to-peak carrier frequency deviation

were $2Af$, then, using Carson's rule, the modulated carrier would have a bandwidth $2(Af + 2(1/2T_b))$ with $d(k)$ as the modulating signal, as in BFSK; and $2(Af) + 2(l/4T_b)$ with $v_D(k)$ as the modulating signal.

Tamed FM

A great deal of effort has been expended to find an arrangement, following the pattern of Fig. 5.35 which will yield a $v_D(k)$ with maximum compression of bandwidth in comparison to $d(k)$. Although the optimum arrangement is yet to be found, the arrangement of Fig. 5.37 does offer a significant improvement over the duobinary arrangement of Fig. 5.35. The arrangement (i.e. filter) of Fig. 5.37 is often used to encode a baseband waveform intended to FM modulate a carrier. When so employed it restrains (i.e. tames) the frequency excursions of the FM signal and the technique is referred to as "tamed FM".

To compare the schemes of Figs 5.35 and 5.37 we shall calculate the transfer function $H_T(f)$ of the taming filter and $H_D(f)$ of the duobinary filter. We keep in mind that if $B(f)$ is the Fourier transform $F(b(t))$ then the Fourier transform of $b(t - kT_b)$ is $B(f) e^{-j2\pi f kT_b}$. We have then in Fig. 5.37,

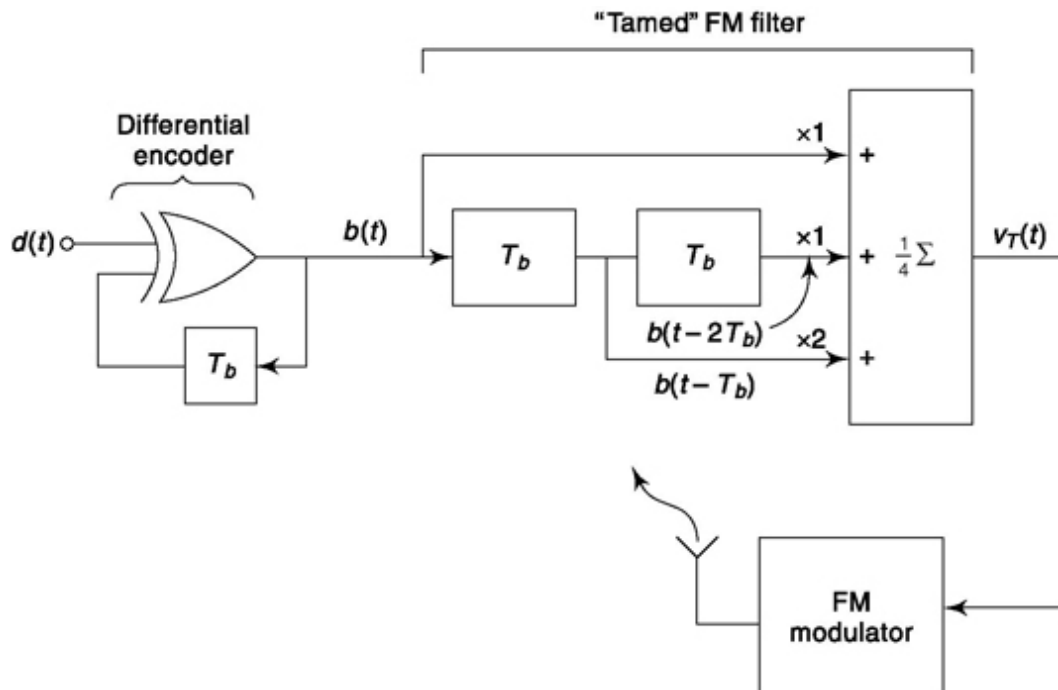


Fig. 5.37 "Tamed" FM encoder.

$$v_T(t) = \frac{1}{4} [b(t) + 2b(t - T_b) + b(t - 2T_b)] \quad (5.97)$$

With $V_T(f) \equiv \mathcal{F}(v_T(t))$, we then have that the transform of the *taming* filter is:

$$\begin{aligned} H_T(f) &= \frac{V_T(f)}{B(f)} = \frac{1}{4} [1 + 2e^{-j2\pi f T_b} + e^{-j4\pi f T_b}] \\ &= \left(\frac{1 + e^{-j2\pi f T_b}}{2} \right) = \frac{1}{2} e^{j2\pi f T_b} \cos^2 \pi f T_b \end{aligned} \quad (5.98)$$

and

$$|H_T(f)|^2 = \cos^4 \pi f T_b \quad (5.99)$$

In the same way we can calculate $H_D(f)^2$ for the duobinary filter of Fig. 5.35. We find

$$|H_D(f)|^2 = \cos^2 \pi f T_b \quad (5.100)$$

The power spectral density of the bit stream $b(t)$ is [see Eq. (5.8)]

$$G_b(f) = V_b^2 T_b \left(\frac{\sin \pi f T_b}{\pi f T_b} \right)^2 \quad (5.101)$$

in which V_b is the amplitude of a bit. Thus altogether the power spectral densities of the duobinary encoded waveform $v_D(t)$ and the tamed FM encoded waveform $v_T(t)$ are then:

$$G_D(f) = H_D(f)^2 G_b(f) = V_b^2 T_b \left(\frac{\sin \pi f T_b}{\pi f T_b} \right)^2 \cos^2 \pi f T_b \quad (5.102)$$

$$G_T(f) = H_T(f)^2 G_b(f) = V_b^2 T_b \left(\frac{\sin \pi f T_b}{\pi f T_b} \right)^2 \cos^4 \pi f T_b \quad (5.103)$$

It can be shown (see Prob. 5.36) that in the frequency range $0 \leq f < f_b/2$ a larger fraction of the total power is contained in the TFM waveform than in the duobinary waveform.

A Comparison of Narrowband FM systems

The great merit of FM over AM is that FM allows us to suppress the effects of noise albeit at the expense of bandwidth. There are, however, frequent occasions when FM is used in preference to AM for an entirely different purpose.

We have already noted that as a matter of practice, the amplitude variations in an AM signal may be a source of difficulty. Such signals when amplified by nonlinear amplifiers (as is generally required for high power efficiency) generate spurious out-of-band spectral components which are filtered out only with difficulty. Even AM systems such as BPSK and QPSK which do not, in principle, generate signals with amplitude variation, do, as a matter of practice, generally have such variation. Further, BPSK and QPSK

generate discontinuities in the carrier phase, which are a further source of difficulty. When it is necessary to avoid such amplitude variations and phase discontinuities, FM is the solution, for the FM waveform

$$v(t) = A \cos (\omega_0 t + k \int m(t) dt) = A \cos \Phi(t) \quad (5.104)$$

has a constant amplitude. Also, no matter how discontinuous may be the modulating waveform, no matter how abruptly $m(t)$ may jump, the phase $\Phi(t)$ is absolutely continuous.

When FM is used principally to avoid amplitude variation and phase discontinuity, narrowband FM is usually employed. For example, we have seen that MSK is an FSK (frequency shift keying) system and hence is an FM system in which $f_M = 1/2T_b = f_b/2$ and $\Delta f = f_b/4$. Hence, the bandwidth, using Eq. (5.92), is

$$B = 2 \left(\frac{f_b}{4} \right) + 2(f_b/2) = 1.5f_b \quad (5.105)$$

If data, $d(k)$, of bit duration T_b is encoded by a duobinary filter before being used to frequency modulate a carrier then, as we have seen, it is reasonable to take f_M in Eq. (5.93), to be $f_M = 1/4T_b$. If we take $\Delta f = f_M/4$ then we have

$$B = 2\Delta f + 2f_M = 2(f_b/4) + 2(1/4T_b) = f_b \quad (5.106)$$

If we were to draw, for the taming filter of Fig. 5.37, waveforms of $d(k)$, $b(k)$ and $v_T(k)$ comparable to Fig. 5.36 we would again come to the conclusion that $f_M = 1/4 T_b$ just as in the duobinary case. On this basis, for the taming filter as for the duobinary filter, again with $\Delta f = f_b/4$,

$$B = \frac{1}{T_b} = f_b \quad (5.107)$$

The two cases yield the same estimated bandwidth because of the crudeness of the estimate. Actually, in the taming filter case, the sidelobes outside the bandwidth range are substantially reduced in comparison with the duobinary filter.

The power spectral density for duobinary—FM, tamed FM, and MSK are compared in Fig. 5.38.

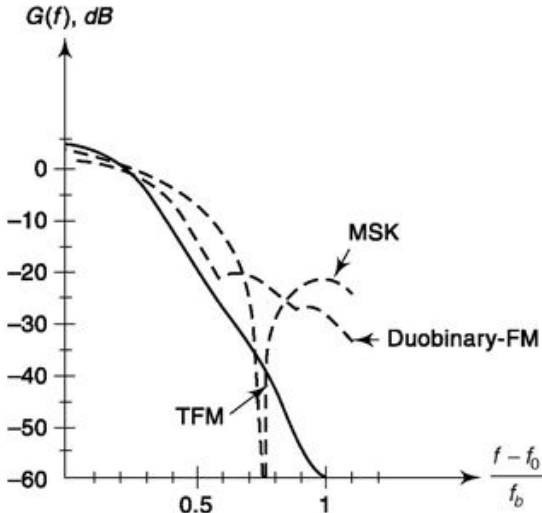


Fig. 5.38 Spectrum of MSK, duobinary FM and TFM.

5.10.2 Nyquist Criterion

We have observed that if we are interested in constraining the bandwidth of a modulated carrier, especially in AM, we must look to the baseband signal. Now the power spectral density of the baseband waveform is determined by the waveform associated with an *individual bit* (or symbol). For example in QPSK, this waveform is rectangular, in MSK it is a half cycle of a sinusoid, etc. We observe that this waveform for an individual bit, or symbol, is a waveform *of finite extension of time*; its duration being the bit or symbol time. Any such waveform of limited time duration has a spectrum which, in principle at least, extends *throughout the frequency range*, i.e. from $f = -'$ to $+'$. It appears, accordingly, that while some waveforms may be better than others, there is no waveform that will completely eliminate interchannel interference.

It occurs to us that we may be able to minimize the spectrum of a signal by passing the baseband waveform through a low-pass filter to remove the offending spectral range of the baseband waveform. However, any such filtering will increase the time extension of the baseband bit waveform so that it will overlap neighboring bit intervals causing *intersymbol interference*. In short, any unfiltered baseband waveform must cause some interchannel interference and if we filter it, we can reduce the interchannel interference but only at the expense of causing intersymbol interference.

We have already noted, in connection with our discussion of the sampling theorem (Sec. 4.2.2) that an impulse of unit strength when applied to a “brick wall filter” with transfer characteristic $H_B f$

$$H_B(f) = \begin{cases} 1 & |f| \leq f_c \\ 0 & \text{elsewhere} \end{cases} \quad (5.108a)$$

as shown in Fig. 5.39a, produces a response which is

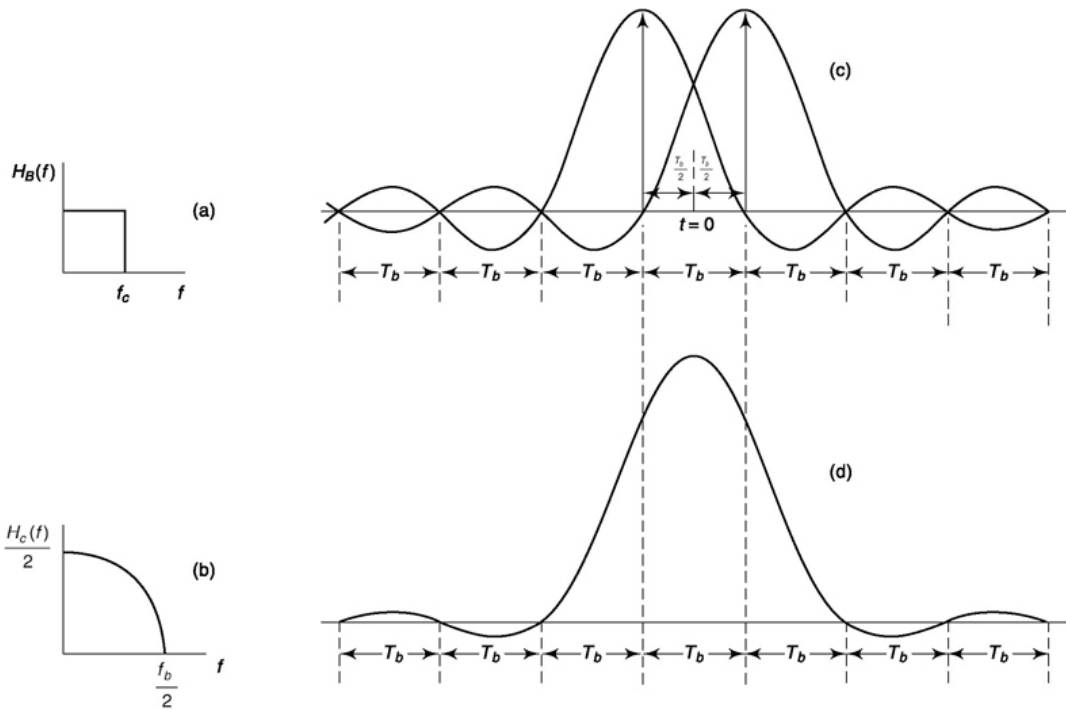
$$h_B(t) = 2f_c \frac{\sin 2\pi f_c t}{2\pi f_c t} \quad (5.108b)$$

This response displays a maximum at $t = 0$ and is zero at multiples of the time $1/2f_c$. Hence, if impulses are generated at time $t = k/2f_c$ (k an integer) then, at the time of peak response to any particular impulse, the response to all other impulses will be zero. Hence, even if all the individual responses are superimposed, we shall be able, by sampling at times $t = k/2f_c$, to observe a response proportional to the k th impulse, without interference from the waveforms due to other impulses.

The above discussion is generalized in *Nyquist first criterion* for distortionless transmission as this: “a wave will be said to be nondistorting when the value at the mid-instant of any time unit is proportional to the magnitude factor for the corresponding element.” That is, the contribution from other signaling elements must be zero at the midpoint of the signaling interval. This is mathematically stated in Eq. (5.109). Here, $p(t)$ represents the required pulse shape for zero ISI and $P(f)$ represents required frequency domain characteristics, T_b the time period of pulse and n sampling index.

$$p(nT_b) = \begin{cases} 1, & n=0 \\ 0, & n \neq 0 \end{cases} \quad \text{or} \quad \sum_{n=-\infty}^{\infty} P\left(f - \frac{n}{T_b}\right) = T_b \quad (5.109)$$

Note that, Nyquist pulse (fulfilling criteria Eq. (5.109)) can take any value between $(n-1)T < t < nT$ but needs to be zero at $t = nT$ when $n \neq 0$. Clearly, the sinc pulse discussed before can be considered as Nyquist pulse which avoids ISI. Note that, the frequency domain representation of sampled data signal is periodic in frequency domain.



19 (a) Brickwall filter; (b) Cosine filter; (c) Shifted versions of two impulse response of a brickwall filter. (d) Impulse response of a cosine filter.

We can apply these considerations to our present concern in the following way: Let us represent the bits in our data stream by impulses, a positive impulse for logic 1, a negative impulse for logic

0, the impulses being separated by the bit time T_b . Let us pass the bit stream through a brickwall filter of cut off frequency $f_c = 1/2T_b = f_b/2$. The filtering will allow us to suppress interchannel interference. While the bit waveform will now be of infinite extent we will still be able to avoid intersymbol interference by sampling at $t = k/f_b$.

The use of a brickwall filter which cuts off at $f_c = f_b/2$ has associated with it a number of awkward features. First of all, it is very difficult to construct a good approximation to such a filter (the ideal filter itself is, of course, unrealizable). Secondly, we observe, from Eq. (5.108b) that the amplitude of each of the successive peaks falls off slowly, i.e., only linearly with time. Hence, intersymbol interference, even between bits which are greatly separated in time, can result if the sampling operation is not timed with great precision. That is, the intersymbol interference is very sensitive to timing errors.

5.10.3 Cosine Filters

The preceding discussion shows we need to look to other filters. A filter of interest in this regard is the “cosine” filter with transfer characteristics shown in Fig. 5.39b,

$$H_C(f) = \begin{cases} 2 \cos \pi f T_b & \text{for } f \leq f_b/2 \\ 0 & \text{for } f > f_b/2 \end{cases} \quad (5.110)$$

or equivalently

$$H_C(f) = [H_B(f)][2 \cos \pi f T_B] \quad (5.111)$$

Equation (5.111) can be rewritten as

$$H_C(f) = H_B(f)(e^{j\pi f T_b} + e^{-j\pi f T_b}) \quad (5.112a)$$

Accordingly, the response of the cosine filter is the response of a cascade of two filters, one with transfer characteristic $H_B(f)$ (with $f_c = f_b/2$) and a second with transfer characteristic given by $2 \cos \pi f T_b$. We recall further that if a time function $q(t)$ has a Fourier transform $Q(f)$ then $Q(f)e^{-j2\pi fT}$ is the transform of $q(t - T)$. Thus, altogether we have that

$$h_C(t) = h_B(t + T_b/2) + h_B(t - T_b/2) \quad (5.112b)$$

The two parts of $h_C(t)$ are drawn in Fig. 5.39c and the total response is shown in Fig. 5.39d. The response is still non-causal, since, as we note, there is a response before $t = 0$. This noncausal feature is a result of the fact that, while we have not assumed that the filter response falls from $H_C(f) = 1$ to $H_C(f) = 0$ precipitously at cut-off, we have persisted in assuming that the filter cuts off completely at $f_b/2$. Nonetheless, a real filter can be constructed which approximates the unrealizable filter of Eq. (5.110).

Observe that the side peaks in the complete response $h_C(t)$ are smaller than the side peaks of the response $h_B(t)$. Such is the case because the side peaks in $h_C(t)$ are the *differences* of the side peaks in $h_B(t)$. This point is also brought out when it is shown (Prob. 5.37) that the response $h_C(t)$ of the cosine filter is:

$$h_C(t) = \frac{4f_b \cos \pi f_b t}{\pi(1 - 4f_b^2 t^2)} \quad (5.113)$$

From Eq. (5.113) we observe that the sidelobes fall off as the square of the time rather than linearly with time as does $h_B(t)$ given in Eq. (5.108b). This smaller peak will reduce the sensitivity to errors in the time at which the sampling operation is performed. We observe further, however, that the central peak of $h_C(t)$, being of duration $3T_b$, is 1.5 times as wide as the central peak of $h_B(t)$ which has a duration $2T_b$.

Note that, $H_c(f)$ discussed here belongs to a more general family of filters called raised cosine filter which is defined as

$$H(\omega) = \begin{cases} 1, & 0 \leq |\omega| \leq (1 - \alpha)W \\ 0.5[1 - \sin\{\pi(|\omega| - W)/(2\alpha\omega)\}], & (1 - \alpha)W \leq |\omega| \leq (1 + \alpha)W \\ 0, & |\omega| > (1 + \alpha)W \end{cases} \quad (5.114)$$

and its impulse response,

$$h(t) = \frac{1}{T_b} \left(\frac{\sin Wt}{Wt} \right) \left[\frac{\cos \alpha Wt}{1 - (2\alpha Wt/\pi^2)} \right] \quad (5.115)$$

where, $\omega = 2\pi f$, W = cut-off frequency in radian and α = roll-off factor that decides sharpness or smoothness of the filter. For $\alpha = 0$, the above represents an ideal LPF (brick-wall filter) and for $\alpha = 1$, it gives full cosine roll-off with $H(W) = 0.5$ (Fig. 5.40). The sinc multiplying factor of impulse response ensures this to be Nyquist pulse with zero at $t = W/\pi$. The last term there is a sinusoidal function that decays with time exponentially. The bandwidth for above filter for extreme two cases of $\alpha = 0$ and 1 are W and $2W$ respectively. And for any in between values of α this is given by

$$\text{bandwidth} = (1 + \alpha)W \text{ in radian} \quad (5.116a)$$

Now, W is related with digital signal rate f_b as $W = 2\pi(f_b/2)$. Hence, the above can be rewritten as

$$\text{bandwidth} = (1 + \alpha)f_b/2 \text{ in Hz} \quad (5.116b)$$

For full cosine roll off, $\alpha = 0$ and bandwidth = $f_b/2$.

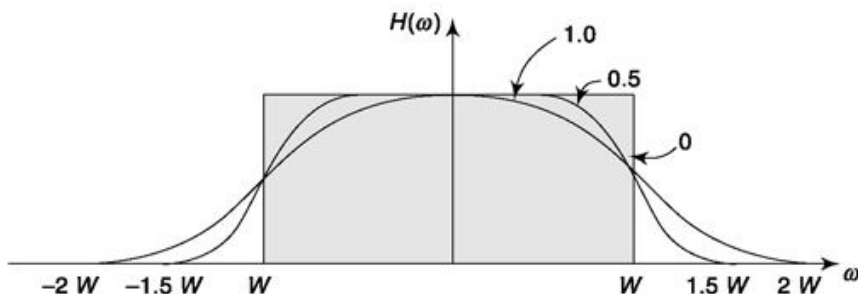


Fig. 5.40 Raised cosine filter characteristics.

Note that $\alpha = 0$ is impossible to implement. Some video systems use $\alpha = 0.11$ though typical values are in the range $\alpha = 0.35-0.5$.

It is worth noting at this point that *Nyquist's second criterion* for distortionless transmission is that the interval, between the instants when the received wave passes through the mean value, shall be the same as the corresponding interval at the transmitting end. A receiving device which responds

to the values of the wave at the ends of the time units, instead of the middle, will give distortionless transmission..." In this case, a time sample is indicated to be taken at the end of the symbol period, rather than at the center. This suggests controlled intersymbol interference at the sampling instant which following solution of simultaneous linear equations asks for frequency spectrum to be like Eq. 6.110.

Note that, the third Nyquist criterion for distortionless digital transmission states that "the area under the received wave shall have the same value as that under the sent wave during each time unit" or symbol period. This is useful in picture transmission or tamed frequency modulation.

Partial Response Signaling

We shall end this discussion with an interesting technique where we allow a controlled amount of intersymbol interference when decoded data is sampled. Let us see how it works. Suppose, that corresponding to each bit of duration T_b , of a data stream we generate a positive impulse of strength $+I$ whenever the bit is at logic 1 and a negative impulse $-I$ whenever the bit is at logic 0. Suppose, further, that these impulses are applied to the input of the cosine filter. In Fig. 6.41 we have drawn the filter responses individually to five successive positive impulses. For simplicity, we have in each

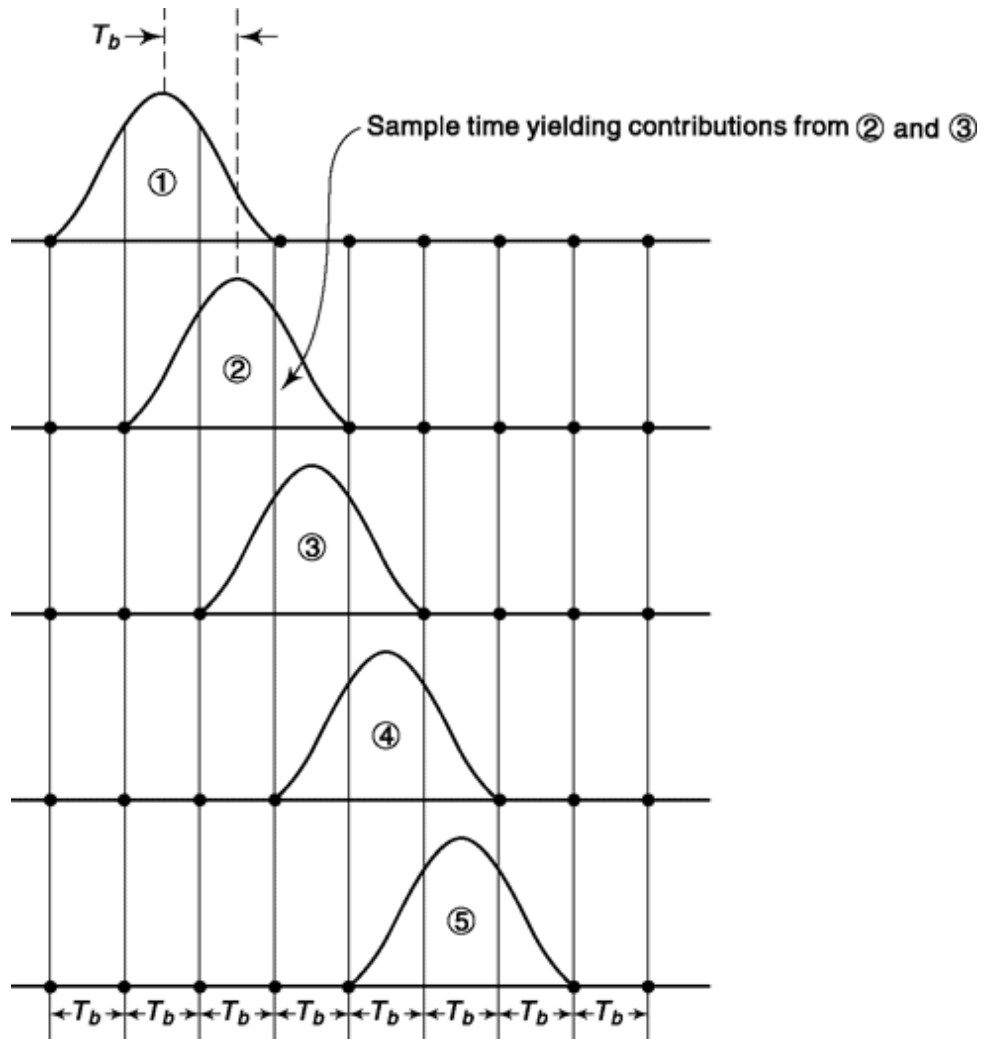


Fig. 5.41 Filter responses of five separate impulses.

case drawn only the central lobe and we have indicated by dots all the places where the individual response waveforms pass through zero. Where there is no dot, the waveforms has a finite value. The peaks of the responses are separated by times T_b and the widths of the central lobes are $3T_b$. The total response is, of course, simply the sum of the individual responses.

We can make the following observations from Fig. 5.41:

1. If we sample the total response at a time when an individual response is at its peak, the sample will have contributions from *all* the individual responses.
2. There is *no* possible time at which a sample of the total response is due only to a single individual response.

3. Importantly, if we sample the total response midway between times when the individual responses are at peak value, i.e. at $t = (2k - 1)T_b/2$, then the sample value will have contributions in equal amount from *only the two individual responses* that straddle the sampling time. These sampling times are indicated in Fig. 5.41 by the light vertical lines. One such sampling time, yielding contributions from individual responses 2 and 3 is explicitly marked. It can be calculated from Eq. (5.108b) that at the sampling time the contribution from each of the straddling individual responses will be a voltage If_b . Note that in sampling at the indicated times, we sample when the individual responses are *not* at peak value. For this reason, the present signal processing is referred to as *partial-responses signaling*.

In partial-response signaling, we shall transmit a signal during each bit interval that has contributions from two successive bits of an original baseband waveform. But as we have seen from our discussion of duobinary coding, this superposition need not prevent us from disentangling the individual original baseband waveform bits. A complete (baseband) partial-response signaling communications system is shown in Fig. 5.42. It is seen to be just an adaptation of duobinary encoding and decoding.

The cosine filter that we described above [see Eq. (5.96)] employed a delay and an advance of the impulse by amount $T_b/2$, the total time between delayed and advanced impulses being T_b . Since, in the real world, a time advance is not possible, we have employed only a delay by amount T_b . The response of the cosine filter of Fig. 5.39b will be the same as the response of Eq. (5.96) except that the present filter response will be delayed by a time T_b . The brickwall filter at the receiver input serves to remove any out of band noise added to the signal during transmission. It can be shown, following the procedure of Sec. 5.10.1, that the output data $d(k) = d(k)$.

5.10.4 Quadrature partial Response (QpR) Encoder Decoder

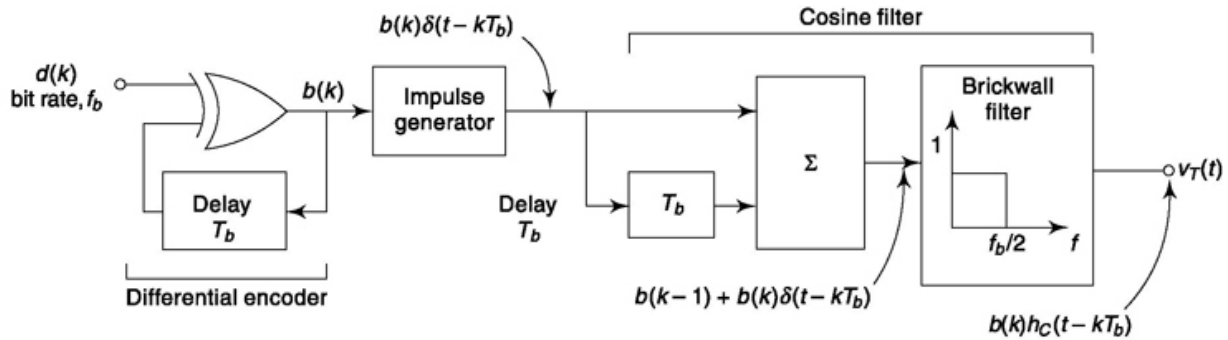
The baseband partial response (duobinary) signal may be used to amplitude or frequency modulate a carrier. If amplitude modulation is employed, either double sideband suppressed carrier DSB/SC or quadrature amplitude modulation QAM can be employed.

For the case of DSP-SC the duobinary signal, $v_T(t)$, shown in Fig. 5.42, is multiplied by the carrier $\sqrt{2} \cos \omega_0 t$. The resulting signal is

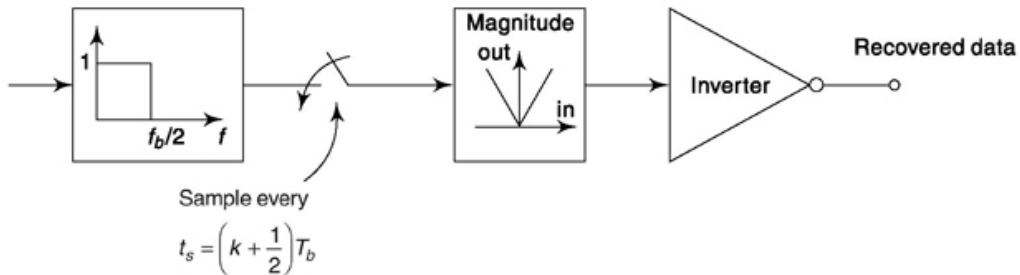
$$v_{\text{DSB}}(t) = \sqrt{2} v_T(t) \cos \omega_0 t \quad (5.117)$$

The bandwidth required to transmit the signal is twice the bandwidth of the baseband duobinary signal which is $f_b/2$. Hence the bandwidth B_{DSB} of an amplitude modulated duobinary signal is

$$B_{\text{DSB}} = 2(f_b/2) = f_b \quad (5.118)$$



(a) Encoder



(b) Decoder

Fig. 5.42 Duobinary encoder and decoder using cosine filter.

If the duobinary signal is to amplitude modulate two carriers in quadrature, the circuit shown in Fig. 5.43 is used and the resulting encoder is called a “quadrature partial response” (QPR) encoder.

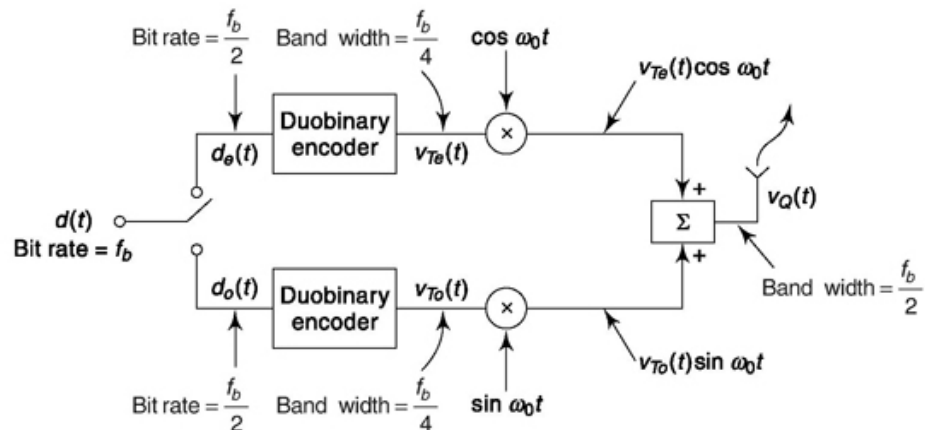


Fig. 5.43 QPR encoder.

Figure 5.43 shows that the data $d(t)$ at the bit rate f_b is first separated into an even and an odd bit stream $d_e(t)$ and $d_o(t)$ each operating with the bit rate $f_b/2$. Both $d_e(t)$ and $d_o(t)$ are then separately duobinary encoded into signals $v_{Te}(t)$ and $v_{To}(t)$. Each duobinary encoder is similar to the encoder shown in Fig. 5.42a except that each delay is now $2T_b$ rather than T_b , the data rate of the input is $f_b/2$ rather than f_b and the bandwidth of the brick wall filter is now $1(f_b/2) = f_b/4$ rather than $f_b/2$. Thus the bandwidth required to pass $v_{Te}(t)$ or $v_{To}(t)$ is $f_b/4$. Each duobinary signal is then modulated using the quadrature carrier signals $\cos w_0 t$ and $\sin w_0 t$.

The bandwidth of each of the quadrature amplitude modulated signals is

$$B_{QPR} = 2(f_b/4) = f_b/2 \quad (5.119)$$

Hence the total bandwidth required to pass a QPR signal is also B_{QPR} since the two quadrature components occupy the same frequency band.

It should be noted that if QPSK, rather than QPR, were used to encode the data $d(t)$, the bandwidth required would be $B_{QPSK} = f_b$. However, if 16 QAM or 16 PSK were used to encode the data the required bandwidth would be $B_{16QAM} = B_{16PSK} = f_b/2$. Thus the spectrum required to pass a QPR signal is similar to that required to pass 16 QAM or 16 PSK. However, the QPR signal displays no (or in practice very small) sidelobes which makes QPR the encoding system of choice when spectrum width is the major problem. The drawback in using QPR is that the transmitted signal envelope is not a constant but varies with time.

QPR Decoder

A QPR decoder is shown in Fig. 5.44. As in 16-QAM and 16-PSK to decode (see Secs. 5.5 and 5.6) the input signal, $vg(t)$ is first raised to the fourth power, filtered and then frequency divided by

4. The result yields the two quadrature carriers: $\cos w_0 t$ and $\sin w_0 t$. The detailed derivation of this result is left to Prob. 5.38. Using the two quadrature carriers we demodulate $vg(t)$ and obtain the two

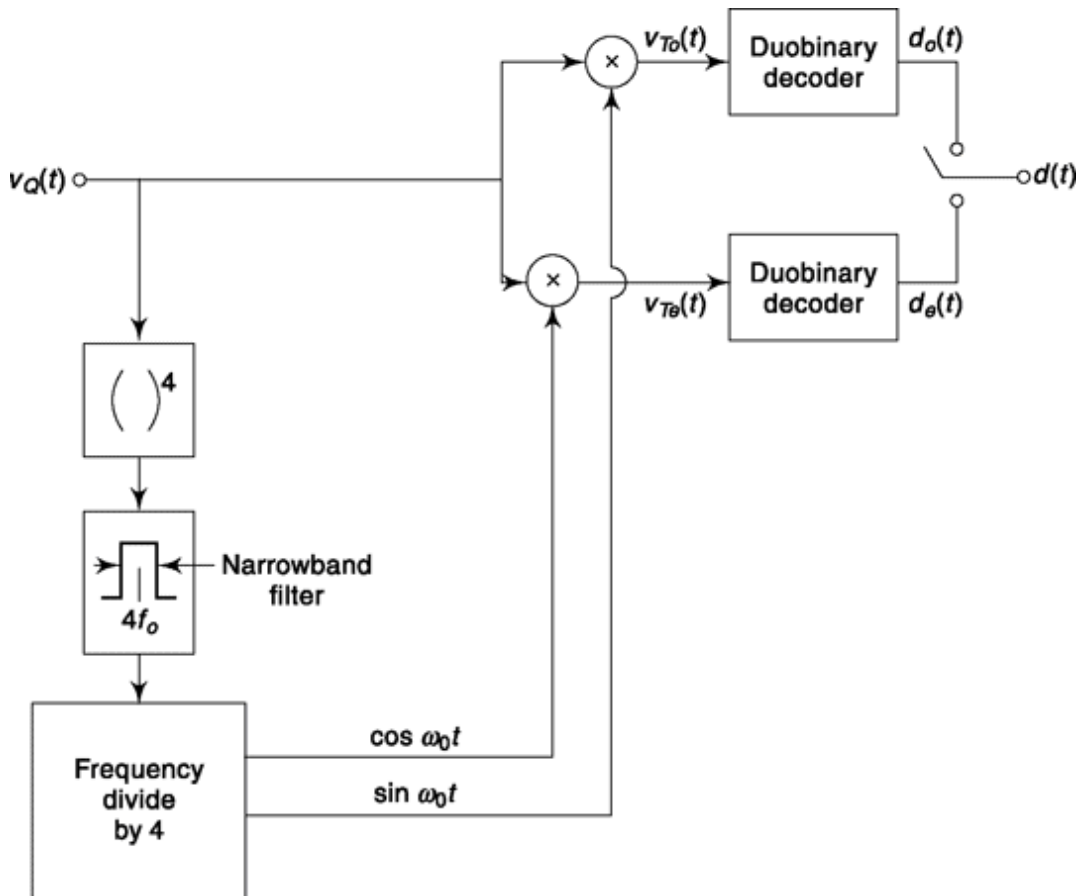


Fig. 5.44 QPR decoder.

baseband duobinary signals $v_{Te}(t)$ and $v_{To}(t)$. Duobinary decoding then takes place; each duobinary decoder being similar to the decoder shown in Fig. 5.42 except that they operate at $f_b/2$ rather than at f_b . The reconstructed data $d_o(t)$ and $d_e(t)$ is then combined to yield the data $d(t)$.

Example 5.5

Show how duobinary decoding is done when input $\{d(k)\} = \{0, 1, 1, 1, 0, 1, 0, 1, 1, \dots\}$ is (a) precoded and (b) not precoded. (c) Show in each case what happens if 4th bit is detected wrongly.

Solution

- (a) The data sent when precoded from Eq. 5.94
 $v_D(k) = b(k) + b(k - 1)$ where, $b(k) = d(k) \oplus b(k - 1)$

If storage element is initialized with logic 0 and considering polar signal $\{0 \rightarrow -1, 1 \rightarrow +1\}$
 $\{b(k)\} = \{-1, -1, 1, -1, 1, 1, -1, -1, 1, -1, \dots\}$
 $\{v_D(k)\} = \{X, -2, 0, 0, 0, 2, 0, -2, 0, 0, \dots\}$ where X signifies first value as don't care, not of use.
Following finding of magnitude and inverting we get decoded output as

$$\{\hat{d}(k)\} = \{0, 1, 1, 1, 0, 1, 0, 1, 1, \dots\}$$

- (b) When not precoded Ex-OR gate is not there,
 $v_D(k) = d(k) + d(k - 1)$

Then, polar $\{d(k)\} = \{-1, 1, 1, 1, -1, 1, -1, 1, \dots\}$ and $\{v_D(k)\} = \{-2, 0, 2, 2, 0, 0, 0, 0, 2, \dots\}$

Decoding rule without precoding is as follows : If $v_D(k) = 2$, then bit = 1, if $v_D(k) = -2$, then bit = 0 and if $v_D(k) = 0$, then bit is reverse of the previous.

Using this we get, $\{\hat{d}(k)\} = \{0, 1, 1, 1, 0, 1, 0, 1, 1, \dots\}$

- (c) When precoded if 4th bit is erroneous received
 $v_D(k) = 0$ in place of 2.

Then, received $\{v_D(k)\} = \{X, -2, 0, 0, 0, 0, 0, -2, 0, 0, \dots\}$

Example 5.6

(a) A telephone line of bandwidth 4 kHz required to transmit data at 6 kbps using raised-cosine pulses. Determine the roll-off factor, a . (b) What data rate is supported for $a = 0.25$ and full roll-off.

Solution

- (a) From Eq. (5.116b), Bandwidth = $(1 + \alpha) f_b/2$
or $4000 = (1 + \alpha) 6000/2$ $(1 + \alpha) = 4/3 \rightarrow \alpha = 0.33$

- (b) Now, $4000 = (1 + 0.25) f_b/2$ or, $f_b = 8000/1.25 = 6400$ kbps

For full roll-off, $\alpha = 1.0$. Then $4000 = (1 + 1) f_b/2$ or, $f_b = 4000$ kbps

SELF-TEST QUESTION

10. Can duobinary encoding be called correlative coding?
11. Does precoding stage in duobinary signaling prevent error propagation?
12. Does Nyquist third criterion say that contribution from other symbols should be zero at the midpoint of a symbol?

5.11 SOME ISSUES IN TRANSMISSION AND RECEPTION

In this section we would like to discuss certain issues related to transmission of line coded data. We postponed this discussion in Chapter 4, since we wanted to discuss ISI and Nyquist pulses before that. Application of certain issues discussed in this section is shown in MATLAB examples.

5.11.1 Regenerative Repeater

When a line coded digital signal (say PCM) is transmitted over a channel, it is attenuated, filtered and corrupted by noise. Consequently, for a long path length the data is highly distorted and it cannot be satisfactorily recovered at the receiving end. The repeater for digital transmission can be regenerative unlike analog system that not only transmits an amplified version of the input data but a cleaner one too by reshaping and retiming it. Refer to our discussion in Sec. 4.1 of Chap. 4 which is one important motivation behind embracing digital communication system. To put in brief, regenerative repeater in digital communication system can separate noise from the data and then amplify and retransmit it.

Figure 5.45 shows the typical block diagram of a regenerative repeater. The amplifier block amplifies the signal. The filter block has a transfer function which is close approximation of the inverse of the channel transfer function. The aim of course, is to despread the signal and get its original shape as it was admitted into channel. We'll talk more about it little later. The next block is sample and hold. Since the pulse available is not completely rectangular in shape we would like to make the decision when its amplitude is likely to be maximum and not when it is crossing zero. After recovery of clock (discussed in Chap. 10) we use it to synchronize the sampling of the signal and

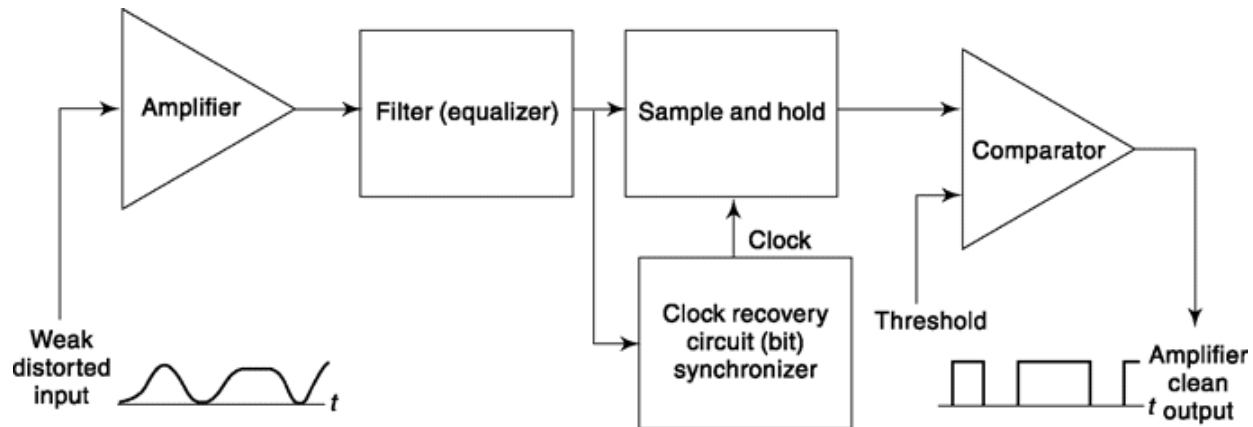


Fig. 5.45 A block diagram of regenerative repeater.

hold it briefly for making decision. The decision is made through a comparator. If the voltage held is above a threshold then it is considered as logic 1 and comparator output is a rectangular pulse, clean, devoid of any noise. If it is below threshold it is a logic 0 and comparator output is held low. The comparator output is held in both the cases for one bit period, i.e. till the next sampling instant. The threshold could be midway of two logic levels that is for unipolar $[0, + V]$ signal $+ V/2$ and bipolar $[-V, +V]$ signal zero or ground. Before we discuss equalizer let us see something called Eye Pattern.

5.11.2 Eye pattern: Noise, Jitter and Other Channel Effects

The effect of channel filtering and channel noise can be seen by observing the received line code on an analog oscilloscope. The noisy, dispersed pulse input is given to the vertical input of the oscilloscope. The horizontal input is connected to a time base generator which provides trigger through a sawtooth-like waveform having same time period as incoming data. The resulting displays are called eye patterns. A typical eye pattern is shown in Fig. 5.46. An eye pattern carries lot of information about the quality of the incoming pulse and state of the channel which is useful for the detection of digital input. Before we explain them let us discuss what it should look like in ideal case. Ideally, if the incoming pulses are rectangular the diagram will be of rectangular shape of width that of one time period. This will be so because of the random nature of the data and the data rate is much higher compared to our persistence in vision. But due to spread of the pulse the pattern won't be rectangular and will take the shape of an eye. There may be asymmetry in the shape which portrays nonlinear nature of the channel. The

more linear the channel is, the more symmetric is the shape of eye. Now, if the pulses are Nyquist pulses and there is no noise then the eye in its maximum position will be fully open with no blurring. This is because Nyquist pulses at sampling instances show zero ISI, i.e. neighboring pulses do not interfere. But in reality we do not get Nyquist pulses (Refer to Sec. 5.10.2 for a detailed discussion) and there are ISI which causes blurring as shown in the diagram. Again the more the ISI, the more is the blurring. How does noise effect eye pattern? The presence of noise tends to make the eye close and make decision or detection difficult. The mid-point of voltage of eye-diagram can be used as decision threshold as it gives maximum noise margin (the amount of additional noise that can be tolerated) when eye is maximally open. This also gives the

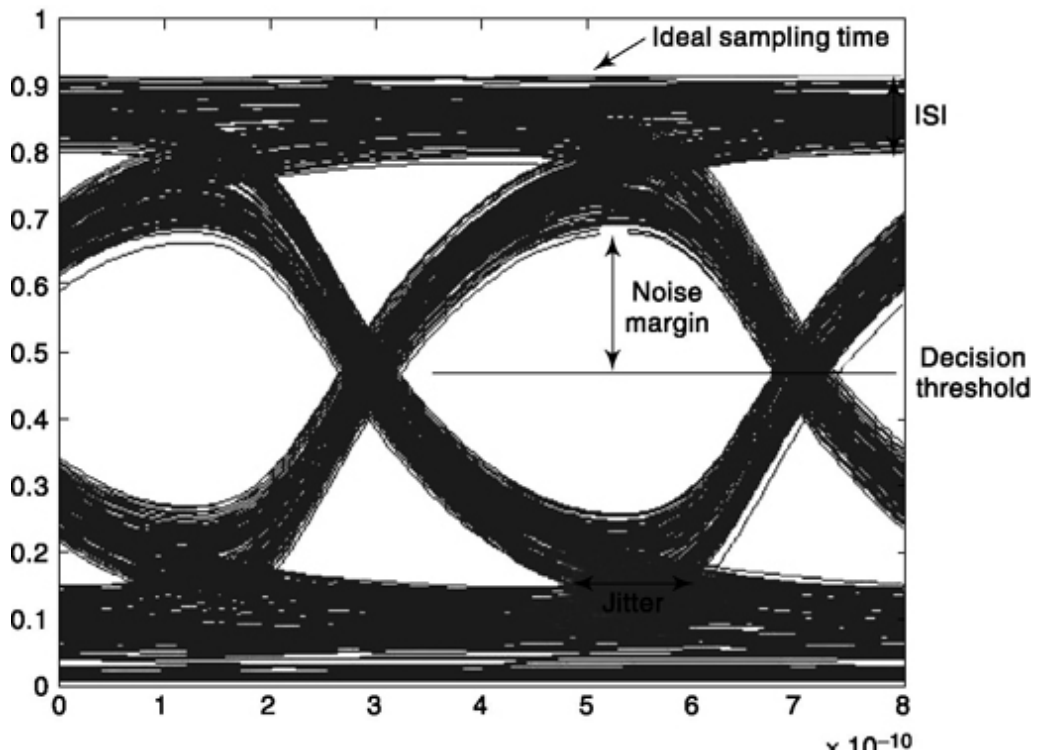


Fig. 5.46 A typical eye diagram for digital data propagating through a channel.

precise instance when the sampling is to be done (maximum open) to get best result. If it is done closer towards zero crossing, the probability of error in detection will increase. The sensitivity to timing error is given by the slope of the open eye (evaluated at the zero-crossing point). Also it is interesting to note, as shown in the diagram that there is a timing *jitter* i.e. positions of the incoming pulses are not very precise. Such deviation is attributed to channel, post processing as well as presence of long chains of

0's and 1's in the digital data. We discussed *scrambler* in Chap. 4 which breaks such chain and helps in reducing jitter. In clock recovery (discussed in Chap. 10), *early-late gate synchronization* (Sec. 10.5.2) helps in reducing effect of jitter. In case of M-ary signaling the eye pattern consists of M-1 eyes stacked up one after another in vertical direction.

5.11.3 Equalizer

We have already seen the need of equalizer in discussing regenerative repeater. This helps in regaining the pulse shape by filtering the signal by a filter, the characteristics which is close approximation of the inverse of the channel or distortion media/process. This is usually done through transverse filtering which uses weighted tap delay lines. The weights on the tap are adjusted in such a manner that the pulse shape is best and ISI is minimized. Eq. (5.120) shows the input-output relation of the tap delay filter shown in Fig. 5.47.

$$y(t) = \sum_{n=-N}^N C_n b(t - nT_b) \quad (5.120)$$

where, $b(t)$ is distorted data input, $y(t)$ filtered output, C_n is weight of n th filter, N is number that indicates number of locations on which zero is forced on either side of the filter in *zero crossing*

Fig. 5.47 Block diagram of a tap delay equalizer.

equalizer, (discussed next) otherwise it indicates that total number of tap weights are $2N + 1$ a total number of delay elements $2N$. Each delay element delays the input to it by an amount T_b whi is time period of the digital data. There can be different methods to choose these tap weights.

Zero Forcing Equalizer

As already stated the filter taps are so adjusted that the equalizer output is forced to zero at N samp points on each side as given in Eq. 5.121. This is an approximated version of Nyquist pulse whi requires it to be zero at all sample points from '-' to '+'. This approximation is required as otherwi for finite number of coefficients we need to solve infinite number of linear equations.

$$y(t) = \begin{cases} 1 & t=0 \\ 0 & t=\pm T_b, \pm 2T_b, \dots, \pm NT_b \end{cases} \quad (5.121)$$

Expanding Eq. (5.120) and using condition of Eq. (5.121) for $2N + 1$ zero crossing points symmetrically placed about $t = 0$ we get,

$$\begin{bmatrix} b(0) & b(-T_b) & \dots & b(-2NT_b) \\ b(T_b) & b(0) & \dots & b[-(2N+1)T_b] \\ \dots & \dots & \dots & \dots \\ b(NT_b) & b[(N-1)T_b] & \dots & b(-NT_b) \\ \dots & \dots & \dots & \dots \\ b(2NT_b) & b[(2N-1)T_b] & \dots & b(0) \end{bmatrix} \begin{bmatrix} C_{-N} \\ C_{-N+1} \\ \dots \\ C_0 \\ \dots \\ C_N \end{bmatrix} = \begin{bmatrix} 0 \\ 0 \\ \dots \\ 1 \\ \dots \\ 0 \end{bmatrix} \quad (5.122)$$

Thus we have $2N + 1$ independent equations in (5.122) and as many number of unknown tap weights C_i which are uniquely determined by solving above.

Mean square Equalizer

Instead of forcing zero crossing this method tries to minimize mean square error by a set of output samples solving simultaneous equations.

Adaptive Equalizer

This is useful when channel characteristics is changing. This involves sending pre-assigned pulses at periodic intervals prior to data transmission which adjusts tap weights by an iterative procedure that minimizes ISI.

5.12 ORTHOGONAL FREQUENCY DIVISION MULTIPLEXING (OFDM)

Orthogonal Frequency Division Multiplexing (OFDM) is a relatively new entrant to the field of digital communication but is finding more and more use due to its high spectral efficiency, robustness against interfering signal and to a great extent in avoiding multipath problems. Multipath problems arises when a signal arrives at a destination following multiple paths (say, reflections against walls or trees) and the resulting phase differences of the superimposed signal distorts it. Today Wireless Local Area Network (WLAN), Mobile Broadband Wireless Access (MBWA), Digital Audio and Video Broadcast (DAB and DVB), 3rd and 4th Generation Cellular Standard, Asymmetric Digital Subscriber Line (ADSL), Power Line Communication (PLC), etc., rely on OFDM; such is the strength of this method.

OFDM uses a subcarrier-based communication concept where the subcarriers are orthogonal to each other over the symbol period. This is possible when carriers are harmonic of each other. We discussed orthogonal representation of signals in Sec. 1.5, and Eq. (1.170) gives the orthogonality condition. In OFDM, each of the subcarriers carries a part of the message and together they deliver the entire message. Refer to Fig. 5.48 for a simplistic representation of this concept. There, instead of squeezing 4 bits within a period T_s by modulating a carrier, we use four orthogonal subcarriers, each of which carry 1 bit of information spread over entire T_s .

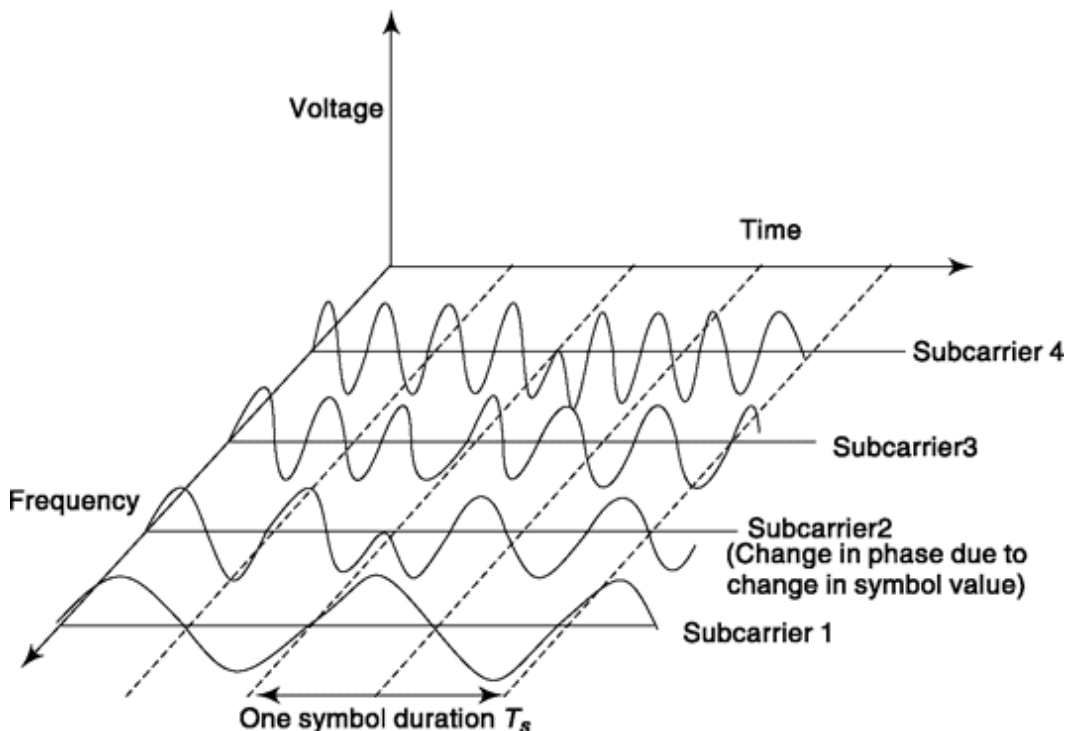


Fig. 5.48 The concept of orthogonal multi carrier based communication in OFDM

Final OFDM signal will be summation of these four signals. The mutual orthogonality of sub carriers help in achieving superior performance of OFDM. The subcarrier can be modulated by a message following any of the modulation techniques say BPSK, QPSK, etc. For example, in WLAN (IEEE 802.11 a/g), subcarrier modulation can be of four types: BPSK, QPSK, 16-QAM and 64-QAM. If channel condition is good, 64-QAM can be used for highest data rate, else other techniques are used with decrease in data rate, the BPSK being the most noise resilient but offering lowest data rate of the four. In this standard, the spacing between subcarriers is 312.5

kHz and with 64 subcarriers, it occupies a bandwidth of $64 \times 312.5 = 20$ MHz.

In developing the theory for OFDM, we shall consider that we have partial information of the channel, i.e. we know the maximum delay the channel can offer and let it be M times the sample time. From our discussion of Sec. 4.6.1, we can modify Eq. (4.47) to describe the channel as

$$H(z) = \sum_{k=0}^M h(k) z^{-k} \quad (5.123)$$

where M is known and $h(0), h(1), \dots, h(M)$ are unknown. If we represent symbols that are input to the channel by $s(k)$ and noise that gets added in travelling through the channel as $\eta(k)$ then the convolution Eq.(5.38) can be used to describe channel output as

$$y(k) = \sum_{i=0}^M h(i) s(k-i) + \eta(k) \quad (5.124)$$

Let us consider that we obtain N outputs from Eq. (5.124) where $N > M$ (it will soon become clear why we have greater-than condition). On expansion of each term, we arrive at the following matrix representation

$$\begin{bmatrix} y(N) \\ y(N-1) \\ \vdots \\ y(M) \\ \vdots \\ y(1) \end{bmatrix}_{N \times 1} = \begin{bmatrix} h(0) & h(1) & \dots & h(M) & \dots & \dots \\ \vdots & h(0) & h(1) & \dots & h(M) & \dots \\ \vdots & \vdots & \vdots & \ddots & \vdots & \vdots \\ \vdots & \dots & h(0) & h(1) & \dots & h(M) \\ \vdots & \vdots & \vdots & \ddots & \vdots & \vdots \\ \vdots & \dots & \dots & h(0) & h(1) & \dots & h(M) \end{bmatrix}_{N \times (N+M)} \begin{bmatrix} s(N) \\ s(N-1) \\ \vdots \\ s(0) \\ \vdots \\ s(-M-1) \end{bmatrix}_{(N+M) \times 1} + \begin{bmatrix} \eta(N) \\ \eta(N-1) \\ \vdots \\ \eta(M) \\ \vdots \\ \eta(1) \end{bmatrix}_{N \times 1} \quad (5.125)$$

In Eq. (5.125), the input vector is $(N + M)$ long where $[s(N) \ s(N-1) \ \dots \ s(1)]^T$ belongs to the data of the present block and $[s(0) \ \dots \ s(-M-1)]^T$, i.e. M data from the previous block. In OFDM, these M data are replaced by zeros or cyclic prefixes. We consider cyclic prefix here so that the signal

vector becomes $[s(N) \ s(N-1) \ \dots \ s(1) \ s(N) \ s(N-1) \ \dots \ s(N-M+1)]^T$. Putting this in Eq. (5.125), and performing multiplication and reorganizing the product, we get Eq. (5.126) where a cyclic matrix (we term as \mathbf{H}_c) appears which is $N \times N$.

$$\begin{bmatrix} y(N) \\ y(N-1) \\ \vdots \\ y(M) \\ y(M-1) \\ y(M-2) \\ \vdots \\ y(1) \end{bmatrix}_{N \times 1} = \begin{bmatrix} h(0) & h(1) & \dots & \dots & h(M) & 0 & 0 & \dots & \dots & 0 \\ 0 & h(0) & (h1) & \dots & \dots & h(M) & 0 & \dots & \dots & 0 \\ \vdots & \vdots \\ 0 & \dots & \dots & 0 & 0 & h(0) & h(1) & \dots & \dots & h(M) \\ h(M) & 0 & \dots & \dots & 0 & 0 & h(0) & h(1) & \dots & h(M-1) \\ h(M-1) & h(M) & 0 & \dots & \dots & 0 & 0 & h(0) & \dots & h(M-2) \\ \vdots & \vdots \\ h(1) & h(2) & \dots & \dots & h(M) & 0 & \dots & \dots & 0 & h(0) \end{bmatrix}_{N \times N} + \begin{bmatrix} s(N) \\ s(N-1) \\ \vdots \\ s(M) \\ s(M-1) \\ s(M-2) \\ \vdots \\ s(1) \end{bmatrix}_{N \times 1} \begin{bmatrix} n(N) \\ n(N-1) \\ \vdots \\ \eta(M) \\ \eta(M-1) \\ \eta(M-2) \\ \vdots \\ \eta(1) \end{bmatrix}_{N \times 1} \quad (5.126)$$

Then, we can write, $y = \mathbf{H}_c \mathbf{s} + \boldsymbol{\eta}$
Recall our discussion on DFT in Sec. 4.1.3. We have defined there

$$\mathbf{W}_N = \begin{bmatrix} 1 & 1 & \dots & 1 \\ 1 & W_N^1 & \dots & W_N^{(N-1)} \\ \vdots & \vdots & \ddots & \vdots \\ 1 & W_N^{(N-1)} & W_N^{2(N-1)} & W_N^{(N-1)^2} \end{bmatrix} \text{ where } W_N = e^{-j2\pi/N}$$

and found $\mathbf{W}_N^* \mathbf{W}_N = N \mathbf{I}_{N \times N}$
Using, Eq. (4.15a), we can find DFT coefficients of $h(k)$ as

$$H(q) = \sum_{k=0}^{N-1} h(k) e^{-j2\pi q k / N}, \quad q = 0, 1, 2, \dots, N-1 \quad (5.128a)$$

In matrix notation, this can be written as $\mathbf{H} = \mathbf{W}_N \mathbf{h}$ (5.128b)

Also note from Eq.(5.128a), $H(-q) = H(N - q)$ (5.129)

We continue our analysis of Eq. (5.127). Postmultiplying \mathbf{H}_c with \mathbf{W}_N^{-1} and using Eq. (5.128) and Eq. (5.129), we get something very interesting. We find that

$$\mathbf{H}_c \mathbf{W}_N^{-1} = \mathbf{W}_N^{-1} \mathbf{D} \quad (5.130)$$

where the diagonal matrix \mathbf{D} is defined as, $\mathbf{D} = \begin{bmatrix} H(N) & 0 & .. & 0 \\ 0 & H(N-1) & .. & 0 \\ .. & .. & .. & .. \\ 0 & 0 & 0 & H(1) \end{bmatrix}$

Then

$$\mathbf{H}_c = \mathbf{W}_N^{-1} \mathbf{D} \mathbf{W}_N \quad (5.131)$$

and Eq. (5.127) becomes

$$\mathbf{y} = \mathbf{W}_N^{-1} \mathbf{D} \mathbf{W}_N \mathbf{s} + \boldsymbol{\eta} \quad (5.132)$$

We treat \mathbf{s} as OFDM transmission symbol and let us define digital information we want to send as $\{b(k)\}$ or \mathbf{b} in vector form. This \mathbf{b} could be a mapped version of binary data stream, say \mathbf{d} where two digits of \mathbf{d} give one value of b if QPSK is employed; the mapping is 3 to 1 for 8-PSK, 4 to 1 for 16-PSK, etc. Now, if \mathbf{s} is obtained from \mathbf{b} by IDFT then from Eq. (4.17), we can write,

$$\mathbf{s} = \frac{1}{N} \mathbf{W}_N^* \mathbf{b} = \mathbf{W}_N^{-1} \mathbf{b} \quad (5.133)$$

or

$$\mathbf{b} = \mathbf{W}_N \mathbf{s} \quad (5.134)$$

Combining Eq. (5.132) and Eq. (5.134), $\mathbf{y} = \mathbf{W}_N^{-1} \mathbf{D} \mathbf{b} + \boldsymbol{\eta}$ (5.135)

or

$$\mathbf{W}_N \mathbf{y} = \mathbf{D} \mathbf{b} + \mathbf{W}_N \boldsymbol{\eta} \quad (5.136)$$

If we perform DFT on received OFDM symbols \mathbf{y} , we get $\hat{\mathbf{y}} = \mathbf{W}_N \mathbf{y}$ and for noise vector a similar operation yields $\hat{\boldsymbol{\eta}} = \mathbf{W}_N \boldsymbol{\eta}$

Then Eq. (5.136) becomes $\hat{\mathbf{y}} = \mathbf{D} \mathbf{b} + \hat{\boldsymbol{\eta}}$ (5.137)

or

$$\begin{aligned} \hat{y}(N) &= H(N)b(N) + \hat{\eta}(N) \\ \hat{y}(N-1) &= H(N-1)b(N-1) + \hat{\eta}(N-1) \\ \hat{y}(1) &= H(1)b(1) + \hat{\eta}(1) \end{aligned} \quad (5.138)$$

This is equivalent to having N independent subchannels, each of which offers a gain $H(k)$, a scalar quantity. We shall take up discussion on noise later. Suffice it to say that $\hat{\boldsymbol{\eta}}$ elements or noises are independent and one symbol does not influence the other. The message $b(k)$ will take k -th channel and ride the subcarrier frequency $f_k = \frac{k}{NT_s}$. Thus, OFDM converts a channel with maximum delay MT_s or order M offering intersymbol interference to N parallel independent subchannels with no intersymbol interference.

Now we can draw the OFDM transmission-reception block diagram as shown in Fig. 5.49. The signal constellation mapper, included in serial to parallel converter block, generates symbol depending on type of digital modulation used. The parallel to serial block for actual radio communication has two parallel path where one does digital to analog conversion of the real

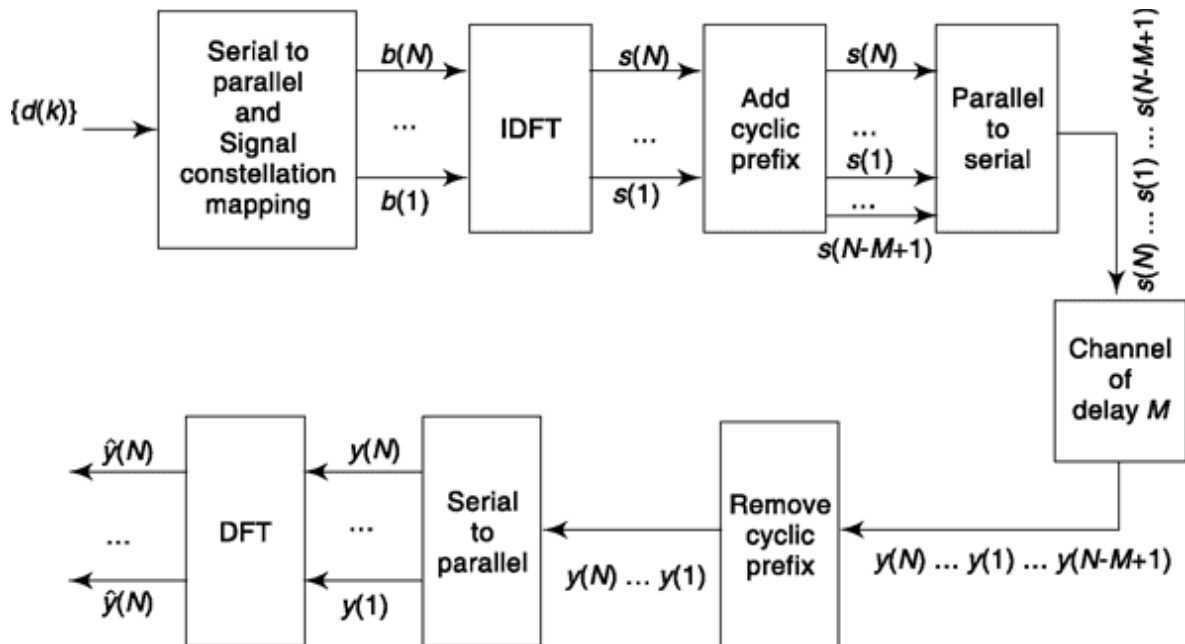


Fig. 5.49 OFDM Transmission and Reception

part of IFFT coefficients and the other for imaginary part. These are then quadrature modulated and fed to the channel. The reverse of this operation is done in the receiver side.

Note that OFDM can be considered a special case of Discrete Multitone Signaling (DMT) where the data rate on each subcarrier is varied according to prevailing SNR on these frequencies. A higher SNR qualifies for a higher data rate. There is yet another technique called OFDMA where the final letter ‘A’ stands for access. In our discussion, we considered that one user is using all the subcarrier frequencies. OFDMA is a multiple-access scenario where subcarrier frequencies are divided among more than one user.

FACTS AND FIGURES

The viability of OFDM theory was first established by Robert W. Chang of Bell Lab in 1966 and subsequently he became the first to receive a US patent on this. The use of Discrete Fourier Transform in OFDM was the next important milestone and it was proposed by S. B. Weinstein and P. M. Ebert in 1971. In 1980, Peled and Ruiz first used the concept of cyclic prefix. In 1994, Digital Audio Broadcasting standard using OFDM came followed by Digital Video Broadcasting standard in 1995. The first Wireless LAN standard using OFDM was introduced in 1999 as IEEE 802.11a followed by IEEE 802.11g in 2002 and IEEE 802.11n in 2004.

The concept of multicarrier communication and parallel subchannels existed before OFDM. One such system was proposed as a military application in 1957 and was called Kineplex. Developed by Collins Radio Company, it was used for data transmission over high-frequency radio channels. This was the time when punched cards were used for data reading and punching (writing). The Kinocard converter Kineplex and IBM punch was proposed as one end-to-end system. The justification for using Kinocard converter read like this, “The wide use of the punched card as a versatile and reliable source document has produced the need to duplicate its information content at remote locations. The Kinocard converter system permits”

Example 5.7

Find spectral efficiency of OFDM in terms of bits/sec/ Hz if BPSK modulation is used.

Solution

In BPSK, a binary data stream modulates the carrier. Let us consider NRZ waveform modulating each subcarrier.

If there are N subcarriers then symbol duration $T_s = N T_b$

or symbol frequency $f_s = f_b / N$

If waveforms make excursions from $+\sqrt{P_s}$ to $-\sqrt{P_s}$

then from Eq. (5.8) power spectral density of each OFDM symbol,

$$G_s(f) = P_s T_s \left(\frac{\sin \pi f T_s}{\pi f T_s} \right)^2 \quad (5.139)$$

For a subcarrier frequency f_i , the PSD will be a shifted version of this and can be written as

$$G_i(f) = P_s T_s \left(\frac{\sin \pi (f - f_i) T_s}{\pi (f - f_i) T_s} \right)^2 \quad (5.140)$$

Since OFDM is a summation of these subcarrier signals,

$$G_{OFDM}(f) = \sum_{i=1}^N G_i(f) = P_s T_s \sum_{i=1}^N \left(\frac{\sin \pi (f - f_i) T_s}{\pi (f - f_i) T_s} \right)^2 \quad (5.141)$$

To maintain orthogonality, subcarriers are f_s apart.

$$\text{Bandwidth of OFDM} = Nf_s + f_s$$

The additional f_s term comes from the endmost carrier (at edge) extending its null bandwidth up to f_s .

Substituting, $f_s = f_b / N$, we get

$$\text{OFDM bandwidth} = (N + 1)f_b / N \approx f_b \text{ for large } N.$$

$$\begin{aligned}\text{Spectral efficiency} &= \text{No. of bits carried per unit bandwidth} \\ &= \text{Data rate/bandwidth} = f_b / f_b \\ &= 1 \text{ bit/sec/Hz (for large } N).\end{aligned}$$

Refer to Prob. 38 for a smaller value of N

Example 5.8

Consider data needs to be sent at a rate 100 kbits/sec in a multipath environment where maximum path difference is 6 km. If guard interval to avoid ISI is one-eighth of the OFDM symbol period, calculate the minimum number of OFDM subcarriers needed.

Solution

Maximum delay = Maximum path difference/Velocity of radio wave

$$= 6/300000 = 20 \text{ microsecond}$$

Guard interval ≥ 20 microseconds

OFDM symbol duration $\geq 8 \times 20 = 160$ microseconds

Given, data rate = 100 kbits/second

Duration of data bit = $1/100000 = 10$ microseconds

Number of subcarriers $\geq 160/10 = 16$

Minimum number of subcarriers needed = 16

SELF-TEST QUESTION

13. A decision threshold in the final comparator stage of regenerative repeater helps to produce clean digital signal. Is that so?

14. In eye pattern noise is not related to opening or closing of eye. Is that true?

15. Equalizer should have a transfer function that is inverse of the channel. Is that correct?

MATLAB

The following experiments illustrate many important concepts of this chapter. You will note that we have shown certain error values as simulation result. If you do it yourself the result may vary little due to randomness of data generation function. However, this variation is small. For more representative error calculation, run each simulation 10 times or more and then average the result.

```

% Experiment 24

% Here we find scatterplot of M symbols in PSK (M-PSK) and QASK (M-QASK),
% We use MATLAB in-built function psk.m and qam.m for respective cases.
% For QASK power is normalized as described in the text by using another
% in-built function modnorm.m while the scatterplot is plotted by function
% scatterplot.m. To know more about them use help <function_name> at MATLAB
% command prompt

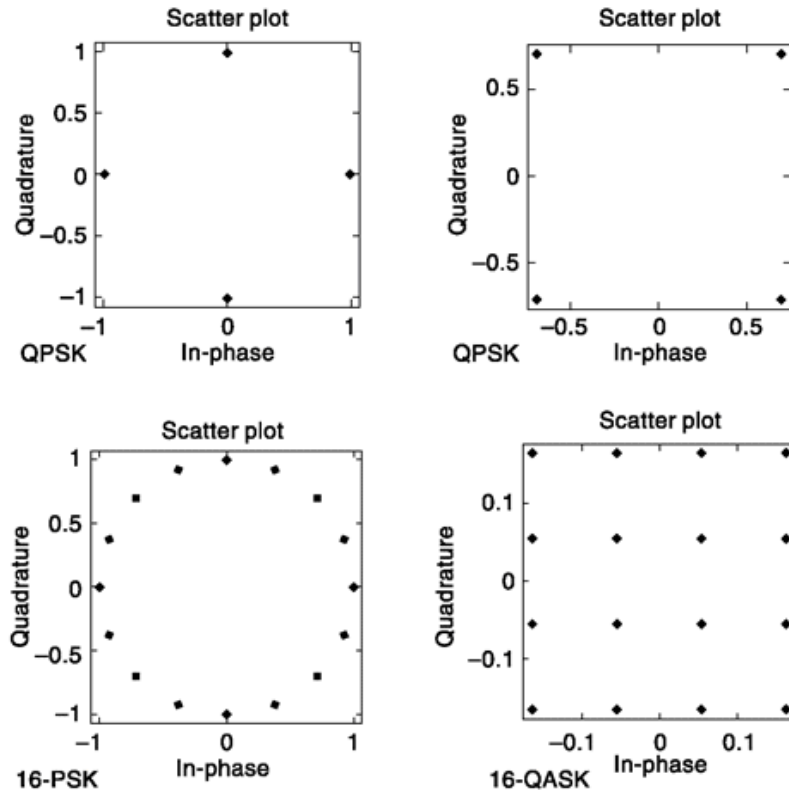
M = 4; x = [0:M-1];
scatterplot(pskmod(x,M)); %plotting the constellation

y = qammmod(x,M); k = modnorm(y, 'peakpow', 1);
y = k*y; scatterplot(y); % scaling and plotting

M = 16; x = [0:M-1];
scatterplot(pskmod(x,M));

y = qammmod(x,M); k = modnorm(y, 'peakpow', 1);
y = k*y; scatterplot(y);

```



```

%Experiment 25
% This experiment shows QPSK modulation demodulation for two different
% noise levels. Noise added is by awgn.m, random message is generated by

```

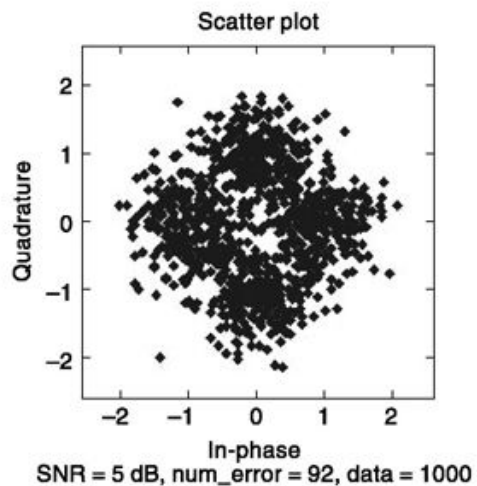
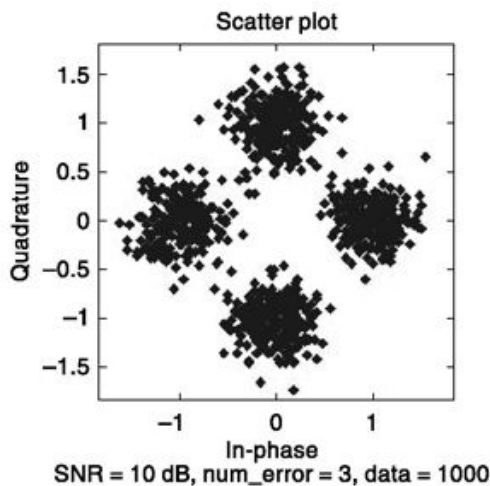
```

% randint.m; pskmod.m and pskdemod.m does modulation and demodulation
% respectively. Total no. of wrongly corrected and hence error rate is
% given by symerr.m

M = 4; x = randint(1000,1,M); % 1000 random quaternary data is generated
y1 = pskmod(x,M); %modulation
yln = awgn(y1,10,'measured'); % SNR of 10 dB
scatterplot(yln);
y1r=pskdemod(yln,M); %demodulation
[num_error,er_rate]=symerr(x,y1r) % no semicolon, result echoed

yln = awgn(y1,5,'measured'); % SNR of 5 dB
scatterplot(yln);
y1r=pskdemod(yln,M);
[num_error,er_rate]=symerr(x,y1r)

```



```
%Experiment 26
```

```

% This experiment shows QASK modulation demodulation for two different
% noise levels. Noise added is by awgn.m, random message is generated by
% randint.m; qammod.m and qamdemod.m does modulation and demodulation
% respectively. Total no. of wrongly corrected and hence ER_RATE is given by
% symerr.m

M = 4; x = randint(1000,1,M); % 1000 random quaternary data is generated
y1 = qammod(x,M); %modulation
yln = awgn(y1,10,'measured'); % SNR of 10 dB
scatterplot(yln);
y1r=qamdemod(yln,M); %demodulation
[num_error,er_rate]=symerr(x,y1r) % no semicolon, result echoed

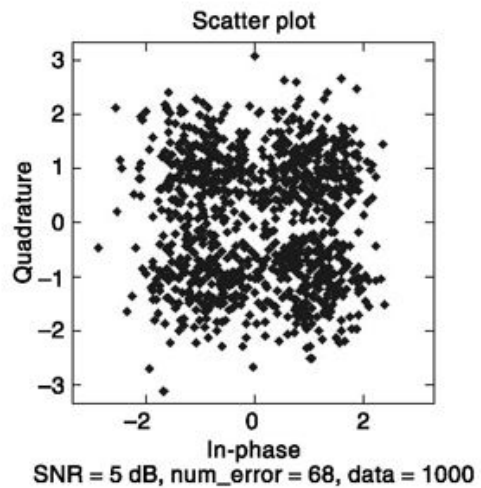
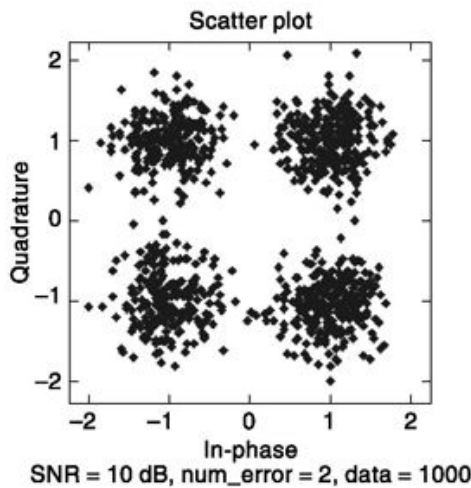
yln = awgn(y1,5,'measured'); % SNR of 5 dB
scatterplot(yln);

```

```

y1r=qamdemod(yln,M);
[num_error,er_rate]=symerr(x,y1r)

```



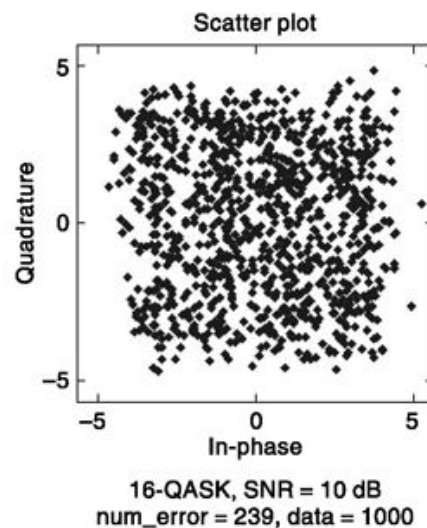
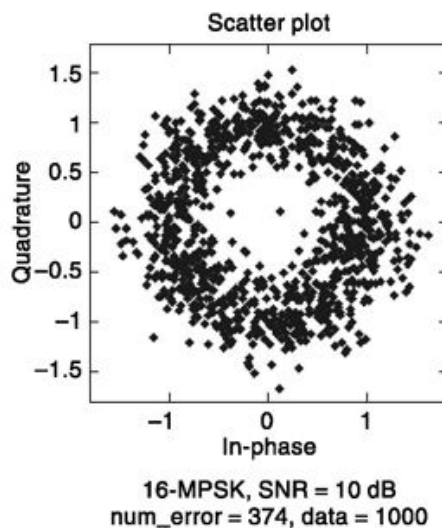
```
%Experiment 27
```

```
% Comparison of 16-MPSK and 16-QASK
```

```

M = 16; x = randint(1000,1,M); % 1000 random quaternary data is generated
y1 = pskmod(x,M); % 16-MPSK modulation
yln = awgn(y1,10,'measured'); % SNR of 10 dB
scatterplot(yln);
y1r=pskdemod(yln,M); %16-MPSK demodulation
[num_error,er_rate]=symerr(x,y1r) % no semicolon, result echoed

```



```

y2 = qammod(x,M); %16-QASK modulation
y2n = awgn(y2,10,'measured'); % SNR of 10 dB
scatterplot(y2n);
y2r=qamdemod(y2n,M); %16-QASK demodulation
[num_error,er_rate]=symerr(x,y2r) % no semicolon, result echoed

%Experiment 28

% Here, we show FSK modulation(fskmod.m) and demodulation(fskdemod.m)
% The syntax is like this fskmod(input,no.of symbol,freq. separation, no.of
% sample per symbol, sampling frequency)
% symbol rate = sampling frequency/no.of sample per symbol

M = 2; x = randint(1000,1,M); % 1000 random quaternary data is generated
y1 = fskmod(x,M,10,5,50); % frequency difference(10) integer times bit rate
y1n = awgn(y1,5,'measured'); % SNR of 5 dB
y1r=fskdemod(y1n,M,10,5,50);
[num_error,er_rate]=symerr(x,y1r) % error echoed

M = 4; x = randint(1000,1,M); % quaternary
y1 = fskmod(x,M,10,5,50); % frequency difference(10) integer times bit rate
y1n = awgn(y1,5,'measured'); % SNR of 5 dB
y1r=fskdemod(y1n,M,10,5,50);
[num_error,er_rate]=symerr(x,y1r)

y1 = fskmod(x,M,5,5,50);%frequency separation less & noninteger times bit rate
y1n = awgn(y1,5,'measured'); % SNR of 5 dB
y1r=fskdemod(y1n,M,5,5,50);
[num_error,er_rate]=symerr(x,y1r)

y1 = fskmod(x,M,15,5,50);%frequency separation more & noninteger times bit rate
y1n = awgn(y1,5,'measured'); % SNR of 5 dB
y1r=fskdemod(y1n,M,15,5,50);
[num_error,er_rate]=symerr(x,y1r)

```

Errors echoed at MATLAB command prompt are as follows. Compare this with theory how frequency separation affects. If frequency separation is integer times the bit rate result is better. You can play with SNR value and check performance.

```

num_error = 0, er_rate = 0
num_error = 1, er_rate = 0.001
num_error = 18, er_rate = 0.018
num_error = 10, er_rate = 0.01

```

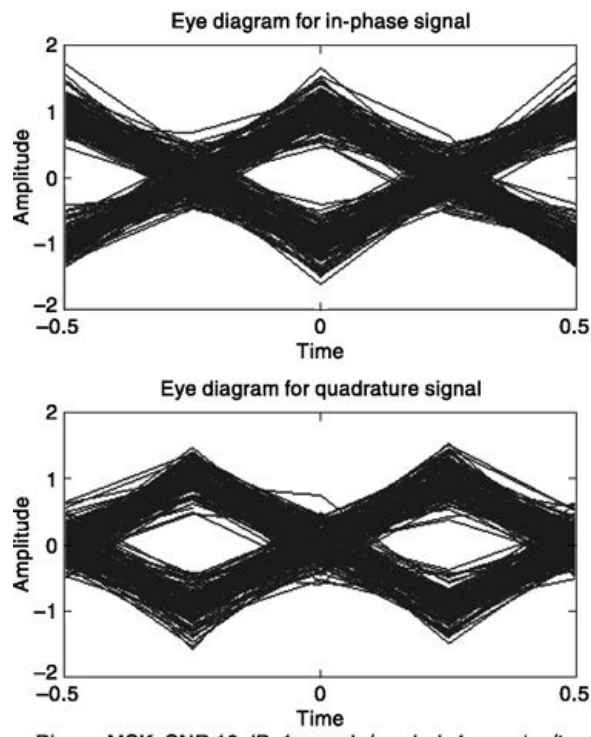
%Experiment 29

```

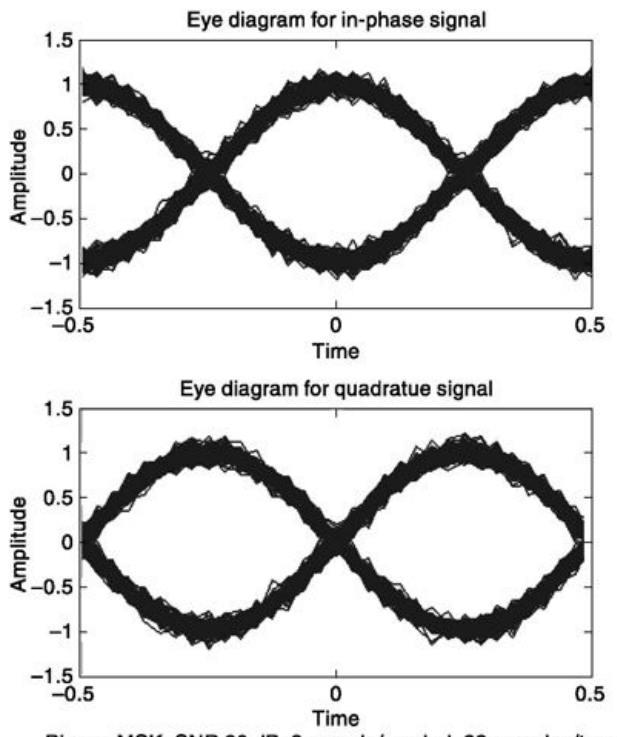
% Here, we show MSK modulation(mskmod.m) and demodulation(mskdemod.m)
% The syntax is like this mskmod(input,no.of sample per symbol)

% We also show how eyediagram is plotted using eyediagram.m.
% Syntax, eyediagram(x, N) where x=noisy input, N=No. of samples per trace.

```



Binary, MSK, SNR 10 dB, 1 sample/symbol, 4 samples/trace



Binary, MSK, SNR 20 dB, 8 sample/symbol, 32 samples/trace

```

M = 2; x = randint(1000,1,M); % 1000 random quaternary data is generated

y1 = mskmod(x,1); % one sample per symbol, modulation
y1n = awgn(y1,5,'measured'); % SNR of 5 dB
y1r=mskdemod(y1n,1); % Demodulation
[num_error,er_rate]=symerr(x,y1r) % Error calculation

y1 = mskmod(x,1); % One sample per symbol
y1n = awgn(y1,10,'measured'); % SNR of 10 dB
y1r=mskdemod(y1n,1);
[num_error,er_rate]=symerr(x,y1r)
eyediagram(y1n,4) % Eyediagram, 4 sample per trace of 10dB SNR data

y1 = mskmod(x,8); % Eight samples per symbol
y1n = awgn(y1,20,'measured'); % SNR of 20 dB
eyediagram(y1n,32); % Eyediagram 32 samples per trace

```

Errors echoed at MATLAB command prompt are as follows. You can play with SNR value, no. of samples per symbol and check performance

```

num_error = 11, er_rate = 0.011
num_error = 1, er_rate = 0.001

% Experiment 30

% Study the effect of Equalizer. Two matlab functions are used.
% EQOBJ = LINEAREQ(NWEIGHTS, ALG) constructs a symbol-spaced linear
% equalizer object. NWEIGHTS = no. of complex weights. ALG an adaptive
% algorithm object which uses LMS with training rate = 0.01
% Y = EQUALIZE(EQOBJ, X) processes the baseband signal vector X with
% equalizer object EQOBJ, and outputs the equalized signal vector Y.

M = 4; x = randint(2000,1,M); % 2000 quaternary message symbol
y = pskmod(x,M); % Modulate using QPSK
trainlen = 100; % Length of training sequence for LMS algo. of equalizer
channel = [.95; .4; .3; .1+.2i]; % Defining Channel
yr = filter(channel,1,y); % Introducing channel distortion

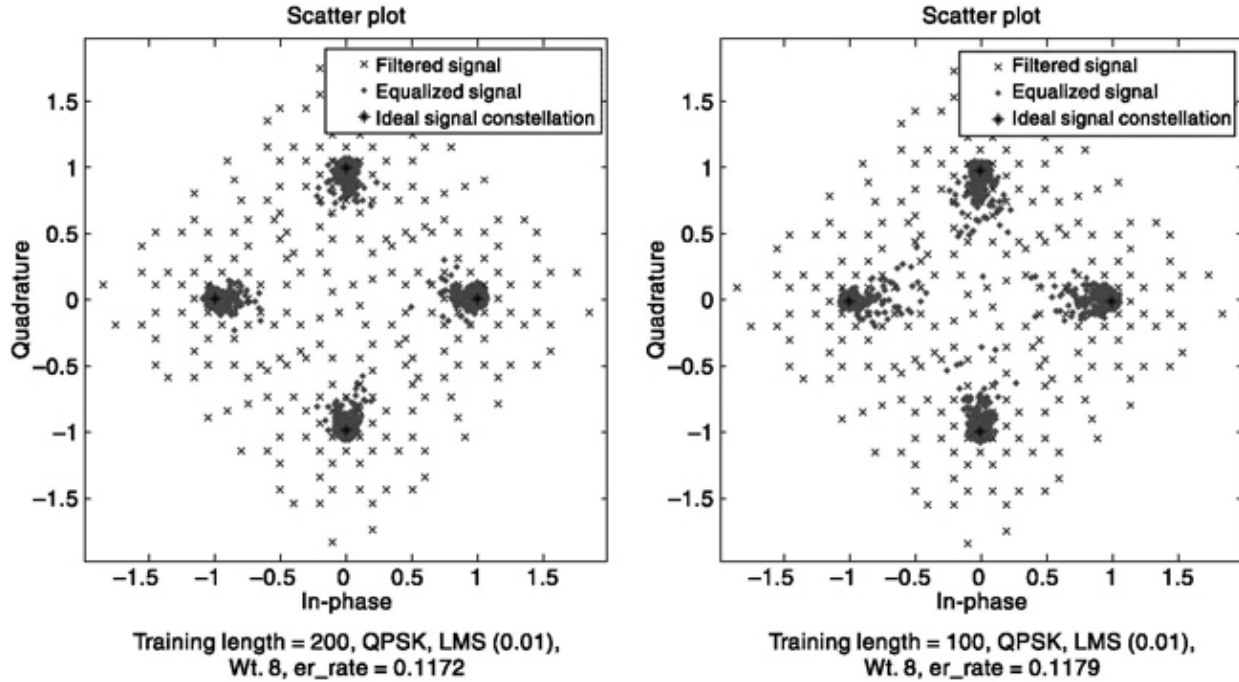
eq1 = lineareq(8, lms(0.01)); % Creates an equalizer object
eq1.SigConst = pskmod([0:M-1],M); % Sets signal constellation
[symbolest,yr_eq] = equalize(eq1,yr,y(1:trainlen)); % Equalizes

% Plot signals
h = scatterplot(yr,1,trainlen,'bx'); hold on;
scatterplot(symbolest,1,trainlen,'g.',h);
scatterplot(eq1.SigConst,1,0,'r*',h);
legend('Filtered signal','Equalized signal','Ideal signal constellation');
hold off;

xr_noeq = pskdemod(yr,M); % Demodulate unequalized signal
xr_eq = pskdemod(yr_eq,M); % Demodulate detected signal from equalizer

% Error calculation
[ne_noeq,er_rate_noeq] = symerr(xr_noeq(trainlen+1:end),x(trainlen+1:end))
[ne_eq, er_rate_eq] = symerr(xr_eq(trainlen+1:end),x(trainlen+1:end))

```



The above shows scatter plot for training length 200 and 100 respectively. You can play with this length, learning rate and other parameters and verify the performance.

SUMMARY

Carrier modulation for passband transmission of digital signal is introduced with BPSK modulation. This is followed by its useful variant DPSK and further improved DEPSK. The bandwidth reduction in QPSK is compared with signal space representation. How far the advantages of QPSK can be extended to MPSK is discussed next. QASK and its extension M-QASK provide interesting alternatives in signal space in terms of distinguishability of a signal. BFSK and MFSK are introduced next and compared with phase shift counterparts. The advantages of MSK and comparison with QPSK come as the final topic of digital carrier modulation technique. The importance of pulse shaping in reduction of inter channel and inter symbol interference is discussed next. Duobinary coding is discussed in detail and comparison with binary, polybinary presented. This is followed by Nyquist criteria for zero ISI, nyquist pulses, cosine filters and partial response filtering that culminates into quadrature partial response encoder and decoder. Regenerative repeater and role of eye diagram, equalizer in digital transmission is discussed at the end.

PROBLEMS

5.1 A binary NRZ data stream of 10^4 bits/sec is transmitted by a carrier of $0.5 \cos(2\pi 10^6 t)$ using BPSK modulation. Find (i) total power needed for transmission, and (ii) power at frequencies 1 MHz, 1.005 MHz, 1.01 MHz, 1.015 MHz and 1.02 MHz.

5.2 For the signal in Prob. 1, how much energy is contained in a bit duration? How much is the distance in signal space for two binary symbols?

5.3 The bit stream $d(k)$ is to be transmitted using DPSK. If $d(k)$ is 001010011010, determine the transmitted bit stream $b(t)$. Show how receiver decodes to get back the original data.

5.4 In Prob. 3, show how detection of $d(k)$ suffers if (i) 4th bit of received $b(k)$ is erroneous, and (ii) both 4th and 5th bits of received $b(k)$ are erroneous.

5.5 Consider that the bit stream $d(k)$ is to be transmitted using DEPSK. If $d(k)$ is 001010011010, determine transmitted bit stream $b(k)$. Show how the receiver decodes to get back the original data.

5.6 In Prob. 5, show how detection of $d(k)$ suffers if (i) 4th bit of received $b(k)$ is erroneous and (ii) both 4th and 5th bits of received $b(k)$ are erroneous. Compare this with the result of Prob. 4.

5.7 Show that for MPSK transmission of NRZ signals, the Power Spectral Density (PSD) is given by

$$G_{MPSK}(f) = \frac{P_s T_s}{2} \left\{ \left(\frac{\sin \pi(f - f_0)t}{\pi(f - f_0)t} \right)^2 + \left(\frac{\sin \pi(f + f_0)t}{\pi(f + f_0)t} \right)^2 \right\}$$

5.8 Consider QPSK transmission instead of BPSK for Prob. 1 and find total power and power at respective frequencies.

5.9 Find distance in signal space between symbols for QPSK, 16-PSK, 64-PSK transmission of an NRZ data stream of 10^4 bits/sec and 10^6 Hz carrier frequency.

5.10 Consider a sinusoidal carrier frequency of 1 MHz. If binary data stream sent is 1000110111001001 at the rate of 1000 bits/sec, what will be the modulated waveforms for BPSK, QPSK, 8-PSK and 16-PSK modulation?

5.11 Represent the data stream of Prob. 10 using a 16-QAM signal constellation diagram of Fig. 5.18.

5.12 How does the representation in Prob. 11 change if a 16-QAM constellation diagram used is as shown in Fig. P5.12?

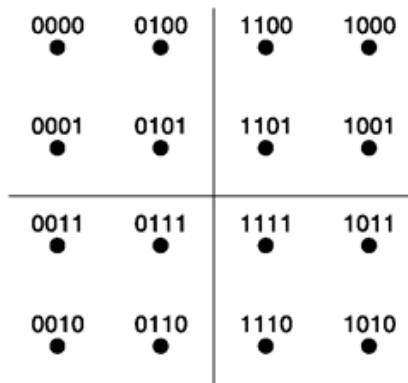


Fig. p5.12 Constellation diagram of 16-QAM for Prob. 12

5.13 For transmission of an NRZ data stream of 10^4 bits/sec and carrier frequency 10^6 Hz, find the distance in signal space if 16-QAM is used. Compare this with 16-PSK. What is the largest separation of two symbols in these two cases? (Note that the distance between signal space in general refers to distance between adjacent symbols or minimum distance.)

- 5.14 For the signal in Prob. 13, find the bandwidth required for transmission if BPSK, QPSK, 16-PSK, 16-QAM is used for modulation.
- 5.15 Compare the result of Prob. 14 along with distance in signal space between symbols if BFSK and 16-FSK is employed.
- 5.16 Consider the signal and carrier of Prob. 13. If MSK is employed, what would be the bandwidth and distance between symbols in signal space? Compare these with QPSK.
- 5.17 Consider speech signal is bandlimited up to 3.4 kHz. It is sampled at 8 kHz rate and quantized into 4096 levels. Calculate the data rate of the digital signal. Find the bandwidth of the modulated signal if baseband signal is represented by NRZ waveform and modulation scheme used is BPSK.
- 5.18 Find the bandwidth of the modulated signal in Prob. 17 if modulation scheme used is BFSK when (i) there is minimum overlap between spectrum of two levels, and (ii) the difference between high and low frequency is 50 kHz.
- 5.19 Find the bandwidth of the modulated signal in Prob. 17 if (i) QPSK, (ii) 16-PSK, and (iii) 64-PSK is used. Compare the effect on distinguishability in these cases and the probability of error.
- 5.20 Compare corresponding results of Prob. 19 with digital modulation schemes 16-FSK and 64-FSK. Arrange 16-PSK, 64-PSK, 16-FSK and 64-FSK in order of bandwidth required and probability of error.
- 5.21 Find the bandwidth of the modulated signal in Prob. 17 if modulation scheme used is 16-QAM. How does it compare in terms of probability of error and bandwidth with corresponding PSK and FSK modulation schemes?
- 5.22 Consider that there is a constraint on available transmission bandwidth and a maximum of 40 kHz can be used. The other condition is data to be sent is at the rate 10 kbits/sec over a carrier frequency of 1 MHz. What is the minimum value of M if M -PSK communication is employed? Now if available bandwidth increases to 50 kHz, how can it help in lowering probability of error?
- 5.23 Show how a duobinary signal is sent when precoder (Ex-OR) gate is used for binary data stream $\{d(k)\} = \{001010011010\}$. Show how decoding is done to get back the original data.
- 5.24 In Prob. 23, show how detection of $d(k)$ suffers if (i) 4th bit of received duobinary signal is erroneously detected as next nearest magnitude, and (ii) both 4th and 5th bits of received signal is detected erroneously as the next nearest magnitude.
- 5.25 Show how a duobinary signal is sent when precoder (Ex-OR) gate is *not* used for binary data stream $\{d(k)\} = \{001010011010\}$. Show how decoding is done to get back the original data.
- 5.26 In Prob. 24, show how detection of $d(k)$ suffers if (i) 4th bit of received duobinary signal is erroneously detected as the next nearest magnitude, and (ii) both 4th and 5th bits of received signal is detected erroneously as next nearest magnitude.
- 5.27 Consider a Nyquist pulse with roll-off factor 0.25 is used in Prob. 17 instead of the NRZ waveform. What will be the bandwidth of the signal after BPSK modulation? How does bandwidth change if the roll-off factor used is 0.5? From these results, comment on the spectrum efficiency of NRZ waveform and Nyquist pulse waveform. Does a change in baseband waveform alter probability of error?

- 5.28 Spectral efficiency of a modulation scheme when given by bits/second/Hz represents how many bits can be sent per second per Hz of available bandwidth. Give this spectral efficiency for BPSK, QPSK, 16-PSK if (i) NRZ pulse, and (ii) Nyquist pulse is used.
- 5.29 Calculate spectral efficiency in bits/sec/Hz for NRZ pulse and Nyquist Pulse are used for 16-QAM modulation.
- 5.30 A more realistic approach of calculating spectral efficiency is to consider roll-off in a raised cosine filter instead of brick-wall filter which is impossible to implement. Calculate spectral efficiency for roll-off factors 0.3 and 0.5 for BPSK, QPSK, 16-PSK.
- 5.31 From Fig. 5.32, find spectral efficiency of MSK signal in bits/sec/Hz.
- 5.32 In BPSK transmission, there are three eye openings in the horizontal direction. What is the time period of X -axis waveform in the oscilloscope?
- 5.33 In a M -PSK transmission, there are 7 eyes in the vertical direction. What is the value of M ? Will there be any change in number of eyes if M -QAM is used instead of M -PSK?
- 5.34 Draw the eye pattern of a duobinary signal.
- 5.35 For a Nyquist pulse sent through a channel, the voltage received at bit intervals are (with increasing time)

$$\dots, 0, 0, 0, 0.2, 0.6, 1.0, -0.1, -0.2, 0, 0, \dots$$

Find the coefficients of a zero-forcing three-tap equalizer for this channel.

- 5.36 For a similar condition as in Prob. 35 show how to design a three-tap equalizer if voltage received are

$$\dots, 0, 0, 0, 0, 0.3, 1.0, -0.1, 0, 0, 0, \dots$$

- 5.37 Write the equation of the equalizer for Prob. 36. Then show how the received voltages get modified when passes through this equalizer. Does it solve ISI completely?
- 5.38 Draw the spectrum of a BPSK modulated OFDM system with two subcarriers. Find bandwidth and spectral efficiency of it. How does it compare with spectral efficiency calculated in Example 5.7?
- 5.39 Instead of OFDM that uses two subcarriers as in Prob. 38, consider frequency division multiplexing is used. How would the spectrum look like then and what would have been the spectral efficiency?
- 5.40 In IEEE 802.11a, system employing OFDM spectral efficiency falls in the range 0.3–2.7 bits/sec/Hz. If channel bandwidth available is 20 MHz, how much data rate is supported?
- 5.41 Further to data given for IEEE 802.11a system in Prob. 40, consider that it employs 64 point FFT. Find the duration of each OFDM symbol.
- 5.42 Consider data needs to be sent in a multipath environment where maximum path difference is 12 km. If guard interval to avoid ISI is one-eighth of the OFDM symbol period, calculate the data rate that can be supported if number OFDM subcarriers used is thirty-two.
- 5.43 For 1 Mbit/sec, OFDM transmission with 64 subcarriers how much of path difference in a multipath environment can be allowed? Consider guard time interval of one-eighth of OFDM symbol period.

6

RANDOM VARIABLES AND PROCESSES

CHAPTER OBJECTIVE

In discussions so far, we have noted that a message signal is not deterministic in nature, so also is the noise that interferes with the message. A completely predictable or deterministic message signal does not require to be sent and information is contained in the randomness of data. It is generally possible to predict the future values of a random process with a certain probability of being correct. In this chapter, we'll present elementary ideas of probability theory and apply them to describe a random process. The aim is to develop the necessary background for subsequent chapters and we'll avoid exhaustive details which may be found in a dedicated course on probability theory. Illustrations focus description of digital signal and digital communication receiver design. Besides numerical examples, the chapter also presents a variety of MATLAB based simulations.

FACTS AND FIGURES

In the year 1654, “a gambler’s dispute” led to the creation of a mathematical theory of probability by two famous French mathematicians, Blaise Pascal and Pierre de Fermat. They exchanged seven letters on this between July and October of that year. One topic in these letters was like this: Two players agree to play a series of fair games until one wins a total of N games. If the play is interrupted when one player has won N_1 ($N_1 < N$) and the other N_2 ($N_2 < N$), how will the stake be divided?

Born in 1777 at Brunswick, Germany, Karl Friedrich Gauss started attending elementary school at the age of seven. Here in one class, to keep his students busy, the teacher asked them to sum integers from 1 to 100. Gauss did it instantly by spotting that the sum was 50 pairs of numbers, each pair summing to 101. Fondly called the ‘Prince of Mathematics,’ Gauss

lends his name to an often used ‘Gaussian’ probability distribution which was first introduced by de Moivre in 1734 and subsequently used by Laplace in 1783 to study measurement of errors and by Gauss in 1809 to analyse astronomical data.

6.1 PROBABILITY

The concept of probability occurs naturally when we contemplate the possible outcomes of an experiment whose outcome is not always the same. Suppose that one of the possible outcomes is called A and that when the experiment is repeated N times the outcome A occurs N_A times. The relative frequency of occurrence of A is N_A/N , and this ratio N_A/N is not predictable unless N is very large. For example, let the experiment consist of the tossing of a die and let the outcome A correspond to the appearance of, say, the number 3 on the die. Then in 6 tosses, the number 3 may not appear at all, or it may appear 6 times, or any number of times in between. Thus with $N = 6$, N_A/N may be 0 or $1/6$, etc., up to $N_A/N = 1$. On the other hand, we know from experience that when an experiment, whose outcomes are determined by chance, is repeated *very many times*, the relative frequency of a particular outcome approaches a fixed limit. Thus, if we were to toss a die very many times we would expect that N_A/N would turn out to be very close to $1/6$. This limiting value of the relative frequency of occurrence is called the probability of outcome A , written $P(A)$, so that

$$P(A) = \lim_{N \rightarrow \infty} \frac{N_A}{N} \quad (6.1)$$

In many cases the experiments needed to determine the probability of an event are done more in thought than in practice. Suppose that we have 10 balls in a container, the balls being identical in every respect except that 8 are white and 2 are black. Let us ask about the probability that, in a single draw, we shall select a black ball. If we draw blindly, so that the color has no influence on the outcome, we would surely judge that the probability of drawing the black ball is $2/10$. We arrive at this conclusion on the basis that we have postulated that there is absolutely nothing which favors one ball over another. There are 10 possible outcomes of the experiment, that is, any of the 10 balls may be drawn; of these 10 outcomes, 2 are favorable to our interest. The only reasonable outcome we can imagine is that, in very many

drawings, 2 out of 10 will be black. Any other outcome would immediately suggest that either the black or the white balls had been favored. These considerations lead to an alternative definition of the probability of occurrence of an event A , that is

$$P(A) = \frac{\text{number of possible favorable outcomes}}{\text{total number of possible equally likely outcomes}} \quad (6.2)$$

It is apparent from either definition, Eq. (6.1) or (6.2), that the probability of occurrence of an event P is a positive number and that $0 \leq P \leq 1$. If an event is not possible, then $P = 0$, while if an event is certain, $P = 1$.

6.1.1 Mutually Exclusive Events

Two possible outcomes of an experiment are defined as being *mutually exclusive* if the occurrence of one outcome precludes the occurrence of the other. In this case, if the events are A_1 and A_2 with probabilities $P(A_X)$ and $P(A_2)$, then the probability of occurrence of *either* A_1 or A_2 is written $P(A_1 \text{ or } A_2)$ and given by

$$P(A_1 \text{ or } A_2) = P(A_1) + P(A_2) \quad (6.3)$$

This result follows directly from Eq. (6.1). For suppose that in a very large number N of repetitions of the experiment, outcome A_1 had occurred N_1 times and outcome A_2 had occurred N_2 times. Then A_1 or A_2 will have occurred $N_1 + N_2$ times and

$$P(A_1 \text{ or } A_2) = \frac{N_1 + N_2}{N} = \frac{N_1}{N} + \frac{N_2}{N} = P(A_1) + P(A_2) \quad (6.4)$$

As an example of the calculation of the probability of mutually exclusive events, we ask, in connection with the tossing of a die, about the probability that either a 1 or a 2 will appear. Since the probability of either event is $1/6$ and since, one having occurred the other cannot take place, the probability of one or the other is $1/6 + 1/6 = 1/3$.

6.1.2 Joint Probability of Related and Independent Events

Suppose that we contemplate two experiments A and B with outcomes A_1, A_2, \dots and B_j, B_2, \dots . The probability of the joint occurrence of, say, A_j and B_k is written $P(Aj \text{ and } B_k)$ or more simply $P(Aj, B_k)$.

It may be that the probability of event B_k depends on whether A_j does indeed occur. For example, imagine 4 balls in a box, 2 white and 2 black. The probability of drawing a white ball is 1/2. If, having drawn a ball, we replace it and draw again, then we are repeating the same experiment and the probability of drawing a white ball is again 1/2. Suppose, however, that the first ball drawn is not replaced. Then if we draw a second ball, we shall be performing a new experiment. If the first ball drawn was white, the probability of a white draw in the second experiment is 1/3. If the first ball drawn was black, the probability of a white draw in the second experiment is 2/3. Here, then, we have a situation in which the outcome of the second experiment is *conditional* on the outcome of the first experiment. The probability of the outcome B_k , given that A_j is known to have occurred, is called the *conditional probability* and written $P(B_k|A_j)$.

Suppose that we perform N times (N a very large number) the experiment of determining which pairs of outcomes of experiment A and B occur jointly. Let N_j be the number of times A_j occurs with or without B_k , N_k the number of times B_k occurs with or without A_j , and N_{jk} the number of times of joint occurrence. Then

$$P(B_k|A_j) = \frac{N_{jk}}{N_j} = \frac{N_{jk}/N}{N_j/N} = \frac{P(A_j, B_k)}{P(A_j)} \quad (6.7)$$

Similarly, we have, since $N_{jk} = N_{kj}$,

$$P(A_j|B_k) = \frac{N_{kj}}{N_k} = \frac{N_{kj}/N}{N_k/N} = \frac{P(A_j, B_k)}{P(B_k)} \quad (6.8)$$

From Eqs (6.7) and (6.8), we have

$$P(A_j, B_k) = P(A_j)P(B_k|A_j) = P(B_k)P(A_j|B_k) \quad (6.9)$$

so that

$$P(A_j|B_k) = \frac{P(A_j)}{P(B_k)} P(B_k|A_j) \quad (6.10)$$

which result is known as *Bayes theorem*.

It is apparent that Eq. (6.10) applies equally well to the case of a *single* experiment whose outcome is characterized by two events. This result follows from a simple restatement of the considerations leading up to Bayes' theorem. We need only view the successive performance of experiment A followed by experiment B as a single joint experiment. If we consider the

example of the 2 white and 2 black balls in a box, it is obvious that the probability of picking a black ball (second experiment) after having picked a white ball (first experiment) is the same as the probability that, in picking 2 balls (joint experiment), we find the first white and the second black.

6.1.3 Statistical Independence

Suppose, as before, that A_j and B_k are the possible outcomes of two successive experiments or the joint outcome of a single experiment. And suppose that it turns out that the probability of the occurrence of outcome B_k simply does not depend at all on which outcome A_j accompanies it. Then we say that the outcomes A_j and B_k are *independent*. In this case of complete independence

$$P(B_k|A_j) = P(B_k) \quad (6.11)$$

and Eq. (6.9) yields

$$P(A_j, B_k) = P(A_j)P(B_k) \quad (6.12)$$

Expressed in words: when outcomes are independent, the probability of a joint occurrence of particular outcomes is the product of the probabilities of the individual independent outcomes. This result may be extended to any arbitrary number of outcomes. Thus,

$$P(A_j, B_k, C_l, \dots) = P(A_j)P(B_k)P(C_l) \cdots \quad (6.13)$$

Example 6.1

The set of all possible outcomes of an event is defined by a sample space S . Two events A and B occurring in S are related in probability space by following three axioms. (i) $P(S) = 1$, (ii) $0 \leq P(A) \leq 1$ also $0 \leq P(B) \leq 1$ and (iii) probability of any of A or B occurring $P(A \cup B) = P(A) + P(B)$ if A and B are mutually exclusive.

Solution

- (a) Figure 6.1a represents the Venn diagram when A and B are mutually exclusive and Fig. 6.1b when they are not. Since S defines the full sample space $P(S) = 1$; A or B are always a subset of $S(A \subset S \text{ or } B \subset S)$ hence their maximum are 1 and minimum is zero occurrence case.
- (b) From Fig. 6.1b, we find that probability of any of A or B occurring $P(A \cup B)$ is the entire space covered by the lines. This total space is sum of space covered by A and B individually

minus the checkered region in between which otherwise gets counted twice. This space that defines joint occurrence of A and B is represented by $A \cap B$.

Thus, if A and B are not mutually exclusive,
$$P(A \cup B) = P(A) + P(B) - P(A \cap B)$$

$$\begin{aligned} \text{Now } P(A \cap B) &= P(A) + P(B) - P(A \cup B) \\ &= 0.2 + 0.4 - 0.5 \\ &= 0.1 \end{aligned}$$

None of A or B are occurring is defined by the space $= S - A \cup B$

$$\begin{aligned} \text{Hence, its probability } &= P(S) - P(A \cup B) \\ &= 1 - 0.5 = 0.5 \end{aligned}$$

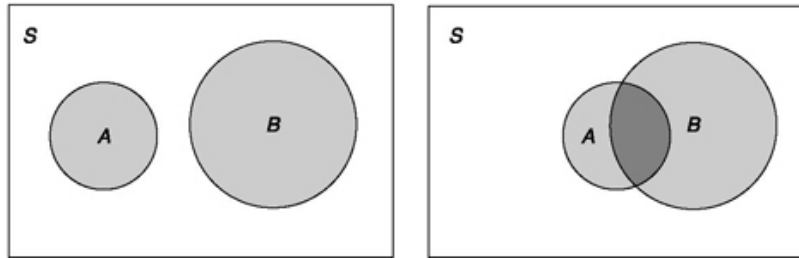


Fig. 6.1 Venn diagram of (a) mutually exclusive event, and (b) general cases.

Example 6.2

What is the probability that A will occur if B has already occurred and the reverse for data given in Example 6.1. Hence, verify Bayes ' theorem.

Solution

Probability that A will occur if B has already occurred

$$= P(A|B)$$

From definition, $P(A|B) = P(A, B)/P(B)$

$$P(B) \neq 0 \text{ [From Eq. 6.7]}$$

$$= P(A \cap B)/P(B)$$

[From Venn diagram, Fig.6.1b]
 $= 0.1/0.4 = 0.25$

Similarly,

Probability that A will occur if B has already occurred

$$= P(B/A) = P(A \cap B)/P(A)$$

$$= 0.1/0.2 = 0.5$$

Bayes' theorem says that $P(A/B) = \frac{P(A)}{P(B)} P(B/A) =$

[From Eq. 6.10]

Substituting,

$$\text{RHS} = \frac{0.2}{0.4} 0.5 = 0.25 = \text{LHS} \quad \text{Hence, verified.}$$

SELF-TEST QUESTION

1. Probability can be defined as limiting value of the relative frequency of occurrence. Is it true?
2. Is Bayes theorem related to joint probability?
3. If A and B are statistically independent, then $P(B/A)$ is same as which of $P(A)$ and $P(B)$?

6.2 RANDOM VARIABLES

The term random variable is used to signify a *rule* by which a real number is assigned to each possible outcome of an experiment. Let the possible outcomes of an experiment be identified by the symbols l . These symbols need not be numbers. For example, the experiment might consist of running a horse race where the outcome of interest is the name of the winner. The symbols l might then be the names of the horses. Let us now arbitrarily establish some rule by which we assign real numbers $X(l)$ to each possible outcome. Then the *rule* or *functional relationship* represented by the symbol $X()$ is called a *random variable*. When used in this sense, the term random variable is a misnomer, since $X()$ is not a variable at all and is in no way random, being a perfectly definite rule.

By a rather easy extension of meaning, the term random variable is also used to refer to a *variable* which may assume any of the *numbers* $X(l)$. When used in this sense, the random variable may be represented by the symbol $X(l)$.

In many cases, the identifying symbols l may turn out to be numbers. To illustrate this point, consider that we perform the experiment of measuring a random voltage V between a set of terminals and find a number of possible outcomes v_1 , v_2 or v_3 . Then for identifying symbols for the outcomes we would rather naturally be led to use the numbers themselves; that is, we would use $l_1 = v_1$, $l_2 = v_2$ and $l_3 = v_3$. Further, we might very naturally use a rule in which the number assigned to an outcome is the very same number used for identifications. We would then have $X(l) = X(v_i) = v_i$. With these considerations in mind, we might well refer to the random voltage itself as a random variable and represent it by the symbol V .

A random variable may be *discrete* or *continuous*. If in any finite interval $X(l)$ assumes only a finite number of distinct values, then the random variable is *discrete*. An example of an experiment which yields such a discrete random variable is the tossing of a die. If, however, $X(l)$ can assume any value within an interval, the random variable is continuous. Thus suppose we fire a bullet at a target. Because of wind currents and other unpredictable influences the bullet may miss its mark, and the magnitude of the miss will be a *continuous random variable*.

6.2.1 Cumulative Distribution Function

The *cumulative distribution function* associated with a random variable is defined as the probability that the outcome of an experiment will be one of the outcomes for which $X(l) < x$, where x is any given number. This probability will depend on the number x and also on $X(\cdot)$, that is, on the rule by which we assign numbers to outcomes. Thus, we use the symbol $F_X(\cdot)(x)$ to represent the cumulative distribution function, and we have the definition.

$$F_{X(\cdot)}(x) \equiv P[X(\lambda) \leq x] \quad (6.14)$$

Observe that in Eq. (6.14) we used the symbol $X(\cdot)$ to represent a rule and the symbol $X(\lambda)$ to represent a variable which ranges over the numbers assigned to possible outcomes. If a different rule $Y(\cdot)$ were used to assign numbers, $F_{Y(\cdot)}(x)$ would differ from $F_{X(\cdot)}(x)$ for the same x . It is for this reason that the subscript $X(\cdot)$ is included in the notation $F_{X(\cdot)}(x)$. Generally, for simplicity of notation, Eq. (6.14) is written more simply in the form

$$F_X(x) \equiv P(X < x) \quad (6.15)$$

Even further, when there is only a single random variable under discussion and no ambiguity will result, we shall drop the subscript X and use the symbol $F(x)$ to represent the cumulative distribution function.

The cumulative distribution function has the properties

$$0 \leq F(x) \leq 1 \quad (6.16a)$$

$$F(-\infty) = 0 \quad F(\infty) = 1 \quad (6.16b)$$

$$F(x_1) \leq F(x_2) \quad \text{if } x_1 < x_2 \quad (6.16c)$$

The property in Eq. (6.16a) follows from the fact that $F(x)$ is a probability. The property in Eq. (6.16b) follows from the fact that $F(-\infty)$ includes no possible events, while $F(\infty)$ includes all possible events. Finally Eq. (6.16c) holds since for $x_1 < x_2$, $F(x_2)$ includes as many or more of the possible outcomes as does $F(x_1)$.

The features of the cumulative distribution function, as well as the concept of a random variable, will be clarified in the course of the following illustrative discussion: We consider the experiment which consists of rolling of 2 dice. There are 36 possible outcomes since each die may show the numbers 1 through 6. These 36 outcomes may be represented by 36 symbols λ_{ij} , where, say, i is the number that shows on the first die, and j the number that shows on the second die. Suppose however that our interest in the outcome extends only to knowing the sum of the numbers appearing on the dice. Then we may use as our random variable the function $N(\lambda_{ij})$ defined by $N(\lambda_{ij}) = i + j$. Observe that in doing so we are assigning the same number to $N(\lambda_{ij})$ and to $N(\lambda_{ji})$. Let

$$n \equiv N(\lambda_{ij}) = i + j$$

Then each integral value of n from $n = 2$ to $n = 12$ corresponds to outcomes which we care to distinguish from one another. The probabilities $P(n)$ are readily calculated. We find $P(1) = 0$, $P(2) = P(12) = 1/36$, $P(3) = P(11) = 2/36$, $P(4) = P(10) = 3/36$, $P(5) = P(9) = 4/36$, $P(6) = P(8) = 5/36$, and $P(7) = 6/36$.

Let us calculate, as an example, the cumulative distribution function $F(n)$ for, say, $n = 3$. We have from the definition of Eq. (6.15)

$$F(3) = P[N(\lambda_{ij}) \leq 3] = P(n \leq 3) \quad (6.17)$$

since $N(\lambda_{ij}) \equiv n$. We must now add up the probabilities of all outcomes corresponding to $n \leq 3$. We find that

$$F(3) = P(1) + P(2) + P(3) = 0 + 1/36 + 2/36 = 3/36 \quad (6.18)$$

In a similar way, $F(n)$ for other values of n may be determined. $F(n)$ is plotted as a function of n in Fig. 6.2 Note that $F(n)$ satisfies all the conditions given in Eq. (6.16a to c) above. Observe also that there is a significance to $F(n)$ for non-integral values of n . Note also that if the function $N(\lambda_{ij})$ had been selected in a different manner, say, $N'(\lambda_{ij})$, $F_{N'}(n)$ would be different from $F_N(n)$.

6.2.2 probability Density Function

The *probability density function* (pdf) $f_X(x)$ is defined in terms of the cumulative distribution function $F_X(x)$ as

$$f_X(x) = \frac{d}{dx} F_X(x) \quad (6.19)$$

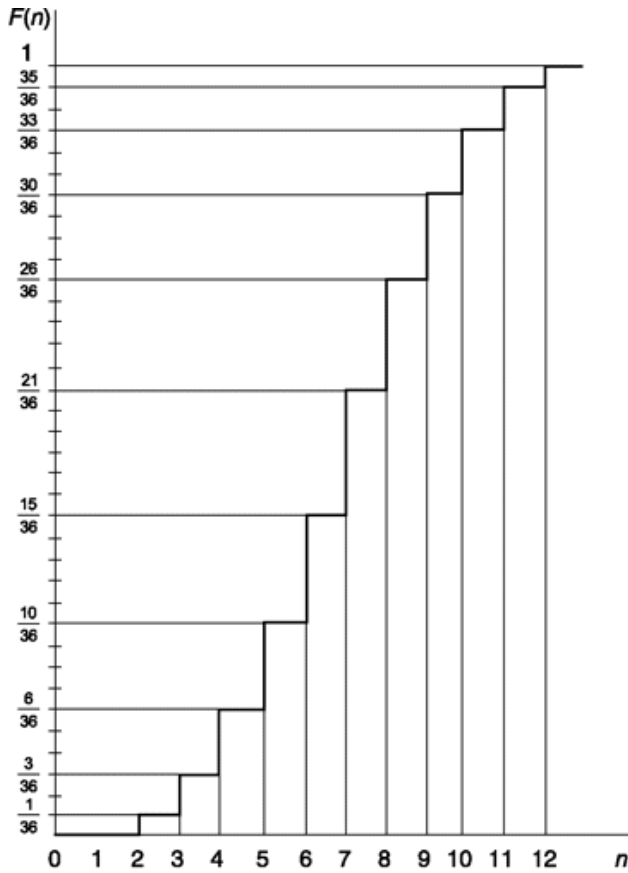


Fig. 6.2 Cumulative distribution function associated with rolling two dice.

[Having made the point in Eq. (6.19) that $f_X(x)$, like $F_X(x)$, requires a subscript in principle, we shall again omit it where no confusion will result]. Thus, $f(x)$ is simply the derivative of the cumulative distribution function $F(x)$. The pdf has the following properties:

$$(a) \quad f(x) \geq 0 \quad \text{for all } x \quad (6.20)$$

This results from the fact that $F(x)$ increases monotonically, for as x increases, more outcomes are included in the probability of occurrence represented by $F(x)$.

$$(b) \quad \int_{-\infty}^{\infty} f(x) dx = 1 \quad (6.21)$$

This result is to be seen from the fact that

$$\int_{-\infty}^{\infty} f(x) dx = F(\infty) - F(-\infty) = 1 - 0 = 1 \quad (6.22)$$

$$(c) \quad F(x) = \int_{-\infty}^x f(x) dx \quad (6.23)$$

This result follows directly from Eq. (6.19).

The pdf corresponding to the cumulative distribution function of Fig. 6.2 is shown in Fig. 6.3. Since the derivative of a step of amplitude A is an impulse of strength $I = A$, we have $f(2) = 1/36 8(n - 2)$, $f(3) = 2/36 S(n - 3)$,

etc. In Fig. 6.3 the height of the arrow is proportional to the strength of the impulse.

As we have already noted, a random variable may be discrete or continuous. The random variable associated, in the discussion above, with the tossing of 2 dice is a discrete random variable. The corresponding cumulative distribution function increases by steps as in Fig. 6.2, and the probability density displays impulses as in Fig. 6.3. With a continuous random variable, on the other hand, the cumulative distribution function and the probability density will generally be *smooth* as shown by the typical plots of Fig. 6.4.

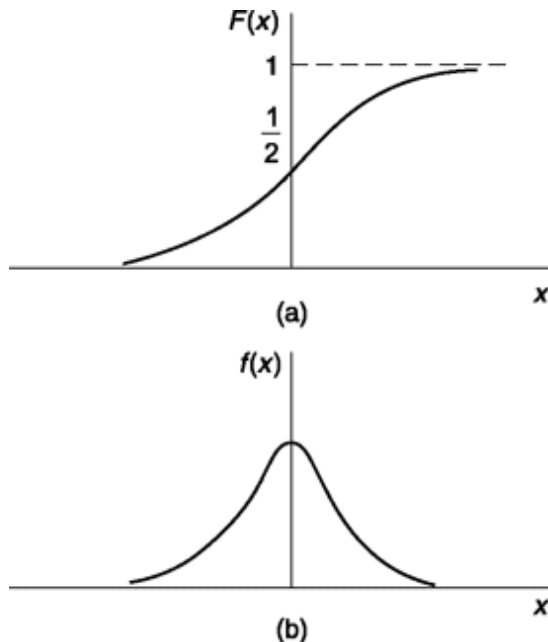


Fig. 6.4 (a) A continuous cumulative distribution function, and (b) the corresponding probability density function.

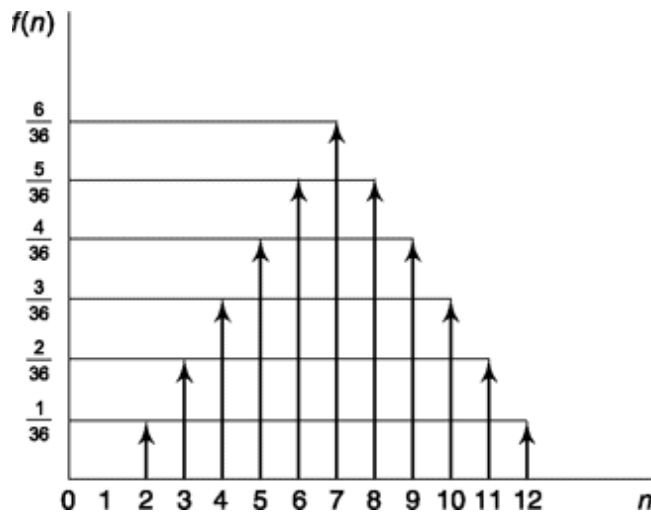


Fig. 6.3 The probability density function corresponding to the cumulative distribution function of Fig. 6.2. The heights of the arrows represent the strengths of impulses.

6.2.3 Relation Between Probability and Probability Density

From Eqs (6.14) and (6.23), we find that the probability of the outcome X being less than or equal to x_1 is

$$P(X \leq x_1) = F(x_1) = \int_{-\infty}^{x_1} f(x) dx \quad (6.24)$$

Similarly, the probability that the outcome X is less than or equal to x_2 is

$$P(X \leq x_2) = F(x_2) = \int_{-\infty}^{x_2} f(x) dx \quad (6.25)$$

The probability that the outcome lies in the range $x_1 \leq X \leq x_2$ is

$$P(x_1 \leq X \leq x_2) = P(X \leq x_2) - P(X < x_1) \quad (6.26)$$

Note that the second term of the right-hand side of Eq. (6.26) is $P(X < x_1)$ and not $P(X \leq x_1)$. The exclusion of the equal sign is necessary since $P(x_1 \leq X \leq x_2)$ includes the possibility that X is exactly $X = x_1$. Using Eqs (6.24) and (6.25) with Eq. (6.26), we have

$$P(x_1 \leq X \leq x_2) = \int_{-\infty}^{x_2} f(x) dx - \int_{-\infty}^{x_2-\varepsilon} f(x) dx = \int_{x_1-\varepsilon}^{x_2} f(x) dx \quad (6.27)$$

where ε is a number which in the limit may approach zero and is introduced simply to exclude $x = x_1$ from the range of integration. If $f(x)$ is everywhere finite, then ε need not be included in Eq. (6.27). Changing the limit by an infinitesimal amount will change the integral only infinitesimally. If, however, the probability density contains impulses as in Fig. 6.3, and if there is an impulse at $x = x_1$, then the presence of the ε reminds us to include this impulse when evaluating Eq. (6.27). For the case where $f(x)$ has no impulses, we have the result which expresses the most important property of the probability density, namely,

$$P(x_1 \leq X \leq x_2) = \int_{x_1}^{x_2} f(x) dx \quad (6.28)$$

or

$$P(x \leq X \leq x + dx) = f(x) dx \quad (6.29)$$

Example 6.3

Consider the probability density $f(x) = ae^{-b|x|}$, where X is a random variable whose allowable values range from $x = -\infty$ to $x = +\infty$. Find (a) the cumulative distribution function $F(x)$, (b) the relationship between a and b , and (c) the probability that the outcome X lies between 1 and 2.

Solution

(a) The cumulative distribution function is

$$\begin{aligned} F(x) = P(X \leq x) &= \int_{-\infty}^x f(x) dx = \int_{-\infty}^x ae^{-b|x|} dx \\ &= \begin{cases} \frac{a}{b} e^{bx} & x \leq 0 \\ \frac{a}{b}(2 - e^{-bx}) & x \geq 0 \end{cases} \end{aligned}$$

(b) In order that $f(x)$ be a probability density, it is necessary that

$$\int_{-\infty}^{\infty} f(x) dx = \int_{-\infty}^{\infty} ae^{-b|x|} dx = \frac{2a}{b} = 1$$

so that $a/b = \frac{1}{2}$.

(c) The probability that X lies in the range between 1 and 2 is

$$P(1 \leq X \leq 2) = \frac{b}{2} \int_1^2 e^{-b|x|} dx = \frac{1}{2} (e^{-b} - e^{-2b})$$

6.2.4 Joint Cumulative Distribution and probability Density

It may be necessary to identify the outcome of an experiment by two (or more) random variables. These random variables may or may not be independent of one another. The concepts of cumulative distribution and probability density are readily extended to such cases.

For the case of a single random variable, Eq. (6.29) expresses, in terms of the probability density, the probability that the random variable X lies in the range $x < X < x + dx$. Correspondingly, for two random variables X and Y ,

the probability that $x \leq X \leq x + dx$ while at the same time $y \leq Y \leq y + dy$ is written

$$P(x \leq X \leq x + dx, y \leq Y \leq y + dy) = f_{XY}(x, y) dx dy \quad (6.30)$$

A comparison of a probability density $f_X(x)$, involving a single random variable, and a density $f_{XY}(x, y)$ involving two variables, is indicated in Fig. 6.5. Part (a) shows a portion of a *curve* which is a plot of $f_X(x)$ as a function of x . Part (b) shows a portion of a *surface* which is a plot of $f_{XY}(x, y)$ as a function of the two variables x and y . The *area* indicated in (a) is the probability that $x \leq X \leq x + dx$, while the *volume* indicated in (b) is the probability that $x \leq X \leq x + dx$ and that $y \leq Y \leq y + dy$.

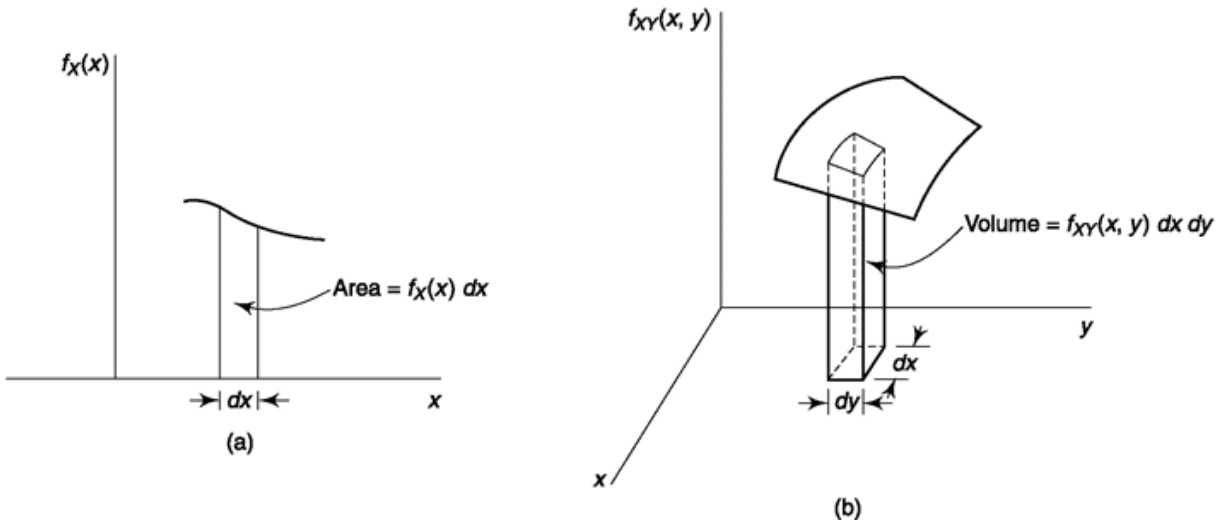


Fig. 6.5 A comparison between a probability density function involving a simple random variable in (a) and a density function involving two random variables as in (b).

Extending Eq. (6.30) to a finite interval, we have, in correspondence with Eq. (6.28),

$$P(x_1 \leq X \leq x_2, y_1 \leq Y \leq y_2) = \int_{y_1}^{y_2} \int_{x_1}^{x_2} f_{XY}(x, y) dx dy \quad (6.31)$$

The cumulative distribution function is

$$F_{XY}(x, y) = P(X \leq x, Y \leq y) = \int_{-\infty}^y \int_{-\infty}^x f_{XY}(x, y) dx dy \quad (6.32)$$

If we should be concerned only with the cumulative probability up to, say, some value of x quite independently of y , we would write

$$F_X(x) = P(X \leq x, -\infty \leq Y \leq \infty) = \int_{-\infty}^{\infty} \int_{-\infty}^x f_{XY}(x, y) dx dy \quad (6.33)$$

The probability density corresponding to $F_X(x)$ in Eq. (6.33) is

$$f_X(x) = \frac{d}{dx} F_X(x) = \int_{-\infty}^{\infty} f_{XY}(x, y) dy \quad (6.34)$$

If the random variables X and Y are *independent*, then by an easy extension of the considerations of Sec. 6.1.3, the probability given in Eq. (6.30) may be written as a product in which each factor involves only one random variable. That is, we may write

$$P(x \leq X \leq x + dx, y \leq Y \leq y + dy) = [f_X(x) dx][f_Y(y) dy] \quad (6.35)$$

The function $f_X(x)$, which is given by Eq. (6.34), depends only on x and need bear no simple relationship to $f_{XY}(x, y)$ given in Eq. (6.30). A similar comment applies, of course, to $f_Y(y)$. We then have, from Eqs (6.30) and (6.35), that, if X and Y are independent,

$$f_{XY}(x, y) = f_X(x)f_Y(y) \quad (6.36)$$

Further, we have, when X and Y are independent,

$$P(x_1 \leq X \leq x_2, y_1 \leq Y \leq y_2) = \left[\int_{x_1}^{x_2} f_X(x) dx \right] \left[\int_{y_1}^{y_2} f_Y(y) dy \right] \quad (6.37)$$

Henceforth, where no confusion will be caused thereby, we shall drop the subscripts from the probability density functions even when more than one such function is involved. Thus we shall write $f_X(x) = f(x)$, $f_Y(y) = f(y)$, and $f_{XY}(x, y) = f(x, y)$. Thus the symbol $f(\)$ represents not a particular probability density but rather a probability density function in general. And the particular random variable or variables referred to are to be determined by the argument of the function.

Example 6.4

The joint probability density of the random variables X and Y is

$$f(x, y) = \frac{1}{4}e^{-|x|-|y|} \quad -\infty < x < \infty, -\infty < y < \infty$$

- (a) Are X and Y statistically independent random variables?
- (b) Calculate the probability that $X \leq 1$ and $Y \leq 0$.

Solution

- (a) Since $f(x, y)$ can be written as

$$f(x, y) = \frac{1}{2}e^{-|x|} \frac{1}{2}e^{-|y|} = f(x)f(y)$$

X and Y are statistically independent.

$$\begin{aligned} \text{(b)} \quad P(X \leq 1, Y \leq 0) &= \int_{-\infty}^1 dx \int_{-\infty}^0 dy f(x, y) \\ &= \int_{-\infty}^1 \frac{1}{2}e^{-|x|} dx \int_{-\infty}^0 \frac{1}{2}e^{-|y|} dy \\ &= \left(\frac{2-e^{-1}}{2} \right) \frac{1}{2} = \frac{1}{4}(2-e^{-1}) \end{aligned}$$

6.2.5 a digital Communication example: development of an Optimal receiver

As we noted in the introductory paragraphs of Chap. 1, one of our principal interests is the transmission of signals from place to place in a manner which suppresses the effects of noise to the maximum extent possible. In the simplest case the medium over which signals are transmitted is simply a length of a pair of wires, the signal being applied directly at one end and being received at the other. In the more general case, before application to the transmitting medium, the signal may be elaborately processed and modified (a process called *modulation*) in a manner calculated to suppress noise. Correspondingly at the receiving end, it will be necessary to undo the

modulation (by a process called *demodulation*) to recover the original signal. As the signal, modulated or not, traverses the transmission medium (wires, or free space as in radio, etc.) noise will be added to the signal. Generally, as well, the process of demodulation will also add noise. Hence as finally received and perceived, the signal will be “corrupted” or “contaminated” by noise from a number of sources. Everything that intervenes between the very original signal at the transmitting end and the final recovered signal at the receiving end, including the modulation equipment, the demodulation equipment, the transmission medium and all the noise sources that corrupt the signal is referred to as the *channel*.

Often the transmitted signal is a more or less continuous waveform as in the case where speech or the music output of a microphone is applied directly to the transmitting end of a channel. In other cases we may want to use a channel to transmit *digital* information, that is, a sequence in time of bits-logical 0's and 1's. Thus in successive intervals we want to transmit one of the two possible *messages*, the message m_0 that the bit 0 is intended, or the message m_1 that the bit 1 is intended. The two possible messages might be represented at the transmitting end by two distinct waveforms, each limited in time duration to the interval allocated to a bit. At the receiving end we might devise a system whereby the message m_0 , when received, generates some voltage, say r_0 , which may be as simple as a dc voltage, while m_1 when received generates a voltage r_1 .

In the absence of noise, the message m_0 generates r_0 and m_1 generates r_1 , each with complete certainty. However, because of noise, errors may occur. Even though the message sent is m_0 the received indication might be r_1 , and correspondingly the message m_1 may generate r_0 . We shall assume, for generality, that the probability of an error is dependent on which message was sent and we introduce the following conditional probabilities called the *transition* probabilities:

$$\begin{aligned} P(r_0|m_0) &= \text{probability that } r_0 \text{ is received given that } m_0 \text{ is sent,} \\ P(r_1|m_0) &= \text{probability that } r_1 \text{ is received given that } m_0 \text{ is sent,} \\ P(r_0|m_1) &= \text{probability that } r_0 \text{ is received given that } m_1 \text{ is sent,} \\ P(r_1|m_1) &= \text{probability that } r_1 \text{ is received given that } m_1 \text{ is sent.} \end{aligned}$$

We also allow for the general case that the messages m_1 and m_0 do not occur with equal frequency and we introduce the probabilities $P(m_1)$ and $P(m_0)$

which are the probabilities that m_1 and m_0 are the messages respectively intended in an arbitrary message interval. These probabilities $P(m_1)$ and $P(m_0)$ are called the *a priori* probabilities. With these probability definitions the two-message system we have described can be represented as in Fig. 6.6.

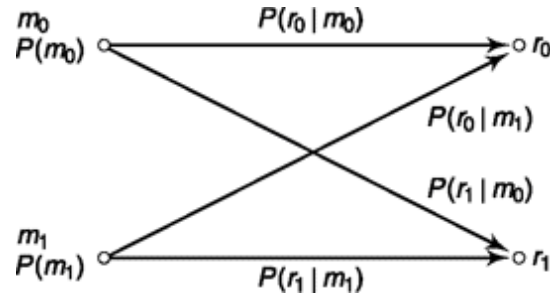


Fig. 6.6 A representation of a two-message communication system.

From an observed response, r_1 or r_0 , we cannot determine with certainty which of the messages was sent. Let us then develop an algorithm which will serve to allow an opinion about the message intended with *maximum probability that our opinion is correct*. Consider then that say r_0 is received. We then have to compare the conditional probabilities, called the *a posteriori* probabilities:

$P(m_0|r_0)$ = probability that m_0 is the message given that r_0 is received;
 $P(m_1|r_0)$ = probability that m_1 is the message given that r_0 is received.

Clearly if $P(m_0|r_0) > P(m_1|r_0)$ then we should decide that m_0 is intended and if the inequality is reversed we should decide for m_1 . Altogether then our algorithm should be:

If r_0 is received:

$$\text{choose } m_0 \text{ if } P(m_0|r_0) > P(m_1|r_0) \quad (6.38a)$$

$$\text{choose } m_1 \text{ if } P(m_1|r_0) > P(m_0|r_0) \quad (6.38b)$$

When the inequality is reversed, the choice is reversed and if the inequality is replaced by an equality we are at liberty to make either choice.

If r_1 is received:

$$\text{choose } m_0 \text{ if } P(m_0|r_1) > P(m_1|r_1) \quad (6.39a)$$

$$\text{choose } m_1 \text{ if } P(m_1|r_1) > P(m_0|r_1) \quad (6.39b)$$

A receiver which operates in accordance with this algorithm is said to “maximize the *a posteriori* probability” (m.a.p.) of a correct decision and is called an *optimum* receiver. The algorithm can be expressed in terms of the a priori and the transition probabilities. For example, starting with Eq. (6.38a) and multiplying both sides by $P(r_0)$ we have the result that, if r_0 is received, m_0 should be chosen if

$$P(m_0|r_0)P(r_0) > P(m_1|r_0)P(r_0) \quad (6.40)$$

From the general result given by Eq. (6.9), we have that Eq. (6.40) can be rewritten

$$P(r_0|m_0)P(m_0) > P(r_0|m_1)P(m_1) \quad (6.41)$$

Correspondingly, if r_1 is received we choose m_1 only if

$$P(r_1|m_1)P(m_1) > P(r_1|m_0)P(m_0) \quad (6.42)$$

Example 6.5

Apply the optimum-receiver algorithm to the case $P(m_0) = 0.7$, $P(m_1) = 0.3$, $P(r_0|m_0) = 0.9$, $P(r_1|m_0) = 0.1$, $P(r_0|m_1) = 0.4$, $P(r_1|m_1) = 0.6$.

$(0.9)(0.7) > (0.4)(0.3)$
Hence we would select m_0 whenever r_0 is received.
Also we find that Eq. (6.42) is valid since
 $(0.6)(0.3) > (0.1)(0.7)$
Hence we should select m_1 whenever r_1 is received.

Solution

We find that Eq. (6.41) is valid since

It is interesting to note that if the a priori probabilities are far from equal, then it may turn out that the algorithm will prescribe that one message be selected no matter what the received indication. For example, if we set $P(m_0) = 0.9$ and $P(m_1) = 0.1$ the optimum receiver will *always* select m_0 regardless of whether r_0 or r_1 is received.

Having established an algorithm for the optimum receiver, it is next of interest to know how effective the algorithm will be in yielding the correct determination. We accordingly want to calculate the probability $P(c)$ that a

correct determination will result. The probability of an error is $1 - P(c) = P(e)$.

Example 6.6

Referring to Example 5, calculate $P(c)$ and $P(e)$. Solution

The probability that the transmitted signal is correctly read at the receiver is equal to the probability that m_0

was sent when r_0 was read plus the probability that m_1 was sent when r_1 was read. Hence,

$$P(c) = P(r_0|m_0)P(m_0) + P(r_1|m_1)P(m_1) \quad (6.43)$$

In the present case we find

$$P(c) = (0.9)(0.7) + (0.6)(0.3) = 0.81$$

and $P(\epsilon) = 0.19$

It can happen that even in a case in which only two messages are contemplated, that because of noise, the receiver may generate more than just two responses. Such a situation is considered in the next example.

Example 6.7

In the system represented in Fig. 6.7, m_0 would generate r_0 , and m_1 would generate r_1 with certainty if there were no noise and r_2 would never occur. For the situation depicted in Fig. 6.7,

(a) find the optimum receiver, and (b) calculate the probability of error.

Solution

(a) We find that

$$P(r_0|m_0)P(m_0) > P(r_0|m_1)P(m_1)$$

since $(0.6)(0.6) > (0)(0.4)$

Hence, we select m_0 whenever r_0 is received. We also find that

$$P(r_1|m_1)P(m_1) > P(r_1|m_0)P(m_0)$$

since $(0.7)(0.4) > (0.2)(0.6)$

Hence we select m_1 whenever r_1 is received. To decide how to assign r_2 we compare $P(r_2|m_0)$ with $P(r_2|m_1)P(m_1)$. We find

$$P(r_2|m_0)P(m_0) = P(r_2|m_1)P(m_1)$$

since $(0.2)(0.6) = (0.3)(0.4)$

We can accordingly make either assignment and we arbitrarily associate r_2 with m_0 .

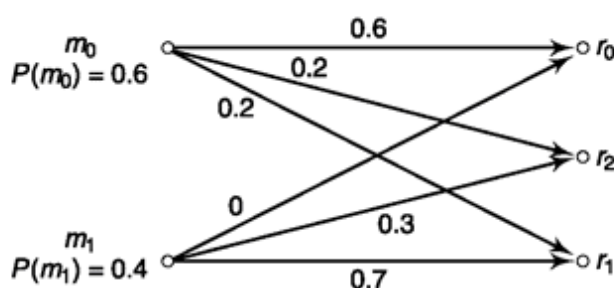


Fig. 6.7 Communication system for Example 6.7. Transition probabilities $P(r|fm)$ and a priori probabilities $P(m)$ are given.

(b) The probability of being correct is

$$\begin{aligned} P(c) &= P(r_0|m_0)P(m_0) + P(r_1|m_1)P(m_1) \\ &\quad + P(r_2|m_0)P(m_0) \\ &= (0.6)(0.6) + (0.7)(0.4) + (0.2)(0.6) \\ &= 0.76 \end{aligned} \tag{6.44}$$

and $P(\epsilon) = 0.24$.

Alternatively, we can calculate the probability of error by adding the probabilities that incorrect decisions are made. We then have, by simply interchanging m_1 and m_0 in Eq. (6.44)

$$\begin{aligned} P(\epsilon) &= (0)(0.4) + (0.2)(0.6) + (0.3)(0.4) \\ &= 0.24 \end{aligned}$$

In the general case, there can be K messages m_1, \dots, m_K and J received responses r_1, \dots, r_J . The optimum receiver is, of course, still designed in accordance with the rule:

If r_j is received, choose m_k if

$$P(m_k|r_j) > P(m_i|r_j) \quad \text{for all } i \neq k \quad (6.45)$$

6.2.6 Average Value of a Random Variable

Consider now that we have the values and their associated probabilities of a discrete random variable. The possible numerical values of the random variable X are x_1, x_2, x_3, \dots , with probabilities of occurrence $P(x_1), P(x_2), P(x_3) \dots$. As the number of measurements N of X becomes very large, we would expect that we would find the outcome $X = x_1$ would occur $NP(x_1)$ times, the outcome $X = x_2$ would occur $NP(x_2)$ times, etc. Hence, the arithmetic sum of all the N measurements would be

$$x_1 P(x_1)N + x_2 P(x_2)N + \dots = N \sum_i x_i P(x_i) \quad (6.46)$$

The *mean* or *average value* of all these measurements and hence the average value of the random variable is calculated by dividing the sum in Eq. (6.46) by the number of measurements N . The mean of a random variable X is also called the *expectation* of X and is represented either by the notation \bar{X} or by $E(X)$. We shall use these notations interchangeably. Thus, using m to represent the value of the average or expectation of X , we have, from Eq. (6.46),

$$\bar{X} \equiv E(X) = m = \sum_i x_i P(x_i) \quad (6.47)$$

To calculate the average for a continuous random variable, let us divide the range of the variable into small intervals Δx . Then from Eq. (6.29) the probability that X lies in the range between x_i and $x_i + \Delta x$ is $P(x_i \leq X \leq x_i + \Delta x) \equiv P(x_i)$ is given approximately by

$$P(x_i) = f(x_i) \Delta x \quad (6.48)$$

Substituting Eq. (6.48) into Eq. (6.47), we have

$$m = \sum_i x_i f(x_i) \Delta x \quad (6.49)$$

In the limit, as $\Delta x \rightarrow 0$ and is replaced by dx , the summation in Eq. (6.49) becomes an integral, and

$$m = \int_{-\infty}^{\infty} x f(x) dx \quad (6.50)$$

In general, the average value, or expectation, of a function $g(X)$ of the random variable X is

$$\overline{g(X)} = E[g(X)] = \int_{-\infty}^{\infty} g(x) f(x) dx \quad (6.51)$$

If the function $g(X)$ is X raised to a power, that is, $g(X) = X^n$, the average value $E(X^n)$ is referred to as the *nth moment* of the random variable. For this reason, the average value \bar{X} is also called the *first moment* of X .

If a random variable Z is a function of two random variables X and Y , say $Z = w(X, Y)$, then by an extension of the above discussion it may be shown that

$$\bar{Z} = \int_{-\infty}^{\infty} \int_{-\infty}^{\infty} w(x, y) f_{XY}(x, y) dx dy \quad (6.52)$$

In particular, if $Z = XY$, then

$$\bar{Z} = \int_{-\infty}^{\infty} xy f_{XY}(x, y) dx dy \quad (6.53)$$

and if X and Y are independent random variables, then from Eq. (6.36)

$$\bar{Z} = \int_{-\infty}^{\infty} xy f_X(x) f_Y(y) dx dy \quad (6.54a)$$

$$= \int_{-\infty}^{\infty} xf_X(x) dx \int_{-\infty}^{\infty} yf_Y(y) dy = \bar{X}\bar{Y} = m_x m_y \quad (6.54b)$$

6.2.7 Variance of a Random Variable

In Fig. 6.8 are shown two probability density functions $f(x)$ and $f'(x)$ for two random variables X and X' . As a matter of simplicity, we have drawn them of the same general form and have drawn them symmetrically about a common average value m . But these features are not essential to the ensuing discussion. Rather, the important point is that $f(x)$ is *narrower* than is $f'(x)$. Suppose, then, that experimental determinations were made of X and X' yielding numerical outcomes x and x' . We would surely find that, on the average, x would be closer to m than x' would be to m' . Thus in comparing X and X' , we find that the outcomes of X have a higher probability of occurring in a smaller range. In other words, if a number of determinations were made of X and X' , we would expect to find that the outcomes of X would *cluster* more closely around m than would be the case for X' .

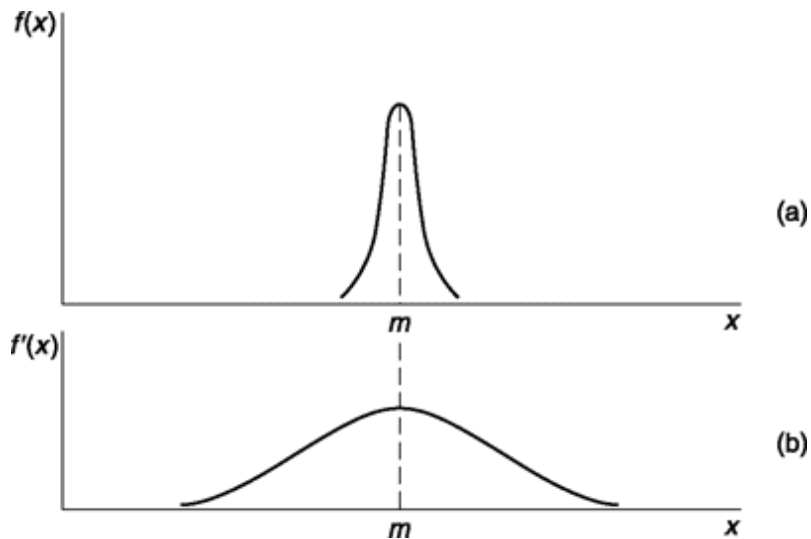


Fig. 6.8 Two probability density functions corresponding to random variables with different variances.

It is convenient to have a number which serves as a measure of the “width” of a probability density function. We might suggest as a candidate for such a number the average value of $(X - m)$ that is, $\overline{X - m}$. However, $\overline{X - m} = 0$, since positive and negative contributions from the portions of $f(x)$ above and below x cancel. A second possibility is $\overline{|X - m|}$, since taking the absolute value of $X - m$ would avoid the cancellation. However, a more useful measure is the square root of the average value of $(X - m)^2$, that is, of the second moment of $X - m$. This second moment is represented by the symbol σ^2 and is called the *variance* of the random variable. Thus,

$$\sigma^2 \equiv E[(X - m)^2] = \int_{-\infty}^{\infty} (x - m)^2 f(x) dx \quad (6.55)$$

Writing $(x - m)^2 = x^2 - 2mx + m^2$ in the integral of Eq. (6.55) and integrating term by term, we find

$$\sigma^2 = E(X^2) - 2m^2 + m^2 \quad (6.56a)$$

$$= E(X^2) - m^2 \quad (6.56b)$$

The quantity σ itself is called the standard deviation and is the *root mean square* (rms) value of $(X - m)$. If the average value $m = 0$, then

$$\sigma^2 = E(X^2) \quad (6.57)$$

Example 6.8

Find if the value of a is fixed where probability distribution function of X is defined as $f_X(x) = ae^{-0.2x}$ for $x > 0$ and zero elsewhere.

Solution

From definition, $\int_{-\infty}^{\infty} f_X(x)dx = 1$

or $\int_0^{\infty} ae^{-0.2x} dx = 1$

or $a \cdot \left[\frac{e^{-0.2x}}{-0.2} \right]_0^{\infty} = \frac{a}{0.2} = 1, \quad \text{Thus } a = 0.2.$

Example 6.9

Find mean and variance of random variable X which is uniformly distributed between a and b , $a < b$.

Solution

Since X is uniformly distributed $f_X(x) = \frac{1}{b-a}$ for $a \leq x \leq b$
and zero elsewhere.

From definition,

$$\text{mean} = m = \int_{-\infty}^{\infty} xf_X(x)dx$$

$$\begin{aligned}
&= \int_a^b x \frac{1}{b-a} dx = \frac{1}{2} \cdot \frac{x^2}{b-a} \Big|_a^b \\
&= \frac{1}{b-a} \cdot \frac{b^2 - a^2}{2} = \frac{a+b}{2}
\end{aligned}$$

From definition, variance

$$\begin{aligned}
\sigma^2 &= \int_{-\infty}^{\infty} (x - m)^2 f_X(x) dx = \int_{-\infty}^{\infty} x^2 f_X(x) dx - m^2 \\
&= \int_a^b x^2 \frac{1}{b-a} dx - m^2 = \frac{1}{b-a} \cdot \frac{x^3}{3} \Big|_0^b - m^2 \\
&= \frac{1}{b-a} \cdot \frac{b^3 - a^3}{3} - \frac{(a+b)^2}{4} \quad [\text{substituting } m] \\
&= \frac{b^2 + a^2 + ab}{3} - \frac{a^2 + b^2 + 2ab}{4} \\
&= \frac{4b^2 + 4a^2 + 4ab}{12} - \frac{3a^2 + 3b^2 + 6ab}{12} \\
&= \frac{(b-a)^2}{12}
\end{aligned}$$

SELF-TEST QUESTION

4. A random variable cannot be discrete. It is always continuous. Is it correct?
5. The maximum slope of cumulative distribution function $F((x))$ corresponds to maxima of probability density function $f(x)$. Is it correct?
6. When does the joint probability density function $f(j(x,y))$ become same as product of individual probability density functions $f(x)$ and $f_7(y)$?
7. What is standard deviation?

6.3 USEFUL PROBABILITY DENSITY FUNCTIONS

The probability density functions are important as they represent the uncertainty around a signal in a close form mathematical equation. This helps in estimation of the message content or calculating probability of error.

Here, we discuss some of the commonly used probability density functions in communication context.

6.3.1 The Gaussian probability Density

The *Gaussian* (also called *normal*) probability density function is of the greatest importance because many naturally occurring experiments are characterized by random variables with a Gaussian density. It is of special relevance to us because the random variables of concern to us will be described by, almost exclusively, the Gaussian density function. A further importance is attached to the Gaussian density because it is involved in a remarkable theorem called the *central-limit theorem* which we discuss in Sec. 6.4.4.

The Gaussian probability density function is defined as

$$f(x) = \frac{1}{\sqrt{2\pi\sigma^2}} e^{-(x-m)^2/2\sigma^2} \quad (6.58)$$

and is plotted in Fig. 6.9. In using the symbols m and σ^2 in Eq. (6.58), we have taken cognizance of the fact that m and σ^2 are indeed the average value and variance associated with $f(x)$. Thus, we find that

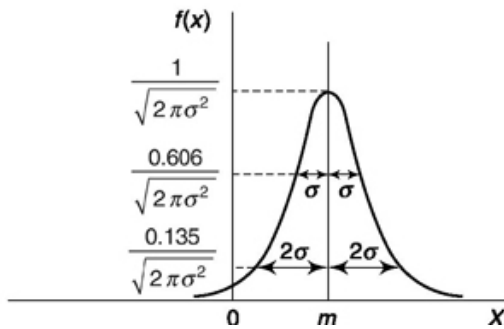


Fig. 6.9 The Gaussian density function.

$$\bar{X} = \int_{-\infty}^{\infty} \frac{x e^{-(x-m)^2/2\sigma^2}}{\sqrt{2\pi\sigma^2}} dx = m \quad (6.59)$$

and

$$E[(X-m)^2] = \int_{-\infty}^{\infty} \frac{(x-m)^2 e^{-(x-m)^2/2\sigma^2}}{\sqrt{2\pi\sigma^2}} dx = \sigma^2 \quad (6.60)$$

It may also be verified that

$$\int_{-\infty}^{\infty} x f(x) dx = 1 \quad (6.61)$$

as is required for a probability density function.

As is indicated in Fig. 6.9, when $x - m = \pm s$, that is, at values of x separated from m by the standard deviation, $f(x)$ has fallen to 0.606 of its peak value. When $x - m = \pm 2s$, $f(x)$ falls to 0.135 of the peak value, and at $x - m = 3 s$ (not shown in the figure), $f(x)$ has fallen to 0.01 of the peak value.

6.3.2 Cumulative Gaussian Probability: The Error Function

The cumulative distribution corresponding to the Gaussian probability density, for $m = 0$, is

$$P(X \leq x) = F(x) = \int_{-\infty}^x \frac{e^{-x^2/2\sigma^2}}{\sqrt{2\pi\sigma^2}} dx \quad (6.62)$$

The integral in Eq. (6.62) is not easily evaluated. It is, however, directly related to the *error function*, tabulated values of which are readily available in mathematical tables.² The error function of u , written $\text{erf } u$, is defined as

$$\text{erf } u \equiv \frac{2}{\sqrt{\pi}} \int_0^u e^{-u^2} du \quad (6.63)$$

The error function has the values $\text{erf } (0) = 0$ and $\text{erf } (\infty) = 1$. The *complementary error function*, written $\text{erfc } u \equiv 1 - \text{erf } u$ and is given by

$$\text{erfc } u \equiv 1 - \text{erf } u = \frac{2}{\sqrt{\pi}} \int_0^\infty e^{-u^2} du \quad (6.64)$$

The cumulative distribution $F(x)$ of Eq. (6.62) may be expressed in terms of the error function and the complementary error function. For $x \geq 0$ we write

$$F(x) = \int_{-\infty}^x \frac{e^{-x^2/2\sigma^2}}{\sqrt{2\pi\sigma^2}} dx = \int_{-\infty}^\infty \frac{e^{-x^2/2\sigma^2}}{\sqrt{2\pi\sigma^2}} dx - \int_x^\infty \frac{e^{-x^2/2\sigma^2}}{\sqrt{2\pi\sigma^2}} dx \quad (6.65)$$

The first term of the right-hand side of Eq. (6.65) is the integral from $-\infty$ to $+\infty$ of the probability density $f(x)$ and hence has the value 1. If we let $u \equiv x/\sqrt{2\sigma}$. Eq. (6.65) becomes

$$F(x) = 1 - \frac{1}{2} \left(\frac{2}{\sqrt{\pi}} \int_{x/\sqrt{2\sigma}}^\infty e^{-u^2} du \right) = 1 - \frac{1}{2} \text{erfc} \left(\frac{x}{\sqrt{2\sigma}} \right) \quad (6.66)$$

For $x \leq 0$, since tabulated values of $\text{erfc}(x|x|/\sqrt{2}\sigma) = \text{erfc } u$ are readily available only for positive u , we proceed as follows:

$$F(x) = F(-|x|) = \int_{-\infty}^{-|x|} \frac{e^{-x^2/2\sigma^2}}{\sqrt{2\pi\sigma^2}} dx = \frac{1}{\sqrt{\pi}} \int_{-\infty}^{-|x|/\sqrt{2}\sigma} e^{-u^2} du \quad (6.67)$$

Letting $\xi = -u$ yields

$$F(x) = \frac{1}{2} \left(\frac{2}{\sqrt{\pi}} \int_{|x|/\sqrt{2}\sigma}^{\infty} e^{-\xi^2} d\xi \right) = \frac{1}{2} \text{erfc} \left(\frac{|x|}{\sqrt{2}\sigma} \right) \quad (6.68)$$

The error function and complementary error function may be used for many additional useful calculations in connection with the Gaussian density. A matter of interest, for example, is the probability that a measurement will yield an outcome that falls within a certain range about the average value of the random variable. Since the “width” of the probability density depends on the standard deviation σ , we ask for the probability $P(m - k\sigma \leq X \leq m + k\sigma)$, that is, the probability that the random variable X is not further from $x = m$ than $k\sigma$, where k is a constant number. It may be shown (Prob. 6.33) that

$$P_{\pm k\sigma} \equiv P(m - k\sigma \leq X \leq m + k\sigma) = \text{erf} \left(\frac{k}{\sqrt{2}} \right) \quad (6.69)$$

For future reference some values of $P_{\pm k\sigma}$ are tabulated here.

k	$P_{\pm k\sigma}$	k	$P_{\pm k\sigma}$
0.5	0.383	2.5	0.988
1.0	0.683	3.0	0.997
1.5	0.866	3.5	0.9995
2.0	0.955	4.0	0.99994

Observe how small is the likelihood that a measured value will fall outside the range ± 3 s.

As a further example of a probability calculation, consider the following situation: Across a set of terminals there appears a voltage V which is either $V = v_0$ volts or $V = 0$ volt. One of the two possible constant voltages is transmitted over wires from a distance point to alert us as to which of the two possible situations prevails there. We are to determine the situation by performing the experiment of making an instantaneous measurement of the voltage across the terminals. A difficulty arises because superimposed on the constant 0 or v_0 volts is noise. We assume that the noise has a Gaussian probability density and zero average value. Because of the noise our measurement will, in general, yield neither the result 0 volt nor v_0 volts. What procedure are we to use to make a decision? What is the probability that our decision will be in error?

When the transmitted voltage is 0 volt, the terminal voltage is $V = N$, where N is the Gaussian random variable representing the noise. Hence, V is

also a Gaussian random variable with probability density as indicated in Fig. 6.10. When the transmitted voltage is v_0 , then $V = v_0 + N$. In this latter case, V is a Gaussian random variable with mean v_0 but with the same variance as in the former case (Prob. 6.29). The probability density of $V = v_0 + N$ is also shown in Fig. 6.10. On the basis of the symmetry in Fig. 6.10 it is apparent that the decision level should be $V = v_0/2$. That is, when we measure V to be $V < v_0/2$, we should decide that the transmitted voltage is 0 volt, and when $V > v_0/2$, we should decide that v_0 volts was transmitted.

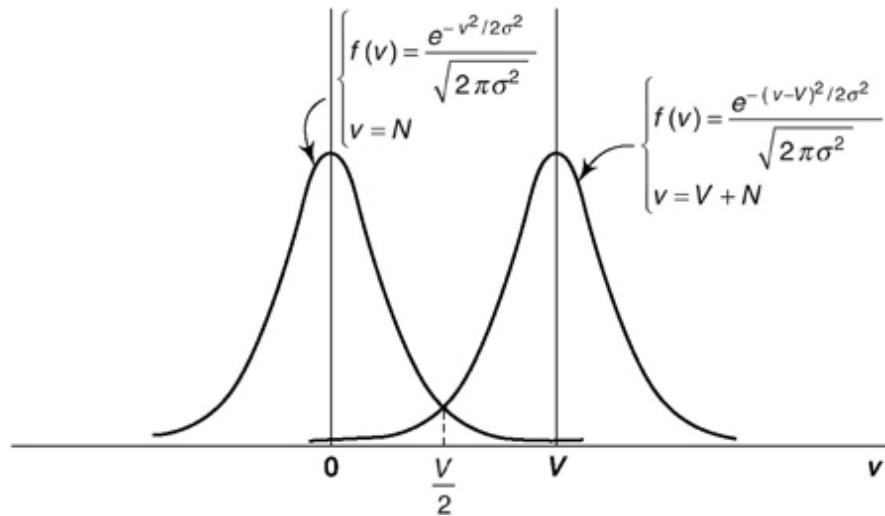


Fig. 6.10 Probability density function of a Gaussian random variable N and of the sum $v_0 + N$.

When v_0 volts is transmitted, the probability of making an error is the probability $P(V = v_0 + N < v_0/2)$, for, if $v_0 + N < v_0/2$, the v_0 volt transmission will be mistaken for a 0 volt transmission. This *probability of error* is

$$P_{\text{error}} = P\left(V = v_0 + N < \frac{v_0}{2}\right) = P\left(N < -\frac{v_0}{2}\right) = \int_{-\infty}^{-v_0/2} \frac{e^{-n^2/2\sigma^2}}{\sqrt{2\pi\sigma^2}} dn \quad (6.70)$$

Letting $u \equiv -n/\sqrt{2\sigma}$, we find

$$P_{\text{error}} = \frac{1}{\sqrt{\pi}} \int_{v_0/(2\sqrt{2\sigma})}^{\infty} e^{-u^2} du = \frac{1}{2} \operatorname{erfc} \frac{v_0}{2\sqrt{2\sigma}} \quad (6.71)$$

Similarly 0 volt will be mistaken for v_0 volts if the noise is *positive* and greater in magnitude than $v_0/2$. Since the Gaussian density is symmetrical, the probability that either transmission will be mistaken for the other is the

same and is given by Eq. (6.71). Finally, then, P_{error} in Eq. (6.71) gives the probability of an error *without reference* to which voltage is transmitted.

We may note that, because of the manner in which the error probabilities are related to the error function, this function is appropriately named.

6.3.3 The Rayleigh probability Density

We consider now the Rayleigh probability density function. The Rayleigh density is of interest to us principally because of a special relationship which it holds to the Gaussian density. For reasons which will be apparent shortly, we use the symbol R to represent the random variable and r to represent the value assumed by the variable. The Rayleigh density is defined by

$$f(r) = \begin{cases} \frac{r}{\alpha^2} e^{-r^2/2\alpha^2} & 0 \leq r \leq \infty \\ 0 & r < 0 \end{cases} \quad (6.72)$$

Note particularly that $f(r)$ is nonzero only for positive values of r . A plot of $f(r)$ as a function of r is shown in Fig. 6.11. It attains a maximum value $1/(\alpha\sqrt{e})$ at $r = \alpha$. It may be verified that the mean value $\bar{R} = \sqrt{\pi/2}\alpha$, the mean-square value $\bar{R^2} = 2\alpha^2$, and the variance $\sigma_r^2 = (2 - \pi/2)\alpha^2$.

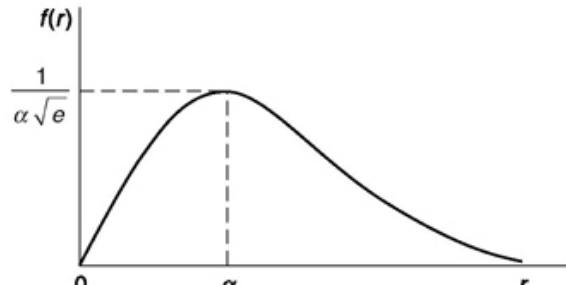


Fig. 6.11 The Rayleigh density function.

Now let X and Y be two independent Gaussian random variables each with average value zero and each with variance s^2 . The joint density function is, using Eq. (6.36),

$$f(x, y) = f(x)f(y) = -\frac{e^{-x^2/2\sigma^2}}{\sqrt{2\pi\sigma^2}} \frac{e^{-y^2/2\sigma^2}}{\sqrt{2\pi\sigma^2}} = \frac{e^{-(x^2+y^2)/2\sigma^2}}{2\pi\sigma^2} \quad (6.73)$$

If we should now make a plot of $f(x, y)$ as a function of x and y , we should find a bell-shaped surface above the xy plane. The probability

$$P(x \leq X \leq x + dx, y \leq Y \leq y + dy) = f(x, y) dx dy \quad (6.74)$$

has the significance indicated in Fig. 6.5b. That is, to find the probability specified in Eq. (6.74), we mark off an area $dx dy$ on the xy plane, and the probability specified is equal to the volume above the surface area $dx dy$ and below the surface $f(x, y)$.

Suppose, however, that to locate a point on the xy plane we use not the x and y coordinates but rather the coordinates r and θ , where r is the length of the radius vector to the point from the coordinate system origin and θ is the angle measured from the x axis as shown in Fig. 6.12. A differential area in such an r, θ coordinate system is $r dr d\theta$. The volume above this area is then equal to the probability $P(r \leq R \leq r + dr, \theta \leq \Theta \leq \theta + d\theta)$. Since $r^2 = x^2 + y^2$, we have, from Eqs (6.73) and (6.74), that

$$\begin{aligned} P(r \leq R \leq r + dr, \theta \leq \Theta \leq \theta + d\theta) &= \frac{e^{-r^2/2\sigma^2}}{2\pi\sigma^2} r dr d\theta \\ &= \left(\frac{re^{-r^2/2\sigma^2}}{\sigma^2} dr \right) \left(\frac{d\theta}{2\pi} \right) \end{aligned} \quad (6.75)$$

Hence, it appears that the probability specified in Eq. (6.75) can be expressed in terms of the probability density functions associated with two *independent* random variables R and Θ . The probability densities are

$$f_R(r) = \begin{cases} \frac{re^{-r^2/2\sigma^2}}{\sigma^2} & r \geq 0 \\ 0 & r < 0 \end{cases} \quad (6.76)$$

and $f_\Theta(\theta) = \frac{1}{2\pi} \quad -\pi \leq \theta \leq \pi \quad (6.77)$

The independence is apparent from the fact, as appears in Eq. (6.75), that the joint density $f_{R,\Theta}(r, \theta)$ appears as the product $f_R(r)f_\Theta(\theta)$.

We note that $f_R(r)$ is precisely the Rayleigh density with $\sigma^2 = \alpha^2$, while $f_\Theta(\theta)$ is a uniform density independent of the angle θ . We observe in Fig. 6.11 that the most probable value of r is $r = \alpha = \sigma$.

Rayleigh distribution is useful in describing signal passing through a narrowband noisy channel and fading in mobile radio that occurs due to multipath propagation.

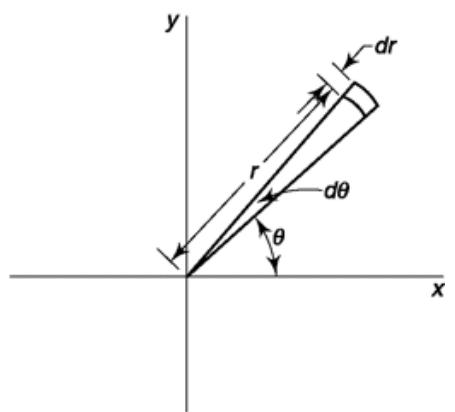


Fig. 6.12 Cartesian and polar representation of an area.

6.3.4 The Rician Distribution

The Rician distribution is useful in analysis of carrier sinusoidal signal passing through narrowband noisy channel or in a signal fading model having a dominant component as found in line-of-sight communication. This is expressed as follows:

$$f_X(x) = \frac{x}{\sigma^2} e^{-\frac{x^2 + a^2}{2\sigma^2}} I_0\left(\frac{ax}{\sigma^2}\right) \quad (6.78)$$

or in normalized form, $f_X(x) = \frac{x^2 + 0^2}{xe^{-\frac{x^2}{2}}} I_0(ax) \quad (6.79)$

where, I_0 represents modified Bessel function of the first kind, zeroeth order, σ is the standard deviation of the underlying Gaussian process and a is amplitude of the sinusoid or a^2 is sum of square of means of two independent Gaussian processes. The plot of $f_X(x)$ vs. x looks like right shifted version of Rayleigh distribution, the higher the value of a , the more the shift. However, as a increases, it approaches Gaussian distribution while at $a = 0$, it is same as Rayleigh distribution.

Estimation of mean and variance for Rician distribution is rather complicated but its second moment can be represented as $E[X^2] = 2\sigma^2 + a^2$.

6.3.5 The Binomial and poisson Distribution

The binomial distribution is derived for discrete two state experiments (also known as *Bernoulli trial*) and useful in the context of a digital transmission. Consider, a random variable that can take only two values say, correct and incorrect—the example could be whether through a communication channel message has reached correctly or not. If probability of reaching correctly is say q , then probability of an error in the message reached is $(1 - q)$. Out of n attempts the probability of message reaching correctly for k times is given by binomial distribution as follows

$$p_x(k) = {}^n C q^k (1 - q)^{nk} \quad (6.80)$$

where trials are all independent and the value q remains constant over all trials. The term nC_k in factorial form can be represented as ${}^nC_k = \frac{n!}{k!(n-k)!}$

The mean and variance of binomial distribution can be calculated as $m = nq$ and $\sigma^2 = nq(1-q)$.

Poisson distribution can be related to emission of electron (or shot noise), arrival of telephone call or data transmission when error rate is low. Consider an experiment where probability of occurrence of an event in a very small interval of time δT is given by $\lambda\delta T$. If successive occurrences are statistically independent then the probability of k occurrences in time T is given by Poisson distribution as

$$p_\lambda(k) = \frac{\alpha^k}{k!} e^{-\alpha} \text{ where, } \alpha = \lambda T \quad (6.81)$$

The mean and variance of Poisson distribution can be calculated as $m = \alpha$ and $\sigma^2 = \alpha$.

Note that, in binomial distribution if no. of trials (n) is large and q very small then it can be approximated by simpler Poisson distribution with $\alpha = nq$.

Example 6.10

A voltage signal is sent from a transmitter which is either zero or V volt. The signal is corrupted by zero mean Gaussian noise in the channel of variance σ^2 . The receiver detects presence of V if received voltage is above threshold $V/2$. Find probability of error if (a) $V = 4$, $\sigma^2 = 2$, (b) $V = 2$, $\sigma^2 = 2$, (c) $V = 4$, $\sigma^2 = 4$, (d) $V = 8$, $\sigma^2 = 2$.

Solution

$$\text{From Eq. 6.71, we find } P_{\text{error}} = \frac{1}{2} \operatorname{erfc} \frac{V}{2\sqrt{2}\sigma}$$

Substituting and using error function table in Appendix A2,

$$\begin{aligned} \text{for (a) } P_{\text{error}} &= \frac{1}{2} \operatorname{erfc} \frac{4}{2\sqrt{2}\sqrt{2}} = \operatorname{erfc}(1.0)/2 \\ &= [1 - \operatorname{erf}(1.0)]/2 = [1 - 0.8427]/2 = 0.0787 \end{aligned}$$

$$\begin{aligned} \text{for (b) } P_{\text{error}} &= \frac{1}{2} \operatorname{erfc} \frac{2}{2\sqrt{2}\sqrt{2}} = \operatorname{erfc}(0.5)/2 \\ &= [1 - \operatorname{erf}(0.5)]/2 = [1 - 0.5205]/2 = 0.2398 \end{aligned}$$

$$\begin{aligned} \text{for (c) } P_{\text{error}} &= \frac{1}{2} \operatorname{erfc} \frac{4}{2\sqrt{2}\sqrt{4}} = \operatorname{erfc}(0.707)/2 \\ &\approx [1 - \operatorname{erf}(0.7)]/2 = [1 - 0.6778]/2 = 0.1611 \end{aligned}$$

$$\begin{aligned} \text{for (d) } P_{\text{error}} &= \frac{1}{2} \operatorname{erfc} \frac{8}{2\sqrt{2}\sqrt{2}} = \operatorname{erfc}(2.0)/2 \\ &= [1 - \operatorname{erf}(2.0)]/2 = [1 - 0.9953]/2 = 0.0024 \end{aligned}$$

Note that, increase in signal energy or decrease in noise variance (or energy) reduces probability of error. Probability of error increases if signal energy is reduced or noise energy is increased.

Example 6.11

The probability of error in transmission of digital data through a noisy channel is $P_e = 0.001$. If each transmission is an independent event (a) what is the probability that out of 10 transmissions 9 are correct and 1 is incorrect? (b) what is the probability that more than two are erroneous out of 100 transmissions and (c) more than one are erroneous out of 100 transmissions?

Solution

- (a) From Binomial distribution (Eq. 6.80)

$$\begin{aligned} p_X(1) &= {}^{10}C_1(0.001)^1(1-0.001)^{10-1} \\ &= \frac{10!}{1!(10-1)!} 10^{-3}(0.999)^9 \\ &= 10^{-2} \cdot 0.991 = 0.00991 \end{aligned}$$

- (b) Required probability = 1 – Probability of less than or equal to two error in transmission

$$\begin{aligned} &= 1 - p_X(0) - p_X(1) - p_X(2) \\ &= 1 - {}^{100}C_0(0.001)^0(1-0.001)^{100} \\ &\quad - {}^{100}C_1(0.001)^1(1-0.001)^{99} \\ &\quad - {}^{100}C_2(0.001)^2(1-0.001)^{98} \end{aligned}$$

Since, calculation of above is cumbersome we may use Poisson distribution (Eq. 6.81) to approximate above. Then, $\alpha = nq = 100 \times 0.001 = 0.1$

Required probability

$$\begin{aligned} &= 1 - \frac{0.1^0}{0!} e^{-0.1} - \frac{0.1^1}{1!} e^{-0.1} - \frac{0.1^2}{2!} e^{-0.1} \\ &= 1 - 0.90483(1 + 0.1 + 0.005) \\ &= 1 - 0.99984 \\ &= 0.00016 \end{aligned}$$

(c) From (b), required probability

$$\begin{aligned} &= 1 - \frac{0.1^0}{0!} e^{-0.1} - \frac{0.1^1}{1!} e^{-0.1} \\ &= 1 - 0.90483(1 + 0.1) \\ &= 1 - 0.9953 \\ &= 0.0047 \end{aligned}$$

Note the order of change in probability of error between (b) and (c).

SELF-TEST QUESTION

8. Is it true that Gaussian probability density function is also known as normal density?
9. How are error function $\text{erf}(u)$ and complementary error function $\text{erfc}(u)$ related?
10. Does binomial distribution approximates Poisson distribution?
11. Does Rayleigh distribution consider two signal components, each having Gaussian distribution?

6.4 USEFUL PROPERTIES AND CERTAIN APPLICATION ISSUES

In this section we discuss few interesting things. If two random variables are summed up how the probability distribution function changes or what will be its mean and variance. The central limit theorem tells how the sum of large number of random variables shows Gaussian characteristic. Tchebycheff's inequality and its use in calculating error probability for finite number of samples are taken up next followed by an illustrative discussion on signal determination in presence of noise.

6.4.1 Mean and Variance of the sum of Random Variables

Let X and Y be two random variables with means m_x and m_y . Let $Z = X + Y$ and have the mean m_z . Then $m_z = m_x + m_y$. This result follows directly from the definition of the mean. We have, using Eqs (6.52) and (6.50), that

$$\begin{aligned}
m_z &= \int_{-\infty}^{\infty} \int_{-\infty}^{\infty} (x + y)f(x, y) dx \\
&= \int_{-\infty}^{\infty} \int_{-\infty}^{\infty} xf(x, y) dx dy + \int_{-\infty}^{\infty} \int_{-\infty}^{\infty} yf(x, y) dx dy \quad (6.82a) \\
&= m_x + m_y \quad (6.82b)
\end{aligned}$$

Expressed in words, *the mean of the sum is equal to the sum of the means*. This result holds whether the variables X and Y are independent or not.

We calculate next the second moment of $Z = X + Y$. In this calculation, however, we shall restrict ourselves to the circumstance that X and Y are *independent*. We have

$$\overline{Z^2} = \overline{(X + Y)^2} = \int_{-\infty}^{\infty} \int_{-\infty}^{\infty} (x + y)^2 f(x, y) dx dy \quad (6.83)$$

Because of the *independence* of X and Y , $f(x, y) = f(x)f(y)$ so that

$$\begin{aligned}\overline{Z^2} &= \int_{-\infty}^{\infty} x^2 f(x) dx \int_{-\infty}^{\infty} f(y) dy + \int_{-\infty}^{\infty} y^2 f(y) dy \int_{-\infty}^{\infty} f(x) dx \\ &\quad + 2 \int_{-\infty}^{\infty} x f(x) dx \int_{-\infty}^{\infty} y f(y) dy\end{aligned}\quad (6.84)$$

However

$$\int_{-\infty}^{\infty} f(x) dx \int_{-\infty}^{\infty} f(y) dy = 1 \quad (6.85)$$

so that

$$\overline{Z^2} = \overline{X^2} + \overline{Y^2} + 2 \overline{XY} \quad (6.86)$$

If either \overline{X} or \overline{Y} or both are zero, then $\overline{Z^2} = \overline{X^2} + \overline{Y^2}$. In this case we also have from Eq. (6.57) that

$$\sigma_z^2 = \sigma_x^2 + \sigma_y^2 \quad (6.87)$$

This result can be obtained directly by calculating $\sigma_z^2 = \overline{(Z - m_z)^2}$.

6.4.2 Probability Density of Sum of Random Variables

We now calculate the probability density $f(z)$ of $Z = X + Y$ in terms of the joint density $f(x, y)$. Assume an arbitrary value of Z and call it z . Then the region $Y \leq z - X$ is shown as the shaded region in Fig. 6.13. Hence the probability that $Z \leq z$ is the same as the probability that $Y \leq z - X$ independently of the value of X , that is, for $-\infty \leq X \leq +\infty$. This probability is

$$F(z) = P(Z \leq z) = P(X \leq \infty, Y \leq z - X) \quad (6.88)$$

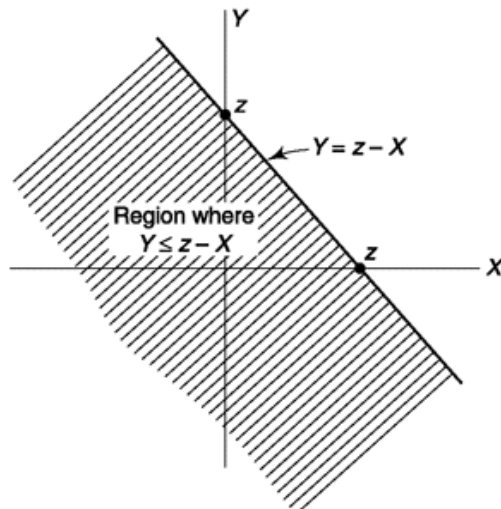


Fig. 6.13 Related to the calculation of the probability density of a sum of random variables.

Using Eq. (6.32), we have

$$F(z) = \int_{-\infty}^{\infty} dx \int_{-\infty}^{z-x} f(x, y) dy \quad (6.89)$$

The probability density of Z is found by differentiating $F(z)$ with respect to z . We then have

$$f(z) = \frac{dF(z)}{dz} = \int_{-\infty}^{\infty} f(x, z-x) dx \quad (6.90)$$

which expresses $f_Z(z)$ in terms of $f_{XY}(x, y = z - x)$.

When X and Y are *independent*, $f(x, y) = f(x)f(y)$, and Eq. (6.90) may be written

$$f(z) = \int_{-\infty}^{\infty} f(x)f(z-x) dx \quad (6.91)$$

Comparing Eq. (6.91) with Eq. (1.124), we recognize that $f(z)$ is the *convolution* of $f(x)$ and $f(y)$.

As a most important consequence of the result given in Eq. (6.91), let us consider the case where $f(x)$ and $f(y)$ are both Gaussian densities.

$$f(x) = \frac{e^{-x^2/2\sigma_x^2}}{\sqrt{2\pi\sigma_x^2}} \quad (6.92)$$

$$f(y) = \frac{e^{-y^2/2\sigma_y^2}}{\sqrt{2\pi\sigma_y^2}} \quad (6.93)$$

Then $f(z)$ is given by

$$f(z) = \frac{1}{2\pi\sigma_x\sigma_y} \int_{-\infty}^{\infty} e^{-x^2/2\sigma_x^2} e^{-(z-x)^2/2\sigma_y^2} dx \quad (6.94)$$

If we define a variable u by

$$u \equiv \left(\frac{1}{\sigma_x^2} + \frac{1}{\sigma_y^2} \right)^{1/2} x - \frac{z}{\sigma_y^2(1/\sigma_x^2 + 1/\sigma_y^2)^{1/2}} \quad (6.95)$$

then we find, after some algebraic manipulation, that Eq. (6.94) may be written

$$f(z) = \frac{e^{-z^2/2(\sigma_x^2 + \sigma_y^2)}}{\sqrt{2\pi(\sigma_x^2 + \sigma_y^2)}} \int_{-\infty}^{\infty} \frac{e^{-u^2/2}}{\sqrt{2\pi}} du \quad (6.96)$$

The definite integral in Eq. (6.96) has the value 1. Hence, if $\sigma^2 \equiv \sigma_x^2 + \sigma_y^2$, Eq. (6.96) becomes

$$f(z) = \frac{e^{-z^2/2\sigma^2}}{\sqrt{2\pi\sigma^2}} \quad (6.97)$$

which is a Gaussian density function. Thus we have the extremely interesting and important result: Given two independent Gaussian random variables, the sum of these variables is itself a Gaussian random variable. We note, of course, that the variance σ^2 of the sum variable is the sum $\sigma_x^2 + \sigma_y^2$ of the individual variables. This result, $\sigma^2 = \sigma_x^2 + \sigma_y^2$, applies for independent random variables generally, not just Gaussian variables. Further, in the discussion above we assumed, for simplicity, that the variables X and Y had zero mean. For if we

had assumed average values m_x and m_y for X and Y , then we would have found that Z had an average value $m_z = m_x + m_y$ and Eq. (6.97) would become

$$f(z) = \frac{e^{-(z-m_z)^2/2\sigma^2}}{\sqrt{2\pi\sigma^2}} \quad (6.98)$$

This result, concerning the sum of independent Gaussian random variables, may be extended somewhat. If X_1 is a Gaussian random variable, then, as may be easily verified, if c_1 is a constant, c_1X_1 is also a Gaussian variable. It follows, by extension of the result above for two independent Gaussian random variables, that a linear combination of independent Gaussian variables is also Gaussian. Explicitly, if X_1, X_2, X_3, \dots are independent Gaussian variables and c_1, c_2, c_3, \dots are constants, then

$$X = c_1X_1 + c_2X_2 + c_3X_3 \dots \quad (6.99)$$

is also a Gaussian random variable. Our proof does not extend to the case of *dependent* Gaussian variables. However, it is interesting to note that, even in the case where the Gaussian variables are dependent, a linear combination of such variables is still Gaussian. In general, the probability density function of a sum of variables of like probability density does not preserve the form of the probability density of the individual variables. Indeed, as shown in Sec. 6.4.4, X tends to become Gaussian if a large number of random variables are summed, regardless of their probability density.

6.4.3 Correlation between Random Variables

The *covariance* μ of two random variables X and Y is defined as

$$\mu \equiv E\{(X - m_x)(Y - m_y)\} \quad (6.100)$$

If X and Y are independent random variables, we find, using Eq. (6.36) and (6.52), that

$$\begin{aligned} \mu &= E\{(X - m_x)(Y - m_y)\} \\ &= \int_{-\infty}^{\infty} (x - m_x)f(x) dx \int_{-\infty}^{\infty} (y - m_y)f(y) dy \\ &= (m_x - m_x)(m_y - m_y) = 0 \end{aligned} \quad (6.101)$$

This result is rather to have been expected on intuitive grounds. For, as assumed, when an experiment is performed to determine a joint outcome specified by the set of numbers x and y , the outcome y is in no way

conditional on the outcome x . Hence we would find that a particular outcome x_1 would occur jointly sometimes with a value y which was positive with respect to its average m_y , and sometimes with a value y negative with respect to m_y . In the course of many experiments with the outcome x_1 , the sum of the numbers $x_1(y - m_y)$ would add up to zero.

On the other hand, suppose X and Y were dependent. Suppose, for example, that outcome y was conditioned on the outcome x in such a manner that there was an enhanced probability that $(y - m_y)$ was of the same sign as $(x - m_x)$. In such a case we would anticipate that the expected value $E\{(X - m_x)(Y - m_y)\} > 0$. Similarly, if there were an enhanced probability that $(x - m_x)$ and $(y - m_y)$ were of opposite sign, we would expect $E\{(X - m_x)(Y - m_y)\} < 0$.

As we have seen, it is easy enough to invent random variables which are uncorrelated but are nevertheless dependent. It is even possible to do so when the random variables are Gaussian. On the other hand, the random variables of interest to us will be variables which occur in the description of such natural physical processes as noise, such variables are Gaussian. It does indeed turn out that, with such Gaussian random variables, an absence of correlation does imply independence. We shall therefore generally assume that two Gaussian random variables, for which the covariance $m = 0$, are independent variables.

As an extreme case, let us assume the maximum possible dependency between X and Y . Let us assume that $X = Y$ or $X = -Y$. In these cases we would find (with $m_x = m_y = 0$)

$$E\{XY\} = E(X^2) = E(Y^2) = \sigma_x^2 = \sigma_y^2 = \sigma_x \sigma_y \quad (6.102)$$

or

$$E\{XY\} = E\{-X^2\} = E\{-Y^2\} = -\sigma_x^2 = -\sigma_y^2 = -\sigma_x \sigma_y \quad (6.103)$$

Consider then the quantity ρ defined by

$$\rho \equiv \frac{\mu}{\sigma_x \sigma_y} \quad (6.104)$$

This number ρ is called the *correlation coefficient* between the variables X and Y and serves as a measure of the extent to which X and Y are dependent. From Eqs (6.102) to (6.104) we have that ρ falls in the range

$$-1 \leq \rho \leq +1 \quad (6.105)$$

When X and Y are independent, $\rho = 0$. When $X = Y$, $\rho = 1$; when $X = -Y$, $\rho = -1$. If X and Y are neither identical nor independent, then ρ will have a magnitude between 0 and 1. When $\rho = 0$, the random variables X and Y are said to be *uncorrelated*.

When random variables are independent, they are uncorrelated. However, the fact that they are uncorrelated does not ensure that they are independent. A simple illustrative example will establish this point.

Example 6.12

Let Z be a random variable with probability density $f(z) = \frac{1}{2}$ in the range $-1 \leq z \leq 1$. Let the random variable $X = Z$ and the random variable $Y = Z^2$.

Obviously X and Y are not independent since $X^2 = Y$. Show, nonetheless, that X and Y are uncorrelated.

Solution

We have

$$E\{Z\} = \int_{-1}^1 \frac{1}{2} dz = 0 \quad (6.106)$$

Since $X = Z$, $E\{X\} = E\{Z\} = 0$. Since $Y = Z^2$, $E\{Y\} = E\{Z^2\}$, so that

$$E\{Y\} = \int_{-1}^1 \frac{1}{2} z^2 dz = \frac{1}{3} \quad (6.107)$$

The covariance μ is

$$\begin{aligned} \mu &= E\{(X - m_x)(Y - m_y)\} = E\left\{(X)\left(Y - \frac{1}{3}\right)\right\} \\ &= E\left\{XY - \frac{1}{3}X\right\} \end{aligned} \quad (6.108a)$$

$$= E\left\{Z^3 - \frac{1}{3}Z\right\} = \int_{-1}^1 \frac{1}{2} \left(z^3 - \frac{z}{3}\right) dz = 0 \quad (6.108b)$$

Hence $\rho = 0$, and the variables are uncorrelated.

As we have seen, it is easy enough to invent random variables which are uncorrelated but are nevertheless dependent. It is even possible to do so when the random variables are Gaussian. On the other hand, the random variables of interest to us will be variables which occur in the description of such natural physical processes as noise, such variables are Gaussian. It does indeed turn out that, with such Gaussian random variables, an absence of correlation does imply independence. We shall therefore generally assume that two Gaussian random variables, for which the covariance $m = 0$, are independent variables.

6.4.4 The Central Limit Theorem

The result of the previous section concerning the probability density of the sum of Gaussian random variables is a special case of the *central-limit theorem*. The so-called central-limit theorem is actually a group of related theorems which are collectively grouped under a single name. We shall not even undertake to state these theorems precisely, let alone undertake to prove them. For our purposes it will be adequate to note that the central-limit theorem indicates that the probability density of a sum of N independent random variables tends to approach a Gaussian density as the number N increases. The mean and variance of this Gaussian density are respectively the sum of the means and the sum of the variances of the N independent random variables. The theorem applies even when (with a few special exceptions) the individual random variables are not Gaussian. In addition, the theorem applies in certain special cases even when the individual random variables are not independent.

As an illustration of the central-limit theorem consider the case where the individual random variable has a uniform (constant) probability density as shown in Fig. 6.14a. Note here that the area under the density has been adjusted to unity. Then, as indicated by Eq. (6.91), if there were two terms in the sum, the density of the sum would be determined as the convolution of the density in Fig. 6.14a with itself. The result of such a convolution is indicated in Fig. 6.14b. Similarly, the density of a sum of the three random variables is the convolution of the density in Fig. 6.14b with the density in Fig. 6.14a. The result (Prob. 6.45) is shown in Fig. 6.14c. Note that even for this sum of only three terms the result suggests a Gaussian density. In the limit, as more and more terms are added, the density would indeed become Gaussian.

6.4.5 Tchebyheff's Inequality

We have noted that the variance of a random variable measures the “width” of the probability density function. Tchebycheff’s rule expresses this same quality of the variance in an alternative manner. In Fig. 6.15 we have drawn a density function which, for simplicity, is assumed to be symmetrical about a mean value of zero; these features however are not essential to the discussion. The probability that a sample of the random variable X should have a value x such that $|x| > e$ is equal to the area of the shaded regions. We should, of course, expect that the probability $P(|x| > e)$ will decrease as

e increases. Further, since the variance measures the width of the density function about the mean we further expect that $P(|x| > e)$ should decrease as c^2 decreases. Both of these expectations are to be seen in Tchebycheff's rule which, however, yields not an exact value for $P(|x| > e)$ in terms of c^2 and e but rather an upper bound (or limit). Specifically, Tchebycheff's rule is an inequality given by

$$P(|x| \geq \varepsilon) \leq \frac{\sigma^2}{\varepsilon^2} \quad (6.109)$$

To prove this inequality, we start with Eq. (6.55) which defines σ^2 . Assuming $m = \bar{x} = 0$, we have

$$\sigma^2 = \int_{-\infty}^{+\infty} x^2 f(x) dx \quad (6.110a)$$

$$= \int_{-\infty}^{-\varepsilon} x^2 f(x) dx + \int_{-\varepsilon}^{+\varepsilon} x^2 f(x) dx + \int_{+\varepsilon}^{+\infty} x^2 f(x) dx \quad (6.110b)$$

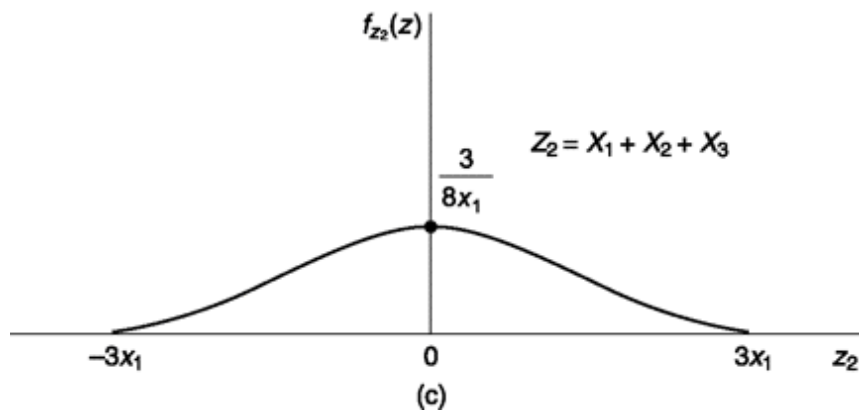
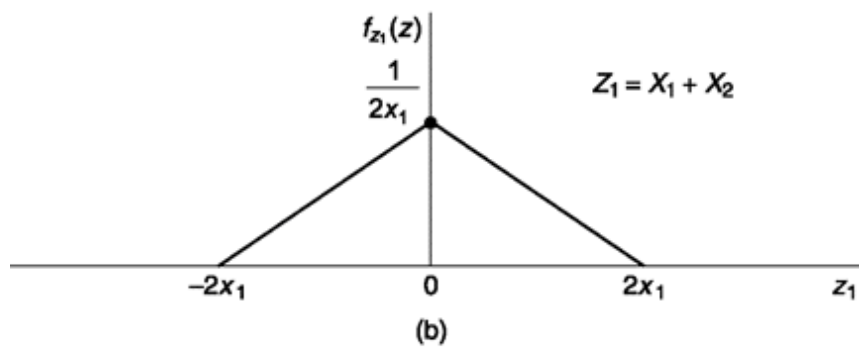
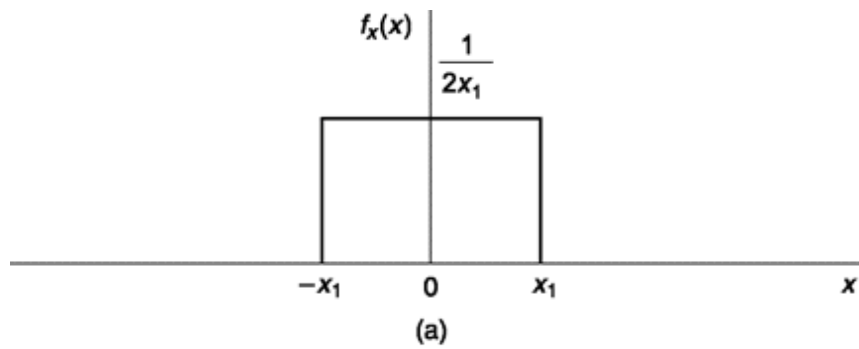


Fig. 6.14 (a) A random variable X has a uniform probability density, (b) The probability density of the random variable $X_1 + X_2$. (c). The density of the random variable $X_1 + X_2 + X_3$.

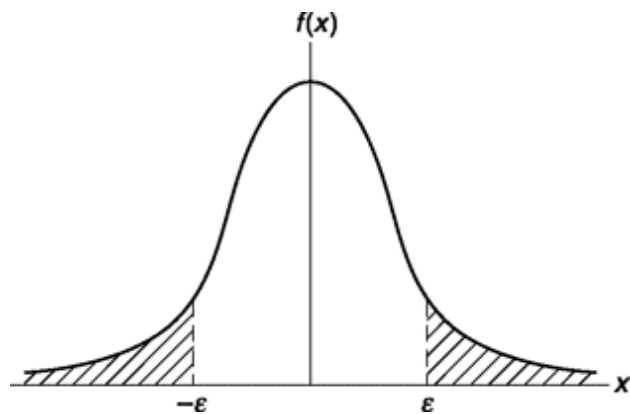


Fig. 6.15 A probability density function.

Since $x^2 \geq 0$ and $f(x) \geq 0$ for all x we have that

$$\int_{-\varepsilon}^{\varepsilon} x^2 f(x) dx \geq 0 \quad (6.111)$$

so that Eq. (6.110b) can be written

$$\sigma^2 \geq \int_{-\infty}^{-\varepsilon} x^2 f(x) dx + \int_{+\varepsilon}^{\infty} x^2 f(x) dx \quad (6.112)$$

In the ranges $-\infty \leq -\varepsilon$ and $\varepsilon \leq x \leq \infty$

$$x^2 \geq \varepsilon^2 \quad (6.113)$$

Therefore, if we replace x^2 by ε^2 in Eq. (6.112) the sum of the two integrals in the right-hand side cannot be increased. Hence, with this substitution, the inequality persists and we have

$$\sigma^2 \geq \varepsilon^2 \left[\int_{-\infty}^{-\varepsilon} f(x) dx + \int_{+\varepsilon}^{+\infty} f(x) dx \right] \quad (6.114)$$

But

$$P(x \leq -\varepsilon) = \int_{-\infty}^{-\varepsilon} f(x) dx \quad (6.115)$$

and

$$P(x \geq +\varepsilon) = \int_{\varepsilon}^{\infty} f(x) dx \quad (6.116)$$

Thus Eq. (6.114) can be written as

$$\frac{\sigma^2}{\varepsilon^2} \geq P(x \leq -\varepsilon) + P(x \geq \varepsilon) = P(|x| \geq \varepsilon) \quad (6.117)$$

and the rule is proved. In Sec. 6.4.6 we shall apply the inequality in a communications example.

6.4.6 Error probability as Measured by Finite samples

We noted in Sec. 6.2.5 how a communications channel is used to transmit, in successive intervals, a sequence of messages. We noted there, further, that because of noise, some errors will be made at the receiver as messages will be incorrectly read and will be confused with one another. If we were to establish the probability of error P_e by experiment we would read a very large number N of messages and take note of the number of instances N_e in which errors were made. In principle it would be required that N be infinite since by definition (see Eq. 6.1) the error probability is

$$P_e \equiv \lim_{N \rightarrow \infty} \frac{N_e}{N} \quad (6.118)$$

In a real situation, we shall find that we have to deal with a finite number of messages N . In such a case, of finite N , the ratio N_e/N need not equal P_e .

Thus if $P_e = 1/1000$, then, in a particular experiment where 1000 received messages are read we would anticipate, as the most likely outcome, that one error will be made. However, it is possible that no errors are made or two or three or more errors are made. The estimate p of the probability of error

$$p \equiv \frac{N_e}{N} \quad (6.119)$$

for a finite N is a random variable. If we perform again and again, the experiment of measuring p by noting errors in finite sequences of messages of length N we shall have an array of values for p . If we perform the experiment a limitless number of times and take the average of the results then we shall have p . But since p like P_e is determined on the basis of examination of a limitless number of messages it is intuitively clear that

$$\bar{p} = P_e \quad (6.120)$$

It is useful to know in connection with a single experiment which measures p , how close p comes to P_e and with what probability. For this purpose, we apply Tchebycheff's inequality (Sec. 6.4.5) to the random variable $|p - P_e| \equiv x$. We need accordingly, as is seen in Eq. (6.109) to evaluate

$$\sigma_x^2 = \overline{(p - P_e)^2} \quad (6.121)$$

We have

$$\sigma_x^2 = \overline{p^2 - 2pP_e + P_e^2} = \overline{p^2} - 2\bar{p}P_e + P_e^2 \quad (6.122)$$

The quantity \bar{p} is given by Eq. (6.120) and since we assume P_e known we have now only to calculate $\overline{p^2}$.

With a view towards calculating $\overline{p^2}$ let us associate a sequence of messages by a corresponding sequence of numerical digits d_i ; the digit $d_i = 0$ if the corresponding message is received correctly and $d_i = 1$ if an error is made. The usefulness of this association is that in a sequence of length N , the sum of the digits d_i divided by N is precisely p , i.e.

$$p = \frac{1}{N} \sum_{i=1}^N d_i \quad (6.123)$$

we then have

$$p^2 = \frac{1}{N^2} \left(\sum_{i=1}^N d_i \right) \left(\sum_{j=1}^N d_j \right) \quad (6.124a)$$

$$= \frac{1}{N^2} \sum_{i=1}^N d_i^2 + \frac{1}{N^2} \sum_{i=1}^N \sum_{j=1}^N d_i d_j \quad i \neq j \quad (6.124b)$$

The first member on the right-hand side of Eq. (6.124b) is $1/N^2$ times the sum which occurs due to the multiplication of each digit by itself, while the second term is $1/N^2$ times the sum which accrues when each digit is multiplied by every *other* digit. We now have

$$\overline{p^2} = \frac{1}{N^2} \sum_{i=1}^N \overline{d_i^2} + \frac{1}{N^2} \sum_{i=1}^N \sum_{j=1}^N \overline{d_i d_j} \quad i \neq j \quad (6.125)$$

We calculate $\overline{d_i^2}$ by writing

$$\overline{d_i^2} = (1)^2 P(d_i = 1) + (0)^2 P(d_i = 0) = P(d_i = 1) = P_e \quad (6.126)$$

We further consider that the events of errors being made in two messages are entirely independent of one another. In this case, using the result given in Eq. (6.54), we find

Example 6.13

Consider a system in which $P_e = 10^{-4}$ and no. of experiments conducted = 4×10^5 . What is the probability that estimated probability of error p does not differ from P_e by more than 50 percent?

Solution

Here, $\epsilon = 50 \times 10^{-4} = 0.5 \times 10^{-3}$ and $N = 4 \times 10^5$
From Eq. 6.131, $P(|p - 10^{-4}| \geq 0.5 \times 10^{-4}) \leq \frac{10^{-4}}{4 \times 10^2 \times (0.5 \times 10^{-4})} = 0.1 = 10\%$

Rather generally, values of $e = P_e/2$ and $P(|p - P_e| > e) < 10\%$ are acceptable. In this case, as is readily verified, the number of messages which must be included in a sequence is

$$N @ 40/P_e \quad (6.132)$$

In conclusion, the Tchebycheff inequality provides an upper bound on the probability of p differing from P_e by more than an amount e . However, tighter bounds, such as the Chernov bound,⁴ do exist. Using this bound, however, is often quite complicated, since the result depends on parameters other than c^2 . For this reason, the Tchebycheff inequality is very popular among communications engineers.

6.4.7 Digital Communication Example Continued: Detection in presence of Noise

In Sec. 6.2.5 we considered a communication channel in which one or another of a discrete number of messages is presented at the input sending end. Some fixed time interval T is allocated to the

transmission of a single message, the messages being distinguished from one another through the fact that different waveforms are used to represent the different messages. The observed response generated at the receiving end by virtue of the processing performed by the channel is quite generally a fixed voltage which persists nominally for the time T allocated to a message. Because of noise, the observed response does not establish with certainty which message was transmitted. We have, however, determined a procedure for estimating which message was transmitted, the procedure assuring minimum likelihood of error. For a response r_j we formed the quantities $P(m_k)P(r_j|m_k)$ for all values of k , that is, for all possible messages, and we estimated that the message sent was the one for which $P(m_k)P(r_j|m_k)$ was a maximum.

Now let us consider a situation in which, in the absence of noise, each message m_k causes the generation of a signal s_k and a unique response r_k .

However, in this case, when noise is superimposed on s_k , the response is a continuous random variable which we call R (with sample values r).

When R is a continuous random variable, the probability that the generated response is precisely some fixed number r is zero. We ask instead about the probability that the response is in the range r to $r + dr$. Having observed a response in the range r to $r + dr$ we shall decide which is the transmitted message by comparing values of

$$P(m_k)P(r \leq R \leq r + dr|m_k) = P(m_k)f_R(r|m_k) dr \quad (6.133)$$

Suppose that there were an interval during which no signal was transmitted. In this case, at the receiver the total receiver response R would be only due to the noise; that is, $R = N$. This noise N can be characterized by a probability density function $f_N(n)$. Very frequently the noise has a Gaussian density function as illustrated in Fig. 6.16a. The shaded area at $N = n$ represents the probability that N is in the range n to $n + dn$.

Next, let the signal m_k be transmitted so that a voltage s_k is applied at the channel input. This voltage s_k will be added to the noise, n , and the voltage $r = s_k + n$ is received. The probability $P(r \leq R \leq r + dr|m_k)$ is then as shown in Fig. 6.16b. Accordingly, with message m_k , the probability that R is at r within the range dr is the same as the probability that, N is at n within the range dn . In short, given that message m_k was transmitted and that a total response R was received,

$$P(r \leq R \leq r + dr|m_k) = P(n \leq N \leq n + dn) \quad n + s_k = r \quad (6.134)$$

and therefore

$$f_R(r|m_k) dr = f_N(n) dn \quad (6.135)$$

Substituting Eq. (6.135) into Eq. (6.133) we see that we decide which is the transmitted message by comparing values of $P(m_k)f_N(n)$.

In summary, consider signals m_k which generate received voltages s_k to which noise is added, the noise having a density function $f_N(n)$ where $n = r - s_k$. To find the best decision we make plots, for each m_k , of the quantities $P(m_k)f_N(r - s_k)$. For any received response r , the message to be selected is the one for which $P(m_k)f_N(r - s_k)$ is the largest. As an example, consider that we have two signals, m_1 with probability $P(m_1) = \frac{1}{4}$ and m_2 with $P(m_2) = \frac{3}{4}$. Let $s_1 = -1$ and $s_2 = +1$. Plots for $f_N(n)$, $P(m_1)f_N(r + 1)$ and $P(m_2)f_N(r - 1)$ are given in Fig. 6.17. If the received total response is $r > \rho$ then the decision should be made that m_2 was sent and if $r < \rho$ than m_1 was sent. Note that if m_2 was indeed sent, but the response is $r < \rho$, then we would mistakenly judge that m_1 had been sent. Thus the shaded area in Fig. 6.17 measures the probability that m_2 was transmitted and read as m_1 .

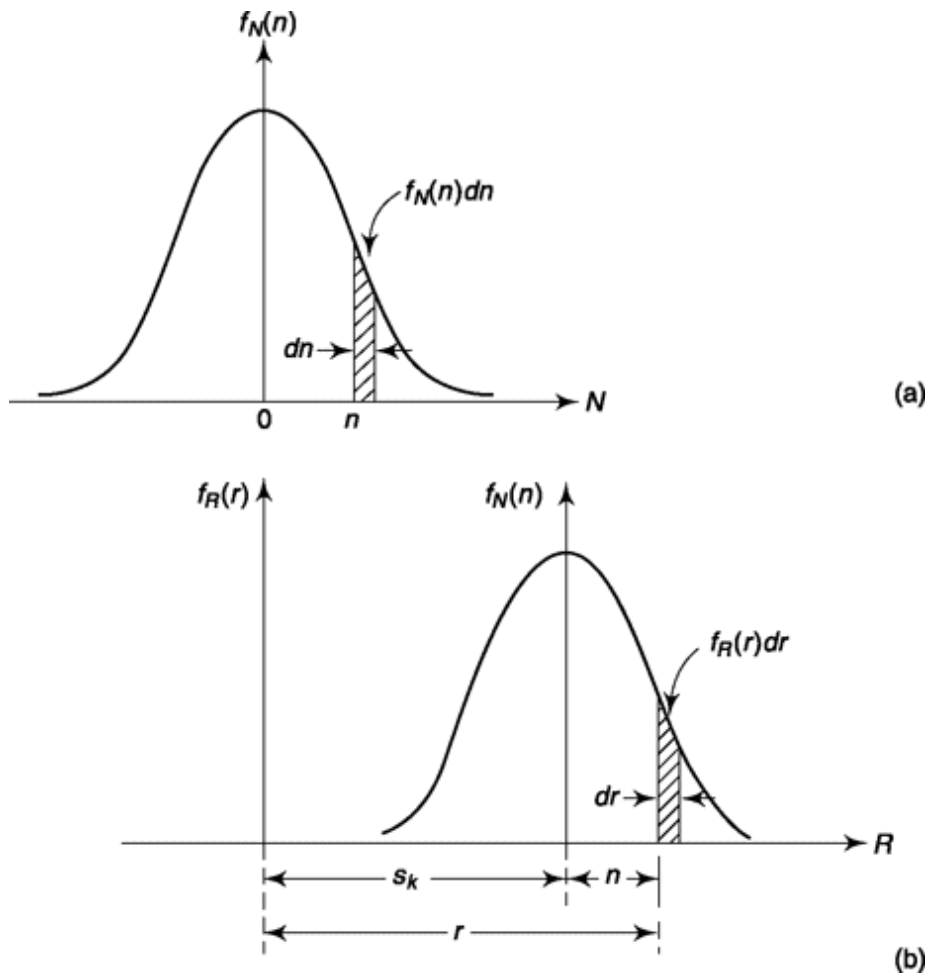


Fig. 6.16 (a) Probability density of noise, N . (b) Probability density of the received voltage $R = s_k + N$.

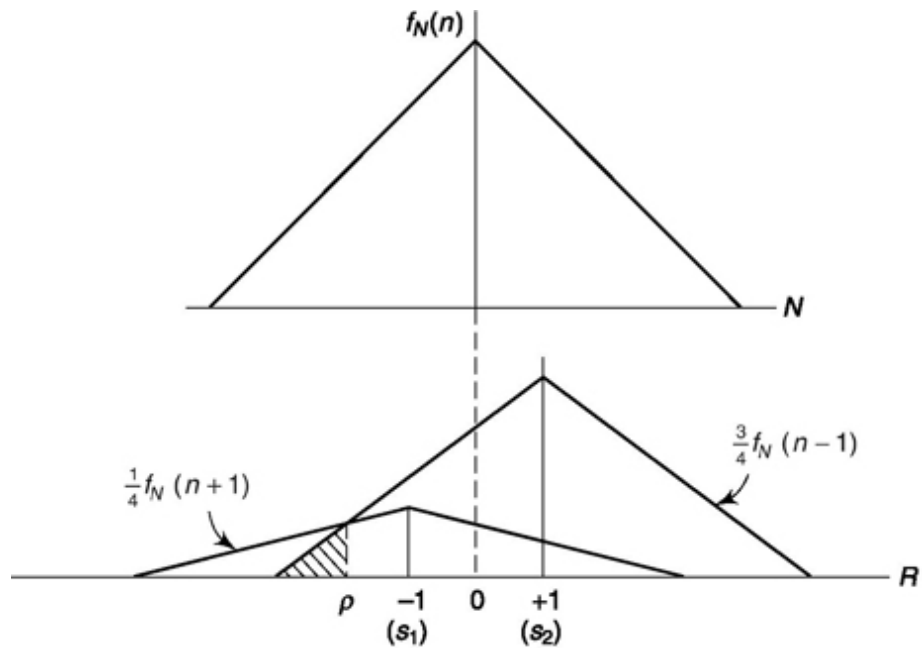


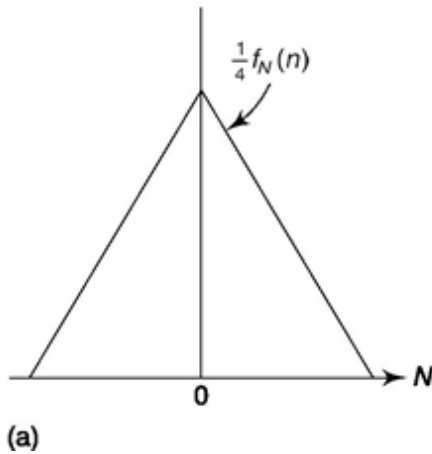
Fig. 6.17 Probability density for unequal *a priori* probabilities.

Example 6.14

Consider a situation in which one of the four messages m_1, m_2, m_3, m_4 are sent yielding receiver response s_1, s_2, s_3, s_4 respectively with $P(m) = 1/4$ (Fig. 6.18). The pdf $f_N(n)$ is shown in Fig. 6.18a. The boundaries of the received response R at which decisions change are marked p_{12}, p_{23}, p_{34} . Find the probability of error in receiving these messages.

Solution

The sum of the two shaded areas shown, each of area Δ , equals the probability $P(E, m_2)$ that m_2 is transmitted and that the message is erroneously read. Thus $P(E, m_2) = 2\Delta$. The remaining area under $\frac{1}{4}f_N(r - s_2)$



is the probability that m_2 is transmitted and is correctly read. This probability is $P(C, m_2) = \frac{1}{4} - 2\Delta$. We find of course that $P(E, m_3) = P(E, m_2)$. But it is most interesting to note that when we evaluate $P(E, m_1)$ or $P(E, m_4)$ there is only a single area Δ involved. Hence $P(E, m_1) = P(E, m_4) = \frac{1}{2} P(E, m_2) = \frac{1}{2} P(E, m_3)$. Thus, we arrive at the most interesting result that given four equally likely messages, when we make boundary decisions which assure minimum average likelihood of error, the probability of making an error is not the same for all messages. Of course, this result applies for any number of equally likely messages greater than two.

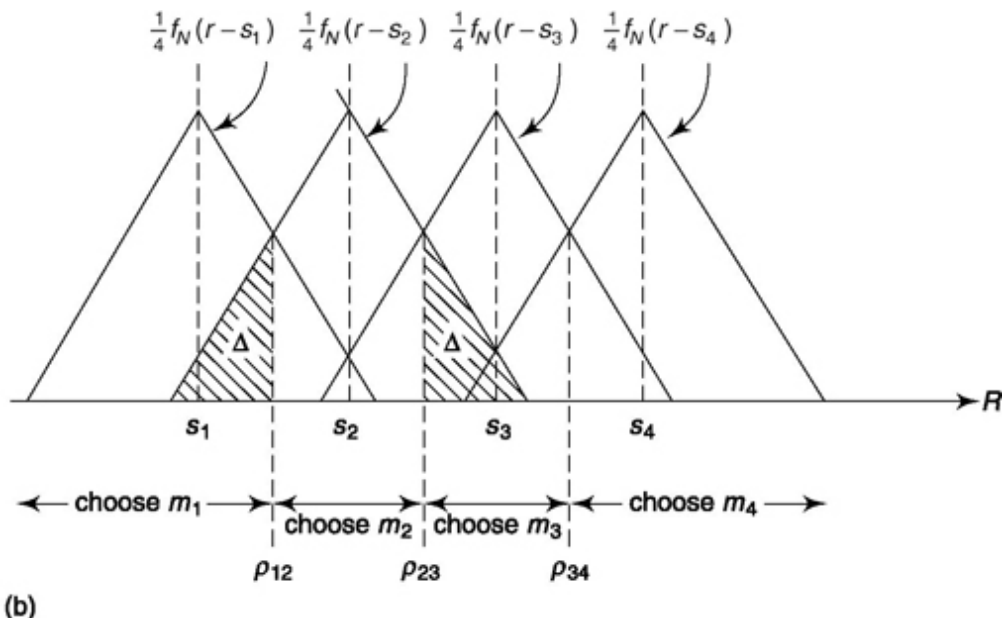


Fig. 6.18 Probability density when four signals are transmitted. (a) Probability density of $f_2(r)$ when noise alone is received, (b) Probability density when one of four signals is transmitted and received in noise.

The probability that a message is read correctly is

$$\begin{aligned}
 P(C) &= P(C, m_1) + P(C, m_2) + P(C, m_3) + P(C, m_4) \\
 &= \left(\frac{1}{4} - \Delta\right) + \left(\frac{1}{4} - 2\Delta\right) + \left(\frac{1}{4} - 2\Delta\right) + \left(\frac{1}{4} - \Delta\right) \\
 &= 1 - 6\Delta
 \end{aligned}$$

Thus the probability of an error is

$$P(E) = 1 - P(C) = 6\Delta$$

Example 6.15

Show that, $(E[XY])^2 < E[X^2]E[Y^2]$ where X and Y are real random variables with finite second moments.

Solution

Let, $Z = X - aY$

$$\text{Since, } E[Z^2] \geq 0, E[(X - aY)^2] \geq 0$$

$$\text{or } E[X^2] - 2aE[XY] + a^2E[Y^2] \geq 0$$

$$\text{or } E[X^2] \geq 2aE[XY] - a^2E[Y^2]$$

$$\text{or } E[X^2]E[Y^2] \geq 2aE[XY]E[Y^2] - a^2E[Y^2]^2$$

The above relation is true for any value of a . By choosing, $a = E[XY]/E[Y^2]$ we get,

$$E[X^2]E[Y^2] \geq 2(E[XY])^2 - (E[XY])^2$$

$$\text{or } E[X^2]E[Y^2] \geq (E[XY])^2 \quad (6.136)$$

Note that, the above inequality is also known as Cauchy-Schwartz inequality.

SELF-TEST QUESTION

12. Like mean can we say that second moment for sum of two random variables are same as sum of individual second moments?
13. Is it true that sum of two Gaussian random variables whether dependent or independent is a Gaussian random variable?
14. What is the significance of central limit theorem?
15. To design decision threshold for a discrete message receiver a priori probability of the messages and noise density function are important. Is the statement correct?

6.5 RANDOM PROCESSES

To determine the probabilities of the various possible outcomes of an experiment, it is necessary to repeat the experiment many times. Suppose that we are interested in establishing the statistics associated with the tossing of a die. We might proceed in either of two ways. On one hand, we might use a single die and toss it repeatedly. Alternatively, we might toss simultaneously a very large number of dice. Intuitively, we would expect that both methods would give the same results. Thus, we would expect that a single die would yield a particular outcome, on the average, of 1 time out of

6. Similarly, with many dice we would expect that 1/6 of the dice tossed would yield a particular outcome.

Analogously, let us consider a random process such as a noise waveform $n(t)$ mentioned at the beginning of this chapter. To determine the statistics of the noise, we might make repeated measurements of the noise voltage output of a single noise source, or we might, at least conceptually, make simultaneous measurements of the output of a very large collection of statistically identical noise sources. Such a collection of sources is called an *ensemble*, and the individual noise waveforms are called *sample functions*. A statistical average may be determined from measurements made at some fixed time $t = t_1$ on all the sample functions of the ensemble. Thus, to determine, say, $n^2(t)$, we would, at $t = t_1$, measure the voltages $n(t_1)$ of each noise source, square and add the voltages, and divide by the (large) number of sources in the ensemble. The average so determined is the *ensemble average* of $n^2(t_1)$.

Now $n(t_1)$ is a random variable and will have associated with it a probability density function. The ensemble averages will be identical with the statistical averages computed earlier in Secs. 6.2.6 and 6.2.7 and may be represented by the same symbols. Thus, the statistical or ensemble average of $n^2(t_j)$ may be written $E[n^2(t)] = n^2(t_1)$. The averages determined by measurements on a single sample function at successive times will yield a *time average*, which we represent as $(n^2(t))$.

In general, ensemble averages and time averages are not the same. Suppose, for example, that the statistical characteristics of the sample functions in the ensemble were changing with time. Such a variation could not be reflected in measurements made at a fixed time, and the ensemble averages would be different at different times. When the statistical characteristics of the sample functions do not change with time, the random process is described as being *stationary*. However, even the property of being stationary does not ensure that ensemble and time averages are the same. For it may happen that while each sample function is stationary the individual sample functions may differ statistically from one another. In this case, the time average will depend on the particular sample function which is used to form the average. When the nature of a random process is such that ensemble and time averages are identical, the process is referred to as

ergodic. An ergodic process is stationary, but, of course, a stationary process is not necessarily ergodic.

We shall have a broader classification of random processes in Sec. 6.5.2 after we define autocorrelation of a random process. We note that these moments are independent of t_1 and hence independent of time.

Example 6.16

Consider the random process

$$V(t) = \cos(\omega_0 t + \Theta) \quad (i)$$

where Θ is a random variable with a probability density

$$\begin{aligned} f(\Theta) &= \frac{1}{2\pi} & -\pi \leq \theta \leq \pi \\ &= 0 & \text{elsewhere} \end{aligned}$$

- (a) Show that the first and second moments of $V(t)$ are independent of time.
- (b) If the random variable Θ in Eq. (i) is replaced by a fixed angle θ_0 , will the ensemble mean of $V(t)$ be time independent?
- (a) Choose a fixed time $t = t_1$. Then

$$E\{V(t_1)\} = \int_{-\pi}^{\pi} \frac{1}{2\pi} \cos(\omega_0 t_1 + \theta) d\theta = 0$$

$$\text{and } E\{V^2(t_1)\} = \int_{-\pi}^{\pi} \frac{1}{2\pi} \cos^2(\omega_0 t_1 + \theta) d\theta = \frac{1}{2}$$

In a similar manner it can be established that all of the moments and all other statistical characteristics of $V(t)$ are independent of time. Hence $V(t)$ is a stationary process.

- (b) Since Θ is known, $V(t)$ is deterministic. For example, if $\Theta = 300^\circ$
 $E\{V(t)\} = V(t) = \cos(\omega_0 t + 300^\circ)$ is constant. Thus, $V(t)$ is not stationary.

Example 6.17

A voltage $V(t)$, which is a Gaussian ergodic random process with a mean of zero and a variance of 4 volt^2 , is measured by a dc meter, a true rms meter, and a meter which first squares $V(t)$ and then reads its dc component.

Solution

(a) The dc meter reads

$$\langle V(t) \rangle = E\{V(t)\}$$

since $V(t)$ is ergodic. Since $E\{V(t)\} = 0$, the dc meter reads zero.

(b) The true rms meter reads

$$\sqrt{\langle V^2(t) \rangle} = \sqrt{E\{V^2(t)\}}$$

since $V(t)$ is ergodic. Since $V(t)$ has a zero mean, the true rms meter reads $\sigma = 2$ volts.

(c) The square and average meter (a full-wave rectifier meter) yields a deflection proportional to

$$\langle v^2(t) \rangle = E\{V^2(t)\} = \sigma^2 = 4$$

6.5.1 autocorrelation and power spectral Density of random processes

A random process $n(t)$, being neither periodic nor of finite energy has an autocorrelation function defined by Eq. (1.19). Thus,

$$R(\tau) = \lim_{T \rightarrow \infty} \frac{1}{T} \int_{-T/2}^{T/2} n(t)n(t+\tau) dt \quad (6.137)$$

In connection with deterministic waveforms we were able to give a physical significance to the concept of a power spectral density $G(f)$ and to show that $G(f)$ and $R(\tau)$ constitute a Fourier transform pair. As an extension of that result we shall *define* the power spectral density of a random process in the same way. Thus, for a random process we take $G(f)$ to be

$$G(f) = \mathcal{F}[R(\tau)] = \int_{-\infty}^{\infty} R(\tau) e^{-j\omega\tau} d\tau \quad (6.138)$$

It is of interest to inquire whether $G(f)$ defined in Eq. (6.138) for a random process has a physical significance which corresponds to the physical significance of $G(f)$ for deterministic waveforms.

For this purpose consider a *deterministic* waveform $v(t)$ which extends from $-\infty$ to ∞ . Let us select a section of this waveform which extends from $-T/2$ to $T/2$. This waveform $v_T(t) = v(t)$ in this range, and otherwise $v_T(t) = 0$. The waveform $v_T(t)$ has a Fourier transform $V_T(f)$. We recall that $|V_T(f)|^2$ is the energy spectral density; that is, $|V_T(f)|^2 df$ is the normalized energy in the spectral range df . Hence, over the interval T the normalized power density is $|V_T(f)|^2/T$. As $T \rightarrow \infty$, $v_T(t) \rightarrow v(t)$, and we then have the result that the physical significance of the power spectral density $G(f)$, at least for a deterministic waveform, is that

$$G(f) = \lim_{T \rightarrow \infty} \frac{1}{T} |V_T(f)|^2 \quad (6.139)$$

Correspondingly, we state, without proof, that when $G(f)$ is defined for a random process, as in Eq. (6.138), as the transform of $R(\tau)$, then $G(f)$ has the significance that

$$G(f) = \lim_{T \rightarrow \infty} E \left\{ \frac{1}{T} |N_T(f)|^2 \right\} \quad (6.140)$$

where $E\{ \}$ represents the ensemble average or expectation and $N_T(f)$ represents the Fourier transform of a truncated section of a sample function of the random process $n(t)$.

The autocorrelation function $R(\tau)$ is, as indicated in Eq. (6.137), a *time average* of the product $n(t)$ and $n(t + \tau)$. Since we have assumed an ergodic process, we are at liberty to perform the averaging over any sample function of the ensemble, since every sample function will yield the same result. However, again because the noise process is ergodic, we may replace the time average by an ensemble average and write, instead of Eq. (6.137),

$$R(\tau) = E\{n(t)n(t + \tau)\} \quad (6.141)$$

The averaging indicated in Eq. (6.141) has the following significance: At some *fixed* time t , $n(t)$ is a random variable, the possible values for which are the values $n(t)$ assumed at time t by the individual sample functions of the ensemble. Similarly, at the *fixed* time $t + T$, $n(t + t)$ is also a random variable. It then appears that $R(t)$ as expressed in Eq. (6.141) is the covariance between these two random variables.

Suppose then that we should find that for some t , $R(t) = 0$. Then the random variables $n(t)$ and $n(t + t)$ are uncorrelated, and for the Gaussian process of interest to us, $n(t)$ and $n(t + t)$ are independent. Hence, if we should select some sample function, a knowledge of the value of $n(t)$ at time

t would be of no assistance in improving our ability to predict the value attained by that same sample function at time $t + T$.

The physical fact about the noise, which is of principal concern in connection with communications systems, is that such noise has a power spectral density $G(f)$ which is uniform over all frequencies. Such noise is referred to as “white” noise in analogy with the consideration that white light is a combination of all colors, that is, colors of all frequencies. Actually as is pointed out in Sec. 15.3, there is an upper-frequency limit beyond which the spectral density falls off sharply. However, this upper-frequency limit is so high that we may ignore it for our purposes.

Now, since the autocorrelation $R(t)$ and the power spectral density $G(f)$ are a Fourier transform pair, they have the properties of such pairs. Thus, when $G(f)$ extends over a wide frequency range, $R(t)$ is restricted to a narrow range of t . In the limit, if $G(f) = I$ (a constant) for all frequencies from $-' < f < +'$, then $R(t)$ becomes $R(t) = I d(t)$, where $d(t)$ is the delta function with $d(t) = 0$ except for $t = 0$. Since, then, for white noise, $R(t) = 0$ except for $t = 0$, Eq. (6.141) says that $n(t)$ and $n(t + t)$ are uncorrelated and hence independent, no matter how small is t .

6.5.2 Classification of random processes

We have already discussed stationarity and ergodicity in Sec. 6.5 while defining random processes. We look into subdivision of that and other classification in this subsection.

strict-sense stationary

A random process $X(t)$ is called strict sense stationary(SSS) if its statistics does not change with shift of origin, i.e. its n -th order density function can be written as,

$$f_X(x_1, x_2, \dots, x_n; t_1, t_2, \dots, t_n) = f_X(x_1, x_2, \dots, x_n; t_1 + T, t_2 + T, \dots, t_n + T) \quad (6.142)$$

where, $f_X(x_1, x_2, \dots, x_n; t_1, t_2, \dots, t_n) = \frac{\partial^n F_X(x_1, x_2, \dots, x_n; t_1, t_2, \dots, t_n)}{\partial x_1 \partial x_2 \dots \partial x_n}$

while n -th order distribution $F_X(x_1, x_2, \dots, x_n; t_1, t_2, \dots, t_n) = P[X(t_1) \leq x_1, X(t_2) \leq x_2, \dots, X(t_n) \leq x_n]$

Thus, for SSS, first order density $f_X(x_1; t) = f_X(x_1)$ [By putting $t_1 = t$ and $T = t_1$]

Second order density $f_X(x_1, x_2; t_1, t_2) = f_X(x_1, x_2, t)$ [putting $T = -t_1$]

Wide-sense Stationary

A random process $X(t)$ is called wide sense stationary (WSS) if Mean, $E[X(t)] = m$ (constant) and Autocorrelation, $E[X(t)X(t + \tau)] = R_{XX}(\tau)$

i.e. autocorrelation depends only on time difference. Putting $\tau = 0$, we get

$$E[X^2(t)] = R_{XX}(0) \quad (6.143)$$

i.e. average power of WSS is constant and independent of time.

Multiple Random Process

Now, two processes are called jointly WSS, if each is WSS and their cross correlation depends only on time difference.

$$R_{XY}(t, t + \tau) = E[X(t)Y(t + \tau)] = R_{XY}(\tau) \quad (6.144)$$

Also, $G_{XY}(f)$ and $R_{XY}(\tau)$ are Fourier transform pair such that

$$R_{XY}(\tau) = R_{XY}(-\tau) \text{ and } G_{XY}(f) = G_{XY}(-f)$$

Ergodic Random Process

A stationary process $X(t)$ is called ergodic (or ergodic in mean) if time average is same as ensemble average, i.e. $\langle x(t) \rangle = E[X(t)] = m$. It is called ergodic in autocorrelation if $\langle x(t)x(t + \tau) \rangle = E[X(t)X(t + \tau)] = R_{XX}(\tau)$.

Band Pass Random Process

A bandpass (or bandlimited) random process $x(t)$ can be expressed in terms of in-phase and in-quadrature components as shown in Eq. (1.169)

$$X(t) = X_c(t) \cos(2\pi f_c t) + X_s(t) \sin(2\pi f_c t) \quad (6.145)$$

If $x(t)$ is a bandpass signal and is input to the BPF of Fig. 1.27c of Chapter 1, and their bandwidths are same then the output will be unaltered $x(t)$. Since multiplication by $\cos(2\pi f_c t)$ at the input side shifts the bandpass signal by $+f_c$ and $-f_c$ along frequency axis and LPF1 filters out only the low frequency components, we can write PSD for in-phase component as

$$G_{X_c}(f) = G_X(f + f_c) + G_X(f - f_c) \text{ for } |f| \leq B \text{ and zero elsewhere.}$$

Similarly, for quadrature component,

$$G_{X_s}(f) = G_X(f + f_c) - G_X(f - f_c) \text{ for } |f| \leq B \text{ and zero elsewhere.}$$

It can also be shown that, $\langle X_c(t) X_c(t) \rangle = R_{X_c X_s}(0) = 0$

and if $G_X(f)$ is symmetrical about f_c , $R_{X_c X_s}(\tau) = 0$

Gaussian Random Process

A random process $X(t)$ is called Gaussian process if $X = [X(t_1) \ X(t_2) \ \dots \ X(t_n)]^T$ has a jointly multi-variate Gaussian density function given by

$$f_X(\mathbf{X}) = \frac{1}{(2\pi)^{n/2} |\det \mathbf{C}|^{1/2}} e^{-\frac{1}{2} (\mathbf{x} - \boldsymbol{\mu})^T \mathbf{C}^{-1} (\mathbf{x} - \boldsymbol{\mu})} \quad (6.146)$$

where, $\mathbf{x} = [x_1 \ x_2 \ \dots \ x_n]^T$, $\mu = E[X]$ and $\mathbf{C} = \begin{pmatrix} C_{11} & \cdots & C_{1n} \\ \vdots & \ddots & \vdots \\ C_{m1} & \cdots & C_{mn} \end{pmatrix}$ such that C_{ij} is covariance of $X(t_i)$

and $X(t_j)$. Note that, $C_{ij} = R_{XX}(t_i, t_j) - \mu_i \mu_j$

A Gaussian process is completely specified by its set of means and autocorrelations. If the input to a linear system is Gaussian, the output is also Gaussian. Finally, if a Gaussian process is WSS then it is also SSS.

White Noise

A random process $X(t)$ is called white noise when its PSD, $G(f) = \eta/2$, i.e. constant over entire frequency spectrum and mean is assumed to be zero.

From inverse Fourier transform, autocorrelation $R(\tau) = \frac{\eta}{2} \delta(\tau)$

The *band-limited* white noise has similar flat spectrum but only over the pass band.

6.5.3 PSD of Sequence of Random Pulses

We shall occasionally need to have information about the power spectral density of a sequence of random pulses such as is indicated in Fig. 6.19. In fact, the digital message signals discussed in previous chapters are a special case of this. Let us first consider that the pulses are of the same form but have random amplitudes and statistically independent random times of occurrence. The waveform (the random process) is stationary so that the statistical features of the waveforms are time invariant. Correspondingly, there is an invariant *average* time of separation T_s between pulses. We further assume that there is no overlap between pulses.

If the Fourier transform of a single sample pulse $P(t)$ is $P(j\omega)$ then Parseval's theorem [Eq. (1.136)] states that the normalized energy of the pulse is

$$E_1 = \int_{-\infty}^{\infty} P_1(f) P_1^*(f) df = \int_{-\infty}^{\infty} |P_1(f)|^2 df \quad (6.147)$$

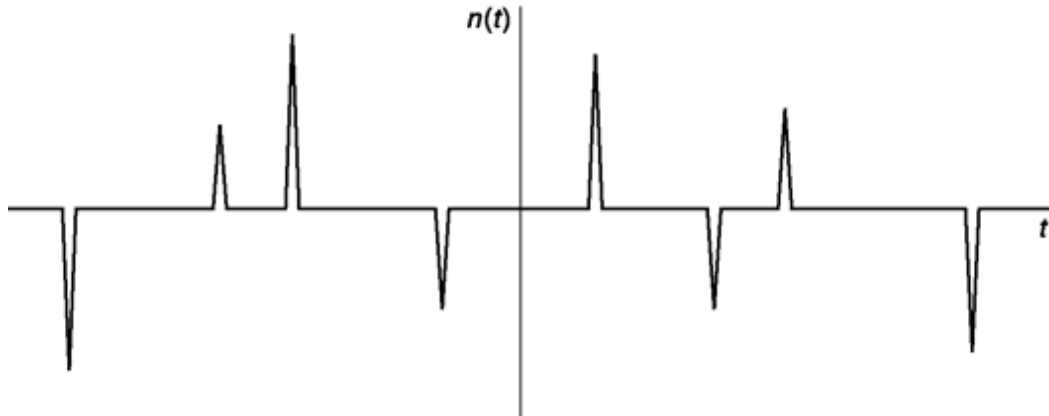


Fig. 6.19 Pulses of random amplitude and time of occurrence.

The energy in the range df at a frequency f is

$$dE_1 = |P_1(f)|^2 df \quad (6.148)$$

Now consider a sequence of n successive pulses. Since we assume that the pulses do not overlap, the energy in the range df at the frequency f due to the n pulses is:

$$dE = dE_1 + dE_2 + \dots + dE_n = \{|P_1(f)|^2 + |P_2(f)|^2 + \dots + |P_n(f)|^2\} df \quad (6.149)$$

The average value $\overline{|P(f)|^2}$ of the sequence of n pulses is, by definition

$$\overline{|P(f)|^2} \equiv \frac{1}{n} \{ |P_1(f)|^2 + |P_2(f)|^2 + \dots + |P_n(f)|^2 \} \quad (6.150)$$

so that dE in Eq. (6.149) can be written

$$dE = n \overline{|P(f)|^2} df \quad (6.151)$$

The average time of separation between pulses is T_s so that n pulses will occur in a time nT_s . The differential energy in the band df contained in the time interval nT_s is, from Eq. (6.151)

$$\frac{dE}{nT_s} = \frac{1}{nT_s} n \overline{|P(f)|^2} df = \frac{1}{T_s} \overline{|P(f)|^2} df \quad (6.152)$$

The power spectral density in the frequency range df is $G(f) = (dE/nT_s)/df$. Hence, from Eq. (6.152), $G(f)$ is:

$$G(f) = \frac{1}{T_s} \overline{|P(f)|^2} \quad (6.153)$$

Hence, whenever we make an observation or measurement of the pulse waveform which extends over a duration long enough so that the average observed pulse shape, such as their amplitudes, widths and spacings are representative of the waveform generally, we shall find that Eq. (6.153) applies.

In the special case in which the individual pulses are impulses of strength I , then, since in this case $P(f) = I$, we shall have:

$$G(f) = \frac{I^2}{T_s} \quad -\infty < f < \infty \quad (6.154)$$

6.5.4 PSD of Digital Data

Let us consider that digital data is transmitted serially over a communication channel one bit at a time at a rate f_b bits/s. Thus the time $T_b = 1/f_b$ is allocated to the transmission of each bit. In the simplest case the bit logic level 1 is represented by sustaining a fixed voltage V_b for the time T_b and logic level 0 is represented by the fixed voltage $-V_b$ for the time T_b .

Digital transmission systems are usually *synchronous*, that is, they operate in conjunction with a *clock* waveform. A clock is a regular periodic waveform, whose period is equal to the bit time T_b . The clock serves many purposes in a digital system but, so far as our present concerns are involved, we note that the clock serves both to establish the duration T_b and also to mark the beginning and end of the interval allocated to each bit. In a transmission system there must be a clock waveform at both the sending end and at the receiving end and these clocks must be synchronized with one another.

In Fig. 6.20, we have indicated a clock waveform which marks off the bit intervals and we have also indicated two formats by which the bits (logic 1 and 0) are distinguished from one another. In

(a) and (b) we show the scheme already referred to. Here logic 1 is represented by the voltage V_b held for the duration of a clock cycle and logic 0 by the voltage $-V_b$ held for an equal time. This scheme is characterized as a *non-return-to-zero* (NRZ) representation for a reason that will be apparent shortly. A second scheme identified by the name *biphase* is shown in (c) and (d). Here the digital bits are represented by waveforms which are at V_b for half the cycle and at $-V_b$ for the other half.

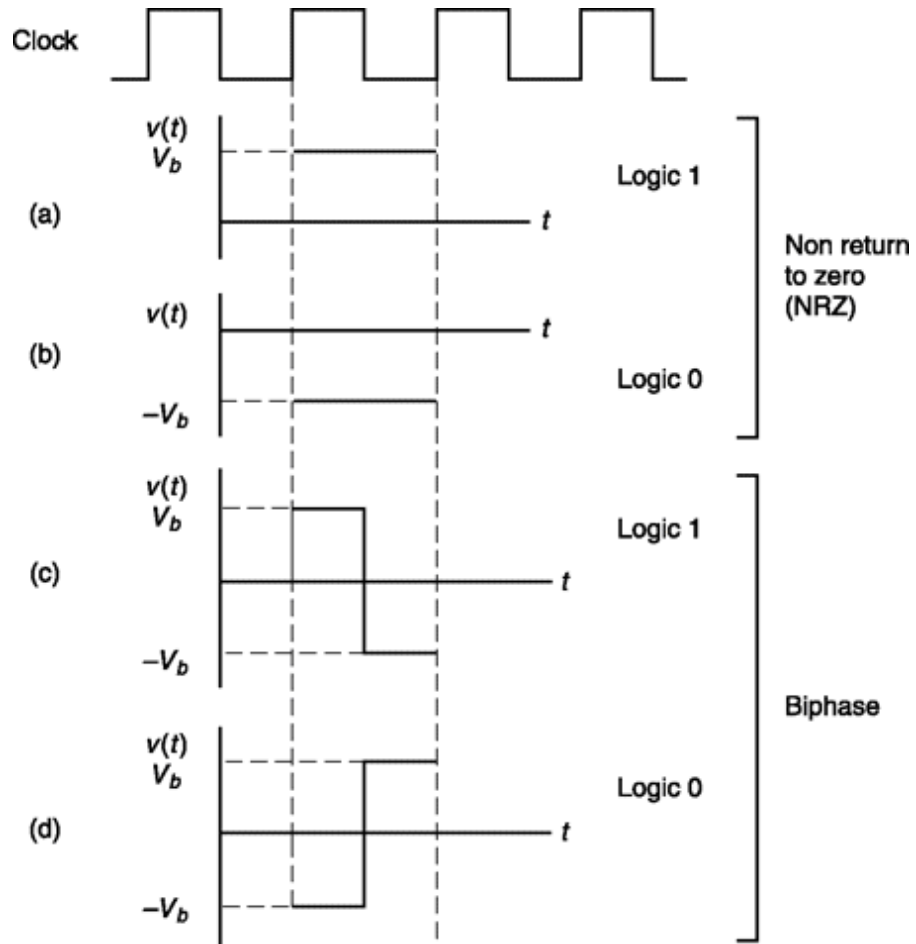


Fig. 6.20 Clock waveform, NRZ and biphase data.

In Fig. 6.21 we again show the clock waveform and show also the waveform generated in the transmission of the sequence ... 10111001... using the NRZ and the biphase formats. Observe that in the NRZ format, when a sequence of like bits is encountered, the signal sustains a fixed level $+V_b$ or $-V_b$, the voltage never returning to the zero voltage level, hence the name NRZ. In the biphase format the signal is identical to the clock waveform or reversed from the clock depending on whether the bit is a 1 or a 0. Further, in the biphase format the signal passes through zero at least once per clock cycle. Since the biphase signal voltage *changes level more frequently* than does the NRZ signal we naturally expect that the spectrum of the biphase signal will have higher frequency components than are present in the NRZ signal.

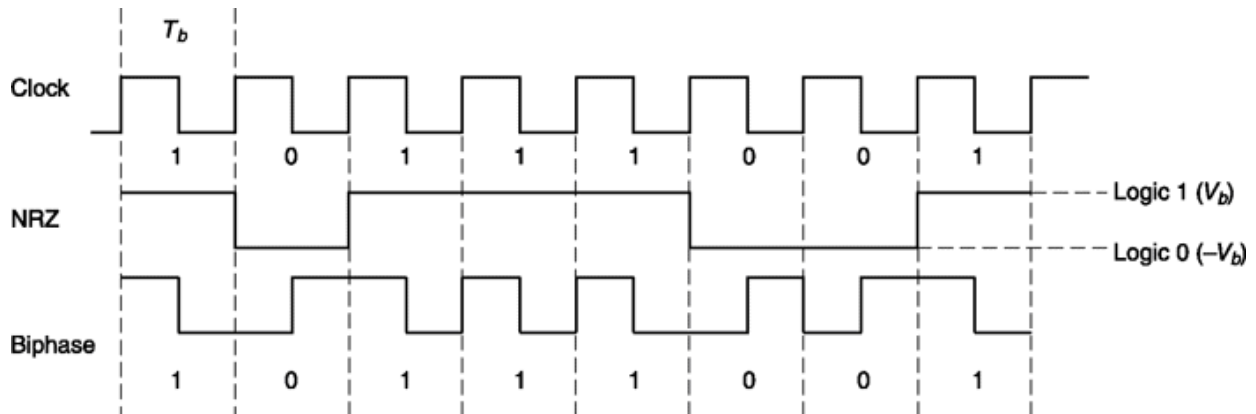


Fig. 6.21 NRZ and biphase data stream.

Of interest to us are the power spectral densities of the NRZ and biphase signals and a comparison between them. To find these spectral densities we use Eq. (6.153):

$$G(f) = \frac{\overline{|P(f)|^2}}{T_s} \quad (6.155)$$

In the present case the mean time between bits, $T_s = T_b$ and for NRZ, with $t = 0$ placed at the center of the bit,

$$p(t) = \begin{cases} \pm V_b & |t| \leq T_b/2 \\ 0 & \text{elsewhere} \end{cases} \quad (6.156)$$

Thus

$$P(f) = \pm V_b \int_{-T_b/2}^{T_b/2} e^{-j2\pi f t} dt = \pm V_b T_b \frac{\sin \pi f T_b}{\pi f T_b} \quad (6.157)$$

Substituting Eq. (6.157) into Eq. (6.155) and noting that in this case the average value of $|P(f)|^2$ is simply $|P(f)|^2$, we have

$$G(f) = V_b^2 T_b \left(\frac{\sin \pi f T_b}{\pi f T_b} \right)^2 \quad (6.158)$$

This power spectral density is plotted in Fig. 6.22. It has a maximum at $f = 0$ and is $G(f) = 0$ at all multiples of $f_b (= 1/T_b)$. The peak between f_b and $2f_b$ occurs at $f = 1.5f_b$ and is 14 dB lower than the peak at $f = 0$. It is left as a student exercise (by consulting a table of integrals) to verify that the total power in an NRZ signal is reduced by only 10 percent if the signal is passed through an ideal lower-pass filter with cutoff at $f = f_b$. Thus 90 percent of the power is in the main lobe centered around $f = 0$. It is to be noted however that the NRZ signal has no dc component. In the frequency range from $f = 0$ to $f = \pm \Delta f$ the power is $2G(f) \Delta f$ and in the limit as $\Delta f \rightarrow 0$ this power becomes zero. (If there were a dc component $G(f)$ would be impulsive at $f = 0$.) This result is, of course, to be anticipated since we would expect the NRZ signal to spend, on the average, equal time at the two levels.

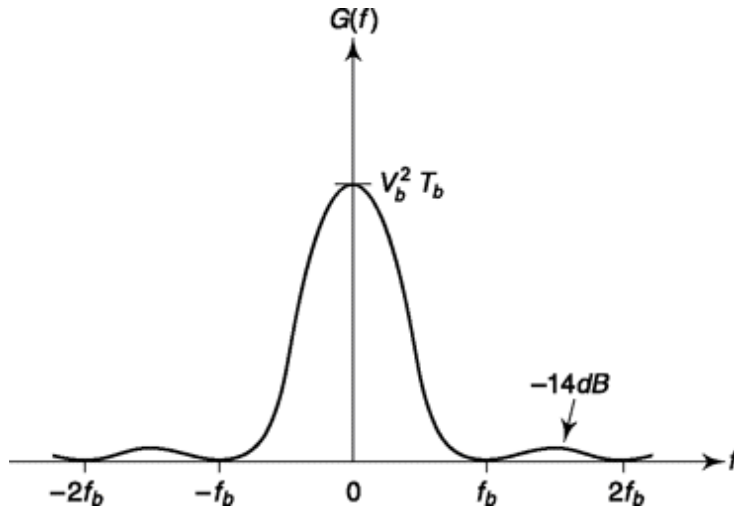


Fig. 6.22 Power spectral density of NRZ data. In the biphase case we have

$$P(f) = \int_{-T_b/2}^0 \pm V_b e^{-j2\pi ft} dt - \int_0^{T_b/2} \pm V_b e^{-j2\pi ft} dt \quad (6.159a)$$

$$= j(\pm V_b) T_b \frac{\sin^2 \pi f T_b / 2}{\pi f T_b / 2} \quad (6.159b)$$

so that

$$\overline{|P(f)|^2} = V_b^2 T_b^2 \left[\frac{\sin^2 \pi f T_b / 2}{\pi f T_b / 2} \right]^2 \quad (6.160)$$

and the power spectral density is

$$G(f) = V_b^2 T_b \left[\frac{\sin^2 \pi f T_b / 2}{\pi f T_b / 2} \right]^2 \quad (6.161)$$

$G(f)$, as given in Eq. (6.161) is plotted in Fig. 6.23. Note that here the principal lobes extend from $f = 0$ to $f = 2f_b$ and have peaks at approximately $\pm 3f_b/4$. At $f = 0$, $G(f) = 0$. It can be verified that if biphase data is transmitted through an ideal low-pass filter, with cutoff at frequency $2f_b$, 95 percent of the power will be passed. However, if the filter cuts-off at f_b then only approximately 70 percent of the power is passed.

6.5.5 Transmission of a random process Through Linear systems

Consider, a random process $X(t)$ is applied to a linear time invariant system with impulse response $X(t)$ and frequency response $H(f)$. Then the output $F(t)$ from convolution,

$$Y(t) = \int_{-\infty}^{\infty} h(\lambda) X(t - \lambda) d\lambda$$

Then,

$$E[Y(t)] = \int_{-\infty}^{\infty} h(\lambda) E[X(t - \lambda)] d\lambda$$

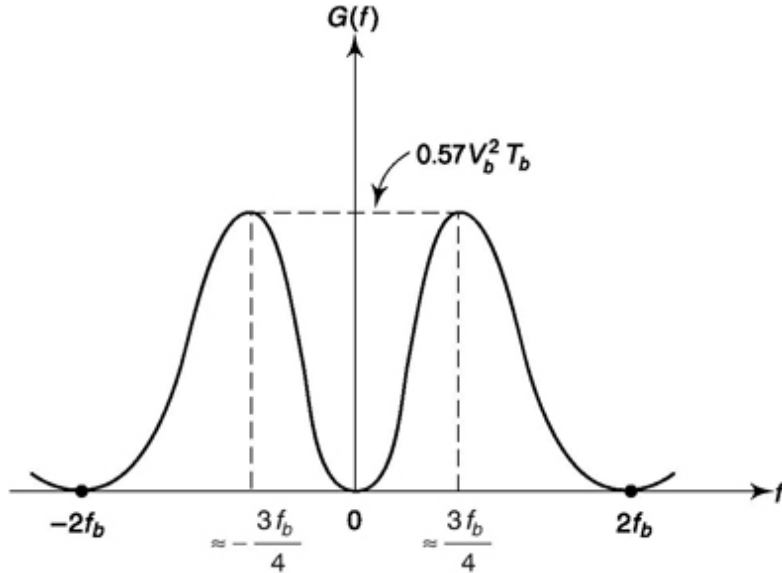


Fig. 6.23 Power spectral density of biphase data.

If,

$$E[X(t)] = m, \text{ constant as in case of WSS then,}$$

$$E[Y(t)] = m \int_{-\infty}^{\infty} h(\lambda) d\lambda = mH(0)$$

Again,

$$Y(t + \tau) = \int_{-\infty}^{\infty} h(\lambda) X(t + \tau - \lambda) d\lambda$$

Now,

$$\begin{aligned} R_Y(\tau) &= \langle Y(t)Y(t + \tau) \rangle \\ &= \left\langle \int_{-\infty}^{\infty} h(\lambda_1) X(t - \lambda_1) d\lambda_1 \int_{-\infty}^{\infty} h(\lambda_2) X(t + \tau - \lambda_2) d\lambda_2 \right\rangle \\ &= \int_{-\infty}^{\infty} \int_{-\infty}^{\infty} h(\lambda_1) h(\lambda_2) \langle X(t - \lambda_1) X(t + \tau - \lambda_2) \rangle d\lambda_1 d\lambda_2 \\ &= \int_{-\infty}^{\infty} \int_{-\infty}^{\infty} h(\lambda_1) h(\lambda_2) R_X(\tau + \lambda_1 - \lambda_2) d\lambda_1 d\lambda_2 \end{aligned}$$

Thus, if input to the system is WSS then output is also WSS.

The above integral can be shown as double convolution as given next

$$R_Y(\tau) = h(\tau) * h(-\tau) * R_X(\tau) \quad (6.162)$$

Taking Fourier transform of both sides of Eq. (6.162) and noting convolution in time domain is multiplication in frequency domain,

$$G_Y(f) = |H(f)|^2 G_X(f) \quad (6.163)$$

6.5.6 Weiner-Hopf Filter: Optimum Filtering to reduce total Output Noise

Here, we discuss one technique to reduce noise added to a signal by passing through a filter. Since, in all practical cases a filter induces some amount of distortion in the signal we'll include that also

or discussion. The simplest way to calculate distortion, D is to subtract the original message from filter output which can be written in frequency domain as (since convolution in time domain is multiplication in frequency domain)

$$D(f) = H(f)M(f) - M(f) = [H(f) - 1]M(f)$$

re $H(f)$ is filter transfer function and $M(f)$ is the spectrum of message signal $m(t)$. Now, we calculate additive noise power N_A and distortion signal power N_D at the output of the filter. If $G_M(f)$ is the input signal power spectral density and $G_N(f)$ that of additive noise at the input to filter then we can write,

$$N_D = \frac{1}{2\pi} \int_{-\infty}^{\infty} G_M(f)|H(f) - 1|^2 df \text{ and } N_A = \frac{1}{2\pi} \int_{-\infty}^{\infty} G_N(f)|H(f)|^2 df \quad (6.164)$$

the total noise due to additive and distortion at the output side can be written as

$$\begin{aligned} N_o &= N_D + N_A \\ &= \frac{1}{2\pi} \int_{-\infty}^{\infty} [G_M(f)|H(f) - 1|^2 + G_N(f)|H(f)|^2] df \end{aligned} \quad (6.165)$$

The Weiner-Hopf filter attempts to minimize this total output noise power and is known as an optimum filter in this sense. The following calculation shows how the transfer function of optimum filter can be derived. Note that, $H(f)$ in general is a complex quantity while $G_M(f)$ and $G_N(f)$ are real quantities as they represent input signal and noise power respectively.

From complex algebra, $|a - b|^2 = a^*a - a^*b - ab^* + b^*b$ where* refers to complex conjugate. So, expanding the above equation,

$$\begin{aligned} N_o &= \frac{1}{2\pi} \int_{-\infty}^{\infty} [G_M(f)[H(f)H^*(f) - H(f) - H^*(f) + 1] + G_N(f)|H(f)|^2] df \\ &= \frac{1}{2\pi} \int_{-\infty}^{\infty} [G_M(f)[|H(f)|^2 - H(f) - H^*(f) + 1] + G_N(f)|H(f)|^2] df \\ &= \frac{1}{2\pi} \int_{-\infty}^{\infty} [[G_M(f) + G_N(f)]|H(f)|^2 - H(f)G_M(f) - H^*(f)G_M(f) + G_M(f)] df \\ &= \frac{1}{2\pi} \int_{-\infty}^{\infty} \left[\{G_M(f) + G_N(f)\}[|H(f)|^2 \right. \\ &\quad \left. - \frac{H(f)G_M(f)}{G_M(f) + G_N(f)} - \frac{H^*(f)G_M(f)}{G_M(f) + G_N(f)} + \frac{G_M(f)}{G_M(f) + G_N(f)} \right] df \\ &= \frac{1}{2\pi} \int_{-\infty}^{\infty} \left[\{G_M(f) + G_N(f)\}[|H(f)|^2 \right. \\ &\quad \left. - \frac{H(f)G_M(f)}{G_M(f) + G_N(f)} - \frac{H^*(f)G_M(f)}{G_M(f) + G_N(f)} + \frac{G_M(f)[G_M(f) + G_N(f)]}{G_M(f) + G_N(f)^2} \right] df \\ &= \frac{1}{2\pi} \int_{-\infty}^{\infty} \left[\{G_M(f) + G_N(f)\}[|H(f)|^2 \right. \end{aligned}$$

$$\begin{aligned}
& - \frac{H(f)G_M(f)}{G_M(f)+G_N(f)} - \frac{H^*(f)G_M(f)}{G_M(f)+G_N(f)} + \frac{G_M^2(f)}{G_M(f)+G_N(f)^2} \Bigg] + \frac{G_M(f)G_N(f)}{G_M(f)+G_N(f)} \Bigg] df \\
& = \frac{1}{2\pi} \int_{-\infty}^{\infty} [\{G_M(f) + G_N(f)\}|H(f) - \frac{G_M(f)}{G_M(f)+G_N(f)}|^2 + \frac{G_M(f)G_N(f)}{G_M(f)+G_N(f)}] df
\end{aligned}$$

We find that output noise N_o is minimum if,

$$H(f) = \frac{G_M(f)}{G_M(f)+G_N(f)} = H_{\text{optimum}}(f) \quad (6.166)$$

and then $N_o = \frac{1}{2\pi} \int_{-\infty}^{\infty} \frac{G_M(f)G_N(f)}{G_M(f)+G_N(f)} df \quad (6.167)$

The equation 6.166 shows that if $G_M(f) @ G_N(f)$ then $H(f) <_x 1$, i.e. no attenuation and if $G_M(f) ! G_N(f)$ then $H(f) <^* 0$ then infinite attenuation. This means that, to minimize total output noise, the optimum filter uses a transfer function that allows higher proportion of signal energy to pass where it is relatively strong compared to input noise and impedes the rest. As we discussed before the realizability issue limits optimal performance in most of the practical cases.

6.5.7 Effect of First Order R-C, R-L Filters on Digital Data

In Sec. 6.5.4 we noted that NRZ data has a power spectral density whose principal lobe has a peak at $f = 0$ while for biphase data the principal lobe has a peak at $f \sim 3f_b/4$. We therefore anticipate that, for effective transmission of NRZ data, greater demands are made on the ability of the channel to transmit lower frequencies than for biphase data. To explore the matter in an easy manner, we consider now the effect on digital transmission of the most rudimentary high-pass and low-pass filters.

The rudimentary high-pass filters are shown in Fig. 6.24a and b. They are characterized in the frequency domain, as shown in Fig. 6.24c by a 3 dB frequency f at which the transmission ratio V_o/V_i falls to $0.707 = (1/\sqrt{2})$. In the *R-C* circuit $f = 1/2\pi RC$ and in the *R-L* circuit $f = 1/2\pi(L/R)$. In the time domain, as indicated in Fig. 6.24d the filters are characterized by a time constant t which is

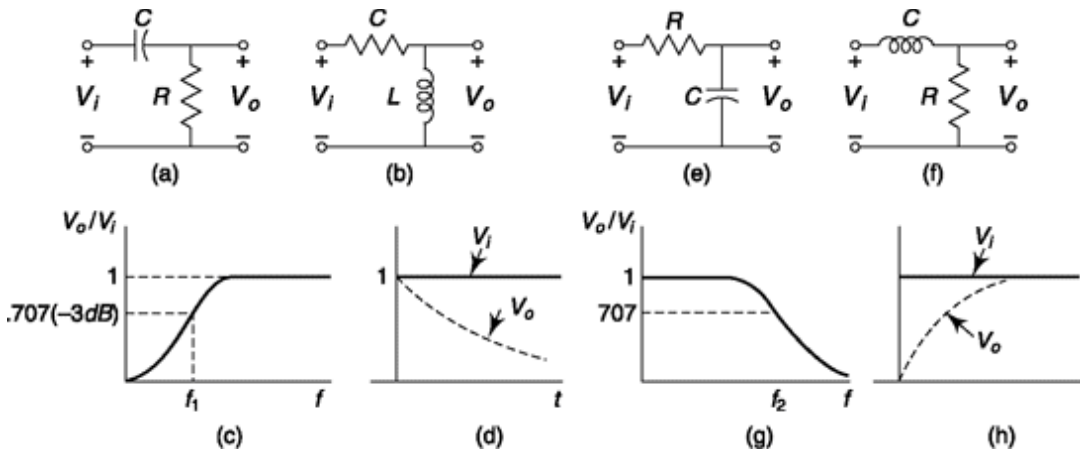


Fig. 6.24 Response of filters.

$t = RC$ or $t = L/R$. In either case $f_x t = 1/2p$. The response of the filters to an applied step voltage is, as shown, an exponential decay to zero voltage with time constant t .

The rudimentary low-pass filters are shown in Fig. 6.24e and f. The 3 dB frequency is now $f_2 = 1/2pRC$ or $f_2 = 1/2p(R/L)$ and the time constant is again $t = RC$ or $t = L/R$. The response to a step voltage is an exponential rise to the voltage of the step with a time constant t .

In Fig. 6.25, against the timing reference of a clock waveform, we have drawn an NRZ data stream which, at the transmitter, consists of alternating 1's and 0's and then a sustained sequence of 1's. We consider that the channel can be approximated by the high-pass filter shown in Fig. 6.24a. The dashed waveform is the received signal response. Note that when the transmitted signal V sustains a fixed level $+V_b$ or $-V_b$ the received signal V_o decays towards zero. So long as the fixed level is sustained for only one clock interval and assuming, as we have, that t and T_b are comparable, there is no serious deterioration of the signal. What starts out as a flat top develops a tilt but there will clearly be no difficulty in distinguishing a bit of logic level 1 from a bit of logic level 0. On the other hand, after a long sequence of 1's (or 0's) the received signal may approach so close to zero that, particularly in the presence of noise, a correct reading of the bit is not certain. This problem would not develop in biphase transmission where the transmitted waveform never sustains a fixed level for more than one clock cycle. (Quantitative details concerning the waveform in Fig. 6.25 including the displayed overshoots are left for a student exercise. See Prob. 6.60.)

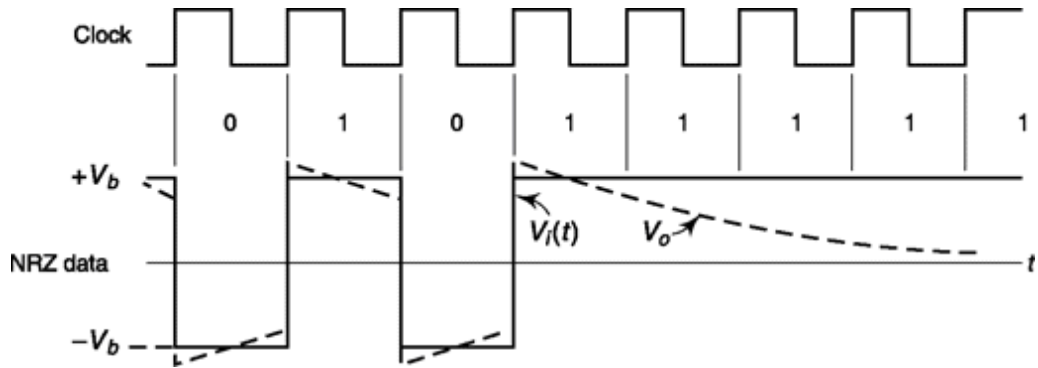


Fig. 6.25 Tilt of NRZ signal produced by high-pass filter.

In Fig. 6.26, we show a biphase data stream consisting of alternating 1's and 0's and then a sustained sequence of 1's. Let us here consider that the channel can be approximated by the low-pass filter shown in Fig. 6.24e. Again we see that the waveform is most adversely affected during a sequence of similar bits. Between transitions of the original waveform V the received waveform V_o heads asymptotically toward $+V_b$ or $-V_b$. When 1's and 0's alternate this asymptotic rise or fall can persist for a full clock period T_b . When 1's or 0's are sustained available time is reduced to one-half period.

Altogether, then, it appears that if a channel is able to transmit *direct current* and is limited at high frequencies, NRZ transmission may be advantageous. If, however, *dc* transmission is not possible, biphase transmission will be needed and we shall also have to take into account that a higher frequency cutoff will have to be provided. We may also note, incidentally, that the low-pass filter of Fig. 6.24b serves as an equivalent circuit for devices that involve magnetic circuits such as transformers, tape recorders, etc.

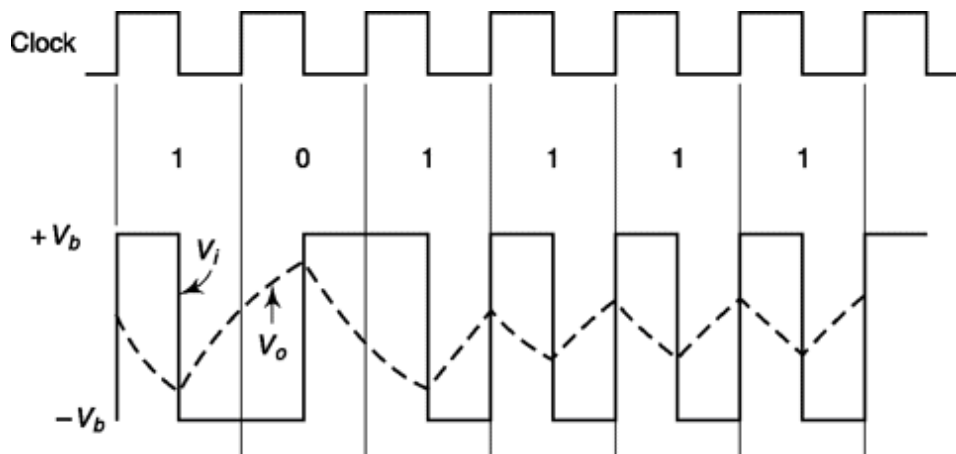


Fig. 6.26 Effect of biphase passed through a low-pass filter.

Example 6.18

Consider a random binary process X , synchronous with clock assumes any of the two values +1 or -1 with equal probability. At any clock trigger, arriving at an interval of T , the transition probabilities are also equal. Find autocorrelation function $R_X(t)$.

Solution

From Eq. (6.158),

$$\begin{aligned} \text{the PSD } G_X(f) &= V_b^2 T_b \left(\frac{\sin \pi f T_b}{\pi f T_b} \right)^2 \Big|_{V_b=1, T_b=T} \\ &= T \left(\frac{\sin \pi f T}{\pi f T} \right)^2 \end{aligned}$$

$$\text{Thus } R_X(\tau) = F^{-1}[G_X(f)]$$

$$= F^{-1} \left[T \left(\frac{\sin \pi f T}{\pi f T} \right)^2 \right] = \begin{cases} 1 - |\tau|T & |\tau| < T \\ 0 & |\tau| > T \end{cases}$$

[From Additional Problem 16 of Chapter 1]

Example 6.19

Consider a random process, $X(t) = A \cos(\omega t + \theta)$ where θ is a uniform random variable in the range $[-\pi, \pi]$ and A, ω are constant. Find if $x(t)$ is WSS.

Solution

Since θ is uniformly distributed, its pdf, $f_\theta(\theta) = \frac{1}{2\pi}$ for $-\pi \leq \theta \leq \pi$ and 0 elsewhere.

$$\text{Then, mean } m = E[X(t)] = \int_{-\infty}^{\infty} A \cos(\omega t + \theta) f_\theta(\theta) d\theta$$

$$= \frac{A}{2\pi} \cos(\omega t + \theta) d\theta = 0$$

And autocorrelation

$$\begin{aligned} R(\tau) &= E[X(t) X(t + \tau)] \\ &= \frac{A^2}{2\pi} \int_{-\pi}^{\pi} \cos(\omega t + \theta) \cos[\omega(t + \tau) + (\theta)] d\theta \\ &= \frac{A^2}{2\pi} \int_{-\pi}^{\pi} \frac{1}{2} [\cos \omega t + \cos(2\omega t + 2\theta + \omega\tau)] d\theta \\ &= \frac{A^2}{2} \cos \omega\tau \end{aligned}$$

Since, mean is constant and autocorrelation depends on time difference only, $x(t)$ is WSS.

Example 6.20

Given, a WSS random process $X(t)$ with mean $E[X(t)] = m$. This is applied as input to an LTI system with impulse response $h(t) = e^{-at} u(t)$. Find mean of the output.

Solution

1

From Example 1.18 of Chapter 1, $H(w) = \frac{1}{a + jw}$

If $Y(t)$ is output of LTI system, required mean $E[y(t)] = mH(0) = m/a$

Example 6.21

The message, a random process $M(t)$ is mixed with a white

channel noise $N(t)$. If $S_M(\omega) = \frac{I}{1 + \omega^2}$ and $S_N(\omega) = 0.2$,

- find optimal filter that maximizes output SNR. Is the filter realizable?

Solution

From Sec. 6.5.5,

$$H(\omega) = \frac{S_M(\omega)}{S_M(\omega) + S_N(\omega)}$$

$$= \frac{1}{1 + \omega^2}$$

Substituting, $H(\omega) = \frac{1}{1 + \omega^2} + 0.2$

$$= \frac{5}{6 + \omega^2} = \frac{5}{2\sqrt{6}} \cdot \frac{2\sqrt{6}}{(\sqrt{6})^2 + \omega^2}$$

$$\text{or } h(t) = \frac{5}{2\sqrt{6}} e^{-\sqrt{6}|t|}$$

[From Example 1.20 of Chapter 1.]

The filter is non-causal and hence not realizable [Refer to discussion on ideal and practical filter after Example 1.23 of Chapter 1]. However, a delayed truncated version of $h(t)$ can approximate optimal filter.

SELF-TEST QUESTIONS -

16. Can we say that random variables are instances of a random process (or stochastic process)?
17. For which random process ensemble average is always equal to time average - stationary or ergodic?
18. A NRZ signal passes 90 percent of power while passing through an ideal LPF filter of cut-off frequency f_b where clock frequency is f_b but biphase signal passes 70 percent. Is it correct?
19. Is a band pass signal defined by in-phase and in-quadrature components?
20. If the input to a linear system is Gaussian, the output need not be Gaussian. Is it true?

FACTS AND FIGURES -

The concept of negative numbers appears for the first time in history in the Chinese text *Nine Chapters on the Mathematical Art* that dates back to the Han Dynasty (202 BC-220 AD). In this text, two different colours were put to represent two types of numbers—red for positive and black for negative. The Indian mathematician Brahmagupta in a treatise written in 628 AD showed the use of negative numbers in the solution of quadratic equations. He termed positive numbers ‘fortunes’, negative numbers ‘debt’ and wrote, “A debt cut off from nothingness becomes a credit; a credit cut off from nothingness becomes a debt.”

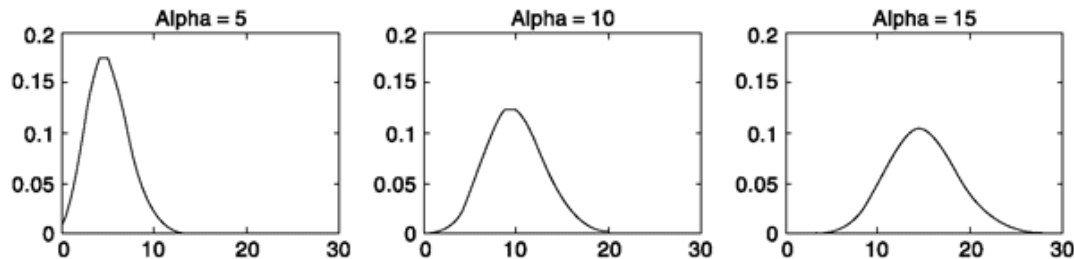
In Europe, Fibonacci used the concept of negative numbers in describing financial problems in his 1202 AD work. In the 15th century, Nicolas Chuquet used ‘absurd numbers’ that were nothing but negative numbers as

exponents. But till the 17th century, the concept of negative numbers were unwelcome among European mathematicians. Francis Maseres, an English mathematician, wrote in 1759 AD, “(The negative numbers) darken the very whole doctrines of the equations and make dark of the things which are in their nature excessively obvious and simple.”

Matlab —

Here we show simulation of different probability distribution functions, its histogram representation, calculation of autocorrelation by writing a MATLAB function and find relationship between autocorrelation and PSD.

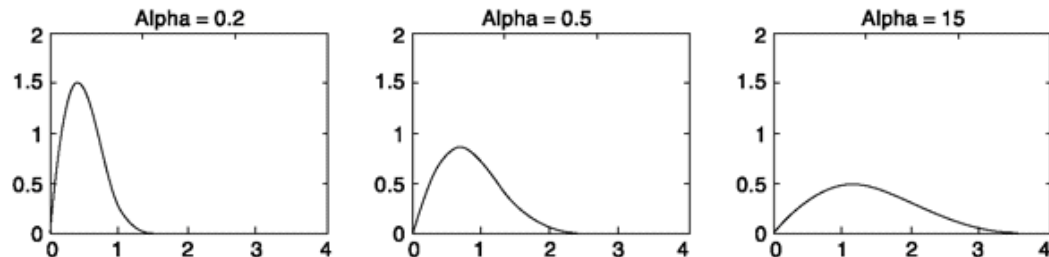
```
%Experiment 7
%Generating Poisson distribution function for different alpha
x = 0:30;
y = poisspdf(x,5); % poisspdf is in built function
subplot(131); plot(x,y); axis([0 30 0 0.2]);title ('alpha=5');
y = poisspdf(x,10);
```



```
subplot(132); plot(x,y), axis([0 30 0 0.2]);title ('alpha=10');
y = poisspdf(x,15);
subplot(133); plot(x,y), axis([0 30 0 0.2]);title ('alpha=15');
```

%Experiment 8

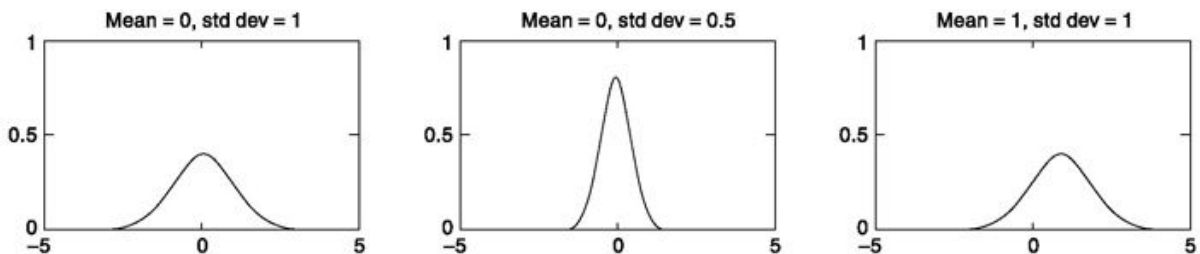
```
%Generating Rayleigh distribution function for different alpha
x = 0:0.05:4;
y = raylpdf(x,0.4); % raylpdf is in built function
subplot(131); plot(x,y); axis([0 4 0 2]);title ('alpha=0.4');
y = raylpdf(x,0.7);
subplot(132); plot(x,y), axis([0 4 0 2]);title ('alpha=0.7');
```



```
y = raylpdf(x,1.2);
subplot(133); plot(x,y), axis([0 4 0 2]);title ('alpha=1.2');
```

%Experiment 9

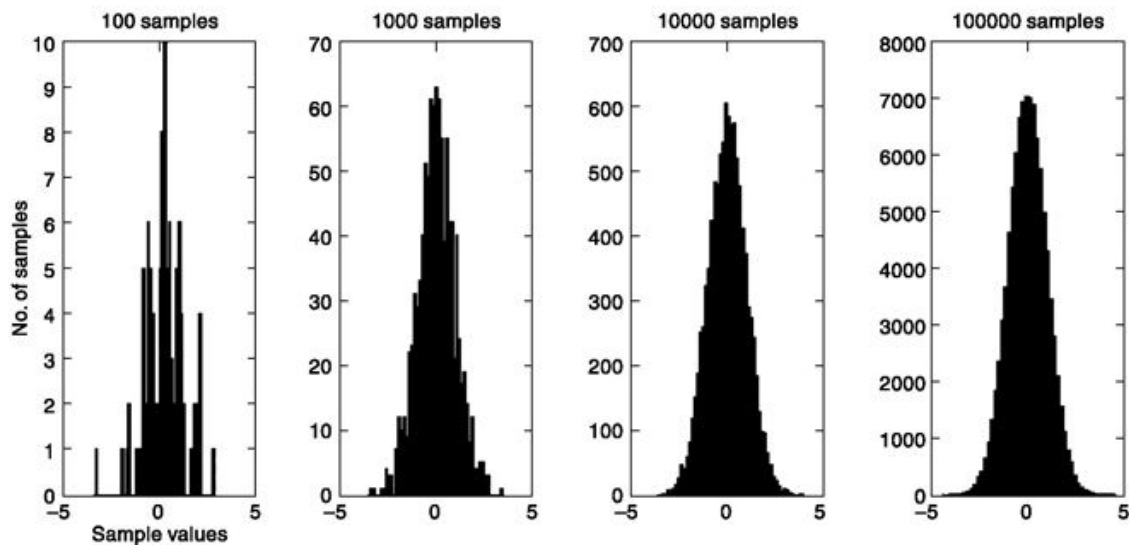
```
%Generating Gaussian distribution function for different alpha
x = -5:0.05:5;
y = normpdf(x,0,1); % mean=0, std deviation=1 normpdf is in built function
subplot(131); plot(x,y); axis([-5 5 0 1]);title ('mean=0, std dev=1');
y = normpdf(x,0,0.5);
subplot(132); plot(x,y), axis([-5 5 0 1]);title ('mean=0, std dev=0.5');
y = normpdf(x,1,1);
subplot(133); plot(x,y), axis([-5 5 0 1]);title ('mean=1, std dev=1');
```



```
% Experiment 10
```

```
% Generating sample values for random distribution and use of histogram
% that shows that when no. of samples are large the pdf is approximated.
% This is shown for normal(Gaussian distribution) but holds true for all.

y = normrnd(0,1,1,100); %Mean=0, std. =1, Generates data for 1 row, 100 col
x=min(y):(max(y)-min(y))/50:max(y); %Creates 51 equispaced bins
subplot(141); hist(y,x), title('100 samples')
xlabel('sample values'); ylabel('No. of samples')
```



```
y = normrnd(0,1,1,1000);
x=min(y):(max(y)-min(y))/50:max(y);
subplot(142); hist(y,x), title('1000 samples')
y = normrnd(0,1,1,10000);
x=min(y):(max(y)-min(y))/50:max(y);
subplot(143); hist(y,x), title('10000 samples')
y = normrnd(0,1,1,100000);
x=min(y):(max(y)-min(y))/50:max(y);
subplot(144); hist(y,x), title('100000 samples')
```

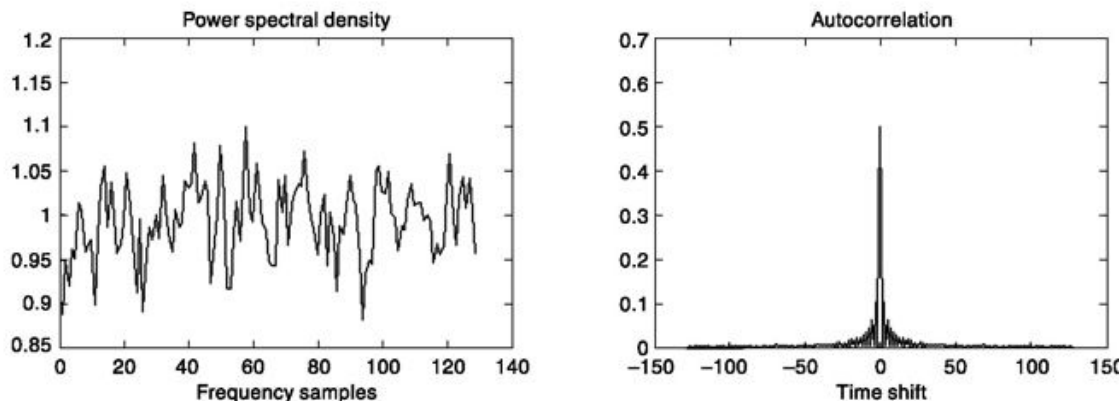
Note that total number of samples in each case (given as title to each plot) should be sum total of No. of samples contained in each of these 51 bins.

```

% Experiment 11
% Plotting power spectral density and autocorrelation function for
% normal(Gaussian) distribution

y = normrnd(0,1,1,100000); %Generates 100000 samples, mean=0, std. dev.=1
Gy=psd(y); % Returns power spectral density of Y, note that it is real +ve
Ry=abs(ifft(Gy,256)); % 256 points, abs. value as inv fft of real is complex
Ry=[Ry(130:256)' Ry(1:129)']; %Shifting the origin;
t=-127:1:128; %Defining time shift for autocorrelation function Ry
subplot(121); plot(Gy); xlabel('frequency samples'); title('Power spectral
density');
subplot(122); plot(t,Ry); xlabel('time shift'); title('Autocorrelation');

```



```

%Experiment 12a
% To write a function that calculates discrete time autocorrelation
% for a given time shift. This is used in Experiment 12.

function Rx=autocorr(x,t) % x=signal,t=time shift,Rx=autocorrelation value
le=length(x);

if t==0
x1=x; %No shift is necessary
Rx=x*x1'/(norm(x)*norm(x1)); %From definition, norm(x) returns magn. of x.
end

if t>0
x1=[x(t+1:le) zeros(1,t)]; % left shift
Rx=x*x1'/(norm(x)*norm(x1));
end

if t<0
t=-t; x1=[zeros(1,t) x(1:le-t)]; % right shift
Rx=x*x1'/(norm(x)*norm(x1));
end

% Experiment 12
% This generates autocorrelation value using function autocorr.m

```

SUMMARY

The chapter begins with a description of probability theory followed by a discussion of random variables and its properties. A short but useful discussion on commonly used probability distribution functions were presented next that includes Gaussian, Rayleigh, Rician, Poisson distribution. Random processes and its various classifications are discussed highlighting the relation between autocorrelation and power spectral density. A discussion on transmission of random process through linear time invariant system is followed by design of an optimal filter that minimizes total output power of the filter. Besides numerical examples, a large number of case studies from practical communication field have been taken up to illustrate various concepts and use of random variables and processes.

PROBLEMS

- 6.1 Six dice are thrown simultaneously. What is the probability that at least 1 die shows a 3?
- 6.2 A card is drawn from a deck of 52 cards.
 - (a) What is the probability that a 2 is drawn?
 - (b) What is the probability that a 2 of clubs is drawn?
 - (c) What is the probability that a spade is drawn?
- 6.3 A card is picked from each of four 52-card decks of cards.
 - (a) What is the probability of selecting at least one 6 of spades?
 - (b) What is the probability of selecting at least 1 card larger than an 8?

- 6.4 A card is drawn from a 52-card deck, and without replacing the first card a second card is drawn. The first and second cards are not replaced and a third card is drawn.
- If the first card is a heart, what is the probability of the second card being a heart?
 - If the first and second cards are hearts, what is the probability that the third card is the king of clubs?
- 6.5 Two factories produce identical clocks. The production of the first factory consists of 10,000 clocks of which 100 are defective. The second factory produces 20,000 clocks of which 300 are defective. What is the probability that a particular defective clock was produced in the first factory?
- 6.6 One box contains two black balls. A second box contains one black and one white ball. We are told that a ball was withdrawn from one of the boxes and that it turned out to be black. What is the probability that this withdrawal was made from the box that held the two black balls?
- 6.7 Two dice are tossed.
- Find the probability of a 3 and a 4 appearing.
 - Find the probability of a 7 being rolled.
- 6.8 A card is drawn from a deck of 52 cards, then replaced, and a second card drawn.
- What is the probability of drawing the same card twice?
 - What is the probability of first drawing a 3 of hearts and then drawing a 4 of spades?
- 6.9 A die is tossed and the number appearing is n_i . Let N be the random variable identifying the outcome of the toss defined by the specifications $N = n_i$ when n_i appears. Make a plot of the probability $P(N \leq n_i)$ as a function of n_i .
- 6.10 A coin is tossed four times. Let H be the random variable which identifies the number of heads which occur in these four tosses. It is defined by $H = h$, where h is the number of heads which appear. Make a plot of the probability $P(H \leq h)$ as a function of h .
- 6.11 A coin is tossed until a head appears. Let T be the random variable which identifies the number of tosses t required for the appearance of this first head. Make a plot of the probability $P(T \leq t)$ as a function of t up to $t = 5$.
- 6.12 An important probability density function is the Rayleigh density
- $$f(x) = \begin{cases} xe^{-x^2/2} & x \geq 0 \\ 0 & x < 0 \end{cases}$$
- Prove that $f(x)$ satisfies Eqs (6.20) and (6.21).
 - Find the distribution function $F(x)$.
- 6.13 Refer to Fig. 6.2.
- Find $P(2 < n \leq 11)$.
 - Find $P(2 \leq n < 11)$
 - Find $P(2 \leq n \leq 11)$.
 - Find $F(9)$.
- 6.14 Refer to the Rayleigh density function given in Prob. 6.12. Find the probability $P(x_1 < x \leq x_2)$, where $x_2 - x_1 = 1$, so that $P(x_1 < x \leq x_2)$ is a maximum. Hint: Find $P(x_1 < x \leq x_2)$; replace x_2 by $1 + x_1$, and maximize P with respect to x_1 .
- 6.15 Refer to the Rayleigh density function given in Prob. 6.12. Find
- $P(0.5 < x \leq 2)$.
 - $P(0.5 \leq x < 2)$.

- 6.16 The joint probability density of the random variables X and Y is $f(x, y) = ke^{-(x+y)}$ in the range $0 \leq x \leq \infty$, $0 \leq y \leq \infty$, and $f(x, y) = 0$ otherwise.
- Find the value of the constant k .
 - Find the probability density $f(x)$, the probability density of X independently of Y .
 - Find the probability $P(0 \leq X \leq 2; 2 \leq Y \leq 3)$.
 - Are the random variables dependent or independent?
- 6.17 X is a random variable having a Gaussian density. $E(X) = 0$, $\sigma_x^2 = 1$. V is a random variable having the values 1 or -1, each with probability $\frac{1}{2}$.
- Find the joint density $f_{X,V}(x, v)$.
 - Show that $f_V(v) = \int_{-\infty}^{\infty} f_{X,V}(x, v) dx$.
- 6.18 The joint probability density of the random variables X and Y is $f(x, y) = xe^{-x(y+1)}$ in the range $0 \leq x \leq \infty$, $0 \leq y \leq \infty$, and $f(x, y) = 0$ otherwise.
- Find $f(x)$ and $f(y)$, the probability density of X independently of Y and Y independently of X .
 - Are the random variables dependent or independent?
- 6.19 (a) In a communication channel as represented in Fig. 6.6 $P(r_0|m_0) = 0.9$, $P(r_1|m_0) = 0.1$, $P(r_0|m_1) = 0.4$, and $P(r_1|m_1) = 0.6$. On a single set of coordinate axes make plots of $P(m_0|r_0)$, $P(m_1|r_0)$, $P(m_0|r_1)$ and $P(m_1|r_1)$ as a function of $P(m_0)$. Mark the range of m_0 for which the algorithm of Eq. 6.38(a) and (b) prescribes that we choose m_0 if r_0 is received and m_1 if r_1 is received, the range for which we choose m_0 no matter what is received and the range for which we choose m_1 no matter what is received.
- (b) Calculate and plot the probability of error as a function of $P(m_0)$.
- 6.20 (a) For the channel and message probabilities given in Fig. P6.20, determine the best decisions about the transmitted message for each possible received response.

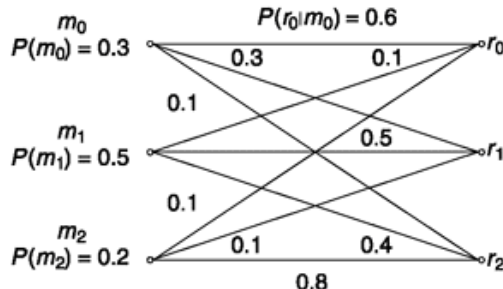


Fig. P6.20

- With decisions made as in part (a) calculate the probability of error.
- Suppose the decision-making apparatus at the receiver were inoperative so that at the receiver nothing could be determined except that a message had been received. What would be the best strategy for determining what message had been transmitted and what would be the corresponding error probability?

6.21 If $f_x(x) = \frac{1}{\sqrt{2\pi}} e^{-x^2/2}$ for all x , show that

- (a) $E(X^{2n}) = 1 \cdot 3 \cdot 5 \cdots (n-1)$, $n = 1, 2, \dots$
- (b) $E(X^{2n-1}) = 0$, $n = 1, 2, \dots$

6.22 Compare the most probable [$f(x)$ is a maximum] and the average value of X when

$$(a) f_{x_1}(x) = \frac{1}{\sqrt{2\pi}} e^{-(x-m)^2/2} \quad \text{for all } x$$

$$(b) f_{x_2}(x) = \begin{cases} xe^{-x^2/2} & \text{for } x \geq 0 \\ 0 & \text{elsewhere} \end{cases}$$

6.23 Calculate the variance of the random variables having densities:

$$(a) \text{ The Gaussian density } f_{x_1}(x) = \frac{1}{\sqrt{2\pi}} e^{-(x-m)^2/2}, \text{ all } x.$$

$$(b) \text{ The Rayleigh density } f_{x_2}(x) = xe^{-x^2/2}, x \geq 0.$$

$$(c) \text{ The uniform density } f_{x_3}(x) = 1/a, -a/2 \leq x \leq a/2.$$

6.24 Consider the Cauchy density function

$$f(x) = \frac{K}{1+x^2} \quad -\infty \leq x \leq \infty$$

(a) Find K so that $f(x)$ is a density function.

(b) Find $E(X)$.

(c) Find the variance of X . Comment on the significance of this result.

6.25 The random variable X has a variance σ^2 and a mean m . The random variable Y is related to X by $Y = aX + b$, where a and b are constants. Find the mean and variance of Y .

6.26 A probability density function $f(x)$ is uniform over the range from $-L$ to $+L$.

(a) Calculate and plot the probability $P[|x| \leq \varepsilon]$ as a function of ε .

(b) Calculate and plot the quantity σ^2/ε^2 and verify that Tchebycheff's rule is valid in this case.

6.27 Refer to the Gaussian density given in Eq. (6.58).

(a) Show that $E((X-m)^{2n-1}) = 0$.

(b) Show that $E((X-m)^{2n}) = 1 \cdot 3 \cdot 5 \cdots (n-1)\sigma^2$.

6.28 Given a Gaussian probability function $f(x)$ of mean value zero and variance σ^2 .

(a) As a function of σ , plot the probability $P[|x| \geq \varepsilon]$.

(b) Calculate and plot the quantity σ^2/ε^2 and verify that Tchebycheff's rule is valid in this case.

6.29 A random variable $V = b + X$, where X is a Gaussian distributed random variable with mean 0 and variance σ^2 , and b is a constant. Show that V is a Gaussian distributed random variable with mean b and variance σ^2 .

6.30 The joint density function of two dependent variables X and Y is

$$f(x, y) = \frac{1}{\pi\sqrt{3}} e^{-2(x^2-xy+y^2)/3}$$

(a) Show that, when X and Y are each considered without reference to the other, each is a Gaussian variable, i.e. $f(x)$ and $f(y)$ are Gaussian density functions.

(b) Find σ_x^2 and σ_y^2 .

6.31 Obtain values for and plot $\operatorname{erf} u$ versus u .

6.32 On the same set of axes used in Prob. 6.31 plot e^{-u^2} and $\operatorname{erfc} u$ versus u . Compare your results.

6.33 The probability

$$P_{\pm k\sigma} \equiv P(m - k\sigma \leq X \leq m + k\sigma) = \int_{m-k\sigma}^{m+k\sigma} \frac{e^{-(x-m)^2/2\sigma^2}}{\sqrt{2\pi}\sigma} dx$$

(a) Change variables by letting $u = x - m/\sqrt{2\sigma}$.

(b) Show that $P_{\pm k\sigma} = \operatorname{erf}(k/\sqrt{2})$.

6.34 Show that a random variable with a Rayleigh density as in Eq. (6.72) has a mean value $R = \sqrt{(\pi/2)\alpha}$, a mean square value $R^2 = 2\alpha^2$, and a variance $\sigma^2 = (2 - \pi/2)\alpha^2$.

6.35 (a) A voltage V is a function of time t and is given by

$$V(t) = X \cos \omega t + Y \sin \omega t$$

in which ω is a constant angular frequency and X and Y are independent Gaussian variables each with zero mean and variance σ^2 . Show that $V(t)$ may be written

$$V(t) = R \cos(\omega t + \Theta)$$

in which R is a random variable with a Rayleigh probability density and Θ is a random variable with uniform density.

(b) If $\sigma^2 = 1$, what is the probability that $R \geq 1$?

6.36 Derive Eq. (6.87) directly from the definition $\sigma_z^2 = E\{(Z - m_z)^2\}$.

6.37 $Z = X_1 + X_2 + \dots + X_N$, $E(X_i) = m$.

(a) Find $E(Z)$.

$$(b) \text{ If } E(X_i X_j) = \begin{cases} 1 & j = i \\ \rho & j = i \pm 1 \\ 0 & \text{otherwise} \end{cases}$$

find (1) $E(Z^2)$ and (2) σ_z^2 .

6.38 The independent random variables X and Y are added to form Z . If

$$f_X(x) = xe^{-x^2/2} \quad 0 \leq x \leq \infty \quad \text{and} \quad f_Y(y) = \frac{1}{2}e^{-|y|} \quad |y| < \infty$$

find $f_Z(z)$.

6.39 The independent random variables X and Y have the probability densities

$$\begin{aligned} f(x) &= e^{-x} & 0 \leq x \leq \infty \\ f(y) &= 2e^{-2y} & 0 \leq y \leq \infty \end{aligned}$$

Find and plot the probability density of the variable $Z = X + Y$.

6.40 The random variable X has a probability density uniform in the range $0 \leq x \leq 1$ and zero elsewhere. The independent variable Y has a density uniform in the range $0 \leq y \leq 2$ and zero elsewhere. Find and plot the density of $Z = X + Y$.

6.41 The N independent Gaussian random variables X_1, \dots, X_N are added to form Z . If the mean of X_i is 1 and its variance is 1, find $f_Z(z)$.

6.42 Two Gaussian random variables X and Y , each with mean zero and variance σ^2 , between which there is a correlation coefficient ρ , have a joint probability density given by

$$f(x, y) = \frac{1}{2\pi\sigma^2\sqrt{1-\rho^2}} \exp - \left[\frac{x^2 - 2\rho xy + y^2}{2\sigma^2(1-\rho^2)} \right]$$

(a) Verify that the symbol ρ in the expression for $f(x, y)$ is indeed the correlation coefficient. That is, evaluate $E\{XY\}/\sigma^2$ and show that the result is ρ as required by Eq. (6.104).

(b) Show that the case $\rho = 0$ corresponds to the circumstance where X and Y are independent.

6.43 The random variables X and Y are related to the random variable Θ by $X = \sin \Theta$ and $Y = \cos \Theta$. The variable Θ has a uniform probability density in the range from 0 to 2π . Show that X and Y are not independent but that, nonetheless, $E(XY) = 0$ so that they are uncorrelated.

6.44 The random variables X_1, X_2, X_3, \dots are dependent but uncorrelated. $Z = X_1 + X_2 + X_3 + \dots$. Show that $\sigma_z^2 = \sigma_1^2 + \sigma_2^2 + \sigma_3^2 + \dots$.

6.45 The random variables X_1, X_2, X_3 are independent and each has a uniform probability density in the range $0 \leq x \leq 1$. Find and plot the probability density of $X_1 + X_2$ and $X_1 + X_2 + X_3$.

6.46 Verify Eq. (6.132).

6.47 In a communication system used to transmit a sequence of messages, it is known that the error probability is 4×10^{-5} . A sample survey of N messages is made. It is required that, with a probability not to exceed 0.05, the error rate in the sample is not to be larger than 5×10^{-5} . How many messages must be included in the sample?

6.48 A communication channel transmits, in random order, two messages m_1 and m_2 . The message m_1 occurs three times more frequently than m_2 . Message m_1 generates a receiver response $r_1 = -1$ V while m_2 generates $r_2 = +1$ V. The channel is corrupted by noise n with a uniform probability density which extends from $n = -1.5$ V to $n = +1.5$ V.

(a) Find the probability that m_1 is mistaken for m_2 and the probability that m_2 is mistaken for m_1 .
(b) What is the probability that the receiver will determine a message correctly?

6.49 A communication channel transmits, in random order, two messages m_1 and m_2 with equal likelihood. Message m_1 generates response $r_1 = -1$ V at the receiver and message m_2 generates $r_2 = +1$ V. The channel is corrupted with Gaussian noise with variance $\sigma^2 = 1$ volt 2 . Find the probability that the receiver will determine a message correctly.

6.50 A communication channel transmits, in random order, two messages m_1 and m_2 . The message m_1 occurs three times more frequently than m_2 . Message m_1 generates a receiver response $r_1 = +1$ V while m_2 generates $r_2 = -1$ V. The channel is corrupted by noise n whose probability density has the triangular form shown in Fig. 6.17 with $f_N(n) = 0$ at $f_N(n) = -2$ V and at $f_N(n) = +2$ V.

(a) What are the ranges of r for which the decision is to be made that m_1 was transmitted and for which the decision is to be made that m_2 was transmitted?
(b) What is the probability that the message will be read correctly?

- 6.51 The function of time $Z(t) = X_1 \cos \omega_0 t - X_2 \sin \omega_0 t$ is a random process. If X_1 and X_2 are independent Gaussian random variables each with zero mean and variance σ^2 , find
 (a) $E(Z)$, $E(Z^2)$, σ_z^2 , and
 (b) $f_Z(z)$.
- 6.52 $Z(t) = M(t) \cos(\omega_0 t + \Theta)$. $M(t)$ is a random process, with $E(M(t)) = 0$ and $E(M^2(t)) = M_0^2$.
 (a) If $\Theta = 0$, find $E(Z^2)$. Is $Z(t)$ stationary?
 (b) If Θ is an independent random variable such that $f_\Theta(\theta) = 1/2\pi$, $-\pi \leq \theta \leq \pi$, show that $E(Z^2(t)) = E(M^2(t))E(\cos^2(\omega_0 t + \Theta)) = M_0^2/2$. Is $Z(t)$ now stationary?
- 6.53 Refer to Prob. 6.51. Find $R_z(\tau)$.
- 6.54 A random process $n(t)$ has a power spectral density $G(f) = \eta/2$ for $-\infty \leq f \leq \infty$. The random process is passed through a low-pass filter which has a transfer function $H(f) = 2$ for $-f_M \leq f \leq f_M$ and $H(f) = 0$ otherwise. Find the power spectral density of the waveform at the output of the filter.
- 6.55 White noise $n(t)$ with $G(f) = \eta/2$ is passed through a low-pass RC network with a 3 dB frequency f_c .
 (a) Find the autocorrelation $R(\tau)$ of the output noise of the network.
 (b) Sketch $\rho(\tau) = R(\tau)/R(0)$.
 (c) Find $\omega_c \tau$ such that $\rho(\tau) \leq 0.1$.
- 6.56 Consider a train of rectangular pulses. The k th pulse has a width τ and a height A_k . A_k is a random variable which can have the values 1, 2, 3, ..., 10 with equal probability. Assuming statistical independence between amplitudes and assuming that the average separation between pulses is T_s , find the power spectral density $G_n(f)$ of the pulse train.
- 6.57 A pulse train consists of rectangular pulses having an amplitude of 2 volts and widths which are either 1 μs or 2 μs with equal probability. The mean time between pulses is 5 μs . Find the power spectral density $G_n(f)$ of the pulse train.
- 6.58 Consider the power spectral density of an NRZ waveform as given by Eq. (6.158) and as shown in Fig. 6.22. By consulting a table of integrals, show that the power of the NRZ waveform is reduced by only 10 percent if the waveform is passed through an ideal low-pass filter with cutoff at $f = f_b$.
- 6.59 Consider the power spectral density of a biphase waveform as given by Eq. (6.161) and as shown in Fig. 6.23. By consulting a table of integrals, show that, if the waveform is passed through an ideal low-pass filter with cutoff at $2f_b$, 95 percent of the power will be passed. Show also that, if the filter cutoff is set at f_b , then only 70 percent of the power is transmitted.
- 6.60 An NRZ waveform consists of alternating 0's and 1's. The bit interval is 1 μs and the waveform makes excursions between +1 V and -1 V. The waveform is transmitted through an RC high-pass filter of time constant 1 μs . Draw the output waveform and calculate numerical values of all details of the waveform.
- 6.61 An NRZ waveform consists of alternating 0's and 1's. The bit interval is 1 μs and the waveform make excursions between +1 V and -1 V. The waveform is transmitted through an RC low-pass filter of time constant 1 μs . Draw the output waveform and calculate numerical values of all details of the waveform.
- 6.62 A random process $X(t)$ is defined as, $X(t) = A \cos(\omega t + \theta)$ where ω and θ are constant and A , a random variable uniformly distributed over $[-1, 1]$. Determine whether $X(t)$ is WSS.

Ans. No.

6.63 If $X(t)$ and $Y(t)$ are WSS random process show that $|R_{XY}(\tau)| \leq \sqrt{R_{XX}(0)R_{YY}(0)}$.

6.64 A WSS random process $X(t)$ with autocorrelation $R_{XX}(\tau) = 0.5e^{-2|\tau|}$ is fed as input to an LTI system with impulse response $h(t) = e^{-t}u(t)$. If $Y(t)$ is system output find its autocorrelation.

$$\text{Ans. } R_{YY}(\tau) = \frac{1}{3}e^{-|\tau|} - \frac{1}{6}e^{-2|\tau|}$$

6.65 The input $X(t)$ to a first-order RC low-pass filter is a white noise process as defined in Sec.

6.5.2. If $Y(t)$ is the output find its mean square value. Ans. $\frac{\eta}{4RC}$

6.66 A bandlimited random process $X(t)$ is defined within $|f| \leq B$ by white noise of PSD, $G(f) = \eta/2$. Find its autocorrelation function. Ans. $R_X(\tau) = \eta B \operatorname{sinc}(2\pi B\tau)$

REFERENCES

1. Mood, A., and F. Graybill: "Introduction to the Theory of Statistics," McGraw-Hill Book Company, New York, 1963.
2. Peirce, B O.: "A Short Table of Integrals," Ginn and Company, Boston, 1956.
3. Papoulis, A.: "Probability, Random Variables, and Stochastic Processes," McGraw-Hill Book Company, 1965.
4. Wozencraft, J and I Jacobs: "Communications Engineering," John Wiley and Sons, New York, 1966.

7

MATHEMATICAL REPRESENTATION OF NOISE

CHAPTER OBJECTIVE

In this chapter, we extend our discussion of the previous chapter to describe the random noise. The common sources of electrical noise affecting communication systems are usually modeled as Additive White Gaussian Noise (AWGN) that exhibits a flat power spectrum and Gaussian distribution of amplitude. We focus on this type of noise here and start with a discussion on sources of noise and frequency domain representation. A study on effect of filtering as noise passes through different processing blocks and superposition with other signals are presented. The chapter also discusses in depth the quadrature components of noise and its usefulness in describing narrowband noise. The orthonormal representation of noise shows that noise components that are orthogonal to a signal is irrelevant in the context. The chapter as a whole serves as foundation material to discuss effect of noise in analog and digital modulation or transmission which is taken up in subsequent chapters. Besides numerical examples, the chapter also presents MATLAB based simulations.

FACTS AND FIGURES

The Federal Standard 1037C of telecommunications standard relates various noise with different colours in the following way. The white noise has flat power density spectrum in linear frequency space, pink noise is flat in logarithmic frequency space, brown (or red) noise has power density decreasing in logarithmic frequency space at 6 dB per octave, for blue noise it increases at 3 dB per octave, for purple (or violet) it increases at 6 dB per octave rate, for grey noise it reduces first and then increases.

The most basic shot-noise statistics, namely the mean and variance, were reported by Campbell in 1909. In 1918, Schottky reported his investigation

on shot noise that comes from spontaneous current fluctuations in electric conductors. In 1944-45, Rice gave rigorous analysis of shot noise when the underlying Poisson process has a constant intensity. He showed that as the intensity tends to infinity, the probability distribution of the shot noise tends to a normal distribution.

7.1 SOME SOURCES OF NOISE

One source of noise is the constant agitation which prevails throughout the universe at the molecular level. Thus, a piece of solid metal may appear to our gross view to be completely at rest. We know, however, that the individual molecules are vibrating about their positions of equilibrium in a crystal lattice, and that the conduction electrons of the metal are wandering randomly throughout the volume of the metal. Similarly the molecules of an enclosed gas are in constant motion, colliding with one another and colliding also with the walls of the container. These agitations of molecules are called *thermal agitations* because they increase with temperature.

Let us consider a simple resistor. It is a resistor, or rather a conductor, because there are within it conduction electrons which are free to wander randomly through the entire volume of the resistor. On the average these electrons will be uniformly distributed through the volume, as will positive ions, and the entire structure will be electrically neutral. However, because of the random and erratic wanderings of the electrons, there will be *statistical fluctuations* away from neutrality. Thus at one time or another the distribution of charge may not be uniform, and a voltage difference will appear between the resistor terminals. The random, erratic, unpredictable voltage which so appears is referred to as *thermal resistor noise*. As is to be expected, thermal resistor noise increases with temperature. Resistor noise also increases with the resistance value of the resistor, being zero in a perfect conductor.

A second type of noise results from a phenomenon associated with the flow of current across semiconductor junctions. The charge carriers, electrons or holes, enter the junction region from one side, drift or are accelerated across the junction, and are collected on the other side. The average junction current determines the average interval that elapses between the times when two successive carriers enter the junction. However, the exact interval that elapses is subject to random statistical fluctuations. This randomness gives rise to a type of noise which is referred to as *shot*

noise. Shot noise is also encountered as a result of the randomness of emission of electrons from a heated surface and is consequently also associated with thermionic devices.

When a signal reaches a receiver it may well arrive very greatly attenuated. It is therefore necessary to provide amplification. This amplification is accomplished in circuits using active devices (transistors, etc.) and resistors. Hence, the signal becomes corrupted by *thermal* and *shot* noise. Even more, the signal may have been contaminated by noise as a result of many types of random disturbances superimposed on the signal during the course of its transfer over the communication channel. The contamination of the signal may take several forms. The noise may be added to the signal, in which case it is called *additive* noise, or the noise may multiply the signal, in which case the effect is called *fading*.

We shall confine our interest, for the most part, albeit not exclusively, to noise which may be described as an ergodic random process. The characteristic of ergodicity of interest here is that an ergodic process is also stationary, that is, statistical averages taken over an ensemble representing the processes yield a result that is independent of the time at which the averages are evaluated. We shall further assume, except where specifically noted, that the probability density of the noise is Gaussian. In very many communication systems and in a wide variety of circumstances the assumption of a Gaussian density is justifiable. On the other hand, it needs to be noted that such an assumption is hardly universally valid. For example, if Gaussian noise is applied to the input of a rectifier circuit, the output is not Gaussian. Similarly, it may well be that the noise encountered on a telephone line or on other channels consists of short, pulse-type disturbances whose amplitude distribution is decidedly not Gaussian.

7.2 FREQUENCY-DOMAIN REPRESENTATION OF NOISE

In a communication system noise is often passed through filters. These filters are usually described in terms of their characteristics in the frequency domain. Hence, to determine the influence of these filters on the noise, it is convenient to have a *frequency-domain characterization* of the noise.¹ We shall now establish such a frequency-domain characterization. On the basis of this representation we shall be able to define a *power spectral density* for a noise waveform that has characteristics similar to those of the power

spectral density of a deterministic waveform. Our discussion will be somewhat heuristic.

Let us select a particular sample function of the noise, and select from that sample function an interval of duration T extending, say, from $t = -T/2$ to $t = T/2$. Such a noise sample function $n^{(s)}(t)$ is shown in Fig. 7.1a. Let us generate, as in Fig. 7.1b, a periodic waveform in which the waveform in the selected interval is repeated every T seconds. This periodic waveform $n_T^{(s)}(t)$ can be expanded in a Fourier series, and such a series will properly represent $n^{(s)}(t)$ in the interval $-T/2$ to $T/2$. The fundamental frequency of the expansion is $Af = 1/T$, and, assuming no dc component, we have

$$n_T^{(s)}(t) = \sum_{k=1}^{\infty} (a_k \cos 2\pi k \Delta f t + b_k \sin 2\pi k \Delta f t) \quad (7.1)$$

or alternately

$$n_T^{(s)}(t) = \sum_{k=1}^{\infty} c_k \cos (2\pi k \Delta f t + \theta_k) \quad (7.2)$$

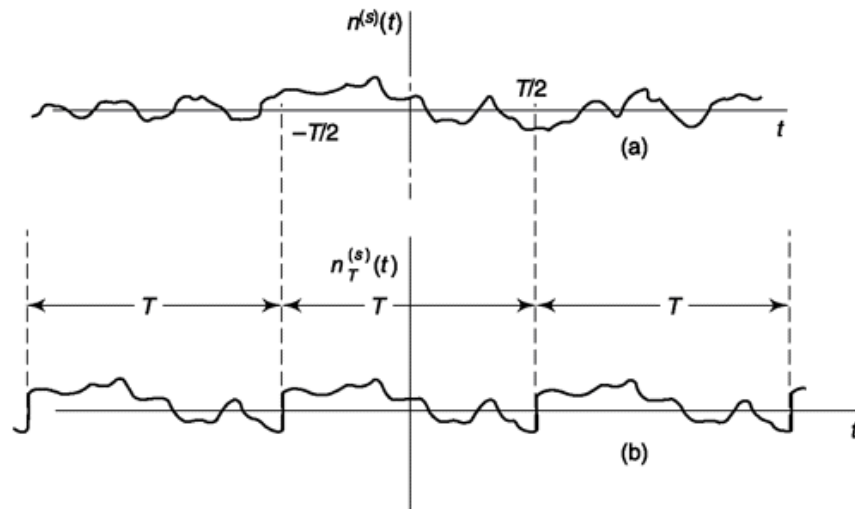


Fig. 7.1 (a) A sample noise waveform. (b) A periodic waveform is generated by repeating the interval in (a) from $-T/2$ to $T/2$.

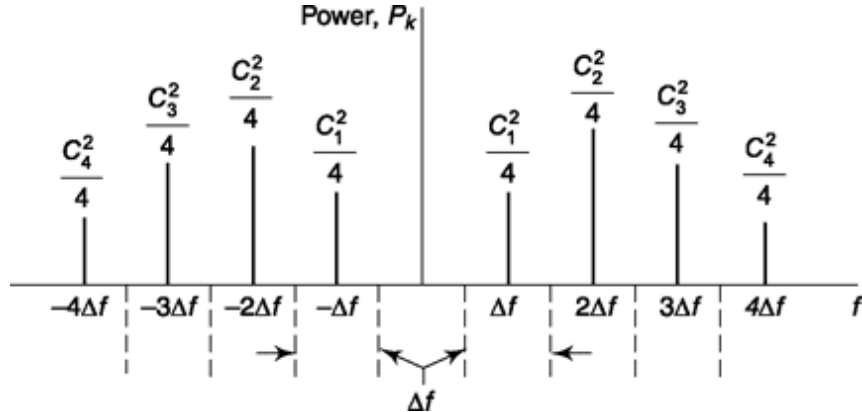


Fig. 7.2 The power spectrum of the waveform n_T .

in which a_k , b_k and c_k are the constant coefficients of the spectral terms and d_k is a phase angle. Of course,

$$c_k^2 = a_k^2 + b_k^2 \quad (7.3)$$

and

$$\theta_k = -\tan^{-1} \frac{b_k}{a_k} \quad (7.4)$$

The power spectrum of the expansion is shown in Fig. 7.2. The power associated with each spectral term is $c_k^2/2 = (a_k^2 + b_k^2)/2$. Since a two-sided spectrum is shown, each power spectral line is of height $c_k^2/4$. The frequency axis has been marked off in intervals Δf , and a power spectral line is located at the center of each interval. We now define the power spectral density at the frequency $k \Delta f$ as the quantity

$$G_n(k \Delta f) \equiv G_n(-k \Delta f) \equiv \frac{c_k^2}{4 \Delta f} = \frac{a_k^2 + b_k^2}{4 \Delta f} \quad (7.5)$$

The total power P_k associated with the frequency interval Δf at the frequency $k \Delta f$ is

$$P_k = 2G_n(k \Delta f) \Delta f \quad (7.6)$$

One-half of the power, $P_k/2 = G_n(k \Delta f) \Delta f$, is associated with a spectral line at frequency $k \Delta f$, the other half with a line at frequency $-k \Delta f$. Thus $G_n(k \Delta f) \equiv G_n(-k \Delta f)$ is equal to the power in the positive or negative interval divided by the size of the interval. Hence, $G_n(k \Delta f)$ is the (two-sided) mean power spectral density within each interval.

For a particular sample function of the noise one obtains specific values of coefficients a_k and b_k in Eq. (7.1) [or coefficients c_k and angles θ_k in Eq. (7.2)]. Different sample functions will result in different coefficients. If we propose that the representations of Eq. (7.1) or (7.2) are to represent generally the random process under discussion, i.e., the periodic noise, we need but consider that the a_k 's, b_k 's, c_k 's and θ_k 's are not fixed numbers but are instead *random variables*. Finally, let us allow that $T \rightarrow \infty$ ($\Delta f \rightarrow 0$), so that the periodic sample functions of the noise revert to the actual noise sample functions. We then have that the noise $n(t)$ is to be represented as

$$n(t) = \lim_{\Delta f \rightarrow 0} \sum_{k=1}^{\infty} (a_k \cos 2\pi k \Delta f t + b_k \sin 2\pi k \Delta f t) \quad (7.7)$$

or as

$$n(t) = \lim_{\Delta f \rightarrow 0} \sum_{k=1}^{\infty} c_k \cos(2\pi k \Delta f t + \theta_k) \quad (7.8)$$

We continue to accept Eq. (7.5) as the definition of the power spectral density of the noise $n(t)$, except that we now replace c_k^2 by $\overline{c_k^2}$, that is, by the expected or ensemble average value of the square of the random variable c_k . Further, as $\Delta f \rightarrow 0$, the discrete spectral lines get closer and closer, finally forming a continuous spectrum. In Eq. (7.5) we therefore replace $k \Delta f$ by the continuous frequency variable f . From Eq. (7.3), we also have that

$$\overline{c_k^2} = \overline{a_k^2} + \overline{b_k^2} \quad (7.9)$$

so that finally Eq. (7.5) becomes

$$G_n(f) = \lim_{\Delta f \rightarrow 0} \frac{\overline{c_k^2}}{4\Delta f} = \lim_{\Delta f \rightarrow 0} \frac{\overline{a_k^2} + \overline{b_k^2}}{4\Delta f} \quad (7.10)$$

Note that the power in the frequency range from f_1 to f_2 is

$$P(f_1 \rightarrow f_2) = \int_{-f_2}^{-f_1} G_n(f) df + \int_{f_1}^{f_2} G_n(f) df = 2 \int_{f_1}^{f_2} G_n(f) df \quad (7.11)$$

while the total power P_T is

$$P_T = \int_{-\infty}^{\infty} G_n(f) df = 2 \int_0^{\infty} G_n(f) df \quad (7.12)$$

7.2.1 The Effect of Filtering on probability Density of Gaussian Noise

We shall now show that if, as in Fig. 7.3a, Gaussian noise $n_l(t)$ is applied to the input of a filter, the output noise $n_o(t)$ is also Gaussian. Let the impulse response of the filter be $h(t)$. Then, applying

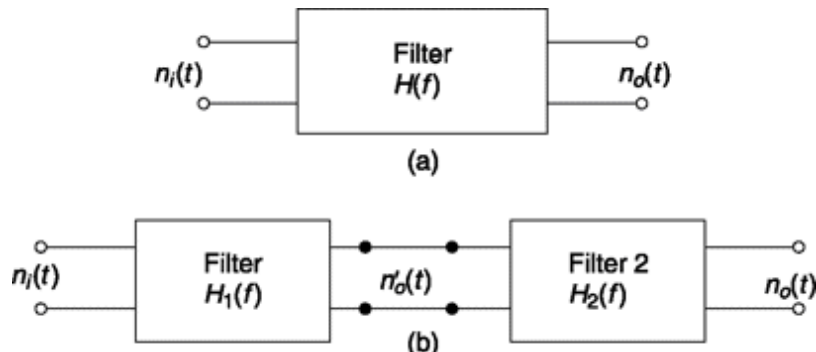


Fig. 7.3 (a) Gaussian noise (t) is applied to a linear filter whose output is $n_o(t)$. (b) The filter in (a) is split into two parts.

Eq. (1.131) to the present situation, we have that

$$n_o(t) = \int_{-\infty}^{\infty} n_i(\tau)h(t - \tau) d\tau = \int_{-\infty}^t n_i(\tau)h(t - \tau) d\tau \quad (7.13)$$

In Eq. (7.13), we have taken cognizance of the fact that, in general, the upper limit may actually be set at $\tau = t$, since the variable of integration is τ and $h(t - \tau) = 0$ for $\tau > t$. Equation (7.13) expresses the output $n_o(t)$ as the superposition of a succession of impulses of strength $n_i(\tau) d\tau$ applied at the filter input. This point is emphasized by rewriting Eq. (7.13) in the form

$$n_o(t) = \lim_{\Delta\tau \rightarrow 0} \sum_{k=-\infty}^{k=t/\Delta\tau} n_i(k \Delta\tau)h(t - k \Delta\tau) \Delta\tau \quad (7.14)$$

in which k ranges over integral values. In the limit $k \Delta\tau$ reverts to the continuous variable τ , and the summation reverts to the integral. In Eq. (7.14), $n_i(k \Delta\tau)$ is a random variable. That is, the noise is represented by an ensemble of sample functions, and the value of $n_i(k \Delta\tau)$ depends on the sample function we consider. On the other hand, the quantities $h(t - k \Delta\tau)$ are fixed, deterministic numbers, regulated by the nature of the filter.

Let us assume that the input noise is white and Gaussian. Then, as discussed in Sec. 6.5.1, the past history of the noise waveform provides no information about its future behavior. That is to say, on any one sample noise waveform of the ensemble, successive noise voltage values are independent of one another no matter how small the interval $\Delta\tau$ between voltage determinations. Hence, the random variables $n_i(k \Delta\tau)$ and $n_i(l \Delta\tau)$ are independent except for the case where $k = l$. Thus, at any time, with $t = t_0$, $n_o(t) = n_o(t_0)$, as given by Eq. (7.14), is a linear superposition of independent Gaussian random variables. Hence, as discussed in Sec. 6.4.2, $n_o(t_0)$ is a Gaussian random variable, and $n_o(t)$ is a Gaussian random process.

Now suppose that the filter of transfer function $H(f)$ is split into two parts, as shown in Fig. 7.3b, with $H(f) = H_1(f)H_2(f)$. Then if $n_i(t)$ is white and Gaussian, both $n'_o(t)$ and $n_o(t)$ are, on the basis of the above discussion, Gaussian, albeit, in general, not white. Further, since both $n'_o(t)$ and $n_o(t)$ are Gaussian, we have the result that nonwhite Gaussian noise, when applied to a linear filter, yields an output noise which is again Gaussian. Strictly, we have established this last result only for the case where the nonwhite Gaussian noise input is itself derived by filtering white noise. But this result is quite general for our purposes.

Equation (7.14) may be applied directly to filter 2 in Fig. 7.3b by simply replacing the impulses $n_i(k \Delta\tau)$ by the impulses $n'_i(k \Delta\tau)$. However, since $n'_o(t)$ is not white noise, successive noise voltage values are *not* independent of one another; that is, the random variable $n'_o(k \Delta\tau)$ and $n'_o(l \Delta\tau)$ are Gaussian but not independent. Nonetheless, we found that $n_o(t)$ is Gaussian. Hence we deduce that a linear superposition of *dependent* Gaussian random variables is still Gaussian.

7.2.2 Spectral Components of Noise

We have represented noise $n(t)$ as a superposition of noise spectral components. The spectral component associated with the k th frequency interval is given, in the limit as $Df \rightarrow 0$, by $n_k(t)$ written as

$$n_k(t) = a_k \cos 2\pi k \Delta f t + b_k \sin 2\pi k \Delta f t \quad (7.15)$$

or as

$$n_k(t) = c_k \cos (2\pi k \Delta f t + \theta_k) \quad (7.16)$$

The spectral components which compose a deterministic waveform are themselves deterministic. The spectral components, as in the present case, which compose noise, are themselves random processes. Thus, in Eqs (7.15) and (7.16), a_k , b_k , c_k , and θ_k are random variables, and $n_k(t)$ represents an ensemble of sample functions, one sample function for each possible set of values of a_k and b_k or of c_k and θ_k . The sample functions are each deterministic waveforms. They are, as a matter of fact, pure sinusoids differing from one another in phase and amplitude, depending on the value of θ_k and c_k . The random process $n_k(t)$ is stationary; that is, its statistical properties do not change with time. However, it is not ergodic; that is, the time averages of the individual sample function of the ensemble are different from one another.

We now look at some of the properties of the random variables a_k and b_k . The normalized power P_k (variance) of $n_k(t)$ is determined by taking the average over the *ensemble* of $[n_k(t)]^2$. We find from Eq. (7.15), that

$$\begin{aligned} P_k = \overline{[n_k(t)]^2} &= \overline{a_k^2} \cos^2 2\pi k \Delta f t + \overline{b_k^2} \sin^2 2\pi k \Delta f t \\ &\quad + 2\overline{a_k b_k} \sin 2\pi k \Delta f t \cos 2\pi k \Delta f t \end{aligned} \quad (7.17)$$

As noted, $n_k(t)$ is a stationary process, so that $\overline{[n_k(t)]^2}$ does not depend on the time selected for its evaluation. We are therefore at liberty to evaluate P_k by substituting in Eq. (7.17) a value $t = t_1$ for which $\cos 2\pi k \Delta f t_1 = 1$, in which case $\sin 2\pi k \Delta f t_1 = 0$. We then have

$$P_k = \overline{a_k^2} \quad (7.18)$$

Similarly we may show that $P_k = \overline{b_k^2}$ so that

$$\overline{a_k^2} = \overline{b_k^2} \quad (7.19)$$

From Eqs (7.6), (7.9), (7.18), and (7.19) we have

$$P_k = 2G_n(k \Delta f) \Delta f = 2G_n(-k \Delta f) \Delta f = \overline{a_k^2} = \overline{b_k^2} = \frac{\overline{a_k^2}}{2} + \frac{\overline{b_k^2}}{2} = \frac{\overline{c_k^2}}{2} \quad (7.20)$$

Since $\overline{a_k^2} = \overline{b_k^2}$ Eq. (7.17) may be written as

$$P_k = \overline{a_k^2} (\cos^2 2\pi k \Delta f t + \sin^2 2\pi k \Delta f t) + 2\overline{a_k b_k} \sin 2\pi k \Delta f t \cos 2\pi k \Delta f t \quad (7.21a)$$

Thus

$$P_k = \overline{a_k^2} + 2\overline{a_k b_k} \sin 2\pi k \Delta f t \cos 2\pi k \Delta f t \quad (7.21b)$$

We note, however, from Eq. (7.18) that $P_k = \overline{a_k^2}$ independently of time. In order that Eq. (7.21a) be consistent with this result, we require that

$$\overline{a_k b_k} = 0 \quad (7.22)$$

Thus, the coefficients a_k and b_k are *uncorrelated*.

We may also establish that the coefficients a_k and b_k are Gaussian. For this purpose we use Eq. (7.15) and substitute for t a value $t = t_1$, for which $\cos 2\pi k \Delta f t_1 = 1$ and $\sin 2\pi k \Delta f t_1 = 0$. Then

$$n_k(t_1) = a_k \quad (7.23)$$

Now $n_k(t_1)$ is a Gaussian random variable. We have this result from the consideration that $n_k(t)$ may be viewed as the output of a very narrowband filter whose input is Gaussian noise. As discussed in Sec. 7.2.1 such a noise output is Gaussian, and the noise voltage at any time, as at $t = t_1$ above, has a Gaussian probability density. Hence, Eq. (7.23) says that a_k is also a Gaussian random variable. It is, of course, similarly established that b_k is Gaussian.

We note also that since $n_k(t)$ is the output of a narrowband filter at frequency $k \Delta f$, it has no dc component. Hence, from Eq. (7.23) a_k has no dc component; that is, $\overline{a_k} = 0$, and, of course, similarly $\overline{b_k} = 0$.

Finally, let us consider two spectral components of noise, one at frequency $k \Delta f$ and the other at frequency $l \Delta f$. Then

$$n_k(t) = a_k \cos 2\pi k \Delta f t + b_k \sin 2\pi k \Delta f t \quad (7.24)$$

and

$$n_l(t) = a_l \cos 2\pi l \Delta f t + b_l \sin 2\pi l \Delta f t \quad (7.25)$$

If we form the product $n_k(t)n_l(t)$ from Eqs (7.24) and (7.25), we find that the product has four terms (products of sinusoids), all of which are time-dependent, provided that $k \neq l$. The coefficients of these terms are $a_k a_l$, $a_k b_l$, $b_k a_l$, and $b_k b_l$. Now let us take the ensemble average of the product, that is, $\overline{n_k(t)n_l(t)}$. Then, again, because of the stationary character of the random processes involved, this ensemble average must be time-independent. Hence, we have that

$$\overline{a_k a_l} = \overline{a_k b_l} = \overline{b_k a_l} = \overline{b_k b_l} = 0 \quad (7.26)$$

That is, each of the coefficients a_k and b_k is uncorrelated with each of the coefficients a_l and b_l .

In summary, we find that we have described noise in the following manner. Noise $n(t)$ is a Gaussian, ergodic, random process. It may be represented as a linear superposition of spectral components of the form given in Eq. (7.15) with the understanding, of course, that the description becomes more precise as $\Delta f \rightarrow 0$. The coefficients a_k and b_k are Gaussian random variables of average value zero and equal variance (normalized power) related to the two-sided power spectral density as in Eq. (7.20). The coefficients a_k and b_k are uncorrelated with one another and are uncorrelated also with the coefficients of a spectral component at a different frequency.

We may now deduce some statistical characteristics of interest concerning the c_k 's and θ_k 's in the noise spectral component representation of Eq. (7.16). We note from Eqs (7.3) and (7.4) that the c_k 's and θ_k 's are related to the a_k 's and b_k 's in precisely the manner in which the random variables R and θ of Sec. 6.3.3 are related to the Gaussian variables X and Y . From the results of Sec. 6.3.3 we find (Prob. 7.5) that the c_k 's have a Rayleigh probability density

$$f(c_k) = \frac{c_k}{P_k} e^{-ck^2/2P_k} \quad c_k \geq 0 \quad (7.27)$$

where P_k [Eq. (7.20)] is the normalized power in the spectral range Δf at the frequency $k \Delta f$. Similarly, the angle θ_k has a uniform probability density

$$f(\theta_k) = \frac{1}{2\pi} \quad -\pi \leq \theta_k \leq \pi \quad (7.28)$$

Furthermore, the amplitude c_k and phase θ_k are independent of one another and are independent as well of the amplitude and phase of a spectral component at a different frequency.

7.2.3 Response of a Narrowband Filter to Noise

If the representation of noise as a superposition of spectral components is a reasonable one, we should expect that when noise is passed through a narrowband filter the output of the filter should look rather like a sinusoid. We find that such is indeed the case, for we find that the output of a narrowband filter with noise input has the appearance shown in Fig. 7.4. The output waveform looks like a sinusoid except that, as expected, the amplitude varies randomly. The spectral range of the *envelope* of the filter output encompasses the spectral range from $-B/2$ to $B/2$, where B is the filter bandwidth. The average frequency of the waveform is the center frequency f_c of the filter. If $B \gg f_c$, the envelope changes very “slowly” and makes an appreciable change only over many cycles. Thus, while the spacings of the *zero crossings* of the waveform are not precisely constant, the change from cycle to cycle is small and when averaged over many cycles is quite constant at the value $1/2f_c$. Finally, we may note that as B becomes progressively smaller, so also does the average amplitude, and the waveform becomes more and more sinusoidal.

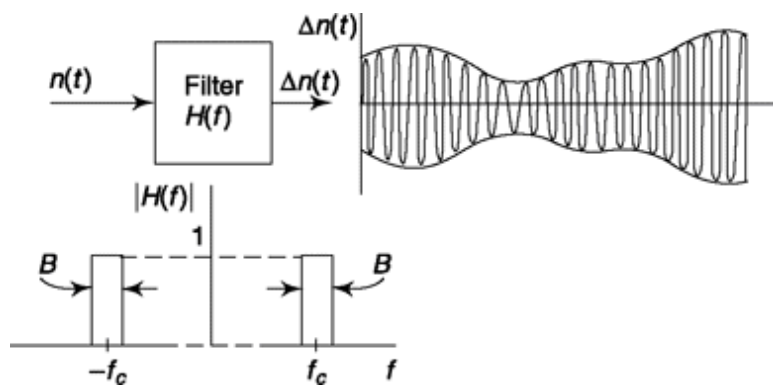


Fig. 7.4 Response of a narrowband filter to noise.

7.2.4 Effect of a Filter on psD of Noise

Let a spectral component of noise $n_k(t)$ given by Eq. (7.15) be the input to a filter whose transfer function at the frequency $k \Delta f$ is

$$H(k \Delta f) = |H(k \Delta f)| j = |H(k \Delta f)| / j \quad (7.29)$$

The corresponding output spectral component of noise will be $n_{k_o}(t)$

$$n_{k_o}(t) = |H(k \Delta f)| a_k \cos(2pk \Delta f t + j) + |H(k \Delta f)| b_k \sin(2pk \Delta f t + j) \quad (7.30)$$

The power P_{k_i} associated with $n_{k_i}(t)$ is, from Eq. (7.20),

$$P_{k_i} = \frac{\overline{a_k^2} + \overline{b_k^2}}{2} \quad (7.31)$$

Since $|H(k \Delta f)|$ is a deterministic function, $\overline{[|H(k \Delta f)| a_k]^2} = |H(k \Delta f)|^2 \overline{a_k^2}$ and $\overline{[|H(k \Delta f)| b_k]^2} = |H(k \Delta f)|^2 \overline{b_k^2}$. Hence, comparing Eq. (7.30) with Eq. (7.15), we find that the power P_{k_o} associated with $n_{k_o}(t)$ is

$$P_{k_o} = |H(k \Delta f)|^2 \frac{\overline{a_k^2} + \overline{b_k^2}}{2} \quad (7.32)$$

Finally, then, from Eqs (7.31) and (7.32), using also Eq. (7.20), we have that the power spectral densities at input and output, $G_{n_i}(k \Delta f)$ and $G_{n_o}(k \Delta f)$, are related by

$$G_{n_o}(k \Delta f) = |H(k \Delta f)|^2 G_{n_i}(k \Delta f) \quad (7.33)$$

In the limit as $\Delta f \rightarrow 0$ and $k \Delta f$ is replaced by a continuous variable f , Eq. (7.33) becomes

$$G_{n_o}(f) = |H(f)|^2 G_{n_i}(f) \quad (7.34)$$

Note the similarity between this result and Eq. (1.81), which applies to a deterministic waveform.

We got this relation by convolution for a transmission of a random process through a linear system in Sec. 6.5.6.

SELF-TEST QUESTION

1. Which of thermal noise and shot noise is related to non-uniform distribution of charge on a conductor due to random, erratic wandering of electrons?
2. Is it true that both white and non-white Gaussian noise input to a filter produce a non-white Gaussian noise at its output?
3. Which of Rayleigh and uniform probability density is followed by magnitude part of Gaussian noise spectrum?
4. If noise is fed as input to a narrowband filter, it gives a sinusoid like output. Is that correct?

5. Does PSD estimation of output of a filter follow similar mathematical relation for both deterministic and noise input?

Example 7.1

Explain the difference between white and nonwhite Gaussian noise.

Solution

If $X(t_1)$ and $X(t_2)$ two independent zero mean random process then from Eq. (6.101)

$$E[X(t_1)X(t_2)] = E[X(t_1)]E[X(t_2)] = 0 \quad \text{for } t_1 \neq t_2$$

$$\text{Now, } R_{XX}(t_1, t_2) = E[X(t_1)X(t_2)]$$

$$\begin{aligned} \text{or } R_{XX}(\tau) &= E[X(t)X(t + \tau)] \quad \text{putting } t_1 - t_2 = \tau \\ &= R_{XX}(0)\delta(\tau) \end{aligned}$$

The PSD of $X(t)$ from Fourier transform of $R_{XX}(\tau)$ is given by $S_{XX}(f) = R_{XX}(0) = \text{constant over all frequency}$ and hence called white.

The above independence condition if maintained by any noise generating random process including

Gaussian will give flat white noise spectrum. In Gaussian noise, if this condition is maintained we get white Gaussian noise but if not, e.g. passing it through a filter (has memory) we get nonwhite Gaussian noise.

Note that, if the noise instances are independent as above but not zero mean (e.g. digital unipolar signal) then the spectrum will appear flat but a large dc or zero frequency component will accompany. (Refer to MATLAB Experiment 33 at the end of this chapter.)

Example 7.2

The autocorrelation function of a noise signal is triangular and defined as

$$R_n(\tau) = \begin{cases} (1-|\tau|) & \text{for } |\tau| < 1 \\ 0 & \text{for } |\tau| > 1 \end{cases}$$

Find its noise spectrum.

Solution

Noise power spectrum is obtained by Fourier transform of $R_n(\tau)$. Refer to Fig. 7.5. The triangular signal

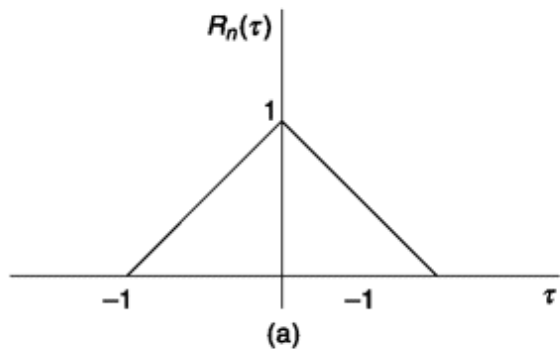


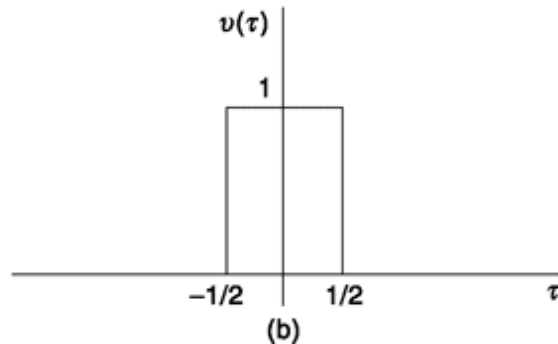
Fig. 7.5 Noise signal for Example 7.2

in Fig. 7.5a can be obtained by convolving two rectangular pulses each of which is as shown in Fig. 7.5b. Note that, the width of the rectangular pulse is 1/2 as convolution does expand the signal. (Refer to Sec. 1.2.3 and Example 1.7 of Chapter 1.)

Since, convolution in time domain is equivalent to multiplication in frequency domain, we'll get necessary noise power spectrum by squaring the Fourier transform of the rectangular pulse of Fig. 7.5b.

$$\begin{aligned} \text{Now, } V(f) &= \int_{-\infty}^{\infty} v(\tau) e^{-j2\pi f\tau} d\tau \\ &= \int_{-1/2}^{1/2} 1 \cdot e^{-j2\pi f\tau} d\tau \\ &= \frac{e^{-j2\pi f\tau}}{j2\pi f} \Big|_{-1/2}^{1/2} = \frac{\sin \pi f}{\pi f} = \text{sinc}(f) \end{aligned}$$

Then power spectrum, $G_n(f) = V(f) \times V(f) = \text{sinc}^2(f)$



7.3 SUPERPOSITION OF NOISES

The power spectral density was introduced in Sec. 1.3.4 and also discussed in previous section. The concept of a power spectrum is useful because it allows us to resolve a deterministic waveform, or a random process, $f(t)$ into a sum

$$f(t) = f_1(t) + f_2(t) + \dots \quad (7.35)$$

in such a manner that *superposition of power* applies, i.e. the power off(t) is the sum of the powers of $f_1(t)$, $f_2(t)$,.... When a deterministic waveform is resolved into a series of spectral components, superposition of power applies

because of the orthogonality of spectral components of different frequencies. This point was discussed in Sec. 1.3.3.

We have also represented a noise waveform as a superposition of spectral components, all of which are harmonics of some fundamental frequency Df which, in the limit, approaches zero. Hence,

up to the present point, this feature alone would have been enough to justify superposition of noise power as expressed in Eqs (7.11) and (7.12). But suppose that we have two noise processes $n_1(t)$ and $n_2(t)$, whose spectral ranges overlap in part or in their entirety. Then the power P_{12} of the sum $n_x(t) + n_2(t)$ would be

$$P_{12} = E\{[n_1(t) + n_2(t)]^2\} = E[n_1^2(t)] + E[n_2^2(t)] + 2E[n_1(t)n_2(t)] \quad (7.36a)$$

$$= P_1 + P_2 + 2E[n_1(t)n_2(t)] \quad (7.36b)$$

where P_1 and P_2 are the powers, respectively, of the noise processes $n_x(t)$ and $n_2(t)$, and $\leq[n_x(t) n_2(t)]$, which is the expected value of the product, is the *cross correlation* of the processes. Thus, superposition of power, $P_{12} = P_1 + P_2$, continues to apply, provided the processes are *uncorrelated*. Such would be the case, for example, if $n_x(t)$ and $n_2(t)$ were the thermal noises of two different resistors even in the same frequency bands.

7.3.1 Mixing Noise with sinusoid

A situation often encountered in communication systems is one in which noise is mixed with (i.e. multiplied by) a deterministic sinusoidal waveform. Let the sinusoidal waveform be $\cos 2\pi f_0 t$. Then the product of this waveform with a spectral noise component, as given by Eq. (7.15), yields

$$\begin{aligned} n_k(t) \cos 2\pi f_0 t &= \frac{a_k}{2} \cos 2\pi(k \Delta f + f_0)t + \frac{b_k}{2} \sin 2\pi(k \Delta f + f_0)t \\ &\quad + \frac{a_k}{2} \cos 2\pi(k \Delta f - f_0)t + \frac{b_k}{2} \sin 2\pi(k \Delta f - f_0)t \end{aligned} \quad (7.37)$$

Thus, the mixing gives rise to two noise spectral components, one at the sum frequency $f_0 + k \Delta f$ and one at the difference frequency $f_0 - k \Delta f$. In addition, the amplitudes of each of the two noise spectral components generated by mixing has been reduced by a factor of 2 with respect to the original noise

spectral component. Hence, the variances (normalized power) of the two new noise components are smaller by a factor of 4. Accordingly, if the power spectral density of the original noise component at frequency $k \Delta f$ is $G_n(k \Delta f)$, then, from Eq. (7.37), the new components have spectral densities

$$G_n(k \Delta f + f_0) = G_n(k \Delta f - f_0) = \frac{G_n(k \Delta f)}{4} \quad (7.38)$$

In the limit as $\Delta f \rightarrow 0$, we replace $k \Delta f$ by the continuous variable f , and Eq. (7.38) becomes

$$G_n(f + f_0) = G_n(f - f_0) = \frac{G_n(f)}{4} \quad (7.39)$$

In words, given the power spectral density plot $G_n(f)$ of a noise waveform $n(t)$, the power spectral density of $n(t) \cos 2\pi f_0 t$ is arrived at as follows: divide $G_n(f)$ by 4, shift the divided plot to the left by amount f_0 , to the right by amount f_0 , and add the two shifted plots.

Now consider the following situation: We have noise $n(t)$ from which we single out two spectral components, one at frequency $k \Delta f$ and one at frequency $l \Delta f$. We mix with a sinusoid at frequency f_0 , with f_0 selected to be midway between $k \Delta f$ and $l \Delta f$; that is, $f_0 = \frac{1}{2}(k + l) \Delta f$. Then the mixing

will give rise to *four* spectral components, two difference-frequency components and two sum-frequency components. The two difference-frequency components will be at the same frequency $p \Delta f = f_0 - k \Delta f = l \Delta f - f_0$. However, we now show that these difference-frequency components are uncorrelated. Representing the spectral components at $k \Delta f$ and $l \Delta f$ as in Eqs (7.24) and (7.25), we find that the difference-frequency components are

$$n_{p1}(t) = \frac{a_k}{2} \cos 2\pi p \Delta f t - \frac{b_k}{2} \sin 2\pi p \Delta f t \quad (7.40)$$

and $n_{p2}(t) = \frac{a_l}{2} \cos 2\pi p \Delta f t + \frac{b_l}{2} \sin 2\pi p \Delta f t \quad (7.41)$

where $n_{p1}(t)$ is the difference component due to the mixing of frequencies f_0 and $k \Delta f$, while $n_{p2}(t)$ is the difference component due to the mixing of frequencies f_0 and $l \Delta f$. If we now take into account, as we have established in Sec. 7.2.2, that $\overline{a_k a_l} = \overline{a_k b_l} = \overline{b_k a_l} = \overline{b_k b_l} = 0$, then we find from Eqs (7.40) and (7.41) that

$$E[n_{p1}(t)n_{p2}(t)] = 0 \quad (7.42)$$

Thus, as discussed in connection with Eq. (7.36), superposition of power applies, and the power at the difference frequency due to the superposition of $n_{p1}(t)$ and $n_{p2}(t)$ is

$$E\{[n_{p1}(t) + n_{p2}(t)]^2\} = E\{[n_{p1}(t)]^2\} + E\{[n_{p2}(t)]^2\} \quad (7.43)$$

Thus, mixing noise with a sinusoidal signal results in a frequency shifting of the original noise by f_0 . The variance of the shifted noise is found by adding the variance of each new noise component. Thus we see that the principle stated immediately after Eq. (7.39) applies even when there is overlap in the two shifted power spectral density plots.

7.3.2 mixing Noise with Noise

We consider now the result of multiplying two spectral components of noise. Representing the spectral components as in Eq. (7.16), we find that the product of two components, one at the frequency $k \Delta f$, the other at the frequency $l \Delta f$ is

$$\begin{aligned} n_k(t)n_l(t) &= \frac{1}{2} c_k c_l \cos [2\pi(k+l) \Delta f t + \theta_k + \theta_l] \\ &\quad + \frac{1}{2} c_k c_l \cos [2\pi(k-l) \Delta f t + \theta_k - \theta_l] \end{aligned} \quad (7.44)$$

The multiplication thus gives rise to two new spectral components of noise, one at the sum frequency $(k+l) \Delta f$ and one at the difference frequency $(k-l) \Delta f$. The terms in Eq. (7.44) are of the form of Eq. (7.16), except that $\frac{1}{2} c_k c_l$ replaces c_k , and θ_k in Eq. (7.16) is replaced by $\theta_k + \theta_l$ in one case and $\theta_k - \theta_l$ in the other. Since θ_k and θ_l have uniform probability densities, it is intuitively apparent from the principle of *minimum astonishment* that $\theta_k + \theta_l$ and $\theta_k - \theta_l$ also have uniform densities.

(A more formal proof is possible; see Prob. 7.10.) Hence the normalized power associated with each of the terms in Eq. (7.44) may be deduced as for the spectral component of Eq. (7.16). We then have, using Eq. (7.20),

$$P_{k+l} = P_{k-l} = \frac{1}{2} \overline{\left(\frac{1}{2} c_k c_l \right)^2} \quad (7.45)$$

Since c_k and c_l are independent random variables,

$$P_{k+l} = P_{k-l} = \frac{1}{8} \overline{c_k^2} \overline{c_l^2} = \frac{1}{2} P_k P_l \quad (7.46)$$

7.4 LINEAR FILTERING OF NOISE

Thermal noise has a power spectral density which is quite uniform up to frequencies of the order of 10^{13} Hz. Shot noise has a power spectral density which is reasonably constant up to frequencies which are of the order of the reciprocal of the transit time of charge carriers across the junction. Other noise sources similarly have very wide spectral ranges. We shall assume, in discussing the effect of noise on communication systems, that we have to contend with *white* noise. White noise is noise whose power spectral density is uniform over the entire frequency range of interest. The term *white* is used in analogy with white light, which is a superposition of all visible spectral components. Thus, we assume, as shown in Fig. 7.6, that over the entire spectrum, including positive and negative frequencies,

$$G_n(f) = \frac{\eta}{2} \quad (7.47)$$

in which η is a constant (see Sec. 15.3).

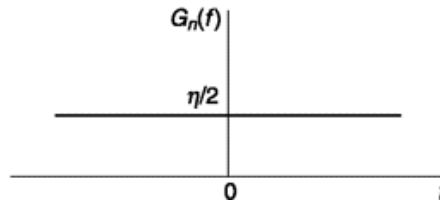


Fig. 7.6 Power spectral density of white noise.

In order to minimize the noise power that is presented to the demodulator of a receiving system, we introduce a filter before the demodulator as indicated in Fig. 7.7. The bandwidth B of the filter is made as narrow as possible so as to avoid transmitting any unnecessary noise to the demodulator. For example, in an AM system in which the baseband extends to a frequency of f_M , the bandwidth $B = 2f_M$. In a wideband FM system the bandwidth is proportional to twice the frequency deviation.

It is useful to consider the effect of certain types of filters on the noise. One of the filters most often used is the simple RC low-pass filter.

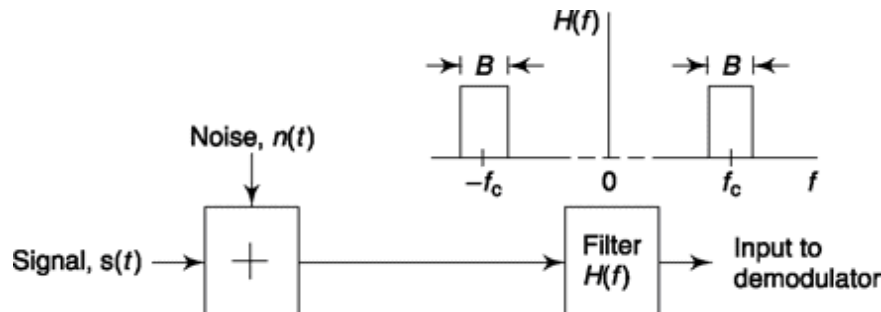


Fig. 7.7 A filter is placed before a demodulator to limit the noise power input to the demodulator.

THE RC LOW-PASS FILTER

An RC low-pass filter with a 3 dB frequency f_c has the transfer function

$$H(f) = \frac{1}{1 + jf/f_c} \quad (7.48)$$

If the input noise to this filter has a power spectral density $G_{n_i}(f)$ and the power spectral density of the output noise is $G_{n_o}(f)$, then, using Eq. (7.34), we have

$$G_{n_o}(f) = G_{n_i}(f)|H(f)|^2 \quad (7.49)$$

If the noise is white, $G_{n_i}(f) = \eta/2$ for all frequencies, Eq. (7.49) becomes

$$G_{n_o}(f) = \frac{\eta}{2} \frac{1}{1 + (f/f_c)^2} \quad (7.50)$$

The noise power at the filter output N_o is

$$N_o = \int_{-\infty}^{\infty} G_{n_o}(f) df = \frac{\eta}{2} \int_{-\infty}^{\infty} \frac{df}{1 + (f/f_c)^2} \quad (7.51)$$

Changing variables to $x \equiv f/f_c$, and noting that $\int_{-\infty}^{\infty} dx/(1 + x^2) = \pi$, we have

$$N_o = \frac{\pi}{2} \eta f_c \quad (7.52)$$

The Rectangular (Ideal) Low-pass Filter

A *rectangular* low-pass filter has the transfer function

$$H(f) = \begin{cases} 1 & |f| \leq B \\ 0 & \text{elsewhere} \end{cases} \quad (7.53)$$

Assuming that the noise input to the filter is *white*, the output-power spectral density is

$$G_{n_o}(f) = \begin{cases} \frac{\eta}{2} & -B \leq f \leq B \\ 0 & \text{elsewhere} \end{cases} \quad (7.54)$$

The output noise power is

$$N_o = \eta B \quad (7.55)$$

A Rectangular Bandpass Filter

A rectangular bandpass filter is shown in Fig. 7.8. The bandwidth of the filter is $f_2 - f_1$. Then, with a *white* noise input, the output-noise power is

$$N_o = 2 \frac{\eta}{2} (f_2 - f_1) = \eta (f_2 - f_1) \quad (7.56)$$

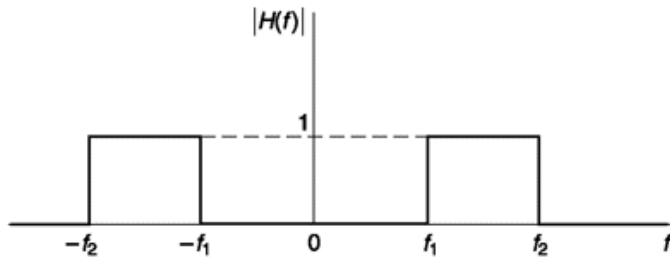


Fig. 7.8 A rectangular bandpass filter.

A Differentiating Filter

A differentiating filter is a network which yields at its output a waveform which is proportional to the time derivative of the input waveform. As discussed in Sec. 1.3.5, such a network has a transfer function $H(f)$ which is proportional to the frequency; that is,

$$H(f) = j2\pi\tau f \quad (7.57)$$

where τ is a constant factor of proportionality. If white noise with $G_{n_i}(f) = \eta/2$ is passed through such a filter, then the output-noise-power spectral density is

$$G_{n_o}(f) = |H(f)|^2 G_{n_i}(f) = 4\pi^2 \tau^2 f^2 \frac{\eta}{2} \quad (7.58)$$

If the differentiator is followed by a rectangular low-pass filter having a bandwidth B , as described by Eq. (7.53), the noise power at the output of the low-pass filter is

$$N_o = \int_{-B}^B 4\pi^2 \tau^2 f^2 \frac{\eta}{2} df = \frac{4\pi^2}{3} \eta \tau^2 B^3 \quad (7.59)$$

An Integrator

Let noise $n(t)$ be applied to the input of an integrator at time $t = 0$. We calculate the noise power at the integrator output at a time $t = T$. The result will be of interest in connection with the discussion of the *matched filter* in Chap. 11.

A network which performs the operation of integration has a transfer function $1/j\omega\tau$. A delay by an interval T is represented by a factor $e^{-j\omega T}$. Hence, a network which performs an integration over an interval T may be represented by a network whose transfer function is

$$H(f) = \frac{1}{j\omega\tau} - \frac{e^{-j\omega T}}{j\omega\tau} = \frac{1 - e^{-j\omega T}}{j\omega\tau} \quad (7.60)$$

where τ is a constant. We find, with $\omega = 2\pi f$, that

$$|H(f)|^2 = \left(\frac{T}{\tau}\right)^2 \left(\frac{\sin \pi Tf}{\pi Tf}\right)^2 \quad (7.61)$$

The noise power output of such a filter with white input noise of power spectral density $\eta/2$ is (using $x \equiv \pi Tf$)

$$N_o = \int_{-\infty}^{\infty} \frac{\eta}{2} |H(f)|^2 df = \frac{\eta}{2} \left(\frac{T}{\tau}\right)^2 \int_{-\infty}^{\infty} \left(\frac{\sin \pi Tf}{\pi Tf}\right)^2 df \quad (7.62a)$$

$$= \frac{\eta T}{2\pi\tau^2} \int_{-\infty}^{\infty} \left(\frac{\sin x}{x}\right)^2 dx \quad (7.62b)$$

The definite integral in Eq. (7.62b) has the value π , so that finally

$$N_o = \frac{\eta T}{2\tau^2} \quad (7.63)$$

It is instructive to obtain Eq. (7.63) by a calculation in the time domain. If an input noise *sample* to the integrator is $n_i(t)$ and the corresponding output of the integrator is $n_o(T)$ then

$$n_o(T) = \frac{1}{\tau} \int_0^T n_i(t) dt \quad (7.64)$$

Note that $n_o(T)$ is a random variable since T is a constant.

The expected value (ensemble average) of the random variable $n_o(T)$ is

$$m_{n_o} = E[n_o(T)] = E\left\{\frac{1}{\tau} \int_0^T n_i(t) dt\right\} \quad (7.65a)$$

In general, as discussed in Sec. 6.2.6, if $f(x)$ is the probability density of a random variable x , and $u(x)$ is some function of x , then

$$E[u(x)] = \int_{-\infty}^{\infty} u(x)f(x) dx \quad (7.65b)$$

Correspondingly, we have in the present case, that

$$m_{n_o} = \int_{-\infty}^{\infty} dn_i f(n_i) \left\{ \frac{1}{\tau} \int_0^T n_i(t) dt \right\} \quad (7.65c)$$

Interchanging the order of integration (see Prob. 7.15) yields

$$m_{n_o} = \frac{1}{\tau} \int_0^T dt \left\{ \int_{-\infty}^{\infty} n_i f(n_i) dn_i \right\} \quad (7.66)$$

But the integral in brackets is the mean value of n_i , i.e.

$$m_{n_i} = E(n_i) = \int_{-\infty}^{\infty} n_i f(n_i) dn_i \quad (7.67)$$

Assuming, as before, that the average value of the input noise $m_{n_i} = 0$, we see that the average value of the output noise $m_{n_o} = 0$ as well.

The normalized noise power N_o corresponding to the random variable $n_o(T)$ is equal to the variance of $n_o(T)$ (see Sec. 6.2.7). Thus,

$$N_o = \sigma_{n_o}^2 = E\{[n_o(T)]^2\} = E\left\{ \frac{1}{\tau^2} \int_0^T n_i(t) dt \cdot \int_0^T n_i(\lambda) d\lambda \right\} \quad (7.68)$$

where t and λ are dummy variables of integration. N_o can be rewritten as

$$N_o = E\left\{ \frac{1}{\tau^2} \int_0^T \int_0^T n_i(t) n_i(\lambda) dt d\lambda \right\} \quad (7.69)$$

If we define

$$\alpha \equiv n_i(t) \quad \text{and} \quad \beta \equiv n_i(\lambda)$$

Equation (7.69) can be written as

$$N_o = \frac{1}{\tau^2} \int_{-\infty}^{\infty} f(\alpha, \beta) \left\{ \int_0^T dt \int_0^T d\lambda \alpha \beta \right\} d\alpha d\beta \quad (7.70)$$

Interchanging the order of integration (see Prob. 7.16) yields

$$N_o = \frac{1}{\tau^2} \int_0^T dt \int_0^T d\lambda \int_{-\infty}^{\infty} \alpha \beta f(\alpha, \beta) d\alpha d\beta \quad (7.71)$$

But

$$R_{n_i}(t - \lambda) = E[n_i(t)n_i(\lambda)] = E(\alpha\beta) = N_o \quad (7.72)$$

where $R_{n_i}(t - \lambda)$ is the autocorrelation function of $n_i(t)$.

We recall (see Eq. 6.141) that the correlation and the power spectral density are Fourier transform pairs. Since for white noise the power spectral density is $G(f) = \eta/2$, we have

$$E[n_i(t)n_i(\lambda)] = R_{n_i}(t - \lambda) = \mathcal{F}\{G(f)\} = \int_{-\infty}^{\infty} \eta/2 e^{-j2\pi f(t - \lambda)} df = (\eta/2) \delta(t - \lambda) \quad (7.73)$$

Altogether, then we have, from Eq. (7.71) and (7.72) that

$$N_o = \frac{1}{\tau^2} \int_0^T dt \int_0^T d\lambda (\eta/2) \delta(t - \lambda) \quad (7.74a)$$

$$= \frac{1}{\tau^2} \int_0^T dt \cdot \eta/2 = \frac{\eta T}{2\tau^2} \quad (7.74b)$$

in agreement with Eq. (7.63).

7.4.1 Noise Bandwidth

Consider that white noise is present at the input to a receiver and a filter with transfer function $H(f)$ centered at f_0 , such as is indicated by the solid plot of Fig. 7.9, is being used to restrict the noise power actually passed on to the receiver. Now contemplate a rectangular filter as shown by the dotted plot in Fig. 7.9. This filter is also centered at f_0 . Let the rectangular filter bandwidth B_N be adjusted so that the real filter and the rectangular filter transmit the same noise power. Then the bandwidth B_N is called the *noise bandwidth* of the real filter. The noise bandwidth, then, is the bandwidth of an idealized (rectangular) filter which passes the same noise power as does the real filter.

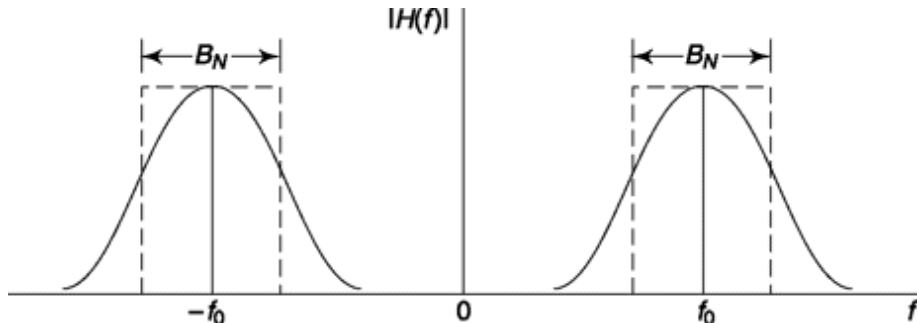


Fig. 7.9 Illustration of the noise bandwidth of a filter.

We illustrate the concept of noise bandwidth by considering the case of the low-pass RC filter with transfer function as given by Eq. (7.48). For this filter, $H(f)$ attains its maximum value $H(f) = 1$ at $f = 0$. As given by Eq. (7.52), with white-noise input of power spectral density $\eta/2$, the noise output of the filter is

$$N_o(RC) = \frac{\pi}{2} \eta f_c \quad (7.75)$$

In the presence of such noise, a rectangular low-pass filter with $H(f) = 1$ over its bandpass B_N would yield an output-noise power

$$N_o(\text{rectangular}) = \frac{\eta}{2} 2B_N = \eta B_N \quad (7.76)$$

Setting $N_o(RC) = N_o(\text{rectangular})$, we find the noise bandwidth to be

$$B_N = \frac{\pi}{2} f_c \quad (7.77)$$

Thus, the noise bandwidth of the RC filter is $\pi/2$ ($= 1.57$) times its 3 dB bandwidth f_c .

SELF-TEST QUESTION

6. Is it true that power of sum of two noise waveforms is equal to sum of individual powers?
7. Mixing noise with sinusoidal signal results in frequency shifting of original noise. Is that correct?
8. Can it be said that thermal noise and shot noise are essentially white noise?
9. Which of integration and differentiation accentuates the effect of noise?

Example 7.3

Given a white noise of magnitude $h = 0.001 \text{ mW/Hz}$ is fed to following. (a) an RC low pass filter of $R = 1000 \text{ ohms}$ and $C = 0.1 \text{ mF}$, (b) an ideal low pass filter of bandwidth=1000 Hz and (c) a differentiator followed by an ideal low-pass filter defined in (b). For differentiator consider proportionality constant $t = 0.01$ unit. Find output noise power in each case. How does result change in each case if low pass cutofffrequency is doubled in each case?

Solution

$$(a) \text{ Cutoff frequency, } f_c = \frac{1}{2\pi RC}$$

$$= \frac{1}{2\pi \times 1000 \times 0.1 \times 10^{-6}} = \frac{5000}{\pi} \text{ Hz}$$

From Eq.(7.52), noise power at filter output

$$= \frac{\pi}{2} \eta f_c = \frac{\pi \times 0.001 \times 5000}{2 \times \pi} = 2.5 \mu\text{W}$$

If cutoff frequency is doubled output power will be doubled to $2.5 \times 2 = 5 \mu\text{W}$

- (b) From Eq. (7.55), output noise power = $\eta B = 0.001 \times 1000 = 1 \mu\text{W}$

If cutoff frequency is doubled output power will be doubled to $1 \times 2 = 2 \mu\text{W}$

- (c) From Eq. (7.59),

$$\text{output noise power} = \frac{4\pi^2}{3} \eta \tau^2 B^3 = \frac{4\pi^2}{3}$$

$$= (0.001)(0.01)^2(1000)^3 = 1.316 \mu\text{W}$$

If cutoff frequency is doubled output power will increase by a factor of $2^3 = 8$ to $1.316 \times 8 = 10.528 \mu\text{W}$

Note the rise in noise power when differentiator is used.

Example 7.4

A low-pass (within 4000 Hz) signal of strength 0.001 W passes through a distorting channel defined as $H(f) = \frac{4000}{j4000 + f}$ and is also corrupted with a additive white Gaussian noise of magnitude 10^{-8} W/Hz . At the receiver side, there is an equalizer which exactly matches the channel within frequency of interest (upto 4000 Hz) and zero elsewhere. Find SNR at the output of equalizer.

Solution

An equalizer when exactly matches channel has a transfer function which is inverse of channel and the signal at its output is undistorted signal. Hence signal energy at equalizer output, $S = 0.001$ W.

Noise at equalizer output,

$$\begin{aligned}
 N &= \int_{-\infty}^{\infty} 10^{-8} |H_{eq}(f)|^2 df \\
 &= 10^{-8} \int_{-4000}^{4000} \left| \frac{4000 j + f}{4000} \right|^2 df \\
 &= 2 \times 10^{-8} \int_0^{4000} \left(1 + \frac{f^2}{16 \times 10^6} \right) df \\
 &= 2 \times 10^{-8} \left(f + \frac{f^3}{3 \times 16 \times 10^6} \right) \Big|_0^{4000} \\
 &= 2 \times 10^{-8} \left(4000 + \frac{4000^3}{3 \times 16 \times 10^6} \right) \\
 &= \frac{32 \times 10^{-5}}{3} \text{ W}
 \end{aligned}$$

Thus, SNR at equalizer output,

$$\frac{S}{N} = \frac{0.001 \times 3}{32 \times 10^{-5}} = 9.7197 \text{ dB}$$

7.5 QUADRATURE COMPONENTS OF NOISE

We have represented noise $n(t)$, as in Eq. (7.7), as the superposition of spectral components of noise in the expression

$$n(t) = \lim_{\Delta f \rightarrow 0} \sum_{k=1}^{\infty} (a_k \cos 2\pi k \Delta f t + b_k \sin 2\pi k \Delta f t) \quad (7.78)$$

It is sometimes more advantageous to represent the noise through an alternative representation given by

$$n(t) = n_c(t) \cos 2\pi f_0 t - n_s(t) \sin 2\pi f_0 t \quad (7.79)$$

in which f_0 is an arbitrary frequency. The representation of Eq. (7.79) is frequently used with great convenience in dealing with noise confined to a relatively narrow frequency band in the neighborhood of f_0 . For this reason Eq. (7.79) is often referred to as the *narrowband* representation. The term *quadrature component* representation is also often used because of the appearance in the equation of sinusoids in quadrature.

We may readily transform Eq. (7.78) into Eq. (7.79) and, in doing so, arrive at explicit expressions for $n_c(t)$ and $n_s(t)$. Let us select f_0 to correspond to $k = K$; that is, we set

$$f_0 = K \Delta f \quad (7.80)$$

Adding $2\pi f_0 t - 2\pi K \Delta f t = 0$ to the arguments in Eq. (7.78), we have

$$n(t) = \lim_{\Delta f \rightarrow 0} \sum_{k=1}^{\infty} \{a_k \cos 2\pi[f_0 + (k - K) \Delta f]t + b_k \sin 2\pi[f_0 + (k - K) \Delta f]t\} \quad (7.81)$$

Using the trigonometric identities for the cosine of the sum of two angles and for the sine of the sum of two angles, it is readily verified that $n(t)$ is indeed given by Eq. (7.79), provided that $n_c(t)$ and $n_s(t)$ are taken to be

$$n_c(t) = \lim_{\Delta f \rightarrow 0} \sum_{k=1}^{\infty} [a_k \cos 2\pi(k - K) \Delta f t + b_k \sin 2\pi(k - K) \Delta f t] \quad (7.82)$$

and

$$n_s(t) = \lim_{\Delta f \rightarrow 0} \sum_{k=1}^{\infty} [a_k \sin 2\pi(k - K) \Delta f t - b_k \cos 2\pi(k - K) \Delta f t] \quad (7.83)$$

Like $n(t)$, so also $n_c(t)$ and $n_s(t)$ are stationary random processes which are represented as linear superpositions of spectral components. We recall, from Sec. 7.2.2, that the a_k 's and b_k 's are Gaussian random variables of zero mean and equal variance and that, further, the a_k 's and b_k 's are uncorrelated. We may then readily establish (Probs. 7.79 to 7.81) that $n_c(t)$ and $n_s(t)$ are Gaussian random processes of zero mean value and of equal variance and that, further, $n_c(t)$ and $n_s(t)$ are uncorrelated.

To see the significance of the quadrature representation of noise, let us use it in connection with narrowband noise. We observe in Eqs (7.82) and (7.83) that a noise spectral component in $n(t)$ of frequency $f = k \Delta f$ gives rise in $n_c(t)$ and $n_s(t)$ to a spectral component of frequency $(k - K) \Delta f = f - f_0$.

Suppose then that the noise $n(t)$ is narrowband, extending over a bandwidth B . And suppose that f_0 is selected midway in the frequency range of the noise. Then the spectrum of the noise $n(t)$ extends over the range $f_0 - B/2$ to $f_0 + B/2$. On the other hand, the spectrum of $n_c(t)$ and $n_s(t)$ extends over only the range from $-B/2$ to $B/2$. By way of example, if the noise $n(t)$ is

confined to a frequency band of only 10 kHz centered around $f_0 = 10$ MHz, then while $n(t)$ is a superposition of spectral components around the 10 MHz frequency, $n_c(t)$ and $n_s(t)$ change only insignificantly during the time the sinusoid of frequency f_0 executes a full cycle.

In view of the slow variations of $n_c(t)$ and $n_s(t)$ relative to the sinusoid of frequency f_0 , it is reasonable and useful to give the quadrature representation of noise an interpretation in terms of phasors and a phasor diagram. Thus, in Eq. (7.79) the term $n_c(t) \cos 2pf_0t$ is of frequency f_0 and of relatively slowly varying amplitude $n_c(t)$. Similarly, the term $-n_s(t) \sin 2pf_0t$ is in quadrature with the first term and has a relatively slowly varying amplitude $n_s(t)$. In a coordinate system rotating counterclockwise with angular velocity $2pf_0$, these phasors are as represented in Fig. 7.10. These two phasors of varying amplitude give rise to a resultant phasor of amplitude $r(t) = [n_c^2(t) + n_s^2(t)]^{1/2}$ which makes an angle

$$\theta(t) = \tan^{-1} [n_s(t)/n_c(t)] \quad (7.84)$$

with the horizontal. With the passage of time, the end point of this resultant phasor wanders about randomly over the phasor diagram.

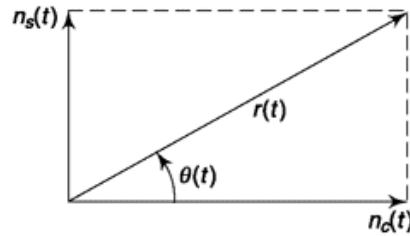


Fig. 7.10 A phasor diagram of the quadrature representation of noise.

We shall find the quadrature representation is useful generally in the analysis of noise and the phasor interpretation is especially useful in discussing angle modulation communications systems.

7.5.1 Power Spectral Density of Quadrature Components

To determine the power spectral density of $n_c(t)$, let us select from the original noise $n(t)$ those spectral components corresponding to $k = K + \lambda$ and $k = K - \lambda$, where λ , like k and K , is an integer. Since $k = K$ corresponds to the frequency f_0 , the selected components correspond to frequencies $f_0 + \lambda \Delta f$ and $f_0 - \lambda \Delta f$. These two frequencies give rise to four power spectral lines in a two-sided power spectral density plot as shown in Fig. 7.11. In this figure, we have assumed band-limited noise. However, for the sake of generality we have not assumed that the power spectral density is uniform in the band, nor have we assumed that the frequency $f_0 = K \Delta f$ is located at the center of the band.

We now select from $n_c(t)$, as given by Eq. (7.82), that part, $\Delta n_c(t)$, corresponding to our selection of frequencies, $f_0 \pm \lambda \Delta f$, from $n(t)$. We find

$$\begin{aligned} \Delta n_c(t) &= a_{K-\lambda} \cos 2\pi\lambda \Delta ft - b_{K-\lambda} \sin 2\pi\lambda \Delta ft \\ &\quad + a_{k+\lambda} \cos 2\pi\lambda + \Delta ft + b_{K+\lambda} \sin 2\pi\lambda \Delta ft \end{aligned} \quad (7.85)$$

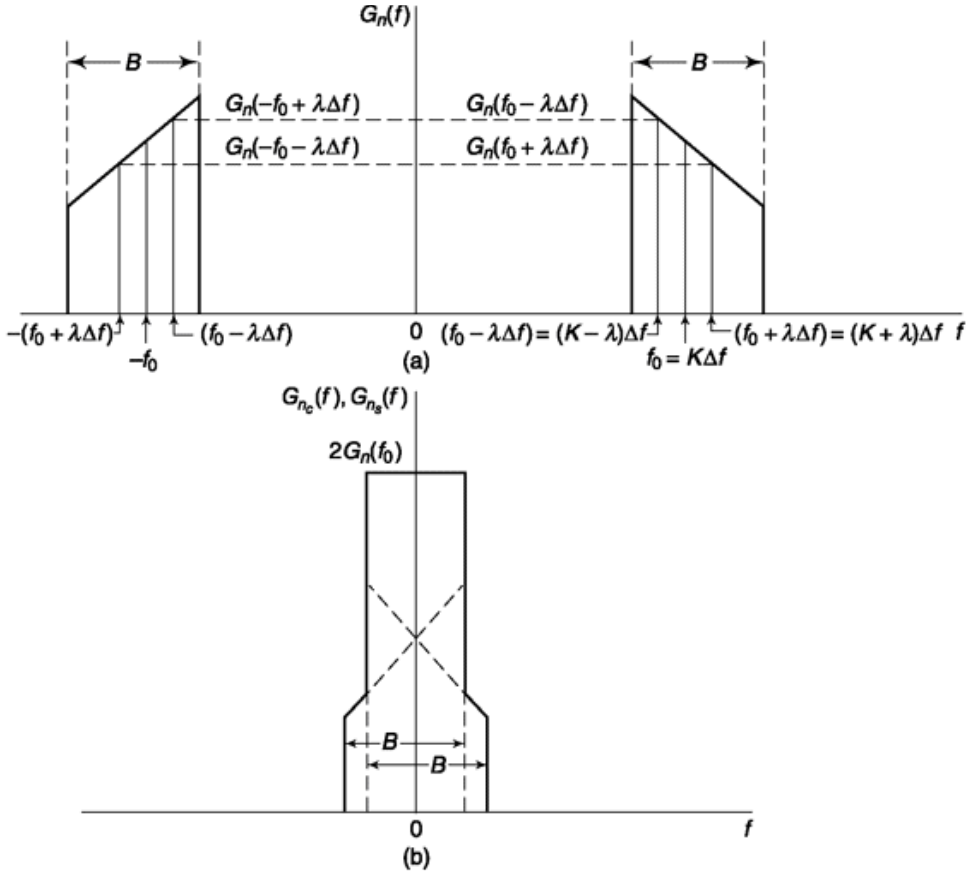


Fig. 7.11 (a) Power spectrum of bandlimited noise. (b) Power spectral density of n_c and n_s .

Note that all four terms in Eq. (7.85) are of the same frequency $\lambda \Delta f$. These four terms represent four uncorrelated random processes, since the a 's and b 's are uncorrelated random variables. Hence we may find the power P_λ of $\Delta n_c(t)$ by determining the ensemble average of $[\Delta n_c(t)]^2$. Since $\Delta n_c(t)$ is a stationary random process, the ensemble average can be calculated at any time $t = t_1$. Following the procedure employed in Sec. 7.2.2, we choose t_1 so that $\lambda \Delta f t_1$ is an integer. Then

$$\Delta n_c(t_1) = a_{K-\lambda} + a_{K+\lambda} \quad (7.86)$$

and

$$P_\lambda = E\{[\Delta n_c(t_1)]^2\} = E[(a_{K-\lambda} + a_{K+\lambda})^2] \quad (7.87)$$

Using Eq. (7.26), which says that $E(a_{K-\lambda} a_{K+\lambda}) = 0$, we have, from Eq. (7.87), that

$$P_\lambda = \overline{a_{K-\lambda}^2} + \overline{a_{K+\lambda}^2} \quad (7.88)$$

From Eqs (7.20) and (7.88), we then find

$$P_\lambda = 2 G_{n_c}(\lambda \Delta f) \Delta f = 2G_n[(K - \lambda) \Delta f] \Delta f + 2G_n[(K + \lambda) \Delta f] \Delta f \quad (7.89)$$

Hence,

$$G_{n_c}(\lambda \Delta f) = G_n[(K - \lambda) \Delta f] + G_n[(K + \lambda) \Delta f] \quad (7.90)$$

We now set $K \Delta f = f_0$ and replace $\lambda \Delta f$ by a continuous frequency variable f , and we have, from Eq. (7.90),

$$G_{n_c}(f) = G_n(f_0 - f) + G_n(f_0 + f) \quad (7.91)$$

In a similar manner we may deduce an identical result for $G_{n_s}(f)$, namely,

$$G_{n_s}(f) = G_n(f_0 - f) + G_n(f_0 + f) \quad (7.92)$$

Expressed in words, Eqs (7.91) and (7.92) say, that to find the power spectral density of $n_c(t)$ or of $n_s(t)$ at a frequency f , add the power spectral densities of $n(t)$ at the frequencies $f_0 - f$ and $f_0 + f$. In view of this result, and in view of the symmetry of a two-sided power spectral density plot as in Fig. 7.11, it may readily be verified that the plot of $G_{n_c}(f)$ or $G_{n_s}(f)$ may be constructed from the plot of $G_n(f)$ in the following manner:

1. Displace the positive-frequency portion of the plot of $G_n(f)$ to the left by amount f_0 so that the portion of the plot originally located at f_0 is now coincident with the ordinate.
2. Displace the negative-frequency portion of the plot of $G_n(f)$ to the right by an amount f_0 .
3. Add the two displaced plots. The result of applying this procedure to the plot of Fig. 7.11a is shown in Fig. 7.11b.

A case of special interest is considered in the following example.

Example 7.5

White noise with power spectral density $\eta/2$ is filtered by a rectangular bandpass filter with $H(f) = 1$, centered at f_0 and having a bandwidth B . Find the power spectral density of $n_c(t)$ and $n_s(t)$. Calculate the power in $n_c(t)$, $n_s(t)$ and $n(t)$.

Solution

Since the filter is rectangular with $H(f) = 1$, the power spectral density of the output noise $n(t)$ is

$$G_n(f) = \begin{cases} \frac{\eta}{2} & f_0 - \frac{B}{2} \leq |f| \leq f_0 + \frac{B}{2} \\ 0 & \text{elsewhere} \end{cases} \quad (7.93)$$

Hence, $G_n(f_0 + f) = G_n(f_0 - f)$, and the spectral density of $n_c(t)$ and $n_s(t)$ is

$$\begin{aligned} G_{n_c}(f) &= G_{n_s}(f) = G_n(f_0 - f) + G_n(f_0 + f) \\ &= \frac{\eta}{2} + \frac{\eta}{2} = \eta \quad |f| \leq \frac{B}{2} \end{aligned} \quad (7.94)$$

Note the extremely important result that the magnitude of $G_{n_c}(f) = G_{n_s}(f)$ is *twice* the magnitude of $G_n(f_0 + f)$.

The power (variance) of $n_c(t)$, and of $n_s(t)$, is

$$\sigma_{n_c}^2 = \sigma_{n_s}^2 = \int_{-B/2}^{B/2} G_{n_c}(f) df = \eta B \quad (7.95)$$

The power (variance) of $n(t)$ is

$$\begin{aligned} \sigma_n^2 &= \int_{-f_0 - B/2}^{-f_0 + B/2} G_n(f) df + \int_{f_0 - B/2}^{f_0 + B/2} G_n(f) df \\ &= 2 \frac{\eta}{2} B = \eta B \end{aligned} \quad (7.96)$$

Thus, the power of $n_c(t)$, $n_s(t)$ and $n(t)$ are each equal.

7.5.2 probability Density of Quadrature Components and Time Derivatives

We have noted that $n_c(t)$ and $n_s(t)$ are Gaussian random processes with mean values of zero. If the noise $n(t)$ has a power spectral density $h/2$ over a bandwidth B , then, as noted in the preceding

example, $\sigma_{n_c}^2 = \sigma_{n_s}^2 = \eta B$. Using Eq. (7.85) with $m = 0$, we find that the probability densities of the random variables n_c and n_s [that is, $n_c(t)$ and $n_s(t)$ at any fixed time] are given by

$$f(n_c) = \frac{1}{\sqrt{2\pi\eta B}} e^{-n_c^2/2\eta B} \quad (7.97a)$$

$$f(n_s) = \frac{1}{\sqrt{2\pi\eta B}} e^{-n_s^2/2\eta B} \quad (7.97b)$$

Since $n_c(t)$ and $n_s(t)$ are Gaussian, the time derivatives $\dot{n}_c(t)$ and $\dot{n}_s(t)$ are also Gaussian, because the operation of differentiation is an operation performed by a linear filter (Eq. 7.57), and from Sec. 7.2.1 we know that filtering Gaussian noise does not change its probability density. To write the probability densities of $\dot{n}_c(t)$ and $\dot{n}_s(t)$, we first evaluate their variances $\sigma_{\dot{n}_c}^2$ and $\sigma_{\dot{n}_s}^2$. Noting that differentiation is equivalent to multiplying each spectral component by $j\omega$, we find

$$G_{\dot{n}_c}(f) = |j\omega|^2 G_{n_c}(f) = 4\pi^2 f^2 G_{n_c}(f) \quad (7.98)$$

so that, using Eq. (7.94), we find

$$\sigma_{\dot{n}_c}^2 = \int_{-B/2}^{B/2} G_{\dot{n}_c}(f) df = \int_{-B/2}^{B/2} 4\pi^2 f^2 \eta df = \frac{\pi^2}{3} \eta B^3 \quad (7.99)$$

with an identical result for $\sigma_{\dot{n}_s}^2$. Hence, we find

$$f(\dot{n}_c) = \frac{\exp\{-\dot{n}_c^2/[(2\pi^2/3)\eta B^3]\}}{\sqrt{(2\pi^3/3)\eta B^3}} \quad (7.100)$$

with a similar expression for $f(\dot{n}_s)$. Assuming that the four random variables n_c , n_s , \dot{n}_c and \dot{n}_s are independent, the joint distribution function for the four variables is the product of the individual densities. Hence, from Eqs (7.97) and (7.99) we find

$$f(n_c, n_s, \dot{n}_c, \dot{n}_s) = \frac{\exp[-(n_c^2 + n_s^2)/2\eta B] \exp[-(\dot{n}_c^2 + \dot{n}_s^2)/(2\pi^2/3)\eta B^3]}{[(2\pi^2/\sqrt{3})\eta B^2]^2} \quad (7.101)$$

We shall have occasion to use Eq. (7.101) in Chap. 10 in connection with an analysis of threshold effects in frequency modulation.

In arriving at Eq. (7.101), we assumed that the four random variables involved were independent. That such is indeed the case may be verified in the manner indicated in Prob. 7.28.

7.6 REPRESENTATION OF NOISE USING ORTHONORMAL COORDINATES

In our discussion of the frequency-domain representation of noise we saw that a noise process can be represented as a sum of orthonormal functions. These orthonormal functions are the sines and cosines. In our discussion of the Gram-Schmitt technique, where our interest concerned a waveform

defined over a time interval T , we pointed out that limitless other functions, orthonormal over T , are also possible. We consider here some features of the representation of noise in terms of orthonormal functions.

If $u_i(t)$ are a set of orthonormal functions in the interval T then in that interval, noise $n(t)$ is

$$n(t) = \sum_{i=0}^{\infty} n_i u_i(t) \quad (7.102)$$

in which n_i is the coefficient of the i th component and is evaluated in the usual manner, that is,

$$n_i = \int_0^T n(t) u_i(t) dt \quad (7.103)$$

If the noise $n(t)$ is a Gaussian random process with a mean value of zero then n_i is a Gaussian random variable with a zero mean value.

We shall now determine the correlation between coefficients say n_i and n_j . We have

$$n_i n_j = \int_0^T n(t) u_i(t) dt \int_0^T n(\lambda) u_j(\lambda) d\lambda \quad (7.104a)$$

$$= \int_0^T dt \int_0^T d\lambda n(t) n(\lambda) u_i(t) u_j(\lambda) \quad (7.104b)$$

where t and λ are dummy variable of integration. We now take the ensemble average of both sides of Eq. (7.104b). Interchanging the order of averaging and integrating as in Sec. 7.4, we have

$$E(n_i n_j) = \int_0^T dt \int_0^T d\lambda E[n(t)n(\lambda)] u_i(t) u_j(\lambda) \quad (7.105)$$

Since the noise process is ergodic, Eq. (6.141) applies and we have that the autocorrelation of the process is

$$R(t - \lambda) = E[n(t)n(\lambda)] \quad (7.106)$$

Further, assuming white noise of power spectral density $G(f) = \eta/2$ we have, as in Eq. (7.73) that

$$R(t - \lambda) = \eta/2 \delta(t - \lambda) \quad (7.107)$$

From Eqs (7.104), (7.105), and (7.106) we have that

$$E(n_i n_j) = \int_0^T dt \int_0^T d\lambda \eta/2 \delta(t - \lambda) u_i(t) u_j(\lambda) \quad (7.108)$$

$$= \eta/2 \int_0^T u_i(t) u_j(t) dt = \begin{cases} \eta/2 & \text{if } i = j \\ 0 & \text{if } i \neq j \end{cases} \quad (7.109)$$

We shall have occasion in Sec. 11.2 in our study of the probability of error to make use of the fact that the additive white Gaussian noise $n(t)$ can be represented as Eq. 7.102 where the n_i form a set of statistically independent random variables, each with a mean of zero and a variance of $\eta/2$.

7.6.1 Irrelevant Noise Components

In Sec. 1.5 we considered the situation where we have M signals s_l ($l = 1, 2, \dots, M$) defined over an interval T . We showed that each of these signals could be represented as a superposition of N orthonormal waveforms $u_i(t)$ ($i = 1, 2, \dots, N$). The signals s_l being given, the orthonormal waveforms u_i were generated through the Gram-Schmitt technique. We have then

$$s_l(t) = \sum_{i=1}^N s_{il} u_i(t), \quad l = 1, 2, \dots, M \quad (7.110)$$

the s_{il} being time-independent coefficients. For example, in QPSK $M = 4$ and $N = 2$.

In the absence of noise, it is a rather trivial task to determine at a receiver, which signal $s_l(t)$ was transmitted. In the presence of noise, the receiver system of Fig. 7.12 is optimum in the sense that it maximizes the probability of being correct. In this system, we make available at the receiver, either in fact or in principle, the very same orthonormal signals $u_i(t)$ referred to above. The receiver determines the correlations of the received signal with each of the orthonormal waveforms. On the basis of this examination we assume that the transmitted signal is the one which yields the greatest correlation.

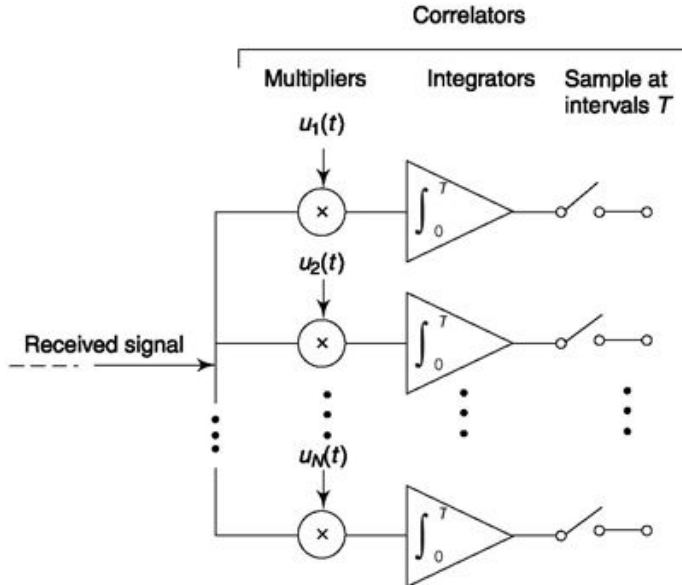


Fig. 7.12 An optimum receiver consists of a bank of correlators.

We noted in the previous section that white noise can also be represented as a superposition of orthonormal components. In the case of white noise an infinite number of orthonormal components are required. Let us now consider that we select an array of orthonormal components, N of which (say the first N) are identical to the N waveforms u_i ($i = 1, 2, \dots, N$) used to represent the possible signals $s_l(t)$. Then the noise is

$$n(t) = \sum_{i=1}^N n_i u_i(t) + \sum_{i=N+1}^{\infty} n_i u_i(t) \quad (7.111)$$

We note that the noise due to the first summation is uncorrelated to the noise terms contained in the second summation. For this reason it is clear that the noise components in the second term of Eq. (7.111) will yield no output at any of the correlators of the receiver of Fig. 7.12. Hence, these components are reasonably referred to as “irrelevant.”

In succeeding sections we shall make use of this result by representing the noise only in terms of the orthonormal components of the signal and we shall ignore the “irrelevant” noise terms.

FACTS AND FIGURES

It was Einstein who while explaining Brownian motion in a paper titled ‘On the Movement of Small Particles Suspended in a Stationary Liquid Demanded by the Molecular-Kinetic Theory of Heat.’ saw that the idea of noise could prove the existence of atoms. It was the year 1905, also known as *Annus Mirabilis* in Latin which means ‘Miracle Year’. In that year, Einstein published three other papers. In the paper titled ‘On a Heuristic Point of View Concerning the Production and Transformation of Light’, he introduced the concept of photoelectric effect. The paper ‘On the Electrodynamics of Moving Bodies’ introduced special theory of relativity and ‘Does the Inertia of a Body Depend upon Its Energy Content?’ gave the world the famous mass-energy equation, $E = mc^2$.

The mathematics of noise is indebted to the independent work of two contemporary scientists, Einstein and Smoluchowski, among others. Smoluchowski’s work on Brownian motion went further to consider external force, concept of transition probability, etc. In the field of physics and chemistry, related to stochastic processes, he is well known but not as much so in other fields. This is due to his work getting overshadowed by the majestic Einstein. Subrahmanyam Chandrasekhar, Nobel Physics winner of 1983, says, “The theory of density fluctuations as developed by Smoluchowski represents one of the most outstanding achievements . . . (he) is chiefly remembered as the originator (along with Einstein) of the theory of Brownian motion . . . (but) his role as the founder of the present flourishing discipline of stochastic theory is not.”

SELF-TEST QUESTION

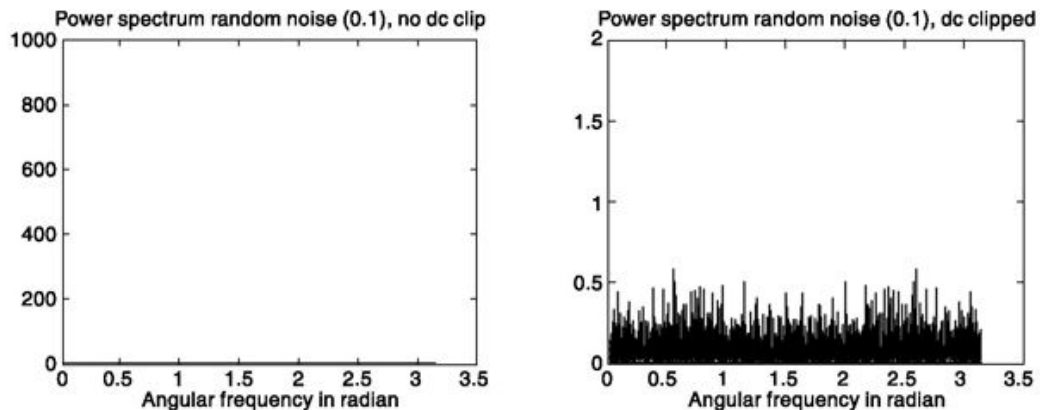
10. Is it true that quadrature components representation helps in addressing narrowband noise?

11. Time derivative of a Gaussian noise does not show Gaussian distribution. Is that correct?

12. Can the noise components orthogonal to the signal of interest be called irrelevant noise components?

MATLAB

```
% Experiment 31
% The following shows power spectrum of random noise that has a dc component
N=4096;
n=rand(N,1); % Generates N random noise elements between 0 and 1
fn=fft(n);
Gn=(abs(fn).^2)/N; % .^ does element wise squaring.
% '.*' stands for element-wise multiplication etc.
```

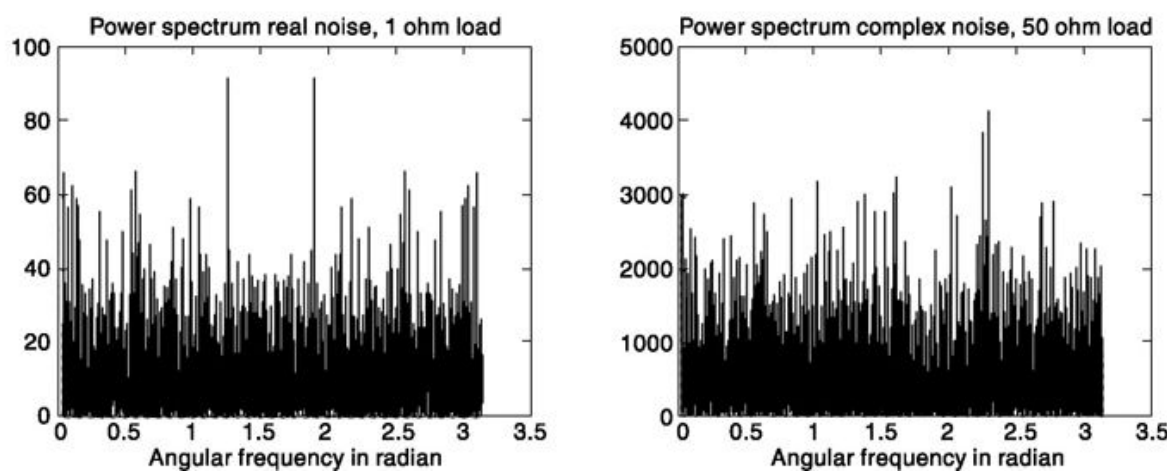


```
w=linspace(0,pi,N); % linspace(X1,X2,N) generates N points between X1 & X2
subplot(121); plot(w,Gn),
title('power spectrum random noise [0,1], no dc clip')
xlabel('angular frequency in radian')
subplot(122); plot(w,Gn), axis([0 3.5 0 2]);
title('power spectrum random noise [0,1], dc clipped')
xlabel('angular frequency in radian')
```

Note that, a high dc value obscures the whiteness of the noise generated.

```
% Experiment 32
% The following shows power spectrum of white gaussian noise accross
% different load

N=4096;
n=wgn(N,1,10); %length Nx1 data of power 10 dBW, load impedance 1 ohm
fn=fft(n);
Gn=(abs(fn).^2)/N;
w=linspace(0,pi,N);
subplot(121), plot(w,Gn);
```



```

title('power spectrum real noise, 1 ohm load')
xlabel('angular frequency in radian')
n=wgn(N,1,10,50,'complex'); %Nx1 complex data of power 10 dBW, load
%impedance 50 ohm
fn=fft(n);
Gn=(abs(fn).^2)/N;
subplot(122), plot(w,Gn);
title('power spectrum complex noise, 50 ohm load')
xlabel('angular frequency in radian')

```

Note the increase in power level and there is no distinction as reference to power spectrum if the noise is real or complex.

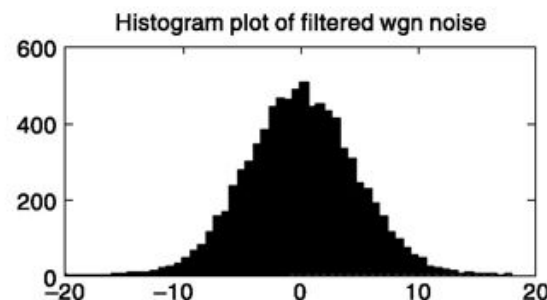
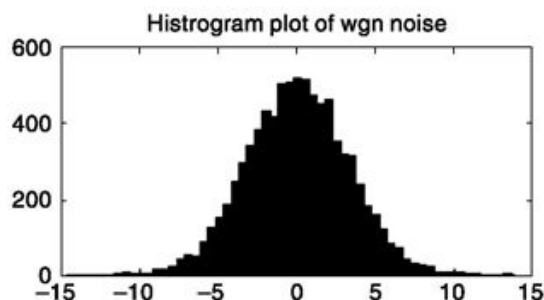
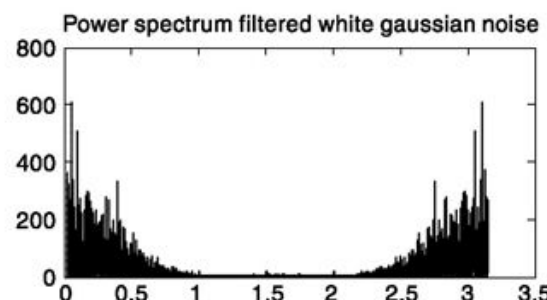
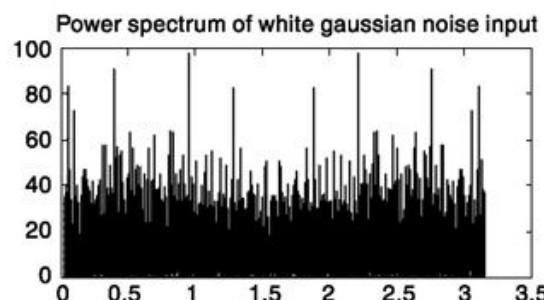
```

% Experiment 33
% The following shows how white gaussian noise becomes non-white as it
% passes through a system of arbitrary transfer function
N=8192;
n=wgn(N,1,10); %length Nx1 data of power 10 dBW, load impedance 1 ohm
fn=fft(n);
Gn=(abs(fn).^2)/N;
w=linspace(0,pi,N);
subplot(221), plot(w,Gn);
title('power spectrum of white gaussian noise input')

%Histogram plot, Refer to Experiment 10 of Ch. 2
x=min(n):(max(n)-min(n))/50:max(n);
subplot(223), hist(n,x), title('Histogram plot of wgn noise');

n1=filter([0.8 0.7 0.4],[1 -0.3],n); % passage through our FIR system
fnl=fft(n1);

```



```

Gn1=(abs(fn1).^2)/N;
subplot(222), plot(w,Gn1);
title('power spectrum filtered white gaussian noise')

%Histogram plot
x=min(n1):(max(n1)-min(n1))/50:max(n1);
subplot(224), hist(n1,x), title('Histogram plot of filtered wgn noise')
Note that the filtered noise is non-white but Gaussian as discussed in theory.

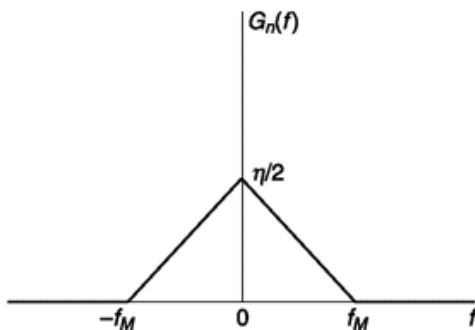
```

SUMMARY

The chapter begins with identifying common sources of noise affecting electrical communication. The discussion on frequency domain representation of noise is followed by the effect of different types of filtering on noise that includes differentiation and integration. In superposition of noise, mixing of noise with sinusoid and another noise source is discussed. It is shown that representation of noise by quadrature components is helpful in characterizing narrowband noise. Various issues related to it including power spectral density, probability density, etc., are discussed. Representing noise in terms of orthonormal components help in identifying irrelevant noise components. This issue is discussed with an example and a correlator scheme. Throughout the discussions reference to white noise is made which is the most common type of noise that interferes with signal in electrical communication.

PROBLEMS

- 7.1 (a) A symmetrical square wave makes excursions between $+V$ and $-V$ volt, where V is a random variable uniformly distributed between 1 V and 2 V. It has a fundamental frequency 10^3 Hz. Make a plot of the two-sided power spectral density of the waveform. Assume that the delay τ between $t = 0$ and a transition is a random variable uniformly distributed between 0 and 1 ms.
- (b) What fraction of the normalized power of the waveform is contained in the frequency range -3×10^3 to $+3 \times 10^3$ Hz?
- 7.2 Noise $n(t)$ has the power spectral density shown.



- (a) Find the normalized power P of the noise in terms of η and f_M . Find P for $\eta = 1 \mu\text{V}^2/\text{Hz}$ and $f_M = 10 \text{ kHz}$.

- (b) Find and plot the autocorrelation function $R_n(t)$ of the noise.

7.3 Gaussian noise $n(t)$ of zero mean has a power spectral density

$$G_n(f) = 2 \mu\text{V}^2/\text{Hz} \quad |f| \leq \text{kHz}$$

$$= 0 \quad \text{elsewhere}$$

- (a) What is the normalized power of the noise?

- (b) Write the probability density function $f(n)$ of the noise.

- (c) The noise $n(t)$ is passed through a filter. The power output of the filter is one-half the power of $n(t)$. Write the probability density function for the output noise of the filter.

7.4 (a) Two Gaussian noise spectral components $n_k(t)$ and $n_l(t)$ are approximated as in Eqs (7.24) and (7.25). The variance of a_k is $a_k^2 = 1$, and the variance of a_l is $a_l^2 = 2$. What is the normalized power of the sum $n_s(t) = n_k(t) + n_l(t)$?

Write the probability density function for the noise waveform $n_s(t)$.

7.5 (a) Gaussian noise in a very narrow spectral range is represented approximately by Eq. (7.15). The normalized power of the noise is $0.01 \mu\text{W}$. Write the expression for the probability density functions of the coefficients a_k and b_k .

- (b) The narrowband noise in (a) is approximated by the representation of Eq. (7.16). Write the expression for the probability density functions of c_k and θ_k .

7.6 White noise with two-sided power spectral density $\eta/2$ is passed through a low-pass RC network with time constant $\tau = RC$ and thereafter through an ideal amplifier with voltage gain of 10.

- (a) Write the expression for the autocorrelation function $R_n(t)$ of the white noise.

- (b) Write the expression for the power spectral density of the noise at the output of the amplifier.

- (c) Write the expression for the autocorrelation of the output noise in (b).

7.7 Consider the noise waveforms $n_1(t), n_2(t), n_3(t), \dots, n_N(t)$ where

$$E[n_j(t)] = 0 \quad j = 1, 2, \dots, N$$

and

$$E[n_j(t)n_k(t)] = \begin{cases} 1 & j = k \\ \frac{1}{2} & |j - k| = 1 \\ 0 & |j - k| > 1 \end{cases}$$

- (a) Calculate the power dissipated in a 1-ohm resistor by the noise

$$n(t) = \sum_{j=1}^N n_j(t)$$

- (b) Assuming that each of the $n_j(t)$ has a Gaussian probability density, write the probability density for $n(t)$.

7.8 Noise $n(t)$ amplitude modulates a carrier having a random phase $v(t) = n(t) \cos(\omega_0 t + \phi)$. Consider that $E[n^2(t)] = \sigma^2$ and that the probability density of the random variable ϕ is $1/2\pi$

from $-\pi$ to π . Assume that $n(t)$ and φ are independent. Show that the power dissipated by $v(t)$ is $E(v^2) = \sigma^2/2$. Is $v(t)$ stationary?

- 7.9 $n(t) = n_1 \cos(\omega_1 t + \varphi_1) + n_2 \cos(k\omega_1 t + \varphi_2)$, where n_1, n_2, φ_1 and φ_2 are uncorrelated. Show that if $v(t) = n(t) \cos(\omega_0 t + \theta)$, where θ is a random variable uniformly distributed from $-\pi$ to π , then $E(v^2) = E(n^2)/2 = \frac{1}{4}[E(n_1^2) + E(n_2^2)]$.

- 7.10 The angles θ_k and θ_l are independent random variables with probability densities which are uniform over all angles. Starting with the convolution integral of Eq. (1.14) show formally that $\theta_k + \theta_l$ and $\theta_k - \theta_l$ also have uniform probability densities. (Hint: Let the probability density be represented by the radius vector r in a cylindrical coordinate system. Then the uniform density over all angles is represented by the radius of a circle of length $1/2\pi$.)

- 7.11 The two-sided power spectral density of noise $n(t)$ is shown in Fig. P7.11.

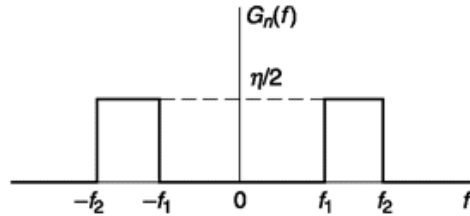


Fig. P7.11

- (a) Plot the power spectral density of the product $n(t) \cos 2\pi f_1 t$.
 (b) Calculate the normalized power of the product in the frequency range $-(f_2 - f_1)$ to $(f_2 - f_1)$.
 (c) Repeat parts (a) and (b) for the product $n(t) \cos 2\pi[(f_2 + f_1)/2]t$.
- 7.12 A noise waveform $n(t)$ has the bandlimited power spectral density shown in Fig. P7.12, with $a = 10^{-6} \text{ V}^2/\text{Hz}$ and $f_M = 10^4 \text{ Hz}$. Plot the power spectral density of $n(t) \sin 2\pi \times 10^6 t$ and find its normalized power over all frequencies.

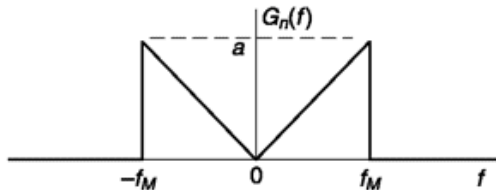


Fig. P7.12

- 7.13 A white-noise current source having a power spectral density $G_n(f) = \eta/2$ is filtered by a narrowband, parallel, single-tuned circuit having a resonant frequency at f_0 and a 3 dB bandwidth $B \ll f_0$.
 (a) Find the output voltage noise power.
 (b) Compare your result with Eq. (7.52).
- 7.14 A random process $v(t) = A \cos(\omega_0 t + \Theta)$ where Θ is a random variable uniformly distributed between $-\pi$ and π , is integrated for a time T . Calculate, using Eq. (7.69) the power, N_0 , in the integrator output. Is this result expected?
- 7.15 Show that Eq. (7.66) follows from Eq. (7.65c).

- 7.16 Show that Eq. (7.71) can be obtained from Eq. (7.70).
- 7.17 Calculate the noise bandwidth of a single-tuned RLC filter centered at frequency f_0 and having a 3 dB bandwidth $B \ll f_0$.
- 7.18 Calculate the noise bandwidth of the Gaussian filter $|H(\omega)|^2 = e^{-\omega^2}$
- 7.19 Show that if a_n and b_n are Gaussian, $n_s(t)$ and $n_c(t)$ are Gaussian.
- 7.20 Show that $E(n_c^2) = E(n_s^2)$.
- 7.21 Show that the autocorrelation functions of $n_c(t)$ and $n_s(t)$ are the same.
- 7.22 Show that $E[n_c(t)n_s(t)] = 0$.
- 7.23 Show that $E[n_c(t)n_s(t + \tau)]$ is not always equal to zero. Prove that it is equal to zero when $G_{n_c}(f) = G_{n_s}(f)$ is an even function with respect to f_0 .
- 7.24 Verify that, with $n_c(t)$ and $n_s(t)$ given as in Eqs (7.82) and (7.83), $n(t)$ given by Eq. (7.79) is identical with $n(t)$ given by Eq. (7.78).
- 7.25 Using Eq. (7.79), show that when $E[n_c(t_1)n_s(t_2)] = 0$ [that is, $G_n(f)$ is an even function of f , with respect to f_0], $R_{nn}(\tau) = R_{n_c n_s}(\tau) \cos \omega_0 \tau = R_{n_s n_s}(\tau) \cos \omega_0 \tau$.
- 7.26 Noise $n(t)$ has the power spectral density shown. We write

$$n(t) = n_c(t) \cos 2\pi f_0 t - n_s(t) \sin 2\pi f_0 t.$$

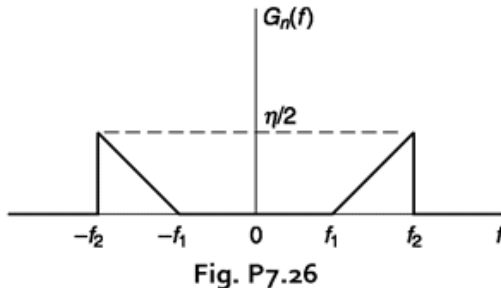


Fig. P7.26

Make plots of the power spectral densities of $n_c(t)$ and $n_s(t)$ for the cases

$$(a) f_0 = f_1 \quad (b) f_0 = f_2 \quad (c) f_0 = \frac{1}{2}(f_2 + f_1)$$

- 7.27 (a) If $G_n(f) = \alpha^2/(\alpha^2 + \omega^2)$, show that $R_n(\tau) = K e^{-\alpha|\tau|}$. Find K .
 (b) If

$$G_n(f) = \frac{\alpha^2/2}{\alpha^2 + (\omega - \omega_0)^2} + \frac{\alpha^2/2}{\alpha^2 + (\omega + \omega_0)^2}$$

show that $R_n(\tau) = K e^{-\alpha|\tau|} \cos \omega_0 \tau$. Here $G_n(f)$ is the spectral density of noise which has been filtered by a narrowband (*symmetrical*) single-tuned filter.

- 7.28 Verify that $n_c(t)$, $n_s(t)$, $\dot{n}_c(t)$ and $\dot{n}_s(t)$ are uncorrelated.
- 7.29 Verify Eq. (7.109).
- 7.30 The signal $\sqrt{2P_s} d(t) \cos(\omega_0 t)$ is received embedded in white Gaussian noise. In order to reduce the probability of error in determining the data $d(t)$ it was proposed that a second receiver be employed using an antenna facing away from the signal, so that only the white Gaussian noise is received.

Can the noise received by this second system help in reducing the error rate by cancelling the noise received with the signal?

REFERENCES

1. Davenport, W., and W. Root: "Random Signals and Noise," McGraw-Hill Book Company, New York, 1958.
2. Papoulis, A.: "Probability, Random Variables, and Stochastic Processes," McGraw-Hill Book Company, New York, 1965.

8

AM RECEPTION PERFORMANCE UNDER NOISE

CHAPTER OBJECTIVE

In Chapter 2, we described amplitude modulation, demodulation and also how a receiver works. In the previous chapter, we characterized noise affecting electrical communication systems. In this chapter, we describe how noise affects reception of amplitude-modulated messages. We investigate single sideband (SSB), double sideband suppressed carrier (DSB-SC) and double sideband with carrier (DSB-C) in detail. For DSB-C, besides synchronous demodulator the performance of cheaper and more convenient alternatives like square-law demodulator and envelop detectors are discussed. The quadrature representation of noise discussed in the previous chapter often proves useful in such analysis. The threshold criterion in DSB-C reception for noncoherent detection is also explained. Besides numerical examples, the chapter also presents MATLAB based simulations highlighting performance of AM systems in noisy environments.

FACTS AND FIGURES

In 1920, a radio station KDKA in Pittsburgh first broadcasted a scheduled commercial program of a radio. It was a 100-watt transmitter on a wooden shack atop of Westinghouse Company's East Pittsburgh plant. The first broadcasting was presidential election returns and occasional music. Throughout the broadcast, the following appeal was interspersed: "... anyone hearing this broadcast please communicate with us, as we are anxious to know how far the broadcast is reaching and how it is being received."

John R. Carson was granted the patent of SSB in 1923 and in the same year, the first transAtlantic radio telephone demonstration used SSB with pilot carrier on a frequency of 52 kHz. By 1927, trans-Atlantic SSB radiotelephony was open for public service. In subsequent years, the use of SSB was limited mainly to low-frequency and wire applications. This was partly due to lack of

interest in conserving spectrum and partly due to belief that FM will have the final say in voice communication which was found incorrect later, especially in long-distance telephony.

8.1 FRAMEWORK FOR AMPLITUDE DEMODULATION

The receiver block diagram of Fig. 2.27, Chapter 2, is reproduced here for convenience. Note that, this is suitable for the reception and demodulation of all types of amplitude-modulated signals. The only essential changes required, to accommodate one type of signal or another, are in the demodulator and in the bandwidth of the IF carrier filter. Hence, from this point our interest will focus on the section of receiver beginning with the IF filter and through to the output.

The signal input to the IF filter is an amplitude-modulated IF carrier. The normalized power (power dissipated in a 1 ohm resistor) of this signal is S_s . The signal arrives with noise. Added, is the noise generated in the RF amplifier and amplified in the RF amplifier and IF amplifiers. The IF amplifiers and mixer are also sources of noise, i.e. thermal noise, shot noise, etc., but this noise, lacking the gain of the RF amplifier, represents a second-order effect. (See Sec. 15.5.4) We shall assume that the noise is Gaussian, white, and of two-sided power spectral density $N_0/2$. The IF filter is assumed rectangular and of bandwidth no wider than is necessary to accommodate the signal. The output baseband signal has a power S_o and is accompanied by noise of total power N_o .

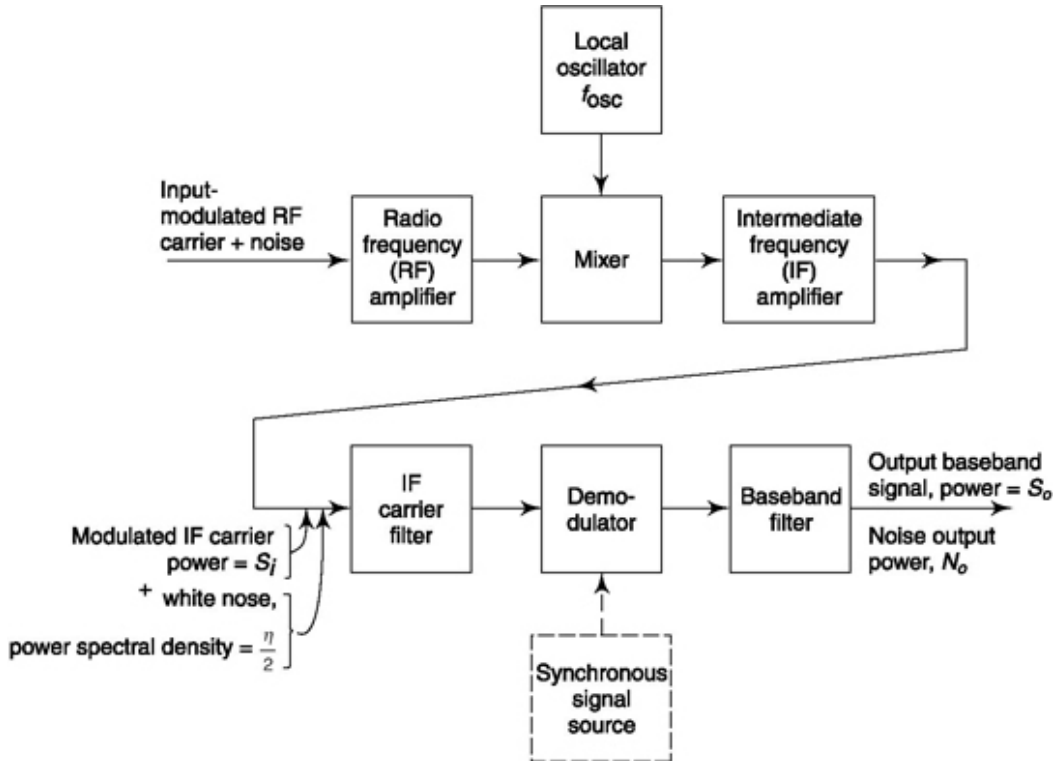


Fig. 8.1 A receiving system for an amplitude-modulated signal.

8.2 SINGLE SIDEBAND SUPPRESSED CARRIER (SSB-SC)

Calculation of Signal power

With a single-sideband suppressed-carrier signal, the demodulator is a multiplier as shown in Fig. 8.2a. The carrier is $A \cos 2\pi f_c t$. For synchronous demodulation the demodulator must be

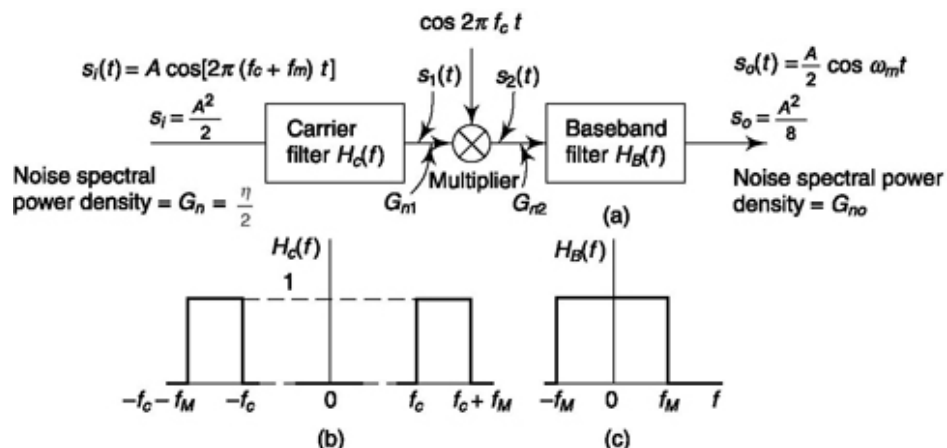


Fig. 8.2 (a) A synchronous demodulator operating on a single-sideband single-tone signal, (b) The bandpass range of the carrier filter, (c) The passband of the lowpass baseband filter.

furnished with a synchronous locally generated carrier $\cos 2\pi f_c t$. We assume that the upper sideband is being used; hence the carrier filter has a bandpass, as shown in Fig. 8.2b, that extends from f_c to $f_c + f_M$, where f_M is the baseband bandwidth. The bandwidth of the baseband filter extends from zero to f_M as shown in Fig. 8.2c.

Let us assume that the baseband signal is a sinusoid of angular frequency f_m ($f_m < f_M$). The carrier frequency is f_c , and, since we have assumed that the upper sideband is being used, the received signal is

$$s_i(t) = A \cos [2\pi(f_c + f_m)t] \quad (8.1)$$

The output of the multiplier is

$$s_2(t) = s_1(t) \cos \omega_c t = \frac{A}{2} \cos[2\pi(2f_c + f_m)t] + \frac{A}{2} \cos 2\pi f_m t \quad (8.2)$$

Only the difference-frequency term will pass through the baseband filter. Therefore the output signal is

$$s_o(t) = \frac{A}{2} \cos 2\pi f_m t \quad (8.3)$$

The input signal power is

$$\frac{1}{2}.$$

which is the modulating signal amplified by

$$S_i = \frac{A^2}{2} \quad (8.4)$$

while the output signal power is

$$S_o = \frac{1}{2} \left(\frac{A}{2}\right)^2 = \frac{A^2}{8} = \frac{S_i}{4} \quad (8.5)$$

Thus

$$\frac{S_o}{S_i} = \frac{1}{4} \quad (8.6)$$

We may readily see that, even though Eq. (8.6) was deduced on the assumption of a sinusoidal baseband signal, the result is entirely general. For suppose that the baseband signal were quite arbitrary in waveshape. Then the single-sideband signal generated by this baseband signal may be resolved into a series of harmonically related spectral components. The input power is the

sum of the powers in these individual components. Next, we note, as was discussed in Chap. 2, that superposition applies to the multiplication process being used for demodulation. Therefore, the output signal power generated by the simultaneous application at the input of many spectral components is simply the sum of the output powers that would result from each spectral component individually. Hence S_t and

S_o in Eqs (8.4) and (8.5) are properly the *total* powers, independently of whether a single or many spectral components are involved.

8.2.1 Calculation of Noise power

We now calculate the output noise N_o . For this purpose, we recall from Sec. 7.3.1 that when a noise spectral component at a frequency f is multiplied by $\cos 2pf_c t$, the original noise component is replaced by two components, one at frequency $f_c + f$ and one at frequency $f_c - f$, each new component having one-fourth the power of the original.

The input noise is white and of spectral density $h/2$. The noise input to the multiplier has a spectral density G_{n1} as shown in Fig. 8.3a. The density of the noise after multiplication by $\cos 2pf_c t$ is G_{n2} as is shown in Fig. 8.3b. Finally the noise transmitted by the baseband filter is of density G_{no} as in Fig. 8.3c. The total noise output is the area under the plot in Fig. 8.3c. We have, then, that

$$N_o = 2f_M \frac{\eta}{8} = \frac{\eta f_m}{4} \quad (8.7)$$

Fig. 8.3 Spectral densities of noises in SSB demodulator. (a) Density G_{n1} of noise input to multiplier, (b) Density G_{n2} of noise output of multiplier, (c) Density G_{no} of noise output of baseband filter.

USE of Quadrature noise Components

It is of interest to calculate the output noise power N_o in an alternative manner using the transformation of Eq. (7.79):

$$n(t) = n_c(t) \cos 2\pi f_c t - n_s(t) \sin 2\pi f_c t \quad (8.8)$$

We now apply Eq. (8.8) to the noise output of the IF filter so that $n(t)$ has the spectral density G_{n1} as in Fig. 8.3a. The spectral densities of $n_c(t)$ and $n_s(t)$ are [see Eqs (7.91) and (7.92)]:

$$G_{n_e}(f) = G_{n1}(f) = G_{n1}(f_c - f) + G_{n1}(f_c + f) \quad (8.9)$$

We observe that for $0 < f < f_M$, $G_{n1}(f_c + f) = h/2$, while $G_{n1}(f_c - f) = 0$, so that $G_n(f)$ and $G((f))$ are as shown in Fig. 8.4.

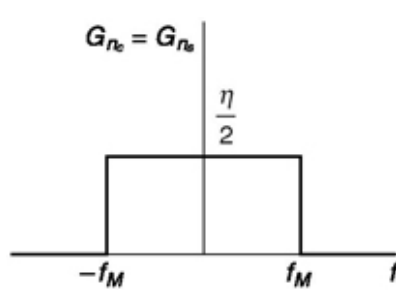


Fig. 8.4 Power spectral densities of G_n and G_{n1} .

Multiplying $n(t)$ by $\cos 2\pi f_c t$ yields

$$\begin{aligned} n(t) \cos 2\pi f_c t &= n_c(t) \cos^2 2\pi f_c t - n_s(t) \sin 2\pi f_c t \cos 2\pi f_c t \\ &= \frac{1}{2} n_c(t) + \frac{1}{2} n_c(t) \cos 4\pi f_c t - \frac{1}{2} n_s(t) \sin 4\pi f_c t \end{aligned} \quad (8.10)$$

The spectral density of $n_o(t)$ is then $G_{no} = \frac{1}{4} G_{n_e} = \frac{1}{4} (\eta/2) = \eta/8$. Hence as before, as shown

in Fig. 8.3c, the spectral density G_{no} is $h/8$ over the range $-f_M$ to f_M , and the total noise is again

$$N_a = hfJ4.$$

Calculation of Signal-to-Noise Ratio (SNR)

Finally we may calculate, using Eqs (8.6) and (8.7), the *signal-to-noise ratio* at the output, S_o/N_o . We have

$$\frac{S_o}{N_o} = \frac{S_i/4}{hf_M/4} = \frac{S_i}{hf_M} \quad (8.12)$$

The importance of SJN_o is that it serves as a *figure of merit* of the performance of a communication system. Certainly, as S_o/N_o increases, it becomes easier to distinguish and to reproduce the modulating signal without error or confusion. If a system of communication allows the use of more than a single type of demodulator (say, synchronous or nonsynchronous), that ratio S_o/N_o will serve as a figure of merit with which to compare demodulators.

We observe from Eq. (8.12) that to increase the output signal-to-noise power ratio, we can increase the transmitted signal power, restrict the baseband

frequency range, or make the receiver quieter.

8.3 DOUBLE SIDEBAND SUPPRESSED CARRIER (DSB-SC)

When a baseband signal of frequency range f_M is transmitted over a DSB-SC system, the bandwidth of the carrier filter must be $2f_M$ rather than f_M . Thus, input noise in the frequency range $f_c - f_M$ to $f_c + f_M$ will contribute to the output noise, rather than only in the range f_c to $f_c + f_M$ as in the SSB case.

Calculation of Noise power

This situation is illustrated in Fig. 8.5a, which shows the spectral density $G_{n1}(f)$ of the white input noise after the IF filter. This noise is multiplied by $\cos w_c t$. The multiplication results in a frequency shift by $\pm f_c$ and a reduction of power in the power spectral density of the noise by a factor of 4. Thus, the noise in region d of Fig. 8.5a shifts to region d shown in Fig. 8.5b. Similarly, regions a , b and c of Fig. 8.5a are translated by $\pm f_c$ and are also attenuated by 4 as shown in Fig. 8.5b. Note that the noise-power spectral density in the region between $-f_M$ and $+f_M$ is $h/4$, while the noise density in the SSB case, as shown in Fig. 8.3c is only $h/8$. Hence the output noise power is twice

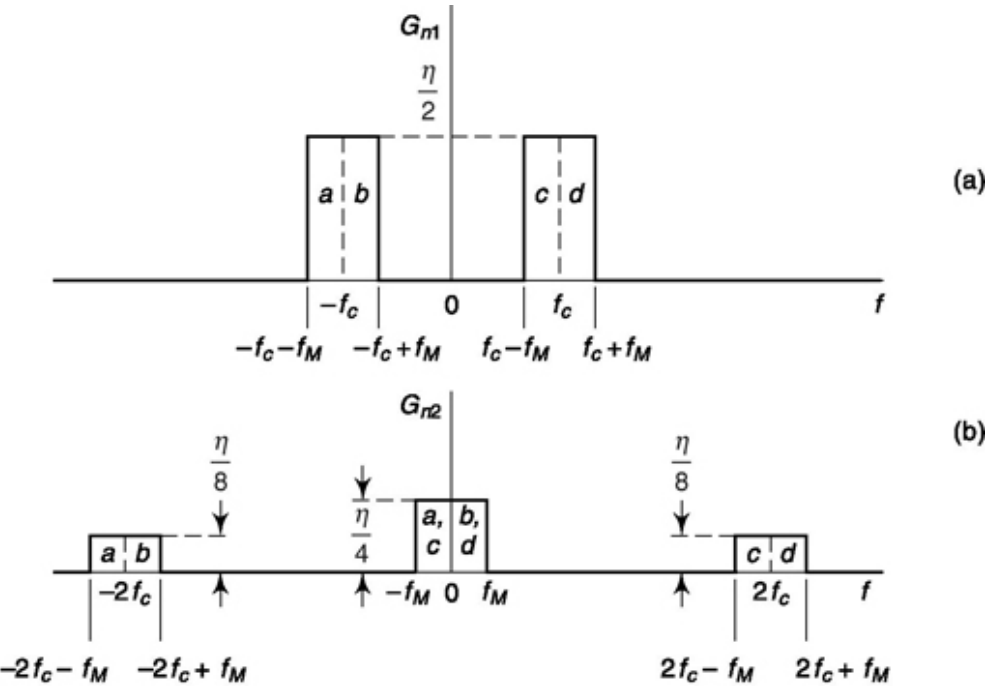


Fig. 8.5 Spectral densities of noise in DSB demodulation. (a) Density G_{ni} of noise at output of IF filter,
 (b) Density G_{n2} of noise output of baseband filter.

as large as the output noise power for SSB given in Eq. (8.5). The output noise for DSB after baseband filtering is therefore

$$N_o = \frac{\eta}{4} (2f_M) = \frac{\eta f_M}{2} \quad (8.13)$$

We can arrive at Eq. (8.13) by using quadrature noise components in a similar manner discussed in the previous section. The only difference lies in considering $G_{no} = \frac{\eta}{4}$, i.e., twice that of SSB-SC value

Calculation of Signal power

We might imagine that for equal received powers, the ratio S_o/N_o for DSB would be only half the corresponding ratio for SSB. We shall now see that such is not the case, and that the ratio S_o/N_o is the *same* in the two cases. Again, without loss in generality, let us assume a sinusoidal baseband signal of frequency $f_m < f_M$. To keep the received power the same as in the SSB case, that is, $S_f = A^2/2$, we write

$$\begin{aligned} s_i(t) &= \sqrt{2} A \cos 2\pi f_m t \cos 2\pi f_c t \\ &= \frac{A}{\sqrt{2}} \cos [2\pi(f_c + f_m)t] + \frac{A}{\sqrt{2}} \cos [2\pi(f_c - f_m)t] \end{aligned} \quad (8.14)$$

The received power is then

$$S_i = \frac{1}{2} \left(\frac{A}{\sqrt{2}} \right)^2 + \frac{1}{2} \left(\frac{A}{\sqrt{2}} \right)^2 = \frac{A^2}{2} \quad (8.15)$$

as in Eq. (8.4).

In the demodulator (multiplier), $s(t)$ is multiplied by $\cos W_c t$. The uppersideband term in Eq. (8.14) yields a signal within the passband of the baseband filter given by

$$s'_o(t) = \frac{A}{2\sqrt{2}} \cos 2\pi f_m t \quad (8.16)$$

The lower-sideband term of Eq. (8.14) yields

$$s''_o(t) = \frac{A}{2\sqrt{2}} \cos 2\pi f_m t \quad (8.17)$$

Observe, most particularly in Eqs (8.16) and (8.17), that $s'_o(t)$ and $s''_o(t)$ are in phase and that hence the output signal is

$$s_o(t) = s'(t) + s''(t) = \frac{A}{\sqrt{2}} \cos 2\pi f_m t \quad (8.18)$$

which has a power

$$S_o = \frac{A^2}{4} = \frac{S_i}{2} \quad (8.19)$$

rather than $S_o = (2/8 = S/4)$ as in Eq. (8.5) for the SSB case. Thus, we see that when a received signal of fixed power is split into two sideband components each of half power, as in DSB, rather than being left in a single sideband, the output signal power increases by a factor of 2. This increase results from the fact that the contributions from each sideband yield output signals which are in phase. A doubling in amplitude causes a fourfold increase in power. This fourfold increase, due to the in-phase addition of s'_o and s''_o , is in part undone by the need to split the input power into two half-power sidebands. Thus, the overall improvement in output signal power is by a factor of 2.

On the other hand, the noise outputs due to noise spectral components symmetrically located with respect to the carrier are uncorrelated with one another. The two resultant noise spectral components in the output, although of the same frequency, are uncorrelated. Hence the combination of the two yields a power which is the sum of the two powers individually, not larger than the sum, as is the case with the signal.

Calculation of signal-to-Noise Ratio

Returning now to the calculation of signal-to-noise ratio for DSB-SC, we find from Eqs (8.13) and (8.19) that

$$\frac{S_o}{N_o} = \frac{S_i}{\eta f_M} \quad (8.20)$$

exactly as for SSB-SC.

Arbitrary Modulating signal

In the discussion in the present section concerning DSB, we have assumed that the baseband signal waveform is sinusoidal. As pointed out in Sec. 8.1, this assumption causes no loss of generality because of the linearity of the

demodulation. Nonetheless it is often convenient to have an expression for the power of a DSB signal in terms of the arbitrary waveform $m(t)$ of the baseband modulating signal. Hence let the received signal be

$$s_i(t) = m(t) \cos 2\pi f_c t \quad (8.21)$$

The power of $s_i(t)$ is

$$S_i \equiv \overline{s_i^2(t)} = \overline{m^2(t) \cos^2 2\pi f_c t} = \frac{1}{2} \overline{m^2(t)} + \frac{1}{2} \overline{m^2(t) \cos(4\pi f_c t)} \quad (8.22)$$

Now $m(t)$ can always be represented as a sum of sinusoidal spectral components. [Of interest, albeit of no special relevance in the present discussion, is the fact that if $m(t)$ is bandlimited to f_M , $m^2(t)$ is bandlimited to $2f_M$. See Prob. 8.7.] Hence, $m^2(t) \cos 4pf_c t$ consists of a sum of sinusoidal waveforms in the frequency range $2f_c \pm 2f_M$. The average value of such a sum is zero, and we therefore have

$$S_i \equiv \overline{s_i^2(t)} = \frac{1}{2} \overline{m^2(t)} \quad (8.23)$$

When the signal $s_i(t)$ in Eq. (8.21) is demodulated by multiplication by $\cos 2pf_c t$, and the product passed through the baseband filter, the output is $s_o(t) = m(t)/2$. The output signal power is

$$S_o = \frac{\overline{m^2(t)}}{4} \quad (8.24)$$

so that, from Eqs (8.23) and (8.24),

$$S_o = \frac{S_i}{2} \quad (8.25)$$

that is, the same result as given in Eq. (8.19) for an assumed single sinusoidal modulating signal.

Example 8.1

A received SSB signal of strength 1 mW has a power spectrum which extends over the frequency range $f_c = 1$ MHz to $f_c = f_m = 1.005$ MHz. The accompanied noise has uniform power spectral density 10^{-9} W/Hz. This is multiplied by a local oscillator of frequency 1 MHz and then followed by a baseband filter of cut-off frequency f_M to get message signal. What is the

message bandwidth? Find the signal and noise energy at the output of baseband filter and calculate the SNR there. How does the SNR change if the bandwidth of the message signal is reduced by 25 percent?

Solution

Single sideband of message is of width $f_M = 1.0005 - 1 \text{ MHz} = 500 \text{ kHz}$

From Eq. (8.6) signal strength at the output of base-

$$\text{band filter} = \frac{1}{4} = 0.25 \text{ mW}$$

From Eq. (8.7) noise strength at the output of baseband

$$1_{\text{filter}} = \frac{10^{-9} \times 500 \times 10^3}{4} = 0.125 \text{ mW}$$

SNR at the filter output = $0.25/0.125 = 2 = 3.01 \text{ dB}$ If baseband filter width remains same as 500 kHz then SNR does not change if bandwidth of message signal is reduced. If baseband filter cutoff frequency is also reduced in-line with message signal the noise reduces by 25 % to $0.125 \times 0.75 = 0.0938$.

Then changed SNR = $0.25/0.0938 = 2.667 = 4.2597 \text{ dB}$

Example 8.2

Repeat Example 8.1 for DSB-SC signal with frequency range $f_c - f_M = 0.995 \text{ MHz}$, $f + f_M = 1.005 \text{ MHz}$. Signal strength and noise power density is same as Example 8.1.

Solution

Single sideband of message is of width $(1.0005 - 0.995)/2 \text{ MHz} = 500 \text{ kHz}$

From Eq. (8.25) signal strength at the output of base-

$$\text{band filter} = \frac{1}{2} = 0.5 \text{ mW}$$

From Eq. (8.13) noise strength at the output of base-

$$\text{band filter} = \frac{10^{-9} \times 500 \times 10^3}{2} = 0.25 \text{ mW}$$

SNR at the filter output = $0.5/0.25 = 2 = 3.01 \text{ dB}$ Similar to SSB demodulation in Example 8.1, if baseband filter width remains same as 500 kHz then SNR does not change if bandwidth of message signal is reduced. If baseband filter cutoff frequency is also reduced in-line with message signal the noise reduces by 25% to $0.25 \times 0.75 = 0.1876$. Then changed SNR = $0.5/0.1876 = 2.667 = 4.2597 \text{ dB}$.

SELF-TEST QUESTION

1. In an AM receiver, it is IF filter and demodulator that differentiates one modulation scheme from another. Is that correct?
2. In SSB reception, signal strength at baseband filter output is half of that at input of carrier filter. Is that true?
3. Does the reduction in frequency range improve SNR of both SSB and DSB-SC reception?
4. Does quadrature components representation of noise alter output SNR of a receiver?

8.4 DOUBLE SIDEBAND WITH CARRIER (DSB-C)

Let us now consider the case where a carrier accompanies the double-sideband signal. Demodulation is achieved synchronously as in SSB-SC and DSB-SC. The carrier is used as a *transmitted reference* to obtain the reference signal $\cos w_c t$ (see Prob. 8.10). We note that the carrier increases the total input-signal power but makes no contribution to the output-signal power. Equation (8.20) applies directly to this case, provided only that we replace S_i by $S_i^{(SB)}$, where $S_i^{(SB)}$ is the power in the sidebands alone. Then

$$\frac{S_o}{N_o} = \frac{S_i^{(\text{SB})}}{\eta f_M} \quad (8.26)$$

Suppose that the received signal is

$$\begin{aligned} s_i(t) &= A[1 + m(t)] \cos 2\pi f_c t \\ &= A \cos 2\pi f_c t + Am(t) \cos 2\pi f_c t \end{aligned} \quad (8.27)$$

where $m(t)$ is the baseband signal which amplitude-modulates the carrier $A \cos 2\pi f_c t$. The carrier power is $A^2/2$. The sidebands are contained in the term $Am(t) \cos 2\pi f_c t$. The power associated with this term is $(A^2/2)\overline{m^2(t)}$, where $\overline{m^2(t)}$ is the time average of the square of the modulating waveform. We then have that the total input power S_i is given by

$$S_i = \frac{A^2}{2} + S_i^{(\text{SB})} = \frac{A^2}{2}[1 + \overline{m^2(t)}] \quad (8.28)$$

Eliminating A^2 , we have

$$S_i^{(\text{SB})} = \frac{\overline{m^2(t)}}{1 + \overline{m^2(t)}} S_i \quad (8.29)$$

or, with Eq. (8.26),

$$\frac{S_o}{N_o} = \frac{\overline{m^2(t)}}{1 + \overline{m^2(t)}} \frac{S_i}{\eta f_M} \quad (8.30)$$

In terms of the carrier power $P_c \equiv A^2/2$, we get, from Eqs (8.28) and (8.30), that

$$\frac{S_o}{N_o} = \overline{m^2(t)} \frac{P_c}{\eta f_M} \quad (8.31)$$

If the modulation is sinusoidal, with $m(t) = m \cos 2\pi f_m t$ (m a constant), then

$$s_i(t) = A(1 + m \cos 2\pi f_m t) \cos 2\pi f_c t \quad (8.32)$$

In this case $\overline{m^2(t)} = m^2/2$ and

$$\frac{S_o}{N_o} = \frac{m^2}{2 + m^2} \frac{S_i}{\eta f_M} \quad (8.33)$$

When the carrier is transmitted only to synchronize the local demodulator waveform $\cos 2\pi f_c t$, relatively little carrier power need be transmitted. In this case $m @ 1$, $m^2/(2 + m^2) @ 1$, and the signal-to-noise ratio is not greatly reduced by the presence of the carrier. On the other hand, when envelope demodulation is used (Sec. 2.3), it is required that $m < 1$. When $m = 1$, the carrier is 100 percent modulated. In this case $m^2/(2 + m^2) = \frac{1}{3}$, so that of the power transmitted, only one-third is in the sidebands which contribute to signal power output.

8.5 COMPARISON OF AM SYSTEMS: A FIGURE OF MERIT

We observe that in each demodulation system considered so far, the ratio S/qf_M appeared in the expression for output SNR [see Eqs (8.12), (8.20), and (8.30)]. This ratio is the output signal power

S_i divided by the product hf_M to give the product hf_M some physical significance, we consider it to be the noise power N_M at the input, measured in a frequency band equal to the *baseband frequency*. Thus,

$$N_M \equiv \frac{\eta}{2} 2f_M = \eta f_M \quad (8.34)$$

The ratio S/hf_M is, therefore, often referred to as the *input signal-to-noise ratio* (SNR) S/N_M . It needs to be kept in mind that N_M is the noise power transmitted through the IF filter only when the IF filter bandwidth is f_M . Thus, N_M is the true input noise power only in the case of single sideband. For the purpose of comparing systems, we introduce the *figure of merit* γ , defined by

$$\gamma \equiv \frac{S_o/N_o}{S_i/N_M} \quad (8.35)$$

The results given above may now be summarized as follows:

$$\gamma = \begin{cases} 1 & \text{SSB-SC} \\ 1 & \text{DSB-SC} \end{cases} \quad (8.36)$$

$$\gamma = \begin{cases} \frac{m^2(t)}{1+m^2(t)} & \text{DSB} \end{cases} \quad (8.37)$$

$$\gamma = \begin{cases} \frac{m^2}{2+m^2} & \text{DSB with sinusoidal modulation} \end{cases} \quad (8.38)$$

$$\gamma = \begin{cases} \frac{m^2}{2+m^2} & \text{DSB with sinusoidal modulation} \end{cases} \quad (8.39)$$

A point of interest in connection with *double-sideband* synchronous demodulation is that, for the purpose of suppressing output-noise power, the carrier filter of Fig. 8.2 is not necessary. A noise spectral component at the input which lies outside the range $f_c \pm f_M$ will, after multiplication in the demodulator, lie outside the passband of the baseband filter. On the other hand, if the carrier filter is eliminated, the magnitude of the noise signal which reaches the modulator may be large enough to overload the active devices used in the demodulator. Hence, such carrier filters are normally included, but the purpose is *overload suppression* rather than *noise suppression*. In single sideband, of course, the situation is different, and the carrier filter does indeed suppress noise.

8.6 THRESHOLD EFFECT IN AM RECEPTION

We have seen in Sec. 2.3 that when synchronous demodulation is not feasible, square-law demodulation or envelope demodulation can be employed. On strong signals (relatively low noise), all demodulators work equally well but for weak signals, synchronous demodulation performs better as the other two show what we now describe as *threshold effect*. In the previous section, we have adopted the figure of merit, the ratio of output SNR to input SNR as a performance measure of the demodulators in the presence of noise and have seen that [Eq. (8.36) to Eq. (8.39)] it is not a function of input signal-to-noise ratio. This means if input SNR is reduced by a certain percentage, the output SNR also reduces by the same percentage. However, as input SNR decreases, there is a point, a threshold at which the output SNR decreases more rapidly. This threshold often marks the limit of usefulness of the demodulator and below the threshold, the performance may be so poor that it is nearly useless. In this section, we briefly describe this effect and make the detailed analysis available in the book website as a supplementary reading material.

Threshold Effect in square Law Demodulator

The input-output relation of a square law device is given by $y = Ix^2$ and is followed by a baseband filter in the demodulator circuit. If the input to the demodulator is $x(t) = ([1 + m(t)] \cos w_c t + n(t))$ then the dropping terms for which PSD falls outside baseband filter and the dc term, we get the signal part as

$$s_o(t) = \lambda A^2 m(t) \left[1 + \frac{m(t)}{2} \right] \quad (8.40)$$

With the assumption $|m(t)| \ll 1$, a condition required to avoid significant signal distortion as discussed in Sec. 2.3.2, we get the output signal power

$$S_o = \lambda^2 A^4 \overline{m^2(t)} \quad (8.41)$$

We avoid the derivation of output noise power which is given in the web supplement and simply report the result here. The total output noise power can be expressed as,

$$N_o = 2\lambda^2 \eta f_M A^2 + 3\lambda^2 \eta^2 f_M^2 \quad (8.42)$$

Considering carrier power $P_c = A^2/2$ and input noise power in the frequency range f_M as $N_M = \eta f_M$, we can write for output SNR,

$$\frac{S_o}{N_o} = \overline{m^2(t)} \frac{P_c}{N_M} \frac{1}{1 + 0.75 N_M / P_c} \quad (8.43)$$

Equations (8.31) and (8.43) are identical except for the factor $1/(1 + 0.75 N_M / P_c)$ which appears for the case of square-law demodulator. When carrier power P_c is large compared to N_M then this extra factor can be ignored and the performance is same as that of a linear synchronous modulator. But as the N_M / P_c term increases, the output SNR starts falling more rapidly and the threshold point is chosen arbitrarily as the one where the performance curve falls away by 1 dB from the linear performance. On this basis, it turns out that the threshold occurs when $P_c / N_M = 4.6$ dB or $P_c = 2.9 N_M$.

Threshold Effect in Envelope Demodulator

Here, a diode demodulator (Sec. 2.3.2) precedes the baseband filter. Representing noise in terms of quadrature components as in Eq. (8.8) and combining in phase and in quadrature components, the ouput signal plus noise just prior to the baseband filter is the envelope (phasor sum)

$$s_2(t) + n_2(t) = \{(A[1+m(t)] + n_c(t))^2 + n_s^2(t)\}^{1/2} \quad (8.44)$$

Assuming $|n_c(t)| \ll A$ and $|n_s(t)| \ll A$, we arrive at the following approximation.

$$s_2(t) + n_2(t) = A[1+m(t)] \left\{ 1 + \frac{2n_c(t)}{A[1+m(t)]} \right\}^{1/2} \quad (8.45)$$

Considering $(1+x)^{1/2} \approx 1 + x/2$ for small x and neglecting dc terms, we get signal power at the output of the baseband filter as

$$S_o = A^2 \overline{m^2(t)} \quad (8.46)$$

Since the PSD of $n_c(t) = \eta$, the output noise power after baseband filtering is

$$N_o = 2\eta f_M \quad (8.47)$$

Then,

$$\frac{S_o}{N_o} = \overline{m^2(t)} \frac{P_c}{N_M} \quad (8.48)$$

and

$$\gamma = \frac{S_o/N_o}{S_i/N_M} = \frac{\overline{m^2(t)}}{1 + \overline{m^2(t)}} \quad (8.49)$$

This result is the same as synchronous demodulation. Now, as input SNR decreases, a point is reached where the output SNR decreases more rapidly. Considering $S_i = A^2/2 = P_c$ and for $S_i/N_M \ll 1$ and $\overline{m^2(t)} \ll 1$, it can be shown that

$$\frac{S_o}{N_o} = \frac{\overline{m^2(t)}}{1.1} \left(\frac{P_c}{N_M} \right)^2 \quad (8.50)$$

This shows a poorer performance than what we get above threshold from Eq. (8.48). In fact, a comparison with Eq. (8.43) shows that a below-threshold envelop detector performs worse than a square-law detector. It is interesting to note that voice signals require nearly 40 dB output SNR for high quality. In that case, both envelope detectors and square-law detectors operate above threshold and are equally good.

Example 8.3

An audio signal of 4 kHz bandwidth is to be transmitted through a channel that introduces 30 dB loss and white noise of power spectral density 10^{-9} W/Hz. Calculate required minimum transmitter power if the message is sent by SSB, DSB-SC and DSB-C modulation. The received output SNR should be more than 40 dB. For DSB-C, energy in sideband is half the energy in carrier.

Solution

From Eq. (8.12) for SSB,

Required minimum output SNR

$$= \frac{S_i}{\eta f_M} = \frac{S_i}{2 \times 10^{-9} \times 4000} = 40 \text{ dB} = 10000$$

Required minimum signal strength at receiver input = $S_t = 0.08 \text{ W}$

Required minimum signal strength at transmitter output = $S_t \times 30 \text{ dB} = 0.08 \times 1000 = 80 \text{ W}$

Following Eq. (8.20) for DSB-SC and proceeding as above, the minimum transmitter power = 80 W For DSB-C, useful energy available in sideband =

$$= \frac{S_i/3}{\eta f_M} = \frac{S_i/3}{2 \times 10^{-9} \times 4000} = 40 \text{ dB} = 10000$$

S/3 Then, required minimum output SNR

Required minimum signal strength at receiver input
= $S_i = 0.24 \text{ W}$

Required minimum signal strength at transmitter output = $S_i \times 30 \text{ dB} = 0.24 \times 1000 = 240 \text{ W}$

Example 8.4

The time average of the square of a modulating message signal of 60 kHz bandwidth is calculated as 0.1 W. The signal is used in DSB-C modulation with carrier power 10 W. If additive white noise power spectral density is 10^{-6} W/Hz , find output SNR for a square demodulator. Also find output SNR if carrier power is reduced by 100 times.

Solution

Given, $\eta/2 = 10^{-6}$, or $\eta = 2 \times 10^{-6}$ so that $N_M = \eta f_M = 2 \times 10^{-6} \times 6 \times 10^4 = 0.12 \text{ W}$

The threshold occurs at carrier power $P_c = 2.9 \times N_M = 2.9 \times 0.12 = 3.48 \text{ W}$

For carrier power of 10 W, from Eq. (8.69) SNR = $0.1 \times 10/0.12 = 9.21 \text{ dB}$

When carrier power is reduced by 100 times $P_c = 10/100 = 0.1 \text{ W}$. This is 12 times less than noise power and

$$\text{from Eq. (8.70) SNR} = \frac{4 \times 0.1 \times (0.1)^2}{3 \times (1.2)^2} = 9.26 \times 10^{-4} \\ = -30.33 \text{ dB.}$$

SELF-TEST QUESTIONS

5. Is the carrier filter in DSB-C reception needed at all for filtering passband signal?

6. What is meant by ‘threshold’ in DSB-C reception?
7. Which of square-law demodulator and envelope demodulator in DSB-C reception shows lower threshold?
8. Is it true that above threshold and for $m^2(t) \neq 1$, envelope demodulator, square-law demodulator and synchronous demodulator perform equally well?

FACTS AND FIGURES

Between 1886 and 1900, many scientists in different parts of the world were involved in the invention of the radio. Heinrich R. Hertz was the first to transmit and receive electromagnetic waves. Nikola Tesla held a demonstration of wireless radio communication in 1893 and the same was done by Oliver Lodge in 1894. In November 1894, Jagadish Chandra Bose became the first to send and receive radio waves over a significant distance. To this the *Daily Chronicle* of England wrote, “The inventor (J.C. Bose) has transmitted signals to a distance of nearly a mile and herein lies the first and obvious and exceedingly valuable application of this new theoretical marvel.”

Bose was not interested in commercially exploiting his invention. Thus, the first patent on wireless telegraphy was awarded to Guglielmo Marconi in England in 1896. Initially, the distance covered by Marconi’s instrument was less and by incorporation of ‘Tesla’s Oscillator’, he succeeded in longdistance communication and a thriving business followed. Back in the US, Tesla filed his patent in 1897 and was granted the same in 1900. Marconi’s first US patent application in the year 1900 got rejected and the patent office observed, “Marconi’s pretended ignorance of the nature of a ‘Tesla oscillator’ being little short of absurd... the term “Tesla oscillator” has become a household word on both continents (Europe and North America)”. In 1904, the US Patent Office reversed its previous decision and gave Marconi a patent for the invention of the radio. Tesla sued Marconi Company for infringement in 1915 and only in 1943, a few months after his death, did the US Supreme Court uphold Tesla’s patent.

MATLAB

```
% Experiment 34

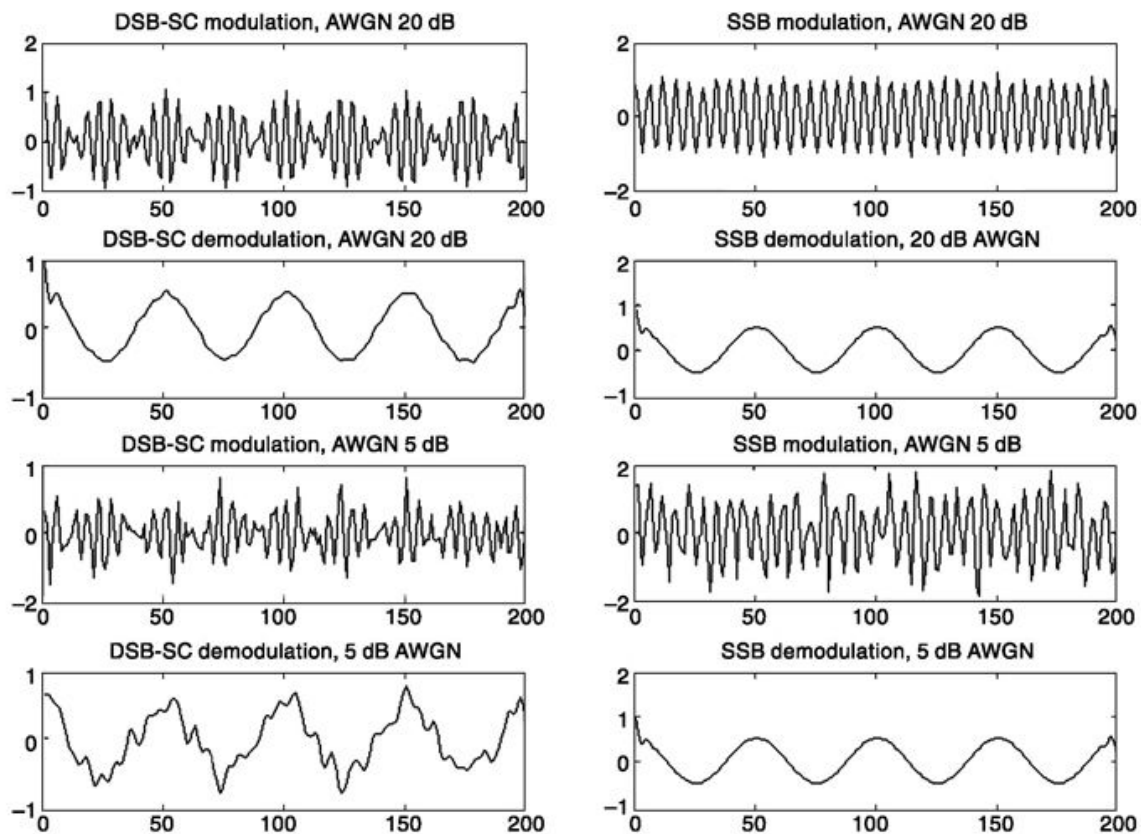
% This is to demonstrate the effect of AWGN noise in DSB-SC and SSB
% transmission and reception. Refer to previous experiments for MATLAB
% functions used here modulate.m, demod.m and awgn.m. You may also use at
% command prompt help <function_name> and press return to know more.

fc=2000;      % Carrier frequency
fs=10000;     % sampling frequency
f=200;        % Single tone modulation

t=0:1/fs:((4/f)-(1/fs));    %Gives exact four cycles of modulating signal
x=cos(2*pi*f*t);

y_dsb_sc = modulate(x,fc,fs,'amdsb-sc');
y(ssb = modulate(x,fc,fs,'amssb');
y_dsb_sc_n=awgn(y_dsb_sc,20,'measured'); %Introduction of AWGN channel noise
subplot(421), plot(y_dsb_sc_n), title('DSB-SC modulation, AWGN 20 dB')
y_ssbn=awgn(y_ssbn,20,'measured'); %Introduction of AWGN channel noise
subplot(422), plot(y_ssbn), title('SSB modulation, AWGN 20 dB')
x1=demod(y_dsb_sc_n,fc,fs,'amdsb-sc');
subplot(423); plot(x1); title('DSB-SC demodulation, 20 dB AWGN')
x2=demod(y_ssbn,fc,fs,'amssb');
subplot(424); plot(x2);title('SSB demodulation, 20 dB AWGN');

y_dsb_sc_n=awgn(y_dsb_sc,5,'measured');
subplot(425), plot(y_dsb_sc_n), title('DSB-SC modulation, AWGN 5 dB')
y_ssbn=awgn(y_ssbn,5,'measured');
subplot(426), plot(y_ssbn), title('SSB modulation, AWGN 5 dB')
x1=demod(y_dsb_sc_n,fc,fs,'amdsb-sc');
subplot(427); plot(x1); title('DSB-SC demodulation, 5 dB AWGN')
```



```

x2=demod(y_ss,fc,fs,'amssb');
subplot(428); plot(x2);title('SSB demodulation, 5 dB AWGN');

% Experiment 35

% This is to demonstrate the effect of AWGN noise in DSB-C
% transmission and reception. Refer to previous experiments for MATLAB
% functions used here modulate.m, demod.m and awgn.m. You may also use at
% command prompt help <function_name> and press return to know more. Ensure
% that function envdet_my.m written for envelop detector in AM demodultion
% at Chapter 3, Experiment 15 is there in the working directory or
% accessible

fc=100000;      % Carrier frequency
fs=1000000;     % sampling frequency
f=1000;          % Tone modulation
m=0.5;           % Modulation index
A=1/m;           % Amplitude of carrier from above relation for modulate.m
opt=-A;          % From definition and syntax of modulate.m

```

```

t=0:1/fs:((4/f)-(1/fs)); %Gives exact four cycles of modulating signal
x=cos(2*pi*f*t);

y = modulate(x,fc,fs,'amdsb-tc',opt);

y_n=awgn(y,20,'measured');
subplot(321), plot(y_n), title('DSB-C modulation, mod. index=0.5, AWGN 20 dB');

x_s=demod(y_n,fc,fs,'amdsb-tc',opt);
subplot(323), plot(x_s), title('DSB-C demodulation, synchronous, AWGN 20 dB');

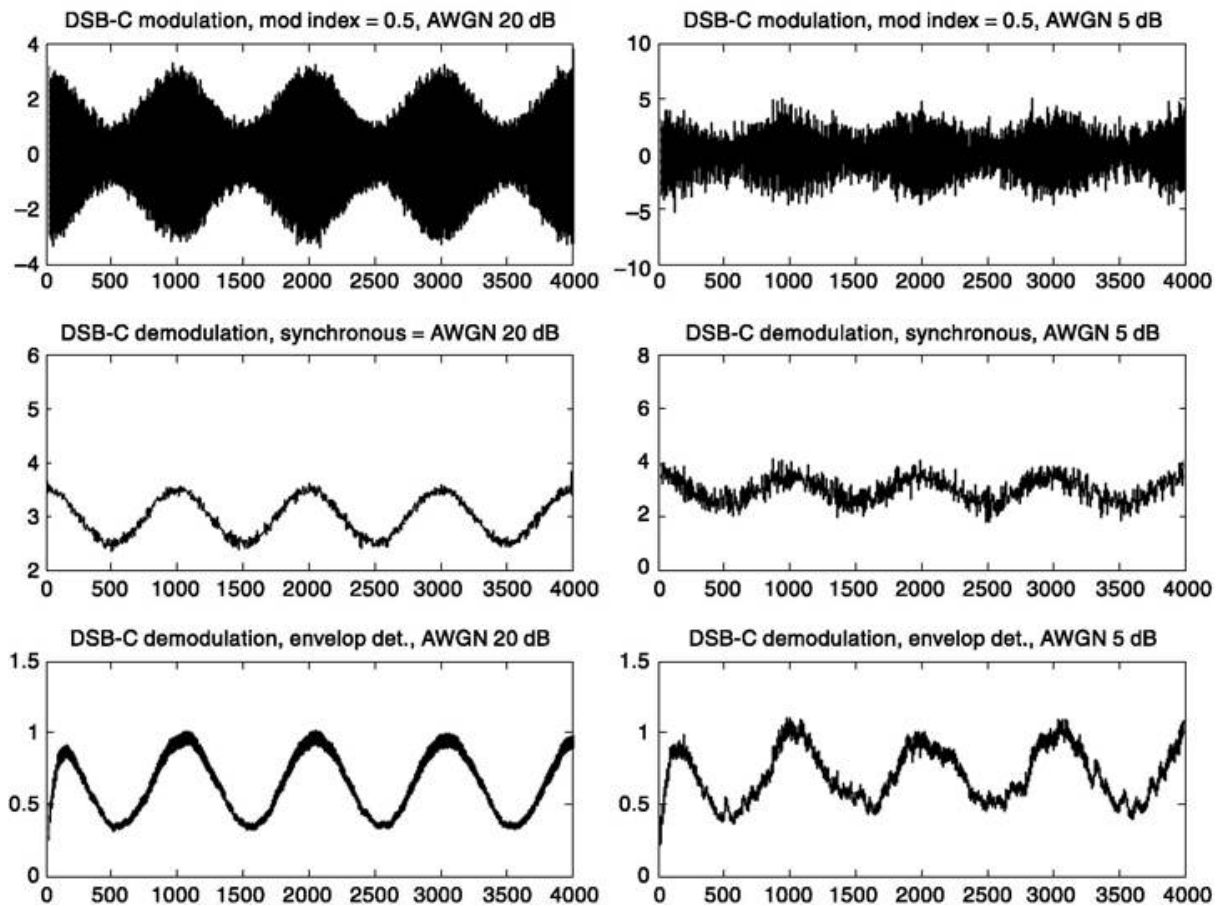
x_e=envdet_my(y_n,f,fs); % Envelop detection by our own coded function
subplot(325), plot(x_e), title('DSB-C demodulation, envelop det., AWGN 20 dB');

y_n=awgn(y,5,'measured');
subplot(322), plot(y_n), title('DSB-C modulation, mod. index=0.5, AWGN 5 dB');

x_s=demod(y_n,fc,fs,'amdsb-tc',opt);
subplot(324), plot(x_s), title('DSB-C demodulation, synchronous, AWGN 5 dB');

x_e=envdet_my(y_n,f,fs);
subplot(326), plot(x_e), title('DSB-C demodulation, envelop det., AWGN 5 dB');

```



SUMMARY

The chapter begins with presentation of common demodulation framework for different kind of amplitude modulated systems which includes discussion

of receiving system introduced in Chap. 2. In each case, received signal and noise power is calculated and signal to noise ratio (SNR) at the final stage (baseband filter) is arrived at. This gives a measure of the noise robustness of a particular modulation scheme. Another measure, called **figure of merit** defined as ratio of output SNR to input SNR of a receiver is also presented. For double sideband with carrier modulation, we can employ convenient noncoherent techniques like square law demodulator or envelope detector. But in noisy condition, both show a threshold effect under which performance starts to degrade more rapidly. It was shown that on this account square law demodulator performs relatively better. Many other practical issues that includes noise overload of amplifier are discussed under various topics.

PROBLEMS

- 8.1 (a) A superheterodyne receiver using an IF frequency of 455 kHz is tuned to 650 kHz. It is found that the receiver picks up a transmission from a transmitter whose carrier frequency is 1560 kHz. Suggest a reason for this undesired reception and suggest a remedy. (These frequencies, 650 kHz and 1560 kHz, are referred to as *image frequencies*. Why?)
- 8.2 Let $g(t)$ be a waveform characterized by a power spectral density $G(f)$. Assume $G(f) = 0$ for $|f| \geq f_1$. Show that the time-average value of $g(t) \cos 2\pi f_c t$ is zero if $f_c > f_1$.
- 8.3 As noted in Sec. 2.4.1, if $m(t)$ is an arbitrary baseband waveform, a received SSB signal may be written $s_i(t) = m(t) \cos 2\pi f_c t + \hat{m}(t) \sin 2\pi f_c t$. Here $\hat{m}(t)$ is derived from $m(t)$ by shifting by 90° the phase of every spectral component in $m(t)$.
- Show that $m(t)$ and $\hat{m}(t)$ have the same power spectral densities and that $\overline{m^2(t)} = \overline{\hat{m}^2(t)}$.
 - Show that if $m(t)$ has a spectrum which extends from zero frequency to a maximum frequency f_M , then $m^2(t)$, $\hat{m}(t)$, and $m(t)\hat{m}(t)$ all have spectra which extend from zero frequency to $2f_M$.
 - Show that the normalized power S_i of $s_i(t)$ is $\overline{m^2(t)} = \overline{\hat{m}^2(t)}$. (*Hint:* Use the result of Prob. 8.2.)
 - Calculate the normalized power S_o of the demodulated SSB signal, i.e. the signal $s_i(t)$ multiplied by $\cos 2\pi f_c t$ and then passed through a baseband filter. Show that $S_o = \overline{m^2(t)}/4$ and hence that $S_o/S_i = \frac{1}{4}$. [*Note:* This problem establishes more generally the result given in Eq. (8.6) which was derived on the basis of the assumption that the modulating waveform is a sinusoid.]
- 8.4 Prove that Eq. (8.11) is correct by sketching the power spectral density of Eq. (8.10).
- 8.5 A baseband signal $m(t)$ is transmitted using SSB as in Prob. 8.3. Assume that the power spectral density of $m(t)$ is

$$G_m(f) = \begin{cases} \frac{\eta_m}{2} \frac{|f|}{f_M} & |f| < f_M \\ 0 & |f| > f_M \end{cases}$$

Find:

- (a) The input signal power.
 - (b) The output signal power.
 - (c) If white Gaussian noise with power spectral density $\eta/2$ is added to the SSB signal, find the output SNR. The baseband filter cuts-off at $f = f_M$.
- 8.6 A received SSB signal has a power spectrum which extends over the frequency range from $f_c = 1$ MHz to $f_c + f_M = 1.003$ MHz. The signal is accompanied by noise with uniform power spectral density 10^{-9} watt/Hz.
- (a) The noise $n(t)$ is expressed as $n(t) = n_c(t) \cos 2\pi f_c t - n_s(t) \sin 2\pi f_c t$. Find the power spectral densities of the quadrature components $n_c(t)$ and $n_s(t)$ of the noise in the spectral range specified as $f_c \leq f \leq f_c + f_M$.
 - (b) The signal plus its accompanying noise is multiplied by a local carrier $\cos 2\pi f_c t$. Plot the power spectral density of the noise at the output of the multiplier.
 - (c) The signal plus noise after multiplication, is passed through a baseband filter and an amplifier which provides a voltage gain of 10. Plot the power spectral density of the noise at the amplifier output, and calculate the total noise output power.
- 8.7 Show that $m^2(t)$ in Eq. (8.22) is bandlimited to $2f_M$.
- 8.8 Repeat Prob. 8.5 if DSB rather than SSB modulation is employed.
- 8.9 A carrier of amplitude 10 mV at f_c is 50 percent amplitude-modulated by a sinusoidal waveform of frequency 750 Hz. It is accompanied by thermal noise of two-sided power spectral density $\eta/2 = 10^{-3}$ watt/Hz. The signal plus noise is passed through the filter shown. The signal is demodulated by multiplication with a local carrier of amplitude 1 volt.
- (a) Find the output signal power.
 - (b) Find the output noise power.

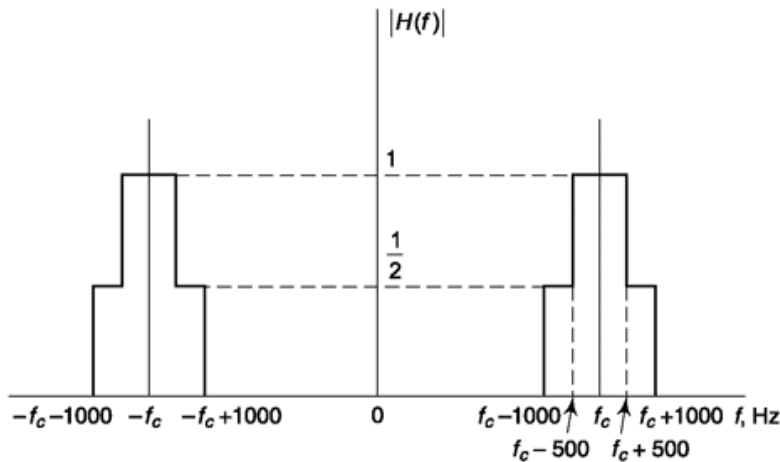


Fig. P8.9

- 8.10 The signal $[\epsilon + m(t)] \cos \omega_c t$ is synchronously detected. The reference signal $\cos \omega_c t$ used to multiply the incoming signal, is obtained by passing the input signal through a narrowband filter of bandwidth B , as shown in Fig. P8.10.
- (a) Calculate S_i .

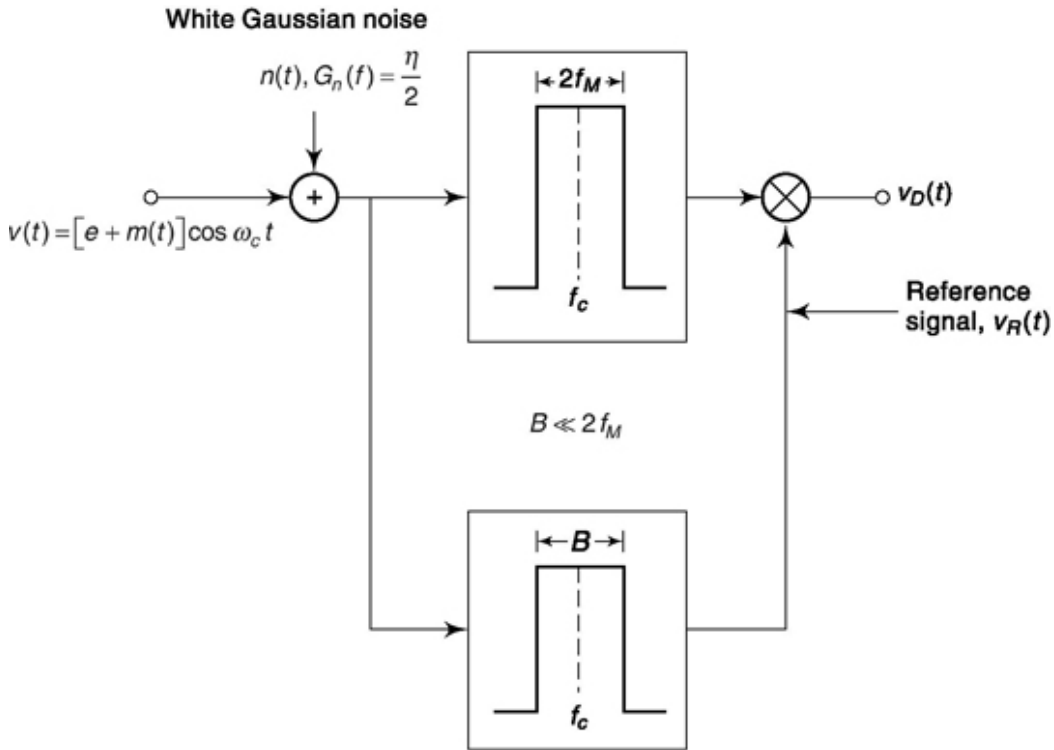


Fig. p8.10

- (c) Comment on the effect of the noisy reference on the output SNR.
- (b) Calculate $v_R(t)$ due to the input signal alone. Calculate the noise power accompanying $v_R(t)$.

8.11 Verify Eqs (8.37) and (8.40).

8.12 (a) Show that the output SNR of a DSB-SC signal which is synchronously detected is independent of the IF bandwidth; i.e. Eq. (8.20) is independent of the IF bandwidth.

(b) Show that the output SNR of an SSB signal which is synchronously detected is dependent on the IF bandwidth. To do this, consider an IF bandwidth which extends from $f_0 - B$ to $f_0 + f_M$, where $f_M > B > 0$. Calculate the output SNR using this bandwidth.

8.13 In the received amplitude-modulated signal $s_r(t) = A[1 + m(t)] \cos 2\pi f_c t$, $m(t)$ has the power spectral density $G_m(f)$ specified in Prob. 8.5. The received signal is accompanied by noise of power spectral density $\eta/2$. Calculate the output signal-to-noise ratio.

8.14 Verify Eq. (8.40) by showing graphically that all the neglected terms have spectra falling outside the range $|f| < f_M$.

8.15 In a DSB transmission, a carrier of 1 MHz frequency and of 2 volts amplitude is amplitude-modulated to the extent of 10 percent by a sinusoidal

baseband signal of frequency 5 kHz. The signal is corrupted by white noise of two-sided power spectral density 10^{-6} watt/Hz. The demodulator is a device whose input/output characteristic is given by $v_o = 3v_i^2$, where v_o and v_i are respectively the output and input voltage. The IF filter, before the demodulator, has a rectangular transfer characteristic of unity gain and 100 kHz bandwidth. By error, the IF filter is tuned so that its center frequency is at 1.002 MHz.

- (a) Calculate the signal waveform at the demodulator output and calculate its normalized power.
- (b) Calculate the noise power at the demodulator output and the signal-to-noise ratio.

8.16 Plot $(1/m^2)$ (S_o/N_o) versus P_c/N_M in Eq. (8.43) and show that the 1-dB threshold occurs when $PJNM = 4.6$ dB.

8.17 Assume that $\overline{m^2(t)} = 0.1$ and that $S_o/N_o = 30$ dB. Find P_c/N_M in Eq. (8.43). Are we above threshold?

8.18 A baseband signal $m(t)$ is superimposed as an amplitude modulation on a carrier in a DSB transmission from a transmitting station. The instantaneous amplitude of $m(t)$ has a probability density which falls off linearly from a maximum at $m = 0$ to zero at $m = 0.1$ volt. The spectrum of $m(t)$ extends over a frequency range from zero to 10 kHz. The level of the modulating waveform applied to the modulator is adjusted to provide for maximum allowable modulation. It is required that under this condition the total power supplied by the transmitter to its antenna be 10 kW. Assume that the antenna appears to the transmitter as a resistive load of 72 ohms.

- (a) Write an expression for the voltage at the input to the antenna.
- (b) At a receiver, tuned to pick up the transmission, the level of the carrier at the input to the diode demodulator is 3 volts. What is the maximum allowable power spectral density at the demodulator input if the signal-to-noise ratio at the receiver output is to be at least 20 dB?

8.19 Plot $(1/m^2)$ (S_o/N_o) versus SJN_M for the envelope demodulator. Assume that $m^2 \neq 1$, and find the intersection of the above-threshold and the below-threshold asymptotes.

8.20 Find the threshold point for an AM envelope detector. In other words, find the input SNR when output SNR of envelope detector falls by 1 dB when compared to a synchronous demodulator.

8.21 Consider the input SNR to be 0 dB. Find output SNR for both square-law demodulator and envelope detector and compare their performances as well as that of a synchronous demodulator.

REFERENCE

1. Davenport, W., and W. Root: "Random Signals and Noise," McGraw-Hill Book Company, New York, 1958.

9

FM RECEPTION PERFORMANCE UNDER NOISE

CHAPTER OBJECTIVE

In this chapter, we discuss the performance of frequency modulation (FM) systems in presence of additive noise. We shall show how in an FM system, an improvement in output signal-to-noise power ratio can be made through the sacrifice of bandwidth and also by inclusion of preemphasis-deemphasis scheme. Like threshold in AM system discussed in the previous chapter, FM too exhibits a threshold below which its performance degrades rapidly. Compared to AM, the threshold effect is much more severe here and occurs at higher level of input signal-to-noise ratio and thus cannot be ignored. The mechanism responsible for such an FM threshold and its relation to occurrence of spikes are presented in detail. Finally, we'll discuss one technique to reduce this threshold by employing feedback. FM threshold can be reduced using phase locked loop (PLL) which we discuss in the next chapter as an important PLL application. Besides numerical examples the chapter also presents MATLAB based simulations highlighting performance of FM systems in noisy environments.

FACTS AND FIGURES

Armstrong demonstrated the utility of FM in the 1930s. The initial success in 1933-1934 leading to commercially sponsored pilot broadcasting services in New York and New England in 1939. Initially, the Radio Corporation of America (RCA) was reluctant to license Armstrong's new technology. The logic put forwarded was that listeners weren't interested in higher quality radio and interested only in cheaper radio sets. In the Second World War, FM had been extremely useful to the allied forces and there was no looking back since then.

Excerpts from the article published in the New York Times on Aug. 2, 1940: "Station W2XOR, New York's first full-time "FM" or staticless radio

broadcaster, went on air last night and was placed in continuous operation, for fifteen hours daily, to carry programs of WOR. ... Major Edwin H. Armstrong, inventor, whose development work is primarily responsible for the "FM" system, pressed a button at the transmitter to start its operation. Thereafter the ceremonies included speeches by Alfred J. McCosker, president of WOR; John Poppele, chief engineer, and others, and music by a symphony orchestra."

9.1 AN FM RECEIVING SYSTEM

The receiving system of Fig. 8.1 may be used with an AM or FM signal. When used to recover a frequency-modulated signal, the AM demodulator is replaced by an FM demodulator such as the limiter-discriminator shown in Fig. 9.1.

The Limiter

In an FM system, the baseband signal varies only the frequency of the carrier. Hence any amplitude variation of the carrier must be due to noise alone. The *limiter* is used to suppress such amplitude-variation noise. In a limiter, diodes, transistors, or other devices are used to construct a circuit in which the output voltage v_1 is related to the input voltage v_i in the manner shown in Fig. 9.2a. The output follows the input only over a limited range. A cycle of the carrier is shown in Fig. 9.2b and the output waveform in Fig. 9.2c. In limiter operation, the carrier amplitude is very large in comparison with the limited range of the limiter, actually much larger than is indicated in Fig. 9.2. As a consequence, the output waveform is a *square* wave. Thus, the output has a waveshape which is nearly entirely independent of modest changes in carrier amplitude. The bandpass filter, following the limiter, selects the fundamental frequency component of the square wave. Therefore, the filter output is again sinusoidal. It has an amplitude which is very nearly independent of the input-carrier amplitude, but does, of course, have the same instantaneous frequency as does the input carrier.

In a physical circuit the limiter and filter generally form an integral unit so that actually there is no point in the limiter-filter combination where the square-wave waveform may be observed.

In this text we shall assume that the discriminator is always preceded by an ideal *hard* limiter, i.e. that the limiter output is a perfect square wave, no

matter how small $v(t)$ may be.

The Discriminator

The discriminator also consists of two component parts. The first of these is a network which, over the range of excursion of the instantaneous frequency, exhibits a transfer characteristic $H(f)$ such that $|H(f)|$ varies linearly with frequency. When the constant-amplitude FM signal passes through this network, it will appear at the output with an amplitude variation (i.e. an envelope) which varies with time precisely as does the instantaneous frequency of the carrier. The baseband signal is now recovered by passing this amplitude-modulated waveform through an envelope demodulator such as the diode detector of Fig. 2.9. The input to the envelope detector is frequency-modulated as well as amplitude-modulated, but the detector does not respond to the frequency modulation.

9.1.1 Mathematical representation of the Operation of the Limiter-discriminator

The frequency-to-amplitude converter necessary to obtain frequency demodulation have an $|H(f)|$ which varies linearly with w over only a limited range, and its slope may be positive or negative. Further, the phase variation of $H(f)$ is of no consequence. However, as a matter of mathematical convenience we shall assume that $H(jw)$ is given by

$$H(j\omega) = j\sigma\omega \quad (9.1)$$

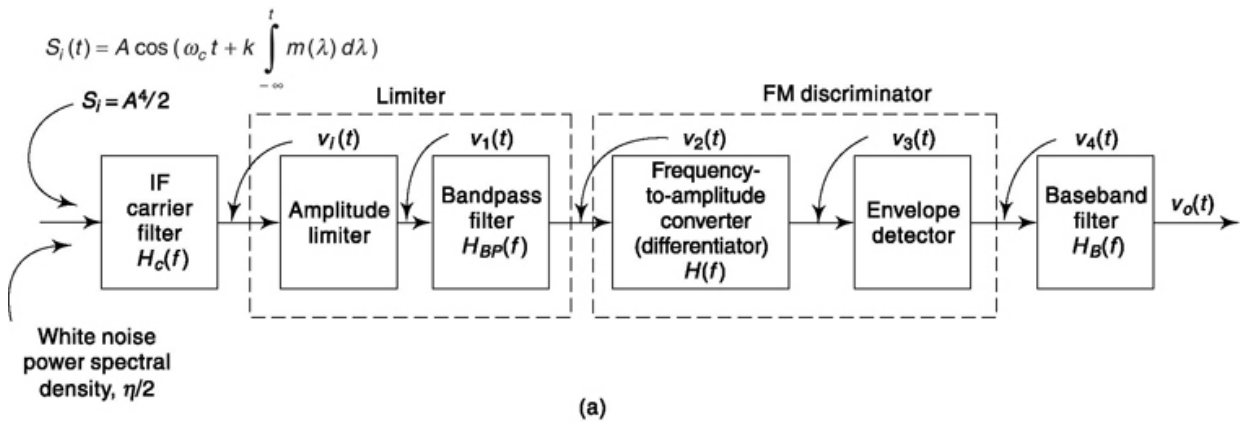


Fig. 9.1 A limiter-discriminator used to demodulate an FM signal.

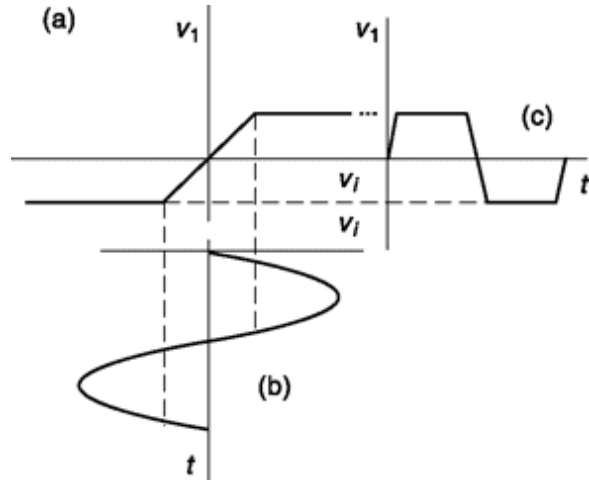


Fig. 9.2 (a) A limiter input-output characteristic. (b) A cycle of the input carrier. (c) The output waveform.

where s is a constant. The advantage of such a selection of $H(jw)$ is that (see Fig. 9.1) the output of the converter $v_3(t)$ is related to the input $v_2(t)$ by the equation

$$v_3(t) = \sigma \frac{d}{dt} v_2(t) \quad (9.2)$$

Equation (9.2) results from the fact that a multiplication by jw in the frequency domain is equivalent to differentiation in the time domain, i.e.

$$\sigma \frac{d}{dt} \Leftrightarrow j\sigma\omega \quad (9.3)$$

Now suppose that the voltage $v_2(t)$ applied to the converter is

$$v_2(t) = A_L \cos [\omega_c t + \phi(t)] \quad (9.4)$$

Here, A_L is the *limited* amplitude of the carrier so that A_L is fixed and independent of the input amplitude, and $\omega_c t + \phi(t)$ is the instantaneous phase. Then from Eq. (9.2),

$$v_3(t) = -\sigma A_L \left[\omega_c + \frac{d}{dt} \phi(t) \right] \sin [\omega_c t + \phi(t)] \quad (9.5)$$

The output of the envelope detector is, using $a = sA_L$,

$$v_4(t) = \sigma A_L \left[\omega_c + \frac{d}{dt} \phi(t) \right] = \alpha \omega_c + \alpha \frac{d}{dt} \phi(t) \quad (9.6)$$

Thus, in summary, we see that if the input waveform to the discriminator is given by Eq. (9.4), the discriminator output is calculated from Eq. (9.6). Note that the discriminator output is proportional to the frequency of the input, df/dt (see Sec. 3.1.1).

9.2 CALCULATION OF SIGNAL TO NOISE RATIO

Let us now consider that the input signal to the IF carrier filter of Fig. 9.1 is

$$s_i(t) = A \cos \left[\omega_c t + k \int_{-\infty}^t m(\lambda) d\lambda \right] \quad (9.7)$$

where $m(t)$ is the frequency-modulating baseband waveform. We assume that the signal is embedded in additive white Gaussian noise of power spectral density $h/2$. The IF carrier filter has a bandwidth $B = 2 Df + 2f_M$ (Carson's rule for bandwidth; see Sec. 3.2.2). This filter passes the signal with negligible distortion and eliminates all noise outside the bandwidth B . The signal with its accompanying noise is ideally limited, discriminated, and after passing through the baseband filter, appears at the output as a signal $s_o(t)$ and a noise waveform $n_o(t)$.

It can be shown that, when the signal-to-noise ratio is high, the noise does not affect the output-signal power. We shall accept this result without giving a proof.¹ In calculating the output-signal power we shall therefore ignore the noise. When the signal $s_i(t)$ in Eq. (9.7) arrives at the output of the limiter shown in Fig. 9.1, the signal is $s_2(t)$ [corresponding to $v_2(t)$] given by

$$s_2(t) = A_L \cos \left[\omega_c t + k \int_{-\infty}^t m(\lambda) d\lambda \right] \quad (9.8)$$

Using the result of Eq. (9.6) and setting

$$\phi(t) = k \int_{-\infty}^t m(\lambda) d\lambda \quad (9.9)$$

we find for the output of the discriminator

$$s_4(t) = \alpha \omega_c + \alpha k m(t) \quad (9.10)$$

The baseband filter rejects the dc component and passes the signal component without distortion. Thus, the output signal is $S_o(t) = \alpha k m(t)$, and the output-signal power is

$$S_o = \alpha^2 k^2 \overline{m^2(t)} \quad (9.11)$$

Output-Noise power

Let us now calculate the noise output of the FM discriminator which results from the presence at the input of white noise having a power spectral density $h/2$. To facilitate the computation, we set the modulation $m(t) = 0$. It can be shown, (although the proof is complex and will not be undertaken here) that the noise output is approximately independent of $m(t)$.¹ The carrier and noise pass through the IF filter $H_c(w)$, which filters the noise. The resulting noise is represented as in Eq. (7.79). Thus the carrier and noise at the limiter input are

$$\begin{aligned} v_i(t) &= A \cos \omega_c t + n_c(t) \cos \omega_c t - n_s(t) \sin \omega_c t \\ &= [A + n_c(t)] \cos \omega_c t - n_s(t) \sin \omega_c t \end{aligned} \quad (9.12)$$

A phasor diagram of the signal and noise is shown in Fig. 9.3. Note that the phasor representing $n_c(t) \cos \omega_c t$ is in phase with the carrier phasor $A \cos \omega_c t$. The phasor representing $n_s(t) \sin \omega_c t$ has

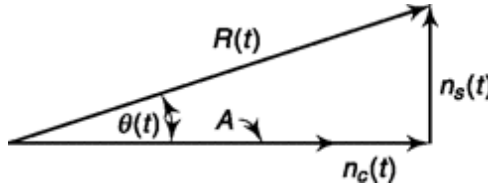


Fig. 93 A phasor diagram of the term in Eq. (9.12).

an amplitude $n_s(t)$ and is in phase-quadrature with the other two terms. The envelope $R(t)$ is easily computed using Fig. 9.3 and is

$$R(t) = \sqrt{[A + n_c(t)]^2 + [n_s(t)]^2} \quad (9.13)$$

Similarly, the phase $d(t)$ is

$$\theta(t) = \tan^{-1} \frac{n_s(t)}{A + n_c(t)} \quad (9.14)$$

Thus, the signal and noise forming $v_i(t)$ can be written as

$$v_i(t) = R(t) \cos [\omega_c t + \theta(t)] \quad (9.15)$$

We ignore the time-varying envelope $R(t)$, since all time variations are removed by the limiter. The output of the limiter-bandpass filter is therefore

$$v_2(t) = A_L \cos [\omega_c t + \theta(t)] \quad (9.16)$$

where again A_L is determined by the limiter, and is a constant.

Let us assume that we are operating under the condition of high-input SNR. Then the noise power is much smaller than the carrier power. In this case we assume that most of the time $|n_c(t)| \gg A$ and $|n_s(t)| \ll A$, on the basis of the justification presented in Sec. 8.4.1. With these assumptions and using the approximation $\tan d \sim d$ for small d , we have, from Eq. (9.14),

$$\theta(t) \approx \frac{n_s(t)}{A} \quad (9.17)$$

Thus, $v_2(t)$ is approximately

$$v_2(t) = A_L \cos \left[\omega_c t + \frac{n_s(t)}{A} \right] \quad (9.18)$$

Comparing Eq. (9.18) with Eq. (9.4) we see that $n_s(t)/A$ is $f(t)$. Then, from Eq. (9.6), we find If we drop the dc term in Eq. (9.19), the noise $n_4(t)$ at the input to the baseband filter is

$$v_4(t) = \alpha \left[\omega_c + \frac{1}{A} \frac{d}{dt} n_s(t) \right] \quad (9.19)$$

The spectral density of $n_s(t)$ is h over the frequency range $|f| < B/2$ (see Sec. 7.5.1). The differentiation is equivalent to passing $n_s(t)$ through a network whose transfer function is $H(jw) = jw$. Hence, as shown in Fig. 9.4a, the operation performed on $n_s(t)$ is equivalent to passing $n_s(t)$ through a network with $H(jw) = jaw/A$. Then $|H(jw)|^2 = a^2 w^2 / A^2$. Therefore, the spectral density of $n_4(t)$ is

$$G_{n4}(f) = \frac{\alpha^2 \omega^2}{A^2} \eta \quad |f| \leq \frac{B}{2} \quad (9.21)$$

This spectral density is plotted in Fig. 9.4b.

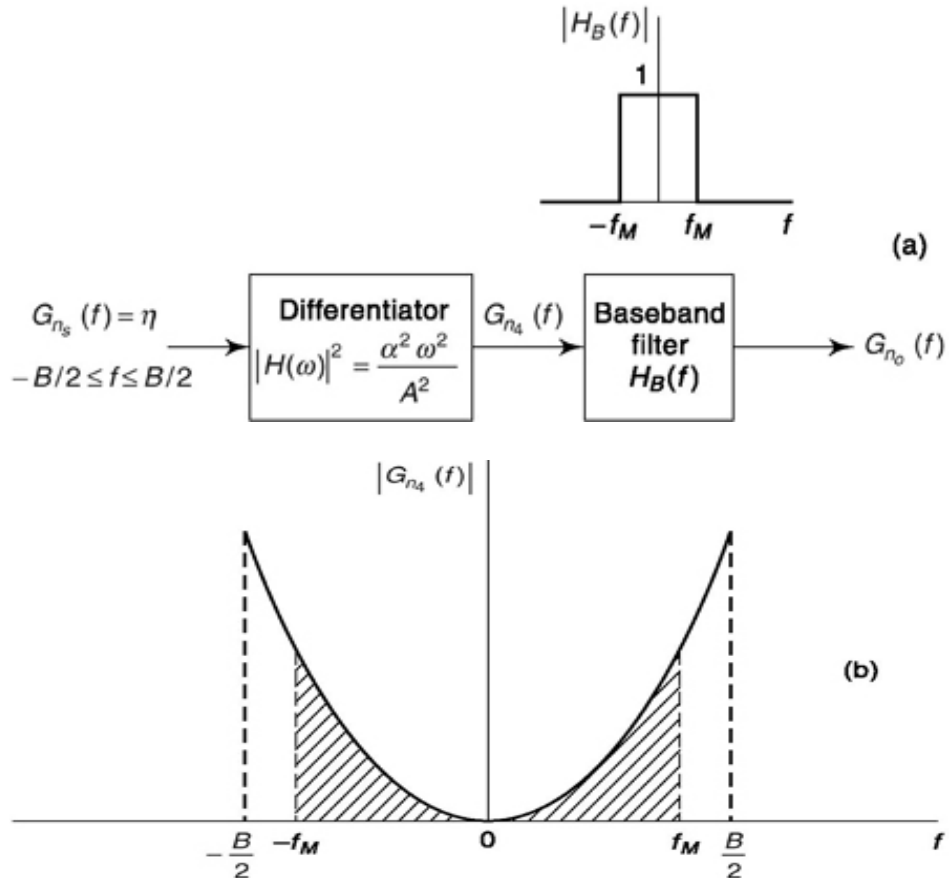


Fig. 9.4 (a) Indicating the operations performed by the discriminator and baseband filter on the noise output of the limiter, (b) The variation with frequency of the power spectral density at the output of an FM demodulator.

Since the baseband filter passes frequencies just up to f_M , only the shaded area in Fig. 9.4b contributes to the output-noise power. This output power can therefore be calculated by computing the shaded area. The output-noise power N_o is

$$N_o = \int_{-f_M}^{f_M} G_{n_4}(f) df = \frac{\alpha^2 \eta}{A^2} \int_{-f_M}^{f_M} 4\pi^2 f^2 df = \frac{8\pi^2}{3} \frac{\alpha^2 \eta}{A^2} f_M^3 \quad (9.22)$$

Output SNR

The output signal-to-noise ratio can now be computed using Eqs (9.11) and (9.22). We find

$$\frac{S_o}{N_o} = \frac{\alpha^2 k^2 \overline{m^2(t)}}{(8\pi^2/3)(\alpha^2 \eta/A^2) f_M^3} = \frac{3}{4\pi^2} \frac{k^2 \overline{m^2(t)}}{f_M^2} \frac{A^2/2}{\eta f_M} \quad (9.23)$$

Now let us consider that the modulating signal $m(t)$ is sinusoidal and produces a frequency deviation Δf . Then the input signal $s_i(t)$ given in Eq. (9.7) may be written [see Eq. (3.13)]

$$s_i(t) = A \cos \left(\omega_c t + \frac{\Delta f}{f_m} \sin 2\pi f_m t \right) \quad (9.24)$$

where f_m is the modulating frequency. Comparing Eq. (9.7) with (9.24), we have, after differentiating the argument, that

$$km(t) = 2\pi \Delta f \cos 2\pi f_m t \quad (9.25)$$

Hence

$$k^2 \overline{m^2(t)} = \frac{4\pi^2 (\Delta f)^2}{2} = 2\pi^2 (\Delta f)^2 \quad (9.26)$$

Substituting this result into Eq. (9.23) yields

$$\frac{S_o}{N_o} = \frac{3}{2} \left(\frac{\Delta f}{f_M} \right)^2 \frac{A^2/2}{\eta f_M} = \frac{3}{2} \beta^2 \frac{S_i}{N_M} \quad (9.27)$$

where $\beta \equiv \Delta f/f_M$ is the modulation index, $S_i = A^2/2$ is the input-signal power, and $N_M \equiv \eta f_M$ is the noise power at the input in the baseband bandwidth f_M . We also have that

$$\gamma_{FM} \equiv \frac{S_o/N_o}{S_i/N_M} \equiv \frac{3}{2} \beta^2 \quad (9.28)$$

which is to be compared with values of g given in Eqs (8.43) and (8.44) for AM systems.

It is to be noted that in Eqs (9.27) and (9.28) the symbol b is being used in a sense which is somewhat different from the sense in which we have used it previously in Chap. 3. Previously, we used b to represent the modulation index associated with a sinusoidal modulating waveform of frequency f_m , that is, $b = Af/f_m$ where Af is the frequency deviation produced by the sinusoidal waveform. In the present instance, $b (= \Delta f/f_M)$ characterizes not a particular sinusoidal modulating waveform but rather a particular set of specifications associated with an FM system. Thus, Eq.

(9.28) has the following interpretation. Suppose that in an FM system whose baseband frequency range is f_M we consider only sinusoidal

modulation. Suppose we assume that independently of the frequency of the modulation its amplitude (and, hence, the frequency deviation Af) is kept fixed. Then, independently of the frequency of the modulation (up to f_M) the performance criterion g will be fixed at $3 b^2/2$.

Note that, we make reference to noise in phase modulation system in Sec. 9.5.

9.3 COMPARISON OF FM AND AM

A comparison of the performances of FM and conventional AM (double sideband with carrier) is of interest. Equation (9.28) applies for sinusoidal frequency modulation of the carrier with modulation index b . Let us compare this result with the corresponding result for sinusoidal amplitude modulation with 100 percent modulation. We find for g_{AM} from Eq. (8.46) that $g_{AM} = 1$, so that from Eq. (9.28)

$$\frac{\gamma_{FM}}{\gamma_{AM}} = \frac{9}{2} \beta^2 \quad (9.29)$$

In the comparison of FM and AM leading to Eq. (9.29), we have assumed in the two cases equal input-noise-power spectral density $h/2$, equal baseband bandwidth f_M , and equal input-signal power S .

Several authors prefer to make the comparison not on the basis of equal signal power but rather on the basis of *equal signal power measured when the modulation $m(t) = 0$* . In this case, as is easily verified (Prob. 9.12), we find that Eq. (9.29) is replaced by

$$\frac{\gamma_{FM}}{\gamma_{AM}} = 3\beta^2 \quad (9.30)$$

A comparison on this basis is not completely fair, however, since the total *transmitted* powers are unequal when the unmodulated carrier powers are the same.

It is clear from either Eq. (9.29) or Eq. (9.30) that FM offers the possibility of improved signal-to-noise ratio over AM. The improvement begins when $9b^2/2 \sim 1$ (Eq. 9.29) or when $3\beta^2 \sim 1$ (Eq. 9.30) corresponding to $b = \sqrt{2}/3 @ 0.5$ or $b = 1/\sqrt{3} @ 0.6$. As b increases, the improvement becomes more pronounced, but this improvement is achieved at the expense of requiring

greater bandwidth. To see the relationship between improvement and bandwidth sacrifice, let us assume that b is large enough so that Carson's rule for bandwidth formula [Eq. (3.25)]

$$B_{FM} = 2(\beta + 1)f_M \quad (9.31)$$

may be approximated by $B_{FM} = 2bf_M$. The bandwidth of the AM system is $B_{AM} = 2f_M$ so that Eq.

(9.29) may be rewritten

$$\frac{\gamma_{FM}}{\gamma_{AM}} = \frac{9}{2} \left(\frac{B_{FM}}{B_{AM}} \right)^2 \quad (9.32)$$

Accordingly, each increase in bandwidth by a factor of 2 increases γ_{FM}/γ_{AM} by a factor of 4 (6 dB).

the noise power is not relatively small, the performance of the FM system degrades rapidly, i.e. the system exhibits a threshold. We shall see in Sec. 9.6 that when the input-noise power is not small in comparison with the input-signal power, the system performance may be improved by restricting the bandwidth, by reducing the modulation index.

We shall now comment briefly on what might appear to be an anomalous situation. We refer to the fact that the performance of the FM system is improved as the bandwidth increases. We might, on intuitive grounds, have expected the opposite effect, since widening the bandwidth admits more noise into the system.

In the AM system the carrier filter bandwidth extends over the range $f_c \pm f_M$, while in FM the bandwidth extends over the range $f_c \pm bfM$. The fact is, however, that noise in the range $f_c \pm b fM$ but outside the range $f_c \pm fM$ does not appear at the output of the FM system. To see this clearly, we refer to Eq. (9.20), which relates the output noise to the quadrature component of the input noise.

This equation indicates that each spectral component of input noise gives rise to an output spectral component of the same frequency. Consider, for example, the pair of noise spectral components at frequencies $f_c \pm f_n$ with $f_M < f_n < b fM$. Such noise components give rise to a baseband noise component at a frequency f_n which will not pass through the baseband filter whose cutoff is at fM . Each such pair of noise spectral components gives rise

to a baseband noise component which is independent of all other noise components. That is, the noise spectral components are not correlated.

On the other hand, let the carrier be FM-modulated by a sinusoidal baseband signal of frequency $f_s > f_M/2$. Then, as discussed in Sec. 3.2 the carrier is accompanied by sidebands separated from the carrier by $\pm f_s$, $\pm 2 f_s$, etc. Except for the sidebands at $\pm f_s$, all other sidebands are separated from the carrier by more than the baseband bandwidth. However, these sidebands are correlated in such a way that the sidebands at, say, $\pm 2 f_s$, do not give rise to a baseband signal at frequency $2f_s$ but serve rather to increase the amplitude of the baseband signal at f_s , as do the higher-order sidebands. Thus, the apparent anomaly is resolved by recognizing that noise outside the range $f_c \pm f_M$ does not pass through the system, while signal sidebands outside this range do contribute to the eventual output signal of the demodulator.

We observe then a characteristic of FM which is not shared by AM. The FM system allows us to sacrifice bandwidth for the sake of improving signal-to-noise ratio. The improvement begins to make itself apparent when $b @ 0.5$ or 0.6 . This value of b is roughly the value of b which establishes the demarcation between “narrowband” and “wideband” FM. Thus, signal-to-noise improvement is a feature of wideband FM not shared by narrowband FM. Equations (9.29) and (9.30) suggest a continuous improvement in performance with increased b (and correspondingly increased bandwidth). Such is indeed the case as long as the noise power admitted by the carrier filter continues to be small in comparison with the signal power. It will be recalled that in deriving Eq. (9.28) we made this assumption of relatively small noise (see Eq. 9.17). When the bandwidth becomes so large that

Example 9.1

(a) Find output SNR of an FM Limiter-Discriminator demodulator when input signal strength = 0.5 W, maximum frequency deviation = 60 kHz, baseband signal cut-off frequency = 15 kHz, received white Gaussian noise power spectral density = 10^{-10} W/Hz and average power of modulating signal = 0.1 W. (b) Find required transmitter power for above if channel has 20 dB loss and required output SNR greater than 40 dB.

Solution

(a) From, Eq. (9.23),

$$\frac{S_o}{N_o} = \left(\frac{3}{4\pi^2} \right) \cdot \left(\frac{k^2 \bar{m}^2(t)}{f_M^2} \right) \cdot \left(\frac{A^2 / 2}{\eta f_M} \right)$$

The last term in the bracket represents received input signal to noise ratio as its numerator gives strength of signal ($S_i = A^2/2$) and denominator strength of noise in the band of interest.

The numerator in the second term is related to maximum frequency deviation Df .

$$\text{Now, } \Delta f = |f - f_c| = |(f_c + k|m(t)|_{\max} - f_c)| = \\ k|m(t)|_{\max} = k \text{ since, message } |m(t)| \leq 1$$

where, f = instantaneous frequency and f_c = carrier frequency.

Thus the above equation can be rewritten as,

$$\frac{S_o}{N_o} = \left(\frac{3}{4\pi^2} \right) \cdot \left(\frac{\Delta f^2}{f_M} \right) \cdot \bar{m}^2(t) \cdot \left(\frac{S_i}{\eta f_M} \right)$$

Example 9.2

Consider Limiter-Discriminator based FM demodulation with a sinusoidal modulation signal with 60 kHz maximum frequency deviation and 15 kHz baseband filter width. Find the Figure of Merit. (a) Compare performance with an AM system if input signal power, noise spectral density and baseband bandwidth are same. (b) How does the value change if bandwidth of incoming FM is double that of AM signal compared to (a)?

Solution

- (a) If input signal $m(t)$ is sinusoidal then **figure of merit** from Eq. (9.28)

$$\gamma_{FM} = \frac{3}{2} \beta^2$$

Here, $\beta = \Delta f/f_M = 60/15 = 4$

Thus $\gamma_{FM} = \frac{3}{2} \times 4^2 = 24$

Comparison for above condition with AM system is given by Eq. (9.29).

Thus, $\frac{\gamma_{FM}}{\gamma_{AM}} = \frac{9}{2} \beta^2 = \frac{9}{2} (4)^2 = 72$

- (b) If bandwidth of incoming FM is doubled then from Eq. (9.31) and Eq. (9.32) it is equivalent to β approximately being doubled in above relation.

Hence, $\frac{\gamma_{FM}}{\gamma_{AM}} = 72 \cdot (2)^2 = 288$

SELF-TEST QUESTION

1. The job of limiter in FM demodulation is to suppress noise associated with amplitude variation. Is that correct?
2. Does FM demodulation involve envelop detection stage used in AM demodulation?
3. In FM demodulation, does b in the relation represent modulation index of sinusoidal FM? $\text{Figure of merit} = \frac{3}{2} \beta^2$
4. At what value of b , does the separation between narrowband FM and wideband FM occur?

9.4 preemphasis, deemphasis and snr improvement

Suppose that we undertake to transmit a baseband signal using FM modulation and naturally require the best possible signal-to-noise ratio for a given carrier power, noise spectral density, IF bandwidth and baseband bandwidth. Then clearly, before applying the baseband signal to the FM

modulator, we shall raise the level of the modulating baseband signal to the maximum extent possible in order to modulate the carrier as vigorously as possible. How shall we know that we have reached the maximum allowable level of the modulating signal? One way of making such a determination is to demodulate the modulated signal and measure the distortion. The distortion occurs because eventually the frequency deviation exceeds the specified IF bandwidth. The modulating signal level may be raised only until the distortion exceeds a specified value.

When, however, the baseband signal happens to be an audio signal, it turns out that something further can be done. An audio signal usually has the characteristic that its power spectral density is relatively high in the low-frequency range and falls off rapidly at higher frequencies. For example, speech has little power spectral density above about 3 kHz. And while music, of course, extends farther into the high-frequency range, the feature still persists that most of its power is in the low-frequency region. As a consequence, when we examine the spectrum of the sidebands associated with a carrier which is frequency-modulated by an audio signal, we find that the power spectral density of the sidebands is greatest near the carrier and relatively small near the limits of the allowable frequency band allocated to the transmission. The manner in which we may take advantage of these spectral features, which are characteristic of audio signals, in order to improve the performance of an FM system, is shown in Fig. 9.5.

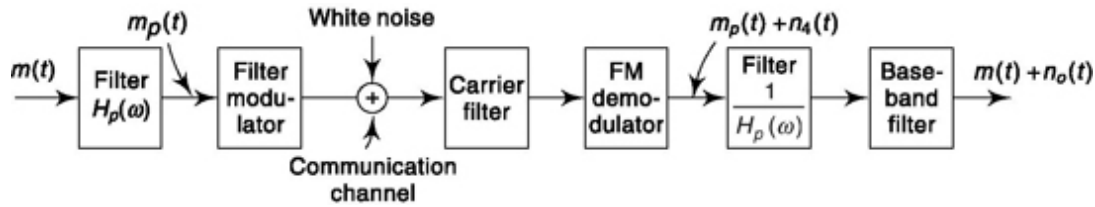


Fig. 9.5 Preemphasis and deemphasis in an FM system.

We observe in Fig. 9.5 that, at the transmitting end, the baseband signal $m(t)$ is not applied directly to the FM modulator but is first passed through a filter of transfer characteristic $H_p(w)$, so that the modulating signal is $m_p(t)$. The modulated carrier is transmitted across a communication channel, during which process, as usual, noise is added to the signal. The receiver is a conventional discriminator except that a filter has been introduced before the baseband filter. The transfer characteristic of this filter is the reciprocal of the characteristic of the transmitter filter. This receiver filter of transfer characteristic $1/H_p(w)$ may equally well be placed after the baseband filter

since both filters are linear. We observe that any modification introduced into the baseband signal by the first filter, prior to modulation, is presently undone by the second filter which follows the discriminator. Hence, the output signal at the receiver is exactly the same as it would be if the filters had been omitted entirely. The noise, however, passes through only the receiver filter, and this filter may then be used to suppress the noise to some extent.

The selection of the transfer characteristic $H_p(w)$ is based on the following considerations. We note that at the output of the demodulator the spectral density of the noise, given by $G_{n4}(f)$ in Eq. (9.21) and shown in Fig. 9.4b, increases with the square of the frequency. Hence the receiver filter will be most effective in suppressing noise if the response of the filter falls off with increasing frequency, that is, if the filter transmission is lowest where the spectral density of the noise is highest. In such a case the transmitter filter must exhibit a rising response with increasing frequency. Let us assume initially that we design the transmitter filter so that it serves only to increase the spectral density of the higher-frequency components of the signal $m(t)$. Such a filter must necessarily increase the power in the modulating signal, thereby increasing the distortion above its specified maximum value. We have, however, noted above that the spectral density of the modulated carrier is relatively small near the edges of the allowed frequency band. We may then expect that such a filter may possibly raise the signal spectral density only near the edges of the allowed frequency band and cause only a small increase in distortion. In this case, we might expect that if the modulating signal power is lowered to decrease the distortion to the allowed value, we end up with a net advantage, i.e., the

improvement due to raising the spectral density near the edges of the allowable band outweighs the disadvantage due to the need to lower the level of the modulating signal. We shall see that such is indeed the case. The premodulation filtering in the transmitter, to raise the power spectral density of the baseband signal in its upper-frequency range, is called *preemphasis* (or *predistortion*). The filtering at the receiver to undo the signal preemphasis and to suppress noise is called *deemphasis*.

SNR Improvement using preemphasis

We recall from Sec. 3.3.3 that the bandwidth occupied by the output of an FM modulator is fixed if the normalized power (or mean square frequency deviation) of the modulating signal is kept fixed (see Prob. 9.16). Hence, referring to Fig. 9.5, we require that the normalized power of the baseband signal $m(t)$ must be the same as the normalized power of the preemphasized signal $m_p(t)$. We begin by expressing the normalized power of a signal in terms of its spectral density. If then $G_m(f)$ is the power spectral density of $m_p(t)$, then the power spectral density of $m_p(t)$ is $|H_p(f)|^2 G_m(f)$, and we require that

$$P_m = \int_{-f_M}^{f_M} G_m(f) df = \int_{-f_M}^{f_M} |H_p(f)|^2 G_m(f) df \quad (9.33)$$

where f_M is the maximum frequency of the modulating signal.

In the absence of deemphasis the output noise is given by N_o in Eq. (9.22).

With the deemphasis filter, the output noise is

$$N_{od} = \left(\frac{\alpha}{A}\right)^2 4\pi^2 \eta \int_{-f_M}^{f_M} f^2 \left|\frac{1}{H_p(f)}\right|^2 df \quad (9.34)$$

The ratio of the noise output without deemphasis to the noise output with deemphasis is $NJN_{od} = R$. From Eqs (9.22) and (9.34) we have

$$R = \frac{(\alpha/A)^2 (4\pi^2 \eta) \int_{-f_M}^{f_M} f^2 df}{(\alpha/A)^2 (4\pi^2 \eta) \int_{-f_M}^{f_M} f^2 / |H_p(f)|^2 df} = \frac{f_M^3 / 3}{\int_0^{f_M} f^2 df / |H_p(f)|^2} \quad (9.35)$$

Since the signal itself is unaffected in the overall process, this quantity R is the ratio by which preemphasis-deemphasis improves the signal-to-noise ratio. We are at liberty to select $H_p(f)$ in Eq. (9.35) arbitrarily, provided only that $H_p(f)$ satisfies the constraint imposed by Eq. (9.33):

In the next section we discuss the application of preemphasis-deemphasis to commercial FM broadcasting.

9.4.1 preemphasis and Deemphasis in Commercial FM Broadcasting

We have noted that the spectral density of the noise at the output of an FM demodulator increases with the square of the frequency. Hence, a

deemphasis network at the receiver will be most effective in suppressing noise if its response falls with increasing frequency. In commercial FM the deemphasis is performed by the simple low-pass resistance-capacitance network of Fig. 9.6a. This network has a transfer function $H_d(f)$ given by

$$H_d(f) = \frac{1}{1 + jf/f_1} \quad (9.36)$$

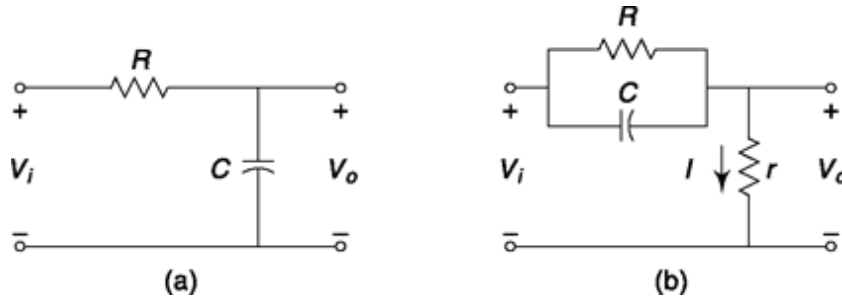


Fig. 9.6 (a) Deemphasis network, and (b) preemphasis network used in commercial radio.

where $f = 1/2\pi RC$. At the transmitter we require an inverse network. A simple network which may be adjusted to provide the required response is shown in Fig. 9.6b. Let us assume that $r \neq R$, and that in the baseband audio-frequency range r is also very small in comparison with the reactance of the capacitance C . In this case we can approximately compute the current $I(f)$ by neglecting the presence of r . We find, for the audio range,

$$I(f) = V_i(f) \left(\frac{1}{R} + j\omega C \right) \quad (9.37)$$

The output voltage $V_o(f) = rI(f)$, and the transfer function $H_p(f) \equiv V_o(f)/I(f)$ is

$$H_p(f) = \frac{r}{R} (1 + j\omega CR) = \frac{r}{R} \left(1 + j \frac{f}{f_1} \right) \quad (9.38)$$

where, as before, $f = 1/2\pi RC$. Hence, $H_p(f)$ has a frequency dependence inverse to $H_d(f)$ as required, in order that no net distortion be introduced into the signal. Thus, $H_p(f)H_d(f) = r/R = \text{constant}$.

Normalized logarithmic plots of H_p and H_d are shown in Fig. 9.7. The transfer function H_d actually has a second breakpoint, as shown, at $f_2 = V_{pt}C$. Since $r \neq R$, $f_2 \neq f_x$, and it is easily arranged that this second breakpoint lie well outside the baseband spectral range and hence be irrelevant.

The improvement in signal-to-noise ratio which results from preemphasis depends on the frequency dependence of the power spectral density of the baseband signal. Let us assume that the spectral density of a typical audio signal, say music, may reasonably be represented as having a frequency dependence given by

$$G_m(f) = \begin{cases} G_0 \frac{1}{1 + (f/f')^2} & |f| \leq f_M \\ 0 & \text{elsewhere} \end{cases} \quad (9.39)$$

where G_0 is the spectral density at low frequencies, while f' is the frequency at which $G(f)$ has fallen by 3 dB from its low-frequency value. Let us further assume that we have adjusted the preemphasis network so that $f' = f$.

The baseband signal to be preemphasized is transmitted through the network of Fig. 9.6b and also through an adjustable gain amplifier. The amplifier will make up for the attenuation produced by the preemphasis network, and its gain is adjusted to the point where the full allowable bandwidth

$$\mathcal{R} = \frac{\tan^{-1}(f_M/f_1)}{3(f_1/f_M)[1 - (f_1/f_M)\tan^{-1}(f_M/f_1)]} \quad (9.43)$$

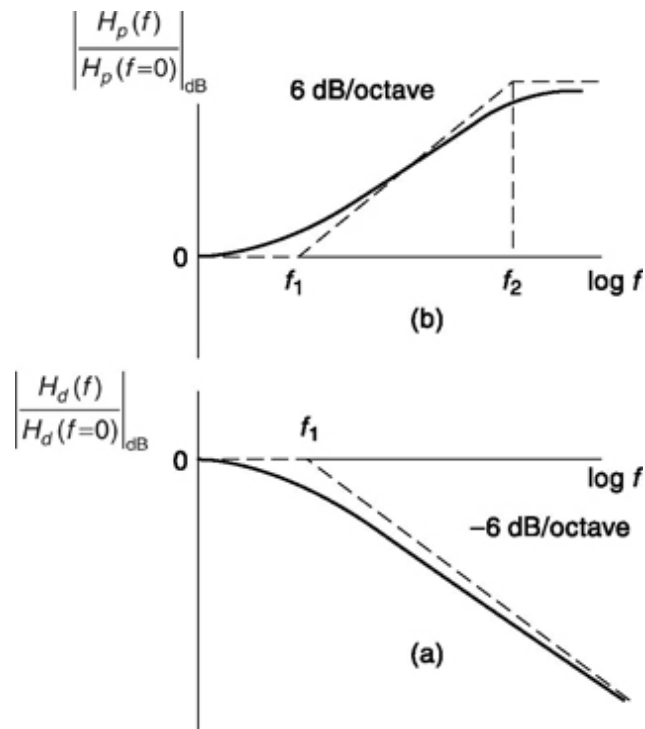


Fig. 9.7 Normalized logarithmic plots of the frequency characteristics of (a) the deemphasis network and (b) the preemphasis network.

is occupied by the modulated carrier. Hence, the baseband signal $m(t)$ passes through a network whose transfer function is

$$H_p(f) = K \left(1 + j \frac{f}{f_1} \right) \quad (9.40)$$

where K is the product of the amplifier gain and the ratio r/R [see Eq. (9.38)]. The coefficient K is adjusted so that the constraint of Eq. (9.33) is satisfied. Using Eq. (9.39) with $f' = f_1$ and using Eq. (9.40), we find by substitution into Eq. (9.33) that K is determined by the condition that

$$P_m = \int_{-f_M}^{f_M} \frac{G_0 df}{1 + (f/f_1)^2} = \int_{-f_M}^{f_M} K^2 G_0 df \quad (9.41)$$

Integrating and solving for K^2 , we find

$$K^2 = \frac{f_1}{f_M} \tan^{-1} \frac{f_M}{f_1} \quad (9.42)$$

Using this value of K , and substituting $H_p(f)$ in Eq. (9.40) into Eq. (9.35), we compute R , the improvement which results from preemphasis and subsequent deemphasis. We find that

$$\mathcal{R} = \frac{\tan^{-1}(f_M/f_1)}{3(f_1/f_M)[1 - (f_1/f_M)\tan^{-1}(f_M/f_1)]} \quad (9.43)$$

If the power in the baseband signal is principally confined to the lower frequencies, so that $f_M/f_1 @ 1$ then R becomes approximately

$$\mathcal{R} \approx \frac{\pi}{6} \frac{f_M}{f_1} \quad (9.44)$$

In commercial FM broadcasting $f_1 = 2.1$ kHz, while f_M may reasonably be taken as $f_M = 15$ kHz. In this case $f_M/f_1 = 7.5$, and from Eq. (9.44) $R @ 4.7$ corresponding to 6.7 dB improvement in the output SNR when using preemphasis. Since output signal-to-noise ratios are typically 40 to 50 dB, this represents an improvement of approximately 15 percent; a significant improvement.

Preemphasis is particularly effective in FM systems which are used for transmission of audio signals. This effectiveness results from the fact that the

spectral density of the audio signal is smallest precisely where the spectral density of the noise is greatest. For, as noted, the audio signal spectral density falls off with increasing frequency while the noise spectral density increases with the square of the frequency. The advantage of using preemphasis is less pronounced in an AM system, such as DSB with carrier, which is employed in commercial AM broadcasting. For in AM the noise spectral density is constant and does not increase with frequency. Preemphasis is also frequently employed in connection with phonographic recording to suppress needle scratch noise.

stereo FM

As noted in Sec. 9.2, and as shown in Fig. 9.4, the noise output of the discriminator in an FM receiver has a parabolic power spectral density in the range $-B/2$ to $B/2$. In commercial FM, the bandwidth is $B = 200$ kHz so that $B/2 = 100$ kHz. In monophonic FM, only the noise in the spectral range of the baseband filter is passed on to the output. In stereo (Sec. 3.3.4), the situation is different. The difference signal $L(t) - R(t)$ as received occupies the frequency range from 23 to 53 kHz. When this difference signal is translated to baseband, so also is the noise in this difference-signal frequency interval. The noise in this difference-signal frequency interval is substantially larger than in the baseband frequency range, because the difference-signal frequency range is twice as large as the baseband range and also because of the parabolic form of the noise power spectral density. As a result, commercial stereo FM is noisier than monophonic FM.

For the sake of the advantage gained thereby, as well as for the sake of compatibility, preemphasis is incorporated in stereo FM just as in monophonic FM. In stereo FM, at the transmitter, the sum signal $L(t) + R(t)$ and the difference signal $L(t) - R(t)$ are passed through identical preemphasis filters. At the receiver the sum and difference signals are passed through identical deemphasis filters before the sum and difference signals are combined to generate the individual signals $L(t)$ and $R(t)$. The preemphasis and deemphasis filters are as shown in Fig. 9.6, with transfer characteristics as indicated in Fig. 9.7. As in monophonic FM, $f_1 = 2.1$ kHz (corresponding to a time constant of 75 ms).

The overall result, taking the preemphasis and deemphasis into account, and assuming a baseband frequency range extending from nominally zero to

15 kHz, is that commercial stereo FM yields a signal-to-noise ratio about 22 dB poorer than monophonic FM. (See Prob. 9.18.) This disadvantage turns out to be tolerable simply because of the high power with which commercial broadcasts are transmitted.

9.5 PHASE MODULATION (PM) AND MULTIPLEXING ISSUES

One method which is used to multiplex voice channels prior to long distance transmission is shown in Fig. 9.8. The speech signals $m_1(t)$, $m_2(t)$, etc., are each bandlimited to 3 kHz and are the baseband signals used to generate a sequence of SSB-SC signals, whose carrier frequencies f_1 , f_2 etc., are

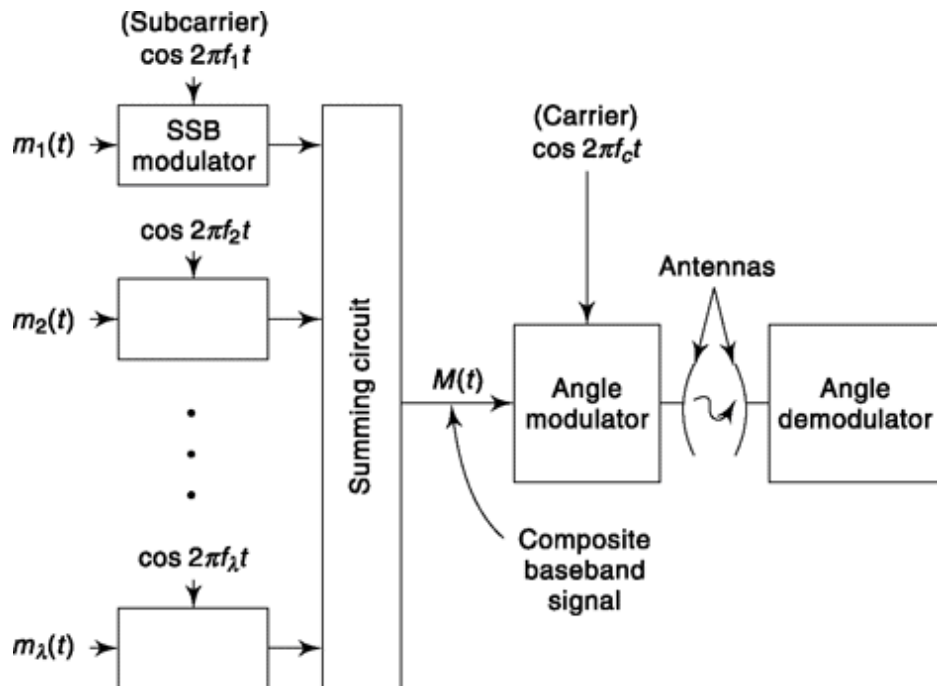


Fig. 9.8 A system of frequency division multiplexing.

separated by 4 kHz. The outputs of the SSB modulators are added, and this sum of signals forms a composite baseband signal that is used to angle-modulate (FM, PM, or some combination of the two) a carrier of frequency f_c . If 1000 speech signals are multiplexed in this way, the baseband signal nominally extends over a bandwidth $1000 \times 4 \text{ kHz} = 4 \text{ MHz}$. The angle modulator excites an antenna whose signal is directed at a receiving antenna. Not indicated in the figure are the repeater stations which may be interposed between initial transmitter and final receiver in a system which connects very distant points. For example, much of the telephone communication

between the United States and Europe presently employs a system as shown in Fig. 9.8, and uses a satellite repeater.

At the receiver, an angle demodulator recovers the composite baseband signal. The individual baseband signals $m_1(t)$, $m_2(t)$, etc., are recovered by synchronous demodulation and by passing the output of each synchronous demodulator through a low-pass filter of bandwidth 3 kHz.

Suppose now that the angle modulator at the transmitter is an FM modulator, that is, the instantaneous frequency of the modulator is directly proportional to the instantaneous magnitude of the composite baseband signal $M(t)$. Then the angle demodulator would be a frequency demodulator, such as the discriminator discussed in Sec. 9.1. However, we have noted in that section that, with white noise present at the input to the discriminator, the spectral density of the noise output is quadratic. As a consequence a channel associated with a higher subcarrier frequency will be *noisier* than a channel associated with a lower subcarrier frequency. That such is the case is easily seen in Fig. 9.9. Here we have plotted the positive half of the parabolic spectral density $G_n(f)$ of the output noise of the discriminator. Two subcarrier frequencies f and f_h are indicated, together with the frequency band occupied by the associated SSB signals (the upper sidebands are arbitrarily chosen). The noise power in each of the individual channels is proportional to its respective shaded area. If then the transmitter power is raised to a level where the signal-to-noise ratio is acceptable in the highest channel, the signal-to-noise ratio in the lower channels will be better than is required.

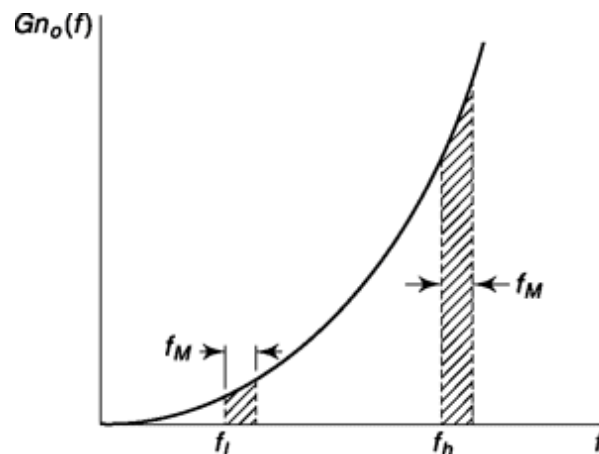


Fig. 9.9 To illustrate that in the multiplex system of Fig. 9.8, using FM, channels associated with high carrier frequencies are noisier than those associated with lower frequencies.

This variation in noise power from channel to channel may be corrected, and the entire system rendered thereby more efficient, by transmitting a carrier which is *phase-modulated* by the composite signal, rather than frequency-modulated. For under these circumstances, we shall be required to use at the receiver a *phase demodulator*. A phase demodulator is a device whose instantaneous output signal is proportional to the instantaneous phase of its input signal. The student may readily verify that a discriminator followed by an integrator constitutes a phase demodulator. The important point, for

our present purpose, about a phase demodulator is that, with such a demodulator, a uniform (white) noise spectral density at the input gives rise to a uniform output-noise spectral density. That such is the case is readily seen from Eq. (9.17). In Eq. (9.17), $d(t) = n_s(t)/A$ is the phase-modulation noise. Since $d(t)$ and $n_s(t)$ are directly related, the form of the power spectral density of each is identical. Hence, in summary, we have the result that if the composite signal $M(t)$ in Fig. 9.8 is transmitted (and necessarily received) as a phase-modulated signal, the noise power in each channel will be the same.

9.5.1 Comparison Between FM and pm in Multiplexing

We noted in the preceding section that phase modulation offers some advantage over frequency modulation in a multichannel FDM system. We compare the two systems now, to see more quantitatively the advantage that accrues from the use of phase modulation.

A frequency-modulation system is shown in Fig. 9.10a and a phase-modulation system is indicated in Fig. 9.10b. We have chosen to construct the phase modulator as a frequency modulator preceded by a differentiator. That such an arrangement does indeed constitute a phase modulator was pointed out in Sec. 3.1.2. Similarly, we have constructed a phase demodulator as a discriminator followed by an integrator. We may view the system of Fig. 9.10b as a frequency-modulation system in which preemphasis and deemphasis have been incorporated. The differentiator is the preemphasis network, and the integrator is the deemphasis network. The combination of preemphasis and deemphasis leaves the signal unaltered; hence the output signal is the same in Fig. 9.10a and b. However, the noise power per channel is the same for each channel in (b), while in (a) the noise is most pronounced in the top channel. Assuming that both channels (a) and

(b), are constrained to use the same bandwidth, we shall now compute the improvement afforded by channel (b) in the signal-to-noise ratio of the top channel.

If there are N channels, the frequency range of the topmost channel of the composite signal $M(t)$ extends from $(N - 1) f_M$ to Nf_M , where f_M is the frequency range of an individual component signal.

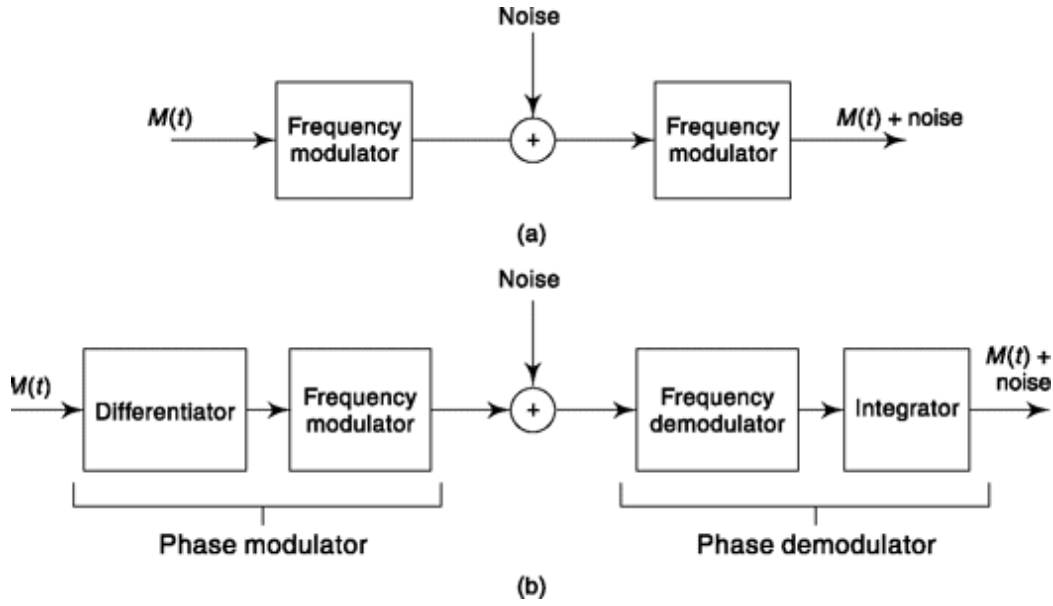


Fig. 9.10 Comparison of an FM system in (a) with a phase-modulation system in (b).

Applying Eq. (9.22) to the present case, we find that, in the absence of deemphasis, the noise output of the top channel is

$$\begin{aligned} N_{o,top} &= 2 \frac{\alpha^2 \eta}{A^2} \int_{(N-1)f_M}^{Nf_M} 4\pi^2 f^2 df \\ &= \frac{8\pi^2 \alpha^2 \eta N^2 f_M^3}{A^2} \end{aligned} \quad (9.45)$$

since $N \gg 1$. The preemphasis (differentiator) circuit has a transfer function whose magnitude squared is

$$|H_p(f)|^2 = 4\pi^2 \tau^2 f^2 \quad (9.46)$$

in which τ^2 is a constant. For the deemphasis filter, we have

$$|H_d(f)|^2 = \frac{1}{|H_p(f)|^2} = \frac{1}{4\pi^2 \tau^2 f^2} \quad (9.47)$$

Applying Eq. (9.33) to the composite signal $M(t)$, we find that the condition of equal bandwidth requires that

$$\int_{-Nf_M}^{+Nf_M} G_M(f) df = \int_{-Nf_M}^{+Nf_M} |H_p(f)|^2 G_M(f) df \quad (9.48)$$

In Eq. (9.48) $G_M(f)$ is the power spectral density of the composite signal. Assuming that $G_M(f)$ is constant, we find by substituting Eq. (9.46) into Eq. (9.48) that

$$\tau^2 = \frac{3}{4\pi^2 N^2 f_M^2} \quad (9.49)$$

In the presence of a deemphasis filter with transfer function $Hd(f)$, the output-noise power of the top channel becomes, from Eq. (9.45),

$$N_{od,top} = 2 \frac{\alpha^2 \eta}{A^2} \int_{(N-1)f_M}^{Nf_M} \frac{4\pi^2 f^2 df}{|H_p(f)|^2} \quad (9.50)$$

The improvement factor \mathcal{R} for the top channel is calculated from Eqs (9.45), (9.47), (9.49), and (9.50). We find

$$\mathcal{R}_{top} = \frac{N_{o,top}}{N_{od,top}} = 3 (= 4.8 \text{ dB}) \quad (9.51)$$

9.5.2 Effect of Transmitter Noise

The discussion of the preceding section is somewhat unrealistic in that it was assumed that the only noise with which we have to contend is noise introduced in the communications channel. Actually, some noise is introduced by the transmitter itself. For example, the frequency modulator may

have some “jitter.” That is, there is some random variation of frequency even in the absence of a modulating signal. Let us represent this jitter as due to a noise voltage present at the input to the frequency modulator, and let us assume for explicitness that the spectral density of this noise voltage is uniform. If we now also assume that the spectral density of the composite baseband signal is also uniform, then the situation with the PM system can be represented as shown in Fig. 9.11a. In this figure the composite input signal is $M(t)$ of spectral density $G_M(f)$, and the output of the amplifier-differentiator is $M'(t)$ of spectral density $G_{M'}(f)$. The transmitter noise $n(t)$ with spectral density $G_n(f)$, is placed at the junction between the amplifier-differentiator and the frequency modulator. The positive-frequency portion of the assumed *flat* power spectral density of $G_M(f)$ is shown in Fig. 9.11b, while the parabolic density of $G_{M'}(f)$ appears in Fig. 9.11c. The noise spectral density is shown in Fig. 9.11d, while finally in Fig. 9.11e we compare the spectral densities of the signal and noise at the input to the frequency modulator.

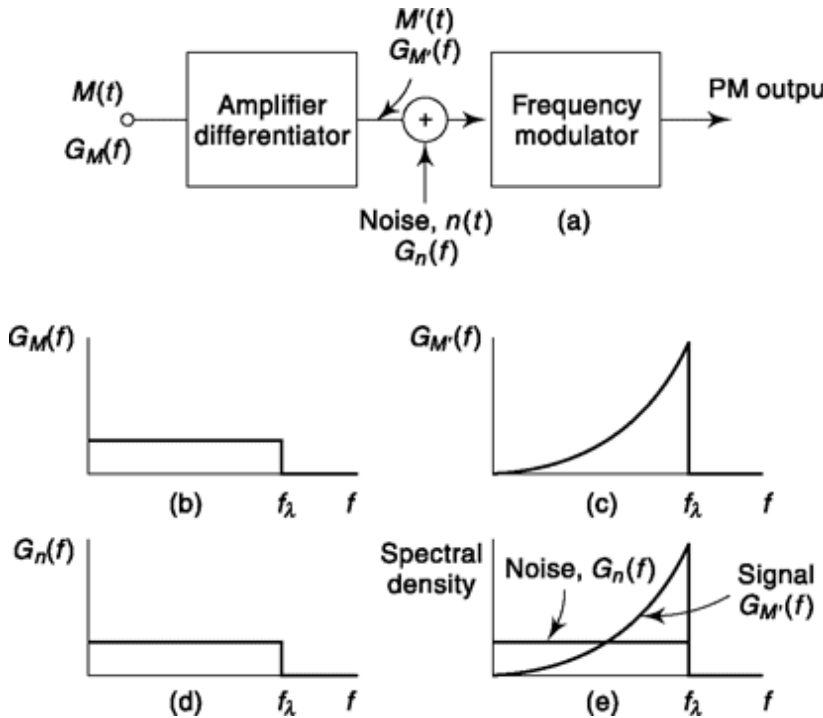


Fig. 9.11 (a) A PM system in which noise is introduced before transmission. (b) The spectral density of the system. (c) The spectral density of the signal after differentiation, (d) The spectral density of the noise. (e) Comparison of spectral densities of signal and noise at input to modulator.

Observe that at the lower frequencies the noise exceeds the signal. To keep the signal level above the noise at low frequencies, it is necessary to modify

the transfer characteristic of the network which precedes the frequency modulator. A suitable network is one whose transfer characteristic increases with frequency to emphasize the high frequencies without suppressing the low frequencies. A network similar to the preemphasis circuit of Fig. 9.6b is suitable. In practice, when such a preemphasis circuit is employed, together with its reciprocal deemphasis circuit, the 4.8 dB advantage quoted above for PM over FM is not realized. In a 1000-channel voice multiplex system the advantage is more nearly 3 or 4 dB.

Example 9.3

An RC filter-based preemphasis-deemphasis is employed in FM system. The deemphasis first order RC filter has $R = 1 \text{ kOhm}$ and $C = 1 \text{ mF}$. Find the gain in dB in an FM broadcasting system which has baseband bandwidth 15 kHz. How is the improvement if baseband bandwidth is increased to 30 kHz.

Solution

Break point for RC filter

$$f_1 = \frac{1}{2\pi RC} = \frac{1}{2\pi(10^3)(0.1 \times 10^{-6})} = 1591.55$$

Thus, $f_1/f_M = 1591.55/15000 = 0.1061$ and $f_M/f_1 = 15000/1591.55 = 9.4248$

From Eq. (9.43),

$$\begin{aligned} \text{gain} &= \frac{\tan^{-1}(9.4248)}{3(0.1061)[1 - 0.1061 \times \tan^{-1}(9.4248)]} \\ &= \frac{1.4651}{0.3183[1 - 0.1061 \times 1.465]} \\ &= 5.4501 = 7.3641 \text{ dB} \end{aligned}$$

Now, $f_M = 30 \text{ kHz}$

i.e. $f_1/f_M = 1591.55/30000 = 0.0531$

and $f_M/f_1 = 30000/1591.55 = 18.8495$

and $\tan^{-1}(18.8495) = 1.5178$

Substituting as above, gain

$$\begin{aligned} &= \frac{1.5178}{0.1591[1 - 0.0531 \times 1.5178]} \\ &= 10.3782 = 10.1604 \text{ dB.} \end{aligned}$$

Example 9.4

(a) Find signal to noise ratio at receiver output of a phase modulated system. Find transmitter power required to have an SNR greater than 40 dB at receiver output for channel having 20 dB loss. Given, frequency of baseband filter = 15 kHz, average modulating signal power = 0.1 W, PM bandwidth = 120 kHz, power spectral density of white noise, $rV2 = 10^{-9}$ W/Hz. (b) Recalculate required transmitter power if signal bandwidth is 60 kHz and compare it with FM transmitter of Example 9.1.

Solution

(a) From Eq. (9.17), $G_n(f) = \frac{\eta/2}{A^2/2} = \frac{\eta}{A^2}$

Then received noise power, $N_o = \int_{-f_M}^{f_M} \frac{\eta}{A^2} df$

$$= \frac{2\eta f_M}{A^2}$$

Received signal power at output (after phase demodulation), $S_o = k_p^2 \bar{m}^2(t)$ where k_p is proportionality constant related to phase modulation.

Required SNR at receiver output,

$$\frac{S_o}{N_o} = \frac{k_p^2 \bar{m}^2(t) A^2}{2\eta f_M} = \frac{k_p^2 \bar{m}^2(t) S_i}{\eta f_M}$$

where S_i is the carrier power, equivalent to received signal energy.

Now, for PM system (from Eq. 3.40), signal bandwidth = $2(1+k_p|m(t)|_{\max})f_M$

Considering $|m(t)| \leq 1$ and substituting,

$$120 = 2(1 + k_p)15$$

$$\text{or } k_p = 3$$

If transmitter power is S_T then $S_T/S_i = 20 \text{ dB} = 100$

Thus, $\frac{S_o}{N_o} > 40 \text{ dB} = 10000$ requires,

$$\frac{k_p^2 \bar{m}^2(t) S_T / 100}{\eta f_M} > 10000$$

$$\text{or } \frac{3^2 \times 0.1 \times S_T / 100}{2 \times 10^{-9} \times 15000} > 10000$$

$$\text{or } S_T > 33.33 \text{ W}$$

$$(b) \text{ Now, } 60 = 2(1 + k_p)15 \\ \text{or } k_p = 1$$

From above, $S_T > 9 \times 33.33 = 300 \text{ W}$. Comparing with Example 9.1, it is seen that PM transmitter require transmitter power which is more than $(300/123.73) = 2.43$ times the FM transmitter power.

SELF-TEST QUESTION

5. The deemphasis filter comes after the FM demodulator and before baseband filter. Is that correct?
6. Preemphasis-deemphasis improves quality of both FM and AM transmission significantly. Is it true?

7. For white noise interference, is it true that noise power spectral density does not vary with frequency at receiver output for phase modulated system while increases in quadratic manner for FM system?

8. How much is the gain in highest frequency band in an FDM system when PM is employed instead of FM?

9.6 THRESHOLD IN FREQUENCY MODULATION

In a communication system in which the modulation is linear and demodulation is accomplished by coherent detection (for example, SSB and DSB-SC), we have the result that [see Eqs (8.43) and (8.44)]

$$\frac{S_o}{N_o} = \frac{S_i}{N_M} \quad (9.52)$$

or equivalently

$$10 \log \frac{S_o}{N_o} \equiv \left[\frac{S_o}{N_o} \right]_{\text{dB}} = \left[\frac{S_i}{N_M} \right]_{\text{dB}} \equiv 10 \log \frac{S_i}{N_M} \quad (9.53)$$

In FM, we have [see Eq. (9.27)] or equivalently

$$\frac{S_o}{N_o} \equiv \frac{3}{2} \beta^2 \frac{S_i}{N_M} \quad (9.54)$$

$$\left[\frac{S_o}{N_o} \right]_{\text{dB}} = \left[\frac{S_i}{N_M} \right]_{\text{dB}} + 10 \log \frac{3}{2} \beta^2 \quad (9.55)$$

In Fig. 9.12 we have plotted Eq. (9.53) in a coordinate system in which the coordinate axes are marked off in decibels. The plot is a straight line passing through the origin. We have also plotted Eq. (9.55) for two values of $\beta \left(> \sqrt{\frac{2}{3}} \right)$. These plots, as indicated by the dashed extensions, are also straight lines. In the FM case a plot for a value of b is raised by the amount $10 \log (3b^2/2)$ above the plot for a linear coherent modulation system. The quantity $10 \log (3b^2/2)$ expresses in decibels precisely the improvement afforded by the FM system in return for a sacrifice of bandwidth.

Experimentally it is determined, however, that the FM system exhibits a threshold. Thus, as indicated by the solid-line plots, for each value of b , as S_i/N_M decreases, a point is reached where

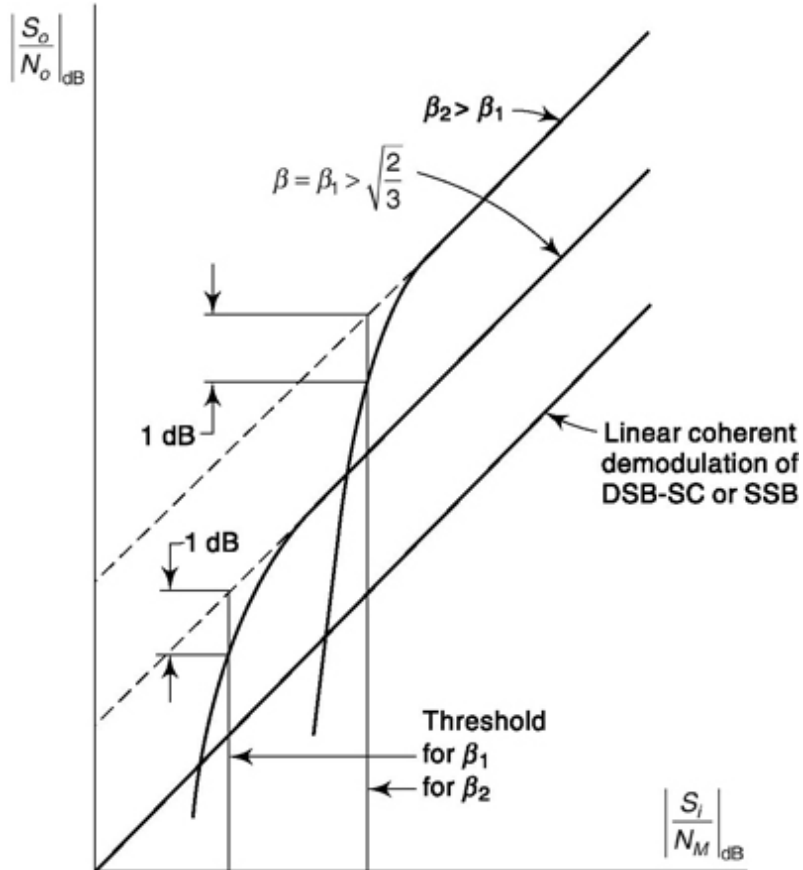


Fig. 9.12 Plots of output signal-to-noise ratio against input signal-to-noise ratio for linear modulation and demodulation and also for an FM system. Illustrating the phenomenon of threshold in FM.

S_o/N_o falls off much more sharply than S_i/N_M . The threshold value of S_i/N_M is arbitrarily taken to be the value at which S_o/N_o falls 1 dB below the dashed extension. We note that for larger b the threshold S/N_M is also higher. Suppose, then, that we are operating with a modulation index b_1 above the threshold for b_1 but below the threshold for b_2 . Suppose, further, that at this input S/N_M we should increase b from b_1 to b_2 hoping thereby to improve the output-signal-to-noise ratio S_o/N_o by a sacrifice of bandwidth. We would find, however, as is apparent from Fig. 9.12, that such a sacrifice of bandwidth would actually decrease the output SNR. Similarly, we see that, if we are operating sufficiently below threshold for any value of b , we do better with a linear coherent system than with an FM system.

The onset of threshold may be observed by examining the noise output of an FM discriminator on a cathode-ray oscilloscope. At high input-signal-to-noise ratios (S_iN_M) the noise displays the usual random-variation characteristic of thermal noise generally. A typical output-noise waveform

has the appearance shown in Fig. 9.13. We can determine experimentally that the instantaneous noise amplitude has a Gaussian probability density as is to be anticipated from the discussion of Sec. 7.2.1. As S_i/N_M decreases, a point is reached where the character of the noise waveform changes markedly. The noise now has the appearance indicated in Fig. 9.14. Here we observe, superimposed on the background thermal-type noise (usually referred to as *smooth* noise), a pulse-type noise waveform. Because of its appearance this new component of noise is often referred to as *spike*

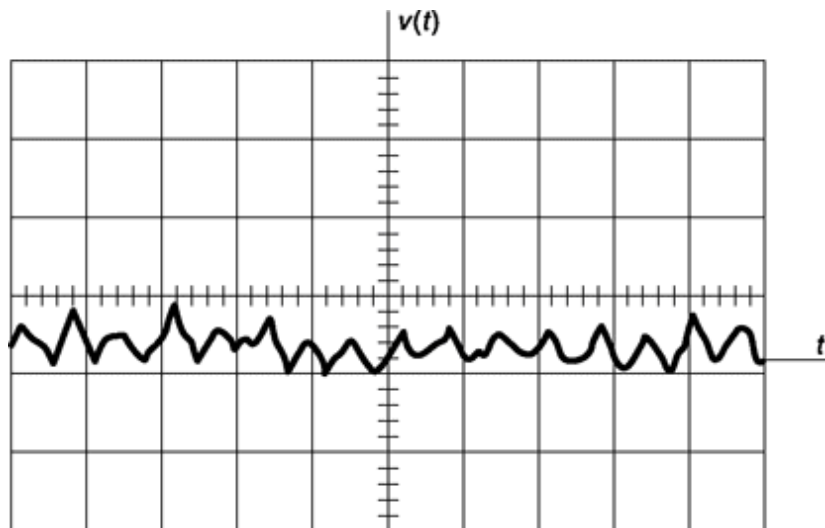


Fig. 9.13 Thermal noise at discriminator output.

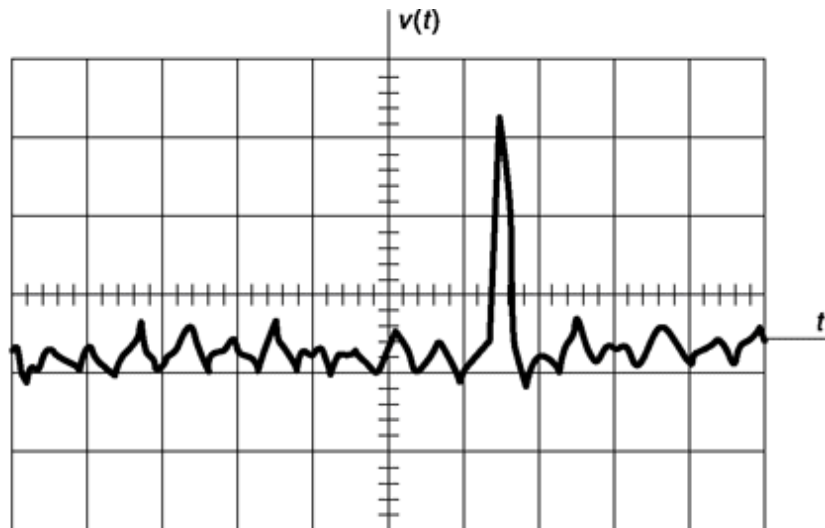
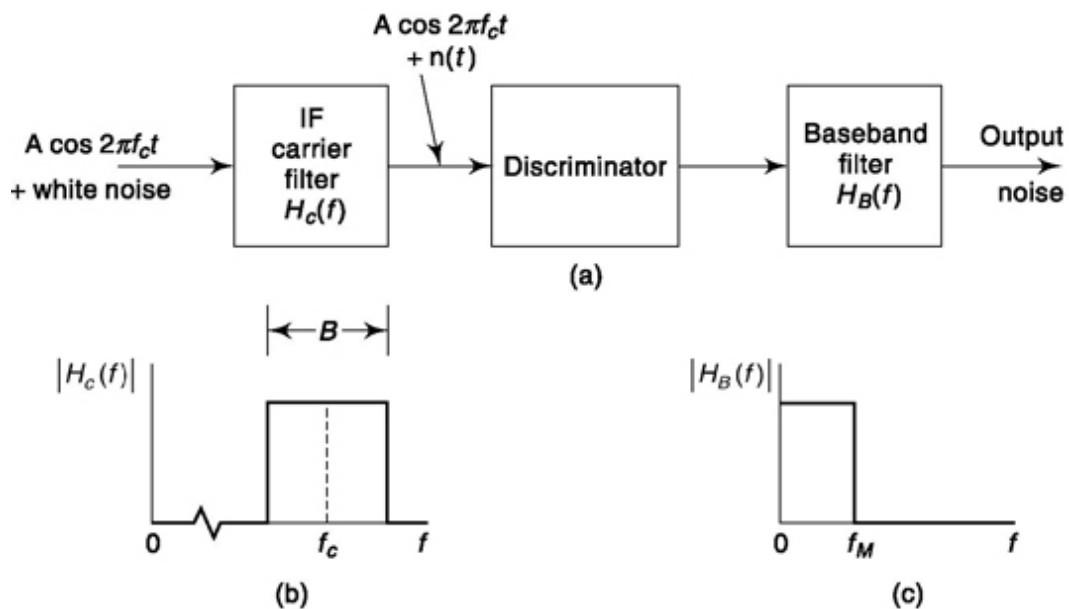


Fig. 9.14 A spike superimposed on a background of smooth (thermal) noise.

noise or *impulse* noise. If we were to listen to the discriminator, we would hear a clicking sound on each occasion that we observed a spike.

The appearance of these spikes denotes the onset of threshold. In succeeding sections we shall discuss the origin of these spikes. We shall show that although the frequency of occurrence of a spike is small, the noise energy associated with a spike is very large compared with the energy of the smooth noise occurring during a comparable time interval. Hence, the *spike* noise greatly increases the total noise output and thereby causes a threshold.

9.6.1 Occurrence of spikes



An FM demodulator consisting of an IF filter, limiter-discriminator, and a baseband filter is shown in Fig. 9.15. The IF filter has a bandwidth B , centered at the IF frequency f_c . The baseband filter extends from $-f_M$ to $+f_M$ but does not pass dc. In order to simplify our discussion, we assume that

Fig. 9.15 (a) An FM discriminator and associated filters. (b) The bandpass range of the carrier filter, (c) The passband of the baseband filter.

the input signal is an unmodulated carrier; that is, $m(t) = 0$, accompanied by white noise. The white noise is filtered and shaped by the IF filter.

In the present and in succeeding sections we shall have occasion to use the quadrature component representation of noise as expressed in Eq. (7.79). It will be convenient to use a notation different from the notation of Eq. (7.79). We shall replace $n_c(t)$ by $x(t)$ and $n_s(t)$ by $y(t)$. In this alternative notation, which is as commonly found in the literature as is the original notation, Eq. (7.79) reads, with $2pf_c$ replaced by w_c ,

$$n(t) = x(t) \cos \omega_c t - y(t) \sin \omega_c t \quad (9.56)$$

The notation of Eq. (9.56) is especially appropriate when $n(t)$ is to be represented as a combination of phasors in a coordinate system rotating counterclockwise with angular frequency ω_c . In such a coordinate system, $n(t)$ is represented by the phasor sum of $x(t)$ in the horizontal direction (i.e. the x direction) and $y(t)$ in the vertical direction (i.e. the y direction). In terms of this new notation, the carrier and noise output of the IF filter, which is the input $v(t)$ to the demodulator, is given by

$$v_i(t) = A \cos \omega_c t + x(t) \cos \omega_c t - y(t) \sin \omega_c t \quad (9.57)$$

This equation can be rewritten in phasor notation as

$$\begin{aligned} v_i(t) &= \operatorname{Re} \{ [A + x(t)] e^{j\omega_c t} + y(t) e^{j[\omega_c t + (\pi/2)]} \} \\ &= \operatorname{Re} \{ e^{j\omega_c t} \underbrace{[A + x(t) + jy(t)]}_{\text{phasors}} \} \end{aligned} \quad (9.58)$$

The phasor $A + x(t)$ lies along the horizontal axis and $y(t)$ lies along the vertical axis.

It is convenient, when discussing the occurrence of spikes, to talk about the *amplitude* of the noise $r(t) = \sqrt{x^2 + y^2}$ and its random phase angle $f(t) = \tan^{-1}(y(t)/x(t))$. [It was shown in Sec. 6.3.3 that the density of $r(t)$ is Rayleigh and that the density of $f(t)$ is $1/2p$ from $-p$ to $+p$.]

The phasor diagram for $v(t)$ is shown in Fig. 9.16. Here we see that the phasor sum of signal A and noise $r(t)$ is defined as $R(t)$. The angle that $R(t)$ makes with the horizontal axis is called $d(t)$. Then

$$A + x + jy = A + r(t) e^{j\phi(t)} = R(t) e^{j\theta(t)} \quad (9.59)$$

and that $v_i(t)$ in Eq. (9.16) is

$$v_i(t) = \operatorname{Re} [e^{j\omega_c t} R(t) e^{j\theta(t)}] = R(t) \cos [\omega_c t + \theta(t)] \quad (9.60)$$

As was discussed in Sec. 9.2, the output of the discriminator is proportional to $0(t) = dd/dt$.

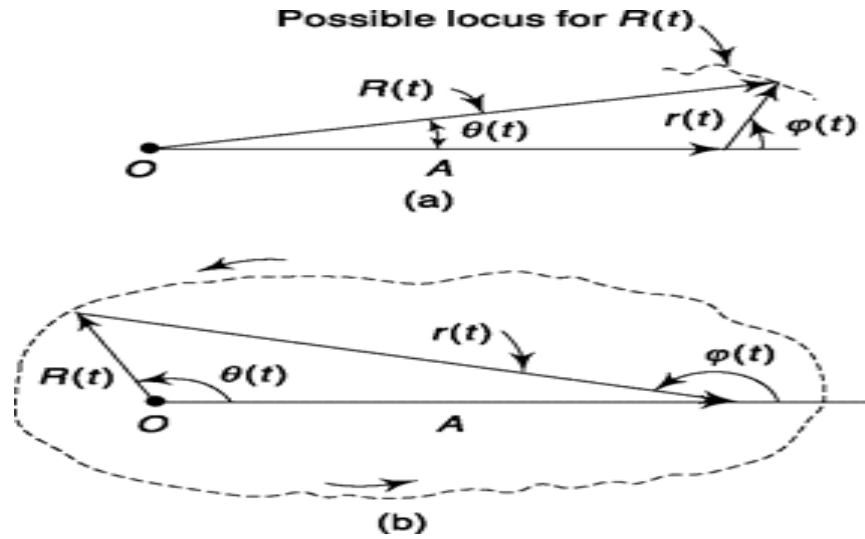


Fig. 9.16 (a) A noise phasor $r(t)$ is added to a carrier phasor of amplitude A . The sum is the resultant phasor $R(t)$. (b) A locus for the end point of $R(t)$ which will give to a spike.

Let us now consider Fig. 9.16a to see how $d(t)$, and hence $\theta(t)$, are affected as the noise $r(t)$ and $f(t)$ vary. If the noise power is small in comparison with the carrier power, we expect that $r(t) \ll A$ most of the time, and that the end point of the resultant phasor $R(t)$ will never wander far from the end point of the carrier phasor. Thus, as $f(t)$ changes, the angle $d(t)$ remains small.

If, however, the ratio S/rf_M decreases, the likelihood of $r(t)$ being much less than A also decreases. When $r(t)$ becomes comparable in magnitude to the carrier amplitude A , the locus of the end point of the resultant phasor $R(t)$ moves away from the end point of the carrier phasor and may, as shown in Fig. 9.16b, even rotate about the origin. The variation of the phase angle $d(t)$, at and near the time of occurrence of this event, is shown in Fig. 9.17a. If the rotation of the end point of $R(t)$ around the origin occurs in the interval between t_1 and t_2 , the angle $d(t)$ changes by 2π rad during

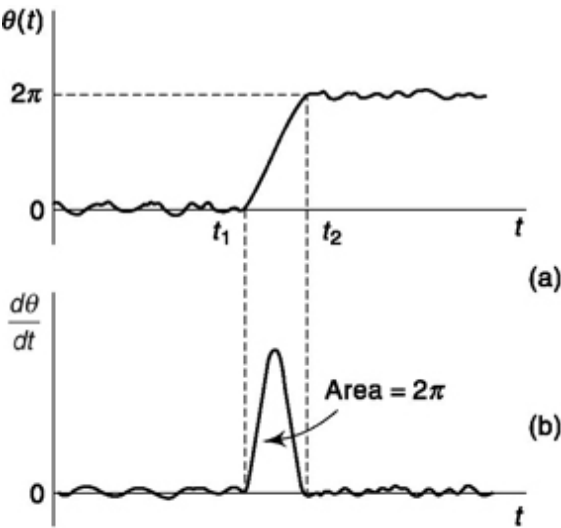


Fig. 9.17 (a) A plot of $\theta(t)$ for a case in which the end point of $R(t)$ in Fig. 9.16b executes a rotation around the origin, (b) A plot of $d\theta/dt$ as a function of time.

this time interval. Preceding t_1 and following t_2 , $r(t) \ll A$, and the usual small random variations of $\theta(t)$ occur.

We are interested in the discriminator output, which is proportional to the instantaneous frequency $d\theta/dt$, and we have therefore plotted $d\theta/dt$ in Fig. 9.17b. Notice that when $\theta(t)$ changes by 2π rad, $d\theta/dt$ appears as a sharp *spike* or *impulse* with area 2π . To show that the area under the spike waveform is indeed 2π , we simply integrate $d\theta/dt$ over the time interval, t_1 to t_2 during which $\theta(t)$ changes by 2π . Thus,

$$\text{Area} = \int_{t_1}^{t_2} \frac{d\theta}{dt} dt = \theta \Big|_{t_1}^{t_2} = 2\pi \quad (9.61)$$

The waveform shown in Fig. 9.17b is the *spike* noise referred to in Sec. 9.6 and is the waveform which is presented to the input of the baseband filter. Since these spikes occur only rarely and are impulse-like in character, they represent a *shot* noise phenomenon. The noise power at the baseband filter output is calculated in Sec. 9.7, using the results given in Sec. 6.5.3.

9.6.2 spike Characteristics

When the noise amplitude $r(t)$ is comparable to the carrier amplitude A , the resultant phasor $R(t)$ may clearly execute all sorts of random, wide-ranging excursions which will cause $\theta(t)$, and hence the frequency $d\theta/dt$, to experience large changes. Why then do we single out for special consideration the excursion which carries the resultant in a complete rotation around the origin? The reason for our special concern may be seen by comparing the noise outputs for the two cases shown in Fig. 9.18a. The path of $R(t)$, marked *spike path*, carries the end point of $R(t)$ completely around

the origin as in Fig. 9.16b and results in a waveform for $O(t)$ as shown in Fig. 9.17a and in a waveform for the discriminator output as shown in Fig. 9.17b. The second path, marked *triplet path*, departs from the spike path only slightly, but, most importantly, it does *not* encircle the origin. For this path, $O(t)$ and the discriminator output appear as shown in Fig. 9.18b and c. Notice that the angle $O(t)$ increases nearly to π , reverses to nearly $-\pi$, and then returns to a small value. The waveform of $O(t)$ displays,

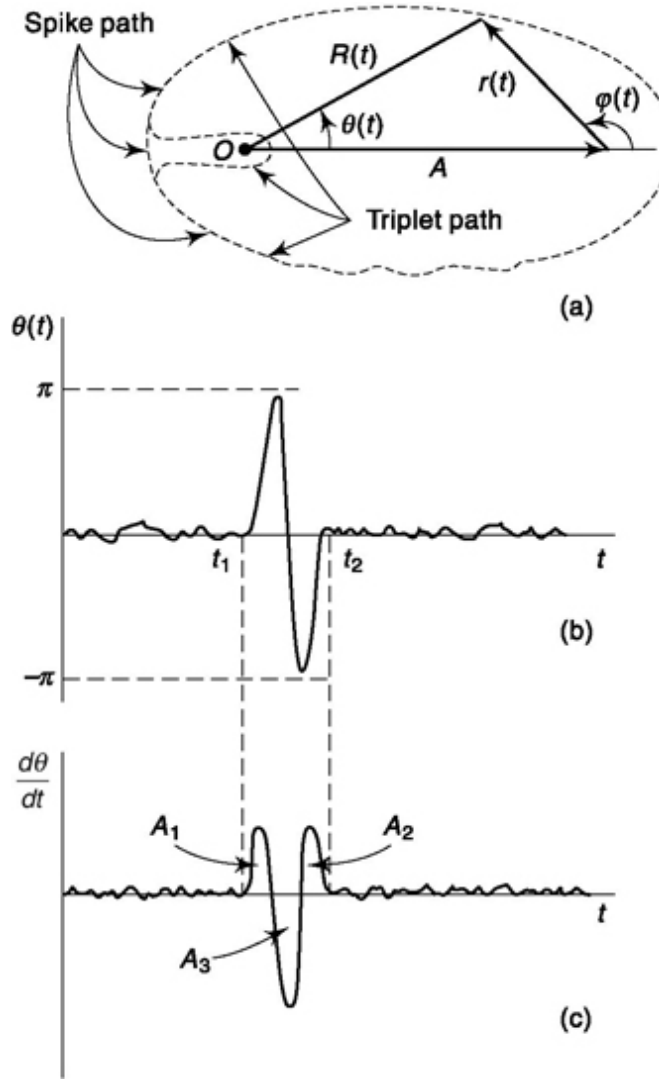


Fig. 9.18 (a) Comparing two nearly identical paths for the end point of $R(t)$. One path encircles the origin, the other does not. (b) and (c) $O(t)$ and dO/dt for the path which does not encircle the origin.

not a simple jump of 2π , but rather a pulse doublet. The waveform of dO/dt displays not a single pulse but rather three pulses, two of positive and one of negative polarity. It is most important to recognize that the total algebraic area under the waveform in Fig. 9.18c is zero. That is, the sum of the

positive areas $A_1 + A_2$ is equal to the negative area A_3 . This can be seen by applying the calculation of Eq. (9.61) to the determination of the total area and noting that the total change in O between t_1 and t_2 is zero.

We can now illustrate how, in an FM system, the noise energy present at the output of the baseband filter shown in Fig. 9.15 is much larger when a spike is generated than when a triplet occurs. We have already noted that if a carrier, accompanied by noise, is passed through a bandpass filter of bandwidth B , the spectral components of the noise output of the discriminator will extend over the frequency range from $-B/2$ to $B/2$. Of this noise, only the part which lies in the range $-f_M$ to f_M will appear at the output of the baseband filter. In Fig. 9.19a and b we have sketched the magnitudes of the Fourier transforms: $F_S(j\omega)$, the spike waveform shown in Fig. 9.17b, and $F_T(j\omega)$, the triplet waveform shown in Fig. 9.18c. We have confined the spectral range to the interval $-B/2$ to $+B/2$

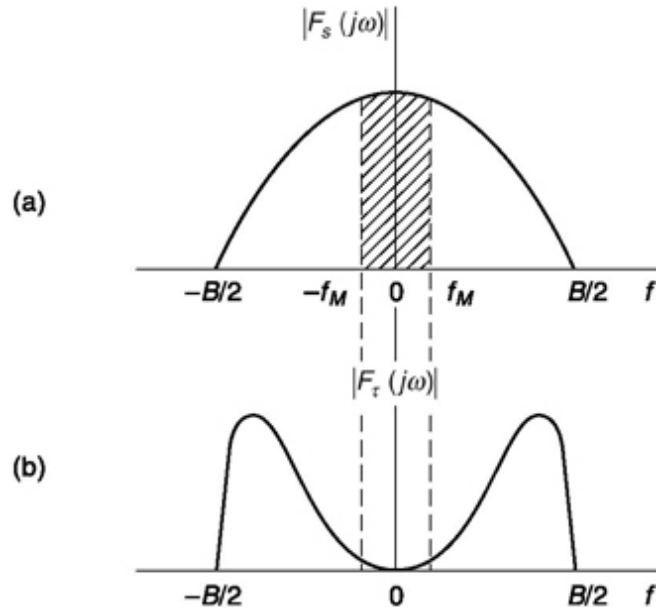


Fig. 9.19 Qualitative plots of the Fourier transform of a pulse type waveform with spectral components limited to range $-B/2$ to $+B/2$. (a) For case where waveform has dc component. (b) For case where dc component is zero.

as required, and have indicated that for the triplet $F_T(jw) = 0$ at $f = 0$, while for the spike $F_S(jw) \neq 0$ at $f = 0$. These features of the transforms, at $f = 0$, are verified in the following way. The Fourier transform of a function $f(t)$ is

$$F(j\omega) = \int_{-\infty}^{\infty} f(t)e^{-j\omega t} dt \quad (9.62)$$

so that

$$[F(j\omega)]_{\omega=0} = \int_{-\infty}^{\infty} f(t) dt = \text{area under } f(t) \quad (9.63)$$

Thus, the value of the transform at $f = 0$ is equal to the area under $f(t)$. As already noted, the spike has a finite area, while the triplet area is zero.

Since the passband of the baseband filter extends only to $f_M + B/2$, only the energy represented by the shaded areas in Fig. 9.19a and b will appear at the filter output. It is apparent from this figure that a spike will contribute much more noise than the triplet. More generally, when the resultant phasor executes any path that carries it around the origin, the corresponding noise energy output will be much larger than any other excursion of comparable wide range which does not succeed in causing an encirclement of the origin.

spike Duration

We may make an order-of-magnitude estimate of the duration of the spike. For this purpose we use the general principle, discussed in Sec. 1.4.5, that when a pulse is made up of spectral components, confined mainly to a frequency range 0 to f_{max} , the time duration of the pulse is of the order of $1/f_{max}$. The spike output of the discriminator has a spectrum that extends over the range 0 to $B/2$, where B is the bandpass of the carrier filter. Hence, we estimate that the spike duration is approximately $2/B$ sec.

Example 9.5

Refer to Fig. 9.12. Consider that FM demodulation scheme b_2 intersects scheme with b_1 ($b_2 > b_1$) at input SNR, a dB and DSB-SC/SSB scheme at b dB. Also consider, FM demodulation scheme b_1 intersects DSB-SC/SSB scheme at c dB. Which of these three schemes would you choose if input SNR is (a) above a dB, (b) between a and b dB, (c) between b and c dB, and (d) below c dB?

Solution:

The scheme that provides highest output SNR in the given range should be chosen. Thus for

- (a) FM scheme with modulation index b_2

- (b) FM scheme with modulation index b_1 (though $b_2 > b_1$)
- (c) FM scheme with modulation index b_1
- (d) DSB-SC/SSB scheme

SELF-TEST QUESTION

9. Does spike or clicking sound indicate onset of threshold in FM reception?
10. Which of Gaussian noise and shot noise characteristics can be associated with spike in FM reception?
11. The *triplet* path in spike does not encircle origin and total area under it is zero while spike path encircles origin and total area under it is $2p$. Is that correct?

9.7 calculation of threshold in an fm discriminator

To calculate the spike noise contribution at the output of an FM discriminator, we need to know the power spectral density of the spike noise. The spike noise is similar to the shot noise discussed in Sec. 6.5.3. We may therefore use the result of Eq. (6.153), which states that the power spectral density is given by

$$G_S(f) = \frac{1}{T_s} \overline{|P(j\omega)|^2} \quad (9.64)$$

where $P(j\omega)$ is the Fourier transform of the spike, and T_s is the mean time interval between spikes. From the discussion of Sec. 9.6.2 we know that $|P(j\omega)|$ will have the general form shown in Fig. 9.19a. For the purpose of calculating noise power at the output of the baseband filter, we need to know $G_S(f)$ only in the range $-f_M$ to $+f_M$. In this range $|P(j\omega)|$ does not change very much, provided that $B/2 @ f_M$. We may therefore assume that $|P(j\omega)|$ is constant and equal to $|P(0)|$, that is, to the value of the Fourier transform at $f = 0$.

Let $O(t)$ in Fig. 9.18 make a rotation by $2p$ so that a spike is formed. Then the waveform of the output-noise voltage spike from the discriminator is

$$[n(t)]_{\text{spike}} = \alpha \frac{d\theta}{dt} \quad (9.65)$$

where α is a constant, i.e. the discriminator constant. From Eq. (9.63), $|P(0)|$ is equal to the area of $[n(t)]_{\text{spike}}$. Since α is a constant and the area under the waveform

$$dO/dt \quad \text{is} \quad 2p, \quad \text{we have}$$

$$|P(0)| = 2\pi\alpha \quad (9.66)$$

Since each spike has the same area, $2p$, the average value of $|P(0)|$ is also given by Eq. (9.66), and from Eq. (9.64)

$$N_S = \frac{4\pi^2 \alpha^2}{T_s} 2f_M \quad (9.68)$$

Thus the total output-noise power due to the spikes is simply

$$\frac{1}{T_s} = \frac{B}{2\sqrt{3}} \operatorname{erfc} \sqrt{\frac{f_M}{B} \frac{S_i}{N_M}} \quad (9.69)$$

The expression for N_s given in Eq. (9.68) is not very useful until we learn how T_s depends on the parameters of the system. It is proven in Sec. 9.7.1 that, for an unmodulated carrier,

$$G_S(f) = \frac{4\pi^2 \alpha^2}{T_s} \quad (9.67)$$

where erfc is the complimentary error function, i.e.

$$\operatorname{erfc} x \equiv \frac{2}{\sqrt{\pi}} \int_x^\infty e^{-\lambda^2} d\lambda = 1 - \frac{2}{\sqrt{\pi}} \int_0^x e^{-\lambda^2} d\lambda \quad (9.70)$$

From Eqs (9.68) and (9.69) we have

$$N_s = \frac{4\pi^2 \alpha^2 B f_M}{\sqrt{3}} \operatorname{erfc} \sqrt{\frac{F_M}{B} \frac{S_i}{N_M}} \quad (9.71)$$

The total output-noise power is $N_o = N_g + N_s$, where N_g is the Gaussian (smooth) noise given by Eq. (9.22), and the noise N_s is the spike noise given by Eq. (9.71). The signal power is given by Eq. (9.11). Combining these equations, we have, with $Sj = A^2/2$ and $N_M = r f_M$,

$$\frac{S_o}{N_o} = \frac{[3 k^2 \overline{m^2(t)} / 4\pi^2 f_M^2] (S_i/N_M)}{(1 + \sqrt{3B/f_M})(S_i/N_M) \operatorname{erfc} \sqrt{(f_M/B)(S_i/N_M)}} \quad (9.72)$$

The threshold effect is evident in Eq. (9.72). At very high $S_i N_M$ the complementary error function approaches zero. The right-hand member of the denominator of Eq. (9.72) becomes zero, and S_o/N_o varies linearly with S_i/N_M . As S_i/N_M decreases, the denominator increases above unity, and S_o/N_o decreases at a more rapid rate than does S_i/N_M .

We shall see in Sec. 9.7.2 that the spike output of a discriminator is very much larger when the input carrier is modulated than when the carrier is not modulated. In deriving Eq. (9.71), we have used Eq. (9.69) which applies only in the absence of modulation, or when the carrier is frequency-modulated to a very slight extent. Thus, Eq. (9.72) is valid only when the bandwidth occupied by the modulated signal is very small in comparison with the bandwidth B of the IF carrier filter.

9.7.1 Calculation of Mean Time Between spikes

In this section we shall calculate the mean time between spikes. We shall derive Eq. (9.6.9), which was used in the preceding section in our calculation of S_o/N_o near threshold.

A phasor diagram of the carrier and noise at the input to the discriminator is shown in Fig. 9.20. The input noise is expressed in terms of the quadrature components $x(t)$ and $y(t)$. In Secs. 9.6.1 and 9.6.2 we showed that a spike resulted in the discriminator output when $O(t)$ rotated $2p$ rad. If the rotation was counter-clockwise so that $O(t)$ increased by $2p$ the spike was positive, and if the rotation was clockwise so that $O(t)$ decreased by $2p$ the spike was negative.

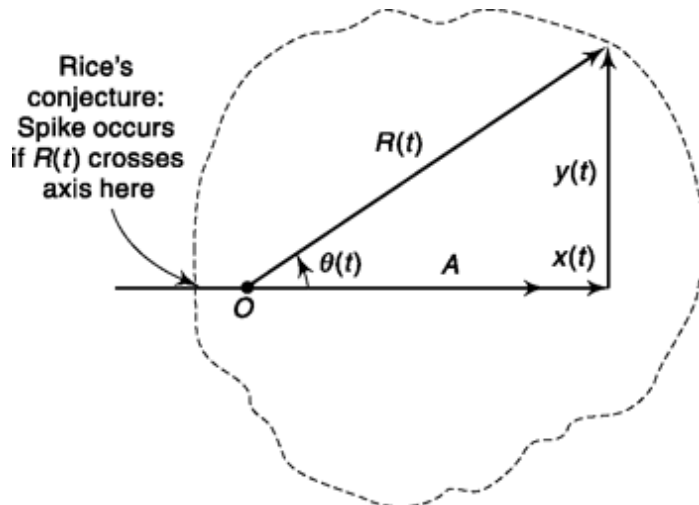


Fig. 9.20 Phasor diagram using quadrature components.

We shall assume that if the end point of $R(t)$ has crossed the horizontal axis so that $O(t)$ passes through p rad, then $O(t)$ will continue to increase (or decrease) giving rise to a positive (or negative) spike. Thus, we assume that to ensure a spike output, it is not actually necessary to observe a complete rotation of $R(t)$, but it is adequate that there be guaranteed a rotation of at least p rad. If, then, at an instant of time $t = t_1$,

$$x(t_1) < -A \quad (9.73a)$$

$$y(t_1) = 0 \quad (9.73b)$$

$$\text{and} \quad y(t_1) < 0 \quad (9.73c)$$

then $\theta(t)$ has increased through π rad, and a positive spike will result. Similarly if, at an instant of time $t = t_2$,

$$x(t_2) < -A \quad (9.74a)$$

$$y(t_2) = 0 \quad (9.74b)$$

$$\text{and} \quad y(t_2) > 0 \quad (9.74c)$$

then $\theta(t)$ has decreased through π rad, and a negative spike results. This hypothesis is due to Rice¹ and has been verified experimentally in a variety of different circumstances.² We shall employ these results in Eqs (9.73) and (9.74), to determine the probability of occurrence of a spike.

Let us consider an interval of time At and calculate the probability P_- of a negative spike occurring during this time interval. This probability is the probability that the conditions given by Eq. (9.74) are satisfied at some instant t_2 within the time interval At . These conditions are illustrated in Fig. 9.21. In this figure we see $R(t)$ and $O(t)$ just after $O(t)$ has decreased through p , which is equivalent to $y(t)$ increasing through zero. It is this increase which results in $y(t_2) > 0$.

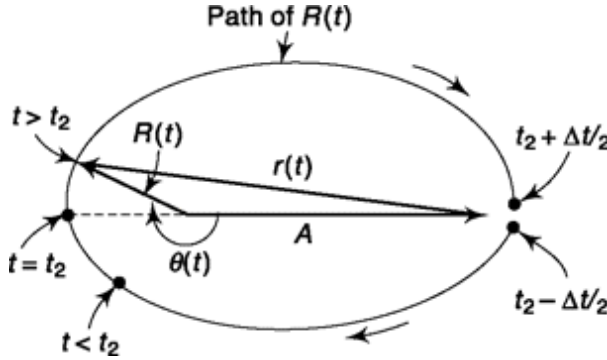


Fig. 9.21 Locus of $R(t)$ and $O(t)$ to cause a negative spike. Thus, we write

$$P_- = P \left[x(t_2) < -A, y(t_2) = 0, \frac{dy}{dt} \Big|_{t_2} > 0 \right] \quad (9.75)$$

In Sec. 7.5.2, we determined the joint probability density of x , x , y and y . In the present instance we need only the joint density of x , y and \dot{y} . Using Eq. (7.101), we have, after replacing n_c and n_s by x and y , respectively

$$f(x, y, \dot{y}) = \frac{\overbrace{e^{-x^2/2\eta B}}^{f(x)} \overbrace{e^{-y^2/2\eta B}}^{f(y)} \overbrace{e^{-\dot{y}^2/(2\pi^2 B^3 \eta/3)}}^{f(\dot{y})}}{\sqrt{2\pi\eta B} \sqrt{2\pi\eta B} \sqrt{2\pi^3 B^3 \eta/3}} \quad (9.76)$$

and

$$P_- = \int_{-\infty}^{-A} dx \int_0^\infty d\dot{y} \int_{-\Delta y/2}^{\Delta y/2} dy f(x, y, \dot{y}) \quad (9.77)$$

Before integrating Eq. (9.77), let us investigate the limits on the integrals to verify that Eq. (9.77) really represents Eq. (9.75). First we see that $\int_{-\infty}^{-A} dx f(x)$ will yield the probability that $x(t_2) < -A$. Next, we note that $\int_{-\Delta y/2}^{\Delta y/2} dy f(y) = f(0) \Delta y$ gives the probability of $y(t_2)$ passing through 0. Finally, we have $\int_0^\infty d\dot{y} f(\dot{y})$, which is the probability of $\dot{y}(t_2)$ being greater than zero. These are exactly the conditions of Eq. (9.75).

We now evaluate Eq. (9.77). The first integral that we determine is

$$\int_{-\Delta y/2}^{\Delta y/2} dy f(y) = f(0) \Delta y \quad (9.78)$$

Referring to Eq. (9.76), we see that $f(0) = 1/\sqrt{2\pi\eta B}$. We next consider the factor Δy . This is the differential change in y occurring during a differential change in time Δt . Thus, we write $\Delta y = (\Delta y/\Delta t) \Delta t$. Since Δy and Δt are differential quantities, $\Delta y/\Delta t$ can be approximated by dy/dt . Equation (9.77) now becomes

$$P_- = \int_{-\infty}^{-A} dx f(x) \int_0^{\infty} d\dot{y} f(\dot{y}) \frac{\Delta t}{\sqrt{2\pi\eta B}} \dot{y} \quad (9.79)$$

The next integral to be evaluated is

$$\int_0^{\infty} d\dot{y} f(\dot{y}) \dot{y} = \int_0^{\infty} d\dot{y} \dot{y} \frac{e^{-\dot{y}^2/(2\pi^2 B^3 \eta/3)}}{\sqrt{2\pi^2 B^3 \eta/3}} \dot{y} \quad (9.80)$$

This integral is easily evaluated after changing the variable of integration to

$$\lambda = \frac{\dot{y}^2}{2\pi^2 B^3 \eta/3} \quad (9.81)$$

Then

$$d\lambda = \frac{\dot{y} dy}{\pi^2 B^3 \eta/3} \quad (9.82)$$

Thus, Eq. (9.80) becomes

$$\sqrt{\frac{\pi B^3 \eta}{6}} \int_0^{\infty} d\lambda e^{-\lambda} = \sqrt{\frac{\pi B^3 \eta}{6}} \quad (9.83)$$

Equation (9.79) now becomes

$$\begin{aligned} P_- &= \int_{-\infty}^{-A} dx f(x) \left(\sqrt{\frac{\pi B^3 \eta}{6}} \frac{\Delta t}{\sqrt{2\pi\eta B}} \right) \\ &= \frac{B \Delta t}{\sqrt{12}} \int_{-\infty}^{-A} dx \frac{e^{-x^2/2\eta B}}{\sqrt{2\pi\eta B}} \end{aligned} \quad (9.84)$$

Again, we make a change in variable of integration. This time, we set

$$\lambda = \frac{-x}{\sqrt{2\eta B}} \quad (9.85)$$

Then

$$P_- = \frac{B \Delta t}{4\sqrt{3}} \int_{\frac{A}{\sqrt{2\eta B}}}^{\infty} \frac{2}{\sqrt{\pi}} d\lambda e^{-\lambda^2} = \frac{B \Delta t}{4\sqrt{3}} \operatorname{erfc} \sqrt{\frac{A^2}{2\eta B}} \quad (9.86)$$

The input-signal power is $S_i = A^2/2$, while the input noise in the baseband bandwidth is $N_M = \eta f_M$. Hence we may rewrite Eq. (9.86) in the form

$$P_- = \left(\frac{B}{4\sqrt{3}} \operatorname{erfc} \sqrt{\frac{f_M}{B} \frac{S_i}{N_M}} \right) \Delta t \quad (9.87)$$

In one second there are $1/\Delta t$ intervals in which a spike might occur. Since P is the probability of occurrence of a negative spike within any such individual interval, the expected number of pulses in a second, N_- , is

$$N_- = \frac{P_-}{\Delta t} \quad (9.88)$$

Hence, N_- is found from Eqs (9.87) and (9.88) to be

$$N_- = \frac{B}{4\sqrt{3}} \operatorname{erfc} \sqrt{\frac{f_M}{B} \frac{S_i}{N_M}} \quad (9.89)$$

From the symmetry displayed in Fig. 9.21, we see that the average number of positive spikes N_+ is the same as the average number of negative spikes N_- . Thus, the total number of spikes occurring per second in the presence of a carrier alone (no modulation) is, on the average,

$$N_c = N_- + N_+ = 2N_- = 2N_+ \quad (9.90)$$

The average time between spikes T_s is as anticipated in Eq. (9.69).

$$T_s = \frac{1}{N_c} = \frac{2\sqrt{3}}{B \operatorname{erfc} \sqrt{(f_M/B)(S_i/N_M)}} \quad (9.91)$$

9.7.2 Effect of Modulation

When the noise spectral components swing the resultant phasor in Fig. 9.16 around the origin in the counterclockwise direction, a positive spike occurs. Similarly, a clockwise rotation produces a negative spike. When the carrier frequency is at the center frequency of the carrier filter, the noise spectral components are symmetrically located in frequency above and below the carrier. In this case, because of the symmetry, positive and negative spikes are equally likely.

Now, however, let us assume that we have *offset* the carrier so that it lies just within the passband of the carrier filter at the lower-frequency limit of the passband. Let us consider a new coordinate system in which the phasor for this offset carrier is at rest. This offset phasor is accompanied by noise spectral components almost all of which are at higher frequency than the carrier and extend over a frequency range, with respect to the carrier, of B rather than $B/2$ as was the case when the carrier was centrally located. In our new coordinate system, all the noise spectral components rotate

counterclockwise. Hence only positive-frequency spikes can occur. Further, since the noise causing the spike has a spectral range B rather than $B/2$ (see Prob. 9.27), the spikes will be narrower than in the case of the symmetrically located carrier. Since the spike area is fixed, the spike amplitude must be larger. Finally, because of the higher relative frequencies of the noise components with respect to the offset carrier, whatever is going to happen will happen more frequently. Hence the rate of occurrence of spikes will increase.

Suppose we use a cathode-ray oscilloscope to examine the output waveform of the discriminator of Fig. 9.15. Let us assume that polarities have been adjusted so that a frequency increase in the carrier produces a positive deflection on the scope. In the case where the carrier is centrally located in the carrier filter passband, the scope trace will display the output noise with an equal frequency of occurrence of positive and negative spikes. As the carrier frequency is lowered, the trace will move downward, and the number of positive and negative spikes will become asymmetrical. The positive spikes will become more frequent and larger in amplitude, while the negative spikes will become smaller and occur less frequently. Eventually, only positive spikes will appear, and the frequency of occurrence of these positive spikes will be greater than the frequency of positive and negative spikes together in the symmetrical case.

When the carrier is modulated, we may view the modulation as simply a continuously varying frequency offset. When the baseband signal appears at the output of the discriminator, negative spikes are encountered most frequently at the positive extremity of the signal, and positive spikes at the negative extremity. The characteristic appearance of a recovered sinusoidal modulation is shown in Fig. 9.22. The important fact to note is not so much the spike polarity; rather, it is the unfortunate fact that in the region of threshold the noise power increases further when the carrier is modulated.

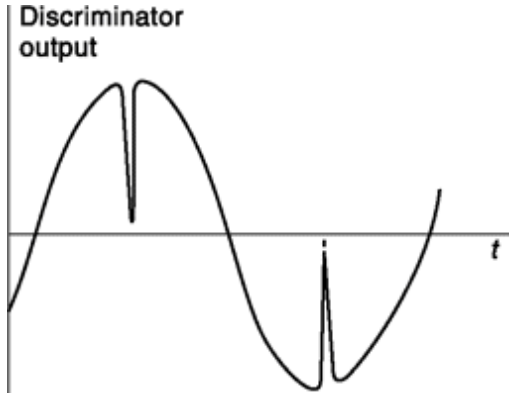


Fig. 9.22 Spikes present on sinusoidal output signal.

When the frequency of the input is offset by an amount $Sf = km(t)/2p$ from the frequency f_c carrier, the number of spikes increases by an amount SN . This increase in SN (in the presence of a carrier which is frequency-modulated) is related to Sf by

$$\delta N = |\delta f| e^{-(f_M/B)(S_f/N_M)} \quad (9.92)$$

The polarity of these *additional* spikes as observed at the discriminator output is always in the direction *opposite* to the polarity of the output signal produced by the offset Sf . The derivation of Eq. (9.92) is an extension of the derivation of Eq. (9.90) and will not be given here. (See Prob. 9.28) Suppose that the input signal is sinusoidally modulated at a frequency $f_m (< f_M)$. Then the input is

$$v(t) = A \cos\left(\omega_c t + \frac{\Delta f}{f_m} \sin 2\pi f_m t\right) \quad (9.93)$$

where Δf is the frequency deviation. Then

$$\delta f = \Delta f \cos 2\pi f_m t \quad (9.94)$$

and the average $|\delta f| = (2/p) Df$. The average value of SN is, therefore,

$$\overline{\delta N} = \frac{2\Delta f}{\pi} e^{-(f_M/B)(S_f/N_M)} \quad (9.95)$$

The total number of spikes per second is $N = N_c + SN$, the latter two terms given, respectively, by Eqs (9.91) and (9.95). It may, however, be verified (Prob. 9.30) that near and below threshold $SN @ N_c$. Therefore the total

average number of spikes is N @ SN. The average time between spikes T_s is,

$$\text{then, } T_s = \frac{1}{N} \approx \frac{1}{\delta N} \quad (9.96)$$

We may now calculate the output SNR of the FM discriminator when demodulating a sinusoidally modulated carrier where

$$\delta f = km(t)/2\pi = \Delta f \cos \omega_m t$$

We use Eqs (9.22), (9.27), (9.68), (9.95) and (9.96) to find

$$\frac{S_o}{N_o} = \frac{\left(\frac{3}{2}\right)\beta^2 (S_i/N_M)}{1 + (12\beta/\pi)(S_i/N_M) \exp\left\{-\frac{1}{2}[1/(\beta+1)](S_i/N_M)\right\}} \quad (9.97)$$

where $b = Df/f_M$.

Equation (9.97) is plotted in Fig. 9.23 for $b = 3$ and $b = 12$. Note that, when we are operating at a value of S/N_M which is above threshold for both values of b , the higher b , corresponding to

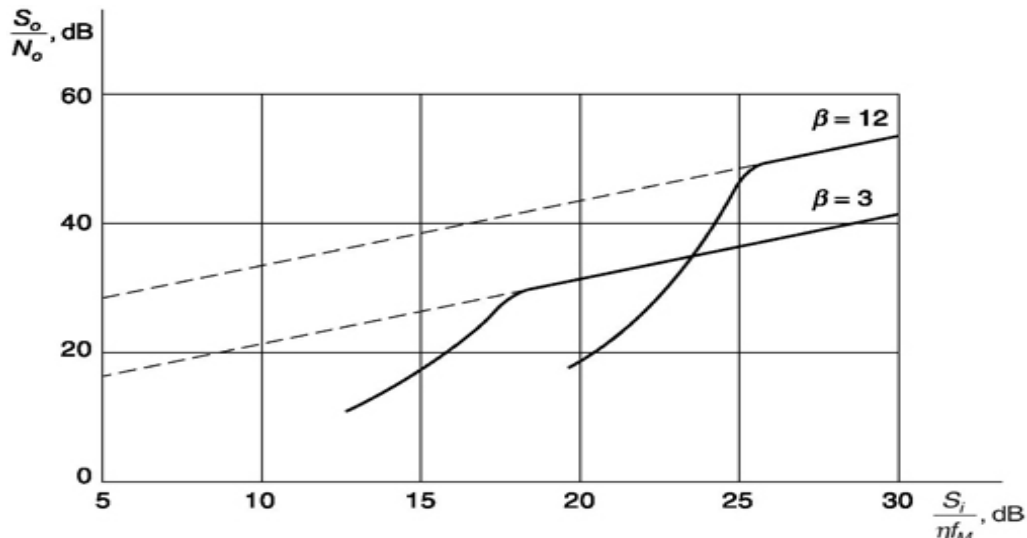


Fig. 9.23 Output SNR of an FM discriminator when demodulating an FM signal which is sinusoidally modulated.

a wider bandwidth, results in an increase in output SNR. On the other hand, at $S/N_M = 20$ dB, the output SNR is higher for $\beta = 3$ than for $\beta = 12$.

If the input signal is modulated by a sample function of a Gaussian random process, we have

$$v(t) = A \cos \left[\omega_c t + k \int_{-\infty}^t m(\lambda) d\lambda \right] + n(t) \quad (9.98)$$

where $km(t)$ is the instantaneous frequency deviation. Hence, the rms frequency deviation produced is

$$(\Delta f)_{\text{rms}} = \sqrt{k^2 \overline{m^2(t)}} / 2\pi \quad (9.99)$$

We begin our calculation of the output SNR by obtaining an expression for the output-signal power. The output-signal power is found from Eqs (9.11) and (9.99):

$$S_o = \alpha^2 k^2 \overline{m^2(t)} = \alpha^2 4\pi^2 (\Delta f_{\text{rms}})^2 \quad (9.100)$$

The FM noise, neglecting spikes, is given by Eq. (9.22):

$$N_G = \alpha^2 \frac{8\pi^2}{3} \frac{\eta f_M^3}{A^2} \quad (9.101)$$

The spike noise is found by combining Eqs (9.68), (9.92) and (9.96), with the result

$$N_S = \alpha^2 (8\pi^2 f_M) |\overline{\delta f}| \exp [-(f_m/B)(S_i/\eta f_M)] \quad (9.102)$$

Here $\delta f = km(t)/2\pi$ is the instantaneous frequency deviation and thus $|\overline{\delta f}|$ is the average value of the magnitude of the instantaneous frequency deviation. Noting that $m(t)$ is Gaussian, we have that δf is Gaussian with an average value of 0 and a standard deviation $(\Delta f)_{\text{rms}}$. Hence,

$$|\overline{\delta f}| = \int_{-\infty}^{\infty} \frac{|\delta f| \exp [-(\delta f)^2 / 2(\Delta f_{\text{rms}})^2]}{\sqrt{2\pi} (\Delta f_{\text{rms}})} d(\delta f) \quad (9.103)$$

This integral can be evaluated by integrating from 0 to infinity and doubling the result. Thus,

$$|\overline{\delta f}| = \sqrt{\frac{2}{\pi}} (\Delta f_{\text{rms}}) \int_0^{\infty} \frac{\delta f}{(\Delta f_{\text{rms}})} \exp [-(\delta f)^2 / 2(\Delta f_{\text{rms}})^2] d(\delta f) \quad (9.104)$$

This integral is directly integrable [change variables to $x = (\delta f)^2 / 2(\Delta f_{\text{rms}})^2$]. The result is

$$|\overline{\delta f}| = \sqrt{\frac{2}{\pi}} (\Delta f_{\text{rms}}) \quad (9.105)$$

Substituting Eq. (9.105) into Eq. (9.102) yields

$$N_S = \alpha^2 (8\pi^2 f_M) \left(\sqrt{\frac{2}{\pi}} (\Delta f_{\text{rms}}) \right) \exp [-(f_m/B)(S_i/\eta f_M)] \quad (9.106)$$

9.8 THE FM DEMODULATOR USING FEEDBACK (FMFB)

An FM modulator using feedback (FMFB) is shown in Fig. 9.24. This modulator decreases the S/N_M at threshold. There is another useful technique to do so by using Phase Locked Loop (PLL). We'll discuss this in next chapter along with PLL's other applications. As we see from the FMFB block diagram, a voltage controlled oscillator or VCO (Refer to discussion of Sec. 3.4.1 of Chapter 3) is frequency modulated by the output signal $v_o(t)$ of the FMFB demodulator. No surprise if you find similarity with Analysis-by-Synthesis approach of Sec. 4.6.4 in the context of vocoder techniques. The input $v_i(t)$ of carrier frequency f_c ($= w_c/2p$) is multiplied with output $v_{osc}(t)$ of VCO. The frequency of the VCO is offset from f_c by an amount f_o . The FMFB includes in its forward transmission path a bandpass filter and also a limiter-discriminator. The bandpass filter, following multiplier, is centred at the offset frequency f_o , and hence passes the difference-frequency output of the multiplier.

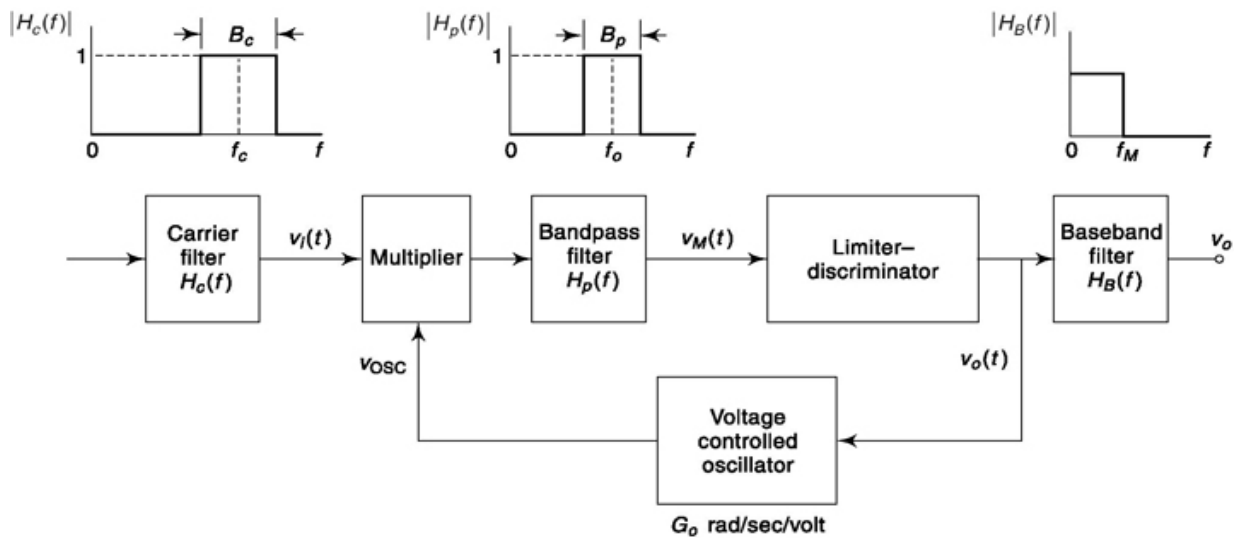


Fig. 9.24 The FM demodulator using feedback.

We show now that the FMFB recovers the baseband signal from an FM modulated carrier, and when operating above threshold yields the same signal-to-noise output as does a simple limiter-discriminator. Let the input signal and noise $v_i(t)$ be

$$v_i(t) = R(t) \sin [\omega_c t + \phi_s(t) + \phi_n(t)] \quad (9.108)$$

where $R(t)$ is the envelope of the carrier signal and the noise, $f_s(t)$ is the angular modulation due to the signal, and $f_n(t)$ is due to the noise. If $v(t)$ were the input to a limiter-discriminator whose baseband output was a times the departure of the instantaneous angular frequency from the carrier frequency w_c , the output voltage of the discriminator $v_o(t)$ would be

$$v_o(t) = \alpha \frac{d}{dt} [\phi_s(t) + \phi_n(t)] \quad (9.109)$$

Returning to the FMFB shown in Fig. 9.24, we represent the VCO output as

$$v_{osc}(t) = B \cos \left[(\omega_c - \omega_0)t + G_0 \int_{-\infty}^t v_o(\lambda) d\lambda \right] \quad (9.110)$$

where B is the VCO amplitude and G_0 , as introduced in Eq. (3.63), is the change in angular frequency of the VCO per unit change in $v_o(t)$. We neglect temporarily the effect of the bandpass filter following the multiplier except to take account of the fact that it passes only the difference-frequency component of the multiplier. On this basis, the product signal $v_M(t)$, which is equal to the low-pass component of $v_i v_{osc}$, is

$$v_M(t) = \frac{AB}{2} \cos \left[\omega_0 t + \phi_s(t) + \phi_n(t) - G_0 \int_{-\infty}^t v_o(\lambda) d\lambda \right] \quad (9.111)$$

This product signal is applied to the limiter-discriminator. The output of the discriminator $v_o(t)$ is then

$$v_o(t) = \alpha \left[\frac{d\phi_s(t)}{dt} + \frac{d\phi_n(t)}{dt} - G_0 v_o(t) \right] \quad (9.112)$$

Solving for $v_o(t)$ yields

$$v_o(t) = \frac{\alpha}{1 + \alpha G_0} \frac{d}{dt} (\phi_s + \phi_n) \quad (9.113)$$

We observe from Eq. (9.113), and from comparing this equation with Eq. (9.109), that the FMFB does indeed demodulate. We see further that the only difference between the output of the discriminator and the FMFB is that the amplitude of output of the FMFB is smaller by the factor $(1 + aG_0)$. Since

both signal and noise have been reduced by the same factor $1/(1 + aG_0)$, the signal-to-noise ratio is the same for the FMFB and the FM discriminator.

We turn our attention now to the bandpass filter and ask how narrow it can be made to pass the signal without undue distortion. Using Eq. (9.113), we may rewrite Eq. (9.111) as

$$v_M(t) = \frac{AB}{2} \cos \left[\omega_0 t + \frac{1}{1 + \alpha G_0} (\phi_s + \phi_n) \right] \quad (9.114)$$

We observe, in comparing Eq. (9.114) with Eq. (9.108), that the feedback has suppressed the frequency deviation, produced by the signal f_s , by the factor $1/(1 + aG_0)$. Consider, for example, that the modulation is sinusoidal. Then $f_s(t) = b \sin \omega_m t$, and the phase of the signal present in the multiplied signal is $f_s(t)/(1 + aG_0) = [b/(1 + aG_0)] \sin \omega_m t$. Hence, if the bandwidth of the carrier filter is B_c and the bandwidth of the bandpass filter preceding the discriminator is B_p then

$$B_p = 2 \left(\frac{\beta}{1 + \alpha G_0} + 1 \right) f_m \quad (9.115)$$

and

$$B_c = 2(\beta + 1) f_m \quad (9.116)$$

so that

$$B_p = \frac{[\beta/(1 + \alpha G_0)] + 1}{\beta + 1} B_c \quad (9.117)$$

If $\beta = 9$ and $\alpha G_0 = 8$, then $B_p = \frac{1}{5} B_c$.

Note that the bandwidths B_p and B_c given by Eqs (9.115) and (9.116) employ Carson's rule for the bandwidth of *rectangular* filters. In practice, the carrier filter with bandwidth B_c is *almost* rectangular. However, the bandpass filter with bandwidth B_p is usually a single-tuned filter, and to pass 98 percent of the signal energy, B_p must be greater than the value given in Eq. (9.115). The reason for employing the single-tuned circuit is related to the fact that the FMFB is a feedback system. If a single-tuned filter is used, the system is stable; if, however, a more sophisticated filter containing many poles is employed, the FMFB may oscillate.

9.8.1 Threshold Extension using FMFB

Let us consider the operation of the FMFB under two conditions of G_0 . First let the VCO sensitivity $G_0 = 0$. Then, referring to Fig. 9.24, we find there is no feedback. The modulation index is not reduced, and $B_p = B_c$ [see Eq. (9.117)]. The VCO now serves only to shift the carrier frequency w_c to an IF frequency w_0 . Therefore, no threshold extension occurs.

Our second condition for G_0 is $G_0 \rightarrow \infty$. Let the output voltage of the VCO be written as

$$v_{\text{osc}}(t) = B \cos [(\omega_c - \omega_0)t + \phi_{\text{osc}}(t)] \quad (9.118)$$

where, comparing Eq. (9.118) with Eq. (9.110), we see that

$$\phi_{\text{osc}}(t) = G_0 \int_{-\infty}^t v_o(\lambda) d\lambda \quad (9.119)$$

Since G_0 is extremely large, $v_o(t)$ must be infinitesimally small for $f_{\text{osc}}(t)$ to remain finite.

Refer now to Eq. (9.112) and replace $G_0 v_o(t)$ by $f_{\text{osc}}(t)$. We have then

$$v_o(t) = \frac{1}{G_0} \frac{d\phi_{\text{osc}}(t)}{dt} = \alpha \left(\frac{d\phi_s}{dt} + \frac{d\phi_n}{dt} - \frac{d\phi_{\text{osc}}}{dt} \right) \quad (9.120)$$

For very large G_0 we can assume $v_o(t) = 0$. Equation (9.120) now becomes

$$\frac{d\phi_{\text{osc}}}{dt} \approx \frac{d\phi_s}{dt} + \frac{d\phi_n}{dt} \quad (9.121)$$

Equation (9.121) shows that when the amount of feedback becomes very large, the frequency of the VCO approaches the sum of the frequency of the input signal and the frequency of the input noise. Note that the output of the multiplier becomes a very narrowband FM signal.

Thus, whenever $f_n(t)$ rotates by 2π , resulting in a discriminator spike, we see from Eq. (9.121) that f_{osc} also rotates by 2π , resulting in a spike in the FMFB. Thus, there is no threshold extension when $G_0 \rightarrow \infty$.

We now show that if G_0 is neither zero nor very large, threshold extension results. We assume first that the modulation is sinusoidal and that the demodulation is performed by a conventional limiter-discriminator circuit. From Eqs (9.90), (9.91) and (9.95) we find that the total average number of spikes per second N is

$$\begin{aligned}
N_{\text{discr}} &= N_c + \overline{\delta N} \\
&= \frac{B}{2\sqrt{3}} \operatorname{erfc} \sqrt{\frac{f_M}{B} \frac{S_i}{N_M} + \frac{2\Delta f}{\pi}} \exp [- (f_M/B)(S_i/N_M)] \quad (9.122)
\end{aligned}$$

In Eq. (9.122), B is the bandwidth of the IF filter and Df is the frequency deviation of the sinusoidally modulated carrier.

In the case of the FMFB, N is also given by Eq. (9.122), provided that B is replaced by B_p (see Fig. 9.24) and Df is multiplied by the factor $1/(1 + aG_0)$. Hence,

$$N_{\text{FMFB}} = \frac{B}{2\sqrt{3}} \operatorname{erfc} \sqrt{\frac{f_M}{B_p} \frac{S_i}{N_M} + \frac{2\Delta f}{\pi(1+aG_0)}} \exp [- (f_M/B_p)(S_i/N_M)] \quad (9.123)$$

Both N_{discr} and N_{FMFB} depend on the ratio S/N_M . It can, however, be shown that S_i/N_M is the same whether measured at the output of the IF filter or at the output of the filter of bandwidth B_p . However, since $B_p < B$ and in addition, since $1 + aG_0 > 1$, we see in comparing Eqs (9.122) and (9.123) that $N_{\text{FMFB}} < N_{\text{discr}}$ and that hence the threshold is extended.

Threshold extension using PLL will be discussed in the next chapter along with other uses of PLL.

Example 9.6

(i) For an FM demodulation system following specification is given. Baseband filter bandwidth = 15 kHz, Carrier filter bandwidth = 60 kHz, RMS frequency deviation = 30 kHz. Find output SNR for input SNR (a) 10 dB, (b) 20 dB and (c) 30 dB. (ii) Cite reason if any of (a)-(c) lie below threshold.

Solution

- (i) From definition, $f_M = 15$ kHz, $B = 60$ kHz, $\Delta f_{\text{rms}} = 30$ kHz

Thus, $\Delta f_{\text{rms}}/f_M = 2$ and $f_M/B = 0.25$

- (a) Input SNR, $\frac{S_i}{\eta f_M} = 10$ dB = 10

Substituting in Eq.(9.107),

Output SNR

$$3 \times 2^2 \times 100 \times 1 + (6/2/p)(2)(1000) \exp[-0.25 \times 1000] = 12000 = 40.7918$$

- (ii) The conditions (b) and (c) are above FM threshold as for those cases denominator in output SNR calculation is practically unity. (a) will be below FM threshold if it is more than 1 dB

dB _____

below the straight line for input SNR vs. output SNR obtained from (b) and (c). If same slope

$$\left(\frac{40.7918 - 30.7918}{30 - 20} = 1 \right) \text{had been followed}$$

for input SNR 10 dB the output SNR would have been $30.7918 - 10 \times 1 = 20.7918$ dB. But output SNR for (a) is 11.3178 dB. Hence at (a) FM receiver is operating below threshold.

SELF-TEST QUESTION

12. Is the spike output of a discriminator much larger if input carrier is modulated?
13. Does the frequency of spike increase if carrier-filter bandwidth increases?
14. The positive and negative spike in FM reception is related to swing of noise plus signal phasor around origin in clockwise and anticlockwise direction respectively. Is the statement correct?
15. In FMFB, bandpass filter bandwidth is less than carrier filter bandwidth and this factor contributes to FM threshold reduction. Is that true?

FACTS AND FIGURES

In June 8, 1919, in an issue of *San Francisco Chronicle*, the author F. A. Collins gave a vivid description of the changes that radio broadcasting would bring about. He wrote, "In the not distant future the newspapers may announce some day, for instance, that the President of the United States will address the people the following morning at 10 o'clock. At the appointed hour 100,000,000 persons scattered throughout the country may listen to his address without missing a word or even the inflection of the speaker's voice." Collins found a lot of utility in having a USD 5 receiver for the citizens that ranged from disaster management to proper functioning of democracy. He continued, "In some hour of great national peril the entire

population can thus be collected and addressed in a few minutes.....it would be possible, for example, for President Wilson on his return from France to discuss the League of Nations in this way with every citizen.”

Within a month of this publication, President Woodrow Wilson made the first attempt by an American President for a nationwide radio broadcast. It was July 4, 1919. President Wilson was making the Independence Day speech aboard the naval ship U.S.S. George Washington. The broadcast was technologically successful, but the president was barely heard as he was too far from the microphone and “the sailors were too intimidated to ask him to move into the proper location.”

MATLAB

- Experiment 3 6
- Frequency modulation and demodulation in noisy condition % Refer to Experiment 18.
- Notice the clicks at input SNR of 5dB

```
fc=10000; % Carrier frequency  
fs=100000; % Sampling frequency  
f1=200; % For single tone message signal  
t=0:1/fs:((2/f1)-(1/fs)); % Gives exact two cycles of modulating signal  
x1=cos(2*pi*f1*t); % single tone message  
kf=2*pi*(fc/fs)*(1/max(max(x1))); %frequency deviation = fc kf=kf*(f1/fc);  
% makes frequency deviation = f1;  
opt=10*kf; % Then deviation = 10*f1  
b=0.1*ones(1,10); a=1; % Defining a moving average filter  
subplot(2 21), plot(x1); title('modulating signal');  
y1=modulate(x1,fc,fs, 'fm',opt) ;  
y1n=awgn(y1,25,'measured');  
x1_recov=demod(yin,fc,fs,'fm',opt);  
x1_recov=filter(b,a,x1_recov);  
subplot(2 22), plot(x1_recov); title('demodulated signal, input SNR = 25dB')
```

```

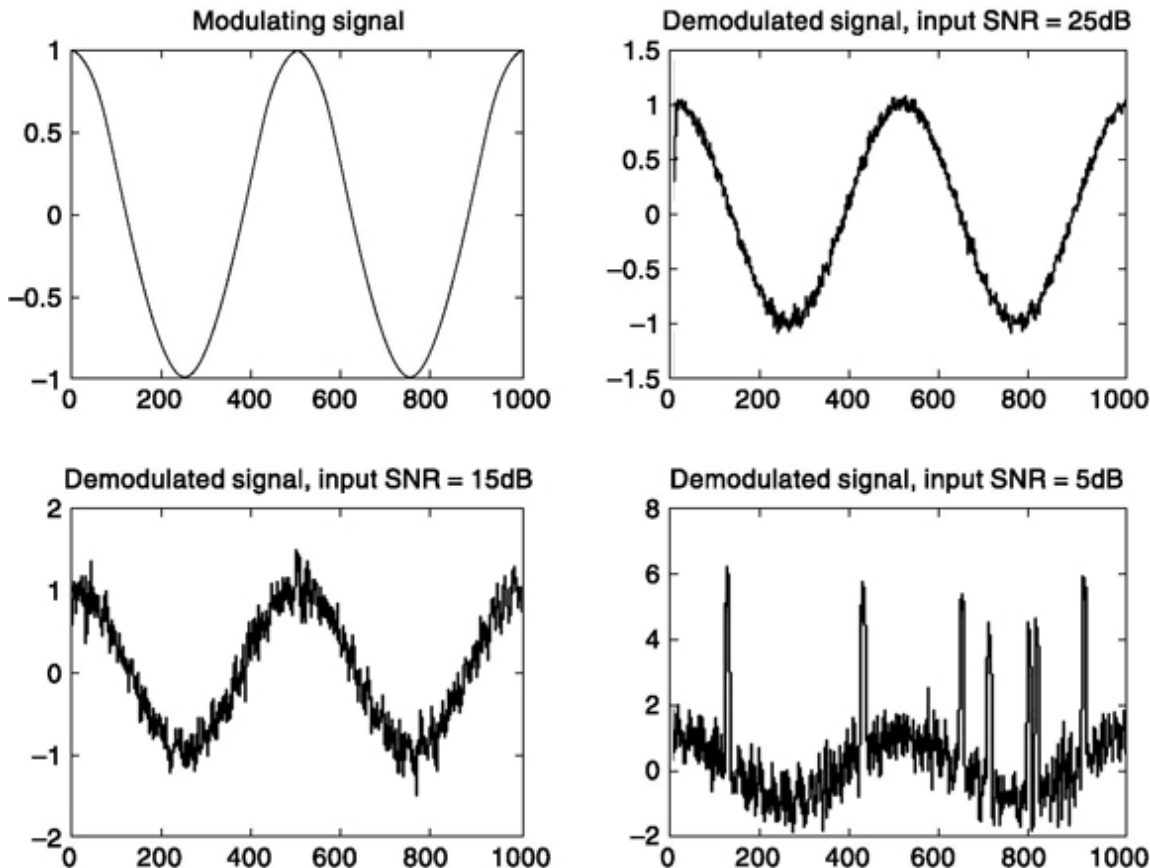
y1n=awgn(y1,15, 'measured' ) ; x1_recov=demod(y1n,fc,fs,'fm',opt);
x1_recov=filter(b,a,x1_recov) ;

subplot(2 2 3), plot(x1_recov); title('demodulated signal, input SNR = 15dB')

y1n=awgn(y1,5, 'measured') ; x1_recov=demod(y1n,fc,fs,'fm',opt);
x1_recov=filter(b,a,x1_recov) ;

subplot(2 2 4), plot(x1_recov); title('demodulated signal, input SNR = 5dB')

```



- Experiment 37
- Reduction in number of spikes in FM demodulation using feedback %
This program calls function myfm_spike.m which calculates spikes % Refer to Section 9.8 of this chapter.

```

clear; fm=15 0 00;

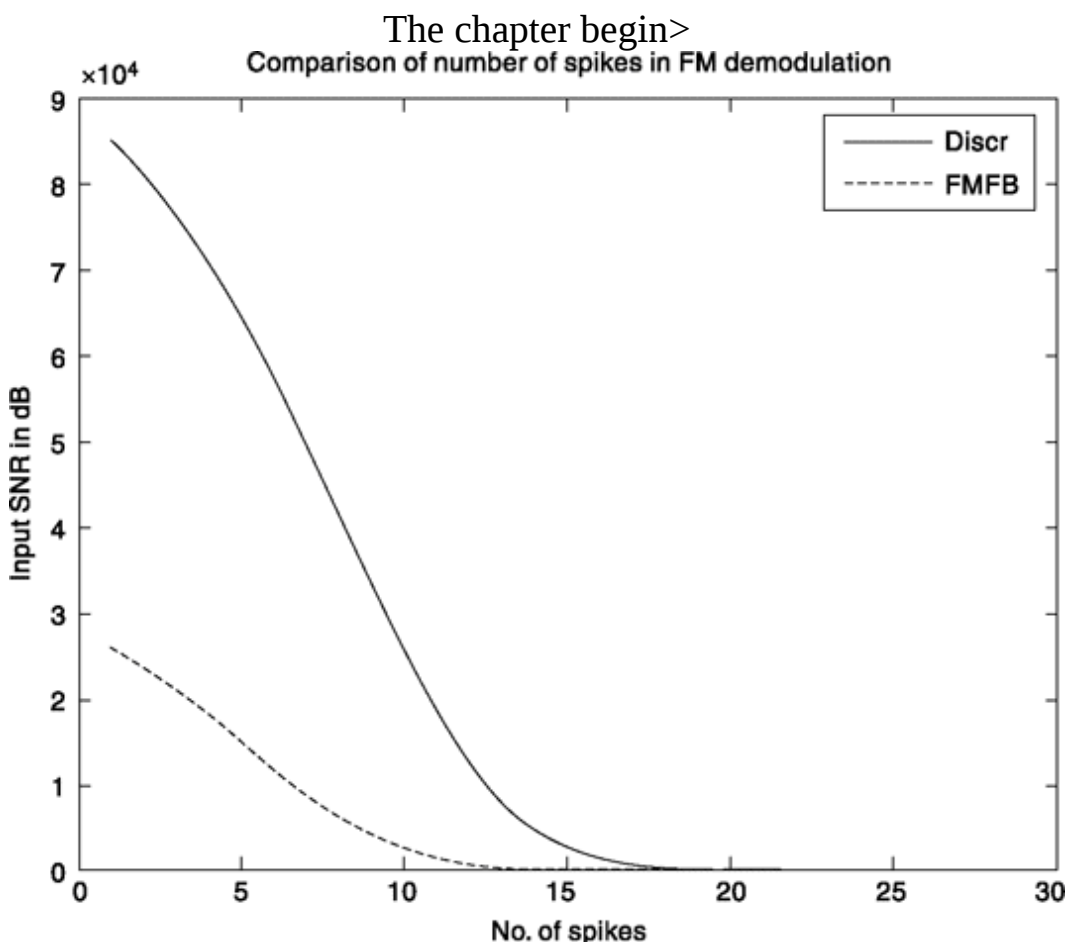
beta=3; % beta =3;
Bp=2*(beta/beta+1)*fm; % Also (1+alpha*G0)=beta
B=2*(beta+1)*fm; df=2*(beta+1)*fm; for i=1:30
SNR=i; % input SNR in dB

```

```

SNRmag=10^A(SNR/10) ;
N_discr(i)=myfm_spike(B,fm,SNRmag,df);
N_FMFB(i)=myfm_spike(Bp,fm,SNRmag,df/3);
end;
ii=1:30;
plot(ii,N_discr,'r-',ii,N_FMFB,'b:'); legend('Discr' , 'FMFB') ;
xlabel('No. of spikes' ) ; ylabel('Input SNR in dB' ) ; title('Comparison of
number of spikes in FM demodulation')

```



- This function is used in calculation of number of spikes and called % by exp37.m. Refer to section 9.8 of this chapter for details.

```

function [N]=myfm_spike(B,fm,SNR,df)
N=(B/(2*sqrt(3)))*erfc(sqrt(fm*SNR/B))+(2*df/pi)*exp(-(fm/B)*SNR);

```

SUMMARY

The chapter begins with the discussion of an FM receiving system that is developed from basic principles. It involves an amplitude limiter and a frequency discriminator. The use of preemphasis and deemphasis to improve system performance is discussed next. Comparison with AM and PM is presented. It is seen that for higher input SNR, FM scores over AM. PM, on the other hand, is useful in frequency division multiplexing as FM tend to perform worse at higher frequency bands due to its rising noise power in output. Like AM, FM too exhibits threshold which is of higher concern in communication context. Threshold phenomena can be related to occurrence of spikes at low input SNR. A detailed discussion on this is presented. Reduction of threshold remains an important concern in FM communication. A technique that uses basic limiter-discriminator circuit but also a feedback through voltage controlled oscillator is discussed. It is shown how occurrence of spikes is reduced by introduction of this feedback which in turn reduces threshold. MATLAB simulation in Experiment 37 gives a clearer idea of this. The other popular threshold reduction technique using phase locked loop is discussed in next chapter.

PROBLEMS

9.1 In an FM receiver, we find it advantageous to use an amplitude limiter. In the “amplitude-modulation” receivers discussed in Chap. 8 we did not find it advantageous to use a “frequency limiter.” Discuss.

9.2 The AM-FM signal $[1 + m(t)] \cos(w_{ct} + b \sin w_M t)$, $|m(t)| < 1$ is ideally limited and then bandpass-filtered. If the bandwidth of the bandpass filter is selected to pass the fundamental frequency and to reject frequencies of the order of $2w_c$, $3w_c$ etc., and, in addition, if the filter bandwidth is also chosen to pass 98 percent of the signal energy contained in the fundamental and its sidebands, find:

- The bandwidth of the filter.
- The minimum ratio of w_c/w_M for a given b -

9.3 (a) The signal $v(t) = 2(1 + 0.1 \cos 2p \times 10^3 t) \cos 2p \times 10^6 t$ is passed through a filter which

removes the lower sideband. Write an expression for the filter output $v_o(t)$ in a form which makes explicitly evident that $v_o(t)$ is an angle-modulated waveform with varying amplitude, that is

$$v_o(t) = A(t) \cos [2\pi \times 10^6 t + \theta(t)]$$

Find $A(t)$ and $d(t)$ and make reasonable approximations to simplify $v_o(t)$.

(b) The waveform $v_o(t)$ is applied to a network whose transfer function is $H(f) = js\omega$ (with $s = 1/2p$ sec) in the frequency range $f_c = 10^6 \pm 100$ Hz and $H(f) = 0$ otherwise. The output of this network is then applied to an envelope demodulator. Write an expression for the output of the demodulator.

9.4 We note from Eq. (9.6) that, since $a = sA_L$, the output of the limiter-discriminator of Fig. 9.1 is $v_4 = sA_L df/dt$. Hence the more severe the limiting, i.e., the smaller A_L , the smaller will be the signal output of the limiter-discriminator. A student commented that limiting should be just barely adequate to remove amplitude variations in order to keep A_L as large as possible. Is this comment valid? Discuss.

9.5 For Eq. (9.27) make a plot of $(S_o/N_o)_{dB}$ against $(S/N_M)_{dB}$ for values of $b = 1, 5, 10, 100$. On the same set of axes include the corresponding plot for synchronous demodulation in a linear system (i.e. SSB or DSD-SC).

9.6 Commercial FM transmission is allocated a bandwidth $B = 200$ kHz. Assume a receiver with a rectangular IF filter of corresponding bandwidth. If the discriminator output is applied directly to a baseband filter with $f_M = 15$ kHz, what fraction of the noise output of the discriminator passes through the filter?

9.7 Consider two frequency-modulated signals, the first where $km(t) = bw_M \cos w_M t$ and the second where $km(t)$ is equal to a Gaussian signal, which is white with power spectral density $h_m/2$, $|f| < f_M$, and zero elsewhere. If the output SNR of each system is the same, calculate the ratio of the IF bandwidths needed to pass 98 percent of the signal energy in each case.

9.8 If the input SNR $Sj/N_M = 30$ dB, calculate S_o/N_o when $km(t) = Bw_M \cos w_M t$ and $b = 1, 5, 10, 100$.

9.9 In an FM system the baseband bandwidth is f_M . The modulation is sinusoidal and the bandwidth B is to be kept constant. Write an expression for g_{FM} , defined in Eq. (9.28) as a function of the modulation index, in terms of B and f_M .

9.10 The input SNR $S/N_M = 30$ dB, and an $S_o/N_o = 48$ dB is required. Find the mean-squared frequency deviation in terms of the frequency range, f_M .

9.11 Verify Eq. (9.29).

9.12 Derive Eq. (9.30).

9.13 A baseband signal $m(t)$ whose spectrum extends to $f_M = 5$ kHz is transmitted by FM. The rms frequency deviation produced by $m(t)$ is 100 kHz. The same signal $m(t)$ is also transmitted by SSB. If the output signal-to-noise ratios for FM and SSB are to be the same, compare the input signal-to-noise ratios for the two types of transmission.

9.14 The power spectral density of a modulating signal $m(t)$ is given by

$$G_m(f) = \frac{G_0}{1 + (f/f_1)^2}$$

where $f_1 \neq f_M$. If a preemphasis circuit is to be used, where $|H_p(f)|^2 = K^2 f^2$, find K^2 if the preemphasis is not to increase the bandwidth.

9.15 If $G_m(f) = h_m/2$, $|f| < f_M$ and zero elsewhere,

$$(a) \text{ Find } \int_{-f_M}^{f_M} |H_p(f)|^2 df$$

(b) If $|H_p(f)|^2 = k_1 f + k_2 f^2$, find k_1 and k_2 to maximize R , subject to the constraint of part a of this problem.

9.16 Consider that a carrier is FM-modulated by a baseband waveform $m(t)$. Let the bandwidth occupied by the FM waveform be defined as in Eq. (3.63):

$$B = 2 \left[\frac{\int_{-\infty}^{\infty} v^2 G(v) dv}{\int_{-\infty}^{\infty} G(v) dv} \right]^{1/2}$$

(a) Show that, in this case, the bandwidth is proportional to the normalized power of $m(t)$, i.e.

$$B = c^2 m^2(t), \text{ with } c^2 \text{ a constant.}$$

(b) Let $m(t)$ have a normalized power of 2 volts² and suppose that the sensitivity of the FM modulator is such that a change by 1 volt in $m(t)$ produces a frequency change of 10 kHz. Find the bandwidth B .

9.17 Preemphasis is to be used in conjunction with a DSB-SC system. The spectral density of the baseband signal, of spectral range f_M , is as given in Eq. (9.39), and the preemphasis filter has the transfer function given in Eq. (9.40). Assume $f_1 = f'$. Impose the constraint that the preemphasis is not to increase the transmitted power. Calculate the preemphasis improvement R and compare with Eq. (9.44).

9.18 (a) In a stereo FM system the baseband spectral range is $f_M = 15$ kHz. Assume that preemphasis

is not used. Find the ratio of the noise output power to the noise power for monophonic transmission. See Fig. 3.16.

(b) Taking preemphasis into account as described in Sec. 9.4.1, show that stereo FM is 22 dB noisier than monophonic FM.

9.19 Plot Eqs (9.43) and (9.44) to determine when Eq. (9.44) can be employed.

9.20 If, in Eq. (9.43), $f_1 = 2.1$ kHz and $f_M = 15$ kHz, calculate R . Compare your result with that given in the text which was obtained using Eq. (9.44).

9.21 (a) One thousand signals are multiplexed by the system of Fig. 9.8. The angle modulator is

a frequency modulator, i.e. the composite baseband signal $M(t)$ frequency modulates the carrier. The lowest SSB carrier frequency is 10 kHz and each baseband signal is allocated 4 kHz. Assume that each baseband signal has the same normalized power. The channel with the least noise turns out to have a signal-to-noise ratio of 80 dB. If a signal-to-noise ratio lower than 20 dB were not acceptable, how many channels of the system would be usable?

(b) Assume instead that $M(t)$ phase-modulates the carrier. Assume also that the total transmitted power is the same as in part (a). Calculate the signal-to-noise ratio in any channel.

9.22 A 4 MHz TV signal, and one thousand 4 kHz audio signals, are multiplexed onto a single FM carrier (the audio signals are SSB-modulated to obtain this goal, the TV signal is left at baseband and is therefore channel 1). The power spectral density of the composite signal is constant over its entire spectral range.

- (a) Find the spectral range of the composite signal.
 - (b) Calculate the output SNR for channel 1, the TV signal, in terms of the input SNR.
 - (c) Calculate the output SNR for the top channel.
- 9.23 (a) A carrier, $A \cos 2\pi f_c t$, is accompanied by noise having quadrature components $x(t)$ and $y(t)$. Assume that for an interval from $t = 0$ to $t = 1$, $x(t)$ and $y(t)$ may be approximated by

$$x(t) = \frac{A}{2} [\sin 2\pi(f_c + f)t]$$

$$y(t) = \frac{A}{2} [\cos 2\pi(f_c + f)t - 1]$$

Draw the path of the resultant phasor $R(t)$ in the phasor diagram of Fig. 9.16. Make a qualitative plot of $d(t)$ and of dQ/dt .

- (b) Repeat (a) if f is replaced by $2f$ in the expression for $y(t)$.
- (c) Repeat (a) if the functions describing $x(t)$ and $y(t)$ are interchanged.
- (d) Repeat (c) if the amplitude A in the expression for $x(t)$ and $y(t)$ is replaced by $3A$.

9.24 Consider a random pulse train where each pulse has a duration $t = 2/B$ and an amplitude pB .

If the average time between pulses is T , and if the pulse train is filtered by a rectangular low-

pass filter of bandwidth f_M ,

- (a) Show that the power measured at the filter output is $(4p^2/T)(2f_M)$, iff $f_M \leq B/2$.
- (b) Obtain an expression for the power measured at the filter output when f_M is not much less than B .

9.25 A random pulse train consists of pulses given by the equation $p(t) = \sin Bt$, $0 < t < 2p/B$,

separated by the average time interval T .

(a) Find $|P(f)|^2$.

(b) If the pulse train is filtered by a low-pass filter with a cutoff frequency f_M ! B, show that the power measured at the filter output is very small in comparison with the power of the pulse train.

9.26 Threshold is defined as the value of S_t/hf_M , which results in S_o/N_o decreasing by 1 dB from

the value

$$\frac{S_o}{N_o} = \frac{3\kappa^2 m^2}{4\pi^2 f_M^2} \frac{S_i}{\eta f_M}$$

(a) Show that when the carrier is unmodulated, threshold is reached when

$$0.26 = \sqrt{3} \frac{B}{f_M} \frac{S_i}{\eta f_M} \operatorname{erfc} \sqrt{\frac{f_M}{B}} \frac{S_i}{\eta f_M}$$

(b) Plot S_t/hf_M at threshold as a function of B/f_M .

9.27 Consider that the signal and noise at the input to an FM system are

$$v_i(t) = \cos(\omega_c t + \Omega t) + x(t) \cos \omega_0 t - y(t) \sin \omega_0 t$$

and that

$$G_x(f) = G_y(f) = \eta \quad -\frac{B}{2} \leq f \leq +\frac{B}{2}$$

(a) Show that $v_i(t)$ can also be written as $v_i(t) = \cos(\omega_c t + \Omega t) + x'(t) \cos(\omega_c t + \Omega t) + y'(t) \sin(\omega_c t + \Omega t)$. Find $x'(t)$ and $y'(t)$.

- (b) Find $G_{x'}(f) = G_y(f)$. Show that if $\Omega = B/2$, the spectral density of x' (and y') extends to B Hz. Comment on the significance of this result with regard to the duration of a spike.
- (c) Find $E[x'(t)y'(t)]$, i.e. show that even though x and y are uncorrelated, x' and y' are correlated.
- 9.28 Using the results of Prob. 9.27 and Eqs (9.73) and (9.74),
- Show that a negative spike occurs when $x' < 1$, y' goes through 0, and $\dot{y}' > 0$.
 - Show also that a positive spike occurs when $x' < -1$, y' goes through 0, and $\dot{y}' < 0$.
 - Using Eq. (9.76) with x replaced by x' , and y by y' , derive Eq. (9.92), where $\delta f = \Omega/2\pi$.
- 9.29 An FM carrier is modulated by the signal $m(t)$, which is Gaussian, and bandlimited to f_M Hz. The instantaneous frequency deviation produced by $m(t)$ is $km(t)$. If the mean value of the square of $km(t)$ is $\overline{(\Delta\omega)^2}$, find $|\overline{\delta f}|$.
- 9.30 An FM carrier is sinusoidally modulated as in Eq. (9.93). Show, using Eqs (9.95) and (9.91), that $\overline{\delta N} \gg N_c$.
- 9.31 Verify Eq. (9.97).
- 9.32 (a) Plot the ratio $S_i/\eta f_M$ at threshold as a function of β [use Eq. (9.97)].
(b) Compare your results with those found in Prob. 9.26b.
- 9.33 The FM signal $v(t) = \cos [\omega_c t + k \int_{-\infty}^t m(\lambda) d\lambda]$ is demodulated using an FM discriminator. If the signal $m(t)$ is Gaussian and is bandlimited to f_M Hz, and $S_i/\eta f_M = 20$ dB, find the maximum rms deviation possible so that the discriminator is operating at threshold.
- 9.34 Show that the ratio $S_i/\eta f_M$ is unchanged when measured after the carrier filter or the bandpass filter shown in Fig. 9.24.
- 9.35 Show that for the FMFB, $\delta N \gg N_c$. Use Eq. (9.123) and plot $N_c/\delta N$ as a function of $S_i/\eta B_p$ with $[(1 + \alpha G_0)B_p]/\Delta f = 4$ (this corresponds to choosing $1 + \alpha G_0 = \beta$, which represents reasonably good design).
- 9.36 Find the threshold extension possible for $\beta = 3$ and 5, if $1 + \alpha G_0 = \beta$.

REFERENCE

1. Sakrison, D: "Communication Theory," John Wiley & Sons; Inc., New York, 1968.

10

PHASE-LOCKED LOOPS

CHAPTER OBJECTIVE

In this chapter, we discuss one of the most versatile devices used in modern electronic communication. Phase Locked Loops (PLL) has the ability to lock to the frequency of an incoming signal, track it and cleanse frequency or phase noise. It can also synthesize frequencies which are some multiple or even fractionally related to a reference frequency. Here, we first introduce the principle of operations of PLL. We describe Analog PLL in detail and its application in improvement of Frequency Demodulation scheme. We follow it up with description of Digital PLL, All Digital PLL and Software PLL. Finally, other important applications of PLL are discussed. Numerical and MATLAB based examples add important insights into functioning of PLL. We introduce the concept of MAT-LAB SIMULINK model here with a frequency demodulation and frequency synthesis experiments.

FACTS AND FIGURES

The history of phase-locked loops goes back to 1932 when an alternative to Armstrong's superheterodyne receiver was investigated which required fewer tuned circuits. In that circuit, a local oscillator was tuned to the desired input frequency and multiplied with the input signal. The resulting output signal included the original audio modulation information. Since the local oscillator would rapidly drift in frequency, an automatic correction signal was applied to the oscillator, maintaining it in the same phase and frequency as the desired signal. The technique was described in 1932, in a paper by H.de Bellescise and became popular later on.

In the 1940s, major use of PLL started in horizontal and vertical sweep of oscillators in the television receivers. In the early 1950s, a "good" phase-locked loop would adjust the television's color within a second. A "fair" phase-locked loop would adjust the color within 10 seconds. Currently, PLLs used in mobile handsets can lock to a channel in less than 1 millisecond of

time. The Bluetooth standard says that a system can hop up to 1600 hops/second. In this case, the PLL can stay on a channel for only 625 microseconds, which states that the PLL used has a lock time only a fraction of this.

10.1 PLL CHARACTERISTICS

The phase-locked loop is a feedback mechanism by which phase error between an input signal and locally generated signal is minimized. If the frequency (and in turn phase) of the input signal changes then the locally generated signal also follows it and in a way remains *locked* to incoming signal. The range over which this is possible gives operating range of the PLL. The basic block diagram of PLL is shown here in Fig. 10.1 and the detailed analysis comes in following sections. The filter following phase error device is essentially a low-pass filter which suppresses phase noise or frequency *jitter* of incoming signal and thus output frequency f_o is a cleaner or more stable version of input frequency f . The output frequency can be a multiple of input frequency when N is any other value than unity. The loop parameters also decide how fast or efficiently f_o adapts to variation in f . The transfer function as a whole can represent a n -th order system. We shall discuss first and second-order PLL in subsequent sections.

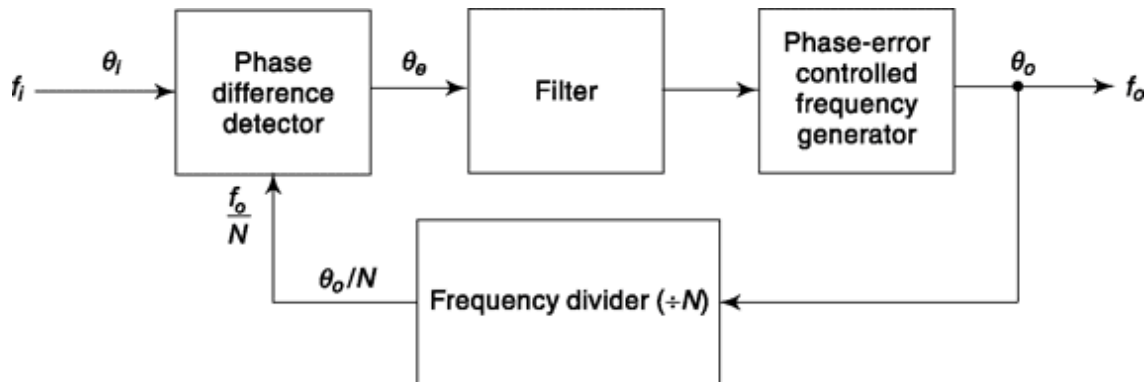


Fig. 10.1 Block-diagram representation of a PLL.

Based on how each of these blocks are realized the PLL often is categorized into (i) Analog PLL (APLL), (ii) Digital PLL (DPLL), (iii) All Digital PLL (ADPLL), and (iv) Software PLL (SPLL). In Analog PLL, all the components are analog in nature. The phase difference is found from a mixer or multiplier. The filter can be a passive or active analog filter while phase-error controlled frequency generator is a Voltage Controlled Oscillator

(VCO), introduced in Sec. 3.4.1. Here, the frequency divider usually operates at a value $N = 1$, i.e. no frequency division takes place making it a unity feedback system. We shall discuss APLL in details in the next section along with its application in Frequency Demodulation. In Digital PLL, except phase-detector block, everything else remains same as APLL. A digital logic device using Flip-Flops and/or Ex-OR gate is used to generate pulses which is in some way related to amount of phase error. These pulses are used to increase or decrease the frequency of a local signal generator. Limiter is used to make the input signal rectangular. This is not a limitation as it is the phase or frequency information of the signal which is of consideration here and not the amplitude. In ADPLL, as the name suggests all the components are digital in nature and this includes replacement of analog filter by a digital one. It deals with discrete signals at every block and the VCO is replaced by Digital Controlled Oscillator (DCO), also called Numerically Controlled Oscillator (NCO). The Software PLL has been made possible by the rapid development of Digital Signal Processing and it is realized using Digital Signal Processors. SPLL provides great design and analysis flexibility, e.g. changes in certain programmable parameters make the PLL behave in a completely different way. We shall discuss more about DPLL, ADPLL and SPLL in later part of this chapter.

In all these applications, the PLL tracks an input signal which is not necessarily the starting frequency of the VCO. Thus, the frequency of VCO is tuned to input frequency by *frequency pull-in* and then VCO phase is adjusted to input phase by *phase lock-in*. The *pull-in frequency range* is the maximum initial frequency difference allowed between input and VCO centre frequency. The *lock-in frequency range* is the frequency over which phase lock-in condition is maintained properly during entire lock-in process while *hold-in frequency range* is the frequency over which lock-in is maintained if input frequency is varied slowly.

10.2 ANALOG PLL AND FREQUENCY DEMODULATION

In this section, we describe the working of Analog PLL and simultaneously present Frequency Demodulation as a typical application of it. We shall see that PLL based FM demodulation is better than conventional method discussed in previous chapter as it extends the FM threshold considerably. We begin with the description of phase difference detector or a phase comparator.

A phase comparator is a device with two input ports and a single output port. If periodic signals of identical frequency but with a timing difference (i.e. a phase difference if the signals are sinusoidal) are applied to the inputs, the output is a voltage which depends on the timing difference. One way in which a phase comparator may be constructed is by the combination of a multiplier and a filter as shown in Fig. 10.2. Here we assume two sinusoidal input voltages of amplitudes A and B , frequency ω , and with time-varying phases $\theta_1(t)$ and $\theta_2(t)$. The student may easily verify (Prob. 10.1) that the output of the multiplier consists of the term

$$v_o = \frac{AB}{2} \sin [\theta_1(t) - \theta_2(t)] = \frac{AB}{2} \sin \psi(t) \quad (10.1)$$

plus other terms whose spectral components cluster around 2ω . Hence, if $d_1(t)$ and $d_2(t)$ have band-widths less than 2ω , a low-pass filter may separate and pass only the term $(AB/2) \sin \psi(t)$. In Fig.

10.2 WE HAVE ASSUMED AN AMPLIFIER WITH A GAIN $2G_p$ IN THE FILTER STAGE OF THE PHASE COMPARATOR SO THAT THE OUTPUT VOLTAGE IS $v_O = ABG_p \sin \psi(t)$. THE COMPARATOR OUTPUT IS PLOTTED IN FIG. 10.3A AS A FUNCTION OF Y.

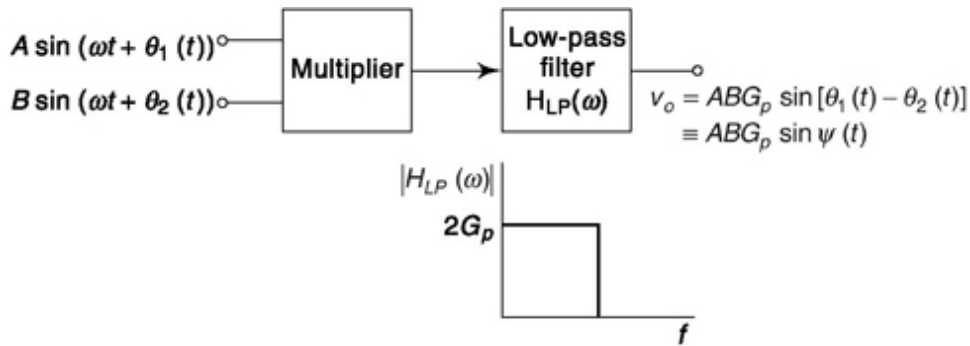


Fig. 10.2 A phase comparator consisting of a multiplier and a filter.

Suppose, however, that we convert the input sinusoids to square waves before application to the multiplier. Such conversion may be achieved by hard limiting and amplifying the input signals. The student may easily verify that if the square waves are clipped so that they have peak amplitudes A and B , the comparator output varies with y in the manner shown in Fig. 10.3b. The plot in Fig. 10.3b displays the same periodicity as does the plot in Fig.

10.3a except that the sinusoidal variation has been replaced by a piecewise-linear variation. Thus,

$$v_o = \begin{cases} ABG_p \frac{\psi}{\pi/2} & |\psi| \leq \frac{\pi}{2} \\ -ABG_p \frac{\psi - \pi}{\pi/2} & \frac{\pi}{2} \leq \psi \leq \frac{3\pi}{2} \\ \text{etc.} & \end{cases} \quad (10.2)$$

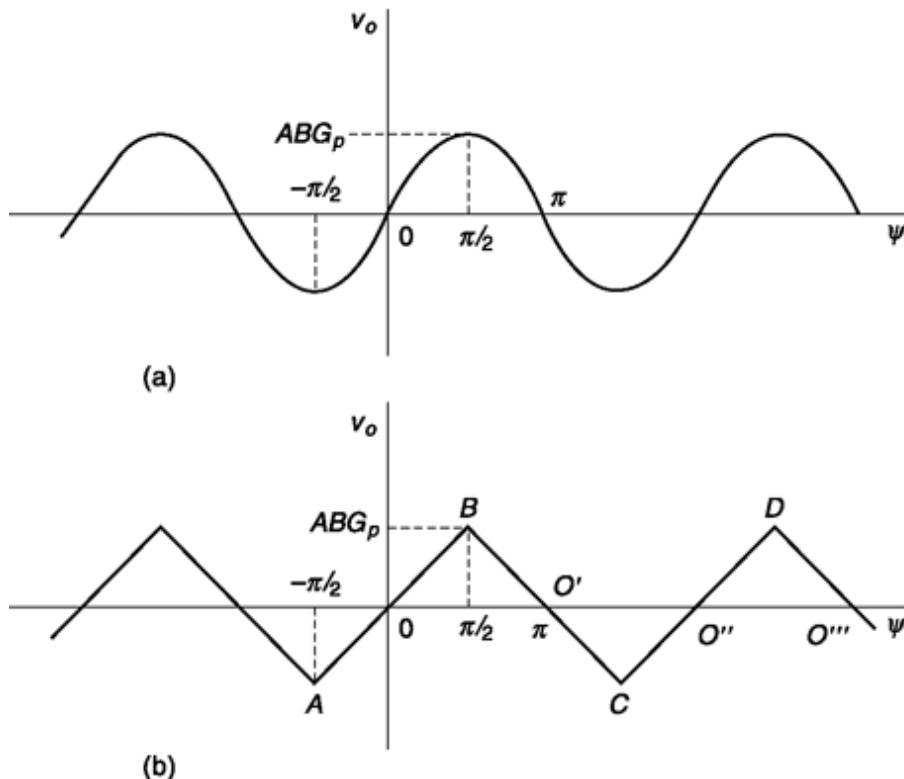


Fig. 10.3 (a) Phase characteristic of the comparator of Fig. 10.2 with sinusoidal inputs. (b) Phase characteristic with square-wave inputs.

A voltage controlled oscillator is a source of periodic signal whose frequency may be determined by the voltage applied to the VCO from external source. In Sec. 3.4.1 of Chap. 3 we have given description of VCO. We reproduce the governing equations here for convenience of PLL analysis. If voltage $v(t)$ is input to VCO and $v_{osc}(t)$ its output then

$$v_{osc}(t) = B \cos \left[\omega_c t + G_0 \int_{-\infty}^t v(\lambda) d\lambda \right] \quad (10.3)$$

where, B is the amplitude of the output of VCO and w_c the angular frequency in absence of any frequency-controlling voltage; G_0 is the frequency sensitivity in radian/volt, i.e. $G_0 = dw/dv$ such that instantaneous angular frequency

$$\omega_i(t) = \omega_c + G_0 v(t) \quad (10.4)$$

In Fig. 10.4, we connect the VCO with phase comparator in the feedback path. Before we analyze it quantitatively in next subsection, let us have a qualitative discussion of its operation and also the way FM demodulation is done. The frequency-modulated carrier $A \sin[\omega_c t + f(t)]$ is applied to one input of the phase comparator. The carrier frequency is ω_c , and if the modulating baseband signal is $m(t)$, then $f(t) = k \int_{-\infty}^t m(\lambda) d\lambda$, with k a constant. Now let us assume that initially $f(t) = 0$, and that we have adjusted the VCO so that when its input voltage $v_o = 0$, its frequency is precisely ω_c , the carrier frequency. Let us further adjust the VCO output signal to have a 900° phase shift relative to the carrier. This phase shift is required so that the comparator output shall be zero when $v_o(t) = 0$. Then the situation we have established is certainly a state of equilibrium. The two inputs to the comparator differ in phase by 900° ; the comparator output, which is the VCO input, is zero. Therefore, this initial setting of the VCO will not be disturbed.

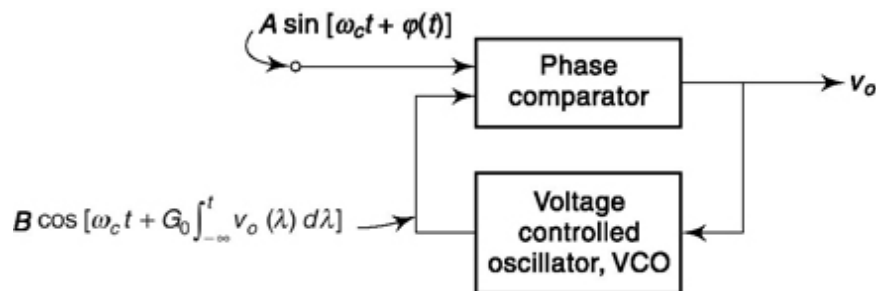


Fig. 10.4 A (first-order) phase-locked loop.

Now let the frequency of the input signal make an abrupt change w at time $t = 0$. Then, beginning at $t = 0$, $f(t) = wt$, since $df/dt = w$. That is, the abrupt frequency change causes the phase $f(t)$ to begin to increase linearly with time. The phase difference at the comparator input will generate a positive output v_o , which will in turn increase the frequency of the VCO. A new equilibrium point will eventually be established in the system, when the frequency of the VCO has been increased to equal the frequency of the input

signal. When equilibrium is established, the input signal and the VCO output will be of identical frequency but no longer different in phase by 900^t . For if the VCO is to operate at a frequency other than its initial frequency w_c , there must be an output v_o , and hence a departure from the 900^t phase difference at the input which yields $v_o = 0$.

The VCO output given in Fig. 10.4 is the same as Eq. (10.3) with v replaced by v_o . If the input and VCO frequencies are to be the same at equilibrium, we require that

$$\frac{d\phi(t)}{dt} = \frac{d}{dt} G_0 \int_{-\infty}^t v_o(\lambda) d\lambda \quad (10.5)$$

Letting $d\phi/dt = \omega$, we have

$$v_o(t) = \frac{\omega}{G_0} \quad (10.6)$$

Thus, the output voltage is proportional to the frequency change as required in an FM demodulator. We see then that if the input-carrier frequency changes continuously, and at a rate which is slow in comparison with the time required for the PLL to establish a new equilibrium operating point, the PLL output is continuously proportional to the *frequency variation* of the carrier.

We readily note that the PLL is a feedback control system in which the error signal is the phase difference between the modulated carrier and the VCO signal. Initially, with an unmodulated carrier, the operating point of the phase comparator may be adjusted to be at the origin in Fig. 10.3a or b. In the presence of modulation the operating point will move up and down along the portion of the plot between $-p/2$ and $p/2$.

10.2.1 ANALYSIS OF THE PHASE-LOCKED LOOP

We now present an elementary analysis of the PLL of Fig. 10.4. We assume for simplicity that the phase characteristic of the phase comparator is *piecewise-linear* as shown in Fig. 10.3b. The results will apply equally well to a PLL using a comparator with the characteristic shown in Fig. 10.3a. From Fig. 10.4 we have that the phase angle difference $y(t)$ is

$$\psi(t) \equiv \phi(t) - G_0 \int_{-\infty}^t v_o(\lambda) d\lambda \quad (10.7)$$

Differentiating Eq. (10.7) and transposing, we have

$$\frac{d\psi}{dt} + G_0 v_o = \frac{d\phi}{dt} \quad (10.8)$$

The output voltage can be eliminated using Eq. (10.2). The result is

$$\frac{d\psi}{dt} + \frac{\psi}{\tau} = \frac{d\phi}{dt} \quad \text{for } |\psi| \leq \frac{\pi}{2} \quad (10.9)$$

where

$$\tau = \frac{\pi}{2ABG_p G_0} \quad (10.10)$$

Since y and v_o are directly related by Eq. (10.2), Eq. (10.9) can also be written as

$$\frac{dv_o}{dt} + \frac{v_o}{\tau} = \frac{1}{G_0 \tau} \frac{d\phi}{dt} \quad \text{for } |\psi| \leq \frac{\pi}{2} \quad (10.11)$$

Equation (10.11) shows explicitly the relationship between the frequency offset dj/dt and the output voltage $v_o(t)$. Equation (10.9) or (10.11) is the differential equation of the PLL. Its solution, subject to the appropriate initial conditions, describes the PLL performance. Parenthetically, we note that with the phase comparator having the sinusoidal characteristic shown in Fig. 10.3a, the equation corresponding to Eq. (10.9) is

$$\frac{d\psi}{dt} + \frac{\sin \psi}{\tau'} = \frac{d\phi(t)}{dt} \quad (10.12)$$

with $t = 1/ABG_p G_0$. For small y , where $\sin y \sim y$, Eq. (10.12) would be identical with Eq. (10.9), except that the time constants would be different, this difference reflecting only the fact that in Fig. 10.3 the slopes at the origin are different in parts (a) and (b).

Suppose that the PLL is operating initially with $y = 0$, that is, the VCO and input-carrier frequency are identical and exactly 900° out of phase. Now let us again ask the question raised before; that is, what happens if the angular frequency of the carrier is abruptly changed by an amount w ($dj/dt = w$)? Subject to these initial conditions, the solution of Eq. (10.9) is

$$\psi = \omega \tau (1 - e^{-t/\tau}) \quad |\psi| \leq \frac{\pi}{2} \quad (10.13)$$

or correspondingly, using Eqs (10.2) and (10.10), the steady-state output voltage v_o is given by

$$v_o = \frac{\omega}{G_0} \quad (10.15)$$

Operating Range

We note that as long as the phase comparator operates in the range AOB in Fig. 10.3b, that is, $|y| < p/2$, the steady-state operating point is given by $y_e = wt$. The range R of the PLL is the angular frequency change w of the input carrier which will just carry the steady-state operating point from O to B or from O to A . This range R is given by

$$R = \omega_{\max} = \frac{\psi_{\max}}{\tau} = \frac{\pi/2}{\tau} = \frac{\pi}{2\tau} \quad (10.16)$$

For the phase comparator of Fig. 10.3a we find R by using Eq. (10.12). Set $df(t)/dt = w$ and $dy/dt = 0$ (steady-state). Then, when $\psi = \pi/2$, $\sin \psi = 1$. Thus, $R = \omega_{\max} = \frac{1}{\tau}$. We observe that the behavior of the PLL is determined entirely by the single parameter t (or t). This parameter depends on the gains G_0 and G_p and also on the amplitudes A and B of the input and VCO signals.

As t becomes progressively smaller, the range of the PLL becomes progressively larger, and the speed with which the PLL responds to a frequency change w increases. The reason the range becomes larger is, as a matter of fact, precisely because the loop does respond faster. A *fast-acting* loop will not permit the phase $f(t)$ to depart appreciably from the phase of the VCO. In the limit, when $t \rightarrow 0$, y will remain close to $y = 0$ and hence close to the origin O in Fig. 10.3b, no matter how large w should become.

Bandwidth

Since the PLL response is given by a linear differential equation, it has the characteristics of a filter. To see that such is the case, let $\Psi(s) \equiv \mathcal{L}[\psi(t)]$ and $\Omega(s) \equiv \mathcal{L}(d\phi/dt) \equiv \mathcal{L}[\omega(t)]$. Then from Eq. (10.9), we have

$$\Psi(s) = \frac{\Omega(s)}{s + 1/\tau} \quad (10.17)$$

The transfer function has a single pole at $s = -1/t$, and the PLL is therefore referred to as a *first-order* PLL.

$$H(s) = \frac{\Psi(s)}{\Omega(s)} = \frac{1}{s + 1/\tau} \quad (10.18)$$

Suppose that the angular frequency variation of the input signal were sinusoidal: $w(t) = Dw_m \cos w_m t$, with Dw_m the amplitude, and w_m the angular frequency of the sinusoidal variation of the instantaneous frequency. Then for a fixed frequency deviation Dw_m , an increase in the modulating frequency w_m results in a decrease in $y(t)$ and hence $v_o(t)$. The angular frequency $(\omega_m)_{3 \text{ dB}}$ at which the response will have fallen by 3 dB is seen from Eq. (10.18) to be

$$(\omega_m)_{3 \text{ dB}} = \frac{1}{\tau} \quad (10.19)$$

A PLL will consequently introduce distortion between the original modulating signal and the signal recovered at the PLL output. The distortion will be the same as would be introduced if the modulating signal had been passed through a low-pass resistance-capacitance network of time constant t . The distortion may be decreased by making the PLL 3 dB cutoff frequency much higher than the highest-frequency spectral component of the modulating signal.

A point worthy of note is to be seen in Eqs (10.16) and (10.19). We observe that a single time constant t determines both the range of the PLL and its frequency response. We are therefore not at liberty, in this first-order loop, to vary these parameters independently. We shall see in Sec. 10.2.4 how this limitation can be remedied.

As long as the operating point of the comparator remains in the range AOB in Fig. 10.3b, the PLL demodulator accomplishes no function which is not performed at least equally well by a conventional discriminator. The PLL displays its special merit, however, precisely when it is operated in such a manner that its operating point ranges outside the limits A and B in Fig. 10.3b. In the next section we discuss such operation.

10.2.2 Stable and Unstable Operating Points

We have seen that in the range AOB in Fig. 10.3b, the differential equation for the PLL is

$$\frac{d\psi}{dt} + \frac{\psi}{\tau} = \frac{d\phi}{dt} \quad (10.20)$$

This equation applies equally well for operation over any positive-slope region in Fig. 10.3b, provided that y measures the departure of the phase from the phase at which the phase characteristic crosses the axis $v_o = 0$. Thus, for example, the equation applies to the region $CO'D$ if y is measured from O'' . Similarly, by retracing the derivation, we find that in a negative-slope region, as, say, $BO'C$, if y is measured from O' , the equation is (see Prob. 10.5)

$$\frac{d\psi}{dt} - \frac{\psi}{\tau} = \frac{d\phi}{dt} \quad (10.21)$$

In Fig. 10.5a we have drawn a portion of the phase-comparator characteristic in which the slope is positive. Let us assume that the input-carrier angular frequency has been offset by an amount w . Then, as given in Eq. (10.15), the new *steady-state* equilibrium is, as shown, at $v_o = w/G_0$, and the corresponding equilibrium value of y is $y_e = wt$ as in Eq. (10.14). Suppose, however, that because of the past history of the PLL, the operating point happens to find itself initially at point X where the phase angle is ψ . We have then from Eq. (10.20) that

$$\frac{d\psi}{dt} = \frac{d\phi}{dt} - \frac{\psi}{\tau} \quad (10.22a)$$

$$= \omega - \frac{\psi}{\tau} \quad (10.22b)$$

$$= \frac{\psi_e}{\tau} - \frac{\psi}{\tau} = \frac{1}{\tau} (\psi_e - \psi) \quad (10.22c)$$

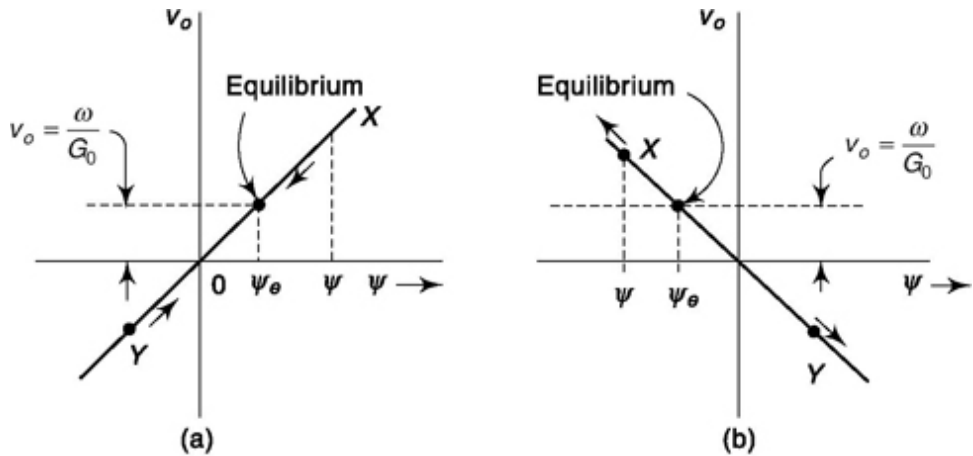


Fig. 10.5 (a) Illustrating that an equilibrium point is stable if the operating point of a PLL is on a positive-slope portion of the phase comparator, (b) Illustrating the instability that results when the operating point is on a negative-slope portion of the comparator.

Now if, as in the case of point X , $y > y_e$, then dy/dt is negative. Hence, the instantaneous operating point X moves to the left along the comparator-phase characteristic. The point X will, as we have already seen, approach the equilibrium point asymptotically, with time constant t . Similarly, if the operating point is at Y , then $y < y_e$, and dy/dt is positive so that again Y approaches the equilibrium point. The equilibrium point is a *stable* point.

Let us now consider the negative-slope portion of the phase characteristic such as $BO'C$ in Fig. 10.3b. Here we use Eq. (10.21) instead of Eq. (10.20). Repeating the above discussion using Fig. 10.5b, we find that initial operating points such as X and Y result in y moving *away* from, not *toward*, the equilibrium point y_e . Thus, in Fig. 10.5b, the equilibrium point is *unstable*. In the next section we apply these simple notions to explain how the PLL acts to suppress spikes.

10.2.3 spike suppression

Let us assume that the input to a PLL is an unmodulated carrier, offset from w_c by an amount w . Let the steady-state output voltage of the PLL corresponding to this offset be $v_o = V_o = \omega/G_0$ as indicated by the dashed horizontal line in Fig. 10.6. That is, the offset w is so large that the horizontal line ZZ' does not intersect the phase characteristic. There are no *actual* equilibrium points. However, two extended equilibrium points have been indicated at points P_2 and P_3 . The point P_2 is the intersection of AOB with ZZ' . An initial operating point P_1 on AOB will move as though headed for

equilibrium at P_2 for, until point B is reached, the PLL does not know that AOB does not continue to P_2 . Similarly, the *equilibrium* point for operation along $BO'C$ is at P_3 .

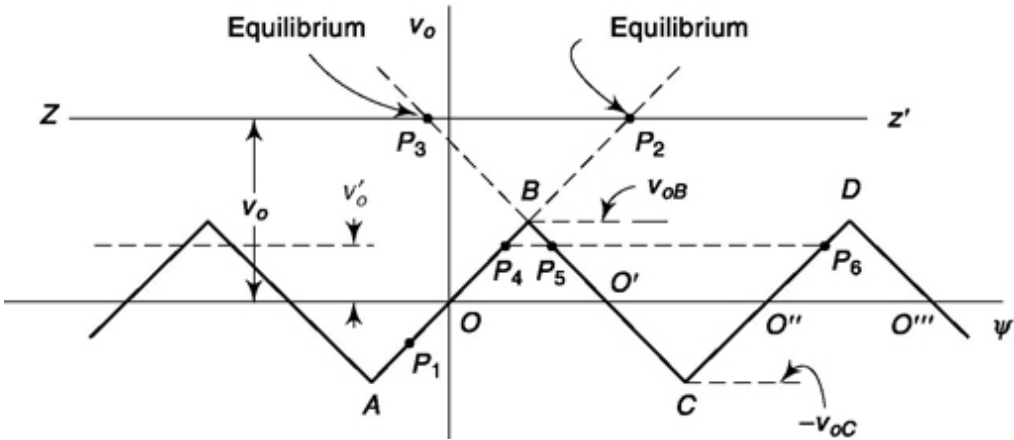


Fig. 10.6 Illustrating the PLL response for various assumed fixed-frequency offsets of the carrier signal.

If the PLL is initially at the origin with $y = 0$, and at time $t = 0$ a phase offset w is added to w_c , the operating point will move from O to B . The operating point cannot remain at B , since B is not an equilibrium point. However, the point B is also on the negative-slope segment $BO'C$. Hence, it will recede from the equilibrium point P_3 and proceed toward C . Continuing in the same way, we see that from C the operating point will go to D , i.e. toward the equilibrium point, and so on. If the output voltage corresponding to the point B is $v_o = v_oB$, then the output voltage will oscillate with excursion from $+v_{oB}$ to $-v_{oB}$. The waveform of this oscillation is easily calculated. Note that y constantly increases and does not oscillate.

Suppose that the offset were such to establish equilibrium at the level V_o as indicated in Fig. 10.6; then if the operating point is initially on AOB , it will settle at P_4 . If the operating point is initially on $BO'C$, it will eventually settle at P_4 or P_6 , depending on whether the initial point is above or below P_5 . If the operating point is initially constrained to be precisely at P_5 , it will remain there only as long as no disturbance displaces it, even ever so slightly. If a disturbance does move the operating point from P_5 , the operating point will end up again at P_4 or P_6 depending on the direction of the disturbance.

After these preliminaries we may turn our attention to the matter of spikes. For this purpose we shall inquire into the response of the PLL to an “artificial” spike. Thus, we consider that the input carrier is at the carrier angular frequency ω_c except for a short time T during which the angular frequency is offset by an amount w . Such artificial spikes are shown by the solid-line plot in Fig. 10.7 in which the offset angular frequency w is plotted as a function of time. In a physical situation the duration T of the spike will be determined by the bandwidth of the IF carrier filter. The spike amplitude w_s will then be determined by the condition that the area under the spike be $2p$, that is, $\omega_s T = 2\pi$.

We have seen [Eq. (10.16)] that the angular frequency corresponding to a steady-state operating point at B in Fig. 10.6 is $\omega_{max} = p/2t$. The dashed waveforms in Fig. 10.7 indicate the PLL responses for three relative values of ω_{max} and ω_s .

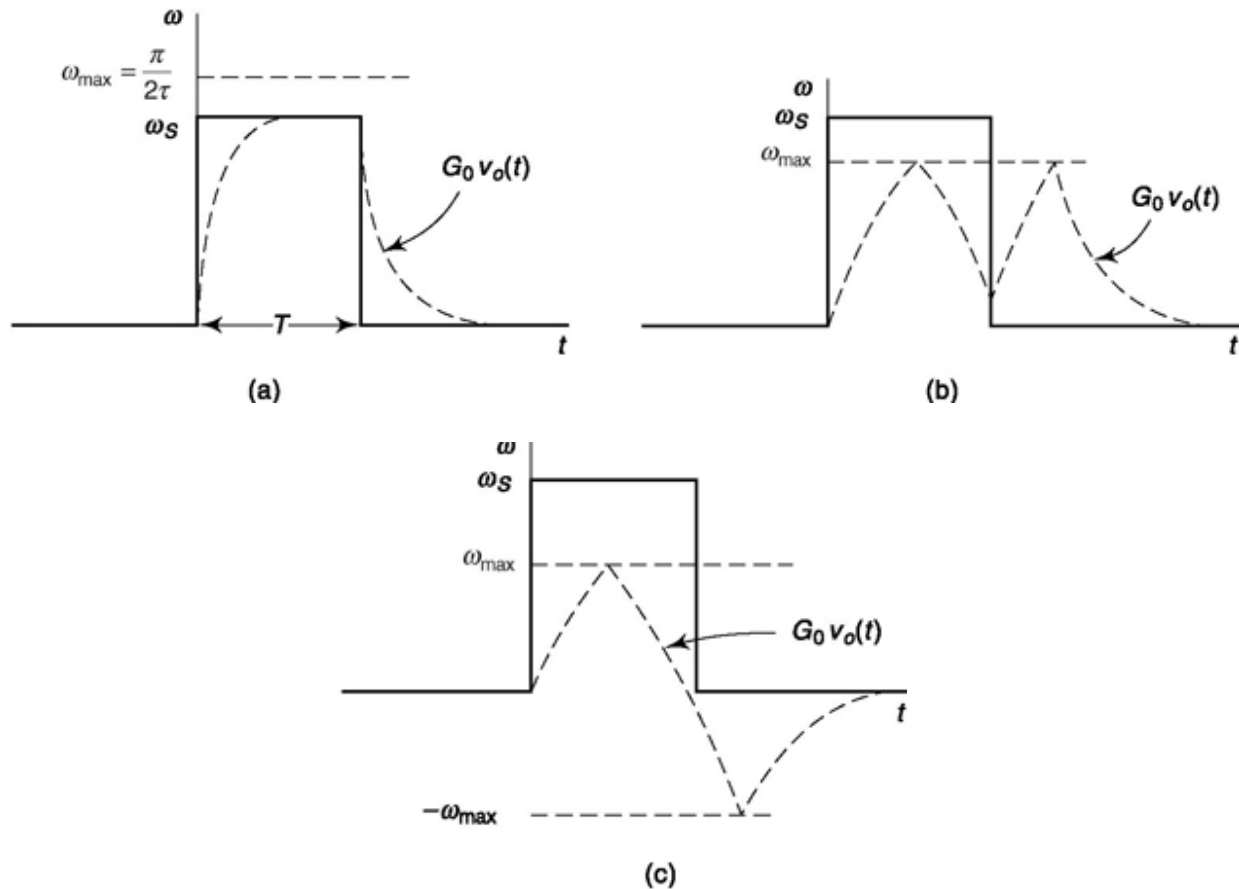


Fig. 10.7 Various possible responses of a PLL to an “artificial” spike. The different cases correspond to different selections of the time constant of the PLL.

Case 1

The steady-state output voltage v_o corresponding to w is $v_o = w/G_0$ [see Eq. (10.15)]. In Fig. 10.7a we assume $w_{\max} > w_S$. The output voltage of the PLL responds to the spike by rising asymptotically with time constant t to the steady-state level $v_o = w_S/G_0$. At this level, the operating point of the PLL has not reached the point B in Fig. 10.6 since we assume that $\omega_{\max} > \omega_S$. At the termination of the spike, the PLL returns to its initial level. The output-voltage waveform v_o has the form of the dashed plot. This output waveform is a replica of the input-spike waveform except rounded because of the time constant of the PLL. In this case, a spike input produces a spike output.

Case 2

Here in Fig. 10.7b, $w_{\max} < w_S$. Hence, the operating point reaches the limit of its range (point B in Fig. 10.6) before it has been able to respond fully to the spike amplitude. After reaching point B , the operating point starts down along $BO'C$. However, the spike ends before the point O' is reached.

When the spike has terminated, w is again equal to zero, and O' is an *unstable* equilibrium point. Thus, the operating point retraces its path back over B and into the positive-slope region, finally returning to the starting point at O . An input spike now yields two spikes at the output.

Note that the change from Case 1 to Case 2 is made by increasing t , thereby lowering w_{\max} and also slowing the response of the PLL.

Case 3

Here in Fig. 10.7c, w_{\max} has been reduced still further and has been set at such a level that the operating point reaches the limit of the range in a time slightly less than one-half the spike duration. Therefore when the spike terminates, the operating point has passed O and hence continues to C and finally settles at O . In this case, a spike input has yielded an output which consists of a positive spike followed by a negative spike. Such an output waveform as indicated by the dashed plot in Fig. 10.7c is called a *doublet*. We may reasonably expect that the total area under a doublet will be near zero. Therefore, the doublet will yield very little energy in the baseband in comparison to the energy yielded by the spike itself. Here, then, qualitatively

is the mechanism by which the PLL suppresses the noise of spikes. The PLL changes spikes into doublets of relatively small energy.

If all the spikes encountered in a physical situation were of precisely the same waveform, then, as the preceding discussion indicates, it would be possible to adjust the time constant t of the PLL so that each spike might be replaced by a doublet. Observe that only a small range of t is suitable. The time constant t must be large enough to avoid the responses indicated in Fig. 10.7a and b. On the other hand, increasing t results in decreasing the PLL bandwidth [Eq. (10.19)]. If the PLL is being used to demodulate a carrier frequency modulated by a baseband signal of bandwidth f_M , then we require that $(1/\tau) \gg f_M$.

Unfortunately, all spikes are not identical. Even in the absence of modulation there will be some variation in spike waveform, and with modulation the spikes will vary considerably during the course of the modulation cycle. Still, as a matter of practice it turns out to be possible to adjust a PLL to convert many of the spikes into doublets and thereby effect a net improvement in performance.

10.2.4 second-Order phase-Locked Loop

We now discuss the second-order PLL, and we shall explain, qualitatively, how the second-order loop manages to suppress spikes more effectively than does the first-order loop.

In Fig. 10.8, the PLL has been modified by the inclusion of a filter. This filter is not to be compared with the filter described in Sec. 10.2 as having been incorporated in the phase comparator. The phase-comparator filter was used to suppress the carrier frequency and its harmonics and hence performs no filtering in the passband of the PLL. Hence, while the phase-comparator filter has absolutely no influence on the PLL performance, the filter introduced in Fig. 10.8 is deliberately introduced to have such influence.

It will be more convenient, in our present discussion, to refer not to the angle-modulated carrier waveforms encountered in the PLL but rather directly to the phases of these waveforms. Thus, in Fig. 10.8, the signal input is $f(t)$ with Laplace transform $F(s)$. The output voltage of the phase comparator is $G_p Y/(s)$, where $y(t)$ is the phase-angle difference at the phase-comparator input, and G_p is a constant of proportionality. The VCO provides

a carrier having a phase proportional to the *integral* of its input voltage $v_o(t)$. Hence the VCO has been characterized as having a transform G_0/s .

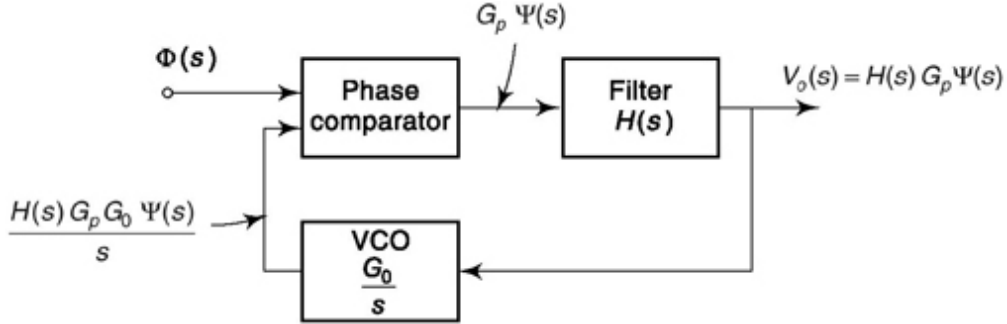


Fig. 10.8 A phase-locked loop which includes a filter.

With $H(s) = 1$, the PLL of Fig. 10.8 is identical with the loop of Fig. 10.4. We have, in this case

$$\Psi(s) \equiv \Phi(s) - \frac{G_p G_0 \Psi(s)}{s} \quad (10.23)$$

Using $s\Phi(s) = \mathcal{L}[d\phi(t)/dt] \equiv \Omega(s)$ and $1/\tau = G_0 G_p$ we find from Eq. (10.23) that

$$\Psi(s) = \frac{s\Phi(s)}{s + G_p G_0} = \frac{\Omega(s)}{s + G_0 G_p} = \frac{\Omega(s)}{s + 1/\tau} \quad |\psi(t)| \leq \frac{\pi}{2} \quad (10.24)$$

exactly as in Eq. (10.17).

Now let us assume a *proportional-plus-integral* filter with $H(s)$ given by

$$H(s) = 1 + \frac{K}{s} \quad (10.25)$$

where K is a constant. We now find that the phase-angle difference $y(t)$ has a transform

$$\Psi(s) = \frac{s^2 \Phi(s)}{s^2 + s/\tau + K/\tau} = \frac{s\Omega(s)}{s^2 + s/\tau + K/\tau} \quad |\psi(t)| \leq \frac{\pi}{2} \quad (10.26)$$

while the output voltage $v_o(t)$ has a transform

$$V_o(s) = G_p H(s) \Psi(s) = \frac{s(s+K)G_p \Phi(s)}{s^2 + s/\tau + K/\tau} = \frac{(s+K)G_p \Phi(s)}{s^2 + s/\tau + K/\tau} \quad (10.27)$$

We observe that the expressions for $\Psi(s)$ and $V_o(s)$ have denominators which, being quadratic in s , give rise to two poles. Hence, the term *second-order*

PLL.

We inquire now, as we did for the first-order loop, about the steady-state response of the second-order loop to an abrupt change of magnitude w in the angular frequency of the input carrier. To make this calculation, we use the *final-value theorem* which states that if $F(s) = L[f(t)]$, then

$$\lim_{s \rightarrow 0} [sF(s)] = \lim_{t \rightarrow \infty} f(t) \quad (10.28)$$

Applying this theorem to $Y(s)$ and $V_o(s)$ in Eqs (10.26) and (10.27) with $W(s) = w/s$, we find

$$\psi(\infty) = 0 \quad (10.29)$$

and

$$v_o(\infty) = G_p \omega \tau \quad (10.30)$$

Thus, we observe from Eq. (10.30) that the steady-state response at the output of the second-order loop is the same as in the first-order loop. However, we see from Eq. (10.29) that the phase difference $y(t)$, unlike the situation obtained in the first-order loop, does not respond with a steady-state displacement from its initial position of equilibrium. Instead, while it may make a transient excursion, it thereafter settles right back to its starting point. Another way of emphasizing this same point is to recognize that the transfer function that relates $Y(s)$ to the input signal $W(s)$ is Eq. (10.26) is the transfer function of a bandpass filter, while the transfer function that relates $V_o(s)$ to $W(s)$ in Eq. (10.27) is the transfer function of a low-pass filter. Therefore, by appropriately selecting the cutoff frequencies of these filters, it is possible to arrange that the output of the PLL respond properly to the modulating signal, while the operating point of the phase comparator responds hardly at all and always hovers close to its initial point of equilibrium.

The relevance of these considerations to spike suppression may now be seen. Consider the first-order loop and let the input be a step in frequency which carries the phase-comparator operating point towards A in Fig. 10.6 and holds it there at point P_1 . If, now, a spike develops because of noise, this spike will be in the direction to drive the operating point in the opposite direction toward B . The spike will not be suppressed unless the operating point does indeed get to point B and beyond toward C , as explained in Sec. 10.23. However, the initial displacement of the operating point away from O towards A due to the input signal makes such spike suppression less likely than if the initial operating point were at point O . On the other hand, in the

second-order loop, after some initial response to the input-frequency step, the phase comparator settles back at point O . Thus if an input spike occurs, that is, $f(t)$ changes by 2π rad, the distance moved to point B and hence the time required to reach point B is less than in the first-order loop. As consequence such a spike has a greater likelihood of suppression.

Third-Order Phase-Locked Loop

Before we go to the next topic, let us briefly look at where third-order PLL could be useful though a discussion on its derivations is beyond the scope of this book. We have seen that second order PLL has zero steady-state error for step change in frequency. But what happens if input frequency changes like a ramp such that $\omega(t) = at$, then $\Omega(s) = a/s^{2\eta}$? Proceeding as before, we can see that

there will be a steady-state error in phase, however small it might be. What if the input frequency is accelerating in nature? We can find that the error will be growing and steady-state error will be infinity. Third-order phase-locked loops provide the desirable characteristic to track an accelerating frequency input with some steady-state error and none for ramp frequency input. In communications, this is an important issue when the receiver or transmitter is in motion. Consider a satellite antenna on the mast of a ship. As the ship moves with waves, the mast moves and resulting displacement is sufficient to generate a considerable frequency ramp. Similarly, Global Positioning Systems (GPS) have significant Doppler shift induced by the satellites moving with respect to the receiver. In all these applications third order PLL is useful.

Example 10.1

(a) Show the transient response of phase error $y(t)$ for step change in frequency at the input of the VCO in Fig. 10.8. (b) Express it in terms of natural frequency and damping factor and show the response for underdamped, overdamped and critical damped case.

Solution

Step change in frequency makes $\Omega(s) = 1/s$

Substituting in Eq. 10.26, $\psi(s) = \frac{1}{s^2 + s/\tau + K/\tau}$

The above equation has two characteristic roots at

$$s = -\frac{1}{2\tau} \pm \frac{1}{2\tau} \sqrt{1-4K\tau} \quad (10.31a)$$

Consider, $4K\tau \neq 1$

Using partial fraction expansion we can write,

$$\begin{aligned} \psi(s) &= \frac{1}{\left(\frac{1}{\tau}\sqrt{1-4K\tau}\right)} \left[\frac{1}{s + \frac{1}{2\tau} - \frac{1}{2\tau}\sqrt{1-4K\tau}} \right. \\ &\quad \left. - \frac{1}{s + \frac{1}{2\tau} + \frac{1}{2\tau}\sqrt{1-4K\tau}} \right] \\ \psi(t) &= \frac{\tau}{\sqrt{1-4K\tau}} \left[e^{-\left(\frac{1}{2\tau}-\frac{1}{2\tau}\sqrt{1-4K\tau}\right)t} \right. \\ &\quad \left. - e^{-\left(\frac{1}{2\tau}+\frac{1}{2\tau}\sqrt{1-4K\tau}\right)t} \right] \end{aligned}$$

$$\text{or} \quad \psi(t) = \frac{\tau}{\sqrt{1-4K\tau}} e^{-\frac{t}{2\tau}} \left[e^{\frac{1}{2\tau}(\sqrt{1-4K\tau})t} \right. \\ \left. - e^{-\frac{1}{2\tau}(\sqrt{1-4K\tau})t} \right] \quad (10.31b)$$

$$\text{If } 4K\tau > 1, \text{ then } \psi(t) = \frac{2\tau}{\sqrt{4K\tau-1}} e^{-\frac{t}{2\tau}} \\ \sin \frac{1}{2\tau}(\sqrt{4K\tau-1})t \quad (10.32)$$

$$\text{If } 4K\tau < 1, \text{ then } \psi(t) = \frac{2\tau}{\sqrt{1-4K\tau}} e^{-\frac{t}{2\tau}} \\ \sinh \frac{1}{2\tau}(\sqrt{1-4K\tau})t \quad (10.33)$$

If $4K\tau = 1$, then both roots are at $s = -\frac{1}{2\tau}$,

$$\text{i.e. } \psi(s) = \frac{1}{\left(s + \frac{1}{2\tau}\right)^2}$$

By inverse Laplace transform, $\psi(t) = te^{-\frac{t}{2\tau}}$ (10.34)

(b) When expressed in terms of natural frequency and damping factor the denominator in the transfer function is expressed as $s^2 + 2\xi\omega_n s + \omega_n^2$

Comparing, natural frequency, $\omega_n = \sqrt{\frac{K}{\tau}}$ and

$$\text{damping ratio } \xi = \frac{1}{2\sqrt{\tau K}} \quad (10.35)$$

$$\text{Then, } 4K\tau = \frac{1}{\xi^2} \quad \text{and} \quad \frac{1}{2\tau} = \omega_n \xi$$

For underdamping $\xi < 1$ (i.e. $4K\tau > 1$),

$$\psi(t) = \frac{1}{\omega_n \sqrt{1-\xi^2}} e^{-\omega_n \xi t} \sin(\omega_n \sqrt{1-\xi^2}) t \quad (10.36)$$

For overdamping $\xi < 1$ (i.e. $4K\tau < 1$),

$$\psi(t) = \frac{1}{\omega_n \sqrt{\xi^2 - 1}} e^{-\omega_n \xi t} \sinh(\omega_n \sqrt{\xi^2 - 1}) t \quad (10.37)$$

$$\text{damping ratio } \xi = \frac{1}{2\sqrt{\tau K}} \quad (10.35)$$

For critical damping, $\xi = 1$ (i.e. $4K\tau = 1$),

$$\psi(t) = te^{-\omega_n \xi t} \quad (10.38)$$

Note that, damping factor gives measure of stability and natural frequency the bandwidth, both of which can be set independently in second-order PLL. Usually, $\omega_n / 2p <$ one-twentieth of reference frequency and $0.45 < \xi < 1.5$.

Define error in frequency $\theta(t) = \omega(t) - \hat{\omega}(t) = d\phi(t)/dt - d\hat{\phi}(t)/dt$

Therefore, $\theta(s) = s[\Phi(s) - \hat{\Phi}(s)] = s\Psi(s)$

Solution

$$\text{From Eq. 10.26, } \frac{\theta(s)}{\Omega(s)} = \frac{s^2}{s^2 + s/\tau + K/\tau} \quad (10.39)$$

Example 10.2

(a) Find steady-state error in the frequency of PLL for a Aw step change in the input frequency. (b) Find expression for transient response if there is a unit step change in frequency where second order PLL is as defined in Fig. 10.8 and loop has damping factor < 1 and natural frequency ω_n .

solution

Define error in frequency $\theta(t) = \omega(t) - \hat{\omega}(t) = d\phi(t)/dt - d\hat{\phi}(t)/dt$

Therefore, $\theta(s) = s[\Phi(s) - \hat{\Phi}(s)] = s\Psi(s)$

$$\text{From Eq. 10.26, } \frac{\theta(s)}{\Omega(s)} = \frac{s^2}{s^2 + s/\tau + K/\tau} \quad (10.39)$$

Steady-state frequency error for frequency change of
say ω , $\Omega(s) = \frac{\omega}{s}$

$$\lim_{t \rightarrow \infty} \theta(t) = \theta(t) = \lim_{s \rightarrow 0} [s\theta(s)] = \lim_{s \rightarrow 0} \frac{s \cdot s^2 \cdot \omega/s}{s^2 + s/\tau + K/\tau} = 0$$

Steady-state frequency error for frequency change of
say ω , $\Omega(s) = \frac{\omega}{s}$

Transient response for unit change in frequency and underdamped case can be found by differentiating phase response in Example 10.1.

$$\theta(t) = d[\psi(t)]/dt = d \left[\frac{1}{\omega_n \sqrt{1-\xi^2}} \right]$$

$$e^{-\omega_n \xi t} \sin(\omega_n \sqrt{1-\xi^2} t) / dt$$

$$\text{or } \theta(t) = \frac{1}{\omega_n \sqrt{1-\xi^2}} e^{-\omega_n \xi t} [\omega_n \sqrt{1-\xi^2} \cos(\omega_n \sqrt{1-\xi^2} t) - (\omega_n \xi) \sin(\omega_n \sqrt{1-\xi^2} t)]$$

For step Dw change in input frequency the transient response of frequency error

$$\theta(t) = \frac{\Delta\omega}{\omega_n \sqrt{1-\xi^2}} e^{-\omega_n \xi t} [\omega_n \sqrt{1-\xi^2} \cos(\omega_n \sqrt{1-\xi^2} t) - (\omega_n \xi) \sin(\omega_n \sqrt{1-\xi^2} t)] \quad (10.40)$$

10.2.5 Output sNR for FM Demodulation by pLL

The input signal to an FM demodulator is

$$v_i(t) = R(t) \cos [\omega_c t + \phi(t)] \quad (10.41)$$

Here, $R(t)$ is the envelope of the waveform which results from the superposition of the carrier of amplitude A and the noise $n(t)$. Similarly, $\phi(t) = \phi_s(t) + \phi_n(t)$, where $\phi_s(t)$ is the angular modulation due to the signal, and $f_n(t)$ due to the noise. Let us ignore, for the present, the effect of the noise on the envelope and assume that $R(t) = A$.

With this assumption, an FM discriminator, when presented with the waveform of Eq. (10.41), will yield an output voltage

$$v_o(t) = \alpha \frac{d\phi(t)}{dt} \quad (10.42)$$

where a is a constant. The student may verify from Eq. (10.11) that the output voltage of a first-order PLL is related to $d\phi(t)/dt$ as indicated in Fig. 10.9 (see Prob. 10.13). The time constant of the RC circuit is equal to the time constant t of the PLL. If we neglect the effect of this low-pass RC circuit, then

$$v_o(t) = \frac{1}{G_0} \frac{d\phi(t)}{dt} \quad (10.43)$$

just as for the discriminator except with a replaced by $1/G_0$. Now both the discriminator and the PLL will be followed by a low-pass baseband filter of cutoff frequency f_M . If, as is always the case, we select the 3 dB frequency of the RC circuit, which represents the phase-locked loop, to be much larger than f_M , then as far as the baseband filter output is concerned, the RC circuit is, indeed of no consequence. Above threshold, where spikes are extremely rare, the discriminator and the PLL, when combined with the baseband filter, process the input waveform, signal plus noise, in exactly the same way. The

output SNR does not depend on the constant a nor on the constant $1/G_0$. Therefore, above threshold, both discriminator and PLL yield the same output SNR.

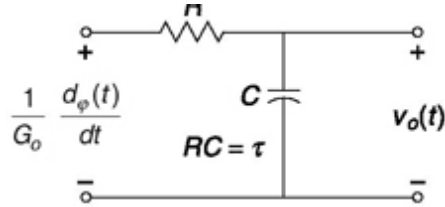


Fig. 10.9 A representation of the relationship between the output voltage v_O of a first-order PLL and the frequency modulation df/dt of an input carrier.

Effect of Limiting

Now let us take account of the fact that the envelope of $v(t)$ in Eq. (10.41) actually varies because of noise. A discriminator is always accompanied in practice by a limiter. Hence the result stated in Eq. (10.42) continues to apply, since the limiter removes all amplitude variation. In the case of the PLL we note from Fig. 10.9 that the carrier amplitude enters only through the time constant t , for as is to be seen in Eq. (10.10) t depends on A . Still, if the 3-dB frequency of the RC filter in Fig. 10.9 is very much larger than the baseband filter cutoff frequency, the small variations in t resulting from the noise can have little effect. At least such will be the case above threshold where the noise power is very small in comparison with the carrier power. Hence, we have the result that above threshold the PLL does not require a limiter, and the result of Eq. (10.43) is valid.

Above threshold, it is immaterial whether we use a limiter. We shall now show qualitatively that below threshold it is advantageous *not* to use a limiter. As explained in Sec. 10.2.3 in connection with Fig. 10.7, it is necessary to restrict the range w_{max} ($= n/2t$) of the PLL in order to achieve spike suppression. Such restriction of the range has the disadvantage that it also restricts the ability of the PLL to follow the frequency deviations of the carrier due to signal modulation. It would therefore be of advantage if we could keep the range large in the absence of a spike and yet be able to restrict the range during the course of the formation of a spike. We may now see that if the PLL is operated without a limiter, the PLL will automatically restrict its own range during a spike.

Referring to Fig. 9.16b, we see that when the noise $r(t)$ is comparable to A , that is, when a spike occurs, then as the resultant $R(t)$ executes a rotation by $2p$, its average magnitude will be smaller than A . [It is of course possible to conceive that $r(t)$ is so large that $R(t)$ is larger than A , but such a situation would have a small probability of occurrence and is therefore of no interest in the present discussion.] Furthermore, since the range $w_{\max} = p/2t$ and t is inversely proportional to the carrier envelope [see Eq. (10.10)], the range of the PLL automatically reduces during a spike. This advantageous operating characteristic of the PLL would be lost if the envelope amplitude were kept constant by the use of a limiter.

Output SNR

We have seen that the number of spikes present at the PLL output is fewer than at the output of the FM discriminator, and threshold *extension* results. The output-noise power due to spikes present at the PLL output is N_S and is found by replacing $1/T_s$ by $N = N_c + SN$, the average number of spikes per second occurring at the PLL output, in Eq. (9.68). The result is

$$N_S = \frac{8\pi^2 f_M N}{G_0^2} \quad (10.44)$$

Note that a is replaced by $1/G_0$ in this equation. Since the PLL suppresses spikes, N is smaller than for the discriminator. Thus, N_S is smaller in the PLL.

From Eqs (9.11) and (9.22) with a replaced by $1/G_0$, and using Eq. (10.44), we have

$$\frac{S_o}{N_o} = \frac{\overline{k^2 m^2(t)}}{(8\pi^2/3) \eta f_M^3 / A^2 + 8\pi^2 f_M N} \quad (10.45)$$

If we simplify and assume sinusoidal modulation, becomes

$$\frac{S_o}{N_o} = \frac{\frac{3}{2} \beta^2 S_i / N_M}{1 + 6(N/f_M)(S_i/N_M)} \quad (10.46)$$

While an analytic expression for N of a PLL has not been determined, computer simulation of the PLL has resulted in the determination of N and of threshold.⁵ The results obtained are shown in Fig. 10.10. We see from this

figure that with $b = 12$, the PLL extends threshold by 3 dB, while with $bi = 3$, threshold extension of 2.5 dB results.

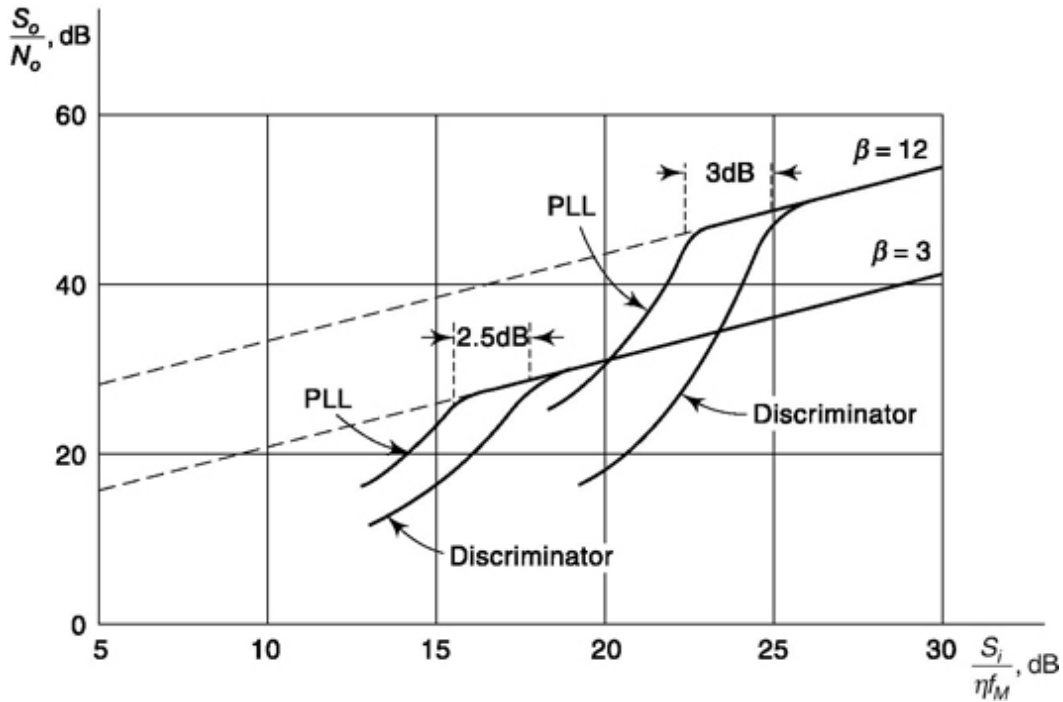


Fig. 10.10 Threshold extension of a PLL.

Example 10.3

- (a) Calculate output SNR of a sinusoidally modulated carrier FM signal when demodulated with phase discriminator and with PLL for input SNR of 30 dB and $b = 10$. (b) Repeat (a) for input SNR of 10 dB.

Solution

(a) Input SNR = 30 dB = 1000

For phase discriminator based demodulation, substituting in Eq. (9.97)

$$\begin{aligned} \text{Output SNR } \frac{S_o}{N_o} &= \frac{1.5 \times 10^2 \times 10^3}{1 + (12 \times 10/\pi)(10^3) \exp[-0.5 \times 10^3/11]} \\ &= 1.5 \times 10^5 = 51.76 \text{ dB} \end{aligned}$$

For PLL based demodulation, substituting in Eq. (10.46)

$$\text{Output SNR } \frac{S_o}{N_o} = \frac{1.5 \times 10^2 \times 10^3}{1 + (12 \times 10/\pi)(10^3) \exp[-0.5 \times 10^3/11]} = 1.5 \times 10^5 = 51.76 \text{ dB}$$

$$\text{Output SNR } \frac{S_o}{N_o} = \frac{1.5 \times 10^2 \times 10^3}{1 + (12 \times 10/\pi)(10^3) \exp[-0.5 \times 10^3/11]} = 1.5 \times 10^5 = 51.76 \text{ dB}$$

SELF-TEST QUESTION

1. In Digital PLL the loop filter is analog in nature. Is that true?
2. What is the difference between lock-in frequency range and hold-in frequency range?
3. Can PLL be called a feedback control system?
4. Does suppression of spikes improve FM demodulation when PLL is used?
5. The steady-state error for both phase and frequency for a step change in frequency at second order PLL input is zero. Is the statement correct?

10.3 DIGITAL PHASE-LOCKED LOOP

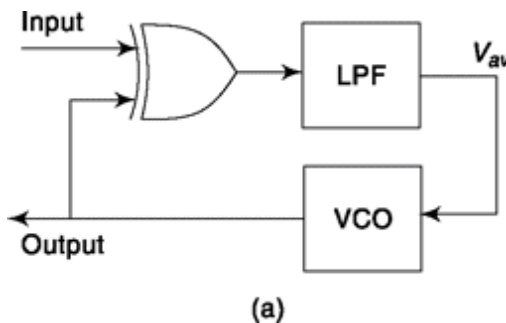
The Digital PLL is different from Analog PLL as it employs a digital phase or phase-frequency error-detection scheme. The input signal is converted to square wave by some mechanism, say hard-limiter and the VCO output can also be generated as a square wave which goes as feedback and compared with input signal. There is an important difference between the phase detector and phase-frequency detector that can be used in DPLL. In the former, the system acts for a limited phase error range say, 0 to 2π and the frequency acquisition range is limited by loop parameters. It usually can lock to a frequency which is close to the VCO free-running frequency. If the input frequency is much different then a special steering mechanism is needed to drive the VCO in correct direction which effectively is an open-loop operation. Once it is in the vicinity, the close loop control takes over and frequency locking takes place. In phase-frequency detector this frequency

steering mechanism is inherent. Let us first discuss phase detectors and then phase-frequency detector.

10.3.1 Digital phase Detector

Fig. 10.11(a), (b) and (c) shows an Ex-OR based phase detector, a typical output of it and the operating point curve respectively. Let us explain how this works. Consider, case I of Fig. 10.11(c) where there is a phase error of $\pi/2$ generating an average voltage $0.5 V_{DD}$ at the LPF output, referred as point D of Fig. 10.11(b). This voltage at the input of VCO generates a signal whose frequency exactly matches the input signal. This is a stable operating condition and the PLL is locked. Consider, case II when VCO output is little ahead in phase compared to case I. Then phase error is less than $\pi/2$, averaging filter output which is also VCO input is less than $0.5 V_{DD}$. This decreases the frequency of VCO and phase lag increases at the rate A_{wt} where A_w is the change in frequency. This continues till phase lag becomes $\pi/2$ (if overshoots, it comes back to stable point as in case III) and VCO input $0.5 V_{DD}$, the stable operating condition. The reverse happens if phase lag is more than $\pi/2$, shown as case III. Now, if the input frequency changes, the PLL will be stable in a new operating point along

straight line AB of Fig. 10.11(c). For the same reason cited in Sec. 10.2.2, the negative slope region AC won't give stable operating point i.e. if disturbed it won't move towards equilibrium point there. Hence, the operating region for this phase detector is 0 to π



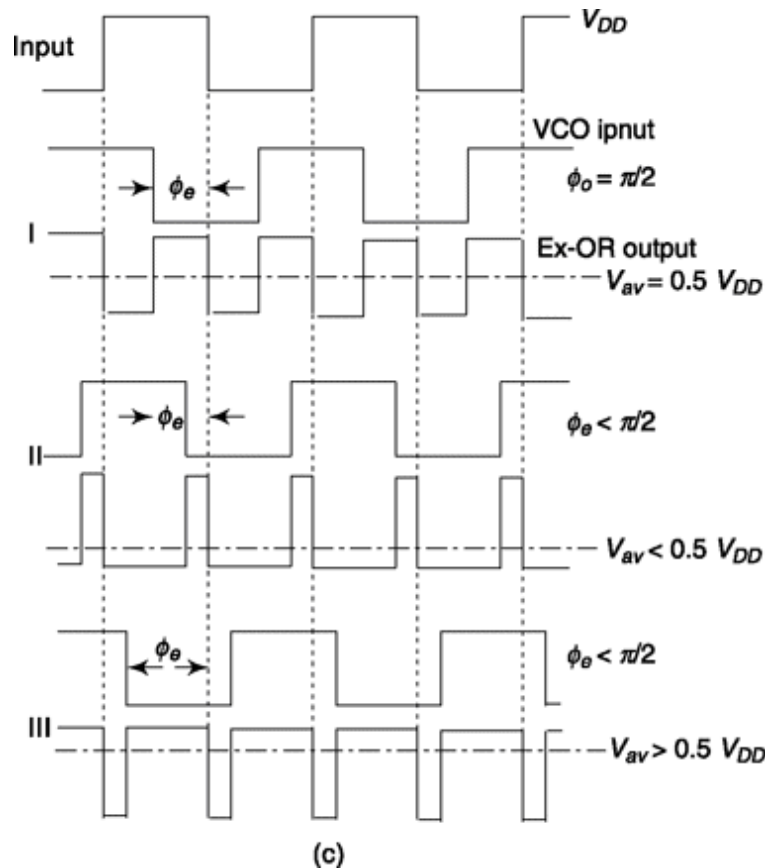


Fig. 10.11 Working of an Ex-OR gate based digital phase comparator.

Let us look at another digital phase detector circuit (Fig. 10.12a) which uses a Flip-Flop that is set and reset at the positive edge of input and feedback (VCO) signal respectively. This is also known as sample-hold phase detector. Figure 10.12(b) shows how it works. It can be seen that the positive edge sets the Flip-Flop which is reset by next positive edge of VCO feedback. Here, it can come after a phase lag between 0 to 2π generating an average voltage 0 to V_{DD} as shown in Fig. 10.11(c). The stable point can be anywhere on positive slope AB. When compared with previous circuit we find it gives a wider operating range of phase 0 to 2π . Also, the signals compared need not be square wave as required in previous case because it acts on the edge and not the levels. This allows duty cycle to be reduced which helps in power management and VCO can be simpler with no strict requirement of 50 percent duty cycle being necessary.

10.3.2 digital phase Frequency detector

The digital phase detectors discussed in previous section and analog-mixer-type phase comparators before, have limited frequency discrimination

properties. Their frequency pull-in ranges in most cases are rather small. The digital sequential circuit based phase-frequency detector (PFD) ensures frequency and phase-lock by itself, irrespective of the initial frequency error of the VCO. Let us discuss one such circuit in this section.

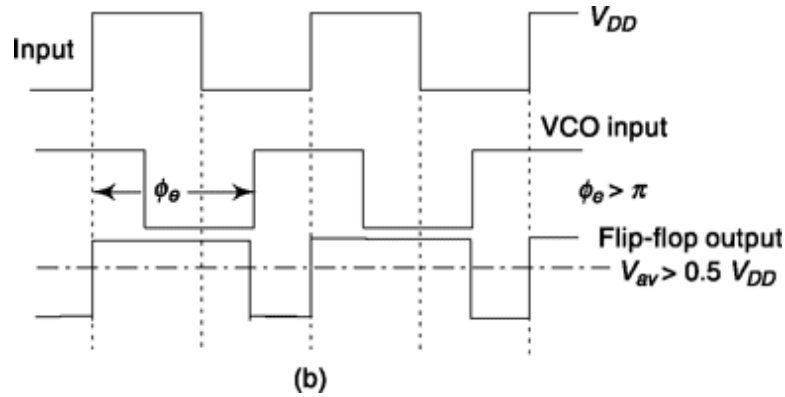
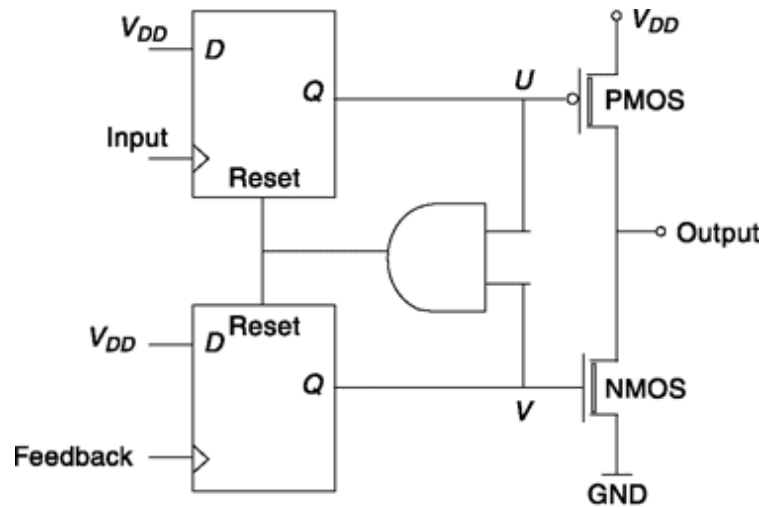
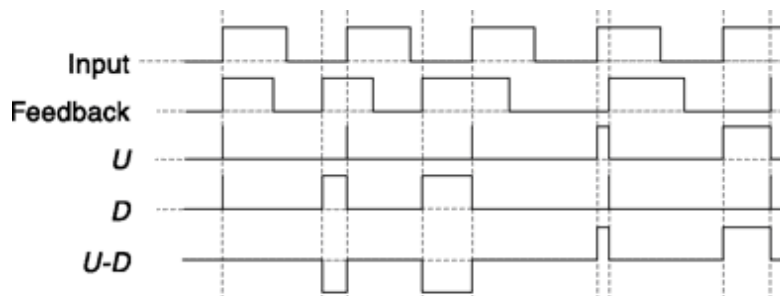


Fig. 10.12 Working of a Flip-Flop based digital phase comparator.

Consider, the circuit shown in Fig. 10.13(a) and its working is shown in Fig. 10.13(b). Both the D Flip-Flops are set to HIGH at positive edge of the clock which is input signal for the top and VCO feedback for the bottom. Both are Reset simultaneously when AND gate output is HIGH, a condition when both the Flip-Flop outputs are HIGH. Thus, both of them remaining HIGH occur for a very short period which is in the order of propagation delay of the AND gate and Flip-Flop. Hence, both PMOS and NMOS are simultaneously **on** only for negligible period of time. Note that, because of the inverter, PMOS is **on** when Flip-Flop output is HIGH. Arguing similarly, PMOS and NMOS will be both **off** when Flip-Flop outputs are LOW (as is the case most of the time) and only one of them is **on** when corresponding Flip-Flop has a HIGH output



(a)



(b)

Fig. 10.13 Working of a sequential logic based digital phase frequency detector.

Let us now study the waveform shown in Fig. 10.13(b) which will explain how the circuit works. In the diagram, the first two positive edges of the input and feedback occur together and both Flip-Flop outputs (top one termed UP abbreviated as U and bottom one DOWN abbreviated as D for some reason which will be clear shortly) U and D go HIGH and are immediately Reset by AND output. Thus $U-D$ is non existent. To start with, we consider feedback frequency is higher than input signal. Thus, next positive edge of feedback comes before input and it makes D to go HIGH. This goes low when positive edge of input signal comes, then U momentarily goes HIGH followed by both U and D going LOW together, reset by AND output. For this excursion, $U-D$ will be a negative going pulse as shown. There is a feedback mechanism which reduces frequency of VCO if $U-D$ is negative and increases frequency if $U-D$ is positive. The extent of decrease/increase is decided by the width of $U-D$. Unlike previous cases, the VCO is lock-in mode when there is no error, i.e. $U-D$ is zero. Now in this case, $U-D$ being negative slows down VCO which comes into effect in next

cycle. But you can see that $U-D$ is still negative there, in fact wider because of the arrival times of the respective

positive edges. This further slows down VCO. In next cycle, we find positive edge of the input occurs earlier than the feedback that makes $U-D$ positive which tries to increase the frequency of VCO by small amount and this goes on till both the signal have same frequency and phase alignment. Note that, even if frequency of one is very large or very small compared to other the $U-D$ will be pulse of very large width with appropriate polarity and within the operating range of the VCO, it will keep changing frequency till the difference goes to zero.

Now how does $U-D$ effect such change? We have seen that U and D are usually not **on** together and most of the time they are LOW when lock-in is established or close to that. If U is HIGH, the PMOS is **on** and NMOS is **off** which charges a capacitor or pumps current into a circuit like a *charge pump*. If D is HIGH the NMOS is **on** and PMOS is **off** which drains the capacitor or sinks current from the circuit. Now, the more the charge is pumped, the more will be the voltage to the input of VCO and the more will be the frequency and vice versa. If $U-D$ is zero, i.e. no charge is pumped or drained the voltage level is maintained at VCO input and the lock-in is established. There are mechanisms employed to arrest the leakage of charge. Around zero phase error, a very small zone, called *dead zone*, is something that is undesirable in such configuration. This is where the loop may fail to react to phase or frequency difference because of the inherent propagation delays. Though it is a small region but being close to lock-in stage, requires some mechanism like providing offset voltage, etc., to alleviate it. From the viewpoint of noise performance, the phase detectors discussed before remain active during a full reference period while PFD is only active during a small fraction of the reference period. The small duty-cycle effectively attenuates its noise contribution to the loop. The spurious contribution of the phase-frequency detector is minimal as it only delivers the amount of energy necessary to compensate for leakage currents after lock-in is established. Being edge triggered device it can work with less than 50 percent duty cycle as in sample-hold phase detector discussed before and with similar benefits.

10.3.3 Frequency dividers

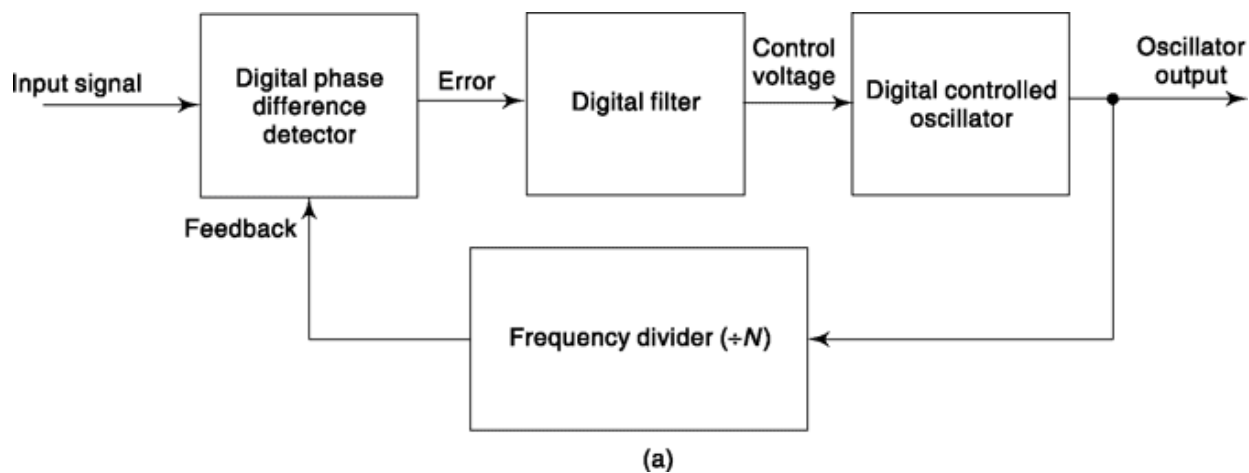
This is though optional has lot of use when PLL is used as a Frequency Synthesizer, one of the many important applications of PLL which we shall discuss later. It can be used in other types of PLL too. When used, the VCO is used to operate at a frequency higher than the reference frequency. The phase or phase-frequency detector input signal comes from the VCO output via a frequency divider which divides the output frequency up to the reference frequency. Flip-Flops when used in toggle mode can divide the frequency, each one by a factor of two. For division of more than two we can use more than one Flip-Flop and with n Flip-Flops, we can divide up to a number 2^n . Using some combinatorial circuits with n Flip-Flops, division by any number from 1 to 2^n can be made possible. Simpler circuits which connect Flip-Flops in the form of a ring can also be used but require more number of such Flip-Flops. This kind of circuits is also known as Counters and for more of counter design aspect we urge you to visit any standard digital logic text. However, we would like to mention here that there can be two distinct varieties known as synchronous and asynchronous counters. Asynchronous circuits are simpler but have longer latency as they do not use common clock.

The counter described above can make integer division. What if we require *fractional divider*? Such a scenario may come if we want a resolution better than what we get by integer division. (Refer to Example 10.7.) Now, no hardware exists which can directly give fractional division. In PLL, this is done by changing the divider in the loop dynamically, between the values N and $N + 1$ in such a way that the ‘average’ division becomes a fraction. If out of F cycles, we divide VCO output by $N+1$ for K times and by N , $F - K$ times, then the average division will be $\frac{(NK + K + NF - NK)/F}{N + K/F}$. The principle used thus is some sort of averaging and the abruptness in the approach leads to spurious signals, which requires spurious compensation circuit to keep it at practical minimum. It is important to note here that four types of VCO are commonly used which in the order of decreasing stability are voltage controlled crystal oscillators (VCXO’s), resonator oscillators, RC multivibrators and YIG-tuned oscillators. The phase stability can be enhanced by a number of ways, e.g. (a) using high Q crystal and circuit, (b) maintaining low noise in the amplifier portion, (c) stabilizing temperature, and (d) keeping mechanical stability.

10.4 ALL DIGITAL PLL AND SOFTWARE PLL

The All Digital PLL (ADPLL) block diagram is shown in Fig. 10.14a. Note that, all the components now are digital. We have already seen how digital phase detector works. The digital loop filter is usually a first or second-order infinite impulse response (IIR) low-pass filter. The filter output is passed to the Digital Controlled Oscillator (DCO) also known as Numerical Controlled Oscillator (NCO). DCO output is fed back usually via a frequency divider to phase comparator. This adjusts phase and frequency to reduce phase error to zero, a condition known as phase lock. The DCO can be developed in the following way. The varactor of VCO which works in the linear region is replaced in DCO by array of say, N-varactors operating in inversion/depletion, i.e. **on/off** region which is decided by N -bit digital word. The frequency acquisition is done in several steps from coarse to finer by setting Most Significant Bits (MSB) first and then Least Significant Bits (LSB). For example, a bluetooth compatible PLL can have 2.4 GHz oscillation frequency and a frequency resolution of 23 kHz. However, this can be further reduced to below 1 kHz by some advanced techniques like sigma-delta modulation. There can be various other configurations of DCO, e.g. odd number of inverters say, 7 connected in the form of a ring can work as an oscillator.

The advantage with ADPLL is its feature like programmability, testability, portability and reduced time to market. It also solves problems like dc drift, calibration difficulty, component saturation, building higher order loops etc. But if one needs to use Digital to Analog converter to generate sinusoidal output, power consumption, jitter, etc., are slightly on the higher side in ADPLL but the gaps are bridged quickly.



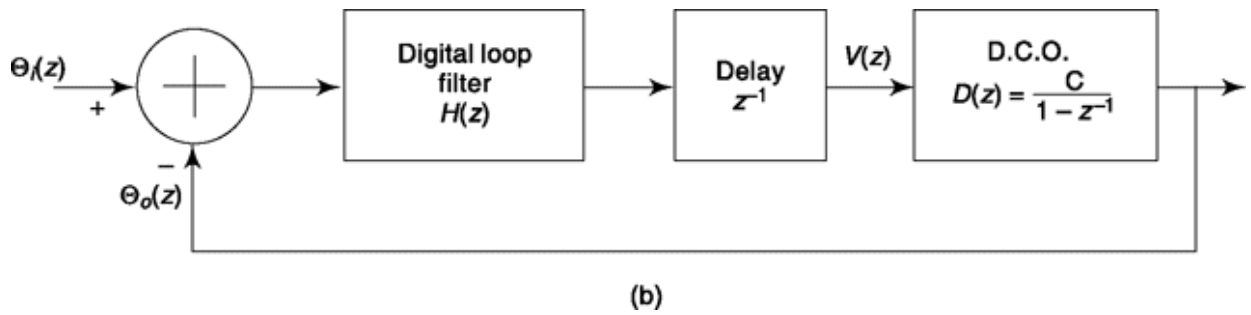


Fig. 10.14 (a) Block diagram representation of ADPLL. (b) ADPLL representation in z-domain.

Software PLL is an all digital implementation of PLL like ADPLL but does not use dedicated digital building blocks. Rather it uses on board capability of general-purpose Digital Signal Processing kits to develop the PLL, e.g. the input signal is sampled by Analog to Digital Converter, Loop filter is replaced by difference equation, etc. The whole thing is made to work by writing appropriate program or codes. The DSP processors are better equipped to handle such tasks with separate program and data memory (Harvard or modified Harvard architecture), pipelined instruction set etc. Because of its huge flexibility it is becoming increasingly popular in Digital Communication applications.

10.4.1 mathematical Analysis of All digital pLL

Here, we try to arrive at a transfer function of All Digital PLL. Refer to Fig. 10.14b where the z-domain representation of an ADPLL is shown. Let us first look at D.C.O. which is described as,

$$D(z) = \frac{\Theta_o(z)}{V(z)} = \frac{C}{1 - z^{-1}} \quad (10.47)$$

or

$$\Theta_o(k) - \Theta_o(k-1) = Cv(k) \quad (10.48)$$

where k is discrete-time index normalized to sampling time period $T = 1$ (else in place of k we should write kT). This means that the change in phase of oscillator output ($\Theta_o(k) - \Theta_o(k-1)$) is proportional to control voltage $v(k)$ with C being the proportionality constant. If control voltage is zero then oscillator output phase is maintained. The one-unit delay having z-domain representation z^{-1} is realized by a register or register array.

With digital loop filter represented by $H(z)$, we can write,

$$\Theta_o(z) = [\Theta_i(z) - \Theta_o(z)][H(z)][z^{-1}] \frac{C}{1-z^{-1}} \quad (10.49)$$

or $(z-1)\Theta_o(z) = C[\Theta_i(z) - \Theta_o(z)][H(z)] \quad (10.50)$

This gives ADPLL input-output relation in the form of a close-loop transfer function as

$$T(z) = \frac{\Theta_o(z)}{\Theta_i(z)} = \frac{CH(z)}{CH(z) + z - 1} \quad (10.51)$$

Rearranging Eq. (10.51), the phase error comes out as

$$E(z) = \Theta_i(z) - \Theta_o(z) = \frac{(z-1)\Theta_i(z)}{CH(z) + z - 1} \quad (10.52)$$

Now, let us find steady-state error for this ADPLL when there is a step change in phase and frequency at the input. We note that the final value theorem of z-transform says,

$$\lim_{k \rightarrow \infty} e(k) = \lim_{z \rightarrow 1} (z-1)E(z) \quad (10.53)$$

A step change in input phase can be represented by $\theta_i(k) = au(k)$ where $u(k)$ is the unit step function

and a is the step size. Then

$$\Theta_i(z) = \frac{az}{z-1} \quad (10.54)$$

From Eq. (10.52), Eq. (10.53) and Eq. (10.54) we get steady-state error e_{ss} as,

$$e_{ss} = \lim_{k \rightarrow \infty} e(k) = \lim_{z \rightarrow 1} \frac{az(z-1)}{CH(z) + z - 1} = 0 \quad (10.55)$$

Next, consider that there is a step change in frequency at time $k = 0$. Then

$Q(k) = bku(k)$ where b is a constant. Now, $\Theta_i(z) = \frac{bz}{(z-1)^2}$ and steady-state error becomes $e_{ss} = \lim_{z \rightarrow 1} \frac{bz}{CH(z) + z - 1} \quad (10.56)$

Now, a pole for $H(z)$ at $z = 1$ will bring a $(z - 1)$ factor in numerator of Eq. (10.56) and make the limiting value zero and hence the steady-state error moves to zero. We can substitute $H(z) = K$ (constant) to get a first-order ADPLL where the denominator of $T(z)$ has highest order of $z = 1$. Example 10.5 describes a second-order system.

Example 10.4

Explain if the following circuit can be used for edge triggered set and edge triggered reset Flip-Flop shown in Fig. 10.12(a).

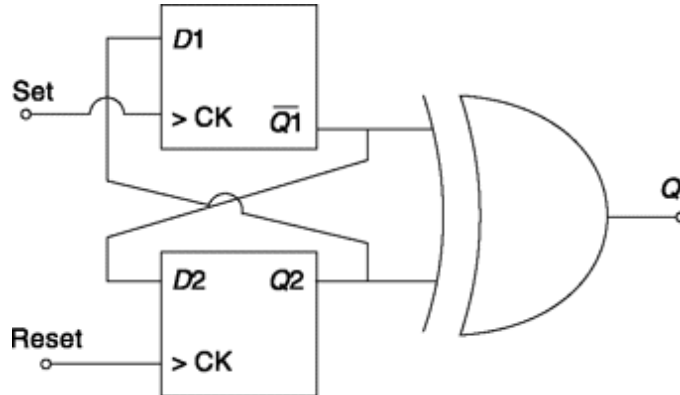


Fig. 10.15 Logic circuit for Example 10.4

Solution

Consider, initially $Q_1 = 0$ and $Q_2 = 1$. Then $Q_1 = 1$ and $Q = \bar{Q}_1 \oplus Q_2 = 1 \oplus 1 = 0$

If ‘Set’ goes HIGH, $Q_2 \rightarrow Q_1 = 1$. Then $\bar{Q}_1 = 0$ and $Q = \bar{Q}_1 \oplus Q_2 = 0 \oplus 1 = 1$

If ‘Set’ goes LOW, still the value of Q is retained at 1.

Now if ‘Reset’ goes HIGH $\bar{Q}_1 \rightarrow Q_2 = 0$. Then $Q = \bar{Q}_1 \oplus Q_2 = 0 \oplus 0 = 0$

If now ‘Reset’ goes LOW, still the value of Q is retained at 0.

If ‘Set’ again goes HIGH, $Q_2 \rightarrow Q_1 = 0$. Then $\bar{Q}_1 = 1$ and $Q = \bar{Q}_1 \oplus Q_2 = 1 \oplus 0 = 1$ and this value is retained till ‘Reset’ is HIGH. This case also shows that if we had started with opposite values of Q_1 and Q_2 similar ‘set’, ‘reset’ characteristics of Q would have been maintained.

If initially, $Q_1 = 0$ and $Q_2 = 0$. Then $\bar{Q}_1 = 1$ and $Q = \bar{Q}_1 \oplus Q_2 = 1 \oplus 0 = 1$

If ‘Set’ goes HIGH, $Q_2 \rightarrow Q_1 = 0$. Then $\bar{Q}_1 = 1$ and $Q = \bar{Q}_1 \oplus Q_2 = 1 \oplus 0 = 1$

Now if ‘Reset’ goes HIGH $\bar{Q}_1 \rightarrow Q_2 = 1$. Then $Q = \bar{Q}_1 \oplus Q_2 = 1 \oplus 1 = 0$

And we are having a situation like before. Similarly for initial value $Q_1 = Q_2 = 1$.

From this discussion, we find Q is set when ‘set’ input goes HIGH and remains there even if it goes LOW and is reset when ‘Reset’ input goes

HIGH and till it is not set again. Clearly this is a case of positive edge-triggered set-reset Flip-Flop discussed in Fig. 10.12(a).

Example 10.5

Consider the loop filter is given by $H(z) = \frac{Az - 1}{z - 1}$ and the proportionality constant of D.C.O. is C. Show that this represents a second-order ADPLL. If sampling period is T, find equivalent s-domain pole positions and comment on transient response, natural frequency.

solution

From Eq. (10.51),

$$T(z) = \frac{C \frac{Az - 1}{z - 1}}{C \frac{Az - 1}{z - 1} + z - 1} = \frac{6z - 2}{z^2 + (AC - 2)z + 1 - C} \quad (10.57)$$

With denominator's highest power being 2, this is a second-order PLL. If two poles are $z = z_1, z_2$ then

$$z_{1,2} = \frac{(2 - AC) \pm \sqrt{(AC - 2)^2 - 4(1 - C)}}{2} \quad (10.58)$$

Now, poles of z-domain get mapped to s-domain by the relation

$$z = e^{sT} \quad (10.59)$$

Thus,

$$s_{1,2} = \frac{1}{T} \ln \left(\frac{(2 - AC) \pm \sqrt{(AC - 2)^2 - 4(1 - C)}}{2} \right) \quad (10.60)$$

From Example 10.1b, in terms of damping coefficient

ξ and natural frequency ω_n , the denominator $H(s)$ can be written as

$$\begin{aligned} (s - s_1)(s - s_2) &= s^2 - (s_1 + s_2)s + s_1 s_2 \\ &= s^2 + 2\xi\omega_n s + \omega_n^2 \end{aligned} \quad (10.61)$$

Using Eq. (10.60) and Eq. (10.61), we can get the natural frequency and damping coefficient.

SELF-TEST QUESTION

6. Which of digital phase detector and digital phase-frequency detector has higher frequency acquisition range?
7. Simple Ex-OR gate based phase detector has operating range 0 to p . Is the statement correct?
8. Can duty cycle of input signal be less than 50 percent in edge-triggered Flip-Flop based digital phase detectors?
9. Is the control voltage output zero for phase-frequency detector when lock-in is established?
10. What is the principle behind design of a fractional divider?

10.5 APPLICATIONS OF PHASE-LOCKED LOOPS

Today, PLL is used in almost all communication devices starting from television set, mobile phone, navigation to satellite. We don't have scope to address each individual case as it will be a subject by itself. Instead, in this section, we shall discuss a few uses of PLL. Use of PLL in FM demodulation is already discussed in detail while describing the working of an analog PLL. In binary FSK demodulation too, this can be used following a simple principle. If PLL is tuned midway between the high and low frequency, a positive error will detect one binary value and a negative error will detect the other. We shall discuss four other applications, namely carrier recovery, clock recovery, frequency synthesis, frequency and phase modulation. There are other applications where PLL is used for designing narrowband filters at very high operating frequency, measuring noise of a signal source, generating multiple clocklike timing signals from a single reference, etc. This way, PLL plays a very important role in both analog and digital modulation.

10.5.1 Carrier Recovery

As we have noted, in many communication schemes it is necessary to regenerate at the receiver a waveform which is synchronous with the transmitter carrier. The method we have described for achieving this carrier recovery is shown in Fig. 10.16. (We disregard temporarily the phase-locked loop and the dashed connections to it.) The receiver signal is initially passed through a bandpass filter to remove the noise outside the band required for

the signal itself. In M-ary PSK, as an example, the signal is next passed through a network whose output is its input raised to the M th power. At the output of the M -power device, there are many spectral components, one of which is a sinusoid of frequency Mf_c , f_c being the carrier frequency. This M -power output signal is then passed through a

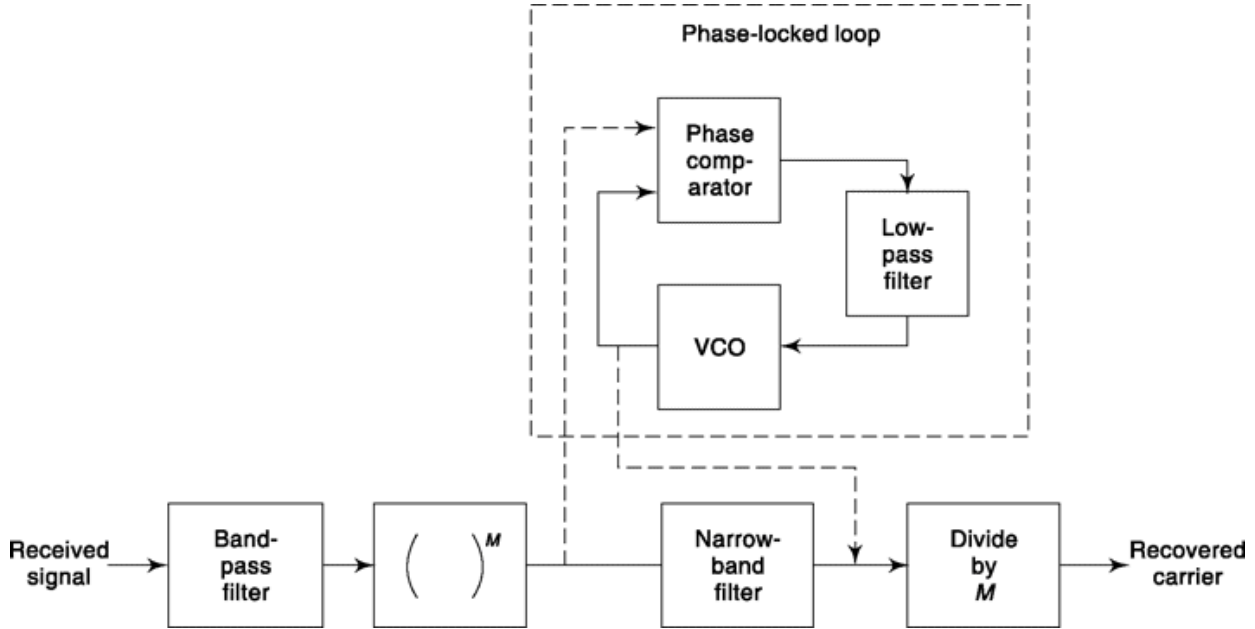


Fig. 10.16 Circuitry for recovering carrier.

narrowband filter to isolate the sinusoid at frequency Mf_c and to remove more of the noise. Finally a divide-by- M circuit yields the desired carrier of frequency f_c .

As a matter of fact, the carrier frequency generated at the transmitter is not constant. It is subject to unpredictable variations, called “jitter” because the oscillator is perturbed by random noise-type disturbances and because of uncontrollable variations in the parameters which determine its frequency. The oscillator frequency drifts back and forth through a frequency deviation $\pm Df$. The nominal frequency at which this frequency drifting occurs be f_d . Normally, Df is much larger than f_d . Typically, in a UHF transmitter, we may find that the frequency drifts by an amount exceeding $Df = 10$ Hz, while the maximum rate of frequency change might be less than 1 Hz. Because of this oscillator jitter the narrowband filter of Fig. 10.16 cannot be made as narrow as we would like. Its bandwidth must be somewhat larger than the width $2M$

Df necessary to accommodate the frequency deviation $\pm Df$ multiplied by M , due to the M -power device.

Now it turns out that we can replace the narrowband filter by a phase-locked loop in the manner shown in Fig. 10.16. The PLL is a filter whose bandpass is determined by the low-pass filter. It can be shown that if the low-pass filter has a transfer function $H(s) = \alpha(1 + 1/s)$ (α a constant) and if

the PLL is adjusted to have a passband $2Mf_d$ (rather than $2MDf$), the PLL will still be able to follow the oscillator jitter. However, so far as noise is concerned, the PLL filter will have the reduced passband $2Mf_d$ and therefore the noise power will be reduced.

The Costas Loop

An alternative circuit by which the carrier of a BPSK received signal may be recovered is the Costas loop, named after its inventor and shown in Fig. 10.17. The circuit involves two PLL's employing a common VCO and loop filter. Let us start by assuming that the VCO is operating at the carrier angular frequency ω_c albeit with an arbitrary phase angle. We shall now be able to see that, in spite

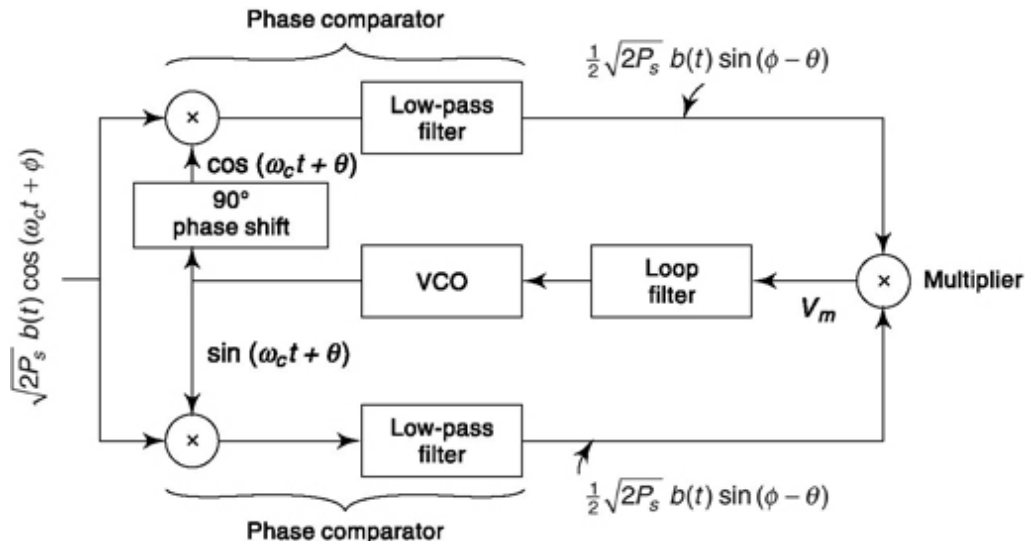


Fig. 10.17 The Costas loop.

of the fact that in the received signal, $b(t)$ is making transitions at random times between ± 1 , the input signal to the VCO will serve to keep the VCO oscillating at the carrier frequency.

The low-pass filters remove the double frequency terms generated in the phase comparators and

make available the waveforms $\frac{1}{2}\sqrt{2P_s}b(t)\cos(\phi - \theta)$ and $\frac{1}{2}\sqrt{2P_s}b(t)\sin(\phi - \theta)$ as shown. The multiplier output signal is then:

$$V_m = \frac{1}{4}(2P_s)b^2(t)\sin(\phi - \theta)\cos(\phi - \theta) \quad (10.62a)$$

$$= \frac{P_s}{4}\sin 2(\phi - \theta) \quad (10.62b)$$

Observe in Eq. (10.47) that, because of the multiplication, the $b(t)$ coefficient has dropped out. Further, we note that if some perturbation should cause the VCO frequency to differ from the carrier frequency, this frequency difference would manifest itself by a progressive change in the phase difference $f - 6$. But a change in $(f - 6)$ will cause a change in V_m which can now serve to increase or decrease the VCO frequency to maintain synchronism. Finally, we note that, as in the case in Fig. 10.16, when the PLL is employed, so in the present case, the required bandwidth required of the Costas loop to accommodate oscillator jitter is determined by f_d and not Af .

10.5.2 Clock Recovery

Clock recovery is important in digital communication to generate important timing information and bit synchronization. For this, we can employ a similar scheme as used for carrier recovery. This is to send the signal through a nonlinear device and select appropriate harmonic with PLL giving stability to the circuit. A better performance can be obtained from *early-late gate* clock recovery circuit which uses PLL loop in an intelligent way. Fig. 10.18(a) shows the circuit diagram for this. Consider first, that the VCO output and input bit stream are in perfect synchronism, timing error $t = 0$, so that both early and late gate integrators integrate data for exactly one half of the period $T/2$ (where T is the symbol duration) on either side of the symbol transition. If the data was positive

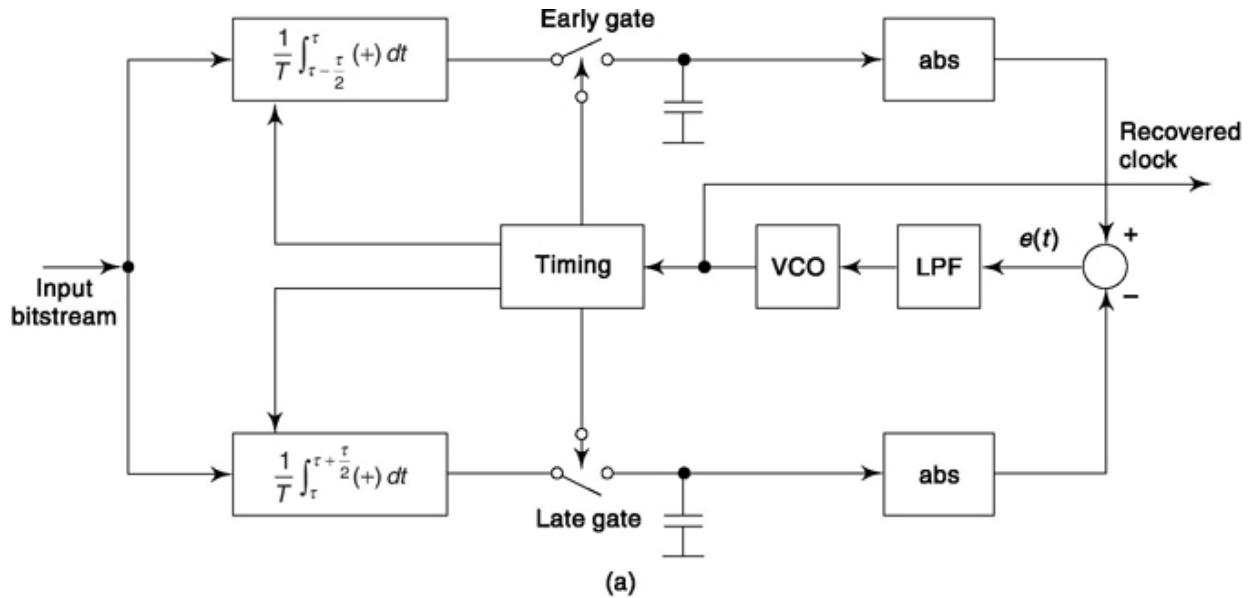


Fig. 10.18 Early-late gate clock recovery circuit and its working.

before transition then early gate dumps into the capacitor accumulated positive voltage. The late gate in turn dumps voltage collected in the other half in which it was fully negative. The capacitors take opposite polarity if transition is reversed. The block ‘abs’ finds absolute value of these two capacitor outputs and being equal for all $t = 0$ case results in error voltage $e(t) = 0$, case I in Fig. 10.18(b). This requires no adjustment in VCO as t is properly estimated. Note that, if in some transition point polarity is not changed the capacitors hold same value (same polarity) and again $e(t) = 0$, the case shown in Fig. 10.18(c).

Let us now see how adjustment is made if there is a timing error $t = -ve$. This means early gate integrator is on for $T/2$ time, entirely before transition where symbol is of a particular polarity and hence, the accumulated voltage will be same as before. But the late gate integrator is on t second before transition and $T/2-t$ second after transition and this is expected to accumulate both positive and negative values, resulting a capacitor voltage whose absolute value is less than before. Now we can see that error $e(t)$ will be positive indicating timing error and increasing frequency of VCO to remove the timing lag. The opposite will happen if VCO goes ahead and $t = +ve$. This is illustrated in 2nd and 3rd plots of Fig. 10.18(b).

remove the timing lag. The opposite will happen if VCO goes ahead and $t = +ve$. This is illustrated in 2nd and 3rd plots of Fig. 10.18(b).

10.5.3 Frequency synthesis

Frequency synthesizers are an essential building block of today's communication systems. Digital tuning is common in television, AM/ FM radios, cellular communication systems and many such applications. The property of making its output frequency an exact multiple of the reference frequency makes the PLL the choicest device for frequency synthesizers. This, in combination with a spectrally pure frequency source like crystal oscillators generate high-quality frequency generators. However, the crystal provides a low frequency which requires to be up-scaled by PLL. A counterbased frequency divider can be used for this which for different count values can generate different output frequency. Figure 10.19 shows basic block diagram of how it operates.

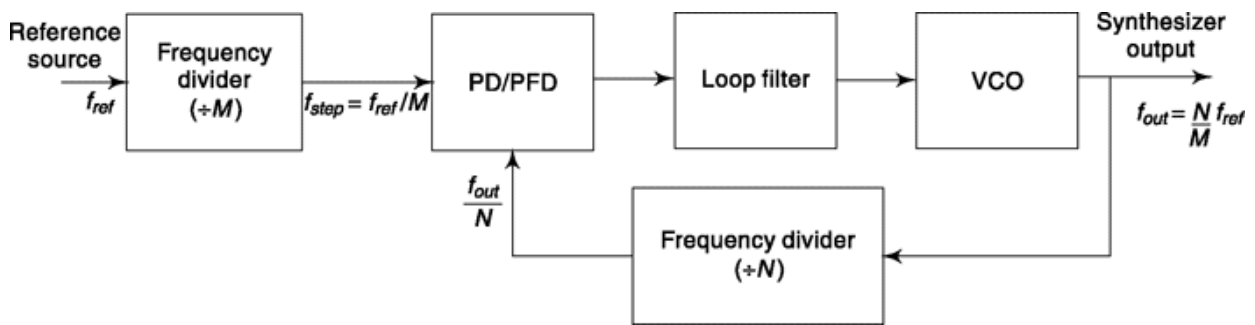


Fig. 10.19 Basic block diagram of a frequency synthesizer.

Let us consider that the reference source generates a stable frequency f_{ref} . This is fed to a frequency divider circuit. If we want a frequency resolution or frequency step as f_{step} then division ratio M is chosen such that

$$f_{\text{step}} = \frac{f_{\text{ref}}}{M} \quad (10.63)$$

This frequency is compared with VCO output frequency divided by a factor of N (by frequency divider in the feedback path) and when a lock is established the two frequencies are equal. If VCO and in turn synthesizer output frequency is f_{out} then

$$f_{\text{out}} = N \times f_{\text{step}} \quad (10.64)$$

and combining Eq. (10.63) and (10.64)

$$f_{\text{out}} = \frac{N}{M} f_{\text{ref}} \quad (10.65)$$

If $f_{ref} = 1$ MHz and $M = 100$ then $f_{step} = 10^6/100 = 10$ kHz. If N is an integer divider then synthesizer output can be varied in steps of 10 kHz. If in-between frequencies are required then fractional frequency divider can be used as discussed in Sec. 10.3.3 or frequency offset can be given through a mixer (multiplying and then filtering one component) before feedback divider block.

When the required N is large, more than one counter is used. Different design alternatives are there for this. Let us present a popular prescaler-based technique here that uses four counters for divide by N block. Let these counters be initially loaded with values A , B , P and $P + 1$ where P stands for prescaler. Then for every $(P + 1)$ count of VCO, counters A and B are decremented by 1 till $A = 0$ which requires $(P + 1)A$ cycles of VCO. Now the P prescalar counter is switched to which decrements remaining of B counter, i.e. $(B - A)$ by 1 for every P cycles of VCO till it is zero requiring $(B - A)P$ cycles of VCO. At this point, the frequency divider block generates one pulse thus requiring $(B - A)P$ cycles of VCO for one pulse output. This makes

$$N = P \times B + A \quad (10.66)$$

We discuss certain design issues using above relations in Example 10.5 and 10.6. Note that, *direct digital synthesis* is a DSP processor based technique for frequency synthesis which uses phase ramp, accumulator, Digital to Analog converter but importantly does not use any feedback like PLL and is yet to become popular.

10.5.4 phase and Frequency Modulation

We have seen PLL can be used in demodulation. Can it be used in phase and frequency modulation? The answer is ‘Yes’. Figure 10.20a shows block diagram of the scheme that can be employed. We have shown FM and PM (dotted line) in same diagram but either of the two is used at a time. If modulating signal appears before loop filter then it acts like a phase modulator but loop filter must be able to pass the message bandwidth. On the other hand, if modulating signal is added before VCO then the arrangement acts like a frequency modulator and of course the message bandwidth should not exceed PLL bandwidth or cutoff frequency.

For mathematical representation of above schemes, we divide VCO into two sections as shown in Fig. 10.20b and consider FM output is available

before integration (w_{out}) and PM output (θ_{out}) after it. In both the cases, it is tapped after VCO block shown in Fig. 10.20a. Then for PM, we can write

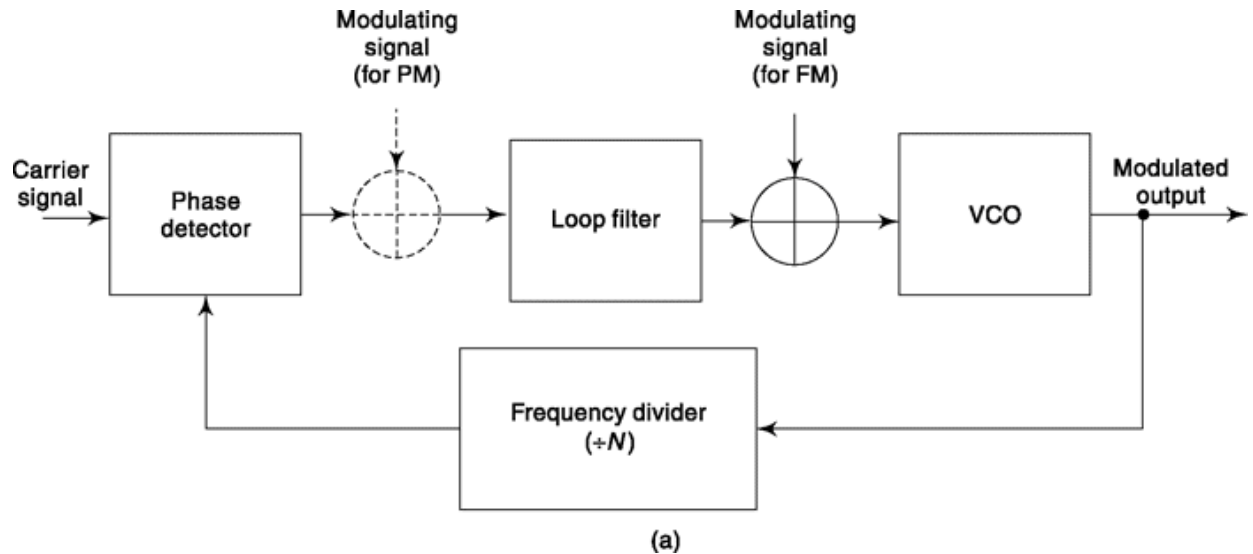
$$\theta_{out}(s) = V_{PM}(s) \cdot H(s) \cdot \frac{G_0}{s} - \theta_{out}(s) \cdot \frac{1}{N} \cdot G_d \cdot H(s) \cdot \frac{G_0}{s} \quad (10.67a)$$

The first term in the right-hand side comes from the forward path and the second term comes from the feedback path. Note that when variation in phase is considered as cases like this, θ_{ref} does not count as it is a constant quantity and the variation we are considering here is over and above θ_{ref} . Simplifying the above equation and in the form of transfer function, we get

$$\frac{\theta_{out}(s)}{V_{PM}(s)} = \frac{G_0 H(s)}{s + \frac{G_0 G_d H(s)}{N}} \quad (10.67b)$$

Similarly, for FM modulated output, we get input-output relation as given next.

$$\frac{\omega_{out}(s)}{V_{FM}(s)} = \frac{s G_0}{s + \frac{G_0 G_d H(s)}{N}} \quad (10.68)$$



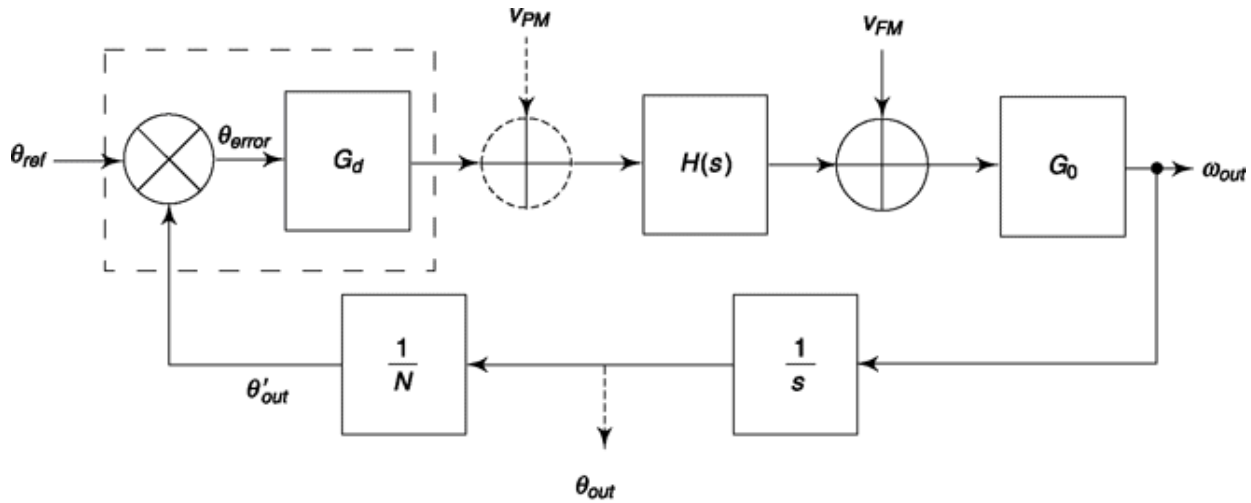


Fig. 10.20 Frequency and phase modulation using PLL.

PLL based FM has use in applications like low-power RF transmission. But when compared to other angle modulation schemes, one must note a different kind of difficulty with PLL. In FM (also in PM) we are trying to change VCO frequency in proportion to the modulating signal applied. The PLL circuit's job is to correct any frequency errors introduced by this modulating signal. If we design the loop filter too well, the quick response will arrest any deviation and hence producing negligible or minimum variation at output. If we relax the requirement to allow more variation to pass uncorrected then PLL lock-in time increases. Ideally, the loop filter should first allow PLL to reach carrier frequency fast and then relax itself to provide higher variation according to modulating signal. There exists two speed PLLs to be of use in such cases.

Example 10.6

For an application, channel spacing is 100 kHz while reference source generates a signal of frequency 10 MHz. If required output is 100.6 MHz and a 64/65 prescaler is used as discussed in Sec. 10.5.3, find the value of A, B and M.

Solution

For divide by M counter, from Eq. (10.63) $M = 10 \text{ MHz}/100 \text{ kHz} = 100$

For divide by N counter, from Eq. (10.64) required
 $N = 100.6 \text{ MHz}/100 \text{ kHz} = 1006$

Given, $P = 64$.

We find, $N/P = 1006/64 = 15.71875$

We truncate this value and set $B = 15$.

Then from Eq. (10.66), $A = N - P \times B = 1006 - 64 \times 15 = 46$

Example 10.7

Consider a frequency synthesizer scheme shown in Fig. 10.21 that generates frequency in the range 2029.9 MHz in step of 0.1 MHz from a 1 MHz reference.

(a) Identify the blocks/value at A, B and C. (b) Find values to be set at programmable quantities when desired output frequency is 25.5 MHz.

Solution

(a) We find there are two phase locked loops, the second one contains an additional ‘Mixer’ block. Between ‘B’ and ‘C’, one is a frequency divider and the other loop filter. Since ‘C’ comes after phase detector it is the low-pass loop filter. Now ‘B’ is a programmable frequency divider in the range $1-1.9 \text{ MHz}/0.1 \text{ MHz} = 10-19$ as its output is to lock to $1 \text{ MHz}/10 = 0.1 \text{ MHz}$, the other input of the phase detector. Finally, A is the output of VCO having frequency $1 \text{ MHz} \times (19-28) = 19-28 \text{ MHz}$ as the frequency divided output of it is locked to 1 MHz reference source.

(b) The output VCO generates 25.5 MHz. ‘A’ takes a value between 19-28 MHz in steps of 1 MHz. The mixer output chooses lower component which has to be within 1-1.9 MHz. Then ‘A’ output should be 24 MHz when mixer output is $25.5-24 = 1.5 \text{ MHz}$ as for any other value it will be out of range. Then first programmable divider has to be set at 24 and ‘B’ has to be set at $1.5/0.1 = 15$.

Example 10.8

Given, reference frequency for a PLL as 0.48 MHz. The programmable frequency divider in the feedback path is set at 2000. (a) What is the output frequency?

(b) What is the frequency resolution if frequency divider changes by integer value? (c) Find the frequency resolution achieved if frequency

divider is set at 2000 for 15 cycles out of 16 cycles and at 2001 in the 16th cycle.

Solution

- (a) Output frequency = $0.48 \text{ MHz} \times 2000$
= 960 MHz
- (b) Since, reference frequency is not subdivided before going to comparator and it is an integer divider in the feedback path the frequency resolution = 0.48 MHz.
- (c) Now the output frequency is averaged as
- $$\frac{2000 \times 15 + 2001 \times 1}{16} \times 0.48 = 960.03 \text{ MHz}$$

This effectively gives a frequency resolution of $960.03 - 960 = 0.03 \text{ MHz}$

SELF-TEST QUESTION

11. What is the use of early-late gate?
12. Can PLL be used for both Frequency Modulation and Demodulation?
13. Can PLL based frequency synthesis be useful in generating multiple clock frequencies from a single source, e.g. in a computer motherboard?
14. What is the use of Costas Loop?

Facts and Figures

The famous Costas loop used for carrier recovery was invented by John P. Costas in the 1950s when he was working in General Electric. He was an undergraduate at Purdue University and a graduate student at Massachusetts Institute of Technology (MIT). Costas served the U.S. Navy as a radar officer during World War II. The Costas loop showed higher sensitivity than the conventional PLL and was particularly suited for carriers that are Doppler-shifted like OFDM, GPS receivers. This is regarded as one that has “a profound effect on modern digital communications.” Costas also contributed to development of sonar systems.

Sundials, water clocks, sand-filled hourglasses were followed by the first mechanical clock in which a weight would slowly descend, thereby moving an hour hand through gears. They were built in tall towers so that the weights would fall a sufficient distance and the amount of time shown would

not be too small. It was considered a great feat to have these clocks off for about two hours a day. Galileo's discovery in 1581 made way for the pendulum clock. In 1900, a fine-tuned pendulum clock would give only 1/100th second of error each day. The quartz crystal clock came later and gives 1/500 of a second error in one year and an atomic clock is off by 1/300 of a second in one million years.

MATLAB

In the first four experiments, to analyze the performance of PLL we follow the method adopted so far, i.e. writing code and storing it in .m file. However, in this chapter, we also exploit MATLAB SIMULINK block sets, a new feature, in last two experiments. These are in-built block-sets available in MATLAB environment which needs to be properly connected and parameterized for an intended application. We discuss how it is done within the experiment.

- Experiment 38
- Here, we show how phase error reduces with time following transfer function described in eqn. (10.26) . The input parameters are K and tau.
- which can be converted to damping factor and natural frequency as given
 - in eqn. (10.35) . We use step input here.
 - We use MATLAB in-built function tf.m to define the PLL transfer function % and lsim.m to simulate its time response.

```
dt = 0.00001;
t = 0:dt:0.004;
u = ones(1,length(t));
K = 10^4; tau = 10^(-4);
sys1 = tf([1 0],[1 1/tau K/tau]); % Defining PLL transfer function
[ph_error t] = lsim(sys1,u,t); % Simulating time response of PLL
subplot(311), plot(t,ph_error); grid;
xlabel('TIME IN SECONDS'), ylabel('AMPLITUDE')
title('Phase Error : K=10000, tau=0.0001, damping=0.5, nat. freq. = 10000 :
step freq. input')

K = 0.25*10^4; tau = 10^(-4);
sys1 = tf([1 0],[1 1/tau K/tau]);
[ph_error t] = lsim(sys1,u,t);
```

- We use MATLAB in-built function tf.m to define the PLL transfer function % and lsim.m to simulate its time response.

```

dt = 0.00001;
t = 0:dt:0.004;
u = t; % generating velocity input
K = 10^4; tau = 10^(-4);
sys1 = tf([1 0],[1 1/tau K/tau]); % Defining PLL transfer function
[ph_error t] = lsim(sys1,u,t); % Simulating time response of PLL
subplot(211), plot(t,ph_error); grid;
xlabel('TIME IN SECONDS'), ylabel('AMPLITUDE')
title('Phase Error : K=10000, tau=0.0001, damping=0.5, nat. freq. = 10000 : velocity freq. input')

```

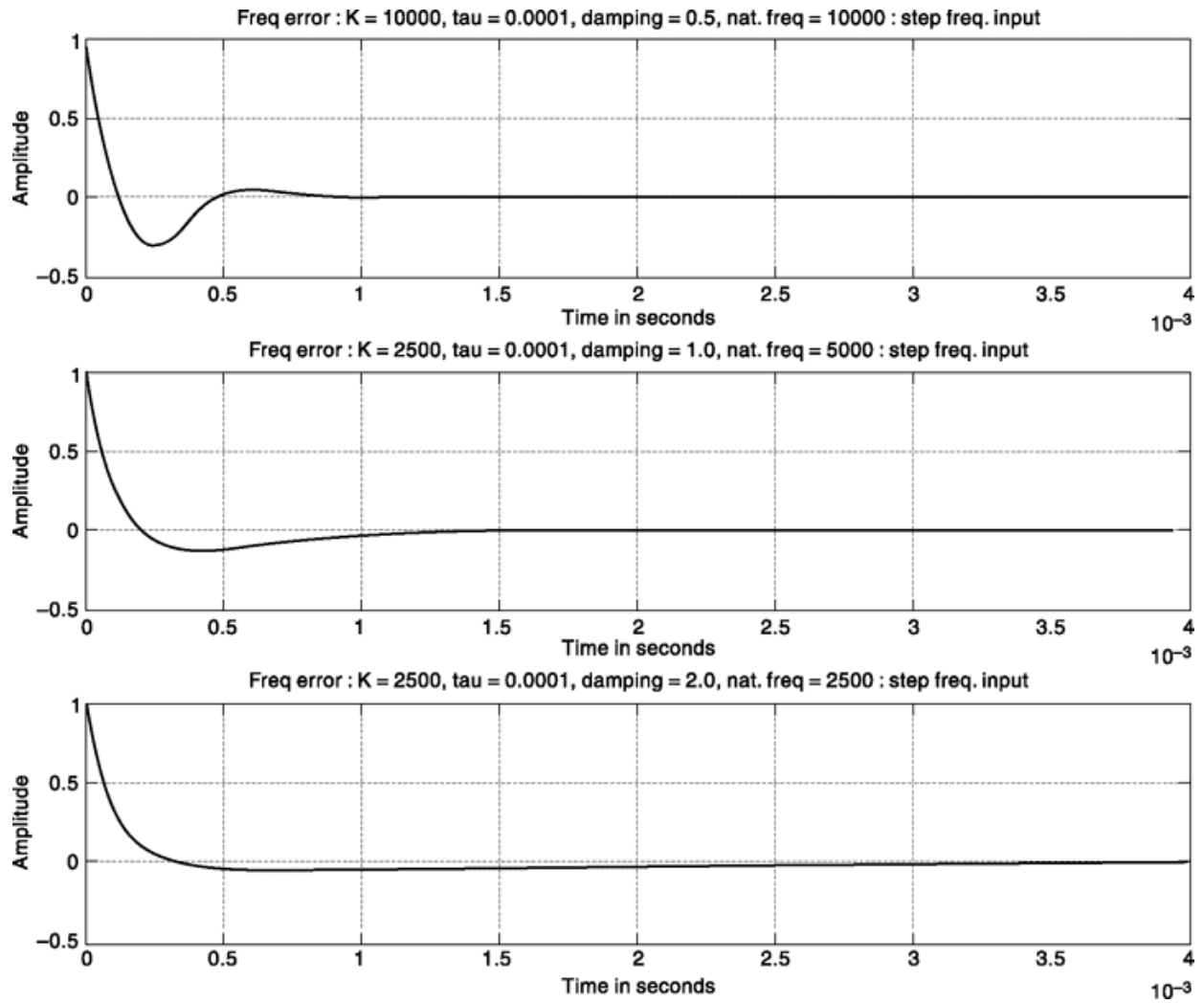
- Experiment 4 0

- Here, we show how frequency error reduces with time following transfer % function described in eqn. (10.26) . The input parameters are K and tau.
- which can be converted to damping factor and natural frequency as given % in eqn. (10.35) . We use step input here.
- We use MATLAB in-built function tf.m to define the PLL transfer function % and lsim.m to simulate its time response.

```
clear; dt = 0.00001; t = 0:dt:0.04; u = ones(1,length(t));
```

```
K = 10^4; tau = 10^(-4); % Defining PLL parameters
```

```
sys1 = tf([1 0 0],[1 1/tau K/tau]); % Defining PLL transfer function
[freq_error t] = lsim(sys1,u,t); % Simulating time response of PLL
subplot(311), plot(t,freq_error); grid;
```



- Here, we show how frequency error reduces with time following transfer % function described in eqn. (10.26) . The input parameters are K and tau.
- which can be converted to damping factor and natural frequency as given % in eqn. (10.35) . We use velocity and acceleration input here.

```
xlabel('TIME IN SECONDS'), ylabel('AMPLITUDE')
title('Freq. Error : K=10000, tau=0.0001, damping=0.5, nat. freq. = 10000 :
step freq. input')
```

- We use MATLAB in-built function tf.m to define the PLL transfer function % and lsim.m to simulate its time response.

```
clear; dt = 0.00001; t = 0:dt:0.0 04;
```

```
u = t; % generating velocity input K = 10 ^A4; tau = 10^A (-4) ;
```

```
sys1 = tf([1 0 0],[1 1/tau K/tau] ) ; % Defining PLL transfer function
[freq_error t] = lsim(sys1,u,t); % Simulating time response of PLL
```

```

subplot(211), plot(t,freq_error); grid; xlabel('TIME IN SECONDS'), ylabel('AMPLITUDE')
title('Freq. Error : K=10000, tau=0.0001, damping=0.5, nat. freq. = 10000 : velocity freq. input')

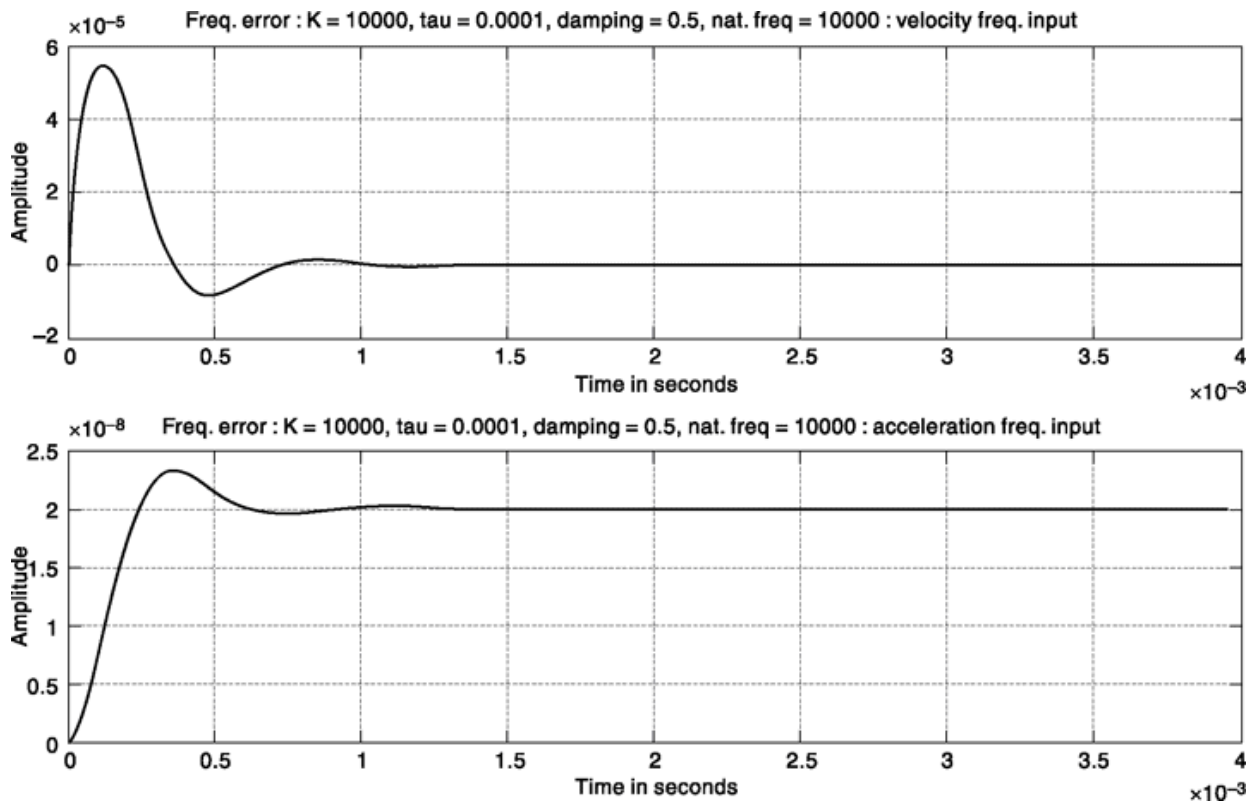
u = t.*t; % generating acceleration input K = 10^A4; tau = 10^A (-4) ;

sys1 = tf([1 0 0],[1 1/tau K/tau]); % Defining PLL transfer function
[freq_error t] = lsim(sys1,u,t); % Simulating time response of PLL

subplot(212), plot(t,freq_error); grid; xlabel('TIME IN SECONDS'), ylabel('AMPLITUDE')
title('Freq. Error : K=10000, tau=0.0001, damping=0.5, nat. freq. = 10000 : acceleration freq. input')

```

Note that, when frequency has a finite steady-state error, phase error (Experiment 39) increases monotonically.

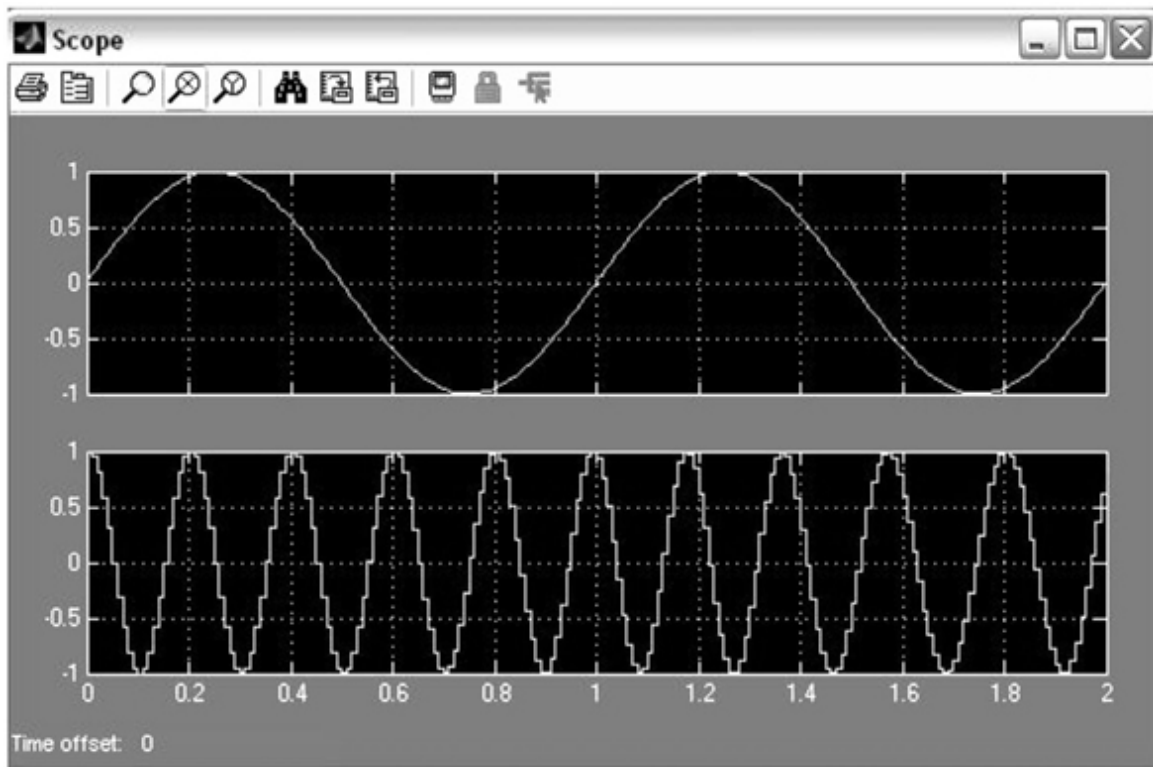


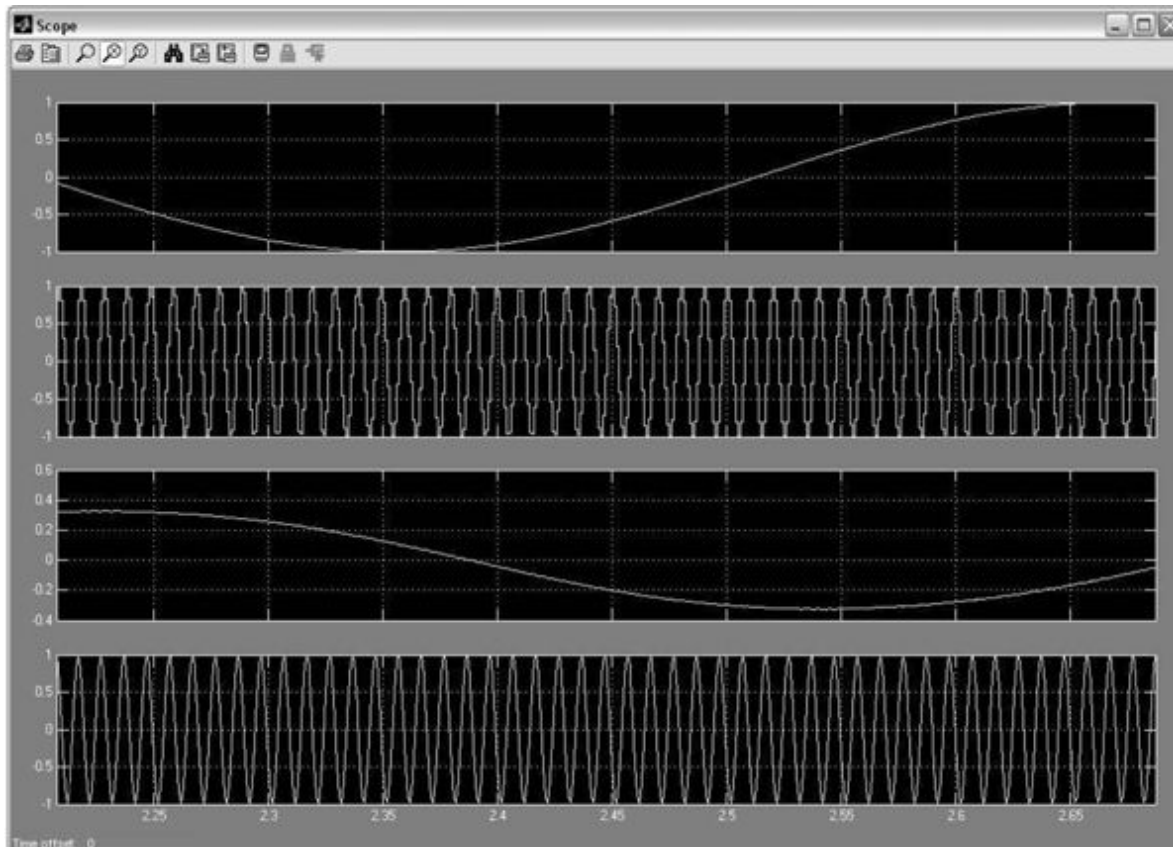
```
% Experiment 42
```

Here, we develop a SIMULINK model of PLL and investigate its frequency tracking ability as well as function as frequency demodulator. We begin by typing ‘simulink’ in MATLAB command window and pressing return. This will open the simulink library browser window. Go to File → new → Model and click left mouse, the model workspace will appear. Using search, find icons shown in the figure, e.g. ‘sine wave’, ‘pll’, etc., and simply drag and drop them one after another in the workspace. Next, you have to set parameters for each block and connect one block to another.

It is easy to recognize each block used in this experiment from its description. A sine wave is used as modulating signal for the FM modulator. The output is shown in the scope. The ‘scope’ icon to start with will have (by default) only one input. We describe below how to connect four inputs to it.

Note that, for this experiment all block parameters are used as available in default except the frequency (rad/sec) of sine wave generator which is set at 10. Also note that, in other blocks frequency parameters are by default expressed in Hz. How to arrive at these parameter settings? Simply double click each block in the workspace and the corresponding window will open as above. As already described, when you first select ‘scope’ block in workspace it has only one input. However, we are interested to see modulating input, Frequency Modulated signal, Demodulated output and also cleaned (purer) carrier frequency. How to do that? Set scope parameters first by double clicking ‘scope’ icon and then in scope window clicking 2nd button from top left. Set ‘number of axes’ = 4 in ‘General’ and uncheck ‘Limit data point to last’ in ‘Data history’. If you place the mouse on each button (don’t need to click), it will describe the function of that.





Connect all the links as shown above by joining corresponding points. This can be done starting from one of the connecting end with left mouse button pressed till you reach the other point. Once this is done, your SIMULINK model is ready for simulation. By default, it runs for 10 seconds. The scope output shown next is for a 3-second simulation. This you can choose by replacing 10 by 3 in the middle of the top workspace buttons. Then simply click the run X button to get output in the scope.

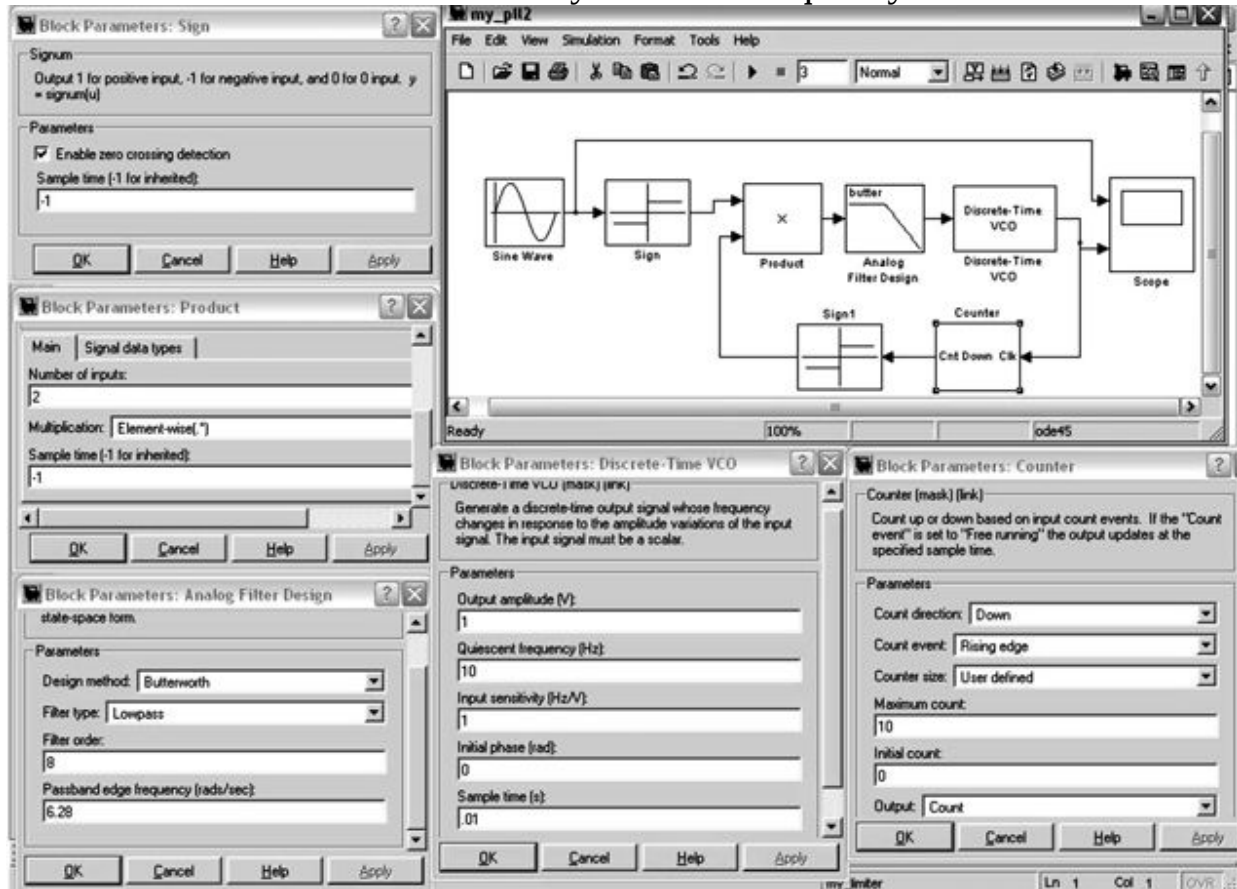
You can see that outputs are generated in 4 axes in same order as it is connected. The first diagram shows we are able to recover the original sinusoidal modulating signal. In the second diagram (by zooming, i.e. clicking x-axis icon with magnifying glass), we can clearly see VCO output has less variation than input in terms of frequency purity. This follows what we discussed in theory.

Once you are satisfied with playing different parameters you can add noise to input through a noise generator block and investigate PLL performance against noisy input.

- Experiment 43

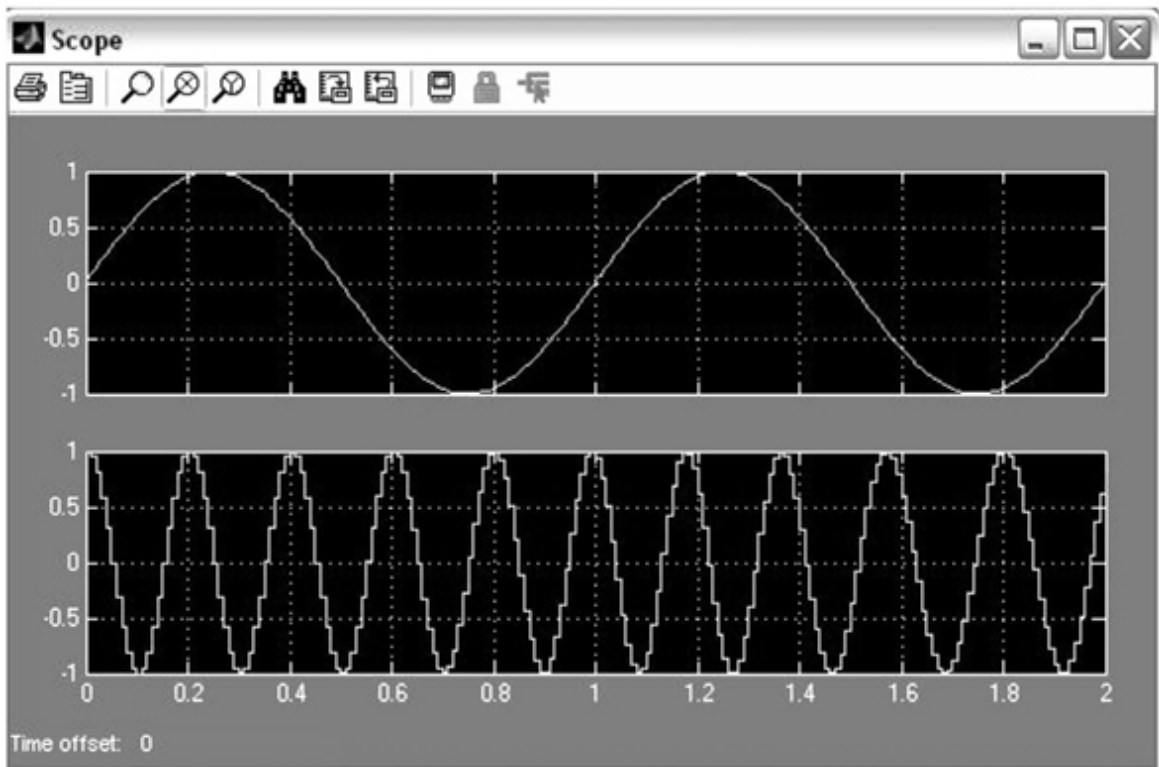
Here, we develop a SIMULINK model of PLL acting as a frequency synthesizer. The output is N times the input frequency. Input frequency is kept 1 Hz (6.28 rad/sec) and output for first case is 10 Hz and second case is 5 Hz. The VCO quiescent (operating) point and counter value are set accordingly. For 10 Hz output, the values chosen for both are 10. Signum function is used to simulate hard limiter behavior and a Butterworth low-pass filter is used as loop filter. The blocks can be found, included and parameterized as discussed in Experiment 42 and as shown next. For rotating a block, select it by left click and press Ctrl+R, else go to Format and click on the appropriate option.

Now for 5 Hz synthesized frequency





Now for 5 Hz synthesized frequency (changing PLL operating point and counter value to 5)



Once again you can play with above and synthesize different frequency outputs from PLL.

SUMMARY

A detailed discussion of Phase-Locked Loops and their applications are presented. After defining basic building blocks, Analog PLL is taken up for detailed analysis. First-and second-order PLLs are thoroughly discussed and important issues of third-order PLL is presented. Ability of PLL to suppress spikes in FM demodulation is shown which results in increase of FM threshold. With introduction of Digital Integrated Circuit based PLLs, Digital PLL has become very popular which differs from Analog PLL by having a digital phase or phase-frequency detector. A detailed discussion on such detectors is presented. The idea of All Digital PLL and Software PLL that offers improved flexibility, testability and other advantages are also discussed. Many interesting applications of PLL are taken up at the end. This includes Carrier recovery, Clock recovery, Frequency synthesis, Frequency and Phase Modulation etc. Both integer and fractional dividers are discussed which is useful in now popular and useful PLL based frequency synthesizers.

PROBLEMS

10.1 Show that if the two inputs to a phase comparator are $V_1(t) = A \cos [w_c t + \theta_x(t)]$ and $V_2(t) = B \cos [w_c t + \theta_2(t)]$, the output of the phase comparator is $v_o(t) = (AB/2) \cos [\theta_x(t) - \theta_2(t)] + (AB/2) \cos [2w_c t + \theta_j(t) + \theta_2(t)]$.

10.2 Show that Eq. (10.2) describes the output of a phase comparator when its input consists of “square” waves rather than sine waves.

10.3 A first-order PLL, with a phase-comparator characteristic as shown in Fig. 10.3b, is initially adjusted so that in the presence of a carrier alone $y = 0$. The VCO has the property that when its input is changed by 1V, its frequency changes by 10^5 Hz. The time constant of the PLL is $t = 10^{-4}$ s.

(a) The carrier is frequency-modulated by a sinusoidal waveform. What is the maximum allowable peak frequency deviation of the carrier if the PLL is to recover the modulating waveform without distortion?

(b) With the frequency deviation at its peak as in (a), make a plot of the PLL output voltage v_n as a function of the frequency of the modulating waveform.

10.4 Derive Eq. (10.12).

10.5 Derive Eq. (10.21).

10.6 A first-order PLL has a phase-comparator characteristic as in Fig. 10.3. The input carrier is unmodulated and the PLL is adjusted so that it is in equilibrium with $y = 0$. By the application of external constraints, the operating point is forced to $y = 3\pi/4$. At the time $t = 0$, these constraints are removed.

(a) Write the differential equation for the phase angle y .

(b) If $t = 10^{-3}$ s, calculate the time at which the operating point reaches B in Fig. 10.3b. Calculate dy/dt at the time the constraints are released and at the time point B is reached.

10.7 A first-order PLL has a phase-comparator characteristic as in Fig. 10.3b. The PLL is adjusted so that, in the presence of a carrier alone, $y = 0$. The time constant of the PLL is $t = 10^{-4}$ s. At time $t = 0$ the carrier is abruptly offset by 5 kHz. Plot y as a function of time up to the point where y attains the value $y = 3\pi/2$.

10.8 A first-order PLL has a phase characteristic as in Fig. 10.3. The PLL is adjusted so that in the presence of a carrier alone $y = -\pi/4$. The time constant of the PLL is $t = 5 \times 10^{-5}$ s and the sensitivity of the VCO is such that a 1V input changes its frequency by 10 kHz. At time $t = 0$ the carrier is abruptly offset by 7.5 kHz (in the direction to increase y) for the interval $0 < t < 10^{-4}$ s. Draw a plot of the output voltage waveform of the PLL.

10.9 A first-order PLL has a phase characteristic as in Fig. 10.3b. In the presence of a carrier alone $y = 0$. The time constant is $t = 10^{-3}$ s and $G_0 = 1$ kHz/volt. At time $t = 0$ the carrier is offset by 0.5 kHz for the interval $0 < t < t_0$, i.e. the frequency of the carrier is modulated by a pulse of duration t_0 .

(a) How long must the pulse last (say $t = t_0$) if at the end of the pulse $y = \pi$ (in which case the subsequent behavior of the PLL is indeterminate).

(b) Assume $t = 0.9t_0$. Draw the waveform at the output of the PLL.

(c) Assume $t = 1.1t_0$. Draw the waveform at the output of the PLL.

10.10 A first-order PLL is used to demodulate the signal $\cos [w_c t + Wt - f_s(t)]$. The VCO is initially operating at a frequency w_c . Assume $W = p/4t$.

(a) Find $v_o(t)$ when $f_s(t) = 0$.

(b) If, after the PLL has reached equilibrium, $f_s(t) = -At$ for $0 < t < 2p/1$ and zero elsewhere, find the minimum value of the product At to *avoid* a spike.

(c) If $f_s(t) = +At$, $0 < t < 2p/1$ and zero elsewhere, find the minimum value of the At product to *avoid* a spike.

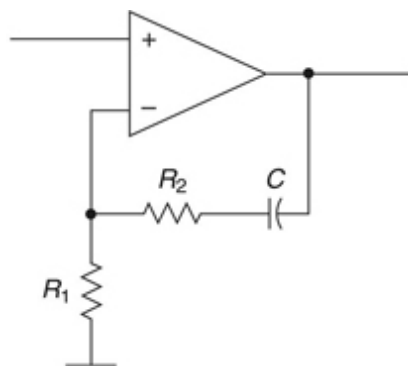
10.11 Find the differential equation of the piecewise-linear second-order PLL in the region in which $p/2 < y < 3p/2$.

10.12 Find the differential equation of the second-order PLL if the phase comparator has a sinusoidal characteristic.

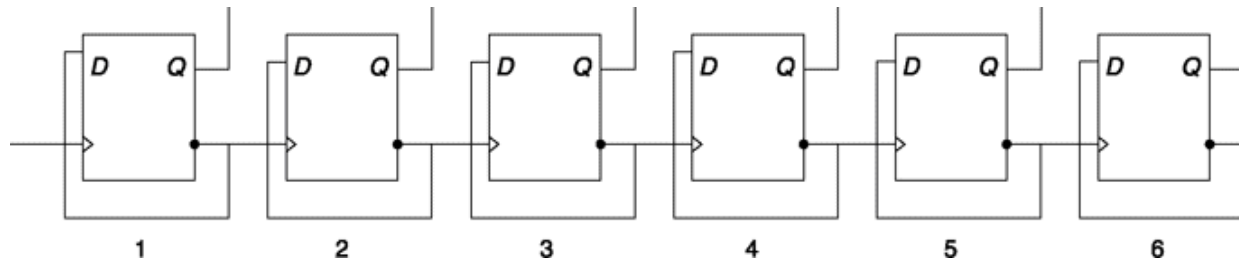
10.13 Show that Fig. 10.9 represents the first-order PLL.

10.14 Plot N/f_M , versus S_t/hf_M at threshold. This is called the *threshold hyperbola* dB and $f_M = 5$ kHz, find N to produce threshold. If $S_i/\eta f_M = 20$

10.15 (a) An active loop filter is given as follows. Find its transfer function $H(s)$. (b) What will be steady-state phase error if this is incorporated in the PLL loop?



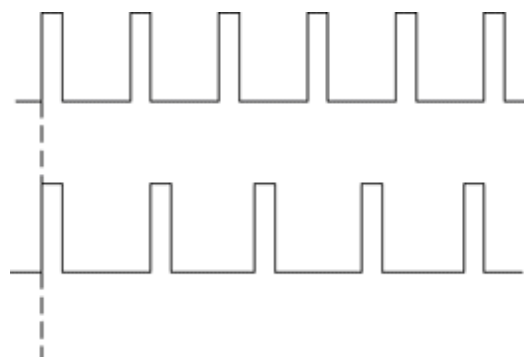
10.16 The following is the logic diagram of a counter. Show wherefrom the output is to be taken if it is used as (a) 32 prescaler, (b) 64 prescaler?



10.17 For an application, channel spacing is 50 kHz while reference source generates a signal of frequency 1 MHz. If required output is 100.25 MHz and a 32/33 prescaler is used as discussed in Sec. 10.5.3, find value of A, B and M.

10.18 For a frequency synthesis application step frequency = 300 kHz. Output frequency range required is 924-927 MHz. With a 64/65 prescaler what range of counter value is needed in A and B? Do you require 8 Flip-Flops for counter B for this?

10.19 If the first waveform is that of input and second that of feedback to a PFD, draw output U and D.



10.20 A step frequency which is input to PLL is 100 kHz. Show how to generate a signal of frequency 1.01 MHz by PLL.

REFERENCES

1. Rice, S. O.: "Time-series Analysis," chap. 25, John Wiley & Sons, Inc., New York, 1963.
2. Schilling, D. L., E. Nelson, and K. Clarke: Discriminator Response to an FM Signal in a Fading Channel, *IEEE Trans. Commun. Tech.*, April, 1967.
F M Discriminator, *IEEE Trans. Commun. Tech*, August, 1967.
Nelson, E., and D. L. Schilling: The Response of an FM Discriminator to a Digital FM Signal in Randomly Fading Channels, *IEEE Trans. Commun. Tech*, August, 1968.
3. Schilling, D. L.: The Response of an APC System to FM Signals and Noise, *Proc. IEEE*, October, 1963.
4. Schilling, D. L., and J. Billing: Threshold Extension Capability of the PLL and the FMFB, *Proc. IEEE*, May, 1964.

5. Osborne, P., and D. L. Schilling: Threshold Response of a Phase Locked Loop, *Proc. Int. Conf. Commun.*, 1968.

6. Hoffman, E., and D. L. Schilling: Threshold of the FMFB, *Proc., Int. Conf. Commun.*, 1969.

11

OPTIMAL RECEPTION OF DIGITAL SIGNAL

CHAPTER OBJECTIVE

In previous chapters, we have seen that digital data can be transmitted directly (baseband) or, as is usually the case, by modulating a carrier (passband). The received signal is corrupted by noise, and hence there is a finite probability that the receiver will make an error in determining within each time interval, whether a 1 or 0 is transmitted. In this chapter, we discuss various issues towards optimal receiver design with an objective to reduce error probability in reception. These include topics like maximum likelihood detector, matched filter, correlator, use of signal space, etc. Next, error probability of different digital modulation schemes under noise is calculated. A comparison that considers signal-to-noise ratio, spectral efficiency and error probability is presented at the end. Besides numerical examples, the chapter also presents MATLAB based simulations where we introduce a new feature, i.e. command line entry of input parameters.

FACTS AND FIGURES

Dwight North was born in Hartford, Connecticut, and was educated at Wesleyan University and at Caltech, from which he received a Ph.D in Physics in 1933. From 1934 until his retirement in 1974, he worked for Radio Corporation of America (RCA). He was the first to formalize the concept of ‘Matched Filter’ which first got published in classified report of RCA Labs in 1943 and later in IEEE Proceedings in 1963. This report introduced not only the matched filter, but also the Rice distribution, the concept of false alarms to set a detection threshold, studies of pre-detection and post-detection integration, etc.

Dr. North’s interest in noise problems was extended to the naming of the street on which he was a longtime resident in Princeton, ‘Random Road’. Interestingly, the term ‘Matched Filter’ was coined by David Middleton and

J.H. Van Vleck, who independently arrived at the same result and published their work in 1946.

11.1 A BASEBAND SIGNAL RECEIVER

Consider that a binary-encoded signal consists of a time sequence of voltage levels +V or -V. If there is a guard interval between the bits, the signal forms a sequence of positive and negative pulses. In either case there is no particular interest in preserving the waveform of the signal after reception. We are interested only in knowing within each bit interval whether the transmitted voltage was +V or -V. With noise present, the received signal and noise together will yield sample values generally different from $\pm V$. In this case, what deduction shall we make from the sample value concerning the transmitted bit?

Suppose that the noise is Gaussian and therefore the noise voltage has a probability density which is entirely symmetrical with respect to zero volts. Then the probability that the noise has increased the sample value is the same as the probability that the noise has decreased the sample value. It then seems entirely reasonable that we can do no better than to assume that if the sample value is positive the transmitted level was +V, and if the sample value is negative the transmitted level was -V. It is, of course, possible that at the sampling time the noise voltage may be of magnitude larger than V and of a polarity opposite to the polarity assigned to the transmitted bit. In this case an error will be made as indicated in Fig. 11.1. Here the transmitted bit is represented by the voltage +V, which is sustained over an interval T from t_1 to t_2 . Noise has been superimposed on the level +V so that the voltage v represents the received signal and noise.

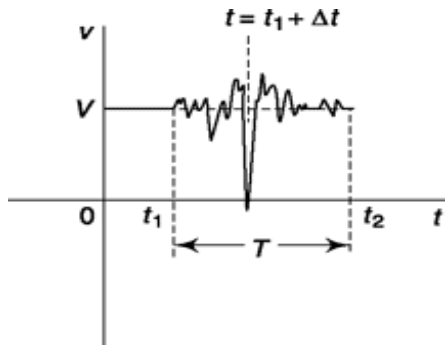


Fig. 11.1 Illustration that noise may cause an error in the determination of a transmitted voltage level.

If now the sampling should happen to take place at a time $t = t_1 + At$, an error will have been made.

We can reduce the probability of error by processing the received signal plus noise in such a manner that we are then able to find a sample time where the sample voltage due to the signal is emphasized relative to the sample voltage due to the noise. Such a processer (receiver) is shown in Fig. 11.2. The signal input during a bit interval is indicated. As a matter of convenience, we have set $t = 0$ at the beginning of the interval. The waveform of the signal $s(t)$ before $t = 0$ and after $t = T$ has not been indicated since, as will appear, the operation of the receiver during each bit interval is independent of the waveform during past and future bit intervals.

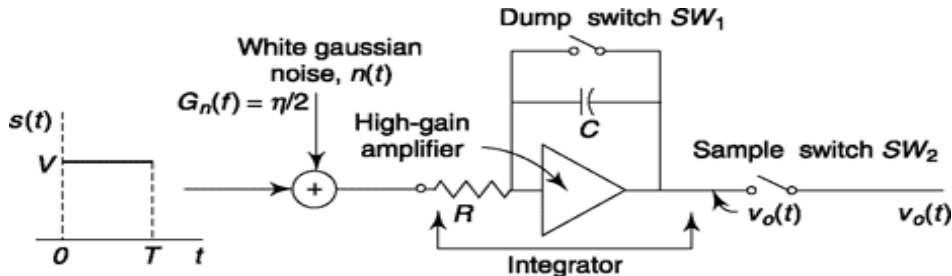


Fig. 11.2 A receiver for a binary-coded signal.

The signal $s(t)$ with added white Gaussian noise $n(t)$ of power spectral density $h/2$ is presented to an integrator. At time $t = 0$ we require that capacitor C be uncharged. Such a discharged condition may be ensured by a brief closing of switch SW_1 at time $t = 0-$, thus relieving C of any charge it may have acquired during the previous interval. The sample is taken at the output of the integrator by closing this sampling switch SW_2 . This sample is taken at the end of the bit interval, at $t = T$. The signal processing indicated in Fig. 11.2 is described by the phrase *integrate and dump*, the term *dump* referring to the abrupt discharge of the capacitor after each sampling.

Peak Signal to RMS Noise Output Voltage Ratio

The integrator yields an output which is the integral of its input multiplied by $1/RC$. Using $t = RC$, we have

$$v_o(T) = \frac{1}{\tau} \int_0^T [s(t) + n(t)] dt = \frac{1}{\tau} \int_0^T s(t) dt + \frac{1}{\tau} \int_0^T n(t) dt \quad (11.1)$$

The sample voltage due to the signal is

$$s_o(T) = \frac{1}{\tau} \int_0^T V dt = \frac{VT}{\tau} \quad (11.2)$$

The sample voltage due to the noise is

$$n_o(T) = \frac{1}{\tau} \int_0^T n(t) dt \quad (11.3)$$

This noise-sampling voltage $n_o(T)$ is a Gaussian random variable in contrast with $n(t)$, which is a Gaussian random process.

The variance of $n_o(T)$ was found in Sec. 7.4 [see Eq. (7.63)] to be

$$\sigma_o^2 = \overline{n_o^2(T)} = \frac{\eta T}{2\tau^2} \quad (11.4)$$

and, as noted in Sec. 7.2.1, $n_o(T)$ has a Gaussian probability density.

The output of the integrator, before the sampling switch, is $v_o(t) = s_o(t) + n_o(t)$. As shown in Fig. 11.3a, the signal output $s_o(t)$ is a ramp, in each bit interval, of duration T . At the end of the interval the ramp attains the voltage $s_o(T)$ which is $+VT/t$ or $-VT/t$, depending on whether the bit is a 1 or a 0. At the end of each interval the switch SW_1 in Fig. 11.2 closes momentarily to discharge the capacitor so that $s_o(t)$ drops to zero. The noise $n_o(t)$, shown in Fig. 11.3b, also starts each interval with $n_o(0) = 0$ and has the random value $n_o(T)$ at the end of each interval. The sampling switch SW_2 closes briefly just before the closing of SW_1 and hence reads the voltage

$$v_o(T) = s_o(T) + n_o(T) \quad (11.5)$$

We would naturally like the output signal voltage to be as large as possible in comparison with the noise voltage. Hence, a **figure of merit** of interest is the signal-to-noise ratio

$$\frac{[s_o(T)]^2}{[n_o(T)]^2} = \frac{2}{\eta} V^2 T \quad (11.6)$$

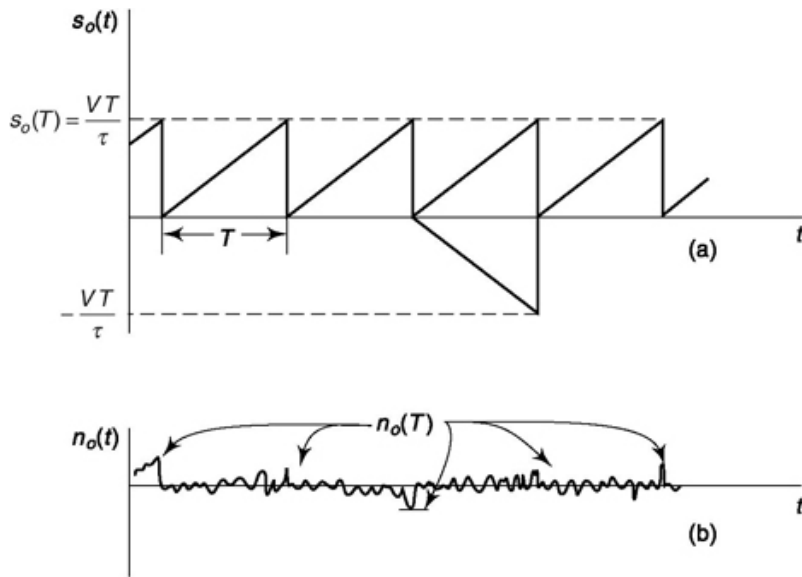


Fig. 11.3 (a) The signal output, and (b) the noise output of the integrator of Fig. 11.2.

This result is calculated from Eqs (11.2) and (11.4). Note that the signal-to-noise ratio increases with increasing bit duration T and that it depends on $V^2 T$ which is the normalized energy of the bit signal. Therefore, a bit represented by a narrow, high amplitude signal and one by a wide, low amplitude signal are equally effective, provided $V^2 T$ is kept constant.

It is instructive to note that the integrator filters the signal and the noise such that the signal voltage increases linearly with time, while the standard deviation (rms value) of the noise increases more slowly, as VT . Thus, the integrator enhances the signal relative to the noise, and this enhancement increases with time as shown in Eq. (11.6).

11.2 PROBABILITY OF ERROR

Since the function of a receiver of a data transmission is to distinguish the bit 1 from the bit 0 in the presence of noise, a most important characteristic is the probability that an error will be made in such a determination. We now calculate this error probability P_e for the integrate-and-dump receiver of Fig. 11.2.

We have seen that the probability density of the noise sample $n_o(T)$ is Gaussian and hence appears as in Fig. 11.4. The density is therefore given by

$$f[n_o(T)] = \frac{e^{-n_o^2(T)/2\sigma_o^2}}{\sqrt{2\pi\sigma_o^2}}$$

where σ_o^2 , the variance, is $\sigma_o^2 = nO(T)$ given by Eq. (11.4). Suppose, then, that during some bit interval the input-signal voltage is held at, say, $-V$. Then, at the sample time, the signal sample voltage is $s_o(T) = -VT/t$, while the noise sample is $n_o(T)$. If $n_o(T)$ is positive and larger in magnitude than VT/t , the total sample voltage $v_o(T) = s_o(T) + n_o(T)$ will be positive. Such a positive sample voltage will result in an error, since as noted earlier, we have instructed the receiver to interpret such

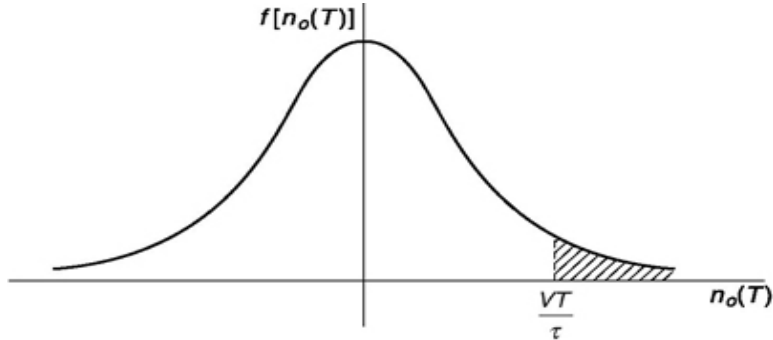


Fig. 11.4 The Gaussian probability density of the noise sample $n_o(T)$.

a positive sample voltage to mean that the signal voltage was $+V$ during the bit interval. The probability of such a misinterpretation, that is, the probability that $n_o(T) > VT/t$, is given by the area of the shaded region in Fig. 11.4. The probability of error is, using Eq. (11.7).

$$P_e = \int_{VT/\tau}^{\infty} f[n_o(T)] dn_o(T) = \int_{VT/\tau}^{\infty} \frac{e^{-n_o^2(T)/2\sigma_o^2}}{\sqrt{2\pi\sigma_o^2}} dn_o(T) \quad (11.8)$$

Defining $x \equiv n_o(T)/\sqrt{2\sigma_o^2}$, and using Eq. (11.4), Eq. (11.8) may be rewritten as

$$P_e = \frac{1}{2} \frac{2}{\sqrt{\pi}} \int_{x=V\sqrt{T/\eta}}^{\infty} e^{-x^2} dx = \frac{1}{2} \operatorname{erfc}\left(V\sqrt{\frac{T}{\eta}}\right) = \frac{1}{2} \operatorname{erfc}\left(\frac{V^2 T}{\eta}\right)^{1/2} = \frac{1}{2} \operatorname{erfc}\left(\frac{E_s}{\eta}\right)^{1/2} \quad (11.9)$$

in which $E_s = V^2 T$ is the signal energy of a bit.

If the signal voltage were held instead at $+V$ during some bit interval, then it is clear from the symmetry of the situation that the probability of error would again be given by P_e in Eq. (11.9). Hence Eq. (11.9) gives P_e quite generally.

The probability of error P_e , as given in Eq. (11.9), is plotted in Fig. 11.5. Note that P_e decreases rapidly as $|E_s|$ increases. The maximum value of P_e is 1. Thus, even if the signal is entirely lost in the noise so that any

determination of the receiver is a sheer guess, the receiver cannot be wrong more than half the time on the average.

11.2.1 Optimum Threshold: Maximum Likelihood Detector and Bayes' Receiver

We have seen in previous section that when binary data 1 and 0 are associated with +V and -V respectively then decision threshold is set at 0. Intuitively we can say that it makes probability of error minimum. Such is the case if both symbols are equally probable and probability densities are symmetric like Gaussian. How to decide decision threshold when apriori probabilities are not equal? Note that in Sec. 6.2.5 and Sec. 6.4.7, we developed the background of this discussion. Here, we develop a general theory for setting such thresholds.

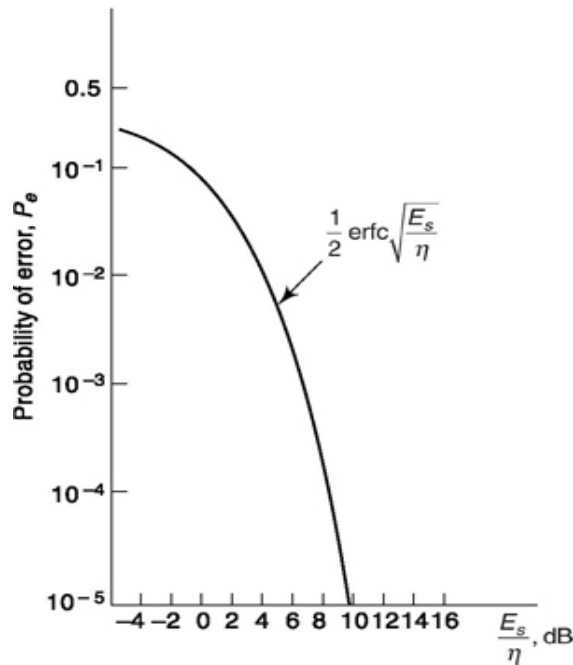


Fig. 11.5 Variation of P_e versus E_s/η -

Consider, when symbol sent is s_x , the probability of receiving voltage v is $P(v/s_x)$ and for symbol sent s_2 it is $P(v/s_2)$. We define apriori probability of presence of these symbols as $P(s_x)$ and $P(s_2)$ respectively. The decision threshold l is such that for $v > l$, symbol s_1 is selected and for $v < l$, symbol s_2 is selected. Then probability of error

$$P_e = P(s_1) \int_{v < \lambda} p(v/s_1) dv + P(s_2) \int_{v > \lambda} p(v/s_2) dv \quad (11.10)$$

Since, some voltage v is received for certain when symbol s_1 is sent we can write

$$\int_{v > \lambda} p(v/s_1) dv + \int_{v < \lambda} p(v/s_1) dv = 1 \quad (11.11)$$

From Eq. (11.10) and (11.11),

$$\begin{aligned} P_e &= P(s_1) \left[1 - \int_{v > \lambda} p(v/s_1) dv \right] + P(s_2) \int_{v > \lambda} p(v/s_2) dv \\ &= P(s_1) + \int_{v > \lambda} [P(s_2)p(v/s_2) - P(s_1)p(v/s_1)] dv \end{aligned} \quad (11.12)$$

Thus, probability of error is minimum if for every $v > \lambda$,

$$P(s_1)p(v/s_1) > P(s_2)p(v/s_2) \quad (11.13)$$

$$\text{or } \frac{p(v/s_1)}{p(v/s_2)} > \frac{P(s_2)}{P(s_1)} \quad (11.14)$$

$$\text{Thus at decision boundary } v = \lambda, \quad \frac{p(\lambda/s_1)}{p(\lambda/s_2)} = \frac{P(s_2)}{P(s_1)} \quad (11.15)$$

Figure 11.6 shows a pictorial presentation of this with symmetrical Gaussian distribution of conditional probabilities. Fig. 11.6a is the case when a priori probabilities are equal. For unequal a priori probabilities we plot $P(s_1)p(v/s_1)$ and $P(s_2)p(v/s_2)$ separately and their intersection as shown in the diagram gives decision threshold according to Eq. (11.15).

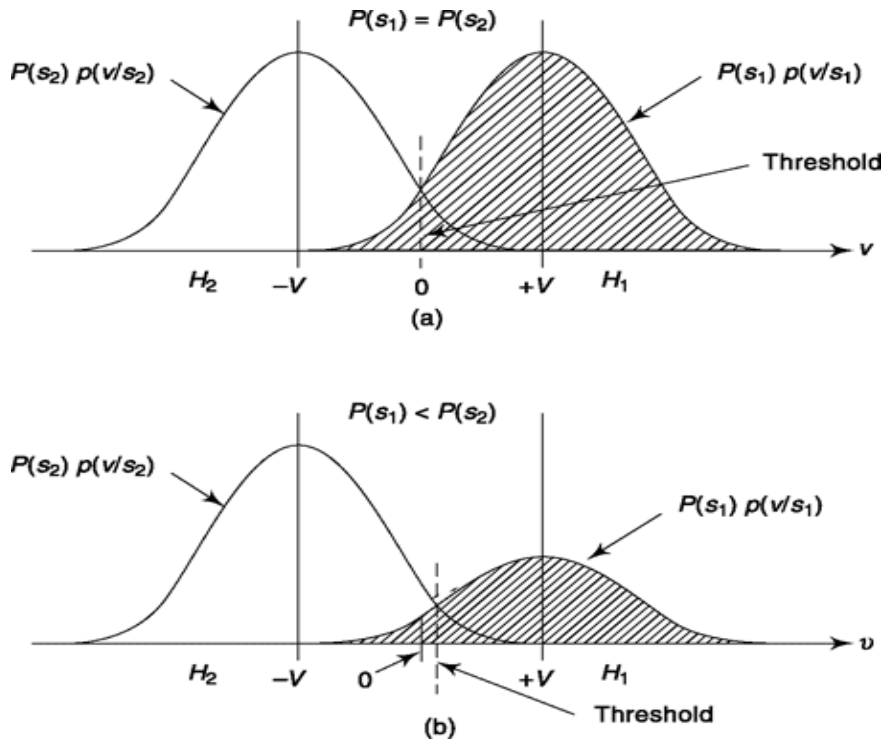


Fig. 11.6 Decision threshold when a priori probabilities are (a) equal, (b) unequal.

Equation (11.14) can be used as maximum likelihood detector. If the condition is valid then symbol sent is most likely to be s_1 when received voltage is v (Hypothesis H_x) and if left-hand side is less than right-hand side symbol sent is most likely to be s_2 with received voltage v (Hypothesis H_2). This is often represented in the form of following equation.

$$\frac{p(v/s_1)}{p(v/s_2)} \stackrel{H_1}{>} \frac{P(s_2)}{P(s_1)} \quad (11.16)$$

This means, if likelihood ratio exceeds ratio of a priori probabilities hypothesis H_1 is chosen, if not then hypothesis H_2 is chosen. If they are equal any of H_1 or H_2 can be chosen and it will contribute equally to probability of error. Example 11.1 shows calculation of optimal threshold and resulting error for Gaussian noise. Example 11.2 incorporates findings of Matched Filter receiver of Sec. 11.1 and arrives at same probability of error as shown in Eq. (11.9) using optimal threshold.

Note that a generalized *Bayes' receiver* may include cost of decision making, more appropriately cost of making a wrong decision by receiver and accordingly decide optimal threshold. If C_{12} is cost of selecting s_1 when s_2 is transmitted and C_{21} is cost of selecting s_2 when s_1 is transmitted then s_1 is

selected by receiver if following condition is fulfilled else symbol s_2 is selected.

$$C_{21}P(s_1)p(v/s_1) > C_{12}P(s_2)p(v/s_2) \quad (11.17)$$

Refer to Example 11.4 for calculation of such decision threshold for Gaussian noise contamination. Note that, in subsequent sections we shall generally discuss receiver design considering prior probabilities and cost to be equal. However, if that is not so, concepts derived here can be used to modify those results.

Example 11.1

(a) Find decision threshold if conditional probability density functions after addition of noise are of Gaussian distribution and voltage V_1 represents symbol s_1 and V_2 symbol s_2 for no noise case. Show the threshold when a priori probabilities are equal for (b) bipolar signal $V_1 = +V$ and $V_2 = -V$, (c) unipolar signal $V_1 = +V$ and $V_2 = 0$

Solution

(a) If noise is Gaussian, then the conditional probabilities will have mean V_1 for symbol s_1 and V_2 for symbol s_2 so that

$$p(v/s_1) = \frac{1}{\sqrt{2\pi\sigma_n^2}} \exp\left[-\frac{(v-V_1)^2}{2\sigma_n^2}\right] \quad (11.18a)$$

$$\text{and } p(v/s_2) = \frac{1}{\sqrt{2\pi\sigma_n^2}} \exp\left[-\frac{(v-V_2)^2}{2\sigma_n^2}\right] \quad (11.18b)$$

Substituting above in Eq. (11.15) and taking log of both sides, we get

$$\begin{aligned} -\frac{(\lambda - V_1)^2 - (\lambda - V_2)^2}{2\sigma_n^2} &= \ln[P(s_2)/P(s_1)] \\ 2\lambda(V_1 - V_2) + (V_1^2 - V_2^2) &= 2\sigma_n^2 \ln[P(s_2)/P(s_1)] \\ \lambda &= [(V_1^2 - V_2^2) + 2\sigma_n^2 \ln\{P(s_2)/P(s_1)\}] / 2(V_1 - V_2) \\ \lambda &= \frac{V_1 + V_2}{2} + \frac{\sigma_n^2 \ln\{P(s_2)/P(s_1)\}}{(V_1 - V_2)} \end{aligned} \quad (11.19)$$

Example 11.2

(a) Calculate generalized expression for probability of error for Example 11.1 when decision threshold is set at optimum value. (b) Find the expression of probability of error when symbols are equally probable, (c) Show for (b) if calculation is done at Matched Filter output discussed in Sec. 11.1, we arrive at same expression as given in Eq. 11.9. Fig. 11.7 gives pictorial presentation of function $\text{erfc}(x)$ and some of its properties.

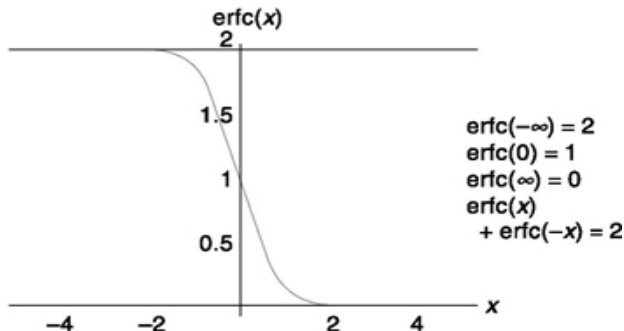


Fig. 11.7 The plot of $\text{erfc}(x)$ vs. x .

Solution

(a) From Eq. (11.10), probability of error

$$P_e = P(s_1) \int_{v < \lambda} p(v/s_1) dv + P(s_2) \int_{v > \lambda} p(v/s_2) dv$$

$$P_e = P(s_1) \int_{v < \lambda} \frac{1}{\sqrt{2\pi}\sigma_n} \exp\left[-\frac{(v-V_1)^2}{2\sigma_n^2}\right] dv + P(s_2) \int_{v > \lambda} \frac{1}{\sqrt{2\pi}\sigma_n} \exp\left[-\frac{(v-V_2)^2}{2\sigma_n^2}\right] dv$$

where, $\lambda = \frac{V_1+V_2}{2} + \frac{\sigma_n^2 \ln\{P(s_2)/P(s_1)\}}{(V_1-V_2)}$

Substituting $\frac{v-V_1}{\sqrt{2}\sigma_n} = y$ in 1st integral and
 $\frac{v-V_2}{\sqrt{2}\sigma_n} = z$ in 2nd integral

$$P_e = \frac{P(s_1)}{\sqrt{\pi}} \int_{v < \lambda_1} \exp[-y^2] dy + \frac{P(s_2)}{\sqrt{\pi}} \int_{v > \lambda_2} \exp[-z^2] dz \quad (11.20)$$

where, $\lambda_1 = \frac{\lambda - V_1}{\sqrt{2}\sigma_n}$

$$= \frac{\frac{V_1+V_2}{2} + \frac{\sigma_n^2 \ln\{P(s_2)/P(s_1)\}}{(V_1-V_2)} - V_1}{\sqrt{2}\sigma_n}$$

$$= \frac{\frac{V_2 - V_1}{2} + \frac{\sigma_n \ln\{P(s_2)/P(s_1)\}}{\sqrt{2}(V_1-V_2)}}{\sqrt{2}\sigma_n}$$

and $\lambda_2 = \frac{\lambda - V_2}{\sqrt{2}\sigma_n}$

$$= \frac{\frac{V_1+V_2}{2} + \frac{\sigma_n^2 \ln\{P(s_2)/P(s_1)\}}{(V_1-V_2)} - V_2}{\sqrt{2}\sigma_n}$$

$$= \frac{\frac{V_1 - V_2}{2} + \frac{\sigma_n \ln\{P(s_2)/P(s_1)\}}{\sqrt{2}(V_1-V_2)}}{\sqrt{2}\sigma_n}$$

$$P_e = \frac{P(s_1)}{2} [\operatorname{erfc}(-\infty) - \operatorname{erfc}(\lambda_1)] + \frac{P(s_2)}{2} \operatorname{erfc}(\lambda_2)$$

$$P_e = \frac{P(s_1)}{2} [2 - \operatorname{erfc}(\lambda_1)] + \frac{P(s_2)}{2} \operatorname{erfc}(\lambda_2) \quad (11.21a)$$

$$P_e = \frac{1}{2} \left[2P(s_1) - P(s_1) \operatorname{erfc} \left(\frac{V_2 - V_1}{2\sqrt{2}\sigma_n} \right) + \frac{\sigma_n \ln \{P(s_2)/P(s_1)\}}{\sqrt{2(V_1 - V_2)}} \right] + P(s_2) \operatorname{erfc} \left(\frac{V_1 - V_2}{2\sqrt{2}\sigma_n} \right) + \frac{\sigma_n \ln \{P(s_2)/P(s_1)\}}{\sqrt{2(V_1 - V_2)}} \right] \quad (11.21b)$$

(b) When $P(s_1) = 0.5$, $P(s_2) = 0.5$. Substituting

$$P_e = \frac{1}{2} \left[1 - 0.5 \times \operatorname{erfc} \left(\frac{V_2 - V_1}{2\sqrt{2}\sigma_n} \right) + 0.5 \times \operatorname{erfc} \left(\frac{V_1 - V_2}{2\sqrt{2}\sigma_n} \right) \right]$$

Since $\operatorname{erfc}(x) = 2 - \operatorname{erfc}(-x)$

$$P_e = \frac{1}{2} \left[1 - 0.5 \times \left\{ 2 - \operatorname{erfc} \left(\frac{V_1 - V_2}{2\sqrt{2}\sigma_n} \right) \right\} + 0.5 \times \operatorname{erfc} \left(\frac{V_1 - V_2}{2\sqrt{2}\sigma_n} \right) \right]$$

$$P_e = \frac{1}{2} \left[\operatorname{erfc} \left(\frac{V_1 - V_2}{2\sqrt{2}\sigma_n} \right) \right] \quad (11.22)$$

(c) For Matched filter discussed in Sec. 11.1, from Eq. (11.2)

$$V_1 = +\frac{VT}{\tau} \text{ and } V_2 = -\frac{VT}{\tau} \text{ such that}$$

$$V_1 - V_2 = \frac{2VT}{\tau}$$

$$\text{From Eq. (11.14), } \sigma_n = \sqrt{\frac{\eta T}{2\tau^2}}$$

$$\begin{aligned} \text{Substituting, } P_e &= \frac{1}{2} \left[\operatorname{erfc} \left(\frac{2VT/\tau}{2\sqrt{2}} \sqrt{\frac{2\tau^2}{\eta T}} \right) \right] \\ &= \frac{1}{2} \operatorname{erfc} \left(\sqrt{\frac{V^2 T}{\eta}} \right) \end{aligned}$$

Hence, proved.

Example 11.3

- (a) Find optimal threshold and probability of error from relations derived from Example 11.2(a) for Gaussian noise contamination when prior probability of $s_1 = 0.4$, noise variance = 10^{-3} and $V_1 = +1V$ and $V_2 = -1V$.
 (b) Find threshold and probability of error if noise variance = 0.1.

Solution

$$P_e = \frac{1}{2} [0.8 - 0.4 \operatorname{erfc}(-2.2361 + 0.0453) \\ - 0.6 \operatorname{erfc}(+2.361 + 0.0453)]$$

$$P_e = \frac{1}{2} [0.8 - 0.4 \times 1.9981 + 0.6 \times 0.0013] \\ = 0.0021$$

Note that in equal probable cases it will be 0 V. Also note that since $P(s_1)$ is smaller than $P(s_2)$ threshold is positive as expected from Fig. 11.6.

Probability of error

$$P_e = \frac{1}{2} \left[2 \times 0.4 - 0.4 \operatorname{erfc} \left(\frac{-2}{2\sqrt{0.002}} + \frac{\ln(1.5)}{2\sqrt{2000}} \right) + 0.6 \operatorname{erfc} \left(\frac{2}{2\sqrt{0.002}} + \frac{\ln(1.5)}{2\sqrt{2000}} \right) \right]$$

$$P_e = \frac{1}{2} [0.8 - 0.4 \operatorname{erfc}(-22.3607 + 0.0045) - 0.6 \operatorname{erfc}(+22.3607 + 0.0045)]$$

$$P_e = \frac{1}{2} [0.8 - 0.4 \times 2 + 0.6 \times 0] \\ = 0 \text{ (negligibly small)}$$

(b) Decision threshold

$$\lambda = \frac{+1-1}{2} + \frac{10^{-1} \ln(0.6/0.4)}{1-0} = 0.0203 \text{ V}$$

Probability of error

$$P_e = \frac{1}{2} \left[2 \times 0.4 - 0.4 \operatorname{erfc} \left(\frac{-2}{2\sqrt{0.2}} + \frac{\ln(1.5)}{2\sqrt{20}} \right) + 0.6 \operatorname{erfc} \left(\frac{2}{2\sqrt{0.2}} + \frac{\ln(1.5)}{2\sqrt{20}} \right) \right]$$

$$P_e = \frac{1}{2} [0.8 - 0.4 \operatorname{erfc}(-2.236) + 0.0453) \\ - 0.6 \operatorname{erfc}(+2.361 + 0.0453)]$$

$$P_e = \frac{1}{2} [0.8 - 0.4 \times 1.9981 + 0.6 \times 0.0013] \\ = 0.0021$$

Example 11.4

(a) Find decision threshold for a generalized Bayes ' receiver for Gaussian noise contamination, voltage V_1 represents symbol s_1 , V_2 symbol s_2 for no noise case.

(b) Find decision threshold under following condition : cost of selecting s_1 when s_2 is transmitted = 0.7, prior probability of s_1 = 0.4, Gaussian noise variance = 10^{-3} and $V_1 = +1V$ and $V_2 = -1V$.

Solution

From Eq. (11.17) at decision boundary, $C_{2l}P(s_x) p^{(v/s_1)} = C_{12}P(s_2)p^{(v/s_2)}$

Substituting using Eq. (11.18a) and (11.18b) and taking natural log of both sides

$$-\frac{(\lambda - V_1)^2 - (\lambda - V_2)^2}{2\sigma_n^2} = \ln \left[\frac{C_{12} P(s_2)}{C_{21} P(s_1)} \right]$$

$$\text{or } 2\lambda(V_1 - V_2) - (V_1^2 - V_2^2) = 2\sigma_n^2 \ln \left[\frac{C_{12} P(s_2)}{C_{21} P(s_1)} \right]$$

$$\text{or } \lambda = \frac{V_1 + V_2}{2} + \frac{\sigma_n^2 \ln \left[\frac{C_{12} P(s_2)}{C_{21} P(s_1)} \right]}{(V_1 - V_2)} \quad (11.23)$$

(b) $C_{12} = 0.7$ then $C_{21} = 1 - 0.7 = 0.3$

$P(s_1) = 0.4$ then $P(s_2) = 1 - 0.4 = 0.6$

Decision threshold

$$\begin{aligned} \lambda &= \frac{1-1}{2} + \frac{10^{-3} \times \ln \left[\frac{0.7 \times 0.6}{0.3 \times 0.4} \right]}{1-(-1)} \\ &= 0.6264 \text{ mV} \end{aligned}$$

Compare this with result obtained in Example 11.3a.

$$-\frac{(\lambda - V_1)^2 - (\lambda - V_2)^2}{2\sigma_n^2} = \ln \left[\frac{C_{12} P(s_2)}{C_{21} P(s_1)} \right]$$

$$\text{or } 2\lambda(V_1 - V_2) - (V_1^2 - V_2^2) = 2\sigma_n^2 \ln \left[\frac{C_{12} P(s_2)}{C_{21} P(s_1)} \right]$$

$$\text{or } \lambda = \frac{V_1 + V_2}{2} + \frac{\sigma_n^2 \ln \left[\frac{C_{12} P(s_2)}{C_{21} P(s_1)} \right]}{(V_1 - V_2)} \quad (11.23)$$

(b) $C_{12} = 0.7$ then $C_{21} = 1 - 0.7 = 0.3$

$P(s_1) = 0.4$ then $P(s_2) = 1 - 0.4 = 0.6$

Decision threshold

$$\lambda = \frac{1-1}{2} + \frac{10^{-3} \times \ln \left[\frac{0.7 \times 0.6}{0.3 \times 0.4} \right]}{1 - (-1)}$$

$$= 0.6264 \text{ mV}$$

Compare this with result obtained in Example 11.3a.

SELF-TEST QUESTIONS

1. In the phrase *integration and dump*, does the term *dump* refer to abrupt discharge of a capacitor?
2. In integration and dump receiver, the integration process enhances signal energy more than noise energy. Is the statement correct?
3. Maximum likelihood detector is an optimal detector in the sense of setting optimal decision threshold that gives minimum error probability. Is that true?
4. If prior probabilities are not equal then the decision threshold can be pushed towards higher probability conditional pdf than equal probable case to get lower probability of error. Is that correct?

11.3 OPTIMAL RECEIVER DESIGN

In the receiver system of Fig. 11.2, the signal was passed through a filter (i.e. the integrator), so that at the sampling time the signal voltage might be emphasized in comparison with the noise voltage. We are naturally led to ask whether the integrator is the optimum filter for the purpose of minimizing the probability of error. We shall find that for the received signal contemplated in the system of Fig. 11.2 the integrator is indeed the optimum

filter. However, before returning specifically to the integrator receiver, we shall discuss optimum filters more generally.

We assume that the received signal is a binary waveform. One binary digit (bit) is represented by a signal waveform $s_x(t)$ which persists for time T , while the other bit is represented by the waveform $s_2(t)$ which also lasts for an interval T . For example, in the case of transmission at baseband, as shown in Fig. 11.2, $s_x(t) = +V$, while $s_2(t) = -V$; for other modulation systems, different waveforms are transmitted. For example, for PSK signalling, $s_x(t) = A \cos w_0 t$ and $s_2(t) = -A \cos w_0 t$; while for FSK, $s_x(t) = A \cos (w_0 + W)t$ and $s_2(t) = A \cos (w_0 - W)t$.

As shown in Fig. 11.8 the input, which is $s_x(t)$ or $s_2(t)$, is corrupted by the addition of noise $n(t)$. The noise is Gaussian and has a spectral density $G(f)$. [In most cases of interest the noise is white, so that $G(f) = r/2$. However, we shall assume the more general possibility, since it introduces no complication to do so.] The signal and noise are filtered and then sampled at the end of each bit interval. The output sample is either $v_o(T) = s_{o1}(T) + n_o(T)$ or $v_o(T) = s_{o2}(T) + n_o(T)$. We assume that immediately after each sample, every energy-storing element in the filter has been discharged.

We have already considered in Sec. 6.4.7, the matter of signal determination in the presence of noise. Thus, we note that in the absence of noise the output sample would be $v_o(T) = s_{o1}(T)$ or $s_{o2}(T)$. When noise is present we have shown that to minimize the probability of error one should assume that $s_x(t)$ has been transmitted if $v_o(T)$ is closer to $s_{o1}(T)$ than to $s_{o2}(T)$. Similarly, we assume $s_2(t)$

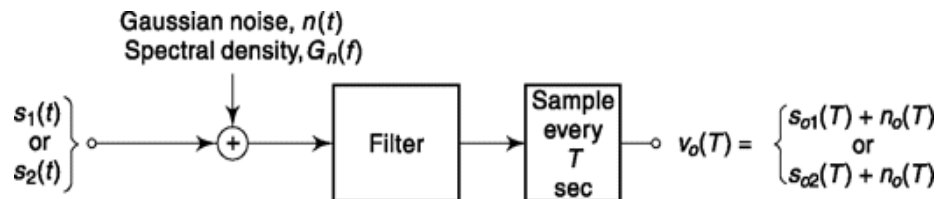


Fig. 11.8 A receiver for binary coded signalling.

has been transmitted if $v_o(T)$ is closer to $s_{o2}(T)$. The decision boundary is therefore midway between $s_{o1}(T)$ and $s_{o2}(T)$. For example, in the baseband system of Fig. 11.2, where $s_{o1}(T) = VT/t$ and $s_{o2}(T) = -VT/t$, the decision boundary is $v_o(T) = 0$. In general, we shall take the decision boundary to be

$$s_o1(T) + s_o2(T)$$

$$vo(T) = -2--(1124)$$

The probability of error for this general case may be deduced as an extension of the considerations used in the baseband case. Suppose that $s_o1(T) > s_o2(T)$ and that $s_2(t)$ was transmitted. If, at the sampling time; the noise $n_o(T)$ is positive and larger in magnitude than the voltage difference

$1 [s_o1(T) + s_o2(T)] - s_o2(T)$, an error will have been made. That is, an error [we decide that $s_x(t)$ is transmitted rather than $s_2(t)$] will result if

$$n_o(T) \geq \frac{s_{o1}(T) - s_{o2}(T)}{2} \quad (11.25)$$

Hence, the probability of error is

$$P_e = \int_{[s_{o1}(T) - s_{o2}(T)]/2}^{\infty} \frac{e^{-n_o^2(T)/2\sigma_o^2}}{\sqrt{2\pi\sigma_o^2}} dn_o(T) \quad (11.26)$$

If we make the substitution $x \equiv n_o(T)/\sqrt{2\sigma_o}$, Eq. (11.26) becomes

$$P_e = \frac{1}{2} \frac{2}{\sqrt{\pi}} \int_{[s_{o1}(T) - s_{o2}(T)]/2\sqrt{2\sigma_o}}^{\infty} e^{-x^2} dx \quad (11.27a)$$

$$P_e = \frac{1}{2} \operatorname{erfc} \left[\frac{s_{o1}(T) - s_{o2}(T)}{2\sqrt{2\sigma_o}} \right] \quad (11.27b)$$

Note that for the case $s_{o1}(T) = VT/t$ and $s_{o2}(T) = -VT/t$, and, using Eq. (11.4), Eq. (11.27c) reduces to Eq. (11.9) as expected.

The complementary error function is a monotonically decreasing function of its argument. (See Fig. 11.5.) Hence, as is to be anticipated, P_e decreases as the difference $s_{oi}(T) - s_{o2}(T)$ becomes larger and as the rms noise voltage σ_o becomes smaller. The optimum filter, then, is the filter which maximizes the ratio

$$\gamma = \frac{s_{o1}(T) - s_{o2}(T)}{\sigma_o} \quad (11.28)$$

We now calculate the transfer function $H(f)$ of this optimum filter. As a matter of mathematical convenience, we shall actually maximize g^2 rather than g

11.3.1 Calculation of the Optimum-Filter Transfer Function $H(f)$

The fundamental requirement we make of a binary encoded data receiver is that it distinguishes the voltages $s_x(t) + n(t)$ and $s_2(t) + n(t)$. We have seen that the ability of the receiver to do so depends on how large a particular receiver can make g . It is important to note that g is proportional not to $s_x(t)$ nor to $s_2(t)$, but rather to the *difference* between them. For example, in the baseband system we represented the signals by voltage levels +V and -V. But clearly, if our only interest was in distinguishing levels, we would do just as well to use +2 volts and 0 volt, or +8 volts and +6 volts, etc. (The +V and -V levels, however, have the advantage of requiring the least average power to be transmitted.) Hence, while $s_x(t)$ or $s_2(t)$ is the received signal, the signal which is to be compared with the noise, i.e. the signal which is relevant in all our error-probability calculations, is the difference signal

$$P(t) \equiv s_1(t) - s_2(t) \quad (11.29)$$

Thus, for the purpose of calculating the minimum error probability, we shall assume that the input signal to the optimum filter is $p(t)$. The corresponding *output signal* of the filter is then

$$P_o(t) \equiv s_{o1}(t) - s_{o2}(t) \quad (11.30)$$

We shall let $P(f)$ and $P_o(f)$ be the Fourier transforms, respectively, of $p(t)$ and $p_o(t)$.

If $H(f)$ is the transfer function of the filter,

$$P_o(f) = H(f)P(f) \quad (11.31)$$

$$\text{and} \quad P_o(T) = \int_{-\infty}^{\infty} P_o(f) e^{j2\pi f T} df = \int_{-\infty}^{\infty} H(f)P(f) e^{j2\pi f T} df \quad (11.32)$$

The input noise to the optimum filter is $n(t)$. The output noise is $n_o(t)$ which has a power spectral density $G_{n_o}(f)$ and is related to the power spectral density of the input noise $G_n(f)$ by

$$G_{n_o}(f) = |H(f)|^2 G_n(f) df \quad (11.33)$$

Using Parseval's theorem (Eq. 1.136), we find that the normalized output noise power, i.e. the noise variance σ_o^2 is

$$\sigma_o^2 = \int_{-\infty}^{\infty} G_{n_o}(f) df = \int_{-\infty}^{\infty} |H(f)|^2 G_n(f) df \quad (11.34)$$

From Eqs (11.32) and (11.34) we now find that

$$\gamma^2 = \frac{p_o^2(T)}{\sigma_o^2} = \frac{\left| \int_{-\infty}^{\infty} H(f)P(f) e^{j2\pi f T} df \right|^2}{\int_{-\infty}^{\infty} |H(f)|^2 G_n(f) df} \quad (11.35)$$

Equation (11.35) is unaltered by the inclusion or deletion of the absolute value sign in the numerator since the quantity within the magnitude sign $p_o(T)$ is a positive real number. The sign has been included, however, in

order to allow further development of the equation through the use of the *Schwarz inequality*.

The *Schwarz inequality* states that given arbitrary complex functions $X(f)$ and $Y(f)$ of a common variable f , then

$$\left| \int_{-\infty}^{\infty} X(f)Y(f) df \right|^2 \leq \int_{-\infty}^{\infty} |X(f)|^2 df \int_{-\infty}^{\infty} |Y(f)|^2 df \quad (1136)$$

The equal sign applies when

$$X(f) = KY^*(f) \quad (11.37)$$

where K is an arbitrary constant and $Y^*(f)$ is the complex conjugate of $Y(f)$.

We now apply the Schwarz inequality to Eq. (11.35) by making the identification

$$X(f) \equiv \sqrt{G_n(f)} H(f) \quad (11.38)$$

and

$$Y(f) \equiv \frac{1}{\sqrt{G_n(f)}} (f) e^{j2\pi Tf} \quad (11.39)$$

Using Eqs (11.38) and (11.39) and using the Schwarz inequality, Eq. (11.36), we may rewrite Eq. (11.35) as

$$\frac{p_o^2(T)}{\sigma_o^2} = \frac{\left| \int_{-\infty}^{\infty} X(f)Y(f) df \right|^2}{\int_{-\infty}^{\infty} |X(f)|^2 df} \leq \int_{-\infty}^{\infty} |Y(f)|^2 df \quad (11.40)$$

or, using Eq. (11.39),

$$\frac{p_o^2(T)}{\sigma_o^2} = \int_{-\infty}^{\infty} |Y(f)|^2 df = \int_{-\infty}^{\infty} \frac{|P(f)|^2}{G_n(f)} df \quad (11.41)$$

The ratio $p_o^2(T)/\sigma_o^2$ will attain its maximum value when the equal sign in Eq. (11.41) may be employed as is the case when $X(f) = KY^*(f)$. We then find from Eqs (11.38) and (11.39) that the optimum filter which yields such a maximum ratio $p_o^2(T)/\sigma_o^2$ has a transfer function

$$H(f) = K \frac{P^*(f)}{G_n(f)} e^{-j2\pi fT} \quad (11.42)$$

Correspondingly, the maximum ratio is, from Eq. (11.41),

$$\left[\frac{p_o^2(T)}{\sigma_o^2} \right]_{\max} = \int_{-\infty}^{\infty} \frac{|P(f)|^2}{G_n(f)} df \quad (11.43)$$

In succeeding sections we shall have occasion to apply Eqs (11.42) and (11.43) to a number of cases of interest.

11.3.2 Optimum Filter Realization using Matched Filter

An optimum filter which yields a maximum ratio $p_o^2(T)/\sigma_o^2$ is called a *matched filter* when the input noise is *white*. In this case $G_n(f) = \eta/2$, and Eq. (11.42) becomes

$$H(f) = K \frac{P^*(f)}{\eta/2} e^{-j2\pi fT} \quad (11.44)$$

The impulsive response of this filter, i.e. the response of the filter to a unit strength impulse applied at $t = 0$, is

$$h(t) = \mathcal{F}^{-1}[H(f)] = \frac{2K}{\eta} \int_{-\infty}^{\infty} P^*(f) e^{-j2\pi fT} e^{j2\pi ft} df \quad (11.45a)$$

$$= \frac{2K}{\eta} \int_{-\infty}^{\infty} P^*(f) e^{j2\pi f(t-T)} df \quad (11.45b)$$

A physically realizable filter will have an impulse response which is real, i.e. not complex. Therefore $h(t) = h^*(t)$. Replacing the right-hand member of Eq. (11.45b) by its complex conjugate, an operation which leaves the equation unaltered, we have

$$h(t) = \frac{2K}{\eta} \int_{-\infty}^{\infty} P(f) e^{j2\pi f(T-t)} df \quad (11.46a)$$

$$= \frac{2K}{\eta} p(T-t) \quad (11.46b)$$

Finally, since $p(t) = s_1(t) - s_2(t)$ [see Eq. (11.29)], we have

$$h(t) = \frac{2K}{\eta} [s_1(T-t) - s_2(T-t)] \quad (11.47)$$

The significance of these results for the matched filter may be more readily appreciated by applying them to a specific example. Consider then, as in Fig. 11.9a, that $s_x(t)$ is a triangular waveform of duration T , while $s_2(t)$, as shown in Fig. 11.9b, is of identical form except of reversed polarity. Then $p(t)$ is as shown in Fig. 11.9c, and $p(-t)$ appears in Fig. 11.9d. The waveform $p(-t)$ is the waveform $p(t)$ rotated around the axis $t = 0$. Finally, the waveform $p(T-t)$ called for as the impulse response of the filter in Eq. (11.46b) is this rotated waveform $p(-t)$ translated in the positive t direction by amount T . This last translation ensures that $h(t) = 0$ for $t < 0$ as is required for a *causal* filter.

In general, the impulsive response of the matched filter consists of $p(t)$ rotated about $t = 0$ and then delayed long enough (i.e. a time T) to make the filter realizable. We may note in passing, that any additional delay that a filter might introduce would in no way interfere with the performance of the filter, for both signal and noise would be delayed by the same amount, and at the sampling time (which would need similarly to be delayed) the ratio of signal to noise would remain unaltered.

11.3.3 probability of Error of the Matched Filter

The probability of error which results when employing a matched filter, may be found by evaluating the maximum signal-to-noise ratio $[p_o^2(T)/\sigma_o^2]_{\max}$ given by Eq. (11.43). With $G_n(f) = \eta/2$, Eq. (11.43) becomes

$$\left[\frac{p_o^2(T)}{\sigma_o^2} \right]_{\max} = \frac{2}{\eta} \int_{-\infty}^{\infty} |P(f)|^2 df \quad (11.48)$$

From Parseval's theorem, we have

$$\int_{-\infty}^{\infty} |P(f)|^2 df = \int_{-\infty}^{\infty} p^2(t) dt = \int_0^T p^2(t) dt \quad (11.49)$$

In the last integral in Eq. (11.49), the limits take account of the fact that $p(t)$ persists for only a time T . With $p(t) = s_1(t) - s_2(t)$, and using Eq. (11.49), we may write Eq. (11.48) as

$$\left[\frac{p_o^2(T)}{\sigma_o^2} \right]_{\max} = \frac{2}{\eta} \int_0^T [s_1(t) - s_2(t)]^2 dt \quad (11.50a)$$

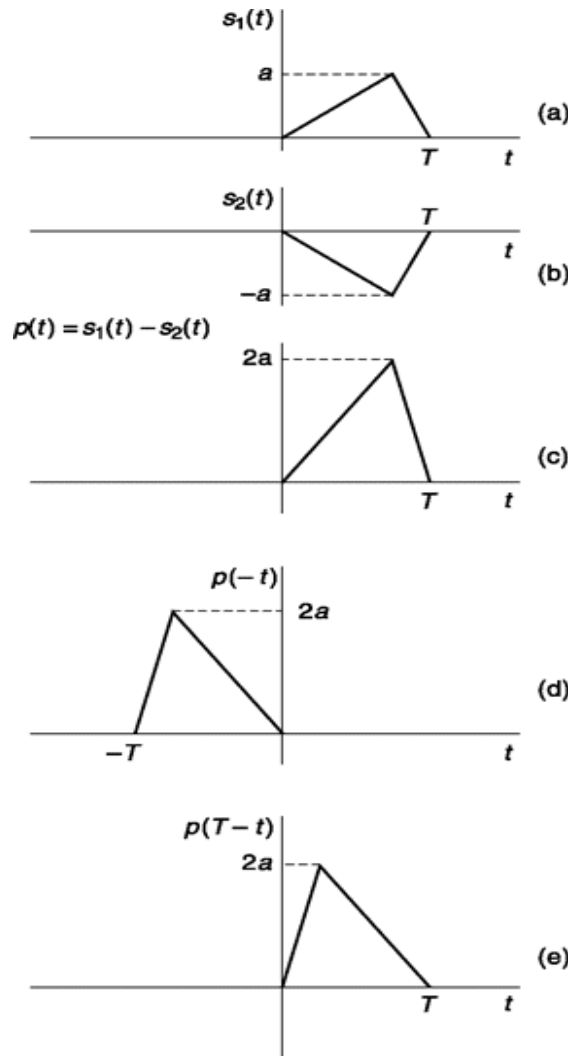


Fig. 11.9 The signals (a) $s_1(t)$, (b) $s_2(t)$, and (c) $p(t) = s_1(t) - s_2(t)$ (d) $p(t)$ rotated about the axis $t = 0$. (e) The waveform in (d) translated to the right by amount T .

$$= \frac{2}{\eta} \left[\int_0^T s_1^2(t) dt + \int_0^T s_2^2(t) dt - 2 \int_0^T s_1(t) s_2(t) dt \right] \quad (11.50b)$$

$$= \frac{2}{\eta} (E_{s1} + E_{s2} - 2E_{s12}) \quad (11.50c)$$

Here, E_{s1} and E_{s2} are the energies, respectively, in $s_x(t)$ and $s_2(t)$, while E_{s12} is the energy due to the correlation between $s_x(t)$ and $s_2(t)$.

Suppose that we have selected $s_x(t)$, and let $s_2(t)$ have an energy E_{s1} . Then it can be shown that if $s_2(t)$ is to have the *same energy*, the optimum choice of $s_2(t)$ is

$$s_2(t) = -s_x(t) \quad (11.51)$$

The choice is optimum in that it yields a maximum output signal $p_o^2(T)$ for a given signal energy. Letting $s_2(t) = -s_1(t)$, we find

$$E_{s1} = E_{s2} = -E_{s12} \equiv E_s$$

and Eq. (11.50c) becomes

$$\left[\frac{p_o^2(T)}{\sigma_o^2} \right]_{\max} = \frac{8E_s}{\eta} \quad (11.52)$$

Rewriting Eq. (11.27b) using $p_o(T) = s_{o1}(T) - s_{o2}(T)$, we have

$$P_e = \frac{1}{2} \operatorname{erfc} \left[\frac{p_o(T)}{2\sqrt{2}\sigma_o} \right] = \frac{1}{2} \operatorname{erfc} \left[\frac{p_o^2(T)}{8\sigma_o^2} \right]^{1/2} \quad (11.53)$$

Combining Eq. (11.53) with (11.52), we find that the minimum error probability $(P_e)_{\min}$ corresponding to a maximum value of $p_o^2(T)/\sigma_o^2$ is

$$(P_e)_{\min} = \frac{1}{2} \operatorname{erfc} \left\{ \frac{1}{8} \left[\frac{p_o^2(T)}{\sigma_o^2} \right]_{\max} \right\}^{1/2} \quad (11.54)$$

$$= \frac{1}{2} \operatorname{erfc} \left(\frac{E_s}{\eta} \right)^{1/2} \quad (11.55)$$

We note that Eq. (11.55) establishes more generally the idea that the error probability depends only on the signal energy and not on the signal waveshape. Previously, we had established this point only for signals which had constant voltage levels.

We note also that Eq. (11.55) gives $(P_e)_{mn}$ for the case of the matched filter and when $s_x(t) = -s_2(t)$. In Sec. 11.2 we considered the case when $s_x(t) = +V$ and $s_2(t) = -V$ and the filter employed was an integrator. There we found [Eq. (11.9)] that the result for P_e was identical with $(P_e)_{\min}$ given in Eq. (11.55). This agreement leads us to suspect that for an input signal where $s_x(t) = +V$ and $s_2(t) = -V$, the integrator is the matched filter. Such is indeed the case. For when we have

$$s_1(t) = V \quad 0 \leq t \leq T \quad (11.56a)$$

and

$$s_2(t) = -V \quad 0 \leq t \leq T \quad (11.56b)$$

the impulse response of the matched filter is, from Eq. (11.47),

$$h(t) = \frac{2K}{\eta} [s_1(T-t) - s_2(T-t)] \quad (11.57)$$

The quantity $s_1(T-t) - s_2(T-t)$ is a pulse of amplitude $2V$ extending from $t = 0$ to $t = T$ and may be rewritten, with $u(t)$ the unit step,

$$h(t) = \frac{2K}{\eta} (2V)[u(t) - u(t-T)] \quad (11.58)$$

The constant factor of proportionality $4KV/\eta$ in the expression for $h(t)$ (that is, the gain of the filter) has no effect on the probability of error since the gain affects signal and noise alike. We may therefore select the coefficient K in Eq. (11.58) so that $4KV/r = 1$. Then the inverse transform of $h(t)$, that is, the transfer function of the filter, becomes, with s the Laplace transform variable,

$$H(s) = \frac{1}{s} - \frac{e^{-sT}}{s} \quad (11.59)$$

The first term in Eq. (11.59) represents an integration beginning at $t = 0$, while the second term represents an integration with reversed polarity beginning at $t = T$. The overall response of the matched filter is an integration from $t = 0$ to $t = T$ and a zero response thereafter. In a physical system, as already described, we achieve the effect of a zero response after $t = T$ by sampling at $t = T$, so that so far as the determination of one bit is concerned we ignore the response after $t = T$.

11.3.4 Optimum Filter Realization using Correlator

We discuss now an alternative type of receiving system which, as we shall see, is identical in performance with the matched filter receiver. Again, as shown in Fig. 11.10, the input is a binary data waveform $s_x(t)$ or $s_2(t)$ corrupted by noise $n(t)$. The bit length is T . The received signal plus noise $v_r(t)$ is multiplied by a locally generated waveform $s_x(t) - s_2(t)$. The output of the multiplier is passed through an integrator whose output is sampled at $t = T$. As before, immediately after each sampling, at the beginning of each new bit interval, all energy-storing elements in the integrator are discharged. This type of receiver is called a *correlator*, since we are *correlating* the received signal and noise with the waveform $s_1(t) - s_2(t)$.

The output signal and noise of the correlator shown in Fig. 11.10 are

$$S_o(T) = \frac{1}{\tau} \int_0^T s_i(t)[s_1(t) - s_2(t)] dt \quad (11.60)$$

$$n_o(T) = \frac{1}{\tau} \int_0^T n(t)[s_1(t) - s_2(t)] dt \quad (11.61)$$

where $s(t)$ is either $s_x(t)$ or $s_2(t)$, and where t is the constant of the integrator i.e. the integrator output is $1/t$ times the integral of its input). We now compare these outputs with the matched filter outputs.

If $h(t)$ is the impulsive response of the matched filter, then the output of the matched filter $v_o(t)$ can be found using the convolution integral (see Sec. 1.4.2). We have

$$v_o(T) = \int_{-\infty}^{\infty} v_i(\lambda)h(t - \lambda) d\lambda = \int_0^T v_i(\lambda) (t - \lambda) d\lambda \quad (11.62)$$

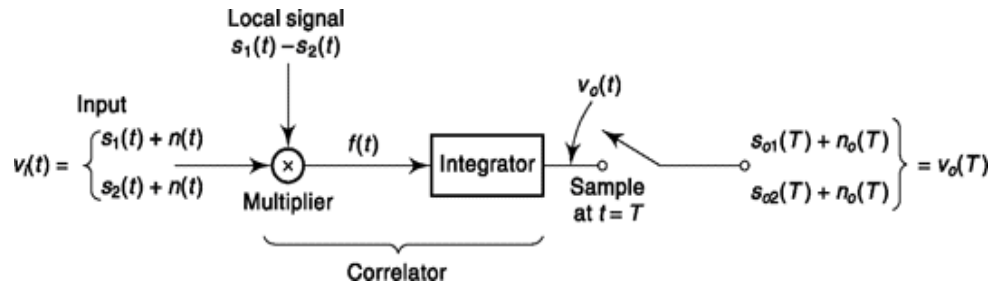


Fig. 11.10 A coherent system of signal reception.

The limits on the integral have been changed to 0 and T since we are interested in the filter response to a bit which extends only over that interval. Using Eq. (11.47) which gives $h(t)$ for the matched filter, we have

$$h(t) = \frac{2K}{\eta} [s_1(T-t) - s_2(T-t)] \quad (11.63)$$

so that $h(t-\lambda) = \frac{2K}{\eta} [s_1(T-t+\lambda) - s_2(T-t+\lambda)] \quad (11.64)$

Substituting Eq. (11.64) into (11.62), we have

$$v_o(t) = \frac{2K}{\eta} \int_0^T v_\lambda(\lambda) [s_1(T-t+\lambda) - s_2(T-t+\lambda)] d\lambda \quad (11.65)$$

Since $v_i(\lambda) = s_i(\lambda) + n(\lambda)$, and $v_o(t) = s_o(t) + n_o(t)$, setting $t = T$ yields

$$s_o(T) = \frac{2K}{\eta} \int_0^T s_i(\lambda) [s_1(\lambda) - s_2(\lambda)] d\lambda \quad (11.66)$$

where $s_i(\lambda)$ is equal to $s_1(\lambda)$ or $s_2(\lambda)$. Similarly, we find that

$$n_o(t) = \frac{2K}{\eta} \int_0^T n(\lambda) [s_1(\lambda) - s_2(\lambda)] d\lambda \quad (11.67)$$

Thus $s_o(t)$ and $n_o(t)$, as calculated from Eqs (11.60) and (11.61) for the correlation receiver, and as calculated from Eqs (11.66) and (11.67) for the matched filter receiver, are identical. Hence, the performances of the two systems are identical.

The *matched filter* and the *correlator* are not simply two distinct, independent techniques which happen to yield the same result. In fact they are two techniques of synthesizing the optimum filter $h(t)$.

Example 11.5

(a) For an equiprobable binary baseband data the optimal receiver receives -5 mV for 0 and +5 mV for 1, corrupted with white noise of PSD 10^{-9} W/Hz. With optimum decision threshold what is the probability of error in reception if data rate is 9600 bits/sec?

(b) Find the percentage increase in error rate if data rate is doubled. (c) If we want probability of error at increased data rate same as (a), what should be input voltage levels?

Solution

- (a) From Eq. (11.58), probability of error for optimal receiver that uses optimal filter and optimal threshold $P_e = 0.5 \operatorname{erfc} \left(\sqrt{\frac{E_s}{\eta}} \right)$ where $\frac{\eta}{2} = 10^{-9}$ W/Hz

With Matched Filter based optimal filter, from
Eq. (11.9),

$$E_s = V^2 T \\ = (0.005)^2 (9600)^{-1} = 0.26 \times 10^{-8}$$

$$\text{Thus, } P_e = 0.5 \operatorname{erfc} \left(\sqrt{\frac{0.26 \times 10^{-8}}{2 \times 10^{-9}}} \right) \\ = 0.5 \operatorname{erfc}(1.1402) = 0.0534$$

- (b) With doubled data rate, effective energy per bit

$$E_s = V^2 T \\ = (0.005)^2 (2 \times 9600)^{-1} = 0.13 \times 10^{-8}$$

$$\text{Then, } P_e = 0.5 \operatorname{erfc} \left(\sqrt{\frac{0.13 \times 10^{-8}}{2 \times 10^{-9}}} \right) \\ = 0.5 \operatorname{erfc}(0.8062) = 0.1271$$

$$\text{Percentage increase in error rate} \\ = 100(0.1271 - 0.0534)/0.0534 \\ = 138.03\%$$

- (c) To restore probability of error input voltage level is to be increased so that E_s is as it was in (a). Since T is halved V is to be increased $\sqrt{2}$ times from definition of E_s . Thus required voltage levels are $\pm 5\sqrt{2}$ mV, i.e. ± 7.07 mV.

SELF-TEST QUESTIONS

5. Does Schwartz inequality contain an equality condition useful for getting optimum filter relation?
6. Can a physically realizable filter have complex impulse response?
7. Is it true that in matched filter error probability depends on signal energy and not on wave shape?
8. Can matched filter and correlator give identical reception performances?

11.4 RECEPTION OF PSK, FSK, QPSK, DPSK SIGNAL

In this section, we discuss how coherent detection is used in optimal reception of PSK, FSK and QPSK modulated signal. We shall use the derivations arrived at in previous section. We shall discuss suboptimal performance of DPSK and noncoherent detection possible with FSK signals.

11.4.1 PSK AND SYNCHRONIZATION ISSUES

An important application of the coherent reception system of Sec. 11.3.3 is its use in phase-shift keying (PSK). Here the input signal is

$$s_1(t) = A \cos \omega_0 t \quad (11.68)$$

or

$$s_2(t) = -A \cos \omega_0 t \quad (11.69)$$

At the receiver a coherent local signal $s_1(t) - s_2(t) = 2A \cos \omega_0 t$ needs to be provided for the multiplier (see Fig. 11.10).

Since, in PSK, $s_1(t) = -s_2(t)$, Eq. (11.55) gives the error probability. Then, in PSK, as in baseband transmission.

$$P_e = \frac{1}{2} \operatorname{erfc} \sqrt{\frac{E_s}{\eta}} \quad (11.70)$$

If a bit duration extends for a time T , which encompasses a whole number of cycles, then the signal energy is $E_s = A^2 T / 2$ so that from Eq. (11.70) the error probability is

$$P_e = \frac{1}{2} \operatorname{erfc} \sqrt{\frac{A^2 T}{2\eta}} \quad (11.71)$$

Imperfect phase synchronization

In PSK, where the signals $s_x(t)$ and $s_2(t)$ are as given in Eqs (11.68) and (11.69), the required local waveform for the correlator which is shown in Fig. 11.10 is given by $s_x(t) - s_2(t) = 2A \cos \omega_0 t$. Then,

when $s_x(t)$ is received, the output of the correlator at the sampling time $t = T$ is $s_{ol}(T) = cA^2 T$, where c is some constant depending on the gain of the integrator. Similarly, $s_{o2}(T) = -cA^2 T$.

Suppose now that the local signal used at the correlator were not $2A \cos \omega_0 t$ as required, but rather $2A \cos (\omega_0 t + f)$ where f is some fixed phase offset. Then, as is easily verified at the sampling instant, the correlator output would become $s_o(T) = \pm 2cA^2 T \cos f$, that is, the output signal is reduced, being multiplied by the factor $\cos f$. In this case, the energy becomes $E_s \cos^2 f$ and Eq. (11.70) would be replaced by

$$P_e = \frac{1}{2} \operatorname{erfc} \sqrt{\frac{E_s}{\eta} \cos^2 \phi} \quad (11.72)$$

while Eq. (11.71) would read

$$P_e = \frac{1}{2} \operatorname{erfc} \sqrt{\frac{A^2 T \cos^2 \phi}{2\eta}} \quad (11.73)$$

The phase shift f increases the probability of error P_e . Typical error probabilities in a communication system range from 10^{-4} to 10^{-7} . In this range, if $f = 250^\circ$, the probability of error is increased by a factor of **10** as compared with the result obtained for $f = 0$.

Imperfect Bit synchronization

The PSK system shown in Fig. 11.10 and characterized by Eq. (11.62) assumes that the *bit synchronizer* at the receiver operates with perfect precision. The bit synchronizer, it will be recalled, is used to assure that the integration starts at $t = 0$ and ends at $t = T$, that is, that the integration extend exactly over the duration of the bit. As a matter of practice, either because of limitations in the synchronizer or because of the influence of noise, the integration may extend not from 0 to T but rather from t to $T + t$. We note that the output noise voltage $n_o(T + t)$ will, of course, not be affected by this overlap since the integration time T remains unchanged. Further, if the two bits overlapped have the same logic value then again the overlap has no affect on the signal voltage $s_o(T + t)$. But, if the overlapped bits are different, the overlap will cause a reduction in $s_o(T + t)$. To see that such is the case, consider that the transmitted signal is $A \cos w_0 t$ in the interval 0 to T and $-A \cos w_0 t$ for T to $2T$. If there is an overlap of amount t then from Eqs (11.66), (11.68), and (11.69),

$$s_o(T + \tau) = \frac{2K}{\eta} \int_{\tau}^T A \cos \omega_0 t [2A \cos \omega_0 t] dt$$

$$\frac{2K}{\eta} \int_T^{T+\tau} A \cos \omega_0 t [2A \cos \omega_0 t] dt \quad (11.74)$$

$$= \frac{2K}{\eta} [A^2(T - \tau) - A^2\tau] = \frac{2K}{\eta} [A^2 T] \left[1 - \frac{2\tau}{T} \right] \quad (11.75)$$

It is readily verified that if the overlap is in the other direction, i.e. the integration extends from $-\tau$ to $T - \tau$, the result is the same, so that more generally Eq. (11.75) becomes

$$s_o(T + \tau) = \frac{2K}{\eta} [A^2 T] \left[1 - \frac{2|\tau|}{T} \right] \quad (11.76)$$

Correspondingly, Eq. (11.70) should be corrected to read

$$P_e = \frac{1}{2} \operatorname{erfc} \sqrt{\left(\frac{E_s}{\eta} \right) \left(1 - \frac{2|\tau|}{T} \right)^2} \quad (11.77)$$

In the range of probabilities of error that are of interest to us, we note that if $t = 0.05T$ the probability of error is increased by a factor of **10**.

If both phase error and timing error are present then Eq. (11.70) becomes

$$P_e = \frac{1}{2} \operatorname{erfc} \left[\left(\frac{E_s}{\eta} \right) (\cos^2 \phi) \left(1 - \frac{2|\tau|}{T} \right)^2 \right]^{1/2} \quad (11.78)$$

11.4.2 Coherent and Noncoherent FSK

In frequency-shift keying (FSK) the received signal is either

$$s_1(t) = A \cos (\omega_0 + \Omega)t \quad (11.79)$$

$$\text{or} \quad s_2(t) = A \cos (\omega_0 - \Omega)t \quad (11.80)$$

As was explained in Sec. 11.3.3, one way of synthesizing the matched filter is to construct the correlation receiver system shown in Fig. 11.10. This receiver will give precisely the same performance as a matched filter, provided that the local waveform is $s_x(t) - s_2(t)$. In FSK the required local waveform is

$$s_1(t) - s_2(t) = A \cos (\omega_0 + \Omega)t - A \cos (\omega_0 - \Omega)t \quad (11.81)$$

probability of Error

In Sec. 11.3.2, we calculated the probability of error for the matched filter and arrived at the result $P_c = \frac{1}{2} \operatorname{erfc} \sqrt{E_s/\eta}$ given in Eq. (11.55). The derivation was general, and would apply in the present case, except for the fact that we had assumed there that $s_x(t) = -s_2(t)$. This assumption is obviously not valid for FSK.

To calculate the probability of error for FSK, we return to a point in the derivation of Sec. 11.3.2 just before the introduction of the assumption $s_x(t) = -s_2(t)$. We start with Eq. (11.50a), which reads

$$\left[\frac{p_o^2(T)}{\sigma_o^2} \right]_{\max} = \frac{2}{\eta} \int_0^T [s_1(t) - s_2(t)]^2 dt \quad (11.82)$$

Substituting $s_x(t)$ and $s_2(t)$ as given in Eqs (11.79) and (11.80) into Eq. (11.82) and performing the indicated integration, we find that

$$\left[\frac{p_o^2(T)}{\sigma_o^2} \right]_{\max} = \frac{2A^2 T}{\eta} \left[1 - \frac{\sin 2\Omega T}{2\Omega T} + \frac{1}{2} \frac{\sin [2(\omega_o + \Omega)T]}{2(\omega_o + \Omega)T} - \frac{1}{2} \frac{\sin [2(\omega_o - \Omega)T]}{2(\omega_o - \Omega)T} - \frac{\sin 2\omega_o T}{2\omega_o T} \right] \quad (11.83)$$

Note that in Sec. 5.3.1, we arrived at this same result using the Gram-Schmitt procedure.

If we assume that the offset angular frequency Ω is very small in comparison with the carrier angular frequency ω_o (a situation usually encountered in physical systems), then the last three terms in Eq. (11.83) each have the form $(\sin 2\omega_o T)/2\omega_o T$. This ratio approaches zero as $\omega_o T$ increases. We further assume, as is generally the case, that $\omega_o T @ 1$. We may therefore neglect these last three terms. We are left with

where the signal energy is $E_s = A^2 T/2$.

$$\left[\frac{p_o^2(T)}{\sigma_o^2} \right]_{\max} = \frac{2A^2 T}{\eta} \left(1 - \frac{\sin 2\Omega T}{2\Omega T} \right) \quad (11.84)$$

The quantity $\left[\frac{p_o^2(T)}{\sigma_o^2} \right]_{\max}$ in Eq. (11.84) attains its largest value when Ω is selected so that $2\Omega T = 3\pi/2$.

For this value of Ω we find

$$\left[\frac{p_o^2(T)}{\sigma_o^2} \right]_{\max} = 2.42 \frac{A^2 T}{\eta} = 4.84 \frac{(A^2/2)T}{\eta} \quad (11.85)$$

The probability of error, calculated using Eq. (11.53) with $[p_o(T)/\sigma_o^2]_{\max}$ as given in Eq. (11.85), is found to be

$$P_e = \frac{1}{2} \operatorname{erfc} \left\{ \frac{1}{8} \left[\frac{p_o^2(T)}{\sigma_o^2} \right]_{\max} \right\}^{1/2} \simeq \frac{1}{2} \operatorname{erfc} \left(0.6 \frac{E_s}{\eta} \right)^{1/2} \quad (11.86)$$

Comparing the probability of error obtained for FSK [Eq. (11.86)] with the probability of error obtained for PSK [Eq. (11.70)], we see that equal probability of error in each system can be achieved if the signal energy in the PSK signal is 0.6 times as large as the signal energy in FSK. As a result, a 2 dB increase in the transmitted signal power is required for FSK. Why is FSK inferior to PSK? The answer is that in PSK $s_x(t) = -s_2(t)$, while in FSK this condition is not satisfied. Thus, although an optimum filter is used in each case, PSK results in considerable improvement compared with FSK.

When one of two *orthogonal* frequencies are transmitted, $2WT = mp$ (m an integer) and

$$P_e = \frac{1}{2} \operatorname{erfc} \left(\frac{E_s}{2\eta} \right)^{1/2} \quad (11.87)$$

Noncoherent Detection of FSK

Since FSK can be thought of as the transmission of the output of either of the two signal sources, the first at the frequency $w_1 = w_0 + W$, and the second at the frequency $w_2 = w_0 - W$, we should think that a reasonable detection system would consist of two bandpass filters, with center frequencies at w_1 and w_2 . The bandwidth of each filter would be adjusted to yield a maximum output when the appropriate signal is received. Thus, when filter H_1 with center frequency $(O_1$ has a larger output than filter H_2 with center frequency w_2 , we would decide that $s_x(t)$ was transmitted. Similarly we would decide that $s_2(t)$ was transmitted when the output of H_2 was greater than the output of H_1 .

When using a filter receiver, we make no use of the *phase* of the incoming signal. Such reception is, therefore, called *noncoherent* detection. The *coherent* matched-filter detector, on the other hand, uses synchronization techniques to determine the phase of the incoming signal. Since some valuable information concerning the signal is not used, the probability of detecting the signal is reduced. The probability of error of noncoherent FSK is found to be²

$$P_e = \frac{1}{2} e^{-E_s/2\eta} \quad (11.88)$$

This probability of error is compared in Sec. 11.7 with the other systems discussed.

11.4.3 suboptimal Reception of Dpsk

The operation of differential phase-shift keying (DPSK) was explained in Sec. 5.2. We shall now show the *suboptimum* nature of DPSK by considering the system in terms of the phasor diagram shown in Fig. 11.11. In Fig. 11.11a, we see that when no noise is present the received phase is either at angle 0 or π . From this we draw a decision boundary at angle $\pi/2$ and decide that a 1 was sent if the phase difference between two consecutive bits differs by less than $\pi/2$, or we decide that a 0 was sent if the phase difference between two consecutive bits differs by more than $\pi/2$.

Figure 11.11b shows three consecutive received bits. Each bit was transmitted as a 1, but because of noise each is perturbed from the horizontal axis as shown. The DPSK receiver compares bit 2 with bit 1, reads an angle d_1 which is less than 90° , and decides that bit 2 is a 1. The DPSK receiver then compares bit 3 with bit 2, reads an angle d_2 which is greater than 90° , and decides that a 0 was transmitted.

The error was due to the fact that the DPSK receiver uses only the previous bit as a reference. This method of operation is analogous to employing *poor* synchronization. If all the previous positive bits were somehow averaged by employing good synchronization, and this average were used as a reference, then the DPSK receiver would have a *stable* reference, and the error described above would not have occurred. As a matter of fact we would then have a PSK system, not a DPSK system. Thus, DPSK is *suboptimum* and results in a higher probability of error than in PSK

where we have a *stable* reference phase (when perfect synchronization is assumed).

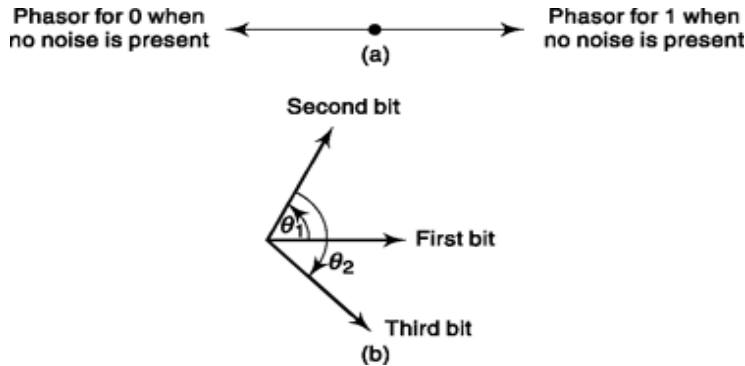


Fig. 11.11 Reception of DPSK. (a) Phasors when no noise is present. (b) Phasors when noise is present.

The calculation of probability of error is complicated and will not be given here.² The result is

$$P_e = \frac{1}{2} e^{-E_s/2\eta} \quad (11.89)$$

11.4.4 QPSK RECEPTION

In previous sections of this chapter we dealt exclusively with binary communication systems, that is, systems in which, in any interval $0 < t < T$, one of two possible messages was transmitted. However, data transmission systems allowing many possible messages in the interval T (so-called M-ary systems, the number of messages being M) are also possible and are widely used. As an example of such a M-ary system we consider 4-phase PSK (QPSK) which, because of its relative simplicity, is very popular (see Sec. 5.4).

In QPSK one of four possible waveforms is transmitted during each interval T . These waveforms are

$$s_i(t) = A \cos\left(\omega_0 t + [2m - 1]\frac{\pi}{4}\right)$$

$$m = 1, 2, 3, 4 \quad 0 \leq t \leq T_s = 2T \quad (11.90)$$

These four waveforms are represented in the phasor diagram of Fig. 11.12. The receiver system is shown in Fig. 11.13. Observe that two correlators are

required and that the local reference waveforms, as indicated also in Fig. 11.12, are $A \cos \omega_0 t$ and $A \sin \omega_0 t$.

Suppose, now, that, in the absence of the noise, signal $s_x(t)$ is received. Let us use the symbol V_o to represent the corresponding output of correlator 1, i.e. $V_o = v_{ol}(T_s)$ when $s_x(t)$ is received. Then, as is readily verified, the output of the two correlators corresponding to each of the four possible signals is as given in Table 11.1.

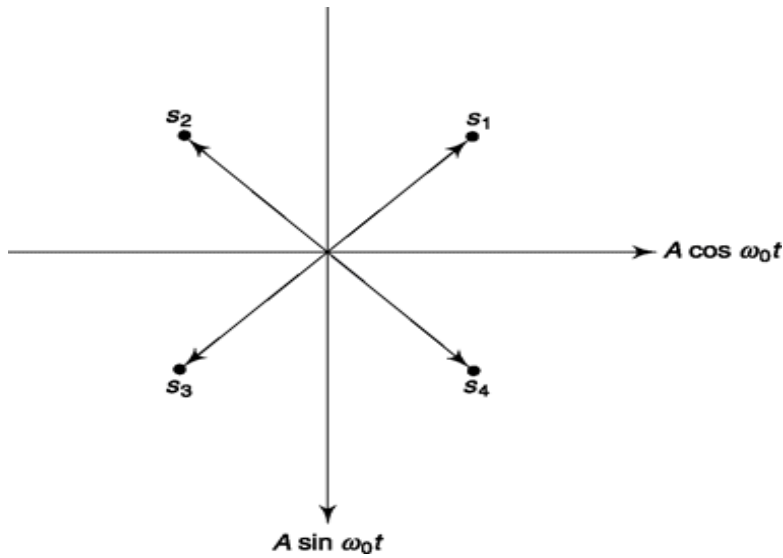


Fig. 11.12 A phasor-diagram representation of the signals in QPSK.

Thus, the transmitted signal may be recognized from a determination of the outputs of *both* correlators. In the presence of noise, of course, there will be some probability that an error will be made by one or both correlators.

We note from Fig. 11.12, that the reference waveform of correlator 1 is at an angle $f = 450^\circ$ to the axes of orientation of all of the four possible signals. Hence, from Eq. (11.73), since $(\cos 450^\circ)^2$

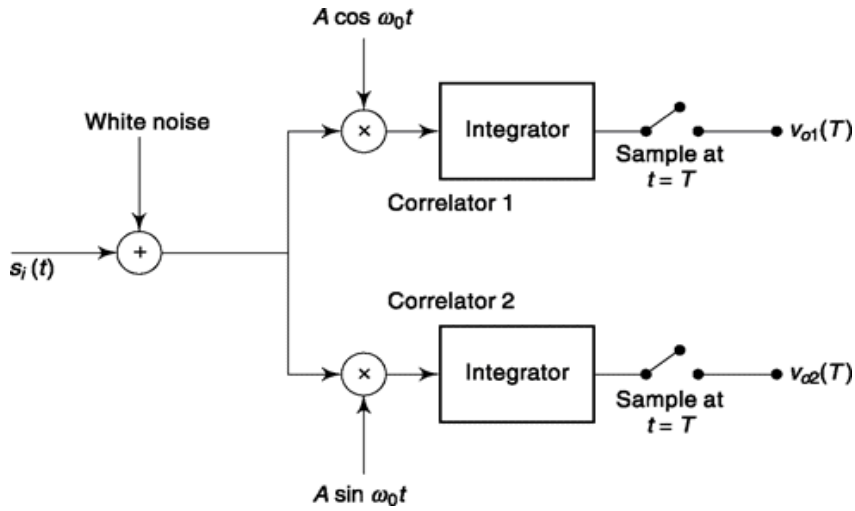


Fig. 11.13 A correlation receiver for QPSK.

Table 11.1

Output	Signal			
	$s_1(t)$	$s_2(t)$	$s_3(t)$	$s_4(t)$
$v_{o1}(T)$	$+V_o$	$-V_o$	$-V_o$	$+V_o$
$v_{o2}(T)$	$-V_o$	$-V_o$	$+V_o$	$+V_o$

$=\frac{1}{2}$ the probability that correlator 1 or correlator 2 will make an error is

$$P'_{e1} = P'_{e2} = \frac{1}{2} \operatorname{erfc} \sqrt{\frac{A^2 T_s}{4\eta}} \quad (11.91)$$

In order to compare this result to the result obtained for BPSK (Eq. 11.71), we simply let the symbol duration $T_s = 2T$ where T is the duration of single bit. Then

$$P'_{e1} = P'_{e2} = \frac{1}{2} \operatorname{erfc} \sqrt{\frac{A^2 T}{2\eta}} = P_e(\text{BPSK}) \quad (11.92)$$

Thus the *bit* probability of error of QPSK and BPSK is the same.

The probability P'_{e2} that correlator 2 will make an error is similarly given by the expression in Eq. (11.91). The probability P_c that the QPSK receiver will correctly identify the transmitted signal is equal to the product of the probabilities that both correlator 1 and correlator 2 have yielded correct results. Thus, using $P'_c = P'_{j1} = P'_{e2}$

$$P_c = (1 - P'_e)(1 - P'_e) = 1 - 2P'_e + P'^2_e \quad (11.93)$$

If, as is normally the case, $P'_e \ll 1$, the last term in Eq. (11.93) may be neglected. Finally, then, the

probability of error of the system is

$$P_e(\text{QPSK}) = 1 - P_c \simeq 2 P'_e = \operatorname{erfc} \sqrt{\frac{A^2 T}{4\eta}} \quad (11.94)$$

Example 11.6

(a) A BPSK signal is received at the input of a coherent optimal receiver with amplitude 10 mV and frequency 1 MHz. The signal is corrupted with white noise of PSD 10^{-9} W/Hz. If data rate is 10^4 bits/sec, find error probability. (b) Find error probability if the local oscillator has a phase shift of $\pi/6$ radian with input signal. (c) Find error probability if there is 10% mistiming in bit synchronization while sampling and
(d) find error probability when both (b) and (c) occur.

Solution

$$\begin{aligned} (a) \quad E_s &= A^2 T / 2 = (0.5)(0.01)^2 (10000)^{-1} \\ &= 0.5 \times 10^{-8} \text{ and } \frac{\eta}{2} = 10^{-9} \text{ W/Hz} \end{aligned}$$

From Eq. (11.70), probability of error

$$\begin{aligned} P_e &= 0.5 \operatorname{erfc} \left(\sqrt{\frac{0.5 \times 10^{-8}}{2 \times 10^{-9}}} \right) \\ &= 0.5 \operatorname{erfc}(1.5811) = 0.0127 \end{aligned}$$

$$(b) \quad \cos(\pi/6) = 0.866$$

From Eq. (11.72) and above result probability of error

$$\begin{aligned} P_e &= 0.5 \operatorname{erfc} \left(\sqrt{\frac{0.5 \times 10^{-8}}{2 \times 10^{-9}} \cos \frac{\pi}{6}} \right) \\ &= 0.5 \operatorname{erfc}(1.5811 \times 0.866) = 0.0264 \end{aligned}$$

$$(c) \quad \text{timing error } \tau = 0.1T, \text{ i.e. } \tau/T = 0.1$$

From Eq. (11.77), probability of error

$$\begin{aligned} P_e &= 0.5 \operatorname{erfc} \left(\sqrt{\frac{0.5 \times 10^{-8}}{2 \times 10^{-9}} [1 - 2 \times 0.1]} \right) \\ &= 0.5 \operatorname{erfc}(1.5811 \times 0.8) = 0.0368 \end{aligned}$$

(d) From Eq. (11.78), probability of error

$$P_e = 0.5 \operatorname{erfc} \left(\sqrt{\frac{0.5 \times 10^{-8}}{2 \times 10^{-9}}} [0.866][1 - 2 \times 0.1] \right)$$

$$= 0.5 \operatorname{erfc}(1.5811 \times 0.866 \times 0.8) = 0.0607$$

Example 11.7

Find error probability for coherent FSK when (a) frequency offset is small, (b) frequencies used are orthogonal.

(c) Also find error probability for noncoherent detection. Use data of Example 11.6a.

Solution

$$E_s = A^2 T / 2 = (0.5)(0.01)^2 (10000)^{-1} = 0.5 \times 10^{-8} \text{ and}$$

$$\frac{\eta}{2} = 10^{-9} \text{ W/Hz}$$

(a) From Eq. (11.86), probability of error

$$P_e = 0.5 \operatorname{erfc} \left(\sqrt{\frac{0.6 \times 0.5 \times 10^{-8}}{2 \times 10^{-9}}} \right)$$

$$= 0.5 \operatorname{erfc}(1.2247) = 0.0416$$

(b) From Eq. (11.87), probability of error

$$P_e = 0.5 \operatorname{erfc} \left(\sqrt{\frac{0.5 \times 10^{-8}}{2 \times 2 \times 10^{-9}}} \right)$$

$$= 0.5 \operatorname{erfc}(1.1180) = 0.0569$$

(c) From Eq. (11.88), probability of error

$$P_e = 0.5 \exp \left(-\frac{0.5 \times 10^{-8}}{2 \times 2 \times 10^{-9}} \right)$$

$$= 0.5 \exp(-1.25) = 0.1433$$

Note how FSK reception performs poorly when compared with PSK (Example 11.6a).

SELF-TEST QUESTIONS

9. How does the phase difference with local signal affect correlator based coherent detection of PSK?
10. Does bit synchronization problem affect signal and noise equally?
11. Which of coherent and noncoherent FSK can give lower probability of error?
12. Is the bit probability of error for PSK same as that of QPSK?

11.5 SIGNAL SPACE REPRESENTATION AND PROBABILITY OF ERROR

In Sec. 6.4.7, we considered a situation in which a number of distinct messages m_k were represented by distinct waveforms s_k each of which has a duration T_b . At the receiver, the signal is processed in such a manner that, in the absence of noise, the received signal s_k generates a response r_k , r_k being a single real number. We saw there how best to determine the message from the generated response in order, with noise present, to minimize the probability of error. We found that if a response r was generated, and if all messages are equally likely, we are to determine the message to be that m_k whose corresponding response r_k yields a minimum difference $|r_k - r|$.

Since message signals can be represented as a linear superposition of orthonormal functions, it is useful to represent the signals as vectors in a signal space. For example, consider the case of BPSK shown in Fig. 11.14. In this simple case, the “signal space” is one dimensional. The signals are s_1 and s_2 , given by

$$\left. \begin{array}{l} s_1 \\ s_2 \end{array} \right\} = b(t) \sqrt{2P_s} \cos \omega_0 t \quad 0 < t \leq T_b \quad (11.95)$$

in which, say $b(t) = +1$ for s_1 and $b(t) = -1$ for s_2 . P_s is the signal power. If we introduce the unit (normalized) vector $u(t) = \sqrt{2/T_b} \cos \omega_0 t$, then

$$\left. \begin{array}{l} s_1 \\ s_2 \end{array} \right\} = b(t) \sqrt{P_s T_b} \sqrt{2/T_b} \cos \omega_0 t = b(t) \sqrt{P_s T_b} u(t) \quad 0 \leq t \leq T_b \quad (11.96)$$

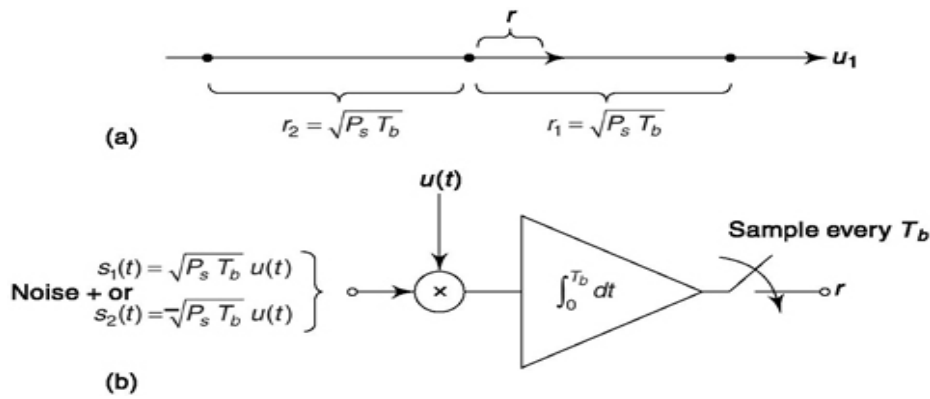


Fig. 11.14 (a) BPSK representation in signal space showing r_1 and r . Received r is drawn for the case where $|r - r_1| < |r - r_2|$ and signal s_1 is determined to have been transmitted. (b) Correlator receiver for BPSK showing that $r = r_1 + n_O$ or $r_2 + n$.

In Fig. 11.14a are shown the signal vectors each of length $\sqrt{P_s T_b}$ measured in terms of the unit vector $u(t) = \sqrt{2/T_b} \cos \omega_0 t$. Processing at the correlator receiver shown in Fig. 11.14b will generate a response r_1 or r_2 for s_1 and s_2 respectively when no noise is present. Now suppose that in some interval, because of noise, a responses generated. If we find $|r - r_1| < |r - r_2|$ then we determine that s_1 was transmitted.

We shall now extend this result, without formal proof, to two-dimensional signal space which we have used to represent BFSK, QPSK and 16 QAM. Specifically a noisy signal response r having been generated, we shall determine, in signal space, the response r_k corresponding to the signal s_k to which r is closest, and we shall then determine that m_k corresponding to s_k was the message that was intended.

11.5.1 probability of Error for BpsK and BFsk bpsk

Using the considerations of the previous section, we shall calculate the error probabilities for synchronous detection in the cases of BPSK. The synchronous detector for BPSK is shown in Fig. 11.14b. Since the BPSK signal is one dimensional, we have from the discussion of Secs. 7.6 and 7.6.1 the result that the only relevant noise in the present case is

$$n(t) = n_o u(t) = n_o \sqrt{2/T_b} \cos \omega_0 t \quad (11.97)$$

in which n_o is a Gaussian random variable of variance $\sigma_o^2 = \eta/2$. Now let us suppose that s_2 was transmitted. The error probability, i.e. the probability that the signal is mistakenly judged to be s_1 is the probability that $n_o > \sqrt{P_s T_b}$. Thus, the error probability P_e is

$$P_e = \frac{1}{\sqrt{2\pi\sigma^2}} \int_{\sqrt{P_s T_b}}^{\infty} e^{-n_o^2/2\sigma^2} dn_o = \frac{1}{\sqrt{\pi\eta}} \int_{\sqrt{P_s T_b}}^{\infty} e^{-n_o^2/2\eta} dn_o \quad (11.98)$$

We let $y^2 \equiv n_o^2/2\sigma_o^2$ and find that

$$P_e = \frac{1}{\sqrt{\pi}} \int_{\sqrt{P_s T_b}/\eta}^{\infty} e^{-y^2} dy = \frac{1}{2} \cdot \frac{2}{\sqrt{\pi}} \int_{\sqrt{P_s T_b}/\eta}^{\infty} e^{-y^2} dy = \frac{1}{2} \operatorname{erfc} \sqrt{\frac{P_s T_b}{\eta}} \quad (11.99)$$

The signal energy is $E_b = P_s T_b$ and the distance between end points of the signal vectors in Fig. 11.14 is $d = 2\sqrt{P_s T_b}$. Accordingly, we find that

$$P_e = \frac{1}{2} \operatorname{erfc} \sqrt{\frac{E_b}{\eta}} = \frac{1}{2} \operatorname{erfc} \sqrt{\frac{d^2}{4\eta}} \quad (11.100)$$

The error probability is thus seen to fall off monotonically with an increase in distance between signals.

BFSK

The case of synchronous detection of orthogonal binary FSK is represented in Fig. 11.15. The signal space is shown in (a). The unit vectors are

$$u_1(t) = \sqrt{\frac{2}{T_b}} \cos \omega_1 t \quad (11.101a)$$

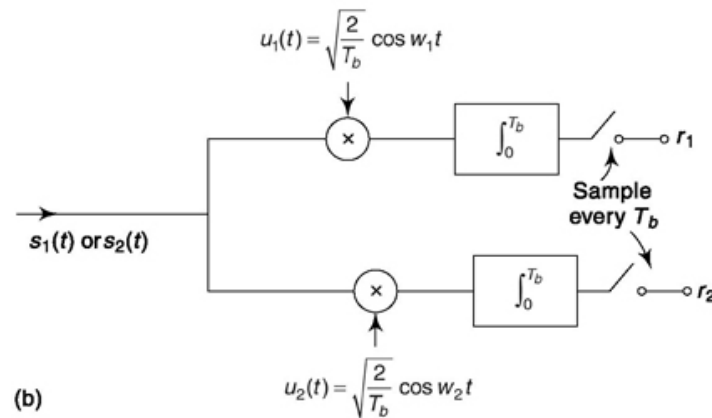
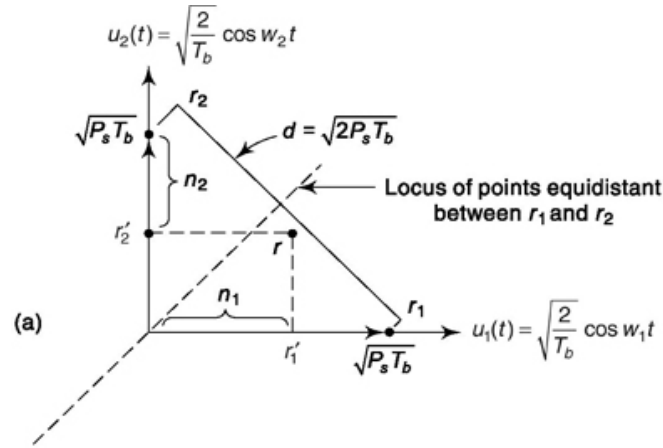


Fig. 11.15 (a) Signal space representation of BFSK. (b) Correlator receiver for BFSK.

and

$$u_2(t) = \sqrt{\frac{2}{T_b}} \cos \omega_2 t \quad (11.101b)$$

orthogonality over the interval T_b having been insured by the selection of ω_1 and ω_2 (see Prob. 11.19). The transmitted signals s_1 and s_2 are of power P_s and are

$$s_1(t) = \sqrt{2P_s} \cos \omega_1 t = \sqrt{P_s T_b} \sqrt{2/T_b} \cos \omega_1 t = \sqrt{P_s T_b} u_1(t) \quad (11.102a)$$

and $s_2(t) = \sqrt{2P_s} \cos \omega_2 t = \sqrt{P_s T_b} \sqrt{2/T_b} \cos \omega_2 t = \sqrt{P_s T_b} u_2(t) \quad (11.102b)$

Detection is accomplished in the manner shown in Fig. 11.15b. The outputs are r_1 and r_2 . In the absence of noise when $s_1(t)$ is received, $r_2 = 0$ and $r_1 = \sqrt{P_s T_b}$. For $s_2(t)$, $r_1 = 0$ and $r_2 = \sqrt{P_s T_b}$. Hence (as in PSK), the vectors representing r_1 and r_2 are of length $\sqrt{P_s T_b}$ as shown in Fig. 11.15a.

Again from the discussion of Sec. 7.6, we have that since the signal is two dimensional, the relevant noise in the present case is

$$n(t) = n_1 u_1(t) + n_2 u_2(t) \quad (11.103)$$

in which n_x and n_2 are Gaussian random variables each of variance $Oj^2 = o2 = h/2$. Now let us suppose that $s_2(t)$ is transmitted and that the observed voltages at the output of the processor are r_j and r_2' as shown in Fig. 11.15a. We find that $r_2' \neq r_2$ because of the noise n_2 and $r_j \neq 0$ because of the noise n_x . We have drawn the locus of points equidistant from r_1 and r_2 and suppose, as shown, that the received voltage r is closer to r_x than to r_2 . Then we shall have made an error in estimating which signal was transmitted. It is readily apparent that such an error will occur whenever $r_1 > r_2 - n_2$ or $r_1 + n_2 > \sqrt{P_s T_b}$. Since n_x and n_2 are uncorrelated, the random variable $n_0 = n_x + n_2$ has a variance $\sigma_o^2 = \sigma_1^2 + \sigma_2^2 = \eta$ and its probability density function is

$$f(n_o) = \frac{1}{\sqrt{2\pi\eta}} e^{-n_o^2/2\eta} \quad (11.104)$$

The probability of error is

$$P_e = \frac{1}{\sqrt{2\pi\eta}} \int_{\sqrt{P_s T_b}}^{\infty} e^{-n_o^2/2\eta} dn_o \quad (11.105)$$

Again we have $E_b = P_s T_b$ and in the present case the distance between r_1 and r_2 is $d = \sqrt{2} \sqrt{P_s T_b}$. Accordingly, proceeding as in Eq. (11.98), we find that

$$P_e = \frac{1}{2} \operatorname{erfc} \sqrt{E_b/2\eta} \quad (11.106a)$$

$$= \frac{1}{2} \operatorname{erfc} \sqrt{d^2/4\eta} \quad (11.106b)$$

Comparing Eqs (11.106b) and (11.100), we see that when expressed in terms of the distance d , the error probabilities are the same for BPSK and BFSK. This result is rather general and does not depend on the special geometries of Figs. 11.14a and 11.15a. In Fig. 11.16, r_1 and r_2 are two signal vector end points located arbitrarily in signal space. The transmitted signal is assumed to be r_1 .

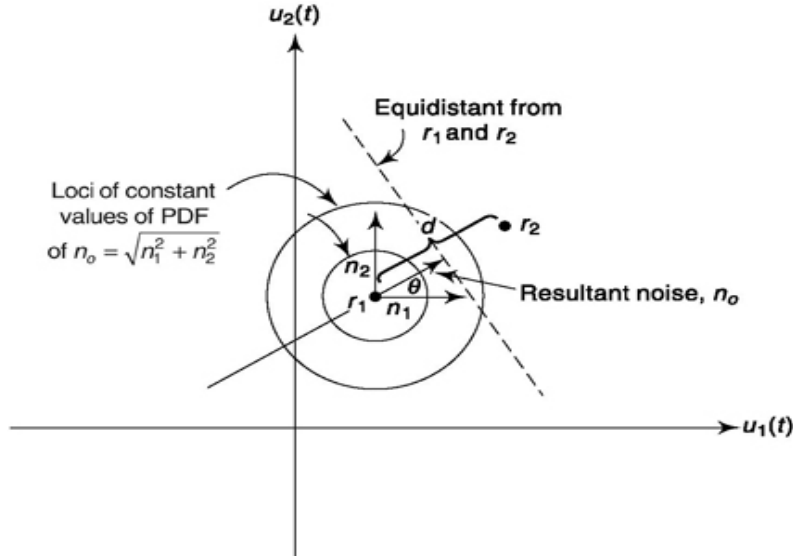


Fig. 11.16 Signal space representation of two signals r_x and r . The loci of constant values of the probability density function (PDF) of n_o are circles with center at r .

Noise components n_x and n_2 displace r_x and if the displacement is large enough to carry the resultant (signal r_1 plus noise) across the (dashed) decision boundary we shall mistakenly estimate that r_2 was transmitted. We note that n_x and n_2 , the random noise amplitudes of the $u_x(t)$ and $u_2(t)$ components, are added to the initial position of r_1 wherever it may be. The displacement of the received voltage caused by the noise components n_1 and n_2 in the direction of r_2 is

$$n_o = n_1 \cos \theta + n_2 \sin \theta \quad (11.107)$$

where n_x and n_2 are independent, Gaussian, random variables of mean zero and of equal variance, $h/2$. Thus n_o is also a Gaussian random variable with mean zero and variance sO , where

$$\begin{aligned} \sigma_o^2 &= E(n_o^2) = E[(n_1 \cos \theta + n_2 \sin \theta)^2] \\ &= E(n_1^2 \cos^2 \theta) + E(n_2^2 \sin^2 \theta) + 2E(n_1 n_2 \sin \theta \cos \theta) \end{aligned} \quad (11.108)$$

Noting that n_1 and n_2 are statistically independent, we have

$$E(n_1 n_2) = 0 \quad (11.109a)$$

Further, n_x and n_y are statistically independent of 6. Thus,

$$E(n_x^2) = E(n_y^2) = \eta/2 \quad (11.109b)$$

and since $E(\cos^2 \theta) = E(\sin^2 \theta) = \frac{1}{2}$, we have

$$E(n_o^2) = \eta/2 \quad (11.110)$$

i.e. the variance of the noise n_o is equal to the variance of n_1 and equal to the variance of n_2 . If we let the distance (voltage) separating r_2 from r_1 be d , the probability of an error P_e is

$$P_e = P\left(n_o > \frac{d}{2}\right) = \int_{(d/2)}^{\infty} \frac{e^{-n_o^2/\eta}}{\sqrt{\pi\eta}} dn_o = \frac{1}{2} \operatorname{erfc} \sqrt{d^2/4\eta} \quad (11.111)$$

as expected.

11.5.2 probability of Error for QpsK

The signal space for QPSK (see Fig. 5.14) is shown again in Fig. 11.17. The unit vectors which establish the coordinate system are

$$u_1(t) = \sqrt{2/T_s} \cos \omega_0 t \quad (11.112a)$$

$$u_2(t) = \sqrt{2/T_s} \sin \omega_0 t \quad (11.112b)$$

in which $T_s = 2T_b$, T_b being the bit time. The relevant noise is

$$n(t) = n_1 u_1(t) + n_2 u_2(t) \quad (11.113)$$

where again n_1 and n_2 are independent, Gaussian random variables of variance $\eta/2$. In the present case, for a reason that will appear shortly, it is more convenient to calculate not the error probability P_e but rather the probability P_c that the decision is *correct*. Thereafter, we can calculate P_e since $P_e = 1 - P_c$. If the transmitted signal is s_1 then a determination will be correct provided that the noise does not move r_1 out of the first quadrant. If such is to be the case we require that

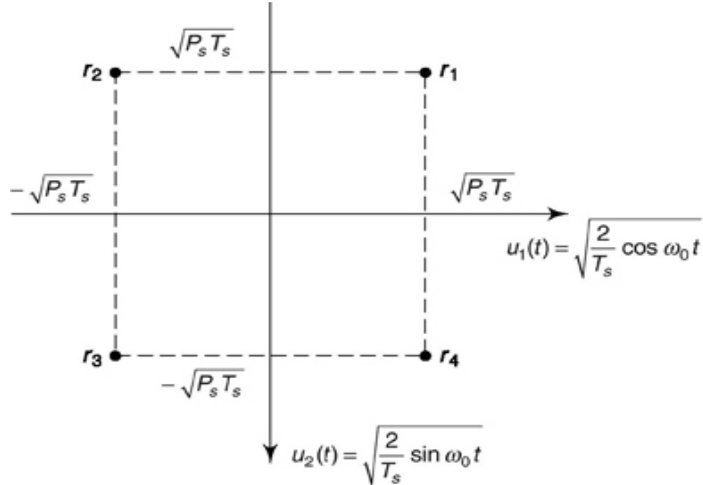


Fig. 11.17 Signal space for QPSK.

both n_1 and n_2 be in the range from $-\sqrt{P_s T_s}$ to infinity. Accordingly, since $d/2 = \sqrt{P_s T_s}$, we have that the probability of a correct decision, given that s_1 was transmitted, is

$$P(c|s_1) = P\left(n_1 > -\frac{d}{2}, n_2 > -\frac{d}{2}\right) = \int_{-d/2}^{\infty} \frac{e^{-n_1^2/\eta}}{\sqrt{\pi\eta}} dn_1 \int_{-d/2}^{\infty} \frac{e^{-n_2^2/\eta}}{\sqrt{\pi\eta}} dn_2 \quad (11.114a)$$

$$= \left[\frac{1}{\sqrt{\pi\eta}} \int_{-d/2}^{\infty} e^{-n_1^2/\eta} dn_1 \right]^2 \quad (11.114b)$$

as can be readily verified (see Prob. 11.24), $P(c|s_1)$ in Eq. (11.114) evaluates to

$$P(c|s_1) = \left[1 - \frac{1}{2} \operatorname{erfc} \sqrt{d^2/4\eta} \right]^2 \quad (11.115)$$

If each signal s_1, s_2, s_3, s_4 are equally likely to be transmitted

$$P_e = 1 - \left[1 - \frac{1}{2} \operatorname{erfc} \sqrt{d^2/4\eta} \right]^2 \quad (11.116)$$

Note that, the above equation when expanded and square of erfc function related term is neglected (in all practical cases very low) gives

$$P_e = \operatorname{erfc} \sqrt{\frac{d^2}{4\eta}} \quad (11.117)$$

11.5.3 probability of Error for MsK

Referring to Fig. 5.32 we see that MSK employs synchronous detection to separate the even and odd bit streams $b_e(t)$ and $b_o(t)$. Furthermore, the correlation interval is $2T_b$ as in QPSK. Thus, to all intents and purposes, the synchronous detector (correlator) could be processing a QPSK signal rather

than an MSK signal. Hence, we would expect that the probability of error of MSK be the same as the probability of error of QPSK:

$$P_{eb}(\text{MSK}) = P_{eb}(\text{QPSK}) = \frac{1}{2} \operatorname{erfc} \sqrt{\frac{E_b}{\eta}} \quad (11.118)$$

To show that such is indeed the case, let us refer to the signal space representation of MSK shown in Fig. 5.30. There we see that $d^2 = 4Eb$ and therefore the symbol error rate of MSK is

$$P_e(\text{MSK}) = 2 \cdot \frac{1}{2} \operatorname{erfc} \sqrt{\frac{d^2}{4\eta}} = \operatorname{erfc} \sqrt{\frac{E_b}{\eta}} \quad (11.119a)$$

Hence, the bit error rate of MSK is

$$P_{eb}(\text{MSK}) = \frac{1}{2} P_e(\text{MSK}) = \frac{1}{2} \operatorname{erfc} \sqrt{\frac{E_b}{\eta}} \quad (11.119b)$$

as expected.

11.6 PROBABILITY OF ERROR CALCULATION FOR M-ARY SIGNAL

The signal space for 16-QASK is shown in Fig. 11.18. We have also marked off the boundaries to which the displacement due to noise must be restricted if an error in message determination is to be avoided. We observe that in the present case we shall have to calculate three different error probabilities because there are three different configurations to the boundaries. Let us use the symbol $P_e(r_1, r_4, r_{13}, r_{16})$ to represent the error probabilities for the four signals in the corners of Fig. 11.18 and similar symbols for the other groupings of signals. Then if all signals are equally likely, the error probability overall would be

$$P_e = \frac{1}{16} [4P_e(r_1, r_4, r_{13}, r_{16}) + 8P_e(r_2, r_3, r_5, r_8, r_9, r_{12}, r_{14}, r_{15}) + 4P_e(r_6, r_7, r_{10}, r_{11})] \quad (11.120)$$

It is apparent that Eq. (11.120), when evaluated, would lead to a rather formidable and awkward expression whose individual terms would have a significance not easily interpretable. Such indeed would be the result as well in a more general case. Further, it is not hard at all to conceive of a case in which an analytic result is not possible and a numerical calculation must be made. Both of these circumstances, complicated expressions or numerical results, have the disadvantage that they limit insight into the merits and

limitations of a system and prevent, as well, an easy comparison of one system with another. Accordingly, we consider now a manner of calculation which leads to an approximate result but does have the feature that it can often circumvent the difficulties we have just described. This calculation leads to the *union-bound approximation*.

To see the nature of the approximation involved we consider the case of QPSK shown again in Fig. 11.19. Assuming r_1 was transmitted let us calculate the probability of an error, the probability of error being that the noise, when added to r_1 yields a vector r that falls outside the upper right quadrant. We calculate first the probability $P(r_2, r_1)$ which we define as the probability that the noise added to r_1 carries the resultant closer to r_2 than to r_1 . Next we calculate $P(r_3, r_1)$ and $P(r_4, r_1)$. Then we ask whether the probability of an error given that r_1 was transmitted, $P(e|s_1)$ is given by

$$P(e|s_1) = P(r_2, r_1) + P(r_3, r_1) + P(r_4, r_1) \quad (11.121)$$

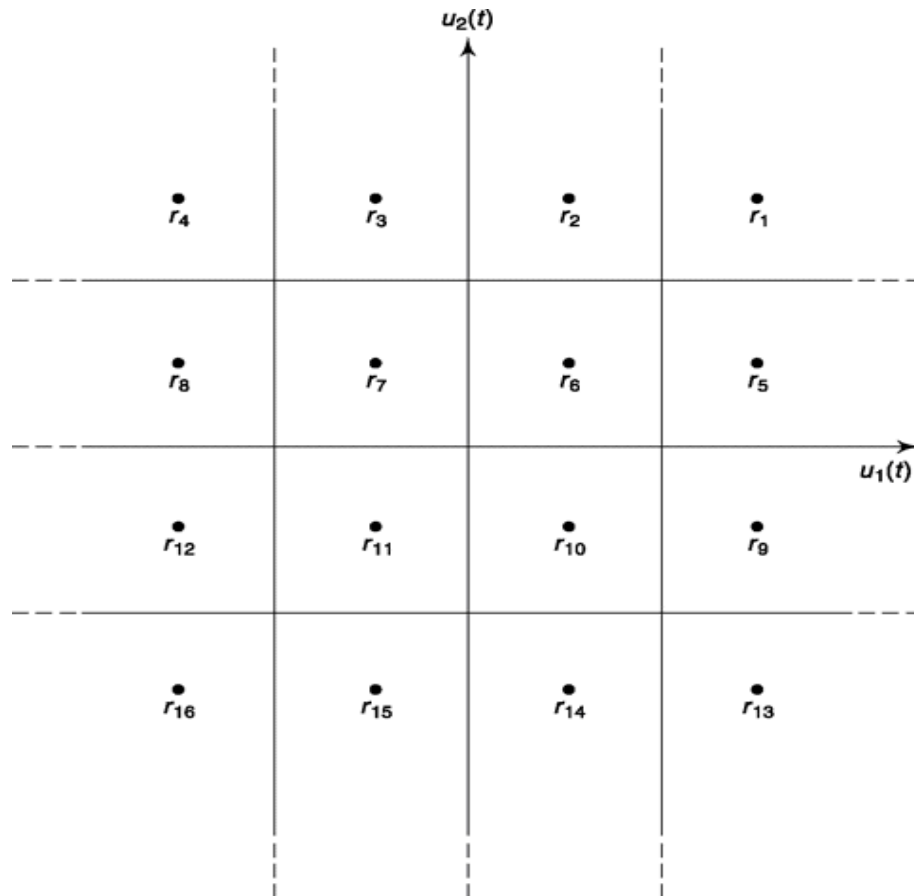


Fig. 11.18 Signal space for 16-QASK.

That is we inquire whether $P(e|s_1)$ is given by the *union* (sum) of these three probabilities. We can see from Fig. 11.19 that such a union involves an approximation. The probability $P(r_2, r_1)$ is the probability that r_1 has been displaced by noise into the region (second and third quadrant) shaded by shading lines which are parallel to the $u_1(t)$ axis. The corresponding shading lines for $P(r_4, r_1)$ are parallel to the $u_2(t)$ axis and the diagonal shading corresponds to $P(r_3, r_1)$. We note that some areas are shaded more than once and hence the sum given in Eq. (11.121) is larger than the correct result and therefore constitutes an *upper bound* on $P(e|s_1)$.

For the case where M signals are used, the union bound approximation yields that the probability of error, given s_1 is transmitted is, using Eq. (11.106b)

$$P(e|s_1) \leq \sum_{k=2}^M \frac{1}{2} \operatorname{erfc} \sqrt{d_{k_1}^2 / 4\eta} \quad (11.122)$$

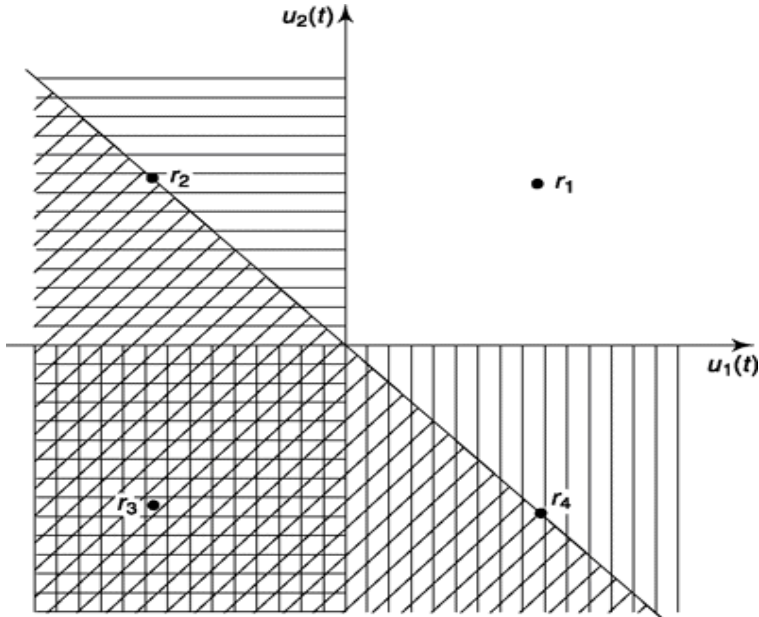


Fig. 11.19 Signal space for QPSK showing approximation made when using the Union Bound.

If there is a symmetry in the M signals so that $P(e|s_k)$ is the same for all k , then we need go no further than Eq. (11.122). Otherwise the error probability without regard to which signal is transmitted will have to be calculated as

$$P_e < \frac{1}{M} \sum_{\substack{j=1 \\ j \neq k}}^M \sum_{k=1}^M \frac{1}{2} \operatorname{erfc} \sqrt{d_{kj}^2 / 4\eta} \quad (11.123)$$

Even when the use of Eq. (11.122) is appropriate, the result often turns out to be too complicated to furnish any useful insight. In such cases, it is common to make a further approximation. The added approximation consists of including in the summation for $P(e|s_1)$ only those terms corresponding to distances between r_1 and its *nearest* neighbors. The justification for such a procedure is to be seen in the following considerations: As a matter of practice, a communications system is useful and of interest only when operated under circumstances where the error probability is very low. Indeed the error probability is usually much less than 10^{-3} . Thus, each term in Eq. (11.122) must then be comparable or smaller than 10^{-3} . Now the complementary error function $\operatorname{erfc} x$ has the property that when $\operatorname{erfc} x$ is small it falls off in value extremely rapidly with increasing x . For example (see Sec. 6.2), if $x = 2.2$, $\operatorname{erfc} x @ 2 \times 10^{-3}$ while if x increases by only 50 percent to $x = 3.3$ we find that $\operatorname{erfc} x = 3.2 \times 10^{-6}$. This rapid decrease becomes even more pronounced as x increases. A further 50 percent increase to $x = 5$ reduces the function to $\operatorname{erfc} x = 1.5 \times 10^{-12}$. Thus, altogether, if the contributions to $P(e|s_1)$ from the closest signal to s_1 is small, the contributions from more distant signals is generally negligible. We now consider some useful results which can be obtained by using the approximation we have discussed.

11.6.1 probability of Error for M-ary psK

The signal space for M-ary PSK is shown in Fig. 5.15. Each signal is represented by an N-bit sequence with $2^N = M$. Each signal is located at a distance $\sqrt{P_s T_s}$ from the origin where $T_s = NT_b$. The signals have an angular separation $2\pi/M$. The signals are located at equal distances from one another around the circumference of a circle of radius $\sqrt{P_s T_s}$. If M is a large number, then the distance d between signals is approximately M and

$$2\pi\sqrt{P_s T_s}/$$

$$d^2 = \frac{4\pi^2 P_s T_s}{M^2} = \frac{4\pi^2 P_s N T_s}{M^2} = \frac{4\pi^2 N E_b}{M^2} \quad (11.124)$$

since $P_s T_b = E_b$ the energy associated with a bit.

Noting the symmetry in the constellation of signals, let us assume that s_1 is transmitted. Thus, taking account of only the two nearest signals to s_1 yields

$$P(e|s_1) \leq P_e \leq 2 \times \frac{1}{2} \operatorname{erfc} \left[\frac{\pi^2 N E_b}{\eta M^2} \right]^{1/2} \quad (11.125)$$

or, using $M = 2^N$, we have

$$P_e = \operatorname{erfc} \left[\frac{\pi^2 N E_b}{\eta 2^{2N}} \right]^{1/2} \quad (11.126)$$

To keep P_e constant as N changes we require that

$$\lambda = \frac{\pi^2 N E_b}{\eta 2^{2N}} = \text{constant} \quad (11.127a)$$

we then have

$$\frac{E_b}{\eta} = \frac{\lambda}{\pi^2} \frac{2^{2N}}{N} \quad (11.127b)$$

Thus the signal energy-to-noise ratio increases nominally in an exponential manner with N for constant P_e .

When M is not so large as to permit the approximation of Eq. (11.124) one can readily show that the distance between adjacent signals can always be obtained from the equation

$$d^2 = 4N E_b \sin^2 \pi/M \quad (11.128)$$

which reduces to Eq. (11.124) for large values of M .

11.6.2 probability of Error for 16-QAM

The signal space for a 16-QASK system is shown in Fig. 11.18. As we already noted, because of the lack of symmetry, Eq. (11.123) must be used to calculate P_e . Still, as an application of Eq. (11.122), let us calculate the error probability for a signal such as s_6 in Fig. 11.18 located at (a, a) in Fig. 5.18. This signal (in common with s_7 , s_{10} , and s_n) has the largest error probability because it has four neighboring signals, each at a minimum distance,

$$d = \sqrt{0.4 E_s} = \sqrt{1.6 E_b} \quad (11.129)$$

Accordingly, we find

$$P_e \leq 4 \times \frac{1}{2} \operatorname{erfc} \left[\frac{1.6E_b}{4\eta} \right]^{1/2} = 2 \operatorname{erfc} \left[0.4 \frac{E_b}{\eta} \right]^{1/2} \quad (11.130)$$

More exact calculations for the present case, using the union bound approximation and also involving no approximation are left as problems (see Probs. 11.27 and 11.28).

11.6.3 probability of Error for Orthogonal M-ary FSK

The signal space for orthogonal M-ary FSK for $M = 3$ is shown in Fig. 5.28. For any number of orthogonal signals M , the distance between signals is

$$d = \sqrt{2E_s} = \sqrt{2NE_b} \quad (11.131)$$

We are not able to draw or visualize a space of more than three dimensions, however, we can conceive of such a space, called a “hyperspace” where the M signals lie. There is complete symmetry among signals; and if we single out any signal, say s_1 , for transmission we have

$$P_e = P(e|s_1) < \frac{(M-1)}{2} \operatorname{erfc} \sqrt{2E_s/4\eta} = \frac{2^N - 1}{2} \operatorname{erfc} \sqrt{NE_b/2\eta} \quad (11.132)$$

Observe, in Eq. (11.132) that the coefficient $(2^N - 1)/2$ causes P_e to increase with increasing N while the factor N in the argument of erfc causes P_e to decrease with increasing N . It is of interest to note that the erfc can overcome the coefficient at large N and that as N increases P_e can be made to become as small as desired. Using the identity

$$2^N = e^{N \ln 2} \quad (11.133)$$

and the approximation valid for large x that

$$\operatorname{erfc} x = \frac{e^{-x^2}}{\sqrt{\pi x}} \quad (11.134)$$

it can be verified (see Prob. 11.30) that P_e may be approximated for large N by

$$P_e < \frac{\exp - N \left[\frac{E_b}{2\eta} - \ln 2 \right]}{2\sqrt{\pi} \sqrt{NE_b/2\eta}} \quad (11.135)$$

Thus, as N increases, P_e decreases so long as

$$\frac{E_b}{\eta} > 2 \ln 2 \approx 1.4 \quad (11.136)$$

As a matter of fact, it can be shown by using a tighter bound than the union bound, that P_e decreases with increasing N so long as

$$\frac{E_b}{\eta} > \ln 2 \approx 0.7 \quad (11.137)$$

11.6.4 Bit-by-bit Encoding versus symbol-by-symbol Encoding

In BPSK and BFSK, we use only *two* waveforms, each persisting for a time T_b . The two waveforms represent the two possible values of a *single* bit. If our communications system needs to accommodate $M = 2^N$ symbols we need to transmit N bits to convey this symbol. In M -ary PSK or M -ary FSK, where M possible symbols are to be accommodated, we transmit one of M distinct waveforms, each time T_s . If the two systems are to be able to transmit messages at the same rate then we require that $T_s = NT_b$. The first method is described as bit-by-bit encoding, and the second is described as symbol-by-symbol encoding. It is clearly of interest to inquire into which method provides the higher probability that the *entire message* is correctly received.

If the message is transmitted through bit-by-bit encoding the probability that the message is correctly received is the probability that *all* of the N bits are correctly received. If P_{eb} is the probability that a bit is received in error then the probability that the entire message is correctly received is

$$P_{c, \text{message}} = (1 - P_{eb})^N \quad (11.138)$$

For BPSK, for example, we have from Eqs (11.138) and (11.100),

$$P_{c, \text{message}} = \left(1 - \frac{1}{2} \operatorname{erfc} \sqrt{E_b/\eta} \right)^N \quad (11.139)$$

It is clear that in bit-by-bit encoding, for fixed P_{eb} , the probability of correctly receiving the message *decreases* with increasing N , and therefore the probability that there is some error in the detected message increases with N .

If, on the other hand, we employ M-ary FSK and encode each of the M messages into its own distinct and individual waveform, the error probability would be given by Eq. (11.132). Then, as we have shown, provided that E_b/h is adequately large, the error probability decreases as N (and hence M) increases. For the case of M-ary PSK, Eq. (11.126) applies and we find that the message error probability increases with increasing N .

11.6.5 Relation Between Bit Error Rate and symbol Error Rate

We have derived a number of expressions which give the *symbol* error probability P_e . If the symbol consists of a single bit, as in BPSK, then, of course, the bit-error probability P_{eb} is the same as the symbol error probability P_e . In the more general case, a system encodes N bits into M symbols with $M = 2^n$. In such cases it is of interest to see what may be determined about P_{eb} from calculations of P_e .

When an N -bit symbol is received with error, it may be that 1 bit or 2 bits or that all N bits are in error. Let us assume that the probability P_e of receiving any of these erroneous symbols is the same. With such an assumption we can without difficulty, relate P_{eb} to P_e . As an example of such a calculation let us consider a case with $M = 4$, $N = 2$ as in QPSK. With such a two-bit transmitted symbol, there are three possible received signals which are erroneous. One such received signal after detection, will have an error in the first bit, a second signal will have an error in the second bit and the third signal will have errors in both bits. The probability of a bit error P_{eb} is then the weighted average:

$$P_{eb} = \frac{\frac{1}{2}P(\text{1st bit error}) + \frac{1}{2}P(\text{2nd bit error}) + \frac{2}{2}P(\text{two-bit error})}{3} \quad (11.140)$$

Since we assume that the three-symbol error probabilities are the same, P_e , Eq. (11.140) becomes:

$$P_{eb} = \frac{2}{3} P_e \quad (11.141)$$

In the general case, it can be shown (Prob. 11.33) that

$$P_{eb} = \frac{M/2}{M-1} P_e \quad (11.142)$$

Actually, errors in received symbols which involve many bit errors and which contribute heavily to P_{eb} are less likely than received symbols with fewer bit errors. Hence, P_{eb} given by Eq. (11.142) is an overestimate, i.e. an upper bound.

Next let us assume that when one of M possible symbols is received and is erroneously decoded, it will be misinterpreted as one or another of only a limited number of the other $M - 1$ symbols. We have already seen in Sec. 11.5.4 that such an approximation is reasonable. There we noted that, in a realistic situation, the probability is overwhelming that a missed symbol will be read as a symbol which is closest in signal space to the symbol which was transmitted. Finally, let us arrange that the symbols are coded in such a manner that closest neighboring symbols differ by only a single bit. Such a coding, using a reflected Grey code, for an eight-symbol PSK system is shown in Fig. 11.20. Here, if s_o is misread, it will be almost inevitable that s_1 or s_7 was transmitted. Under the circumstances just described we have the result that a lower bound on P_{eb} is $P_{eb} = Pe/N$. Altogether, using *Grey coding* and assuming that every signal has an *equal likelihood* of transmission, P_{eb} is bounded as follows:

$$\frac{Pe}{N} \leq P_{eb} \leq \frac{M/2}{M-1} P_e \quad (11.143)$$

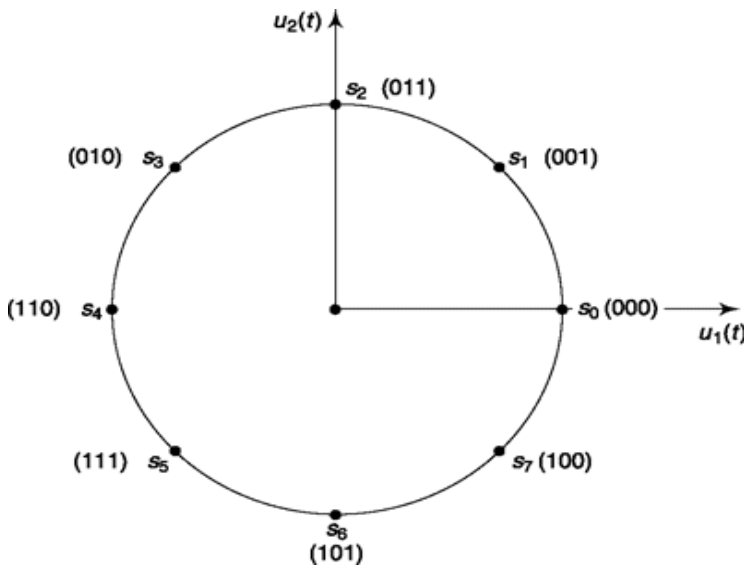


Fig. 11.20 8PSK encoded using the Grey code.

Example 11.8

Find upper limit of error probability in optimal reception of 16-PSK, 16-QASK, orthogonal 16-FSK. Given energy associated with per bit = 5×10^{-8} J and power spectral density of white noise at input 10^{-9} W/Hz.

Solution

$$M = 16, N = \log_2 M = 4, E_b = 5 \times 10^{-8}, \\ \eta = 2 \times 10^{-9}$$

From Eq. (11.126) for 16-PSK, the error limit

$$= \operatorname{erfc} \left[\frac{\pi^2 \times 4 \times 5 \times 10^{-8}}{2 \times 10^{-9} \times 256} \right]^{1/2} = 0.0058$$

From Eq. (11.130) for 16-QASK, the error limit

$$= 2 \times \operatorname{erfc} \left[\frac{0.4 \times 5 \times 10^{-8}}{2 \times 10^{-9}} \right]^{1/2} = 1.55 \times 10^{-5}$$

From Eq. (11.132) for 16-FSK, the error limit

$$= \frac{2^4 - 1}{2} \operatorname{erfc} \left(\sqrt{\frac{4 \times 5 \times 10^{-8}}{2 \times 2 \times 10^{-9}}} \right) = 7.5 \times \operatorname{erfc}(50) = 0$$

(negligibly small 1.14×10^{-22})

Note that, though the above results do not give actual probability of error (only the upper bound) it gives a fairly good idea about their reception performances in terms of error probability.

SELF-TEST QUESTIONS

13. Is the signal space one dimensional for BPSK signal?
14. Does error probability decrease for both BPSK and BFSK with increase in distance between signals in the same monotonic way?
15. Which of lower or upper bound in error probability is referred by union bound approximation?
16. In general, as M increases error probability for M-ary PSK increases while that of M-ary FSK decreases. Is the statement correct?

11.7 PROBABILITY OF ERROR IN A QPR SYSTEM

Figure 11.21 shows a radio communication system employing two quadrature carriers. We have already seen the merit of the use of quadrature carriers in our discussion of QPSK (Sec. 5.4) and other systems, i.e. as compared to a single carrier system, the quadrature carrier system provides two independent channels without any increase in required bandwidth. As a result, we can use the independent channels to transmit alternate data bits and thereby make available for each bit a time interval twice as long as is available with only one carrier.

The input data bits $d(t)$ of duration T_b are presented alternately to the $\cos w_0 t$ and the $\sin w_0 t$ channels and a bit so presented to a channel is not changed for a time $2T_b$. This demultiplexing is represented symbolically by the input switch and the details of a scheme by which the bits can be alternated and held are shown in Fig. 5.10. The data is encoded into an even and an odd baseband signal and these baseband signals amplitude modulate (suppressed carrier) the two carrier waveforms. At the receiver the baseband signal is recovered by synchronous detection and the data is recovered by the usual procedure of sampling each channel at the proper time in each $2T_b$ interval and then taking the magnitude of the sample and inverting it. The even and odd outputs $d_e(t)$ and $d_o(t)$ are multiplexed (interleaved) to reconstruct the original bit stream $d(t)$.

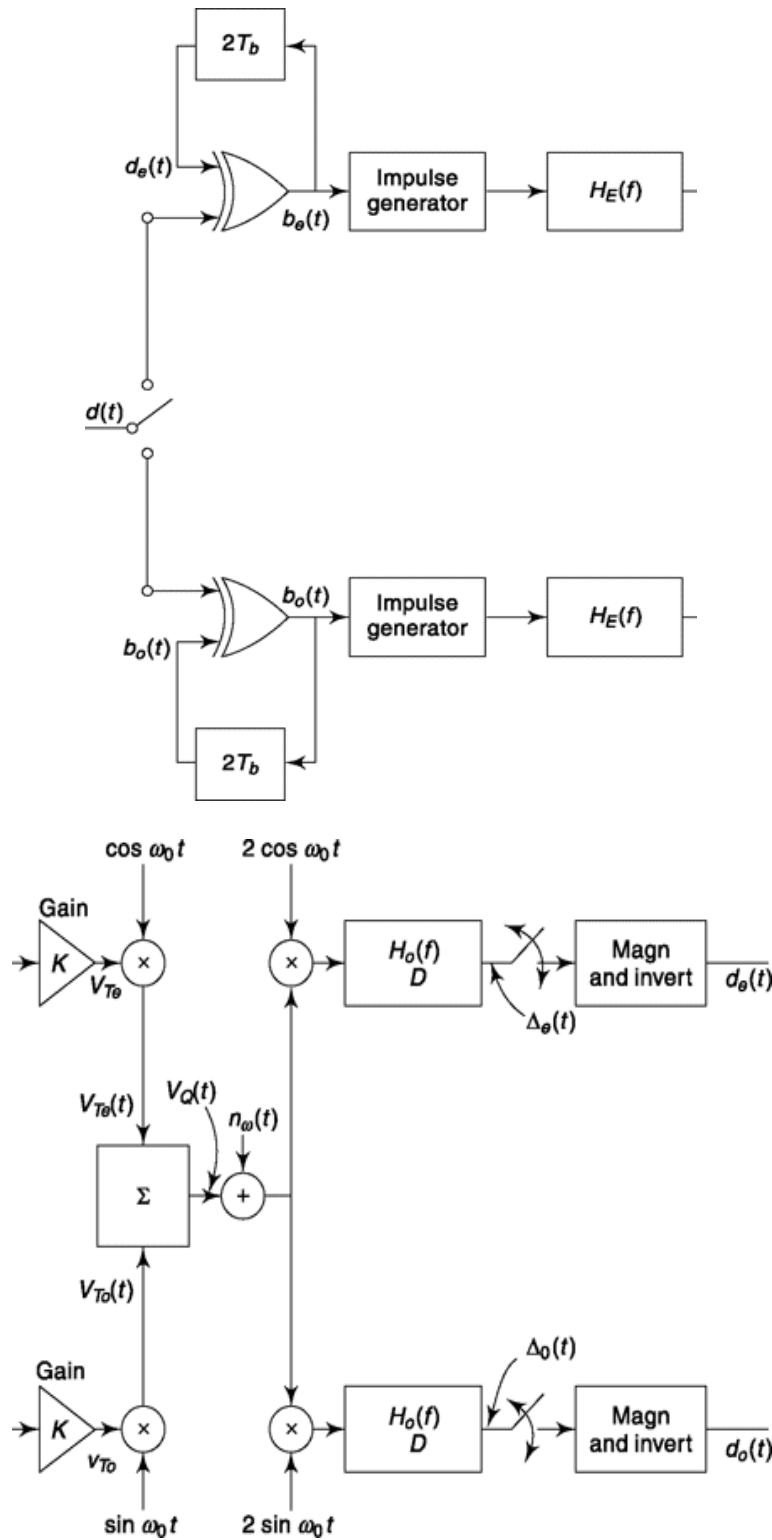


Fig. 11.21 Block diagram of the QPR system.

In Fig. 11.21, the duo binary filter with transfer function $H_C(f)$, given by Eq. (5.110), has been split into two parts, a part $H_E(f)$ associated with the

encoding and a part $H_D(f)$ associated with the decoding. We arrange that

$$H_C(f) = H_E(f)H_D(f) \quad (11.144)$$

Accordingly, if we ignore the noise that is added in transmission, then, except for the fact that the baseband signal has been modulated and then demodulated, we still have exactly the same system as in Fig. 5.39. In the present case, however, because white noise $n_w(t)$ has been added in transmission we have split the filter so that we can arrange that the decoding filter be the *matched filter* for the waveform generated when an impulse is transmitted through the encoding filter.

In the present case, the transfer function $H_C(f)$ of Eq. (5.110) has to be modified by replacing T_b by $2T_b$ (and f_b by $f_b/2$) to take account that each bit is held for a time $2T_b$. Accordingly, we have

$$H_C(f) = 2 \cos 2\pi f T_b \quad |f| \leq f_b/4 \quad (11.145)$$

It turns out that if we select

$$H_E(f) = H_D(f) = \sqrt{H_C(f)} \quad (11.146)$$

then, as is evident, $H_C(f) = H_E(f)H_D(f)$ and as can be verified (see Prob. 11.37) the decoding filter is indeed the matched filter for an impulse transmitted through the encoding filter.

We shall now adjust the gain K so that the modulating baseband signals v_{Te} and v_{To} each have a

normalized power $P_s = vT_e = vj_o$. Assuming impulses of unit strength, the power spectral density of the impulse train applied to the encoding filters is $G(f) = 1/2T_b$. The power spectral density of v_{Te} or of v_{To} is

$$K^2 G(f) |H_E(f)|^2 = \frac{K^2}{2T_b} \cdot 2 \cos 2\pi f T_b = \frac{K^2}{T_b} \cos 2\pi f T_b \quad (11.147)$$

The power in v_{Te} or in v_{To} is calculated by integrating the power spectral density in Eq. (11.149) over the frequency range from $-f_b/4$ to $+f_b/4$. Accordingly, K is determined from the condition that

$$P_s = \int_{-f_b/4}^{+f_b/4} \frac{K^2}{T_b} \cos 2\pi f T_b df \quad (11.148)$$

from which we find

$$K^2 = p T_b^2 P_s \quad (11.149)$$

With K^2 selected as in Eq. (11.149), v_{Te} and v_{To} are each of power P_s and the transmitted signal

$v_Q(t)$ is

$$v_Q(t) = v_{Te} \cos(\omega_0 t + \theta) + v_{To} \sin(\omega_0 t + \theta) \quad (11.150)$$

We see, also that v_Q has a power P_s since

$$\overline{v_Q^2(t)} = \overline{v_{Te}^2} \overline{\cos^2(\omega_0 t + \theta)} + \overline{v_{To}^2} \overline{\sin^2(\omega_0 t + \theta)}$$

and since $\overline{v_{Te}^2} = \overline{v_{To}^2}$, and $\overline{\cos^2(\omega_0 t + \theta)} = \overline{\sin^2(\omega_0 t + \theta)} = \frac{1}{2}$,

$$\overline{v_Q^2} = \overline{v_{Te}^2} = \overline{v_{To}^2} = P_s \quad (11.151)$$

Equation (11.151) is valid because v_{Te} and v_{To} are uncorrelated.

As can be verified, because of the carrier amplitudes selected at the modulator and demodulator as indicated in Fig. 11.21, the demodulator multiplier outputs, neglecting the noise, are precisely v_{Te} and v_{To} . That is, as a matter of computational convenience, we have arranged that the baseband signal applied to the modulating multiplier is recovered unaltered at the output of the demodulating multiplier. We have assumed impulses of unit strength. Such impulses have a Fourier transform of magnitude unity over all frequencies. Hence, altogether, the Fourier transform of the signals $D_e(t)$ and $D_o(t)$ which are to be sampled are

$$\Delta_e(f) = \Delta_o(f) = 1 \cdot K \cdot H_E(f) \cdot H_D(f) \quad (11.152a)$$

$$= KH_C(f) = \sqrt{\pi T_b^2 P_s} \cdot 2 \cos 2\pi f T_b \quad (11.152b)$$

$$= \sqrt{4\pi T_b^2 P_s} \cos 2\pi f T_b \quad |f| \leq f_b/4 \quad (11.152c)$$

Taking the inverse transform (see Prob. 11.37), we find

$$\Delta_e(t) = \Delta_o(f) = \sqrt{\frac{4P_s}{\pi}} \frac{\cos \pi f_b t / 2}{1 - (f_b t)^2} \quad (11.153)$$

Examining Fig. 5.39, we note that when the bit has a duration T_b the sample is to be taken at time $t = T_b/2$. Since, in the present case a bit interval

has the duration $2T_b$, the sampling is to be done at $t = T_b$. We then find that

$$\Delta_e(t = T_b) = \Delta_o(t = T_b) = \sqrt{\frac{\pi P_s}{4}} \quad (11.154)$$

We recall that at each sample time the total output is due to two adjacent input pulses. The total sample value will then be double the value given in Eq. (11.154) if two successive inputs are of the same polarity or will be zero if two successive inputs are of opposite polarity. Altogether then, the outputs are

$$d_e(\text{or } d_o) = \pm \sqrt{\pi P_s} \quad \text{or} \quad 0 \quad (11.155)$$

The white noise has a power spectral density $h/2$. After passing through a demodulator multiplier whose input carrier is $2 \cos w_0 t$ or $2 \sin w_0 t$ the noise will have a density h . After filtering by the decoding filter with transfer function $H_D(f)$ the mean square value of the noise, i.e., its variance squared will be

$$\sigma_N^2 = \int_{-f_b/4}^{+f_b/4} \eta |H_D(f)|^2 df = 4\eta \int_0^{f_b/4} \cos 2\pi f T_b df \quad (11.156a)$$

$$= \frac{2\eta}{\pi T_b} \quad (11.156b)$$

The noise adds to the signal, and the sampling process samples the superposition of the two. An error will be made whenever the noise component of the sample is larger than one half the signal component. Both the white noise and the filtered noise are Gaussian, hence the probability of error P_e is the probability that the noise exceeds $\sqrt{\pi P_s}/2$

$$P_e = \int_{\sqrt{\pi P_s}/2}^{\infty} \frac{e^{-n^2/2\sigma_N^2}}{\sqrt{2\pi\sigma_N^2}} dn \quad (11.157)$$

Defining $x \equiv n/\sqrt{2\sigma_N}$ and using Eq. (11.156b), Eq. (11.157) becomes

$$P_e = \frac{1}{2} \frac{2}{\sqrt{\pi}} \int_{\sqrt{(\pi^2 P_s T_b)/16\eta}}^{\infty} e^{-x^2} dx = \frac{1}{2} \operatorname{erfc} \left[\frac{\pi^2 E_b}{16\eta} \right] \quad (11.158)$$

We note that the channel bandwidth required to transmit a QPR signal is $BW = f/2$ which is the same bandwidth required to transmit 16 QAM or 16

phase PSK. If we compare the probability of symbol error for these systems we find that QPR has a significantly lower error rate. For example, compared with 16 QAM, QPR requires approximately two-thirds the signal-to-noise ratio to achieve the same error rate.

11.8 COMPARISON OF MODULATION SYSTEMS

Table 11.2 presents a summary of the error probability, P_e , and the half-bandwidth of the digital modulation techniques discussed in this chapter for the case of white noise interference. The halfbandwidth, W is the bandwidth of the modulating baseband signal. For SSB modulation, W is the bandwidth of both the modulating baseband signal and the modulated carrier. However, all of the other cases are doubled sideband systems and hence:

$$W = \frac{B}{2} \quad (11.159)$$

B being the (two-sided) bandwidth of the modulated carrier. For the sake of having a uniform basis of comparison, we have in every case tabulated the error probability P_e .

Table 11.2 Summary of P_e and W for Digital Modulation Techniques (M = number of symbols, N = number of bits/symbol, $2^N = M$)

Modulation Technique	P_e	W
BPSK, QPSK, MSK	$\frac{1}{2} \operatorname{erfc} [E_b/\eta]^{1/2}$	f_b/N
MPSK	$\operatorname{erfc} \left[\frac{NE_b}{\eta} \sin^2 \pi/M \right]^{1/2}$	f_b/N
16 QAM	$2 \operatorname{erfc} [0.4_b/E_b/\eta]^{1/2}$	$f_b/4$
Orthogonal MFSK	$\frac{M-1}{2} \operatorname{erfc} [NE_b/2\eta]^{1/2}$	Mf_b/N
QPR	$\frac{1}{2} \operatorname{erfc} \left[\frac{\pi^2}{16} \frac{E_b}{\eta} \right]^{1/2}$	$f_b/4$

In connection with a communication system which is to be designed, it is commonplace that, in addition to such practical constraints as cost, volume, etc., there be a specification on allowable error rate. In such circumstances, plots as shown in Fig. 11.22 are very useful. Here, P_e is fixed at $P_e = 10^{-5}$. As we shall see in Sec. 13.4.1, there is an ultimate limit to the performance

of a communications system. This limit, deduced by Shannon, is given by the inequality:

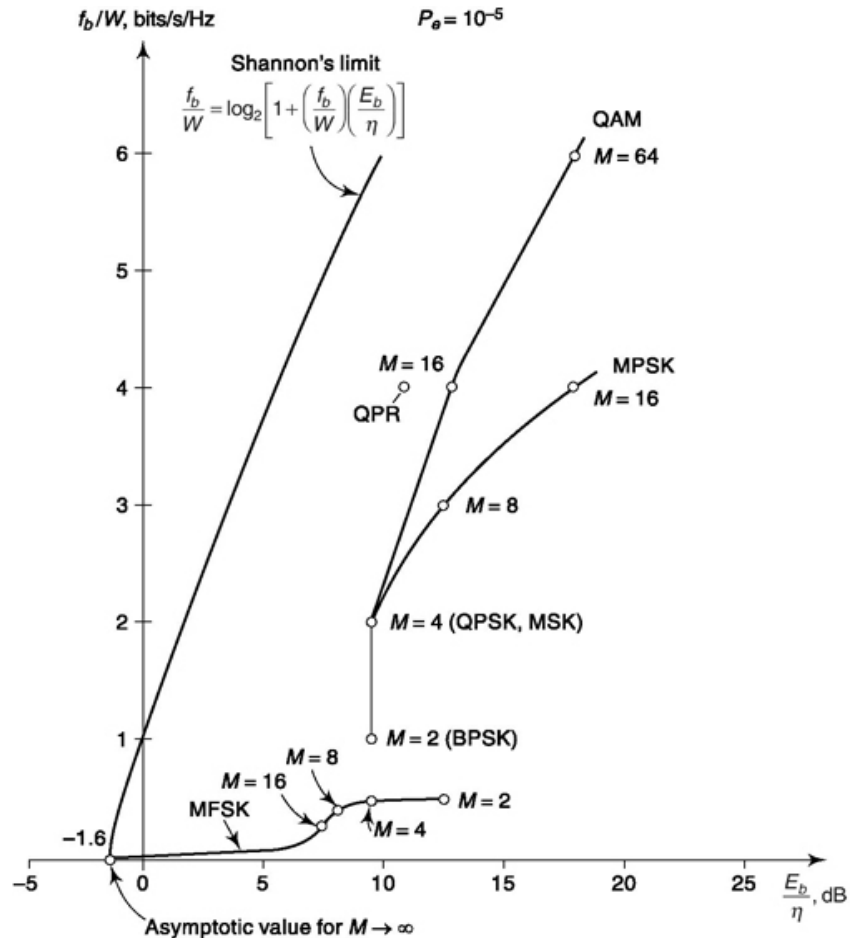


Fig. 11.22 Bits/s/Hz vs. E_b/η for probability of error = 10^{-5} .

$$\frac{f_b}{W} \leq \log_2 \left[1 + \left(\frac{f_b}{W} \right) \left(\frac{E_b}{\eta} \right) \right] \quad (11.160)$$

and is independant of the error probability. We have included a plot of Eq. (11.60) in Fig. 11.22. In Fig. 11.22, as well as for any given error probability, P_e , we shall always find that all modulation schemes yield plots which lie to the *right* of Shannon's limiting plot.

Figure 11.22 shows that QAM more closely approaches Shannon's curve than does MPSK, indicating that QAM is a more efficient system for operation in a white Gaussian noise environment. Note that when we compare MPSK with MFSK (see Table 11.2 and Fig. 11.22), we find that as

M increases the bandwidth of MPSK decreases while the SNR required to obtain $P_e = 10^{-5}$ increases. However, with MFSK, the bandwidth increases while the SNR decreases. In all cases however we note that the *slope* of each curve is positive, so that an increase in f_b/W requires an increase in E_b/h if a constant bit error rate is to be maintained, i.e. for a constant error rate

$$\frac{f_b}{W} \sim \frac{E_b}{\eta} \quad (11.161)$$

If the error rate were, for example, $P_e = 10^{-6}$ each curve would shift approximately 1 dB to the *right*, except of course, for Shannon's curve which is independent of P_e .

Example 11.9

Find probability of error of the QPR system defined in Sec. 11.7 if energy associated with each bit = 5×10^{-8} J and power spectral density of white noise at input 10^{-9} W/Hz. If channel bandwidth is 10 kHz what data rate is supported?

Solution:

$$E_b = 5 \times 10^{-8}, \eta = 2 \times 10^{-9}$$

From Eq. (11.158), probability of error

$$= 0.5 \times \text{erfc} \left[\frac{\pi^2 \times 5 \times 10^{-8}}{2 \times 10^{-9} \times 16} \right]^{1/2} = 1.4 \times 10^{-8}$$

Data rate can be supported up to $= 2 \times 10^4 = 20$ kbps

SELF-TEST QUESTIONS

17. If bit rate is f_b , what channel bandwidth is required for QPR transmission?
18. For a constant bit error rate, is it necessary to increase bit energy to noise ratio to reduce bandwidth requirement?
19. Does Shanon's limit depend on probability of error?
20. The acceptable error probability in data communication is typically 10^{-5} . Is that true?

FACTS AND FIGURES

A controversy that began towards the end of the seventeenth century turned ugly when two of the greatest personalities of science, Newton and Leibniz, accused each other of plagiarism over who ‘invented’ calculus. It was found that Newton had indeed started the work before Leibniz but it was the latter who first got his work published. Whether Leibniz was aware of Newton’s unpublished work remained a contentious issue. Soon it divided the scientific community on national lines and it became a war of Newton’s England vs. Leibniz’s Germany. Today it is regarded that both worked independent of each other and both are held in great respect. Calculus continues with the symbols introduced by them; f as notation for derivative introduced by Newton, J as notation for integral dy and — for differentiation of y with respect to x introduced by Leibniz.

Modern calculus, however, can be linked to many early works scattered across the globe. Calculation of area and volume remain a basic function of integral calculus. Antiphon, Eudoxus and Archimedes, all from Greece (480-212 BC) contributed to these calculations. Liu Hui of China calculated the volume of a cylinder in the third century. Aryabhatta of India in 500 AD showed how to calculate volumes of cubes and gave expressions related to basic differential equations. In eleventh century, Alhacen from Iraq calculated the volume of a paraboloid and derived the formula for sum of fourth power. In the seventeenth century, Isaac Barrow, Pierre de Fermat, Blaise Pascal, John Wallis and others from Europe dwelt on different aspects of derivatives.

MATLAB

We learn a new MATLAB utility in this chapter by which you can enter data/parameter at command prompt. When this is used, you no longer need to change data/parameter values in the original program through MATLAB editor.

```

% Experiment 44
% This calculates probability of error(or upper limit) for different types
% of modulation contaminated by white Gaussian noise. Note that by using
% 'input', data can be entered by user at the command prompt. Press 'Enter'
% after entering input data

% This uses Table 11.2 of the textbook

choice=input('Enter 1:BPSK, 2:QPSK, 3:MSK, 4:16-QASK, 5:QPR, 6:MPSK, 7:ortho. MFSK - ');
SNR=input('Enter Eb/eta ratio i.e. bit energy to twice of PSD - ');

if choice >5
    M = input('Enter no. of symbols in integer power of 2 - ');
end

if choice <4,
    Pe = 0.5*erfc(sqrt(SNR));
end

if choice == 4,
    Pe = 2*erfc(sqrt(0.4*SNR));
end

if choice == 5,
    Pe = 0.5*erfc(sqrt(pi*pi*SNR/16));
end

if choice == 6,
    N = log2(M);
    Pe = erfc(sqrt(N*SNR)*sin(pi/M));
end

if choice == 7,
    N = log2(M);
    Pe = ((M-1)/2)*erfc(sqrt(N*SNR/2));
end

Error_Probability = Pe

```

You can substitute values given in various examples of this chapter and check the result. Below one example is shown where data from Example 6a is used.

>> exp44

```
Enter 1:BPSK, 2:QPSK, 3:MSK, 4:16-QASK, 5:QPR, 6:MPSK, 7:ortho. MFSK - 1
Enter Eb/eta ratio i.e. bit energy to twice of PSD - 2.5
```

```
Error_Probability =
0.0127
```

You can play with above codes and include various effects like phase, bit synchronization.

```

% Experiment 45

% This calculates probability of error vs SNR (from 1 to 25)
% The numbering follows notation of Experiment 44

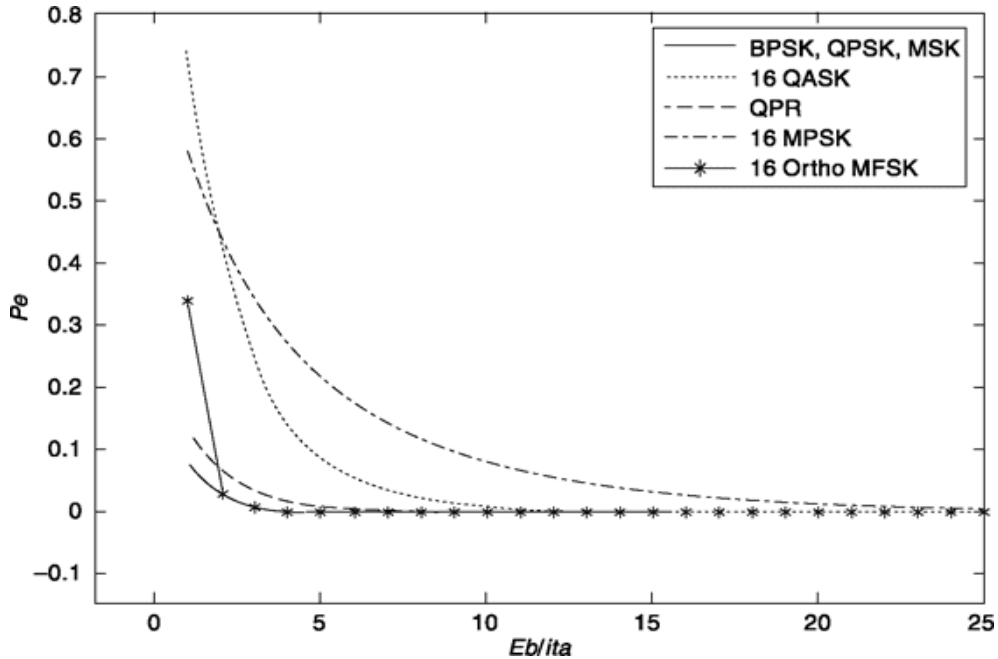
% This uses the Table 11.2 of the text book

SNR=1:25; M=16; N=log2(M);

Pe_1toPe_3=0.5*erfc(sqrt(SNR));
Pe_4 = 2*erfc(sqrt(0.4*SNR));
Pe_5 = 0.5*erfc(sqrt(pi*pi*SNR/16));
Pe_6 = erfc(sqrt(N*SNR)*sin(pi/M));
Pe_7 = ((M-1)/2)*erfc(sqrt(N*SNR/2));

plot(SNR,Pe_1toPe_3,'r-',SNR,Pe_4,'b:',SNR,Pe_5,'g- ',SNR,Pe_6,'c-.',SNR,Pe_7,
'k-*');
legend('BPSK,QPSK,MSK','16QASK','QPR','16MPSK','16OrthoMFSK');
xlabel('Eb/ita')
ylabel('Pe')

```



SUMMARY

The chapter begins with requirement of a baseband receiver and gently introduces concept of matched filter. The theoretical derivation of an optimal filter and how it is implemented through matched filter and correlator are discussed. The logic used applies equally well to both baseband and passband reception of digital data. Probability of error or its upper limit is calculated for different types of transmission mode. Signal space representation of a signal is also used which is particularly useful for M-ary

communication. A discussion on relationship between bit error rate and symbol error rate is presented. In all these derivations, it is assumed that symbols are equiprobable and also the cost of making a wrong decision is same for every circumstances. A discussion on maximum likelihood detector and generalized Bayes' receiver shows how to proceed if it is otherwise. Finally, probability of error of QPR system is presented in full detail followed by comparison of different modulation systems in terms of error probability and bandwidth requirement.

PROBLEMS

11.1 (a) Find the power spectral density $G_n(f)$ of noise $n(t)$ which has an autocorrelation function

$$R_n(\tau) = \sigma^2 e^{-|\tau/\tau_0|}$$

(b) The noise in (a) is applied to an integrator at $t = 0$. Find the mean square value of the noise output of the integrator at $t = T$. $[n_o(T)]^2$

(c) The noise in (a) accompanies a signal which consists of either the voltage $+V$ or the voltage $-V$ sustained for a time T . At time $t = T$, find the ratio of the integrator output due to the signal to the rms noise voltage.

11.2 A received signal $s(t) = \pm V$ is held for an interval T . The signal is accompanied by white Gaussian noise of power spectral density $h/2$. The received signal is to be processed as in Fig. 11.2. However, as an approximation to the required integrator, we use a low-pass RC circuit of 3 dB bandwidth f_c . Calculate the value of f_c for which the signal-to-noise voltage, at the sampling time, will be a maximum. For this value of f_c calculate the signal-to-rms noise ratio and compare with Eq. (11.6) which applies when an integrator is used. Show that for the RC network the signal-to-noise ratio is about 1 dB smaller than for the integrator.

11.3 A signal which can assume one of the voltage $+V$ or $-V$ is transmitted. Consider that the probability of transmitting $+V$ is $\frac{3}{4}$ while the probability of transmitting $-V$ is $\frac{1}{4}$. The signal is accompanied by white Gaussian noise. The signal is accompanied by white Gaussian noise.

(a) Assume that the threshold voltage for decision between the two possible signals is V_t rather than zero volts. Write an expression for the probability that an error in decision will be made. An integrate and dump receiver is used as in Fig. 11.2.

(b) Find V_t such that the probability of error is a minimum and calculate the corresponding probability of error.

11.4 A signal, which can take on the voltages $+V$, 0 , $-V$ with equal likelihood, is transmitted. When received, it is embedded in white Gaussian noise. The receiver integrates the signal and noise for a time T_s .

Write an expression for the threshold voltages $\pm V_s$ so that the probability of error is independent of which signal is transmitted.

11.5 A 1 kbps bipolar binary signal is a ± 1 V pulse is contaminated with white Gaussian noise of variance 0.1. For an integrator and dump type receiver filter find optimum decision threshold if prior probability $P(s_1)$ is (a) 0.2, (b) 0.5 and (c) 0.7.

11.6 Show how optimum threshold changes in previous problem if cost of making a wrong decision when 1 is transmitted is (a) 0.4, (b) 0.5 and (0.6).

11.7 A received signal is either $+2V$ or $-2V$ held for a time T . The signal is corrupted by white Gaussian noise of power spectral density 10^{-4} volt 2 /Hz. If the signal is processed by an integrate and dump receiver, what is the minimum time T during which a signal must be sustained if the probability of error is not to exceed 10^{-4} ?

11.8 A transmitter transmits the signals $\pm V$ with equal probability; the channel noise has the power spectral density $G_n(f) = G_0/[1 + (ff/f_0)]$

(a) Find the transfer function $H(f)$ of the *matched filter*, and comment on its realizability.

(b) Find the average probability of error when using the matched filter.

(c) An integrator is employed rather than the optimum filter. Find its P_e and compare with (b).

11.9 A signal is either $s_1(t) = A \cos 2\pi f_0 t$ or $s_2(t) = 0$ for an interval $T = n/f_0$ with n an integer. The signal is corrupted by white noise with $G_n(f) =$

$h/2$. Find the transfer function of the matched filter for this signal. Write an expression for the probability of error P_e .

11.10 Repeat Prob. 11.9 if the signal is $s(t) = \pm A(1 - \cos 2\pi f_0 t)$.

11.11 Compare the outputs of the MF and the correlator, when the input signal is either $\pm V$, as a function of time t for $0 < t < T$. Assume white Gaussian noise. Are the outputs the same for all t , or just when $t = T$?

11.12 A signal is $s(t) = \pm 2(t/T)$ for $0 < t < T$. The signal is corrupted by white Gaussian noise of power spectral density 10^{-6} volt²/Hz.

(a) Draw the signal waveform at the output of a matched filter receiver.

(b) If the probability of error P_e is to be no larger than 10^{-4} , find the minimum allowable interval T .

11.13 Verify Eq. (11.72).

11.14 Plot Eq. (11.86) versus E_s/h .

11.15 If the frequency offset W in FSK satisfies $WT = np$, $s_1(t)$ and $s_2(t)$ are orthogonal.

(a) Prove this statement.

(b) Calculate P_e .

(c) Plot P_e versus E_s/h and compare with the results given in Eq. (11.86).

11.16 Plot the P_e in binary FSK as a function of WT . Select $E_s/h = 15$.

11.17 Plot Eq. (11.88) versus EJh .

11.18 M-ary PSK involves choosing signals of the form $(\cos \omega_0 t + Q)$ for M values of i .

(a) Show how to choose the Q_t so that the probability of error of each Q_t is the same.

(b) Find the correlator detector.

(c) Obtain an expression for the probability of error.

11.19 Verify the entries in Table 11.1.

11.20 Verify Eq. (11.96).

11.21 Refer to Eq. (11.101a and b). Determine w_2 - such that the unit vectors $u_1(t)$ and $u_2(t)$ are orthonormal.

11.22 (a) If $u_1(t) = \sqrt{2/T_b} \cos(\omega_1 t + \Theta)$ and $u_2(t) = \sqrt{2/T_b} \cos(\omega_2 t + \phi)$ where Θ and ϕ are

independent random variables uniformly distributed between $-p < \Theta, \phi < P$, find $w - W$ so that u_1 , and u_2 are orthonormal.

(b) Compare your answer to the answer obtained for Prob. 11.19. Why do they differ?

11.23 Plot a graph having an ordinate which is f_yW and an abscissa which is E_b/h for BPSK and BFSK for $P_e = 10^{-4}, 10^{-5}$ and 10^{-6} . Use Eqs (11.100) and (11.106a) and the results,

$$f_i(\text{BPSK}) = 2f_b \text{ and } f_i(\text{BFSK}) = 4f_b.$$

11.24 Verify that Eq. (11.114) reduces to Eq. (11.115).

11.25 Equations (11.124) and (11.126) assume that the *arc* of a circle is of the same length as the *chord*. (a) Derive an expression for P_e to replace Eq. (11.126) if the above approximation is *not* made. (b) If the approximation is to be used but the resulting P_e is to be correct to within 50 percent determine the minimum value of M .

11.26 If the probability of BPSK, BFSK and MPSK for $M = 4, 8, 16, 32$ and 64 are to be the same, what is the ratio of their E_b/h compared to $(E_b/h)_{\text{BPSK}}$?

11.27 Calculate P_e for 16 QAM using the Union Bound. Compare your answer with that of Eq. (11.130).

11.28 Calculate P_e for 16 QAM without using the Union Bound approximation.

11.29 (a) Using the Union Bound approximation, calculate P_e for 64 and 256 QAM.

(b) To obtain the same P_e for 16, 64 and 256 QAM determine the ratio of each E_b/h as compared to $(E_b/h)_{\text{BPSK}}$.

11.30 Verify Eq. (11.135).

11.31 A 9.6 kb/s NRZ data stream is to be transmitted over a 2.4 kHz bandwidth channel. What modulation system would you choose if an error rate of 10^{-4} is to be achieved with a minimum signal-to-noise ratio (minimum E_b/h)?

11.32 A 9.6 kb/s NRZ data stream is to be transmitted over a 2.4 kHz bandwidth channel. An error rate of 10^{-4} is desired. Due to channel nonlinearities and its phase characteristics, intersymbol interference (ISI) is produced which results in an “eye pattern” which closes by 3 dB compared to the response obtained when the transmitter is connected directly to the receiver (by-passing the channel) when E_b/h is 12 dB.

Can a modulation system be found to achieve this error rate of 10^{-3} ? What is the value of E_b/h that is needed?

11.33 The probability of a bit being in error is 10^{-3} . (a) If a message consists of 10 bits, calculate the probability of the message being in error. (b) Repeat (a), if the message length is 100, 1000, 10,000. Note how quickly the probability of a message being in error increases toward unity.

11.34 The probability of a bit being in error is 10^{-3} . (a) What is the probability of a 6-bit word containing an error? (b) The bits are grouped so that instead of transmitting 6 bits, bit-by-bit, a 64 phase, 64 PSK signal is sent. (The symbol rate is one-sixth of the bit rate.) Calculate the probability of a 6-bit symbol being in error. (c) Repeat (b) using 64 QAM. (d) Repeat using 64 FSK. (e) Discuss your results.

11.35 Verify Eq. (11.141).

11.36 Consider that bits are grouped so that there are 4 bits/symbol and then modulated using 16 QAM. Following Fig. 11.20 show how to arrange the Grey code so that an error in a symbol will with high probability correspond to an error in only 1 of the 4 bits.

11.37 Prove that $H_D(f)$ as defined by Eqs (11.145) and (11.146) is the matched filter for an impulse transmitted through $H_E(f)$.

11.38 Verify Eq. (11.149).

11.39 Verify Eq. (11.152) and Eq. (11.153).

11.40 Verify Eq. (11.154).

11.41 $D_0(kT_s)$ and $D_s(kT_s)$ can each assume one of three values. Thus, a signal space sketch would indicate nine signal points. Determine the nine signal points in signal space to yield Eq. (11.158).

11.42 A probability of error of 10^{-5} is desired and a channel bandwidth of 20 kHz is available. If the bit rate is 80 kb/s, 16 PSK, 16 QAM, or QPR can be used. Calculate the value of E_b/h required for each of these systems.

11.43 MSK can be viewed as an FM system with a peak frequency deviation of $f/4$. If coherent FM detection is employed as in MFSK (see Sec. 11.4.2), calculate the probability of error.

11.44 MSK can be detected in a noncoherent manner using an FM discriminator. Referring to Fig. 9.15, the 1F filter bandwidth is set to $B = 1.5 f_b$ (since the spectral density of MSK is zero at $f - f_c = 0.75 f_b$, very little required signal power lies outside this region and hence ISI can be neglected). The baseband filter is often replaced by an integrate-and-dump filter, which integrates over each bit, i.e. for a time T_b .

(a) Using Eqs (9.22), (9.27), and (9.92) where $|8f| = f/4$, calculate the probability of error.

(b) Why is $f = f_b/4$? (c) How much degradation is produced when the FM discriminator is employed?

11.45 Using Table 11.2 and Shannon's limit, plot Fig. 11.22 for $P_e = 10^{-6}$.

REFERENCES

1. Stein, S., and J. Jones: "Modern Communication Principles," McGraw-Hill Book Company, New York, 1967.
2. Schwartz, M., W. R. Bennett, and S. Stein: "Communication Systems and Techniques," McGraw-Hill Book Company, New York, 1966.
3. Wozencraft, J., and I. Jacobs: "Communication Engineering," John Wiley and Sons, New York, 1966.

12

NOISE IN PULSE CODE MODULATION AND DELTA MODULATION SYSTEMS

CHAPTER OBJECTIVE

In the previous chapter, we have calculated probability of error or bit error rate for different kinds of digital modulation systems. An error bit is a part of bit stream generated after waveform coding following analog-to-digital conversion. Depending on the location of the error bit in the coded waveform, whether it is a more significant bit or a less significant one, the quality of the signal at the receiver side after digital-to-analog conversion becomes different. We discuss two waveform coding techniques—Pulse Code Modulation (PCM) and Delta Modulation (DM)—in this chapter and calculate the signal to noise ratio at the receiver end for different digital modulation schemes and the probability of error. We take speech as an application example through which we present a comparison of PCM and DM that combines effect of both quantization noise and thermal noise. Finally, noise aspect in Adaptive Delta Modulation (ADM) in relation to its use in a space shuttle flights is presented. Besides numerical examples the chapter also presents MATLAB based simulations.

FACTS AND FIGURES

The credit of PCM invention goes to Alec Reeves, a British Engineer. It was 1937 and he was working for the International Telephone and Telegraph in France. Reeves got a French patent of his invention in 1938 and a USA patent in 1942. Interestingly, unaware of this progress Bell Lab scientists of USA too developed PCM with its first ever implementation in SIGSALY, a communication system used in World War II. On this, the Reeves had the following to say in his 1964 note on “*The past, present and future of Pulse-Code Modulation*”.

“Having got it patented, for understandable reasons I then let the invention slip from my mind until the end of the war; and it was in the U.S.A. during World War II that the next step in PCM’s progress was made. It was in the Bell Telephone Laboratories that this next, important stage was undertaken: a team under Ralph Bown, comprising among others Harold S. Black, carried out practical design studies on PCM for the U.S. Army Signal Corps. It is right that in the records this early Bell work should be stressed; for it was the first time that the principles underlying the new system were translated into hardware.”

12.1 PCM TRANSMISSION

A binary PCM transmission system is shown in Fig. 12.1. The baseband signal $m(t)$ is quantized, giving rise to the quantized signal $m_q(t)$, where

$$m_q(t) = m(t) + e(t) \quad (12.1)$$

The term $e(t)$ is the error signal which results from the process of quantization. The quantized signal is next sampled. Sampling takes place at the Nyquist rate. The sampling interval is $T_s = 1/2f_M$, where f_M is the frequency to which the signal $m(t)$ is bandlimited.

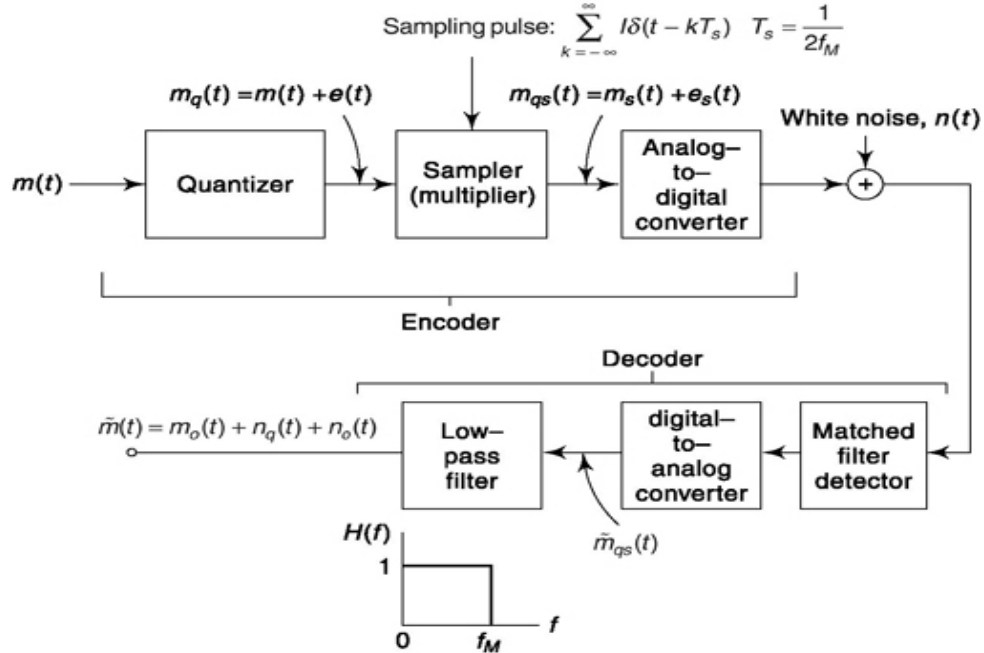


Fig. 12.1 A binary PCM encoder-decoder.

Sampling is accomplished by multiplying the signal $m_q(t)$ by a waveform which consists of a periodic train of pulses, the pulses being separated by the sampling interval T_s . We shall assume that the sampling pulses are narrow enough so that the sampling may be considered as instantaneous. It will be recalled (Sec. 4.1.1) that with such instantaneous sampling, the sampled signal may be reconstructed *exactly* by passing the sequence of samples through a low-pass filter with cut-off frequency at f_M . Now, as a matter of mathematical convenience, we shall represent each sampling pulse as an impulse. Such an impulse is infinitesimally narrow yet is characterized by having a finite area. The area of an impulse is called its *strength*, and an impulse of strength I is written $IS(t)$. The sampling-impulse train is therefore $S(t)$, given by

$$S(t) = I \sum_{k=-\infty}^{\infty} \delta(t - kT_s) \quad T_s = \frac{1}{2f_M} \quad (12.2)$$

From Eqs. (12.1) and (12.2) the quantized signal $m_q(t)$ after sampling becomes $m_{qs}(t)$, written as

$$m_{qs}(t) = m(t)I \sum_{k=-\infty}^{\infty} \delta(t - kT_s) + e(t)I \sum_{k=-\infty}^{\infty} \delta(t - kT_s) \quad (12.3a)$$

$$= m_s(t) + e_s(t) \quad (12.3b)$$

The quantized, sampled signal $m_{qs}(t)$ which consists of the sum of two strength-modulated impulse trains is applied to an analog-to-digital converter. (In a physical system, the input to the A/D converter is a quantized amplitude-modulated *pulse* train.) The binary output of the A/D converter is transmitted over a communication channel and arrives at the receiver contaminated as a result of the addition of white thermal noise $n(t)$. Transmission may be direct, as indicated in Fig. 12.1, or the binary output

signal may be used to modulate a carrier as in PSK or FSK. In any event, the received signal is detected by a matched filter to minimize errors in determining each binary bit and thereafter passed on to a D/A converter. The output of the D/A converter is called $m_{qs}(t)$. [In the absence of thermal noise, and assuming unity gain from the input to the A/D converter to the output of the D/A converter, we would have $m_{qs}(t) = m_{qs}(t)$.] Finally, the signal $m_{qs}(t)$ is passed through the low-pass baseband filter. At the output of this filter we find a signal $m_O(t)$ which, aside from a possible difference in amplitude, has exactly the waveform of the original baseband signal $m(t)$. This output signal, however, is accompanied by a noise waveform $n_q(t)$, which is due to the quantization, and an additional noise waveform $n_{th}(t)$, due to the thermal noise.

12.1.1 Calculation of Quantization Noise

We shall now temporarily ignore the effect of the thermal noise and shall calculate the output power due to the quantization noise in the PCM system of Fig. 12.1.

The sampled quantization error waveform, as given by Eq. (12.3), is

$$e_S(t) = e(t)I \times d(t - kT_S) \quad (12.4)$$

It is to be noted that if the sampling rate is selected to be the Nyquist rate for the baseband signal $m(t)$, the sampling rate will be inadequate to allow reconstruction of the error signal $e(t)$ from its samples $e_S(t)$. That such is the case is readily apparent from Fig. 12.2. In Fig. 12.2a is shown the relationship between $m_q(t)$ and $m(t)$, while in Fig. 12.2b is shown the error waveform $e(t)$ as a function of $m(t)$. The quantization levels are separated by amount S . We observe in Fig. 12.2b that $e(t)$ executes a complete cycle and exhibits an abrupt discontinuity every time $m(t)$ makes an excursion of amount S . Hence, the spectral range of $e(t)$ extends far beyond the bandlimit f_M of $m(t)$.

To find the quantization noise output power N_q , we require the power spectral density of the sampled quantization error $e_S(t)$, given in Eq. (12.4). Since $S(t - kT_S) = 0$ except when $t = kT_S$, $e_S(t)$ may be written

$$e_S$$

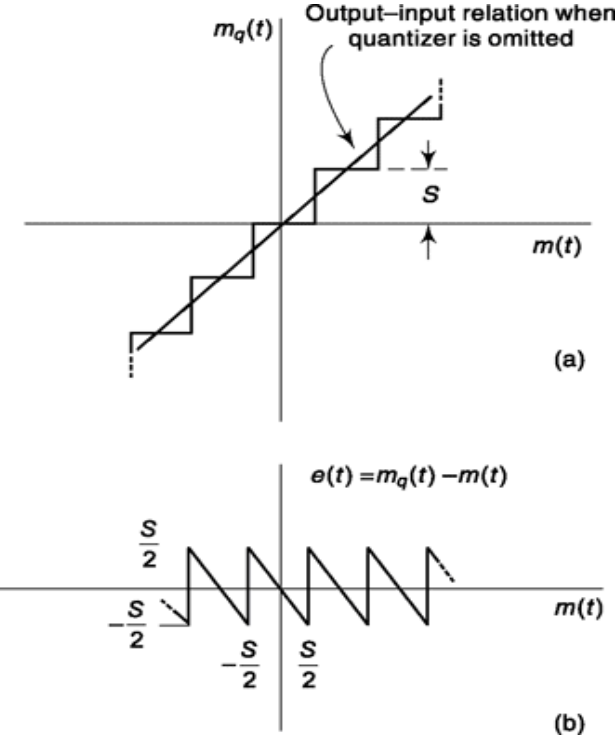


Fig. 12.2 (a) Plot of $m_q(t)$ as a function of $m(t)$. (b) Plot of $e(t)$ as a function of $m(t)$.

$$e_s(t) = I \sum_{k=-\infty}^{\infty} e(kT_s) \delta(t - kT_s) \quad (12.5)$$

The waveform of Eq. (6.53) consists of a sequence of impulses of area (strength) $A = e(kT_s)I$ occurring at intervals T_s . The quantity $e(kT_s)$ is the quantization error at the sampling time and is a random variable. In Sec. 6.53 we calculated the power spectral density of just such a waveform and arrived at the result given in Eq. (6.153). Applying Eq. (6.153) to the present case, we find that the power spectral density $G_e(f)$ of the sampled quantization error is

$$G_{e_s}(f) = \frac{I^2}{T_s} \overline{e^2(kT_s)} \quad (12.6)$$

In Sec. 4.4.2 [see Eq. (4.26)] we found that if the quantization levels are separated by amount S , then the quantization error is given by

$$\overline{e^2(t)} = \frac{S^2}{12} \quad (12.7)$$

Equation (12.6) involves $\overline{e^2(kT_s)}$ rather than $\overline{e^2(t)}$. However, since the probability density of $e(t)$ does not depend on time, the variance of $e(t)$ is equal to the variance of $e(t = kT_s)$. Thus,

$$\overline{e^2(t)} = \overline{e^2(kT_s)} = \frac{S^2}{12} \quad (12.8)$$

From Eqs. (12.6), (12.7), and (12.8), we have

$$G_{e_s}(f) = \frac{I^2 S^2}{T_s 12} \quad (12.9)$$

Finally, the quantization noise N_q is, from Eq. (12.9),

$$N_q = \int_{-f_M}^{f_M} G_{e_s}(f) df = \frac{I^2 S^2}{T_s 12} 2 f_M = \frac{I^2 S^2}{T_s^2 12} \quad (12.10)$$

since $2f_M = 1/T_s$.

Of more interest than the quantization noise given in Eq. (12.10) is the signal-to-quantization noise ratio. To determine this ratio, we calculate, in the next section, the output-signal power expressed in terms of the quantization step size S .

12.1.2 The Output Signal Power

The sampled signal which appears at the input to the baseband filter shown in Fig. 12.1 is given by $m_s(t)$ in Eq. (12.3) as

$$m_s(t) = m(t) I \sum_{k=-\infty}^{\infty} \delta(t - KT_s) \quad (12.11)$$

Since the impulse train is periodic it can be represented by a Fourier series. Because the impulses have a strength (area) I and are separated by a time T_s , the first term in the Fourier series is the dc component which is $1/T_s$. Hence the signal $m_o(t)$ at the output of the baseband filter is

$$m_o(t) = \frac{1}{T_s} m(t) \quad (12.12)$$

Since $T_s = 1/2f_M$, other terms in the series of Eq. (12.11) lie outside the passband of the filter. The normalized signal output power is, from Eq. (12.12),

$$\overline{m_o^2} = \frac{I^2}{T_s^2} \overline{m^2(t)} \quad (12.13)$$

We shall now express $\overline{m^2(t)}$ in terms of the number M of quantization levels and the step size S . To do this we assume that the signal can vary from $-MS/2$ to $+MS/2$, that is, we assume that the instantaneous value of $m(t)$ may fall anywhere in its allowable range of MS volts with equal likelihood. Then the probability density of the instantaneous value of m is $f(m)$ given by

$$f(m) = \frac{1}{MS} \quad (12.14)$$

The variance of $m(t)$, that is, $\overline{m^2(t)}$, is

$$\overline{m^2(t)} = \int_{-MS/2}^{MS/2} m^2 f(m) dm = \int_{-MS/2}^{MS/2} \frac{m^2 dm}{MS} = \frac{M^2 S^2}{12} \quad (12.15)$$

Hence, from Eq. (12.13), the output-signal power is

$$S_o = \overline{m_o^2(t)} = \frac{I^2}{T_s^2} \frac{M^2 S^2}{12} \quad (12.16)$$

From Eqs. (12.10) and (12.16), we find that the signal-to-quantization-noise ratio is

$$\frac{S_o}{N_q} = M^2 = (2^N)^2 = 2^{2N} \quad (12.17)$$

where N is the number of binary digits needed to assign individual binary-code designations to the M quantization levels.

12.1.3 The Effect of Thermal Noise

The effect of additive thermal noise is to cause the matched filter detector of Fig. 12.1 to make an occasional error in determining whether a binary 1 or a binary 0 was transmitted. As we saw in Chap. 11, if the thermal noise is white and Gaussian, the probability of such an error depends on the ratio E_b/h where E_b is the signal energy transmitted during a bit and $h/2$ is the two-sided power spectral density of the noise. The error probability depends also on the type of modulation employed, i.e. direct transmission, PSK, FSK, etc.

Rather typically, PCM systems operate with error probabilities which are small enough so that we may ignore the likelihood that more than a single bit error will occur within a single word. By way of example, if the error probability $P_e = 10^{-5}$ and a word has 8 bits ($N = 8$), we would expect, on the average, that 1 word would be in error for every 12,500 words transmitted. Indeed, the probability of

$$\text{two bits being in error in the same 8 bit word when } P_e = 10^{-5} \text{ is } P_2 = \left(\frac{8}{2}\right)P_e^2(1 - P_e)^6 \approx \frac{28 \times 10^{-10}}{.}$$

Let us assume that a code word used to identify a quantization level has N binary digits. We assume further that the assignment of code words to levels is in the order of the numerical significance of the word. Thus, we assign 00 ... 00 to the most negative level, 00 ... 01 to the next-higher level until the most positive level is assigned the code word 11 ... 11.

An error which occurs in the least significant bit of the code word corresponds to an incorrect determination by amount S in the quantized value $m_S(t)$ of the sampled signal. An error in the next-higher significant bit corresponds to an error $2S$; in the next-higher, $4S$, etc. Let us call the error Dm . Then assuming that an error may occur with equal likelihood in any bit of the word, the variance of the error is

$$\overline{(\Delta m_s)^2} = \frac{1}{N} [S^2 + (2S)^2 + (4S)^2 + (8S)^2 + \dots + (2^{N-1} S)^2] \quad (12.18)$$

The sum of the geometric progression in Eq. (12.18) is

$$\overline{(\Delta m_s)^2} = \frac{2^{2N}-1}{3N} S^2 \cong \frac{2^{2N}}{3N} S^2 \quad (12.19)$$

for $N \geq 2$.

The preceding discussion indicates that the effect of thermal-noise errors may be taken into account by adding, at the input to the A/D converter in Fig. 12.1, an error voltage Dm_S , and by deleting the white-noise source and the matched filter. We have assumed unity gain from the input to the

A/D converter to the output of the D/A converter. Thus, the same error voltage appears at the input to the low-pass baseband filter. The result of a succession of errors is a train of impulses, each of strength IDm_s . These impulses are of random amplitude and of random time of occurrence.

A thermal-noise error impulse occurs on each occasion when a word is in error. With P_e the probability of a bit error, the mean separation between bits which are in error is $1/P_e$ bits. With N bits per word, the mean separation between words which are in error is $1/NP_e$ words. Words are separated in time by the sampling interval T_s . Hence, the mean time between words which are in error is T , given by

$$T = \frac{T_s}{NP_e} \quad (12.20)$$

Again using Eq. (6.153), we find that the power spectral density of the thermal-noise error impulse train is, using Eqs. (12.19) and (12.20),

$$G_{th}(f) = \frac{I^2 \overline{(\Delta m_s)^2}}{T} = \frac{NP_e I^2 \overline{(\Delta m_s)^2}}{T_s} \quad (12.21)$$

Using Eq. (12.19), we have

$$G_{th}(f) = \frac{2^{2N} S^2 P_e I^2}{3 T_s} \quad (12.22)$$

Finally, the output power due to the thermal error noise is

$$N_{th} = \int_{-f_M}^{f_M} G_{th}(f) df = \frac{2^{2N} S^2 P_e I^2}{3 T_s^2} \quad (12.23)$$

since $T_s = 1/2f_M$.

12.1.4 Output signal-to-noise ratio in pCM

The output signal-to-noise ratio, including both quantization and thermal noise, is found by combining Eqs. (12.10), (12.16), and (12.23). The result is

$$\begin{aligned}\frac{S_o}{N_o} &= \frac{S_o}{N_q + N_{th}} = \frac{(I^2/T_s^2)(M^2 S^2/12)}{(I^2/T_s^2)(S^2/12) + (I^2/T_s^2)(P_e 2^{2N} S^2/3)} \\ &= \frac{2^{2N}}{1 + 4P_e 2^{2N}}\end{aligned}\quad (12.24)$$

in which we have used the fact that $M = 2^N$.

In PSK (or for direct transmission) we have, from Eq. (11.70), that

$$(P_e)_{\text{PSK}} = \frac{1}{2} \operatorname{erfc} \sqrt{\frac{E_b}{\eta}} \quad (12.25)$$

where E_b is the signal energy of a bit and $\eta/2$ is the two-sided thermal-noise power spectral density. Also, for coherent reception of FSK we have, from Eq. (11.86), that

$$(P_e)_{\text{FSK}} = \frac{1}{2} \operatorname{erfc} \sqrt{0.6 \frac{E_b}{\eta}} \quad (12.26)$$

To calculate E_b , we note that if a sample is taken at intervals of T_s , and the code word of N bits occupies the entire interval between samples, then a bit has a duration T_s/N . If the received signal power is S_i , the energy E_b associated with a single bit is

$$E_b = S_i \frac{T_s}{N} = S_i \frac{1}{2f_M N} \quad (12.27)$$

Combining Eqs. (12.24), (12.25), and (12.27), we find

$$\left(\frac{S_o}{N_o} \right)_{\text{PSK}} = \frac{2^{2N}}{1 + 2^{2N+1} \operatorname{erfc} \sqrt{(1/2N)(S_i/\eta f_M)}} \quad (12.28)$$

Using Eq. (12.26) in place of (12.25), we have

$$\left(\frac{S_o}{N_o} \right)_{\text{FSK}} = \frac{2^{2N}}{1 + 2^{2N+1} \operatorname{erfc} \sqrt{(0.3/N)(S_i/\eta f_M)}} \quad (12.29)$$

Equations (12.28) and (12.29) are plotted in Fig. 12.3 for $N = 8$. Note that for $S_i/\eta f_M \gg 1$ and $N = 8$

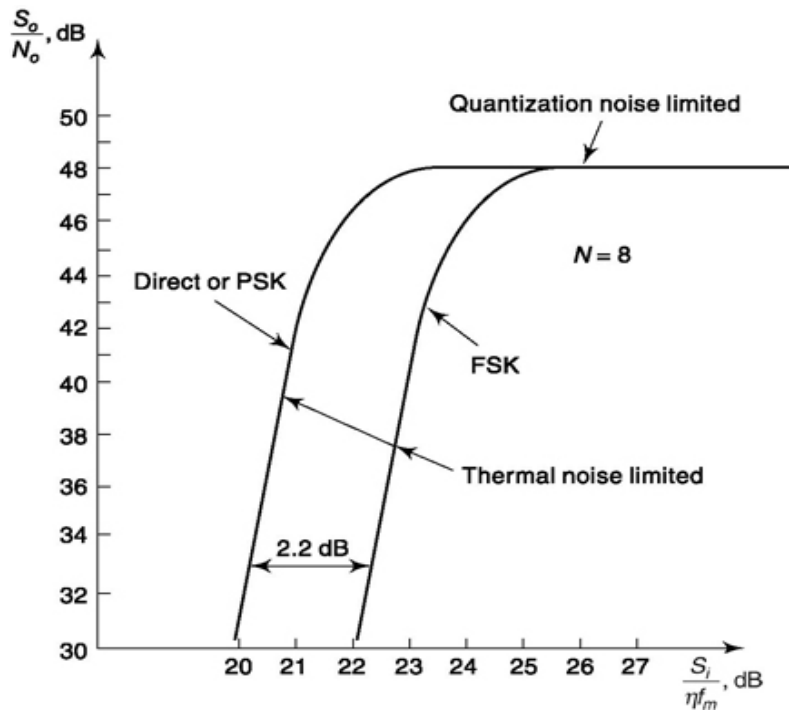


Fig. 12.3 Comparison of PCM transmission systems.

$$\left(\frac{S_o}{N_o} \right)_{PSK, FSK} = 10 \log (2^{16}) = 48 \text{ dB}$$

Observe that both PCM systems exhibit a threshold, the FSK threshold occurring at a S_i/hf_M which is 2.2 dB greater than for PSK. (The threshold point is arbitrarily defined as the S_i/hf_M value at which S_o/N_o has fallen 1 dB from the value corresponding to a large S/hf_M .) Experimentally, the onset of threshold in PCM is marked by an abrupt increase in a *crackling* noise analogous to the clicking noise heard below threshold in analog FM systems.

A comparison of PCM and FM is presented in Sec. 13.16.3.

Example 12.1

Show that for each additional bit used in quantization, the signal to quantization noise ratio is quadrupled.

Solution

From Eq. 12.17, $\left(\frac{S_o}{N_q}\right)_N = 2^{2N}$ where suffix N stands for no. of bits used

Then, $\left(\frac{S_o}{N_q}\right)_{N+1} = 2^{2(N+1)}$. Taking ratio

$$\left(\frac{S_o}{N_q}\right)_{N+1} / \left(\frac{S_o}{N_q}\right)_N = 2^{2(N+1)} / 2^{2N} = 2^2 = 4$$

Hence, shown.

Example 12.2

Find output SNR (in dB) of optimal receiver with PCM coded PSK modulated data. Given, white noise PSD = 10^{-9} W/Hz, baseband cut-off frequency = 4000 Hz and (a) input signal energy 0.001, No. of level used for PCM coding = 8, (b) input signal energy 0.001, No. of level used = 256, (c) input signal energy 0.01, No. of level used = 256. Find input SNR in dB in each case.

Solution

Given, $\eta = 2 \times 10^{-9}$, $f_M = 4000$

(a) $S_i = 0.001$, $M = 8$ then $N = \log_2 8 = 3$.

$$\begin{aligned} \text{Input SNR} &= \frac{S_i}{\eta f_M} \\ &= 10 \log_{10} \left[\frac{0.001}{2 \times 10^{-9} \times 4000} \right] \\ &= 20.97 \text{ dB} \end{aligned}$$

Substituting in Eq. (12.28)

Output SNR

$$= 10 \log_{10} \left[\frac{2^{2 \times 3}}{1 + 2^{2 \times 3+1} \operatorname{erfc} \left(\sqrt{\frac{10^{-3}}{2 \times 3 \times 2 \times 10^{-9} \times 4000}} \right)} \right]$$

$$= 18.06 \text{ dB}$$

- (b) $S_i = 0.001, M = 256$ then $N = \log_2 256 = 8$.

Substituting as above

Output SNR

$$= 10 \log_{10} \left[\frac{2^{2 \times 8}}{1 + 2^{2 \times 8+1} \operatorname{erfc} \left(\sqrt{\frac{10^{-3}}{2 \times 3 \times 2 \times 10^{-9} \times 4000}} \right)} \right]$$

$$= 37.70 \text{ dB}$$

Input SNR same as (a)

- (c) $S_i = 0.001, M = 256$ then $N = \log_2 256 = 8$.

Substituting as above

Output SNR

$$= 10 \log_{10} \left[\frac{2^{2 \times 8}}{1 + 2^{2 \times 8+1} \operatorname{erfc} \left(\sqrt{\frac{10^{-2}}{2 \times 3 \times 2 \times 10^{-9} \times 4000}} \right)} \right]$$

$$= 48.16 \text{ dB}$$

Since signal energy is increased 10 times compared to (a), input SNR will be 10dB more i.e. 30.97 dB

You can compare the result with plot shown in Fig. 12.3.

Again compare with the plot given in Fig. 12.3. Note the drastic fall in performance compared to PSK of Example 12.2 for case (b) as FSK goes below threshold at higher input SNR.

Example 12.3

Repeat Example 2 for PCM coded FSK modulated data.

Solution

- (a) Output SNR

$$= 10 \log_{10} \left[\frac{2^{2 \times 3}}{1 + 2^{2 \times 3+1} \operatorname{erfc} \left(\sqrt{\frac{0.3 \times 10^{-3}}{3 \times 2 \times 10^{-9} \times 4000}} \right)} \right]$$

$$= 18.06 \text{ dB}$$

(b) Output SNR

$$= 10\log_{10} \left[\frac{2^{2 \times 8}}{1 + 2^{2 \times 8+1} \operatorname{erfc} \left(\sqrt{\frac{0.3 \times 10^{-3}}{3 \times 2 \times 10^{-9} \times 4000}} \right)} \right]$$

$$= 23.55 \text{ dB}$$

(c) Output SNR

$$= 10\log_{10} \left[\frac{2^{2 \times 8}}{1 + 2^{2 \times 8+1} \operatorname{erfc} \left(\sqrt{\frac{0.3 \times 10^{-2}}{3 \times 2 \times 10^{-9} \times 4000}} \right)} \right]$$

$$= 48.16 \text{ dB}$$

SELF-TEST QUESTION

1. The quantization error cannot be reconstructed from sampled data. Why?
2. Does probability distribution of quantization noise depend on time?
3. The thermal noise is white, Gaussian. Is it true?
4. In the context of received SNR, which of PSK and FSK performs better?

12.2 DELTA MODULATION (DM) TRANSMISSION

The operation of a delta-modulation communication system was discussed in Sec. 4.7. At that point the discussion was entirely qualitative, and we considered neither quantization nor thermal noise. In the following sections we shall calculate the output signal-to-noise ratio of a DM system taking quantization noise and thermal noise into account.

A delta-modulation system, including a thermal-noise source, is shown in Fig. 12.4. The impulse generator applies to the modulator a continuous sequence of impulses $p(t)$ of time separation t . The modulator output is a sequence of pulses $p_O(t)$ whose polarity depends on the polarity of the difference signal $D(t) = m(t) - m(t)$, where $m(t)$ is the integrator output. We assume that the integrator has been adjusted so that its response to an input impulse of strength I is a step of size S ; that is, $m(t) = (S/I) \int p_O(t) dt$.

A typical impulse train $p_O(t)$ is shown in Fig. 12.5a [actually, of course, the waveform $p_O(t)$ is a train of narrow pulses, each having very small energy]. Before transmission, the impulse waveform will be converted to the two-level waveform of Fig. 12.5b since this latter waveform has much greater power than a train of narrow pulses. This conversion is accomplished by the block in Fig. 12.4 marked "transmitter." The transmitter, in principle, need be nothing more complicated than

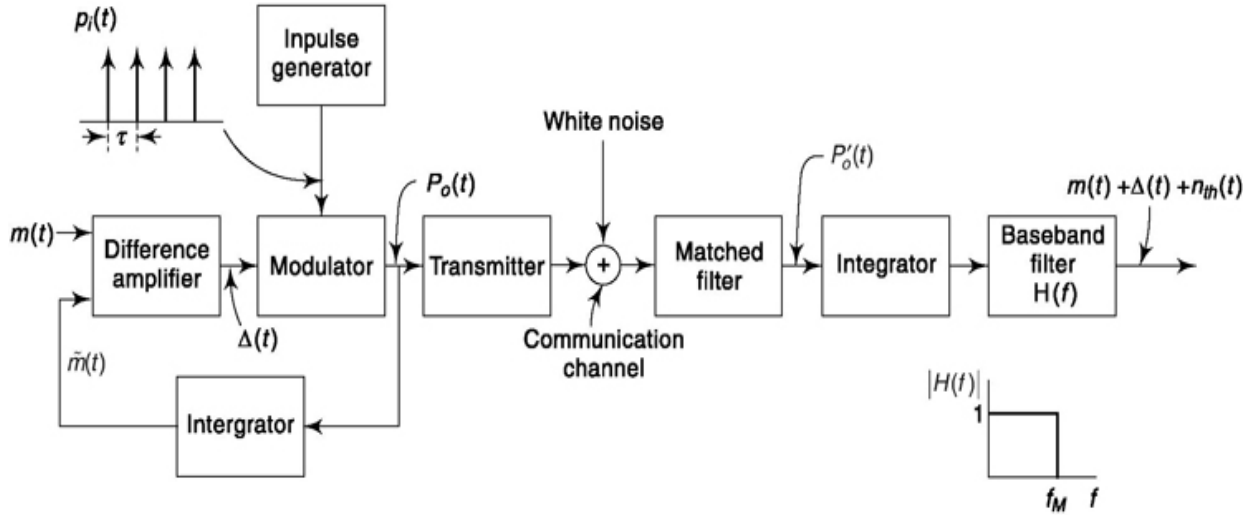


Fig. 12.4 A delta-modulation system.

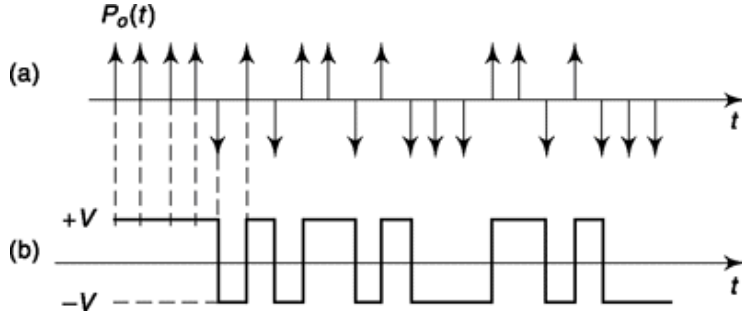


Fig.12.5 (a) A typical impulse train $p_o(t)$ appearing at the modulator output in Fig. 12.5. (b) The two level signal transmitted over the communication channel.

a bistable multivibrator (Flip-Flop). We may readily arrange that the positive impulses set the flip-flop into one of its stable states, while the negative impulses reset the Flip-Flop to its other stable state. The binary waveform of Fig. 12.5b will be transmitted directly or used to modulate a carrier as in PSK or FSK. After detection by the matched filter shown in Fig. 12.4, the binary waveform will be reconverted to a sequence of impulses $p'_o(t)$. In the absence of thermal noise $p'_o(t) = p_o(t)$, and the signal $m(t)$ is recovered at the receiver by passing $m(t)$ through an integrator. We assume that transmitter and receiver integrators are identical and that the input to each consists of a train of impulses of strength $\pm I$. Hence in the absence of thermal noise, the outputs of both integrators are identical.

12.2.1 Quantization Noise in Delta Modulation

To arrive at an estimate of the quantization noise power in delta modulation, we consider the situation represented in Fig. 12.6. Here, in Fig. 12.6a is shown a sinusoidal input signal $m(t)$ and the waveform $m(t)$ which is the delta modulator approximation to $m(t)$. In Fig. 12.6b is shown the error waveform $D(t)$ given by

$$\Delta(t) \equiv m(t) - \bar{m}(t) \quad (12.30)$$

This error waveform is the source of the quantization noise.

We observe that, as long as slope overloading is avoided, the error $D(t)$ is always less than the step size S . (In PCM, the error is always less than $S/2$.) We shall assume that $D(t)$ takes on all values between $-S$ and $+S$ with equal likelihood. That is, we assume that the probability density of $D(t)$ is

$$f(\Delta) = \frac{1}{2S} \quad -S \leq \Delta \leq S \quad (12.31)$$

The normalized power of the waveform $\Delta(t)$ is then

$$\overline{[\Delta(t)]^2} = \int_{-S}^S \Delta^2 f(\Delta) d\Delta = \int_{-S}^S \frac{\Delta^2}{2S} d\Delta = \frac{S^2}{3} \quad (12.32)$$

Our interest is in estimating how much of this power will pass through a base-band filter. For this purpose we need to know something about the power spectral density of $D(t)$.

In Fig. 12.6, the period T of the sinusoidal waveform $m(t)$ has been selected so that T is an integral multiple of the step duration t . (Note that the bit rate $f_b = 1/t$.) We then observe that $D(t)$ is periodic, with fundamental period T , and is, of course, rich in harmonics. Suppose, however, that the period T

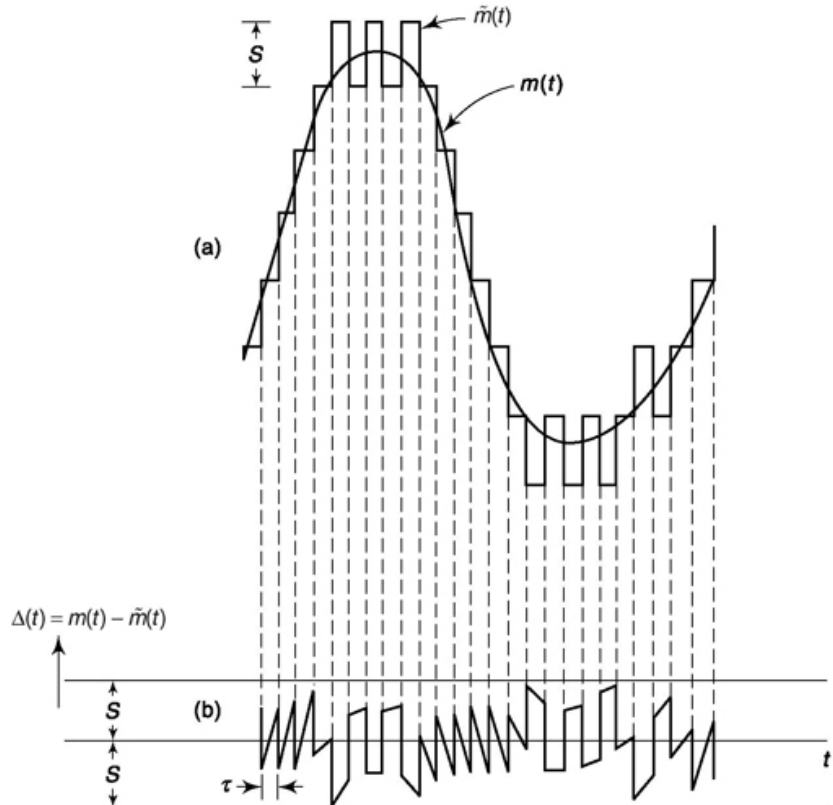


Fig. 12.6 The estimate $m(t)$ and error $D(t)$ when $m(t)$ is sinusoidal.

is changed very slightly by amount ST . Then the fundamental period of $D(t)$ will not be T but will be instead $T \times t/ST$ (Prob. 12.15) corresponding to a fundamental frequency near zero as $ST \rightarrow 0$. And again, of course, $D(t)$ will be rich in harmonics. Hence, in the general case, especially with $m(t)$ a random signal, it is reasonable to assume that $D(t)$ has a spectrum which extends continuously over a frequency range which begins near zero.

To get some idea of the upper-frequency range of the spectrum of the waveform $D(t)$, let us contemplate passing $D(t)$ through a low-pass filter of adjustable cutoff frequency. Suppose that initially the cutoff frequency is high enough so that $D(t)$ may pass with nominally no distortion. As we

lower the cutoff frequency, the first type of distortion we would note is that the abrupt discontinuities in the waveform would exhibit finite rise and fall times. Such is the case since it is these abrupt changes which contribute to the high-frequency power content of the signal. To keep the distortion within reasonable limits, let us arrange that the rise time be rather smaller than the interval t . As was discussed in Sec. 1.4.5, to satisfy this condition, we require that the filter cutoff frequency f_c be of the order of $f_c = 1/t$. Since the transmitted bit rate $f_b = 1/t$, $f_c = f_b$ as expected.

We now have made it appear reasonable, by a rather heuristic argument, that the spectrum of $D(t)$ extends rather continuously from nominally zero up to $f_c = f_b$. We shall assume further that over this range the spectrum is white. It has indeed been established experimentally that the spectrum of $D(t)$ is approximately white over the frequency range indicated.

We may now finally calculate the quantization noise that will appear at the output of a baseband filter of cutoff frequency f_M . Since the quantization noise power in a frequency range f_b is $S^2/3$ as given by Eq. (12.32), the output-noise power in the baseband-frequency range f_M is

$$N_q = \frac{S^2}{3} \frac{f_M}{f_b} = \frac{S^2 f_M}{3 f_b} \quad (12.33)$$

We may note, in passing, that the two-sided power spectral density of $\Delta(t)$ is

$$G_\Delta(f) \simeq \frac{S^2/3}{2 f_b} = \frac{S^2}{6 f_b} \quad -f_b \leq f \leq f_b \quad (12.34)$$

12.2.2 The Output-Signal Power

In PCM, the signal power is determined by the step size and the number of quantization levels. Thus, as in Fig. 12.2, with step size S and M levels, the signal could make excursions only between $-MS/2$ and $+MS/2$. In delta modulation, there is no similar restriction on the amplitude of the signal waveform, because the number of levels is not fixed. On the other hand, in delta modulation there is a limitation on the *slope* of the signal waveform which must be observed if *slope overload* is to be avoided. If, however, the signal waveform changes slowly (i.e. has a frequency content in the lower-baseband range), there is nominally no limit to the signal power which may be transmitted.

Let us consider a *worst case* for delta modulation. We assume that the signal power is concentrated at the *upper end* of the baseband. Specifically, let the signal be

$$m(t) = A \sin \omega_M t \quad (12.35)$$

with A the amplitude and $\omega_M = 2\pi f_M$, where f_M is the upper limit of the baseband frequency range. Then the signal power output power is

$$S_o = \overline{m^2(t)} = \frac{A^2}{2} \quad (12.36)$$

The maximum slope of $m(t)$ is $\omega_M A$. The maximum average slope of the delta modulator approximation $\hat{m}(t)$ is $S/t = Sf_b$, where S is the step size and f_b the bit rate. The limiting value of A just before the onset of slope overload is, therefore, given by the condition

$$\omega_M A = Sf_b \quad (12.37)$$

From Eqs. (12.36) and (12.37) we have that the maximum power which may be transmitted is

$$S_o = \frac{S^2 f_b^2}{2 \omega_M^2} \quad (12.38)$$

The condition specified in Eq. (12.37) is unduly severe. A design procedure, more often employed, is to select the Sf_b product to be equal to the rms value of the *slope* of $m(t)$. In this case the output-signal power can be increased above the value given in Eq. (12.38).

12.2.3 DM Output-signal-to-Quantization-Noise Ratio

The output-signal-to-quantization-noise ratio for delta modulation is found by dividing Eq. (12.38) by Eq. (12.33). The result is

$$\frac{S_o}{N_q} = \frac{5}{8\pi^2} \left(\frac{f_b}{f_M} \right)^3 \cong \frac{3}{80} \left(\frac{f_b}{f_M} \right)^3 \quad (12.39)$$

It is of interest to note that when our heuristic analysis is replaced by a rigorous analysis,¹ it is found that Eq. (12.39) continues to apply, except with the factor 3/80 replaced by 3/64, corresponding to a difference of less than 1 dB.

The dependence of S_o/N_q on the product f_b/f_M should be anticipated. For suppose that the signal amplitude were adjusted to the point of slope overload. If now, say, f_M were increased by some factor, then f_b would have to be increased by this same factor in order to continue to avoid overload [see Eq. (12.38)].

Let us now make a comparison of the performance of PCM and DM in the matter of the ratio S_o/N_q . We observe that the transmitted signals in DM (Fig. 12.5) and in PCM (Fig. 5.15) are of the same waveform, a binary pulse train. In PCM, a voltage level corresponding to a single bit persists for the time duration allocated to one bit of a code word. With sampling at the Nyquist rate, every $1/2f_M$ s, and with N bits per code word, the PCM bit rate is $f_b = 2f_M N$. In DM, a voltage level, corresponding to a single bit, is held for a duration t which is the interval between samples. Thus the DM system operates at a bit rate $f_b = 1/t$.

If the communication channel is of limited bandwidth, then there is the possibility of interference in either DM or PCM. Whether such intersymbol interference occurs in DM depends on the ratio of f_b to the bandwidth of the channel and similarly, in PCM, on the ratio of f_b to the channel bandwidth. For a fixed channel bandwidth, if inter-symbol interference is to be equal in the two cases, DM or PCM, we require that both systems operate at the same bit rate or

$$f_b = f'_b = 2f_M N \quad (12.40)$$

Combining Eq. (12.17) for PCM with Eq. (12.40) yields for PCM

$$\frac{S_o}{N_q} = 2^{2N} = 2^{f_b/f_M} \quad (12.41)$$

Combining Eq. (12.39) with Eq. (12.40) yields for delta modulation

$$\frac{S_o}{N_q} = \frac{3}{\pi^2} N^3 \quad (12.42)$$

Comparing Eq. (12.41) with Eq. (12.42), we observe that for a fixed channel bandwidth the performance of DM is always poorer than PCM. By way of example, if a channel is adequate to accommodate code words in PCM with $N = 8$, Eq. (12.41) gives $(S_o/N_q) = 48$ dB. The same channel used for DM would, from Eq. (12.42), yield $(S_o/N_q) @ 22$ dB.

Comparison of DM and pCM for voice

When the signal to be transmitted is the waveform generated by voice, the comparison between DM and PCM is overly pessimistic against DM. For, as appears in the discussion leading to Eq. (12.37), in our concern to avoid slope overload under any possible circumstance, we have allowed for the very worst possible case. We have provided for the possibility that all the signal power might be concentrated at the angular frequency w_M which is the upper edge of the signal bandwidth. Such is certainly not the case for voice. Actually, for speech, a bandwidth $f_M = 3200$ Hz is adequate and the voice spectrum has a pronounced peak at 800 Hz = $f_M/4$. If we replace w_M by $w_M/4$ in Eq. (12.37), we have

$$\frac{\omega_M}{4} A = Sf_b \quad (12.43)$$

The amplitude A will now be four times larger than before and the allowable signal power before slope overload will be increased by a factor of 16 (12 dB). Correspondingly, Eq. (12.39) now becomes

$$\frac{S_o}{N_q} = \frac{6}{\pi^2} \left(\frac{f_b}{f_M} \right)^3 \cong 0.6 \left(\frac{f_b}{f_M} \right)^3 = 5 N^3 \quad (12.44)$$

It may be readily verified that for $(f_b/f_M) < 8$ the signal-to-noise ratio for delta modulation, SNR(D), given by Eq. (12.44) is larger than SNR(PCM) given by Eq. (12.41). At about $f_b/f_M = 4$ the ratio SNR(D)/SNR(PCM) has a maximum value 2.4 corresponding to a 3.8 dB advantage. Thus if we allow $f_M = 4$ kHz for voice, then to avail ourselves of this maximum advantage afforded by delta modulation we would take $f_b = 16$ kHz. (When using PCM, f_M is usually taken to be 4 kHz even though 3.2 kHz would be adequate for voice.)

In our derivation of the signal-to-noise ratio in PCM we assumed that at all times the signal is strong enough to range widely through its allowable excursion. As a matter of fact, we specifically assumed that the distribution function $f(m)$ for the instantaneous signal value $m(t)$ was uniform throughout the allowable signal range. As a matter of practice, such would hardly be the case. Voice levels wax and wane and it is precisely for this reason that companding is employed as we have discussed in Sec. 4.4.6. The fact is, that commercial PCM systems using companding, are designed so that the signal-to-noise ratio remains at about 30 dB over a 40 dB range of signal power. In short, while Eq. (12.41) predicts a continuous increase in SNR(PCM) with increasing f_b/f_M , this result is for uncompanded PCM, and, in practice SNR(PCM) is approximately constant at 30 dB. The linear DM discussed above has a dynamic range of about 15 dB. In order to widen this dynamic range to 40 dB, as in PCM, one employs adaptive DM (ADM) discussed below, which yields advantages similar to the companding of PCM. When adaptive DM is employed, the SNR of ADM is comparable to the SNR of companded PCM. Today, many systems, such as the Satellite Business System (SBS), employ ADM operating at 32 kb/s rather than companded PCM which operates at 64 kb/s, thereby providing twice as many voice channels in a given frequency band.

DELTA PULSE-CODE MODULATION (DPCM)

In delta modulation, the approximation $m(t)$ is compared with the signal $m(t)$. A correction of fixed magnitude (of step size S) is then made in $m(t)$. The direction of this correction depends on whether $m(t)$ is greater or smaller than $m(t)$. An improved system results if the correction is not of fixed magnitude but rather increases as the error $D(t) = m(t) - m(t)$ increases. Delta pulse-code modulation is just such a system in which, however, the correction is quantized. Delta pulse-code modulation is implemented by replacing the modulator of Fig. 12.6 by an M -level quantizer and sampler. The output of this quantizer-sampler is an impulse whose strength is not fixed, but is proportional to the quantized error. This quantized error sample is also applied to the transmitter. Corresponding to each quantized error sample, the transmitter impresses on the communication channel a binary waveform of N bits ($2^N = M$) which is the binary code representation of the quantized error sample.

12.2.4 The Effect of Thermal Noise in DM

When thermal noise is present, the matched filter in the receiver of Fig. 12.4 will occasionally make an error in determining the polarity of the transmitted waveform. Whenever such an error occurs, the received impulse stream $p'_o(t)$ will exhibit an impulse of incorrect polarity. The received impulse stream is then

$$p'_o(t) = p_o(t) + p_{th}(t) \quad (12.45)$$

in which $p_{th}(t)$ is the error impulse stream due to thermal noise. If the strength (area) of the individual impulses is I , then each impulse in p_{th} is of strength $2I$ and occurs only at each error. The factor of two results from the fact that an error reverses the polarity of the impulse.

The thermal-error noise appears as a stream of impulses of random time of occurrence and of strength $\pm 2I$. The average time of separation between these impulses is t/P_e , where P_e is the bit error probability, and t is the time duration of a bit. If the results of Sec. 6.5.3 [see Eq. (6.153)] are used, the power spectral density of the thermal-noise impulses is

$$G_{pth}(f) = \frac{P_e}{\tau} (2I)^2 = \frac{4I^2 P_e}{\tau} \quad (12.46)$$

Now we have already characterized the integrators (assumed identical in both the DM transmitter and receiver) as having the property that when the integrator input is an impulse of strength I , the output is a step of amplitude S . The Fourier transform of the impulse is I , and the Fourier transform of a step of amplitude S is [using $u(t)$ = unit step]

$$\begin{aligned} \mathcal{F}\{Su(t)\} &= \frac{S}{j\omega} \quad \omega \neq 0 \\ &= S\pi\delta(\omega) \quad \omega = 0 \end{aligned} \quad (12.47)$$

We may ignore the dc component in the transform since such dc components will not be transmitted through the baseband filter. Hence, we may take the transfer function of the integrator to be $H_I(f)$ given by

$$H_I(f) = \frac{S}{I} \frac{1}{j\omega} \quad \omega \neq 0 \quad (12.48a)$$

and

$$|H_I(f)|^2 = \left(\frac{S}{I}\right)^2 \frac{1}{\omega^2} \quad \omega \neq 0 \quad (12.48b)$$

From Eqs. (12.46) and (12.48b) we find that the power spectral density of the thermal noise at the input to the baseband filter is $G_{th}(f)$ given by

$$G_{th}(f) = |H_I(f)|^2 \quad G_{pth}(f) = \frac{4S^2 P_e}{\tau \omega^2} \quad \omega \neq 0 \quad (12.49)$$

It would now appear that to find the thermal-noise output, we need but to integrate $G_{th}(f)$ over the passband of the baseband filter. We have performed similar integrations on many occasions. And, in doing so, we have extended the range of integration from $-f_M$ through $f = 0$ to $+f_M$, even though we recognized that the baseband filter does not pass dc and actually has a low-frequency cutoff f_1 .

However, in these other cases the power spectral density of the noise near $f = 0$ is not inordinately large in comparison with the density throughout the baseband range generally. Hence, if as is normally the case, $f_1 \gg f_M$, the procedure is certainly justified as a good approximation. We observe however, that in the present case [Eq. (12.49)], $G_{th}(f)$ is finite at $\omega = 0$, and more importantly that the integral of $G_{th}(f)$, over a range which includes $\omega = 0$, is infinite.

Let us then explicitly take account of the low-frequency cutoff f_1 of the baseband filter. The thermal-noise output is, using Eq. (12.49) with $\omega = 2\pi f$, and since $f_b = 1/t$,

$$N_{th} = \frac{S^2 P_e}{\pi^2 \tau} \left(\int_{-f_M}^{-f_1} \frac{df}{f^2} + \int_{f_1}^{f_M} \frac{df}{f^2} \right) \quad (12.50a)$$

$$= \frac{2 S^2 P_e}{\pi^2 \tau} \left(\frac{1}{f_1} - \frac{1}{f_M} \right) \quad (12.50b)$$

$$\approx \frac{2 S^2 P_e}{\pi^2 f_1 \tau} \frac{2 S^2 P_e f_b}{\pi^2 f_1} \quad (12.50c)$$

if $f_1 \gg f_M$. Observe that, unlike the situation encountered in all other earlier cases, the thermal-noise output in delta modulation depends on the low-frequency cutoff rather than the high-frequency limit of the baseband range. In many applications such as voice encoding where the voice signal is typically bandlimited from 300 to 3200 Hz, the use of a band pass output filter is commonplace. In this case $f_1 = 300$ Hz.

12.2.5 Output signal-to-Noise Ratio in DM including Thermal Noise

The output SNR is obtained by combining Eqs. (12.33), (12.44), and (12.50c). The result is

$$\frac{S_o}{N_o} = \frac{S_o}{N_q + N_{th}} = \frac{(2S^2/\pi^2)(f_b/f_M)^2}{(S^2 f_M/3f_b) + (2S^2 P_e f_b/\pi^2 f_1)} \quad (12.51)$$

which may be rewritten

$$\frac{S_o}{N_o} = \frac{S_o}{N_q + N_{th}} \cong \frac{0.6(f_b/f_M)^3}{1 + 24P_e(f_b^2/f_M f_1)/4\pi^2} = \frac{0.6(f_b/f_M)^3}{1 + 0.6P_e(f_b^2/f_M f_1)} \quad (12.52)$$

If transmission is direct or by means of PSK,

$$P_e = \frac{1}{2} \operatorname{erfc} \sqrt{\frac{E_s}{\eta}} \quad (12.53)$$

where E_s , the signal energy in a bit, is related to the received signal power S_i by

$$E_s = S_i T_b = S_i/f_b \quad (12.54)$$

Combining Eqs. (12.52), (12.53) and (12.54), we have

$$\frac{S_o}{N_o} = \frac{0.6(f_b/f_M)^3}{1 + [0.3(f_b^2/f_M f_1)] \operatorname{erfc} \sqrt{S_i/\eta f_b}} \quad (12.55)$$

Example 12.4

For DM based voice (300-3200 Hz) transmission required receiver output SNR is greater than 30 dB. Find if both or which of 32 kbps and 64 kbps data rate support this. Given, contaminating white noise PSD = 10 W/Hz and input signal energy 0.001 J.

Solution

Lower cutoff frequency = 300 Hz, upper cut-off frequency = 3200 Hz, For data rate = 32000, substituting in Eq. 12.55 Output SNR

$$= \frac{0.6 \times (32000/3200)^3}{1 + \left[0.3 \times \frac{32000^2}{300 \times 3200} \right] \operatorname{erfc} \left(\sqrt{\frac{0.001}{2 \times 10^{-9} \times 32000}} \right)}$$

$$= 27.78 \text{ dB}$$

For data rate = 64000, similarly,
Output SNR

$$= \frac{0.6 \times (64000/3200)^3}{1 + \left[0.3 \times \frac{64000^2}{300 \times 3200} \right] \operatorname{erfc} \left(\sqrt{\frac{0.001}{2 \times 10^{-9} \times 64000}} \right)}$$

$$= 36.40 \text{ dB}$$

Clearly 64 kbps only fulfills the requirement.

SELF-TEST QUESTIONS

5. In principle, the transmitter of a DM system can simply be a bistable multivibrator. Is that correct?
6. Is it experimentally observed that quantization noise in DM is white in the frequency range of interest?
7. In DM, signal to quantization noise ratio increases eight fold if bit rate is doubled. Explain if true.

8. Is it true that in DM the thermal noise depends on low frequency cutoff of the message signal and not high frequency cutoff?

12.3 COMPARISON OF PCM AND DM

We can now compare the output signal-to-noise ratios in PCM and DM by comparing Eqs. (12.28) and (12.55). To ensure that the communications channel bandwidth required is the same in the two cases, we use the condition, given in Eq. (12.40), that $2N = f_b/f_M$. Then Eq. (12.28) may be written

$$S_o = \frac{2}{\pi} f_b \text{lfM} \quad (12.56)$$

$$N_o = 1 + 2(2f_b^2/f_M) \operatorname{erfc}(\sqrt{S_i/\eta f_b})$$

Equations (12.56) and (12.55) are compared in Fig. 12.7 for $N = 8$ ($f_b(\text{DM}) = 48 \text{ kb/s}$). To obtain the threshold performance of the delta-modulation system, we assume voice transmission where $f_M = 3000 \text{ Hz}$ and $f_1 = 300 \text{ Hz}$. Thus,

$$\frac{f_b}{f_M} = 16 \quad (12.57a)$$

and

$$\frac{f_M}{f_1} = 10 \quad (12.57b)$$

Let us compare the ratios S_o/N_o for PCM and DM for the case of voice transmission. We assume $f_M = 3000 \text{ Hz}$, $f_1 = 300 \text{ Hz}$ and $N = 8$. We then have $f_b = 2Nf_m = 48 \times 10^3 \text{ Hz}$. Using these numbers and recalling that the probability of an error in a bit is we have from Eqs. (12.55) and (12.56) the result

$$P_{eb} = \frac{1}{2} \operatorname{erfc} \sqrt{\frac{S_i}{\eta f_b}},$$

$$\left(\frac{S_o}{N_o} \right)_{\text{DM}} = \frac{2457.6}{1 + 768 \operatorname{erfc} \sqrt{\frac{S_i}{\eta f_b}}} = \frac{2457.6}{1 + 1536 P_e} \quad (12.58a)$$

and for PCM is

$$\left(\frac{S_o}{N_o} \right)_{\text{PCM}} = \frac{65,536}{1 + 131,072 \operatorname{erfc} \sqrt{\frac{S_i}{\eta f_b}}} = \frac{65,536}{1 + 262,144 P_e} \quad (12.58b)$$

When the probability of a bit error is very small, the PCM system is seen to have a higher output SNR than the DM system. Indeed, the output SNR for the PCM system is 48 dB and only about 33 dB for the DM system. However, an output SNR of 30 dB is all that is required in a communication system. Indeed, if companded PCM is employed, the output SNR will decrease by about 12 dB to 36 dB for the PCM system. Thus, while Eq. (12.58b) indicates that the output SNR is higher for PCM, the output SNR, in practice, can be considered as being *comparable*.

With regard to the threshold, we see that when $P_e \sim 10^{-6}$ the PCM system has reached threshold while the DM system reaches threshold when $P_e \sim 10^{-4}$. In practice, we find that our *ear* does not

detect threshold until P_e is about 10^{-4} for PCM and 10^{-2} for DM and ADM. Some ADM systems can actually produce understandable speech at error rates as high as 0.1.

Figure 12.7 shows a comparison of PCM and DM for $N = 8$ and $f_M/f_1 = 10$.

12.4 THE SPACE SHUTTLE ADM

Adaptive Delta Modulation (ADM) has been in use for voice communication in space shuttles. Block diagrams of the transmitter and receiver are shown in Fig. 12.8. The adaptive feature of the system is incorporated in the block labeled “impulse-size algorithm.” The output of this block, at each bit time, is an impulse whose polarity and amplitude depend on the result of the present comparison of $m(t)$ and $m(t)$ and also on the past history of the results of these comparisons. The algorithm block incorporates the memory and logic required to carry out this adaptive determination. The intention of the algorithm is to arrange that the slope overload be reduced in comparison to the overload encountered in linear delta modulation (LDM), thereby increasing the dynamic range of the ADM.

The adaptive feature operates as follows: Consider first the case in which the baseband signal $m(t)$ is a constant, that is unvarying. Then in the steady-state the estimate $m(t)$ simply hunts back and forth across $m(t)$, that is, $m(t)$ alternately overshoots and undershoots $m(t)$. An example of such behavior is seen in Fig. 4.41 which applies to LDM. In the present ADM case, whenever there is a *reversal* in the sign of $m(t) - m(t)$, the algorithm block generates an impulse of minimum size $I_0(kT_S)$ which is adequate when integrated to generate a step S_0 of correspondingly minimum size. The step is positive or negative according to sign [$m(t) - m(t)$]. Such a minimum size step is shown at time 2 in Fig. 12.9a. The step is of minimum size S_0 , because, as we note the sign of $m(t) - m(t)$ has reversed in comparison with time 1. At time 3 we still find that $m(t) > m(t)$. The algorithm correctly interprets this result to indicate that slope overload is being generated, i.e., $m(t)$ is rising too rapidly for $m(t)$ to keep pace with steps of amplitude S_0 . Accordingly, the step size is

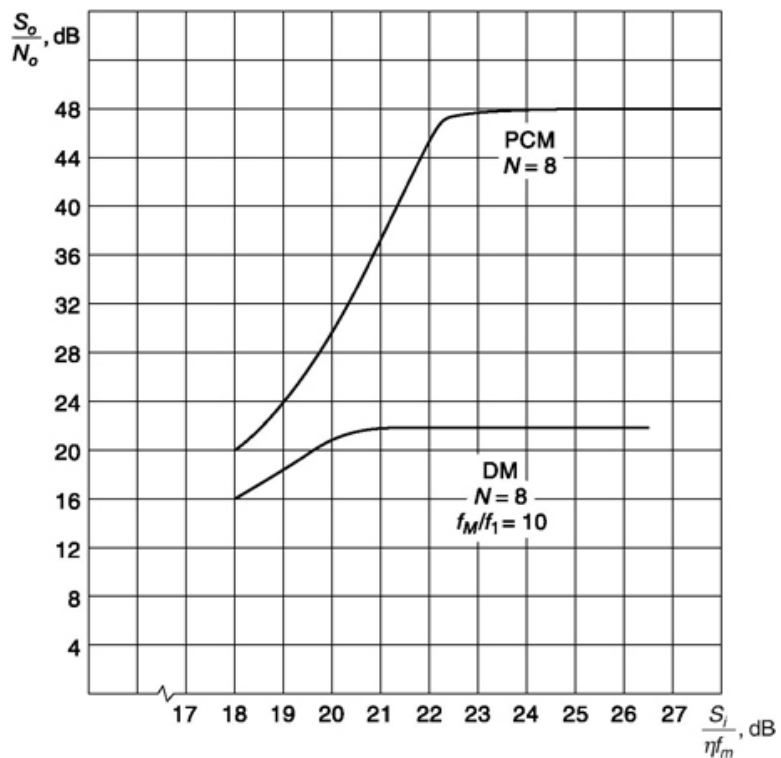


Fig. 12.7 A comparison of PCM and DM.

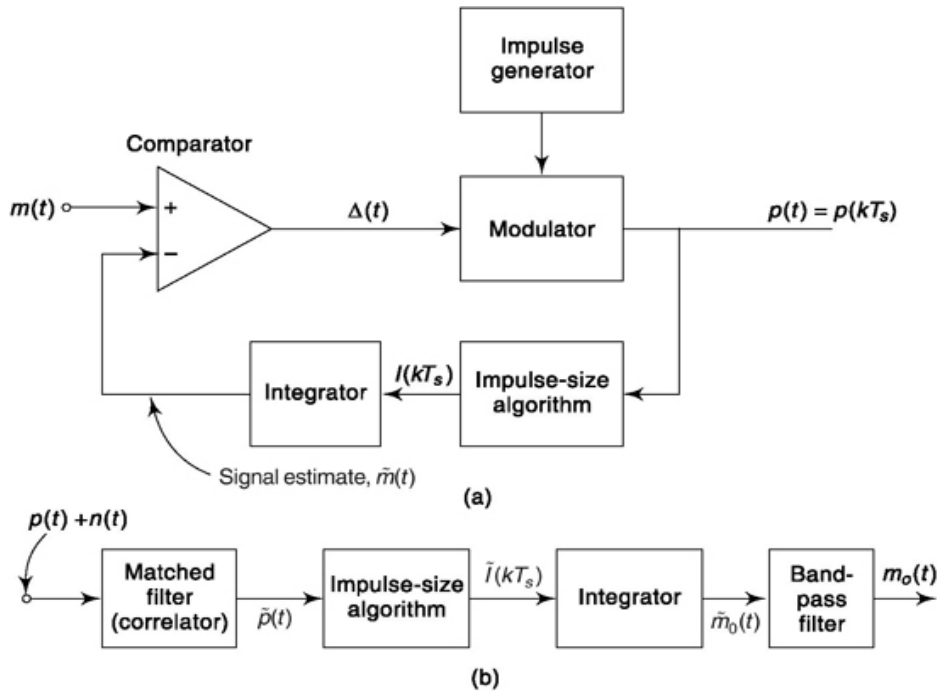


Fig. 12.8 (a) An adaptive delta modulation encoder, (b) Decoder.

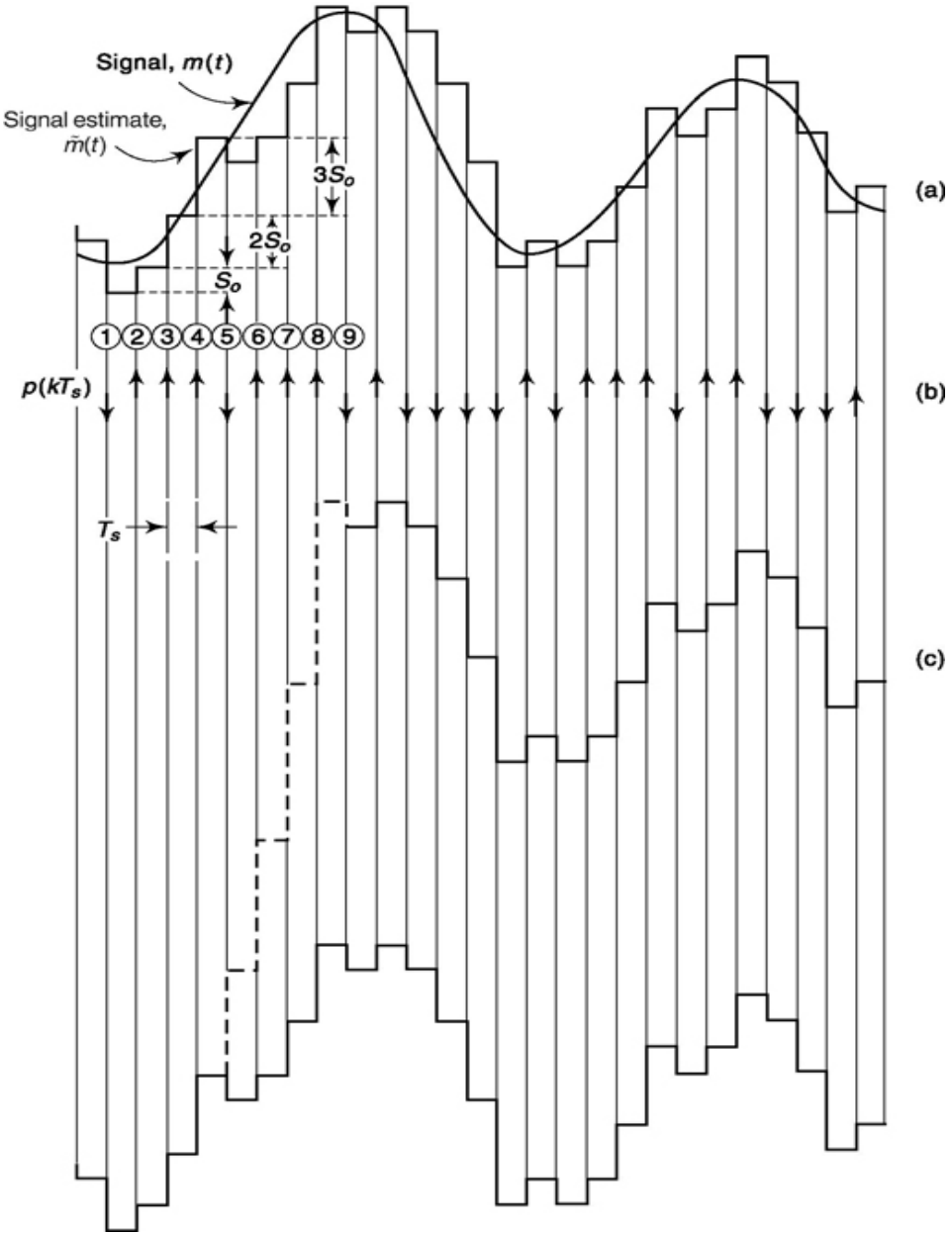


Fig. 12.9 (a) Signal and estimate. (b) Transmitted bit stream. (c) Decoded signal (with and without error).

increased to $2S_o$. At time 4 it is found that still $m(t) > m(t)$ so the step size is increased to $3S_o$. In short, starting at a reversal with step S_o , at each successive sample, if $m(t)$ remains greater than $m(t)$ an additional S_o is added to the step size. At time 5 there is a reversal in sign of $m(t) - m(t)$ so the step reverts to S_o and, of course reverses polarity. The polarities of the impulses output from

$$S(kT_s) = \begin{cases} S_o \operatorname{sgn} p(kT_s) & \text{if } p(kT_s) \neq p[(k-1)T_s] \\ \{S[(k-1)T_s] + S_o\} \operatorname{sgn}(kT_s) & \text{if } p(kT_s) = p[(k-1)T_s] \end{cases} \quad (12.59)$$

Decoder

The ADM receiver (decoder) is shown in Fig. 12.8b. The matched filter regenerates the impulse stream $p(t)$, hopefully without error, in spite of the presence of the thermal noise $n(t)$ at its input. If the effect of the noise is suppressed completely then $p(t) = p(t)$. The algorithm block and the integrator processes $p(t)$ precisely as $p(t)$ is processed at the transmitter. Again, if noise is absent or suppressed $m_o(t) = m(t)$.

the modulation in Fig. 12.9a are shown in Fig. 12.9b. The algorithm can be expressed precisely by the equations

The effect of thermal noise in the Shuttle ADM system is somewhat more severe than it is in the case of LDM. In LDM if the polarity of a received impulse is misinterpreted by the matched filter a corresponding error occurs in the step direction. Correspondingly, there is an offset of amount $2S$ in the regenerated waveform as compared to the original waveform. But since the LDM has no memory the error is not propagated and, aside from the offset the regenerated waveform again immediately follows the original signal. The situation in ADM is shown in Fig. 12.9c. Here we have considered that the negative impulse at time 5 has been misread. We observe that, as a consequence, not only is the resultant step of the wrong polarity but it is also exaggerated in amplitude because the impulse at 5 is read as the fourth successive such impulse. The next successive three positive steps are of the correct polarity but are progressively exaggerated even further. The situation is not corrected until the next impulse reversal at time 5. The overall effect of the noise in ADM is much the same as in LDM, that is simply an offset in the waveform. In ADM, however, the offset will generally be larger and take a somewhat longer time to be corrected. What is important to note is that we can anticipate that generally the shuttle ADM and LDM will have quite similar responses to thermal noise. Interestingly, it turns out that most other ADM schemes described in the literature do not share this feature of responding to noise in a manner similar to LDM.

SELF-TEST QUESTIONS

9. Is it true that for companded PCM the output SNR is comparable to DM?
10. Understable speech is produced in some ADM up to error probability 0.1 while this is 0.01 and
0.0001 for DM and PCM respectively. Is the statement correct?
11. Can thermal noise cause more serious problem in ADM compared to DM?

FACTS AND FIGURES

Electrical communication grew out of the confinement of a national boundary when the first treaty ‘on record’ was signed between Austria and Prussia (consisting of present North Germany and Poland) in 1849. Following this, Berlin and Vienna were connected by telegraph lines. Soon other countries found value in such agreement that set tariff zones, cost structure, standardization of resources, etc., for smooth operation of communication traffic. Twenty European states came together to form the International Telegraph Union (ITU) in 1865 and membership started increasing. Since 1934, ITU

stands for International Telecommunication Union. After the Second World War, ITU became an agency operating under United Nations and is now based in Geneva, Switzerland, with 191 member states and more than 700 sector members/associates.

ITU plays an important role in conflict resolution through ‘cooperation and collaboration’. It gives ‘Recommendation’ which becomes mandatory for the adopting nation. We have noted that two different encoding schemes in PCM telephony found their spread in two distinct geographical regions, A-law in Europe and (-law in North America. Point 3.4 of ITU-T Recommendation G.711, titled ‘Pulse Code Modulation (PCM) of Voice Frequencies’, says “Digital paths between countries which have adopted different encoding laws should carry signals encoded in accordance with the A-law.

Where both countries have adopted the same law, that law should be used on digital paths between them. Any necessary conversion will be done by the countries using the (-law.”

MATLAB

```

% Experiment 46

% This calculates output SNR of receiver for PCM coded PSK or FSK modulated
% data. This uses eqn.(12.28 and 12.29) of the book. Output is expressed in dB

choice=input('Enter 1:PSK, 2:FSK - ');
Si=input('Enter input signal energy - ');
eta=2*input('Enter PSD of input white noise - ');
fm=input('Enter baseband cut-off frequency - ');
N=input('Enter no. of bits used for each sample - ');

if choice == 1,
    outputSNR_PSK =10*log10(2^(2*N)/(1+2^(2*N+1)*erfc(sqrt(Si/(2*N*eta*fm)))));
end

if choice == 2,
    outputSNR_FSK =10*log10(2^(2*N)/(1+2^(2*N+1)*erfc(sqrt(0.3*Si/(N*eta*fm)))));
end

```

The data can be given as discussed in Example 12.2 and output verified as follows.

```

>> exp46
Enter 1:PSK, 2:FSK - 1
Enter input signal energy - 0.001
Enter PSD of input white noise - 0.000000001
Enter baseband cut-off frequency - 4000
Enter no. of bits used for each sample - 3

outputSNR_PSK = 18.0618

```

You can play with various parameters. Also you can write code similar to Experiment 45 of Chapter 11 that gives output SNR for a range of input SNR and accordingly plot input-output SNR.

% Experiment 47

```

% This calculates output SNR of receiver for DM coded PSK modulated
% data. This uses eqn.(12.55) of the book. Output is expressed in dB

Si=input('Enter input signal energy - ');
eta=2*input('Enter PSD of input white noise - ');
fm=input('Enter baseband upper cut-off frequency - ');
f1=input('Enter baseband lower cut-off frequency - ');
fb=input('Enter bit rate - ');

outputSNR_DM_PSK
=10*log10(0.6*((fb/fm)^3)/(1+(0.3*(fb^2)/(fm*f1))*erfc(sqrt(Si/(eta*fb)))));

```

The data can be given as discussed in Example 12.4 and output verified as follows.

```

>> exp47
Enter input signal energy - 0.001
Enter PSD of input white noise - 0.000000001
Enter baseband upper cut-off frequency - 3200
Enter baseband lower cut-off frequency - 300
Enter bit rate - 64000

```

outputs SNR_DM_PSK = 50.4050

SUMMARY

The chapter begins with a discussion of how quantization of message signal in PCM transmission needs to be interpreted as noise and then calculates. This is followed by calculation of quantization noise power. The effect of additive thermal noise on PCM is considered next. SNR at PCM receiver output is calculated that includes both quantization noise and thermal noise. This is used to calculate probability of error for PCM system carrier modulation schemes like PSK, FSK. Next, similar issues like quantization noise, thermal noise and their combined effect in SNR calculation are addressed for DM and corresponding probability of error shown. A comparison of PCM and DM is presented. How noise affects Adaptive DM is discussed through its use in a space shuttle flight.

PROBLEMS

12.1 Suppose that in PCM, the sampling of the quantized waveform is not instantaneous but rather flat-topped. Let the flat-topped sampling pulses have a duration t and an amplitude I/t . For this case find the power spectral density $G_e(f)$ of the sampled quantization error corresponding to Eq. (12.6).

12.2 The signal $m(t)$ is sampled at Q times the Nyquist rate. Find N_q .

12.3 Prove that Eq. (12.16) is valid when M is an even integer.

12.4 Plot Eq. (12.17) as a function of N .

12.5 A signal $m(t)$ is not strictly bandlimited. We bandlimit $m(t)$ and then sample it. Due to the bandlimiting, distortion results even without quantization.

(a) Show that the noise caused by the distortion is $N_D = \int_{f_M}^{\infty} G_m(f) df$, where $G_m(f)$ is the power spectral density of $m(t)$, and f_M is the cutoff frequency of the bandlimiting filter.

(b) If $G_m(f) = G_0 e^{-f^2/2}$ find N_D .

(c) If the signal $m(t)$ is sampled at the Nyquist rate and quantized, find the total output SNR = $S_0/(N_d + N_q)$.

12.6 The thermal-noise error pulse train is *not* an impulse train. Each pulse has the duration $1/2f_M$ if sampling is at the Nyquist rate. The pulse amplitude is proportional to Dm_s .

(a) Find $G_{th}(f)$.

(b) Calculate N_{th} .

12.7 Plot S_0/N_0 in Eq. (12.28) as a function of $S/h f_M$ for $N = 4, 8, 100$.

12.8 Show that threshold is defined by the equation $P_e \sim 1/[(16)2^{2N}]$. Plot P_e versus N .

12.9 Find the output SNR if the binary signal is transmitted using DPSK. Plot your result.

12.10 The signal $m(t)$ is *not* bandlimited. Its power spectral density is $G_m(f) = G_0 e^{-f^2/2f_1}$.

Using the results of Prob. 12.5c, obtain an expression for the output signal-to-noise ratio $S_o/N_o = S_o/(N_d + N_q + Nh)$.

12.11 A signal $m(t)$, bandlimited to 4 kHz, is sampled at *twice* the Nyquist rate and the samples transmitted by PCM. An output SNR of 47 dB is required. Find N and the minimum value of S/h if operation is to be above threshold.

12.12 Two signals $m_1(t)$ and $m_2(t)$, each bandlimited to 4 kHz, are sampled at the Nyquist rate, PCM encoded, and then time-division multiplexed. The output SNR, including thermal-noise effects, of each demultiplexed signal is to be at least 30 dB.

- (a) Sketch the entire transmitter and receiver structure.
- (b) Find N and the minimum $S_i h$ that is required if operation is to be above threshold.

12.13 Let $m(t)$ be a constant M_o .

- (a) Sketch the steady-state error $D(t)$ for the DM shown in Fig. 12.4.
- (b) Calculate the output quantization noise power after filtering. Assume a step size S and that the time between samples is t . Let the filter bandwidth be f_M .

12.14 Let $m(t) = Kt$ where $K = S/t$.

- (a) Sketch $D(t)$ for the DM shown in Fig. 12.4.
- (b) Sketch the filtered output quantization noise power. Let the baseband filter bandwidth be f_M .

12.15 Assume initially that $m(t)$ in Fig. 12.4 is periodic with a period T which is an integral multiple of the sampling interval t . Now let T change, very slightly, by an amount ST . Show that the fundamental period of the error waveform $D(t)$ becomes $(Tt)/ST$.

12.16 The baseband input signal $m(t)$ in Fig. 12.4 is a random waveform with power spectral density which is uniform at $h_m/2$ up to the bandlimit f_M . To keep slope overload within tolerable limits, the design criterion to be used is that S/t is to be equal to the rms value of the slope of $m(t)$. For this condition calculate the maximum power S_o and compare with Eq. (12.38).

12.17 A signal $m(t)$ is to be encoded using either DM or PCM. The signal-to-quantization-noise ratio $S_o/N_q > 30$ dB. Find the ratio of the PCM to DM bandwidths required.

12.18 Plot $\left(\frac{S_o}{N_q}\right)_{PCM}$ versus $\left(\frac{S_o}{N_q}\right)_{DM}$ for equal bandwidths.

12.19 A DPCM system is shown in Fig. P12.19.

- (a) If $m(t) = Kt$, find K_{max} to avoid slope overloading.
- (b) If a two-level quantizer is used, $S/t = K_{max}$. With this value of K_{max} find $17t$, t' being the time interval allowed for a bit in the transmitted PCM waveform.
- (c) Sketch $m(t)$ and $D(t)$, if $S/t = 2K_{max}$.
- (d) Comment on the quantization noise of the DPCM system as compared with the DM system.

12.20 Verify Eq. (12.50c).

12.21 (a) Show that the threshold in DM occurs when $100 P_e \sim (w_M t)^2 (f_1/f_M)$.

(b) Plot P_e versus $w_M t$ for $f_1/f_M = 0.01, 0.04, 0.1$.

12.22 Plot Eq. (12.55) for $w_M t = 10$ and $w_1 t = 0.004$.

12.23 (a) Derive an expression for the output SNR when the binary signal is transmitted using DPSK.
 (b) If $w_m t = 10$ and $w_1 t = 0.04$, compare the thresholds obtained using PSK and DPSK.

12.24 A PCM and a DM system are both designed to yield an output SNR of 30 dB. Let $f_M = 4$ kHz and assume PCM sampling at 5 times the Nyquist rate.

- (a) Compare the bandwidths required for each system.
- (b) If $f_1/f_M = 0.04$, compare the threshold of each system.

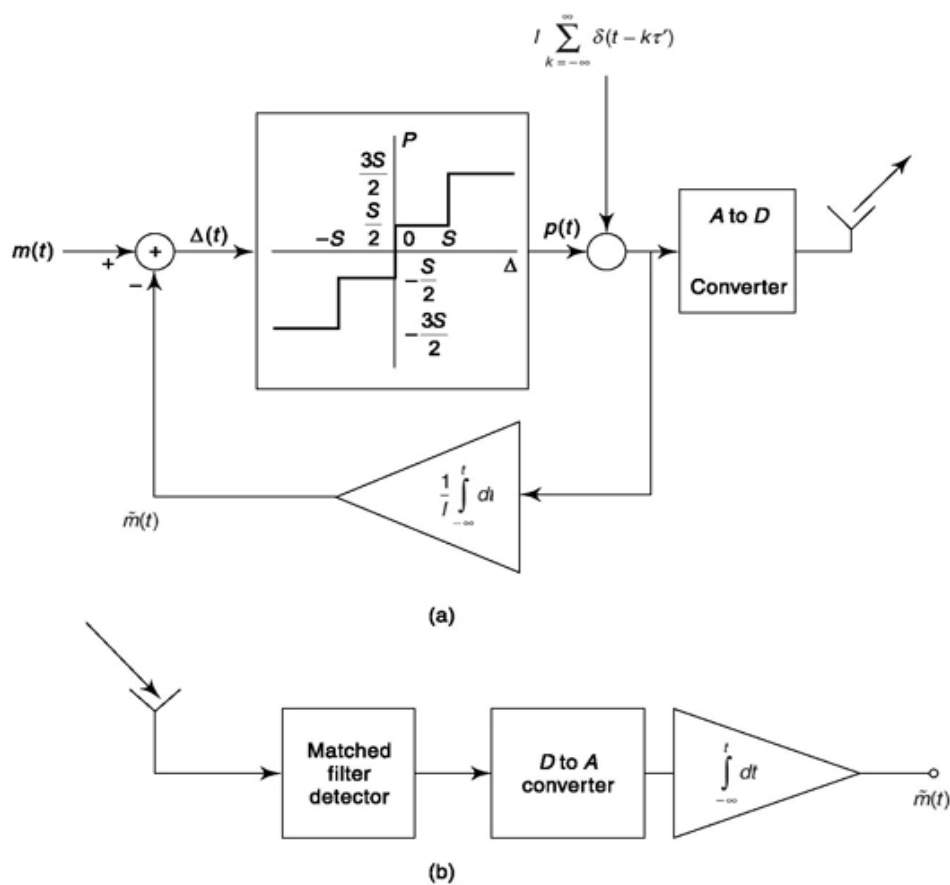


Fig. P12.19 A DPCM system. (a) Encoder, (b) Decoder.

REFERENCES

1. Van de Weg, H: Quantizing Noise of a Single Integration Delta Modulation System with an N-digit Code, *Philips Res. Repr.* 8, pp. 367-385, 1953.
2. Jayant, N.S., and P. Noll: "Digital Coding of Waveforms," Prentice-Hall Inc., New Jersey, 1984.

13

INFORMATION THEORETIC APPROACH TO COMMUNICATION

CHAPTER OBJECTIVE

We have seen that communication systems are limited in their performance by the available signal power, the inevitable background noise, and the need to limit bandwidth. The performance of each of the systems studied is not equal. In this chapter, we discuss information theory that gives an opportunity to know the performance characteristics of an optimum or ideal system that can be used as a comparison tool. Information theory allows us to quantify information content in a message leading to different source coding techniques for efficient transmission of message. Besides numerical examples the chapter also presents MATLAB based simulations highlighting interesting aspects of Information Theory and Coding.

FACTS AND FIGURES

Claude Shannon, the ‘father of information theory’, was born in Michigan, USA, in 1916. Thomas Edison, the prolific inventor, was his childhood hero and was found later to be a distant cousin of him. In 1936, Shannon received two bachelor’s degrees, one in electrical engineering and one in mathematics. His master’s thesis on symbolic analysis of relay and switching circuits was considered “possibly the most important, and also the most famous, master’s thesis of the century” by H. Gardner of Harvard University.

His contribution in communication systems is nicely portrayed in following by Irving Reed, speaking on an international symposium in 1981. “It was thirty-four years ago, in 1948, that Professor Claude E. Shannon first published his uniquely original paper, ‘A Mathematical Theory of Communication’ in the *Bell System Technical Journal*. Few other works of this century have had greater impact on science and engineering. By this landmark paper and his several subsequent papers on information theory, he

has altered most profoundly all aspects of communication theory and practice.” Of the many devices Shannon invented, he was particularly fond of his ‘ultimate machine’ which he always kept on his desk. This was an otherwise featureless box having only one switch to its side. When the switch was flipped, the lid of the box used to open, a mechanical hand reached out, flipped off the switch and retracted back inside the box.

13.1 DISCRETE MESSAGES AND INFORMATION CONTENT

In considering communication systems broadly, we may assume, without loss of generality, that the function of any communication system is to convey, from transmitter to receiver, a sequence of messages which are selected from a finite number of predetermined messages. Thus, within some specified time interval, one of these messages is transmitted. During the next time interval, another of these messages (or possibly the same message) is transmitted. It should be noted that while the messages are predetermined and hence known by the receiver, the message selected for transmission during a particular interval is not known, *a priori*, by the receiver. Thus the receiver does not have the burden of extracting an arbitrary signal from a background of noise, but need only perform the operation of identifying which of a number of allowable messages was transmitted. The job of the receiver is not to answer the question “What was the message?” but rather the question “Which one?” As may well be anticipated the receiver will answer this question by determining the correlation of the received noisy signal with all of the possible predetermined signals individually. The receiver will then decide that the transmitted signal is the predetermined signal with which the noisy received signal has the greatest correlation. Rather generally, the probability that a particular message has been selected for transmission will not be the same for all messages. In this case, we assume that the probability of occurrence of each possible message is known at the receiver.

We recognize that this transmission of known messages is actually nothing more than an extension of the concept of quantization discussed in Sec. 5.1.1. When a signal is quantized, the receiver need determine only which of the quantized levels is encountered at each sampling time. The discrete predetermined messages then consist of those quantization levels which may

be transmitted directly or encoded into anyone of a number of forms. It is to be noted, of course, that such quantization imposes no restriction on the precision with which an arbitrary signal may be transmitted, since, in principle, the number of quantization levels may be increased without limit.

We may be rather free in our interpretation of the term “message.” Thus, suppose that, during some time interval, there is generated at the transmitter one of a number of predetermined waveforms. If the receiver correctly identifies the waveform, then the receiver has received the transmitted message. For example, suppose that a quantization level is encoded into a binary waveform as in binary PCM. Then we may view the quantization level as a message, but we may also view each binary digit as a message. Thus a number of messages conveyed by a succession of binary digits may convey the single message contained in one quantization sample.

13.1.1 The Concept of Amount of Information

Let us consider a communication system in which the allowable messages are m_1, m_2, \dots , with probabilities of occurrence p_1, p_2, \dots . Of course, $p_1 + p_2 + \dots = 1$. Let the transmitter select message m_k , of probability p_k ; let us further assume that the receiver has correctly identified the message. Then we shall say, by way of *definition* of the term *information*, that the system has conveyed an *amount of information* I_k given by

$$I_k \equiv \log_2 \frac{1}{p_k} \quad (13.1)$$

The concept of *amount of information* is so essential to our present interest that it behooves us to examine with some care the implications of Eq. (13.1). We note first that while I_k is an entirely dimensionless number, by convention, the “unit” it is assigned is the *bit*. Thus, by way of example, if $p_k = Y_A$, $I_k = \log_2 4 = 2$ bits. The unit bit is employed principally as a reminder that in Eq. (13.1) the base of the logarithm is 2. (When the natural logarithmic base is used, the unit is the *nat*, and when the base is 10, the unit is the *Hartley* or *decit*. The use of such units in the present case is analogous to the unit *radian* used in angle measure and *decibel* used in connection with power ratios.) The use of the base 2 is especially convenient when binary PCM is employed. For, if the two possible binary digits (bits) may occur with equal likelihood, each with a probability $\frac{1}{2}$, then the correct

identification of the binary digit conveys an amount of information $I = \log_2 2 = 1$ bit.

In the past we have used the term bit as an abbreviation for the phrase *binary digit*. When there is an uncertainty whether the word bit is intended as an abbreviation for binary digit or as a unit of information measure, it is customary to refer to a binary digit as a *binit*. Note that if the probabilities of two possible binites are not equally likely, one binit conveys *more* and one conveys *less* than 1 *bit* of information. For example, if the binites 0 and 1 occur with probabilities of $\frac{1}{4}$ and $\frac{3}{4}$, respectively, then binit 0 conveys information in amount $\log_2 4 = 2$ bits, while binit 1 conveys information in amount $\log_2 \frac{3}{4} = 0.42$ bit.

Suppose that there are M equally likely and independent messages and that $M = 2^N$, with N an integer. In this case the information in each message is

$$I = \log_2 M = \log_2 2^N = N \text{ bits} \quad (13.2a)$$

Suppose, further, that we choose to identify each message by binary PCM code words. The number of binary digits required for each of the 2^N messages is also N . Hence in this case, the information in each message, as measured in bits, is numerically the same as the number of binites needed to encode the messages.

When $p_k = 1$, we have a trivial case since only one possible message is allowed. In this instance, since the receiver knows the message, there is really no need for transmission. We find that $I = \log_2 1 = 0$. As p_k decreases from 1 to 0, I_k increases monotonically, going from 0 to infinity. Thus, a greater amount of information has been conveyed when the receiver correctly identifies a less likely message.

When two independent messages m_k and m_t are correctly identified, we can readily prove that the amount of information conveyed is the sum of the information associated with each of the messages individually. Thus, we note that the individual information amounts are

$$I_k = \log_2 \frac{1}{p_k} \quad (13.2b)$$

$$I_t = \log_2 \frac{1}{p_t} \quad (13.2c)$$

Since the messages are independent, the probability of the composite message is $p_k p_l$, with corresponding information content of messages m_k and m_l is

$$I_{k,l} = \log_2 \frac{1}{p_k p_l} = \log_2 \frac{1}{p_k} + \log_2 \frac{1}{p_l} = I_k + I_l \quad (13.3)$$

It is of interest to note that the term information applied to the symbol I_k in Eq. (13.1) is rather aptly chosen, since there is some correspondence between the properties of I_k and the meaning of the word information as used in everyday speech. For example, suppose that an airplane dispatcher calls the weather bureau of a distant city during daylight hours to inquire about the present weather. If he receives, in response, the message, "There is daylight here," he will surely judge that he has received no information since he was certain beforehand that such was the case. On the other hand, if he hears "It is not raining here," he will consider that he has received information since he might anticipate such a situation with less than perfect certainty. Further, suppose the dispatcher receives some weather information on two different days. Then he might indeed consider that the total information received was the sum of the information received in the individual weather reports.

Furthermore, consider that the weather bureau of a city located in the desert, where it has not rained for 25 years, is called before each flight. The call is required although everyone "knows" that the weather will be clear. However, the day the call is made and the reply is that a very heavy rainstorm is in progress and that the flight must be canceled. The information received is then very great.

13.1.2 average information, Entropy

Suppose we have M different and independent messages m_1, m_2, \dots , with probabilities of occurrence p_1, p_2, \dots . Suppose further that during a long period of transmission a sequence of L messages has been generated. Then, if L is very large, we may expect that in the L message sequence we transmitted $p_1 L$ messages of m_1 , $p_2 L$ messages of m_2 , etc. The total information in such a sequence will be

$$I_{\text{total}} = p_1 I \log_2 \frac{1}{p_1} + p_2 I \log_2 \frac{1}{p_2} + \dots \quad (13.4)$$

The average information per message interval, represented by the symbol H , will then be

$$H \equiv \frac{I_{\text{total}}}{L} = p_1 \log_2 \frac{1}{p_1} + p_2 \log_2 \frac{1}{p_2} + \dots = \sum_{k=1}^M p_k \log_2 \frac{1}{p_k} \quad (13.5)$$

This average information is also referred to by the term *entropy*.

We have seen that when there is only a single possible message ($p_k = 1$), the receipt of that message conveys no information. At the other extreme, as $p_k \rightarrow 0$, $I_k \rightarrow \infty$. However, since

$$\lim_{p \rightarrow 0} p \log \frac{1}{p} = 0 \quad (13.6)$$

the *average* information associated with an extremely unlikely message, as well as an extremely likely message, is zero.

As an example of the dependence of H on the probabilities of messages, let us consider the case of just two messages with probabilities p and $(1 - p)$. The average information per message is

$$H = p \log_2 \frac{1}{p} + (1 - p) \log_2 \frac{1}{1-p} \quad (13.7)$$

A plot of H as a function of p is shown in Fig. 13.1. Note that $H = 0$ at $p = 0$ and at $p = 1$. The maximum value of H may be located by setting to zero dH/dp as calculated from Eq. (13.7). It is then found that, as indicated in the figure, the maximum occurs at $p = 1/2$, that is, when the two messages are equally likely. The corresponding H is

$$H_{\max} = 1/2 \log_2 2 + 1/2 \log_2 2 = \log_2 2 = 1 \text{ bit/message} \quad (13.8)$$

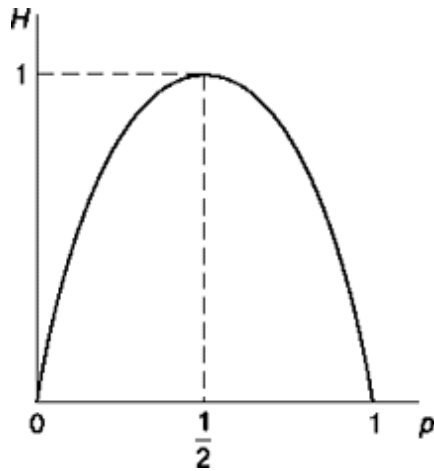


Fig. 13.1 Average information H , for case of two messages, plotted as a function of the probability p of one of the messages.

When there are M messages, it may likewise be proved that H becomes a maximum when all the messages are equally likely. (The student is guided through the details of this proof in Prob. 13.3.) In this case each message has a probability $p = 1/M$ and

$$H_{\max} = \sum \frac{1}{M} \log_2 M = \log_2 M \quad (13.9)$$

since there are M terms in the summation.

13.1.3 Information Rate

If the source of the messages generates messages at the rate r messages per second, then the *information rate* is defined to be

$$R = rH = \text{average number of bits of information/second} \quad (13.10)$$

Example 13.1

An analog signal is bandlimited to B Hz, sampled at the Nyquist rate, and the samples are quantized into 4 levels. The quantization levels Q_1 , Q_2 , Q_3 , and Q_4 (messages) are assumed independent and occur with

Solution

The average information H is

$$H = p_1 \log_2 \frac{1}{p_1} + p_2 \log_2 \frac{1}{p_2} + p_3 \log_2 \frac{1}{p_3} + p_4 \log_2 \frac{1}{p_4}$$

The information rate R is $R = rH = 2B(1.8) = 3.6B$ bits/s *probabilities*
 $p_1 = p_4 = \frac{1}{8}$ and $p_2 = p_3 = \frac{3}{8}$. Find the information rate of the source.

We might choose to transmit the messages, referred to in the above example, by binary PCM. Thus we might identify each message by a binary code as indicated in the following table.

Message	Probability	Binary code
Q_1	$\frac{1}{8}$	0 0
Q_2	$\frac{3}{8}$	0 1
Q_3	$\frac{3}{8}$	1 0
Q_4	$\frac{1}{8}$	1 1

If we transmit 2B messages per second, then, since each message requires 2 bunits, we shall be transmitting 4B bunits per second. We have seen that a bunit is capable of conveying 1 bit of information. Hence with 4B bunits per second we should be able to transmit 4B bits of information per second. We note in the above illustration that we are actually transmitting only 3.6 bits of information per second. We are therefore not taking full advantage of the ability of the binary PCM to convey information. One way to rectify this situation is to select different quantization levels such that each level is equally likely. In this case we would find that the average information per message is

$$H = 4\left(\frac{1}{4} \log_2 4\right) = 2 \text{ bits/message}$$

and

$$R = rH = 2B(2) = 4B \text{ bits/s}$$

Suppose, however, that it was not convenient or appropriate to change the messages. In this case we might seek an alternative coding scheme (rather than binary encoding) in which, on the average, the number of bits per message was fewer than 2 (ideally 1.8). Such a coding scheme is described in Sec. 13.2.

SELF-TEST QUESTION

1. Is it true that a greater amount of information is conveyed when the receiver correctly identifies a less likely message?
2. What is the unit of information?
3. The average information rate is zero for both extremely likely and extremely unlikely message. Is the statement correct?
4. Is it true that average information is maximum when all the messages are equally likely?

13.2 SOURCE CODING AND INCREASE OF AVERAGE INFORMATION

Suppose we have $M = 2^N$ messages, each message coded into N bits. We have seen that if the messages are equally likely the average information per message interval is, from Eq. (13.9), $H = N$. There being N bits in the message, the average information carried by an individual bit is $H/N = 1$ bit. If, however, the messages are not equally likely then H is less than N and each bit carries less than 1 bit of information. The situation can be improved by using a code in which not all messages are encoded into the same number of bits. The more likely a message is, the fewer the number of bits that should be used in its code word. The merit of such a scheme is to some extent intuitively obvious. Witness the fact that in the *Morse* code of telegraphy the most common letter *e* is represented by a single “dot” while the less frequently occurring letters are represented by longer sequences of “dots” and “dashes”. In general, for an average length of binary code word, L we find, $L > H$. This requires rate of binary data transmission to be greater than or equal to information rate.

13.2.1 shannon-Fano Coding

One basic technique by which we may generate such a more “efficient” code is the Shannon-Fano algorithm. An example of the application of this algorithm is given in Fig. 13.2. Here we consider that there are 8 possible messages m_1 through m_8 with probabilities as given. We have ordered the messages in order of decreasing probability. In column 1 we divide the message into two partitions such that the sum of the probabilities of each group are the same. Thus, m_1 in one partition has the probability K and the sum of the probabilities of all the other messages in the second

Message	Probability	I	II	III	IV	V	No of bits/message
m_1	1/2	0					1
m_2	1/8	1	0	0			3
m_3	1/8	1	0	1			3
m_4	1/16	1	1	0	0		4
m_5	1/16	1	1	0	1		4
m_6	1/16	1	1	1	0		4
m_7	1/32	1	1	1	1	0	5
m_8	1/32	1	1	1	1	1	5

Fig. 13.2 An example of the application of the Shannon-Fano algorithm.

partition is also 12. We assign the bit 0 to the message in one partition and we assign the bit 1 to all the messages in the other partition. This process of dividing groups in the same partition into two partitions each with equal sums of probabilities is continued, until each message finds itself alone in a partition. At each partitioning, one group has a zero assigned while a 1 is assigned to the other. In the example of Fig. 13.2 five partitionings are required. We find that m_1 is represented by the single bit 0, m_2 is represented by the 3 bit code 100, etc., up to m_8 whose code is the 5 bit word 11111.

We now find that with this code, the average information per message interval is

$$H = \sum_{i=1}^8 p_i \log_2 \frac{1}{p_i} = \frac{1}{2} \log_2 2 + 2 \times \frac{1}{8} \log_2 2^3 + 3 \times \frac{1}{16} \log_2 2^4 + 2 \times \frac{1}{32} \log_2 2^5 \\ = 2 \frac{5}{16} \quad (13.12)$$

We find further that the average number of bits per message is

$$\text{aver. bits/message} = 1\left(\frac{1}{2}\right) + 3\left(\frac{1}{8}\right) + 3\left(\frac{1}{8}\right) + 4\left(\frac{1}{16}\right) + 4\left(\frac{1}{16}\right) + 5\left(\frac{1}{32}\right) + 5\left(\frac{1}{32}\right) \\ = 2 \frac{5}{16} \quad (13.13)$$

Hence we have the result from Eqs. (13.12) and (13.13) that each binit on the average carries 1 bit of information which is the maximum information that can be conveyed by a binit. If we had not used this more efficient code, we would have required 3 bits per message which is about 30 percent larger than the number $2^5/16$ calculated above.

The saving in average number of bits per message can be put to good advantage in a number of ways. On one hand we may decide to allow more

time per bit thereby reducing bandwidth and improving noise immunity. Or, if we decide to keep the bit rate fixed, we may use bits not used for information transmission to provide error detection, error correction, or both.

The code generation example of Fig. 13.2 is special in that we selected probabilities in such a manner that at each partitioning it was possible to arrange the sum of the probabilities in each group exactly equal. When such is not the case, we partition to satisfy this equal probability condition as nearly as possible. In this more general case, the code efficiency will be reduced.

Example 13.2 shows how to solve a problem when messages do not show such equiprobability as shown here.

13.2.2 Huffman Coding

Huffman coding in general performs better than Shannon-Fano coding and for a source of given entropy gives minimum average word length, hence can be called an optimum code. Like Shannon-Fano coding, the messages are arranged in decreasing order of probability. We use the same message and probability values of example in previous section to illustrate the coding technique. The next step is to combine two messages of lowest probabilities, in this case m_7 and m_8 and write their combined probability as $1/16$ as shown (Fig. 13.3). The combination could be placed anywhere within the group of $1/16$ probabilities. We keep at the top for convenience. We repeat this reduction step again, i.e. combine two more messages of lowest probabilities and continue to do so till only two remain as described in Fig. 13.3. The next step is to encode the messages. We start that from the final reduction and assign bit ‘0’ to the top probability and ‘1’ to the bottom one. Since, in this case the top one never faces any combination on its way back to m_1 , the message m_1 is simply coded as ‘0’. As we follow the bottom probability of last stage we come across a combination in last but one stage and we assign second bit again ‘0’ to top and ‘1’ to bottom and continue to do so at each combination. The encoded message then is represented by the bits it goes through starting from the final reduction. In Fig. 13.3, this is shown by a dotted line for message m_5 . Note that, it crosses 1, then 1, 0, 0 to reach to m_5 . Hence, m_x is coded as 1100. Similarly, one can find the other messages encoded as follows: m_2 -100, m_3 -101, m_4 -1111, m_6 -1101, m_7 -11100, m_8 -11111.

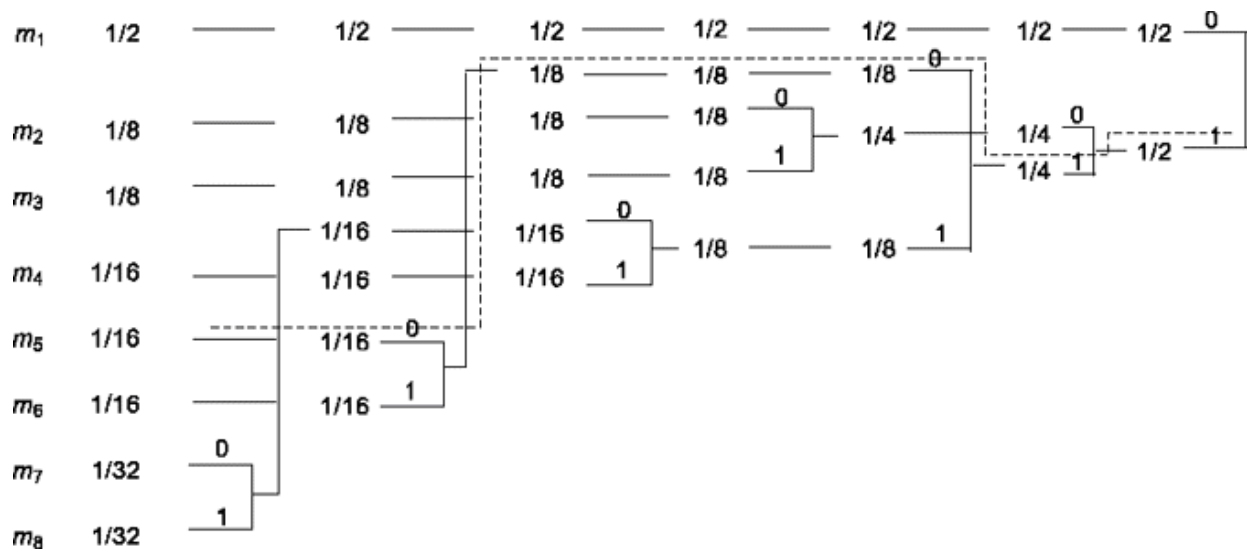


Fig. 13.3 An example of the application of Huffman coding.

Let us, now find average number of bits per message. Following same procedure as in Eq. (13.13) we get,

$$\begin{aligned}\text{av. bits/message} &= 1(1/2) + 3(1/8) + 3(1/8) + 4(1/16) + 4(1/16) + 4(1/16) + 5(1/32) + 5(1/32) \\ &= 2 \frac{5}{16}\end{aligned}$$

This is same as average information per message and thus each binary digit on average carries 1 bit of information giving 100 percent efficiency. Though in this example Shannon-Fano coding equals efficiency of Huffman coding, we shall see in Example 13.2 that the later in general does better.

Some of the limitations in application of Huffman coding are (i) it requires advance knowledge of source probabilities and overhead increases a lot if source probabilities vary with time, (ii) coding efficiency suffers if source probabilities deviate significantly from 2^{-k} where k is an integer, and (iii) length of the code for lowest probability symbol can be quite large.

13.2.3 Lempel-Ziv (LZ) Coding

This is one of the newer coding schemes that does not require prior probabilities of the symbols to be known. Also, contrary to Huffman coding, the code length of symbols or strings of symbols representing one message unit are fixed. The number of codes depends on the codebook (also called dictionary) size. A typical size is 4096 where $\log_2 4096 = 12$ bits represent each message unit. In fact, these 12 bits represent one address of the codebook used for decoding. The encoding process adaptively builds the

codebook from the symbol stream. There are several variants of LZ algorithm to develop this algorithm. We present one scheme of encoding and decoding here with an example.

Consider an input binary data stream 101101000100100010010101... This is to be LZ coded with a maximum codebook size of 7. First, the data stream is parsed into shortest strings which are not repetitive starting from the first binit. This is shown in Fig. 13.4a and turns out to be 1, 0, 11, 01, 00, 010, 0100. Note that the 6th group has 3 digits (010), else it will repeat 01 (prefix) that has already appeared. The next one can be 2 digits (10) which has not come before. Thus, while parsing for each subsequence or phrase, the prefix is already been considered and the last digit is only new, also called *innovation symbol*. This way seven codewords forming the codebook or dictionary is prepared and this is shown in Fig. 13.4b. The next task is to write the prefix and innovation symbol for largest groups of digits possible in a sequential manner and is shown in Fig. 13.4c.

Data	: 1	0	1 1	0 1	0 0	0 1 0	0 1 0 0	0 1 0 0 1	0 1 0 1	...
Parsing	:	<u>1</u>	<u>0</u>	<u>1 1</u>	<u>0 1</u>	<u>0 0</u>	<u>0 1 0</u>	<u>0 1 0 0</u>	<u>0 1 0 0 1</u>	<u>0 1 0 1</u>
Indexing	:	1	2	3	4	5	6	7		
Encoding	:	(0,1)	(0,1)	(1,1)	(2,1)	(2,0)	(4,0)	(6,0)	(7,1)	(6,1)

(a)

Codebook Index	Codebook Entry	Codebook Address
0	START	000
1	1	001
2	0	010
3	11	011
4	01	100
5	00	101
6	010	110
7	0100	111

(b)

Phrase	Previous Entry Coded	Previous Entry Code	Innovation Symb (I.S.)	Encoded Output
1	START	000	1	0001
0	START	000	0	0000
11	1	001	1	0011
01	0	010	1	0101
00	0	010	0	0100
010	01	100	0	1000
0100	010	100	0	1100
01001	0100	111	1	1111
0101	010	110	1	1101

(c)

Received data : 0001 0000 0011 0101 0100 1000 1100 1111 1101
Index, I.S. : 0,1 0,0 1,1 2,1 2,0 4,0 6,0 7,1 6,1
Decoded data : 1 0 11 01 00 010 0100 01001 0101

(d)

Fig. 13.4 LZ Coding: (a) Data stream with parsing, indexing and encoding. (b) Codebook or dictionary preparation with maximum size = 7. (c) Generation of fixed length LZ codes. (d) Decoding of LZ codes.

The LZ coding is done by writing the location or index of the prefix in binary followed by the innovation digit. In this example, total $\log_2 8 + 1 = 4$ bunits are required to describe each phrase and the encoded output from Fig. 13.4c will be 0001, 0000, 0011, 0101, 0100, 1000, 1100, 1111, 1101. Note that for single-digit phrase, we have used 000 as the ‘START’ prefix. All the coded outputs are of fixed length as mentioned before. The decoding is done in a reverse manner. The prefix is used as a pointer to the root phrase and innovation symbol is simply added to it. This is shown in Fig. 13.4d.

At this point, you may wonder how we had a savings in a number of binary digits used. Aren’t we using more number of bunits to describe the original string? You are correct. The coding efficiency is shown when a longer sequence is taken and the data shows some sort of redundancy within it in the form of repetition. You may notice that for the 8th group comprising of 5 bunits, the coded output has only 4 bunits. This coding gain increases when data length increases and becomes asymptotically optimal. Many popular compression techniques like ZIP, GZIP, ARZ, CAB, GIF use LZ coding.

Example 13.2

Five source messages are probable to appear as $m_1 = 0.4$, $m_2 = 0.15$, $m_3 = 0.15$, $m_4 = 0.15$, $m_5 = 0.15$. Find coding efficiency for (a) Shannon-Fano coding, (b) Huffman coding.

Solution

$$\text{Average information} = 0.4 \times \log_2(1/0.4) + 4 \times 0.15 \times \log_2(1/0.15) = 2.171 \text{ bits}$$

(a) Shannon-Fano coding is shown in Fig. 13.5. We try to break the probabilities in two equal halves to the extent possible. In second stage we could combine m_3 and m_4 instead of m_4 and m_5 which would generate same coding efficiency. The final

code of each message is shown in last column combining all the bits.

Average code word length = $0.4 \times 2 + 2 \times 0.15 \times 2 + 2 \times 0.15 \times 3 = 2.3$ bits

$$\text{Coding efficiency} = 2.171/2.3 = 0.9439 = 94.39\%$$

		Coding		
m_1	0.4	0	0	00
m_2	0.15	0	1	01
m_3	0.15	1	0	100
m_4	0.15	1	0	101
m_5	0.15	1	1	11

Fig. 13.5 Shannon-Fano coding of Example 13.2

(b) The Huffman coding is shown in Fig. 13.6. We start pairing bottommost probabilities. The encoded messages following each link is derived in bottom-right part of the figure Average codeword length = $0.4 \times 1 + 4 \times 0.15 \times 3 = 2.2$ bits

$$\text{Coding efficiency} = 2.171/2.2 = 0.9868 = 98.68\%$$

In general, Huffman coding gives equal or better coding efficiency compared to Shannon-Fano coding.

Example 13.3

A data stream to be coded is 18 repeating '10' starting with 1. (a) Show how parsing is done in LZ coding of this data. (b) If number of prefix used is 8, show how this data is encoded.

Solution

(a) Parsing is done as follows: 1, 0, 10, 101, 01, 010, 1010, 10101, ...

(b) Prefix and corresponding sequential location is as follows. Since 8 prefix is used that includes 1 for the start we use first $8 - 1 = 7$ parsed data as prefix

1:001, 0:010, 10:011, 101:100, 01:101, 010:110, 1010:111, ...

Thus, encoded message considering last bit as innovation symbol in each phrase and before that there is prefix which is represented by location index can be written as follows.

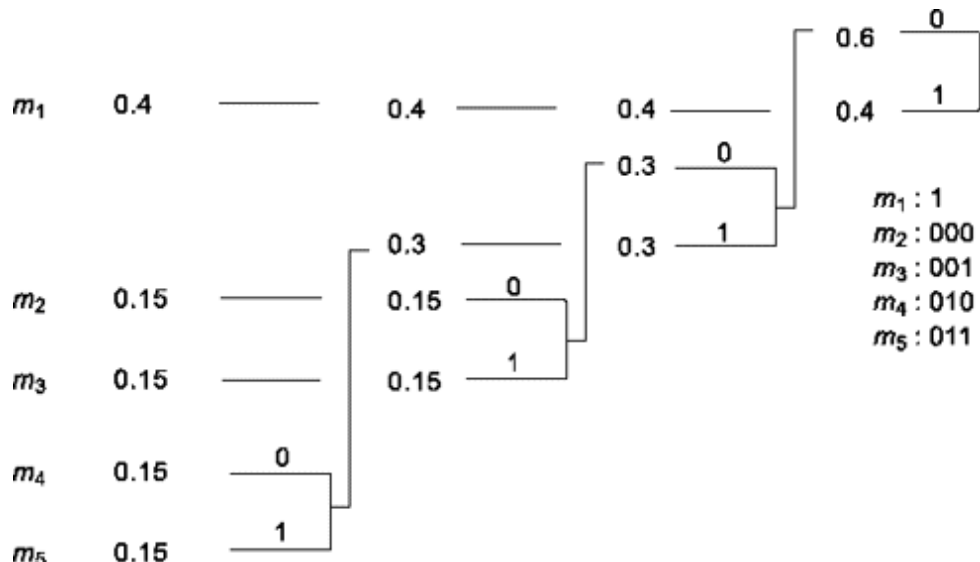


Fig. 13.6 Huffman coding for Example 13.2

0001, 0000, 0010, 0111, 0101, 1100, 1000,
1111, ...

Note that, the coding efficiency begin to appear at later part of the string, e.g. the last 5 digit (10101) is coded by 4 (1111) in LZ.

SELF-TEST QUESTION

5. Is it logical in source coding to assign less probable symbol longer string and more probable ones shorter?

6. Can average bits/message exceed average information per message interval?
7. Is coding efficiency of Shannon-Fano coding better than Huffman coding?
8. Where is LZ coding useful?

13.3 SHANNON'S THEOREM, CHANNEL CAPACITY

The importance of the concept of information rate is that it enters into a theorem due to Shannon³ which is fundamental to the theory of communications. This theorem is concerned with the rate of transmission of information over a communication channel. While we have used the term communication channel on many occasions, it is well to emphasize at this point, that the term, which is something of an abstraction, is intended to encompass all the features and component parts of the transmission system which introduce noise or limit the bandwidth. Shannon's theorem says that it is possible, in principle, to devise a means whereby a communications system will transmit information with an arbitrarily small probability of error provided that the information rate R is less than or equal to a rate C called the *channel capacity*. The technique used to approach this end is called *coding* and is discussed in the beginning of next chapter. The idea is to introduce redundancy so that even if some of the messages are erroneously detected, together it is able to carry the information across. This requires transmission of more number of symbols due to redundancy introduced. This lowers the efficiency of the code in terms of average information per symbol. We talk more about this later. To put the matter more formally, we have the following:

Theorem

Given a source of M equally likely messages, with $M \geq 1$, which is generating information at a rate R . Given a channel with channel capacity C . Then, if

$$R \leq C$$

there exists a *coding* technique such that the output of the source may be transmitted over the channel with a probability of error in the received message which may be made arbitrarily small.

Note that the unit of R and C are bits per second where bit is the unit of information and not binary digit. The message symbols can be binary and with a lower coding efficiency due to introduction of redundancy each binary digit or binit will carry less than one bit of information. To send 1 bit/s of information we have to send more than 1 binit/s. For a noiseless channel, probability of error will be zero and we can achieve 1 bit of information per binit. We shall derive this later in this chapter.

13.3.1 Capacity of Gaussian Channel

A theorem which is complementary to Shannon's theorem and applies to a channel in which the noise is Gaussian is known as the Shannon-Hartley theorem.

Theorem

The channel capacity of a white, bandlimited Gaussian channel

$$C = B \log_2 \left(1 + \frac{S}{N} \right) \text{ bits/s} \quad (13.14)$$

where B is the channel bandwidth, S the signal power, and N is the total noise within the channel bandwidth, that is, $N = hB$, with $h/2$ the (two-sided) power spectral density.

This theorem, although restricted to the Gaussian channel, is of fundamental importance. First, we find that channels encountered in physical systems generally are, at least approximately, Gaussian. Second, it turns out that the results obtained for a Gaussian channel often provide a *lower bound* on the performance of a system operating over a non-Gaussian channel. Thus, if a particular encoder-decoder is used with a Gaussian channel and an error probability P_e results, then with a non-Gaussian channel another encoder-decoder can be designed so that the P_e will be smaller. We may note that channel capacity equations corresponding to Eq. (13.14) have been derived for a number of non-Gaussian channels.

The derivation of Eq. (13.14) for the capacity of a Gaussian channel is rather formidable and will not be undertaken. However, the result may be made to appear reasonable by the following considerations. Suppose that, for the purpose of transmission over the channel, the messages are represented by fixed voltage levels. Then, as the source generates one message after

another in sequence, the transmitted signal $s(t)$ takes on a waveform similar to that shown in Fig. 13.7.

The received signal is accompanied by noise whose root-mean-square voltage is s . The levels have been separated by an interval Is , where l is a number presumed large enough to allow recognition of individual levels with an acceptable probability of error. Assuming an even number of levels, the levels are located at voltages $\pm ls/2$, $\pm 3ls/2$, etc. If there are to be M possible messages, then there must be M levels. We assume that the messages and hence the levels occur with equal likelihood. Then the average signal power is

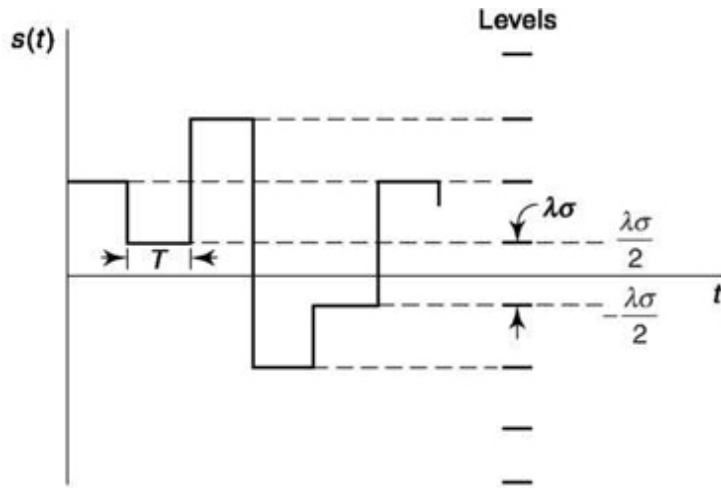


Fig. 13.7 A sequence of messages is represented by waveform $s(t)$ which assumes voltage levels corresponding to the messages.

where $N = s^2$ is the noise power. Each message is equally likely and therefore conveys an average amount of information

$$S = \frac{2}{M} \left\{ \left(\frac{\lambda\sigma}{2} \right)^2 + \left(\frac{3\lambda\sigma}{2} \right)^2 + \dots + \left[\frac{(M-1)\lambda\sigma}{2} \right]^2 \right\} \quad (13.15a)$$

The number of levels for a given average signal power is, from Eq. (13.15b),

$$M = \left(1 + \frac{12S}{\lambda^2 \sigma^2} \right)^{1/2} = \left(1 + \frac{12}{\lambda^2} \frac{S}{N} \right)^{1/2} \quad (13.16)$$

$$H = \log_2 M = \log_2 \left(1 + \frac{12}{\lambda^2} \frac{S}{N} \right)^{1/2}$$

$$= \frac{1}{2} \log_2 \left(1 + \frac{12}{\lambda^2} \frac{S}{N} \right) \text{ bits/message} \quad (13.17)$$

To find the information rate of the signal waveform $s(t)$ of Fig. 13.7, we need to estimate how many messages per unit time may be carried by this signal. That is, we need to estimate the interval T which should be assigned to each message to allow the transmitted levels to be recognized individually at the receiver, even though the bandwidth B of the channel is limited. Now the principal effect of limited bandwidth on the signal waveform $s(t)$ will be a *rounding* of the initially abrupt transitions from one level to another. We saw in Sec. 1.4.5 that when an abrupt step is applied to an ideal low-pass filter of bandwidth B , the response has a 10 to 90 percent rise time t given by $t = 0.44/B$. We may then reasonably estimate that if we set $T = t$, we shall be able to distinguish levels *reliably*. Since our discussion is heuristic, let us, as a matter of convenience, take $T = t = 0.5/B$. The message rate is then

$$r = \frac{1}{T} = 2B \text{ messages/s} \quad (13.18)$$

which is equal, as we might expect, to the Nyquist sampling rate. Since the transmission of any of the M messages is equally likely,

$$H = \log_2 M$$

Thus our channel is transferring information at a rate $R = rH$. Since we have presumably taken what precautions are necessary to ensure that the channel is just able to allow the transmission with acceptable probability of error, $R \sim C$. The channel capacity is, therefore, found by combining Eqs. (13.17) and (13.18):

$$C \approx R = rH = B \log_2 \left(1 + \frac{12}{\lambda^2} \frac{S}{N} \right) \quad (13.19)$$

Comparing Eq. (13.19) with Eq. (13.14) of the Shannon-Hartley theorem, we observe that the results would be identical if we set $12/\lambda^2 = 1$, that is, $\lambda = 3.5$.

This heuristic discussion leading to Eq. (13.19) was undertaken to make the Shannon-Hartley theorem [Eq. (13.14)] rather intuitively acceptable. It needs to be emphasized, however, that Eq. (13.19) specifies the rate at which information may be transmitted with *small* error, while the Shannon-Hartley theorem contemplates that, with a sufficiently sophisticated transmission

technique, transmission at channel capacity is possible with arbitrarily small error.

13.3.2 Bandwidth-s/N Trade-off

The Shannon-Hartley theorem, Eq. (13.14); indicates that a noiseless Gaussian channel ($S/N = \infty$) has an infinite capacity. On the other hand, while the channel capacity does increase, it does not become infinite as the bandwidth becomes infinite because, with an increase in bandwidth, the noise power also increases. Thus for a fixed signal power and in the presence of white Gaussian noise the channel capacity approaches an upper limit with increasing bandwidth. We now calculate that limit. Using $N = hB$ in Eq. (13.14), we have

$$C - B \log_2 \left(1 + \frac{S}{\eta B} \right) = \frac{S}{\eta} \frac{\eta B}{S} \log_2 \left(1 + \frac{S}{\eta B} \right) \quad (13.20a)$$

$$= \frac{S}{\eta} \log_2 \left(1 + \frac{S}{\eta B} \right)^{\eta B/S} \quad (13.20b)$$

We recall that $\lim_{x \rightarrow 0} (1+x)^{1/x} = e$ (the Naperian base), and identifying x as $x = S/hB$, we find that Eq. (13.20b) becomes

$$C_\infty = \lim_{B \rightarrow \infty} C = \frac{S}{\eta} \log_2 e = 1.44 \frac{S}{\eta} \quad (13.21)$$

The Shannon-Hartley principle also indicates that we may trade off bandwidth for signal-to-noise ratio and vice versa. For example, if $S/N = 7$ and $B = 4$ kHz, we find $C = 12 \times 10^3$ bits/s. If the SNR is increased to $S/N = 15$ and B decreased to 3 kHz, the channel capacity remains the same. With a 3 kHz, bandwidth the noise power will be % as large as with 4-kHz. Thus the signal power will have to be increased by the factor $\left(\frac{3}{4} \times \frac{15}{7}\right) = 1.6$. Therefore, the 25 percent reduction in bandwidth requires a 60 percent increase in signal power.

It is of great interest, and even a little surprising, to recognize that the trade off between bandwidth and signal-to-noise ratio is not limited by a lower limit on bandwidth. Specifically, suppose that we want to transmit a signal whose spectral range extends up to a frequency f_M . Let us quantize the signal so that we may determine an information rate for the signal, and let us

assume that the channel has a channel capacity greater than the signal information rate. Now, however, suppose that it turns out that the bandwidth B of the channel is less than f_M . Say, as an extreme example, that the bandwidth is 1 Hz while f_M is 1000 Hz. Then is it really possible, in principle, to receive the signal with arbitrarily small probability of error? The answer is yes, provided that the channel capacity is greater than the transmitted data bit rate.

To make the idea somewhat more acceptable that such errorless signal reception is indeed possible, consider the extreme case where there is no noise at all. Suppose that the signal with $f_M = 1000$ Hz is transmitted through a channel which can be represented as a low-pass RC circuit with cut off at 1 Hz. Then the received signal will be greatly attenuated and severely distorted. If, however, there is no noise, then we are entirely free to make up for the attenuation by the use of an amplifier and to correct the frequency distortion by the use of an equalizer. The signal is then recoverable precisely as it was transmitted.

13.4 USE OF ORTHOGONAL SIGNALS TO ATTAIN SHANNON'S LIMIT

In the preceding section we saw that in the (trivial) case of no noise the channel capacity was infinite, and that no matter how restricted the bandwidth was, it was always possible to receive a signal without error, as predicted by the Shannon limit. In the present section we shall discuss one possible method of attaining performance predicted by Shannon's theorem in the presence of Gaussian noise. We shall see that, to obtain errorless transmission for $R < C$ requires an extremely complicated communication system. In physically realizable systems, therefore, we must accept a performance less than optimum.

Orthogonal signals

The system we are to describe involves the use of a set $s_1(t), s_2(t), \dots$ of orthogonal signals. Such signals $s(t)$, defined as being orthogonal over the interval 0 to T , have the property that

$$\int_0^T s_i(t)s_j(t) dt = 0 \quad \text{for } i \neq j \quad (13.22)$$

A familiar example of a set of orthogonal signals is M-ary FSK, whose probability of error we have calculated in Sec. 11.5.4. Because of the importance of the result and the fact that the probability of error obtained using the Union Bound is “too loose” we now proceed with an alternate derivation of P_e .

We shall assume that the amplitudes of the signals have been adjusted so that in every case

$$\int_0^T s_i^2(t) dt = E_s \quad (13.23)$$

that is, each signal has the same energy E_s in the interval T and also the same power $P_s = E_s/T$.

13.4.1 Matched-Filter Reception

Let us assume that our message source generates M messages, each with equal likelihood. Let each message be represented by one of the orthogonal sets of signals $s_1(t), s_2(t), \dots, S_M(t)$. The message interval is T . The signals are transmitted over a communications channel where they are corrupted by additive white Gaussian noise. As shown in Fig. 13.8, at the receiver a determination of which message has been transmitted is made through the use of M matched filters, that is, correlators. Each correlator consists of a multiplier followed by an integrator. The local inputs to the multipliers are, as shown, the signals $s(t)$. Suppose then, in the absence of noise, that the signal $s(t)$ is transmitted, and the output of each integrator is sampled at the end of a message interval. Then, because of the orthogonality condition of Eq. (13.22), all integrators will have zero output, except that the i th integrator output will be E_s , as given by Eq. (13.23).

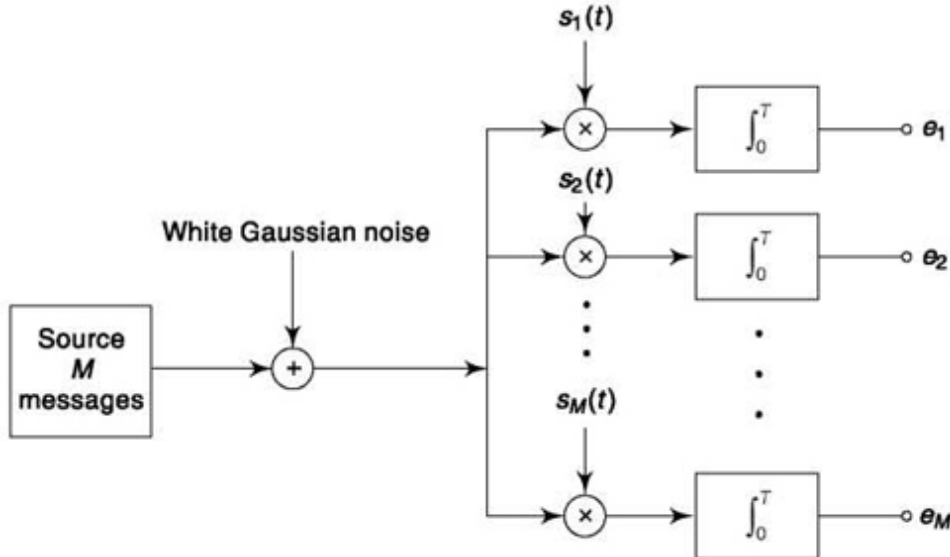


Fig. 13.8 The messages of a source are represented by orthogonal signals $s_1(t)$, ... $s_2(t)$, ... $s_M(t)$. Reception is accomplished by the use of correlation detectors (matched filters).

In the presence of an additive noise waveform $n(t)$, the output of the l th correlator ($l \in \{1, 2, \dots, M\}$) will be

$$e_l = \int_0^T n(t)s_l(t) dt \equiv n_l \quad (13.24)$$

This quantity n_l is a random variable. In Prob. 13.12 the student is guided through a proof that (a) the random variable n_l is Gaussian, (b) that it has a mean value zero, (c) that it has a mean-square value, i.e., a variance s^2 given by

$$\sigma^2 = \frac{\eta E_s}{2} \quad (13.25)$$

and (d) that $E(e_l e_m) = 0$; that is, the outputs of the matched filter are independent. The Gaussian character and zero mean value of n_l do not depend on the form of the deterministic signal $s_l(t)$. The variance s^2 depends only on the signal energy. Since we have selected the orthogonal signals $s_1(t)$, $s_2(t)$, ..., to have the same energy [Eq. (13.23)], the noise sample value at the output of each correlator will have the same statistical properties.

The correlator corresponding to the transmitted message $s_i(t)$ will have an output

$$e_i = \int_0^T (s_i(t) + n(t)) s_i(t) dt \quad (13.26a)$$

from Eqs. (13.23) and (13.24). Again n_t is a random variable with statistical properties identical with those specified for n_l .

13.4.2 Calculation of Error Probability

To determine which message has been transmitted, we shall compare the matched-filter outputs e_1, e_2, \dots, e_M . We shall decide that $s(t)$ has been transmitted if the corresponding output e_t is larger than the output of any other filter. We shall now calculate the probability that such a determination will lead to an error.

The probability that some arbitrarily selected output e_t is less than the output e_i is

$$P(e_t < e_i) = \frac{1}{\sqrt{2\pi\sigma^2}} \int_{-\infty}^{e_i} e^{-e_t^2/2\sigma^2} de_t \quad (13.27)$$

in which s^2 is given by Eq. (13.25). Observe, in Eq. (13.27), that $P(e_t < e_i)$ depends only on e_i and does not depend on which output e_t ($t \neq i$) has been selected for comparison with e_i .

The probability that, say, e_x and e_2 are *both* smaller than e_i is

$$P(e_1 < e_i \text{ and } e_2 < e_i) = P(e_1 < e_i)P(e_2 < e_i) \quad (13.28a)$$

$$= [P(e_1 < e_i)]^2 = [P(e_2 < e_i)]^2 \quad (13.28b)$$

since e_x and e_2 are independent (Prob. 13.12), and as we have noted, $P(e_t < e_i)$ does not depend on e_i . Hence, the probability P_L that e_i is the largest of the outputs is

$$\begin{aligned} P_L &\equiv P(e_i > e_1, e_2, \dots, e_{i-1}, e_{i+1}, \dots, e_M) \\ &= \left(\frac{1}{\sqrt{2\pi\sigma^2}} \int_{-\infty}^{e_i} e^{-e_t^2/2\sigma^2} de_t \right)^{M-1} \end{aligned} \quad (13.29a)$$

$$= \left(\frac{1}{\sqrt{2\pi\sigma^2}} \int_{-\infty}^{E_s + n_i} e^{-e_t^2/2\sigma^2} de_t \right)^{M-1} \quad (13.29b)$$

from Eq. (13.26c). If we let $x \equiv e_t/(\sqrt{2}\sigma)$, Eq. (13.29b) becomes

$$P_L = \left(\frac{1}{\sqrt{\pi}} \int_{-\infty}^{\sqrt{E_s/\eta} + n_i/\sqrt{2}\sigma} e^{-x^2} dx \right)^{M-1} \quad (13.30)$$

where we have used Eq. (13.25) to show that $E_s/((2 s)) = (E_s/h)$. Observe that P_L depends on the two deterministic parameters EJh and M and on the single random variable, $n_jyfl s$; that is,

$$P_L = P_L \left(\frac{E_s}{\eta}, M, \frac{n_i}{\sqrt{2}\sigma} \right)$$

To find the probability that e_t is the largest output without reference to the noise output n_t of the i th correlator, we need but average P_L over all possible values of n_i . This average is the probability that we shall be correct in deciding that the transmitted signal corresponds to the correlator which yields the largest output. Let us call this probability P_c . The probability of an error is then $P_e = 1 - P_c$.

We have seen that n_t is a Gaussian random variable with zero mean and variance s^2 . Hence the average value of P_L , considering all possible values of n_i , is

$$P_c = 1 - P_e = \frac{1}{\sqrt{2\pi\sigma^2}} \int_{-\infty}^{\infty} P_L(E_s/\eta, M, n/\sqrt{2}\sigma) e^{-n_i^2/2\sigma^2} dn_i \quad (13.31)$$

If we let $y = n/(\sqrt{2}s)$, Eq. (13.31) becomes, using Eq. (13.30),

$$1 - P_e \equiv P_c = \left(\frac{1}{\sqrt{\pi}} \right)^M \int_{-\infty}^{\infty} e^{-y^2} \left(\int_{-\infty}^{\sqrt{E_s/\eta} + y} e^{-x^2} dx \right)^{M-1} dy \quad (13.32)$$

The integral in Eq. (13.32) is rather formidable. It has been approximated using the Union Bound and the result presented in Eq. (11.135). It has also been evaluated⁴ by numerical integration by computer, and the results for several values of M are shown in Fig. 13.9. Here the ordinate is the error probability P_e . We may note that it appears from Eq. (13.32) that P_e is a function of E_s/h and M . The abscissa of the plot of Fig. 13.9 has been marked off in units of the ratio $E_s/h \log_2 M$. Note that $(\log_2 M)/T = R$, the rate of information transfer (since each of the M signals has equal probability

of occurrence), so that the quantity $E_s/(h \log^2 M) = S_i/hR$, where $S_i = E_s/T$ is the signal power.

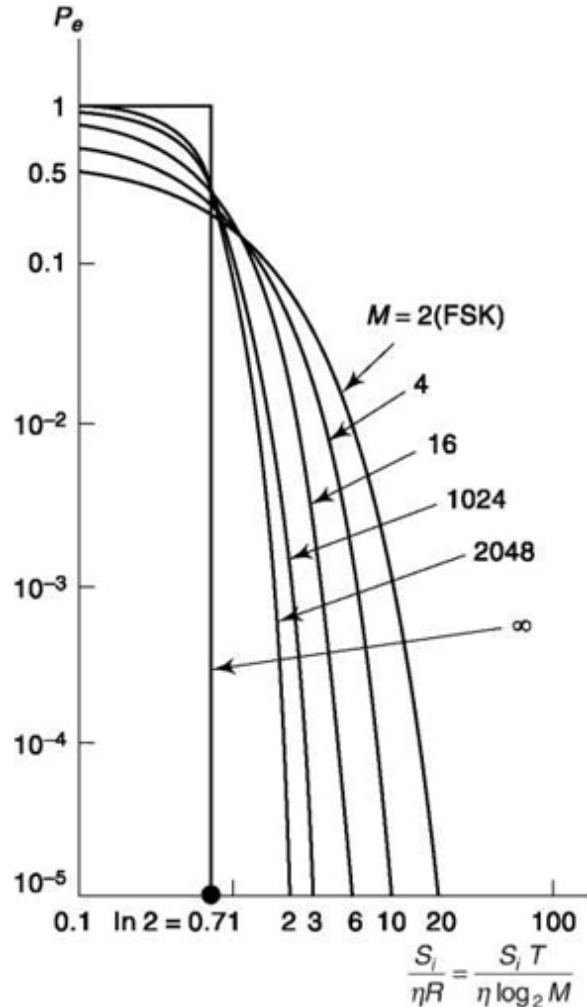


Fig. 3.9 Probability of error with orthogonal signals (Courtesy of A. J. Viterbi, "Principles of Coherent Communications," McGraw-Hill Book Co., 1966.)

13.4.3 Efficiency of Orthogonal signal Transmission

We observe that for all M , P_e decreases as S_i/hR increases. Also, we note that as $S_i/hR \rightarrow 0$, $P_e \rightarrow 0$.

0. The axis $P_e = 0$ does not appear on the plot because of the logarithmic scale of the ordinate. In the plot for $M \rightarrow \infty$, $P_e = 0$, provided that

$$\frac{S_i}{\eta R} \geq \ln 2 \quad (13.33)$$

and $P_e = 1$ otherwise. It is interesting to note that using the Union Bound, we found that $P_e \leq 0$, provided that [see Eq. (11.136)]

$$\frac{E_s}{\eta \log_2 M} = \frac{S_t}{\eta R} > 2 \ln 2 \quad (13.34)$$

Thus, the Union Bound was too loose by 3 dB. In general, as M increases, S_t/h must also increase to keep P_e small, otherwise P_e increases.

Some of the features in Fig. 13.9 are certainly to have been anticipated readily enough on a qualitative basis. Thus, we note that for fixed M and R , P_e decreases as the signal power S_t goes up or as the background noise density h goes down. Similarly, we note that for fixed S_t , h and M , the P_e decreases as we allow more time T (that is, decreasing R) for the transmission of a single message. This result is to have been anticipated as an easy generalization of our earlier discussion (Sec. 11.1) concerning baseband binary PCM transmission [see particularly Eq. (11.6) and the ensuing comments].

However, the real usefulness to us of the results given in Fig. 13.9 is that, in the first place, they allow us the satisfaction of verifying, in this one special case, the validity of Shannon's principle and of the Shannon-Hartley result for channel capacity. In the second place, they allow us a basis on which to make an engineering judgement concerning how much complexity is warranted in terms of the reduction in error which results therefrom. We consider now the first point.

13.4.4 shannon Limit

Let us assume that our signal source generates four equally likely messages $m_1(t)$, $m_2(t)$, $m_3(t)$, $m_4(t)$ and a time $T = 1$ s is to be allowed as the transmission interval for a message. We shall refer to these messages as elemental messages in the sense that they extend over the smallest time interval in which some information may be conveyed. The transmission rate is $R = (\log_2 4)/1 = 2$ bits/s. Let us assume that $S/h = 10$ s⁻¹. Then $S/hR = 5$, and, as indicated on the plot of Fig. 13.9, we may expect an error probability $P_e \sim 10^{-2}$. At the receiver we require four matched filters. If we assume for simplicity that 4-ary FSK is being used the channel bandwidth is approximately 8 Hz.

Now let us join two successive intervals into an extended interval of length $2T = 2$ s. Since four messages are possible in each interval T , there are $4 \times 4 = 16$ message combinations, i.e., new orthogonal messages possible in the extended interval. We now consider $2T$ as the message interval, and the transmission rate R is, of course, unaltered, for we now have $R = (\log_2 16)/2 = 2$ bits/s as before. If we transmit using these sixteen new orthogonal messages, then we shall complicate the receiver very seriously, since we now require sixteen matched filters in place of the original four. The advantage which accrues to us in return for this added complexity is to be seen by referring again to Fig. 13.9. For now we find, with $S/hR = 5$ again, that the error probability has been reduced to $P_e @ 5 \times 10^{-4}$. However, now the required bandwidth is approximately 16 Hz.

If we extend our message intervals to $3T$, $4T$, etc., the number of composite messages increases correspondingly to 64, 256, etc., reducing the error probability further, but correspondingly increasing the number of matched filters required, as well as the bandwidth needed. In the limit as the number of message intervals increases without bound, $M ('$, and the error probability P_e will approach zero provided that Eq. (13.33) is satisfied. The required bandwidth is now infinite. From this condition we may calculate the maximum allowable errorless transmission rate R_{\max} , which, by definition, is the channel capacity C . We find

$$R_{\max} = C = \frac{S_i}{\eta} \frac{1}{\ln 2} = \frac{S_i}{\eta} \log_2 e = 1.44S/\eta \quad (13.35)$$

Equation (13.35) is in agreement with Eq. (13.21) which we deduced from the Shannon-Hartley theorem for a channel of unlimited bandwidth.

When we transmit elemental messages, then, of course, some information is received in each elemental interval T . Suppose, however, we form composite messages each of which extends over many time intervals. Then no information will be received except at the termination of the extended interval. At this termination, all the information in all the intervals will be received at once. In the limit as we increase the number of intervals without bound, and hence let $M ('$, to reduce the error probability to zero, we find that we must wait a time $T ('$ before we receive any information.

In summary, we have examined one possible way of achieving errorless transmission. We have shown that such transmission is possible through the

use of orthogonal signals and matched filters over a channel of unlimited bandwidth. We have also calculated the channel capacity and arrived at a result which is consistent with the Shannon-Hartley theorem.

Trade-offs

The plots of Fig. 13.9 may be used not only to illustrate some general principles as we have already done, but also to determine what advantage results in one direction as a result of a sacrifice in another direction. By way of example, suppose we are required to transmit information at some fixed information rate R , in the presence of a fixed background-noise power spectral density, with an error probability $P_e = 10^{-5}$. Suppose we use $M = 2$. Then, from Fig. 13.8 we find that $S/hR \sim 20$. Now consider what happens if M is increased to $M = 4$. Then to keep R fixed, T must be increased by the factor $(\log_2 4/\log_2 2) = 2$. Again referring to Fig. 13.9, we see that S/hR can now be reduced to 10 and still result in $P_e = 10^{-5}$. Since h and R are fixed, S_i can be halved (reduced by 3 dB). Thus, to increase the number of messages while maintaining the same information rate R and P_e required that the time T be increased; however, the required signal power can be decreased.

13.5 MUTUAL INFORMATION AND CHANNEL CAPACITY

In this section, we take up mutual dependence of source message and received message considering the channel can cause misrepresentation due to presence of noise. We shall further consider channel to be discrete, memoryless so that it is specified by a set of conditional probabilities between input and output; output at any time being function of only current input. Fig. 13.10 shows a channel that has two inputs, two outputs defined by transition probability matrix $P(Y/X)$ as

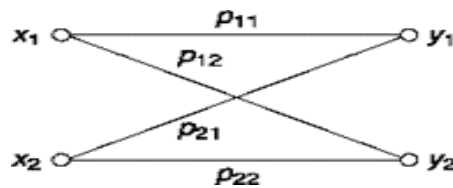


Fig. 13.10 Channel diagram.

$$P(Y/X) = \begin{pmatrix} p(y_1/x_1) & p(y_2/x_1) \\ p(y_1/x_2) & p(y_2/x_2) \end{pmatrix} \quad (13.36)$$

In the channel diagram, the transition probabilities are shown as $py = p(y/x)$. Note that, if there are m inputs and n outputs then transition matrix will be of size $m \times n$. Now, if we define input probabilities as $P(X) = [P(x_1), P(x_2)]$ then output probability

$$P(Y) = [P(y_1) \quad P(y_2)] = P(X)P(Y/X) \quad (13.37)$$

Expanding our definition of entropy given in Eq. (13.5) and representing joint probabilities as

$$p(xi, yi),$$

average uncertainty of source, $H(X) = \sum_{i=1}^m p(x_i) \log_2 \frac{1}{p(x_i)}$ (13.38)

average uncertainty of received symbol, $H(Y) = \sum_{j=1}^n p(y_j) \log_2 \frac{1}{p(y_j)}$ (13.39)

average uncertainty of received symbol when X is transmitted,

$$H(Y/X) = \sum_{i=1}^m \sum_{j=1}^n p(x_i, y_j) \log_2 \frac{1}{p(y_j/x_i)} \quad (13.40)$$

Note that unit is bits per message symbol where bit is the unit of information. For noise-free channel, the elements of the transition matrix in Eq. (13.36) are two valued: 1 or 0. This makes one of the term in each product under summation of Eq. (13.40) zero as

$$p(x_i, y_j) = p(x_i)p(y_j/x_i)$$

That makes average uncertainty of received symbol zero. Similarly, for noise free condition, uncertainties defined by Eq. (13.41) and Eq. (13.42) will also be zero. average uncertainty in transmitted symbol when Y is received,

$$H(X/Y) = \sum_{i=1}^m \sum_{j=1}^n p(x_i, y_j) \log_2 \frac{1}{p(x_i/y_j)} \quad (13.41)$$

average uncertainty in communication is given by joint entropy,

$$H(X, Y) = \sum_{i=1}^m \sum_{j=1}^n p(x_i, y_j) \log_2 \frac{1}{p(x_i, y_j)} \quad (13.42)$$

Having defined all these terms we are in a position to define mutual information. The decrease in receiver's uncertainty about the transmitted symbol when an output is received is described as the measure of mutual information between input and output. This is the amount of information received by the receiver in terms of bits per symbol. Mathematically, mutual information

$$I(X; Y) = H(X) - H(X|Y) \quad (13.45)$$

$$\text{From Eq. (13.43) and (13.44), } I(X; Y) = H(Y) - H(Y|X) \quad (13.46)$$

$$\text{also } I(X; Y) = H(X) + H(Y) - H(X, Y) \quad (13.47)$$

Note that mutual information is always positive as $H(X) > H(X|Y)$. This is because uncertainty in the input is less if output is known.

The channel capacity per message symbol for which the unit is bits/symbol is defined as the maximum value of mutual information and can be written as,

$$C_m = \max[I(X; Y)] \quad (13.48)$$

Since the transition probabilities defining the channel are fixed, the maximization is done over source probabilities (Eq. 13.44) and with that maximum value substituted, the channel capacity is seen to depend on channel transition probabilities only. The relation between channel capacity C (for which the unit is information bits/sec) and channel capacity per message symbol C_M is given by

$$C = rC_M \quad (13.49)$$

where r = message symbol transmitted per second. Let us study C_M further. Consider, in the channel described by Fig. 13.9, if the message sent is x_1 and y_2 is received, then it is an error. The probability of such event, or the channel transition probability $p(y_2/x_1) = p_{12} = P_e$ or probability of error. Similarly, if the message sent is x_2 and the message received is y_1 that also is an error. For a binary symmetric channel for that probability too, we can write $p(y_1/x_2) = p_{21} = P_e$. This gives the relationship (See Example 13.6) between channel capacity per binit (binary digit) C_M and P_e as

$$C_M = 1 + P_e \log_2 P_e + (1 - P_e) \log_2 (1 - P_e) \quad (13.50)$$

The plot of C_M vs. P_e is shown in Fig. 13.11. This is a U-shaped curve with a minimum of C_M occurring at $P_e = 0.5$. Then if the message x_1 is transmitted, there is an equal probability of it being received as either y_x or y_2 , i.e. they are equally likely and thus information received about the source is zero. The $P_e = 0$ condition refers to no error or a noiseless channel. Then the capacity is at maximum with 1 binit carrying 1 bit of information. Interestingly, the capacity is again maximum for $P_e = 1$. This is the case when the channel makes errors in all the transmissions with certainty. For a binary transmission, this amounts to the complement of the message received without error on all occasions. Thus, the received symbol gives the information of the transmitted message with certainty and C_M is at maximum.

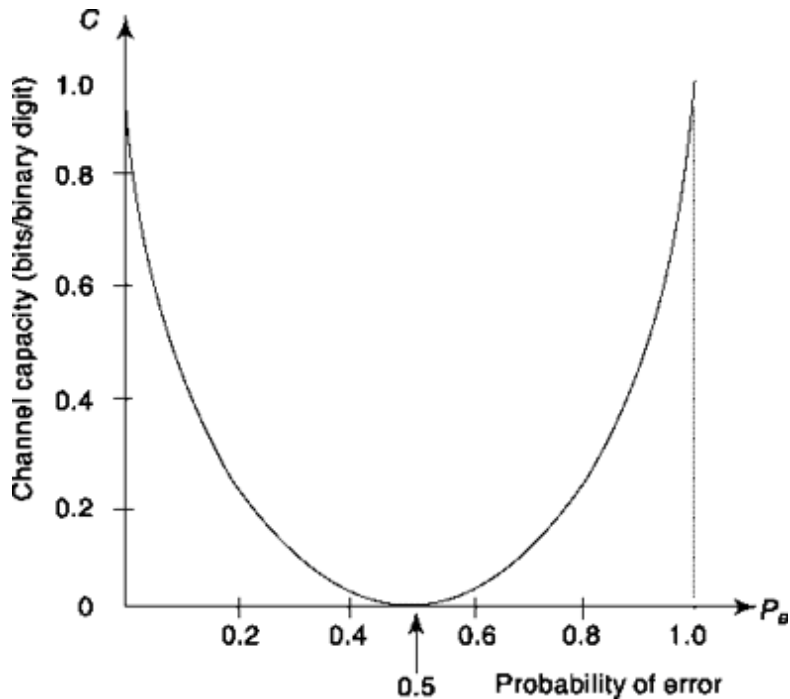


Fig. 13.11 Probability of error vs. channel capacity for a binary symmetric channel.

13.6 RATE DISTORTION THEORY AND LOSSY SOURCE CODING

We discussed lossless source coding in Sec. 13.2 and have seen that the rate of binary data transmission must be greater than or equal to information rate. Next we saw that for a noisy channel, error is a must if information

transmission rate is more than the channel capacity. Even when it is below channel capacity, there can be error which is arbitrarily low if there is adequate redundancy in the code word. This again increases the need of sending more number binary digits per second. Now, consider the case where there is a limitation on the amount of data we can send per second due to non-availability of adequate resources. This amounts to not being able to provide enough binary digits to code information bits which is known as lossy source coding or operating at higher than channel capacity. Can such transmission be permitted or considered useful? Yes, provided we are ready to accept some distortion between the transmitted and received message and the distortions are within acceptable limit. For speech or image transmission, as long as distortions are below human perception threshold, we do not experience any problem and the compression achieved in lossy source coding reduces transmission rate. Rate distortion theory deals with two main issues, (i) given a maximum data transfer rate (R) how to minimize distortion (D), and (ii) given a distortion, how to minimize data transfer rate.

Figure 13.12a shows this concept of distortion between transmitted symbol X and received symbol Y and Fig. 13.12b shows a typical R - D trade-off curve which allows rate to fall as more and more distortion is allowed.

From Eq. (13.45 and 13.46). $I(X; Y) = \sum_{i=1}^m \sum_{j=1}^n p(x_i, y_j) \log_2 \frac{p(x_i, y_j)}{p(x_i)p(y_j)}$ (13.51)

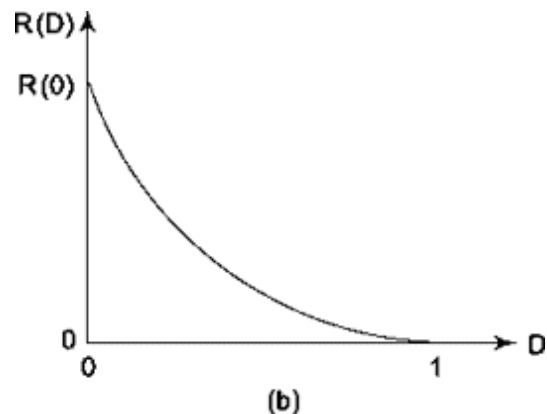
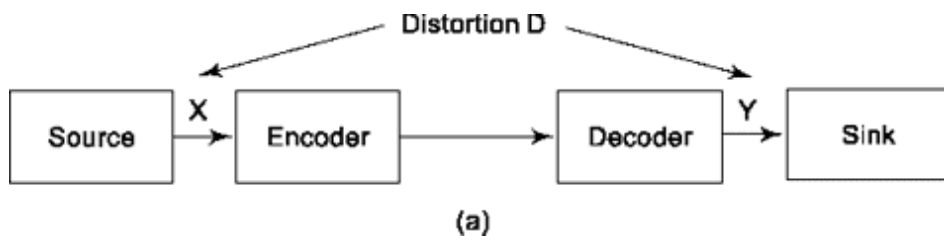


Fig. 13.12 (a) Overview of rate distortion, (b) Rate vs. Distortion curve.

For sent symbol x , if received symbol is yj then let per symbol distortion be $d(x, yj)$ such that $d(x, yj) > 0$, the equality holds when the symbols are same. In image coding, Hamming distortion d_H defined by Eq.(13.52) and in speech coding, squared error distortion d_{sq} defined by Eq. (13.53) are popular.

$$d_H(x, y) = \begin{cases} 0 & \text{for } x = y \\ 1 & \text{for } x \neq y \end{cases} = x \oplus y \quad (13.52)$$

$$d_{sq}(x, y) = (x - y)^2 \quad (13.53)$$

The average distortion considering joint probabilities of x_t and yy occurrences is defined as

$$D_{av} = \sum_{i=1}^m \sum_{j=1}^n p(x_i, y_j) d(x_i, y_j) \quad (13.54)$$

Thus, distortion criterion to be followed for average distortion is to be less than or equal to some maximum distortion D , i.e. $D_{av} \leq D$, and for a given maximum distortion, the rate distortion function gives the lower bound of the transmission bit rate as defined next.

$$R(D) = \min_{D_{av} \leq D} [I(X; Y)] \quad (13.55)$$

$$R(D) = H(X) - \max [H(X - Y|Y)] \quad (13.56)$$

$$D_{av} \leq D$$

Since $H(X/Y) = H(X - Y|Y)$, we can write,

If distortion $X-Y$ is independent of received symbol Y (in ideal cases), then we can further simplify above as

$$R(D) = H(X) - \max_{D_{av} \leq D} [H(X - Y)] \quad (13.57)$$

and this gives Shannon's lower bound,

$$R(D) \geq H(X) - \max_{D_{av} \leq D} [H(X - Y)] \quad (13.60)$$

The rate distortion function of a Gaussian source with zero mean and variance s^2 is given by Eq.

(13.61) where squared error is used as distortion measure. The x in Eq. (13.53) represents sample value and y represents its quantized version.

$$R(D) = \begin{cases} \frac{1}{2} \log_2 \left(\frac{\sigma^2}{D} \right), & 0 \leq D \leq \sigma^2 \\ 0, & D > \sigma^2 \end{cases} \quad (13.61)$$

By inverting the relation, we can write

$$D(R) = \sigma^2 2^{-2R} \quad \text{for } 0 \leq D \leq \sigma^2 \quad (13.62)$$

This says that for every additional bit of information, the distortion reduces by 4 times. Equation (13.61) further says that for $D = \sigma^2$, $R = 0$ and for $D = 0$, $R = \infty$. In Example 13.9, we calculate rate distortion function of a binary symmetric source with Hamming distance as distortion measure. The application of rate distortion theory is found in transfer of audio, image, etc., where a certain amount of distortion is permissible. Also when we consider a continuous source, the entropy is infinite. If we transmit it as a discrete signal encoding in finite number of bits, we always incur some distortion and it will be a lossy coding. Even for discrete signals, if we can reduce source entropy by allowing some distortion, the transmission rate can be reduced. Such indeed is the objective of lossy source encoders. Examples include MP3 in audio, and JPEG in image. They cleverly utilize limitation of human perception in introducing distortion and are thereby able to compress the data.

Example 13.4

Find capacity of Gaussian channel of bandwidth 4 kHz with noise PSD 10^{-9} W/Hz when signal energy is (a) 0.1 J and (b) 0.001 J. (c) How does channel capacity change in (b) if bandwidth is increased to 10 kHz?

Solution

(a) From Eq. (13.20),

$$\begin{aligned} C &= 4000 \times \log_2 \left(1 + \frac{0.1}{2 \times 10^{-9} \times 4000} \right) \\ &= 5.44 \times 10^4 \text{ bits/sec} \end{aligned}$$

(b) Similarly,

$$\begin{aligned} C &= 4000 \times \log_2 \left(1 + \frac{0.001}{2 \times 10^{-9} \times 4000} \right) \\ &= 2.79 \times 10^4 \text{ bits/sec} \end{aligned}$$

c) Here, $B = 8000$. Then

$$C = 10000 \times \log_2 \left(1 + \frac{0.001}{2 \times 10^{-9} \times 10000} \right)$$

$$= 5.67 \times 10^4 \text{ bits/sec}$$

Note that a 100 times fall in energy is more than compensated by increasing bandwidth by 2.5 times.

Example 13.5

For a television transmission, the required number of brightness level = 16, pixels per picture frame = 10^6 , frames transmitted per second = 30 and SNR = 30 dB. Find minimum bandwidth required.

Solutions

From definition, 30 dB = 1000

Information per pixel = $\log_2 16 = 4$ bits/pixel

Information per picture frame = 4×10^6 bits/frame

Information rate = $4 \times 10^6 \times 30 = 12 \times 10^7$ bits/s

Channel capacity, $C \geq 12 \times 10^7$ bits/s

By definition, $C = B \log_2 (1 + \text{SNR})$ where B = bandwidth

Therefore, $B \log_2 (1 + 1000) \geq 12 \times 10^7$

or $B \geq 1.212 \times 10^7$ Hz

Minimum bandwidth required = 12.12 MHz.

[as joint prob. is summed over all inputs] or $H(X, Y) = H(X/Y) + H(Y)$ [from Eq. 13.39] Hence, shown.

Example 13.6

Show that $H(X, Y) = H(X/Y) + H(Y)$

Solutions

From Eq.(13.39),

$$H(X, Y) = \sum_{i=1}^m \sum_{j=1}^n p(x_i, y_j) \log_2 \frac{1}{p(x_i, y_j)}$$

$$\text{or } H(X, Y) = - \sum_{i=1}^m \sum_{j=1}^n p(x_i, y_j) \log_2 [p(x_i|y_j)p(y_j)]$$

since, $p(x_i, y_j) = p(x_i|y_j)p(y_j)$

$$\begin{aligned} \text{or } H(X, Y) &= - \sum_{i=1}^m \sum_{j=1}^n p(x_i, y_j) \log_2 p(x_i|y_j) \\ &\quad - \sum_{i=1}^m \sum_{j=1}^n p(x_i, y_j) \log_2 p(y_j) \end{aligned}$$

$$\begin{aligned} \text{or } H(X, Y) &= H(Y/X) - \sum_{j=1}^n \left[\sum_{i=1}^m p(x_i, y_j) \right] \log_2 p(y_j) \\ &\quad [\text{from Eq. 13.41}] \end{aligned}$$

$$\text{or } H(X, Y) = H(Y/X) - \sum_{j=1}^n p(y_j) \log_2 p(y_j)$$

Example 13.7

Consider channel diagram of Fig. 13.10. If $p(x_1) = \alpha$, $p_{12} = p_{21} = \beta$, find the channel capacity.

Solution

Given, $p(x_1) = \alpha$, then $p(x_2) = 1 - \alpha$

$p(y_2/x_1) = \beta$ then $P(y_1/x_1) = 1 - \beta$

and $p(y_1/x_2) = \beta$ i.e. $P(y_2/x_2) = 1 - \beta$

From Eq. (13.48) channel capacity is $I(X; Y)$ maximized over input probabilities, i.e. a . Therefore, let us first calculate $I(X; Y)$ and then substitute value of a that maximizes it giving an expression of channel capacity which is function of p .

$$p(x_1|y_1) = p(x_1)p(y_1/x_1) = \alpha(1 - \beta) \quad (13.63a)$$

$$p(x_1|y_2) = p(x_1)p(y_2/x_1) = \alpha\beta \quad (13.63b)$$

$$p(x_2|y_1) = p(x_2)p(y_1/x_2) = (1 - \alpha)\beta \quad (13.63c)$$

$$\text{and } p(x_2|y_2) = p(x_2)p(y_2/x_2) = (1 - \alpha)(1 - \beta) \quad (13.63d)$$

Expanding Eq. (13.40) for $m = 2$ and $n = 2$,

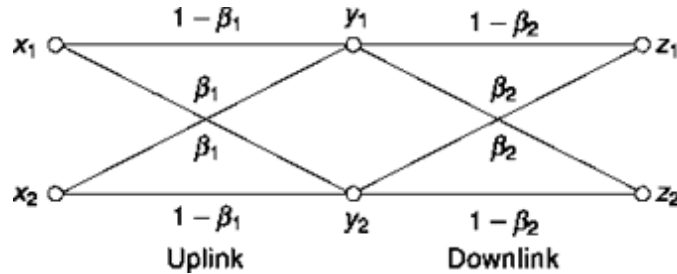
$$H(Y/X) = -p(x_1, y_1)\log_2 p(y_1/x_1) - p(x_1, y_2)\log_2 p(y_2/x_1) - p(x_2, y_1)\log_2 p(y_1/x_2) - p(x_2, y_2)\log_2 p(y_2/x_2)$$

Substituting,

$$\begin{aligned} H(Y/X) &= -\alpha(1-\beta)\log_2(1-\beta) - \alpha\beta\log_2\beta \\ &\quad - (1-\alpha)\beta\log_2\beta - (1-\alpha)(1-\beta)\log_2(1-\beta) \\ \text{or } H(Y/X) &= -(1-\beta)\log_2(1-\beta) - \beta\log_2\beta \quad (13.64) \end{aligned}$$

From Eq.(13.37).

$$\begin{aligned} P(Y) &= P(X)P(Y/X) \\ &= |p(y_1) - p(y_2)| \end{aligned}$$



$$= |\alpha - (1-\alpha)| \begin{pmatrix} 1-\beta & \beta \\ \beta & 1-\beta \end{pmatrix}$$

$$= |\alpha + \beta - 2\alpha\beta - \alpha + \beta - 2\alpha\beta|$$

$$H(Y) = 2 \times (\alpha + \beta - 2\alpha\beta) \log_2 \frac{1}{\alpha + \beta - 2\alpha\beta} \quad (13.65)$$

Now, from Eq. (13.48) channel capacity $CM = \max[I(X; Y)]$ w.r.t. a

or $CM = \max[H(Y) - H(Y/X)]$ [from Eq. 13.46] Thus, RHS is maximum if $H(Y)$ is maximum which occurs if $\alpha = 0.5$ (as $H(Y/X)$ does not contain α). Then from Eq. (13.65), $H(Y) = 1$. Using this and Eq. (13.64), Channel capacity

$CM = 1 + (1 - b) \log_2(1 - b) + b \log_2 b$ (13.66) Note that a channel with such transition probability is also known as Binary Symmetric Channel (BSC).

Example 13.8

Consider a two hop satellite channel as shown in Fig. 13.13 along with transition probabilities. Find its channel capacity.

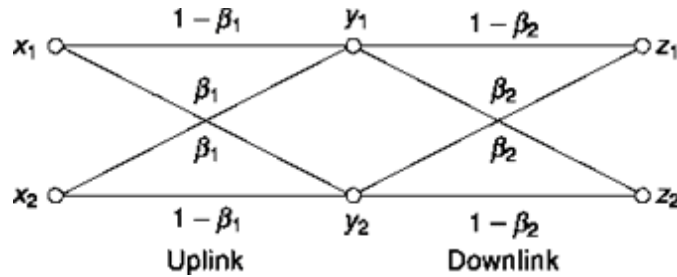


Fig. 13.13 Two hop satellite channels for Example 13.8.

Solution

We solve this first by obtaining an equivalent single hop channel and then if it's BSC by applying equation 13.66.

From Eq. (13.37), in first hop, between intermediate output y_i and input x_i , we can write

$$P(Y) = P(X)P(Y/X) \quad (13.67)$$

Similarly, in the second hop, between intermediate output z_i and input y_i , we can write

$$P(Z) = P(Y)P(Z/Y) \quad (13.68)$$

Combining Eq.(13.57) and (13.59)

$$P(Z) = P(X)P(Y/X)P(Z/Y) = P(X)P(Z/X)$$

where, $P(Z/X) = P(Y/X)P(Z/Y)$ (13.69)

Substituting values from channel data,

$$P(Z/X) = \begin{pmatrix} 1 - \beta_2 & \beta_2 \\ \beta_2 & 1 - \beta_2 \end{pmatrix} \begin{pmatrix} 1 - \beta_1 & \beta_1 \\ \beta_1 & 1 - \beta_1 \end{pmatrix}$$

(13.70)

or $P(Z/X)$

$$= \begin{pmatrix} (1 - \beta_2)(1 - \beta_1) + \beta_2 \beta_1 & (1 - \beta_2)\beta_1 + \beta_2(1 - \beta_1) \\ \beta_2(1 - \beta_1) + (1 - \beta_2)\beta_1 & \beta_2 \beta_1 + (1 - \beta_2)(1 - \beta_1) \end{pmatrix}$$

or $P(Z/X)$

$$= \begin{pmatrix} 1 - (\beta_1 + \beta_2 - 2\beta_1\beta_2) & \beta_1 + \beta_2 - 2\beta_1\beta_2 \\ \beta_1 + \beta_2 - 2\beta_1\beta_2 & 1 - (\beta_1 + \beta_2 - 2\beta_1\beta_2) \end{pmatrix}$$

(13.71)

Hence, the equivalent is a binary symmetric channel. Substituting, $p = \beta_1 + \beta_2 - 2p_1p_2$ in Eq. (13.56) we get channel capacity for this two-hop satellite channel

$$\begin{aligned}
C_M &= 1 + (1 - (\beta_1 + \beta_2 - 2\beta_1\beta_2))\log_2 \\
&\quad (1 - (\beta_1 + \beta_2 - 2\beta_1\beta_2)) + (\beta_1 + \beta_2 \\
&\quad - 2\beta_1\beta_2)\log_2(\beta_1 + \beta_2 - 2\beta_1\beta_2) \quad (13.72)
\end{aligned}$$

Example 13.9

Find the rate distortion function of a binary symmetric source (BSS) for distortion $D < 0.5$. Consider Hamming distortion measure.

Solution

Expected proportion of error is the distortion $D >$

$$P(X \neq Y)$$

For BSS, $H(X) = \log_2 2 = 1$

Now,

$$\begin{aligned}
I(X; Y) &= H(X) - H(X|Y) \\
&= 1 - H(X \oplus Y|Y) \\
&\geq 1 - H(X \oplus Y) \\
&\geq 1 - H(D) \\
R(D) &= \min[I(X; Y)] = 1 - H(D)
\end{aligned}$$

Since $H(D)$ is a binary entropy function,

$$\text{or} \quad R(D) = 0$$

$$\text{At } D = 0, H(D) = 0 \text{ and } R(D) = 1.$$

Between $D = 0$ and $D = 0.5$, $H(D)$ monotonically decreases from 1 to 0.

SELF-TEST QUESTION

9. Can application of Shannon-Hartley theorem give lower bound of performance for non Gaussian channel?
10. Can there be a trade-off between signal to noise ratio and bandwidth in calculation of channel capacity?
11. The Shannon limit is practically not achieved as it requires extremely complicated communication system. Do you agree?
12. Does knowledge of output of a channel decrease uncertainty of input to channel?

13. Can we send information at a higher rate than channel capacity if certain amount of distortion is allowed?

14. Is it true that reduction of source entropy can lead to data compression?

13.7 INFORMATION THEORY AND OPTIMUM MODULATION SYSTEM

A generalized communication system is shown in Fig. 13.14. The baseband signal $m(t)$ of bandwidth f_M is encoded or modulated, or both, onto a carrier and is then transmitted over a channel of bandwidth B . Noise is added on the channel, and when the modulated/encoded signal arrives at the receiver it has a signal-to-noise ratio S_i/N_i at the receiver input. Here N_i is the noise power, at the receiver input, in the bandwidth B , that is $N_t = hB$. The output signal obtained after decoding or demodulation, or both, is $m(t) + n_o(t)$, where $n_o(t)$ is the noise that accompanies the *output* signal. The output signal-to-noise ratio is S_o/N_o , and the output waveform $m(t)$ is bandlimited to f_M .

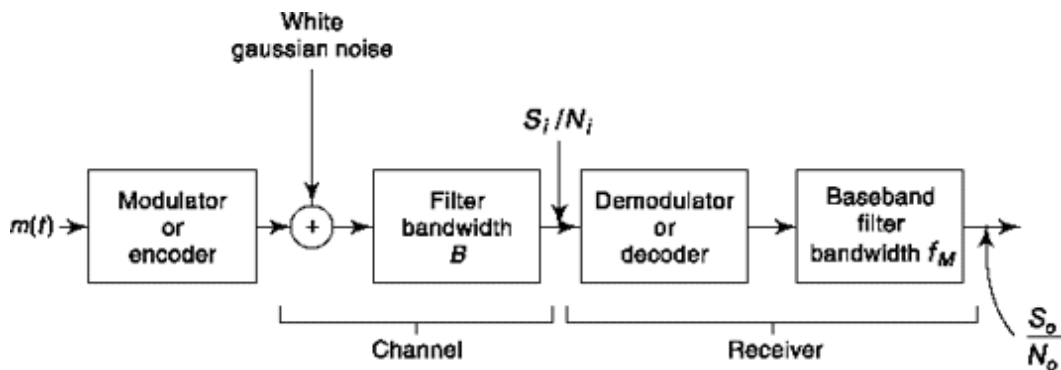


Fig. 13.14 A generalized communication system.

From the Shannon-Hartley theorem, Sec. 13.3.1, the maximum rate at which information may be arriving at the receiver is

$$C_i = B \log_2 \left(1 + \frac{S_i}{N_i} \right) \quad (13.73)$$

while the maximum rate at which information may be issuing from the receiver is

$$C_o = f_M \log_2 \left(1 + \frac{S_o}{N_o} \right) \quad (13.74)$$

We now introduce the concept of an *optimum* or *ideal* modulation or encoding system as one in which $C_o = C$. Such a system is defined as one in which the rate of information output of the receiver is equal to the rate of information input to the receiver. That is, no information is lost as the information passes through the receiver, nor is any information accumulated in the receiver. We assume that this feature of the receiver persists at all rates of information flow up to the maximum as determined by the Shannon-Hartley theorem.

Setting $C_i = C_o$ and solving for S_o/N_o , we find

$$\frac{S_o}{N_o} = \left(1 + \frac{S_i}{N_i} \right)^{B/f_M} - 1 \quad (13.75)$$

An essential feature of the communication system represented in Fig. 13.14 is that while the baseband signal is bandlimited to f_M , we deliberately arranged that the encoded signal should occupy

a larger bandwidth B . The *bandwidth expansion factor* B/f_M is a most important parameter of the system, and it is useful to rewrite Eq. (13.75) in a manner to emphasize this point. The input noise $N_i = hB$, and if we call the input-signal power S_i , we may write

$$\frac{S_i}{N_i} = \frac{S_i}{\eta B} = \frac{f_M}{B} \frac{S_i}{\eta f_M} \quad (13.76)$$

and from Eq. (13.75)

$$\frac{S_o}{N_o} = \left(1 + \frac{f_M}{B} \frac{S_i}{\eta f_M} \right)^{B/f_M} - 1 \quad (13.77)$$

Equation (13.77) characterizes the *optimum* communication system. For a given ratio S/hf_M and a given bandwidth expansion factor B/f_M , any *physical* communication system will yield a smaller S_o/N_o . Plots of S_o/N_o as a function of S/hf_M for various values of B/f_M are given in Fig. 13.15.

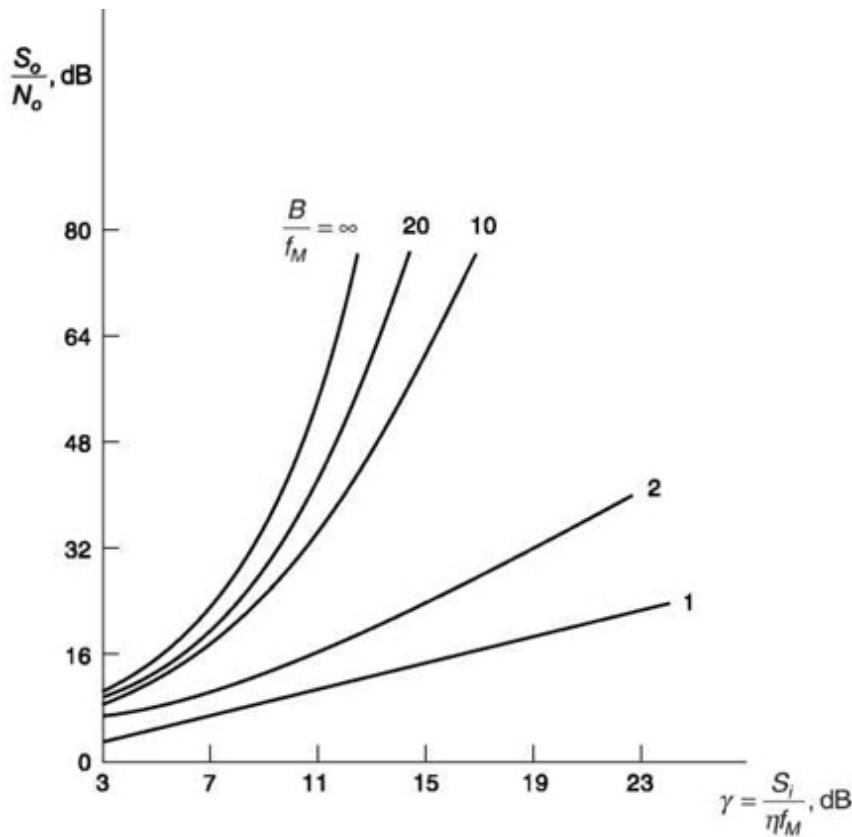


Fig. 13.15 Signal-to-noise ratio characteristic of an optimum communication system.

Equation (13.77) allows us to determine the extent to which we may improve the performance of an ideal system by making a sacrifice in bandwidth. It is of interest to compare the ideal system with frequency modulation, which is a practical system in which such bandwidth sacrifice is made. From Eq. (13.77) if $S_i/N_i \gg 1$, then

$$\frac{S_o}{N_o} \approx \left(\frac{f_M}{B} \cdot \frac{S_i}{\eta f_M} \right)^{B/f_M} \quad (13.78)$$

On the other hand, it may be verified (Prob. 13.60) that in a wideband FM system

$$\frac{S_o}{N_o} = \frac{3}{4} \left(\frac{B}{f_M} \right)^2 \frac{S_i}{\eta f_M} \quad (13.79)$$

Thus, while the performance of the ideal system increases exponentially with bandwidth expansion, the performance of an FM system increases only with the square of the bandwidth expansion factor. Thus, for $B/f_M > 1$ the

performance of the ideal system increases much more rapidly with increase in S/hf_M than does the FM system.

13.7.1 A Comparison of Amplitude Modulation system with Optimum system

In Chap. 8 we arrived at the following results for the amplitude-modulation systems studied there. Single sideband, $B/f_M = 1$

$$\frac{S_o}{N_o} = \frac{S_i}{\eta f_M} \quad (13.80)$$

Double sideband, no carrier, synchronous detection, $B/f_M = 2$

$$\frac{S_o}{N_o} = \frac{S_i}{\eta f_M} \quad (13.81)$$

Square-law detection, $\overline{m^2(t)} \ll 1$, $B/f_M = 2$

$$\frac{S_o}{N_o} = \overline{m^2(t)} \frac{S_i}{\eta f_M} \frac{1}{1+3/4S_i/\eta f_M} \quad (13.82)$$

Linear envelope detection, $\overline{m^2(t)} \ll 1$, $B/f_M = 2$

$$\text{Above threshold } \frac{S_o}{N_o} = \overline{m^2(t)} \frac{S_i}{\eta f_M} \quad (13.83)$$

$$\text{Below threshold } \frac{S_o}{N_o} = \frac{\overline{m^2(t)}}{1.1} \left(\frac{S_i}{\eta f_M} \right)^2 \quad (13.84)$$

It is of interest to compare the performance of these systems with the performance of an ideal system with the same bandwidth expansion factor. In SSB, $B/f_M = 1$. If we set $B/f_M = 1$ in Eq. (13.77), which applies to the ideal system, we find that Eq. (13.77) reduces precisely to Eq. (13.80), which applies to SSB. Hence, SSB is an *ideal* system. The plots of S_o/N_o vs. S_i/N_i , for $B/f_M = 1$ and for $B/f_M = 2$, shown in Fig. 13.15, are reproduced in Fig. 13.16. The plot for $B/f_M = 1$ applies both to the ideal system for $B/f_M = 1$ and also to SSB.

Equation (13.81) for the DSB system is identical with Eq. (13.80) for SSB. Hence, again the plot in Fig. 13.16 for $B/f_M = 1$ applies to DSB. However, in DSB, $B/f_M = 2$. Hence if DSB were an

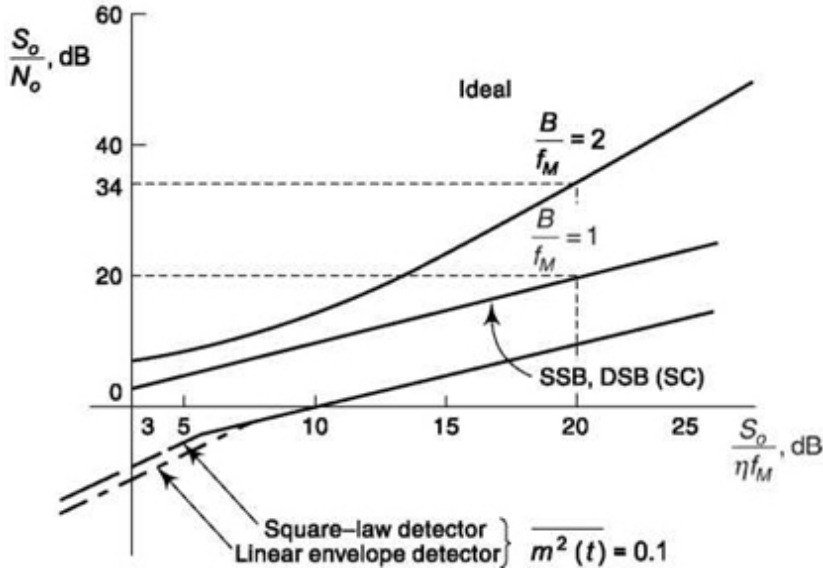


Fig. 13.16 A comparison of AM systems.

optimum system, the plot corresponding to $B/f_M = 2$ would apply. DSB is therefore not an optimum system. By way of example, if $S/\eta f_M$ is chosen to be 20 dB, then the output S_o/N_o is also 20 dB. If, however, DSB were optimum, the output signal-to-noise ratio would be larger by 14 dB.

The performance curves for the asynchronous square-law and linear envelope detector are also given in Fig. 13.16 for $m^2(t) = 0.1$ ($= -10$ dB). The performance of these systems is seen to be poor in comparison with the optimum system for $B/f_M = 2$.

13.7.2 A Comparison of FM systems

The output SNR of each of the FM systems considered in Chapters 9 and 10 are the same above threshold. The result, for sinusoidal modulation, is [see Eq. (9.27)]

$$\frac{S_o}{N_o} = \frac{3}{2} \beta^2 \frac{S_i}{\eta f_M} \quad (13.85)$$

where $b = Df/f_M$, and Df is the frequency deviation. To relate b and the bandwidth expansion factor, we note that $B = 2(b + 1)f_M$. Thus,

$$\frac{B}{f_M} = 2(\beta + 1) \quad (13.86)$$

The expression for the output signal-to-noise ratio of the discriminator, including the effect of sinusoidal modulation and valid both above and below threshold, is found by combining Eqs. (9.97) and (13.86). We find

$$\frac{S_o}{N_o} = \frac{(3/2)\beta^2 (S_i/\eta f_M)}{1 + (12\beta/\pi)(S_i/\eta f_M) \exp[-(f_M/B)(S_i/\eta f_M)]} \quad (13.87)$$

This equation is plotted in Fig. 13.17 for $b = 3$ and 12 . The output SNR characteristics of the optimal demodulator and the second-order phase-locked loop are sketched on the same set of axes. The

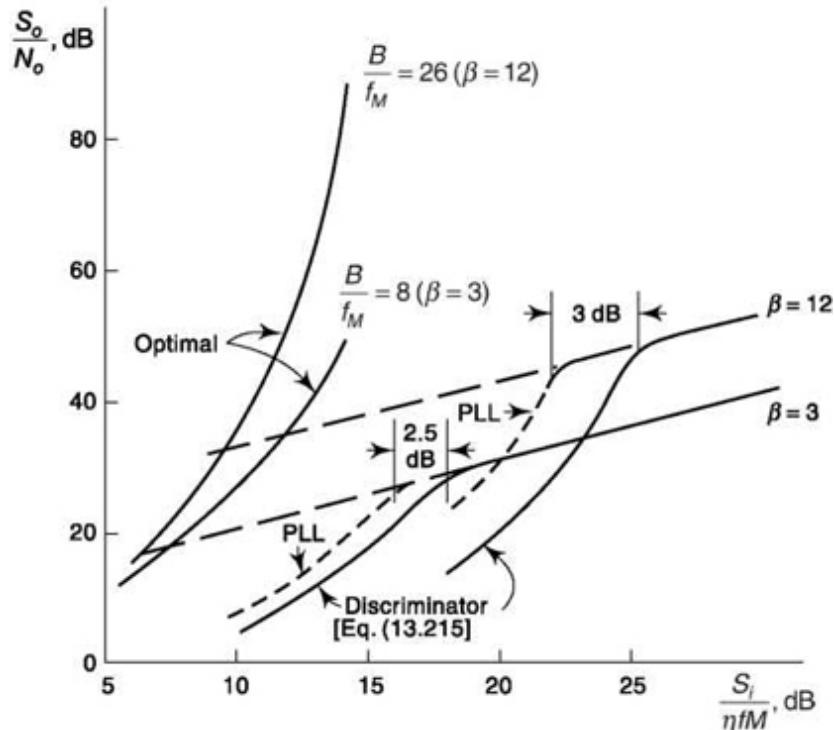


Fig. 13.17 Comparison of FM demodulators including the effect of sinusoidal modulation.

threshold extension presented for the PLL was obtained experimentally and theoretically verified.⁶ We note that the PLL results in a 3 dB threshold extension when $b = 12$, and a 2 dB threshold extension when $b = 3$. We note that the performance of FM systems falls substantially short of the performance of ideal systems.

13.7.3 Comparison of PCM and FM Communication systems

The transmission of analog signals by modulating a binary PCM signal onto a PSK or FSK carrier was studied in Sec. 12.1.4. In Fig. 12.3, we saw

that the threshold of FSK was 2.2 dB greater than the threshold using PSK. In Fig. 13.18 we compare PCM-PSK, the FM discriminator, and the optimal demodulator. The PCM characteristics are obtained from Eq. (12.24).

Consider the two FM discriminator characteristics first. When $b = 12$, the threshold occurs at 25 dB, and when $b = 3$, threshold occurs at 18 dB. To compare these results with PCM, we consider both threshold and the bandwidths necessary for transmission, i.e. the bandwidth expansion factor. We note that a bandwidth expansion factor $B/f_M = 8$ in PCM (which corresponds to $b = 3$) results in an output SNR which is approximately equal to that of the discriminator operating with $b = 12$, $B/f_M = 2(12 + 1) = 26$. Thus, to obtain an output SNR of 48 dB requires a $B/f_M = 26$ when using a discriminator, and a $B/f_M = 8$ when employing PCM-PSK. Hence 3.25 times more bandwidth is required of the discriminator.

If an output SNR of 28 dB is all that is required, the FM discriminator with $b = 3$, $B/f_M = 8$, can be employed. However, the results can be obtained using PCM-PSK with $B/f_M = 5$. In this case the FM discriminator requires only 1.6 times more bandwidth. Thus, we see that the improvement of PCM over the discriminator increases with increased bandwidth expansion.

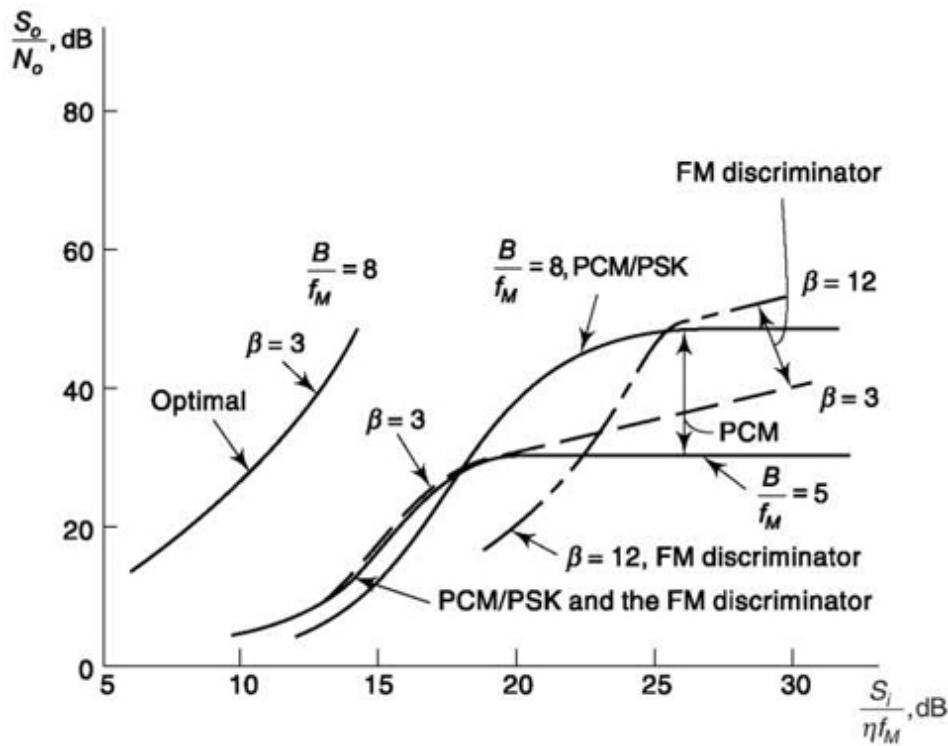


Fig. 13.18 Comparison of PCM-PSK, FM using discriminator demodulation, and the optimal system.

Comparing the PCM system with the optimal system for $B/f_M = 8$ indicates that the PCM system operating at threshold requires a signal-to-noise ratio which is 11 dB greater than required by the optimal demodulator threshold.

13.8 FEEDBACK COMMUNICATION

Many communication systems provide a two-way communication link. That is, not only is station *A* able to transmit and station *B* to receive, but station *A* is able also to receive and station *B* to transmit. In such a two-way link, it is possible to incorporate *feedback* and thereby improve the performance of the communication system. We shall consider a type of feedback communication system, referred to as an *information-feedback* system, which is especially effective when transmission in one direction is much more reliable than transmission in the other direction. Such a situation might well result if one station were a fixed ground-based station while the other station was located in an airplane or a satellite. The ground-based station, having no essential limitations on weight, might be able to transmit hundreds of kilowatts of power while the station in space might be limited to tens of watts. We discuss now how feedback may be used to reduce the average energy required to transmit a bit of information from the low-powered station to the high-powered station, while maintaining a low probability of error.

13.8.1 system Description

An information-feedback communication system is shown in Fig. 13.19. The two transceivers (transmitter-receiver combinations) are coupled through two communication channels. Over one channel, transceiver 1 (with low-power transmitter) transmits information to transceiver 2. We have

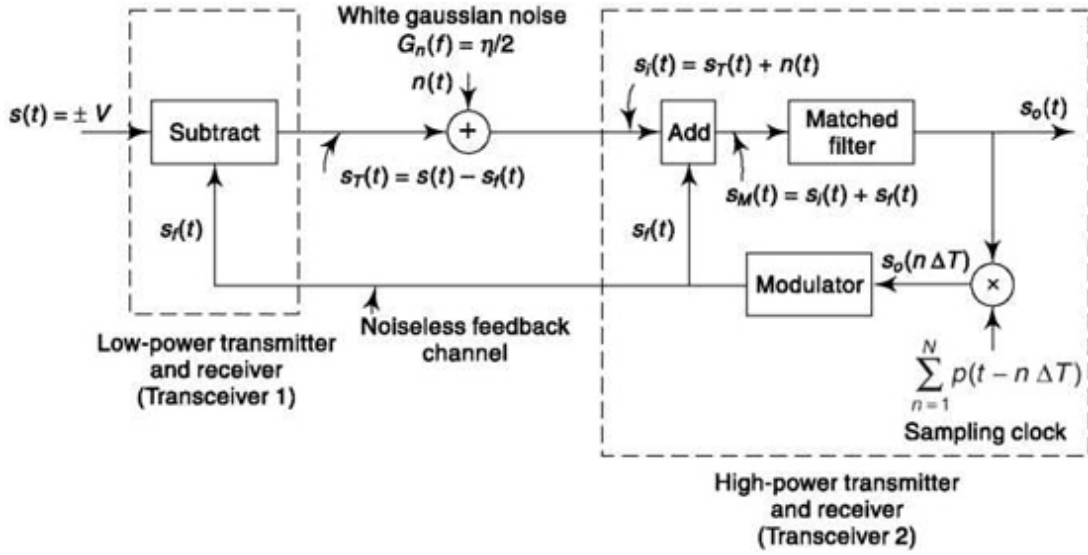


Fig. 13.19 An information-feedback communication system.

included a noise source in this channel. Over the second channel (the feedback channel), the transceiver 2 transmits back to transceiver 1. We have assumed that the transmitter in transceiver 2 has so much transmitter power available that we may ignore the effect of noise on the feedback channel. Thus we allow the possibility that receiver 2 may make an error in determining the transmission of transmitter 1. However, we assume that receiver 1 will receive the transmission of transmitter 2 with perfect reliability, that is, with negligible probability of error.

We assume transmission by binary pulse-code modulation. The baseband signal $s(t)$ is a sequence of voltage levels $+V$ or $-V$ held for intervals T and representing binary 1's and 0's. For simplicity, we assume transmission at baseband, although in a physical system the baseband signal may be used to modulate a carrier, as in PSK or FSK. We now describe the operation of the system.

Since transmission is at baseband, the matched filter in the receiver is the *integrate and dump* filter described in Sec. 11.1. At the beginning of the interval T allocated to a bit, the output of the matched filter is zero. The interval T is divided into N subintervals, each of duration $\Delta T = T/N$, by the sampling clock pulses which occur at intervals of ΔT . The modulation provides a feedback voltage $s_f(t)$ which, like the baseband signal $s(t)$, is $s_f(t) = +V$ or $s_f(t) = -V$. The feedback signal is $s_f(t) = +V$ when the modulator input $s_o(n \Delta T)$ is positive and $s_f(t) = -V$ when $s_o(n \Delta T)$ is negative.

Now suppose that, during some bit interval T , the signal $s(t) = +V$ is transmitted. At the beginning of this interval, i.e., at $t = 0$, $s_o(t) = 0$. This output is sampled and the sample $s_o(t = 0) = 0$. The modulator output $s_f(t) = 0$. Thus, during the first subinterval, from $t = 0$ to $t = AT$, there is no feedback signal. During this subinterval the input to the matched filter is (refer to Fig. 13.18)

$$s_M(t) = s_f(t) = s_T(t) + n(t) = s(t) + n(t) \quad (13.88)$$

At the end of this subinterval the output of the matched filter is again sampled. Let us suppose that it turns out that $s_o(AT)$ is positive. That is, let us suppose that at $t = AT$ the matched filter *correctly* decides that the transmission is $s(t) = +V$. Then $s_f(t) = +V$. The transmitted signal in the second subinterval, from $t = AT$ to $t = 2AT$, would then be

$$s_T(t) = s(t) - s_f(t) = V - V = 0 \quad (13.89)$$

Accordingly, we see that during this second subinterval the transmitter will be turned off. On the other hand, the input to the matched filter will be

$$s_M(t) = s_f(t) + s_f(t) = s_T(t) + n(t) + s_f(t) \quad (13.90a)$$

$$= s(t) - s_f(t) + n(t) + s_f(t) \quad (13.90b)$$

$$= s(t) + n(t) \quad (13.90c)$$

precisely as in Eq. (13.88). Thus the matched filter will not “know” that the transmitter has been turned off. The signal plus noise present at the input to the filter will always be independent of the feedback signal. This result is apparent from Eq. (13.90) as well as from Fig. 13.18. For we see that the feedback signal is both added and subtracted from the filter input. Thus the matched filter will continue to integrate the signal plus noise $s(t) + n(t)$ in a manner which is entirely independent of the feedback signal.

Next, let us suppose that it turns out that $s_o(DT)$ is negative. That is, let us suppose that at $t = AT$ the matched filter *incorrectly* decides that the transmission is $s(t) = -V$. In this case we find $s_f(t) = -V$, and the transmitted signal during the subinterval $t = DT$ to $t = 2AT$ will be

$$s_T(t) = s(t) - s_f(t) = V - (-V) = 2V \quad (13.91)$$

In this case the transmitted signal voltage is doubled, and the transmitted signal power is increased by a factor of four. But again, as in the previous

case, the input to the matched filter will remain as $s,At) = s(t) + n(t)$, independent of the feedback.

The process we have described over the first two subintervals continues over the remaining intervals up to the time T . Interval by interval the transmitter is **turned off** or **on** to a high power, depending on the preliminary and tentative estimates made by the matched filter at intervals of AT . However, a final determination of the transmitted bit is made only by examining the matched filter at the end of the bit interval, at $t = T$. As noted, the input to the matched filter is independent of the feedback. Hence the probability of an error in the determination of a bit is *exactly the same* as if no feedback were employed. This error probability is given by [see Eq. (11.9)]

$$P_e = \frac{1}{2} \operatorname{erfc} \sqrt{\frac{V^2 T}{\eta}} \quad (13.92)$$

The merit of the information feedback system, then, lies not in that it reduces the probability of error, but rather that, for a fixed probability of error, the feedback system may use less average energy per bit than a system without feedback. For if the preliminary estimates of the matched filter, made at intervals DT , are rather more frequently right than wrong, the transmitter may be **turned off** often enough to produce a saving in energy.

13.8.2 Calculation of Average Transmitted signal Energy Per Bit

We now calculate the average signal energy per bit, that is, the energy transmitted in the interval T . We assume arbitrarily that $s(t) = +V$. Since $+V$ and $-V$ are transmitted with equal probability, this assumption does not affect the generality of the result.

$$\text{is } E_1 = V^2 AT \quad (13.93)$$

During the second interval AT , $s_T(t) = 0$ if the decision made by the matched filter at $t = AT$ was correct. In this case no energy is transmitted. If however, the decision was incorrect, $s_T(t) = 2V$ and the energy $(2V)^2 AT$ is transmitted. Since the probability of an incorrect decision after processing the signal and noise for time AT is q_1 , where

$$q_1 = \frac{1}{2} \operatorname{erfc} \sqrt{\frac{V^2 \Delta T}{\eta}} \quad (13.94)$$

the average energy transmitted during the second AT second interval is

$$E_2 = (2V)^2 \Delta T q_1 \quad (13.95)$$

Similarly, the average energy transmitted during the nth AT second interval is

$$E_n = (2V)^2 \Delta T q_{n-1} \quad (13.96)$$

where

$$q_{n-1} = \frac{1}{2} \operatorname{erfc} \sqrt{\frac{V^2(n-1) \Delta T}{\eta}} \quad (13.97)$$

The average energy transmitted in the interval T is E_T , given by

$$E_T = E_1 + E_2 + \dots + E_N \quad (13.98a)$$

$$= V^2 \Delta T + (2V)^2 \Delta T q_1 + \dots + (2V)^2 \Delta T q_{N-1} \quad (13.98b)$$

$$= V^2 \Delta T + 2V^2 \Delta T \sum_{n=2}^N \operatorname{erfc} \sqrt{\frac{V^2(n-1) \Delta T}{\eta}} \quad (13.98c)$$

For any given N , the total energy per bit E_T may be calculated from Eq. (13.98c). We find, for example (Prob. 13.29), that for $N = 2$, and if $V^2 T / 2h \approx 1$, that the feedback provides a 3 dB improvement. That is, the energy E_T is only one-half the energy that would be required, without feedback, for the same error probability.

It is of interest to explore the improvement possible in the limiting case as N becomes very large. For this purpose, we introduce the variable

$$x_n \equiv \frac{V^2(n-1) \Delta T}{\eta} \quad (13.99)$$

so that

$$\Delta x \equiv x_{n+1} - x_n = \frac{V^2 \Delta T}{\eta} \quad (13.100)$$

We note also that

$$\operatorname{erfc} \sqrt{x_n} \equiv \frac{2}{\sqrt{\pi}} \int_{\sqrt{x_n}}^{\infty} e^{-u^2} du \quad (13.101)$$

Substituting Eqs. (13.100) and (13.101) into Eq. (13.98c), we find

$$E_T = \eta \left(\Delta x + \sum_{n=2}^N \frac{4}{\sqrt{\pi}} \Delta x \int_{\sqrt{x_n}}^{\infty} e^{-u^2} du \right) \quad (13.102)$$

In the limit as $N \rightarrow \infty$, Δx and ΔT may be replaced by the differentials dx and dt and the summation in Eq. (13.102) replaced by an integral. We then find (Prob. 13.30) that

$$E_T = \frac{4\eta}{\sqrt{\pi}} \int_0^{V^2 T / \eta} dx \int_{\sqrt{x}}^{\infty} e^{-u^2} du \quad (13.103)$$

This integral may be evaluated (Prob. 13.31) with the result

$$E_T = \eta \left(\frac{-2}{\sqrt{x}} \sqrt{\frac{V^2 T}{\eta}} e^{-V^2 T / \eta} + \operatorname{erfc} \sqrt{\frac{V^2 T}{\eta}} + \frac{2V^2 T}{\eta} \operatorname{erfc} \sqrt{\frac{V^2 T}{\eta}} \right) \quad (13.104)$$

For $V^2 T / \eta \gg 1$ (or, more specifically, for $V^2 T / \eta > 3$) the first and third terms in Eq. (13.104) may be neglected in comparison with the second term. Furthermore, $\operatorname{erf} \sqrt{V^2 T / \eta} \approx 1$. Hence, we then find

$$E_T \approx \eta \quad (13.105)$$

From Eqs. (13.92) and (13.105) we may now deduce the following interesting result. The error probability may be made arbitrarily small by increasing V . However, provided $V^2 T / \eta \leq 1$, the required average energy per bit is constant at $E_T = h$ and does not depend on the error probability P_e . Thus the characteristic of the transmitter which determines the extent to which the error probability may be reduced is not the power it can transmit but rather its *peak power*, i.e. the peak value V^2 which the transmitter can attain.

13.8.3 Comparison of Information Rate with Channel Capacity

It is of interest to compare the performance of an information-feedback communication system with the performance of an ideal system. The system of Fig. 13.19 is a binary PCM system. For such a system, the rate of information transmission R as given by Eq. (13.10) with $M = 2$ is

$$R = \frac{1}{T} \log_2 M = \frac{1}{T} \quad (13.106)$$

the channel capacity for a Gaussian channel is [Eq. (13.21)]

$$C = 1.44 \frac{P_s}{\eta} \quad (13.107)$$

in which P_s is the input power at the receiver. From Eqs. (13.106) and (13.107), setting $R = C$, we find that in a system with ideal coding an arbitrarily small error probability is attainable with a power P_s that satisfies the condition

$$P_s T = \frac{1}{1.44} \eta = 0.69 \eta \quad (13.108)$$

The quantity $P_s T$ is the energy associated with a bit of duration T . We have found that the information-feedback system is capable of attaining arbitrarily small error with an energy per bit given by $E_T = h$. Hence we find that the feedback system requires an energy per bit which is only 1.44 times greater (~ 1.5 dB) than required by an optimal system.

SELF-TEST QUESTIONS

15. Does an optimum or ideal system require rate of information output of the receiver same as rate of information input to the receiver?
16. Which of SSB and DSB in AM modulation is considered as an optimum system?
17. Does PCM-PSK perform better than FM discriminator?
18. Is information feedback system (based on feedback communication system) suitable for analysis of communication between ground station and satellite?
19. Can feedback system use less average energy per bit for a fixed probability error compared to without feedback system?
20. How much more power information feedback system take if compared with optimum system?

FACTS AND FIGURES

Robert Fano, born in Turin, Italy, emigrated to the United States at the age of 22. He studied in MIT where he became a faculty member in 1947. Besides his interest in computers, together with Shannon he invented Shannon-Fano coding, a near-optimal lossless source coding. He was instrumental in popularizing Information Theory and was amongst the first to introduce a course on that in 1950. David Huffman, a native of Ohio, joined this course in 1951 at MIT after serving U.S. Navy and completing M.S. from Ohio State University. Huffman preferred submitting a term paper instead of

taking the final examination in Fano's course. The topic was finding the most efficient coding symbol for messages.

Huffman worked for months on the project and reached nowhere. Frustrated, he was on the verge of giving up when 'there was the absolute lightning of sudden realization'. Huffman got the solution of the optimal coding algorithm by taking a bottom-up strategy compared to top-down approach taken by Shannon-Fano and pursued by others. He moved from least frequent messages to most frequent in assignment of symbols. In the words of Huffman, "It was the most singular moment of my life." Huffman joined the faculty of MIT in 1953.

MATLAB

- Experiment 4 8
- This shows how Huffman encoding and decoding can be done.
- We use the data given in Example 13.2 of this Chapter and compare its result
- with simulation output. In built function huffmandict.m creates the dictionary or coding strategy. It outputs binary coding of each symbol (in a cell structure, value seen by double-clicking the cell in workspace window) and average code length. The encoding of actual data is done by huffmanenco.m using this dictionary and decoding is done by huffmandeco.m

```
symbols = [1:5]; % Distinct symbols that data source can produce p = [.4 .15 .15 .15]; % Probability distribution of symbols [dict,avglen] = huffmandict(symbols,p) % Creating dictionary
```

```
avginfo=0;
```

```
for i=1:length(p)
```

```
avginfo=avginfo+p(i)*log2(1/p(i)); end; avginfo
```

```
coding_efficiency=avginfo*1000/avglen
```

```
sig = randsrc(1,100,[symbols; p]); % Creating data using symbol probability  
code = huffmanenco(sig,dict); % Encoding the data using dictionary
```

```
decoded = huffmandeco(code,dict); % Decoding the data using dictionary  
isequal(sig,decoded) % Outputs 1 if decoding is correct
```

When this program is run, the following is available at command window.
dict =

```
|1| | 1|  
|2| |1x3 double|  
|3| |1x3 double|  
|4| |1x3 double|  
|5| |1x3 double|  
  
avglen = 2.2000  
avginfo = 2.1710  
coding_efficiency = 98.6796  
ans = 1
```

You can see that the result exactly matches what we got in Example 13.2.
Now you can play with number of symbols, their probabilities and find out
coding efficiency and related issues.

- Experiment 4 9
- Lossy source coding for an image file using JPEG standard
- Distortion measure uses a perceptual distortion model
- An image under the filename exp49.bmp is drawn and stored in 24-bit format

```
fid=fopen('exp49.bmp'); %fid and fread combination opens a file as binary  
A=fread(fid); %This is to know the number of bits used
```

```
B=imread('exp49.bmp'); %This reads the file as an image as pixels
```

• This writes the file in JPEG format where quality taken as 75 percent
imwrite(B, 'exp49_75.jpg', 'jpg', 'quality', 75);

```
f_id=fopen('exp49_75.jpg');
```

```
A_75=fread(fid); % This will give size in binary for the compressed file
```

```
B_75=imread('exp49_75.jpg');
```

• Repeated for 25 percent quality

```
imwrite(B, 'exp49_25.jpg', 'jpg', 'quality', 25); f_id=fopen('exp49_25.jpg');
```

```

A_25=fread(fid);
B_25=imread('exp4 9_25.jpg');
• Repeated for 5 percent quality
imwrite(B, 'exp4 9_05.jpg', 'jpg', 'quality', 5); fid=fopen('exp49_05.jpg');
A_05=fread(fid);
B_05=imread('exp4 9_05.jpg');
whos % This gives sizes of all active variables in this workspace

```

Executing this code returns the following in command window.

Name	Size	Bytes	Class
A	504294x1	4034352	double array
A_05	5657x1	45256	double array
A_25	10178x1	81424	double array
A_75	18392x1	147136	double array
B	382x439x3	503094	uint8 array
B_05	382x439x3	503094	uint8 array
B_25	382x439x3	503094	uint8 array
B_75	382x439x3	503094	uint8 array
fid	1x1	8	double array

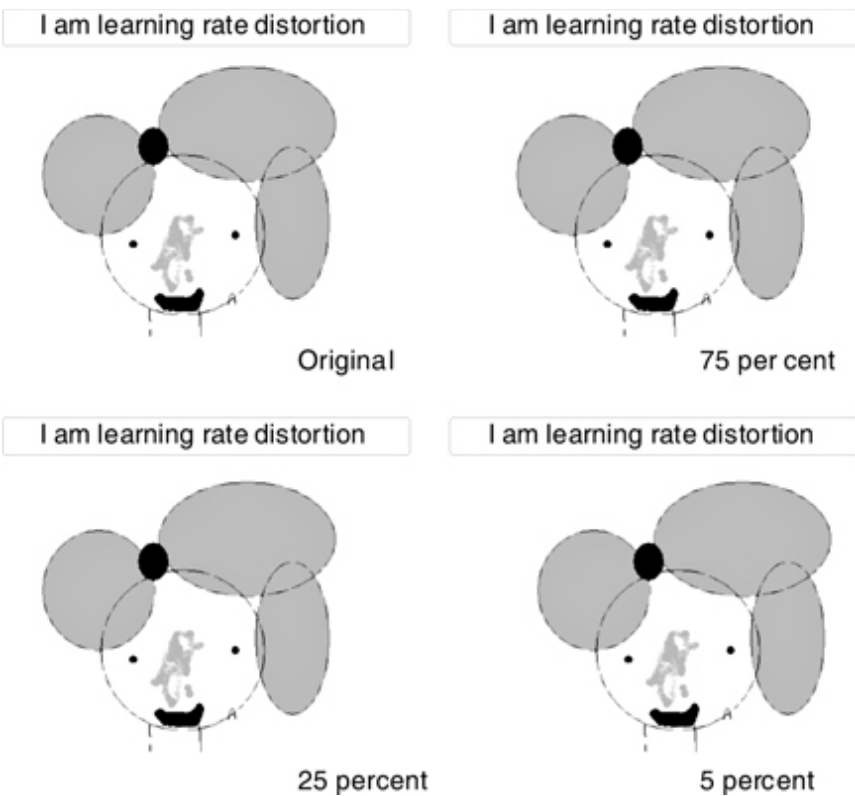
```

Grand total is 2550898 elements using 6320552 bytes
Grand total is 3579117 elements using 7502988 bytes

```

We can find that size in binary reduces as more loss is allowed for lower quality. The original .bmp file of size 504294 reduces to 18392 for 75 percent quality JPEG and 5657 for 5 percent quality JPEG. Incidentally, the number of pixels remains the same; 382x493x3 refers to 382 pixel in x direction, 493 pixel in y direction and 3 colours.

You must be interested to have a look at these pictures, original and lossy. The same is reproduced below. You can find how quality suffers with increase in compression.



Matlab Example 49 output in Fig.

SUMMARY

The chapter begins with the concept of amount information and means to quantify it. It shows how different source coding techniques like Shannon-Fano, Huffman, Lempel-Ziv coding improve transmission efficiency. Shannon's classic theorem and its influence on derivation of channel capacity are discussed next along with bandwidth-SNR trade-off. Orthogonal signal transmission and its relation to Shannon's limit and related trade-offs are taken up next. The effect of mutual information on channel capacity is described and rate distortion theory is introduced to show how it improves data rate when some data loss is acceptable. An optimum system is derived from information theory and is compared against popular techniques like amplitude modulation, frequency modulation, etc. Finally, an information feedback communication system is discussed and a comparison is presented. MATLAB examples demonstrate use of information theory in improving communication efficiency.

PROBLEMS

13.1 One of four possible messages Q_1 , Q_2 , Q_3 , and Q_4 , having probabilities $1/8$, $3/8$, $3/8$, and $1/8$, respectively, is transmitted. Calculate the average information per message.

13.2 One of the possible messages Q_1 , to Q_5 having probabilities $1/2$, $1/4$, $1/8$, $1/16$, $1/16$, respectively, is transmitted. Calculate the average information.

13.3 Messages Q_1 , ..., Q_M have probabilities p_1 , ..., p_M of occurring.

- (a) Write an expression for H .
- (b) If $M = 3$, write H in terms of p_1 , and p_2 by using the result that $p_1 + p_2 + p_3 = 1$.
- (c) Find p_1 , and p_2 for $H = H_{\max}$ by setting $dH/dp_1 = 0$ and $dH/dp_2 = 0$.
- (d) Extend the result of (c) to the case of M messages.

13.4 A code is composed of dots and dashes. Assume that the dash is 3 times as long as the dot and has one-third the probability of occurrence.

- (a) Calculate the information in a dot and that in a dash.
- (b) Calculate the average information in the dot-dash code.
- (c) Assume that a dot lasts for 10 ms and that this same time interval is allowed between symbols. Calculate the average rate of information transmission.

13.5 In Example 13.1 we saw that the four messages have different probabilities and that as a result we transmit 4B binary digits per second and convey only 3.6B bits of information. Consider transmitting Q_1 , Q_2 , Q_3 and Q_4 by the symbols 0, 10, 110, 111.

- (a) Is this *code* uniquely decipherable? That is, for every possible sequence is there only one way of interpreting the message?
- (b) Calculate the average number of code bits per message. How does it compare with $H = 1.8$ bits per message?

13.6 Consider the four messages of Example 13.1. Let Q_1 , Q_2 , Q_3 , Q_4 have probabilities $1/2$, $1/4$, $1/8$, $1/8$.

- (a) Calculate H .
- (b) Find R if $r = 1$ message per second.

(c) What is the rate at which binary digits are transmitted if the signal is sent after encoding Q_1, \dots, Q_4 as 00, 01, 10, 11?

(d) What is the rate, if the code employed is 0, 10, 110, 111?

13.7 Consider five messages given by the probabilities $1/2, 1/4, 1/8, 1/16, 1/16$.

(a) Calculate H .

(b) Use the Shannon-Fano algorithm to develop an efficient code and, for that code, calculate the average number of bits/message. Compare with H .

13.8 Compare coding efficiency of Shannon-Fano coding and Huffman coding when five source messages have probabilities $m_1 = 0.4, m_2 = 0.15, m_3 = 0.15, m_4 = 0.15, m_5 = 0.15$.

13.9 A Gaussian channel has a 1-MHz bandwidth. If the signal-power-to-noise power spectral density $S/h = 10^5$ Hz, calculate the channel capacity C and the maximum information transfer rate R .

13.10 Suppose 100 voltage levels are employed to transmit 100 equally likely messages. Assume $l = 3.5$ and the system bandwidth $B = 10^4$ Hz.

(a) Calculate S/h , using Eq. (13.70).

(b) If an integrate-and-dump filter is employed to determine which level is sent, calculate the probability of an error when sending the k th level. Assume that the only errors possible are in choosing the $k - 1$ or the $k + 1$ levels.

13.11 (a) Plot channel capacity C versus B , with $S/h = \text{constant}$, for the Gaussian channel.

(b) If the channel bandwidth $B = 5$ kHz and a message is being transmitted with $R = 10^6$ bits per sec find S/h for $R < C$.

13.12 (a) Why is n_l , in Eq. (13.24), Gaussian?

(b) Find $E(n_l)$ by interchanging integration and ensemble averaging. Why is this permitted?

(c) Show that $E(n_l^2) = \int_0^T dt \int_{-\infty}^{\infty} d\lambda E[n(t)n(\lambda)|s_l(t)s_l(\lambda)]$.

13.13 Show the following by changing variables: (a) That as in Eq. (13.30),

$$P_L = \left(\frac{1}{\sqrt{\pi}} \int_{-\infty}^{\sqrt{E_s(\eta+\eta_r)} / \sqrt{2\sigma}} e^{-x^2} dx \right)^{M-1}$$

(b) That as in Eq. (13.30)

$$P_c = \left(\frac{1}{\sqrt{\pi}} \right)^M \int_{-\infty}^{\infty} dy e^{-y^2} \left(\int_{-\infty}^{\sqrt{E_s(\eta+\eta_r)} / \sqrt{2\sigma}} e^{-y^2} dy \right)^{M-1}$$

$$(c) \frac{E_s}{\sqrt{2\sigma}} = \frac{E_s}{\eta} = \frac{S_i T}{\eta} = \frac{S_i}{\eta R} \log_2 M$$

13.14 If $S_i/h = \text{constant}$, plot T versus M for $P_c = 10^{-5}$ from Fig. 13.8.

13.15 An analog signal has a 4 kHz bandwidth. The signal is sampled at 3 times the Nyquist rate and quantized using 256 quantization levels. The S/h ratio at the receiver is $S/h = 1$ MHz.

- (a) Calculate the time T between samples.
- (b) The quantized and sampled signal is encoded into a binary PCM waveform. Calculate the number of bits N and find the P_e .
- (c) The quantized and sampled signal is encoded into 1 of 256 orthogonal signals. Find P_e .

13.16 Show that $T/\log M = \text{duration of a bit of a binary encoded signal}$.

13.17 Show that, $H(X, Y) = H(Y/X) + H(X)$

13.18 Consider a binary channel as shown in Fig. 13.9 with $p_{11} = 0.9$, $p_{22} = 0.8$. Find output probabilities if input is equiprobable. Also find joint input-output probabilities.

13.19 Show that (a) $H(X/Y) = H(X - Y/Y)$, (b) $I(X; Y) = I(Y, X)$.

13.20 For a BSC with equiprobable input find mutual information when (a) $p_{12} = 0.5$ and (b) $p_{12} = 0.5$.

13.21 Find channel capacity of a BSC for condition stated in Problem 5.

13.22 (a) Using Eq. (13.77), find $\lim S/N_o B/f_M$ ()

13.23 Verify Eq. (13.79). Hint: Use Eq. (9.23) and recognize that $k^2 m^2(t) = 4\pi^2 \Delta f_{\text{rms}}^2$. Assume that $B = 2 \Delta f$.

13.24 Plot S_o/N_o versus Sj/N , for the ideal and FM systems. Assume that $B/f_M = 2b$. Choose $b = 10$ and 100.

13.25 (a) Plot S_o/N_o and B/f_M versus S/hf_M at the threshold of an FM discriminator. The abscissa of the graph should be S/hf_M at threshold, and the two ordinate axes should be S_o/N_o and B/fM .

(b) For each value of S_o/N_o (and its corresponding value of B/f_M), calculate and plot the value of S/hf_M required by the ideal demodulator.

(c) Compare the results obtained in (a) and (b).

13.26 A signal $m(t)$ is Gaussian and bandlimited to 100 kHz. The sensitivity of the FM modulator $k = 10^{-6}$ rad(sec)(volt). An output SNR of 40 db is required.

(a) Calculate the rms frequency deviation, if a minimum S/hf_M is to be employed.

(b) Calculate S/hf_M .

(c) Calculate B, the IF bandwidth.

(d) Calculate the S/hf_M required by the ideal demodulator to give $S_o/N_o = 40$ dB for the same value of B . Compare results.

13.27 (a) Repeat Prob. 13.26 assuming that $m(t)$ is PCM-encoded and then transmitted using PSK.

(b) Compare results for Probs. 13.26 and 13.27.

13.28 (a) Plot S_o/N_o and N versus S_i/hf_M at threshold for PCM.

(b) Compare your results with those obtained in Prob. 13.25.

(c) When would you use PCM rather than FM?

13.29 Show that, for $N = 2$ and when $V^2T/h \leq 1$, the information-feedback communication system allows a 3 dB reduction in energy per bit for a fixed error probability.

13.30 Show that in the limit as $N \rightarrow \infty$, Eq. (13.102) may be replaced by Eq. (13.103).

13.31 Evaluate Eq. (13.103):

$$E_T = \frac{4\eta}{\sqrt{\pi}} \int_0^{V^2T/\eta} dx \int_{\sqrt{x}}^{\infty} du e^{-u^2}$$

This evaluation is most easily accomplished by interchanging the order of integration. Refer to Fig. P13.31a. Here we see that the shaded area

represents the region of integration of Eq. (13.231), i.e. we integrate over x for $0 < x < V^2 T / \eta$, and over u for $sfx < u < '$. The solid

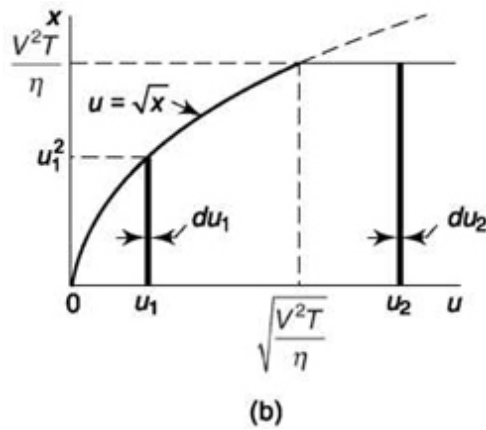
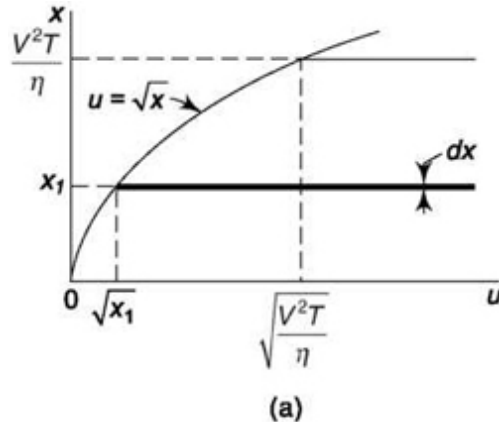


Fig. P13.31

line at $x = x_1$, of thickness dx , illustrates that in Eq. (13.103) we integrate first over u and then over x . Now refer to Fig. P13.31b. Here the shaded area is the same as in Fig. P13.31a. However, we are now integrating first over x , from $0 < x < u^2 < V^2 T / \eta$ and then over u , from 0 to infinity. Show that using this new order of integration yields

$$\begin{aligned} E_T &= \frac{4\eta}{\sqrt{\pi}} \left(\int_0^{\sqrt{V^2 T / \eta}} du_1 e^{-u_1^2} \int_0^{u_1^2} dx + \int_{\sqrt{V^2 T / \eta}}^{\infty} du_2 e^{-u_2^2} \int_0^{\sqrt{V^2 T / \eta}} dx \right) \\ &= \frac{4\eta}{\sqrt{\pi}} \left(\int_0^{\sqrt{V^2 T / \eta}} du_1 u_1^2 e^{-u_1^2} + \frac{V^2 T}{\eta} \int_{\sqrt{V^2 T / \eta}}^{\infty} du_2 e^{-u_2^2} \right) \end{aligned}$$

Complete your evaluation of E_T by integrating both integrals. To do this change variables, so that

$$x = u_1 \quad \text{and} \quad dy = 2u_1 e^{-u_1^2} du_1$$

Show that

$$E_T = \eta \left(\frac{2}{\sqrt{\pi}} \frac{\sqrt{V^2 T}}{\eta} e^{-V^2 T / \eta} + \operatorname{erf} \sqrt{\frac{V^2 T}{\eta}} + \frac{2V^2 T}{\eta} \operatorname{erfc} \sqrt{\frac{V^2 T}{\eta}} \right)$$

REFERENCES

1. Sakrison, D.: "Communication Theory," John Wiley & Sons, Inc., New York, 1968.
2. Wozencraft, J., and I. Jacobs: "Principles of Communication Engineering," John Wiley & Sons, Inc., New York, 1965.
3. Shannon, C. E.: A Mathematical Theory of Communications, *BSTJ*, vol. 27, pp. 379-623, 1948. Shannon, C. E.: Communication in the Presence of Noise, *Proc. IRE*, vol. 37, p. 10, 1949.
4. Viterbi, A.: "Principles of Coherent Communications," McGraw-Hill Book Company, New York, 1966.
5. Viterbi, A. T., and J. K. Omura: "Principles of Digital Communications," McGraw-Hill Book Company, New York, 1979, Chap. 5.
6. Osborne, P., and D. L. Schilling: Threshold Response of a Phase Locked Loop, *Proc. Intl. Conf. Commun.*, 1968.
7. Ungerboeck, G.: "Channel Coding with Multilevel/Phase Signals," *IEEE Trans. on Information Theory*, January 1982, pp. 55-67.
8. Calderbank, R., and J. E. Mazo: "A New Description of Trellis Codes," *IEEE Trans. on Information Theory*, November 1984, pp. 784-791.

14

ERROR-CONTROL CODING

CHAPTER OBJECTIVE

The noise in a transmission channel induces error in the symbols transmitted and the higher the noise, the more is the error. In this chapter, we discuss techniques to reduce this error through coding of transmitted messages. The central idea is to introduce redundancy in an intelligent way. We begin with an introduction to error-control codes and discuss the difference between error-detection codes and error detection cum correction codes. The major part of our discussion is on Forward Error Correction (FEC) codes where no feedback is necessary. Towards the end, we discuss Automatic Repeat Request (ARQ) system where based on error detection feedback, the message is retransmitted. In FEC, we discuss different varieties of block codes. This is followed by discussion on burst-error correction and convolutional coding. Then two new coding systems, Turbo Codes and Low Density Parity Check Codes, are introduced which are gaining popularity. The chapter ends with a description of Trellis-Decoded Modulation and MATLAB examples.

FACTS AND FIGURES

Initially, the popularity of source coding and its data compression ability overshadowed the importance of Shannon's channel capacity theorem on noisy channel. Shannon's superior at Bell Labs, John Pierce, played down the importance of this theorem, saying: "just use more bandwidth and more power." In a 2001 interview, Fano went on to add, "there was no limitation then—you could do whatever you needed in terms of reliable communication without long encoding. And besides, even if you wanted to, you were very badly limited by equipment complexity and cost..."

However, the launch of *Sputnik* by Russia in 1957 changed the ground scenario. Space launches and space communication became a priority in U.S. and NASA was established by National Aeronautics and Space Act on July 29, 1958. The limitation on the power available at spaceships and

weights of the power supply showed that ‘just use more power’ cannot be the solution. Error Control Coding or Channel coding in spite of its complexities appeared as viable alternative for reliable communication. Each dB coding gain saved USD 1 million in mission cost in 1960. That a small cell-phone device today uses coding to enhance its performance owes it to space missions to give this field its first real impetus. Deep space communication and coding, nicely observed by Professor James Massey, is a ‘marriage made in heaven.’

14.1 INTRODUCTION TO ERROR-CONTROL CODES

The block-diagram representation of a digital communication system is shown in Fig. 14.1. The ADC/ DAC block is required if message is accepted/delivered in analog form. The source coding increases information per bit by removing redundancy. We discuss error-control codes or channel coding in this chapter. The noise in channel introduces error in detection and to combat that channel coding is employed. Channel coding puts additional digits in the data stream that is helpful in error control. This can be seen as increase of redundancy and a sacrifice in information rate. However, here the redundancy is introduced methodically and is superior to redundancy removed in the source-coding process. The modulator modulates a carrier in passband communication and is useful in using communication resources like spectrum, power in an efficient manner. The reverse of the above like demodulation, channel decoding, source decoding is done at the receiver side.

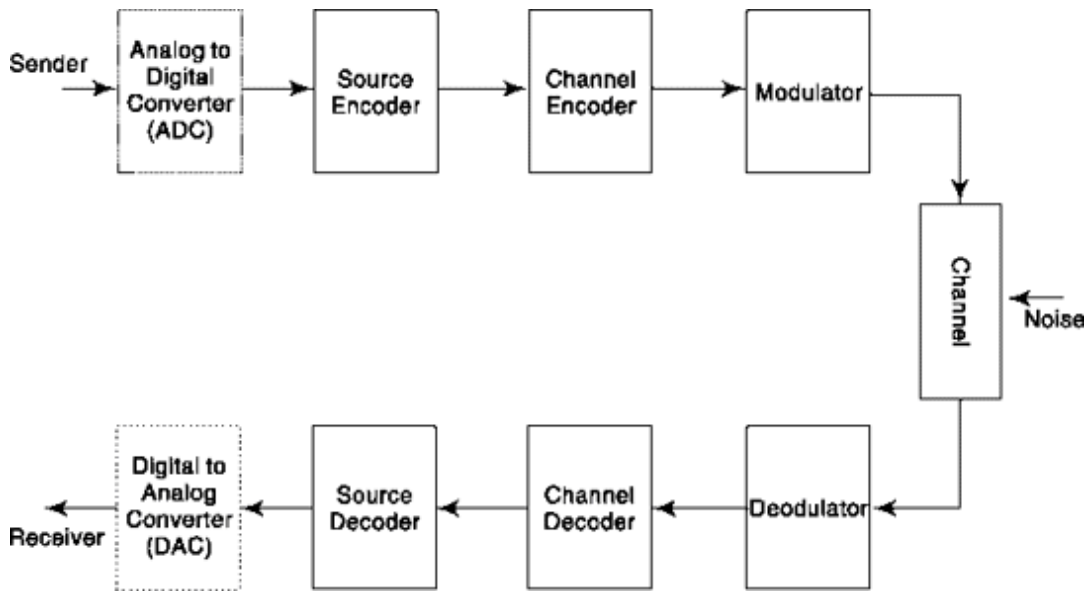


Fig. 14.1 Block-diagram representation of a digital communication system. ADC/DAC is discussed in Chapter 4, source coding in Chapter 13, channel or error-control coding in Chapter 14, digital modulation in Chapters 5 and 11.

Coding has the usefulness that it allows us to increase the rate at which information may be transmitted over a channel while maintaining a fixed error rate. Alternatively, coding allows us to reduce the information bit error rate while maintaining a fixed transmission rate. More generally, coding allows us, in principle, but up to the Shannon limit, to design a communication system in which both information bit rate and error rate are arbitrarily specified but subject to constraint of bandwidth. The price we pay for seeking to reach closer to the Shannon limit, is increased hardware complexity both at the transmitter where the encoding is done and at the receiver where the decoding is effected. In principle, with ingenious enough coding and unlimited complexity, we would be able to reach the Shannon limit. That is, we would be able to transmit at channel capacity and with an error rate which may be made as small as desired.

In Section 13.4, we studied one method of improving the efficiency of operation of a communication channel by transmitting a code signal which consisted of 1 of M orthogonal signals. That is, given a channel of capacity C , we examined one procedure for transmitting information at a rate as nearly equal to C as possible with a minimum likelihood of error. However, this technique required infinite bandwidth. We now consider alternative, more efficient methods of coding signals, to permit us to detect errors and correct errors caused by noise. Error control coding or simply coding accomplishes its purpose through the deliberate introduction of redundancy

into messages. For example, *orthogonal* signaling required the transmission of 1 of M orthogonal messages. If each of these orthogonal messages were transmitted using binary digits, it can be shown that M binary digits/message are required. If, however, the original M quantization levels were binary-encoded, then only $N = \log_2 M$ binary digits/message are required. The excess number of binary digits required for orthogonal encoded signals is $M - N$. Hence, the coding will produce an effective redundancy of $M - N$. As an additional example, consider that we are transmitting information by means of binary PCM. Then we transmit a stream of binary digits, 0 or 1, and our concern is not to confuse a 0 for a 1, or a 1 for a 0. Suppose that when a 0 is to be transmitted, we transmit instead a sequence of three 0's, that is, 000, and transmit 111 to represent the digit 1. These triplets of 0's or 1's are certainly redundant, for two of the 0's in 000 add no information to the message. Suppose, however, that the signal-to-noise ratio on the channel is such that we can be nearly certain that not more than one error will be made in a triplet. Then, if we received 001, 010, or 100, we would be rather certain that the transmitted message was actually 000. Similarly, if we received 011, 101, or 110, we would be rather certain that the message was actually 111. Thus the redundancy, *deliberately introduced*, has enabled us to detect the occurrence of an error and even to correct the error.

The introduction of redundancy, however, cannot *guarantee* that an error will be either detectable or correctable, for errors are caused by the *unpredictable* random process called noise. Hence, while the noise level, as we assumed, may be low enough so that more than a single error is *unlikely*, there is always a finite possibility that two errors will occur. In this case we would know that an error had occurred but we would be inclined to read a 0 as a 1 and a 1 as a 0. Even more, there is always the possibility, however small, that three errors had been made. In this case, not only would we misread the digit, but we would not even suspect that an error had been made. We are thus led to the conclusion that while coding may allow a great deal of detection and correction, it ordinarily cannot detect or correct all errors.

An essential feature which results from the introduction of redundancy is that not all sequences of symbols constitute a bona fide message. For example, with a triplet of binary digits, eight combinations are possible. However, only two of these combinations, that is, 000 and 111, are recognized as words which convey a message. The remaining combinations

are not in our “dictionary.” It is this fact that certain words are not in our “dictionary” that allows us to detect errors. Corrections are made on the basis of a similarity between unacceptable and acceptable words.

There is a correspondence between the redundancy deliberately introduced in coding messages prior to transmission over a channel and the redundancy which is part of language. For example, suppose that on a page of printed text we encounter the word *ekpensive*. We would immediately recognize that the printer had made an error since we know that there is no such word. If we were inclined to judge it unlikely that the printer had made an error in more than one letter, we would easily recognize the word to be *expensive*. On the other hand there is always the possibility that more than one error was made and that the intended word was, say, *offensive*. And in this latter case, of course, we would not make the proper correction.

In language, redundancy extends beyond combinations of letters in a word. It extends to entire words, and beyond to phrases and even sentences. For example, if we had come across the sentence “the army launched an offensive,” we would not have much difficulty in recognizing that the proper correction of the last word is *offensive*, in spite of the fact that corrections in three letters are called for. In this case we would be taking advantage of the redundancy in the sentence.

Now let us return briefly to the binary PCM transmission scheme we described above, in which three bits 000 or 111 were transmitted as a code to represent the bits 0 and 1, respectively. If the redundant message is to be transmitted at the same rate as the original binary signal, we shall have to transmit three bits in the time T otherwise allocated to a single bit. As we have seen on many occasions when the time allocated to a bit transmission decreases, the error rate increases. Hence, the required increased bit rate will undo some of the advantage that will accrue from redundancy coding. We shall however, of course, find that coding may yield a very worthwhile net advantage.

14.1.1 Error Probability with Repetition in the Binary Symmetric Channel

In Fig. 14.2 we represent the transmission of a bit over a *binary symmetric channel* (BSC). The probability $P(0)$ that a 0 was transmitted is the same as the probability $P(1)$ that a 1 was transmitted, i.e. $P(0) = P(1) = 1$. There is a

probability p of an error in transmission, i.e. that a 0 was transmitted and a 1 received or vice versa. The probability of correct transmission is $1 - p$. Suppose, as we have described, when a 0 is to be transmitted we transmit instead a sequence of M 0's and similarly a 1 is replaced by a sequence of M 1's. At the receiver we shall interpret the received sequence to represent a 0 or a 1 if more than half the bits in the sequence are 0's or 1's respectively. To avoid ambiguity we shall select M to be an odd number.

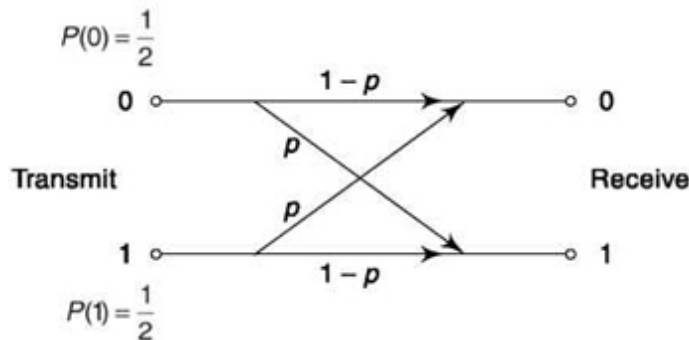


Fig. 14.2 The binary symmetric channel.

Consider, as an example, the case $M = 3$. An error will result if all three bits of the sequence are in error or if any two bits of the sequence are in error. The probability that all three are wrong is p^3 . Now suppose next that a 0 was transmitted and was incorrectly read at the receiver because the received sequence was 110. The probability of such an occurrence is the probability that two bits in the sequence were incorrectly received while one bit was correctly received. This probability is $p^2(1 - p)$. There are two additional similar sequences, making a total of three, that will yield an error, i.e. 101 and 011. Hence altogether, the error probability that the transmitted bit will be received in error is

$$P_e(M) = \sum_{i=1}^{M+1/2} \binom{M}{i} p^i (1-p)^{M-i} \quad (14.3)$$

We find that if $p = 0.01$, $P_e(M = 3) = 3 \times 10^{-4}$. If $M = 5$ we find by a similar calculation that

$$P_e(M = 5) = p^5 + 5p^4(1-p) + \frac{5 \cdot 4}{2!} p^3(1-p)^2 \quad (14.2)$$

In Eq. (14.2), the first term is the probability that all five bits in the sequence are wrong, while the second and third terms are, respectively, the probabilities that four and three bits in the sequence are wrong. In the general case, as can be verified (see Prob. 14.17)

$$P_e(M=3) = p^3 + 3p^2(1-p) \quad (14.1)$$

where, as usual the symbol . represents the number of combinations of M things taken i at a

time. In Fig. 14.3 we have plotted $P_e(M)$ as a function of $1/M$ for the case $p = 0.01$. As is suggested by the plot and as can be verified, with increasing M , P_e decreases without limit as is predicted by Shannon's theorem.

When a bit of duration t is replaced by a sequence of M bits each of the same duration t , then, of course, the rate at which information is transmitted is reduced by the factor $1/M$. For this reason such a code is called a "rate $1/M$ " code. If we propose to keep the information rate constant then the bit duration must be reduced to t/M . Such a reduction will require that the bandwidth be increased by the factor M .

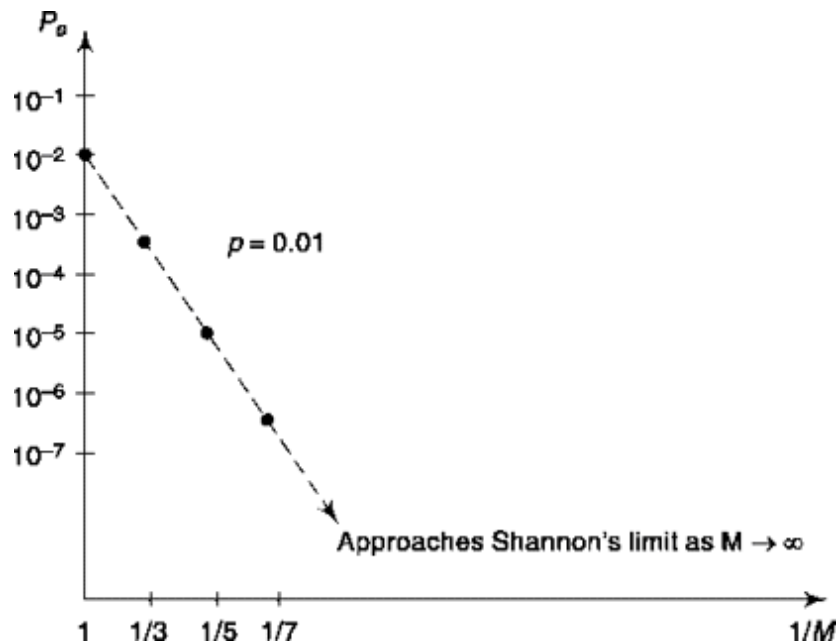


Fig. 14.3 Plot of P_e of BSC as a function of number of repetitions M .

14.1.2 Parity Check Bit Coding for Error Detection

The simplest error-detecting technique consists in adding an extra binary digit at the end of each word. This extra bit is called a parity-check bit and is chosen to make the number of 1's in each word an even number. Thus consider a case in which there are only sixteen ($= 2^4$) possible messages to be transmitted. These sixteen messages could be encoded into four bits. In adding an extra bit, the fifth bit, we now have $2^5 = 32$ possible words, only

sixteen of which are to be recognized as messages conveying information. Thus the parity-check bit has introduced redundancy. If an odd number of the first four bits were 1's, we would add a 1. Thus 1011 would become 10111. If an even number of the first four bits were 1's, we would add a 0. Thus 1010 would become 10100.

The parity-check bit is rather universally used in digital computers for error detection. This check bit will be effective if the probability of error in a bit is low enough so that we may ignore the likelihood of more than a single bit error in a word. If such a single error occurs, it will change a 0 to a 1 or a 1 to a 0 and the word, when received, would have an odd number of 1's. Hence it will be known that an error has occurred. We shall not, however, be able to determine which bit is in error. An error in two bits in a word is not detectable, since such a double error will again yield an even number of 1's.

14.1.3 block Coding for error detection and Correction

Consider that a message source can generate M equally likely messages. Then initially we represent each message by k binary digits with $2^k = M$. These k bits are the information bearing bits. We next add, to each k bit message, r redundant bits (parity check bits). Thus, each message has been expanded into a codeword of length n bits with

$$n = k + r \quad (14.4)$$

the total number of possible n bit codewords is 2^n while the total number of possible messages is 2^k . There are, therefore, $2^n - 2^k$ possible n bit words which do not represent possible messages.

Codes formed by taking a *block* of k information bits and “adding” r ($= n - k$) redundant bits to form a codeword are called *block* codes and designated (n, k) codes. In this section we shall discuss *systematic* codes only. When an n bit codeword consists of k information bits and r redundant bits the code is said to be *systematic*. A *nonsystematic* code has n bits in the codeword and k information bits which are *not* explicitly presented in the codeword. Such codes are discussed in Sec. 14.3.

A $(7, 4)$ systematic code has four information bits which distinguish from one another the sixteen ($= 2^4$) possible messages. There are seven bits in each codeword so that each codeword has three redundant bits. If the codeword with n bits is to be transmitted in no more time than is required for

the transmission of the k information bits and if T_b and T_c are the bit durations in the uncoded and coded word, then it is required that

$$nT_c = kT_b \quad (14.5)$$

We define the *rate of the code* to be

$$R_c \equiv k/n$$

Accordingly, with $f_b = 1/T_b$ and $f_c = 1/T_c$ we have

$$\frac{f_c}{f_b} = \frac{T_b}{T_c} = \frac{n}{k} = \frac{1}{R_c} \quad (14.6)$$

14.1.4 The Hamming Distance, d_{\min}

Consider that C_i and C_j are any two codewords in a particular block code. Then these codewords will differ in some bit positions and we represent by the symbol d_{ij} the number of such positions with differences. Thus, suppose

$$\begin{aligned} C_i &= 1 & 0 & 0 & 0 & 1 & 1 & 1 \\ C_j &= 0 & 0 & 0 & 1 & 0 & 1 & 1 \end{aligned}$$

Then we observe that these codewords differ in the leftmost bit position and in the bit positions fourth and fifth from the left. Accordingly, $d_{ij} = 3$. Assume that we have determined d_{ij} for each pair of codewords. Then the minimum value of the d_{ij} 's is called the *Hamming distance*, d_{\min} . It is rather intuitively clear that when we try to determine, which of two or more codewords, a received “codeword” represents when some of the received codeword's bits may be misread because of noise, the likelihood of a successful determination will be greater for words which have a larger number of bit differences. The greatest likelihood of confusion between words will be encountered for a codeword pair for which d_{ij} is a minimum. Hence, the Hamming distance d_{\min} establishes an upper limit to the effectiveness of a code. We shall describe below two important properties of the parameter d_{\min} :

1. Suppose that there are D errors in a received codeword. Then provided that

$$D \leq d_{\min} - 1 \quad (14.7)$$

we shall be able to *detect*, with certainty, that the received codeword is not valid, i.e. not a word in our vocabulary.

2. If there are t errors in the received word, then provided

$$2t + 1 \leq d_{\min} \text{ (odd);} \quad 2t + 2 \leq d_{\min} \text{ (even)} \quad (14.8)$$

we shall not only be able to establish that the received word is not valid but also *correct* the errors, i.e. we shall be able to regenerate the original correct codeword.

Thus with $d_{\min} = 7$ we can detect a nonvalid word even if as many as six errors have been made and, if no more than three errors have been made we can determine the correct codeword. Finally, it is to be noted that Eqs. (14.7) and (14.8) apply in worst-case conditions. In many cases even more errors can be detected or corrected than indicated by those equations.

14.2 UPPER BOUND OF THE PROBABILITY OF ERROR WITH CODING

In Fig. 14.4, we have codewords transmitted over a communications channel. We should like to direct our attention to the matters pertaining to the use of codes without the distraction of having to take into account the characteristics of modulation-demodulation scheme. For this reason, we assume that transmission takes place at baseband. The waveform $c_i(t)$ makes excursions between +1 and -1 corresponding to logic 1 and 0 respectively. The waveform $y(t)$ therefore has a signal power P_s . A complete codeword is comprised of a sequence of n bits each allocated the bit time T_c . White noise of power spectral density $h/2$ is added to the signal waveform $yfP(c_i(t))$. At each sampling time we shall have made a *hard* decision, i.e. an irrevocable decision about *each individual bit*. We then store bit after bit until we have assembled an entire codeword. Finally, we pass the codeword

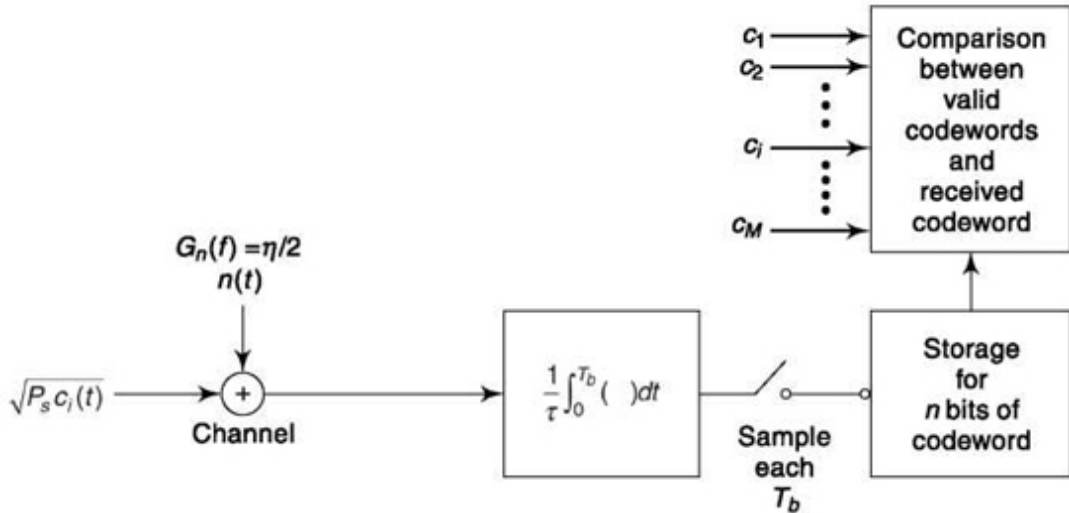


Fig. 14.4 A system incorporating hard-decision decoding.

to appropriate hardware which compares the received codeword with all the valid codewords. The codeword chosen is the one which differs from the received codeword in the fewest number of bits. In this comparison we shall correct errors if they do not exceed the limits of Eq. (14.8).

We note that two decisions are made when using hard decision decoding: the first is a decision concerning each bit and the second is a decision to determine which codeword compares most favorably to our reconstructed word. It is well known that to minimize the probability of an error one should correlate the received signal and noise with all possible signals and then choose the signal yielding the highest correlation. Such a technique does not suggest making a decision in each bit but only *one* final decision. The problem with such a single correlation technique, which is called *soft-decision* decoding is that the resulting hardware is extremely complex. However, it does provide approximately 2 to 3 dB of improvement and is therefore used when needed.

14.2.1 soft decision decoding

The scheme for soft-decision decoding is shown in Fig. 14.5. Here the demodulated baseband signal plus noise $J_p c(t) + n(t)$ is correlated with each of the possible waveforms $c_1, c_2, \dots, c, \dots, c_M$. Decoding is carried out by seeking maximum correlation between the incoming signal and the locally generated codewords. The received codeword $yffS c(t)$ (plus noise) is applied to a bank of correlators consisting of a multiplier followed by an integrator. The integration interval is $nT_c = T_n$ and the integrator output is sampled each

T_n . In the correlator the incoming signal in noise $\sqrt{P_s} c_i(t) + n(t)$ is first multiplied by each of the locally generated waveforms c_1, c_2, \dots, c_M . We assume that $c_i(t)$ takes on the voltages ± 1 . In general, if the transmitted codeword is c , the sampled outputs are

$$v_j = \begin{cases} \frac{\sqrt{P_s} T_n}{\tau} + n_j & i = j \\ \frac{\sqrt{P_s} T_n}{\tau} (n - 2d_{ij}) + n_j & i \neq j \\ = \frac{\sqrt{P_s} T_n}{\tau} \left(1 - \frac{2d_{ij}}{n}\right) + n_j \end{cases} \quad (14.9a)$$

$$(14.9b)$$

$$(14.9c)$$

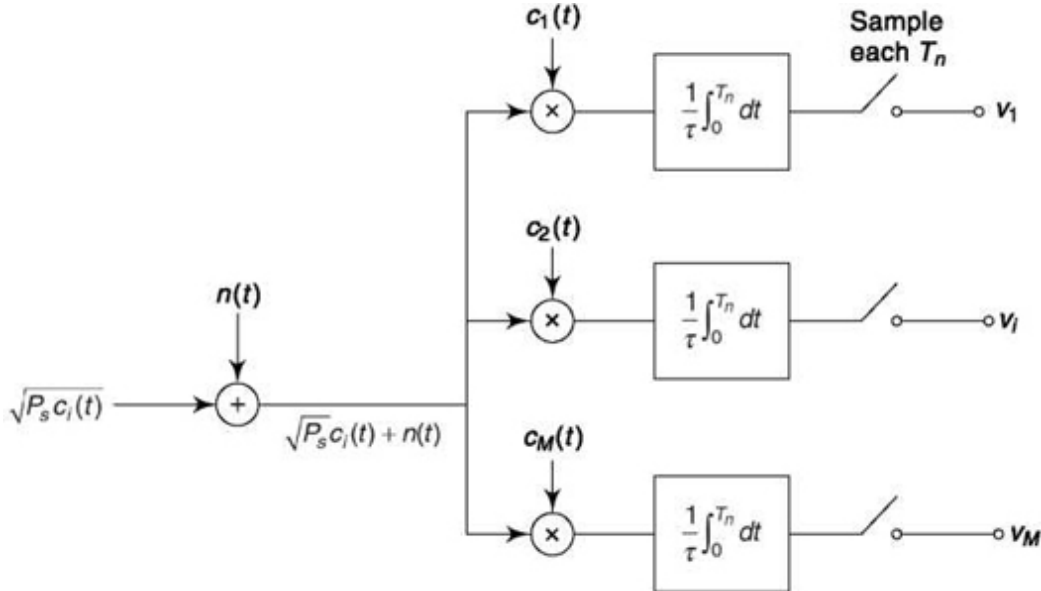


Fig 14.5 A system incorporating soft-decision decoding.

where d_{ij} is the distance (number of bit differences) between c_i and c_j and

$$n_i = \frac{1}{\tau} \int_0^{T_n} n(t)c_i(t) dt \quad (14.10a)$$

$$n_j = \frac{1}{\tau} \int_0^{T_n} n(t)c_j(t) dt \quad (14.10b)$$

are the values of the noise output at the sampling times.

Equation (14.9) confirms that so far as the deterministic portions of v_i and v_j are concerned the larger is d_j the greater is the difference between v_t and

vj . If we should arrange that for all codewords the distance $dj = n/2$ then we find from Eq. (14.9b) that the deterministic portion of $vj = 0$. In such coding the number n is an even number and any two codewords differ by $n/2$ bits. In this case the integrated product of any two different codewords yields a zero result. Hence, such a code is referred to as an *orthogonal* code.

We have from Eq. (14.10)

$$n_i^2 = \frac{1}{\tau} \int_0^{T_n} n(t)c_i(t) dt \cdot \frac{1}{\tau} \int_0^{T_n} n(t)c_i(t) dt \quad (14.11)$$

Since the name of the variable of integration does not affect the value of the definite integral we have

$$n_i^2 = \frac{1}{\tau} \int_0^{T_n} n(t)c_i(t) dt \cdot \frac{1}{\tau} \int_0^{T_n} n(\lambda)c_i(\lambda) d\lambda \quad (14.12a)$$

$$= \frac{1}{\tau} \int_0^{T_n} dt \int_0^{T_n} n(t)n(\lambda)c_i(t)c_i(\lambda) d\lambda \quad (14.12b)$$

and the expected value $E(n_i^2)$ is

$$E(n_i^2) = E\left[\frac{1}{\tau^2} \int_0^{T_n} dt \int_0^{T_n} n(t)n(\lambda)c_i(t)c_i(\lambda) d\lambda\right] \quad (14.13)$$

We now take account of the facts: (1) since $c_i(t)c_i(X)$ are deterministic waveforms $E[c_i(t)c_i(1)] = c_i(t)c_i(1)$, (2) that $c_i(t)$ is not correlated with the noise $n(t)$, so that after interchanging expectation with integration we find

$$E(n_i^2) = \frac{1}{\tau^2} \int_0^{T_n} dt \int_0^{T_n} E[n(t)n(\lambda)]|c_i(t)c_i(\lambda)| d\lambda \quad (14.14)$$

For white Gaussian noise of power spectral density $\eta/2$, we have

$$E[n(t)n(\lambda)] = (\eta/2) \delta(t - \lambda) \quad (14.15)$$

Hence, Eq. (14.14) becomes

$$E(n_i^2) = \frac{1}{\tau^2} \int_0^{T_n} dt \int_0^{T_n} (\eta/2) c_i(t)c_i(\lambda)\delta(t - \lambda) d\lambda \quad (14.16a)$$

$$= \frac{1}{\tau^2} \int_0^{T_n} (\eta/2)c_i^2(t) dt \quad (14.16b)$$

Correspondingly, we find that

$$E(n_j^2) = \frac{1}{\tau^2} \int_0^{T_n} (\eta/2)c_j^2(t) dt \quad (14.17)$$

and since $c_i^2(t) = c_j^2(t) = 1$, we have

$$E(n_i^2) = E(n_j^2) = \frac{\eta T_n}{2\tau^2} \quad (14.18)$$

If we now undertake to calculate $E(n_i n_j)$ we find that all of the steps beginning with Eq. (14.11) and leading to Eq. (14.18) are duplicated with the exception that one of the c 's in each equation is replaced by a c . Thus, Eq. (14.16b) becomes

$$E(n_i n_j) = \frac{1}{\tau^2} \int_0^{T_n} (\eta/2) c_i c_j dt = \frac{\eta}{2\tau^2} \int_0^{T_n} c_i c_j dt \quad (14.19)$$

Applying now the same consideration which led to Eq. (14.9b) we have the result that

$$E(n_i n_j) = \frac{\eta T_n}{2\tau^2} (n - 2d_{ij}) = \frac{\eta T_n}{2\tau^2} \left(1 - \frac{2d_{ij}}{n} \right) \quad (14.20)$$

In the system of Fig. 14.10, if there were no noise and if c_t were the transmitted codeword then v_t would be larger than any other output. In the presence of noise we shall then make the judgement that, if v_t is the largest of the outputs at the sampling time, then the transmitted codeword was c . An upper bound to the probability P_e , that an error is made in decoding a codeword, can be obtained using the *union bound*, which was discussed in Sec. 11.6. The Union Bound is the *sum* of the probabilities that $v_1 > v_2$, $v_2 > v_3$, etc. Thus

$$P_e \leq \sum_{j=1}^M P(v_j > v_i) \quad i \neq j \quad (14.21)$$

The probability that $v_j > v_i$ is

$$P(v_j > v_i) = P\left[\frac{\sqrt{P_s} T_n}{\tau} \left(1 - \frac{2d_{ij}}{n} \right) + n_j > \frac{\sqrt{P_s} T_n}{\tau} + n_i \right] \quad (14.22)$$

Letting $n_0 = n_j - n_i$, Eq. (14.22) becomes

$$P(v_j > v_i) = P\left(n_0 > \frac{2\sqrt{P_s} T_n}{\tau n} d_{ij} \right) \quad (14.23)$$

The variance $\sigma_{n_0}^2$ of the Gaussian random variable n_0 is

$$\sigma_{n_0}^2 = E(n_0^2) = E[(n_j - n_i)^2] = E(n_j^2) + E(n_i^2) - 2E(n_j n_i) \quad (14.24)$$

Using the results given in Eqs. (14.18) and (14.20), we find that

$$\sigma_{n_0}^2 = \frac{2\eta T_n}{\tau^2} \frac{d_{ij}}{n} \quad (14.25)$$

Therefore,

$$P(v_j > v_i) = \int_{2\sqrt{P_s T_n d_{ij} / \eta n}}^{\infty} \frac{\exp(-n_0^2 / 2\sigma_{n_0}^2)}{\sqrt{2\pi\sigma_{n_0}^2}} dn_0 \quad (14.26)$$

Proceeding as we have on a number of other occasions we make the substitution $x^2 = n_0^2 / 2\sigma_{n_0}^2$ and we find that Eq. (14.26) becomes

$$P(v_j > v_i) = \frac{1}{2} \frac{2}{\sqrt{\pi}} \int_{\sqrt{T_n d_{ij} P_s / \eta n}}^{\infty} e^{-x^2} dx \quad (14.27a)$$

$$= \frac{1}{2} \operatorname{erfc} \left[\frac{P_s T_n d_{ij}}{\eta n} \right]^{1/2} \quad (14.27b)$$

Finally, from Eqs. (14.21) and (14.27b) we have

$$P_e \leq \sum_{j=1, j \neq i}^M \frac{1}{2} \operatorname{erfc} \left[\frac{P_s T_n d_{ij}}{\eta n} \right]^{1/2} \quad (14.28)$$

Since $d_{ij} \geq d_{\min}$, we also have

$$P_e \leq \frac{(M-1)}{2} \operatorname{erfc} \left[\frac{P_s T_n d_{\min}}{\eta n} \right]^{1/2} \quad (14.29)$$

To put this result in a more useful form, we note that for large M , $M - 1 = M$ and that $M = 2^k$. Also we recall that $T_n = nT_c$; and from Eq. (14.5) $nT_c = kT_b$, T_c being the bit duration in the coded word and T_b , the bit duration in the uncoded word. Further, P_s is the normalized signal power and $P_s T_b$ is the normalized bit energy E_b in a bit of the uncoded word. Altogether, we find that

$$P_e \leq \frac{2^k}{2} \operatorname{erfc} \left[\frac{E_b}{\eta} \left(\frac{k}{n} \right) d_{\min} \right]^{1/2} \quad (14.30)$$

14.2.2 Hard Decision Decoding

In the beginning of this section 14.2, we have introduced hard decision decoding and its block diagram through Fig. 14.4. As we have noted, in hard-decision decoding, an irrevocable decision is made about each individual bit, the entire codeword is then assembled and this “codeword” is then compared with each valid codeword. From Sec. 11.5.1, we have the result that with coherent detection, the probability that an individual bit is erroneously decoded is

$$p = \frac{1}{2} \operatorname{erfc} \sqrt{\frac{P_s T_c}{\eta}} = \frac{1}{2} \operatorname{erfc} \sqrt{\frac{E_b}{\eta} \cdot \left(\frac{k}{n}\right)} \quad (14.31)$$

If a coding scheme can correct t errors, then the probability that an n -bit codeword is in error is the probability that more than t errors have occurred in n bits. This probability is

$$P_e = \sum_{i=t+1}^n \binom{n}{i} p^i (1-p)^{n-i} \quad (14.32)$$

where p is the probability that i bits are in error, $(1 - p)$ is the probability that the remaining $n - i$ bits are correct and . is the number of combinations of n things taken i at a time. This number is $\binom{n}{i}$

$$\binom{n}{i} = \frac{n!}{(n-i)!i!} \quad (14.33)$$

and is the number of ways in which i bits can be incorrect in a block of n -bits.

For small P_e (in which case p must also be small) P_e can be approximated by the first term of the sum, so that

$$P_e \approx \binom{n}{t+1} p^{t+1} (1-p)^{n-t-1} \quad (14.34)$$

In Prob. 14.9 the student is guided through a calculation to verify that Eq. (14.34) can be approximated by

$$P_e \approx \frac{2^k}{2} \exp - \left\{ (t+1) \left(\frac{E_b}{\eta} \right) \left(\frac{k}{n} \right) \right\} \approx \frac{2^k}{2} \exp - \left\{ \frac{E_b}{\eta} \left(\frac{k}{n} \right) \frac{d_{\min}}{2} \right\} \quad (14.35)$$

since $d_{\min} \approx 2t$.

For large values of E_b/η , the probability of error for soft and hard decision decoding are seen from Eqs. (14.30) and (14.35), to behave asymptotically (i.e., for large values of E_b/η) as

$$P_{e_{\text{soft}}} < \frac{2^k}{2} e^{(-kd_{\min}/n)(E_b/\eta)} \quad (14.36)$$

Thus soft-decision decoding can provide a 3 dB coding gain compared to hard-decision decoding.

The difficulty encountered in performing the n correlations, each for a time $T_n = kT_b$ which is required for soft-decision decoding often inclines code designers to employ hard-decision decoding.

14.3 BLOCK CODES—CODING AND DECODING

A block code (like any code) is an *invention*. Its merit depends on the ingenuity and insight of its inventor. There are few rules for creating good and effective codes. The mathematical framework in terms of which we shall describe the block codes is useful for systematization, organization and comparison of codes and also for the purpose of clarifying the mechanics of encoding and decoding.

In a block code, as we have noted, a codeword has the form

$$a_1 \ a_2 \ a_3 \dots \ a_k \ c_1 \ c_2 \dots \ c_r \quad (14.38)$$

There are k information bits, r parity bits and the codeword has $n = k + r$ bits. There are $M = 2^k$ valid codewords. The uncoded word is

$$\bar{A} = [a_1 \ a_2 \ \dots \ a_k] \quad (14.39)$$

14.3.1 Encoding Block Codes

The generation of a block code starts with a selection of the number r of parity bits to be added and thereafter with the specification of an H matrix

$$\bar{H} = \left[\begin{array}{cccc|cccc} h_{11} & h_{12} & \dots & h_{1k} & 1 & 0 & 0 & \dots & 0 \\ h_{21} & h_{22} & \dots & h_{2k} & 0 & 1 & 0 & \dots & 0 \\ \vdots & \vdots & \ddots & \vdots & \vdots & \vdots & \vdots & \ddots & \vdots \\ h_{r1} & h_{r2} & \dots & h_{rk} & 0 & 0 & 1 & \dots & 0 \end{array} \right] \quad (14.40)$$

$\underbrace{\hspace{1cm}}_{r \times k}$ $\underbrace{\hspace{1cm}}_{r \times r}$

\bar{h} submatrix Identity submatrices, \bar{I}

We observe that H consists of an $r \times k$ submatrix \bar{h} , and an $r \times r$ identity submatrix. In the expression (14.38) and Eq. (14.39) the a 's and c 's are logical variables with possible values 0 or 1. Correspondingly the h 's in Eq. (14.40) are *constant* logical variables with values 0 or 1. The merit of the block code depends on the ingenuity with which the h 's have been selected.

If the entries in the matrix of Eq. (14.40) and in other matrices we encounter were numbers, then the process of finding an element in a product matrix would consist in forming the arithmetic sum of arithmetic products. In the present case, since we deal with logical variables it turns out that the arithmetic product is replaced by the logical product, i.e. the AND operation and the arithmetic sum is replaced by the EXCLUSIVE-OR operation. We recall that these logical operations are defined as follows

<u>AND</u>	<u>EXCLUSIVE-OR</u>	
$0 \cdot 0 = 0$	$0 \oplus 0 = 0$	
$0 \cdot 1 = 0$	$0 \oplus 1 = 1$	
$1 \cdot 0 = 0$	$1 \oplus 0 = 1$	
$1 \cdot 1 = 1$	$1 \oplus 1 = 0$	(14.41)

The transpose of the H matrix, that is the matrix derived from H by interchanging rows and columns is

$$\bar{H}^T = \left[\begin{array}{cccc} h_{11} & h_{21} & \dots & h_{r1} \\ h_{12} & h_{22} & \dots & h_{r2} \\ \hline h_{1k} & h_{2k} & \dots & h_{rk} \\ 1 & 0 & \dots & 0 \\ 0 & 1 & \dots & 0 \\ 0 & 0 & \dots & 0 \\ 0 & 0 & \dots & 1 \end{array} \right] \left\{ \begin{array}{l} k \times r \\ \bar{h}^T \text{ submatrix} \\ r \times r \\ \text{identity submatrix} \end{array} \right\} \quad (14.42)$$

This transposed matrix H^T consists of an $r \times r$ identity submatrix and a submatrix \bar{h}^T which is the transpose of h .

To generate a codeword T from the uncoded word A given by Eq. (14.39) we form a generator matrix G where

$$\bar{G} = \left[\underbrace{\begin{array}{ccccc} 1 & 0 & 0 & \dots & 0 \\ 0 & 1 & 0 & \dots & 0 \\ 0 & 0 & 0 & \dots & 1 \end{array}}_{k \times k} \quad \underbrace{\begin{array}{cccc} h_{11} & h_{21} & \dots & h_{r1} \\ h_{12} & h_{22} & \dots & h_{r2} \\ \hline h_{1k} & h_{2k} & \dots & h_{rk} \end{array}}_{k \times r} \right] \quad (14.43)$$

Observe that G consists of an identity submatrix, this time of order $k \times k$ and a second submatrix which is the submatrix \bar{h}^T encountered in Eq. (14.42). We can readily verify that

$$\bar{G}\bar{H}^T = 0 \quad (14.44)$$

Thus, if for example, we form $(\bar{G}\bar{H}^T)_{11}$, we get

$$(\bar{G}\bar{H}^T)_{11} = h_{11} \cdot 1 \oplus 1 \cdot h_{11} = 0 \quad (14.45)$$

Similarly, all other elements of $\bar{G}\bar{H}^T$ are zero.

The generator matrix G having been formed, the codeword T corresponding to each uncoded word A is

$$\bar{T} = \bar{A}\bar{G} \quad (14.46)$$

Most importantly, it turns out that the coded words so formed have the property that [see Eq. (14.44)]

$$\bar{T}\bar{H}^T = \bar{A}\bar{G}\bar{H}^T = 0 \quad (14.47a)$$

or (see Prob. 14.18)

$$\bar{T}\bar{H}^T = 0 \quad (14.47b)$$

which, written out at length, means

$$\begin{aligned} h_{11} a_1 \oplus h_{12} a_2 \oplus \dots \oplus h_{1k} a_k \oplus 1 \cdot c_1 \oplus 0 \cdot c_2 \oplus \dots \oplus 0 \cdot c_r &= 0 \\ h_{12} a_1 \oplus h_{22} a_2 \oplus \dots \oplus h_{2k} a_k \oplus 0 \cdot c_1 \oplus 1 \cdot c_2 \oplus \dots \oplus 0 \cdot c_r &= 0 \\ \vdots &\vdots \\ h_{r1} a_1 \oplus h_{r2} a_2 \oplus \dots \oplus h_{rk} a_k \oplus 0 \cdot c_1 \oplus 0 \cdot c_2 \oplus \dots \oplus 1 \cdot c_r &= 0 \end{aligned} \quad (14.48a)$$

For example, the \bar{H} matrix of a (7, 4) Hamming code is

$$\bar{H} = \left[\begin{array}{ccccccc} 1 & 1 & 1 & 0 & 1 & 0 & 0 \\ 1 & 1 & 0 & 1 & 0 & 1 & 0 \\ 1 & 0 & 1 & 1 & 0 & 0 & 1 \end{array} \right] \quad (14.48b)$$

$\underbrace{h}_{r \times r = 3 \times 3 I \text{ matrix}}$

Here the identity matrix is $r \times r = 3 \times 3$ because there are $7 - 4 = 3$ parity bits. The total matrix has seven columns leaving a 3×4 h submatrix. The generator matrix G then consists of a $k \times k = 4 \times 4$ identity matrix together with a submatrix which is the transpose h^T of h so that

$$\bar{G} = \left[\begin{array}{cc} \underbrace{\begin{array}{cccc} 1 & 0 & 0 & 0 & 1 & 1 & 1 \\ 0 & 1 & 0 & 0 & 1 & 1 & 0 \\ 0 & 0 & 1 & 0 & 1 & 0 & 1 \\ 0 & 0 & 0 & 1 & 0 & 1 & 1 \end{array}}_{4 \times 4 \bar{I} \text{ matrix}} & \underbrace{\begin{array}{ccc} 1 & 1 & 1 \\ 1 & 1 & 0 \\ 0 & 0 & 1 \end{array}}_{h^T} \end{array} \right] \quad (14.49)$$

It is readily verified that $GH^T = 0$. The coded words are now determined as

$$\bar{T} = \bar{A}\bar{G} = \overbrace{\begin{bmatrix} a_1 & a_2 & a_3 & a_4 \end{bmatrix}}^{k \text{ bits}} \begin{bmatrix} 1 & 0 & 0 & 0 & 1 & 1 & 1 \\ 0 & 1 & 0 & 0 & 1 & 1 & 0 \\ 0 & 0 & 1 & 0 & 1 & 0 & 1 \\ 0 & 0 & 0 & 1 & 0 & 1 & 1 \end{bmatrix} \quad (14.50)$$

Thus, the uncoded word $\bar{A} = |a_1 \ a_2 \ a_3 \ a_4|$ having been specified, the corresponding coded word is

$$\bar{T} = |a_1 \ a_2 \ a_3 \ a_4 \ c_1 \ c_2 \ c_3| \quad (14.51)$$

where

$$\begin{aligned} c_1 &= a_1 \oplus a_2 \oplus a_3 \\ c_2 &= a_1 \oplus a_2 \oplus a_4 \\ c_3 &= a_1 \oplus a_3 \oplus a_4 \end{aligned} \quad (14.52)$$

It is left as a problem (Prob. 14.16) to verify that for each T so generated, the product $HT^T = 0$ as indicated by Eq. (14.47).

When the codeword corresponding to each uncoded word has been determined, the results can be stored in a memory. Such a memory, in this case a read-only memory (ROM), is shown in Fig. 14.6. The bits $a_1 \ a_2 \dots \ a_k$ of the uncoded words are presented as an address to the memory. At the memory location specified by that address we have stored the n ($= k + r$) bits corresponding to the coded word. The uncoded word bit *serial* bit stream $A(t)$ is converted to a *parallel* bit array (i.e., all bits available at the same time) by a serial-to-parallel converter (i.e., a shift register). The converter is driven by a clock at the uncoded bit rate f_b . When the bits $a_1 \ a_2 \dots \ a_k$ are all available, a READ command is given to the ROM and a LOAD command to the parallel-to-series converter

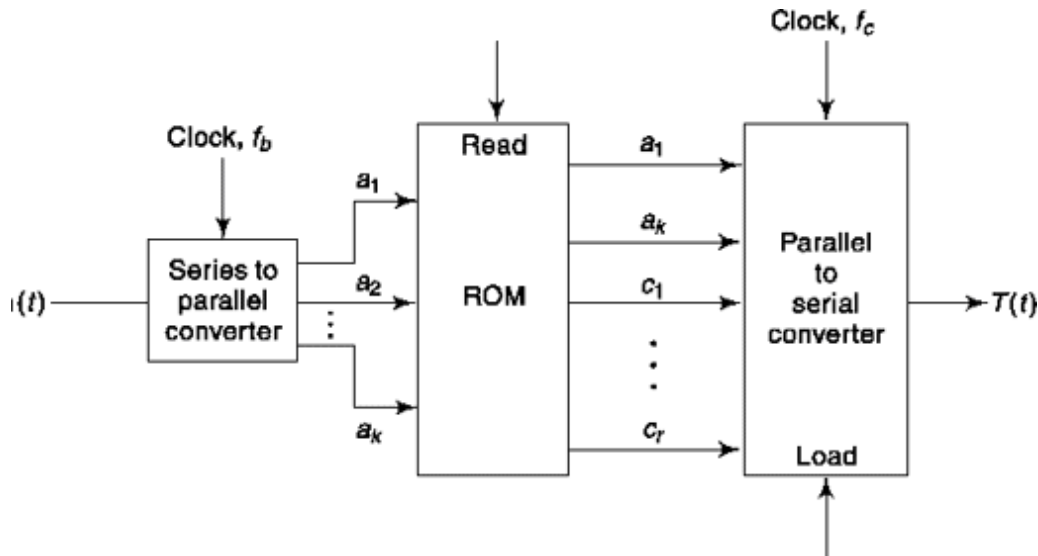


Fig. 14.6 Showing that a read-only memory (ROM) can perform the encoding function.

(i.e., another shift register with a parallel-load facility). The coded word $a_1 a_2 \dots a_k c_1 c_2 \dots c_r$ is thus loaded into the converter. The converter then presents the bits serially at its output. The clock rate for this second converter is f_c , the bit rate for the coded bits. As we have noted before $f/f_b = n/k$.

14.3.2 Decoding Block Codes

Now let the received message be R which may or may not be the transmitted codeword. Suppose that at the receiver we have an appropriate apparatus for forming the product HT^T . If $HT^T \neq 0$ we know that R is not a possible message and one or more bits are in error. Under these circumstances we shall be interested in inquiring into whether we can determine the transmitted codeword and what is the probability that our determination is correct. Even, however, if we find that $HR^T = 0$ we cannot be absolutely certain that R was transmitted, since there is always the possibility that the number of bit errors was so large that the transmitted codeword was transformed into another possible codeword.

We look now into the matter of decoding the received codewords. One possible technique for decoding is to evaluate the correlation of the received codeword with all the possible codewords. This was illustrated earlier in Figs. 14.4 and 14.5. We then assume that the transmitted word was the codeword with which the received codeword exhibits the closest correlation. We have already considered such a procedure in Sec. 14.2. However, the

procedure gets out of hand when the number of bits in a word is large. If the uncoded word has k bits then, excluding the word in which all bits are zero, there are $2^k - 1$ codewords with which comparisons (correlations) have to be made. In some schemes of computer communications, messages (called packets) may contain as many as 1000 bits in which case $2^{1000} - 1$ correlations would be required. One of the primary advantages of *algebraic* codes, whose generation we have just described, is that they allow alternative techniques which reduce very considerably the complexity of decoding.

If \bar{T} is transmitted and $\bar{R} \neq \bar{T}$ is received then

$$\bar{R} = \bar{T} \oplus \bar{E} \quad (14.53)$$

in which \bar{E} is the *error* word. For example, if

$$\bar{T}^T = \begin{vmatrix} 1 \\ 0 \\ 0 \\ 0 \\ 1 \\ 1 \\ 1 \\ 1 \end{vmatrix} \quad (14.54)$$

and an error is made in the fifth place so that

$$\bar{E}^T = \begin{vmatrix} 0 \\ 0 \\ 0 \\ 0 \\ 1 \\ 0 \\ 0 \end{vmatrix} \quad (14.55)$$

then the received codeword will be

$$\bar{R}^T = \begin{vmatrix} 1 \\ 0 \\ 0 \\ 0 \\ 1 \\ 1 \\ 1 \\ 1 \end{vmatrix} \oplus \begin{vmatrix} 0 \\ 0 \\ 0 \\ 0 \\ 1 \\ 0 \\ 0 \end{vmatrix} = \begin{vmatrix} 1 \\ 0 \\ 0 \\ 0 \\ 0 \\ 1 \\ 1 \\ 1 \end{vmatrix} \quad (14.56)$$

Observe from this example that our algebra is such that a 1 in the error word E indicates an error in the corresponding bit position and a 0 indicates that no error has been made.

A first step in the process of decoding is to evaluate the *syndrome* S of the received codeword R . The syndrome is defined as

$$\bar{S} = \bar{H}\bar{R}^T \quad (14.57)$$

If the received word \bar{R} is \bar{T} as transmitted then $\bar{S} = \bar{H}\bar{R}^T = \bar{H}\bar{T}^T = 0$. But if there are errors we find

$$\bar{S} = \bar{H}\bar{R}^T = \bar{H}(\bar{T}^T + \bar{E}^T) \quad (14.58a)$$

$$= \bar{H}\bar{T}^T + \bar{H}\bar{E}^T \quad (14.58b)$$

$$= \bar{H}\bar{E}^T \quad (14.58c)$$

since $H\bar{T}^T = 0$. Accordingly, if the syndrome S is *not* zero then we have an indication that there is one or more errors. If the syndrome is zero then either there are no errors or the errors are so many that a transmitted codeword has been changed to a different codeword. In this latter unlikely, but possible, case, we have from Eq. (14.58c) that $H\bar{E}^T = 0$ so that the error word itself is the same as one of the valid codewords.

When S is not zero, the syndrome provides information about the bit positions in which errors may have been made. For example, let H be the matrix given in Eq. (14.48). Let us assume that a received word is $R = [1000011]$. Forming the syndrome, we find

$$\bar{S} = \bar{H}\bar{R}^T = \begin{vmatrix} 1 & 1 & 1 & 0 & 1 & 0 & 0 \\ 1 & 1 & 0 & 1 & 0 & 1 & 0 \\ 1 & 0 & 1 & 1 & 0 & 0 & 1 \end{vmatrix} \begin{vmatrix} 0 \\ 0 \\ 0 \\ 0 \\ 0 \\ 0 \\ 1 \\ 1 \end{vmatrix} = \begin{vmatrix} 1 \\ 0 \\ 0 \\ 0 \\ 0 \\ 0 \\ 1 \\ 1 \end{vmatrix} \quad (14.59)$$

Since $\bar{S} = \bar{S}\bar{H}^T$, we now have

$$\begin{array}{c|ccccccc|c} & & & & & & & & E_1 \\ & & & & & & & & E_2 \\ 1 & | & 1 & 1 & 1 & 0 & 1 & 0 & 0 \\ 0 & | & 1 & 1 & 0 & 1 & 0 & 1 & 0 \\ 0 & | & 1 & 0 & 1 & 1 & 0 & 0 & 1 \end{array} \left| \begin{array}{c} E_3 \\ E_4 \\ E_5 \\ E_6 \\ E_7 \end{array} \right. \quad (14.60)$$

From Eq. (14.60), we have the three simultaneous equations

$$\begin{aligned} 1 &= E_1 \oplus E_2 \oplus E_3 \oplus E_5 \\ 0 &= E_1 \oplus E_2 \oplus E_4 \oplus E_6 \\ 0 &= E_1 \oplus E_3 \oplus E_4 \oplus E_7 \end{aligned} \quad (14.61)$$

Since there are seven variables E_1 through E_7 and only three equations, a unique solution for the E 's in Eq. (14.61) is therefore not possible. As a matter of fact, it can be shown that there are 2^k different sets of values for the E 's, that is, 2^k different patterns of errors which will satisfy Eq. (14.61). It will be recalled that k is the number of bits in the uncoded word. In the present case $k = 4$ so that there are $2^4 = 16$ different possible error patterns. Five of these patterns are given in Table (14.1). It is left as a student exercise (Prob. 14.17) to verify that the solutions given in Table 14.1 are valid and to find the remaining 11 solutions.

If the probability that a bit in a word is received with an error is p (say $p = 10^{-3}$) then the probability that two bits are in error is $p^2(10^{-6})$ and so on. Accordingly, when we undertake to decide

which error pattern is valid it is eminently most reasonable to decide on that pattern which involves the fewest errors. In the present case where Eq. (14.61) applies, it can be verified that there is only a single error pattern that involves only one error. That pattern is the one given in the first row of Table 14.1. All of the other

Table 14.1 Five patterns of $E_1 E_2 \dots E_7$ which satisfy Eq. (14.61)

E_1	E_2	E_3	E_4	E_5	E_6	E_-
0	0	0	0	1	0	0
1	0	0	1	0	0	0
1	1	1	0	0	0	0
1	0	1	0	1	1	0
0	1	1	0	1	1	1

error patterns involves two or more errors. Accordingly, we accept that the error pattern which is most likely is $E = E_m = [0\ 0\ 0\ 0\ 1\ 0\ 0]$, i.e. the error is in the fifth bit position. Thus, the best estimate \hat{T} about T is the sum of R and the most likely error pattern E_m , so that

$$\hat{T} = \bar{R} + \bar{E}_m \quad (14.62)$$

In the present case, this yields

$$\begin{aligned} \hat{T} &= [1\ 0\ 0\ 0\ 0\ 1\ 1] \oplus [0\ 0\ 0\ 0\ 1\ 0\ 0] \\ &= [1\ 0\ 0\ 0\ 1\ 1\ 1] \end{aligned} \quad (14.63)$$

In the general case, the number, 2^k , of possible error patterns can turn out to be astronomical. For example in the (63,45) BCH code, where $k = 45$ the number of patterns is $2^{45} = 35 \times 10^{12}$. Fortunately, we do not have to find them all to make certain that we have not missed the most likely one. First we note that there is a maximum number t of errors that a code can correct. For this reason let us simply ignore the possibility of errors larger in number than t , since we can do nothing about the matter. For errors fewer or equal to t let us simply explore the possible error patterns by trial and error. For example, in the (7,4) code which we have just used as an example, with H given in Eq. (14.48), $t = 1$. Hence, rather than to undertake to find all error pattern solutions to Eq. (14.61) let us simply try, in turn, all the seven possible error patterns involving only a single error, i.e.

$$[1\ 0\ 0\ 0\ 0\ 0\ 0], [0\ 1\ 0\ 0\ 0\ 0\ 0], \dots, [0\ 0\ 0\ 0\ 0\ 0\ 1].$$

We would then find, as we already have, that $[0\ 0\ 0\ 0\ 1\ 0\ 0]$ is the most likely pattern. In the (63, 45) BCH code it turns out that $t = 3$. Hence, we would first try the 63 error patterns of one error. If none of these was found valid we would then try all possible error patterns of two errors. (⁶³1 The number of these is ${}_2$, i.e. the number of combinations of 63 things taken two at a time. If $V^2 J$ again we met with no success we would look at the patterns with three errors. In total, the number of trials would be

$$\sum_{i=1}^3 \binom{63}{i} = 63 + \frac{63 \cdot 62}{2} + \frac{63 \cdot 62 \cdot 61}{6} = 41,727 \quad (14.64)$$

which is quite an improvement over finding all 35×10^{12} error patterns. There are algorithms which reduces still further the computational complexity.

A block diagram of a method for decoding a received signal is shown in Fig. 14.7. The received serial bit stream is first converted to parallel form so that all bits of the codeword $R_1 R_2 \dots R_m$ are available simultaneously. Since H is fixed and known, the syndrome corresponding to any R can be stored in a ROM, the syndrome calculator. This syndrome is stored at a memory location whose address is arranged to be R itself. Hence, when R appears at the address inputs of the ROM the syndrome is read out. The syndrome has r bits with $r = n - k$. Corresponding to each syndrome, we shall have to determine, as described above, the most likely error pattern. The error pattern, so determined for each syndrome, will be stored in the error-pattern generator ROM at an address which is arranged to be the same as the syndrome. Each output bit, $E_x E_2 \dots E_n$ is applied to one input of an EXCLUSIVE-OR logic gate, the other input of the gate being the corresponding bit of R . If there is an error in a bit, say R , the corresponding error bit E_j will be $E_j = 1$ and the output T will be $T = R^*$ (where * denotes the complement) as required.

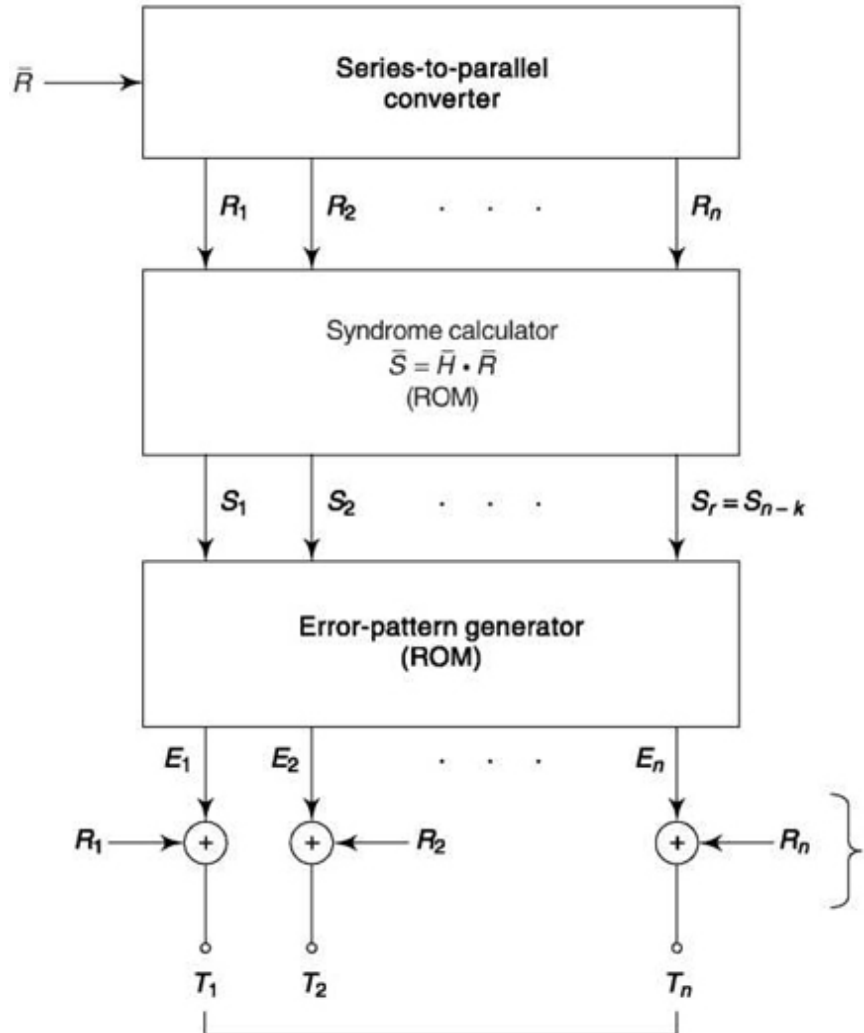


Fig. 14.7 Generic circuit to decode a block code.

It is apparent from the discussion and from the diagram of Fig. 14.7 that the complexity of a decoder grows with increasing codeword size n . However, from our discussion of Shannon's theorem we saw that the error rate can be reduced efficiently by increasing the message size, that is, by making n large. For this reason, the key to efficient communication is linked to the development of electronics which incorporates very large numbers of components and operates at high speed such as VLSI and VHSIC. Also required are efficient algorithms.

14.3.3 single parity-Check bit Code

The single parity-check bit code is an example of a block code. In this case the parity-check is selected to satisfy the equation

$$a_1 \oplus a_2 \oplus \dots \oplus a_k \oplus c_1 = 0 \quad (14.65)$$

Equation (14.65) is the first of the set of Eqs. (14.48) with

$$h_{11} = h_{12} = \dots = h_{1k} = 1$$

All other equations of the set are identically zero. In this case, then, $r = 1$ and $n = k + 1$. Keeping in mind the definition of EXCLUSIVE-OR addition given in Eq. (14.41), we may see that Eq. (14.65) requires that the number of 1's in a word be even, for only the sum of an even number of 1's will add up to zero. If there were an odd number of 1's in the sum of Eq. (14.65), the result would be 1 rather than 0. This code is a single error detecting code and will not correct errors.

14.3.4 Repeated Codes

In a repeated code a binary 0 is encoded as a sequence of $(2t + 1)$ zeros, and a binary 1 as a similar number of 1's. Thus, $k = 1$, $r = 2t$ and $n = 2t + 1$. We considered such encoding in Sec. 14.1. For the case $t = 1$, so that $r = 2t = 2$ and $n = 2t + 1 = 3$. A repeated code is a block code since the redundant bits are determined by Eqs. (14.48). We have $2t$ equations with a_l equal to either 0 or 1, and

$$h_{11} = h_{21} = \dots = h_{r1} = 1$$

while all other h 's are set to zero. The redundant bits are therefore given by

$$\begin{aligned} 0 &= a_1 \oplus c_1 \\ 0 &= a_1 \quad \quad \oplus c_2 \\ &\cdots \cdots \cdots \cdots \cdots \\ 0 &= a_1 \oplus c_{2t} \end{aligned} \tag{14.66}$$

Using again the coding arithmetic of Eq. (14.106), we find that if $a_l = 0$, all the c 's are 0, and if $a_l = 1$, all the c 's are 1. The matrix H for the repeated code with $n = 2t + 1 = 3$ is given by [see Eq. (14.40)]:

$$\bar{H} = \begin{vmatrix} h_{11} & 1 & 0 \\ h_{21} & 0 & 1 \end{vmatrix} = \begin{vmatrix} 1 & 1 & 0 \\ 1 & 0 & 1 \end{vmatrix} \tag{14.67}$$

The ($n = 2t + 1$, $k = 1$) repeated code is capable of correcting t errors. However it requires the use of significant bandwidth as it is a rate $1/(2t + 1)$ code, and therefore such codes are inefficient.

14.3.5 Hadamard Code

The codeword in a Hadamard code are the rows of a Hadamard matrix. The Hadamard matrix is a square ($n \times n$) matrix in which $n = 2^k$ where, as usual, k is the number of bits in the uncoded word. One codeword consists of all zeros and all the other codewords have $n/2$, 0's and $n/2$, 1's. Further, each codeword differs from every other codeword in $n/2$ places and for this reason the codewords are orthogonal to one another.

The Hadamard matrix which provides two codewords is

$$M_2 = \begin{vmatrix} 0 & 0 \\ 0 & 1 \end{vmatrix} \quad (14.68)$$

and the codewords are 00 and 01. The matrix M_4 which provides four codewords is

$$M_4 = \begin{vmatrix} M_2 & M_2 \\ M_2 & M_2^* \end{vmatrix} = \begin{vmatrix} 0 & 0 & 0 & 0 \\ 0 & 1 & 0 & 1 \\ 0 & 0 & 1 & 1 \\ 0 & 1 & 1 & 0 \end{vmatrix} \quad (14.69)$$

in which, as appears, M_2^* is the M_2 matrix with each element replaced by its complement. In general

$$M_{2^n} = \begin{vmatrix} M_n & M_n \\ M_n & M_n^* \end{vmatrix} \quad (14.70)$$

Observe that an $n \times n$ Hadamard matrix provides n codewords each of n bits. To provide for the n different codewords, each with k information bits, each codeword contains $n = 2^k$ bits. Hence, in the n bit codeword there are $r = n - k = 2k - k$ parity bits. Accordingly as k increases, the number of parity bits becomes overwhelmingly large in comparison with the number k of information bits. Correspondingly the rate of the code becomes quite small since

$$R_c = \frac{k}{n} = \frac{k}{2^k} = k2^{-k} \quad (14.71)$$

If, with large k , we propose to transmit coded words at the same rate as uncoded words, the coded transmission will require a bit rate larger than the uncoded bit rate by the factor $1/R_c$. Hence, there would be a corresponding increase in the bandwidth required. This result is consistent with the conclusions we drew in Sec. 14.4 where we took note of the large bandwidth required in orthogonal signalling. Because Hadamard coding makes such

demands on bandwidth it is generally used only where there are no bandwidth restrictions such as in deep space probes.

As we have noted earlier, the Hamming distance of an orthogonal code is

$$d_{\min} = \frac{n}{2} = 2^{k-1} \quad (14.72)$$

Thus the number of errors that can be corrected with a Hadamard code is from Eq. (14.8)

$$t = \frac{3}{4} - 1 - 2^{k-2} - 1 \quad (14.73)$$

Hence to provide for error correction we require that $k > 2$. However, for large k , t increases as 2 so that significant error correction is possible. Hadamard code was used in NASA Mars Mission Mariner 9 to correct picture transmission errors.

14.3.6 Hamming Code

The Hamming code is a code in which $d_{\min} = 3$ so that $t = 1$, i.e. a single error can be corrected. The number n of bits in the codeword, the number k of bits in the uncoded word and the number r of parity bits are related by

$$n = 2^r - 1 \quad (14.74)$$

and

$$k = 2^r - 1 - r \quad (14.75)$$

For $r = 3$ we have a (7,4) code and for $r = 4$ we have a (15,11) code.

The parity check matrix H has r rows and n columns. No column consists of all zeros, each column is unique and each column has r elements: 1's or 0's. The matrix for the (7,4) code is

$$\bar{H} = \underbrace{\begin{vmatrix} 1 & 1 & 1 & 0 & 1 & 0 & 0 \\ 1 & 1 & 0 & 1 & 0 & 1 & 0 \\ 1 & 0 & 1 & 1 & 0 & 0 & 1 \end{vmatrix}}_{\bar{h}} \quad \underbrace{\begin{vmatrix} & & & & & & \\ & & & & & & \\ & & & & & & \end{vmatrix}}_{\bar{f}} \quad (14.76)$$

Observe that if we read the 0's and 1's in Eq. (14.76) as binary numbers then there is a single column corresponding to each of the decimal numbers from 1 through 7. The order of the columns is not of consequence. Of course, different orderings of the rows of H will yield different sets of codewords, but each such set is equally valid. The ordering established in Eq. (14.76) has been selected to separate the h submatrix from the identity

submatrix I and hence give H the form shown in Eq. (14.40). This form is described as the *systematic* form and the corresponding code is called a *systematic code*.

The systematic H matrix for the $(15, 11)$ code is

$$\bar{H} = \begin{bmatrix} 1 & 1 & 1 & 1 & 1 & 1 & 1 & 1 & 0 & 0 & 0 & 0 & 1 & 0 & 0 & 0 \\ 1 & 1 & 1 & 1 & 0 & 0 & 0 & 1 & 0 & 1 & 0 & 0 & 0 & 1 & 0 & 0 \\ 1 & 1 & 0 & 0 & 1 & 1 & 0 & 1 & 1 & 0 & 1 & 0 & 0 & 0 & 1 & 0 \\ 1 & 0 & 1 & 0 & 1 & 0 & 1 & 1 & 1 & 1 & 1 & 1 & 0 & 0 & 0 & 1 \end{bmatrix} \quad (14.77)$$

Observe again that all 4-bit column patterns except the all-zero pattern each appear just once. It is left as a student exercise (Prob. 14.21) to determine the generating matrices for the H given above. The simplicity of the Hamming code makes it a useful error-correction tool. Application includes error correction in semiconductor memories.

14.3.7 Extended Codes

All codes can be *extended*, that is, starting with a parity-check matrix H , a new, extended, matrix H_e can be formed as follows:

$$\bar{H}_v = \begin{vmatrix} & & 0 \\ & & 0 \\ \bar{H} & & \vdots \\ & & 0 \\ 1 & 1 & \cdots & 1 & 1 \end{vmatrix} \quad (14.78)$$

Observe that the extended matrix H_e consists of the H matrix with an added row consisting of all 1's and an added right-hand column consisting of all 0's except for the bottommost element which remains a 1. The extended (7,4) Hamming code matrix is

The matrix H_e defines a $(n + 1, k)$ code. It can be verified (Prob. 14.22) that the extension of a code increases the minimum distance by 1, so that

$$d_{e, \text{min}} = d_{\text{min}} + 1 \quad (14.80)$$

For the extended Hamming code, $d_{e, \text{min}} = 4$. The increase in this case does not improve the error-correcting ability of the code, since with $d_{e, \text{min}} = 4$ we shall still have $t = 1$. However it does allow triple errors to be detected, while only double errors could be detected with $d_{\text{min}} = 3$.

14.3.8 Cyclic Codes

Coding theory is a very sophisticated discipline. We shall not, accordingly, pursue the matter in detail. However, in order to convey an idea of a very large class of codes which are widely used we shall describe rather qualitatively some of the features of *cyclic codes*, stating a number of results and procedures without proof or justification.

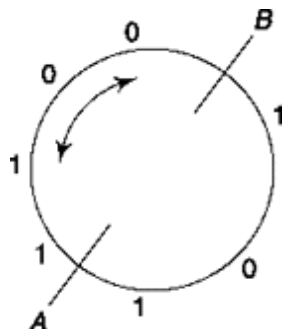


Fig. 14.8 Showing that for a (7,4) Hamming code, a cycle shift in either direction produces a new codeword.

A cyclic code has the property that a cyclic shift of one codeword of the code forms another codeword. The meaning of the term “cyclic shift” is to be seen in Fig. 14.8. Here, a 7-bit word, instead of being written out horizontally, is written out around a circle. Starting at an arbitrary point, say at A, the 7-bit word encountered by a clockwise rotation is 1 1 0 1 0 0 1. Starting at some other arbitrary point, say B, we would read 0 1 1 1 0 1 0. The two words are related in that one is derived from the other by a cyclic shift. There are seven possible starting places in Fig. 14.8. Hence, seven words can be read, each related to the other by a cyclic shift. The order in which the words are generated depends on the direction, clockwise or counterclockwise, of the shift, but the end result of the resultant collection of words is not affected by the shift direction.

Cyclic codes are important because they have algebraic properties which allow them to be easily encoded and decoded. The Hamming code turns out to be an example of such a code type. In the (7,4) Hamming code, there are $2^k = 2^4 = 16$ codewords. It can be verified (Prob. 14.23) that seven of these words are precisely the cyclic-shift related words read from Fig. 14.8. Seven other words in the code are similarly cyclic-shift related. The fifteenth and sixteenth words are 0 0 0 0 0 0 0 and 1 1 1 1 1 1 1 in which a cyclic shift leaves the words unchanged.

To generate a code with $n = 7$ bits, $T(x)$ in Eq. (14.82) must be a polynomial of degree $n - 1 = 6$. Since A is a $k = 4$ bit word, $A(x)$ is of degree $k - 1 = 3$. Hence, we must select a factor from Eq. (14.87) which is of degree 3 so that $T(x)$ be of degree $3 + 3 = 6$. There are two such factors either is suitable, and we arbitrarily select the factor $\lambda_2(x) = (1 \oplus x \oplus x^3)$. Now suppose the uncoded word is $A = [1001]$ then

A procedure for generating an (n, k) cyclic code is the following: The bits of the uncoded word $A = [A_0 A_1, \dots A_{k-1}]$ are written as the coefficients of the polynomial:

$$A(x) = A_0 + A_1x + A_2x^2 + \dots + A_{k-1}x^{k-1} \quad (14.81)$$

The bits of the coded word $\bar{T} = [T_0 T_1 \dots T_{n-1}]$ are written as the coefficients of the polynomial:

$$T(x) = T_0 + T_1x + T_2x^2 + \dots + T_{n-1}x^{n-1} \quad (14.82)$$

We next form the "generating" polynomial $g(x)$ of degree $r = n - k$:

$$g(x) = 1 \oplus g_1x \oplus g_2x^2 \oplus \dots \oplus g_{r-1}x^{r-1} \oplus x^r \quad (14.83)$$

and we determine the values of the coefficients g_1, g_2, \dots, g_{r-1} from the condition that $g(x)$ be a factor of the polynomial

$$f(x) = x^n \oplus 1 \quad (14.84)$$

where n is the number of bits in the codeword. Finally, when $g(x)$ is determined, $T(x)$ is found from the equation

$$T(x) = g(x)A(x) \quad (14.85)$$

As an example of the application of this procedure, let us generate a (7,4) code. Since $n = 7$

$$f(x) = x^7 \oplus 1 \quad (14.86)$$

It can be verified (Prob. 14.24) that the factors of $f(x)$ are

$$f(x) = \lambda_1(x) \cdot \lambda_2(x) \cdot \lambda_3(x) \quad (14.87a)$$

$$= (1 \oplus x)(1 \oplus x \oplus x^3)(1 \oplus x^2 \oplus x^3) \quad (14.87b)$$

$$A(x) = 1 \oplus 0x \oplus 0x^2 + 1 \cdot x^3 = 1 \oplus x^3 \quad (14.88)$$

and the corresponding coded word is

$$T(x) = g(x)A(x) = (1 \oplus x \oplus x^3)(1 \oplus x^3) \quad (14.89a)$$

$$= 1 \oplus x \oplus x^4 \oplus x^6 \quad (14.89b)$$

so that

$$\bar{T} = [1 \ 1 \ 0 \ 0 \ 1 \ 0 \ 1] \quad (14.90)$$

Note that the generated codeword is *not systematic*, that is, it does not appear as the original uncoded word with parity bits added on.

Alternatively, the coded words may be generated by the use of a *generator matrix* as in Eq. (14.46). In the present case, since $k = 4$ and $n = 7$ the generator matrix will have four rows and seven columns. We state without proof that the elements of the matrix are given by the coefficients of the polynomials

$$x^i \lambda(x); \quad i = k - 1, k - 2, \dots, 0 \quad (14.91)$$

$\lambda(x)$ being $\lambda_2(x)$ or $\lambda_3(x)$ of Eq. (14.87b). Each value of i yields the elements of one row. Let us again arbitrarily select $\lambda_2(x)$. Then we find, setting $i = k - 1 = 3$

$$\begin{aligned} x^i \lambda_2(x) &= x^3(1 \oplus x \oplus x^3) = x^3 \oplus x^4 \oplus x^6 \\ &= 0 \cdot x^0 \oplus 0 \cdot x^1 \oplus 0 \cdot x^2 \oplus 1 \cdot x^3 \oplus 1 \cdot x^4 \oplus 0 \cdot x^5 \oplus 1 \cdot x^6 \end{aligned} \quad (14.92)$$

Thus the elements of the first row are 0 0 0 1 1 0 1. The elements of the second row are found by setting $i = 2$, etc. Altogether we find that the generator matrix G_2 , corresponding to $\lambda_2(x)$, is

$$\bar{G}_2 = \begin{vmatrix} 0 & 0 & 0 & 1 & 1 & 0 & 1 \\ 0 & 0 & 1 & 1 & 0 & 1 & 0 \\ 0 & 1 & 1 & 0 & 1 & 0 & 0 \\ 1 & 1 & 0 & 1 & 0 & 0 & 0 \end{vmatrix} \quad (14.93)$$

It is now readily verified that forming $T = AG_2$ does indeed yield the codeword given above in Eq. (14.90).

The Golay Code

Another example of a cyclic code is the *Golay code*. The Golay code is a (23,12) cyclic code whose generating function is

$$g(x) = x^{11} \oplus x^9 \oplus x^7 \oplus x^6 \oplus x^5 \oplus x \oplus 1 \quad (14.94)$$

The extended form of the code is a (24,12) code. For the unextended Golay code $d_{\min} = 7$ and for the extended code $d_{\min} = 8$. The distinctive

feature of this code is that it is the only known code of codeword length 23 which is able to correct $t = 3$ errors. NASA's Voyager 1 and 2 mission to Jupiter and Saturn used Golay codes which gave higher data rate compared to Hadamard code used in the Mariner mission.

14.3.9 BCH Codes

The *Bose, Chaudhuri and Hocquenghem* (BCH) codes form a large class of error correcting codes. The Hamming code, discussed earlier, and the Reed-Solomon code to be discussed subsequently are two special cases of this powerful error correction coding technique.

The BCH code employs k information bits, r parity check bits and therefore the number of bits in a codeword is $n = k + r$. Furthermore, the number of errors t which can be corrected in an n -bit codeword is

$$t = r/m \quad (14.95)$$

where m is an integer related to the number of bits n in the codeword by the formula

$$n = 2^m - 1 \quad (14.96)$$

The Hamming code, where $n = 2^r - 1$, is seen to be a BCH code where $m = r$ so that $t = 1$.

To see the capability of the BCH code relative to the (23,12) Golay code let $t = 3$. Then, from Eq. (14.67), $m = r/3$. If $n = 31$ (no integer value of m , when substituted into Eq. (14.86) will make n equal to 23) then $m = 5$ and $r = 15$ thus $k = 16$ and the code is a (31,16) BCH code. Note that the

code rate is $R_c = \frac{16}{31} \approx \frac{1}{2}$ but if we define the code efficiency as $E = t/n$ then $E = \frac{3}{31} \approx 10\%$; for

Example 14.1

An even parity bit is added to 3-bit codes before transmission. Find the probability of an undetected symbol error if the probability of symbol error rate is (a) $p = 0.1$ and (b) $p = 0.01$. Assume all symbol errors are independent.

Solution

With single parity bit added, the code size = 4. An error evades parity check if any 2 or all 4 symbols of the code arrived are erroneous.

Probability of any m symbol from n are erroneous

$$= {}^nC_m p^m (1-p)^{n-m} \quad (14.98)$$

Thus, the probability of error going undetected,

$$P_{\text{undet_err}} = {}^4C_2 p^2(1-p)^2 + {}^4C_4 p^4$$

or, $P_{\text{undet_err}} = 6p^2(1-p)^2 + p^4$

(a) Required probability of error in detection

$$\begin{aligned} &= 6(0.1)^2(1-0.1)^2 + (0.1)^4 \\ &= 0.0486 + 0.0001 = 0.0487 \end{aligned}$$

(b) Required probability of error in detection

$$\begin{aligned} &= 6(0.01)^2(1-0.01)^2 + (0.01)^4 \\ &= (5.8806 + 0.0001)10^{-4} = 5.8807 \times 10^{-4} \end{aligned}$$

Note that, it is the first term, i.e. error coming from mis-detection of two symbol errors that contribute significantly to the final error. If it was say, 8-bit code (instead of 3-bit) the first term, ${}^iC_2 p^2(1-p)^6$ would have contributed the most compared to 4, 6, 8 bit errors.

Example 14.2

(a) The parity check matrix H of a linear (7,4) block code is given as follows. Show how data words (a) 0011, (b) 0100 and (c) 0101 are coded. (b) Show how error is detected when 2nd bit is detected erroneously for data word 0011.

$$\bar{H} = \begin{pmatrix} 1 & 0 & 1 & 1 & 1 & 0 & 0 \\ 1 & 1 & 0 & 1 & 0 & 1 & 0 \\ 0 & 1 & 1 & 1 & 0 & 0 & 1 \end{pmatrix}$$

Solution

(a) From Eqs (14.40) and (14.43), we can write generating matrix,

$$\bar{G} = \begin{pmatrix} 1 & 0 & 0 & 0 & 1 & 1 & 0 \\ 0 & 1 & 0 & 0 & 0 & 1 & 1 \\ 0 & 0 & 1 & 0 & 1 & 0 & 1 \\ 0 & 0 & 0 & 1 & 1 & 1 & 1 \end{pmatrix}$$

(i) Coded word = [0 0 1 1] G = [0 0 1 1 0 1 0] Note that, multiplication is logic AND operation and addition is logic Ex-OR operation.

(i) 0011, (ii) 0100. (b) Show how cyclic code is decoded to get data word for previous case (i).

$$\begin{aligned} \text{(ii) Coded word} &= [0 \ 1 \ 0 \ 0] \quad \bar{G} = [0 \ 1 \ 0 \ 0 \ 0 \\ &\quad 1 \ 1] \end{aligned}$$

(b) Transmitted word $\bar{T} = [0\ 0\ 1\ 1\ 0\ 1\ 0]$

Received word $\bar{R} = [0\ 1\ 1\ 1\ 0\ 1\ 0]$

From Eq. (14.57),

$$\bar{S} = \begin{pmatrix} 1 & 0 & 1 & 1 & 1 & 0 & 0 \\ 1 & 1 & 0 & 1 & 0 & 1 & 0 \\ 0 & 1 & 1 & 1 & 0 & 0 & 1 \end{pmatrix}$$

$$[0\ 1\ 1\ 1\ 0\ 1\ 0]^T$$

$$= \begin{pmatrix} 0 \\ 1 \\ 1 \end{pmatrix}$$

Since, syndrome S is having non-zero element, the received code is erroneous.

$$\text{Thus, } A(x) = \frac{T(x)}{g(x)} = \frac{x^2 + x^4 + x^5 + x^6}{1 + x + x^3} \text{ and}$$

$$\begin{array}{c} 1 + x + x^3 \mid x^2 + x^4 + x^5 + x^6 \\ \quad \quad \quad \left| x^2 + x^3 + x^5 \right. \\ \hline \quad \quad \quad x^3 + x^4 + x^6 \\ \hline \quad \quad \quad x^3 + x^4 + x^6 \end{array}$$

Hence, data word = 0011

Note that subtraction is similar to addition and through logic Ex-OR operation.

Example 14.3

(a) For a (7,4) cyclic code, the generating polynomial $g(x) = 1 + x + x^3$. Find the code word if data word is

Data word	1	x	x^2	x^3	$A(x)$	$T(x) = g(x).A(x)$	Code word
(i) 0011	0	0	1	1	$x^2 + x^3$	$x^2 + x^4 + x^5 + x^6$	0010111
(ii) 0100	0	1	0	0	x	$x + x^2 + x^4$	0110100

(a) The data polynomial $A(x)$ and transmission code polynomial $T(x)$ are shown below.

(b) The data word is found by division of $T(x)$ by $g(x)$.

$$\text{Thus, } l(x) = \frac{T(x)}{g(x)} = \frac{x^2 + x^4 + x^5 + x^6}{1 + x + x^3} \text{ and}$$

$$\begin{array}{r} 1 + x + x^3 \mid x^2 + x^4 + x^5 + x^6 \\ \quad\quad\quad\left| \begin{array}{l} x^2 + x^3 + x^5 \\ \hline x^3 + x^4 + x^6 \end{array} \right. \\ \hline x^3 + x^4 + x^6 \end{array}$$

Hence, data word = 0011

Note that subtraction is similar to addition and through logic Ex-OR operation.

SELF-TEST QUESTIONS -

1. Coding detects and corrects error by deliberate introduction of redundancy into messages. Is that true?
2. In coded signal, all sequences of symbols do not constitute bona fide message. Is the statement correct?
3. In block-code generation, arithmetic product operation is replaced by Ex-OR and arithmetic addition is replaced by AND. Is that correct?
4. Does soft decision decoding provide 2-3 dB improvement over hard decision decoding?
5. Does bandwidth restriction limits use of Hadamard code?
6. In systematic code, the coded message has original uncoded words followed by parity bits while in non systematic codes, it is not necessary. Do you agree?

14.4 BURST ERROR CORRECTION

The parity bits added in the block codes discussed above will correct a limited number of bit errors in each codeword. However, there are occasions when the *average* bit error rate is small, yet the error correcting codes discussed in Sec. 14.3 are not effective in correcting the errors because the errors are *clustered*. That is, examination of a received bit stream will show that in one region a large percentage of bits are in error, thereby precluding error correction using the techniques of Sec. 14.3, while in another region there are few and perhaps no errors.

Since the bit errors are closely clustered we say that the errors occur in *bursts*. Examples of the sources of such bursts are the following: (a) In

magnetic tape or compact disc recording and playback there may occur, for mechanical reasons, intervals when the spacing between head and tape/ disc is incorrect or it may be that some small section of the tape is simply defective. In either case a burst of errors will occur. (b) Static (i.e. non-thermal noise), such as results in radio transmission due to lightning, causes bursts of errors as long as it lasts. (c) There are channels in which the level of the received signal power waxes and wanes with time. In such *fading* channels bursts of errors are likely to occur when the received power is low.

14.4.1 Block Interleaving

A primary technique which is effective in overcoming error bursts, is *interleaving*. The principle of interleaving is illustrated in Fig. 14.9. As shown in Fig. 14.9a, before the data stream is applied to the channel the data goes through a process of interleaving and error correction coding. At the receiving end the data is decoded, i.e. the data bits are evaluated in a manner to take advantage of the error correcting and detecting features which result from the coding and the process of interleaving is undone. As represented in Fig. 14.9b a group of kl data bits is loaded into a shift register which

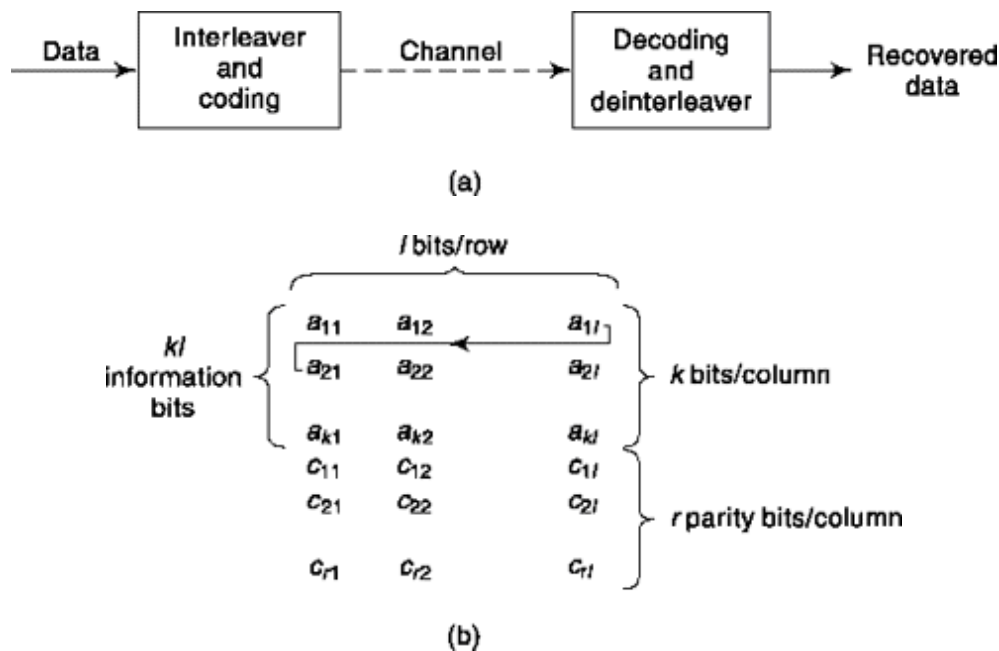


Fig. 14.9 (a) Interleaving used to contend with burst errors. (b) Organization of information and parity bits in interleaving.

is organized into k rows with l bits per row. The data stream is entered into the storage element at a_{n1} . At each shift each bit moves one position to the

right while the bit in the rightmost storage element moves to the leftmost stage of the next row. Thus, for example, as indicated by the arrow, the content of a_u moves to a_{21} . When kl data bits have been entered, the register is full, the first bit being in a_{kl} , and the last bit in a_n . At this point the data stream is diverted to a second similar shift register and a process of coding is applied to the data held stored in the first register. In this coding process, the information bits in a column (e.g., $a_n, a_{21}, \dots, a_{k1}$) are viewed as the bits of an uncoded word to which parity bits are to be added. Thus, the codeword $a_u a_n a_{21} \dots a_{k1} c_{11} c_{21} \dots c_{r1}$ is formed, thereby generating a codeword with k information bits and r parity bits. Observe that the information bits in this codeword were l bits apart in the original bits stream.

When the coding is completed, the entire content of the $k \times l$ information register as well as the $r \times l$ parity bits are transmitted over the channel. Generally, the bit-by-bit serial transmission is carried out row by row, that is in the order

$$c_{rl} \dots c_{r1} \dots c_{1l} \dots c_{11} a_{kl} \dots a_{k1} \dots a_{2l} \dots a_{21} a_{1l} \dots a_{12} a_{11}.$$

Note that the data is transmitted in exactly the same order it entered the register, however, now parity bits are also transmitted. The received data is again stored in the same order as in the transmitter and error correction decoding is performed. The parity bits are then discarded and the data bits shifted out of the register.

To see how interleaving affects bursts of errors, consider that the code incorporated into a codeword (a column in Fig. 14.9b) is adequate to correct a single error. Next suppose that in the transmitted data stream there occurs a burst of noise lasting for I consecutive coded bits. Then because of the organization displayed in Fig. 14.9b it is clear that only one error will appear in each column and this single error will be corrected. If there are $l + 1$ consecutive errors then one column will have two errors and correction will not be assured. In general, if the code is able to correct t errors then the process of interleaving will permit the correction of a burst of B bits with

$$B \leq II \quad (14.99)$$

14.4.2 Convolutional Interleaving

An alternative interleaving scheme, convolutional interleaving, more commonly used in digital television system, is shown in Fig. 14.10. The four

switches operate in step and move from line-to-line at the bit rate of the input bit stream $d(k)$. Thus, each switch makes contact with line 1 at the same time, then moves to line 2 together, etc., returning to line 1 after line l . The cascade of storage elements in the lines are shift registers. Starting with line 1, on the transmitter side, which has no storage elements, the number of elements increases by s as we progress from line to line. The last line l has $(l - 1)s$ storage elements. The total number of storage elements in each line (transmitter plus receiver side) is, in every case, the same. Hence, in each line there are a total of $(l - 1)s$ storage elements.

To describe the timing of operations in the interleaver, let us consider a single line l_i on the transmitter side. Suppose that during the particular bit interval of bit $d(k)$ there is switch contact, at input and output sides of line l_i . At the end of the bit interval, a clock signal causes the shift register of line l_i (and line l_i only), to enter into the leftmost storage element the bit on the input side of the line and to start moving the contents of each of its storage elements one bit to the right. That process having started, a synchronous clock advances the switches to the next line $l_i + x$. When

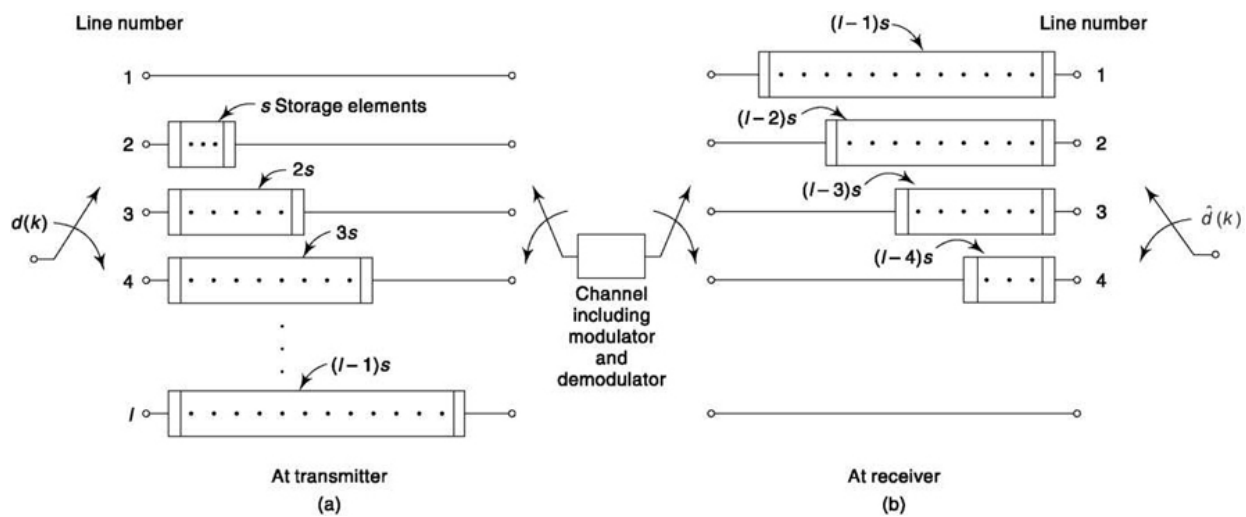


Fig. 14.10 Convolutional interleaving (a) at transmitter, (b) at receiver.

the shift register response is completed, there will be a new bit at the output end of the line, l_i . However, because of the propagation delay through the storage elements, the switch at the output end of the line will have already lost contact with line l_i , before the new bit has appeared at the line output. In summary, during the interval of input $d(k)$, during which the switches were connected to line l_i , there is one-bit shift of the shift register on line l_i which

accepts bit $d(k)$ into the register. However, the fact that such a shift took place is not noticed on the output switch until the *next* time the switch makes contact with line l_i . We observe also that while the clock that drives the switches has a clock rate f_b , which is the bit rate, the clocks that drives the shift registers have a rate f_b/l . The shift registers are not driven in unison, but rather in sequence, each register being activated as the switches are about to break contact with its line.

Now let us consider that, initially, all the shift registers in the transmitter and the receiver are short circuited. If bit $d(k)$ occurs when all the switches are on line l_i , then the corresponding received bit $d(k)$ will appear immediately. The next input bit $d(k + 1)$ will be the next received bit except that it will be transmitted over line l_{i+1} , and so on. In short, the received sequence $d(k)$ will be the same as the transmitted sequence. With the shift registers in place in the transmitter and receiver, each of the l lines will have the same delay $(l - 1)s$ and therefore the output sequence will still be identical to the input sequence. Of course, however, $d(k)$ will be delayed with respect to $d(k)$ by the amount $(l - 1)s$.

The sequence in which the bits will be transmitted over the channel is different. This sequence will be interleaved. Suppose that two successive bits in the input bit stream are $d(k)$ and $d(k + 1)$. Then it can be verified that if in the interleaved stream we continue to refer to the first bit as $d(k)$, the bit which was originally $d(k + 1)$ will instead be $d(k + 1 + ls)$. Thus if $l = 5$ and $s = 3$, there will be $ls = 15$ bits interposed between two bits that were initially adjacent to one another. See Prob. (14.29).

In comparison with a block interleaver, the convolutional interleaver has the following advantages: For the same interleaving distance less memory is required; the interleaving structure can be changed easily and conveniently by changing the number of lines l and, or, the incremental number of elements per line, s .

14.4.3 The Reed-Solomon (RS) Code

The block codes we have described so far are organized on the basis of individual bits. Thus typically a codeword has k individual information bits, r individual parity bits and a total of $n (= k + r)$ individual bits in a codeword. The Reed-Solomon (RS) block code, useful in error correction in compact disc, satellite communication, etc., is organized on the basis of

groups of bits. Such groups of bits are referred to as *symbols*. Thus, suppose we store sequences of m individual bits which appear serially in a bit stream and thereafter operate with the m -bit sequence rather than the individual bits. Then we shall be dealing with m -bit *symbols*. Since we deal only with symbols we must consider that if an error occurs even in a *single* bit of a symbol, the entire symbol is in error. The RS code has the following characteristics: The RS code has k information *symbols* (rather than bits), r parity *symbols* and a total codeword length of $n (= k + r)$ *symbols*. It has the characteristic that the number of symbols in the codeword is arranged to be

$$n = 2^m - 1 \quad (14.100)$$

The RS code is able to correct errors in t symbols where

$$t = r/2 \quad (14.101)$$

As an example, assume that $m = 8$, then $n = 2^8 - 1 = 255$ symbols in a codeword. Suppose further that we require that $t = 16$, then $r = 2t = 32$ and $k = n - r$ is

$$k = 255 - 32 = 223 \text{ information symbols/codeword} \quad (14.102)$$

The code rate is

$$R_c = \frac{k}{n} = \frac{223}{255} \approx \frac{7}{8} \quad (14.103)$$

The total number of bits in the codeword is $255 \times 8 = 2040$ bits/codeword.

Since the RS code of our example can correct sixteen symbols it can correct a burst of $16 \times 8 = 128$ consecutive bit errors. If we use the RS code with the interleaving as described above, then using Eq. (14.99) the number of correctable *symbols* is $l t$ and the number of correctable bits is

$$B = m l t \quad (14.104)$$

with $m = 8$, $t = 16$ and $l = 10$, $B = 1280$ bits.

The organization of an RS block code with $m = 8$, $k = 233$, $r = 32$ utilizing interleaving to a depth of $l = 4$ is shown in Fig. 14.11.

$l = 4$ symbols/row			
$a_{1,1}$	$a_{1,2}$	$a_{1,3}$	$a_{1,4}$
$a_{2,1}$	$a_{2,2}$	$a_{2,3}$	$a_{2,4}$
:	:	:	:
$a_{223,1}$	$a_{223,2}$	$a_{223,3}$	$a_{223,4}$
$c_{1,1}$	$c_{1,2}$	$c_{1,3}$	$c_{1,4}$
$c_{2,1}$	$c_{2,2}$	$c_{2,3}$	$c_{2,4}$
:	:	:	:
$c_{32,1}$	$c_{32,2}$	$c_{32,3}$	$c_{32,4}$

Each entry represents an 8-bit symbol

$k = 223$ Information symbols/column

$k = 32$ parity symbols/column

Fig. 14.11 The organization of an RS code with $m = 8$, $k = 223$, and $r = 32$. Here a_{11} , etc. is an 8-bit information symbol and c_{11} etc. is an 8-bit parity symbol. The interleaving depth is $l = 4$. There are $233 \times 8 \times 4 = 7136$ information bits and $32 \times 8 \times 4 = 1024$ parity bits.

It is interesting to note that while the (255,223) RS code can correct 128 consecutive bit errors it must then have an *error-free* region of $255 - 16 = 239$ symbols (1912 bits). Further, if the errors are random, and there is, at most, one error per symbol, then the RS code can correct only sixteen bit errors in 2040 bits. Clearly the RS code is *not* an efficient code for correcting random errors.

14.4.4 Concatenated Codes

The use of nonbinary codes (i.e., codes based on symbols rather than on individual bits such as the RS code) is an effective way of dealing with error bursts. As we have noted, the RS code turns out to be an especially effective and useful code when m (the symbol length) is much larger than unity. The RS code is important because there is available an efficient hard-decision decoding algorithm which makes it possible to employ long codes. A second, effective, way of dealing with bursts is interleaving. However, nonbinary codes and interleaving are not particularly effective in dealing with random errors which affect only a single bit or only a small number of consecutive bits. When we must contend with both burst and random errors it is useful to cascade coding which is effective with bursts and coding useful with random errors. Such cascading of codes is called *concatenation*.

To illustrate the technique of concatenation, let us start with the coding represented in Fig. 14.11. Here we have used an RS code with $k = 223$, $r = 32$, $m = 8$ and we have used interleaving with $l = 4$. Now let us add further coding to each of the 255 rows of Fig. 14.11 using the (7,4) Hamming code. To effect this additional coding, we add three parity symbols to each row so

that now the pattern of Fig. 14.11 is expanded to $4 + 3 = 7$ columns. The number of information bits remains

$$k = 223 \times 8 \times 4 = 7136 \text{ information bits}$$

The number of parity bits due to the RS coding is, as before

$$r(\text{RS}) = 32 \times 8 \times 4 = 1024 \text{ RS parity bits}$$

The number of bits added by the Hamming coding is

$$r(\text{H}) = 255 \times 8 \times 3 = 6120 \text{ Hamming parity bits}$$

The code rate of the concatenated coding is

$$R_c = \frac{k}{k + r(\text{RS}) + r(\text{H})} \approx \frac{1}{2}$$

$$B = 8 \times 4 \times 16 = 512 \text{ bits}$$

with concatenation we have

$$B = 8 \times 7 \times 16 = 896 \text{ bits}$$

However, in the first case we have a block length

$$n = 8 \times 4 \times 255 = 8160 \text{ bits}$$

In the second case, we have

$$n = 8 \times 7 \times 255 = 14,280 \text{ bits}$$

The effectiveness of the coding against bursts is reasonably measured by the ratio B/n and we find that this ratio is the same with or without concatenation, that is, $512/8160 = 896/14,280$. Since for the sake of minimizing hardware, we might well be inclined to use the shorter block length, it appears that, so far as burst error connection is concerned, the concatenation is actually somewhat disadvantageous. However, the concatenated code can also correct random errors if they are spaced so that no more than one bit is in error out of seven. Thus, concatenation allows correction of a burst of 896 errors and one error in seven bits in the remaining $14,280 - 896 = 13,384$ bits. Without concatenation the remaining 13,384 bits would have to be error free.

14.5 CONVOLUTIONAL CODING

Convolutional coding is an alternative to block coding of digital messages. It can offer higher coding gain for both hard and soft kind of decoding.

14.5.1 Code generation

A convolutional code is generated by combining the outputs of a K-stage shift register through the employment of v EXCLUSIVE-OR logic summers. Such a coder is illustrated in Fig. 14.12 for the case $K = 4$ and $v = 3$. Here M_x through M_4 are 1-bit storage (memory) devices such as Flip-Flops. The outputs v_1 , v_2 and v_3 of the adders in Fig. 14.12 are

$$v_1 = s_1 \quad (14.105a)$$

$$v_2 = s_1 \oplus s_2 \oplus s_3 \oplus s_4 \quad (14.105b)$$

$$v_3 = s_1 \oplus s_3 \oplus s_4 \quad (14.105c)$$

The operation of the encoder proceeds as follows: We assume that initially the shift register is clear. The first bit of the input data stream is entered into M_x . During this message bit interval, the commutator samples, in turn, the adder outputs v_1 , v_2 and v_3 . Thus, a single bit yields, in the present case, three coded output bits. The encoder is therefore of rate $1/3$. The next message bit then enters M_j , while the bit initially in M_x transfers to M_2 , and the commutator again samples all the v adder outputs. This process continues until eventually the last bit of the message has been entered into M_j . Thereafter, in order that every message bit may proceed entirely through the shift register, and hence be involved in the complete coding process, enough 0's are added to the message to transfer the last message bit through M_4 , and, hence, out of the shift register. The shift register then finds itself in its initial “clear” condition.

It may be verified, by way of example, that, for the encoder of Fig. 14.12, if the input bit stream to the encoder is given by the 5-bit sequence

$$m = 1 \ 0 \ 1 \ 1 \ 0 \quad (14.106)$$

then the coded output bit stream is

$$c = 111 \ 010 \ 100 \ 110 \ 001 \ 000 \ 011 \ 000 \ 000 \quad (14.107)$$

If the number of bits in the message stream is L , the number of bits in the output code is $v(L + K)$. As a matter of practice however, L is ordinarily a very large number while K is a relatively small number. Hence $v(L + K) \approx vL$. Thus, the number of code bits is v times the number of message bits, v being the number of commutator segments. Accordingly, also, the rate of the code is $1/v$.

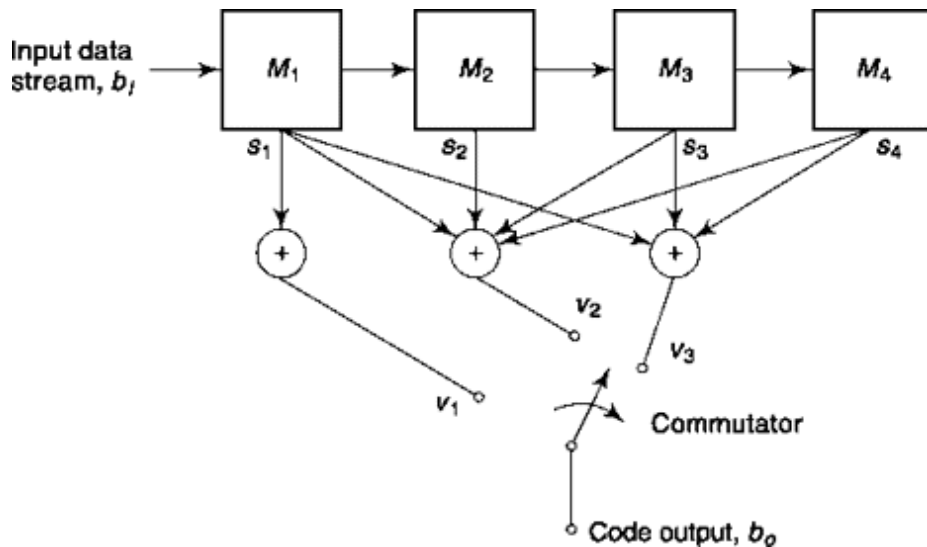


Fig. 14.12 An example of a convolutional coder.

Note the continuity of operation of the convolutional encoder. Even if the input message bit stream were to consist of millions of bits, the stream would be run continuously through the encoder. Each bit remains in the shift register for as many message bit intervals as there are stages in the shift register. Hence each input bit influences K groups of v bits.

The coded output depends on the number K of shift-register stages, on the number of EXCLUSIVE-OR adders used and on the connections of the register stages to the adders. With a view toward searching out optimal encoders, exhaustive computer analyses have been undertaken. Some results, for rate 1/2 coders (two adders) are given in Table 14.2. A 1 in the table indicates a connection to an adder while a 0 indicates that no connection is made.

Table 14.2 Optimum Configurations for Rate 1/2 Convolutional Coders
Code Generator Connections (M_1, M_2, \dots, M_K)

K (Number of Register Stages)	v_1	v_2
3	1, 1, 1	1, 0, 1
4	1, 1, 1, 1	1, 1, 0, 1
5	1, 1, 1, 0, 1	1, 0, 0, 1, 1
6	1, 1, 1, 0, 1, 1	1, 1, 0, 0, 0, 1
7	1, 1, 1, 1, 0, 0, 1	1, 0, 1, 1, 0, 1, 1
8	1, 1, 1, 1, 1, 0, 0, 1	1, 0, 1, 0, 0, 1, 1, 1

Thus, by way of example, for the case $K = 5$, stages 1, 2, 3 and 5 should be connected to the adder which generates v_1 while stages 1, 4 and 5 should be

connected to the adder for v_2 . More extensive tables are available in the literature.

14.5.2 Decoding Convolutional Code

The Code Tree

With a view towards exploring procedures for decoding a convolutional code, we consider the code tree of Fig. 14.13. This code tree applies to the convolutional encoder of Fig. 14.12, for which $K = 4$ and $v = 3$, and which is constructed for the case $L = 5$ corresponding to a 5-bit message sequence. We now discuss the interpretation of the code tree.

The starting point on the code tree is at the left and corresponds to the situation before the occurrence of the first message bit. The first message bit may be either a 1 or a 0. We adopt the convention that, when an input bit is a 0, we shall diverge upward from a node of the tree, and when the input bit is a 1 we shall diverge downward. Suppose then that the first input bit is 1. Then entering the tree at node A, we move downward to the lower branch and to node B. Now from Eqs. (14.106) and (14.107) we note that when the first input bit is 1, the output of the coder is 111. Hence the lower branch associated with node A in Fig. 14.13 has correspondingly been marked 111. Suppose, to continue, that the second input bit is 0. Then we now diverge upward from node B. We find, again, as to be noted from Eqs. (14.106) and (14.107), that, when the first two input bits to the encoder are 10, the encoder output during this second input message bit interval is 010. Hence the upper branch diverging from node B is correspondingly marked 010. Continuing in this fashion we find that the message $m = 10110$ of Eq. (14.106) indicates a downward divergence from node C to node D, a downward divergence from D to E, an upward divergence from node E, and from there out to the end of one of the branches of the tree. The path through the tree is shown by the dashed line.

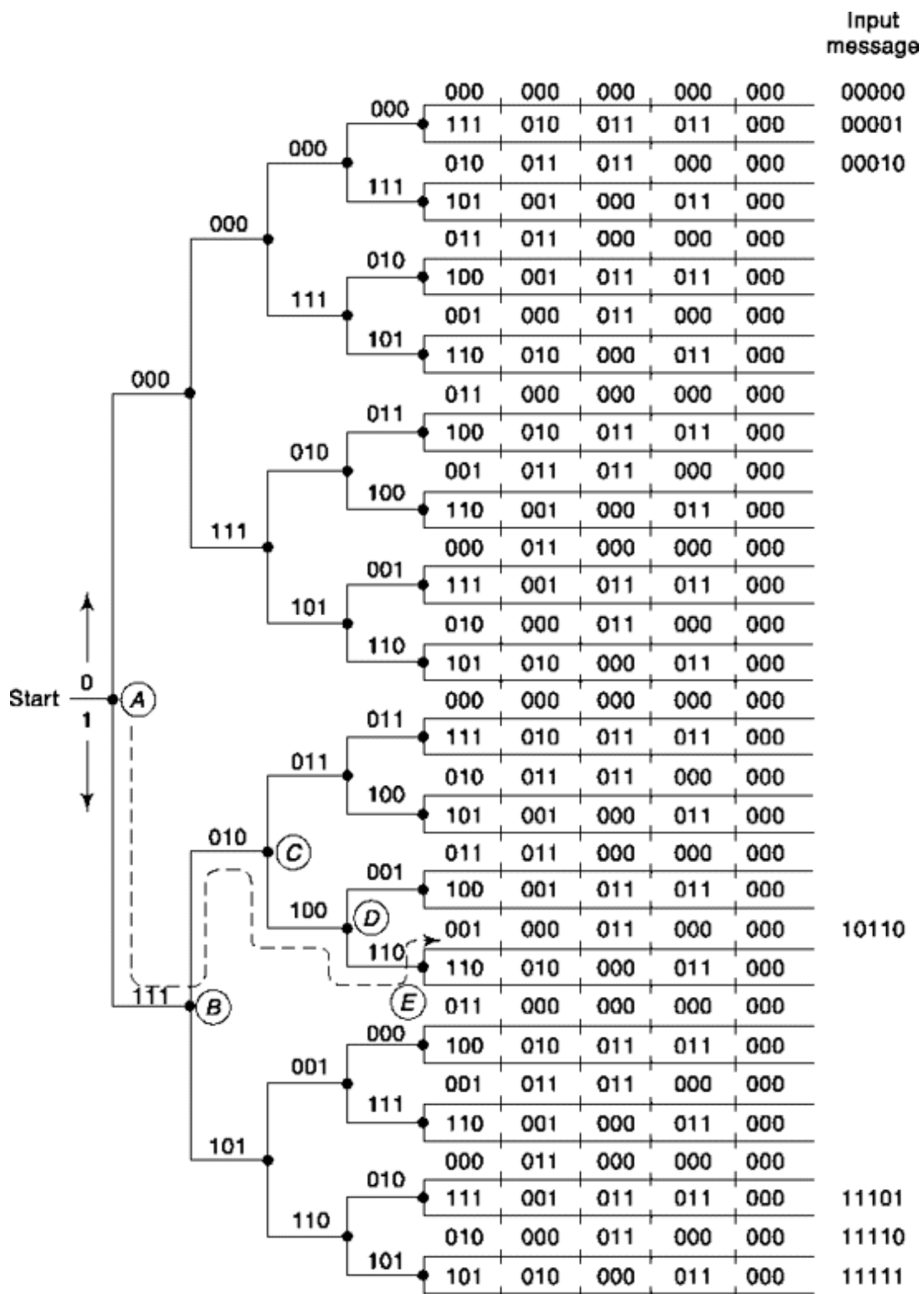


Fig. 14.13 Code tree for encoder of Fig. 14.12.1: $K = 4, L = 5, v = 3$. (from Ref.2.)

Reading, in order, the bits encountered from entrance to exit of the tree, we find precisely the code given in Eq. (14.107) for the message of Eq. (14.106).

Note that any path through the tree passes through only as many nodes (L) as there are bits in the input message. The node corresponds to a point where alternate paths are possible depending on whether the next message bit is 1 or 0. The extension of the terminal branches of the tree corresponds to the process of clearing the last message bit through the shift register.

Decoding in the Presence of Noise

In the absence of noise, the codeword will be received as transmitted. In this case it is a simple matter to reconstruct the original message. We simply follow the codeword through the code tree v bits at a time. The message is then reconstructed from the path taken through the tree, or, equivalently, from the terminal branch of the tree at which the path is completed. But suppose that; on account of noise, the word received is not as transmitted. How shall we undertake to reconstruct the transmitted code word in a manner which, hopefully, will correct errors? A recommended procedure is the following:

Consider the first message bit. This first message bit has an effect only on the first Kv bits in the code word. Thus, with $K = 4$ and $v = 3$, as for the tree of Fig. 14.13, the first digit has an effect only on the first 4 groups of 3 digits. Hence, to deduce this first bit, there is no point in examining the code word beyond its first 12 digits. On the other hand, we would not be taking full advantage of the redundancy of the code if we undertook to decide about the first message bit on the basis of anything less than an examination of the first 12 bits of the code. We see from the code tree of Fig. 14.13 that there are 16 possible combinations of the first 12 digits which are acceptable code words. These combinations correspond to the 16 possible (incomplete) paths through the code tree which penetrate into the tree only to the extent of passing the first 4 nodes. Let us then compare the first 12 bits of the received code with the 12 bits of each of the 16 acceptable possible paths. We next take a count, for each of the 16 paths, of the number of discrepancies between bits of the received code word and the acceptable codeword corresponding to each path. If now the path that yields the minimum number of discrepancies is a path which diverges upward from the first node (node A in Fig. 14.13), we make the decision that the first message bit is 0. And, of course, if this path diverges downward from node A, we decide that the first bit is 1. Thus, we see that a decision about the first message bit is not made until after a complete exploration of all possible paths which penetrate into

the tree to the extent of including K nodes or equivalently Kv digits. It will be recognized that the operation of convolutional decoding described here is a digital operation which corresponds to the analog correlation detection process described in Sec. 11.3.4.

The second message bit is decided upon in the same manner. Thus, referring to Fig. 14.13, suppose it turns out that, using the above procedure, we decide that the first message bit is 1. Then we start at node B and again examine the 16 paths starting at node B and penetrating into the code tree to the extent of $Kv = 12$ code bits. We compare the 12 code bits corresponding to each of these 16 paths with the 12 received code bits after *discarding the first 3 received code bits*. A decision about the second message bit is now made on the basis of the same criterion used to decide about the first bit. Successive message bits are decoded in the same manner.

In summary, the decoding procedure is the following: The i th message bit m_t is decoded on the basis of previous decisions about the message bits m_1, m_2, \dots, m_{i-1} and on the basis of an examination of the Kv digit span of the received code word that is influenced by m_i . The previous decisions determine the starting node, the i th starting node, for the K node section of the code tree to be examined. Thereafter, m_i itself is decoded by determining which one of the 2^K branch sections of the code tree diverging from the i th starting node exhibits the fewest discrepancies when compared with the Kv digit span of the received code word that is influenced by m . If this section of the code tree diverges upward from the i th starting node, the i th message digit is 0; otherwise it is 1.

It turns out that when a message is decoded in the manner we have just described, the probability that a bit in the decoded message is in error decreases exponentially with K . Hence, there is an interest in making K as large as possible. On the other hand, as noted, the decoding of each bit requires an examination of the 2^K branch sections of the code tree. Hence, for large K , the above, general, decoding procedure may involve such a lengthy procedure that it is simply not feasible. We therefore consider next a *sequential* decoding scheme that remains manageable even when K is large.

14.5.3 sequential Decoding

The principal advantage of sequential decoding is that such decoding generally allows the decoder to avoid the lengthy process of examining

every branch of the 2^K possible branches of the code tree in the course of decoding a single message bit. In sequential decoding, at the arrival of the first v code bits, the encoder compares these bits with the two branches which diverge from the starting node. If one of the branches agrees exactly with these v code bits, then the encoder follows this branch. If, because of noise, there are errors in the received bits, the encoder follows the branch, in comparison with which the received bits exhibit the fewer discrepancies. At the second node, a similar comparison is made between the diverging branches and the second set of v code bits, and so on, at succeeding nodes.

Now suppose that in the transmission of any v bits, corresponding to some tree, branch errors have found their way into more than half the bits. Then at the node from which this branch diverges the decoder will make a mistake. In such a case, the entire continuation of the path taken by the encoder must be in error. Consider, then, that the decoder keeps a record, as it progresses, of the total number of discrepancies between the received code bits and the corresponding bits encountered along its path. Then, after having taken a wrong turn at some node, the likelihood is very great that this total number of discrepancies will grow much more rapidly than would be the case if the decoder were following the correct path. The decoder may be programmed to respond to such a situation by retracing its path to the node at which an apparent error has been made and then taking the alternate branch out of that node. In this way the decoder will eventually find a path through K nodes. When such a path is found, the decoder decides about the first message digit on the basis of the direction of divergence of this path from the first node. Similarly, as before, the second message is determined on the basis of a path searched out by the decoder, again K branches long, but starting at the second starting node and on the basis of the received code bit sequence with the first v bits discarded.

We consider now how the decoder may judge that it has made an error and taken a wrong turn. Let the probability be p that a received code bit is in error, and let the encoder already have traced out a path through l nodes. We assume $l < K$, so that the decoder has not yet made a decision about the message bit in question. Since every branch is associated with v bits, then, on the average over a long path of many branches, we would expect the total number of bit differences between the decoder path and the corresponding received bit sequence to be $d(l) = plv$ even when the correct path is being followed. In Fig. 14.14 we have plotted $d(l)$ in a coordinate system in which

the abscissa is l , the number of nodes traversed, and the ordinate is the total bit error that has accumulated. We would expect that, if the encoder were following the correct path, the total bit errors accumulated would oscillate about $d(l)$. On the other hand, shortly after a wrong decoder decision has been made, we expect the accumulated bit error to diverge sharply as indicated. A *discard level* has also been

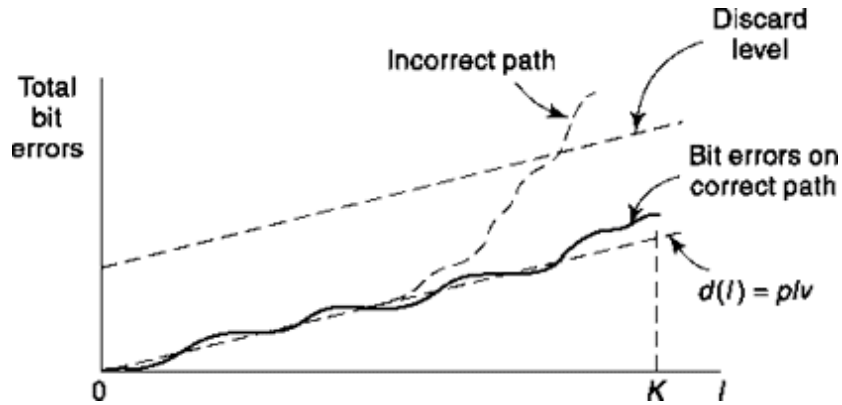


Fig. 14.14 Setting the threshold in sequential decoding.

indicated in the figure. When the plot of accumulated errors crosses the discard level, the decoder judges that a decoding error has been made. The decoder then returns to the nearest *unexplored* branch and starts moving forward again until, possibly, it is again reversed because the discard level is crossed. In this way, after some trial and error, an entire K -node section of the code tree is navigated. And at this point, a decision is made about the message bit associated with this K -node section of the tree. In Fig. 14.14 the discard level line does not start at the origin in order to allow for the possibility that the initial bits of the received code sequence may be accompanied by a burst of noise.

The great advantage of sequential decoding of a convolutional code is that such decoding makes it unnecessary, generally, to explore everyone of the 2^K paths in the code tree section. Thus, suppose it should happen that the decoder takes the correct turn at each node. Then, in this case, the decoder will be able to make a decision about the message bit in question on the basis of a *single* path. Let us assume that at some node the decoder errs and must return to this node to take an alternative branch. Then even the information that an error has been made is useful because thereafter the decoder may exclude from its searchings all paths which diverge in the original direction from this node. The end result is that sequential decoding

may generally be accomplished with very much less computation than the direct decoding discussed earlier.

14.5.4 State and Trellis Diagrams

A node, in the tree diagram of Fig. 14.13, is a point from which a branch diverges in one direction or the other depending on whether the next message bit is a 1 or a 0. Thus, the number of new nodes at each stage increases exponentially with the number of input bits. However, as we shall see, there is a great deal of redundancy in the tree diagram. To reduce this redundancy we consider a structure referred to as a *trellis*. The trellis avoids the redundancy of the tree while allowing, as does the tree, an effective representation of the response of a convolutional coder to an input bit stream.

Consider the convolutional coder of Fig. 14.15. It is a rate 1/2 encoder with $v_1 = s_1 \oplus s_3$ and $v_2 = s_1 \oplus s_2 \oplus s_3$. In any clock interval k , the outputs v_1 and v_2 depend on the bit moved into the encoder at the start of that interval and depend also on the past history which the encoder has experienced, i.e., on the sequence of earlier input bits. This past history is recorded in the content of memory bits M_1 and M_2 . Following the terminology associated with sequential logic systems, we use the term *states* to characterize the individual possible past histories of the system which are relevant to the future response of the

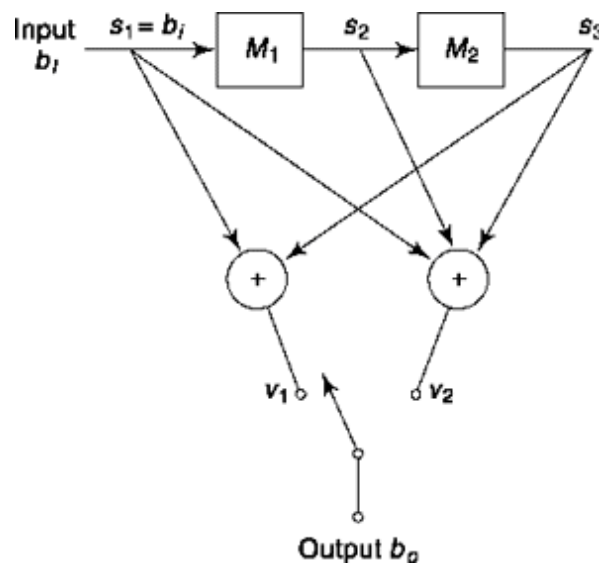


Fig. 14.15 A convolutional coder.

system. Accordingly, we find that the encoder of Fig. 14.15 has four states a , b , c and d corresponding to $M_1M_2 = 00, 01, 10$ and 11 , respectively.

One way in which we can represent the response of the encoder to an arbitrary input sequence is through the *state diagram* of Fig. 14.16. Here the four states are shown, and transitions from state-to-state are represented by arrows. The dashed arrows represent state-to-state transitions which result from inputs and the solid arrows from 1 inputs. Each arrow is also marked with the encoder output v_1v_2 determined by the state and the next input. Thus, for example, suppose that during clock interval k the encoder is in state a ($M_1M_2 = 00$) and the next input bit is a 1 transferred into M_1 at the beginning of clock interval $k + 1$. Then this input will cause the encoder to make a transition to state c ($M_1M_2 = 10$) in which state it will remain for the duration of clock interval $k + 1$ and further, during this interval the output will be $v_1 v_2 = 11$

An alternative representation is shown in Fig. 14.17. In this *trellis structure* the states, each of which appears just once in the state diagram of Fig. 14.16, are duplicated for each new clock cycle. The possible state transitions from clock cycle k to clock cycle $k + 1$ are shown as are the corresponding outputs. The symbolism follows the convention used in Fig. 14.16. The transitions and outputs from $k + 1$ to $k + 2$ (not shown) are, of course, duplicates of the transitions and outputs from k to $k + 1$. Finally, we note that, if the encoder has n memory elements, the number of states is 2^n . There is a one-to-one correspondence between the states of Figs. 14.16 and 14.17 and the nodes of the tree diagram of Fig. 14.13. Since in the tree diagram, the nodes proliferate without limit, it is clear that, as the tree expands, the same set of nodes reappear time and again.

Suppose that we start at an arbitrary state, say state b during interval k in Fig. 14.17. The next input bit will carry the encoder over one of 2 branches either to state a or to state c where it will remain during interval $k + 1$. The second bit will carry the encoder from $k + 1$ to $k + 2$ over one of four possible branches, two from state a and two from state c . During interval $k + 2$, any of the four states is possible. Since the number of branches leaving each state is two, the number of branches from $k + 2$ to $k + 3$ is $4 \times 2 = 8$. Thereafter, the number of branches available is always eight. Altogether then the total number of paths through the trellis from its start, at $k = 1$, to its end

at $k = L$ is 2^{L-1} . We note the rapid (exponential) increase of paths with increasing L .

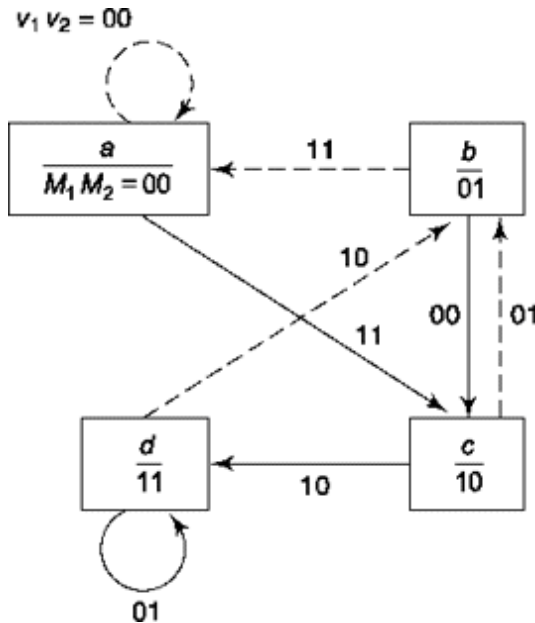


Fig. 14.16 The state diagram for the coder of Fig. 14.15.

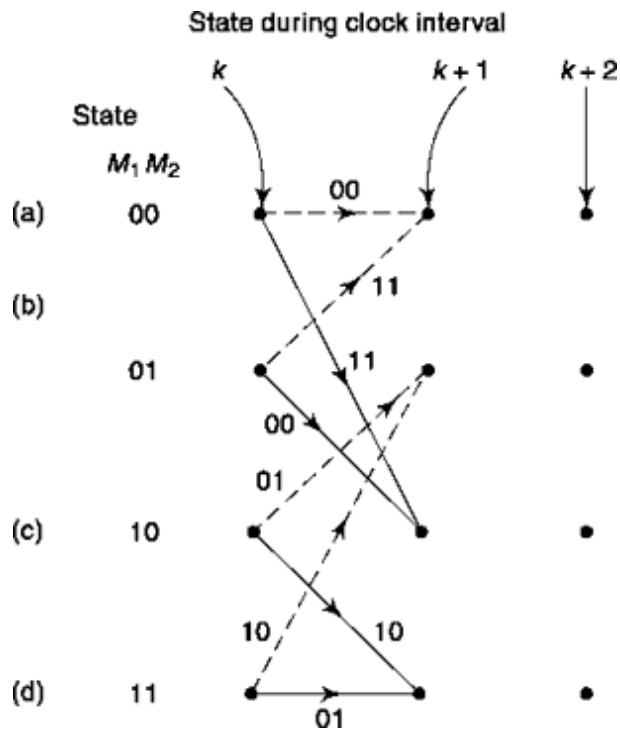


Fig. 14.17 A trellis diagram for the coder of

14.5.5 The Viterbi Algorithm

As noted, a common procedure with a convolutional coder is to start with the coder cleared, then to run a block of information bits through the encoder and finally to add 0 bits as needed to return the codes to the cleared state. Under such circumstances, a decoding procedure which readily recommends itself and which, as a matter of fact yields a decoded output with the minimum likelihood of error, is the following: Let us consider *all possible paths* through the coder from the starting point to the end point. Each possible input information bit sequence generates its own path. For each such path let us determine the corresponding sequence of coder output bits. Next let us compare each one of these output sequences with the actual received sequence. If we find that the received sequence is exactly identical to a sequence corresponding to some particular path through the coder then we shall assume that the information input sequence is the one corresponding to that particular path. If we find no exact correspondence then we shall assume the input sequence to be the one whose path generates the *fewest bit discrepancies* when compared to the received sequence. We have, however, noted that the number of paths increases exponentially with sequence length. Hence, the suggested procedure seems hardly to be feasible except for very short sequences. However, it turns out, through the application of an algorithm due to Viterbi, that many paths may be discarded thereby rendering the procedure much more useful.

To illustrate and explain the Viterbi algorithm, let us use the encoder of Fig. 14.15. We assume that the encoder is initially cleared, i.e. the encoder is in state a (Fig. 14.17) with $M_1M_2 = 00$. Now let there be presented at the encoder a sequence of five information bits, and let it be that the corresponding *received* v_{1R}, v_{2R} bits (not the transmitted encoder output bits) are

$$v_{1R}, v_{2R} = 10\ 00\ 10\ 00\ 00 \quad (14.108)$$

It is readily apparent at the outset that at least one and possibly more errors must have been introduced in transmission. For, as appears in Fig. 14.17 starting from state a , if the first information bit

were a 0 the first two received bits should have been $v_{1R}, v_{2R} = 00$, while if the first information bit had been a 1 the first two received bits should have been $v_{1R}, v_{2R} = 11$. In either case $v_{1R}, v_{2R} \neq 10$.

First, without reference to the received sequence, let us trace the possible paths through the encoder states as shown in the trellis of Fig. 14.18. Starting at state a , in clock interval $k = 1$, a 0 (dashed line) will cause an output 00, as indicated and will carry the encoder again to state a . A 1 (solid line) will generate an output 11 and will carry the encoder to state c . Using the information provided in Fig. 14.17, the remainder of the transitions shown in Fig. 14.18 can be verified. Next, taking account of the received sequence, we have indicated in parenthesis in Fig. 14.18 the number of bit discrepancies in each clock cycle between the bits associated with the paths in the trellis diagram and the actual received bits. Thus, starting at state a with $k = 1$, a 0 input to the encoder should generate an output 00. Since the actual output is 10 the number of bit discrepancies is one. In the next interval the input 0 should again yield an output 00 and since the corresponding set of received bits is indeed 00, there are no discrepancies. Finally, we have also indicated in Fig. 14.18, in circles, the *cumulative* number of bit discrepancies encountered in reaching any state. Thus, to reach state c at $k = 3$ we go first from a at $k = 1$ to a at $k = 2$ encountering one discrepancy and then to c encountering two more discrepancies for a cumulative sum of three discrepancies. The states at $k = 4$ can be reached by *two* paths and we have noted the cumulative discrepancies for *both* paths.

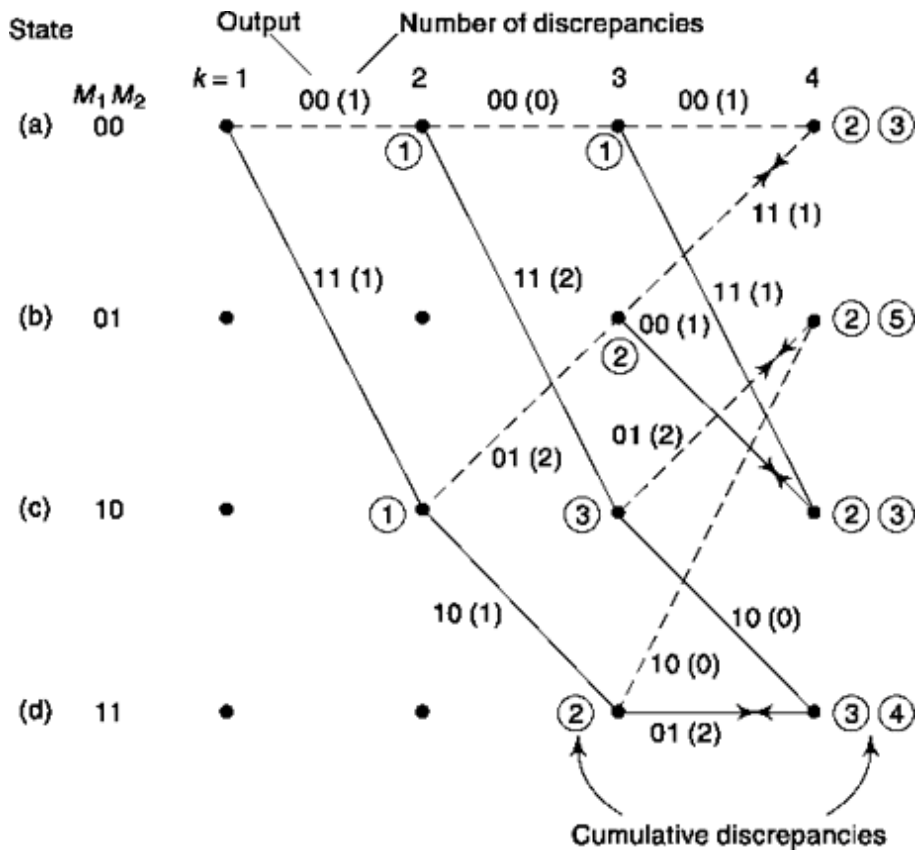


Fig. 14.18 Showing the possible paths through the trellis of Fig. 14.17.

The important point that needs now to be noted is the following: Suppose we consider any complete paths through the entire trellis from state a at $k = 1$ back to state a at $k = L$. Suppose, for example that the path passes through state b at $k = 4$. Let us assume that the path from state b at $k = 4$ to the end of the trellis is known, but, that to go from state a at $k = 1$ to state b at $k = 4$, we are free to select either of the two available paths. Our interest lies in the *complete* path which has the smallest cumulative discrepancy. The number of discrepancies accumulated beyond state b is fixed by the fixed path selected. Hence, the *complete* path of interest is the path whose cumulative discrepancy up to state b at $k = 4$ is the smaller. On this basis, one of the two paths leading to state b can be discarded. We accordingly keep the path to b with cumulative discrepancy 2 and *discard* the path with cumulative discrepancy 5. This discard can be accomplished without affecting any other paths by deleting the transition from c at $k = 3$ to b at $k = 4$. The cross marks through that transition in Fig. 14.18 indicates that discard. Other discards of transitions leading to other states is similarly indicated. We now observe that there are only four paths leading to the states at $k = 4$ rather than the sixteen that we would otherwise have. The same algorithmic processes can be

applied at $k = 5$, etc. That is, at each state which is reached by two paths, one of the paths can be discarded so that, as we proceed through the trellis, we need only keep account of four paths. Of course, in the general case, the number of paths which survive is equal to the number of states.

The four *surviving* paths which reach $k = 4$ in Fig. 14.18 are redrawn in Fig. 14.19. It is left as a student exercise (Prob. 14.34) to extend the trellis of Figs. 14.19. It will then be verified that, for the output sequence of Eq. (14.108), the path through the trellis corresponding to an input bit stream consisting of all 0's yields the minimum number of bit discrepancies. With such a result we would then decide that the input information sequence was all 0's. If, indeed, in a real situation, the input sequence was all 0's then the received sequence, as is readily verified, should also be all 0's. If then, because of noise, the received sequence was as given in Eq. (14.108), the coder would have corrected two errors.

As a result of the reduction of paths entering each node from 2 to 1, there are only four paths at each value of k . However, when the information bit stream is long, the amount of information that must be stored, in memory, to record the four possible bit streams, and the error associated with each, becomes enormous. For example, if data is sent at the rate of 10 Mb/s for one second, 10 M bits of data is transmitted. The memory must therefore store more than 40 M bits of data.

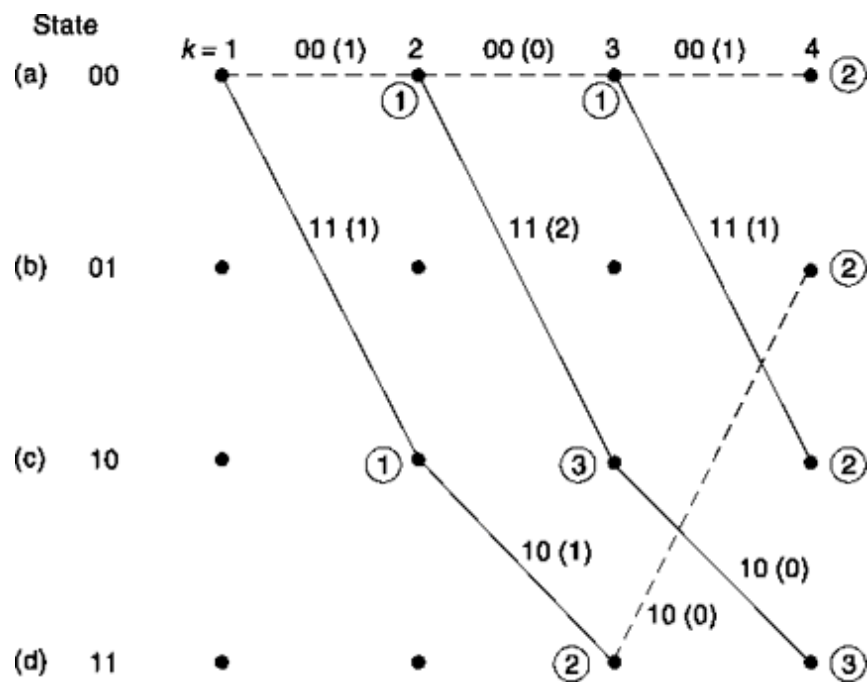


Fig. 14.19 The surviving paths through the trellis of Fig. 14.18.

To reduce the data-handling capability required of the decoder, the Viterbi algorithm presents a suboptimum procedure which truncates the trellis after L nodes. Typically, $L = 5K$ where K is the *constraint length*, i.e. the number of memory elements. Thus, if $K = 7$, $L = 35$ bits. When truncating the trellis we look at the trellis after L bits are received. We then choose that path (remember there are four paths) with the fewest errors and delete the remaining three paths. In this manner the memory is reduced to somewhat more, than L bits as after each decision the $L/2$ data information bits are outputted from the system.

The reason that the Viterbi truncation technique is sub-optimum is that we are choosing the minimum number of errors from among the paths terminating at nodes a , b , c and d when $K = L$. Such a comparison is not optimum since each node yields a distinct path and is then not comparable. An optimum system would make a decision only after receiving the entire message.

14.5.6 probability of Error of Convolutional Codes

The calculation of the probability of error of a convolutional code is beyond the scope of this text and the interested reader is referred to the references [5]. For the special case of a rate 1, constraint length $K = 7$ code, the probability of a bit error is upper bounded by

$$P_b < 36D^{10} + 211D^{12} + 1404D^{14} + 11,633D^{16} + \dots \quad (14.109)$$

where

$$D = 2\sqrt{p(1-p)} \quad (14.110a)$$

and

$$p = \frac{1}{2} \operatorname{erfc} \sqrt{\frac{E_b}{\eta}} \quad (14.110b)$$

14.6 COMPARISON OF ERROR RATES IN CODED AND UNCODED TRANSMISSION

In this section we compare block-coded and uncoded systems to obtain some idea of their relative error rates. We do this under the condition that the rate of information transmission (messages or words per unit time) is the same in the two cases. Then, coded or uncoded, a word must have the same duration T_w . Since the coded word has more digits than does the uncoded word, the bit duration T_c in the coded case must be less than the bit duration

T_b in the uncoded case. We have seen, however, that as the bit duration decreases, the probability of error in a bit increases. We have then to inquire whether coding yields a net advantage. For the sake of being specific, we shall compare k -bit uncoded transmission with transmission using an (n, k) block code. We shall, of course, assume that the signal power P_s and the thermal-noise power spectral density h are the same in both cases.

We shall use the symbols p and p_c to represent, respectively, the probability of error in a bit in (c) the uncoded and coded cases, reserving the symbols P_e and P_e for the probability of error of an uncoded or coded word. The energy in a bit in the uncoded case is $E_s = P_s T J k$ and $= P_s T J n$ in the coded case. Hence, from Eq. (11.55), assuming matched-filter reception,

$$p = \frac{1}{2} \operatorname{erfc} \sqrt{\frac{P_s T_w}{k \eta}} \quad (14.111)$$

and

$$p_c = \frac{1}{2} \operatorname{erfc} \sqrt{\frac{P_s T_w}{n \eta}} \quad (14.112)$$

In the uncoded case, a word will be in error if one or more digits are in error. The probability that a digit is not in error is $1 - p$. The probability that all k digits are not in error is $(1 - p)^k$. The probability of at least one bit error, and hence a word error, is

$$P_e = 1 - (1 - p)^k \approx kp \quad (14.113)$$

since typically $kp \sim 10$ or smaller.

Consider using a (7,4) single error correcting Hamming code. Then a word error occurs only if two or more errors occur. It may be verified (Prob. 14.37) that if $p_c \ll 1$ the likelihood of more than two errors is entirely negligible in comparison with the likelihood that one or two errors will occur. For $n = 7$ (7 digits in the coded word), the probability of just two errors, and hence the probability of a word error, is

$$P_e^{(c)} = \binom{7}{2} (1 - p_c)^5 p_c^2 \quad (14.114)$$

where $\binom{7}{2}$ is the number of combinations of seven things taken two at a time.

Since $\binom{7+6}{2} = 21$ and assuming that $p_c \ll 1$, we have

$$P_e^{(c)} \cong 21 p_e^2 \quad (14.115)$$

From Eqs. (14.111) and (14.113) with $k = 4$, we have

while from Eqs. (14.112) and (14.115) we find

$$P_e^{(uc)} = 5.25 \left(\operatorname{erfc} \sqrt{\frac{P_s T_w}{7\eta}} \right)^2 \quad (14.117)$$

For the purpose of comparing the performance of coded and uncoded transmission, Eqs. (14.116) and (14.117) are plotted in Fig. 14.20. Note that when $P_s T_w/r = EJr$ is greater than 9 dB, coded transmission results in lower probability of error than uncoded transmission. The difference, however, is not significant until E_s/r exceeds 16 dB. When E_s/r is less than 9 dB, the coded system has a higher probability of error than does the uncoded system.

Note that coding is not a cure-all. The complicated and expensive coding and decoding equipment needed does not yield significant improvement in this example until E_s/r is large. Here we see that at a probability of error in a word of 10^{-6} , the E_s/r difference between systems is only about 1 dB. Before deciding to employ coding, we should therefore carefully analyze the system response, with and without coding, to determine if the improvement obtained is worth the complication and expense.

The reader may well inquire at this point about why one studies coding if our improvement is only 1 dB. The answer is that the improvement may be considerably greater than 1 dB depending on the coding technique employed and the length of the code.

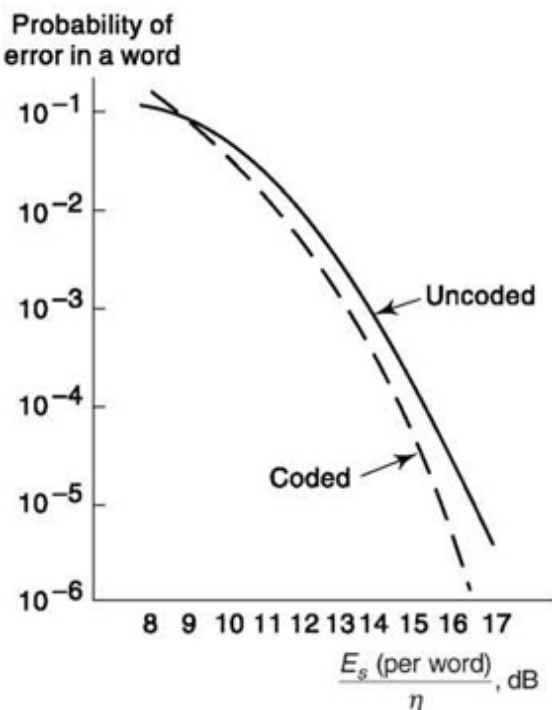


Fig. 14.20 Probability of error for an uncoded (4 bit) and a coded (7 bit) system.

Table 14.3 compares several coding techniques when using BPSK or QPSK modulation on a Gaussian channel. The *coding gain* is used as the basis of comparison. The coding gain refers to the number of dB that the signal-to-noise ratio, E_b/h , can be reduced from the value required when there is no coding and still provide the same bit error rate, P_b . Then to achieve the *same* P_b , the coding gain A is

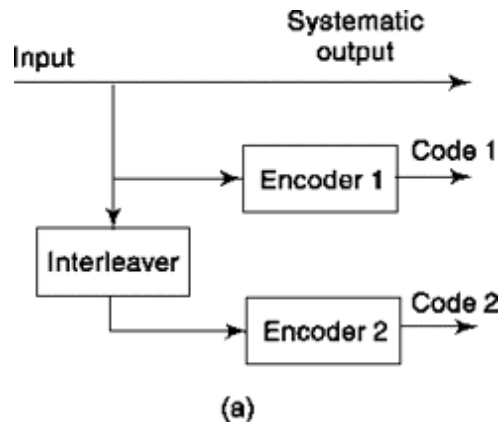
$$A = \frac{(E_b/\eta)_{\text{uncoded}}}{(E_b/\eta)_{\text{coded}}} \quad (14.118)$$

Table 14.3 Comparison of Coding Techniques on a Gaussian Channel

Coding technique	Coding gain (dB)	
	$P_b = 10^{-5}$	$P_b = 10^{-8}$
Block codes (hard decision)	3–4	4.5–5.5
Convolutional coding with sequential decoding (hard decision)	4–5	6–7
Convolutional coding with Viterbi decoding (hard decision)	4–5.5	5–6.5
Block codes (soft decision)	5–6	6.5–7.5
Convolution encoding with sequential decoding (soft decisions)	6–7	8–9
Concatenated codes (RS and convolutional coding with Viterbi decoding) (hard decisions)	6.5–7.5	8.5–9.5

14.7 TURBO CODES

Turbo codes are a relatively new development which gets very close to Shannon's limit. This is formed by *parallel* concatenation of two encoded data separated by an interleaver. Although various forms of Turbo codes have been used since its emergence in 1993, it is systematic in general, i.e. input-bits also occur in the output and the interleaver is pseudo random in nature. The arrangement is shown in Fig. 14.21a which makes two encoder outputs uncorrelated. The encoder as can be seen from one typical representation (Fig. 14.21b) is a convolution coder with feedback and is also known as *recursive systematic convolution* (RSC) coder. The data is usually processed as block, the size determined by the interleaver size and the frames are terminated (i.e. encoders are forced to a known state after each block) with termination tail appended to encoded data. If block size is large, then the RSC codes appear nearly random to the channel and from coding theory the more random is the code, the closer it is to Shannon's channel capacity.



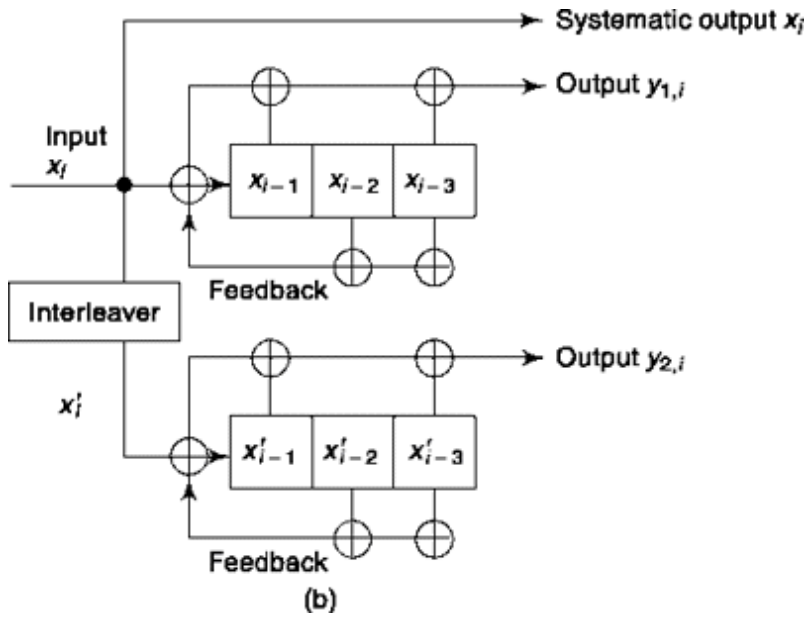


Fig. 14.21 (a) Turbo encoder block diagram. (b) A typical encoder.

One would definitely believe that the Turbo codes are difficult to decode. But in spite of the randomness in data, it has information and structure for a decoder to work it out. The term ‘Turbo’ is coined to refer to the decoding process which reminds one ‘turbo engine’ principle involving feedback. The decoding strategy uses some sort of soft decision and information exchange in the form of soft inputs between two decoders; the analogy used by the proposer of this method is decoding of a crossword puzzle. One uses both ‘down’ and ‘across’ clues to arrive at a word. The ‘down’ clue may suggest one word with some confidence (soft decision) and may be few other words. A clue from a ‘across’ word may improve the confidence and vice versa. After few iterations, one is able to make a hard decision about a word. Similar method is adopted in Turbo decoding. The information available from a priori probabilities are used in addition to current observation at decoder output to generate posterior probabilities. Of two outputs, one may be decoded and its output can be used as a priori probability to next decoder (Fig. 14.22) for decoding second encoded sequence.

The above equation says when we gain some information from one decoder (the ratio can be positive or negative), it gets added through a feedback as shown and helps to make decision (soft). After few iterations, based on whether $r(b_i)$ is positive or negative, a decision on b_t is taken: 1 if positive, 0 if negative. In one implementation, to prevent positive feedback a priori, probabilities to the decoder

is subtracted from decoder output $r(b_i)$ and $r(b)$ is forwarded to the next stage.

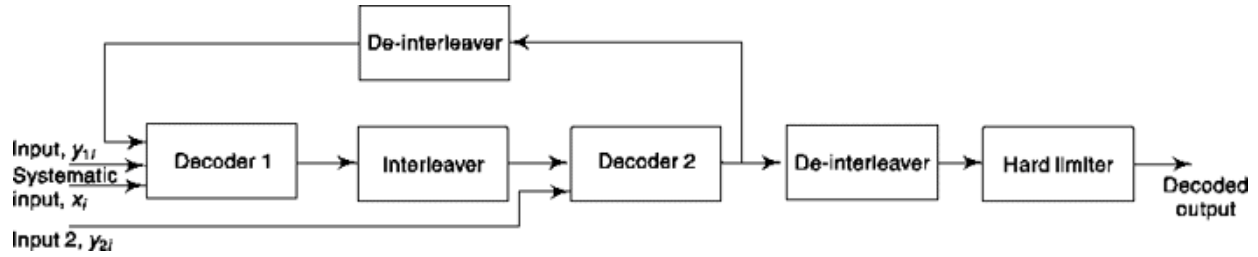


Fig. 14.22 Block diagram of a turbo decoder.

We define posterior probability for i -th bit b_i and conditional probability as

$$\Gamma(b_i) = \log \frac{\Pr(b_i=1, \text{observation})}{\Pr(b_i=0, \text{observation})} \text{ and } \bar{\Gamma}(b_i) = \log \frac{\Pr(\text{observation}/b_i=1)}{\Pr(\text{observation}/b_i=0)} \text{ respectively.}$$

We know from Eq. (6.9), $P(A,B) = P(A)(B/A)$. Combining apriori probabilities and information gained from current observation followed by log of their ratio we get,

$$\Gamma(b_i) = \log \frac{\Pr_{\text{apriori}}(b_i=1)}{\Pr_{\text{apriori}}(b_i=0)} + \log \frac{\Pr(\text{observation}/b_i=1)}{\Pr(\text{observation}/b_i=0)} \quad (14.119a)$$

$$\text{or, } \Gamma(b_i) = \log \frac{\Pr_{\text{apriori}}(b_i=1)}{\Pr_{\text{apriori}}(b_i=0)} + \bar{\Gamma}(b_i) \quad (14.119b)$$

The performance of Turbo Coder is near optimal for high SNR and converges quickly. For low SNR, it takes relatively more iterations to converge and the error rate reduces with more number of iterations. Today, turbo codes are vital in deep space missions to cellular communications down earth.

14.8 LOW DENSITY PARITY CHECK CODES

Low Density Parity Check (LDPC) codes belong to the family of linear block codes that is near optimal. Its performance is comparable to Turbo codes in digital communication systems affected by high noise. We have seen that a linear block code is represented by (n, k) where n is the codeword length and k is the length of information bit and $(n - k)$ bits are used for parity. Compared to Turbo codes, the decoding of LDPC codes is simpler and easier to implement in hardware due to implicit parallelism. LDPC codes also give lower error floor and higher code rate. However, all these advantages come when code length is quite large, i.e. $n > 1000$, and also the

design of encoder for LDPC codes is more complex than Turbo codes. In this discussion, we shall use a smaller code length to keep things tractable and for the purpose of understanding.

Let us start with the parity check matrix H of $(7,4)$ the block code given by Eq. (14.48b) of Sec.

14.3.1 as LDPC code. This is reproduced in Fig. 14.23a. Let a_t represent the number of 1s in the

$$\bar{H} = \begin{bmatrix} 1 & 1 & 1 & 0 & 1 & 0 & 0 \\ 1 & 1 & 0 & 1 & 0 & 1 & 0 \\ 1 & 0 & 1 & 1 & 0 & 0 & 1 \end{bmatrix}$$

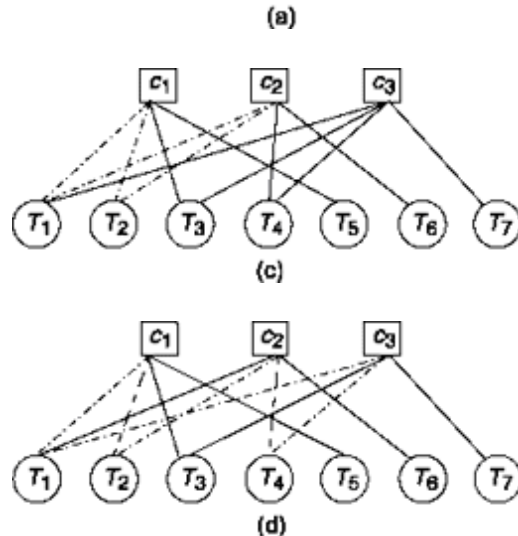


Fig 14.23 (a) A parity check matrix H of $(7,4)$ block code, (b) Tanner graph of H , the square box represents check node and circles represents bit node. (c) Presence of a cycle of 4 shown by dash-dot lines, (d) Presence of a cycle of 6.

i -th row and b_j represent the number of 1s in the j -th column. The encoding process of LDPC code requires the parity check matrix H to be *sparse* or of low density. This means H will consist of only a small number of 1s and mostly 0s. The abundance of 0s reduces the computational effort. The encoding also requires $a_i \leq n$ and $b_j \leq n$. If $a_i = a$ (constant) and $b_j = b$ (constant) for all rows and columns, it is called regular LDPC code. If not, it is known as irregular LDPC code. In our example, H matrix $a_t = 4$ for all rows but $b_j = 3$ for $j = 1$, i.e. 1st column $b_j = 2$ for remaining columns. The third requirement is to avoid short cycles. Let us understand short cycles through what is known as Tanner graph introduced by R. M. Tanner in 1981.

Incidentally, LDPC code was first introduced by R. G. Gallager in 1963 but was not found effective due to presence of short cycles.

In Fig. 14.23b, we draw the Tanner graph of H matrix of Fig. 14.23a. The top square nodes represent parity check bits c , and the bottom circular nodes represent code bits T_j . A connection or edge exists between c_t and T_j if corresponding element of H matrix $h_{jt} = 1$, else there is no edge. If we follow the first row of H , we get all the edges of c_1 check bit node. The four 1s are at place

1, 2, 3 and 5 and the accordingly connection is made from c_1 to T_1, T_2, T_3 and T_5 . Similarly, other edges are connected and we get the final Tanner graph of H as shown in Fig. 14.23b. A cycle exists in Tanner graph if connected edges form a closed loop that start and end in the same node. The number of edges traversed in closing a loop gives the length of the cycle. In Fig. 14.23c and 14.23d, two cycles of lengths 4 and 6 are shown using dash-dot lines. It is left as a student exercise to find other cycles and their lengths from this Tanner graph.

As has already been mentioned, LDPC coding requires avoidance of short cycles. This is to make decoding easier. A cycle of 4 can be avoided if no two columns overlap at two places. But it would be useful to avoid cycles of 6, 8 too. We have also noted that the advantage of LDPC code lies for high values of n and when $a_t \ll n$ and $b_j \ll n$. A computer-based search technique is more suited to encode LDPC codes.

Hard Decision Decoding

There are different decoding algorithms for LDPC codes but each is based on message-passing operation along the edges of a Tanner graph. In this, messages pass from the check node and bit node iteratively and each node decides locally what to pass based on information available to it in that iteration. Let us discuss one method named the *bit-flipping algorithm* where a binary message is passed as hard decision from check nodes to bit nodes. The decision is arrived at by parity-check equation or modulo-2 sum of the incoming bit values. A bit node flips or alters its current value if *majority* of the messages from all connected check nodes reaching the bit node along the edges are different from the current bit value. Let us continue with the H matrix of Sec. 14.3.1 shown in Fig. 14.23. We consider the erroneous code word [1 0 0 0 0 1 1] of Eq. (14.56) from Sec. 14.3.2 and see how the error in

the 5th bit is corrected through message passing following bit-flipping algorithm. Figure 14.24 gives a Tanner graph based representation of the steps. In Fig. 14.24a, we write the erroneous code word in bit nodes. We use solid lines if a check node receives a 1 from a bit node and a dotted line if it receives 0. In Fig. 14.24b, we show how the binary decision made at a check node is passed to a bit node as a message along the edges. We use the earlier notation of representing 1 by solid lines and 0 by dotted lines. The arrow direction indicates the direction of information whether it is from bit node to check node or reverse in a particular stage of iterative algorithm. Now let us see how a check node makes decision. Let us represent an edge by S_{ij} that connects i-th check node to j-th bit node. Then for this Tanner graph (Fig. 14.24b),

$$\epsilon_{11} = T_2 \oplus T_3 \oplus T_5 = 0 \oplus 0 \oplus 0 = 0$$

Accordingly, e_n is represented by dotted line in Fig. 14.24b indicating binary message 0 is passed from 1st check node to 1st bit node as decision. Similarly,

$$S_{12} = T_1 \oplus T_3 \oplus T_5 = 1 \oplus 0 \oplus 0 = 1 \text{ (a solid line connecting 1st check node to 2nd bit node)}$$

$$\begin{aligned}\epsilon_{13} &= T_1 \oplus T_2 \oplus T_5 = 1 \oplus 0 \oplus 0 = 1 \\ \epsilon_{15} &= T_1 \oplus T_2 \oplus T_3 = 1 \oplus 0 \oplus 0 = 1\end{aligned}$$

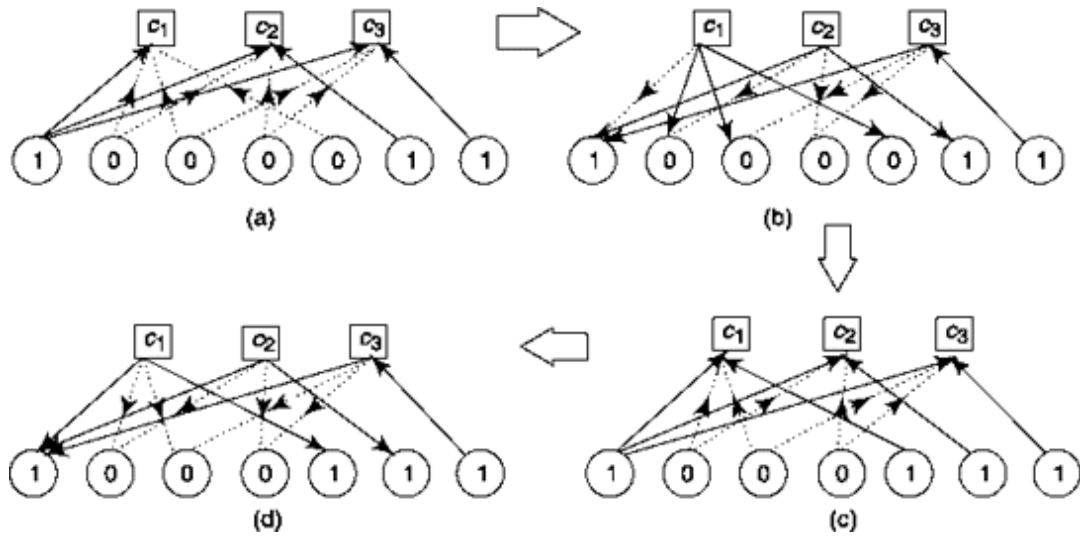


Fig. 14.24 Hard decision decoding by bit-flipping algorithm. A solid line indicates message passed is 1 and a dotted line indicates message passed is 0. The arrowhead shows the direction of message whether from bit node to check node or reverse. (a) to (d) gives snapshots of different stages of the algorithm.

Next, for edges passing messages from 2nd check node to connected bit nodes, we can write

$$\begin{aligned}\varepsilon_{21} &= T_2 \oplus T_4 \oplus T_6 = 0 \oplus 0 \oplus 1 = 1 \\ \varepsilon_{22} &= T_1 \oplus T_4 \oplus T_6 = 1 \oplus 0 \oplus 1 = 0 \\ \varepsilon_{24} &= T_1 \oplus T_2 \oplus T_6 = 1 \oplus 0 \oplus 1 = 0 \\ \varepsilon_{26} &= T_1 \oplus T_2 \oplus T_4 = 1 \oplus 0 \oplus 0 = 1\end{aligned}$$

For edges passing messages from 3rd check node to connected bit nodes, these are

$$\begin{aligned}\varepsilon_{31} &= T_3 \oplus T_5 \oplus T_7 = 0 \oplus 0 \oplus 1 = 1 \\ \varepsilon_{33} &= T_1 \oplus T_5 \oplus T_7 = 1 \oplus 0 \oplus 1 = 0 \\ \varepsilon_{35} &= T_1 \oplus T_3 \oplus T_7 = 1 \oplus 0 \oplus 1 = 0 \\ \varepsilon_{37} &= T_1 \oplus T_3 \oplus T_5 = 1 \oplus 0 \oplus 0 = 1\end{aligned}$$

In the next step of the algorithm, we compare current value at a bit node and messages arriving through edges to that bit node. If the majority of the messages arriving is in disagreement with the current value, the bit is flipped. For T_x bit node, we find one 0 and two 1s arrive as messages and the current value is 1. So, it need not be flipped. For T_2 bit node we find one 0 and one 1 arrive as messages and the current value is 0. Since the majority should disagree to qualify a flip, this bit value too is not flipped. Proceeding in this manner, we find that for the T_5 bit node, the only edge passing a message disagrees and thus this bit value is to be flipped. This is shown in Fig. 14.24c. We keep iterating the above steps till it converges or a specific number of iterations is reached. In this example, we arrive at Fig. 14.24d following Fig. 14.24c where all the current bit values are in agreement with the binary decisions passed. Hence, the corrected code word is [1 0 0 0 1 1 1]. This is also verified from Eq. (13.119).

Soft Decision Decoding

In soft decision decoding, the message is passed in the form of a probability which is also termed *belief propagation*. This kind of decoding is more complex but yields better result for LDPC codes. Sum-Product decoding is one such iterative technique which we describe briefly here. The input to a sum-product decoder is the parity check matrix H , log likelihood ratio (LLR) of *a priori* probabilities of code bits and maximum number of

iterations. The output of the decoder is maximum *a posterior* probabilities (MAP) of code bits. LLR is the natural logarithm of the ratio of two complementary probabilities like probability of j -th code bit is 1 to probability of j -th code bit is 0 that may be subject to certain condition. Thus, a positive sign of LLR means the numerator probability is higher and it helps taking a decision in favor of that. Similarly, a negative sign helps in taking a decision in favor of the denominator. The magnitude of LLR gives the degree of confidence in that decision. The other advantage of taking log is that the multiplication becomes addition in the log domain which is easier to implement.

Let us continue with the discussion on sum-product algorithm. While received code bit probabilities (depends on condition of communication channel) comprise what is known as *intrinsic* information, the extra information available from fulfillment of check bit constraints constitute *extrinsic* information. In other words, the extrinsic information passed from i -th check bit node to j -th code bit node is the LLR of the probability that j -th code bits satisfy the i -th parity check. The total LLR of each code bit is the sum of all LLRs coming from all connected check nodes in the form of messages along edges. The j -th bit node sends back to i -th check node this sum of LLRs minus LLRs recently received from i -th check node (as i -th check node already has the information it sent). This message passing between bit node and check node goes on till the maximum number of iterations is reached.

Example 14.4

Write the A convolutional coder output equations from data given in first row of Table 14.2. What is the number of bits in output code? Show the output when input to this is 101.

Solution

The output equations are as follows.

$$v_1 = s_1 \oplus s_2 \oplus s_3 \quad (14.12(a))$$

$$v_2 = s_1 \oplus s_3 \quad (14.12(b))$$

Thus the output is 11 10 00 10 11 00

Example 14.5

Show how output can be generated by defining a generator matrix for Example 14.4.

Solution

The generator matrix requires impulse response of the coder. This is the output generated when the initially reset coder is fed with a single 1. The no. of bits in the output code = $2(1 + 3) = 8$

Input	s_1	s_2	s_3	v_1	v_2	Output
initial	0	0	0	0	0	
1	1	0	0	1	1	11
0	0	1	0	1	0	10
0	0	0	1	1	1	11
0	0	0	0	0	0	00

Therefore, impulse response is 11101100

Then generator matrix.

$$G = \begin{pmatrix} 1 & 1 & 1 & 0 & 1 & 1 & 0 & 0 & 0 & 0 & 0 \\ 0 & 0 & 1 & 1 & 1 & 0 & 1 & 1 & 0 & 0 & 0 \\ 0 & 0 & 0 & 0 & 1 & 1 & 1 & 0 & 1 & 1 & 0 \end{pmatrix}$$

Note that, in G , impulse responses appear in a staggered (staggered by number of outputs) manner in each row while the rest of the elements are 0.

Now, output is $b_o = b_i G$ (14.122)

where, input $b_i = [1 \ 0 \ 1]$

Thus output

$$= [1 \ 0 \ 1] \begin{pmatrix} 1 & 1 & 1 & 0 & 1 & 1 & 0 & 0 & 0 & 0 & 0 \\ 0 & 0 & 1 & 1 & 1 & 0 & 1 & 1 & 0 & 0 & 0 \\ 0 & 0 & 0 & 0 & 1 & 1 & 1 & 0 & 1 & 1 & 0 \end{pmatrix} \\ = [1 \ 1 \ 1 \ 0 \ 0 \ 0 \ 1 \ 0 \ 1 \ 1 \ 0 \ 0]$$

Note that, product is logic AND and addition is logic Ex-OR operation.

The output obtained is exactly same as Example 14.4.

SELF-TEST QUESTIONS

7. Can fading channel cause burst error?
8. Is it true that convolutional interleaving requires less memory and offers more flexibility compared to block interleaving?

9. Which of Reed-Solomon and concatenated codes is more efficient in correcting random errors?
10. Does Viterbi algorithm avoids exhaustive search in convolutional coder?
11. What is special in the convolution coder used in Turbo codes?

14.9 AUTOMATIC REPEAT REQUEST (ARQ)

There are two basically different techniques available for controlling transmission errors. The first technique involving the coding schemes, which have been the subject of our interest up to the present, is referred to as *forward-error correction* (FEC). In an FEC scheme we depend on the coding to allow error *correction*. The FEC method has the limitation that if the errors are too numerous, the code will not be effective. Further, to achieve low error rates, it is necessary to add a relatively large number of redundant bits. As a result, the efficiency of the code (i.e., the rate = k/n) is low. It also turns out that good codes invariably involve long codewords whose processing requires complex and expensive hardware. Hence, it is not surprising that, in spite of the very great merit and extensive application of coding, an alternative scheme is also extensively employed.

The alternative scheme is referred to as *automatic-repeat-request* (ARQ) and is used primarily when extremely low error rates are required. In this system, the receiver is not called upon to *correct* but only to *detect* errors. When an error is detected in a word, the receiver signals back to the transmitter and the word is transmitted again. In an ARQ system, then, a *feedback* channel must be provided. Since coding allows more error detection than error correction, ARQ makes more effective use of the coding.

There are three basic ARQ systems. They are (a) *stop-and-wait ARQ*, (b) *go-back N ARQ*, and (c) *selective-repeat ARQ*.

The *stop-and-wait* ARQ system is the simplest to implement and is represented in Fig. 14.25a. The transmitter sends a codeword to the receiver during the time T_w . The receiver receives and processes the received word and if the receiver detects no error, it then sends back to the transmitter a positive-acknowledgement (ACK) signal. Upon receipt of the ACK signal, the transmitter sends the next word. If the receiver does detect an error, it returns to the transmitter a negative-acknowledgement (NAK) signal. In this

case, the transmitter transmits the same message and then waits again for an ACK or NAK response before undertaking further transmission. The elapsed time between the end of transmission of one word and the start of transmission of the next word is T_I . Clearly, the limitation of such a system is that it must stand by idly without transmission while waiting for an ACK or NAK. Nonetheless this system is effectively used in many data systems including IBM's Binary Synchronous Communication (BISYNC) protocol.

The *go-back N* ARQ scheme is represented in Fig. 14.25b. The transmitter sends messages, one after another, without delay and does not wait for an ACK signal. When, however, the receiver detects an error in a message, say message i , a NAK signal is returned to the transmitter. In response to the NAK, the transmitter returns to codeword i and starts all over again at that word. In Fig. 14.25b we have assumed that the propagation delay and the processing at the receiver occupies an interval of such length that when an error is detected in word i the number N of words that are sent over again is $N = 5$. The go-back-N system is readily implemented, and, as we shall see, it is a significant improvement over the stop-and-wait system. The go-back-N scheme is used in many data systems.

The *selective-repeat* ARQ system is represented in Fig. 14.25c. Here the transmitter sends messages in succession, again without waiting for an ACK after each message. If the receiver detects that there is an error in codeword i , the transmitter is notified. The transmitter retransmits codeword i and thereafter returns immediately to its sequential transmission. The selective ARQ, as might well be anticipated, has the highest transmission efficiency of the three systems but, on the other hand, it is the most costly to implement.

14.9.1 performance of ARQ systems

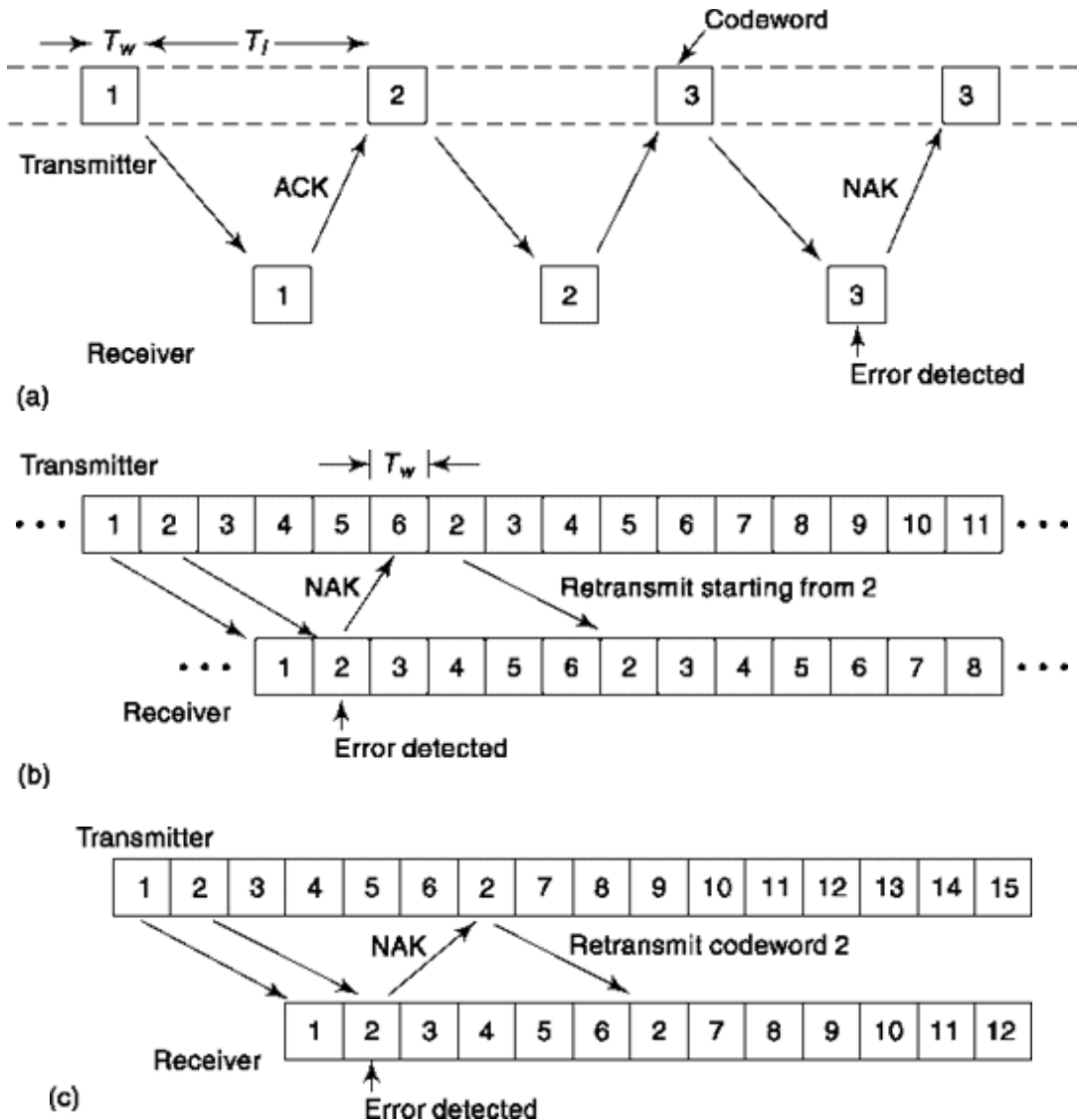


Fig. 14.25 (a) Stop-and-wait ARQ. (b) Go-back NARQ. (c) Selective-repeat ARQ.

14.9.1 Performance of ARQ Systems

The performance of ARQ systems is measured in two ways, by the *probability of error* and by the *transmission efficiency*.

Probability of Error

In an ARQ system, block codes are used for error detection. As discussed earlier, whenever an error is detected, a NAK is returned to the transmitter and the message is repeated. Thus, the only time that a received message is in error is when a received message has a sufficient number of errors and

looks like a different codeword. In such a case, an ACK is returned and therefore an error is made.

To illustrate this point, consider that the messages 0 and 1 are encoded prior to transmission using a (3, 1) repeated code. Thus, one of the codewords 000 or 111 is transmitted. If the receiver receives 001, 010, 100, 110, 101 or 011, a NAK is returned to the transmitter. If, however, either

000 or 111 is received, an ACK is returned. If a 000 was transmitted and a 111 received an error will be made. Thus, if the message 000 is transmitted there are $2^3 = 8$ possible received words and an error is made only when the message 111 is received. If all eight messages were equally likely to be received the probability of error would be $P_e = 1/8$. However, in order for a received word to be in error, all three bits must be in error. Since such an event is *less* likely than any of the other seven possible received words, the probability of error is *less* than 1/8 and we say that P_e is *upper bounded* by 1/8, that is, $P_e < 1/8$.

Let us now generalize our discussion to an arbitrary (n, k) block code. There are now 2^n possible received words and of these there are 2^k codewords. Thus, if a codeword is transmitted, an error will occur if one of the other $2^k - 1$ codewords is received. To upper bound P_e we again assume that all 2^n possible received words are equally likely. Then P_e is

$$P_e \leq \frac{2^k - 1}{2^n} \approx 2^{-(n-k)} \quad (14.123)$$

Example 14.6

If a (1023,973) BCH code is used for error detection, the probability of error P_e is bounded by

$$P_e \leq 2^{-50} \approx 10^{-15}$$

Throughput

The *throughput efficiency* is defined as the ratio of the average number of information bits accepted at the receiver per unit of time to the number of information bits that would be accepted per unit of time if ARQ were not used. While all the ARQ systems yield the same error rate, the throughput efficiencies are different.

Throughput of the stop-and-wait ARQ

Let P_A be the probability that the receiver accepts the message on any particular transmission. Then the probability that only a single transmission is all that is needed for acceptance is P_A . The probability that two transmissions will be required is $(1 - P_A)P_A$ that is, the product of the probability $(1 - P_A)$ that the first transmission was rejected and P_A the probability that it was accepted on the second try. The average number of transmissions required for acceptance of a single word is the sum of the products of the number of transmissions j and the probability of requiring j transmissions, $P_A(1 - P_A)^{j-1}$. Thus (see Prob. 14.43),

$$\bar{N}_{sw} = 1 \cdot P_A + 2 \cdot P_A(1 - P_A) + 3P_A(1 - P_A)^2 + \dots \quad (14.124a)$$

$$= \frac{1}{P_A} \quad (14.124b)$$

We note from Fig. 14.25 that the total time devoted to a single attempt to get the receiver to accept a word is $T_w + T_l$. Hence, on average, the time required to transmit one word is

$$\bar{T}_{sw} = \frac{T_w + T_l}{P_A} \quad (14.125)$$

If ARQ is not used and no coding bits were added to the k information bits, the time needed to transmit the k bits would be

$$T_k = \frac{k}{n} T_w \quad (14.126)$$

The throughput efficiency of the stop-and-wait ARQ system is

$$\eta_{S\&W} = \frac{T_k}{\bar{T}_{sw}} = \frac{k}{n} \frac{P_A}{1 + \frac{T_l}{T_w}} \quad (14.127)$$

Throughput of Go-Back-N ARQ

In this system, when the transmitter is informed that an error has been detected in a particular word, retransmission is required of that word and of the $N - 1$ words that followed. Hence, the retransmission involves N words. Thus, if a word is received in error, N words are retransmitted. Thus, the total number of words transmitted is $N + 1$. If the same word is again in error, the N words are repeated once again, etc. Following the analysis used

in the stop-and-wait ARQ we find that the average number of word transmissions required for the acceptance of a single word is

$$N_{GBN} = 1 \times P_A + (N+1)P_A(1-P_A) + (2N+1)P_A(1-P_A)^2 + \dots \quad (14.128a)$$

$$= 1 + \frac{N(1-P_A)}{P_A} \quad (14.128b)$$

Correspondingly the average time to transmit one word is

$$\bar{T}_{GBN} = T_w \left(1 + \frac{N(1-P_A)}{P_A} \right) \quad (14.129)$$

and

$$\eta_{GBN} = \frac{T_k}{\bar{T}_{GBN}} = \frac{k}{n} \frac{1}{1 + \frac{N(1-P_A)}{P_A}} \quad (14.130)$$

Selective Repeat ARQ

The mean time for transmission of a word T_{SR} in this selective-repeat case is calculated exactly as in the stop-and-wait case except that T_I is set to zero. Hence, we find

$$\bar{T}_{SR} = T_w / P_A \quad (14.131)$$

and

$$\eta_{SR} = \frac{T_k}{\bar{T}_{SR}} = \frac{k}{n} P_A \quad (14.132)$$

Example 14.7

As an example, to compare throughput efficiencies, let us assume that $T_w = 10$ ms, a BCH (1023,973) code is used, $P_A = 0.99$ and $T_I = 40$ ms. Let us further assume that $N = 4$ so that the retransmission time in the go-back-N system is the same as the idle time in the stop-and-wait system. We then find,

$$\begin{aligned} \eta_{GBN} &= \frac{k}{n} \cdot \frac{1}{1 + \frac{N(1-P_A)}{P_A}} \\ &= \frac{973}{1023} \cdot \frac{1}{1 + \frac{4(0.01)}{0.99}} = 0.915 \quad (14.134) \end{aligned}$$

Thus, there is a significant improvement obtained by using the go-back-# algorithm rather than the stop-and-wait algorithm. However, the improvement made in using the selective repeat algorithm is often not deemed worth the additional complexity.

14.10 TRELLIS-DECODED MODULATION

In this section, we shall describe a communication scheme which involves trellis decoding (Sec. 14.5.4) together with a judicious selection of the signal waveforms used to represent messages. We shall consider a simple example of the method which, when applied in a more sophisticated manner, can yield the same noise immunity as would result from increasing the signal power of uncoded data by more than 6 dB without increasing the channel bandwidth.

To illustrate the communication technique, we employ, as an example, the transmission system shown in Fig. 14.26a. The data stream $d(k)$, as well as the data stream delayed by one bit time, $d_D(k) = d(k - 1)$

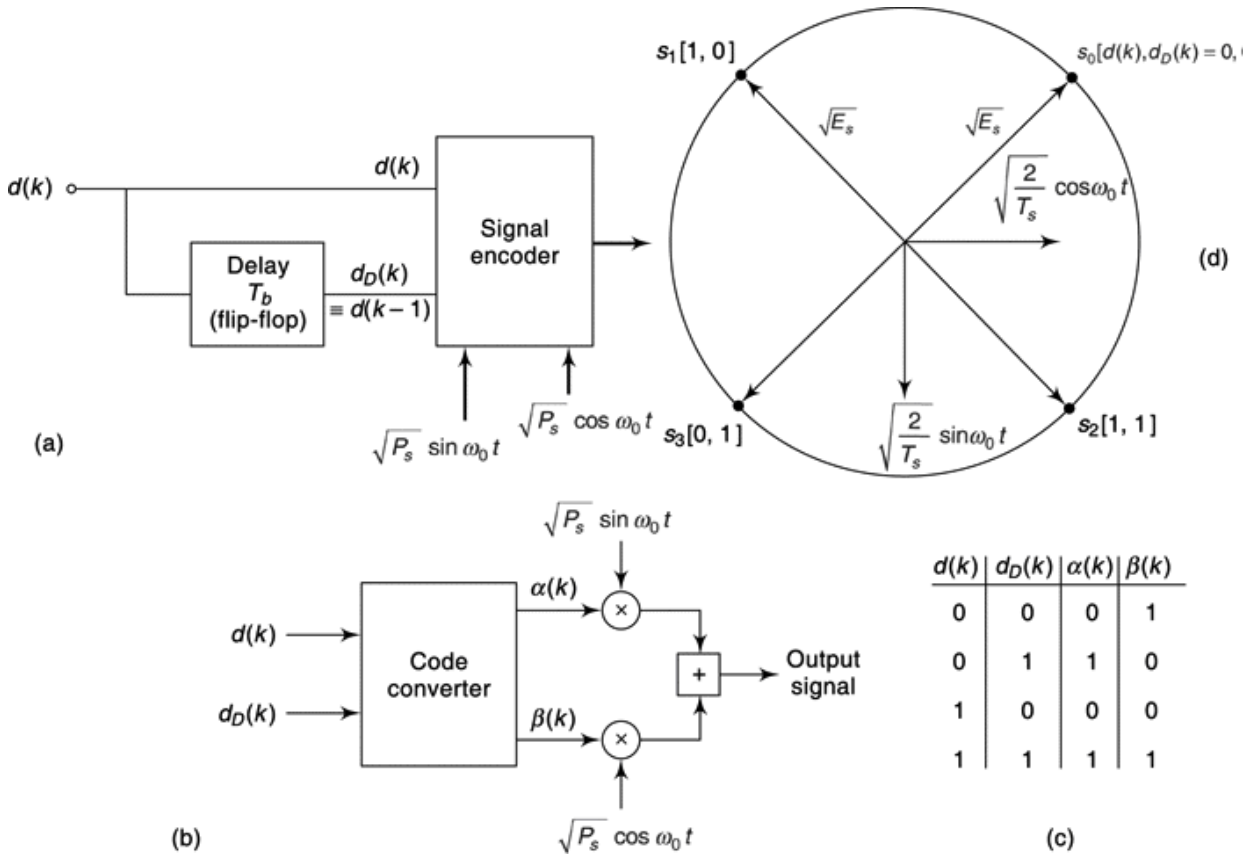


Fig. 14.26 (a) Transmitter of trellis-demodulation communication system. (b) The signal encoder.

(c) Truth table of code converter of (b). (d) Signal space representation of generated signals.

are applied to the signal encoder shown in Fig. 14.26b. It consists of a code converter and a pair of multipliers (mixers). The code converter is characterized by the truth table given in Fig. 14.26c. We shall subsequently discuss the reason for using this particular truth table. As usual, corresponding to the logic levels 1 and 0, we take the voltage levels of $a(k)$ and $b(k)$ to be +1 and -1 volt. The

carrier inputs to the signal encoder are $J_p S \cos w_0 t$ and $yffS \sin w_0 t$, P_s being the carrier power and w_0 being the carrier angular frequency. The signals which can be generated by the encoder are shown in the signal space diagram of Fig. 14.26d. The values of $d(k)$ and $d_D(k)$ corresponding to each signal are also specified. A signal persists for one bit interval and has an energy $E_s = P_s T_b$, T_b being the duration of the bit interval.

In Fig. 14.27 are shown a typical bit stream $d(k)$, the corresponding delayed stream $d_D(k)$, and the generated signals $s_0, s_x, s_2, s_3, s_x, \dots$. As can be observed from Figs. 14.27 and 14.26d, s_0 corresponds to $d(k)$, $d_D(k) = 00$, s_x to 10, etc. Note that each signal s_t corresponds to a pair of bits and not just to the data bit itself.

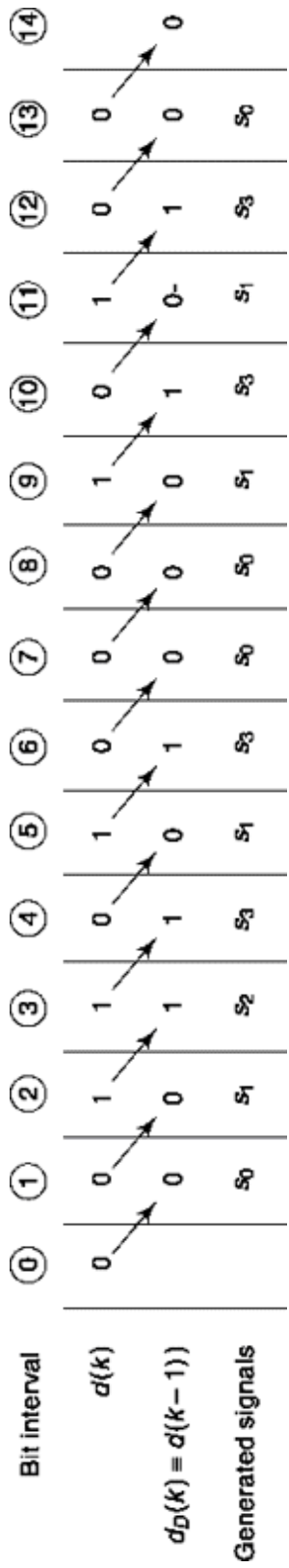
The correlator portion of the receiver is shown in Fig. 14.28. It consists of four correlators which determine the correlation of the received signal with each of the signals s_0 through s_3 . As usual we assume that, in transmission, white noise $n(t)$ of power spectral density $G(f) = r/2$ has been added to the signal. In the absence of noise, at each sampling time we would find that one correlator yielded an output voltage corresponding to complete correlation while the other three generated an output of zero volts corresponding to zero correlation. With noise, we would still anticipate that generally the output of the correlator corresponding to the transmitted signal would yield an output higher than the output of each of the other three correlators. In any event, at each sampling time we observe and record in a memory all the correlator *discrepancies*. We use the term correlator “discrepancy” to refer to the amount by which the correlator output voltage is different from what it would be if the correlation were perfect. (The hardware, memory, etc., needed to take note of and to store these discrepancies are not indicated on the figure.)

The transmitter shares with convolutional encoders the feature of a storage element (i.e. the delay element, generally a Flip-Flop). The output signal depends on both the bits at the input and output of the storage element. Accordingly, as in the case of convolutional encoder-decoder schemes, the sequence of events from one bit interval to the next bit interval can be represented on a trellis diagram. The trellis diagram, shown in Fig. 14.29a has two states, states 0 and 1, corresponding to the state of the flip-flop, shown in Fig. 14.26a.

Starting at state 0 at the beginning of interval 1, suppose that the data bit $d(1)$ is $d(1) = 0$. Then, as appears in Fig. 14.27, the signal generated during interval 1 will be s_0 and at the end of the interval the system will again be in state 0. The starting points and transitions corresponding to the other signals s_x , s_2 and s_3 are also shown in Fig. 14.26a. Observe that not every sequence of signals is possible. For, when the system is in state 0, the next signal can be only s_0 or s_x ; and when the system is in state 1, the next signal can be only s_2 or s_3 . The path through the trellis, corresponding to the signal sequence shown in Fig. 14.27, is shown in Fig. 14.29b.

Now let us consider the situation represented in Fig. 14.30. Here, before transmitting a message, we start at the transmitter with a bit sequence of all 0's so that the message signal sequence is all s_0 's. The first *message* signal will be either s_0 or s_x so that in the receiver, at the end of message bit interval 1, we need only inquire about the outputs of the s_0 and the s_1 correlators. At the end of interval 1 the receiver may find the system to be in state 0 or state 1 so that in the second interval the message signal may be s_0 , s_x , s_2 or s_3 . It appears that there are four paths through the trellis

from the beginning of the trellis through bit interval 2. But if we now invoke the Viterbi algorithm, we have the result that two of the paths through bit interval 2 can be discarded, leaving only two paths through the trellis. The decision about which paths the receiver should discard are made on



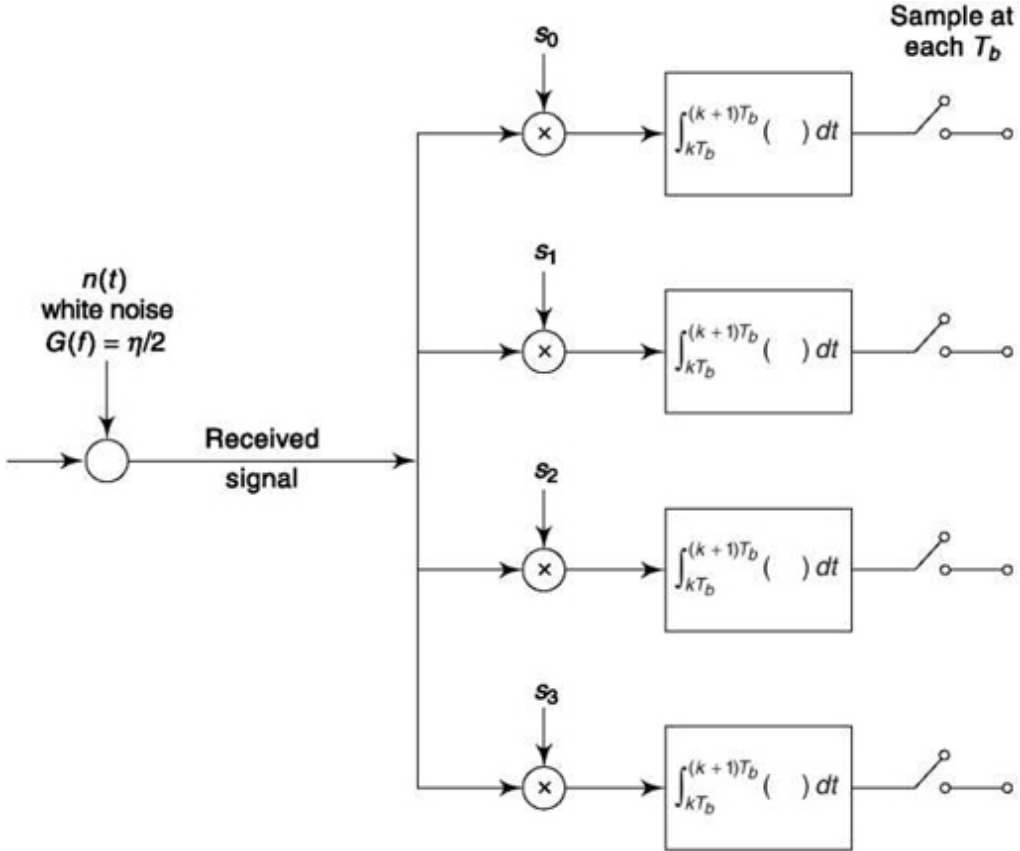


Fig. 14.28 The correlator portion of the Trellis-demodulation receiver.

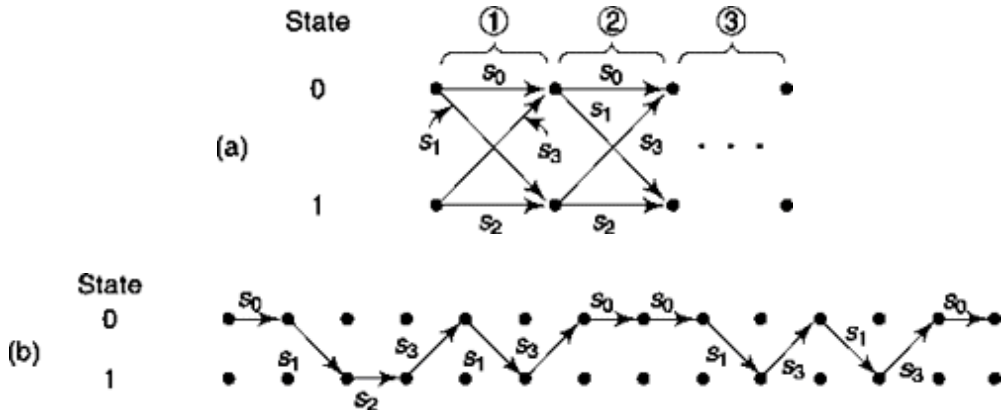


Fig. 14.29 (a) The trellis for the encoder of Fig. 14.26. Possible transitions are shown. (b) The path through the Trellis corresponding to the signal sequence of Fig. 14.27.

the basis of the sum of the discrepancies registered at the correlator outputs in the two bit intervals 1 and 2. In the same manner, as we proceed further through the trellis only two paths will survive after each interval, these being the paths for which the *accumulated* discrepancies are the smallest. Finally, at message end, the system will return permanently to state 0 and we shall then select as the valid path, the path with minimum discrepancy.

The path we finally select as valid, is of course, not guaranteed to be completely correct. Rather it is, based on our observations, the most likely set of signals that could be transmitted. We shall

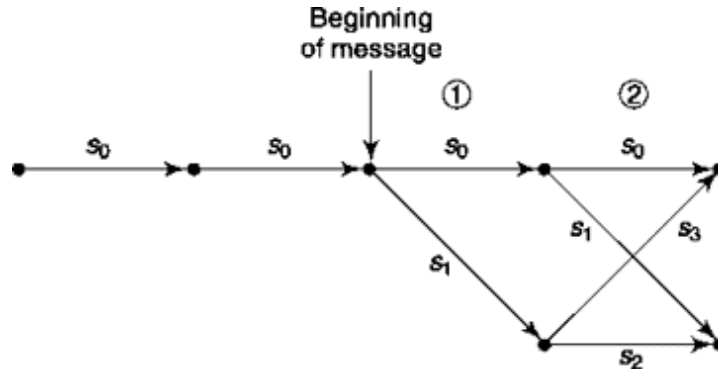


Fig. 14.30 Possible paths through the Trellis for a message starting at the point indicated after a sequence of all zeros.

now consider the types of errors that are possible, their probabilities of occurrence and their effect on the average probability that a transmitted bit is received in error.

Figure 14.31 shows a possible received signal sequence. The solid line indicates the transmitted sequence while the dashed lines indicate possible receiver determinations. In Fig. 14.31a, because of noise, the receiver has incorrectly decided that the path $s_1 - s_2$ was transmitted rather than $s_0 - s_x$. In Fig. 14.31b the receiver has incorrectly decided that path $s_l - s_3 - s_l$ was transmitted. Note that an incorrect path involving only one bit interval is not possible. We would expect that errors in a “good” communication system would occur rather infrequently. Hence, path errors involving many successive signals will be progressively less probable as the number of successive signals increases. Hence, the most likely error is as shown in Fig. 14.31a. In this case, to calculate the error probability, we consider that in two successive intervals, the transmitted signals are s_0 and s_1 . In the first interval we must compare the result of correlating the received signal with s_0 and with s_x . In the second interval we must compare the result of correlating the received signal with s_l and with s_2 . Referring now to Fig. 14.32, it is to be seen that the probability of error is the probability that $I_2 > I_1$, that is

$$P_e = p(I_2 > I_1) \quad (14.136)$$

We first evaluate I_1 :

$$I_1 = \int_0^{T_b} s_0^2(t) dt + \int_{T_b}^{2T_b} s_1^2(t) dt + \int_0^{T_b} n(t)s_0(t) dt + \int_{T_b}^{2T_b} n(t)s_1(t) dt \quad (14.137)$$

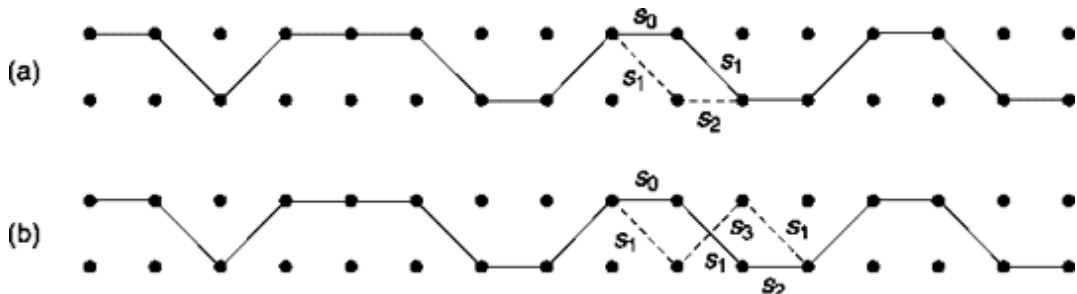


Fig. 14.31 The solid line is the transmitted sequence. The dashed line departure represents errors in the receiver determination, (a) Errors in two successive signal determinations, (b) Three successive errors.

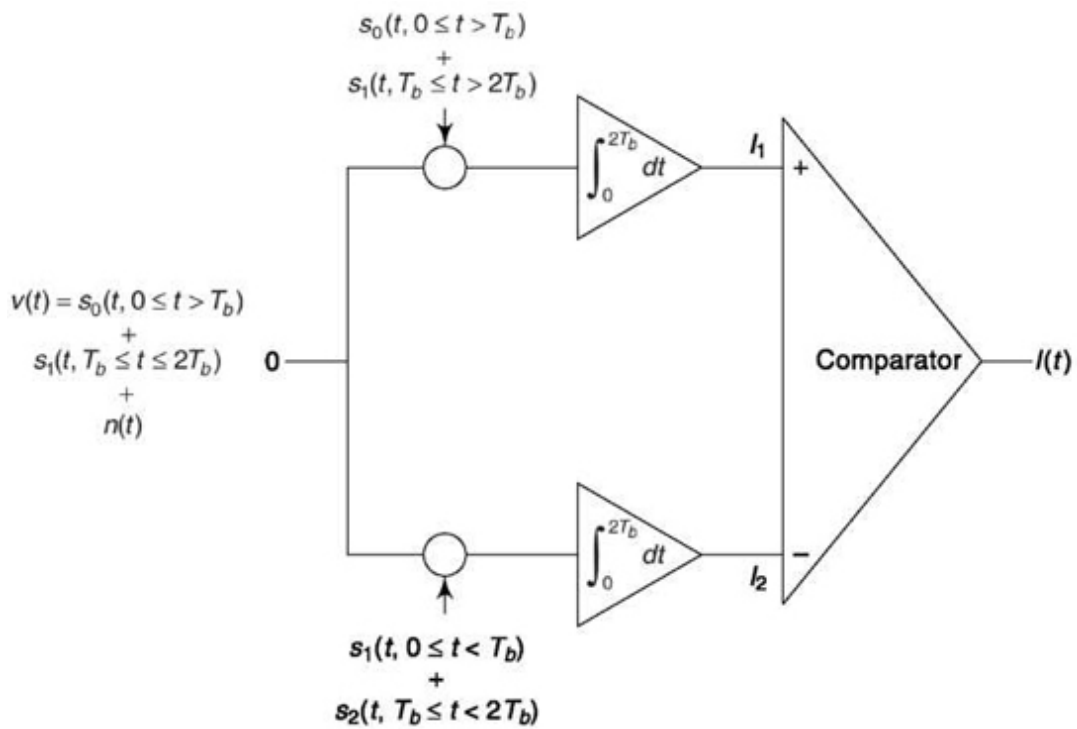


Fig. 14.32 Indicating the correlation and comparison which is required to determine the most likely path in Fig. 14.31a.

Since each signal s_0 , s_x , s_2 , and s_3 have equal power P_s ,

$$I_1 = 2E_b + N_0^{(1)} + N_1^{(2)} \quad (14.138)$$

where

$$N_0^{(1)} = \int_0^{T_b} n(t)s_0(t) dt \quad (14.139)$$

and where the notation $N^{(1)}$ refers to the correlation between $n(t)$ and $s_0(t)$ over the *first* interval and N to the correlation between $n(t)$ and $s_x(t)$ over the *second* interval.

In the *second* interval the correlation between $n(t)$ and $s_x(t)$ is

$$N_1^{(2)} = \int_{T_b}^{2T_b} n(t)s_1(t) dt \quad (14.140)$$

The noise terms $N^{(1)}$ and $N^{(2)}$ are uncorrelated, Gaussian, random variables, each with mean zero and variance a^2 where

$$\begin{aligned} \sigma^2 &= E[N_0^{(1)}]^2 = E[N_1^{(2)}]^2 = E\left\{\int_0^{T_b} dt \int_0^{T_b} d\lambda s_0(t)s_0(\lambda)n(t)n(\lambda)\right\} \\ &= \int_0^{T_b} dt \int_0^{T_b} d\lambda s_0(t)s_0(\lambda)E(n(t)n(\lambda)) \end{aligned} \quad (14.141)$$

We have from Eq. (7.73) that

$$E(n(t)n(\lambda)) = (\eta/2) \delta(t - \lambda) \quad (14.142)$$

Substitution of Eq. (14.141) into Eq. (14.142) yields

$$\sigma^2 = \eta E_b / 2 \quad (14.143)$$

Similarly, taking into account that $s_0(t)$ and $s_x(t)$ are orthogonal and that $s_2(t) = -s_x(t)$, we find that

$$\begin{aligned} I_2 &= \int_0^{T_b} s_0(t)s_1(t) dt + \int_{T_b}^{2T_b} s_1(t)s_2(t) dt + \int_0^{T_b} n(t)s_1(t) dt \\ &\quad + \int_{T_b}^{2T_b} n(t)s_2(t) dt = 0 - E_b + N_1^{(1)} + N_2^{(2)} \end{aligned} \quad (14.144)$$

where

$$N_1^{(1)} = \int_0^{T_b} n(t)s_1(t) dt \quad (14.145)$$

and

$$N_2^{(2)} = \int_{T_b}^{2T_b} n(t)s_2(t) dt \quad (14.146)$$

we note that $Nj^{(1)}$ and $Nj^{(2)}$ are uncorrelated Gaussian random variables, each with zero mean and variance

$$\sigma^2 = \eta E_b / 2 \quad (14.147)$$

It is important to note here that while $N0^1$ and $Nj^{(2)}$, $Nj^{(1)}$ and $N2^2$, $N0^r >$ and $NT >$ and $Nj^{(2)}$ and $N2^1$, and, $N0^1$ and $N2^{(1)}$ are each uncorrelated pairs,

$Nj^{(2)}$ and Np are correlated. The correlation between them is

$$E(N_1^{(2)} N_2^{(2)}) = \int_{T_b}^{2T_b} dt \int_{T_b}^{2T_b} d\lambda s_1(t) s_2(t) E(n(t)n(\lambda)) \quad (14.148)$$

Using Eq. (14.142b) and $s_2(t) = -s_1(t)$, we have

$$E[N_1^{(2)} N_2^{(2)}] = -(\eta/2) \int_{T_b}^{2T_b} s_1^2(t) dt = -\eta E_b/2 \quad (14.149)$$

The probability of error is the probability that $I_2 > I_1$. Using Eqs. (14.245) and (14.239) yields

$$\begin{aligned} P(I_2 > I_1) &= P(-E_b + N_1^{(1)} + N_2^{(2)} > 2E_b + N_0^{(1)} + N_1^{(2)}) \\ &= P(N_1^{(1)} + N_2^{(2)} - N_0^{(1)} - N_1^{(2)} > 3E_b) \end{aligned} \quad (14.150)$$

The superposition of the noise components

$$N_T = N_1^{(1)} + N_2^{(2)} - N_0^{(1)} + N_1^{(2)} \quad (14.151)$$

that appears in Eq. (14.150) is a Gaussian random variable with zero mean and variance $sT = E(N_T)^2$. This variance is readily evaluated by taking account of the fact that only $Nj^{(2)}$ and $N_2^{(2)}$ are correlated and that the variance of each of the four noise components is given by Eq. (14.147). We then find that

$$\begin{aligned} \sigma_T^2 &= E(N_T^2) = 4\sigma^2 - 2E(N_1^{(2)} N_2^{(2)}) \\ &= 4\sigma^2 - 2(-\sigma^2) \\ &= 6\sigma^2 = 3\eta E_b \end{aligned} \quad (14.152)$$

Hence, P_e is

$$\begin{aligned} P_e &= P(N_T > 3E_b) \\ &= \int_{3E_b}^{\infty} \frac{e^{-N_T^2/2\sigma_T^2}}{\sqrt{2\pi\sigma_T^2}} dN_T \end{aligned} \quad (14.153)$$

Letting $x^2 = N_T^2/2\sigma_T^2$ yields

$$P_e = \frac{1}{2} \frac{2}{\sqrt{\pi}} \int_{\sqrt{(9E_b^2/6\eta E_b)}}^{\infty} e^{-x^2} dx = \frac{1}{2} \operatorname{erfc}\left[1.5 \frac{E_b}{\eta}\right]^{1/2} \quad (14.154)$$

If data were being transmitted at the same rate using QPSK, we would have the result

$$P_e = \frac{1}{2} \operatorname{erfc}\left[\frac{E_b}{\eta}\right]^{1/2} \quad (14.155)$$

Hence, for the same P_e , QPSK would require signal power 1.5 (1.7 dB) times larger than trellis-decoded modulation.

We note that in general, the relationship between P_e and minimum distance d_{\min} , is

$$P_e = \frac{1}{2} \operatorname{erfc} \sqrt{d_{\min}^2 / 4\eta} \quad (14.156)$$

Comparing Eq. (14.156) with Eq. (14.154) yields

$$d_{\min}^2 = 6E_b \quad (14.157)$$

This value of is not simply related to the distances between signals shown in Fig. 14.26d. The reason for this situation is that P_e in Eq. (14.154) results from a correlation calculation which extends over two bit intervals (see Fig. 14.31a). If d_{lin}^2 were computed using the equation:

From these considerations, we generalize and state, without proof^{7, 8}, the valid result that where multiple bit intervals are involved in trellis demodulation, the quantity is the sum of the square of the distance between signals in each bit interval. (d_{\min} is thus the “Euclidian” distance between signals.)

Finally we note that the result given in Eq. (14.154) depends on the placement of the signals in signal space (see Fig. 14.26d). For example if the code converter were modified so that s_2 were to correspond to $d(k)$, $d_D(k) = 0, 1$ and s_3 were to correspond to $d(k)$, $d_D(k) = 1, 1$ then P_e would increase significantly (see Prob. 14.44). In a more sophisticated case, the placement of signals in signal space is determined by a computer search.

Example 14.8

Find power required for a 1 MHz transmitter that gives arbitrarily small error for (a) information-feedback system and (b) optimal system. Given, additive white noise power spectral density = 10^{-9} W/Hz.

Solution

Bit interval	$T = \frac{1}{10^6} = 10^{-6}$ sec,
	$\eta = 2 \times 10^{-9}$ W/Hz

Noting that power required $P_s = E_b/T$ where E_b = Energy per bit

(a) from Eq. (14.233),

$$P_s = \frac{E_b}{T} = \frac{\eta}{T} = \frac{2 \times 10^{-9}}{10^{-6}} = 0.002 \text{ W}$$

(b) from Eq. (14.236),

$$P_s = \frac{0.69\eta}{T} = \frac{0.69 \times 2 \times 10^{-9}}{10^{-6}} = 0.00138 \text{ W}$$

Example 14.9

If energy per bit = 10^{-8} J and additive white noise power spectral density = 10^{-9} W/Hz, find probability of error for trellis-decoded modulation. Compare it with QPSK modulation.

Solution

Given, $E_b = 10^{-8}$ J and $\eta = 2 \times 10^{-9}$ W/Hz

From Eq. (14.255) for trellis-decoded modulation, Probability of error

$$= \frac{1}{2} \operatorname{erfc} \left(\frac{1.5 \times 10^{-8}}{2 \times 10^{-9}} \right)^{1/2} = 5.3756 \times 10^{-5}$$

To compare with QPSK modulation Eq.(14.257) can be used to calculate probability of error

$$= \frac{1}{2} \operatorname{erfc} \left(\frac{10^{-8}}{2 \times 10^{-9}} \right)^{1/2} = 7.8270 \times 10^{-4}$$

Thus, in trellis-decoded modulation error is nearly 14.56 times less than QPSK modulation.

SELF-TEST QUESTIONS

12. The coding for ARQ system requires only error detection and not error correction. Is the statement correct?
13. Which of stop-and-wait, go-back N and selective-repeat ARQ has highest transmission efficiency?
14. Does an optimum or ideal system require rate of information output of the receiver same as rate of information input to the receiver?
15. Is information feedback system (based on feedback communication system) suitable for analysis of communication between ground station and satellite?

16. In trellis-decoded modulation, can the sequence of events from one bit interval to the next bit interval be represented on a trellis diagram?

FACTS AND FIGURES

In the late sixties, a view point emerged among the experts of information theory, mostly from MIT that coding has reached saturation and hints were given to young scientists to work on “more promising fields such as vacuum tubes.” The dampener was the high equipment cost of coding and decoding in spite of the presence of an elegant theory. In a 1971 coding workshop held in St. Petersburg, Florida, attended by who’s who of that time in coding theory, a talk was titled ‘Coding is dead’ and the conclusion reached in the workshop was ‘whatever was achievable has been achieved already.’

The advent of semiconductor devices and integrated circuit technology brought down the cost of hardware and revived interest in coding. Two of the later developments, Turbo Codes and Low Density Parity Check Codes, brought coding close to Shannon’s Limit. Information theorists in a 2001 IEEE International Symposium again declared that the field is dead. Unlike the 1971 workshop, the issue here was not hardware limitation but reaching the limit of channel capacity. To this, Dave Forney of MIT said, “the field has been declared dead again and again. ... each time that it’s declared dead, something new comes along.”

MATLAB

- Experiment 5 0
- Use of Hamming Code and Block Interleaving for Burst Error Correction % (section 14.7)
- This shows for burst error how interleaving, i.e. spreading the error improves probability of error. This uses (7,4) hamming code which can correct upto 3 bit errors. The burst error used affects 6 bits at a stretch, 2 in one block and 4 in next block. The in-built function encode.m is used for encoding and decode.m is used for decoding. The random interleaving is done by randintrlv.m and deinterleaving by randdeintrlv.m using same seed.

```

seed1 = 1428; % Random number seed for random message generation
seed2 = 5975; % Random number seed for interleaving and deinterleaving
n = 7; k = 4; % Parameters for Hamming code

inp_msg = randint(k*500,1,2,seed1); % Input message to encode
op_code = encode(inp_msg,n,k, 'hamming/binary'); % Encoded output

errors = zeros(size(op_code)) ;
errors(n-2:n+3) = [1 1 1 1 1 1]; % Burst error affecting adjacent blocks

```

- First we find probability of error when interleaver is not used
 $code_error = \text{bitxor}(op_code, errors)$; % Introduction of burst error
 $decoded_inp = \text{decode}(code_error, n, k, 'hamming/binary')$; % Decoded input
 $\text{disp}('Number of errors and error rate, without interleaving:');$
 $[num_no_interleav, rate_no_interleav] = \text{biterr}(inp_msg, decoded_inp)$
- Next we find probability of error using interleaver

```

inter_op_code = randintrlv(op_code,seed2); % Interleaving of output code
inter_op_err = bitxor(inter_op_code,errors); % Introduction of burst error
deinter_op = randdeintrlv(inter_op_err,seed2); % Deinterleaving
decoded_inp_inter = decode(deinter_op,n,k,'hamming/binary');
disp('Number of errors and error rate, with interleaving:');
[num_interleav,rate_interleav] = biterr(inp_msg,decoded_inp_inter)

```

Running this code we get error, rate 0.002 without interleaver and 0 with interleaver. You can play with various parameters and burst error length to further explore the effect of interleaving.

- Experiment 51
- This shows use of convolutional code with viterbi decoding for a 1/2 convolutional decoder. The configuration used is taken from Table 13.2, 2nd row of section 14.7.1. In built functions convenc.m and vitdec.m are used for it. The polynomial structure of encoder is described by trellis using function poly2trellis.m. There, the first argument describes no. of memory elements used (if there are more than one input, it will be an array describing memory elements for each input)

- and the next argument shows how memory outputs are connected to adder.
- If a memory element is connected it is considered as 1, if not 0. Thus in this example it is 1111 and 1101. The argument enters this value in octal(starting from rightmost) as 17 and 15. If more than one input is used then it will be a matrix showing connections similarly in octal.
- We also explore the effect of data corruption and viterbi decoder depth. len = 1000;

```

inp_msg = randint(len,1); % Random binary input message
trel = poly2trellis([4],[17 15]); %trellis for 2nd row of Table 14.2
code = convenc (msg, trel) ; % Encode the message and output it
rec_code=code; % received code under no noise
decoded = vitdec(rec_code,trel,5,'cont','hard'); %Decoding Viterbi of depth 5
[num_nonoi, ratio_nonoi]=biterr(decoded(5+1:end),msg(1:end-5))%5      data rejected
rec_code = rem(code + randerr(2*len,1,[0 1;.97 .03]),2);%
Error bit prob. 0.03
decoded = vitdec(rec_code,trel,5,'cont','hard');
[num_pe03, ratio_pe03] = biterr(decoded(5+1:end),msg(1:end-5))
rec_code = rem(code + randerr(2*len,1,[0 1;.94 .06]),2);%
Error bit prob. 0.06
decoded = vitdec(rec_code,trel,5,'cont','hard');
[num_pe0 6, ratio_pe0 6] = biterr(decoded(5+1:end),msg(1:end-5))
rec_code = rem(code + randerr(2*len,1,[0 1;.9 .1]),2); % Error bit prob. 0.1
decoded = vitdec(rec_code,trel,5,'cont','hard');
[num_pe10_vit5, ratio_pe10_vit5 ] = biterr(decoded(5 + 1:end) ,msg(1:end-5) )

```

```

decoded = vitdec(ncode,trel,2,'cont','hard'); %Decoding Viterbi of depth 2
[num_pe10_vit2, ratio_pe10_vit2] = biterr(decoded(2+1:end),msg(1:end-2))

decoded = vitdec(ncode,trel,8,'cont','hard'); %Decoding Viterbi of depth 8
[num_pe10_vit8, ratio_pe10_vit8 ] = biterr(decoded(8 + 1:end) ,msg(1:end-8) )

```

If this code is run, the output typically gives

```

num_nonoi = 0 ratio_nonoi = 0 num_pe03 = 2 ratio_pe03 = 0.0020
num_pe06 = 29

```

```

ratio_pe06 = 0.0291
num_pe10_vit5 = 103
ratio_pe10_vit5 = 0.1035
num_pe10_vit2 = 120
ratio_pe10_vit2 = 0.1202
num_pe10_vit8 = 86
ratio_pe10_vit8 = 0.0867

```

Note that, due to random nature of the data and error introduced the value will differ from one simulation to other. You can play with various parameters of above as well as many different structures including 2/3 convolution coder which takes 2 input and generates 3 outputs.

SUMMARY

The chapter begins with an introduction to error-control coding that shows how calibrated introduction of redundancy can reduce error in transmission. This also tells how error detection is different from error detection and correction. An upper bound on probability of error for coded transmission is arrived at. A discussion on block codes shows its simplicity as well as effectiveness. Techniques like Hadamard, Hamming, Cyclic, BCH and other algebraic codes are discussed. Burst error is a common phenomena in digital transmission in which errors are clustered. A variety of codes used for burst error corrections are discussed, e.g. block interleaving, convolutional interleaving, Reed-Solomon code, etc. Convolutional coding and decoding is discussed in details which shows use of trellis diagrams and Viterbi algorithm. A simple introduction to now popular Turbo Coding and Low Density Parity Check codes are made. A competitive technique to forward error correction code is discussed which uses different types of Automatic-

Repeat-Request systems. Finally, Trellis-Coded Modulation presents an efficient coding system suitable for band limited channels.

PROBLEMS

14.1 We transmit either a 1 or a 0, and add redundancy by repeating the bit.

(a) Show that if we transmit 11111 or 00000, then 2 errors can be corrected.

(b) Show that in general if we transmit the same bit $2t + 1$ times we can correct up to t errors.

14.2 Verify Eq. (14.3).

14.3 Show that a parity-check bit can be inserted which makes the number of 1s *odd* and that this detects errors.

14.4 An 8-bit binary code has a parity-check bit added. How many codewords are now available that are not used.

14.5 Verify Eq. (14.18).

14.6 Verify Eq. (14.20).

14.7 Consider that an orthogonal code is used with soft decision decoding.

(a) If the probability of error in a codeword is to be 10^{-7} , find the number of information bits/codeword k as a function of EJh . (b) Will coding always improve performance? *Hint:* Use Ea. (14.30).

14.8 For small values of p , Eq. (14.32) can be approximated by Eq. (14.34). To verify this, evaluate the ratio of the second term of the sum in Eq. (14.32) to the first term. When this ratio is much less than unity, Eq. (14.34) can be employed. Show that if $p \leq t/n$, Eq. (14.34) is

14.9 (a) Show that we can approximate p in Eq. (14.34) by

$$p \approx \frac{1}{2} e^{-(E_b/\eta)(k/n)}$$

for large values of E_b/η (i.e., small values of p), and let

$$(1-p)^{n-t-1} \approx 1 - (n-t-1)p$$

(b) Now show that the number of ways that t errors can occur $\binom{n}{t+1}$ can be bounded by $2^k - 1$.

(c) Verify Ea. (14.35)

14.10 A (24,12) code capable of correcting $t = 3$ errors using hard decisions, has a $d_{\min} = 7$. (a) Plot P_e as a function of E_b/h using Eqs. (14.30) and

(14.34). (b) When $P_e = 10^{-5}$ what is the difference, in dB, between E_b/h required for soft and hard decisions?

14.11 The numbers 0 to 7 are binary-encoded.

- (a) Write the 3 binary digits for each decimal number.
- (b) Add a single parity-check bit to each code word.
- (c) Each 4-bit code word forms a T matrix. Show that if $H = [1111]$, $HT = 0$ for each T . Also show that if a single error occurs, $HT = 1$.

14.12 The repeated code symbols 111 and 000 are the two values of T . Find H using Eq. (14.40). Show that

$$HT = 0.$$

14.13 The repeated code symbols are 11111 and 00000. Find the H matrix.

14.14 Using H as given by Eq. (14.48) and G given by Eq. (14.49), show that $GH^T = 0$.

14.15 Generate all 16 codewords for the Hamming code described by the G matrix given by Eq. (14.49).

14.16 Show that $HT^T = 0$ where H is given by Eq. (14.48) and T is given in Prob. 14.15.

14.17 Find all 16 entries to Table 14.1.

14.18 (a) Verify that the transpose of the transpose of a matrix is the original matrix, i.e. $(X^T)^T = X$

(b) Show that if the product $XY = 0$ then also $Y^T X^T = 0$.

14.19 The code word transmitted is either $T_1 = 111$ or $T_2 = 000$. The H matrix is given by Eq. (14.67). The signal 101 is received. Show that $HR = S$ shows where the error is located.

14.20 (a) Construct all eight, 8-bit codewords for the Hadamard code. (b) How many errors can be detected?

(c) How many errors can be corrected? (d) Show that the four, 4-bit Hadamard codewords given in Eq. (14.69) can detect one error but can correct no errors.

14.21 (a) Find the generating matrix of the H matrix given in Eq. (14.77). (b) If the information word is $A = 00101100111$ find the codeword T .

14.22 Verify that H_e as given in Eq. (14.79) has a minimum distance of 4.

14.23 Verify that cyclic shifts of the Hamming codeword 1110100 are also Hamming codewords.

14.24 Show that the factors off(x) of Eq. (14.86) are as shown in Eq. (14.87).

14.25 If an uncoded word is 111100101110 (a) find the 23 bit Golay codeword using Eq. (14.94).

(b) How would you implement codeword generation using a ROM?

14.26 It is desired to determine a BCH code having *approximately* 1000 bits in a codeword with the capability of correcting three errors. (a) Find d_{\min} . (b) Find m. (c) Find r. (d) Find k. (e) What is the rate of the code?

14.27 The ability of a code to correct errors can be increased by the use of *erasure* information. For example consider that a received codeword is $R = 1 \ x \ 00111$ where the symbol x denotes that the receiver “was not sure” if the second bit was a 1 or a 0. If the code employed is a Hamming code, then the codeword $T = AG$ is given by Eq. (14.50). Equation (14.50) provides seven equations, one for each bit in T . However, we only want to determine, $A = a_1 \ a_2 \ a_3 \ a_4$, which consists of only four bits. Hence, we can discard any three equations. In this case we assume $R = T$ but the second bit is unknown.

(a) Show that using equations 1, 3, 4 and 5 yields the correct decoded word.

(b) In general, for a (n, k) code capable of correcting t errors, how many erasures can occur in a received codeword and still result in correctly decoding the word if there are no bits detected incorrectly?

(c) Show that, in general, a decoder can correct a codeword having E erasures and e errors if $r > n - k = E + 2e$ where $e < t$.

(d) Usually, when erasures are employed, thresholds are set so that the probability of a bit error is much less than the error rate required. For example, if the error rate of a bit in the codeword is $P_{ec} = 10^{-11}$ and the probability of an erasure is $q = 10^{-3}$, calculate the probability of a received codeword being incorrectly decoded. Assume that the code can correct $t = 5$ errors.

14.28 The (31, 15) RS code is very popular. (a) How many bits are there in a symbol? (b) How many symbols can be corrected in a codeword?

14.29 (a) Sketch the convolutional interleaver and deinterleaver if $l = 5$ and $s = 3$.

(b) Show that there are 15 bits now separating two bits that were initially adjacent to one another.

14.30 Find the output sequence of the shift register connected as in Eq. (14.105) for the input given in Eq. (14.105). Thereby verify Eq. (14.106).

14.31 Verify that the tree shown in Fig. 14.13 yields the same output as the encoder shown in Fig. 14.12.

14.32 The signal 001 101 001 000 100 is received by the tree shown in Fig. 14.13. How many discrepancies are found by the time the output is reached? How many discrepancies if the correct path is always taken?

14.33 In connection with the tree of Fig. 14.13, we note that a double error coming first leads us along an incorrect path. What is the effect of a double error coming last? Consider, for example, that the signal 111 101 001 000 100 is transmitted and the signal 111 101 001 000 111 is received.

14.34 Extend the trellis of Fig. 14.18. For the output sequence of Eq. (14.108), find the path through the trellis having the minimum number of bit discrepancies.

14.35 (a) Calculate the upper bound on the bit error rate for a rate $\frac{1}{2}$, constraint length 7 convolutional code using Eq. (14.109) when $p = 10^{-2}$.

(b) Plot P_b vs. p for $p = 10^{-2}, 10^{-3}, 10^{-4}$.

(c) Compare (b) with the result obtained for the (24, 12), $t = 3$, Golay code.

14.36 Show that for hard decision decoding of a (7, 4) Hamming code the probability of 2 or more errors is at least a factor of 10 less than the probability of a single error if $p < P_0$. Find P_0 .

14.37 The binary digits 1 and 0 are transmitted by repeating the digits three times: 111 and 000.

- (a) Calculate the probability of error in receiving the uncoded 1, in terms of ST/h , where T is the duration of the word.
- (b) Calculate the probability of error in receiving the coded 1(111), in terms of ST/h .
- (c) Plot the probability of error of (a) and (b) as a function of ST/h , and compare.

14.38 Data having a bit rate 20 kb/s is to be transmitted. The value of $E_b/h = 8$ dB. Compare the probability of a *bit* being in error if (a) no coding is used, but QPSK is employed; (b) rate -1 Golay code is used and 16 PSK is then employed (interleaving is used so that bit errors are independent). Note that the bandwidths required of (a) and (b) are the same.

14.39 A 1 or 0 is to be sent using a repeated code 111 or 000 respectively. The probability of a bit being in error is p . Find the probability of an undetected error. *Hint:*

$$P_e = P(\text{undetected error}|111 \text{ is sent})P(111 \text{ being sent}) + P(\text{undetected error}|000 \text{ is sent})P(000 \text{ being sent})$$

$$P(\text{undetected error}|111) = P(\text{undetected error}|000)$$

Next find Show that $P_e = p^3$ and not $2^{-k} = 1/4$

Explain why the bound given by Eq. (14.123) is so loose.

14.40 A (7, 4) Hamming code is used for error detection. The probability of a bit error is p . (a) Calculate the probability of an undetected error. (b) How does your result compare to the bound given by Eq. (14.123)? Explain.

14.41 A 16 cycle redundancy check (CRC) is an IC which supplies 16 parity check bits to each k information bit word to form an $n = k + 16$ bit codeword for error detection: (a) What is the probability of an undetected error? (b) What is the probability of detecting an error?

14.42 Assume that a BCH (1023,973) code is used for error detection and that $P_A = 0.99$ and $T_I = 50$ ms. If $T_w = 50$ ms, compare the throughput efficiencies of the stop-and-wait, go-back N and selective-repeat systems. Assume that the time to transmit or to receive is 25 ms.

14.43 Verify Eq. (14.124b). *Hint:* From the series given in Eq. (14.124a), factor out P_A , then let $(1 - P_A) = y$ and show that the resulting series in y is

given by $\frac{d}{dy} \left(\frac{y}{(1-y)} \right)$.

14.44 Figure 14.31a shows only one path containing double errors. (a) How many paths exist that contain double errors? (b) Calculate the minimum distance of each path? (c) Is any distance found in (a) less than $d_{\min} = \sqrt{6E_b/\eta}$?

14.45 Consider the signal, $A(t)$, generated by transmitting a voltage $A(k)$ during the time interval $kT_b < t < (k + 1)T_b$, where $k = 0, 1, 2, \dots$, and $A(k) = d(k - 1) - 3 d(k) d(k - 1) d(k - 2)$. Here $d(k)$ is the present data bit, $d(k - 1)$ is the preceding bit and $d(k - 2)$ precedes $d(k)$ by two bits. Let $d(k)$, $d(k - 1)$ and $d(k - 2)$ have the values ± 1 and occur with equal likelihood.

- (a) Show that $A(k)$ can have one of four voltages, ± 2 V and ± 4 V.
 - (b) Find the average power, P_s , in $A(t)$.
 - (c) Show that $A(k)$ can be generated using two delay units, two EXCLUSIVE-OR gates and an adder.
 - (d) Since there are two delay (storage) elements, the trellis code will have four states: 00, 01,
- 10, 11. Draw the trellis.
- (e) Show that the minimum error paths have a duration $3T_b$.
 - (f) Show that $d = 8E_b$, where $E_b = P_s T_b$. Note that by using this trellis code we gain 3 dB in signal power as contrasted with using BPSK.

15

COMMUNICATION SYSTEMS AND COMPONENT NOISES

CHAPTER OBJECTIVE

A received signal, whether it arrives over a wired communication channel or wireless antenna, is accompanied by noise. As the signal is processed by the various stages of the receiver, each stage superimposes additional noise on the signal. This chapter discusses various parameters like noise temperature, noise figure, etc., to characterize such noise and determine overall signal to noise ratio (SNR) of a communication system. This helps to find required minimum power level at the point of transmission that will ensure a final receiver output signal with acceptable SNR. Besides numerical examples the chapter also presents MATLAB based simulations on certain aspects of the discussion.

FACTS AND FIGURES

Thevenin's theorem, one of the most celebrated results of electric circuit theory, provides a two-parameter characterization of the behavior of an arbitrarily large circuit when seen across two of its terminals. This was formulated by Leon Thevenin (1857-1926), a French telegraph engineer at the age of 26. His discovery met initially with skepticism and controversy within the engineering establishment of that time.

Norton's theorem is an extension of Thevenin's theorem that talks about current equivalence instead of voltage equivalence and was introduced in 1926 in the same month separately by Hans Ferdinand Mayer (1895-1980) in Europe and Edward Lawry Norton (1898-1983) in USA. Mayer was the only one of the two who actually published on this topic, but Norton made known his finding through an internal technical report at Bell Labs. In some places, the equivalent circuit developed from this is known as Mayer-Norton equivalent.

15.1 RESISTOR NOISE

As we have already noted in Sec. 7.1, resistors are a source of noise. The conductivity of a resistor results from the availability, within the resistor, of electrons which are free to move, and the resistor

noise is due precisely to the random motion of these electrons. This random agitation at the atomic level is a universal characteristic of matter. It accounts for the ability of matter to store the energy which is supplied through the flow of heat into the matter. This energy, stored in the random agitation, is made manifest generally by an increase in temperature. Thus resistor noise as well as other noise of similar origin is called *thermal* noise.

It has been determined experimentally that the noise voltage $v_n(t)$ that appears across the terminals of a resistor R is Gaussian and has a mean-square voltage, in a narrow frequency band df , equal to

$$\overline{v_n^2} = 4kTR df \quad (15.1)$$

where T is the temperature in degrees Kelvin, and k is the Boltzmann constant $k = 1.38 \times 10^{-23}$ J/K. At room temperature, taken as $T_0 = 290$ K, we have $kT_0 \sim 4 \times 10^{-21}$ W/s. Experiments indicate further that $\overline{v_n^2}$ is independent of the center frequency f_0 of the filter having the bandwidth df , for values of f_0 between 0 Hz and approximately 10 GHz [see Sec. 15.3 for a discussion of the limitations to Eq. (15.1)]. Thus, we conclude that for the communication systems employed today (excluding optical communication systems), the normalized power supplied by $v_n(t)$ is also independent of f_0 , and hence the power spectral density of the noise source is approximately white and equal to

$$G_v(f) = \frac{\overline{v_n^2}}{2df} = 2kTR \quad (15.2)$$

The *noisy* resistor R can be represented by the equivalent circuit shown in Fig. 15.1. Here the physical resistor shown in Fig. 15.1a has been replaced in Fig. 15.1ft by a Thevenin circuit representation consisting of a *noiseless* resistor in series with a noise voltage source $v_n(t)$ having the mean-square voltage

$\overline{v_n^2} = 4kTR \Delta f$. If the terminals in Fig. 15.1ft were short-circuited, a noise current $i_n(t)$ would flow having a mean-square value

$$\overline{i_n^2} = \frac{\overline{v_n^2}}{R^2} = \frac{4kTR \Delta f}{R^2} = 4kTG \Delta f \quad (15.3)$$

where $G = 1/R$ is the conductance of the resistor. The Thevenin equivalent in Fig. 15.1ft therefore corresponds to the Norton equivalent representation shown in Fig. 15.1c.

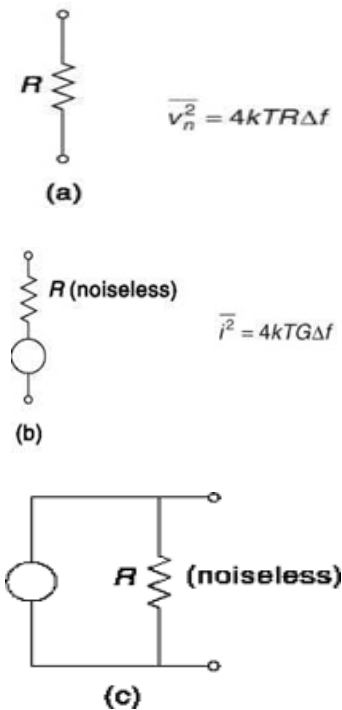


Fig. 15.1 A physical resistor in (a) of resistance R and at a temperature T is replaced in (b) by a Thevenin equivalent representation consisting of the noiseless resistor in series with a noise source. In (c) a Norton equivalent representation is shown.

15.1.1 Multiple-Resistor Noise sources

We saw in Sec. 6.4.1 that the sum of two (or more) independent Gaussian random processes is itself a Gaussian random process and that, further, the variance of the sum is equal to the sum of the variances of the individual processes. This result may be applied to the calculation of the noise power generated by combinations of resistors. Consider, for example, the case of two resistors, of resistances R_1 and R_2 both at the temperature T , connected in series. The mean-square values of the noise generated by each of the

resistors and measured in the frequency band df are $\overline{v_{n1}^2} = 4kTR_1 df$ and $\overline{v_{n2}^2} = 4kTR_2 df$. Then, the mean-square voltage measured across the series combination of R_1 and R_2 is $\overline{v_n^2} = \overline{v_{n1}^2} + \overline{v_{n2}^2}$, where

$$\begin{aligned}\overline{v_n^2} &= \overline{v_{n1}^2} + \overline{v_{n2}^2} = 4kTR_1 df + 4kTR_2 df \\ &= 4kT(R_1 + R_2) df\end{aligned}\quad (15.4)$$

This result have been anticipated since it indicates that two noisy resistors R_1 and R_2 can be replaced by a single noisy resistor $R = R_1 + R_2$. The mean-square noise voltage due to R is given by Eq. (15.4).

Rather obviously, this discussion can be extended to an arbitrary network of resistors, all at the same temperature T . If the resistance seen looking into some set of terminals is $R = 1/G$, then the open-circuit mean-square noise voltage at those terminals is $vI = 4kTR df$, and the mean-square short-circuit current is $i_n^2 = 4kTG df$.

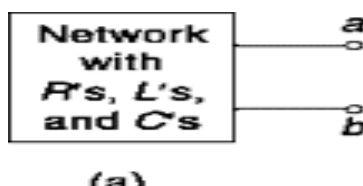
15.2 NETWORKS WITH REACTIVE ELEMENTS

Consider a network composed of resistors, inductors and capacitors as indicated in Fig. 15.2a. We arbitrarily select a set of terminals $a-b$ and inquire now about an appropriate equivalent circuit to represent these terminals as a noise source.

The impedance $Z(f)$ seen looking back into these terminals $a-b$ is generally a function of frequency and has a real and an imaginary part. That is,

$$Z(f) = R(f) + jX(f) \quad (15.5)$$

where $R(f)$ is the resistive (real) component of the impedance, and $X(f)$ is the imaginary (reactive) component. We therefore replace the network by the equivalent circuit shown in Fig. 15.2b in which the resistance $R(f)$ and the reactance $X(f)$ are noiseless and the voltage source has a mean-squared value $\overline{V_s^2}$ which is to be determined.



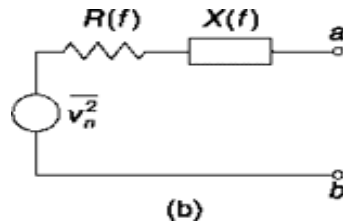


Fig. 15.2 (a) A network containing resistors, capacitors and inductors with terminals *a* and *b*. **(b)** An equivalent circuit representing the terminals as a noise source.

In Fig. 15.3, we have bridged a load resistor R_1 across the terminals *a*-*b* of the network of Fig. 15.2. This load resistor is represented by a noiseless resistor R_1 in series with a noise generator of mean-squared voltage $\bar{v_{n1}^2}$. We assume that all the parts of the circuit of Fig. 15.3 are at the same temperature in thermal equilibrium. In this case the power delivered by $Z(f)$ to R_1 must equal the power delivered by R_1 to $Z(f)$. To show that this is indeed the case, consider what occurs if there is a net power flow from $Z(f)$ to R_1 . Then the temperature of R_1 would increase, thereby exceeding the temperature of $Z(f)$. However, we have assumed that $Z(f)$ and R_1 are the same temperature in thermal equilibrium. Hence the power flow to R_1 from $Z(f)$ must equal the power flow to $Z(f)$ from R_1 to maintain this equilibrium condition.

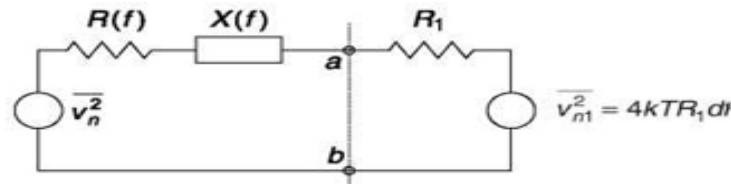


Fig. 15.3 A load resistor R_1 is bridged across the terminals *a*-*b* of Fig. 15.2.

The mean-squared current due to the source v^2j is

$$\bar{i_n^2} = \frac{\bar{v_{n1}^2}}{[R_1 + R(f)]^2 + [X(f)]^2} \quad (15.6)$$

and that due to the source v^2 is

v_n

$$\bar{i_n^2} = \frac{\bar{v_n^2}}{[R_1 + R(f)]^2 + [X(f)]^2} \quad (15.7)$$

From the condition that there be no net transfer of power, we have

$$\overline{i_n^2} R(f) = \overline{i_n^2} R \quad (15.8)$$

From Eqs. (15.6), (15.7) and (15.8), and using $v^2 j = 4kT R_1 df$, we find

$$\overline{v_n^2} = 4kT R(f) df \quad (15.9)$$

Correspondingly, the two-sided power spectral density of the open-circuit voltage in Fig. 15.2 is

$$G_v(f) = 2kT R(f) \quad (15.10)$$

15.2.1 An Application to RC Circuit

As an example of a noise calculation and also because the result is of interest in itself, we calculate the mean-squared noise voltage $\overline{v_n^2}$ at the terminals of the *RC* circuit shown in Fig. 15.4a.

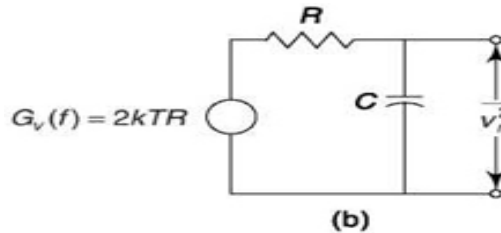
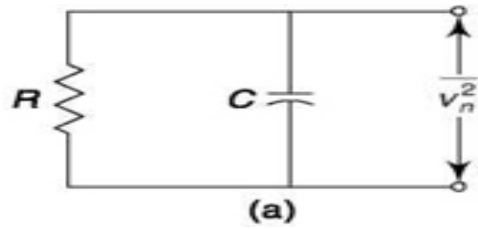


Fig. 15.4 (a) An *RC* circuit. (b) The equivalent representation in which the resistor is replaced by a noise generator and a noiseless resistor.

Looking back into the terminals of the *RC* circuit, we calculate that the resistive component of the impedance seen is

$$R(f) = \frac{R}{1 + 4\pi^2 f^2 R^2 C^2} \quad (15.11)$$

Applying Eq. (15.10) to the entire frequency spectrum, we find

$$\overline{v_n^2} = 2kT \int_{-\infty}^{\infty} \frac{R df}{1 + 4\pi^2 f^2 R^2 C^2} = \frac{kT}{C} \quad (15.12)$$

The calculation of $v^2 n$ may be performed in an alternate manner. In Fig. 15.4b we have replaced

the noisy resistor by a noise generator of power spectral density $G_v(f) = 2kTR$ and a noiseless resistor. The RC combination has a transfer function $H(f)$ from noise generator to output terminals given by

$$H(f) = \frac{1}{1 + j2\pi f RC} \quad (15.13)$$

The power spectral density of the output noise is $G_v(f) |H(f)|^2$, and v_n^2 is given, as before, by

$$\overline{v_n^2} = 2kTR \int_{-\infty}^{\infty} \frac{df}{1 + 4\pi^2 f^2 R^2 C^2} = \frac{kT}{C} \quad (15.14)$$

Equation (15.14) may be written

$$\frac{1}{2} C \overline{v_n^2} = \frac{1}{2} kT \quad (15.15)$$

in which the left-hand member is the average energy stored on the capacitor. This result is an example of the famous equipartition theorem of classical statistical mechanics. The equipartition theorem states that a system in equilibrium with its surroundings, all at a temperature T , shares in the general molecular agitation and has an average energy which is $\propto kT$ for each degree of freedom of the system. Thus, an atom of a gas, which is free to move in three directions, has three

degrees of freedom and correspondingly has an average kinetic energy which is $3 \times \frac{1}{2} kT = \frac{3}{2} kT$. At the other extreme, a macroscopic system such as a speck of dust suspended in a gas similarly flits about erratically and has an average energy associated with this random motion of $32 kT$. Since the dust speck is much more massive than an atom, the average velocity of the dust speck will be correspondingly much smaller. As another example, consider a wall galvanometer, which, being free only to rotate, has a single degree of freedom. The kinetic energy associated with such rotation is $\frac{1}{2} I\dot{\theta}^2$ where I is the moment of inertia and $\dot{\theta}$ is the angular velocity. Such a galvanometer shares

in the thermal agitation of the air in which it is suspended, and $\overline{\dot{\theta}^2} = \frac{1}{2} kT$. If the beam of light

reflected from the galvanometer mirror is brought to focus on a scale sufficiently far removed, the slight random rotation of the galvanometer may be observed with the naked eye. Altogether, it is interesting to note that the noise generated by a resistor is not a phenomenon restricted to electrical systems alone, but is a manifestation of, and obeys, the same physical laws that characterize the general thermal agitation of the entire universe.

Returning now to the RC circuit of Fig. 15.4, we observe that it has one degree of freedom, i.e. the circuit has one mesh, and a single current is adequate to describe the behavior of the system. On this basis, then, Eq. (15.15) is seen to be an example of the equipartition theorem.

15.3 AVAILABLE POWER

The *available power* of a source is defined as the maximum power which may be drawn from the source. If, as in Fig. 15.5, the source consists of a generator v_s in series with a source impedance $Z_s = R + jX_s$, then maximum power is drawn when the load is $Z_L = R - jX_s$, that is, $Z_L = Z^*$ the complex conjugate of Z_s . The available power is, therefore,

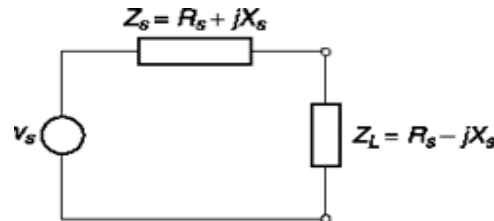


Fig. 15.5 A source of impedance Z_s is loaded by a complex conjugate impedance $Z_L = Z^*$ in order to draw maximum power.

$$P_a = \frac{\overline{v_s^2}}{4R_s} \quad (15.16)$$

Note that the available power depends only on the resistive component of the source impedance.

Using Eq. (15.16), we have that the available thermal-noise power (actual power not normalized power) of a resistor R in the frequency range df is

$$P_a = \frac{4k T R df}{4R} = kT df \quad (15.17)$$

The two-sided available thermal-noise power spectral density is

$$G_a = \frac{P_a}{2 df} = \frac{kT}{2} \quad (15.18)$$

Observe that G_a does not depend on the resistance of the resistor but only on the physical constant k and on the temperature. If the source consists of a combination of resistors (all at temperature T) together with inductors and capacitors, then in Eq. (15.17) the R in the numerator and the R in the denominator are both replaced by $R(f)$, where $R(f)$ is the (usually frequency-dependent) resistive component of the impedance seen looking back into the network. These $R(f)$'s will cancel, as do the R 's. Hence, whether the network is a single resistor or a complicated RLC network, the available noise-power spectral density is $G_a = kT/2$ quite independently of its component values and circuit configuration.

Equation (15.18) expresses the available noise-power spectral density as predicted by the principles of classical physics, which also predict that this value of G_a applies at all frequencies; i.e. the noise is, white. This result is manifestly untenable, since it predicts that the total available power

$$P_a = \int_{-\infty}^{\infty} G_a(f) df \quad (15.19)$$

is infinite. This prediction was one of a series of similar inconsistencies which were, in part, responsible for the development of the branch of physics called quantum mechanics. The quantum mechanical expression for $G_a(f)$ is

$$G_a(f) = \frac{hf/2}{e^{hf/kT} - 1} \quad (15.20)$$

in which $h = 6.62 \times 10^{-34}$ J/s is Planck's constant. Equation (15.18) yields a finite value for P_a and reduces to Eq. (15.20) when $hf \gg kT$.

The power spectral density of Eq. (15.20) is plotted in Fig. 15.6. Note that the density is lower than $kT/2$ by 1 dB or more only when $f > 4.3 \times 10^9 T$, which at room temperature, $T_0 @ 2900^\circ K$, corresponds to $f > 1.3 \times 10^{12} = 1.3 \times 10^3$ GHz. Hence we may certainly use $G_a = kT/2$ at radio and even microwave frequencies (~ 10 GHz). Note that a microwave receiver may employ a maser amplifier operating at a temperature as low as 4 K in order to minimize the noise due to the amplifier. Even at these low temperatures, it is still appropriate to assume that the noise is white. At optical frequencies this assumption is no longer valid, and Eq. (15.20) must be employed.

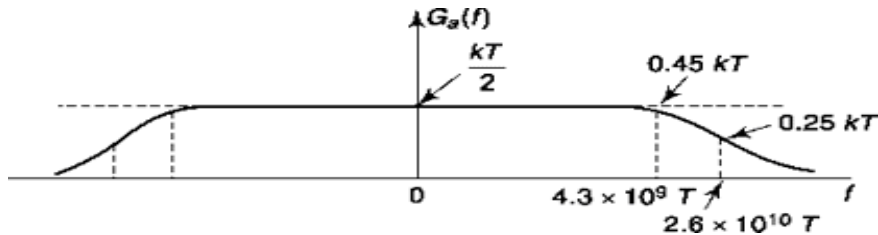


Fig. 15.6 Available power spectral density of thermal noise as given by Eq. (15.20).

15.4 NOISE TEMPERATURE

Solving Eq. (15.17) for T , we have

$$T = \frac{P_a}{k df} \quad (15.21)$$

When we apply Eq. (15.21) to a passive *RLC* circuit in which the noise is due entirely to the resistors, then T is the actual common temperature of the resistors. Consider, however, the noise which may appear across a set of terminals connected to a more general type of circuit, including possibly active devices.

Suppose that we measure the available power at the terminals and find that the noise is white, i.e. the available power P_a increases in proportion to the bandwidth, so that P_a/df is the same at all frequencies. We may then take Eq.

(15.21) to be the definition of the noise temperature of the network. The noise temperature of the network need not be the temperature of any part of the network.

Consider, for example, the simple idealized situation represented in Fig. 15.7. Here a resistor R , which is a thermal-noise source at a temperature T , is connected to the input terminals of an amplifier of gain A . We assume that the input impedance of the amplifier is infinite and assume further, for simplicity, that the amplifier output resistance is a *noiseless* resistor R_o . Then the noise power, in a frequency range df , available at the amplifier output terminals is

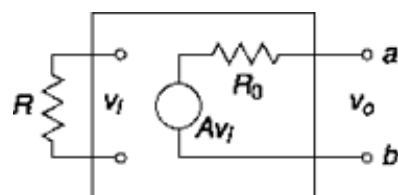


Fig. 15.7 Illustrating that the noise temperature seen looking back into set of terminals $a-b$ may assume any value.

$$P_a = \frac{\overline{v_o^2}}{R_o} = \frac{kT R A^2 df}{R_o} \quad (15.22)$$

The noise temperature seen looking back into these terminals is, using Eq. (15.21),

$$T_n = \frac{P_a}{k df} = A^2 \left(\frac{R}{R_o} \right) T \quad (15.23)$$

Thus, depending on the gain A and the ratio R/R_o , this noise temperature may assume any value including even $T_n = 0$.

As a further example to illustrate the concept of noise temperature, consider an antenna which may consist of nothing more than a loop of wire. If we assume that the wire has zero resistance, then the antenna by itself will generate no noise. Noise may, however, be induced in the antenna from a number of sources, some atmospheric and some man-made, including lightning, automobile ignition systems, fluorescent lights, etc. The spectral density of such noise falls off above about 50 MHz. Thus, while an AM radio may be affected by such noise, commercial FM, operating at higher carrier frequencies, is not appreciably affected. A second source of noise is the thermal radiation of any physical body which is at a temperature other than 0 K. Thus the earth, the atmosphere, the sun, the stars and other cosmic bodies are all sources of noise. If it were possible to shield an antenna completely from all noise sources, then the antenna noise temperature would be zero. (It should also be noted that in this case the antenna would receive no signals either.) Otherwise, if, in the frequency range of interest, the available power spectral density of the antenna noise is constant, then Eq. (15.21) may be used to determine the antenna noise temperature. That is, if in a frequency band B the available noise power is P_a , then the antenna noise temperature is T (antenna) = P_a/kB .

Example 15.1

Find the thermal noise voltage measured at room temperature (270°C) by a measuring equipment of bandwidth 10 MHz in each of the three cases shown in Fig. 15.8.

Solution

For (a), equivalent resistance seen at the output = $10 + 10 = 20$ ohms

From Eq. (15.1), rms noise voltage at output

$$= \sqrt{4 k T R d f}$$

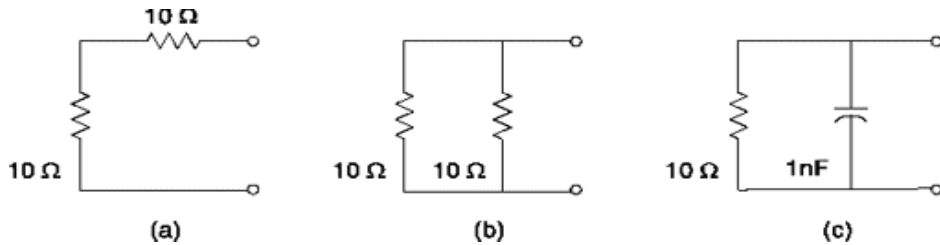


Fig. 15.8 Circuits for Example 15.1

$$= \sqrt{4 \times 1.38 \times 10^{-23} \times (273 + 27) \times 20 \times 10^7}$$

$$= 1.82 \mu\text{V}$$

For (b), equivalent resistance at the output

$$= \frac{10 \times 10}{10 + 10}$$

$$= 5 \text{ ohms}$$

rms noise voltage at output

$$= \sqrt{4 \times 1.38 \times 10^{-23} \times (273 + 27) \times 5 \times 10^7}$$

$$= 0.91 \mu\text{V}$$

For (c), from Eq. (15.12)

$$\bar{v}_n^2 = 2 \times 1.38 \times 10^{-23} \int_{-10^7}^{10^7} \frac{10}{1 + (2\pi \times 10 \times 10^9)^2 f^2} df$$

$$= 27.6 \times 10^{-23} \int_{-10^7}^{10^7} \frac{1}{1 + (2\pi \times 10^{-8})^2 f^2} df$$

$$= \frac{4.3927 \times 10^{-19}}{2\pi \times 10^{-8}} \tan^{-1}(2\pi \times 10^{-8} x) \Big|_{-10^7}^{10^7}$$

$$= 0.6991 \times 10^{-11} \times 2 \times 0.5610$$

$$= 7.884 \times 10^{-10}$$

Thus, rms noise voltage = $\sqrt{7.884 \times 10^{-10}} = 28.01 \mu\text{V}$

SELF-TEST QUESTIONS

- Is the resistor noise because of random motion of electrons?

2. The noise voltage across a resistor terminal is experimentally found as Gaussian. Is the statement correct?
3. What does equipartition theorem say on relation between average energy and degree of freedom?
4. Does available power depend only on resistive component of source impedance?
5. Can noise temperature be zero?

15.5 TWO PORTS: EQUIVALENT NOISE TEMPERATURE AND NOISE FIGURE

Received signals may be processed in a variety of ways. For example, the signal may need to be amplified through a number of amplifier stages or the signal may need to be subjected to frequency conversion to an intermediate frequency, as in a superheterodyne receiver. Each of these processing stages has input and output terminals, i.e. each is a two-port network. Each such two-port may, in general, contain resistors and active devices which are sources of noise. The signal at the input to a two-port will be accompanied by noise and will be characterized by some signal-to-noise ratio. Because of the noise sources within the two-port, the signal-to-noise ratio at the output will be

lower than at the input. It is a great convenience to have available a means of describing the extent to which a signal is degraded in passing through a two-port. There are two methods which are commonly employed for this purpose. In one method, the two-port is characterized in terms of an *effective input noise temperature*; in a second method the two-port is characterized by a *noise figure*.

In preceding sections we have described noise sources in terms of their available noise power. In order to continue conveniently to use this concept when two-ports are involved, it is useful to introduce, in connection with two-ports, the idea of the *available gain* of a two-port. The available gain $g_a(f)$ is generally frequency-dependent and is defined as

$$g_a(f) = \frac{\text{available power spectral density at the two-port output}}{\text{available power spectral density at the source output}} \quad (15.24)$$

Thus $g_a(f)$ is the ratio of available output power in a small frequency range df to the available source power in this same range.

A point which is immediately apparent from the definition of Eq. (15.24) is that the available gain is not a characteristic of a two-port alone, but depends on the driving source as well. The available gain does not depend on the two-port load. To consider the matter further, consider the situation represented in Fig. 15.9. Here, 2 two-port networks, say two amplifiers, are in cascade, the first being driven by a source of impedance R . The available gain of the first two-port depends on R as well as on the two-port itself. The available gain of the second depends on the output impedance R_{o1} of the first two-port, which may in turn depend on R . In the general case of a cascade of N two-ports, the available gain of the last two-port depends, in principle, on all the preceding $N - 1$ two-ports as well as on the source. Of course, in a two-port cascade encountered in practice, the situation may not be as complicated as suggested here. It may turn out, to a good approximation, that the output impedance of a stage is influenced only slightly by its driving source. In spite of the possible complexity associated with calculating the available gain, particularly of a later stage in a cascade, fortunately the overall available gain of a cascade is related in a very simple manner to the available gains of the individual stages. It may be verified (Prob. 15.7) that if the available gains of an N -stage cascade are $g_{a1}, g_{a2}, \dots, g_{aN}$, then the overall available gain is the product

$$g_a = g_{a1}, g_{a2}, \dots, g_{aN} \quad (15.25)$$

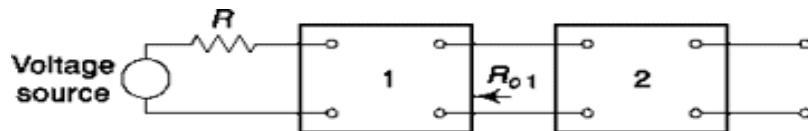


Fig. 15.9 A cascade of two-ports driven by a source of impedance R .

The concept of available gain is especially useful because it permits us to write generalized results for the noise characteristics of two-ports in very simple form.

For example, we note that if a source of available-power spectral density $G_a(f)$ is connected to the input of a two-port of available gain $g_a(f)$, the available-power spectral density at the output is $G_a(f)g_a(f)$, and the total available output power is

$$P_{ao} = \int_{-\infty}^{\infty} G_d(f) g_d(f) df \quad (15.26)$$

If the source has a noise temperature T , then $G_d(f) = kT/2$, and

$$P_{ao} = \frac{kT}{2} \int_{-\infty}^{\infty} g_d(f) df \quad (15.27)$$

15.5.1 Noise bandwidth

Bandpass amplifiers, as well as other two-ports of restricted bandpass, will typically have available gains with a frequency dependence such as illustrated by the solid-line plot of Fig. 15.10. We have indicated a passband characteristic which is symmetrical about some frequency f_0 , since this is the type of characteristic most frequently encountered. However, this symmetry is not essential to the present discussion.

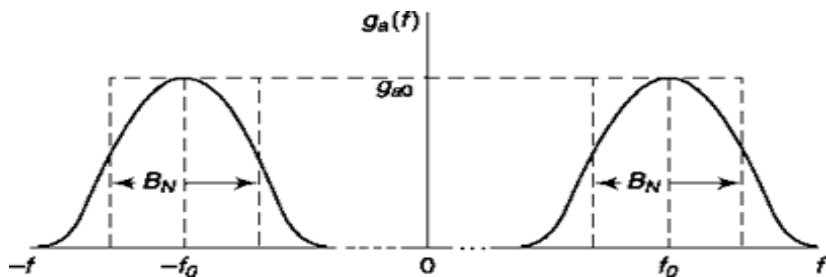


Fig. 15.10 Illustrating the concept of noise bandwidth.

If this two-port is driven by a thermal-noise source of temperature T , the two-port output available power will be

$$P_{ao} = \frac{kT}{2} \int_{-\infty}^{\infty} g_d(f) df \quad (15.28)$$

It is frequently convenient to replace the actual available-gain characteristic by rectangular characteristic, as shown by the dashed plot, which is equivalent for the purpose of computing available output-noise power. Such a rectangular characteristic would have to have a bandwidth B_N determined by the condition of equal available noise output for the two cases, that is, B_N would be determined by

$$P_{ao} = g_{ao} k T B_N = \frac{kT}{2} \int_{-\infty}^{\infty} g_d(f) df \quad (15.29)$$

where g_{ao} is the constant value of $g(f)$ over the passband for the rectangular characteristic. The bandwidth B_N is called the *noise bandwidth*

and, from Eq. (15.29), is given by

$$B_N = \frac{1}{2g_{ao}} \int_{-\infty}^{\infty} g_a(f) df \quad (15.30)$$

In Fig. 15.10 we have selected g_{ao} to equal the value of g_a at $f = f_0$. Hence the noise bandwidth which results is the noise bandwidth with respect to the frequency f_0 . Customarily, as indicated, f_0 is selected to be the frequency at which $g_a(f)$ is a maximum.

15.5.2 effective input noise Temperature

Consider that a two-port is driven by a noise source that has a noise temperature T . Then the source behaves like a resistor at temperature T , and from Eq. (15.18) the available noise-power spectral density of the source will be $kT/2$. If the available gain of the two-port is g_a , and if the two-port itself is entirely noise-free, then the available two-sided power spectral density at the two-port output would be

$$G'_{ao} = g_a(f) \frac{kT}{2} \quad (15.31)$$

However, because the two-port itself will contribute noise, the available output noise power will be G_{ao} , which is larger than G'_{ao} . We may choose to make it appear that the two-port itself is noise-free, and to account for the increased noise by assigning to the source a new noise temperature higher than T by an amount T_e . We would then have

$$G_{ao} = g_a(f) \frac{k}{2} (T + T_e) \quad (15.32)$$

The temperature T_e is called the *effective input-noise temperature* of the two-port. It is to be kept in mind, however, that T_e , like the available gain, depends on the source as well as on the two-port itself.

Example 15.2

An antenna has a noise temperature $T_{ant} = 10$ K. It is connected to a receiver which has an equivalent noise temperature $T_e = 140$ K. The midband available gain of the receiver is $g_{ao} = 10^{10}$ and, with respect to its

midfrequency, the noise bandwidth is $B_N = 1.5 \times 10^5$ Hz. Find the available output noise power.

Solution

The available power spectral density of the antenna is $kT_{\text{ant}}/2$. By the definition of equivalent noise temperature T_e , the noise of the receiver may be taken into account by increasing the source temperature by T_e . Hence the effective source temperature is $T = T_{\text{ant}} + T_e$, and the effective available noise-power spectral density at the input to the receiver is

$$G_a(f) = \frac{k}{2} (T_{\text{ant}} + T_e) \quad (15.33)$$

The available noise power at the output is, using Eq. (15.29),

$$\begin{aligned} P_{ao} &= g_{ao} k(T_{\text{ant}} + T_e) B_N \\ &= 10^{10} \times 1.38 \times 10^{-23} \times 150 \times 1.5 \times 10^5 \\ &= 3.1 \mu\text{W} \end{aligned} \quad (15.34)$$

15.5.3 noise Figure

Let us assume that the noise present at the input to a two-port may be represented as being due to a resistor at the two-port input, the resistor being at room temperature T_0 (usually taken to be $T_0 = 2900^\circ\text{K}$). If the two-port itself were entirely noiseless, the output available noise-power spectral density would be $G_{ao} = g_a(f)(kT_0/2)$. However, the actual output noise-power spectral density is G'_{ao} , which is greater than G'_{ao} . The ratio $G_{ao}/G'_{ao} = F$ is the *noise figure* of the two-port, that is,

$$F(f) = \frac{G_{ao}}{G'_{ao}} = \frac{G_{ao}}{g_a(f)(kT_0/2)} \quad (15.35)$$

If the two-port were noiseless, we would have $F = 1$ (0 dB). Otherwise $F > 1$. Using Eq. (15.32) with $T = T_0$, and Eq. (15.35), we find that the noise figure F and the effective temperature T_e are related by

$$T_e = T_0(F - 1) \quad (15.36)$$

$$\text{or } F = 1 + \frac{T_e}{T_0} = \frac{T_e + T_0}{T_0} \quad (15.37)$$

The noise figure as defined by Eq. (15.35) is referred to as the *spot noise figure*, since it refers to the noise figure at a particular “spot” in the frequency spectrum. If we should be interested in the *average noise figure* over a frequency range from f_1 to f_2 , then, as may be verified (Prob. 15.15), this average noise figure \bar{F} is related to $F(f)$ by

$$\bar{F} = \frac{\int_{f_1}^{f_2} g_a(f) F(f) df}{\int_{f_1}^{f_2} g_a(f) df} \quad (15.38)$$

Two-ports are most commonly characterized in terms of noise figure when the driving noise source is at or near T_0 , while the concept of effective noise temperature T_e is generally more convenient when the noise temperature is not near T_0 .

When following a signal through a two-port, we are not so much interested in the noise level as in the signal-to-noise ratio. Consider, then, the situation indicated in Fig. 15.11. Here the noise at the two-port input is represented as being due to a resistor R so that the available input-noise-power spectral density is $G(\cdot) = kT/2$. A signal is also present at the input with available power spectral density $G^{(*)}$. The available output-signal-power spectral density is

$$G_{du}^{(s)} = g_a G_{af}^{(s)} \quad (15.39)$$

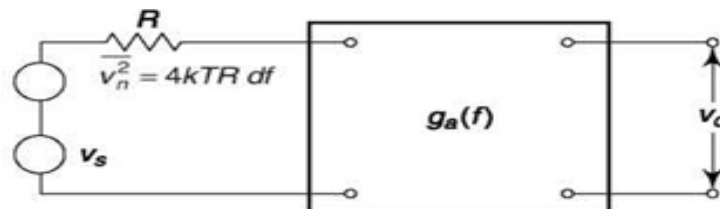


Fig. 15.11 A signal v_s and a noise source are superimposed and applied at the input of a two-port of available gain $g_a(f)$.

However, because of the noise added by the two-port itself, the available output-noise spectral density is

$$G_{du}^{(n)} = g_a F G_{af}^{(n)} \quad (15.40)$$

Combining Eqs. (15.39) and (15.40), we have an alternative interpretation of the spot noise figure, that is,

$$F(f) = \frac{G_{dt}^{in}/G_{dt}^{out}}{G_{ao}^{in}/G_{ao}^{out}} \quad (15.41)$$

Thus, F is a ratio of ratios. The numerator in Eq. (15.41) is the input-signal-to-noise power spectral density ratio, while the denominator is the output-signal-to-noise power spectral density ratio.

Let us assume that in a frequency range from f_1 to f_2 , the power spectral densities of signal and noise are uniform. In this case it may be verified (Prob. 15.17) that the average noise figure \bar{F} defined by Eq. (15.38) has the significance

$$\bar{F} = \frac{S_t/N_o}{S_o/N_o} \quad (15.42)$$

where S_t and N_t are, respectively, the total input available signal and noise powers in the frequency range f_1 to f_2 , and similarly S_o and N_o are the total output available signal and noise powers.

The noise figure F (or \bar{F}) may be expressed in a number of alternative forms which are of interest. If the available gain g_a is constant over the frequency range of interest, so that $F = \bar{F}$, then $S_o = g_a S_t$. In this case Eq. (15.42) may be written as

$$F = \frac{1}{g_a} \frac{N_o}{N_t} \quad (15.43)$$

Further, the output noise N_o is

$$N_{tp} = g_a (F - 1) N_t \quad (15.46)$$

$$N_o = g_a N_t + N_{tp} \quad (15.44)$$

where $g_a N_t$ is the output noise due to the noise present at the input, and N_{tp} is the additional noise due to the two-port itself. Combining Eqs. (15.43) and (15.44), we have

$$F = 1 + \frac{N_{tp}}{g_a N_t} \quad (15.45)$$

or, the noise due to the two-port itself may be written, from Eq. (15.45), as

$$N_o = g_a N_i + N_p \quad (15.44)$$

15.5.4 noise Figure and equivalent noise temperature of a Cascade

In Fig. 15.12 is shown a cascade of 2 two-ports with a noise source at the input of noise temperature T_0 . The individual two-ports have available gains g_{a1} and g_{a2} and noise figures F_1 and F_2 . If the input-source noise power is N_t , the output noise due to this source is $g_{a1} g_{a2} N_t$. The noise output of the first stage due to the noise generated within this first two-port is $g_{a1}(F_1 - 1)N_t$, from Eq. (15.46). The corresponding noise at the output of the second stage is $g_{a1} g_{a2}(F_1 - 1)N_t$. Again, using Eq. (15.46), we find that the noise output due to the noise generated within the second two-port is $g_{a2}(F_2 - 1)N_t$. The total noise output is therefore

$$N_o = g_{a1} g_{a2} N_t + g_{a1} g_{a2}(F_1 - 1)N_t + g_{a2}(F_2 - 1)N_t \quad (15.47)$$

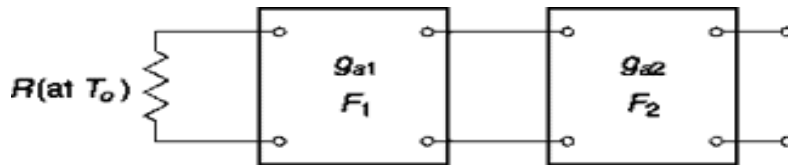


Fig. 15.12 A noise source at temperature T_0 derives a cascade of two ports.

If the two-ports are characterized by equivalent temperatures rather than noise figures, then the equivalent temperature of the cascade, T_e , is related to the equivalent temperatures and available gains of the individual stages by

If we use Eq. (15.43), the overall noise figure of the cascade is

$$F = \frac{1}{g_a} \frac{N_o}{N_t} = \frac{1}{g_{a1} g_{a2}} \frac{N_o}{N_t} \quad (15.48)$$

$$= F_1 + \frac{F_2 - 1}{g_{a1}} \quad (15.49)$$

from Eq. (15.47). If the calculation leading to Eq. (15.49) is extended to a cascade of k stages, the result is

$$T_e = T_{e1} + \frac{T_{e2}}{g_{a1}} + \frac{T_{e3}}{g_{a1} g_{a2}} + \dots + \frac{T_{ek}}{g_{a1} g_{a2} \dots g_{a(k-1)}} \quad (15.51)$$

Equation (15.51) may be established by combining Eq. (15.50) with Eq. (15.49) (see Prob. 15.22).

Suppose that the individual two-ports have comparable noise figures or equivalent temperatures. Then, especially if the gains are large, the contribution to the net output noise of succeeding stages in the cascade becomes progressively smaller. A very effective practice, for the purpose of securing a low-noise receiving system, is to design the first stage of the cascade with a low equivalent temperature and a high gain. A gain of 30 dB is not uncommon. Similarly, equivalent temperatures as low as $T_s = 4$ K are obtained by cooling the amplifier with liquid nitrogen.

15.5.5 An Example of a Receiving system

The receiver shown in block diagram form in Fig. 15.13 is rather typical of microwave receivers such as are used for *satellite communication*. In such cases, it is certainly justifiable to take considerable pains to keep the noise figure of the receiver as low as possible. For variety, and also to be consistent with practice, we have characterized the noisiness of the first amplifier in terms of a noise temperature, while the other stages have been characterized by a noise figure. We calculate now the overall noise figure of the receiver. The antenna does not enter the calculation, since it is considered the driving source and not part of the receiver. Using Eqs. (15.37) and (15.50), we have

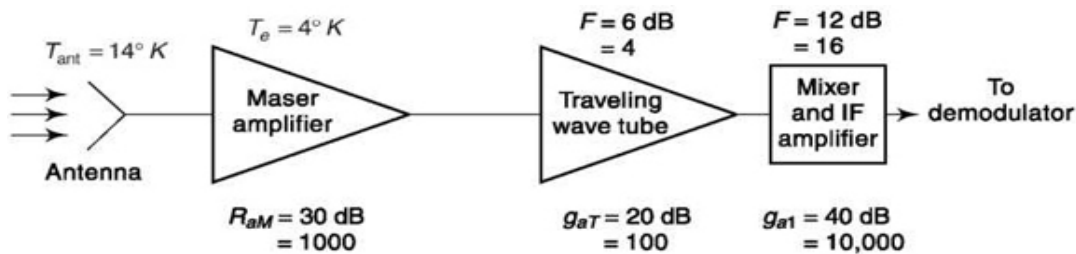


Fig. 15.13 A typical microwave receiver.

$$F(\text{receiver}) = \left(1 + \frac{4}{290}\right) + \frac{4 - 1}{1,000} + \frac{16 - 1}{100,000} = 1.017 (= 0.05 \text{ dB}) \quad (15.52)$$

From Eq. (15.36) the equivalent temperature of the receiver is

$$\begin{aligned} T_e(\text{receiver}) &= T_0 |F(\text{receiver}) - 1| \\ &= 290(0.017) = 4.93 \text{ K} \end{aligned} \quad (15.53)$$

Note that, because of the high gain of the first amplifier stage, the travelling wave tube amplifier, the mixer, and the IF amplifier increase the effective receiver temperature only 0.93 K above the temperature of the maser amplifier.

The available noise power present at the demodulator input in the bandwidth B is

$$P_a = \frac{k}{2} [T_{\text{ant}} + T_e(\text{receiver})](2B)g_d(\text{receiver}) \quad (15.54)$$

The available gain of the receiver is $30 + 20 + 40 = 90 \text{ dB} = 10^9$; hence

$$P_a = 1.38 \times 10^{-23}(14 + 4.93) \times 10^9 B$$

$$\sim 2.6 \times 10^{-13} B \text{ watts} \quad (15.55)$$

Because of the high gain which precedes the demodulator, the noise which may be introduced by the demodulator or any succeeding processing will not further degrade the signal-to-noise ratio of the signal.

In the receiver of Fig. 15.13 each of the stages provides some bandlimiting, and the IF amplifier may well consist of a number of stages, each one of which is bandlimited. Conceptually, however, it is very convenient to consider that all the stages of the system are of unlimited bandwidth and that bandlimiting is done in a single IF filter at the output end of the IF amplifier. Under these circumstances the noise input to this IF filter would have a white (uniform) spectral density. We have, as a matter of fact, throughout this text assumed that such was the case when we assumed that our communication channel was characterized by a two-sided noise-power spectral density $G_n(f) = h/2$ [see Eq. (7.47)]. It is now of interest, in connection with the receiver of Fig. 15.13 to inquire into the magnitude of $h/2$. From the result given in Eq. (15.55) we have

$$G_n(f) \equiv \frac{\eta}{2} = \frac{P_a}{2B} = \frac{2.6 \times 10^{-13} B}{2B} = 1.3 \times 10^{-13} \text{ watt/Hz} \quad (15.56)$$

As a further example of the performance of the system of Fig. 15.13 consider that the receiver is being used to receive a frequency-modulated signal with a baseband frequency range $f_M = 4 \text{ MHz}$. The received signal power at the demodulator is S_d . Let us assume that, in order to keep the discriminator operating above threshold, we require $S_d/hf_M = 20 \text{ dB}$. What

then must be the value of available signal power at the output of the antenna? Since

$$\frac{S_i}{\eta f_M} = \frac{S_i}{2.6 \times 10^{-13} \times 4 \times 10^6} \geq 100 (= 20 \text{ dB}) \quad (15.57)$$

we find

$$S_i \geq 10.4 \times 10^{-5} \text{ watt} \quad (15.58)$$

Since the receiver gain is 90 dB ($= 10^9$), the required minimum available signal power at the antenna must be

$$S_i(\text{antenna}) = \frac{10.4 \times 10^{-5}}{10^9} = 10.4 \times 10^{-14} \text{ watt} \quad (15.59)$$

SELF-TEST QUESTIONS

6. Is it so that available PSD at the output of 2-port network is product of source PSD and available gain?
7. Which of effective noise temperature and noise figure is preferred in characterizing a 2-port network operating near room temperature?
8. Is the contribution to equivalent temperature in cascaded network lower in succeeding stages?

15.6 ANTENNAS

An antenna, as a noise source, is characterized by a noise temperature. The two-ports of a receiving system, so far as their noise generation is concerned, are characterized by equivalent input-noise temperatures or by noise figures. We have seen how, in terms of these characterizations, we may determine the signal power required to be available from a receiving antenna to ensure an acceptable signal-to-noise ratio. We refer briefly to the manner in which the transmission performance of an antenna system is characterized, so that, given the required available power at the receiving antenna, we may determine the power required to be radiated by the transmitting antenna.

Consider a transmitting antenna which radiates a power P_T , and assume that the power is radiated uniformly in all directions, that is, *isotropically*. The power incident on an area A oriented perpendicularly to the direction of power flow, and at a distance d from the transmitting antenna, is

$$P_R = \frac{P_T}{4\pi d^2} A \quad (15.60)$$

Equation (15.60) may be used to define an effective area A_e of an antenna. Thus, if the available power from a receiving antenna is P_R when the antenna is a distance d from an isotropic antenna transmitting a power P_T , then the effective area of the receiving antenna is

$$A_e \equiv 4\pi d^2 \frac{P_R}{P_T} \quad (15.61)$$

The effective area of an antenna is related principally to the physical shape and dimensions of the antenna. Thus, for example, for a parabolic disk antenna the effective area is generally in the range 0.5 to 0.6 of the physical area of the disk.

Real antennas do not radiate isotropically but are rather directional. This directivity is of advantage when we are interested in transmitting from one antenna to a *particular* receiving antenna. In such a case we would be interested in making the transmitting antenna as directional as possible, and we would orient the transmitting antenna to radiate with maximum intensity towards the receiving antenna. A typical antenna-radiation pattern of a directional antenna is shown in Fig. 15.14. If we draw a line, in an arbitrary direction, from the antenna to the antenna pattern, the length of the line is proportional to the radiant power density in that direction. As indicated, the radiated power is principally confined to a *main lobe*, while some power is also radiated in the direction of the *side lobes*. The *beam width* of the antenna is defined as the angle, at the antenna, between directions in which the radiated-power density is down 3 dB from the maximum. The direction of maximum radiation is referred to as the 0 dB direction. In a highly directional antenna, beam widths of 10°, with side lobes down 30 dB to 50 dB as indicated, are feasible.

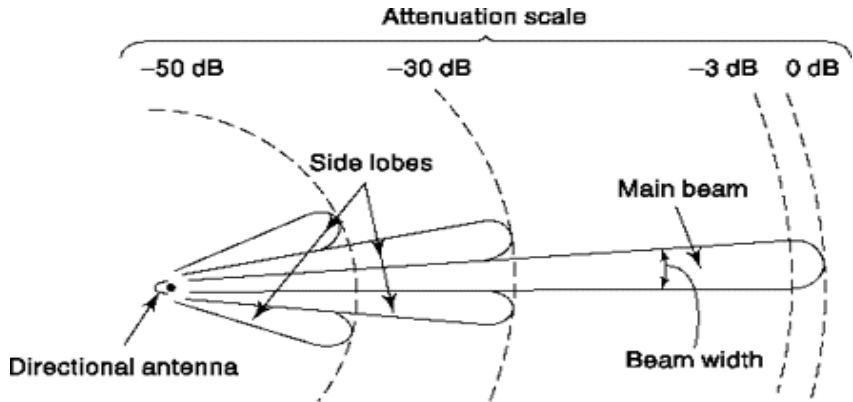


Fig. 15.14 Transmission pattern of a highly directional antenna.

There is a reciprocity relationship between an antenna used for radiation and the same antenna used for reception. An antenna has the same directivity pattern in the two cases. Thus, a highly directional antenna radiates principally in one direction, and when used for reception it similarly absorbs most of the radiant energy from this same direction. Hence, for communication between two particular antennas, and to minimize interference and spurious signals, it is advantageous that both antennas be directional and, of course, with main lobes oriented toward one another.

The extent to which the principal direction of an antenna is favored is measured by the *antenna gain*. Thus, suppose that an isotropic radiator would radiate a power per unit solid angle of P_i when

furnished with a power P (that is, $P_t = P/4\pi$). If a directional antenna radiates a power per unit solid angle p_m in the direction of most intense radiation, then the antenna gain K is defined by

$$K \equiv \frac{p_m}{p_i} \quad (15.62)$$

It turns out that the gain of an antenna and its effective area are related by

$$K = \frac{4\pi A_e}{\lambda^2} \quad (15.63)$$

where λ is the wavelength of the radiation. Note that, for fixed λ , the gain increases with effective area and hence with the physical dimensions of the antenna. A large antenna, therefore, absorbs more power and can also be made more directional than a small antenna.

Consider now a receiving antenna of effective area A_{eR} facing a transmitting antenna of gain K_T . Then from Eq. (15.60) and from the

definition of antenna gain we find that the received power is

$$P_R = \frac{P_T}{4\pi d^2} A_{eR} K_T \quad (15.64)$$

where K_T is the gain of the transmitting antenna. Applying Eq. (15.63) to the receiving antenna, i.e. replacing K by K_R and A_e by A_{eR} and combining this result with Eq. (15.64), we have

$$\frac{P_R}{P_T} = \frac{K_T K_R}{(4\pi d/\lambda)^2} \quad (15.65)$$

Thus we find that the received-to-transmitted power ratio P_R/P_T depends on the ratio d/l which is called the *effective distance* and on the gains K_T and K_R of the two antennas.

Example 15.3

The available power required at a receiving antenna is 10^{-6} watt (that is, -60 dB with respect to 1 watt). Transmitting and receiving antennas have gains of 40 dB each. The carrier frequency used is 4 GHz, and the distance between antennas is 30 miles. Find the required transmitter power.

Solution

Using Eq. (15.65), we have (1.6×10^3 m = 1 mile)

$$10 \log P_R = 10 \log P_T + 10 \log K_T \\ + 10 \log K_R - 20 \log \left(4\pi \frac{d}{\lambda} \right) \quad (15.66)$$

$$-60 = 10 \log P_T + 40 + 40 \\ - 20 \log \left[4\pi \frac{30 \times 1.6 \times 10^3}{(3 \times 10^8) / (4 \times 10^9)} \right]$$

$$-60 = 10 \log P_T + 40 + 40 - 1.38$$

so that

$$10 \log P_T = -2$$

or $P_T = -2$ dB (15.67)

That is, P_T is 2 dB below 1 watt or $P_T = 0.64$ watt.

15.6.1 An example: Satellite-to(Earth) Communication System

For the sake of tying together a number of ideas developed in this chapter as well as several of the concepts encountered in connection with frequency modulation, let us undertake some calculations on a proposed satellite-to-

earth communication system as represented in Fig. 15.15. We propose a system with the following specifications:

1. Frequency modulation is to be used to transmit from the satellite a TV signal with $f_M = 4 \text{ MHz}$ on a carrier of frequency $f_c = 3 \text{ GHz}$.
2. The satellite antenna gain is to be $K_T = 20 \text{ dB}$, while the receiving antenna on the ground is to have $K_R = 50 \text{ dB}$. (Note that the earth-bound antenna may be much larger than the satellite antenna and hence may have a larger gain.) The satellite is assumed to be at a distance of $32 \times 10^6 \text{ m} (= 20,000 \text{ miles})$.
3. The noise temperature of the receiving antenna is to be $T_{\text{ant}} = 14 \text{ K}$.
4. The receiver (a cooled maser amplifier is employed) is to have a total noise figure $F = 0.2 \text{ dB} (1.047)$, and the overall available gain of the receiver up to the demodulator is to be $ga = 70 \text{ dB}$.
5. The demodulated signal-to-noise ratio is to be $S_o N_o = 40 \text{ dB}$.

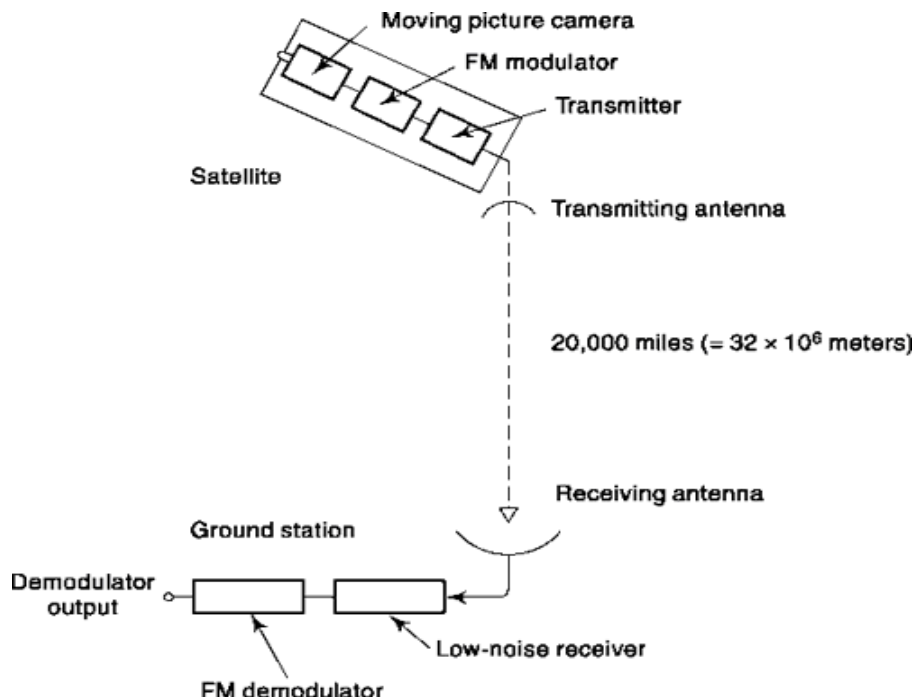


Fig. 15.15 A satellite communication system.

We are to find:

1. The rms frequency deviation (A_{rms})
2. The IF bandwidth

3. The minimum required transmitter power

For simplicity we shall assume that demodulation is performed by an FM discriminator. To minimize the required transmitted power, we assume operation at or just above threshold. We shall further assume that the TV signal can be approximated by a Gaussian process. Thus, the received FM signal can be written as

$$v(t) = A \cos \omega_c t + k [m(l) dl + n(t)] \quad (15.68)$$

where $m(t)$ is the TV signal. Hence, the rms frequency deviation produced is

$$(\Delta f)_{\text{rms}} = \frac{\sqrt{k^2 m^2(t)}}{2\pi} \quad (15.69)$$

From Eq. (9.107) we have

$$\frac{S_o}{N_o} = \frac{3(\Delta f_{\text{rms}}/f_M)^2 (S_i/\eta f_M)}{1 + 6\sqrt{2/\pi} (\Delta f_{\text{rms}}/f_M) (S_i/\eta f_M) e^{-(f_M/B)(S_i/\eta f_M)}} \quad (15.70)$$

Equation (15.70) is a function of the input SNR S_i/hf_M and the rms modulation index Af_{rms}/f_M [note that using Eq. (3.58) $B/f_M = 4.6Af_{\text{rms}}/f_M$]. Thus, for a given output SNR, an infinite number of combinations of these ratios are possible. However, we have a constraint in our problem; that is, we are to operate at or above threshold. Let us solve Eq. (15.70) subject to the constraint that we are operating *at* threshold. The 1 dB dropoff associated with threshold, as noted in Fig. 9.12, occurs when the denominator in Eq. (15.70) has the value 1.26. Hence, at threshold, since an output SNR of 40 dB ($= 10^4$) is required, we have, from Eq. (15.70), the following two results:

$$0.26 = 6\sqrt{\frac{2}{\rho}} \frac{\Delta f_{\text{rms}}}{f_M} \frac{S_i}{\eta f_M} e^{-(f_M/4.6\Delta f_{\text{rms}})(S_i/\eta f_M)} \quad (15.71)$$

$$3 \left(\frac{\Delta f_{\text{rms}}}{f_M} \right)^2 \frac{S_i}{\eta f_M} = 1.26 \times 10^4 \quad (15.72)$$

Equations (15.71) and (15.72) can be solved by solving Eq. (15.72) for S_i/hf_M and substituting this result in Eq. (15.71), thereby eliminating S_i/hf_M . The resulting equation is

It may be shown (Prob. 15.26) that this equation has the solution

$$\frac{\Delta f_{\text{rms}}}{f_M} \approx 4.5 \quad (15.74)$$

$$13 \times 10^{-6} \frac{\Delta f_{\text{rms}}}{f_M} = e^{-(9.13)(f_M/\Delta f_{\text{rms}})^4} \quad (15.73)$$

The corresponding input SNR is

$$\frac{S_i}{\eta f_M} = 23 \text{ dB} \quad (15.75)$$

Good design requires that a margin of safety be employed to ensure operation at or above but not below threshold. We therefore decrease the ratio $\Delta f_{\text{rms}}/f_M$, making it

$$\frac{\Delta f_{\text{rms}}}{f_M} = 4 \quad (15.76)$$

The input SNR required to obtain an $S_0/N_0 = 40$ dB is still

$$\frac{S_i}{\eta f_M} = 23 \text{ dB} \quad (15.77)$$

since we are now operating above threshold.

The IF bandwidth can now be calculated by letting

$$B = 4.6\Delta f_{\text{rms}} = 18.4f_M = 73.6 \text{ MHz} \quad (15.78)$$

We now determine only the required transmitter power, to complete our design. We begin this calculation with Eq. (15.77). Thus,

$$\frac{S_i}{\eta} = 23 \text{ dB} + 10 \log f_M = 89 \text{ dB} \quad (15.79)$$

The noise-power spectral density $h/2$ at the input to the IF filter was shown in Sec. 15.5 to be a function of the noise figure (equivalent temperature) of the receiver and the receiver gain. Using Eqs. (15.33) and (15.56), we have

$$\eta = k(T_{\text{ant}} + T_c)g_a(f) \quad (15.80)$$

where, from the problem specifications,

$$T_{\text{ant}} = 14 \text{ K}$$

$$T_e = T_0(F - 1) = 290(1.047 - 1) \approx 13.6 \text{ K}$$

$$g_a(f) = 70 \text{ dB}$$

Thus

$$\eta = 1.38 \times 10^{-23} (27.6) g_a(f) = 38 \times 10^{-23} g_a(f) \quad (15.81)$$

We can now compute the signal power measured at the HF filter. We find [Eq. (15.79)]

$$S_i = 89 \text{ dB} + 10 \log \eta \approx (89 - 224) \text{ dB} + 10 \log g_a(f) \quad (15.82)$$

The input-signal power measured at the *antenna* is $S_i g_i(f)$. This result, in decibels, is

$$(S_i)_{\text{antenna}} = (S_i)_{\text{HF filter}} - 10 \log g_a(f) = -135 \text{ dB} \quad (15.83)$$

The transmitter power required to deliver a signal power of -135 dB and meeting the problem specifications is found from Eq. (15.65).

$$P_T = P_R \frac{(4\pi d/\lambda)^2}{K_T K_R} \quad (15.84)$$

Performing the calculations in decibels yields

$$\begin{aligned} 10 \log P_T &= 10 \log P_R + 20 \log \left(\frac{4\pi d}{\lambda} \right) - 10 \log K_T - 10 \log K_R \\ &= -135 + 20 \log \left[\frac{4\pi \times 32 \times 10^6}{(3 \times 10^8)/(3 \times 10^9)} \right] - 20 - 50 \end{aligned}$$

Thus

$$P_T = -13 \text{ dB} \quad (15.85)$$

Hence $P_T \geq 50 \text{ mW}$ must be transmitted.

SELF-TEST QUESTIONS

9. Does an antenna has same directivity both for transmission and reception?
10. Which of satellite antenna and earth station antenna has higher gain?

FACTS AND FIGURES

The first satellite, Sputnik-1, was launched on October 4, 1957, by the Soviet Union. A month later, Sputnik-2 made Lyka, a dog, history for being the first living being in space. On January 31, 1958, Explorer-1 was launched by the

United States that discovered magnetic radiation belts around the earth. This was named the Van Allen belt after the principal investigator of the project from University of Iowa. The first communication satellite, SCORE, was launched on December 18, 1958, by the United States. This coincided with Christmas with President Eisenhower delivering this message to all through this satellite, “Peace on Earth, goodwill toward men.”

On August 20, 1964, eleven participating countries formed the International Telecommunications Satellite Organization (Intelsat). The first satellite, Intelsat-I, also called Early Bird, catered 150 telephone circuits and 80 hours of television service from its geostationary orbit. In less than ten years, the number of participating countries in Intelsat grew to eighty. It was privatized in 2001 and today it operates a fleet of more than fifty satellites. In 1969, the Intelsat-III series provided coverage to Indian Ocean for the first time and a complete global network was established. This came useful after a few days when people the world over watched Neil Armstrong setting foot on the moon on July 20, 1969 with his famous words “That’s one small step for (a) man, one giant leap for mankind.”

MATLAB

```

% Experiment 52

% This calculates total (equivalent) noise figure or total (equivalent)
% noise temperature of two port cascaded network. The choice and data can
% be given at command prompt. Equations 15.50 and 15.51 of section
% 15.5.4 are used.

choice=input('Enter 1 if overall noise figure, 2 if eqv. noise temp. - ');
N = input('Enter no. of stages - ');

if choice == 1,
    for i=1:N
        disp('Enter following data for stage - '); disp(i);
        F(i)=input('Enter noise fig. - '); % Data entry
        Ga(i)=input('Enter gain - ');
    end;
end
if choice == 2,
    for i=1:N
        disp('Enter following data for stage - '); disp(i);
        T(i)=input('Enter noise temp. - '); % Data entry
        Ga(i)=input('Enter gain - ');
    end;
end

if choice == 1,
    F_total=F(1); temporary=1; % Realizing eqn. 15.50
    for i=2:N
        for j=1:i-1
            temporary=temporary*Ga(j);
        end;
        F_total=F_total+(F(i)-1)/temporary;
    end;
    F_total %Displaying result
end

if choice == 2,
    T_total=T(1); temporary=1; % Realizing eqn. 15.51
    for i=2:N
        for j=1:i-1
            temporary=temporary*Ga(j);
        end;
        T_total=T_total+T(i)/temporary;
    end;
    T_total % Displaying result
end

```

One typical run of above program with data entry is shown as follows.

```

>> exp52
Enter 1 if overall noise figure, 2 if eqv. noise temp. - 1
Enter no. of stages - 3
Enter following data for stage -
    1
Enter noise fig. - 1.1
Enter gain - 2
Enter following data for stage -
    2
Enter noise fig. - 1.2
Enter gain - 3
Enter following data for stage -
    3
Enter noise fig. - 1.5
Enter gain - 20
F_total = 1.2417

% Experiment 52

% This calculates required transmitter power of a transmitting antenna.
% This uses (eqn.15.65) of section 15.6.

PR=input('Required power at receiving antenna in Watt - ');
KR=input('Receiving antenna gain in dB - ');
KT=input('Transmitting antenna gain in dB - ');
f=input('Carrier frequency in GHz - ');
d=input('Distance between two antennas in KM - ');

KTabs=10^(KT/10);
KRabs=10^(KR/10);
lambda=3*10^8/(f*10^9);
dsi=d*10^3;

PT=PR* (4*pi*dsi/lambda)^2/(KTabs*KRabs); % Realizing eqn. (15.65)
disp('Required transmitter power in Watt - '); disp(PT);

```

A typical run of the program is shown below. The data used are of Example 15.3.

```

>> exp53
Required power at receiving antenna in Watt - 10^-6
Receiving antenna gain in dB - 40
Transmitting antenna gain in dB - 40
Carrier frequency in GHz - 4
Distance between two antennas in KM - 48
Required transmitter power in Watt - 0.6468

```

SUMMARY

The chapter begins with a discussion of resistor as a source of noise and also shows how noise affects when there is a network of multiple resistors and resistors with reactive elements. The concept of available thermal noise power and noise temperature is described. Two-port networks are the

basic building block of any receiving system. A detailed discussion on noise available at the two port network output and its bandwidth are

presented. Noise figure and concept of equivalent noise temperature are introduced which effectively characterize a cascaded network. The noise performance of antenna in communication is presented with system level calculations.

PROBLEMS

15.1 The three resistors are at a temperature T . A bandlimited rms voltmeter is placed across ab , bc , and ac in succession.

- (a) Is $\overline{V_{ac}}(\text{rms}) = \overline{V_{ab}}(\text{rms}) + \overline{V_{bc}}(\text{rms})$? Why, or why not?
- (b) Is $\overline{V_{ac}^2} = \overline{V_{ab}^2} + \overline{V_{bc}^2}$? Why or why not?
- (c) Calculate $\overline{V_{ac}}(\text{rms})$ read by a meter having a bandwidth B , if R_a and R_c are at temperature T , and R_b is at temperature T_b . Give your answer in terms of symbols.

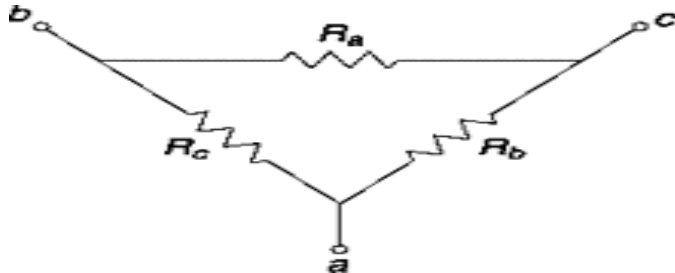


Fig. p.15.1

15.2 A parallel RLC circuit centered at 3 GHz has a bandwidth of 10 MHz. If the resistance R is 10 kilohms, calculate $R(f)$ and the power spectral density $G_v(f)$ of the noisy circuit.

15.3 (a) Develop an expression for the power spectral density of the noise voltage e_n .

(b) The noise voltage e_n is passed through a low-pass filter with cutoff frequency at $(O_c$ and then through an amplifier of gain $A = 9$. Develop an expression for the total noise output power of the amplifier.

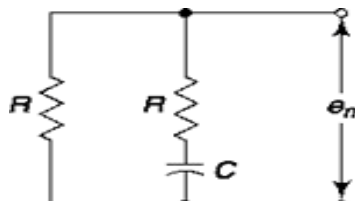


Fig. p.15.3

15.4 Refer to Fig. 15.4a. Assume that the resistor has an inductance L in series with it. Find $R(f)$, $G_v(f)$ and $v^2 n$ when the integral is over all frequencies.

15.5 Comment on the difference between $G_a(f) = kT/2$ in Eq. (15.18) and $G_v(f) = 2kTR(f)$ in Eq. (15.10).

15.6 If $T = 4$ K, find $G_a(f)$ from Eq. (15.20) when the wavelength $l \sim 1$ mm, 1 mm. Is the noise white in these regions?

15.7 Verify Eq. (15.25).

15.8 Calculate the noise bandwidth of a parallel RLC filter having a 3 dB bandwidth B .

15.9 Calculate the noise bandwidth of an RC low-pass filter having a 3 dB bandwidth f_c .

15.10 A Gaussian filter has the characteristic

- (a) Calculate the 3 dB bandwidth.
- (b) Calculate the noise bandwidth.

15.11 An antenna is connected to a receiver having an equivalent noise temperature $T_e = 100$ K. The available gain of the receiver is $g_a(f) = 10^8$ and the noise bandwidth is $B_N = 10$ MHz. If the available output-noise power is 10 mW. find the antenna temperature.

15.12 An antenna has a noise temperature $T_{\text{ant}} = 4$ K. It is connected to a receiver which has an equivalent noise temperature $T_e = 100$ K; the midband available gain of the receiver is $g_{a0} = 10^{10}$, and can be represented by a parallel RLC filter having a 3 dB bandwidth of 10 MHz. Find:

- (a) B_N .
- (b) The available output-noise power.

15.13 (a) Explain why F cannot be less than 1.

- (b) Verify Eqs. (15.36) and (15.37).

15.14 The noise figure of an amplifier is 0.2 dB. Find the equivalent temperature T_e .

15.15 Show that the average value of the noise figure is given by Eq. (15.38).

15.16 The noise present at the input to a two-port is 1 mW. The noise figure F is 0.5 dB. The receiver gain $g_a = 10^{10}$. Calculate:

- (a) The available noise power contributed by the two-port.
- (b) The output available noise power.

15.17 Show that Eq. (15.42) applies under the conditions specified in the text.

15.18 With the entire setup operating at 290 K the measured noise figure of the amplifier circuit is $F = 3$ and the voltmeter reads 12 volts. When the resistor R_s alone is cooled to 25 K, what will be the reading of the voltmeter?



Fig. P.15.18

15.19 The entire setup is at $T = 290$ K. Boltzmann's constant $k = 1.38 \times 10^{-23}$. When $e = 0$ V, the voltmeter reads 3 volts. When $e = 10$ mV rms, the voltmeter reads 5 volts. Find the noise figure F .

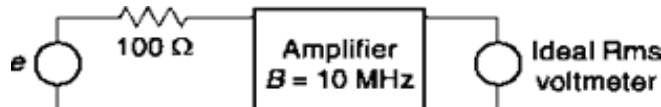


Fig. P.15.19

15.20 A noisy amplifier has flat gain from 0 to B Hz and zero gain above B Hz, source impedance R_s , and load impedance R_L . When the input voltage is zero, it is found that P_o watts are dissipated in the load impedance. When the input voltage is white noise with (one-sided) spectral density h (volts) 2 /Hz, the power dissipated in the load is $2P_o$. Find an expression for the noise figure of the amplifier.

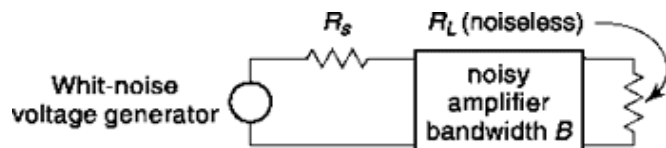


Fig. p.15.20

- 15.21 Derive Eqs. (15.49) and (15.50).
- 15.22 Derive Eq. (15.51).
- 15.23 Refer to Fig. 15.13. Let $T_{\text{ant}} = 10 \text{ K}$, $T_e(\text{maser}) = 4 \text{ K}$ with a gain of 20 dB, the Travelling Wave Tube (TWT) has a noise figure $F = 3 \text{ dB}$ and a gain $g_a = 40 \text{ dB}$, and a mixer and IF amplifier with $F = 10 \text{ dB}$ and a gain $g_{aT} = 60 \text{ dB}$. Calculate the available noise power at the receiver output.
- 15.24 Repeat Prob. 15.23. Now, however, consider that the available noise power at the receiver output, measured in a noise bandwidth of 10 MHz, is 1 mW. Find the value of T_{ant} .
- 15.25 Verify Eqs. (15.71) and (15.72).
- 15.26 Find r.m.s. modulation index of frequency modulated satellite-to-earth communication system using data of Sec. 15.6.1.
- 15.27 How does the required transmitter power change in satellite-to-earth communication example of Sec. 15.6.1 if noise temperature of receiving antenna reduces to 10 K?

16

SPREAD SPECTRUM MODULATION

CHAPTER OBJECTIVE

In this chapter, we discuss a relatively new modulation technique where the spectrum of the modulated signal is spread to cover a wider range of frequency spectrum. This is done over and above the common modulation schemes discussed in previous chapters and offer features like resistance to jamming, transparency to unfriendly receiver, etc. We discuss two popular spread spectrum techniques, Direct Sequence and Frequency Hopping with their advantages and disadvantages. Applications like Code Division Multiple Access (CDMA), Ranging are presented. Finally, we discuss acquisition and tracking of spread spectrum signals. Besides numerical examples the chapter also presents MATLAB based simulations highlighting generation and use of spread spectrum signal.

FACTS AND FIGURES

MGM movie star Hedy Lamarr and music composer George Antheil were awarded a US Patent in 1942 for their “Secret Communications System” which essentially was a frequency hopping spread spectrum system. The idea was developed to guide torpedoes to their target without being intercepted by the enemy, by sending messages between a transmitter and receiver over multiple radio frequencies in a random pattern. Lamarr learnt about the problem at defence meetings she had attended with her husband, an arms manufacturer. Rather than developing the patent commercially, they gave it away to the US government for the war effort.

Most of the work done in Spread Spectrum throughout the '50s, '60s and '70s was heavily backed by the military and drowned in secrecy. Spread Spectrum was first used for commercial purposes in the 1980s when Equatorial Communications of Mountain View, CA used Direct Sequence for multiple access communications over synchronous satellite transponders.

16.1 USE OF SPREAD SPECTRUM

Spread spectrum is a technique whereby an already modulated signal is modulated a *second* time in such a way as to produce a waveform which interferes in a barely noticeable way with any other signal operating in the same frequency band. Thus, a receiver tuned to receive a specific AM or FM broadcast would probably not notice the presence of a spread spectrum signal operating over the same frequency band. Similarly, the receiver of the spread spectrum signal would not notice the presence of the AM or FM signal. Thus, we say that interfering signals are *transparent* to spread spectrum signals and spread spectrum signals are transparent to interfering signals.

To provide the “transparency” described above the spread spectrum technique is to modulate an already modulated waveform, either using amplitude modulation or wideband frequency modulation, so as to produce a very wideband signal. For example, an ordinary AM signal utilizes a bandwidth of 10 kHz. Consider that a spread spectrum signal is operating at the same carrier frequency as the AM signal and has the same power P_s as the AM signal but a bandwidth of 1 MHz. Then, in the 10 kHz bandwidth of the AM signal, the power of the second signal is $P_s \times (10^4/10^6) = P_s/100$.

Since the AM signal has a power P_s the interfering spread spectrum signal provides noise which is 20 dB *below* the AM signal.

What are some of the applications of spread spectrum modulation? The widest application at this time is its use in military communications systems where spread spectrum serves two functions. The first is that it allows a transmitter to transmit a message to a receiver without the message being detected by a receiver for which it is not intended, i.e., the transmission is transparent to an unfriendly receiver. To achieve this transparency, the spread spectrum modulation decreases the transmitted power spectral density so that it lies well below the thermal noise level of any unfriendly receiver. The second major application of spread spectrum is found, when, as a matter of fact, it turns out not to be possible to conceal the transmission. Police radars can employ spread spectrum to avoid detection by radar detectors employed by drivers. In such a case the operator of an unfriendly receiver might attempt to begin transmitting an interfering signal to block communication between transmitter and receiver. Here again, spread

spectrum acts to reduce the effective power of the interference so that communication can proceed with minimal interference.

In the commercial communications field spread spectrum has many applications, a major application being the transmission of a spread spectrum signal on the same carrier frequency as an already existing microwave signal. By communicating in this manner additional signals can be transmitted over the same band thereby increasing the number of users.

In addition, spread spectrum is used in satellite communications, cellular telephony, Global Positioning Systems (GPS) etc. which we discuss in brief in the next chapter.

16.2 DIRECT SEQUENCE (DS) SPREAD SPECTRUM

A Direct Sequence (DS) spread spectrum signal is one in which the amplitude of an already modulated signal is amplitude modulated by a very high rate NRZ binary stream of digits. Thus, if the original signal is $s(t)$, where

$$s(t) = \sqrt{2 P_s} d(t) \cos \omega_0 t \quad (16.1)$$

(a binary PSK signal), the DS spread spectrum signal is

$$v(t) = g(t)s(t) = \sqrt{2 P_s} P g(t)d(t) \cos \omega_0 t \quad (16.2)$$

where $g(t)$ is a *pseudo-random* noise (PN) binary sequence having the values ± 1 .

The characteristics of $g(t)$ are extremely interesting and are discussed in some detail in Sec. 16.4. Here we merely assume that $g(t)$ is a binary sequence as is the data $d(t)$. The sequence $g(t)$ is generated in a deterministic manner and is repetitive. However, the sequence length before repetition is usually extremely long and to all intents and purposes, and without serious error, we can assume that the sequence is truly random, i.e. there is no correlation at all between the value of a particular bit and the value of any other bits. Furthermore, the bit rate f_c of $g(t)$ is usually much greater than the bit rate f_b of $d(t)$. As a matter of fact the rate of $g(t)$ is usually so much greater than f_b , we say that $g(t)$ “chops the bits of data into *chips*”, and we call the rate of $g(t)$ the *chip rate* f_c , retaining the words, *bit rate*, to represent f_b .

To see that multiplying the BPSK sequence $s(t)$ by $g(t)$ spreads the spectrum we refer to Fig. 16.1 which shows a data sequence $d(t)$, a pseudo-random (often called a pseudo-noise or PN) sequence $g(t)$ and the product sequence $g(t)d(t)$. Note that (as is standard practice) the edges of $g(t)$ and $d(t)$ are aligned, that is, each transition in $d(t)$ coincides with a transition on $g(t)$. The product sequence is seen to be similar to $g(t)$, indeed if $g(t)$ were truly random, the product sequence would be another random sequence $g'(t)$ having the *same* chip rate f_c as $g(t)$. Since the bandwidth of the BPSK signal $s(t)$ is nominally $2f_b$ (see Fig. 5.2) the bandwidth of the BPSK spread spectrum signal $v(t)$ is $2f_c$ and the spectrum has been spread by the ratio f_c/f_b . Since the power transmitted by $s(t)$ and $v(t)$ is the same, i.e. P_s , the power spectral density $G_s(f)$ is reduced by the factor f_b/f_c .

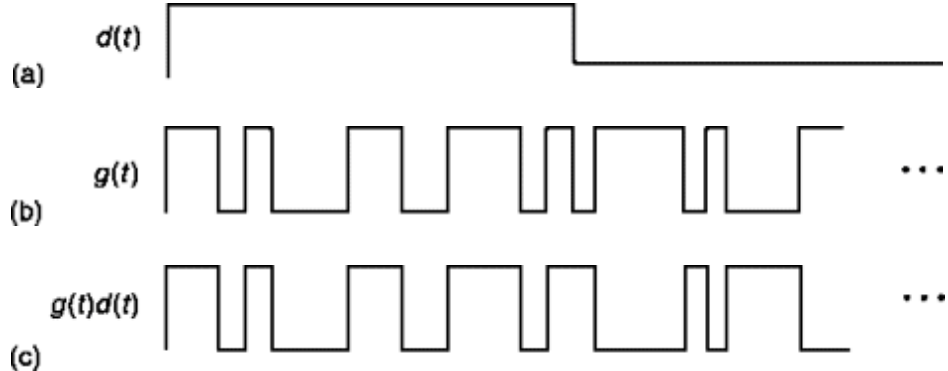


Fig. 16.1 (a) The waveform of the data bit stream $d(t)$. (b) The chipping waveform $g(t)$. (c) The waveform of the product $g(t)d(t)$.

To recover the DS spread spectrum signal, the receiver shown in Fig. 16.2 first multiplies the incoming signal with the waveform $g(t)$ and then by the carrier $\cos w_0 t$. The resulting waveform is then integrated for the bit duration and the output of the integrator is sampled, yielding the data $d(kT_b)$. We note that at the receiver it is necessary to regenerate both the sinusoidal carrier of frequency w_0 and also to regenerate the PN waveform $g(t)$.

16.2.1 Effect of Thermal Noise

Having noted that spread spectrum techniques can suppress the effect of an interfering deterministic signal, we may wonder whether the technique can serve, as well to reduce the disturbance generated by thermal noise. As we shall now see, such is not the case.

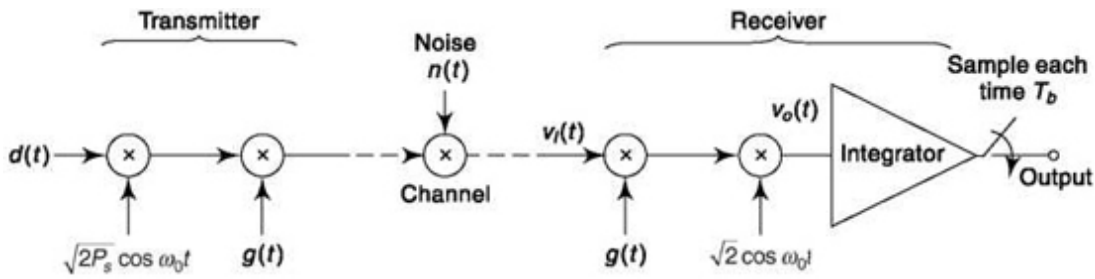


Fig. 16.2 A BPSK communication system incorporating a spread spectrum technique.

In Fig. 16.2 is shown a BPSK communication system incorporating a spread-spectrum technique. The data waveform $d(t)$ is an NRZ bit stream which makes excursions between +1 and -1 at the rate f_b while the chipping waveform makes excursions between +1 and -1 at the rate f_c . Observe that in the overall transmission, the input signal is twice multiplied by $g(t)$, and, since $g^2(t) = 1$ there is no net effect on the received output signal. The noise $n(t)$ introduced in the channel is chipped at the receiver before reaching the integrator. That is, at nominally random times, the polarity of the noise waveform is reversed. It is intuitively clear that the reversal has no effect on the power spectral density or the probability density function of the Gaussian noise. Hence both the signal and the statistical properties of the noise are unaffected by the spread-spectrum technique and the overall performance of the system is not affected. As in BPSK without spread spectrum, the error probability (see Sec. 11.4.1) is

$$P_e = \frac{1}{2} \operatorname{erfc} \sqrt{E_b / \eta} \quad (16.3)$$

where as before E_b is the bit energy and $h/2$ is the two-sided power-spectral density of the noise.

16.2.2 Single-Tone Interference and Jamming

Consider next that the DS spread spectrum signal is interfered with by a sinusoidal signal of normalized power P_J at the carrier frequency f_0 . That is in Fig. 16.2, the noise $n(t)$ is replaced by the

waveform $JlP_J \cos(\omega_0 t + Q)$. The input to the receiver is then

$$v_r(t) = \sqrt{2 P_s} d(t)g(t) \cos \omega_0 t + \sqrt{2 P_J} \cos(\omega_0 t + \theta) \quad (16.4)$$

Taking account of the fact that $g^2(t) = 1$, the signal $v_0(t)$ that appears at the input to the integrator is

$$v_0(t) = \sqrt{P_s} d(t)(1 + \cos 2\omega_0 t) + P \sqrt{P_J} g(t)(1 + \cos 2\omega_0 t) \cos \theta - \sqrt{P_J} g(t) \sin 2\omega_0 t \sin \theta \quad (16.5)$$

As we have noted on other occasions, it is normal practice to arrange that the bit duration be some multiple of the half period of the carrier period $1/f_0$. Hence, as usual, the terms in Eq. (15.4), in which $\cos 2\omega_0 t$ or $\sin 2\omega_0 t$ is a factor, will yield no voltage at the integrator output. Our interest then remains with the waveform

$$v'_0(t) = \sqrt{P_s} d(t) + \sqrt{P_J} g(t) \cos \theta \quad (16.6)$$

It is of interest to note that at the input to the receiver, as appears in Eq. (16.4), the information signal, which has $g(t)$ as a factor, is a wide spectrum signal while the interfering signal is a singlefrequency sinusoidal waveform. On the other hand, in Eq. (16.6) the information signal, involving now only $d(t)$ and not $g(t)$ is a signal whose bandwidth has been greatly compressed. The interfering signal which in Eq. (16.4) had a spectrum which consisted of an impulse at $f=f_0$, in Eq. (16.6) appears as a wideband signal. Using the results of Sec. 6.1.1 (see also Prob. 16.4), we readily find that the power spectral density of the interfering signal in Eq. (16.6) is

$$G_J(f) = \frac{P_J \overline{\cos^2 \theta}}{2 f_c} \left(\frac{\sin \pi f / f_c}{\pi f / f_c} \right)^2 \quad (16.7)$$

The integrator has characteristics not unlike a low-pass filter. As a matter of fact, it can be verified (Prob. 16.5) that an integrator whose integration period is T_b is approximately equivalent to a low-pass filter with cutoff at frequency f_b ($=1/T_b$). Since $f_b \ll f_c$, then, in the frequency range $\pm f_b$, $G_J(f)$ in Eq. (16.7) has, approximately, the constant value

$$G_J(f) = \frac{P_J \overline{\cos^2 \theta}}{2 f_c} : |f| \leq f_b \quad (16.8)$$

Now we have noted that the effective information signal which appears at the input to the integrator in Fig. 16.2 is the same as it would be if the spread spectrum feature had not been incorporated in the system. If the interfering

signal were thermal noise $n(t)$ of power spectral density $h/2$, the noise signal at the integrator would also have the power spectral density $h/2$. In this case, the probability of error at the output of the integrate and dump filter would be, as we have often noted,

$$P_e = \frac{1}{2} \operatorname{erfc} \sqrt{\frac{E_b}{\eta}} \quad (16.9)$$

In the present case, where the interfering signal is sinusoidal, we can continue to apply Eq. (16.9). We simply replace $h/2$ by $G_J(f)$, from Eq. (16.8), in Eq. (16.9). Hence, we find

$$\begin{aligned} P_e &= \frac{1}{2} \operatorname{erfc} \sqrt{\frac{E_b}{\eta}} = \frac{1}{2} \operatorname{erfc} \sqrt{\frac{E_b f_c}{P_J \cos^2 \theta}} = \frac{1}{2} \operatorname{erfc} \sqrt{\frac{P_s T_b f_c}{P_J \cos^2 \theta}} \\ &= \frac{1}{2} \operatorname{erfc} \sqrt{\left(\frac{P_s}{P_J}\right) \left(\frac{f_c}{f_b}\right) \cdot \frac{1}{\cos^2 \theta}} \end{aligned} \quad (16.10)$$

The angle d is the phase of the jamming sinusoidal waveform with respect to the phase of the information signal carrier. There is no reason to expect any correlation between the phases of jamming and signal carriers. Hence we consider that d is a random variable all of whose possible values are equally likely. In this case we have that $\overline{\cos^2 \theta} = \frac{1}{2}$ and we have

$$P_e = \frac{1}{2} \operatorname{erfc} \sqrt{2 \left(\frac{P_s}{P_J}\right) \left(\frac{f_c}{f_b}\right)} \quad (16.11a)$$

$$= \frac{1}{2} \operatorname{erfc} \sqrt{P_s \sqrt{\frac{P_J}{2(f_c/f_b)}}} \quad (16.11b)$$

The quantity

$$P_{J,\text{eff}} = \frac{P_J}{2 \left(\frac{f_c}{f_b}\right)} \quad (16.12)$$

is called the *effective jamming power* since it is this power, in comparison to the signal power P_s that determines the error probability generated by the

jamming. The ratio f_c/f_b measures the extent to which the effect of the (mean) jamming power $P_j/2$ is reduced by the chipping and is called the *processing gain* G_p , i.e.

$$G_p \equiv f_c/f_b \quad (16.13)$$

The results presented above are entirely valid if the chipping waveform $g(t)$ is of frequency very much higher than the bit frequency and if $g(t)$ is a truly random sequence. On the other hand when these conditions are not met it may actually turn out that Eq. (16.10) is overly pessimistic. For example, if the length of the pseudo-random sequence before repeating is no longer than the duration of a bit, the error probability is significantly smaller than given in Eq. (16.10).

16.3 SPREAD SPECTRUM AND CODE DIVISION MULTIPLE ACCESS (CDMA)

In this section, we describe a method for multiple access communications which on principle allows more than one sender use the same channel for transmission with potential problem of collision when sent simultaneously. This scheme employs spread spectrum and is called *Code Division Multiple Access* (CDMA). The advantage of a CDMA system is that collisions are not destructive, i.e. each of the signals involved in a collision would be received with only a slight increase in error rate.

In CDMA, each user is provided with an individual and distinctive PN code. These codes are almost uncorrelated with one another (see Sec. 16.6) and for the purpose of our explanation we shall assume that the sequences are indeed uncorrelated. To illustrate the principle of operation of CDMA consider that at a given time, each of k users is transmitting data at the same carrier frequency f_0 , using DS spread spectrum, and his particular code $g_i(t)$. Then, each receiver is presented with the same input waveform,

$$v(t) = \sum_{i=1}^k \sqrt{2P_s} g_i(t) d_i(t) \cos(\omega_0 t + \theta_i) \quad (16.14)$$

where each signal is assumed to present the same power P_s to the receiver, each pseudo-random sequence $g(t)$ has the same chip rate f_c and $d_i(t)$ is the data transmitted by user i . The data rate for each user is the same, f_b . Also θ_i

is a random phase, statistically independent of the phase of each of the other users. Thermal noise is omitted to simplify the discussion.

If the receiver is required to receive each of the k users it needs k correlators. At receiver 1, the signal of Eq. (16.14) will be multiplied by $g_x(t)$ and also by $\sqrt{2} \cos(\omega_0 t + \theta_1)I$ to generate the signal v'_{01} which is to be applied to the integrate and dump circuit. As before, we drop from v'_{01} those components which will not make their way through the integrator and we shall be left with

$$v'_{01} = \sum_{i=1}^k \sqrt{P_s} g_1(t) g_i(t) d_i(t) \cos(\theta_i - \theta_1) \quad (16.15a)$$

$$= \sqrt{P_s} d_1(t) + \sum_{i=2}^k \sqrt{P_s} g_1(t) g_i(t) d_i(t) \cos(\theta_i - \theta_1) \quad (16.15b)$$

We assume that all the g 's make transitions at the same time. In this case the product $g_1(t)g_i(t)$ has the same chip rate f_c as has any of the g_i 's individually. And to the extent that the g_i 's individually are random sequences so also is the product $g_1(t)g_i(t) = g_{1i}(t)$. Writing also $\cos(0_i - d_1) = \cos d_{1i}$, Eq. (16.15b) becomes

$$v'_{01} = \sqrt{P_s} d_1(t) + \sum_{i=2}^k \sqrt{P_s} g_{1i}(t) \cos \theta_{1i} \quad (16.16)$$

Comparing Eq. (16.16) with Eq. (16.6) we see that they are similar, except that Eq. (16.16) has $k - 1$ independent interfering signals while Eq. (16.6) is for a single interfering signal. Since the power spectral density of one interferer is given by Eq. (16.8), letting $P_J = P_s$ and $\cos^2 \theta = V$, the total power spectral density of $k - 1$ independent interferers is the sum of the power spectral densities. The total power spectral density of the $k - 1$ interferers in Eq. (16.16) is therefore

$$v'_{01} = \sqrt{P_s} d_1(t) + \sum_{i=2}^k \sqrt{P_s} g_{1i}(t) \cos \theta_{1i} \quad (16.16)$$

The probability of a bit being in error is found using Eq. (16.11a), by letting $P_J = (k - 1)P_s$:

$$P_e = \frac{1}{2} \operatorname{erfc} \sqrt{2 \left(\frac{1}{k-1} \right) \left(\frac{f_c}{f_b} \right)} \quad (16.18)$$

Thus in a slotted CDMA system, to insure a low probability of error, the gain, f_c/f_b , must be adjusted so that

$$\frac{f_c}{f_b} \ll (k-1)/2 \quad (16.19)$$

In Eq. (16.14) we assumed that each transmitted signal presented the same power P_s to the receiver. There are many practical situations where such is not the case. When transmitting to a satellite, there may be high-power as well as low-power transmitters. Also, in ground communication, one user may be close to the receiver while another user may be far from the receiver.

When an unwanted user's received power is much larger than the received power presented by the desired user, errors can occur. This problem is referred to in the literature as the *near-far problem*, and limits the utility of DS systems to applications where each user's received power is approximately the same. In modern systems this problem is addressed by adaptive power control.

16.3.1 Multipath Fading and Rake Receiver

Multipath fading is a phenomena where signals starting from a source take different paths through various reflections and refractions to reach the destination. At the destination, we have the sum total of various versions of the signal coming via different paths with different attenuations and delays. These attenuations and delays again can change due to change in refraction index of propagation media or change of reflecting surfaces (e.g. reflection from a moving vehicle). From our discussion, we can find that the delayed version has low autocorrelation with the original signal, more so if the delay exceeds chip duration. Then it is treated as an interfering signal and is rejected in the same manner. However, a better method is available today to utilize the power available in the signal coming from multiple paths. This is accomplished in a *rake receiver* which is a bank of correlation receiver, each correlated to delays (adjustable) of different arriving paths. Finally, the outputs of the correlators, which are coherent, are added with improved reception quality.

Refer to Fig. 16.3 that gives the block diagram of one realization of a rake receiver. The multipath signal is first fed to a block of delay elements working in parallel. These parallel blocks are often known as *fingers*. The number of such fingers, N , can vary depending on the number of different

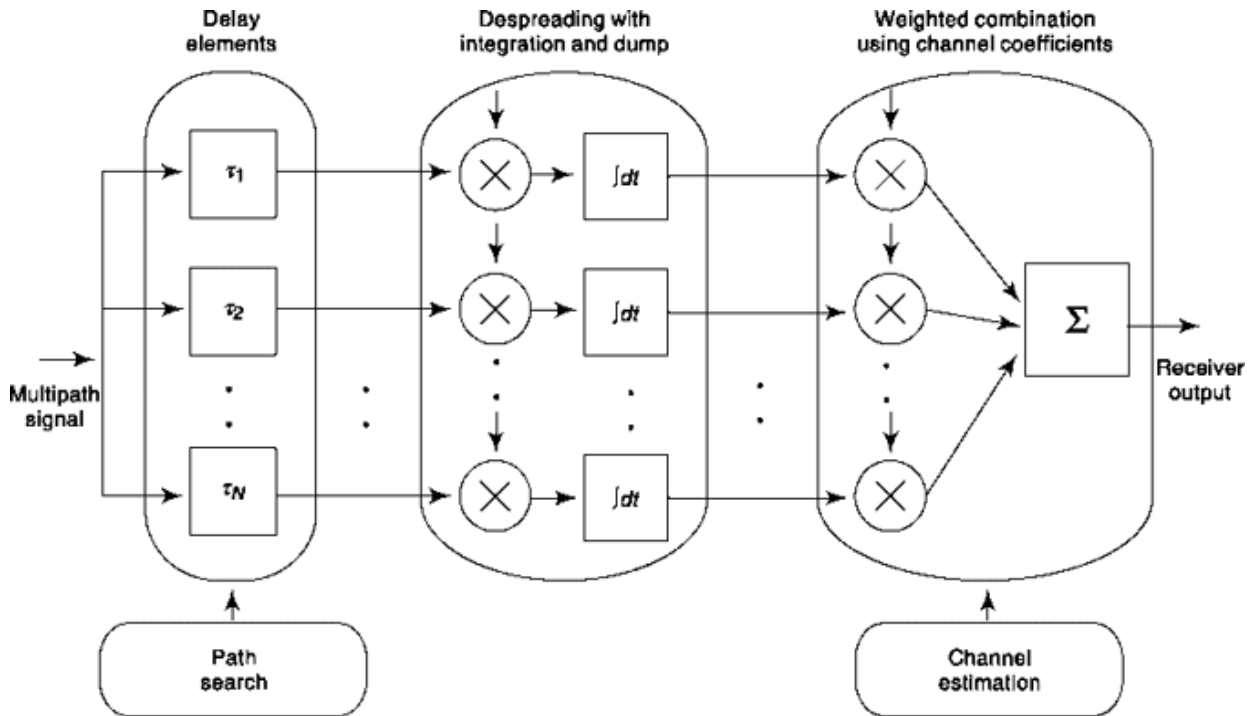


Fig. 16.3 Block-diagram representation of a rake receiver

paths expected (typically 2 to 8). The path-search block estimates the delays in each path. The delayed versions of the input signal are then despread by multiplying with spreading code and this is followed by integrate and dump filter which operates over one symbol period. If the input data is a scrambled one then despreading and descrambling can be combined. The channel-estimation block gives channel coefficients of each path which is proportional to its strength. These weights are used in a combiner and the process is known as Maximum Ratio Combining (MRC). If the same weights are used in different paths then it is known as Equal Gain Combining (EGC). MRC performs better than EGC for Rayleigh fading channel which represents a mobile communication environment better. The rake receiver made spread spectrum system efficient by taking care of the multipath problem and is a part and parcel of today's cell phones.

16.4 RANGING USING DS SPREAD SPECTRUM

Another application of DS spread spectrum is for *ranging*. In this application, illustrated in Fig. 16.4, a DS signal

$$s(t) = \sqrt{2 P_s} g(t) \cos \omega_0 t \quad (16.20)$$

is transmitted. The signal is reflected from the intended target and received $T_1 + T_2$ seconds later

as $r(t)$,

$$r(t) = a \cos(t - T_1 - T_2) \quad (16.21a)$$

where a represents the signal attenuation and Q is a random phase caused by the time delay, i.e. $Q = -\omega_0 (T_1 + T_2)$. The carrier $\sqrt{2} \cos \omega_0 (t - T_1 - T_2)$ is determined using a squaring circuit (not shown in Fig. 16.4) or equivalent (see Sec. 10.5.1) and the PN sequence $g(t - T_1 - T_2)$ is extracted.

The PN waveform $g(t - T_1 - T_2)$ having been recovered, is correlated with the waveform $g(t - D)$ which is the PN waveform delayed by a *known* time interval D . The correlation function $R_g(D)$, which is the output v_o of the integrator in Fig. 16.4 is

$$v_o = R_g(D) = \int_0^{LT_c} g(t - T_1 - T_2) g(t - D) dt \quad (16.22)$$

The integration interval in Eq. (16.22) extends over the length of the PN sequence. This length is given by the product of the number of bits in the sequence (i.e. the sequence length L) and the period T_c of the chipping.

The special and important characteristic of the PN waveform in the present application is that the correlation $R_g(D)$ is negligibly small if the difference it delays, i.e. $D - (T_1 + T_2)$ exceeds the chip duration and $R_g(D)$ is a maximum when $D = T_1 + T_2$. Accordingly, in Fig. 16.3, the range is determined by adjusting D to maximize v_o . If the velocity of light is $c = 3 \times 10^8$ m/s and $T_1 = T_2$, the range of the target is

$$d = \frac{1}{2} c D \quad (16.23)$$

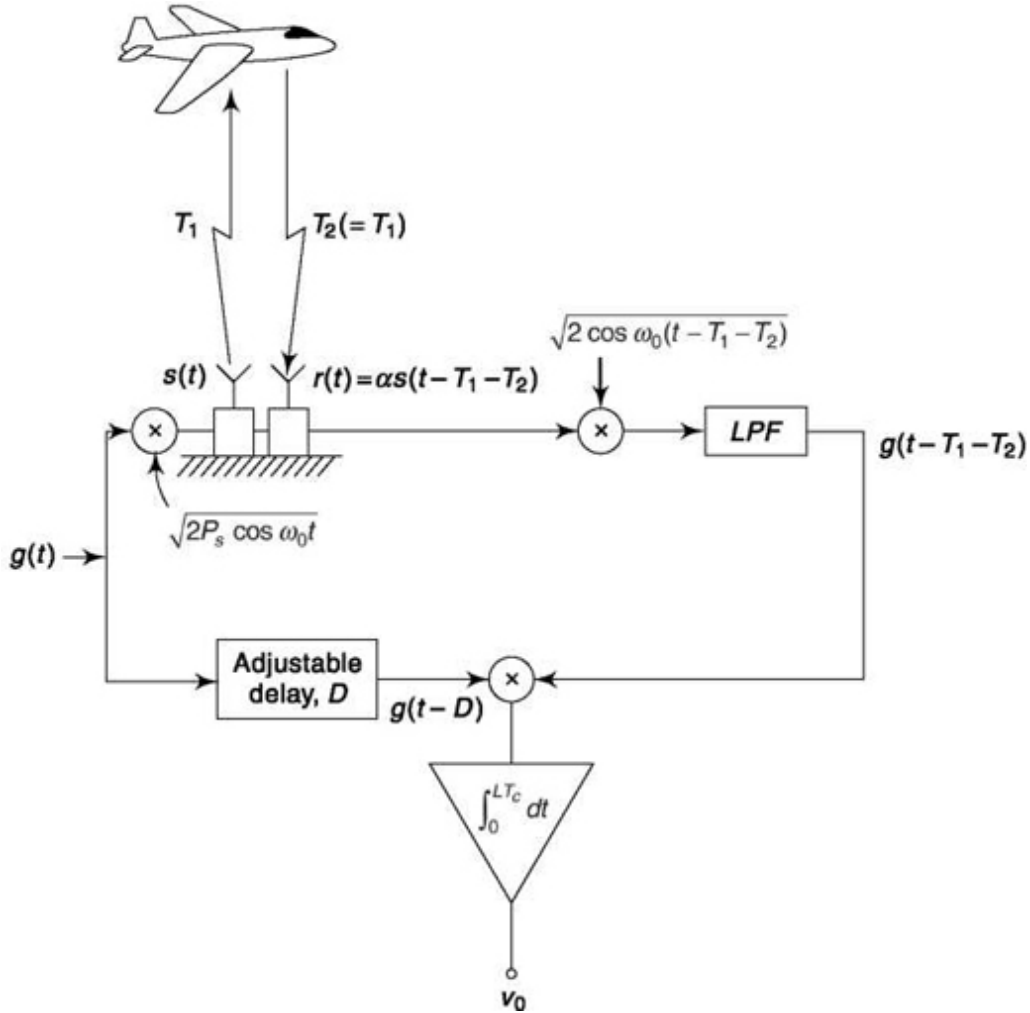


Fig. 16.4 Ranging using DS spread spectrum.

Furthermore, the precision of the measurement is the chip duration $\pm T_c$ which corresponds to a distance $cT_c/2$ so that

$$d = \frac{c}{2}(D \pm T_c) \quad (16.24)$$

and the measurement accuracy can be improved by decreasing T_c relative to D .

Example 16.1

The signal power received for a desired signal of 100 Kb/s bit rate signal is 1 mW. The chip frequency used is 100 MHz. A jamming signal is employed at the carrier frequency, the received power of which is 1 W. Find (a) processing gain, (b) error probability without jamming and with jamming. Noise power spectral density = 10^{-9} W/Hz.

Solution

Given, $f_b = 10^5$, $f_s = 10^8$, $P_s = 0.001$,
 $P_j = 1$, $\eta = 2 \times 10^{-9}$ W/Hz
(a) Processing gain = $f_c/f_b = 10^8/10^5 = 1000$

$$\text{Bit interval } T = \frac{1}{10^5} = 10^{-5} \text{ sec.}$$

$$\begin{aligned}\text{Energy per bit, } E_b &= P_s T = 0.001 \times 10^{-5} \\ &= 10^{-8}\end{aligned}$$

Using Eq. (16.9), Error probability

$$\begin{aligned}\text{without jamming} &= \frac{1}{2} \operatorname{erfc} \sqrt{\frac{10^{-8}}{2 \times 10^{-9}}} \\ &= 0.00078\end{aligned}$$

$$\begin{aligned}\text{with jamming} &= \frac{1}{2} \operatorname{erfc} \sqrt{\frac{10^{-8}}{1/(2 \times 10^{-9})}} \\ &= 0.0228\end{aligned}$$

Example 16.2

A DS spread spectrum system of chip rate 10 MHz is used for ranging. If the reflected wave is received after 0.1 milisecond, find the probable distance of the target.

$$\begin{aligned}\text{Chip period } T_c &= 1/f_c = 1/10^7 = 10^{-7} \text{ s} \\ \text{From Eq.(16.23), the estimated distance} \\ &= 0.5 \times 3 \times 10^8 \times 10^{-4} = 1.5 \times 10^4 \text{ m} = 15 \text{ km} \\ \text{From Eq.(16.24), the tolerance} \\ &= 0.5 \times 3 \times 10^8 \times 10^{-7} \text{ m} = 15 \text{ m} \\ \text{Thus, the target is between } 15000 - 15 \\ &= 14985 \text{ m and } 15000 + 15 \\ &= 15015 \text{ m of the source.}\end{aligned}$$

SELF-TEST QUESTIONS

1. Can interfering signals be considered transparent to spread spectrum signals and vice versa?
2. Is the sequence length before repetition of a pseudorandom sequence used in spread spectrum extremely large?
3. What is ‘near-far’ problem?
4. How chip duration is related to measurement accuracy in Ranging by DS spread spectrum?

16.5 FREQUENCY HOPPING (FH) SPREAD SPECTRUM

Frequency Hopping (FH) spread spectrum is a FM or FSK technique while D spread spectrum, described in Sec. 16.2, is an AM (or PSK) technique.

The signal to be frequency hopped is usually a BFSK signal although M-ary FSK, MSK or TFM can be employed. Considering that BFSK is used, we have that the original signal, before spread spectrum is applied, is

$$s(t) = \sqrt{2 P_s} \cos(\omega_0 t + d(t)\Omega t + \theta) \quad (16.25)$$

where $d(t)$ is the data to be transmitted. The FH modulation is then applied by varying the carrier frequency so that the resulting FH spread spectrum is

$$v(t) = \sqrt{2 P_s} \cos(\omega_f t + d(t)\Omega f t + \theta) \quad (16.26)$$

Here the FH signal has a carrier frequency $f = w/2p$ which changes at the hopping rate f_H , i.e. the carrier frequency f changes each T_H seconds. The frequency chosen for each T_H is selected in a pseudo-random manner from a specified set of frequencies. Typically, 32-500 different frequencies are used to form this set.

The primary advantage of FH is that it enables the transmitter to change its carrier frequency and thereby avoid an otherwise in-band interfering signal. For example, consider that the FH signal spends an equal time at each of 1000 frequencies $f_1, f_2, \dots, f_{1000}$. Also assume that BFSK is employed. The

FH rate of the data is f_b , the bandwidth used by the signal (see Sec. 5.3.1), at any carrier frequency f_i , is $B = 4f_b$. Now assume that there is an interfering signal having a bandwidth $B = 4f_b$ and a fixed center frequency f_j . If frequency hopping were not employed and the interference were located at the transmitted signal's carrier frequency, i.e. $j = i$, then if the interfering signal power were sufficiently large the probability of error would be $P_e = 0.5$ since under these circumstances we could do no better than to guess. (In a military system, the interferer determines the signal's carrier frequency and purposely transmits at that frequency to block or *jam* the communications.) By employing FH and using say 1000 frequencies, the probability of the same interferer causing an error is reduced to $P_e = 1/2000 = 5 \times 10^{-4}$ (note that thermal noise is ignored since it is considered to be a second-order effect when "jamming" is present).

The Need for Coding

A probability of error of 5×10^{-4} is often considered to be very large and would render such a system useless for data transmission. As a result, FH

systems employ error correction coding to reduce the probability of error.

In the above discussion we assumed that when the FH signal “lands” at f a single error could occur. Very often, however, the bit rate f_b of the BFSK data is much greater than the hopping rate f_H . For example, it is not uncommon to transmit 10 bits/hop. In such a case, errors, due to jamming, occur in *bursts* and either interleaving and/or Reed-Solomon coding (Sec. 14.4) is employed. To further protect the data from random errors produced by thermal noise, which we have previously omitted from our discussion, one often employs concatenated coding (Sec. 14.4).

The Near-far problem

In Sec. 16.2, we noted that DS systems were affected by a near-far problem in which the receiver will receive significant noise from a signal transmitted by a nearby interferer and may not receive successfully the signal transmitted by a distant desired transmitter. The cause of the problem is that both signals are located in the *same* frequency band. In an FH system, if the receiver and transmitter are tuned to frequency f and the interfering signal at frequency f_{nf} then BFSK demodulator does not even know of the presence of the interferer since its spectrum is not in the signal bandwidth. Thus, there is *no* near-far problem when using FH.

Spectrum of FH Spread Spectrum

To determine the spectrum of a FH/BFSK system consider that the bit rate is equal to the hop rate,

i.e. there is 1 bit transmitted/hop. Then, if there were no hopping, the spectrum would be that of BFSK which is shown in Fig. 16.5a. When FH is employed the BFSK signal is repeated at each of the K hopping frequencies f_1, f_2, \dots, f_K . If the frequencies are contiguous the spectrum is as shown in Fig. 16.5b and the bandwidth is

$$\text{BW} = 4kf_b \quad (16.27)$$

Detection of a FH/BFSK Signal

A FH/BFSK modulation/demodulation system is shown in Fig. 16.6. Note that there are two sections to the modulator, the first being the BFSK

modulator and the second the frequency-hopped modulator. In practice, the two modulators are combined into a single, FM, modulator using a *frequency synthesizer*.

The received signal $v(t)$ is embedded in both the thermal noise $n(t)$ and an interference $I(t)$, which we assumed, earlier, to be

$$I(t) = \sqrt{2P_s} \cos(\omega_i t) \quad (16.28)$$

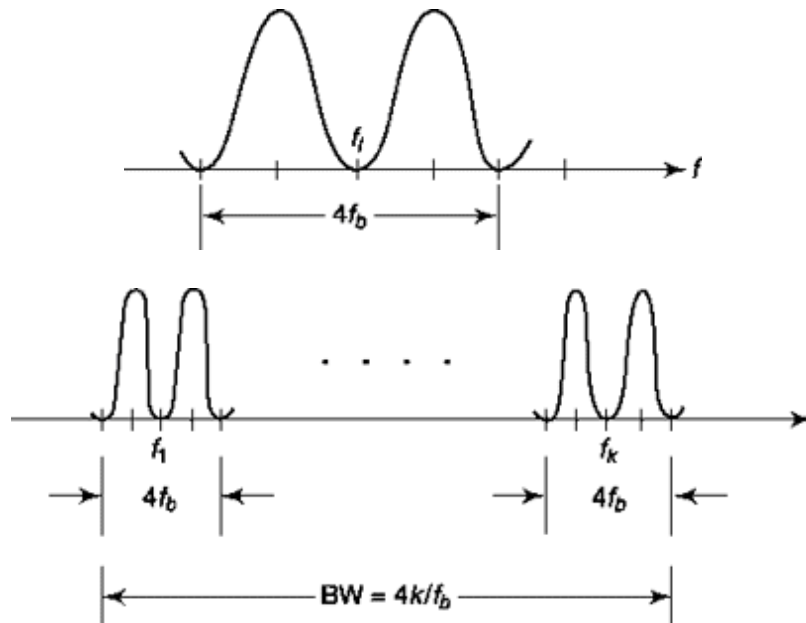
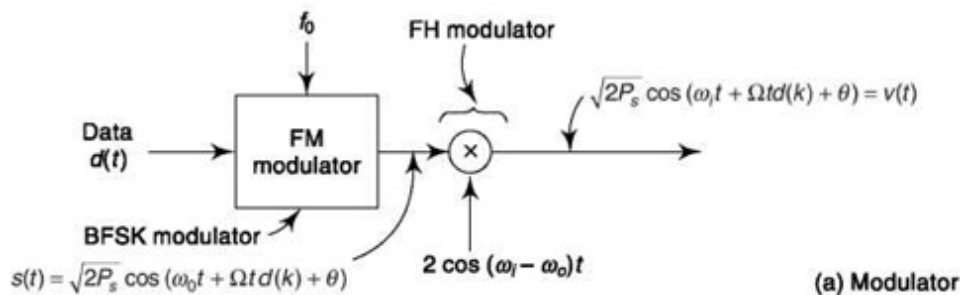


Fig. 16.5 Spectrum of FH/BFSK.



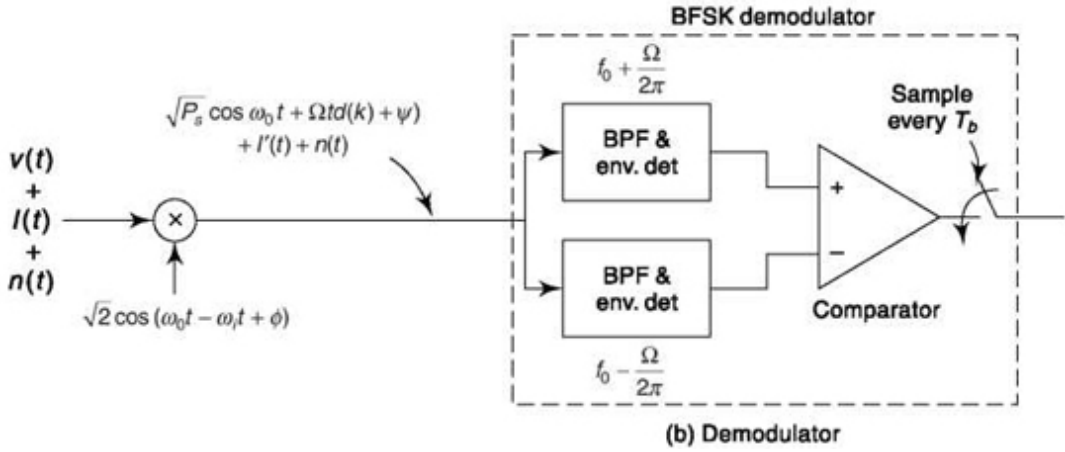


Fig. 16.6 *FH/BFSK modulation/demodulation system.*

The received waveform, shown in Fig. 16.6b, is first detected and shifted to a constant intermediate frequency (IF), f_0 . The resulting waveform is passed through the BFSK detector shown. Note that the interference $I(t)$ can affect the output only if its spectral density is large at frequency f_i .

$$I(t) = \sqrt{2 P_i} \cos \omega_i t \quad (16.28)$$

The major problem area in the use of spread spectrum is synchronization. Note that in Fig. 16.6b we have assumed that the received carrier frequency and the receiver's locally generated carrier frequency is the same; i.e. w . In addition, we have assumed that whenever the transmitted carrier frequency changes, the receiver's locally generated carrier frequency also changes by an appropriate amount. Should this not be the case, the error rate would increase significantly, rendering the system unusable. The synchronization problem is studied in Secs. 16.7 and 16.7.2.

16.6 PSEUDORANDOM (PN) SEQUENCES: GENERATION AND CHARACTERISTICS

A piece of hardware which is widely used to generate PN sequences is shown in Fig. 16.7. It consists initially of a shift register. We have selected type-*D* Flip-Flops and arranged that each data input except D_o is the Q output of the preceding Flip-Flop. The input D_o is the output of a parity generator. A parity generator (generally constructed of an array of EXCLUSIVE-OR logic gates, see Prob. 16.10) generates an output which is at logic 0 when an *even* number of inputs are at logic 0 and generates an output which is at logic 1 when an *odd* number of inputs are at logic 1. The

parity generator inputs are the outputs of the Flip-Flops. We have shown a portion of each connection to the parity generator input as dashed in order to indicate that not all outputs Q need be connected to the parity generator. As a matter of fact, the character of the PN sequence generated depends on the number N of Flip-Flops employed and on the selection of which Flip-Flop outputs are connected to the parity generator. (An alternative PN generator is shown in Prob. 16.11).

The *state* of a sequential system such as in Fig. 16.7 is specified by stating the logic values of all the Q 's of the Flip-Flops. During the course of a clock cycle the state of the shift register remains fixed, but, in general, the state changes at each advance from one clock cycle to the next. A register of N flip flops has 2^N states from $Q_0QQ_2 \dots Q_{N-1} = 000 \dots 0$ to $Q_0QQ_2 \dots Q_{N-1} = 111 \dots 1$. It is clear that the hardware of Fig. 16.7 cannot generate a truly random sequence since it is a deterministic structure. It is also clear that whatever the sequence of states through which the sequence generator progresses, the sequence will repeat. That is, it will be periodic. Such is the case because each state is uniquely determined by the immediately preceding state. Thus, each time the generator arrives at some particular state, the subsequent sequences of states will always be the same.

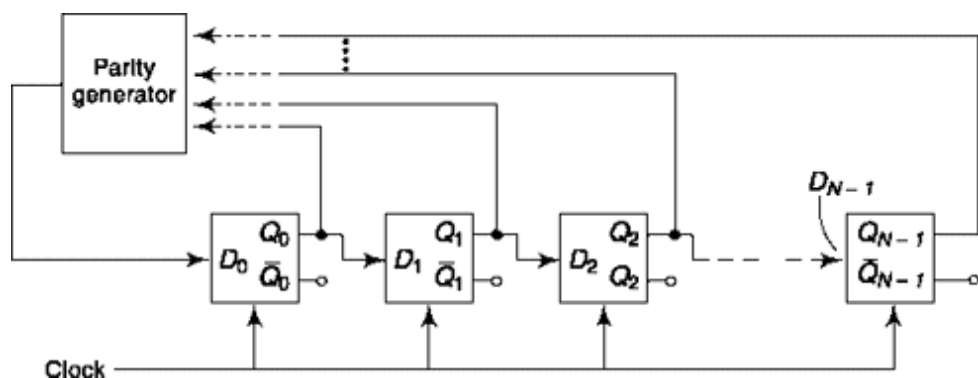


Fig. 16.7 A pseudo-random sequence generator.

While, as we have noted, a truly random sequence is not possible, we may intuitively anticipate that a sequence with a long enough period will have some of the characteristics of a random sequence. The first step in that direction is taken by using a large number of Flip-Flops. For, if we can make the sequence generator go through all its states the sequence length will be 2^N . With present-day MOS large scale integration, it is reasonable to have a 2000 Flip-Flop register on a single chip. Actually the maximum sequence length is $2^N - 1$ since the state 000 ... 0 must be excluded. Such is the case

because, as is easily verified, if the register should ever arrive at this all zero state, it will remain in that state permanently. We shall now set down some of the characteristics (in some cases, without proof) of the PN sequences produced by the generator of Fig. 16.7.

Sequence Length

It is always possible to find a set of connections from Flip-Flop outputs to parity generator which will yield a maximal length of sequence,

$$L = 2^N - 1 \quad (16.29)$$

For the cases $N = 1$ through $N = 15$ one logic design for maximal length sequences is given in Table 16.1.

Table 16.1

N	D_o for $L = 2^N - 1$
1	Q_0
2	$Q_0 \oplus Q_1$
3	$Q_1 \oplus Q_2$
4	$Q_2 \oplus Q_3$
5	$Q_2 \oplus Q_4$
6	$Q_4 \oplus Q_5$
7	$Q_5 \oplus Q_6$
8	$Q_1 \oplus Q_2 \oplus Q_3 \oplus Q_7$
9	$Q_4 \oplus Q_8$
10	$Q_6 \oplus Q_9$
11	$Q_8 \oplus Q_{10}$
12	$Q_1 \oplus Q_9 \oplus Q_{10} \oplus Q_{11}$
13	$Q_0 \oplus Q_{10} \oplus Q_{11} \oplus Q_{12}$
14	$Q_1 \oplus Q_{11} \oplus Q_{12} \oplus Q_{13}$
15	$Q_{13} \oplus Q_{14}$

Independence of Sequences

For a particular logic design of the parity generator, as for example the designs of Table 16.1, sequences are available at each Flip-Flop output Q and at each Flip-Flop complementary output \bar{Q} . Clearly these sequences are not independent. One may be derived from another by a simple shift in time or by complementing each bit or both. There are, however, other logic designs (i.e. other connections to the parity generator) which do yield

sequences which have small correlation to one another. The number of such sequences has an upper bound S given by

$$S \leq \frac{L-1}{N} \quad (16.30)$$

The equal sign applies when L is a prime number. These independent sequences can be divided into two equal groups so that each number of one group has a *mirror image* in the other group. Mirror image sequences have the same bit sequence when one is read forward in time and the other is read backward in time.

Example 16.3

If $N = 13$, $L = 2^{13} - 1 = 8191$. This value for L is prime so that

$$S = \frac{8191 - 1}{13} = 630 \quad (16.31)$$

Hence there are $630/2 = 315$ basic sequences and 315 mirror images.

Example 16.4

As can be verified (Prob. 16.12) if, in Fig. 16.7, $N = 3$ and if the connection from Q_0 is omitted, as in Fig. 16.8a the sequence generated at Q_n is

1 1 1 0 0 1 0 1 1 1 ...

If, on the other hand the connection from Q_1 is omitted, as in Fig. 16.8b, the sequence is

1 1 1 0 1 0 0 1 1 1 ...

Number of 1's and 0's in a Maximal sequence
which is recognized as the mirror image.

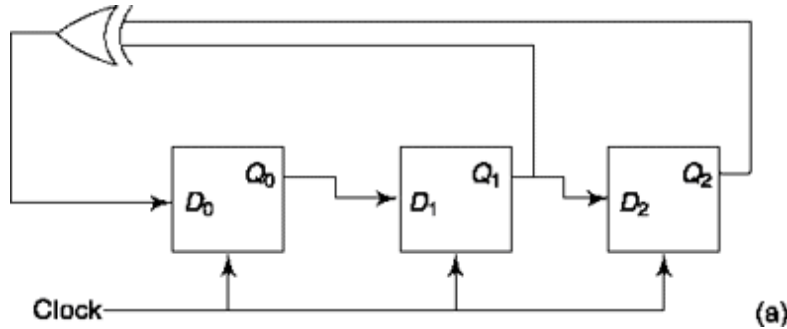


Fig. 16.8 PN generation which generate mirror image sequences.

Number of 1's and 0's in a Maximal Sequence

If the PN generator sequenced through all its states, then the number of states would be an even number and the sequence available at any Q or \bar{Q} output would contain the same number of 1's and 0's. Since, however, the all-zero state is excluded, there are an odd number of states. Correspondingly, the sequence will have one more 1's than 0's or one more 0's than 1's depending on when the sequence is taken from a Q or \bar{Q} output.

Clustering in a pN Sequence

One way in which the generator of Fig. 16.7 gives evidence of the fact that its sequences are not truly random is that its sequences display *clusters*. A cluster is a run of identical bits that occur in sequence. The clustering exhibited by a generator as in Fig. 16.7 using N Flip-Flops is given in Table 16.2. Thus, in the example given above, we encounter the sequence 1 1 1 0 0 1 0 in the case $N = 3$. This sequence has one cluster of $N (= 3)$ 1's, one cluster of $N - 1 (= 2)$ 0's and one cluster of $N - 2 (= 1)$ 1's and one cluster of $N - 2 (= 1)$ 0's.

Table 16.2 Clustering Produced by the Generator of Fig. 16.7 when Connected for Maximum Sequence Length

Number of Clusters	Length of Cluster	Bit value if Q output is used
1	N	1
1	$N - 1$	0
1	$N - 2$	1
1	$N - 2$	0
2	$N - 3$	1
2	$N - 3$	0
4	$N - 4$	1
4	$N - 4$	0

Properties of Shifted Sequences

Let $g(i)$ represent a PN sequence. Then $g(i + j)$ represents the same sequence except shifted by j chips. If we view the chip values of the sequence as logic variables with logic values 1 or 0 then it turns out that

$$g(i) \oplus g(i + j) = g(i + k) \quad (16.32)$$

That is, the EXCLUSIVE-OR operation, applied chip by chip to a sequence $g(i)$ and the same sequence except shifted by j bits, gives rise to the sequence $g(i)$ shifted by k bits. It turns out further, that in Eq. (16.32), we cannot further specify k except to note that $k \neq 0$ and $k \neq j$.

Next let us view $g(i)$ as a waveform which makes excursions between +1 volt and -1 volt corresponding to logic 1 and logic 0. Then using Eq. (16.32) it can be shown (Prob. 16.14) that

$$g(i) \times g(i + j) = -g(i + k) \quad (16.33)$$

Here, the left-hand side involves the arithmetic product.

Autocorrelation of a pN Sequence

The autocorrelation function $R_d(t)$ of a truly random data sequence $d(t)$ with bit duration T_b is defined as

$$R_d(\tau) = E\{d(t)d(t + \tau)\} \quad (16.34)$$

and has the form shown in Fig. 16.9 when $d(t) = \pm 1$ volt. The autocorrelation function $R_{PN}(t)$ of a PN sequence is

$$R_{PN}(\tau) = E\{g(t)g(t + \tau)\} \quad (16.35)$$

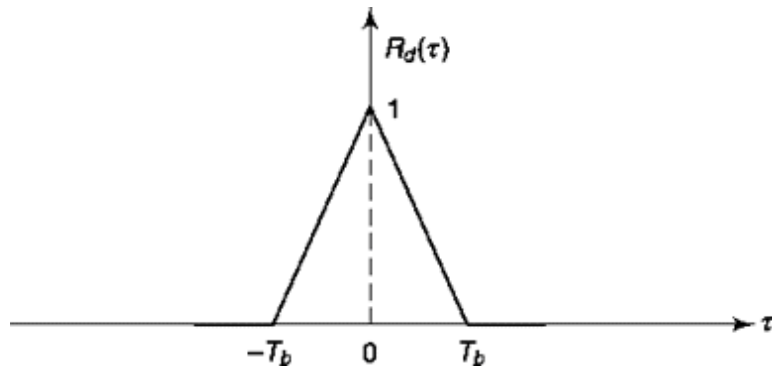


Fig. 16.9 Autocorrelation function of random data $d(t)$ having the values, $d = \pm 1$.

where $g(t)$ assumes the values $g(t) = \pm 1$ volt. As might be expected $(_{PN}(0)) = 1$. We now calculate $(_{pn}(t))$ for $t = nT_c$, where n is an integer and T_c is the chip duration. From Eq. (16.33) we have that

$$R_{PN}(\tau - nT_c) = E\{g(t)g(t + nT_c)\} = E\{-g(t + kT_c)\} \quad (16.36)$$

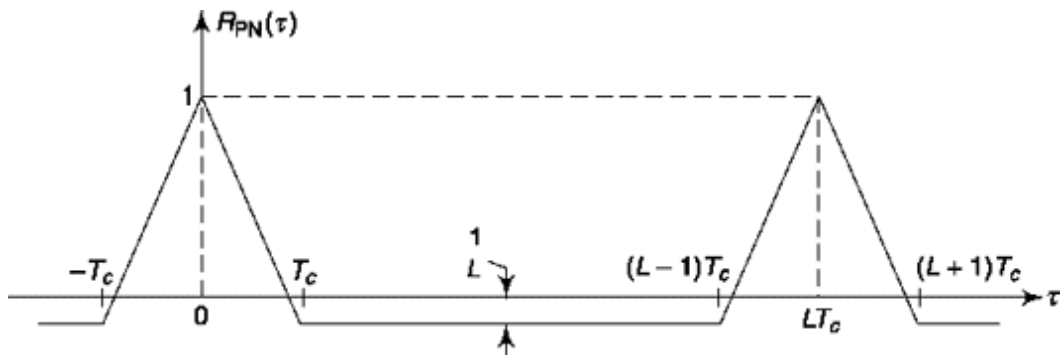


Fig. 16.10 Autocorrelation function of a PN sequence.

Now $g(t + kT_c)$ is a PN sequence and, in the course of L chips there is one more 1 than 0. Hence the average value of $-g(t + kT_c)$ is $-1/L$ as shown in Fig. 16.10. Finally, since the sequence has a period LT_c so too has $(_{PN}(t))$.

power spectral Density

We now determine the power spectral density $G_{PN}(f)$ of the pseudo-random noise sequence. The power spectral density $G_{PN}(t)$ is the Fourier transform of $(_{PN}(t))$. Since $(_{PN}(t))$ is periodic with period LT_c , $G_{PN}(f)$ must consist of impulses at multiples of the frequency $1/LT_c$. $G_{PN}(f)$ will also display an impulse at $f = 0$ since the impulse $G_{PN}(0)$ is the dc power of the PN frequency. The PN sequence $g(t)$ consists of excursions between $+V$ (logic 1) and $-V$ (logic 0). In a sequence of L chips there is one more logic 1 than logic 0, hence the dc voltage of $g(t)$ is V/L and the normalized dc power in V^2/L^2 . Hence $G_{PN}(0) = (V^2/L^2)5f$. Finally, we recall that if $g(t)$ were truly random its power spectral density would have the form $[(\sin pf/f_c)/(pf^l f_c)]^2$. Altogether, then, the spectral density $G_{PN}f$ is as shown in Fig. 16.11 and can be shown to be

$$G_{PN}(f) = \frac{V^2}{L^2} \delta(f) + \frac{V^2}{L} \sum_{i=-\infty}^{\infty} \delta\left(f + i\frac{f_c}{L}\right) \left[\frac{\sin \pi(f + if_c/L)}{\pi(f + if_c/L)} \right]^2 \quad (16.37)$$

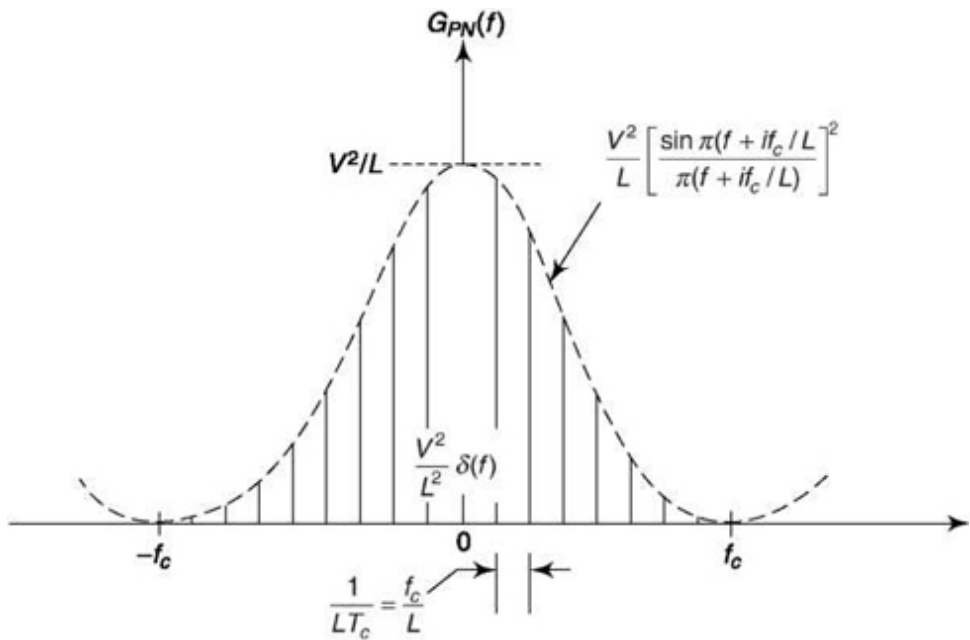


Fig. 16.11 Power spectral density of a PN sequence.

SELF-TEST QUESTION

5. DS spread spectrum is related to AM or PSK while FH spread spectrum is related to FM or FSK. Is the statement correct?
6. Is FH spread spectrum system prone to burst error?
7. Which of DS and FH spread spectrum is prone to near-far problem?
8. If N Flip-Flops are used to generate the PN sequence and T_c the chip period, what is the maximum time after which the PN sequence repeats itself?

16.7 SYNCHRONIZATION IN SPREAD SPECTRUM SYSTEMS

As we saw in Chap. 5, noncoherent communication systems such as FSK require *bit synchronizers* to allow signal recovery at the receiver. Coherent systems require, in addition, *carrier and phase synchronization* to permit the modulated received signal to be mixed down to baseband. In spread-spectrum systems, a third synchronizer is required to allow the regeneration at the receiver of a duplicate of the chipping waveform used at the transmitter. We consider, in succeeding sections, synchronization procedures for FH and OS spread-spectrum systems.

Note that, the term *acquisition* is referred to coarse synchronization and *tracking* is used to refer fine synchronization.

16.7.1 Acquisition of an FH Signal

A block diagram of the *acquisition* (coarse synchronization) circuit for a FH signal is shown in Fig. 16.12 and its waveforms are shown in Fig. 16.13. The acquisition circuit shown in Fig. 16.12 is seen to be similar to the Frequency Demodulator Using Feedback described in Sec. 9.8. The circuit consists of a mixer (multiplier), a bandpass filter centered at an IF frequency f_0 and having a

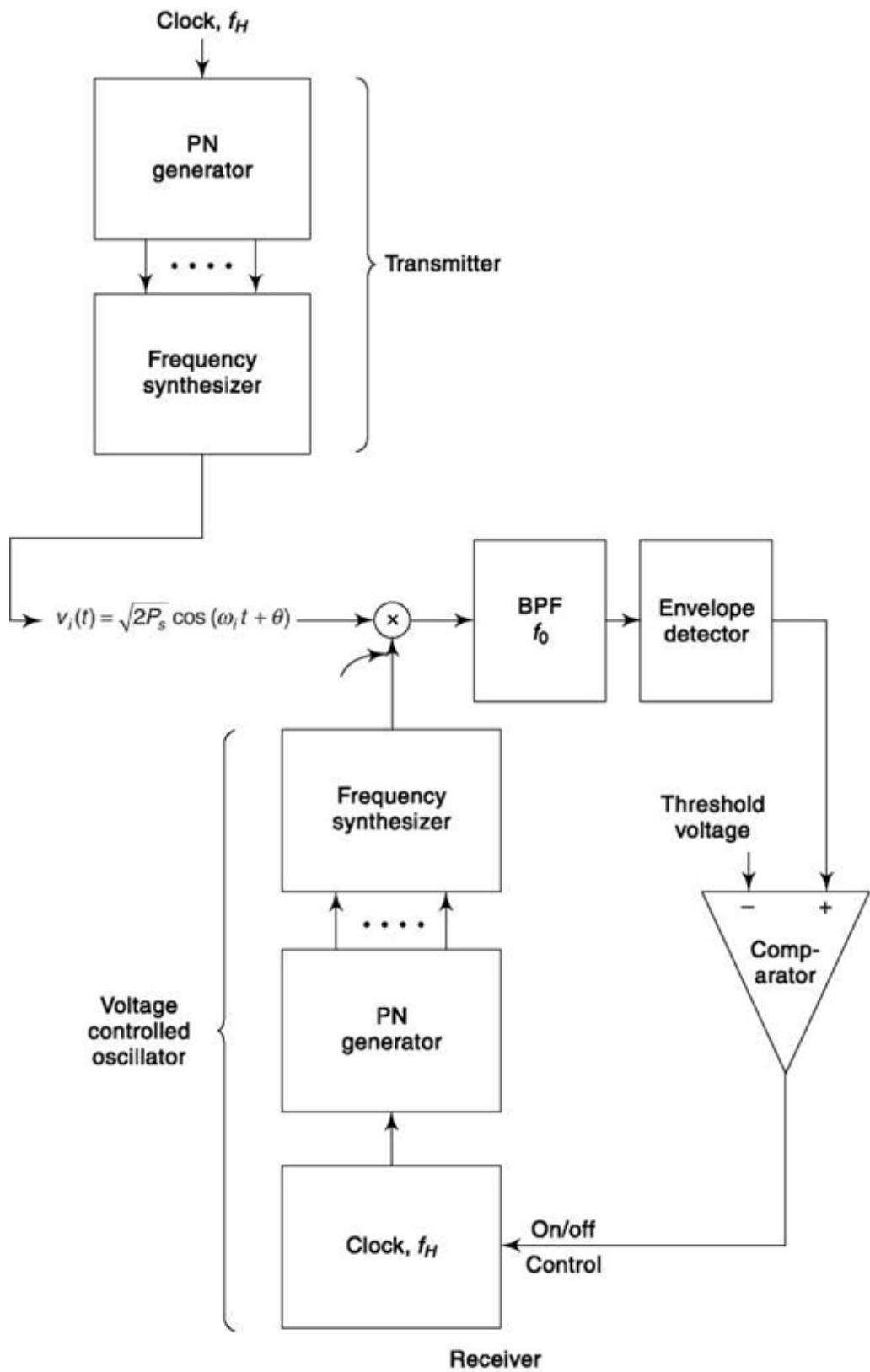


Fig. 16.12 Acquisition circuit (camp-and-wait) for a FH signal.

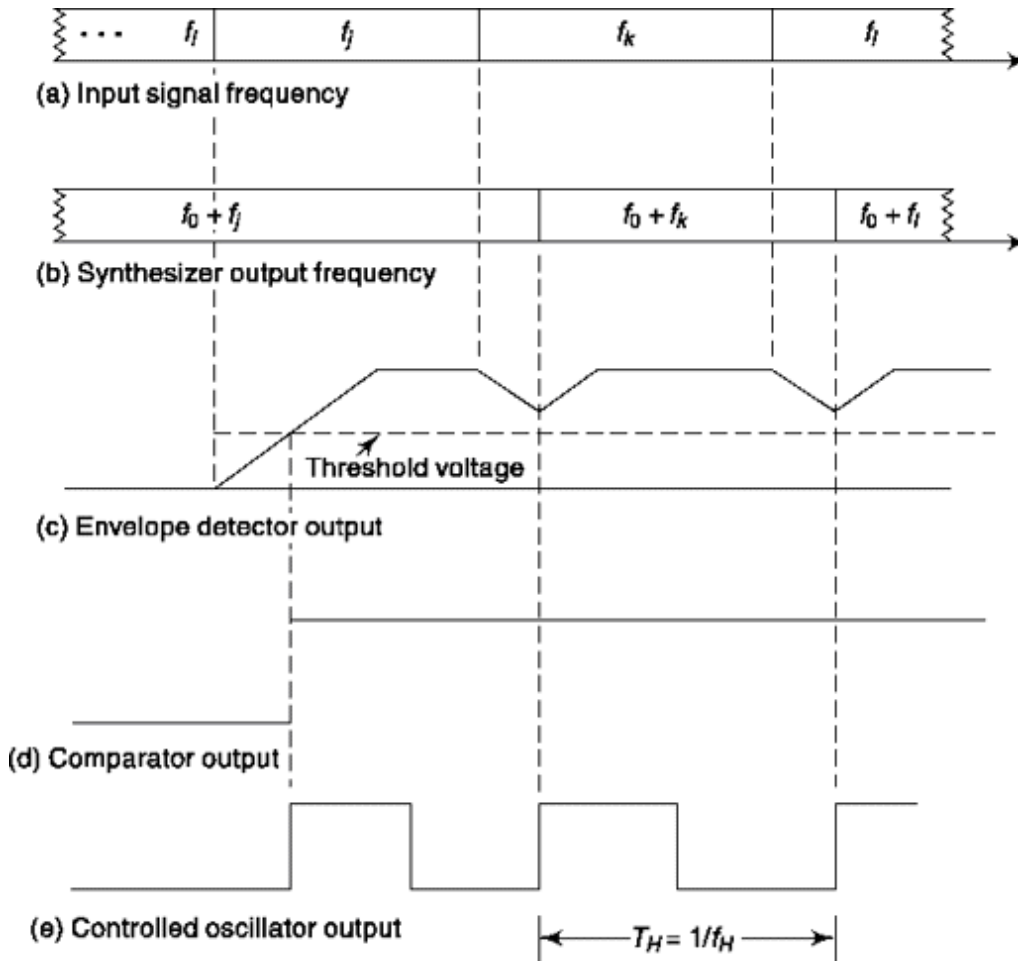


Fig. 16.13 Waveforms for the acquisition circuit of Fig. 16.12.

bandwidth equal to twice the hopping rate ($B = 2f_h$), an envelope detector-comparator (rather than an FM limiter-discriminator) and a voltage controlled oscillator (VCO).

The VCO consists of a clock, PN generator and frequency synthesizer. The clock is either *off* or *on*, in which case clock pulses at the hopping rate f_H are delivered to the PN generator.

The PN generator and frequency synthesizer are identical in the transmitter and receiver. The frequency synthesizer is merely an oscillator whose frequency can be controlled by the digital signal applied to it by the PN generator. Thus, as the PN generator moves through each of its states, dwelling in each state for a time $T_H = 1/f$, the frequency synthesizer hops from frequency f_1 to $f ..$ to f_N , back to f_1 , etc.

The purpose of the network in Fig. 16.12 is to arrange that the receiver PN generator falls into synchronism with the transmitter PN generator.

Accordingly, let us assume that initially the receiver synthesizer is providing the frequency $f + f$ while the received frequency is, say, $f \neq f$. At the mixer output the difference frequency $f + f - f$ will not pass through the bandpass filter whose pass region is narrowly centered around f and the output of the envelope detector will be zero. The detector output is compared with a threshold voltage by the comparator. A comparator, it will be recalled accept two input voltages and provides an output which assumes one of two voltages, depending on which input is the larger. It is arranged that when the detector output is less than the threshold voltage, the on/off control voltage applied to the controlled oscillator keeps that oscillator *turned off*. Hence, as long as the received frequency is *not* equal to f the PN generator does not cycle through its states and the receiver synthesizer holds at the frequency $f_0 + f_j$. Thus, the synthesizer remains *camped* at $f_0 + f$, on account of which the name *Camp-and-Wait* is used to characterize the technique. When finally the received frequency is f_j the difference signal passes through the filter, the detector output rises above the threshold, the comparator output changes, the controlled oscillator is turned on and the receiver PN generator is advanced through its states in synchronism with the transmitter generator. Waveforms for the system are shown in Fig. 16.13. In (a) is shown the received signal hopping from frequency to frequency while as in (b) the receiver synthesizer frequency remains camped at $f_0 + f_j$. When, in (a), the awaited frequency f_j appears, then as shown in (c) the envelope detector output begins to change. When the threshold voltage is reached the comparator output changes as in (d) and (e) the voltage controlled clock turns on and provides the clock waveform needed to drive the PN generator. At each positive transition of the clock, except the first transition, the PN generator advances to its next state and the frequency synthesizer advances to its next frequency. (It is necessary to incorporate provisions, not shown, to arrange that the first clock transition should not advance the PN generator.)

We have deliberately provided, as is to be seen in the waveforms, that the change in detector output be relatively slow. Such a feature is not difficult to incorporate because the output hardware component of the detector is a capacitor. Because of this relative sluggishness, the time at which the receiver PN generator changes state lags behind the time of state change of the transmitter generator. On the other hand because of this very sluggishness the detector output will remain above threshold and will keep

the controlled oscillator running even during the intervals, which occur one per oscillator cycle, when the two PN generators are not in the same state.

16.7.2 Tracking of an FH Signal

To effect fine synchronization we need to replace the voltage controlled clock shown in Fig. 16.12 (which can only be turned on and off) by a voltage-controlled oscillator (VCO) whose frequency can be adjusted above and below the hopping frequency. We require further that the VCO frequency be controlled by a voltage which measures that phase difference between the two PN generators. The phase discrepancy can then be used to speed up or slow down the VCO as required to reduce the phase error. Such a system is, in short, an automatic feedback control system, or more specifically, a phase-locked loop.

Such a phase-locked loop is shown in Fig. 16.14. The frequency synthesizer and PN generator shown here are the same as in Fig. 16.12. The bandpass filter bandwidth is now widened to pass the data, i.e. $B = 2Df$. The on-off controlled oscillator is replaced by a VCO which operates at a frequency which is nominally f_H but which can be varied continuously about f_H by the control signal furnished by the low-pass filter. As a matter of convenience we shall assume that the clock waveform furnished by the VCO makes excursions between +1 volt and -1 volt. The envelope detector in the present case, unlike the situation which prevailed in the coarse synchronizer, has a fast response. As a matter of fact, for simplicity in the waveforms of Fig. 16.15 we have assumed that the envelope detector output responds immediately to the bandpass filter output. However, this feature is not essential for operation of the system. The *gate* between the envelope detector and low-pass filter is a *transmission gate*. When there is an output provided by the envelope detector, the VCO clock waveform is transmitted through the gate and is not transmitted when the detector output is zero. Altogether we can characterize the operation of this gate as a process of multiplication if we take

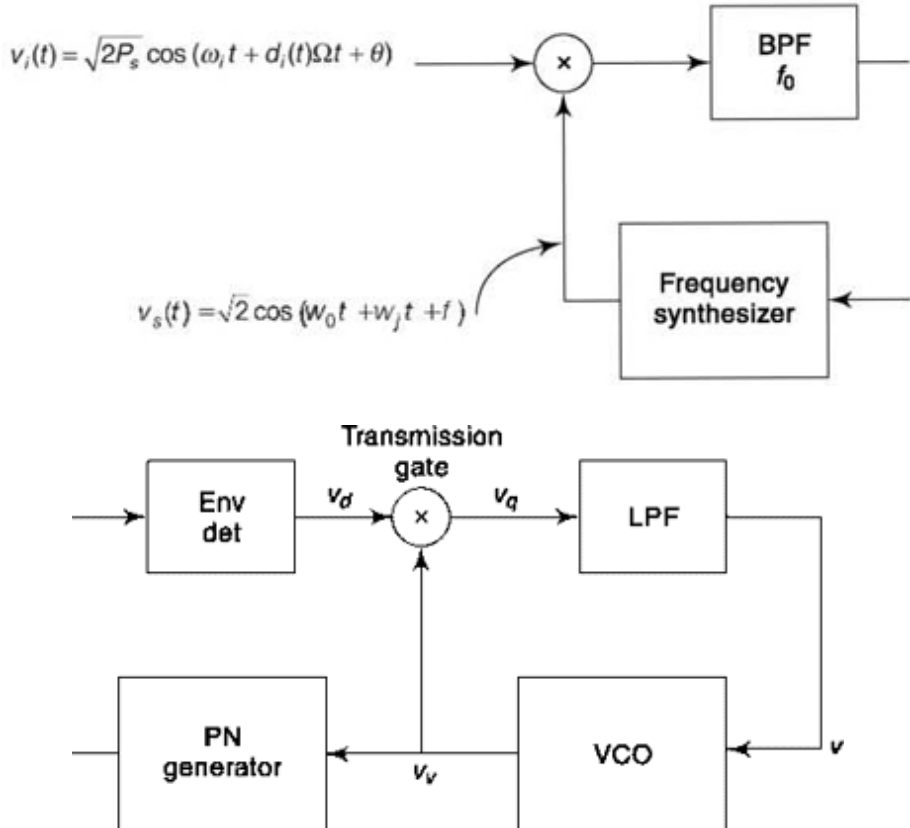


Fig. 16.14 Early-late gate tracking circuit.

the VCO clock to make excursions between ± 1 V and the envelope detector output to be 0 when there is no output and 1 when there is an output.

Waveforms describing the circuit operation are shown in Fig. 16.15. Here, as in Fig. 16.14, we assume the presence of an input data stream which shifts the transmitter frequencies by amount $W/2p = Df$ from the frequencies provided by the frequency synthesizer. So long as these shifts keep the received frequencies within the range of the bandpass filter, the operation of the synchronizer will be in no way influenced.

In Fig. 16.15a and b we assume that coarse synchronization has been established between the receiver PN generator and the transmitter generator with a lag of amount t . During the intervals of duration t when the generators are not in the same state, the envelope detector output, shown in (c), is at 0 volts; the envelope detector is at 1 volt when the states are the same. The VSO clock waveform is shown in

(d) and the product $v_g = v_v v_d$ is shown as the three-level waveform in (e). This transmission gate output is applied to the low-pass filter. The low-pass filter output, which is the average value of its input, serves as the control

voltage v_c to the VCO. If the VCO output is symmetrical and $t = 0$ then v_c will be equal to zero. Depending, however, on whether the receiver PN generator lags (is late) or leads (is early), the control voltage v_c will be of one polarity or the other to increase or decrease the

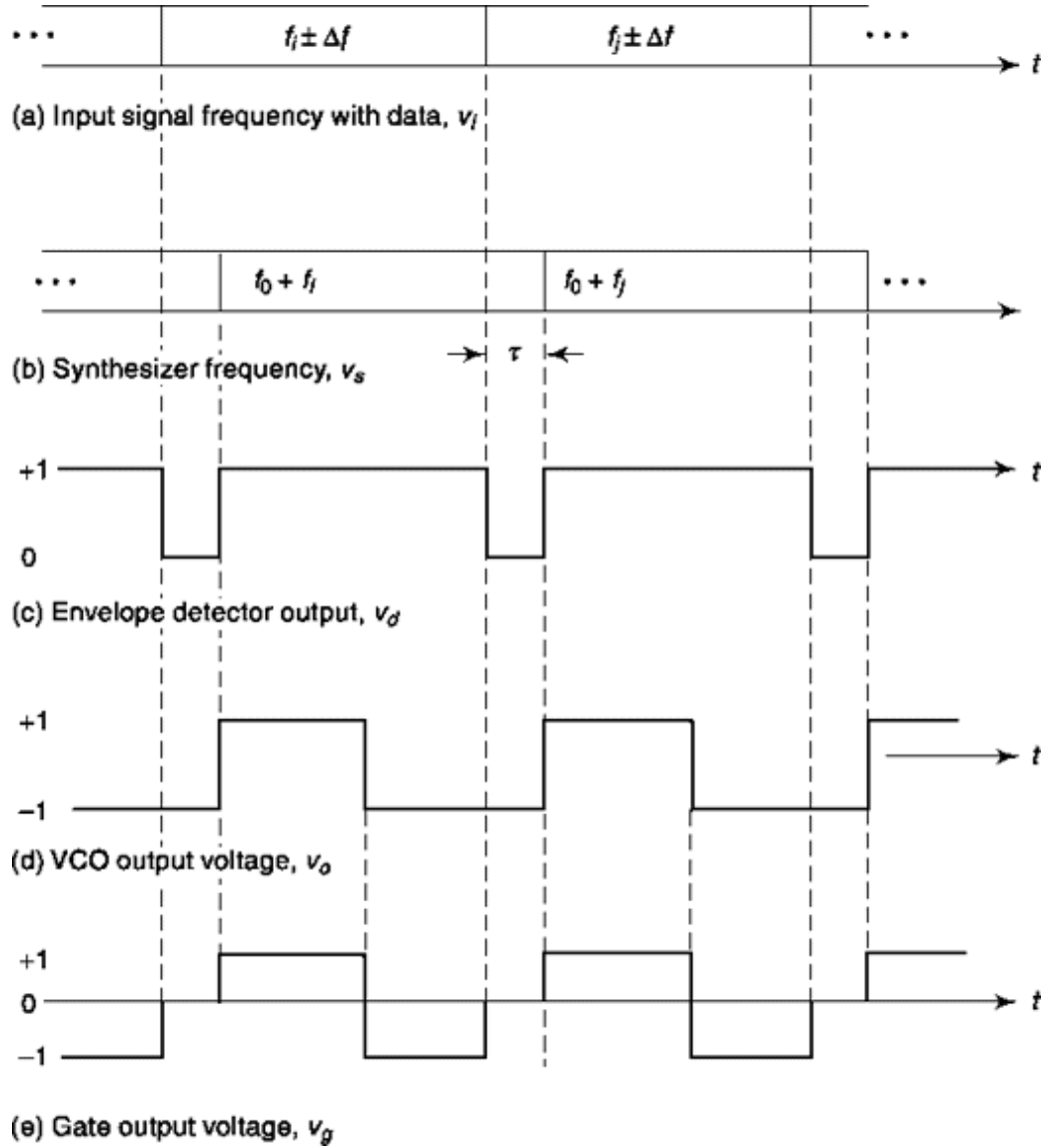


Fig. 16.15 E-L gate waveforms.

VCO frequency, moving it always in the direction to reduce t . This fine synchronization scheme, called an *Early-Late gate* will sustain synchronization even in the presence of disturbances, provided that $|t|$ remains less than T_H . Otherwise synchronization will be lost, and the whole process beginning with coarse synchronization will start all over again.

16.7.3 Acquisition of a DS Signal

The *Serial-Search* technique carried out by the arrangement of Fig. 16.16 is used to establish acquisition of a DS signal. During the acquisition process data is not superimposed on the chipped carrier so that the received signal is

$$v_i = V2P_s g(t)\cos(w_0 t + \theta)$$

Initially, the switch S is in position 1 making connection to a fixed voltage source (corresponding to logic 1) which enables the AND gate. The oscillator, operating at the chipping frequency f_c provides the clock waveform to drive the PN generator. Let us assume that the receiver PN generator and the transmitter generator are not in synchronism, i.e. not in the same state at the same time. Then the product waveform $v_r(t)$ is itself a DS waveform which encompasses a wide spectral range. Because its power is spread over a wide spectrum, its power spectral density is small. Accordingly little power will be available at the output of the bandpass filter (centered at f_0) and the output of the envelope detector will be correspondingly low. The envelope detector output is integrated for a time nT_c , that is some number n of clock cycles depending on the noise. In the absence of synchronization, the integrator output will not be large enough to exceed the comparator reference voltage. In this case, and by mechanisms not shown, the switch S will be thrown to position 2, disabling the AND gate and stopping the sequencing of the PN generator. In this way the receiver PN generator will then be allowed to step back some cycles with respect to the transmitter generator. Then the accumulated output of the integrator is *dumped* and the switch is thrown back to position 1 to try again. By this

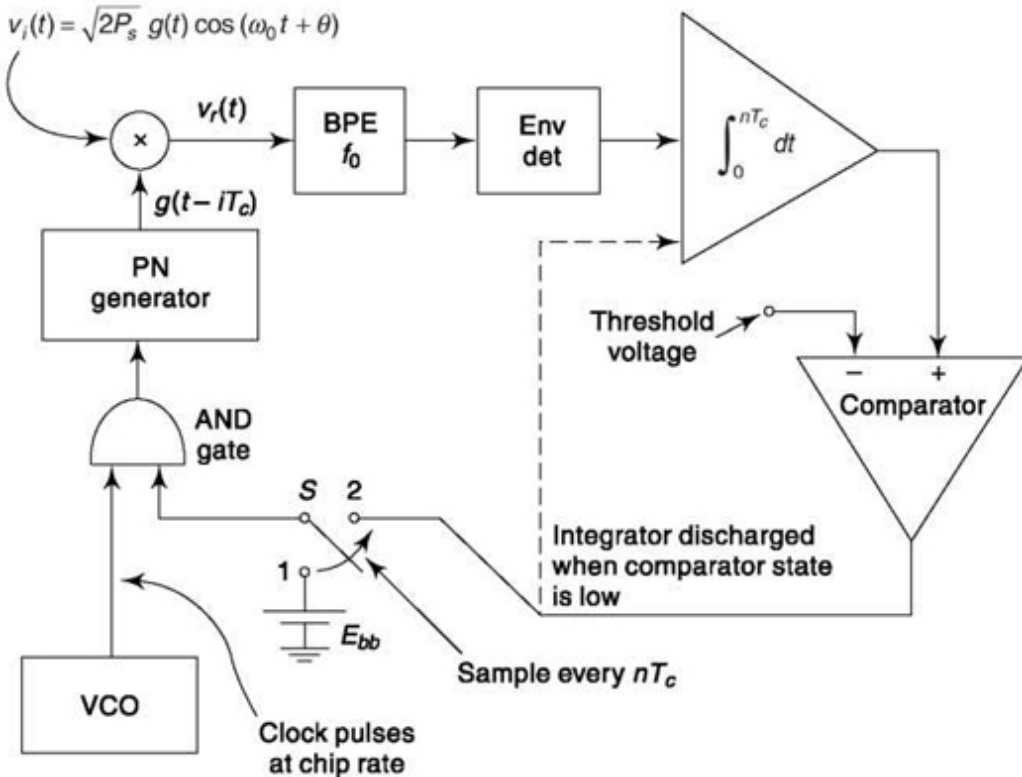


Fig. 16.16 Direct sequence acquisition circuit.

repeated trial-and-error process, acquisition will eventually be established as evidenced at the output of the comparator. For at acquisition, the product $g(t)g(t - iT_c)$ becomes $g^2(t) = 1$ since $i = 0$ and the input v_r to the bandpass filter is simply $\sqrt{2P_s} \cos(\omega_0 t + \theta)$. The envelope detector output is now high, the integrator output is high and the comparator voltage goes to its high state. Acquisition having been established, synchronization continues by tracking (fine synchronization) the signal.

16.7.4 Tracking of a DS signal

A circuit which is often used to track a DS signal is the Delay Locked Loop (DLL) shown in Fig. 16.17. The input signal in this case involves both the chipping waveform $g(t)$ and the data stream $d(t)$. Since we assume acquisition has occurred, the receiver PN generator is generating a sequence in step with the input sequence but of course there may be a time lead or lag so that we consider at the outset that the receiver generator generates $g(t + t)$. Additional hardware is incorporated in the receiver generator so that actually it makes available two waveforms one delayed and one advanced by amount

$T_c/2$ from $g(t + t)$, i.e. $g(t + t + T_c/2)$ and $g(t + t - T_c/2)$ as indicated in Fig. 16.17.

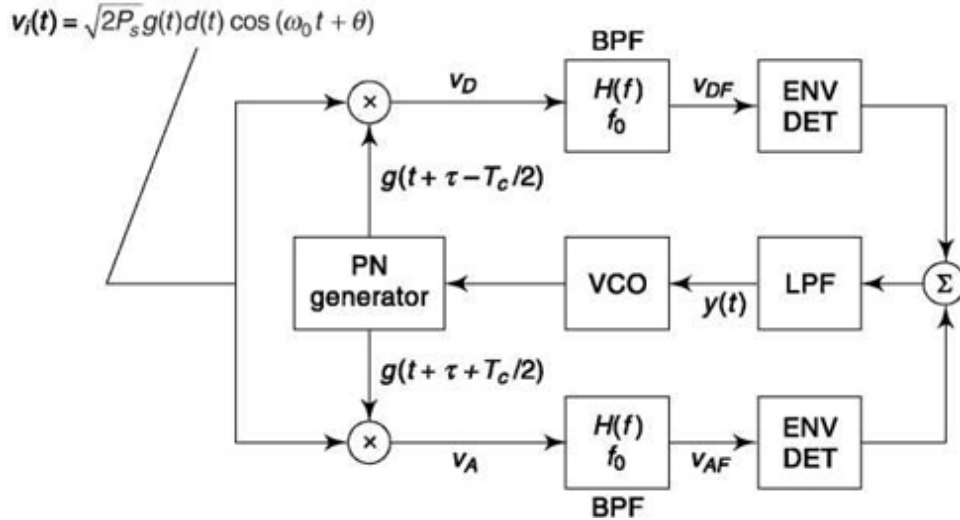


Fig. 16.17 A delay locked loop (DLL) used to track a DS signal. The waveforms v_D and v_A in Fig. 16.17 are then given by

$$v_D(t) = \sqrt{2 P_s} g(t) g(t + \tau - T_c/2) d(t) \cos(\omega_0 t + \theta) \quad (16.39)$$

and

$$v_A(t) = \sqrt{2 P_s} g(t) g(t + \tau + T_c/2) d(t) \cos(\omega_0 t + \theta) \quad (16.40)$$

These signals are passed through identical bandpass filters each having a bandwidth equal to $B = 2f_b$. Thus the bandwidth of each filter is much less than the bandwidth needed to transmit a PN sequence and only the average value of the product $g(t)g(t + T_c/2)$ is passed. The filter outputs can then be written as

$$v_{DF}(t) \approx \sqrt{2 P_s} [g(t)g(t + \tau - T_c/2)] d(t) \cos(\omega_0 t + \theta) \quad (16.41)$$

and

$$v_{AF}(t) \approx \sqrt{2 P_s} [g(t)g(t + \tau + T_c/2)] d(t) \cos(\omega_0 t + \theta) \quad (16.42)$$

We recognize that the average value of the product of the PN sequence and a shifted version of the same sequence is the autocorrelation function (see Sec. 16.4). That is

$$R_g(\tau \pm T_c/2) = \overline{g(t)g(t + \tau \pm T_c/2)} \quad (16.43)$$

The envelope detectors extract the envelopes of $v_{DF}(t)$ and $v_{AF}(t)$ thereby removing the data $d(t)$. The result is

$$V_D(t) = |R_g(\tau - T_c/2)| \quad (16.44)$$

$$\text{and } V_d(t) = |R_g(\tau + T_c/2)| \quad (16.45)$$

The average voltages $V_D(t)$ and $V_A(t)$ are then subtracted and low pass filtered to extract as much noise as possible. The input voltage to the VCO, $y(t)$, is $y(t) = |R_g(\tau - T_c/2)| - |R_g(\tau + T_c/2)|$ (16.46)

Equation (16.46) is sketched in Fig. 16.18 at a function of t . Note if t is positive, a positive voltage will appear at the VCO input, increasing its frequency and thereby decreasing t . Similarly if t is negative a negative voltage is generated at the VCO input, decreasing the VCO rate and thereby increasing t .

Finally, we note by way of overview, that the FH and DS synchronization circuits presented above are only examples of many which are used. Also, it is to be noted that some spread spectrum systems combine both FH and DS.

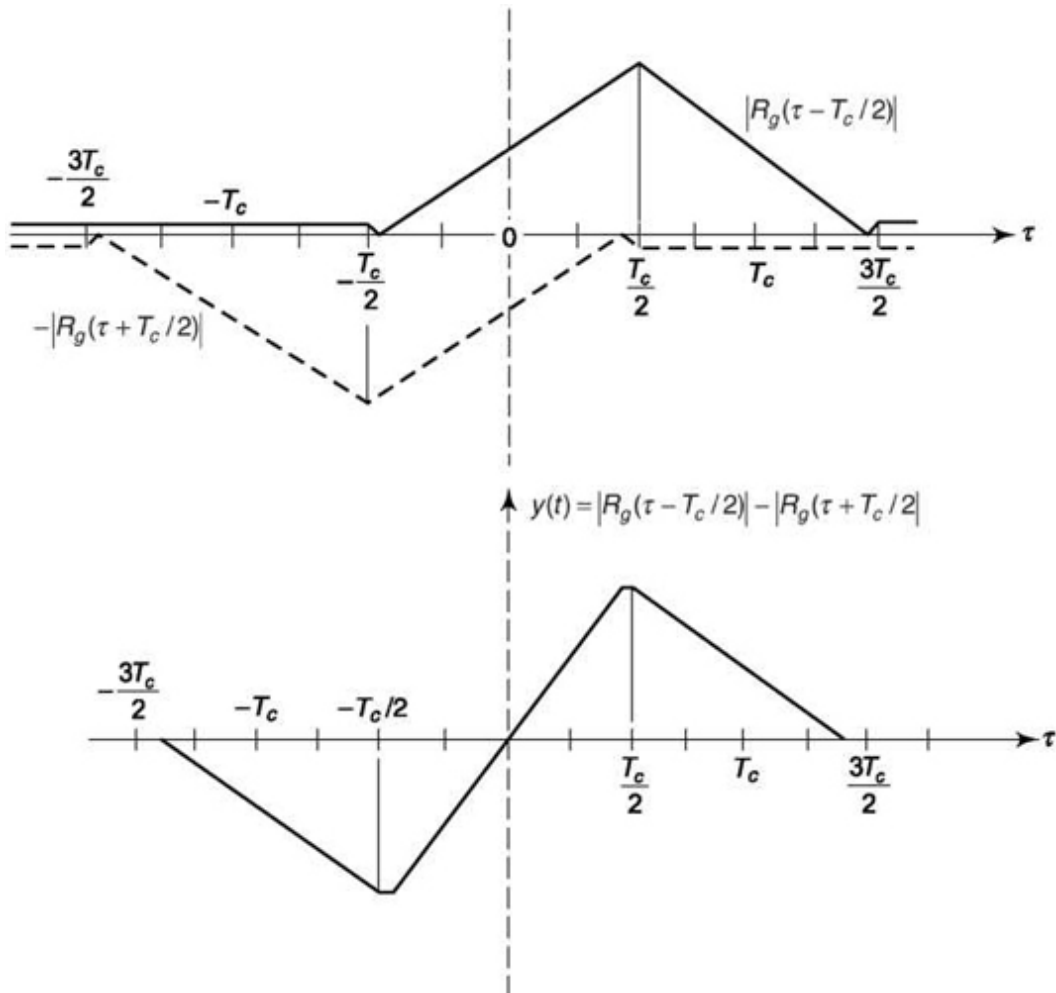


Fig. 16.18 VCO input voltage, $y(t)$.

SELF-TEST QUESTION

9. Does acquisition in FH spread spectrum system require the receiver PN generator to fall in synchronism with transmitter PN generator?
10. Does tracking of FH system utilizes PLL principle?
11. Which of FH and DS spread spectrum system uses serial-search technique?

FACTS AND FIGURES

The first operational spread spectrum system was named Lincoln F9C and was built for the US army in MIT Lincoln Lab. Its first transcontinental field trial took place in August, 1954. The system used frequency-shift data modulation at about 22 ms/bit rate over 10 kHz bandwidth. Four counters of fixed periods 117, 121, 125 and 128 were employed and the four 7-bit outputs were combined to generate a 28-bit signal. This was followed by an array of AND logic gates and bandpass filters to generate the spread spectrum signal. To avoid jamming, a changeable punched card was used as security key to the input of AND gates.

The F9C system was descendent of a secret project NOMAC, an abbreviation of NOise Modulation And Correlation. A correlation-based rake receiver later improved the performance of this system against multipath fading. In a separate development, the company Sylvania was entrusted with a surface-to-surface missile development work in 1946. They found noise modulation useful from ‘anti-jamming and security aspects’. To highlight the effect of correlation, in a 1950 meeting, Sylvania played this jingle: “*Correlation is the best /It outdoes all the rest / Use it in your guided missile / And all they'll hear will be a whistle / Whistle, whistle, whistle ...*”

MATLAB

```

% Experiment 54

% This shows generation of DS spread spectrum signal (Section 16.2 of book)

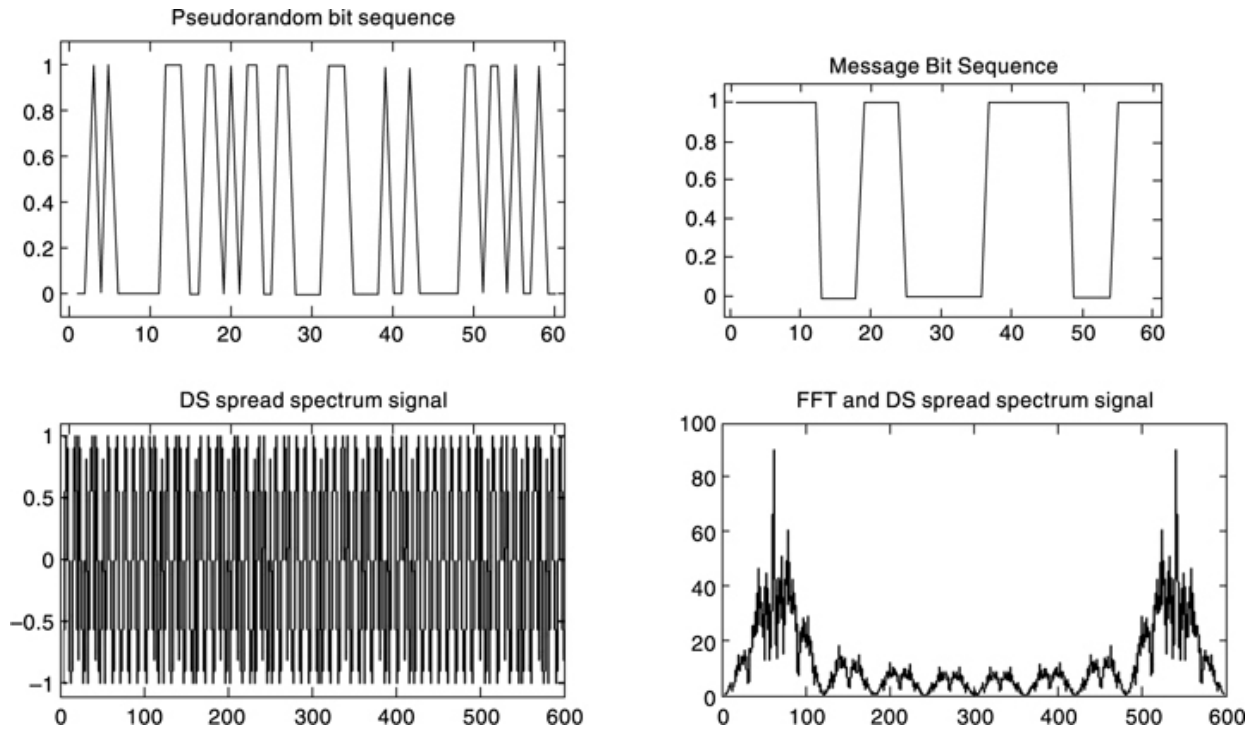
pnsig=round(rand(1,60)); % Generating the PN sequence for spreading
subplot(221),plot(pnsig);
axis([-1 61 -0.1 1.1]);title('Pseudorandom Bit Sequence');

msg=round(rand(1,10)); % Generating the bit seq with each message 6 samples
long bitseq=[];
for i=1:10
    if msg(i)==0
        sig=zeros(1,6);
    else
        sig=ones(1,6);
    end
    bitseq=[bitseq sig];
end
subplot(222),plot(bitseq);
axis([-1 61 -0.1 1.1]); title('Message Bit Sequence');

spread_sig=bitxor(bitseq,pnsig); % Spreading:XORing the message with the PN seq

% BPSK Modulation of spread data for transmission
ds_ss=[]; % initializing DS SS signal
fc=10000; fs=100000; % fc=carrier freq, fs=sampling freq used
t=0:1/fs:1/fc-1/fs;
m1=cos(2*pi*fc*t); m2=cos(2*pi*fc*t+pi); % BPSK signals
for i=1:60
    if spread_sig(1,i)==0
        ds_ss=[ds_ss m1];
    else
        ds_ss=[ds_ss m2];
    end
end
subplot(223),plot(ds_ss);
axis([-1 601 -1.1 1.1]); title('DS Spread Spectrum Signal');
% Frequency spectrum of DS SS signal
subplot(224),plot(abs(fft(ds_ss))), title('FFT of DS Spread Spectrum Signal');

```



```
% Experiment 55
% This shows the finding target distance (ranging) using DS spread spectrum
% Section 16.4 of Book

fc=input('Give chip frequency in MHz - ');
D=input('Give the delay where correlation is maximum in millisecond - ');
c=3*10^8;

Tc=1/(fc*10^6); D=D*10^-3;
d1=c*(D+Tc)/2;
d2=c*(D-Tc)/2;
disp('The target is within following two distances in kilometer ');
disp([d1 d2]/1000);
```

When this program is run with specifications of Example 16.2 the following is obtained.

```
>> exp55
Give chip frequency in MHz - 10
Give the delay where correlation is maximum in millisecond - 0.1
The target is within following two distances in kilometer
15.0150 14.9850
```

SUMMARY

The chapter begins with an introduction of spread spectrum systems and discusses certain common application areas. Direct Sequence (DS) spread spectrum system is presented which includes a discussion on how thermal

noise and single tone interference affects it. Next, the idea of Code Division Multiple Access (CDMA) is introduced that uses spread spectrum and is useful in multiple access communications. Application of DS spread spectrum in ranging is shown. This is followed by discussion on Frequency Hopping (FH) spread spectrum and its various characteristics. Pseudorandom signal remains an important component in spread spectrum system. Generation and characterization of pseudorandom signal in frequency domain is discussed. Finally, a detailed description of synchronization techniques for both DS and FH systems is given which involves coarse synchronization or acquisition and fine synchronization or tracking.

PROBLEMS

16.1 Consider that the signal-to-noise ratio of a received signal not employing spread spectrum is $E_b/h = 10$ dB. If the signal is spread using a chip rate $f_c = 10^4 f_b$, calculate the ratio of the peak power spectral density of the spread signal $G_s(d)$ to the power spectral density of thermal noise, $h/2$.

16.2 A received spread spectrum signal is embedded in noise $v_1(t) = \sqrt{2P_s} d(t)g(t) \cos \omega_0 t + n(t)$

where the bit rate $f_b = 20$ kb/s and the chip rate $f_c = 2$ Mb/s. The ratio of the power spectral density of the signal to the noise is 10^{-3} .

- (a) Calculate $h/2$ in terms of P_s .
- (b) A receiver set at f_0 has a 4 MHz bandwidth. The receiver is followed by a square low amplifier and a low pass filter of bandwidth $B_0 = 100$ kHz.
 (1) Calculate the signal-to noise ratio of the filter output. (2) Calculate the probability of detecting the presence of the DS signal.

16.3 (a) Prove that the variance of the thermal noise at the integrator output, in Fig. 16.2, is $s_n = hT_b$. (b) Verify Eq. (16.3).

16.4 Verify Eq. (16.7).

16.5 Find the square of the magnitude of the transfer function $H(f)$ of an integrator with input/ output characteristic Determine the approximate cutoff

frequency of this

$$\text{filter. } y(t) = \frac{1}{2} \int_0^{T_b} x(t) dt.$$

16.6 When the second term of Eq. (16.6) is integrated, as in Fig. 16.2, the

$$n_0(T_b) = \frac{1}{\tau} \int_0^{T_b} dt g(t) \sqrt{P_j \cos^2 \theta} = \frac{\sqrt{P_j \cos^2 \theta T_b}}{\tau} \sum_{i=1}^{f_c/f_b} g_i$$

integrator output is

- (a) Verify this result.
 - (b) If we assume that each g_i is independent with equal likelihood of being ± 1 , what can be said of the probability density of $n_0(T_b)$? Explain.
 - (c) $n_0(T_b)$ is approximately Gaussian, yet
- $$|n_0(T_b)| \leq \frac{AT_b}{\tau} \frac{f_c}{f_b}, A = \sqrt{P_j \cos^2 \theta}$$

Explain,

- (d) What is the mean value of $n_0(T_b)$? What is the variance of $n_0(T_b)$?
- (e) What is the probability that $n_0(T_b) > (P_s T_b)/t$. Compare this answer with that obtained in Eq. (16.10).

16.7 If a possibility of error $P_e = 10^{-3}$, determine the processing gain required for a CDMA system to have 20 simultaneous users.

16.8 Direct sequence spread spectrum is to be used for ranging. The approximate distance to be measured is 10 km to a resolution of 1 m. Determine the required chip rate f_c .

16.9 FH/BFSK spread spectrum is to be used. The bit rate is 20 kb/s. The available bandwidth is 8 MHz.

- (a) Calculate the bandwidth required to pass the FM signal.
- (b) To combat interference, a (31,15) RS code is used. There is interference over 20 percent of the frequency band. Perfect symbol interleaving can be assumed so that symbol errors in each RD codeword can be considered independent.
 1. Calculate the maximum number of hopping frequencies used.
 2. How many bits are there in each hop?
 3. What is the hopping rate?

16.10 Draw a PN generator as in Fig. 16.6 for $N = 5$. Using Table 16.1, show how the parity generator is constructed.

16.11 An alternative PN generator is shown in Fig. P16.11.

$$b_i = \begin{cases} \text{connected to the feedback loop} & i = N-1-j \\ \text{connected to ground} & i \neq N-1-j \end{cases}$$

where j represents each subscript of Q_j shown in Table 16.1 for the value of N used.

If $N = 5$, show that connecting b_0 and b_2 to the feedback path, and b_1 and b_3 to ground yield the same sequence as Prob. 16.10.

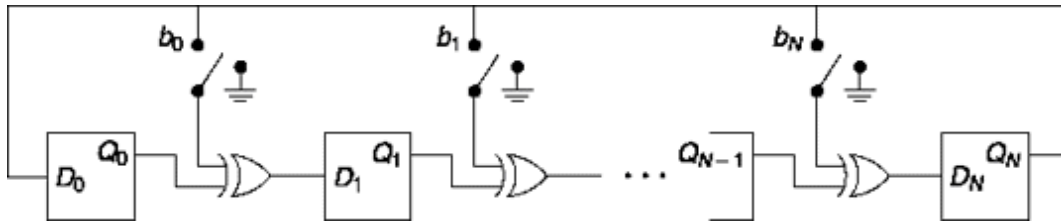


Fig. P16.11

16.12 Verify that Fig. 16.8 are mirror images of one another.

16.13 For $N = 13$, plot the probability that a cluster of length l occurs as a function of the length l . Comment on the density if N (∞).

16.14 Verify Eq. (16.33).

16.15 The power spectral density of an unknown DS signal is observed. The spectrum at $f = 0$ is 1 mW, the spectrum goes through zero at 20.47 MHz from the carrier frequency of 1 GHz and the spacing between spectral lines is 10 kHz.

What is the received power, the chip rate, and the number N of shift registers forming the PN sequence?

16.16 Verify analytically the result shown in Fig. 16.9.

16.17 Verify Eq. 16.37.

16.18 The camp and wait acquisition circuit shown in Fig. 16.12 waits at frequency $f_2 + f_0$ for f_2 to arrive. The hopping rate is 1000 hops/s. If the input signal-to-noise ratio $P_s T_H/h = 10$ dN calculate the probability of not detecting the signal when f arrives. State assumptions.

16.19 Verify Eqs. (16.44) and (16.45).

16.20 Consider a delay locked loop is used for tracking a Direct Sequence Spread Spectrum Signal (Fig. 16.17). Show how to obtain the voltage waveform at VCO output.

17

MISCELLANEOUS TOPICS IN COMMUNICATION SYSTEMS

CHAPTER OBJECTIVE

This chapter provides a glimpse of many developing areas in the field of electronic communication. Each of these topics qualifies as a separate subject and may be a part of core or elective in different branches of study. The topic ‘telephone switching’ describes principle ideas behind it and also covers digital switching. In computer communication, a brief idea of packet switching, types of networks and network protocols are presented followed by various digital interfaces like ISDN, ATM, ADSL etc. A short discussion on optical communication shows how high bit rate data transfer is done through fibre optic cables. Next, we present the mobile telephone system and the cellular concept. Mobile systems based on FDMA-TDMA and CDMA are described in brief. Fundamental issues in satellite communication are discussed along with a relatively new application GPS.

FACTS AND FIGURES

In 1904, Christian Huelsmeyer showed how radio echo can be used to detect ships from a distance up to 3000 m. He designed his *telemobiloscope*, a transmitter-receiver system to detect distant metallic objects as an anti-collision device. In a public demonstration, Huelsmeyer showed how a bell started ringing when a ship came within range and the bell stopped when the ship moved away. To avoid interference or detection of spurious signals by the telemobiloscope, he devised the following protocol. The receiver treats echo to a first transmission signal valid if it gets another echo from a second transmission after a predetermined interval. Huelsmeyer received a US patent for this device on January 16, 1906.

The first fully automatic mobile phone system was developed by Ericsson and commercially released in Sweden in 1956. Each phone used to weigh 40 kg. This was an 160 MHz system and called *Mobiltelefonisystem A* or MTA.

It had approximately 125 subscribers. An upgraded version of this phone called *Mobiltelefonisystem B* or MTB was introduced in 1962. This used transistors which helped in reducing the weight of each phone to 9 kg. This service lasted till 1983 and had about 600 subscribers. Today each of the three largest mobile phone operators in the world has more than 300 million subscribers each.

17.1 TELEPHONE SWITCHING

If we require only two telephone stations, then the system in Fig. 17.1 is, at least in principle, adequate for the purpose of providing telephone communications. The inductor L offers no dc resistance but is nominally an open circuit at voice frequencies. The transmitter consists of a box containing a powder of small carbon granules. One side of the enclosure is flexible and is mechanically attached to a diaphragm on which sound waves impinge. The sound vibrates the diaphragm, the diaphragm causes the carbon granules to compress or allow them to expand, and there is a consequent decrease or increase in the resistance of the carbon granules in the box. The carbon granule box with diaphragm is, of course, a microphone. It is not a microphone intended for high-fidelity sound reproduction, but when used with an external battery, the resistance changes cause corresponding changes in current and the signal so generated is very much stronger than is available from more sophisticated high-fidelity microphones.

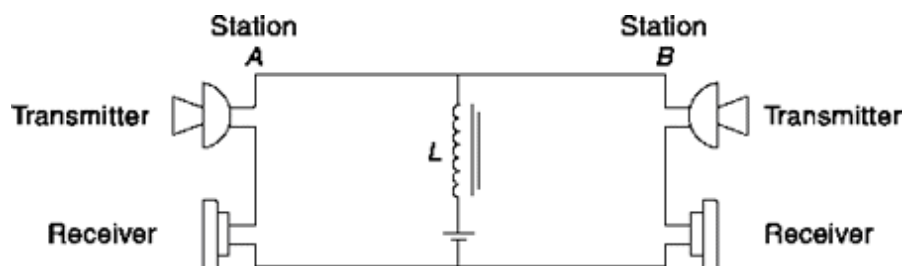


Fig. 17.1 A telephone communication system between two stations.

The receiver is an electromagnet with an accompanying magnetic diaphragm. The received changes in current, cause changes in the force of the electromagnet which produce corresponding displacements of the receiver diaphragm. In the circuit of Fig. 17.1, there is a quiescent current flowing even in the absence of sound. This quiescent current is necessary for faithful sound reproduction. The receiver diaphragm must always be

displaced in one direction from its unstressed position. In more sophisticated and more practical systems than indicated in Fig. 17.1, where there is no quiescent current in the receiver, this biasing "tug" on the diaphragm is provided by supplementing the electromagnet with a permanent magnet.

In the system of Fig. 17.1, the sound incident on the transmitter at station *A* will be heard not only at the receiver at station *B* but at the receiver at *A* as well. This sound, heard at the sound generating station, is called a *sidetone*. Some sidetone is useful. In the absence of sidetone, when the speaker does not hear himself in the earpiece, he unconsciously raises his voice to an unnecessarily high level. Too much sidetone, correspondingly, prompts the talker to reduce his voice level excessively.

How do more than two people connect to each other in a telephone talk? In Fig. 17.2 there is shown a system with four telephone stations. The scheme shown allows any station to call any other station to undertake a conversation while leaving the remaining two stations to communicate at the same time if they choose. Each station is furnished with two inputs, one by which it is *signaled* that a call is being made to it and one over which it can talk. The *signal* and *talk* lines and switches are shown only in connection with station *A*, but it is to be understood that each station is similarly equipped. While only a single wire interconnection between stations is shown, at least two wires are needed, and more may be used if multiple connections between stations are intended. The switches will need

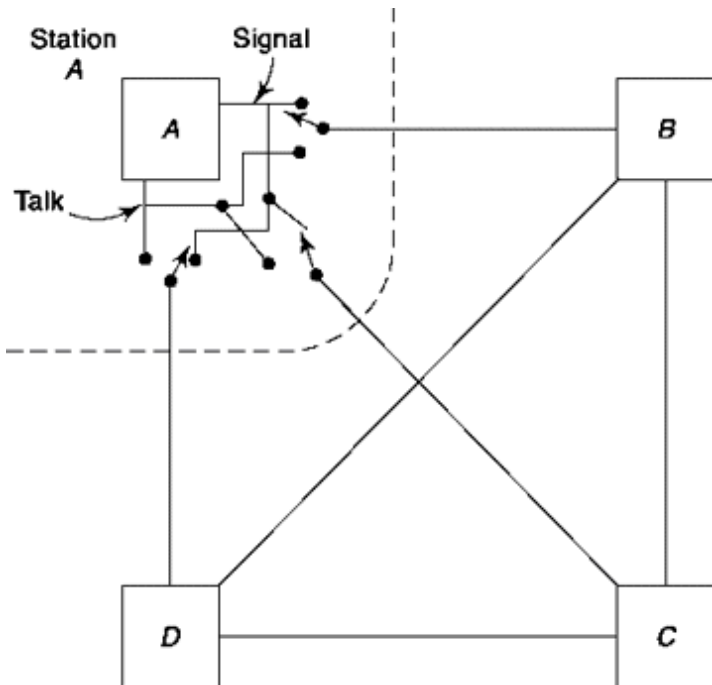


Fig. 17.2 A switching system in which each station provides its own switching.

to be correspondingly modified to show these extra connections. When the system is not carrying a conversation, all switches are in the signalling position so that any party can call any other party. Signals between the calling and called party having been exchanged, both parties will switch to the talk position. Presumably they will disable their call indicator (light, bell, etc.) to avoid interruption. The internal workings of the station are not of present interest to us. With some ingenuity we could devise a number of feasible schemes to allow both signalling and talking over the same wires, to provide "station busy" indications, etc. As a matter of fact, the system can be made effective and, at the present time, is used for intraoffice communication in small businesses. However, our present interest is simply to note that in this system *each station provides its own switching*. If there are N stations then the number of switches is $N(N - 1)$ and the number of interconnecting wires between stations is $N(N - 1)/2$. Note that since it is communications across a *distance* that we are dealing with, the path length of such interconnections will be *long*.

An improvement with respect to the total length of the interconnecting wires and number of switches results when individual station switching is replaced by *central switching*. A central switching arrangement is shown in Fig. 17.3. All of the switches are now located at one central location called a switching *exchange* and the system is referred to as *central* switching. The

crosses at the exchange indicate normally open switches (for two or more wires) which can be closed to provide a completed communication path for two subscribers. For the purpose of signalling, to indicate that a connection is called for, each subscriber is connected to a *control* facility which will close switches as required. This control can be provided by a human operator or by automatic machinery. The connections from the subscribers to the exchange are called subscriber loops. The system of switches which effect the interconnections between subscribers is referred to as the switch *matrix*. Thus, the essential components of an exchange are the *control* and the *switch matrix*. We observe that with central switching, as compared with station switching, the number of long interconnecting wires is reduced from $N(N - 1)/2$ to N and the number of switches is reduced from $N(N - 1)$ to $N(N - 1)/2$.

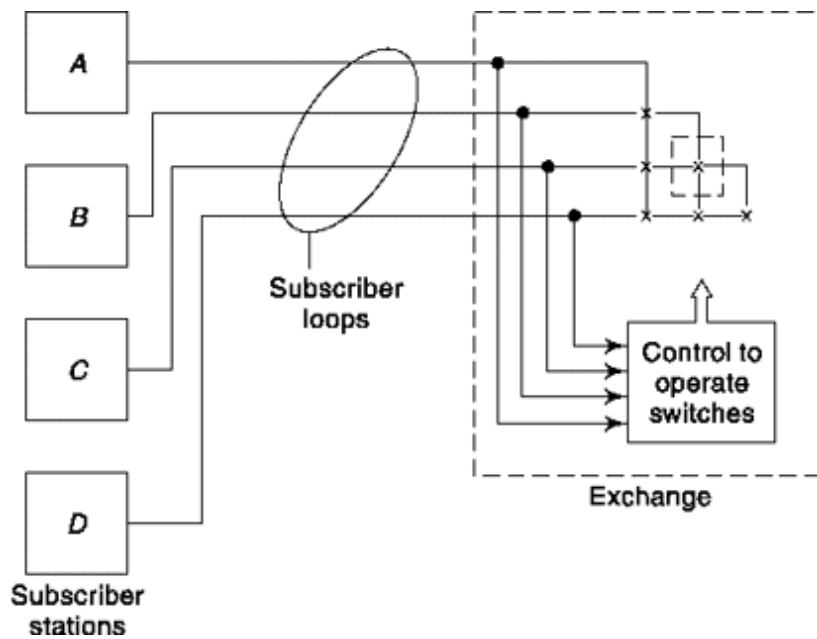


Fig. 17.3 A central exchange system. Closing the contacts in the dashed square connects subscribers B and C.

17.1.1 A Telephone Exchange

It is easy to understand that switching at telephone exchange is automated to effectively connect millions of telephone subscribers. We illustrate the switching at exchange with a simple human operated system in Fig. 17.4. In fact, this used to be the practice in early days of telephone service. Here the control is provided by a human operator and the elements of the switch assemblies are plugs and jacks. Each subscriber has a transmitter-receiver

which is bridged across the subscriber's loop and a capacitatively coupled bell similarly bridged. The line lamp relay coil serves as the inductor L shown in Fig. 17.1. All of the remaining hardware is located at the exchange, and, with the exception of the ringing generator, the operator's head set and the battery, all of the exchange equipment is duplicated for each subscriber. We have identified the subscriber whose equipment appears in the diagram as subscriber *A* and a second subscriber as subscriber *B*.

To initiate a call, subscriber *A* lifts the transmitter-receiver from its *cradle*. The cradle switch, held open by the weight of the transmitter-receiver, then closes, bridging the transmitter-receiver across the subscriber's loop. The *ring* key is normally connected to the plug side so that the closing of the cradle switch causes a dc current provided by the battery to flow through the line lamp relay coil. (The capacitor in series with the bell assures that no dc bell current will flow except when the cradle switch closes.) The excitation of the line lamp relay causes the line lamp to illuminate. The lamps are labelled to identify the caller. When the operator sees subscriber *A*'s lamp light, she closes the "speak" key connected to subscriber *A* and asks "number please." *A* says he wants to talk to *B*. The operator then throws ring key *B* (not shown) to the ringing generator side. (This key is spring loaded so that it remains in the ringing position only while being held.) The ringing generator provides an ac current which passes through the bell capacitor at *B*'s subscriber station. If *B* does not pick up the phone after a reasonable time, the operator reports to *A* that the call cannot be completed. (The speak keys are also spring loaded and provide connection to the subscribers only while being held.)

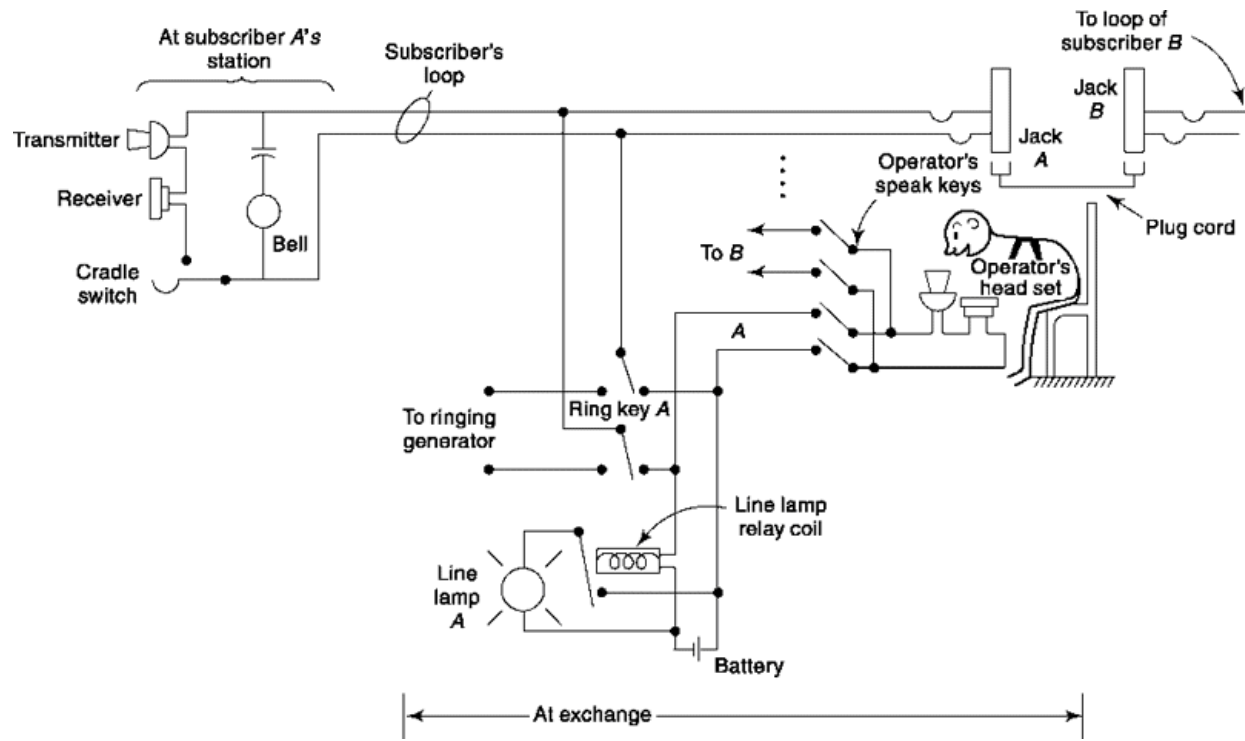


Fig. 17.4 A simple exchange operated by a human operator.

If *B* lifts his phone from its cradle, the operator will be so informed because *B*'s line lamp (not shown) will go on. In this case, the operator will connect jack *A* to jack *B*, and then say to *A* "go ahead please." So long as *A* and *B* are in communication, the line lamps of both will be lit. When both hang up, the lamps will go out, and the operator will disconnect the jacks. If only one party hangs up, the operator can ring the other party to remind him to do the same.

17.1.2 Hierarchy of switching Offices

There are in excess of 150 million phones in the United States alone. While, in principle, it is possible to arrange that a single switching exchange accommodate all these phones, we need hardly belabor the point that it is not practical to do so. For, suppose that there were a single exchange at some central location, say at Chicago. Then with $N @ 150 \times 10^6$ subscribers, there would be N connections to the exchange and the number of switch assemblies would be $N(N - 1)/2 @ 10^{16}$ switches. Two subscribers *A* and *B* located on the same street in Los Angeles would communicate over a 4000 mile line extending to Chicago and back again. Over such a long path the voice signal levels would frequently have to be passed through repeaters (amplifiers). The need for repeaters would in turn require one

communication path to carry A's voice to B and a second path from B to A. Hence, at a minimum, four wires would be required. On the other hand, we have noted, as in Fig. 17.4, that when no amplification is required, two wires are adequate to accommodate a two-way communication.

To circumvent the difficulties just described and to accommodate to changes in available equipment and subscriber requirements, operating switching systems employ a hierarchy of switching offices. The first levels of the hierarchy is to be seen in Fig. 17.5. The solid circles represent *end offices* to which individual subscribers are directly connected. The connection from subscriber to end office is referred to as a *subscriber loop*. If two subscribers are connected to the same end office then that office alone provides the necessary switching service for these two. In Fig. 17.5 we contemplate a number of end offices clustered into three relatively distantly separated locations. Where a number of end offices are located in the same general area, the need for multiple offices will have arisen either because the subscribers are not close enough to one another or are too numerous to be serviced by a single end office or for both of these reasons. The end offices in the same area will be interconnected by trunks (shown dashed) so that subscribers serviced by nearby end offices may be interconnected. For the purpose of allowing communication between distant clusters of end offices, toll offices have been provided. The end offices in one area are connected to a nearby toll office and the toll offices are, in turn, interconnected through toll-connecting trunks. While, for the sake of simplicity, we have not so indicated, depending on geography and customer usage, it may happen that an end station will be connected to more than one toll station and also end stations connected to different toll stations may also be connected by an end office to end office trunk.

A very populous area, such as a large city, will have many end offices. Much of the traffic will involve calls between subscribers in the city and hence between end offices. To facilitate this end office to end office traffic a *tandem* switching office may be provided as shown in Fig. 17.5 for one group of end offices. Calls between subscribers connected to different end offices in the city will go by way of a tandem office. Intercity calls will use a toll office.

In the United States there are thousands of end offices, each one of which must be connected to at least one toll office. The number of such toll offices

is consequently so large that it would still be prohibitive to provide interconnections from every such toll office to every other. Accordingly

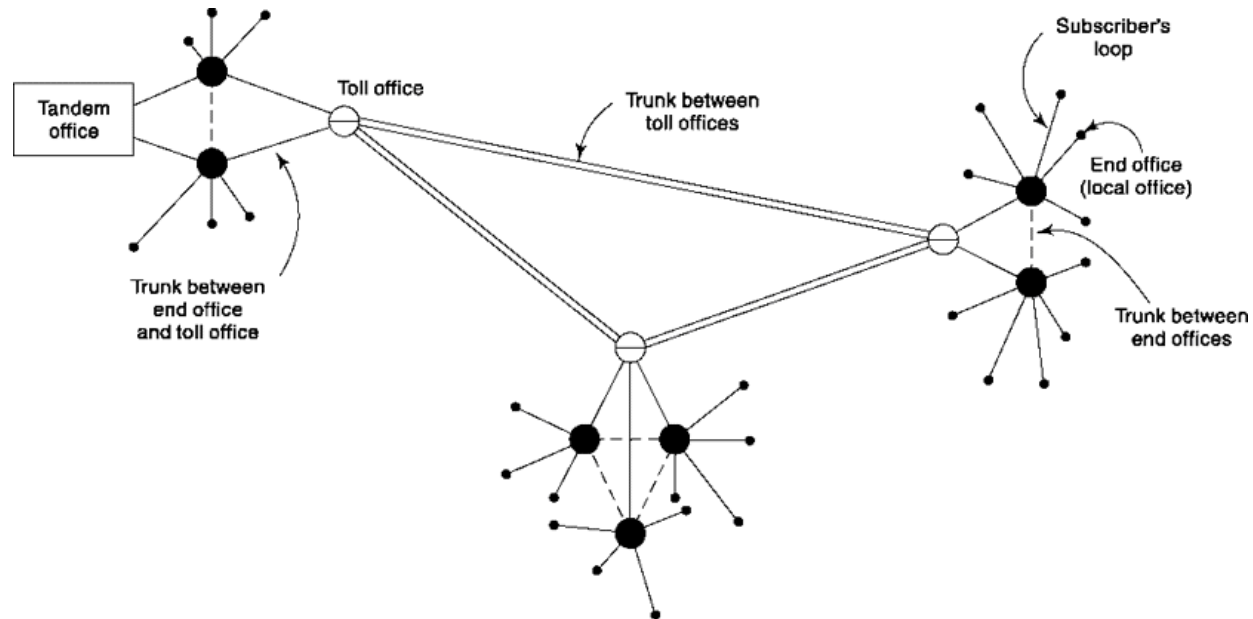


Fig. 17.5 Illustrating interconnections of subscribers to end offices, end offices to toll offices, and trunks between toll offices.

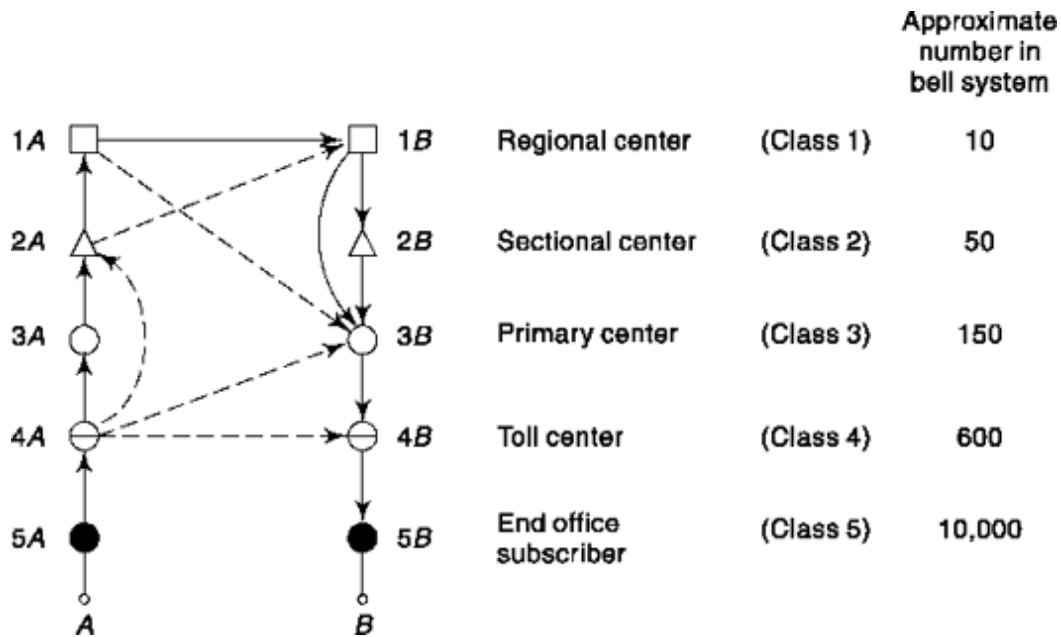


Fig. 17.6 The hierarchy of switching centers showing possible interconnections.

the hierarchy is continued so that altogether there are five *classes* of switching facilities. These are identified by name and class number in Fig. 17.6. As noted, there are about 10,000 end offices in the Bell system in the United States and progressively fewer centers as we go up in the hierarchy,

there being only ten regional centers. The tandem offices, which may interconnect end offices, are not shown.

Suppose that subscriber *A* in Fig. 17.6 wants to call subscriber *B* in a distant location and there is no direct connection between their end offices. End office *A* is certainly connected to some toll center (4*A*) which is certainly connected to some primary center (3*A*), etc., and finally all regional centers are accessible to one another. Hence if there is no alternative, the call can be routed through all of the centers shown: from 5*A* to 1*A* through all the intermediate centers then to 1*B* and finally to 5*B* again through all the *B* intermediate centers. This path, being a route of last resort, adequate facility is incorporated to assure that the possibility of blocking is very small.

On the other hand, depending on the locations of the various centers, it may be that toll centers 4*A* and 4*B* are connected. In such a case the call will be routed over the shorter path 5*A* (4*A* (4*B* (5*B* as shown by one of the dashed paths in Fig. 17.6. If there is no 4*A* to 4*B* connection there may be a connection from toll center 4*A* to primary center 3*B* giving rise to an alternative route which again circumvents the very long route up and down the entire hierarchy. As we have noted, every toll center will have a direct route to a primary center. But, again depending on location, a toll center may also have a connection to a sectional center such as from 4*A* to 2*A*. And it may be that center 2*A* is connected not only to 1*A* but to 1*B* as well. We have assumed that there is no direct connection between end offices 5*A* and 5*B*, but otherwise many other interconnections may be available, some of which are shown by the dashed lines in Fig. 17.6, any one or combination of which may shorten the path from *A* to *B*. The dashed connections will generally be heavily utilized and hence attempted calls through them may frequently be blocked. As noted, if all attempts to find a shortened path meet with failure, the long path up and down the hierarchy will be employed. Typically, each caller may be routed through as many as seven possible paths,

starting with the shortest and proceeding to the longest, in an attempt to complete the connection. If all seven paths are blocked a “busy-circuit” signal, is returned to the caller, which indicates that the caller should redial at a later time.

17.1.3 Two and Four-wire Connections

We have seen as in Fig. 17.4 that a single loop (two wires) is all that is required to provide complete service to a subscriber. Such is the case so long as the transmission distance is short enough so that no amplification is required to make up for the attenuation over the transmission path. Thus, generally when two subscribers are served by the same local exchange only two-wire interconnections are required. When amplification is needed, as when a toll call is involved, then gain must be provided for each of the two directions of signal transmission. There are available two terminal repeaters, which can simply be bridged across a two-wire line, which can provide gain in the two directions simultaneously. However, as a matter of practicality such two-way repeaters lack reliability and dependable stability and are generally not used. Instead, as shown in Fig. 17.7 separate one-way repeater amplifiers are used, one to amplify the signal generated at station A and to be transmitted to B and a second for the B to A transmission.

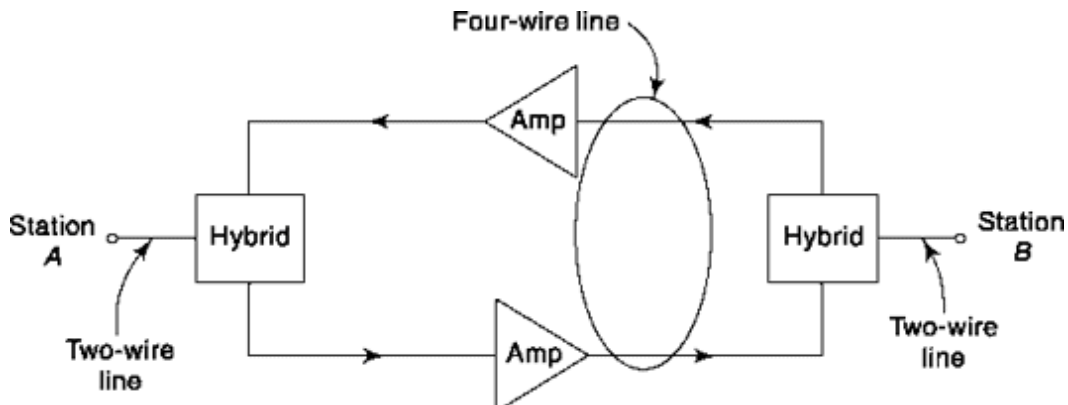


Fig. 17.7 The four-wire connection which is required when amplification must be provided.

We observe that each amplifier's output is connected to the input of the other amplifier. Such an arrangement will result in oscillations, in spite of the *hybrid*, which ideally should isolate the input and output lines. The oscillations produce a loud, sustained, tone referred to frequently as "singing." In a telephone system, the transmitted voice signal from A reaches B and is amplified and returned to the receiver at A. Thus, this system also produces a loud and annoying "echo."

An echo produced by the circuit shown in Fig. 17.7 can be suppressed using the circuit shown in Fig. 17.8. In this circuit assume that A is transmitting to B. If the received voltage, at point q, exceeds the preset threshold voltage V_q then a loss L_B is inserted in the path from B to A to

attenuate the “echo” signal. When A is not talking, the threshold voltage is not exceeded and the loss is reduced so that speaker B can send a signal to A .

One major drawback of this technique is that if A and B speak simultaneously (a situation which occurs more often than you may think), speaker B ’s voice may be attenuated by the large loss L_B introduced by speaker A , thereby producing *clipping*. “Clipping” may sometimes be heard on long distance calls when the *echo-suppressor* is not operating properly.

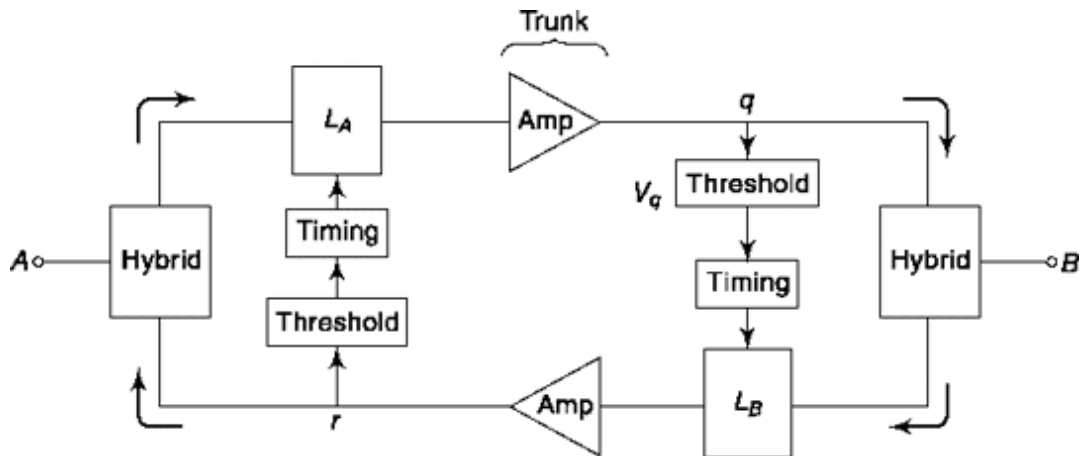


Fig. 17.8 Basic concept of an echo suppressor.

Figure 17.9 is an echo suppressor designed to permit two speakers to talk “naturally”, i.e. both speakers are able to talk simultaneously without noticeable clipping and without noticeable echo.

In this figure, a differential amplifier measures the relative voltage levels between points a and b . If speaker A is talking, the voltage at a exceeds the voltage at b and L_A is reduced while L_B is increased to reduce the echo. If speaker B interrupts so that both speakers are talking simultaneously the voltage at b becomes comparable to the voltage at a , the difference amplifier output becomes small and both loss elements L_A and L_B are reduced. The echo now is not heard since the voice signal of speaker B is louder than the echo of speaker A .

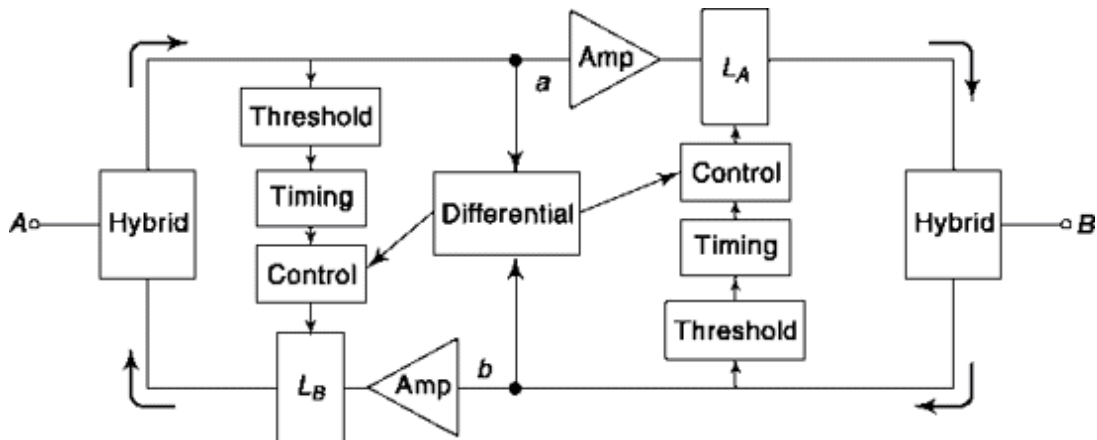


Fig. 17.9 Balanced echo suppressor.

It is clearly more expensive and complicated to switch four-wire lines than two-wire lines. Two separate paths through the switching matrices must be established and twice as many contact points are involved. We can however avoid four-wire switching by converting to two-wire lines, performing the required switching and then, if necessary convert back to four-wire lines. Such a procedure is used very sparingly however, because each such conversion saves switching complexity only at the expense of adding echo suppressors. Further, the balance provided by the echo suppressors which is necessary to avoid echo is never perfect so that as a matter of practice it is difficult to suppress an echo if too many conversions are used.

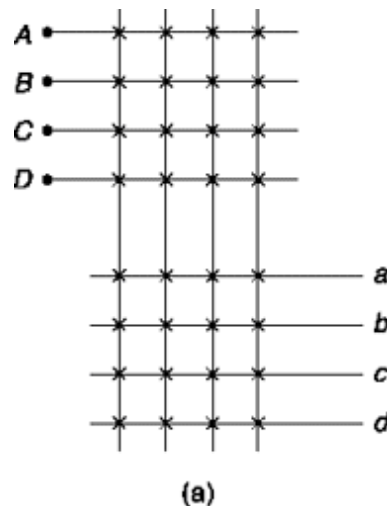
17.1.4 space and Time switching

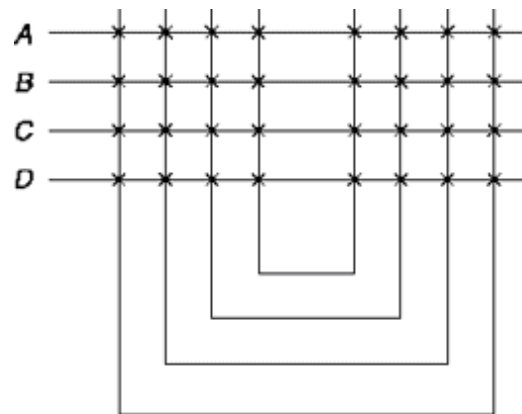
A simple illustration of space switching is shown in Fig. 17.10. It is a two stage matrix that exists between two stations providing four paths between (A, B, C, D) and (a, b, c, d) . Consider, A wants to connect to a . Then, any of the four lines between two stations can be chosen and corresponding space-switches at cross-points are to be turned on to establish the connection. Could it work with less number of switches and reduce the cost? It can. For example, consider A can be connected only via first vertical line, B second line, etc. Then in the top matrix only one switch at cross-point of A and first vertical line would require. But, a failure of that switch would completely disconnect A . Also to take care of random failures of switches, a certain amount of redundancy is necessary to be built-in. Similar question may be asked if we can reduce the number of lines between two stations which will reduce the channel cost. In that case, calls are to be blocked if all four subscribers of one station want to connect to their counterpart in the other

station simultaneously. In actual practice, multiple stage switching is done with judicious choice of different parameters.

The previous type of switching is also known as space-multiplexing. Switching can also be done by time-multiplexing. This is illustrated in Fig. 17.11. The subscriber's lines are labelled 1, 2,..., N and are all joined to a common bus through *analog* gates. The gates can be *open* to allow for signal transmission or *closed* to prevent transmission. (These gates can be viewed simply as switches. If so, then the gate is *open* when the switch is *closed* and the gate is *closed* when the switch is *open*) The *gate control lines* serve to control the gates, i.e. to close and open the switches.

If we want to allow subscriber k to transmit a signal to subscriber l then we must allow subscriber l to sample the signal from subscriber k at the Nyquist rate or more frequently. We have already noted that in voice telephony a sampling rate of 8000 Hz (i.e. every 125 ms) is adequate. To permit the sampling we must open for signal transmission the two gates, one in subscriber k 's line and one in the line of subscriber l . The length of time t during which this connection can be allowed to persist is, of course, determined by the number of subscribers who share the bus. If there are N subscribers then there can be at most $N/2$ simultaneous connections. If, say, we require that $t = 5$ ms then the number of connections will be $N/2 = 125/5 = 25$ and the number of subscribers who can be served is $N = 50$.





(b)

Fig. 17.10 Two stage matrices used to provide multiple paths.

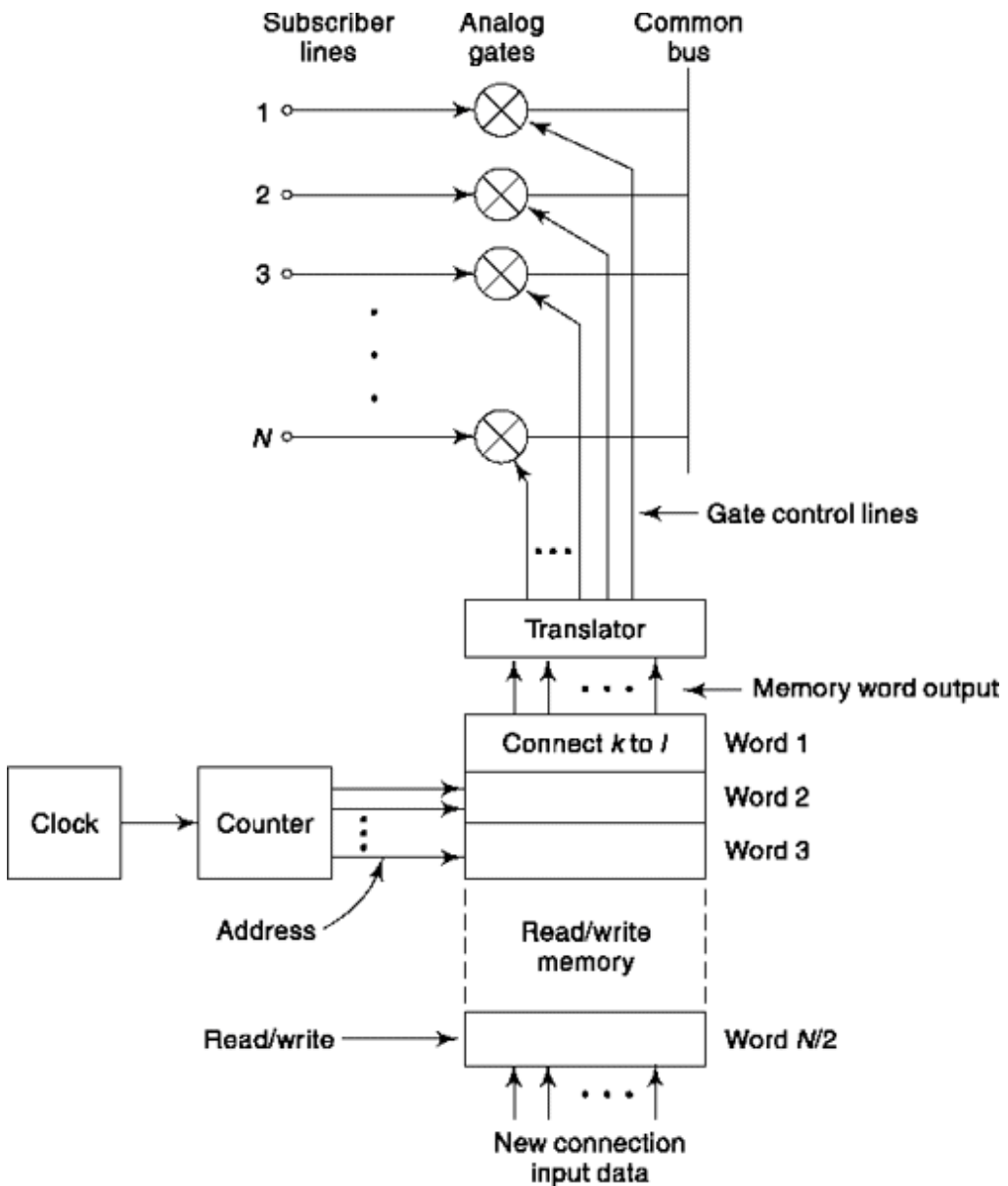


Fig. 17.11 Analog time-division multiplexing used for switching.

The read/write memory (also called a random-access memory, RAM) in Fig. 17.11 has a capacity of $N/2$ words. Each word is a coded instruction indicating which analog gates are to be open for transmission. Thus word 1, as shown, holds the instruction that subscriber k is to be connected to subscriber l . When this word is read out of the memory it is applied to a *translator* which decodes the instruction and sets its output *gate control lines* so that only gates k and l are open for transmission. The address specifying the word which is to be read is provided by a counter of modulo $N/2$. The counter is advanced through its states by a clock which runs at a rate to insure that it provides each address from 1 to $N/2$ every 125 ms. Thus the

clock frequency is $8000 (N/2) = 4000 N = 200$ kHz, if $N = 50$, as in the example above. Each word in the memory holds an instruction specifying which gates are to be open. Of course when some subscribers lines are idle there will be memory word locations specifying that no gate is to be open. When a call is initiated or terminated, it is necessary to change the corresponding word. Accordingly, the memory is provided with facility not only to be read but also with facility to allow new words to be written into it. This “new connection” data input is indicated in Fig. 17.11. Of course, depending on the past history of call connections the instruction “connect k to l ” can appear in anyone of the memory locations. There is no reservation of memory locations for particular subscriber pairs.

17.1.5 time slot interchanging

For digital signal, the idea of time division multiplexing can be enhanced to time-slot interchanging. The basics of switching by time-slot interchanging is illustrated in Fig. 17.12. At the transmitting side, a multiplexer and A/D converter multiplexes and encodes signals from N subscribers. At the receiving end the inverse process is carried out. The multiplexer and demultiplexer switches maintain a fixed synchronism so that the switches contact terminals 1 at the same time, terminals 2 at the same time, etc. If there were a direct connection, as indicated by the dashed line, the single channel shown would carry N signals but there would be no provision for switching.

To provide for switching, a *slot-content memory* is provided. This memory has N word locations, i.e., as many as there are time slots, and each location can accommodate all the bits in a time slot. The time slot counter runs at the time-slot rate, that is, it increments its count by one at the end of each time slot. This counter provides the address at which a memory input word is to be written into the memory. Accordingly, we can arrange that the content of slot 1 will be *written* into memory location

1, the content of slot 2 in location 2, etc. that is, successive slot contents are *written* sequentially into the memory. (Actually to write a word into the memory it is generally necessary that all the bits of the word be available in parallel, that is, all at the same time.) Figure 17.12 indicates that the bits in a time slot are available only serially, i.e. in sequence, one at a time. Accordingly, it will be necessary to interpose, before the memory, a piece of hardware to convert from serial to parallel. A shift register driven by a clock

at the bit rate can serve for this purpose. For the sake of simplicity we have not included such provision in Fig. 17.12.

There is a second memory in the system. This memory is the control (slot interchange information) memory and it holds, not the content of the slots, but holds addresses of the slot content memory from which words are to be *read*. The control memory also has N word locations and a word needs to accommodate many bits as needed to write the number N . The time-slot counter which provides *writing* addresses for the slot-content memory provides reading address for the control memory. Observe that, quite arbitrarily, we have written the address 7 in memory location 1 of the control memory. Accordingly, during the first time slot of the frame, the *content of slot 1 will be written* into the slot content memory but during this first time the *word in memory location 7 will read* from the memory. This word is the content of slot 7. Hence, altogether we have interchanged the contents of slots 1 and 7. Thus, we have arranged the transmitting subscriber 7 has been switched to receiving subscriber 1. Correspondingly, on the basis of the addresses we have arbitrarily written into the control memory, we have switched N to 2, 18 to 3, ..., 6 to N. The interchange are also shown by the numbering of slots in the input and output frames.

Observe that, in this scheme, each subscriber at either end is assigned a fixed time slot. Switching is not effected by changing the assigned time slot but rather by interchanging the content of a time slot. Note further that the channel of Fig. 17.12 provides for only one-way communication. For two-way communication a second channel is required. If in one channel, the content of, say, slot 3 is moved to slot 12, then in the second channel the content of 12 must be moved to slot 3. When a

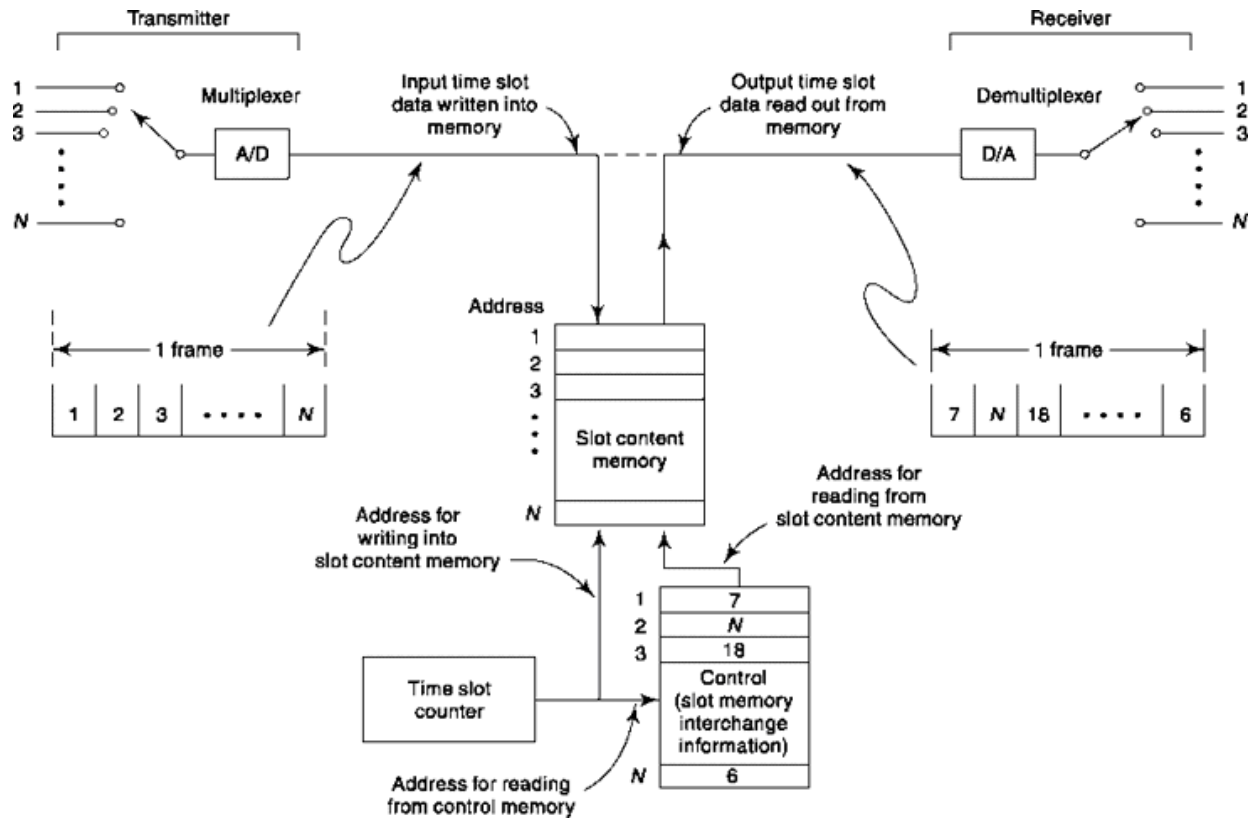


Fig. 17.12 Illustrating the principle of time-slot interchanging.

new call is initiated and the corresponding connections have to be made, this switching function is effected by changing the address data in the control memory.

In the arrangement of Fig. 17.12 writing into the slot-content memory is sequential and reading is random, leading to what is referred to as “output time slot interchanging”. The alternative possibility, sequential reading and random writing that is “input time-slot interchanging” is equally feasible.

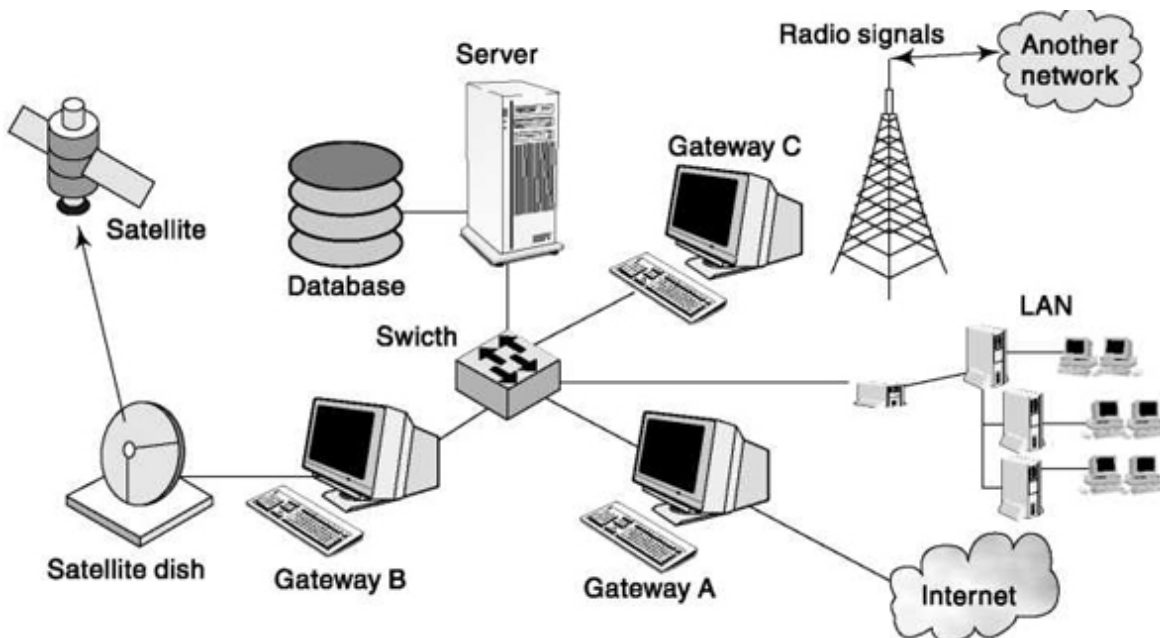
Note that, for digital signal combined space and time switching is employed in actual practice.

SELF-TEST QUESTION

1. How important is the level of side tone in a telephone receiver?
2. Is central switching effective in reducing length of interconnections?
3. What is a subscriber's loop?
4. Which of 2 and 4-wire lines is more expensive to switch?
5. Which of analog and digital signals can use time slot interchanging?

17.2 COMPUTER COMMUNICATION

Computers are commonplace today and an important means of digital data storage and processing. To share this data with another computer located in a nearby or a far-off place, a network is needed that requires switching and appropriate protocol of data transfer. The communication can be among computers hosted within a building through a Local Area Network (LAN) or across continents through Internet which is a complex network of many networks. Figure 17.13 gives a broad picture of modern computer communication system. A *switch* is a sophisticated, specialized computer which provides switching facility to make the connection required. A *gateway* or *router* is a computer node that serves as an entrance to another network and vice versa. Generally, lines joining terminals to a local computer need not be required to transmit data at a high rate and a relatively modest bandwidth is adequate. High speed, i.e. wide bandwidth lines, are needed to interconnect switching networks.



17.2.1 types of Networks

There are three basic types of communication networks in service. These are: *circuit (line) switching*, *message switching* and *packet switching*.

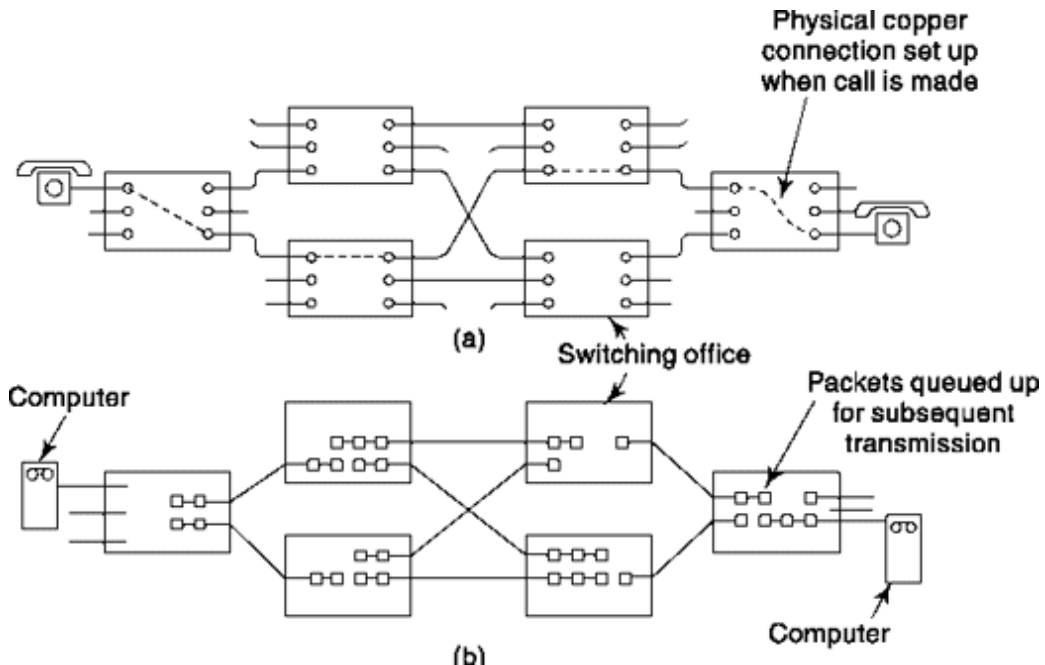
Circuit switching

In *circuit switching*, the hosts which are to communicate are connected by a wire path which is dedicated to the communicating pair, without interruption, for the entire duration of the transmission. This type of system is entirely analogous to a telephone switching system. The entire wire path remains allocated to the single set of users until released and, during this time, no other potential user can use any part of the wire path, not even during intervals when the path happens to be idle. Figure 17.14a illustrates the major principle of circuit switching. Here a suitable path is established by physical wire connections and maintained until disconnected by the users.

Message switching

A distinctive feature of computer communication which makes it quite different from telephone communications, is that, in computer communication, transmission generally occurs in relatively short bursts separated by long intervals of no transmission. Typically, a line connecting two computers may be in use only 1 percent of the time allocated. Such a manner of use is clearly uneconomical since, of course, the users must be charged for the entire time of allocation.

Message switching used in conjunction with a network offers the possibility of greatly improved economy. To see how message switching works consider that computer *A* needs to transmit data to computer *B*. Consider, further, that the communication will consist of relatively short messages separated by long intervals when there is no transmission. Suppose that the transmission path selected is *A* (*X* (*Y* (*Z* (*B*. Note that the lines from *X* to *Y* and from *Y* to *Z* can be used as part of a connection from many computers to many other computers.



In circuit switching there is no transmission until a *complete* connection is established between users. In message switching, at any particular time, no such complete connection is needed. Instead computer A will transmit a message to switching center X where it will be *stored* in a *buffer*. This stored message will be kept waiting in the buffer at X until the line from X to Y is not required for some other prior transmission. When that line becomes available the message at X will be transmitted to Y. Again, after storage and a possible delay to wait for available open time, the message will go from Y to Z and then to computer C. This system has the disadvantage that there will be a delay between the time of transmission and the time of reception of a message. On the other hand, the long distance, fast, expensive lines between switching computers will be idle for shorter intervals. For example, when the line from X to Y is not transmitting a message from A to B it can be used to relay a message between other computers. In the total transmission of a message from A to B it will generally be that, at any particular time, only one of the lines between switching computers will be involved with that message, the other lines in the overall path of connection being released to handle other messages between other computers. Since the system involves *storing* and subsequent forwarding of messages, a message-switched network is referred to as a *store and forward* network.

packet-switched Network

Message switching has a number of features which are less than desirable. (1) A message may be very long (many hundreds of thousands of bits) or very short (of the order of thousands of bits). To accommodate the long message, large buffers need to be available. The hardware of these buffers is wasted when short messages are received. (2) Even if a line is available, a switching computer will not begin to relay a message until the entire message has first been received. Accordingly, if the message duration is T_m and it must be relayed R times, then even ignoring waiting time, the delay will be RT_m since at each relay the entire message is stored before being forwarded to the next node. For long messages and many relays this long delay time can become inconvenient. (3) It may be that a link between centers is needed very briefly to accommodate a very short message but the link is busy transmitting a very long message. It would be useful if it were possible to interrupt the long message briefly to allow transmission of the short message. Unfortunately, it is not easily feasible to incorporate such a feature in a message-switched system. Hence it is possible that short messages may be delayed for a time which is long in comparison with the message lengths while the system is “tied-up” processing a long message.

A *packet-switched* network undertakes to circumvent the less desirable features of message switching by subdividing messages into packets. A typical packet may be 1024 bits long. The message is then transmitted packet by packet. Like the messages in message switching, each packet must be stored in buffers at the nodes of the subsystem and then forwarded. Packet-switching like message switching, is therefore a *store and forward* system. In some packet-switched systems, different packets of a single message may arrive at a destination by different routes and with different delays. It is also entirely possible that the packets of a message may arrive out of order. Packet switching is represented in Fig. 17.14b where the small squares in the switching computers represent the individual packets.

Each unit of transmission, whether the message in message switching, or the packet in packet switching, must include not only the information bits but additional bits referred to as *overhead* information. These overhead bits must identify the *destination* of a unit (message or packet) so that each switching center will know how further to route the unit, the *source* of the unit so that acknowledgement is possible, and the *user identification* so that the user can be charged for services. Further, *synchronization bits*, also part of the overhead, must be included to identify the *beginning* and *end* of a unit.

In packet switching, as mentioned above, it may happen that different packets of a message may travel over different routes and therefore arrive out of order. Accordingly packets must be *numbered* so that they may be reassembled in proper sequence.

In a message switched system the overhead information must be appended to each message, while in packet switching each packet must be accompanied by overhead bits. Thus, if there is more than one packet/message the packetized message had more overhead. Accordingly with respect to message switching, packet switching has two disadvantages: (1) To transmit a given amount of information per unit time, packet switching requires that bits be transmitted at a more rapid rate than is required in message switching. (2) The switching hardware needed to packetize, add overhead, depacketize and reassemble is more complicated and must operate more rapidly than the corresponding hardware needed in message switching.

On the other hand, in spite of the fact that packet switching requires more overhead bits, it is entirely possible that packet switching will transmit a given amount of information in less time than message switching. This feature results from the fact that a switching computer cannot begin to retransmit a message (relatively long) or a packet (relatively short) until the *entire* message or packet has been received. Let us assume that a message of B bits is to be relayed from one to another of a series of switching computers using *message switching*. There are to be $K + 1$ computers involved in the overall transmission from the source computer C_0 to the destination computer C_K over K transmission facilities (links). We neglect the time of propagation over the links and assume that the only delay is caused by the bit duration $T_b = 1/f_b$. The number of overhead bits needed is b . The total transmission has $B + b$ bits and will be transmitted from one computer to the next in a time $(B + b)/f_b$. There being K links, the total time required for transmission of the message without packetizing is

$$T_M = K[(B + b)/f_b] \cong K \frac{B}{f_b} \quad (17.1)$$

since, ordinarily $B @ b$. Next, let us consider that the message has been divided into P packets each with a number of bits per packet B/P , and let us assume that the number of overhead bits needed is again b as before. The total number of bits in the packet is then $(B/P) + b$. To transmit this packet

over the K links will require a time as given by Eq. (17.1) except with B replaced by B/P . Hence the time required for the first transmitted packet to arrive at its destination is $K[(B/P) + b]/f_b$. The next packet is processed immediately after the first and will arrive after the first by a time $[(B/P) + b]/f_b$. Since, after the first, there are $p - 1$ further packets, the total time needed to transmit the entire message by packets is

$$T_p = K[(B/P) + b]/f_b + (P - 1)[(B/P) + b]/f_b \quad (17.2)$$

To find the value of P which minimizes T_p we set to zero the derivation of T_p with respect to P . We find that T_p is minimum when

$$P^2 = (K - 1) \frac{B}{f_b} \quad (17.3)$$

and that correspondingly

$$T_{p,\min} = K \frac{b}{f_b} \left[\sqrt{\frac{B}{b}} + \sqrt{K-1} \right]^2 \quad (17.4)$$

If $B/b @ K$ then

$$T_{p,\min} \cong \frac{B}{f_b} \quad (17.5)$$

and, in this case, referring to Eq. (17.1) we note $T_{p,\min}/T_M = 1/K$. If there is a finite propagation time t associated with propagation over a link, then T_p and T_M will be increased by the amount Kt .

17.2.2 Design Features of a Computer Communication Network

A computer communication network is designed such that:

- (a) communications between sources and destinations are available to a large number of users at a relatively low cost;
- (b) the time required to process a transmission from source-to-destination, which is called the *response time* should be less than some specified value. There are several ways of specifying response time such as: (1) that the average response time of the network be less than some given value, (2) that the probability that a response time exceeds a time T_0 is less than, say, 1 percent, etc.;

(c) the *throughput* S is greater than some specified value. The throughput is the number of packets that are successfully *received* per unit of time. In any computer communication system, we find that as more users enter the network and the total number of packets transmitted per unit time by these users increases, the more packets are received per unit time until a point is reached where congestion limits the rate at which packets can be received correctly. Clearly, we would like this rate to be as high as possible;

(d) the network should continue to operate even if a few nodes or links fail, and that the response time and throughput in such a “stressed” network should not be significantly degraded.

In order to accomplish these design objectives the designer of a computer communication network must consider:

Topological design

Topological analysis investigates different ways of interconnecting terminals and computers, i.e. different network designs. Such design is very dependent on the geographical location of these *resources* (as the terminals and computers are called).

Figure 17.15 shows the four basic topological structures. Figure 17.15a is a *star* connection. Here, the outputs of terminals located in one location are multiplexed to form a single high speed bit stream. The multiplexer shown is called a *remote concentrator*. The outputs of the remote concentrators are then connected to the computer (central processor).

Figure 17.15b shows a *tree* configuration. In this system, terminals are multiplexed into remote concentrators which are then multiplexed into another remote concentrator, etc., until we finally reach the central processor which routes the message to the appropriate host.

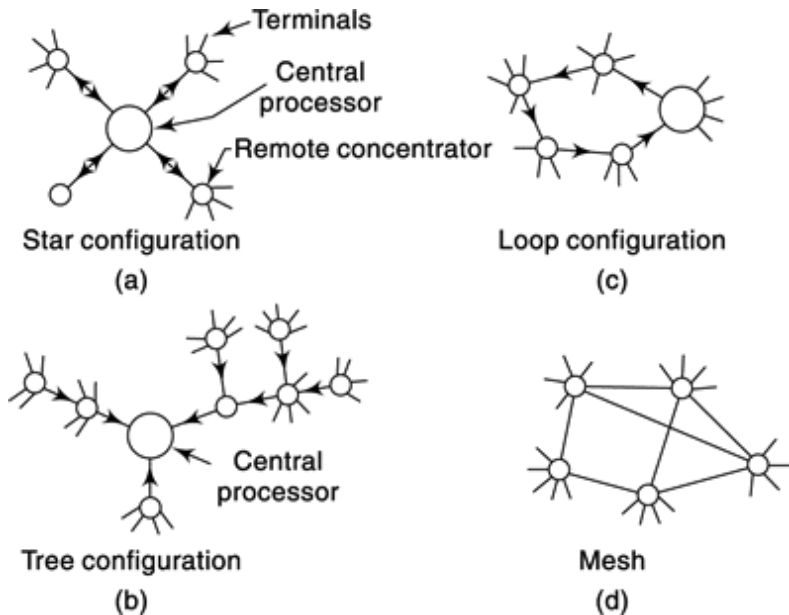


Fig. 17.15 *Different topological configurations.*

Figure 17.15c is a *loop* configuration, where the remote concentrators form a loop with the central concentrator. Figure 17.15d is a *mesh* configuration. Most networks employ the mesh configuration either by itself or in combination with one or more of the other configurations thereby forming a hybrid configuration.

A basic problem with the star and tree configuration is that if a node or link fails, computers on one side of the failure are unable to communicate with computers on the other side of the failure. The mesh configuration has low response time and is robust against node or link failure.

Line Capacity Allocation

The tree connection and the star connection result in heavy traffic along links that input the central processor. Such links must be capable of carrying the traffic, and wideband cable, filter optic cable or a wideband radio or satellite channel is often used. The network cost depends to some degree on the type of links employed and the bandwidth of these links.

Routing procedures

A routing procedure is required to insure that the sender reaches its destination within the specified response time and takes a path which enables the network to carry a maximum number of users. There are many

different routing procedures (algorithms), several of which are briefly discussed below, for the typical mesh network shown in Fig. 17.16:

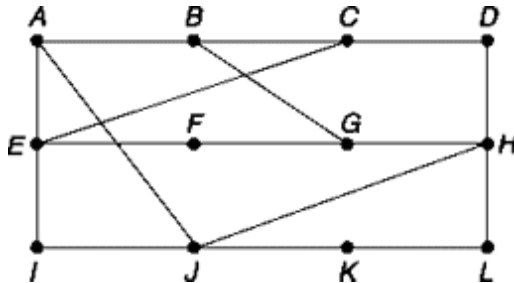


Fig. 17.16 A typical data communications network.

1. *Flooding*. This technique is used primarily when a message from one node must be certain to reach one or more specified nodes in a network. Suppose, for example, that in Fig. 17.16 a message from node *A* must reach node *L*. Then to *flood* the network, the message is sent on each outgoing link, in this case to *E*, *J* and *B*. Each of these nodes forward the message on each outgoing link except for the link over which it arrived, i.e. *B* forwards the message to *G* and *C*, etc. As a result of flooding the network, the message has an extremely high probability of being received correctly in a reasonable time at its destination. The technique is robust, i.e. node or link failure will not dramatically affect the response time period. However, flooding results in traffic congestion since a large number of duplicate packets are transmitted.

2. *Random Walk*. Using this technique a packet stored at a node is forwarded at random over any available path. For example, a packet at *H* will be forwarded at random to either node *G*, *D*, *L* or *J*. This technique is robust since node failure does not alter possible transmission to other nodes. In addition, only one packet is transmitted from node-to-node thereby helping to avoid unnecessary congestion. However, since the motion of a packet is random, there is no guarantee that the packet will be delivered in a reasonable time.

3. *Fixed Routing*. In this technique each node is furnished a table of routes which has been predetermined, usually on the basis of previous traffic flow. This technique is useful when the traffic is well estimated a priori. However, it does not operate properly when there are large random variations in the traffic pattern.

4. *Centralized Adaptive Routing*. In this technique, each node is furnished a table of routes. This table is continually altered as a result of instructions

furnished by a “supervisory” computer which monitors the traffic at each node. This technique is adaptive to network traffic changes and therefore helps to minimize congestion. However, there is a delay in the determination and distribution of table updates.

5. *Isolated Adaptive Routing.* Here the table of routes at each node is continually upgraded by information the node gathers by itself. One way for this to occur is (see Fig. 17.16) for packets from any node, say from nodes B , E and J , to node A to carry within the packet an entry as to the buffer availability at that node. If, say, node B has not transmitted to node A in a “long” time interval, A assumes that node B is not working and will not route messages to node B . This procedure does not require a supervisory computer, but, on the other hand no node has a global picture of the traffic in the network.

Flow Control procedures

After the routing technique has been decided upon, it is necessary to establish the procedure by which we can assure smooth traffic flow and avoid “bottlenecks” and “deadlocks.” Flow control procedures include selecting the multiplexing scheme including determining the number of links that can be combined at a multiplexer, the *access* technique used to input the messages on each link to the multiplexer, as well as the buffer size needed at each multiplexer.

To illustrate two *access* techniques, *polling* and *random access*, refer to Fig. 17.17. Here, signal packets S_1, S_2, \dots, S_k are stored in the input buffers of the concentrator. The access technique determines the strategy by which the stored packets are outputted through the output buffer B_o . In a *polling* technique each of the input buffers are interrogated, in order, to determine if a packet is present. If a packet is present in, say, buffer B_i it is forwarded to B_o and then the next buffer, B_{i+1} , is interrogated, etc. This technique is often used when packets are present on a regular basis. If packets

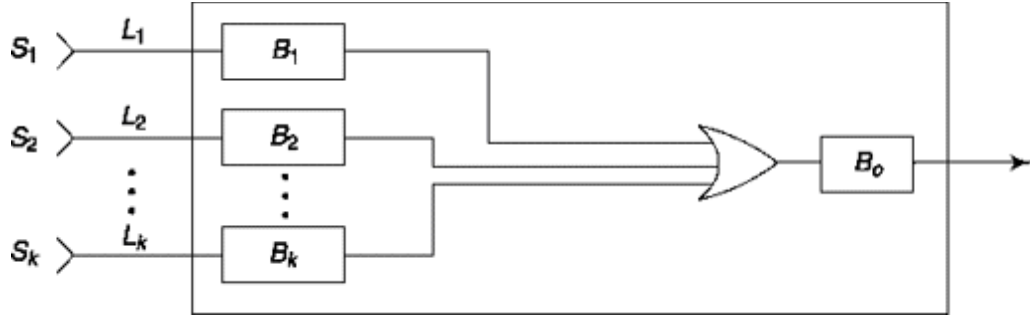


Fig. 17.17 Concentrator (multiplexer) access.

occur only rarely on any of the input links, so that a single packet may be stored in only one of the input buffers, but the probability is very small of more than one packet being stored simultaneously in the concentrator's buffers, then *random access* can be employed to speed throughput through the concentrator. In a random access technique, any packet in any input buffer moves directly to the output buffer. It does *not* wait. One way to avoid a collision between a packet entering \$B_o\$ from say, \$B_t\$ and a packet which might be just leaving \$B_j\$ is to disable each buffer once a packet starts to enter \$B_o\$. This type of monitoring and control is often done using a microcomputer which is a part of the concentrator.

17.2.3 Network protocols

In order for a network to accommodate a number of users efficiently, routing and flow control procedures are to be established and all users of the network must follow these procedures. To reduce the system design complexity, these rules, called *protocols*, are divided into approximately seven areas called *layers* or levels. The set of layers is called the *network architecture*. A brief description of these layers is presented next.

physical layer

The first protocol is called the physical layer and is concerned with the actual transmission of data over physical communication channel. Specifically, the physical layer considers how to set-up a connection and once a connection is set-up what bit rate to use to insure that the resulting error is acceptable.

data-link layer

The second layer carries service request from physical layer to next layer and provides functional means to transfer data between two networks. One important task of this layer is error correction. The error control procedure usually employs Automatic Repeat Request. Data-link layer is concerned with communications between the Interface devices (Interface Message Processor or IMP) of transmitting and receiving computer.

Network layer

The third layer's main concern is *routing*, to control congestion in the network and to control congestion at the receiving IMPs. Congestion control deals with the problem that develops when more packets arrive at an IMP than there are buffers to store them. One way to control congestion is to monitor the traffic at each IMP and not allow data to be forwarded to an IMP that does not have adequate buffer space. The X.25 protocol is an international standard for first three layers.

Transport layer

The fourth layer has the responsibility of providing a reliable and efficient end-to-end transport between users rather than between IMPs. The programs that provide the transport service run on host computers and not on IMPs. This layer makes sure that packets are delivered in order, without loss or duplication and also acts as a multiplexer from host to correct user locations. Certain resources of host such as files, mailboxes, terminals, etc., can be addressed using transport layer. Also buffering, ordering, flow control, synchronizations are effected here.

session layer

The fifth layer is used to allow users to identify themselves when wanting access to the network. This also establishes, manages and terminates a session or connection among applications. In some networks there is no session layer. In these cases the session layer's functions are performed by the transport layer.

presentation layer

The sixth layer performs two main functions: *data encryption* and *word compression*. Data encryption ensures that transmitted message is understood only by the intended receiver. This is also called end-to-end encryption where user can select the encryption technique which is different from *data link encryption* done at data-link level by IMPs. Word compression is used to reduce user data flow and techniques called *run-length coding* is used which detects repetitive patterns and replace it by shorter patterns. The other job of this layer is to relieve the highest application layer of concern regarding syntactical differences in data representation.

Application layer

The seventh and final layer is the user's protocol layer. This presents the set of allowed messages, program employed and partitioning of a problem or data in a data base. It also interfaces to and performs common application services for the application processes. Industry specific protocols such as the banking and airlines industries are typical examples.

Note that while the International Standard organization (ISO) have developed protocol standards, called the *Open System Interconnection* or OSI protocols, which were described before, certain organizations may have their own protocol standards which differ slightly with the seven layer ISO-OSI standard.

17.2.4 LAN, MAN, wAN, Internet

A relatively small and inexpensive digital network used to provide an access is called a *local area network* (LAN). LAN's employ coaxial cable, twisted pair and most recently optical fibres. The LAN is usually 1 to 25 km in length and supports up to several thousand users usually within an office, building or a group of buildings. The LAN, such as Xerox's *Ethernet* can be a single loop network as shown in Fig. 17.18. Here, four nodes are connected to a loop network which allows transmis-

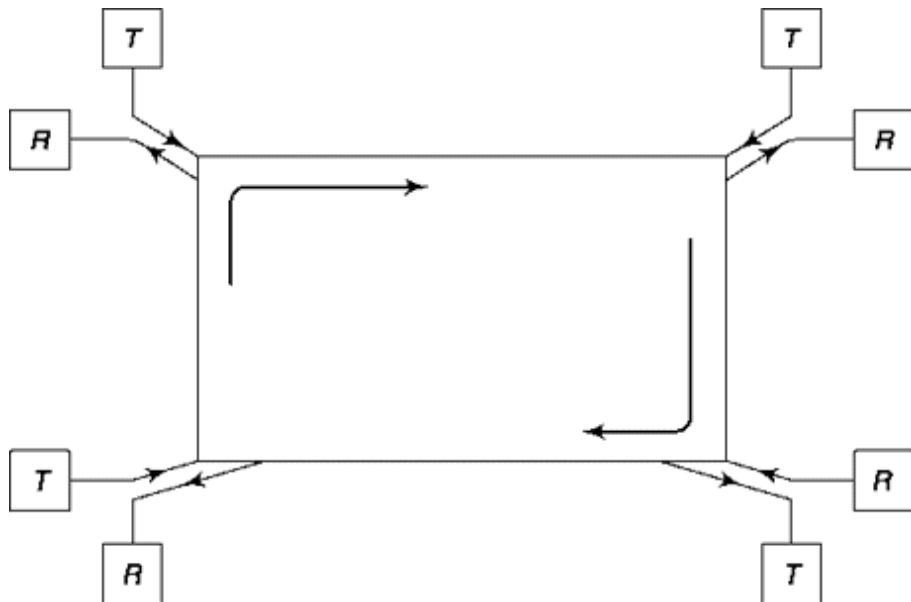


Fig. 17.18 A local area network (LAN).

sion only in clockwise direction. Before transmitting, the user's receiver, shown by receiver box marked R, listens to the channel to see if there are any other transmissions. If no other transmission is sensed, the user transmits. Such a technique is called *carrier sense multiple access* or CSMA. Several versions of *Ethernet* are now available. The popular ones are 10 Mb/s or 100 Mb/s while Gigabit *Ethernet* able to carry up to 10 Gb/s is a relatively new development.

A *metropolitan area network* (MAN) spans a larger geographical area than LAN, ranging from several blocks of buildings to a big city (5-50 km). It is often used as means of interconnecting LANs of an enterprise and usually depends on leased lines. A MAN might be owned and operated by a single organization, but used by many individuals and organizations. MANs might also be owned and operated as public utilities. A MAN usually operates on fibre-optic cables or other digital media providing high-speed connection. The term *wide area network* (WAN) refers to communication link by which an individual computer can communicate with another over a large geographical range like across the state or country. Numerous WANs exist today that include public packet networks, large corporate networks, military networks, banking networks, stock brokerage networks, airline reservation networks, etc. A WAN, like MAN, is not generally owned by a single organization.

The *Internet* is the largest of the WANs covering the globe and is a complex conglomerate of several networks. This is a publicly accessible

network providing large number of useful and popular services such as *E-mail*, *Web browsing*, *File transfer*, *E-Commerce*, *Messaging*, etc. The internet *backbone* to which smaller networks connect to is usually high speed fibre-optic cables laid all over the world by big companies and provide many alternative paths to travel for packetized data. *Internet Protocol* (IP) is used to define the packets for transmission over Internet. This is characterized by five of the seven OSI layers : physical, data-link, network, transport and application. *Transmission Control Protocol* (TCP) is the most used transfer protocol which establishes a virtual connection between transmitting and receiving computers and resends data which is lost. TCP provides flow control, i.e. doesn't overwhelm receiver and congestion control, i.e. slows down sender when network is congested. Applications that use TCP are *HTTP* (Hyper Text Transfer Protocol) for *world wide web*, *FTP* (File Transfer Protocol) for file transfer, *Telnet* for remote log in, *SMTP* (Simple Mail Transfer Protocol) for email services. *User Datagram Protocol* (UDP) is another transfer protocol which is connectionless and does not resend the data that are lost and there is no flow or congestion control. The applications include streaming audio or video, teleconferencing, internet telephony, etc.

17.2.5 IsDN, ATM, DsL, sDH/sONET

Integrated Services Digital Network (ISDN) is a circuit-switched digital interface designed to allow digital transmission of voice and data over ordinary telephone copper wires, resulting in better quality and higher speeds than available with analog systems. This was designed to replace local analog loop of *public switched telephone network* (PSTN). In ISDN, there are generally two types of channels, 'Bearer' also called *B* and 'Delta', popular as *D* channel. *B channels* are used for data that may include voice, and *D channels* are intended for signaling and control but can also be used for data. There is a third type called *H* channel that is used to carry data at higher rate. The ISDN implementations are as follows: (i) Basic rate interface (BRI) or Basic rate access (BRA) consists of two *B* channels, each with bandwidth of 64 kb/s, and one *D* channel with a bandwidth of 16 kb/s, designated as $2B + D$. (ii) Primary rate interface (PRI) or Primary rate access (PRA) has greater number of *B* channels and a *D* channel of bandwidth 64 kb/s. The number of *B* channels in PRI is different in different countries, e.g. in North America and Japan, it is $23B + D$ giving bit rate up to 1.544 Mb/s

(T1 line) and in Europe and Australia it is 30B + D, with an aggregate bit rate of 2.048 Mb/s (E1 line). The H0 channel has higher capacity compared to B and D channel and can transmit data at a rate 384 kb/s suitable for applications like video, digital television etc.

Broadband Integrated Services Digital Network (BISDN) is an ISDN implementation which is developed to manage different types of services at the same time. It is primarily used within network backbones and employs Asynchronous Transfer Mode (ATM). Asynchronous Transfer Mode (ATM) is a cell relay data link layer protocol which encodes data traffic into small 48 bytes of data and 5 bytes of header information, i.e. total 53 bytes, fixed-sized cells. This is used as an alternative to variable sized *packets* (also called *frames*) as in packet-switched networks (such as the Internet Protocol or Ethernet). The idea behind is that the small, constant cell size will allow ATM equipments to transmit video, audio and computer data over the same network, and assure that no single type of data hogs the line. ATM is a connection-oriented technology, in which a virtual connection is established between the two endpoints before the actual data exchange begins. It was designed to implement a low-jitter network interface. There are four kinds of ATM service: (i) Constant Bit Rate (CBR): specifies a fixed bit rate so that data is sent in a steady stream. This is analogous to a leased line. (ii) Variable Bit Rate (VBR): provides a specified throughput capacity but data is not sent evenly. This is a popular choice for voice and videoconferencing data.

(iii) Available Bit Rate (ABR): provides a guaranteed minimum capacity but allows data to be sent as *burst* at higher capacities when the network is free. (iv) Unspecified Bit Rate (UBR): does not guarantee any throughput levels. This is used for applications, such as file transfer, that can tolerate delays.

Digital Subscriber Line (DSL) technology was originally implemented as part of the ISDN specification. DSL or xDSL, is a family of technologies that provide digital data transmission over the wires of a local telephone network. Different variations of DSL (' in xDSL changes) exists such as HDSL where 'H' refers to high data rate, SDSL where 'S' stands for symmetric, ADSL - 'A' for asymmetric, RADSL -RA' for rate adaptive, PDSL - 'P' for powerline, etc. Of these ADSL or *asymmetric digital subscriber line* is very popular providing up to 8Mb/s downstream and 1 Mb/s upstream data rate. The unused high-frequency region in normal

telephone cable (twistedpair) is exploited. The upstream signal uses 25.875-138.8 kHz while downstream signal uses 138-1100 kHz of frequency range which is structured as bins of width 4 kHz. Each bin supports few bits/s (if noisy) to 60 kb/s (if noise free) of data transfer. Note that, normal telephone line provides very high attenuation at higher frequencies. Hence, special amplifiers and frequency compensation techniques are used that takes help of high-speed digital signal processors. Also this limits the distance ADSL can support and it is useful only for short distances, typically less than 5 km.

Synchronous Digital Hierarchy (SDH) or its North American equivalent *Synchronous Optical Network* (SONET) is a standard for connecting fiber-optic transmission systems. This defines a technology for carrying many signals of different capacities through a synchronous, flexible, optical hierarchy. This is accomplished by means of a byte-interleaved multiplexing scheme that can work on data streams of different rates. Byte-interleaving simplifies multiplexing and offers end-to-end network management. SONET uses a concept called pointers to compensate for frequency and phase variations in a dynamic manner which is independent of the content of payload. The data rate supported by the optical carrier (OC) has different levels starting from 51.8 Mb/s or OC-1 to 9.95 Gb/s or OC-192.

17.3 OPTICAL COMMUNICATION

In optical communication, light waves are used for transmission. A light wave is an electromagnetic wave at higher frequency range of the spectrum (3×10^{11} - 3×10^{16} Hz) and can offer a large bandwidth for transmission. Unlike microwaves, the light waves are greatly absorbed by the atmosphere and are not suitable for atmospheric propagation. LASER (Light Amplification by Stimulated Emission of Radiation), if used as a source, can penetrate the atmosphere due to its high intensity and narrowness of the beam; but the requirement that the transmitter and reflector need to be perfectly aligned, maintaining line of sight, limits its use. It has been considered for satellite to satellite communication because it is small, light in weight and can offer high data rate. However, it is vibration causing misalignment, that increases the bit error rate. There have been ground-to-satellite communication experiments too where a satellite was tracked for about 60 percent of the time in good weather conditions.

Light Emitting Diode (LED) based wireless infra-red remote control device and infra-red computer links are useful as short-range communication links. A plastic lens focuses the LED output to obtain a narrow beam. The light is made on-off according to digital binary information which is also known as On-Off Keying (OOK). The communication follows IrDA (Infrared Data Association) Standard. IrDA-Control allows wireless pointing devices like keyboards, mouse, joysticks, etc., to interact with host devices. IrDA-Data defines how two-way infrared data transmission between two devices occurs. LASER based infrared communication also exists but is less popular in comparison.

Optical communication finds wide application when used in guided media. Fiber optic cables are now used to transmit television signals, voice as well as data. We discuss fiber optic communication next.

17.3.1 Optical Communication through Fiber

Among wired communications, optical communication is the most modern with highest capacity. In this, glass is used as a media. Initially, an 800 nm ($1 \text{ nm} = 10^{-9} \text{ m}$) band, also called ‘First Window’ was in use where attenuation was low. As glass purification technology improved, two more windows showing low loss came to use. They are 1300 nm band known as ‘Second Window’ and 1550 nm band called ‘Third Window’; both have approximately 100 nm bandwidth but the latter shows the lowest loss of approximately 0.2 dB/km. In this, frequency bandwidth Df , wavelength bandwidth Dl , wavelength λ , refractive index of the medium m and velocity of light c are related by

$$\Delta f = \frac{c}{\mu} \cdot \frac{\Delta \lambda}{\lambda^2} \quad (17.6)$$

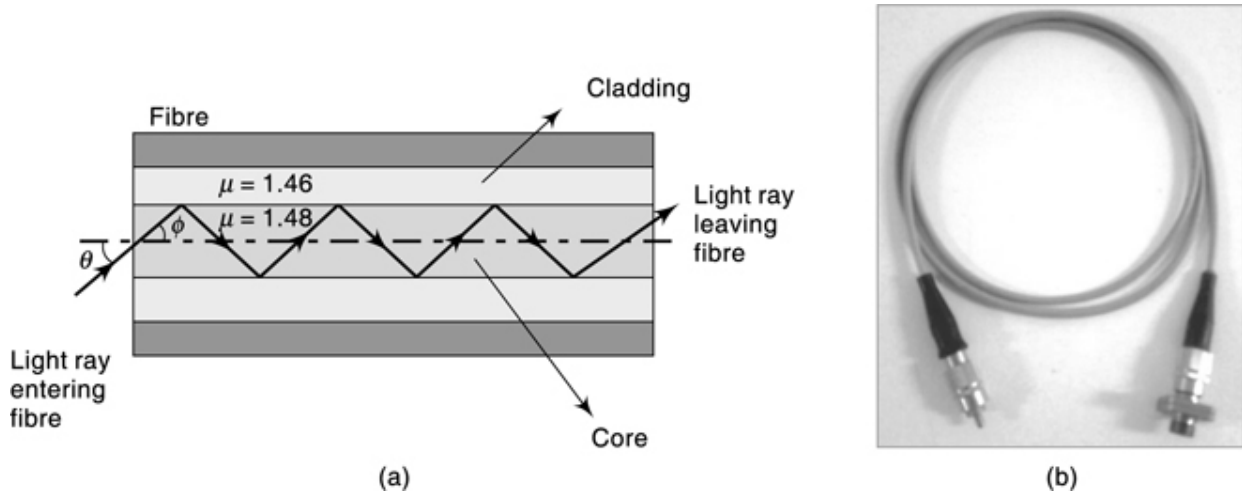
For glass, $m < 1.5$. In the 1550 nm window, substituting we get $Df < 120 \text{ GHz}$. This huge bandwidth capacity makes optical communication through fiber so very useful.

To understand how light propagates through glass, let us use ray model and refer to Fig. 17.19a. Light ray is incident at an angle d and inside glass media the corresponding angle of refraction is f . Glass being optically denser media $d > f$. Inside the fiber, the ray moves along the core of the refractive index m_1 and gets totally reflected against cladding of refractive index m_2 . This type of fiber is known as step index fiber. In graded index fiber, the

refractive index is gradually varied and that gradually bends the light and finally it undergoes total internal reflection when critical angle is exceeded. Critical angle between two media is given by $\sin^{-1} (\mu_2/\mu_1)$. In Fig. 17.19a, the angle ($90 - f$) is the angle of incidence between core and cladding and it must be greater than critical angle to satisfy total internal reflection. If we increase launching angle d then f increases and angle of incidence between core and cladding decreases. This puts a limit on maximum launching angle θ_{\max} which can be calculated as

$$\theta_{\max} = \sin^{-1} (\sqrt{\mu_1^2 - \mu_2^2}) \quad (17.7)$$

Fig. 17.19 (a) Light wave propagation through optical fiber: Ray model (b) An optical fiber cable with connector



Now, the higher the θ_{\max} , the more power can be launched into fiber. *Numerical aperture* of an optical fiber defined by $\sin \theta_{\max}$ is a measure of power-launching efficiency of an optical fiber. Next, consider that a ray is launched at θ_{\max} and the corresponding angle of refraction is ϕ_{\max} . Then this ray travels a distance d/θ_{\max} inside a fiber of length d through total internal reflection. Another ray which is launched at zero angle will travel a distance of d . The velocity of light inside the core is given by c/μ_1 . The time difference between these two rays arriving at the other end gives rise to broadening of the optical pulse and gives rise to *dispersion* and limits rate of data transfer. We can calculate this time difference as

$$\Delta t = \frac{\mu_1 (\mu_1 - \mu_2) d}{\mu_2 c} \quad (17.8)$$

While we want numerical aperture to be as large as possible, i.e. ($m_1 - m_2$) high, it is desirable to have dispersion as minimum as possible that requires ($m_1 - m_2$) to be low. In practice, the difference between refractive indices of core and clad lies within one percent. This gives higher weightage to data rate that can be achieved. For a 1 km long fiber with $m_1 = 1.48$ and $m_2 = 1.46$, we can calculate $\Delta t = 6.73 \times 10^{-8}$ second. Now, bandwidth $Af < 1/\Delta t = 14.85$ MHz. Also from Eq. (17.8), we can write,

$$\Delta f \times d = \text{Constant} \quad (17.9)$$

Dispersion can be reduced in graded index fiber that allows rays that travel more distance to move at higher speed in lower refractive index core before undergoing total internal reflection. This results in lower Δt and increases bandwidth.

17.3.2 Certain issues in Fiber Optic Communication

We have noted that LED and LASER are used as source in the transmitter side. At the receiver-side *photodetector*, a semiconductor-based photodiode converts light into electricity. For long-distance communication to compensate loss, amplification can be done electronically by converting the optical signal to electrical signal and then retransmitting it optically. However, the use of optical domain amplifier is more convenient that does not use electronics. Erbium Doped Fiber Amplifiers (EDFA) has successfully been used in third window (1550 nm). The gain of this amplifier is relatively flat and is independent of data rate.

In fiber optic communication, 10 GHz is considered a high data rate. LED and LASER as a source has a spectral width close to 30 nm (< 3600 GHz) and 2 nm (< 240 GHz) respectively. One can see that message bandwidth is much smaller than carrier. This is quite different from what we have seen earlier where message was much broader. Due to this, for fiber optic communication a message cannot be recovered from spectral domain and demodulation needs to be done in time domain only. Amplitude Modulation or its digital form Amplitude Shift Keying that can use envelope detection is the preferred method.

The attenuation suffered by light signal as it travels through a fiber can be attributed to several reasons: (a) Intrinsic loss or material loss due to impurities like iron, nickel, aluminium, etc., present in the fiber, diffusion of

OH ion that absorbs light and infra-red absorption of glass; (b) Scattering loss due to non-uniform refractive index, known as Rayleigh scattering that is proportional to IT^4 ;

(c) Bending or radiation loss at every bent of the fiber, however small it might be; (d) Micro-bending loss due to surface unevenness that prevents total internal reflection and light leaks out. In addition to all these in power budgeting, one needs to consider losses at connectors. A simple exercise may appear like this. Consider that the transmitter power is -5 dBm. The power required at the receiver is -20 dBm. Loss at each connector is 0.3 dB. Loss at each splice or joint is 0.1 dB. Loss in fiber is 0.5 dB/km. If we keep a contingency of 6 dB then between transmitter and receiver $20 - 5 - 6 = 9$ dB loss can be accommodated. If 10 connectors and 10 splices are used then there is a loss of $10 \times 0.3 + 20 \times 0.1 = 5$ dB. That leaves with $9 - 5 = 4$ dB. Thus, $4/0.5 = 8$ km long fiber can be used for communication.

17.3.3 wavelength division Multiplexing

The aim of Wavelength Division Multiplexing (WDM) in fiber optic communication is to multiplex more than one signal and send them together. In SONET or SDH network, introduced in Section 17.2.6, data is sent through optical fiber using Time Domain Multiplexing (TDM). In WDM, multiple optical TDM data streams are sent along different wavelengths through the same fiber. This helps in increasing capacity of the existing fiber and avoids laying of a new fiber. To transmit data at a rate up to 40 Gbps (Gigabit per second) over a 600 km distance, a fiber optic communication system without WDM may require 16 pairs of fibers and approximately 270 regenerators (optical-electrical-optical). With WDM, the requirement can reduce to a single fiber pair and 4 amplifiers.

In early version of WDM, two channels—one at 1310 nm and the other at 1550 nm—were used that doubled the capacity of a fiber. This improved to 20 nm spacing in ITU G.694.2 standard that places 18 channels in between 1271 nm and 1611 nm. This is known as Coarse WDM (CWDM) in which total source wavelength variation is accounted in two-third of the 20 nm and the rest is guard band. This wider variation allows cheaper LASER source to be used that does not require cooling. CWDM is used for distances up to 50 km in metro network connection with data rates up to 2.5 Gbps. Each of the CWDM channel in a fiber can have a different bit rate.

Note that WDM is equivalent to Frequency Domain Multiplexing (FDM) in optical domain. Dense WDM (DWDM) derives its name from denser spacing of channels. In ITU Grid-C Band, they are spaced 0.77 nm (100 GHz) apart with 72 channels in between 1520.25 nm to 1577.03 nm. There is 50 GHz DWDM that accommodates up to 128 channels. Technologies that are 25 GHz spaced are called Ultra DWDM. DWDM is useful for long-haul networks covering thousands of kilometres with amplification and regeneration en route. It requires a stable LASER source with very small drift, more size, more equipment cost and power requirement but of much higher capacity than CWDM. The capacity for DWDM is up to 10 Gbps per channel.

Before we end our discussion on optical communication, we note the following. Besides higher bandwidth, fibre optic communication offers advantages compared to copper wire like (i) less susceptibility to degradation, (ii) light signals from one fiber do not interfere with light signals in another fiber, (iii) it provides electrical isolation and is immune to electromagnetic interference,

(iv) unaffected by lightning, (v) low power, (vi) less weight, (vii) difficult to tap making it more secure, etc. One major disadvantage is that its termination is complex and requires special tools.

SELF-TEST QUESTION

6. In a packet-switched network, the message packets can follow different routes to arrive at the destination. Is the statement correct?
7. Which of the seven OSI layers does a routing job?
8. In Internet application, which of TCP and UDP protocol is more reliable?
9. Does ADSL offer more data rate for download than upload?
10. Which among ‘noise’ and ‘pulse’ spreads due to dispersion limits the data rate in optical communication through a fiber?

17.4 MOBILE TELEPHONE COMMUNICATION— THE CELLULAR CONCEPT

In cellular mobile communication, *cellular radio network* concept is used that divides each geographical area into small regions called *cells*. Within a

cell all communications are performed using a given bandwidth. Refer to cellular layout shown in Fig. 17.20(a). Generally, the concept used is as follows. Let, in cell A centre frequency f_A is used, in cell B centre frequency f_B is used, etc. If two cells are widely separated, such that a receiving antenna in one cell cannot detect the signal transmitted from the other cell, both cells can be allocated same frequency. In Fig. 17.20a, each pair of cells A_1 and A_2 , B_1 and B_2 , C_1 and C_2 , etc., can use same frequency. This technique, which is designed to conserve frequency spectrum, is called *frequency reuse*. A *cluster* is a group of cells within which no frequency is reused. The bandwidth allocated to each cell is divided into N channels. Thus, if the bandwidth of a cell is B_c , the bandwidth allocated to each user is $B_u = B_c/N$. In Bell System's analog *Advanced Mobile Phone Service* (AMPS) system of 1980's, communication was by frequency modulation and each user's channel was allocated a bandwidth was $B_u = 30$ kHz. Peak frequency deviation was 12 kHz and modulating signal bandwidth was 3 kHz. The total spectrum allocation per cell was 40 MHz so that $4000/(2 \times 30) = 666$ full-duplex (each user can talk and listen simultaneously and hence a factor of 2 in denominator) can be provided in a cell. If more than 666 users need to be accommodated, *cell splitting* is employed where a cell is split into several cells, each with different frequency. Note that, power level needs to be reduced accordingly to reduce the footprint of a spectrum and facilitate frequency reuse. When a mobile phone moves from one cell to another while in use, the conversation is to be *handed off* to the next cell for an uninterrupted service. This is done when the mobile unit starts receiving stronger signal from the cell it is heading to.

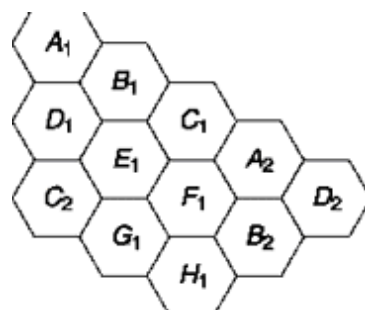


Fig. 17.20(a) A cellular layout.

The components of a cellular system (Fig. 17.21) are as follows. Each mobile *base station* has a cell site *antenna* which transmits to or receives signal from *mobile subscriber unit* (MSU). The *mobile telephone switching*

office (MTSO) is the central office for mobile switching. Through network interface, it can connect to wire line exchanges like public switched telephone network. The MSUs can be of different types based on their applications and transmitted power, e.g. a transportable vehicle mounted unit can typically transmit 3.0 W of power while a mobile handheld unit only 0.5 W. The MSU consists of a transceiver with automatic power control circuit, a PLL based frequency synthesizer and a control unit.

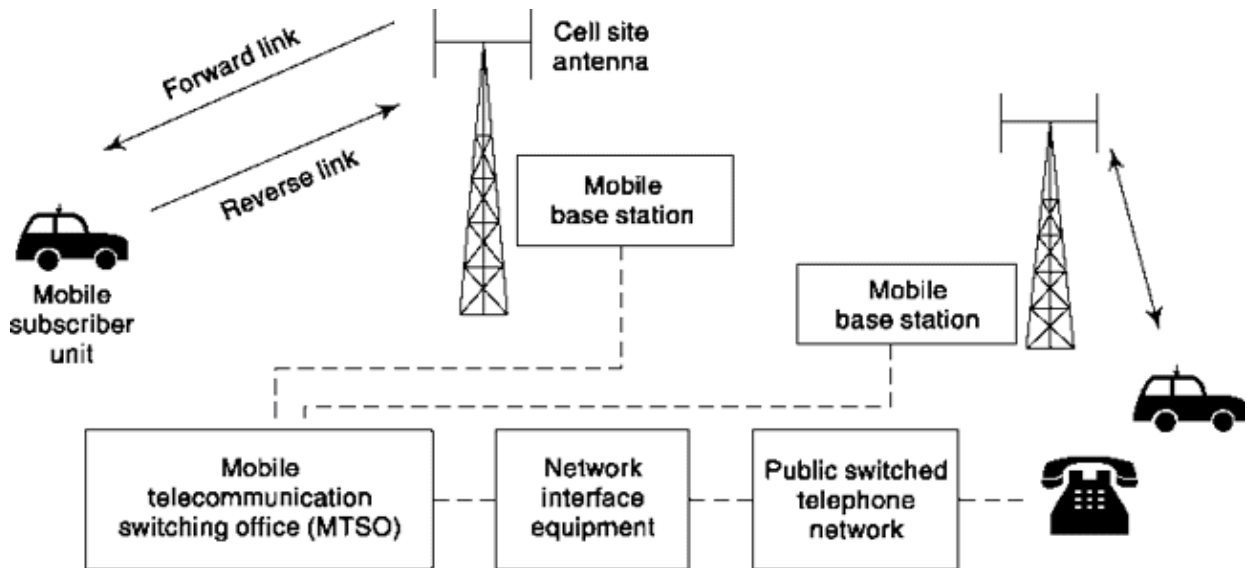


Fig. 17.21 Components of a mobile communication system.

17.4.1 Call set-up in Mobile Communication

There are three different call set-up requirements in mobile communication—mobile to mobile, mobile to fixed and fixed to mobile calls. We briefly describe how it is done taking example of AMPS system cited before.

Mobile-to-Mobile Calls

When a mobile subscriber wants to place a call, the mobile unit first inquires as to the availability of a channel and its center frequency. There are 21 special, *set-up* channels, not intended for communications, but intended instead to determine which center frequency is available. After the appropriate center frequency is determined, the unit then sends a data message containing the user's identification and the number to be called. The bit rate of this message is 10 kb/s. A (63,51) BCH error correcting code

is used and the message is repeated 5 times with majority-rule logic employed to minimize errors in signal amplitude fluctuation (called *fading*) which may occur when tall office buildings are present.

The cell site transmits this data message to a “MTSO” as shown in Fig. 17.22. The MTSO analyzes the identification to insure that it is proper and then analyzes the called number to see if it refers to a mobile or fixed subscriber. If the call is to a mobile unit the MTSO initiates a *paging* process by sending a data message containing the called number to each cell site. Each mobile subscriber’s

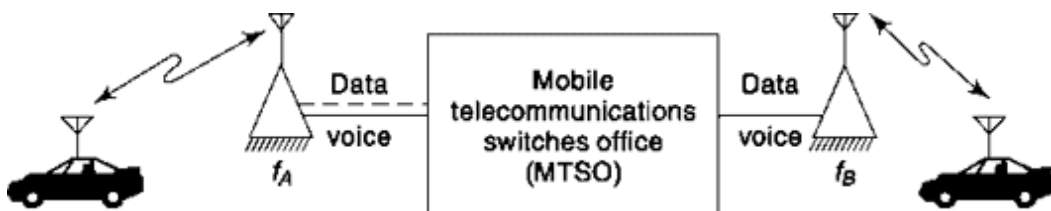


Fig. 17.22 Mobile-to-mobile call.

unit scans, once each minute the set-up channels in the cell in which it is located. The unit, sensing the data message indicating it is being called, responds to the cell site in which the unit is located and then the cell site responds to the MTSO. The MTSO then provides the caller’s cell and the called unit’s cell with voice line connections and the connection is completed and the conversation can begin. When the conversation is terminated and *either* user “hangs-up” the MTSO releases both voice lines.

Mobile-to-Fixed subscriber Calls

When a mobile subscriber calls a fixed subscriber, the cell enters the MTSO as above. Now, however, the MTSO recognizes the number called as being “fixed.” The call is then routed to a class 5 switching office where it is forwarded to its destination. This situation is depicted in Fig. 17.23.

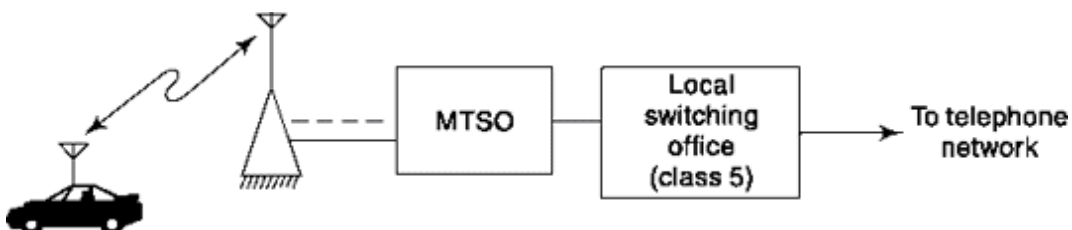


Fig. 17.23 Mobile-to-fixed call.

Fixed-to-Mobile subscriber Calls

When a fixed subscriber calls a mobile subscriber, the call is routed to the appropriate toll office as determined by the area code of the called number. The number dialled indicates that a mobile subscriber is being called and the toll office routes the call to the local office and MTSO. The MTSO then pages the called subscriber as described above and connection is finally completed.

17.4.2 Digital Cellular phone systems: TDMA/GsM, CDMA/cdmaOne

The analog cellular system can handle only limited number of users within a cell and increasing number of cells increases cost. Time Division Multiple Access (TDMA) gives each call a separate time slot so that one bandwidth is time shared by several calls. DAMPS is a digital TDMA architecture on existing AMPS system used in North America and uses same frequency band and channel allocation as AMPS but with 3 to 6 times increased capacity. Extended TDMA (ETDMA) allows up to 15 times more capacity than analog system by efficiently compressing the quiet time in a conversation and providing more number of slots.

The Global System for Mobile communication (GSM), formerly known as Groupe Speciale Mobile is the most widely used mobile communication system in today's world. GSM uses 890-915 MHz frequency range for uplink and 935-960 MHz for downlink. Each of 25 MHz frequency range is divided into 124 carrier frequencies spaced 200 kHz apart. Further to this frequency division TDMA is employed to allow 8 users in each channel by dividing it into time slots. Each time slot is approx. 0.577 millisecond wide and each frame approx. $8 \times 0.577 = 4.615$ millisecond long. The voice is sent digitized (PCM followed by RPE-LPC speech coder) in GSM with basic bit rate of 13 kb/s. The modulation used is MSK (minimum shift keying) with a Gaussian response filter that reduces the bandwidth of the signal to be sent. This is also known as Gaussian MSK (GMSK). Besides telephony GSM offers *short message services* (SMS). The digital nature of GSM allows data, both synchronous and asynchronous, to be transported as a bearer service to or from an ISDN terminal. The data rates supported by GSM are 300 bps, 600 bps, 1200 bps, 2400 bps and 9600 bps. GSM technology is also used in other frequencies like 800, 1800, 1900 MHz etc. The range is typically limited to 35 kilometers due to timing requirements.

In cellular communication user space ‘CDMA’ is a popular term for CDMA based cdmaOne or IS-95 standard. In the previous chapter, we have seen how CDMA uses spread spectrum method with related advantages. In 1990s, a commercial adaptation of CDMA based cellular communication system started. The immediate advantage was increase in number of users in a particular cell. Here, all users use the whole of 1.25 MHz spectrum of a cell but a different pseudorandom code is used for different user to separate his piece of information. Theoretically, one can increase capacity just by providing more number of pseudorandom codes. Practically, it is limited by the amount of interference which include background noise as well as interference from other user’s signal. Ideally, the cell site requires same receiving power from all the users and hence a power control bit is introduced in the communication by which the cell site can increase or reduce the power of mobile unit. Cell site to mobile unit power is controlled by reducing it in steps till the reception error falls below a threshold. The CDMA based system thus as a whole requires to work in as low power level as possible but have higher cell size due to higher capacity. Unlike analog or digital TDMA based system, CDMA based system doesn’t change the frequency moving from one cell to another; the pseudorandom code is transferred from one base station to another and thereby a soft-handover occurs, i.e. communication doesn’t stop even for a small amount of time. Here, certain type of CELP coding is used for voice transmission.

Note that, cellular systems are often divided across generations. First generation or 1G refers to analog system, 2G refers to digital TDMA based GSM or CDMA based cdmaOne system, 3G refers to a faster version of digital system that is capable of applications like video transmission that requires high bit rate. The GSM system for 3G is evolving to W-CDMA or wideband CDMA which replaces TDMA as air interface for radio frequency part of the circuit between mobile unit and active base station. For 3G, cdmaOne, protocol is upgraded to CDMA2000EV. There have been intermediate developments (data rate) between 2G and 3G e.g. 2.5 G like General Packet Radio Service (GPRS) in GSM world and CDMA2001xRTT as upgradation of cdmaOne.

SELF-TEST QUESTION

11. Does cell splitting in cellular communication network require lowering of power for frequency reuse?

12. Does GSM system use both FDMA and TDMA?
13. What does 2G stand for in cellular communication?

17.5 SATELLITE COMMUNICATION

In Chapter 15, we have discussed satellite to earth communication as a case study in communication system noise calculation. We discussed various antenna related issues like directivity, gain etc. there. In this section, we discuss satellite communication in more general terms. Communication satellites are artificial satellites which orbit the earth with different velocities according to their altitudes. The velocity should be such that centripetal force exactly counterbalances gravitational pull of earth. Refer to Fig. 17.24a. Low Earth Orbit (LEO) satellites are at about 500-1500 km above earth's surface and circle the earth once in approximately 90 minutes. Because of this they are available over a geographical region to communicate earth stations (Fig. 17.24b) for a short period of time (15-20 minutes). Also due to their low height, coverage area is less. The atmospheric drag causes orbit deterioration. Of course, cost-wise they are the cheapest, provides high signal strength and less roundtrip delay of signal. These are useful for remote sensing operations and certain types of discontinuous communications. Iridium is an effort to provide continuous communication with LEO satellites that has a constellation of 66 satellites. These satellites can communicate with each other and cover the entire earth.

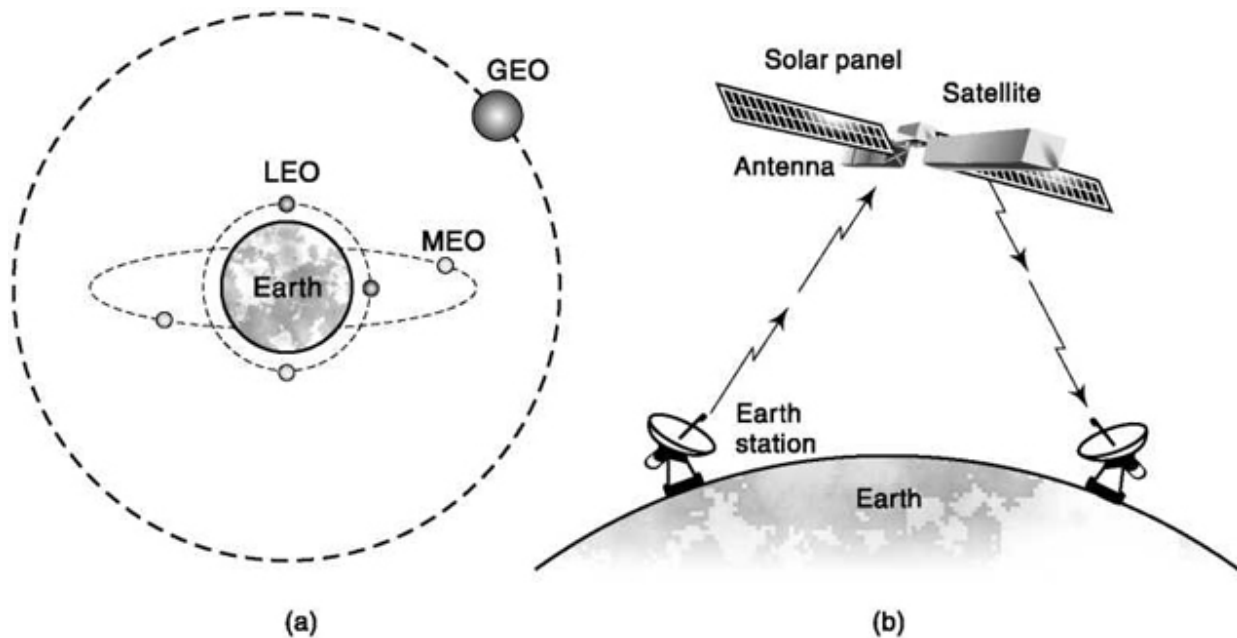


Fig. 17.24 (a) Different communication satellite orbit, (b) A satellite communication system.

Medium Earth Orbit (MEO) satellites are at 8000-18000 km distance from earth's surface. These are functionally similar to LEO with higher distance related advantages and disadvantages. Among advantages it has higher coverage area, more visibility time while disadvantages are more launching cost, more power requirement, more delay, etc. Geo-stationary Earth Orbit (GEO) satellites are functionally different as they are at a height of 35863 km above the earth's surface where its angular velocity exactly matches that of earth so that it appears stationary. This makes these satellites always available at a particular position relative to earth and provides 24 hour view. Also the earth station does not need to track these satellites as in case of LEO and MEO. The higher altitude gives more footprint and three GEO satellites can cover the entire earth except polar region. These are very useful for broadcasting and different multipoint applications. Here, the launching cost and delay are high, also the signal strength is weaker because of increased distance.

Satellites receive power from solar panels but during eclipse (when earth comes between the sun and satellite) it uses storage cells. Alignment of solar panels and the antenna is an important exercise. The satellite is made stable in the orbit by various means like eddy-current, reaction wheel, gyroscopic stabilization etc. Besides circular orbit, there could be elliptical orbits too, e.g. Molniya orbit satellites used by Russia and they can cover polar region.

17.5.1 Communication Between satellite and Earth station

The communication via satellite between earth stations occurs at microwave frequencies where satellites act like a repeater. As we have noted, antenna size depends on frequency, the higher it is the lower the size of antenna. The electronic signal processing if does not support such a high frequency then it needs to be down-converted, processed and then up-converted before relaying. Frequency used to carry message from earth station to satellite is called uplink frequency which is higher than downlink frequency that carries information from satellite to the earth. The other important consideration in choice of frequency is atmospheric absorption which is higher for frequencies greater than 10 GHz. Also resonances of O₂, H₂O molecules cause very high attenuation over certain frequency ranges. Rain, fog, too have a negative effect in this context. Of the various frequency

bands used for satellite communication C band is very popular and Ku band is finding increasing use.

Schematic of a C band satellite transponder is shown in Fig. 17.25. The uplink frequency is taken as 6 GHz (typical). Following Receiver (Rx) antenna, there is a relatively wideband Band Pass Filter (BPF). The signal is amplified by a Low Noise Amplifier (LNA) and down converted by Down Converter (DC) from 6 GHz to 4 GHz, the downlink frequency. At this stage, error correction and amplifications are also done. Frequency demultiplexer divides the signal into different frequency band, the phase error of which is rectified by equalizer. Frequency division is necessary as no single High Power Amplifier (HPA) that amplifies the signal for transmission to earth can give adequate linearity. BPF after HPA removes out of band noise, Transmission (Tx) antenna sends combined signal. In 12 channel C band transponder the input is wideband 500 MHz and each of 12 channels is 36 MHz wide with 4 MHz guard band in between.

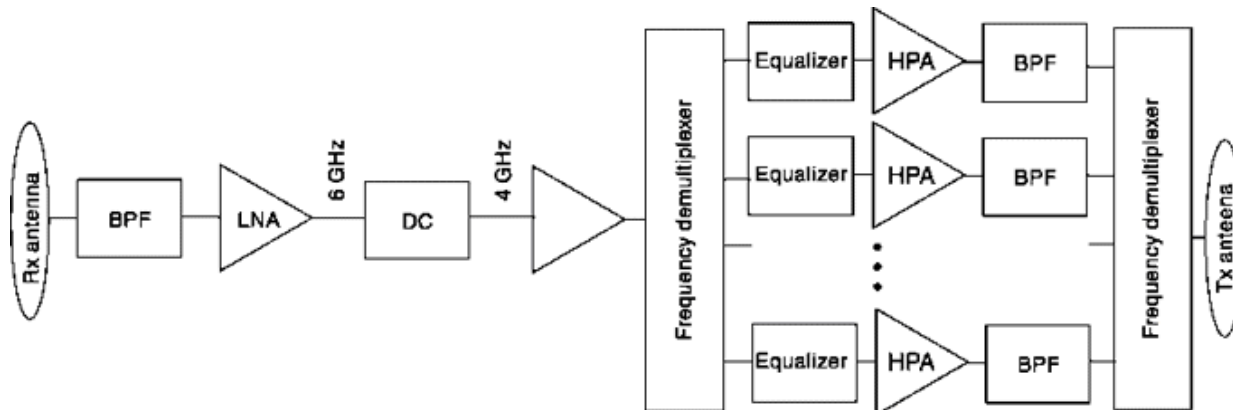
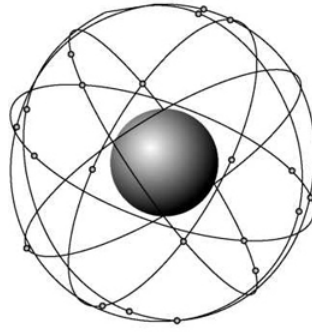


Fig. 17.25 Schematic of a C Band satellite transponder. BPF: Band Pass Filter, LNA: Low Noise Amplifier, DC: Down Converter, HPA : High Power Amplifier.

For Ku band transmission the uplink and downlink frequencies typically are 14 GHz and 11 GHz respectively. There the DC after LNA converts 14 GHz signal to 1 GHz for ease of processing. And Up Converter (UC) between Equalizer and HPA up-scales 1 GHz signal to 11 GHz. Note that, a satellite can communicate to other satellite by microwave, optical laser etc. Besides FDMA, both TDMA and CDMA can be used in satellite communication.

17.5.2 Global positioning system (Gps)

Global Positioning System (GPS) is an important satellite based navigational aid system. GPS receiver receives information from a constellation of 24 satellites (Fig. 17.26a) revolving in 6 orbits (4 in each orbit). This is an outcome of a US Defence project where military use enjoys better position



(a)



Fig. 17.26 (a) GPS satellite constellation, (b) Car navigation using GPS.

resolution compared to civilian applications. The satellites are placed at a height of 20200 km from earth's surface, equipped with very accurate atomic clocks (100000 years to lose 1 second while Quartz crystals loses 1 second in 2 years) and mechanism by which their precise position in the orbit at any instant is known. Few ground stations can communicate with them and send a correction message, if required. To keep the cost down GPS receivers have less precise clock which usually have some offset with the reference atomic clocks. The receiver at any time receives time and position information from four satellites which at any time can be found over any region. These information are used to find three position (x , y , z) coordinates and time offset. The time to travel from satellite to the receiver by the electromagnetic wave is converted to distance. The time offset when included in the equation removes time synchronization related error. In fact, if synchronization was perfect, information from three satellites would have been sufficient to calculate the position as solution to them gives two values one of which is absurd, the other only acceptable.

GPS uses spread spectrum modulation and thus each satellite can use the same frequency without interfering with other. This also prevents unauthorized access and requires less power for its operation. We have noted in previous chapter that spread spectrum technique requires a pseudorandom signal and this is sent by satellite. The same pseudorandom sequence is generated at the GPS receiver and is correlated with the one available from satellite. This helps to measure the delay resulting from amount of travel. Two frequencies are used as carrier of which only one 1.57542 GHz (also called L1) is given to civilian use and gives a position resolution (standard deviation) of about 10m. This is known as Standard Positioning System (SPS). When the other frequency 1.2276 GHz (L2) is also used then error due to atmospheric variations are minimized and resolution is 1m. This is called Precision Positioning System (PPS) and is used by military. Besides this dual tone frequency method, resolution can be improved by using a static object of known position reference. This is called Differential GPS (DGPS) where the reference object periodically sends its location information to nearby satellites. This helps the satellites to understand atmospheric condition through which the signal is traveling. Accordingly correction is made to transmit information to different GPS receivers in that area considering signal travels the same atmosphere and undergoes similar deterioration. The third technique which can give accuracy at centimeter level, millimeter under special cases, uses carrier phase information in an intelligent way.

GPS is now used by ship, aeroplane, car and other moving vehicles as navigational aid. Fig. 17.26b shows a car navigation device where the software uses GPS information and tells the driver his present location and the street ahead. Other applications include tracking delivery vehicles, surveying and geological studies, localization in expeditions, getting accurate time information, estimating velocity etc.

SELF-TEST QUESTION

14. Do GEO satellites require continuous tracking?
15. In satellite communication, which of uplink and downlink frequency is higher?
16. Does a GPS receiver need to communicate with 4 satellites?
17. Is GPS communication spread spectrum modulated?

FACTS AND FIGURES

The concept of packet switching, which is at the heart of computer communication or Internet, was the outcome of a US Defence sponsored research project, DARPA, abbreviation of Defense Advanced Research Projects Agency. DARPA started in 1958 with a mission to prevent technological surprises like launch of Sputnik by Soviet Russia. The first computer network ARPANET, a DARPA initiative, came alive in 1969 with four nodes situated at University of California, Los Angeles; Stanford Research Institute; University of California, Santa Barbara, and University of Utah. The first text sent over the ARPANET was 'lo', the attempt was to send 'login' but the system crashed after first two letters were sent. However, it recovered after an hour and the full text was sent.

Theodore Harold Maiman of Los Angeles, California, took jobs of repairing electrical appliances and radios to support his college study. A B.S. from University of Colorado, he got his M.S. and Ph.D from Stanford University. Maiman is credited as the one who showed first operational LASER on May 16, 1960 in Hughes Research Laboratories. Earlier Einstein gave the theoretical foundation of LASER, Ladenberg showed existence of stimulated emission, Kastler proposed method of optical pumping. Later in 1966, the work of Kao and Hockam showed how a clad glass fiber can be used for communication, and optical communication became a part of reality.

SUMMARY

Different useful application areas under modern electronic communication are presented in brief. In telephone switching, the benefit of central switching is discussed followed by function of a simple exchange and hierarchy of switching offices. The idea of space-time switching and time slot interchanging is introduced and their usefulness discussed. In computer communication, it is described how computers are connected with each other by different types of networks. Network protocols are discussed and concept of LAN, MAN, WAN, Internet introduced. This also discusses digital interfaces like ISDN, ADSL, ATM, SDH or SONET. Basic concepts behind optical communication through fibre optic cables which provides huge bandwidth are presented. In satellite communication, various orbital paths are compared and role of LEO, MEO, GEO satellites discussed. Working of

a C band satellite transponder is cited as an illustration of how satellite communicates to earth. Global Position System (GPS), a modern satellite based navigational aid is described.

PROBLEMS

17.1 The current i_R in the receiver of station B of Fig. 17.1 is

$$i_R = I \frac{R_t}{R_r + R_t}$$

where I is the dc current flowing in the battery, R_t is the variable, voice sensitive resistance of the transmitting microphone and R_r is the receiver impedance.

- (a) Explain why I is approximately constant.
- (b) Why should $R_t \neq R_r$?

17.2 23 ma is required for the carbon transmitter. A 50 V battery with a 400 W short-circuit protection resistance is employed with 26 gauge wire. Neglecting the resistance of the transmitter, calculate the loop distance. *Hint:* Consult a handbook to determine the resistance of 26 gauge wire.

17.3 Explain why it is necessary that in the absence of voice-generated signal current, the diaphragm of a telephone receiver must be displaced from its unstressed position either by a quiescent current or by the presence of a permanent magnet.

17.4 Show that if in Fig. 17.2 there are N stations, there are (a) $N(N - 1)$ switches and (b) $N(N - 1)/2$ interconnections.

17.5 Show that with a central exchange system as in Fig. 17.3 there are (a) $N(N - 1)/2$ switches and N interconnections.

17.6 The system shown in Fig. 17.11 is to be employed. There are 24 subscriber lines which are to be capable of connection with a different set of 24 subscribers.

- (a) How many simultaneous connections can occur?
- (b) What is the duration t that each connection can persist?
- (c) What is the capacity of the R/W memory?
- (d) What is the clock rate?

17.7 A 1000 line, 1000 trunk digital switch is to be built using TSI. Using 8-bit PCM specify

- (a) the size of each memory needed,
- (b) the speed at which the data must be accessed.

17.8 An 8192-bit message is to be transmitted, using message switching over an 8-link path to its destination. After each link there is a switching mode in which a minicomputer stores the message in a buffer and then forwards the message as soon as the message reaches the front of the buffer. The message contains 256 bits used for “overhead.”

Assume that there is no queue in any of the 8 buffers so that as soon as a message is received, the overhead bits are processed and the message is forwarded. Neglect this processing time and the propagation time in a link.

If the bit rate is $f_b = 1 \text{ Mb/s}$ calculate the time for the message to be transmitted from the source to the user.

17.9 If a link is 25 km long, calculate the time required for an 8192 bit message, transmitted at 1 Mb/s to be completely received at the switching mode following the link. Assume the velocity of propagation is $3 \times 10^8 \text{ m/s}$.

17.10 If in Prob. 17.8, propagation delay is not neglected, then calculate the time for the message to be transmitted from source to user if the distance separating switching nodes is 25 km and the velocity of propagation is $3 \times 10^8 \text{ m/s}$.

17.11 A 7936-bit message is to be transmitted over an 8-link path to its destination. Packet switching is to be used and the overhead/packet is 256 bits.

Neglect the processing time and the propagation time. If the bit rate is $f_b = 1 \text{ Mb/s}$

- (a) Calculate the number of packets that the message should be divided into if the time from transmission to reception is to be minimized.
- (b) Calculate this minimum time.
- (c) Compare it to the result obtained for message switching. Which moves more quickly? Why?

17.12 A computer network is shown in Fig. 17.16. Assume the time to travel over any link is T . Flooding is used to transmit a message from A to L . Plot

the number of times the same message reaches L as a function of time, for integral values of T . If the same message arrives at any node i from two different nodes j and k simultaneously, a collision occurs and one can assume that the message never reached node i . Assume that the message was transmitted from A only one time.

17.13 A shortest route is to be selected to transmit a message from A to L . Find the route.

17.14 Random walk is to be used to transmit a message from A to L . For example, the message leaving node A could go to B , E or J , each with probability $1/3$. If the system is designed to avoid returning to a past node, e.g. once at J the packet could go to H , I or L with probability $1/3$, but not return to node A , calculate the probability of a message sent once from node A , reaching node L , as a function of time for integral values of T .

17.15 Signal packets S_1, S_2, \dots, S_{10} enter a concentrator located at node R where they are multiplexed. Packets arrive independently, each with a Poisson density, at the average rate of 1 packet/s, and the time to transmit a packet is 1 ms. What is the probability of two or more packets being in the queue simultaneously?

17.16 Find numerical aperture and maximum launching angle of single step optical fiber with referactive indices of core and cladding 1.48 and 1.46 respectively. How does it change if cladding refractive index is reduced to 1.2?

17.17 Calculate dispersion in two cases defined in Prob. 17.16 for a 10 km long optical fiber. Hence, calculate available bandwidth for both the cases.

17.18 Consider an optical fiber requires one connector and two splices per km when laid in a particular terrain. The losses are 0.4 dB/km along the fiber, 0.1 dB splice and 0.3 dB/connector. If transmitter power is -5 dBm and power required at receiver is -1.8 dBm find the length of fiber that can be used for communication with appropriate power budgeting.

REFERENCES

1. Bellamy, J. *Digital Telephony*, chap. 5; John Wiley and Sons, New York, 1982.

2. Martin, J. *Telecommunications and the Computer*, 2d ed., *Part III: Switching*; Prentice Hall Inc., Englewood Cliffs, N.J., 1976.
3. McDonald, J. C., ed., *Fundamentals of Digital Switching*; Plenum Press, New York, 1983.
4. Hamsher, D. H., ed., *Communication System Engineering Handbook*, chap. 7; McGraw-Hill, New York, 1967.
5. Talley, D., *Basic Electronic Switching for Telephone Systems*; Hayden Book Co., Rochelle Park, N.J., 1975.
6. Fleming, P. Jr, "Principles of Switching," vol. 10, *Lee's abc of the Telephone*; Geneva III, 1979.
7. Flowers, T. H., *Introduction to Exchange Systems*, John Wiley and Sons, New York, 1976.
8. Pearce, J. G., *Telecommunications Switching*, Plenum Press, New York, 1981.
9. Bell Telephone Laboratories, *Engineering and Operations in the Bell System*, 1980, Chap. 9.
10. Joel, Amos E. Jr., ed., *Electronic Switching: Digital Central Office Systems of the World*; IEEE Press, 1981.
11. *Bell System Technical Journal*, January 1979, vol. 58, No. 1.

APPENDIX A

Table A1 ASCII code

Bit Position				7	0	0	0	0	1	1	1	1
4	3	2	1	5	0	1	0	1	0	1	0	1
0	0	0	0	NUL	DLE	SP	0	:a	p	\	p	
0	0	0	1	SOH	DC1	!	1	A	Q	a	q	
0	0	1	0	STX	DC2	"	2	B	R	b	r	
0	0	1	1	ETX	DC3	#	3	C	S	c	s	
0	1	0	0	EOT	DC4	\$	4	D	T	d	t	
0	1	0	1	ENQ	NAK	%	5	E	U	e	u	
0	1	1	0	ACK	SYN	&	6	F	V	f	v	
0	1	1	1	BEL	ETB	'	7	G	W	g	w	
1	0	0	0	BS	CAN	(8	H	X	h	x	
1	0	0	1	IIT	EM)	9	I	Y	i	y	
1	0	1	0	LF	SUB	*	:	J	Z	j	z	
1	0	1	1	VT	ESC	+	:	K	[k	{	
1	1	0	0	FF	FS	'	<	L	\	l	:	
1	1	0	1	CR	GS	-	=	M]	m	}	
1	1	1	0	SO	RS	,	>	N	^	n	~	
1	1	1	1	SI	US	/	?	O	—	0	DEL	

Table A2 The error function

u	$erf(u)$	u	$erf(u)$
0.00	0.00000	1.10	0.88021
0.05	0.05637	1.15	0.89612
0.10	0.11246	1.20	0.91031
0.15	0.16800	1.25	0.92290
0.20	0.22270	1.30	0.93401
0.25	0.27633	1.35	0.94376
0.30	0.32863	1.40	0.95229
0.35	0.37938	1.45	0.95970
0.40	0.42839	1.50	0.96611
0.45	0.47548	1.55	0.97162
0.50	0.52050	1.60	0.97635
0.55	0.56332	1.65	0.98038
0.60	0.60386	1.70	0.98379
0.65	0.64203	1.75	0.98667
0.70	0.67780	1.80	0.98909
0.75	0.71116	1.85	0.99111
0.80	0.74210	1.90	0.99279
0.85	0.77067	1.95	0.99418
0.90	0.79691	2.00	0.99532
0.95	0.82089	2.50	0.99959
1.00	0.84270	3.00	0.99998
1.05	0.86244	3.30	0.999998

Table A3 Value of Bessel functions

$n \backslash \beta$	1	2	3	4	5	6	7	8	9	10
0	0.7652	0.2239	-0.2601	-0.3971	-0.1776	0.1506	0.3001	0.1717	-0.09033	-0.2459
1	0.4401	0.5767	0.3391	-0.06604	-0.3276	-0.2767	-0.004683	0.2346	0.2453	0.04347
2	<u>0.1149</u>	0.3528	0.4861	0.3641	0.04657	-0.2429	-0.3014	-0.1130	0.1448	0.2546
3	0.01956	<u>0.1282</u>	0.3091	0.4302	0.3648	0.1148	-0.1676	-0.2911	-0.1809	0.05838
4	0.002477	0.03400	<u>0.1320</u>	0.2811	0.3912	0.3576	0.1578	-0.1054	-0.2655	-0.2196
5		0.007040	0.04303	<u>0.1321</u>	0.2611	0.3621	0.3479	0.1858	-0.05504	-0.2341
6		0.001202	0.01139	0.04909	<u>0.1310</u>	0.2458	0.3392	0.3376	0.2043	-0.01446
7			0.002547	0.01518	0.05338	<u>0.1296</u>	0.2336	0.3206	0.3275	0.2167
8				0.004029	0.01841	0.05653	<u>0.1280</u>	0.2235	0.3051	0.3179
9					0.005520	0.02117	0.05892	<u>0.1263</u>	0.2149	0.2919
10					0.001468	0.006964	0.02354	0.06077	<u>0.1247</u>	0.2075
11						0.002048	0.008335	0.02560	0.06222	<u>0.1231</u>
12							0.002656	0.009624	0.02739	0.06337
13								0.003275	0.01083	0.02897
14								0.001019	0.003895	0.01196
15									0.001286	0.004508
16										0.001567

Table A4 Integrals

Indefinite integrals

$$\begin{aligned}
 \int u dv &= uv - \int v du \\
 \int uv dx &= u \int v dx - \int \left[\frac{du}{dx} \int v dx \right] dx \\
 \int x \sin(ax) dx &= \frac{1}{a^2} [\sin(ax) - ax \cos(ax)] \\
 \int x \cos(ax) dx &= \frac{1}{a^2} [\cos(ax) + ax \sin(ax)] \\
 \int x \cos(ax) dx &= \frac{1}{a^2} \exp(ax)(ax - 1) \\
 \int x \exp(ax^2) dx &= \frac{1}{2a} \exp(ax^2) \\
 \int x \exp(ax) \sin(bx) dx &= \frac{1}{a^2 + b^2} \exp(ax)[a \sin(bx) - b \cos(bx)] \\
 \int x \exp(ax) \cos(bx) dx &= \frac{1}{a^2 + b^2} \exp(ax)[a \cos(bx) + b \sin(bx)] \\
 \int \frac{dx}{a^2 + b^2 x^2} &= \frac{1}{ab} \tan^{-1}\left(\frac{bx}{a}\right) \\
 \left(\int \frac{xdx}{a^2 + b^2 x^2} \right) &= \frac{1}{2b^2} \ln(a^2 + b^2 x^2) \\
 \int \frac{x^2 dx}{a^2 + b^2 x^2} &= \frac{x}{b^2} - \frac{a}{b^3} \tan^{-1}\left(\frac{bx}{a}\right)
 \end{aligned}$$

Definite integrals

$$\begin{aligned}
 \int_0^\infty \frac{x \sin(ax)}{b^2 + x^2} dx &= \frac{\pi}{2} \exp(-ab), \quad a > 0, b > 0 \\
 \int_0^\infty \frac{\cos(ax)}{b^2 + x^2} dx &= \frac{\pi}{2b} \exp(-ab), \quad a > 0, b > 0 \\
 \int_0^\infty \frac{\cos(ax)}{(b^2 - x^2)^2} dx &= \frac{\pi}{4b^3} [\sin(ab) - ab \cos(ab)], \quad a > 0, b > 0 \\
 \int_0^\infty \sin x dx &= \int_0^\infty \sin^2 x dx = \frac{1}{2} \\
 \int_0^\infty \exp(-ax^2) dx &= \frac{1}{2} \sqrt{\frac{\pi}{a}}, \quad a > 0 \\
 \int_0^\infty x^2 \exp(-ax^2) dx &= \frac{1}{4a} \sqrt{\frac{\pi}{a}}, \quad a > 0
 \end{aligned}$$

Table A5 Series expansions

Taylor series

$$f(x) = f(a) + \frac{f'(a)}{1!}(x-a) + \frac{f''(a)}{2!}(x-a)^2 + \cdots + \frac{f^{(n)}(a)}{n!}(x-a)^n + \cdots$$

where

$$f^{(n)}(a) = \left. \frac{d^n f(x)}{dx^n} \right|_{x=a}$$

MacLaurin series

$$f(x) = f(0) + \frac{f'(0)}{1!}x + \frac{f''(0)}{2!}x^2 + \cdots + \frac{f^{(n)}(0)}{n!}x^n + \cdots$$

where

$$f^{(n)}(0) = \left. \frac{d^n f(x)}{dx^n} \right|_{x=0}$$

Binomial series

$$(1+x)^n = 1 + nx + \frac{n(n-1)}{2!}x^2 + \cdots, \quad |nx| < 1$$

Exponential series

$$\exp x = 1 + x + \frac{1}{2!}x^2 + \cdots$$

Logarithmic series

$$\log(1+x) = x - \frac{1}{2}x^2 + \frac{1}{3}x^3 - \cdots$$

Trigonometric series

$$\sin x = x - \frac{1}{3!}x^3 + \frac{1}{5!}x^5 - \cdots$$

$$\cos x = 1 - \frac{1}{2!}x^2 + \frac{1}{4!}x^4 - \cdots$$

$$\tan x = x + \frac{1}{3}x^3 + \frac{2}{15}x^5 - \cdots$$

$$\sin^{-1} x = x + \frac{1}{6}x^3 + \frac{3}{40}x^5 - \cdots$$

$$\tan^{-1} x = x - \frac{1}{3}x^3 + \frac{1}{5}x^5 - \cdots, \quad |x| < 1$$

$$\text{sinc } x = 1 - \frac{1}{3!}(\pi x)^2 + \frac{1}{5!}(\pi x)^4 - \cdots$$

Table A6 Useful constants

Physical Constants

Boltzmann's constant	$k = 1.38 \times 10^{-23}$ joule/degree Kelvin
Planck's constant	$h = 6.626 \times 10^{-34}$ joule-second
Electron (fundamental) charge	$q = 1.602 \times 10^{-19}$ coulomb
Speed of light in vacuum	$c = 2.998 \times 10^8$ meters/second
Standard (absolute) temperature	$T_0 = 273$ degrees Kelvin
Thermal voltage	$V_T = 0.026$ volt at room temperature
Thermal energy kT at standard temperature	$kT_0 = 3.77 \times 10^{-21}$ joule
One hertz (hz) = 1 cycle/second; 1 cycle = 2π radians	
One watt (W) = 1 joule/second	

Mathematical Constants

Base of natural logarithm	$e = 2.7182818$
Logarithm of e to base 2	$\log_2 e = 1.442695$
Logarithm of 2 to base e	$\log e = 0.693147$
Logarithm of 2 to base 10	$\log_{10} 2 = 0.30103$
Pi	$\pi = 3.1415927$

APPENDIX B

Answers to self-test questions:

Chapter 1

1. Yes
2. No
3. 1-30 GHz
4. Yes, increases if increased
5. $Ayfl$
6. Yes
7. No
8. Yes
9. Yes
10. Yes
11. No
12. Yes
13. Yes
14. Multiplication
15. Total energy is sum of energy of each spectral component
16. Yes
17. Yes
18. Yes
19. Orthogonal set each having unity magnitude
20. If they have $360/3 = 120$ phase . difference

Chapter 2

1. Yes
2. Yes
3. $P(B)$
4. No
5. Yes
6. If X and Y are independent

7. Square root of variance
8. Yes
9. $\text{erfc}(D) = 1 - \text{erf}(i)$
10. No, the reverse
11. Yes
12. When at least one of $E[x]$ or $E[y]$ are zero
13. Yes
14. pdf of sum of N independent random variables approaches Gaussian pdf as N increases even if individual pdfs are not Gaussian
15. Yes
16. Yes
17. Ergodic
18. Yes
19. Yes
20. No, Output will be Gaussian

Chapter 3

1. Yes
2. No
3. amplitude
4. Yes
5. By coherent detection, multiplying with synchronized carrier and then low pass filtering.
6. Yes
7. Yes
8. Yes
9. No
10. Yes
11. No, only video
12. Phase error in synchronizing carrier.
13. Yes
14. No, a balanced system with an unbalanced one.
15. Yes, but gain here refers to concentration of power in one direction compared to average.
16. No, more.

Chapter 4

1. No
2. Yes
3. No, by integrating
4. Theoretically so, practically much less.
5. Since envelop is of constant magnitude energy gets distributed in sidebands.
6. Yes
7. No, $p @ 1$
8. Yes
9. Yes
10. Either multiplying by two the sum of individual deviations or their root mean square value.
11. Yes
12. Yes
13. No, both amplitude and frequency vary.
14. Yes
15. Yes

Chapter 5

1. Yes
2. No
3. No, $> 2f$
4. Yes
5. Yes
6. Yes
7. $x/\sin x$
8. The first proposition
9. Yes
10. Yes
11. No, in uniform quantization
12. Yes
13. Yes
14. Yes

15. c
16. Yes
17. Yes
18. True to the extent that the channel noise affects decoder but not encoder.
19. In RPE pulses occur at regular interval, in MPLP it is not.
20. Yes

Chapter 6

1. Yes
2. Inter channel interference
3. It is not important as what counts
there is transition and not absolute value.
4. Yes
5. No, by a factor of two
6. Yes
7. No
8. Yes
9. Yes
10. Yes, if it is generated by considering correlation between successive intervals.
11. Yes
12. No, the first criterion says that
13. Yes
14. No
15. Yes
7. If multiplicative mixing

Chapter 7

1. Thermal noise
2. Yes
3. Rayleigh
4. Yes
5. Yes
6. Yes

8. Yes
9. Differentiation
10. Yes
11. No. It also shows Gaussian distribution
12. Yes

Chapter 8

1. Yes
2. No, One-fourth
3. Yes
4. No
5. No, but restricts overload of noise.
6. The input SNR below which output SNR falls more rapidly.
7. Square-law demodulator
8. Yes

Chapter 9

1. Yes
2. Yes
3. No, but a similar relation with denominator replaced by bandwidth of baseband filter.
4. 0.5-0.6
5. Yes
6. No, improves FM significantly
7. Yes
8. 4.8 dB
9. Yes
10. Short noise
11. Yes
12. Yes
13. Yes
14. No, Positive spike is for anticlockwise rotation and negative for clockwise rotation.
15. Yes

Chapter 10

1. Yes
2. In the latter frequency is followed when changes are made slowly
3. Yes
4. Yes
5. Yes
6. Phase frequency detector
7. Yes
8. Yes
9. Yes
10. Averaging two integer divided frequencies over a certain number of VCO cycles.
11. Clock recovery, bit synchronization
12. Yes
13. Yes
14. Carrier recovery

Chapter 11

1. Yes
2. Yes
3. Yes
4. No, can be pushed up to a particular value towards other direction to get lower probability of error
5. Yes
6. No
7. Yes
8. Yes
9. Effectively reduces energy per bit and increases probability of error.
10. No, noise remains unaffected, signal strength reduced

Chapter 12

1. It shows abrupt changes and hence requires infinite sampling frequency
2. No
3. Yes
4. PSK
5. Yes

6. Yes
11. Coherent FSR
12. Yes
13. Yes
14. Yes. But for same energy per bit this distance is more for BPSR than BFSK signal
15. Upper bound
16. Yes
17. $-f_b/2$
18. Yes
19. No
20. Yes
7. Yes. Substituting in Eq. 12.39 as done in Example 1
8. Yes
9. Yes
10. Yes
11. Yes

Chapter 13

1. Yes
2. Bit
3. Yes
4. Yes
5. Yes
6. No
7. No
8. Where apriori probabilities are not known and/or where data shows some sort of repetition or redundancy in the digit string.
9. Yes
10. Yes
11. Yes
12. Yes
13. Yes
14. Yes

15. Yes
16. Yes
17. No, just opposite
18. Yes
19. Yes
20. Yes
21. Yes
22. Yes
23. Concatenated codes
24. Yes
25. It is recursive
26. Yes
27. Selective-repeat ARQ
28. Yes
29. Yes
30. Yes

Chapter 14

1. Yes
2. Yes
3. For each degree of freedom, average energy is $0.5 kT$
4. Yes
5. Yes
6. Yes
7. Noise figure
8. Yes
9. Yes
10. Earth station antenna

Chapter 15

1. Yes
2. Yes
3. Performance degradation in DS spread spectrum when unwanted user's received power, located near is much larger than desired user's received power, located far.

4. Measurement accuracy can be improved by reducing chip duration.
5. Yes
6. Yes
7. DS spread spectrum
8. $(2^n - 1) T_C$ second
9. Yes
10. Yes
11. DS spread spectrum

Chapter 16

1. Too low will prompt the speaker too loud and reverse.
2. Yes
3. The connection from subscriber to end office
4. 4 wire lines
5. Digital
6. Yes
7. Network layer
8. TCP
9. Yes
10. Dispersion
11. Yes
12. Yes
13. 2nd Generation and digital service
14. No
15. Uplink frequency is higher
16. Yes
17. Yes
18. Yes

INDEX

2B1Q, 223
16-QAM, 290, 606

A

acquisition, 817
 of a DS Signal, 823
 of an FH Signal, 817
Adaptive
 delta modulation, 238
 delta modulation encoder, 643
 delta modulator, 241
 differential pulse code modulation, 235
 equalizer, 335
 Linear Prediction: Least Mean Square Algorithm, 234
additive noise, 417
Advanced Mobile Phone Service (AMPS), 860
Advantage of the Superheterodyne, 125
A-law compander, 216
algebraic codes, 713
aliasing, 184
All Digital PLL (ADPLL), 524, 545, 547
Alternate Mark Inversion (AMI), 222
Amplitude
 demodulation, 452
 modulation, 95, 682
 modulators, 91
 spectral density, 38
 spectrum, 24
analog, 4
 communication, 4
Digital conversion, 4

PLL (APLL), 524, 525
signals, 14
to Digital, 180
to-digital converter, 213
Angle Modulation, 138
An Integrator, 432
Antenna, 123, 787, 861
antenna gain, 788
antialiasing filter, 184
aperiodic signals, 14
aperture effect, 198
a posteriori probability, 364
Application Layer, 853
Armstrong FM System, 159
Armstrong's, 156
ARQ Systems, 752
Asynchronous Transfer Mode (ATM), 855
attenuation, 3
Autocorrelation, 20, 49, 50, 391
Autocorrelation of a PN Sequence, 815
Automatic Gain Control (AGC), 125
Automatic Repeat Request (ARQ), 751
Available Bit Rate (ABR), 855
available
gain, 780
power, 776
average
distortion, 676
information, 654
power, 12

B

balanced FM demodulator, 162
Balanced Modulator, 91, 269
bandlimited, 46
band pass filter, 9, 32

Band Pass Random Process, 393
bandpass sampling theorem, 186
bandwidth, 3, 10
bandwidth expansion factor, 681, 683
Bandwidth for PAM, 194
Bandwidth of a QASK Signal, 293
bank of correlators, 442
baseband, 90
baseband signal, 3
base station, 861
Bayes' receiver, 577
Bayes' theorem, 354
BCH code, 716, 723, 724
beam width, 788
belief propagation, 749
Bending, 859
Bernoulli trial, 374
Bessel Coefficient, 143
Bessel functions, 143
BFSK, 598, 809
BFSK Receiver, 296
Binary Frequency Shift Keying (BFSK), 294
Binary Phase Shift Keying (BPSK), 269, 598, 801
binary symmetric channel, 674, 701
binomial distribution, 374
biphase, 396
Bipolar NRZ, 220
Bipolar RZ, 222
bit, 6
Bit-by-bit Encoding, 608
Bit Error Rate, 608
bit-flipping algorithm, 748
Bit Rate, 226, 801
Bit Synchronization, 590
bit synchronizer, 271, 817
Block Codes, 710

Block Coding, 703
Block Interleaving, 726
brick wall filter, 322
Broadband Integrated Services Digital Network (BISDN), 855
Burst error, 726

C

call set-up, 861
Camp-and-Wait, 820
carrier, 6
 frequency, 809
 recovery, 549
 signal, 90
Carson's rule, 146
cascade of two ports, 785
causal signal, 15
CDMA, 863
cell splitting, 860
cellular radio network, 860
CELP coder, 250
CELP decoder, 250
Centralized Adaptive Routing, 851
central-limit theorem, 369, 381
central switching, 833
channel, 2
 bandwidth, 3
 capacity, 10, 662, 673, 689
 coding, 10
 vocoder, 244
chip rate, 801
chips, 801
Circuit Switching, 846
Classification of Random Processes, 392
clipping, 839
Clock Recovery, 551
CMI, 223

Coaxial Cables, 7
Code Division Multiple Access (CDMA), 804
Coded Mark Inversion code, 223
Code-Excited Linear Prediction, 249
coder-decoder, 249
Code Tree, 733
coding, 6, 10, 662, 699
coding gain, 744
Coherent Detection, 93
Coherent Detector, 109
communication, 2
communication system, 2
commutator, 193
companding, 215
Comparison between FM and PM, 490
Comparison
 of BFSK and BPSK, 300
 of Coding Techniques, 744
 of DM and PCM, 637
 of FM and AM, 480
 of Modulation Systems, 614
 of Narrowband FM Systems, 320
 of PCM and DM, 641
complementary error function, 370
complex signal, 14
compression, 6
Computer Communication, 845
Concatenated Codes, 730
conditional probability, 353
'Constant Bandwidth' FM, 147
Constant Bit Rate (CBR), 855
Continuously Variable Slope Delta Modulator, 240
converter, 124
Convolution, 18, 43
Convolutional Code, 733, 742

Convolutional Coding, 731
Convolutional Interleaving, 727
Correlation, 18
Correlation coefficient, 19, 380
Correlator, 587
Cosine Filters, 324
Costas Loop, 550
covariance, 379
cross correlation, 18, 427
crosstalk, 180, 194
cumulative distribution function, 356
Cumulative Gaussian Probability, 370
Cyclic Codes, 721

D

Data-link Layer, 852
decibel, 12
Decoder, 213, 643
decoding, 252
Deemphasis, 482
degree of freedom, 775
delta function, 15
Delta modulation, 235
Delta Modulation (DM) Transmission, 632
delta modulator, 235
demodulation, 3
demultiplexing, 3
Dense WDM (DWDM), 859
dependent Gaussian variables, 379
Derivative with Frequency, 42
Derivative with Time, 42
Detection in Presence of Noise, 385
deterministic signal, 15
DFT coefficients, 190
Differential GPS (DGPS), 867
Differentially Encoded Phase Shift Keying (DEPSK), 277
Differential Phase Shift Keying (DPSK), 274, 593

Differential Pulse Code Modulation, 230
Differentiating Filter, 431
digital, 4
digital communication, 4
Digital Controlled Oscillator (DCO), 524, 545
Digital Phase Detector, 541
Digital Phase Frequency Detector, 542
Digital Phase-Locked Loop, 541
Digital PLL (DPLL), 524
digital signals, 14
Digital Subscriber Line (DSL), 855
digital-to-analog (D/A) converter, 213
Dirac-delta function, 15
direct digital synthesis, 554
Direct Sequence (DS) spread spectrum, 800
Dirichlet's conditions, 24
Discrete Fourier Transform, 39
Discrete Multitone Signaling (DMT), 339
Discrete Time Fourier Transform, 39, 190
Discriminator, 473, 683
dispersion, 858
Distinguishability of Signals, 64
Distortion, 2, 46, 675
distortionless transmission, 325
Double Sideband Suppressed Carrier (DSB-SC), 456
Double Side Band—Suppressed Carrier (DSB-SC) Modulation, 88
Double Sideband with Carrier (DSB-C), 95, 460
doublet, 534
DPCM, 638
DSB, 682
DSB-C Demodulator, 98
DSB-C Modulator, 97
DSB-SC Demodulator, 93
DSB-SC Modulator, 90
Duality or Symmetry, 42
Duobinary Encoding, 316

E

Early-Late gate, 823
clock recovery, 551
synchronization, 333
tracking, 821
Earth Station, 865
echo-suppressor, 839
effective distance, 789
effective input-noise temperature, 782
effective jamming power, 804
Effect of Transfer Function, 34
encoder, 212
Encoding, 252
energy signal, 15
energy spectral density, 44, 46, 50
ensemble, 389, 422
ensemble average, 390
entropy, 654
Envelope Demodulator, 463
Envelope Detector, 98, 110
Equal Gain Combining, 807
Equalization, 199
Equalizer, 333
equivalent temperatures, 785
ergodic, 390
Ergodic Random Process, 393
Error-Control Codes, 699
error function, 370
Error Probability, 668
error rate, 6
even signal, 15
Extended Codes, 720
External noise, 3
Extremely High Frequency (EHF), 9
extrinsic information, 749

Eye Pattern, 332

F

fading, 417

fading channels, 726

Fast Fourier Transform, 189

Feedback Communication, 685

Fiber Optic Communication, 858

Figure of Merit, 461, 572

Filtering, 9

Filtering of Noise, 429

final-value theorem, 535

first-order phase-locked loop, 527

Fixed Routing, 851

Flat-Top Sampling, 197

Flooding, 851

FM Broadcasting, 484

FM Demodulator, 160, 538

FM Demodulator using Feedback, 511

FM Modulators, 155

FM Receiving System, 473

FM systems, 683

forward-error correction (FEC), 751

Fourier

expansion, 31

series, 24, 56

transform, 37, 49

Fourier Transform Properties, 41

fractional divider, 545

frame, 226

Frame Synchronization, 226

Frequency

Demodulation, 525

deviation, 140

discriminator, 162

divider, 545

division multiplex (FDM), 194
division multiplexing, 7, 117
 Domain Multiplexing, 859
domain Representation of Noise, 418
Hopping (FH) spread spectrum, 809
Modulation, 138, 554, 681
multiplexing, 86, 117
multiplier, 157
pull-in, 525
reuse, 860
selective network, 160
Shifting, 42
shift keying (FSK), 591
Spectrum, 9
Synthesis, 553
synthesizer, 811
translation, 6, 86, 87
space, 62, 63

G

gateway, 845
Gaussian channel, 663, 689, 744
Gaussian Minimum Shift Keying (GMSK), 311
Gaussian
 noise, 420
 Probability Density, 369
 Random Process, 393
generator matrix, 723
Geo-stationary Earth Orbit (GEO), 865
Global Positioning System (GPS), 866
Global System for Mobile communication (GSM), 863
Golay code, 723
graded index fiber, 857
Gram-Schmidt procedure, 57, 63
Grey coding, 609

guard band, 183
guard time, 197

H

Hadamard code, 719
Hadamard matrix, 719
Hamming
 code, 712, 720
 distance, 704
 distortion, 676
hard decision, 704
hard decision decoding, 705, 709
HDB, 223
heterodyning, 90
hierarchy of switching centers, 838
High Density Bipolar code, 223
high-pass filter, 402
hold-in frequency range, 525
hopping rate, 809
Huffman Coding, 658

I

ideal filter, 9
Impedance Matching Network, 121
independent, 380
independent Gaussian random variables, 379
information, 653
information rate, 11, 655, 689
information theory, 10
infrared, 9
input transducer, 3
instantaneous
 frequency, 138
 phase, 138
integrate and dump, 572
Integrated Services Digital Network (ISDN), 855
Integration, 29, 42

interchannel interference, 272, 322
Interleaving, 167
intermediate frequency, 124
Internal noise, 3
Internet, 854
intersymbol interference, 272, 322, 324, 326
intrinsic information, 749
Inverse Discrete Fourier Transform, 189
Irrelevant Noise Components, 442
Isolated Adaptive Routing, 851

J

jam, 810
jamming, 803
jitter, 333
Joint Cumulative Distribution, 360
joint entropy, 673
Joint Probability, 353

L

LASER, 856
Lempel-Ziv (LZ) Coding, 660
Light Emitting Diode (LED), 856
likelihood ratio (LLR), 749
Limiter, 473
Limiter-Discriminator, 473
linear distortion, 3
Linearity, 42
Linear Predictive Coder, 246
linear predictive encoder, 248, 249
Linear system, 18, 30
linear-time-invariant, 18
Line Coding, 220
LMS algorithm, 234
local area network (LAN), 853
local oscillator, 87, 90
lock-in frequency range, 525
lossy source coding, 675

Low Density Parity Check (LDPC) codes, 746
Low Earth Orbit (LEO), 864
lower-sideband, 90
Low Frequency (LF), 9
low pass filter, 9, 403

M

main beam, 788
Manchester Coding, 223
M-ary FSK, 300, 302
M-ary Phase Shift Keying, 284, 606
M-ary PSK receiver, 288
M-ary PSK transmitter, 287
M-ary Signal, 603
Matched Filter, 432, 583, 587, 667
Matched Filter receiver, 576
material loss, 858
Maximal Sequence, 814
Maximum Likelihood Detector, 574
Maximum Ratio Combining, 807
mean, 366
Mean Square Equalizer, 334
Medium Earth Orbit (MEO), 865
Medium Frequency (MF), 9
MELP, 252
Message Switching, 846
Method, 156
metropolitan area network (MAN), 854
Micro-bending loss, 859
Microwave, 9
microwave receivers, 785
Milimeter waves, 9
Minimum Shift Keying (MSK), 303
Mixed Excitation Linear Prediction, 251
mixing, 90
Mixing Noise with Noise, 428
Mixing Noise with Sinusoid, 427

m-law compandor, 216
mobile subscriber unit (MSU), 861
Mobile Telephone Communication, 860
mobile telephone switching office (MTSO), 861
modulates, 3
Modulation, 6
modulation index, 103, 140
Modulation Index: AM vs. FM, 146
MPLP codec, 249
MSK, 602
MSK as FSK, 305
Multipath fading, 806
Multiple Random Process, 393
multiplexes, 3
Multiplexing, 6, 126
Multi-Pulse Excited Linear Prediction, 247
mutual information, 673
Mutually Exclusive Events, 352

N

Narrowband Angle Modulation, 152
narrowband FM, 149
Narrowbanding, 87
natural sampling, 196
near-far problem, 806, 810
negative correlation, 19
Network Layer, 852
Network Protocols, 852
Noise Bandwidth, 434, 781
Noise, 3
 figure, 780, 782, 785
 power, 454, 456
 suppression, 461
 temperature, 777
 using Orthonormal Coordinates, 440
noncausal signal, 15

noncoherent detection, 593
nonlinear distortion, 3
Nonlinear Modulator, 91
Non-offset QPSK, 281
Non-Orthogonal BFSK, 298
non-return-to-zero, 396
nonsystematic code, 703
normalized energy, 12
normalized power, 12, 31, 422
Norton equivalent, 772
NRZ
 bit stream, 802
 data, 401
 waveform, 272
Numerical aperture, 858
Numerical Controlled Oscillator (NCO), 545
Numerically Controlled Oscillator (NCO), 524
Nyquist
 criterion, 322
 first criterion, 322
 pulse, 322
 rate, 184
 sampling rate, 665
 second criterion, 325
 theory, 14

O

odd signal, 15
OFDMA, 339
offset QPSK, 279
On-Off Keying (OOK), 856
Open System Interconnection, 853
Open Wire Lines, 7
optical communication, 9, 856
Optical Fibre, 8
Optimal Receiver, 362, 580

optimum communication system, 681
Optimum-Filter Transfer Function, 581
orthogonal, 31
Orthogonal BFSK, 297
orthogonal code, 706
Orthogonal Frequency Division Multiplexing (OFDM), 335
orthogonality, 55
Orthogonal
 M-ary FSK, 607
 representation, 54
 Set, 55, 56
 Signals, 666
orthonormal
 set, 55, 56
 vector, 59
Output-Noise Power, 476
Output SNR, 479, 538
output transducer, 3
overload suppression, 461

P

Packet-Switched Network, 847
paging, 861
Paired Cables, 7
Paley-Wiener criterion, 54
Parity Check, 703
parity-check bit code, 718
Parseval's Theorem, 44
Partial Response Signaling, 326
passband, 47
PCM System, 212
PCM Transmission, 624
percentage modulation, 100
periodic
 signals, 14
 waveform, 49

phase

- comparator, 545
- continuity, 308
- demodulator, 163
- deviation, 140
- locked loop, 94, 162, 524, 528, 550
- lock-in, 525
- modulation, 138, 159, 487
- modulator, 163, 554
- spectrum, 24
- phase-shift keying (PSK), 589
- Phase Synchronization, 589
- Phasor Diagram: AM vs. FM, 149
- photodetector, 858
- Physical Layer, 852
- pitch, 244
- PLL, 524
- Poisson distribution, 375
- polling, 851
- positive correlation, 19
- power, 45
 - Amplifier, 120
 - of FM Signal, 144
 - signal, 15
 - spectral density, 44, 50, 392, 398, 418
- Power Spectral Density (PSD), 33
- PPM demodulation, 204
- Practical Filter, 54
- Predictor, 231
- predictor coefficient, 234
- Preemphasis, 482
- Presentation Layer, 853
- Probability, 352, 359
 - density, 359, 360

density function, 357
density of noise, 387
of error, 5, 73, 372, 383, 597
processing gain, 804
proportional-plus-integral filter, 535
PSD, 34
pseudo-random noise, 800
Pseudorandom (PN) Sequences, 812
public switched telephone network (PSTN), 855
pull-in frequency range, 525
Pulse
 Amplitude Modulation, 192
 Averaging Discriminator, 163
pulse-code modulation (PCM), 210
Pulse Position Modulation (PPM), 202
Pulse Width Modulation (PWM), 202
PWM demodulation, 204

Q

QASK Receiver, 293
QPR
 decoder, 330
 encoder, 329
 system, 610
QPSK, 594, 601
 receiver, 282
 transmitter, 279
Quad Cables, 7
Quadrature
 Amplitude Modulation (QAM), 116, 290
 Amplitude Shift Keying (QASK), 290
 Components of Noise, 436
 Noise Components, 455
 Partial Response (QPR), 327
 Phase Shift Keying (QPSK), 278

quantization

- error, 208
- levels, 206
- noise, 4, 207, 625, 634
- of signals, 206

R

radiation loss, 859

Radio, 7

- frequency, 124
 - receiver, 124
 - spectrum, 9
 - transmitter, 119
- rake receiver, 806
- random
- access, 851
 - processes, 389
 - pulses, 394
 - signals, 15
 - variables, 356, 419

walk, 851

ranging, 807

Rate

- distortion function, 676
- distortion theory, 675
- of the code, 703

Rayleigh

- Probability Density, 372
- scattering, 858

Ray model, 857

Reactive Elements, 773

real signals, 14

receiver, 3

receiver for a binary-coded signal, 571

Reception of BPSK, 270

Rectifier Detector, 99
recursive systematic convolution (RSC), 745
Reed-Solomon (RS) Code, 729
regenerative repeater, 4, 331
Regular Pulse Excited, 249
relationship between phase and frequency modulation, 139
repeated code, 718
repeater, 6, 180
requantization, 213
Resistor Noise, 771
Rician Distribution, 374
rise time, 47
RMS power, 12
root mean square, 368
rounding, 664
router, 845

S

sample functions, 27, 389
Sampling of Bandpass Signal, 184
sampling rate, 181
 theorem, 181
 time, 181
Satellite Communication, 864
satellite-to-earth communication system, 790
Scattering loss, 858
Schwarz inequality, 582
Scrambling, 223
Second-Order Phase-Locked Loop, 534
Sequential Decoding, 736
Serial-Search technique, 823
Session Layer, 853
Shannon-Fano Coding, 657
Shannon-Hartley theorem, 663, 680
Shannon limit, 666, 671, 699
Shannon's

equation, 10
lower bound, 676
theorem, 662
short message services (SMS), 863
Short Waves (SW), 9
side lobes, 788
sidetone, 832
signal, 11
bandwidth, 3
energy, 12, 62
Energy Per Bit, 687
Signaling, 226
Signal power, 12, 452, 457
Signal Recovery Through Holding, 200
signal space, 272, 283-285, 290, 297-299, 302, 308, 597
Signal to Noise Ratio, 6, 10, 458, 476
Signal-to-Noise Ratio in DM, 640
Signal-to-Noise Ratio in PCM, 629
Signal-to-Noise Ratio (SNR), 455
signal-to-quantization noise ratio, 215
signal-to-quantization-noise ratio for delta modulation, 636
Single SideBand Modulation (SSB), 105
Single Sideband Suppressed Carrier (SSB-SC), 452
single-sided spectrum, 25
Single-Tone Interference, 802
slope-overload error, 236
slot-content memory, 843
soft-decision, 705
soft-decision decoding, 705
Software PLL, 546
Software PLL (SPLL), 524
source, 2
source coding, 10
Sources of Noise, 417
space-multiplexing, 841

Space Shuttle ADM, 642
spectral
 amplitudes, 24
 component, 24
Spectral Components of Noise, 421
Spectrum of Tone Modulated Signal, 142
Spikes, 496
Spike
 Characteristics, 499
 Duration, 501
 Suppression, 532
Spread spectrum, 799
Square Law Demodulator, 462
Squaring Synchronizer, 94
SSB, 682
 Demodulator, 109
 Modulator, 107
stable point, 531
standard deviation, 368
state diagram, 738
stationary, 390
statistical fluctuations, 417
Statistical Independence, 354
step index fiber, 857
Stereo FM, 487
Stereophonic FM, 164
Strict-sense Stationary, 392
subscriber loop, 836
Sum of Random Variables, 376
superheterodyne system, 124
Super High Frequency (SHF), 9
Superposition of Noises, 426
switch, 845
 matrix, 833
Symbol-by-symbol Encoding, 608

Symbol Error Rate, 608
synchronization problem, 812
Synchronous Digital Hierarchy (SDH), 856
Synchronous Optical Network (SONET), 856
syndrome, 714
systematic code, 703, 720

T

T1 Digital System, 224
Tamed FM, 319
Tchebyheff's Inequality, 381
TDM hierarchy, 228
Telephone
 Exchange, 834
 Switching, 832
Television Broadcasting, 114
The Discrete Fourier Transform, 187
thermal agitations, 417
Thermal Noise, 628, 772, 801
Thermal Noise in DM, 639
Thevenin equivalent, 772
third Nyquist criterion, 326
Third-order Phase-locked Loop, 536
threshold, 631
 effect in AM Reception, 462
 extension, 513
 extension of a PLL, 540
 in an FM Discriminator, 502
 in Frequency Modulation, 494
throughput efficiency, 753
time
 average, 390
 Derivative, 29
Division Multiple Access (TDMA), 862
division multiplexing, 7
Scaling, 17, 29, 42

Shift, 29, 42
Shifting, 17
Slot Interchanging, 843
time-division multiplex (TDM), 194
time-invariant, 18
Time Inversion, 17, 29, 42
time-multiplexing, 841
tracking, 817
Tracking of a DS Signal, 824
Tracking of an FH Signal, 820
transducers, 3
Transmission
 Media, 7
 of a Random Process, 398
transmitter, 3
 Noise, 491
Transport Layer, 853
Trellis-Decoded Modulation, 755
trellis, 737
 decoding, 755
 diagrams, 737
 structure, 738
Turbo Codes, 745
two-port network, 779
two-sided spectrum, 25

U

Ultra High Frequency (UHF), 9
uncorrelated, 380, 422
union-bound approximation, 603
Unipolar NRZ, 220
Unipolar RZ, 220
unit impulse function, 15
unit step function, 15
Unit step function, 16
Unspecified Bit Rate (UBR), 855

upper-sideband, 90

V

Variable Bit Rate (VBR), 855

variance, 368

VCO, 156, 526

Very High Frequency (VHF), 9

Very Low Frequency (VLF), 9

Vestigial SideBand (VSB) Modulation, 112

Viterbi Algorithm, 739

Vocoder, 243

Voice Model, 243

Voltage Controlled Oscillator (VCO), 156, 524, 526

W

Waveguide, 8

Wavelength Division Multiplexing, 859

Weiner-Hopf Filter, 399

White Noise, 394

wide area network (WAN), 854

Wideband FM, 153

Wide-sense Stationary, 392

wired line, 2

wireless, 2

Z

zero crossing equalizer, 333

Zero Forcing Equalizer, 334